MISSION TO EARTH: LANDSAT VIEWS THE WORLD



NATIONAL AERONAUTICS
AND SPACE ADMINISTRATION

NASA SP–360

MISSION TO EARTH: LANDSAT VIEWS THE WORLD

Authors

NICHOLAS M. SHORT, PAUL D. LOWMAN, Jr.,
AND STANLEY C. FREDEN
NASA Goddard Space Flight Center

and

WILLIAM A. FINCH, Jr.
San Diego State University

Scientific and Technical Information Office 1976
NATIONAL AERONAUTICS AND SPACE ADMINISTRATION
Washington, D.C.

The cover picture shows some 34 000 square kilometers (13 000 square miles) of southern California, including Los Angeles (lower right) and other cities of the Los Angeles Basin and San Fernando Valley. The light-colored triangular area in the upper right quarter of the scene is the Mojave Desert, bounded on the southwest by the San Andreas fault and on the northwest by the Garlock fault. The Mojave Desert is separated from the Pacific Ocean in this area by the various mountains making up the Transverse Ranges. The south end of the San Joaquin Valley is visible at upper left, marked by the checkerboard pattern characteristic of farming areas. A more detailed description of this area will be found accompanying plate 129.

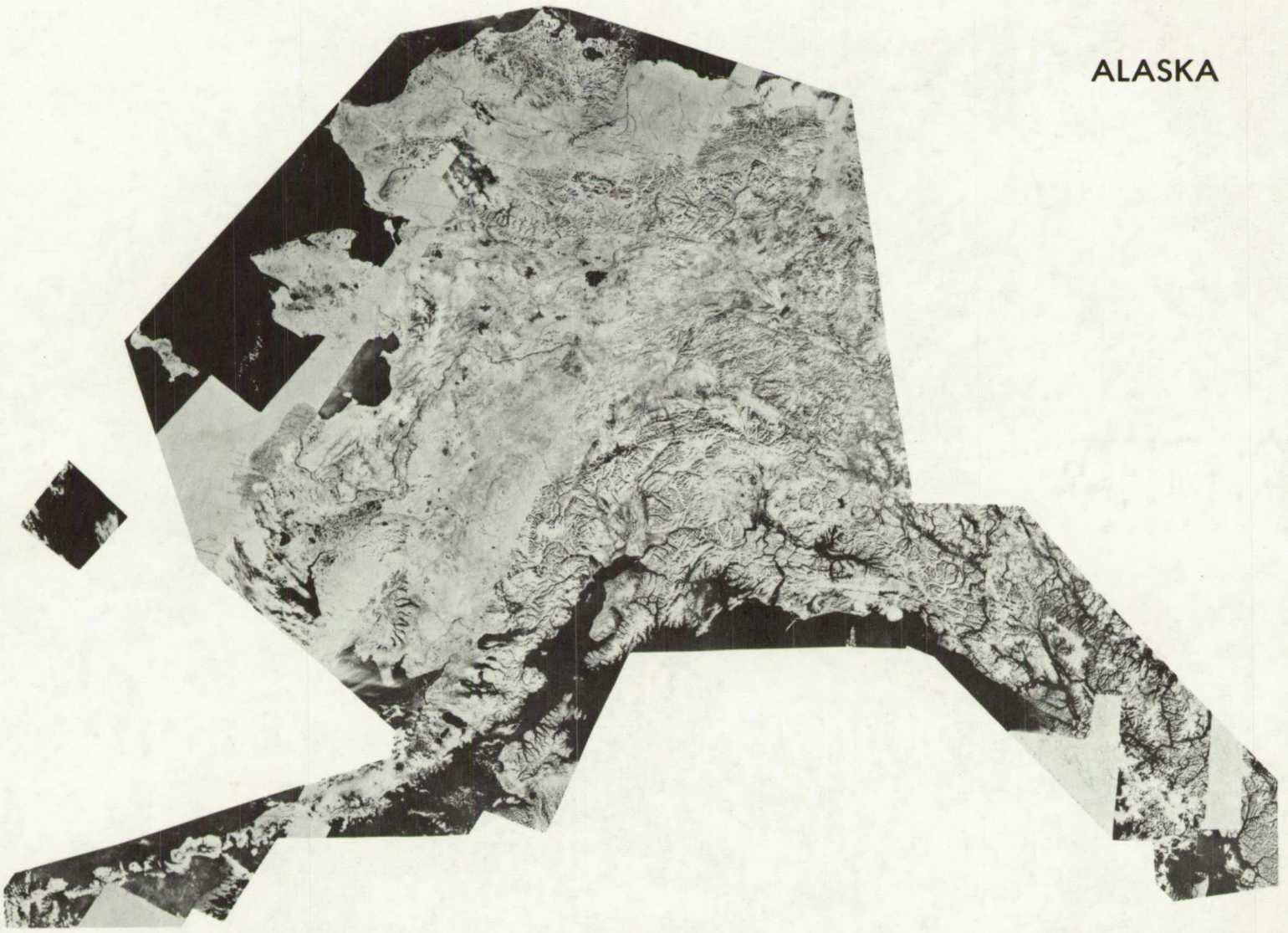
The front endpaper shows the first false color mosaic of the conterminous United States constructed from 569 Landsat images by the General Electric Co. in cooperation with the National Geographic Society and the National Aeronautics and Space Administration. This false color rendition used multispectral scanner bands 4, 5, and 7, displayed in blue, green, and red, respectively.

The first precision black and white photomosaic of the conterminous United States is shown in the back endpaper. This mosaic was compiled using imagery from Landsat 1. The mosaic consists of 595 cloud-free, multispectral scanner band 5 (0.6 to 0.7 micrometer) images obtained during the period from July 25 to November 1, 1972. The Soil Conservation Service of the U.S. Department of Agriculture produced the mosaic for NASA's Goddard Space Flight Center. Mosaics of Alaska and Hawaii appear on the last page before the endpaper in the back of this book.

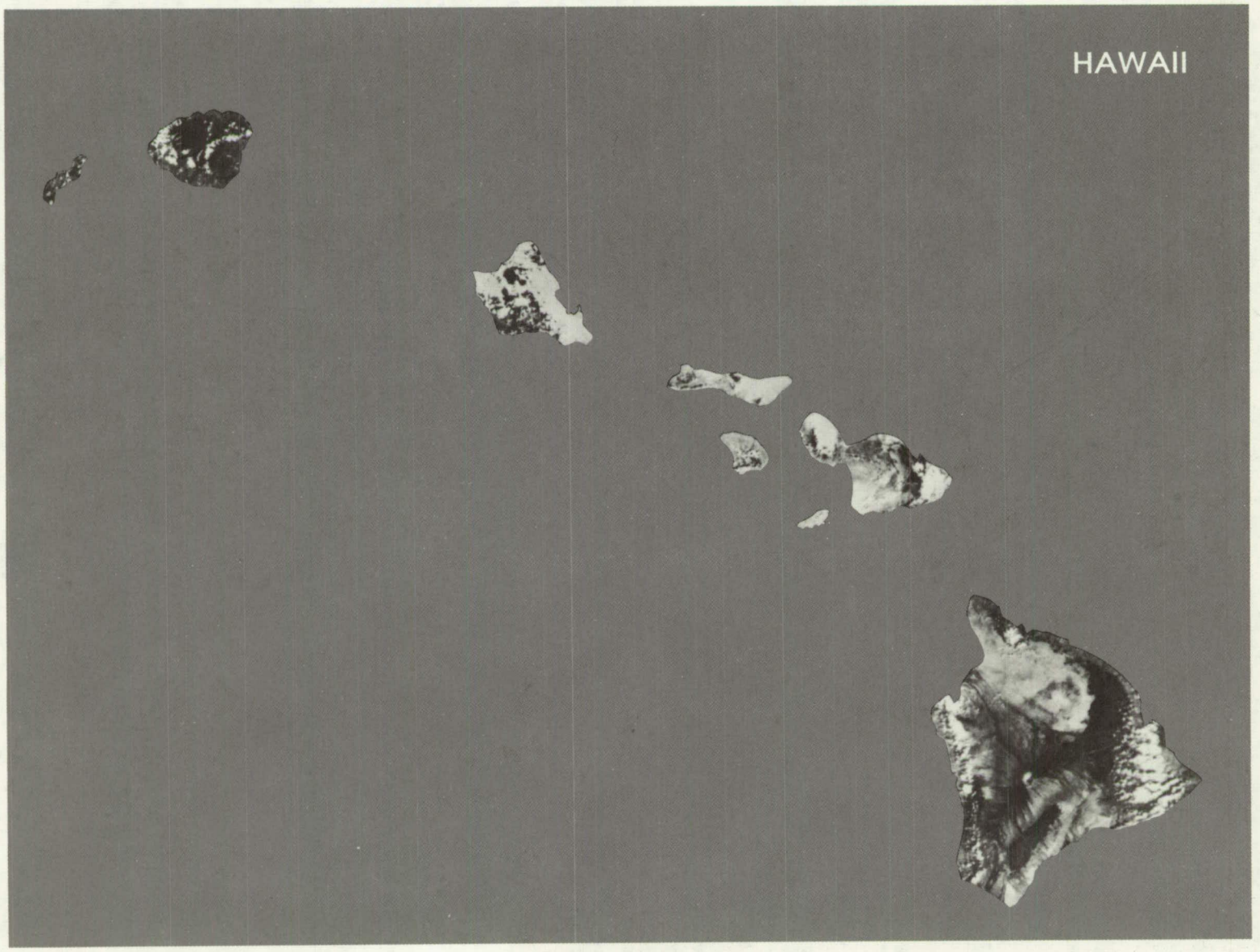
Mission to earth. Landsat views the world.
(NASA SP ; 360)
Includes index.
Supt. of Docs. no.: NAS 1.21:360
1. Earth—Photographs from space. 2. Astronautics in earth sciences. I. Short, Nicholas M. II. Series: United States. National Aeronautics and Space Administration. NASA SP ; 360.
QB637.M57 910'.02'0222 76-608116

For sale by the Superintendent of Documents,
U.S. Government Printing Office, Washington, D.C. 20402
Price $14 Stock Number 033-000-00659-4

ALASKA



HAWAII





This book is dedicated to William Nordberg, whose dynamic leadership contributed greatly to the development of the Landsat system and to the achievement of project objectives. His boundless energy, creative ability, and tireless efforts brought together a large number of technical contributors and data users from all over the world, so that Landsat has truly lived up to its motto, "For the benefit of all mankind."

PAGE MISSING FROM AVAILABLE VERSION

Preface

This book was conceived on the very day the first Landsat (originally called the Earth Resources Technology Satellite or ERTS) images were received, processed, and displayed to the more than 100 expectant scientists and technologists at the Goddard Space Flight Center. Almost immediately after the Landsat 1 image showing the Ouachita Mountains (see p. 84, plate 49) was mounted in a viewer, one of the book's authors—surprised and delighted by the variety and sharpness of the features it contained—announced to his nearby colleagues that "we'd better get started right now in picking the best to come for a picture book."

Nearly 4 years and more than 100 000 images later, the results of that commitment have been assembled into this compendium of outstanding Landsat scenes depicting the Earth's surface from a perspective never before presented in such breadth and detail. Prior to Landsat, synoptic photos that view large areas of the world had been obtained during the Mercury, Gemini, and Apollo missions. Unmanned NASA meteorological satellites in the TIROS and Nimbus series also produced TV and scanner images that covered vast areas of the continents. The Soviets, too, had acquired similar pictures from many of their space efforts. But, for the first time, Landsat images make it possible to visualize essentially the entire global land surface at a scale and resolution that specify many natural and cultural features in man's familiar environments with sufficient clarity to be recognized. In addition to their technical value, Landsat images are almost unique in their esthetic qualities—showing in numerous examples a richness in color and form that rivals the finest of the French impressionist paintings.

Mission to Earth will be published during the year of the bicentennial celebration of the founding of the United States of America. It is fitting, in honor of this event, that almost 40 percent of this book presents outstanding views of the vastness and variety of our country—the wooded Appalachians and industrial lowlands of the east, the rolling glacial hills and scattered lakes of the north country, the pine forests and savannas of the south, the prairies and farms of the midwest and plains, the western mountains and desert basins from Canada to Mexico, and the rugged coastlines along the Pacific. The book, furthermore, appears at about the same time as an excellent companion volume:

> *ERTS-1, A New Window on Our Planet* (R. S. Williams and W. D. Carter, eds.), U.S. Geological Survey Professional Paper 929, 1976

That book reviews in more detail a wide range of examples and case histories that demonstrate the practical applications of Landsat to resources evaluation and decisionmaking in many of the activities—including cartography, geologic mapping, mineral resource evaluation, water inventory, coastal and wetlands management, and land use assessment—that come under the auspices of the Department of the Interior.

Mission to Earth traces its particular lineage to several publications:

> NASA SP–129 and SP–171, *Earth Photographs From Gemini III, IV, and V* and *Earth Photographs From Gemini VI Through XII,* U.S. Government Printing Office, 1967 and 1968
>
> NASA SP–250, *This Island Earth* (O. W. Nicks, ed.), U.S. Government Printing Office, 1970
>
> P. D. Lowman, *The Third Planet,* Weltflugbild Publ., Switzerland, 1972.

In planning the present book, we have generally followed the format and style of these predecessors. However, two important variants have been introduced. First, we have preceded the main "picture gallery" section with a comprehensive introduction explaining the spacecraft and its data-gathering systems, and giving also a broad review of Landsat accomplishments and applications. (Additional technical detail is provided in appendix A.) This properly recognizes that Landsat was designed primarily to collect extensive information about both the spatial and temporal states of the Earth's surface to better assess the natural resources available to mankind. Second, we have expanded the customary lengths of captions accompanying the images to narratives that, hopefully, summarize most of the

basic story present in any scene. Thus, as a rule, a caption will describe the well-known geographic points of interest that locate the scene, its main urban and cultural features, the major farming and industrial activities of the region, and its characteristic natural vegetation. In addition, many aspects of the geology exposed in a scene have been given considerable attention. (See appendix B for a glossary of technical terms.) This, no doubt, reflects the geological background of two of the authors and the physical geography background of a third, but it also stems from the inherent dominance of many scenes by such expansive and imposing features as mountain ranges, depositional landforms, and volcanic fields, which occupy a large fraction of any regional terrain.

The selection process leading to this final collection of exceptional images deserves some explanation. As Landsat 1 continued to send back new imagery, certain individual images were singled out as being special by many interested workers at Goddard, other agencies, the investigator teams, and others in the data user community because of such diverse criteria as geographic location, natural scene content, variety of information relevant to applications, features or events of unusual interest, political importance, public relations value, and explicit beauty. These images, then, became the nucleus of the book; some were added and others deleted over time so as to lead to constant iteration of content and improvement in scene quality. Many of the images that remain in the final version were culled from a large collection. Others were found by frequent "rummaging" through the files of the Landsat Browse Library at the NASA Data Processing Facility (NDPF). Some images were chosen from the collection developed for press releases by Goddard's Public Information Office. Again, other images had been prepared for the user community by several photographic laboratories outside NASA. (See appendix C.)

Ultimately, the makeup of the image sequence depended on three factors. First, we tried insofar as practical to "cover the world" with representative examples. One constraint was to give some preferential coverage to the United States—about 40 percent of the book is devoted to the 50 States. At least one image was selected to include part of each State. The total allotted to each State was fixed by the size of the State (Rhode Island and Delaware essentially fit into single images whereas 13 images embrace only a fraction of Alaska) and by the variety of features we wished to depict (California, for example, required nine images to show most of its major cities and certain natural phenomena). Another constraint involved the attempt to cover the better-known areas elsewhere in the world while showing the considerable variations in regional geographies. Only about 200 scenes could be used to exemplify the remainder of the Earth's continents, which otherwise would require almost 11 000 scenes for complete coverage. Certain areas such as parts of Africa and Canada may seem to be disproportionately covered; this is largely the consequence of either the "photogenic" nature of the regions selected or the availability of extensive coverage. Some parts of the world have not been as well treated in this book simply because of limited coverage from Landsat. Thus, few suitable images were available for much of central Africa and parts of Central and South America, Ireland, and sections of the European Soviet Union and the block of Warsaw Pact nations; this is generally the result of excessive cloud cover or the absence of NASA-sponsored investigations there that called for coverage.

The second factor was based on the availability of appropriate black and white or color composite imagery. Because of uneven quality, it was necessary to reprocess all black and white images to improve scene contrast and definition. The color composites come from several sources. (The sources of the images are listed in appendix C.) Each processing source tends to have its own characteristic color balance. Images produced by one laboratory are recognized by their stronger green and yellow tones whereas those made by another facility emphasize blues and reds. Still other sources might lean toward brighter or more pastel renditions, brown tones, etc. This diversity stems from a current lack of control specifications for color processing of Landsat images; each facility employs some particular equipment and materials to routinely process its images without regard to reproducing to a common standard. The reader will therefore notice several distinct color types in this book. Color variations, of course, can be useful in bringing out certain features within the image, and completely different color combinations are often made for interpretative reasons. (See the introductory chapter.)

The third factor was the suggestion to "inject some variety" into the image sequence to sustain reader interest. This translates into an interspersion of mosaics, montages, enlargements, and repetitive coverage of Landsat imagery into the common mode of presentation. The standard mode is that of the 1:1 000 000 scale format in which the complete scene is 185 km (115 miles) on a side and encompasses about 34 000 km^2 (13 000 sq miles). In this book, the tick marks.

locaters, and other descriptive notation have been removed from the images prepared at the NASA Data Processing Facility (an example of the complete notation appears in fig. 13(*a*)). Some of this information, including geographic center coordinates and Sun azimuth and elevation, is recorded in appendix C. Each normal mode image has been fitted to a reference (letter-number) grid system along its margins. Any feature within the image, when referred to in its caption, can be located to an accuracy within one grid cell using this system. Some scene features spread out over several cells while others may lie more or less astride cell lines or their intersections; the reader must exercise some judgment in finding a specific location. Nonnormal mode images (e.g., mosaics) generally are indexed by sketch maps that locate features identified in the caption text.

Most of the captions were written by Drs. Short, Lowman, and Finch, but "guest" caption writers were sought for some individual or groups of images. The author of each caption is indicated in appendix C.

The ideal way to write a definitive caption free of error is to visit the area under consideration and to interview the local experts. Because this was not possible, the next best alternative was employed, consulting appropriate reference books, drawing upon travel experiences and professional knowledge, and checking with knowledgeable people in the Washington, D.C., area or with foreign visitors to Goddard. Because source books and regional data were often lacking or were notably sparse in the particular kinds of information required, we admit to the likelihood of errors of misidentification, incorrect geographic nomenclature (various atlases used different and inconsistent spellings), and overgeneralizations in regard to geological, agricultural, and natural vegetation features listed as present in the scene (for example, a given crop or forest type that is only a small percentage of the total number of varieties present is normally given coequal listing). Owing to production schedules, we were unable to subject these captions to the same extensive review by outside specialists that we habitually apply to our technical papers. To allow the reader to cross-check the data sources, we here present those principal references employed in preparing the captions:

National Atlas of the United States, U.S. Geological Survey, 1970

The [London] *Times Atlas of the World* (J. Bartholomew, ed.), volumes I to V, Houghton Mifflin Co., Boston, 1957

National Geographic Atlas of the World (F. G. Vosburgh, ed.; rev. 3d ed.), Washington, D.C., 1970

Goode's World Atlas (E. G. Espenshade, Jr., and J. L. Morrison, eds.; 14th ed.), Rand McNally & Co., Chicago, 1974

Advanced Level Geography Series: D. C. Money, *Australia and New Zealand;* H. Robinson, *The Mediterranean Lands;* D. C. Money, *South America;* B. Carlson, *North America;* H. Robinson, *Western Europe;* W. F. Hornby and P. Newton, *Africa; Monsoon Lands* (pt. 1: R. T. Cobb and L. J. M. Coleby; pt. 2: W. B. Cornish); University Tutorial Press, London

Preston, James, *Latin America,* Odyssey Press, 1964

A. B. Mountjoy and C. Embleton, *Africa: A New Geographical Survey,* F. A. Praeger Pub., Inc., 1967

S. P. Suslov, *Physical Geography of Asiatic Russia,* W. H. Freeman and Co., Publ., 1961

L. S. Berg, *Natural Regions of the U.S.S.R.,* Macmillan Co., New York, 1950

D. V. Nalivkin, *The Geology of the U.S.S.R.: A Short Outline,* Pergamon Press, 1960

C. B. Hunt, *Physiography of the United States,* W. H. Freeman and Co., Publ., 1967

W. D. Thornbury, *Regional Geomorphology of the United States,* Wiley-Interscience, 1965

E. Raisz, *Landforms of the United States* (6th rev. ed.), 1960

This book has been oriented toward a wide readership—resource specialists; research professors; college and high school teachers in the relevant disciplines; the serious student in geography, geology, and other fields; the outdoorsman; the traveler; and the general public. As an aid to the reader, in appendix B we have compiled a glossary of terms from the several indicated sources. The reader is advised to become familiar with the geological terms that recur frequently in the captions.

An Educator's Guide for *Mission to Earth: Landsat Views the World* is available from the Educational Programs Office, Code 202.3, Goddard Space Flight Center, Greenbelt, Md. There is no cost for this publication.

The Educator's Guide serves as an educational supplement to *Mission to*

Earth. It provides a general overview of the Landsat program, how the satellite operates, and an explanation of remote sensing and imagery, as well as some suggested classroom uses of the imagery.

Contained within the Guide is a Teacher's Resource Section that includes classroom activities, exercises, and techniques for using the imagery. This section is organized around several major discipline areas; i.e., Earth science, geography, and social studies. To facilitate the use of *Mission to Earth,* the Guide includes a glossary of geological and remote sensing terms that are used in the book.

Some readers will no doubt want to procure copies of individual images displayed in this book or may desire images of other areas of personal interest to them. These readers are encouraged to write to any of the following distribution centers for further information, including catalogs and prices, about Landsat imagery:

EROS Data Center, U.S. Geological Survey, 10th and Dakota Ave., Sioux Falls, S. Dak. 57098

National Climatic Center, Federal Building, Asheville, N.C. 28802

Department of Agriculture, Western Photo Laboratory, ASCS-USDA, 2505 Parleys Way, Salt Lake City, Utah 84109

In closing, we take this opportunity to express our gratitude to the following for their assistance in preparing this book: H. Mathews (formerly of NASA Goddard), A. Anderson, A. Rango, and V. V. Salomonson, all of NASA Goddard, for help in selecting the images; C. Bohn, S. Deremer, and B. Bligh of NASA Goddard for aid in obtaining many of the images; W. Kouns of NASA Goddard for performing several important tabulation and plotting tasks; A. Smith of General Electric Space Sciences, Inc., for helpful services in providing numerous color composite images; and B. M. French of the National Science Foundation for suggesting the title of this book.

Contents

	Page
SURVEY OF THE LANDSAT PROGRAM *Stanley C. Freden*	1
PLATES OF LANDSAT IMAGES	27
APPENDIX A—THE LANDSAT SYSTEM *Stanley C. Freden*	437
APPENDIX B—GLOSSARY OF TECHNICAL TERMS *Paul D. Lowman, Jr., and Margaret A. Tindal*	443
APPENDIX C—INDEX OF PLATES *Nicholas M. Short*	453

*Survey of the Landsat Program**

The now-famous deep space photographs of the Earth from Apollo spacecraft (fig. 1) dramatize the uniqueness of our planet, and especially the fragility of its environment. These photographs have also brought out the global nature of many problems, such as pollution, drought, and climatic changes. Satellites and other space vehicles are naturally suited to study such problems. To use this capability in a practical way, the National Aeronautics and Space Administration (NASA) established the Earth Resources Survey Program in 1965. This program has since evolved into an effort to apply space and aircraft technology to global problems now becoming acute: food production, increasing scarcity of metals and fossil fuel supplies, and environmental degradation, to mention just a few. It is also concerned with acquiring continuing information on such diverse regional activities as forest cutting, changing land use, water storage, and coastal sedimentation effects. The program gathers its data primarily through "remote sensing," the science (or art) of studying objects or areas from a distance.

As generally used, "remote sensing" refers to the recording and analysis of electromagnetic radiation—visible light, infrared radiation, and similar forms of wave-transmitted energy. Remote sensing, strictly speaking, is a new term, not a new science. Astronomy has always depended on sensing at a distance as its main tool, and any table radio is a remote sensing instrument of certain wavelengths of electromagnetic radiation.

The NASA Earth Resources Survey Program is based largely on remote sensing of the Earth's surface from aircraft and spacecraft. Emphasis is placed on detecting and measuring radiation ranging from the ultraviolet through the visible and infrared to the microwave portions of the electromagnetic spectrum. The program relies on a wide variety of instruments and techniques and on advanced communication systems to relay the data to control and processing facilities and on computers to store, process, and analyze the data. Many discipline specialists, such as hydrologists, foresters, and geographers, then interpret the data products and apply the results to the solutions of practical problems in the everyday world. This type of information is also proving valuable to decisionmakers concerned with managing the Earth's resources and environment. The role of NASA is mainly an experimental one demonstrating concepts and feasibility, inasmuch as operational applications of remotely sensed information to fields such as geology, agriculture, and environmental monitoring are the province of other designated governmental agencies and many private organizations in the user community.

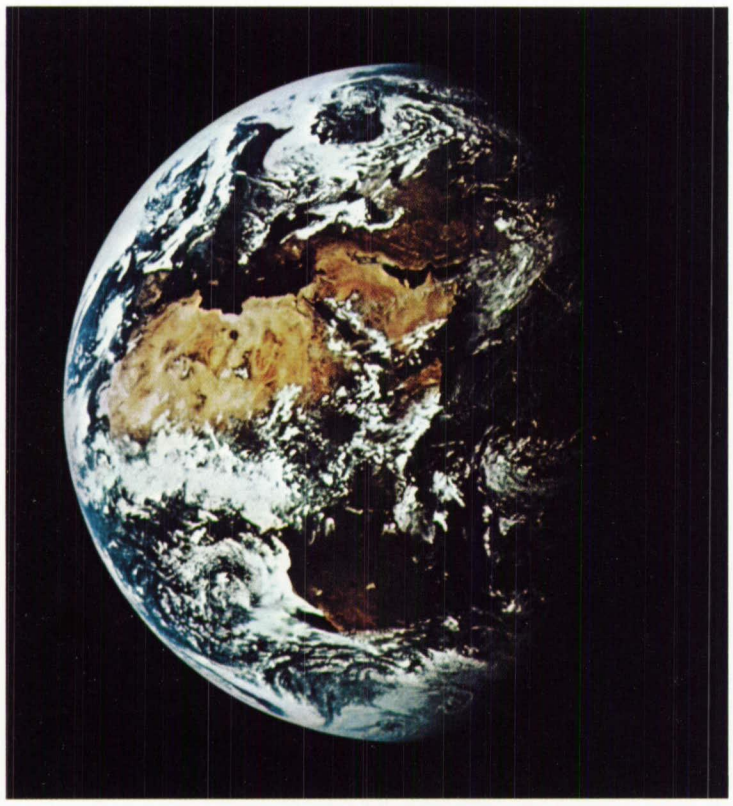


FIGURE 1.—Deep space photo of Earth from Apollo.

* Written by Stanley C. Freden, *Goddard Space Flight Center*.

Since its inception, the Earth Resources Survey Program has included experiments carried out from the Gemini, Apollo, Landsat, and Skylab space missions as well as from aircraft. Clearly, the most significant and widely used mission to date has been the highly successful Landsat (originally named the Earth Resources Technology Satellite, or ERTS). Landsat 1 was launched on July 23, 1972. A second Landsat was placed in orbit on January 22, 1975, so that both spacecraft have now operated simultaneously for more than a year. Designed as a research and development tool to demonstrate the feasibility of systematic remote sensing from Earth orbit for resource and environmental monitoring, the two Landsats have already shown that the application of satellite-acquired data on the Earth's surface is a practical reality. Hundreds of thousands of images of the Earth have been returned by these satellites. This book presents some of the best of this collection.

THE LANDSAT SYSTEM

Basic data on the technical aspects of Landsat, such as orbital parameters, sensor payload, data products, and data handling systems, are reviewed in detail in appendix A. A brief synopsis of the characteristics of the satellite system and the principal data products is given in the next paragraphs.

An artist's rendering of the Landsat 1 spacecraft is shown in figure 2. This satellite moves in an almost perfectly circular orbit at an altitude of 917 km (570 miles) inclined at 81° relative to a plane passing through the Earth's Equator. This near polar orbit is also Sun synchronous, crossing the Equator on the day side of Earth 14 times every day at approximately 9:30 a.m. local time in each transit. Each successive orbit shifts westward about 2875 km (1785 miles) at the Equator. On the following day the next 14 orbits parallel those of the previous day, but each one is offset westward by about 159 km (99 miles). Images obtained for any two adjacent orbits show about 15 percent sidelap at the Equator; this sidelap increases to about 85 percent near the poles. All parts of a large region, e.g., a continent, are imaged during the succession of shifted orbits in a cycle lasting 18 days. Thus, in principle, any area can be imaged every 18 days, but, in practice, cloud cover usually reduces the coverage to some simple multiple of 18, which depends on geographic location and time of year (a

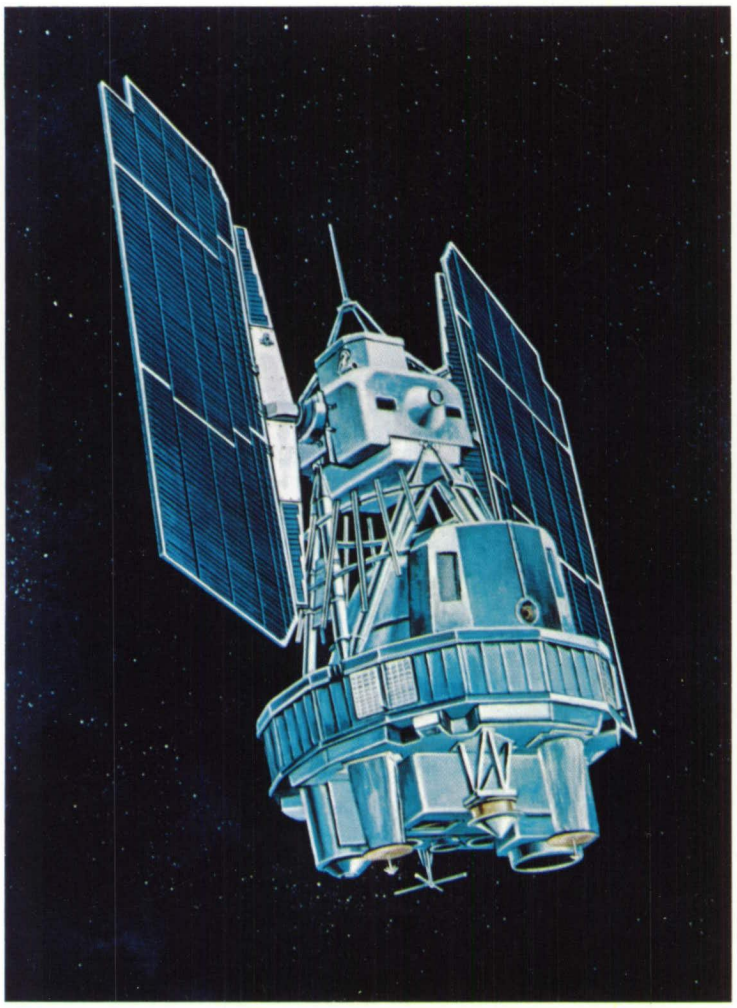


FIGURE 2.—Artist's concept of Landsat 1.

typical case in the eastern United States is 54 days, but this varies with season).

Two imaging sensor systems operate on the Landsats. One, a television camera system referred to by the acronym RBV (for return beam vidicon), was shut down early in the Landsat 1 operation owing to a switching malfunction. The second is a multispectral scanner (MSS) (see Appendix A for an operational description), which produces a continuous image strip built up from successive scan lines extended perpendicular to the forward direction of the satellite's orbital motion. Reflected light from the ground is transferred by an oscillating mirror in the MSS to a recording system after passing through filters that select different wavelength intervals of this light. Each of the four wavelength channels processes a predetermined spectral interval or band (the bands of the MSS are numbered 4, 5, 6, and 7 simply to avoid confusion with the three RBV bands, which are numbered 1, 2, and 3) according to the following arrangement:

MSS band no.	*Wavelength, μm*	*Spectral region*
4	0.5 to 0.6	Green
5	0.6 to 0.7	Red
6	0.7 to 0.8	Near infrared
7	0.8 to 1.1	Near infrared

One principal use of this multispectral capability stems from a basic property of materials. Because various classes of features found on the surface reflect differing amounts of light at different wavelengths or wavelength intervals, they can be separated and identified by their own characteristic reflectance patterns, or spectral "signatures." For example, vegetation typically reflects more green light than red and is very reflective (bright) in the infrared. Many dry soils, by contrast, reflect less light in the green than in the red and moderately more so in the infrared; wet soils show similar patterns of relative reflectance in the four bands but the magnitude or intensity of light reflected in each band is reduced by the general light-absorbing character of water.

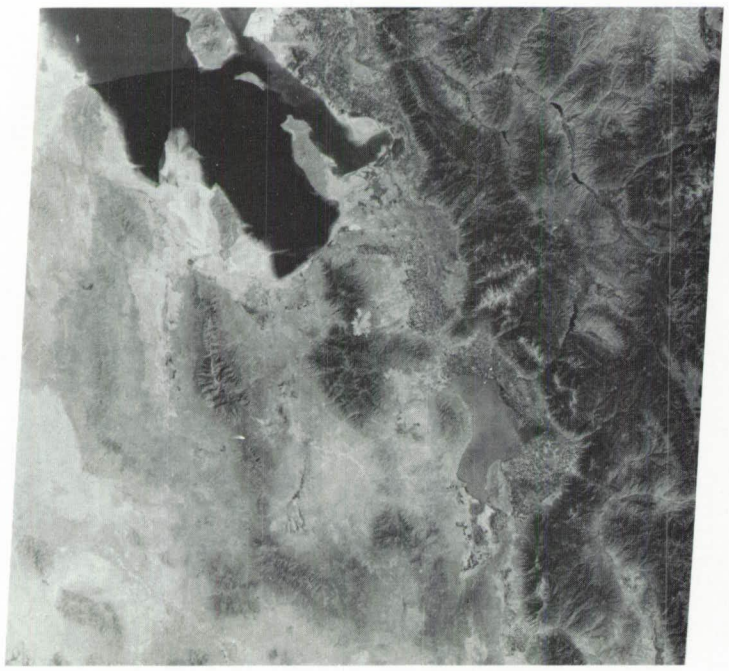
The light reflectance data obtained by the MSS on board Landsat are first converted to electrical signals, which vary in proportion to the intensity measured for each band. These analog signals then are converted into a digital form and transmitted to one of the three receiving stations in the continental United States. (By agreement with other nations, foreign stations are constructed and operated by participating countries. Canada, Brazil, and Italy have each developed a station and Zaire, Iran, and Chile are proceeding with similar developments.) Data from the satellite can be collected by a receiving station over about a 2800-km (1700-mile) radius depending somewhat on antenna size, station elevation, and local terrain features. Wherever a region of the Earth lies beyond a receiving station, data obtained during a Landsat overpass are stored on an onboard tape recorder for playback later when the satellite is within range of one of the U.S. stations.

The digital video data can be re-formatted into computer-compatible tapes (CCT's) and analyzed by investigators and users through a variety of computer-based programs. Alternatively, the digital data can be reconverted at ground-processing facilities into sets of black and white photo images. Each of the four black and white images (fig. 3) represents a particular spectral band; the gray tones associated with individual features vary from one band image to the next in proportion to the amount of light reflected from each small surface area. Color images are made from combinations of individual black and white images by projecting each given band through a particular filter. The usual combination consists of band 4 (green) projected through a blue filter, band 5 (red) projected through a green filter, and band 7 (infrared) projected through a red filter. In this rendition (called a false color image), which is equivalent to the standard false color infrared product of conventional color infrared photography, growing vegetation will appear in various shades of red, rocks and soils will normally show colors ranging from bluish through yellows and browns, water will stand out as blue to black depending on depth and amount of suspended sediment, and cultural features (towns and roads) will usually be recognized by bluish-black tones arranged in characteristic patterns. These general identifying colors will vary somewhat depending on such intrinsic scene factors as angle of illumination (time of year), vegetational differences (season), and atmospheric conditions, as well as on the processing and printing methods and materials used in a particular photo lab.

Several types of photo products are generated from Landsat data. These include positive and negative transparencies and paper prints of different sizes (representing several ground scales) in black and white and in color. The most frequent format—from which most images in this book were reproduced—is the 23-cm (9-in.) print. At that size, the image itself is scaled at 1:1 000 000 or 1 cm of the print matches 1 000 000 cm (10 km) on the ground. (One inch represents 16 miles.) For this scale, the dimensions of the scene outline (whose slanted sides are explained in appendix A) are approximately equivalent to 185 km (115 miles) on a side. A Landsat scene therefore covers approximately 34 225 km² (13 225 sq miles). The effective resolution (in terms of the smallest adjacent ground features that can be distinguished as separate entities) is about 80 m (250 ft); linear features as narrow as 10 m (33 ft) are sometimes visible where they are in sharp contrast to their surroundings (e.g., bridges over water or dirt roads passing through dark brush). Owing to the high altitude of the satellite and the narrow field of view (±5.8°), the shapes, dimensions, and relative locations of individual features remain almost constant over the entire image. Because distortions and



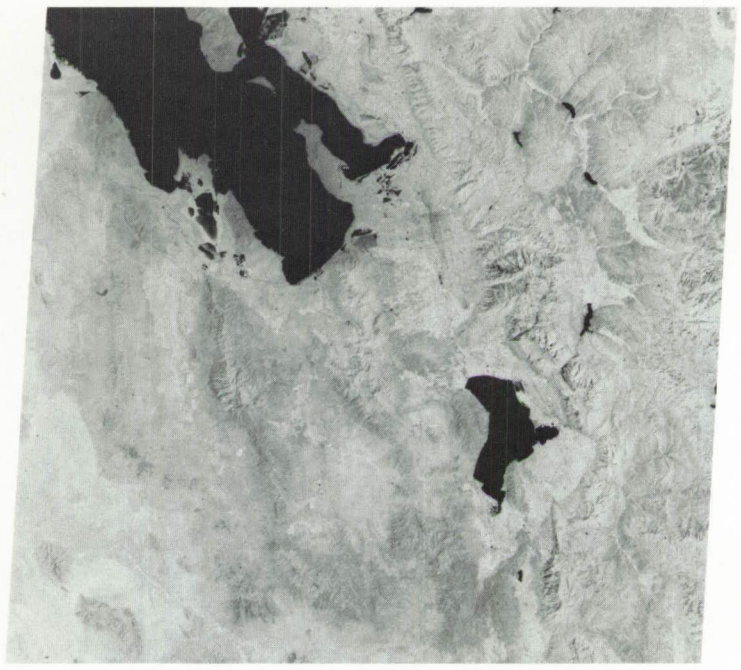
(a)



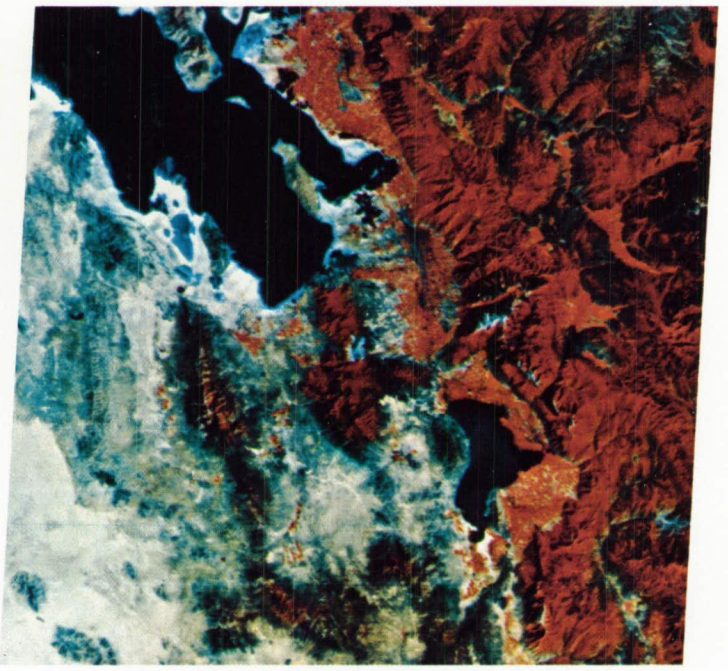
(b)



(c)



(d)



(e)

FIGURE 3.—Landsat spectral bands for the MSS in the Salt Lake City, Utah, area, August 7, 1972. (*a*) Green. (*b*) Red. (*c*) Near infrared. (*d*) Infrared. (*e*) Color composite.

displacement are small, these images are orthographic and meet current national map standards for acceptable fidelity at scales as large as 1:250 000.

The minimal distortion at the edges, together with the capability of images taken at different times of year to be adjusted to similar photographic densities or shading, allows them to be joined in mosaics with very little of the special manipulation often required for aerial photographs. Uniformly toned mosaics of entire States, broad regions, and even continents can be produced from Landsat imagery, as exemplified by the remarkable mosaic of the 48 conterminous States of the United States prepared for NASA by the Department of Agriculture's Soil Conservation Service. (See back endpaper.)

Although Landsat is primarily an imaging system, it is also being employed to relay radio signals sent from data collection platforms (DCP's) on the ground to the regular receiving stations. The DCP's are usually located in isolated or remote areas, where they collect in situ information or make measurements on such diverse physical conditions as water temperature or seismic activity. DCP's are also placed at points where ground data would aid in interpretation of image data or of other aspects of an experiment or application, e.g., sediment density, water depth, or snow depth.

DISCIPLINE APPLICATIONS

Landsat is the first of a generation of unmanned satellites dedicated to repetitive surveillance of the continents and adjacent coastal waters to gather data for a variety of practical applications in Earth resources. For convenience these applications can be classed into six major categories, each coming under the purview of some recognized professional discipline or specialty. For example, information sought by Landsat on the distribution, growth states, and anticipated productivity of both natural and cultivated vegetation can be grouped under the heading of agriculture, forestry, and range resources. This information is of value to diverse users such as agronomists, pedologists, recreational planners, conservationists, economists, park rangers, and water engineers. Likewise, analysis of Landsat data pertinent to landform classification, crustal deformation, dynamic earth-moving processes, and exploration for metals and oil becomes the responsibility of the geology discipline. Some disciplines such as land use and (cartographic) mapping have their own sets of unique applications but also rely upon certain observations and measurements that overlap and are of mutual interest to other disciplines.

Examples of many specific applications within each of the six disciplines are listed in table 1. Many of these examples are treated in some detail in the remaining sections of this chapter, presented in the sequence of the disciplines recorded in the table. Each discipline is reviewed first to define the basis or rationale for using remote sensing from space rather than ground or air surveys to obtain critical data relative to the applications cited. It should be pointed out that Landsat is not the first space system to provide such data. Considerable experience in conducting remote sensing surveillance has accumulated for many years from aerial flights with photo cameras and other sensors; from photo experiments on the Gemini and Apollo missions; and from specialized sensors on Nimbus, TIROS, and other meteorological satellites. Landsat, however, is the first spacecraft capable of producing medium-resolution, multispectral, seasonal images from digital (computer-compatible) data in formats specially tailored to the needs of specialists, technicians, and managers in the Earth resources disciplines.

Many additional examples of applications to agriculture, land use, geology, water resources, oceanography and marine resources, and environment, not mentioned in the remainder of this section, as well as to other disciplines such as geography, meteorology, and history are treated in the captions of the Landsat images selected for this book.

AGRICULTURE, FORESTRY, AND RANGE RESOURCES

Basis for Remote Sensing Applications

The world's population is increasing at a rate of 250 000 young mouths per day; it is estimated that it will increase by as much as three times its current level in the next 50 yr. The food required to feed these many billions must increase by at least the amount of the population rise and, in fact, a sixfold jump in production is necessary to raise the protein level of consumption to that meeting today's U.S. standards for good health. To meet these increasing demands for food and fiber, levels of crop production must be improved through more efficient yields and less undesired loss and through effective conversion of available noncultivated land to well-managed farms. Greater yields and increased acreage as well as more efficient range management are also required for grazing on rangelands to provide higher forage production for the animals consumed in man's food chain.

Even in the most technologically advanced countries, up-to-date and accurate assessments of total acreage of different crops in production, anticipated yields, stages of growth, and condition of health (vigor) are often incomplete or delayed (nontimely) in relation to information needed by agricultural managers. These managers are continually faced with decisions on planting, fertilizing, watering, control of pests and disease, harvesting, storage, evaluation of crop quality, and planning for new areas to cultivate. The resulting information is used to predict marketing factors, evaluate effects of crop failure, assess

TABLE 1.—*Summary of Applications of Landsat Data in the Various Earth Resources Disciplines*

Agriculture, forestry, and range resources	Land use and mapping	Geology	Water resources	Oceanography and marine resources	Environment
(1) Discrimination of vegetative types: Crop types Timber types Range vegetation	(1) Classification of land uses	(1) Recognition of rock types	(1) Determination of water boundaries and surface water area and volume	(1) Detection of living marine organisms	(1) Monitoring surface mining and reclamation
(2) Measurement of crop acreage by species	(2) Cartographic mapping and map updating	(2) Mapping of major geologic units	(2) Mapping of floods and flood plains	(2) Determination of turbidity patterns and circulation	(2) Mapping and monitoring of water pollution
(3) Measurement of timber acreage and volume by species	(3) Categorization of land capability	(3) Revising geologic maps	(3) Determination of areal extent of snow and snow boundaries	(3) Mapping shoreline changes	(3) Detection of air pollution and its effects
(4) Determination of range readiness and biomass	(4) Separation of urban and rural categories	(4) Delineation of unconsolidated rock and soils	(4) Measurement of glacial features	(4) Mapping of shoals and shallow areas	(4) Determination of effects of natural disasters
(5) Determination of vegetation vigor	(5) Regional planning	(5) Mapping igneous intrusions	(5) Measurement of sediment and turbidity patterns	(5) Mapping of ice for shipping	(5) Monitoring environmental effects of man's activities (lake eutrophication, defoliation, etc.)
(6) Determination of vegetation stress	(6) Mapping of transportation networks	(6) Mapping recent volcanic surface deposits	(6) Determination of water depth	(6) Study of eddies and waves	
(7) Determination of soil conditions	(7) Mapping of land-water boundaries	(7) Mapping landforms	(7) Delineation of irrigated fields		
(8) Determination of soil associations	(8) Mapping of wetlands	(8) Search for surface guides to mineralization	(8) Inventory of lakes		
(9) Assessment of grass and forest fire damage		(9) Determination of regional structures			
		(10) Mapping linears (fractures)			

damage from natural disasters, and aid farmers in determining when to plow, water, spray, or cut. Data of this kind are obtained in the United States at the county farm agent level and then collated by the Statistical Reporting Service of the Department of Agriculture. For the aggregated United States, the inventory system is reasonably reliable for most crops but nevertheless is still open to improvements in timeliness, extent of coverage, and correction for nonharvested acreage. In many other parts of the world, the reporting system ranges from adequate to meager to nonexistent. To meet the coming demands of a rapidly burgeoning population, a truly worldwide system is clearly essential.

In past years, aircraft surveys have been used sporadically to assist crop and range managers in gathering useful data. With the advent of a multispectral, repetitive satellite that can image the entire world's land surface a number of times each year, the "dream" of an automated crop inventory capability is now approaching reality. Information from satellites such as Landsat can be integrated into a sophisticated crop assessment system, such as the one outlined in figure 4. Other satellites, including already operational meteorological satellites and some planned for the future, add critical data on weather conditions such as temperature and moisture to the system. The total number of observations and volume of information produced from such a satellite system and from supplemental data sources are tremendous indeed; however, the digital format in which the satellite data are usually recorded allows computers to process these data directly and thereby reduce the vast quantity of ever-flowing information to the precise outputs required by the managers in their continuing decisionmaking.

The principles of remote sensing by which crop and range types are recognized and yields assessed from Landsat observations are relatively simple to explain. First, land given to agriculture is generally easy to identify in a Landsat image because it customarily has uniform or regular boundaries giving rise to well-defined shapes such as rectangles, polygons, and circles. Landsat can recognize many major crop types with accuracies of 90 percent or higher in fields of 80 000 m^2 (20 acres) or larger and can achieve lesser accuracies in fields as small as 20 000 m^2 (5 acres). Fallow or unplanted fields are easily distinguished in false color composites by their characteristic blues, tans, or browns—the specific color depends on the type of soil. Growing crops appear in various shades of pink to red—young plants tend to appear pinkish while many fully matured crops are bright red, and rice appears as dark red (owing to black tones introduced from associated water).

However, crops are best identified from computer-processed digital data that represent quantitative measures of radiance (percentage or intensity of reflected light). In general, all leafy vegetation by itself has a similar reflectance spectrum regardless of plant or crop species. The differences among crops, by which they are separated and identified, result from degree of maturity, percent of canopy cover, and differences in soil type and soil moisture. In practice, the crops are differentiated in the satellite image or the computer data by using training sets; i.e., the spectral signatures or reflectance responses of known specific crop types are determined at several individual fields in the image and closely similar responses are looked for elsewhere in the image or computer data. When data from all four channels of the MSS are used, there are usually enough subtle differences in reflectance from one crop to the next to distinguish them. Also, if certain crops are not separable at one time of the year, they are normally separable at another time due to the differences in planting, maturing, and harvesting dates.

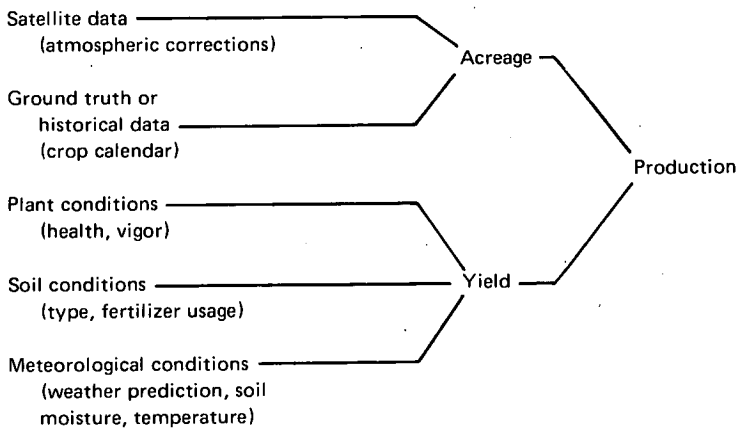


FIGURE 4.—Crop assessment for world food management system.

The degree of maturity and the yield for a given crop also influence the reflectance at any stage of growth. This maturity and yield can be assessed as the history of any crop is traced in terms of its changing reflectances. When a crop is diseased or seriously damaged (as by a hailstorm), its reflectances decrease, particularly in the infrared, allowing the presence of crop stress to be recognized. Lack of available moisture also stresses a crop, which effect again shows up as a reduction of reflected light intensity in the infrared and usually as a drop in reflectance in the green MSS band (4) and a rise in the red MSS band (5). In grasses, bush, and other forage vegetation of the rangeland, the amount of feed available (or biomass) is also estimated by measurements of relative radiance levels.

Landsat has proved effective in recognizing and locating the broadest classes of forest land and timber. Deciduous, evergreen, and mixed (deciduous-evergreen) communities can be separated. Generally, coniferous evergreens appear as darker reds in false color composites and these trees will retain that reddish tone even as deciduous trees or shrubs change from pinks to reds to browns in the composites through a growing season. The total acreage given to forests can be conveniently measured in Landsat images, and changes in these amounts (such as produced by cutting or new seeding) are readily detected. Under certain conditions, timber volume, age of forests, and presence of disease or pest infestations can likewise be determined. Vegetation in varied environments such as river valleys, coastal zones, swamps, or tundra plains has also been identified by its characteristic signatures.

Of interest in agriculture is the ability to recognize the major soil associations and the specific soil types. This has been feasible wherever the soil possesses a distinctive spectral signature and/or supports characteristic, identifiable vegetation.

Examples of Applications

Figure 5 is an example of how Landsat data are used in making crop classifications. Using a computer to process digital MSS data for an agricultural area in Holt County, Nebr., the investigator compared and classified crop types by spectral pattern recognition techniques. Based on ground-truth checking, the accuracy of this method of crop classification was 70 to 90 percent, using single data sets. Using registered data sets from two or more Landsat passes further improves classification accuracy to greater than 90 percent.

NASA, in cooperation with the U.S. Department of Agriculture and the National Oceanic and Atmospheric Administration (U.S. Department of Commerce), has undertaken a demonstration project to determine the capability of Landsat data for use in inventorying a major world food crop. It will be extended to all the major wheat growing areas of the world after initial testing in the United States and Canada. This Large Area Crop Inventory Experiment (LACIE) should provide more accurate and timely assessment of worldwide wheat production to allow for better management of this major world food. Extension to other important agricultural crops is also anticipated in the near future.

The technique, called "clear-cutting" in the timber industry, means cutting down virtually all usable trees in a given area, while leaving untouched all the timber surrounding the clear-

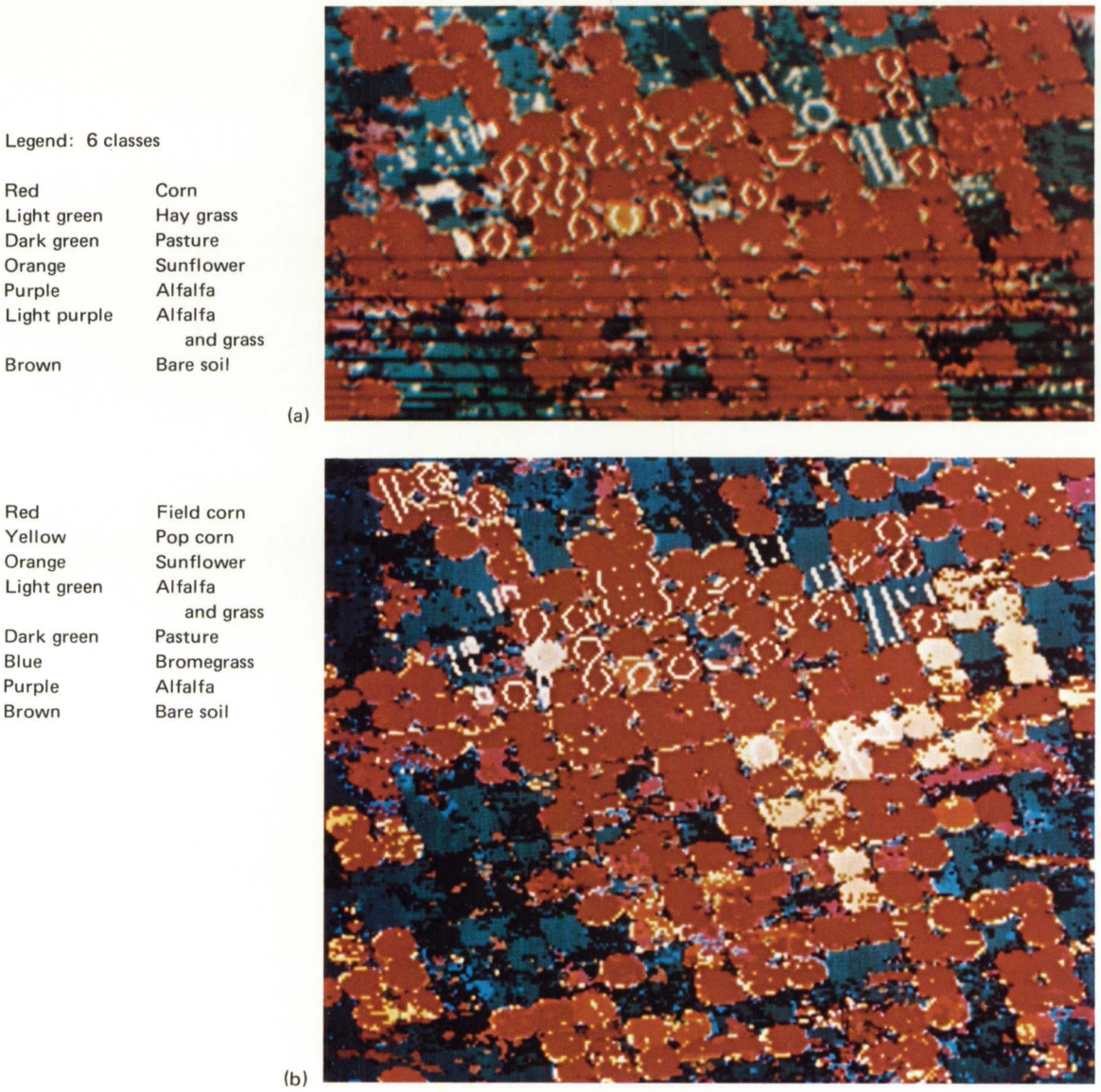


FIGURE 5.—Computer-aided crop classification from Landsat 1 MSS data; Holt County, Nebr. (*a*) July 30, 1972. (*b*) August 16, 1972.

cut area. Although it had been known that clear-cutting techniques were being applied to the heavily forested regions of Oregon, its widespread use was not fully realized until Landsat 1 produced the dramatic scene shown in figure 6. In this scene, with volcanic Mount Hood visible in the left-center and the Columbia River at the top, clear-cut areas are vividly displayed as light patches within the dark red of the forested areas. So numerous are the clear-cut areas that the entire scene assumes a speckled appearance. Imagery such as this can be of considerable value to Federal and State agencies having the responsibility of monitoring and protecting our forest resources.

Figure 7 illustrates another application of Landsat data that will save both time and money for resource management agencies. A fire in the Fiske Creek area of northern California was mapped both by the State's Division of Forestry (fig. 7(*a*)) using conventional techniques and by a Landsat 1 investigator (fig. 7(*b*)) using Landsat imagery (fig. 7(*c*)) taken over the area 10 days after the fire. The accuracy of the Landsat-derived map was checked by low-altitude aircraft photography (fig. 7(*d*)). Not only was the burned area mapped more accurately (53.99 km^2 (13 340 acres) from the Landsat map versus 41.85 km^2 (10 340 acres) from the conventional map), but the cost of producing the Landsat map was one-tenth the cost of producing the State's map.

The Sahel region of Africa has been suffering from drought for the past 5 yr. While studying Landsat imagery of the region, Landsat investigators detected a distinct area of vegetation (dark polygonal area in fig. 8(*a*)) within the semidesert region. The unusual linearity of the area's boundaries, as seen in an aerial photo (fig. 8(*b*)), led to the conclusion that the feature was manmade. On a field trip to the area, investigators discovered that the dark polygonal area is a fenced compound

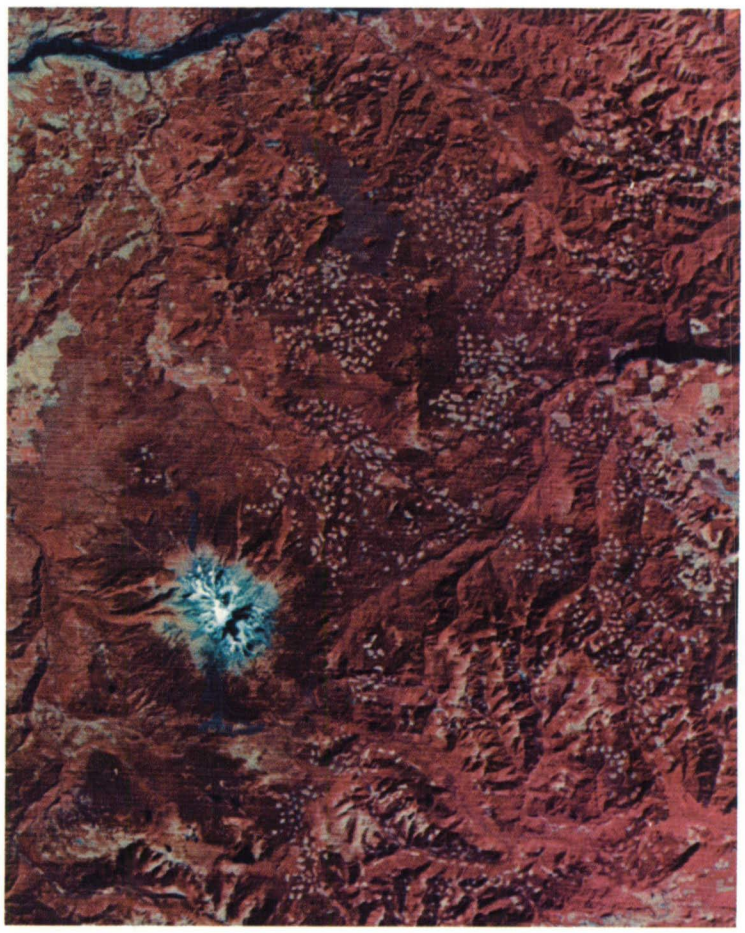


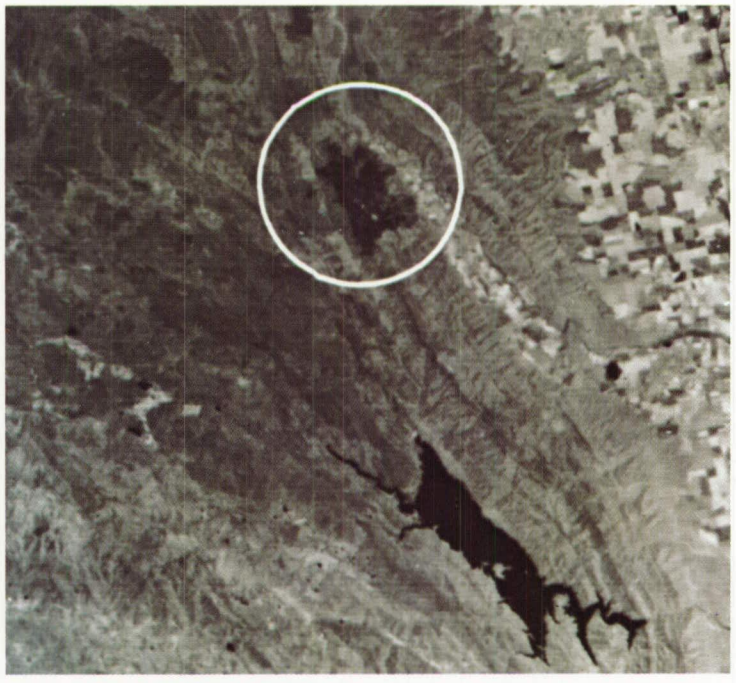
FIGURE 6.—Landsat 1 scene of the forests around Mount Hood, Oreg., showing the extent of clear-cut areas.



(a)



(b)



(c)



(d)

FIGURE 7.—Fiske Creek, Calif., fire scene. (*a*) Burned area as mapped by Division of Forestry personnel. (*b*) Burned area as mapped by Landsat investigators. (*c*) Landsat image of burn scar used to produce map shown in (*b*). (*d*) Low-altitude aircraft photo used to check accuracy of Landsat map.

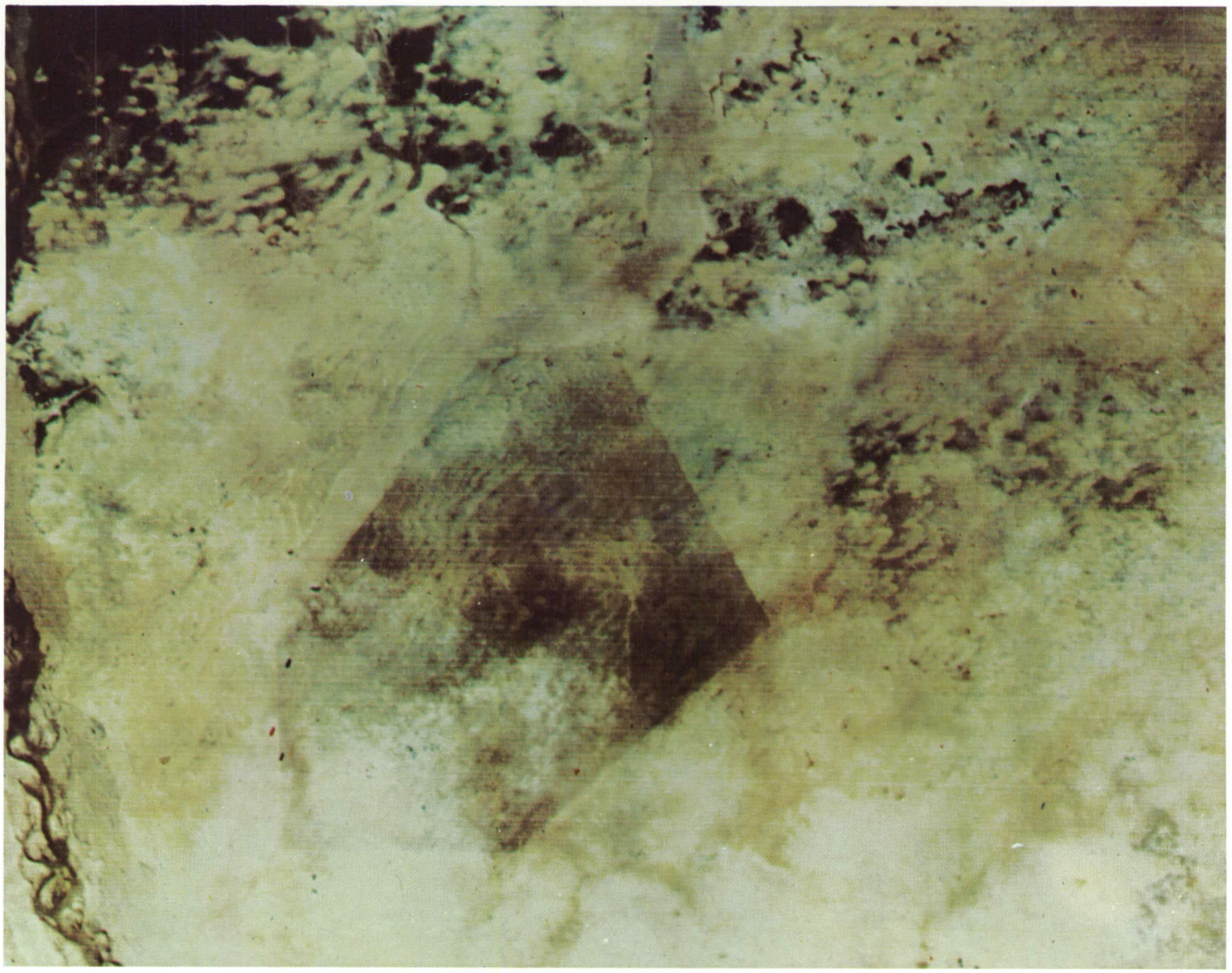
where grazing has been carefully controlled, thus causing it to differ noticeably in vegetative cover from the uncontrolled grazing areas outside its limits (fig. 8(*c*)). The ranch demonstrates that controlled grazing could be sustained even in the semiarid region of the Sahel whereas uncontrolled grazing has led to complete destruction of the vegetative cover with subsequent encroachment of the desert.

LAND USE AND MAPPING

Basis for Remote Sensing Applications

The term "land use" refers both to current use of the land surface by man for his activities and to the natural state or cover of the land where not given over to these activities. "Land use planning" is concerned with achieving the optimum benefits for mankind in the development and management of the land for food, housing, urbanization, manufacture, supply of raw materials, power production, transportation, recreation, and many other activities. This planning allows for controlled growth of populations by matching land use with land capability and by tying specific uses with appropriate natural conditions so as to provide adequate food and materials supplies without significant damage to the environment.

Heretofore, land use planning has been severely hampered both by the lack of up-to-date maps showing what categories are present and changing in an area or large region and by inadequate means to handle and analyze the huge quantities of data involved. The scope of effort and the costs of producing land use maps have prohibited their acquisition for many parts of the United States at useful working scales (e.g., 1:250 000



(a)



(b)



(c)

FIGURE 8.—Vegetated area in the midst of the African desert. (*a*) Portion of Landsat scene showing dark polygonal area with linear features. (*b*) Aerial view of ranch's fence line showing wide variation in vegetative cover. (*c*) Ground photo of fence.

to 1:500 000). The situation for the rest of the world is even less satisfactory. Vast areas of Africa, Asia, and South America are poorly, and often incorrectly, mapped. Over the last 20 yr, a project sponsored by UNESCO has completed a series of land use maps at scales of 1:5 000 000 to 1:20 000 000. Although invaluable as a general record of land use (and for other disciplines including agriculture, hydrology, and geology), these maps are insufficient in detail to assist developers and managers in many of their decisions. Furthermore, frequent changes in land use are hard to plot at these small scales. What clearly must be sought for these planners is a worldwide base map at scales of 1:1 000 000 or larger.

The Landsat system responds to these needs. Man's use of the land can be deduced or inferred indirectly from the identity

and distribution patterns of vegetation, surface materials, and cultural features as interpreted from images or computer-processed displays. This information is usually then depicted on land use maps that locate specific categories of surface features. Evaluation of the maps prepared from Landsat data indicates that all level I land use categories (as defined in the *1974 Land Use Classification Scheme,* U.S. Geological Survey Circular 671) can be correctly identified to an accuracy exceeding 90 percent, and 10 or more level II categories to accuracies of 60 to 90 percent. As a result, much of the United States not yet mapped and vast sections of the rest of the world are now being mapped at scales of 1:1 000 000 to 1:250 000. This approach has been demonstrated to be quite cost effective. For an area including the three southern States of New England (see fig. 9), the relative costs for mapping by ground surveys, high altitude aircraft, and Landsat are estimated to be approximately $20, $6, and $0.40 per square kilometer ($50, $15, and $1 per square mile), respectively. When integrated into a total land use program, which employs additional data from social, economic, and technical studies, a savings of 30 percent or more is accomplished. This savings should increase as more of the data from Landsat and these other sources are processed and stored in computers. This ability to computerize the great quantities of both remote sensing and ground data, and to retrieve them readily in map or table form, stands out as the most significant advance in the Earth resources program to date.

Through both satellite and high resolution aircraft coverage, it is now possible to monitor changing land use patterns, survey environmentally critical areas, and perform land capability inventories on a continuing basis. The high frequency of repetitive coverage provided by Landsat is more than enough to allow an annual updating of current maps. Some categories, such as urban areas and strip mining, may require an even more frequent revision while others, like brushland and rocky areas, probably remain constant for periods of years. Thus, Landsat has provided a versatile new approach to Federal and regional planners within the United States, responding to an awakened concern by this country's citizenry for comprehensive, balanced programs of land use from the national to the local levels.

Examples of Applications

Figure 9 presents the result of one highly successful Landsat 1 investigation in land use classification. This detailed land use map of a three-State area (Massachusetts, Connecticut, and Rhode Island) contains 11 separate land use categories. The map was compiled from several Landsat 1 scenes of the New England area taken during clear weather in mid-October 1972. The spectral images were converted into a false color infrared transparency from which a single photointerpreter, working from the transparency, then produced the land use map in draft form within 3 months. It took only another 2 months to produce the final color-coded map as shown in figure 9. The investigator estimated savings of approximately 90 percent over what the cost would have been had an equivalent map been prepared by conventional means, such as aerial photography.

Figure 10 shows a map depicting the six categories in the Great Dismal Swamp as defined using Landsat computer-compatible tape data. Two categories concern an important element of the swamp, open water and standing water (vegetation growing within the water boundary); the remaining four categories are defined by plant associations. By monitoring the location, extent, and long-term expansion or contraction of these hydric to mesic areas, the need for water management as well as other management techniques necessary to maintain diversity is evidenced. Remote sensing can assist managers in evaluating the long-term impact of alterations within the swamp, subtle changes that might otherwise not be observed by conventional ground reconnaissance, and is proving to be a prac-

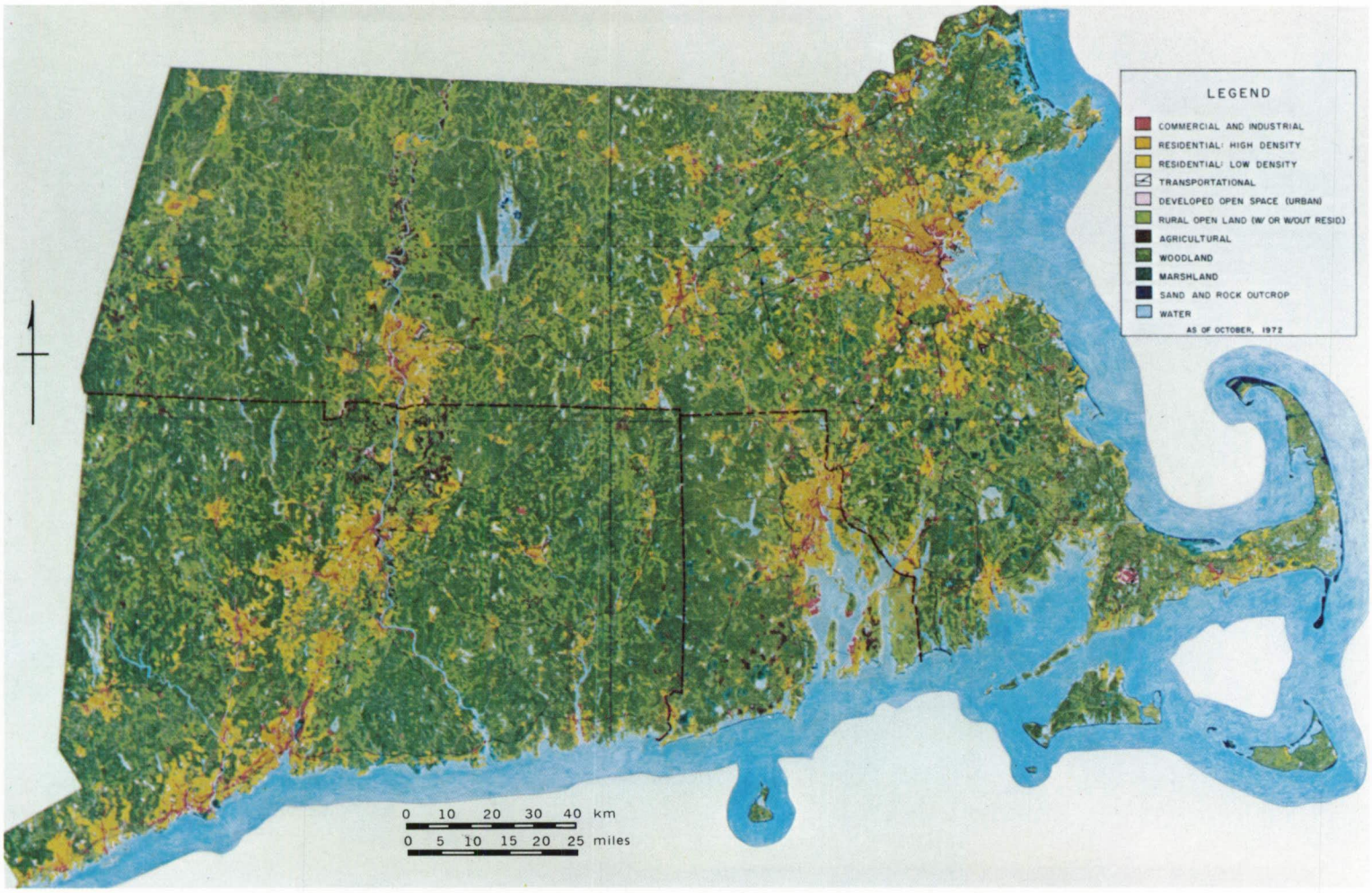


FIGURE 9.—Land use map of three-State area in New England compiled from Landsat 1 imagery.



FIGURE 10.—Computer-generated map of land use categories at the Great Dismal Swamp, Va.

tical tool for monitoring wildland situations where access is difficult.

An example of land use classification in an urban area is shown in figure 11. Here the Twin Cities (Minneapolis-St. Paul) metropolitan area in Minnesota was mapped from a Landsat image into eight categories. Although the fine details in these categories, such as individual buildings, usually cannot be

Legend:

- Central Business District: dominated by very high density commercial, industrial, and institutional buildings, characterized by lack of vegetation
- Commercial-Industrial-Institutional: dominated by either buildings of medium density or land, extensive commercial activity with little vegetation except in newer surburban areas
- Residential 1: dominated by single family dwellings, characterized by a tree canopy
- Residential 2: dominated by moderate-to-low-density single family dwellings, characterized by vegetative cover of grass
- Water: dominated by open water that may contain scattered emergent vegetation
- Extractive: dominated by quarries, gravel pits, and/or landfills, active or inactive
- Forest: dominated by forest, brushland with trees, and/or swamp
- Other: dominated by cropland, grassland (pasture), and marsh

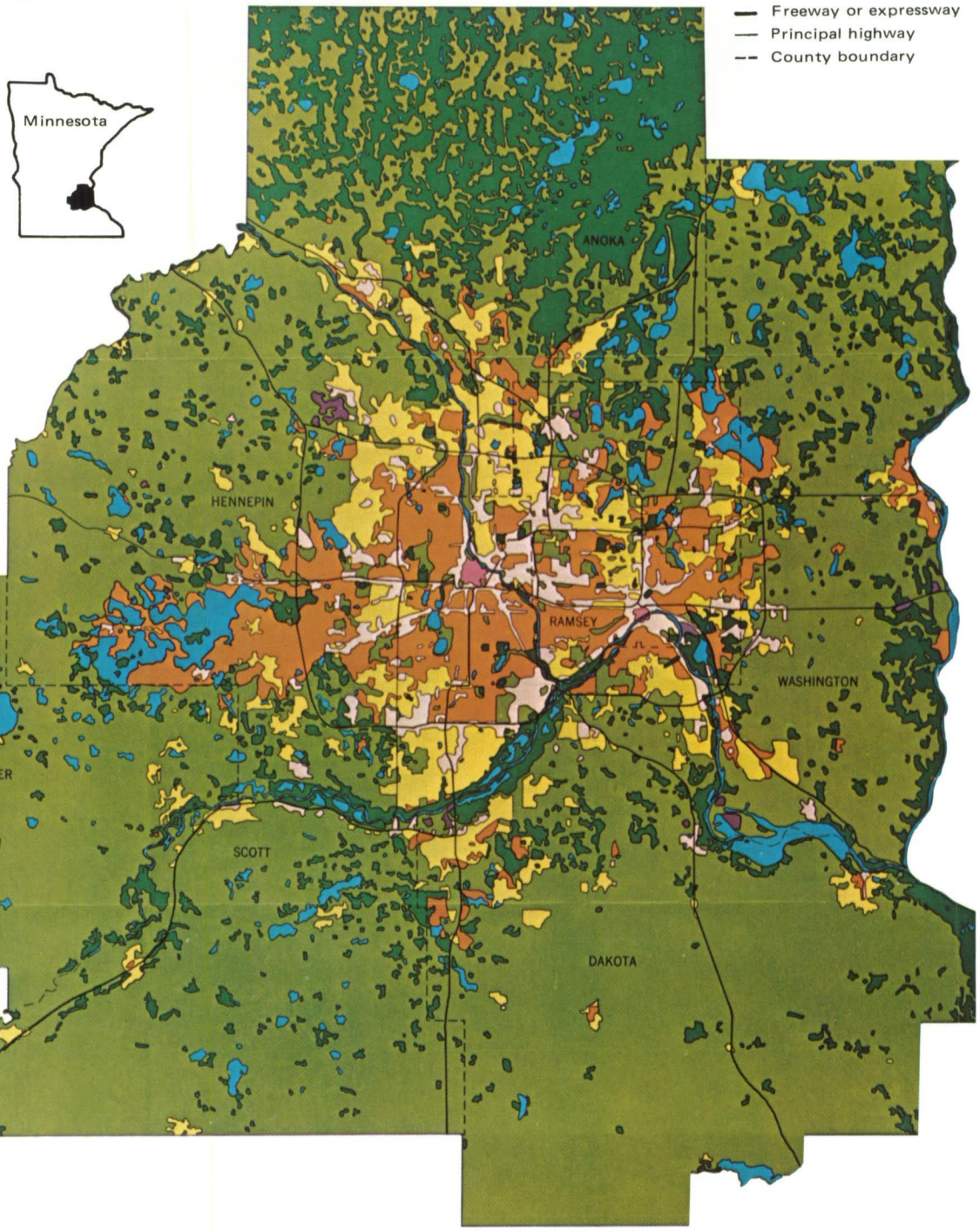


FIGURE 11.—Classification of major land use categories in the Minneapolis-St. Paul region; mapping unit size: 0.16 km² (40 acres).

seen, the general areas containing these specific details can be separated one from another. Thus, the central business district (red) can be distinguished from what is called commercial, industrial, and institutional areas (pink); sparse single family residential areas dominated by trees (orange) can be delineated from moderate density dwellings dominated by grass (yellow), and the extractive areas containing gravel sites (purple) stand out against the water (blue), forested areas (dark green), and cropland (olive green).

Besides classifications of 18 to 20 categories covering features as small as 0.02 km² (5 acres), the Landsat system is providing a series of image mosaics that can serve as a reference photo base on which these categories are directly illustrated or otherwise plotted as overlays. The mosaic of the 48 conterminous States of the United States (see front endpaper) is a prime example; several other mosaics appear in the main section of this book. One reason why individual Landsat images can be joined to neighboring frames lies in the high geometric fidelity of each. After suitable corrections are applied, the images have internal mapping errors of 200 to 450 m (600 to 1500 ft). Images therefore meet or exceed current National Map standards up to scales of 1:250 000. This means, then, that after fitting to the appropriate geodetic grid, these images are equivalent to maps in themselves on which extracted thematic information can be traced or overlaid.

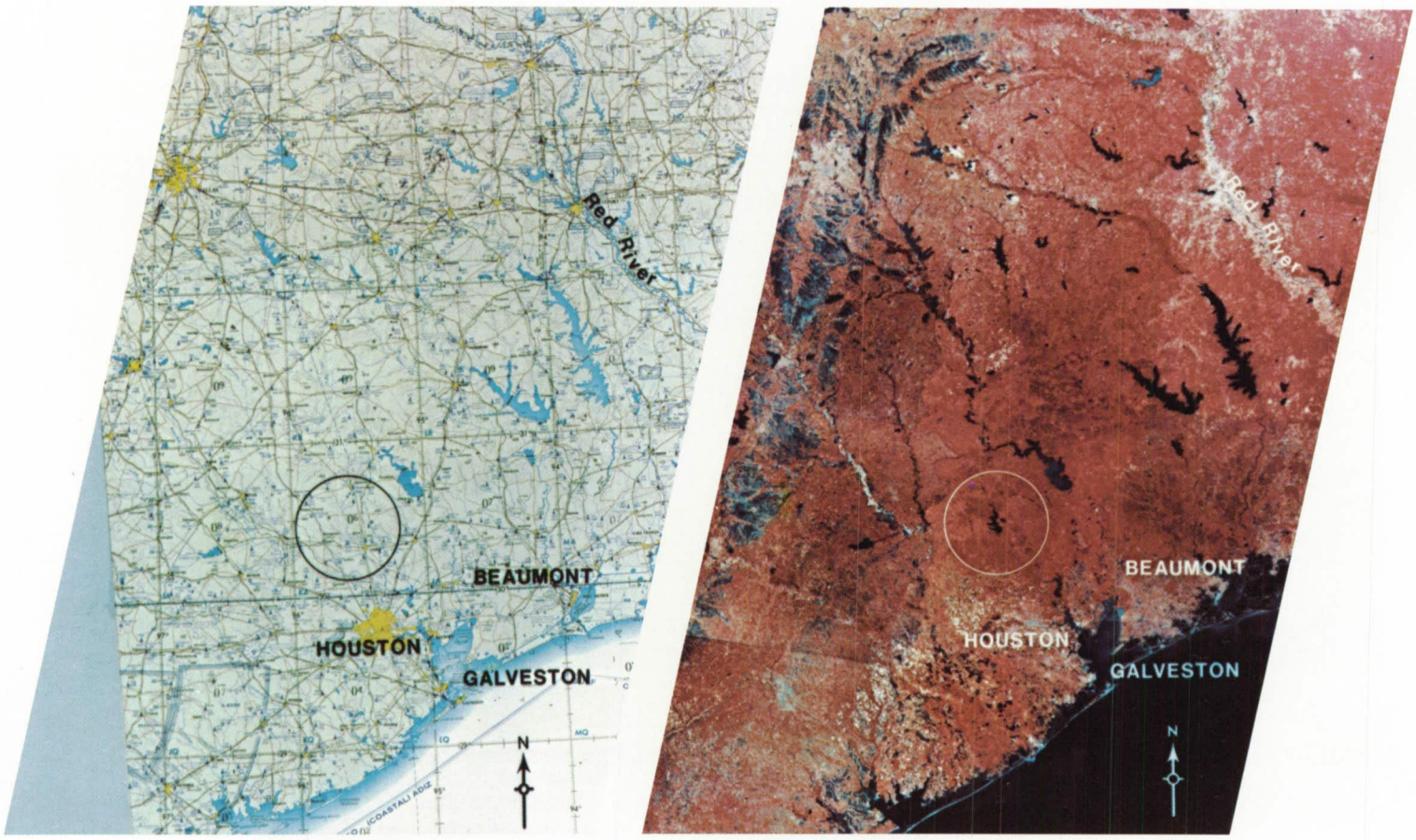
Figure 12 shows the use of Landsat imagery for map updating. The left side of the figure shows a section of a 1973 aeronautical map of the Houston, Tex., area. The right side shows the corresponding Landsat image taken in 1974. The circled area on the image shows a lake not shown on the map. Similar situations have been seen in other States leading to the use of the imagery for direct updating of maps. Note also the difference in the shoreline boundary in the Beaumont area.

GEOLOGY

Basis for Remote Sensing Applications

Geology is the study of the composition, structure, processes of development, and history of the rock materials making up the Earth. The materials visible at the Earth's surface are exposures of a variety of rock units, often layered and complexly deformed, that extend to great depths into the solid crust. The key task of the geologist is to map the location of the rock units where they intersect the surface, from which the three-dimensional distribution of these units at depths can be inferred. From a practical sense in exploring for mineral and petroleum deposits, as well as detection of potential geologic hazards such as earthquakes and volcanoes, the surface geologic maps are the prime data products used. In addition to recording the composition and relative ages of distinguishable rock units, the maps normally also show the structural relations (expressed in folds and faults) among the units and may also indicate areas of alteration or mineralization and areas covered by Recent sediments or soils.

The traditional approach to geologic mapping has involved an on-the-ground search for rock outcrops. In most terrains, these are frequently scattered and isolated and often inaccessible in rugged country. Mapping of large regions commonly requires years of field work. The process can be made faster and more accurate, as well as more economical, if the geologist is given a series of aerial photographs that pinpoint outcrops and express structural configurations. For many decades now, these photographs have served as the visual base from which the maps are made by tracing the recognizable units where exposed. Instead of surveying in these units at many sites, the geologist need only spot check the identity of each



Map

Landsat 1 image

FIGURE 12.—Example of map updating through the use of Landsat imagery. Note new lake north of Houston. The Landsat image shows more detail along the Gulf Coast shoreline than is depicted on the map.

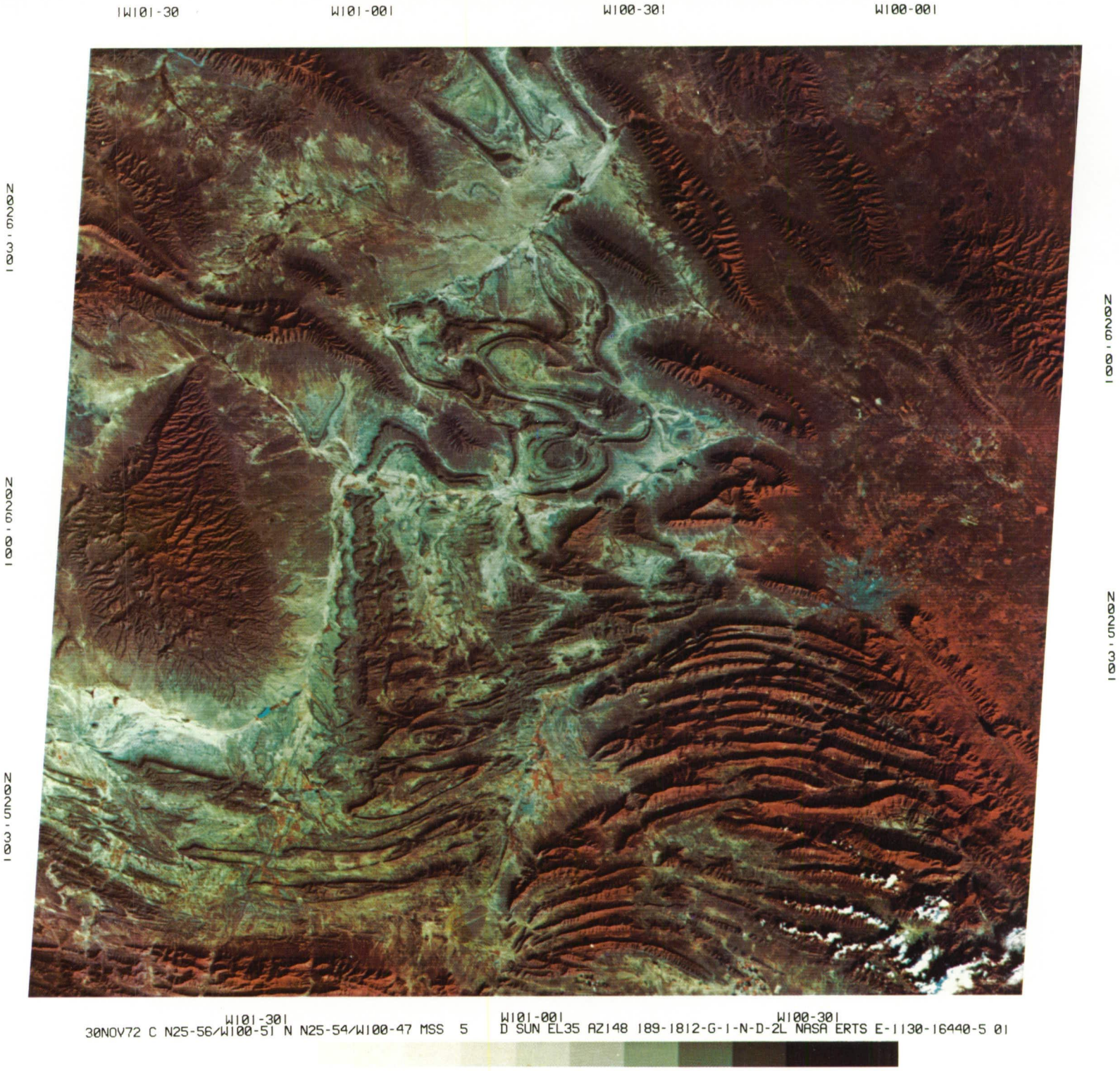
unit at selected localities and then extrapolate the positions of the units throughout the photographs.

While high-resolution aerial photos are a prerequisite to detailed mapping, they have certain inherent limitations, such as vignetting (variations in background tone from center outward) and geometric distortion, that introduce difficulties in joining overlapping views in mosaics to provide a regional picture of larger areas. Such synoptic overviews are particularly valuable in geology because the scales of interrelated landforms, structural deformation patterns, and drainage networks are commonly expressed in tens to hundreds of kilometers; that is, generally in the range covered by space images.

The chief value of Landsat imagery to geological applications therefore lies in the regional aspects presented by individual frames and the mosaics constructed for vast areas extending over entire geologic provinces. For the first time, whole sections of a continent subjected to glaciation can be examined as a unified surface on which different glacial landforms are spatially and genetically interrelated. Deposits of sands in desert environments can be tied to such things as source areas, modifying surface obstructions, and climatic influences.

A frequently reported use of Landsat images in geology results from the remarkable pictorial renditions of a variety of terrains associated usually with structurally complex mountain belts. Geologic and topographic maps tend to subdue the reality of the scene even though they properly record essential information about the surface. Compare, as an example, the superb depiction of the natural physiography of a part of the Sierra Madre Oriental in northern Mexico with the geologic map of the equivalent area (fig. 13).

Landsat images seemingly have the unique ability to single out certain types of linear features of structural significance.



(a)

FIGURE 13.—(*a*) Landsat image 1130–16440, taken on November 30, 1972, of part of the State of Nuevo León in northeast Mexico including the cities of Monterrey and Saltillo. (*b*) Part of a 1:2 000 000 geologic map of Mexico covering the same area shown in (*a*). The tight

Faults and fractures seen at isolated points are frequently misjudged as to the extent and continuity when examined in the field or in individual aerial photos; even where displayed in mosaics, these linear features are often obscured by such differences as angle of illumination and surface conditions that cause irregularities in the aerial mosaic product. But, as seen in space imagery, the trends of these linear features—although they may be broken into unjoined segments—can usually be followed across diverse terrain and vegetation owing to the uniformity of illumination and the integration of patterns and textures intrinsic to the small-scale expression of the scene.

In many instances, these features have been identified with surface traces of faults and fracture zones that control patterns of topography, drainage, and vegetation which serve as clues to their recognition. Many new discoveries of linears are being claimed by Landsat users. In some parts of the world, fivefold or more increases in mapped linears have been reported. The importance of finding these features is that the linears often represent major fracture systems responsible for modern-day earthquakes and for transporting and localizing mineral solutions as ore bodies in the geologic past.

A major objective in geologic mapping is the identification of rock types and alteration products. In general, most layered rocks cannot be directly identified in Landsat imagery because of limitations in spatial resolution and the inherent lack of unique (characteristic) differences in color and brightness of rocks whose types are normally distinguished by mineral and chemical content and grain sizes. Also, it is not possible to determine the stratigraphic age of recognizable surface units directly from Landsat data unless the units can be correlated with those of known age in the scene or elsewhere. Under some circumstances, certain rocks exposed in broad outcrops can be recognized by their spectral properties and by their distinctive topographic expressions (fig. 14). However, in many scenes, the presence of covering soil and vegetation masks the properties favorable to recognition.

Alteration products associated with rocks and ore bodies are often widespread at the surface and may show diagnostic indications in the Landsat images. Investigators have found that by manipulating spectral information from the MSS bands it is possible to extract information (for example, iron oxide surface stains overlying altered ore deposits) unobtainable in a single channel or in a black and white image. Proven data enhancement techniques, such as color additive viewing, band



(b)

folds of the Sierra Madre Oriental (lower right) consist of Jurassic (J) and Cretaceous (Ki) sedimentary rocks. More open folds elsewhere are made up of younger Cretaceous (Ks) rocks. Cenozoic (Cs) sediments fill many of the valleys.



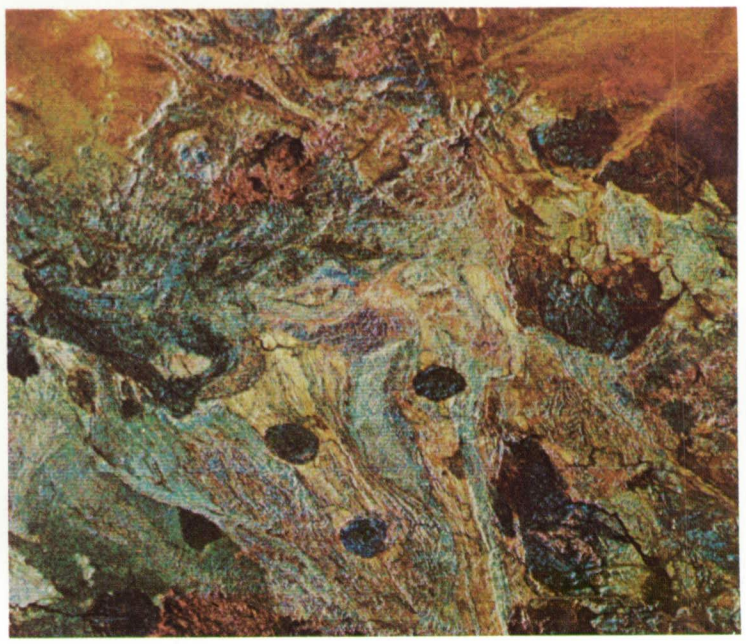
(a)



(b)



(c)



(d)

FIGURE 14.—(*a*) Part of Landsat image 1226–07011 (MSS band 6) showing a region of desert and hills in northwest Saudi Arabia. (*b*) Part of the 1:500 000 scale geologic map of the Hijaz quadrangle covering the area shown in (*a*). (*c*) Computer-processed color composite of the area shown in (*a*); MSS bands 4, 5, and 7 are contrast stretched and projected through blue, green, and red filters; neither this nor the next image have been corrected for aspect (vertical shortening). (*d*) Computer-processed color composite made from the ratio images of bands 4/5, 5/6, and 6/7 projected through blue, green, and red filters; compare the geologic units highlighted by this technique with those mapped in (*b*).

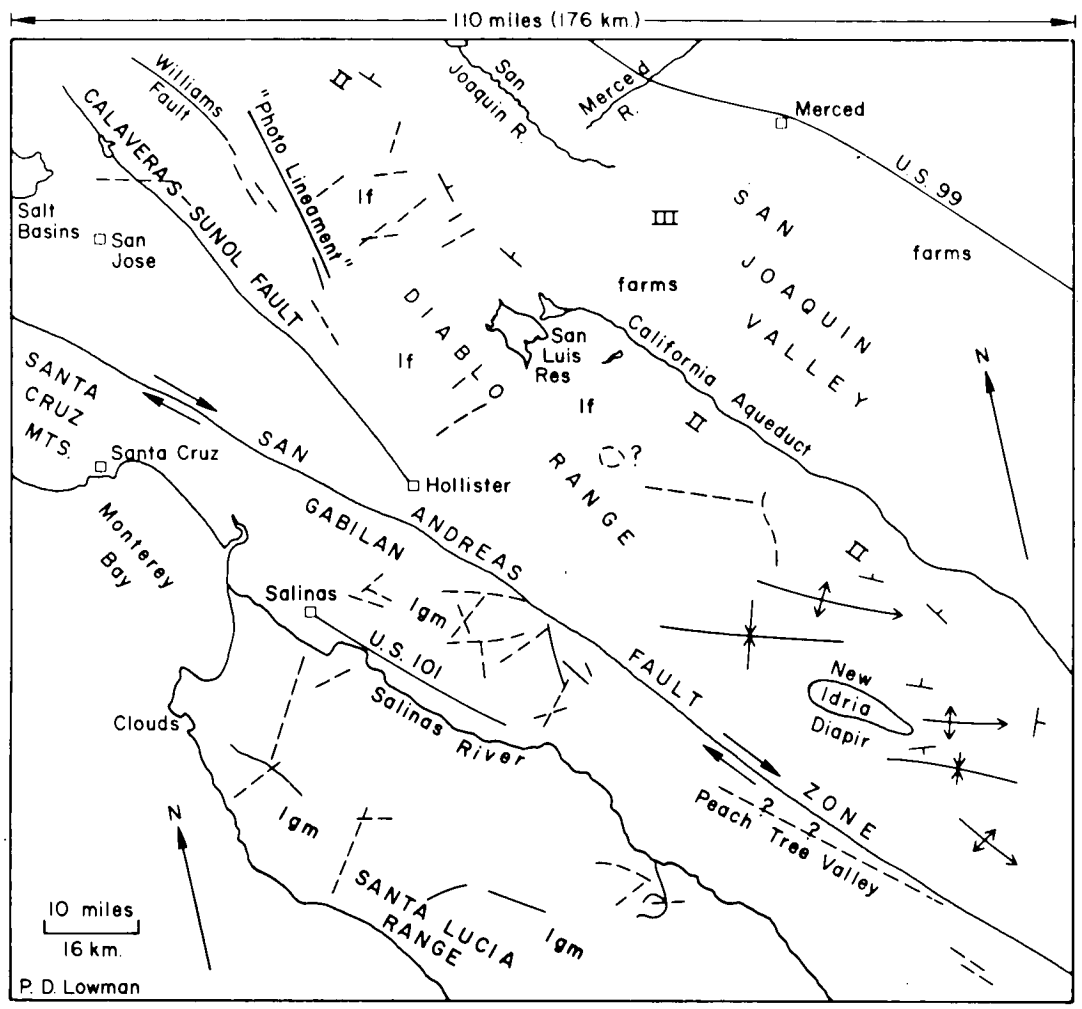
ratioing, and contrast stretching can be used with multiband data.

The ability to use Landsat data for mineral and petroleum exploration and for the detection of geologic hazards should enable Government and industry to reduce or eliminate several phases of their field exploration and mapping efforts at substantial savings in time and money.

Examples of Applications

The first map of any sort ever made from Landsat image (fig. 15) was produced as a sketch map of the California Coast Ranges near Monterey Bay. Finished only 1 week after the spacecraft was launched, it demonstrated the great time savings possible with Landsat imagery. More than 30 lineaments not corresponding to any recorded geologic structures were discovered in this image. These linear features are probably fractures—either faults or joints—and are important for several reasons. They may present problems, such as cave-ins or landslides, to tunneling or roadcut excavations, or, if faults, they act as potential seismic hazards. On the beneficial side, such fractures may be concentrating ground water or may have localized useful minerals such as the mercury deposits known in parts of the region. Their detection as previously unmapped structures makes them prime candidates for close field investigation to assess their economic or engineering importance.

Landsat data are being used to revise and update existing geologic maps. Figure 16(*a*) shows a geologic map of the West Aswan area of Egypt as compiled by the Egyptian Geological Survey prior to the launch of Landsat 1. Because of the extreme importance of the Aswan Dam and its surrounding area to the economy of Egypt, investigators performed a detailed photogeologic analysis of the area using Landsat imagery to locate rock units and detect features that could affect seepage from the reservoir (Lake Nasser), drainage patterns, and other features that might impact future development. Their investigation produced the new and much more detailed geologic map shown in figure 16(*b*). One highly significant result of their



GEOLOGIC SKETCH MAP
CENTRAL COAST RANGES, CALIFORNIA

Legend:

Calaveras Fault — Fault shown on 1:250 000 Geologic Map of California

Photo lineament (fault ?) not shown on Geologic Map of California

Plunging anticline

Plunging syncline

Attitude of strata (schematic)

Scale and orientation shown on map; principal point approximately 36°45'N, 121°10'W. Spacecraft altitude 560 stat. miles (900 km).

III Cenozoic terrestrial sediments

II Late Mesozoic marine sediments (Great Valley sequence)

lgm Granitic-metamorphic core complex with Cretaceous igneous intrusions

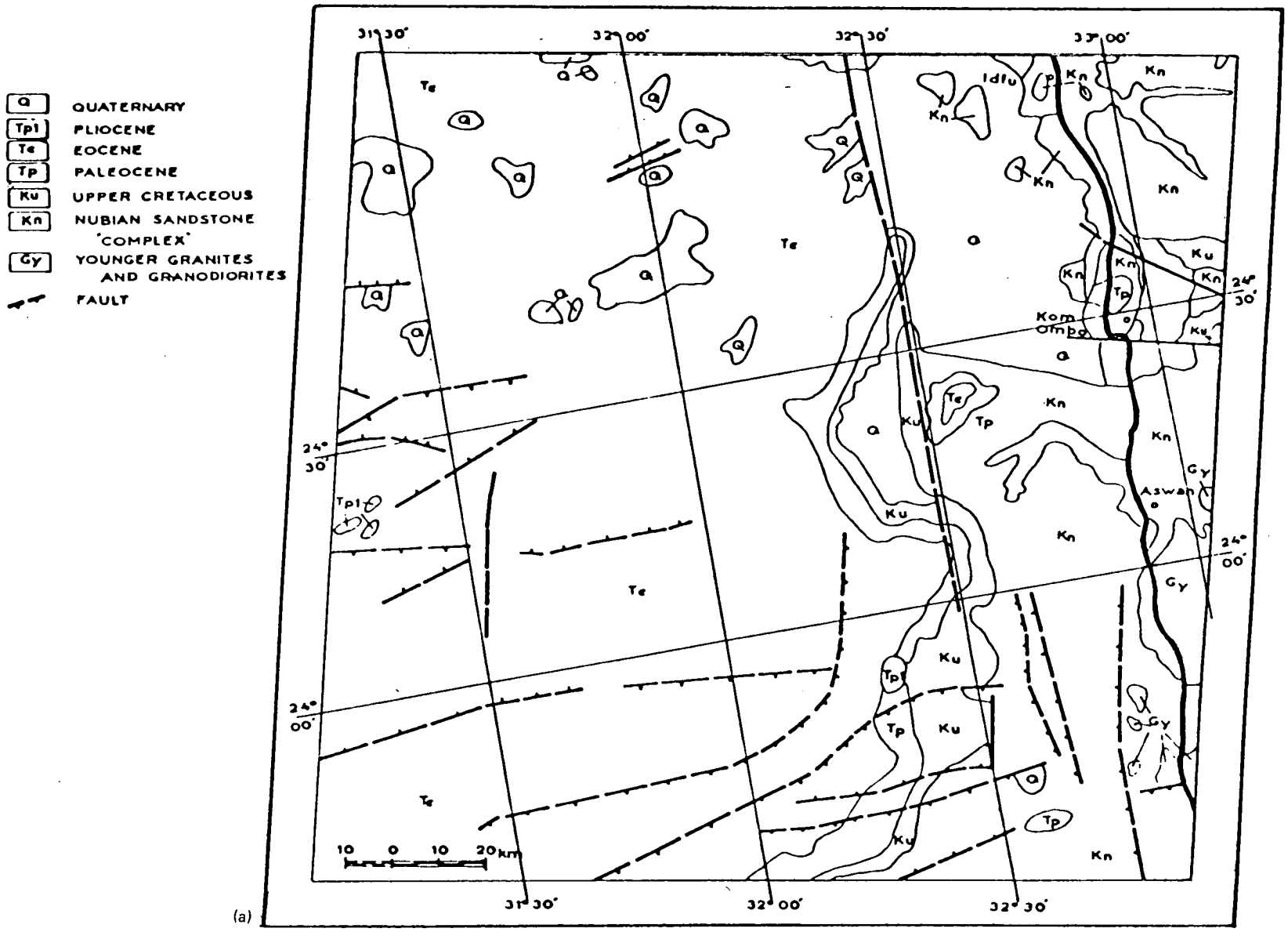
If Franciscan core complex (Mesozoic eugeosynclinal rocks)

FIGURE 15.—This map, prepared within 1 week after the launch of Landsat 1, was the first map of any sort drawn from Landsat images. Covering central California from the Pacific coast to the Sierra Nevada, it shows many lineaments that may be unmapped faults.

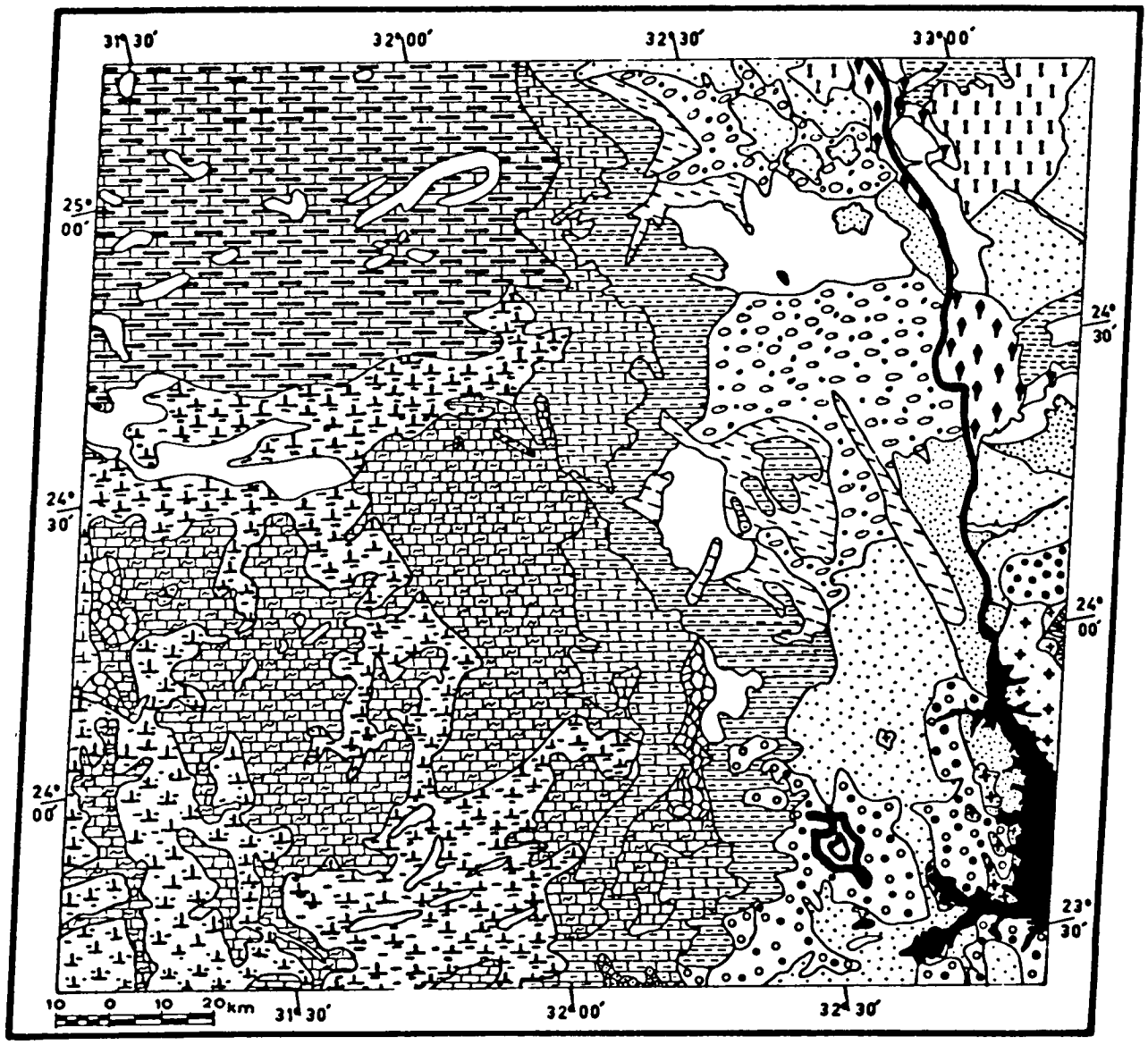
effort was the discovery and mapping of several faults trending in the direction of the reservoir that were not shown on the previous map.

A dramatic example of the use of Landsat images in structural studies is presented in figure 17 showing the Wind River Range in Wyoming. The sketch in figure 17(*a*) describes the extent of the structural geologic mapping completed for this area (of extremely rugged mountainous terrain) over a period of five summers prior to the launch of Landsat 1. Using MSS imagery, the investigator was able to compile the map shown in figure 17(*b*) in less than 1 day. Landsat data are being used to prepare similar geologic structure maps in other parts of the world where such detailed information has long been lacking.

Before a new method or instrument is applied by the mineral exploration industry, it must demonstrate its potential use and economic feasibility. With this in mind, Landsat investigators have designed an experiment to test the application of photo-lineament information obtained from Landsat imagery to the selection of potential target areas for mineral exploration. Using a test site in the mineral-rich central Colorado area, the investigators plotted all recognizable linears as enhanced by snow cover in a Landsat winter scene (fig. 18). Of particular importance were arcuate to circular fractures related to intrusions or volcano roots. Landsat has demonstrated a remarkable facility for emphasizing this type of curvilinear pattern. Next, a number of potential target areas for exploration were selected (without prior knowledge of the location of actual producing mineral districts) wherever there was a high density of intersecting straight and curved lineaments, which, from experience, tends to occur with structurally controlled zones of mineralization. Then, a map of known mineral districts in Colorado was compared with the chosen target areas. As shown in figure 18, 5 of the 10 potential target areas coincide with major mineral districts. This type of analysis of Landsat imagery can be a

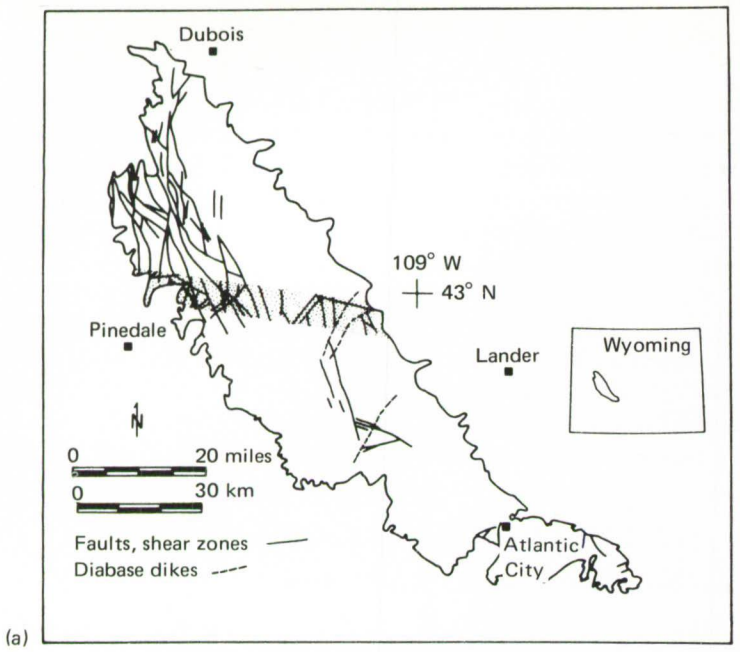


(a)

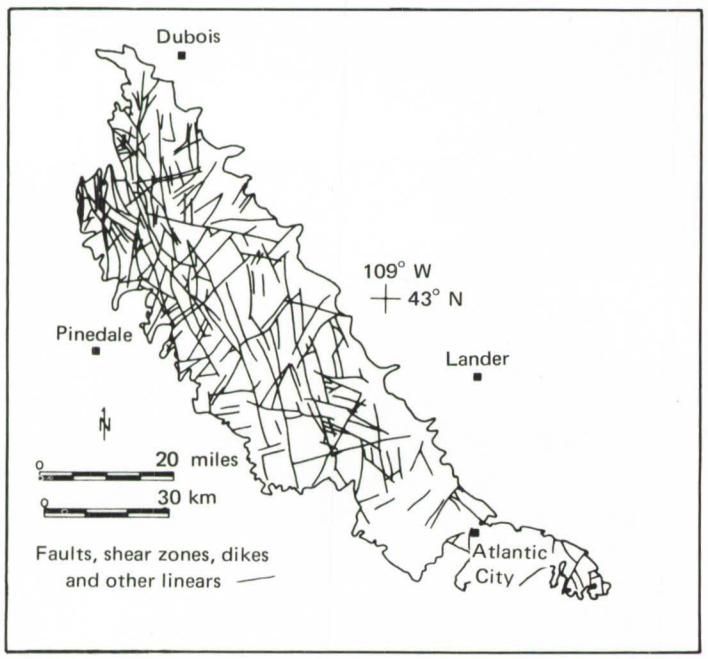


(b)

FIGURE 16.—*(a)* The published geologic map (1972) of the West Aswan area in Egypt. *(b)* Geologic map of West Aswan area showing surface units defined from Landsat imagery. (See legend at bottom of facing page.)



(a)



(b)

FIGURE 17.—Linears of probable geologic nature mapped in the Wind River Range of western Wyoming. (*a*) Linears mapped from ground studies and aerial photography. (*b*) Linears mapped from Landsat imagery.

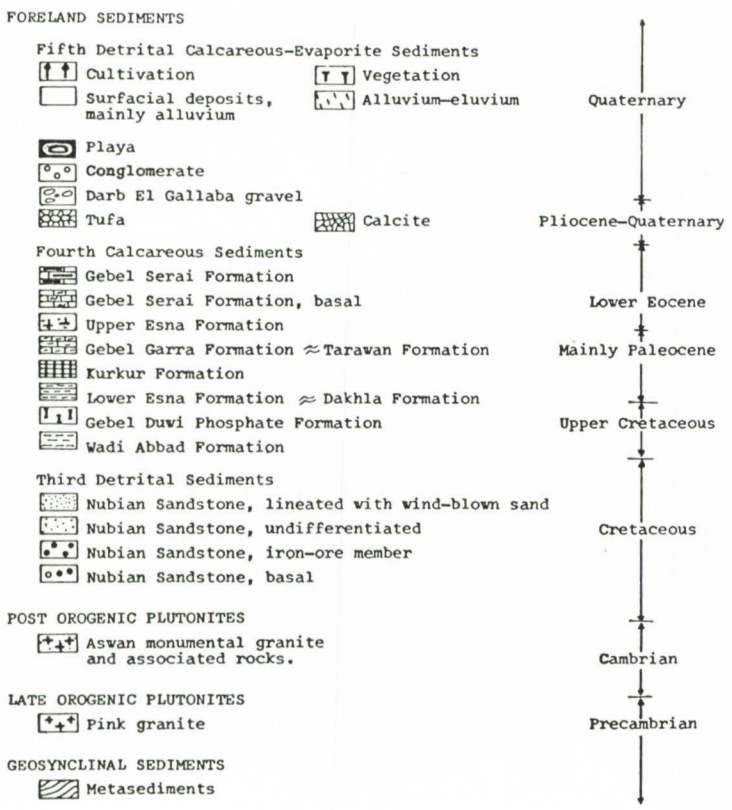




FIGURE 18.—Map of linears identified in a Landsat image (winter, snow-covered scene) of central Colorado. The mining districts (shown in red abbreviations) are as follows: Al—Alma; Br—Breckenridge; BZ—Bonanza; CC—Cripple Creek; Cx—Climax; G-P—Goldbrick-Pitkin; Ko—Kokomo; Lv—Leadville; Mn—Monarch; Mz—Montezuma; SC—Silver Cliff; and Tm—Tomichi.

valuable and inexpensive first step in a mineral exploration program, especially if used in conjunction with other sources of geologic information.

A test of the capability of computer-based enhancement techniques for identifying alteration zones associated with ore bodies has proved successful in a study of a gold and silver mining district in southwest Nevada. A special technique in which color images are reproduced from combinations of photo products generated by ratioing the reflectances of different pairs of MSS bands has been found to bring out subtle variations in the spectral characteristics of several types of common alteration materials occurring with ore bodies. The initial unratioed Landsat color image covering this Nevada mining district and also the reprocessed band ratio product are shown on plates 119 and 120. Careful examination of the color variants in the band ratio image, coupled with field studies and correlation with published map data, has led to a new map in which the different alteration products evident in the image are identified and located.

Landsat data are being applied increasingly to assist in exploration for new supplies of raw materials needed as energy sources. Information about certain types of oil and gas traps is commonly expressed at the surface. Included are direct signs of folds and faults, indicators of gross lithologic changes, and

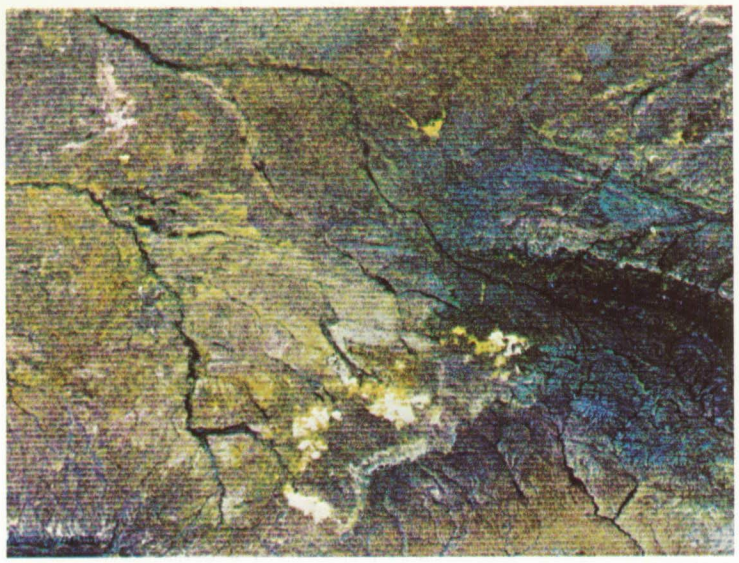


FIGURE 19.—A computer-generated color composite of part of a Landsat image of the Wind River Basin in central Wyoming made by projecting the ratio images of MSS bands 4/6, 6/7, and 5/7 through blue, green, and red filters, respectively. The area shown is the Gas Hills uranium district. Some of the white patches represent surface mines and pits; the bright yellow generally indicates iron oxide alteration products associated with the mine waste dumps and, in places, natural alteration zones.

evidence of thickening of stratigraphic units. Often, indirect clues to underlying structures are revealed by morphological anomalies such as deflected drainage or offset hills. Tonal variations sometimes reveal effects of escaping hydrocarbons. These several types of information have already led some petroleum companies to alter exploration programs; seek new leases; and, in at least one instance, actually test drill to search for possible pay zones. Landsat is also being used in the expanding quest for uranium and other radioactive materials important as nuclear fuels for power plants. Figure 19 shows the results of employing the band ratio technique to define areas of iron concentration that have proved to be telltale signs of alteration associated with sedimentary uranium ores in Wyoming.

WATER RESOURCES (HYDROLOGY)

Basis for Remote Sensing Applications

Hydrology is the applied science concerned with the inland (fresh) waters of the Earth—their occurrences, distribution, and circulation through the never-ending hydrologic cycle. The more information the water manager has about the hydrologic cycle, the better he is able to make decisions allocating our

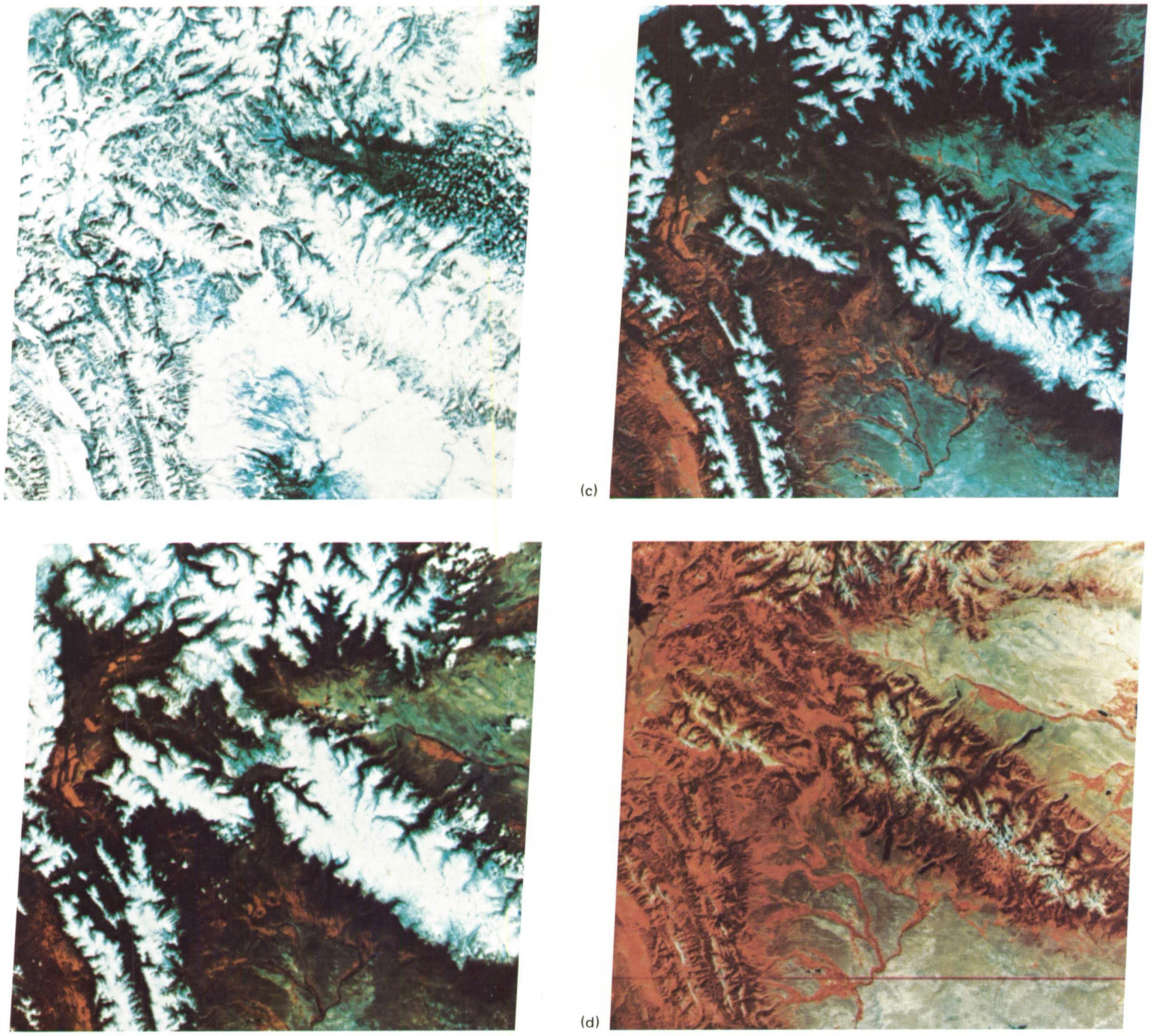


FIGURE 20.—Four Landsat scenes of the Wind River Mountains in Wyoming showing the progress of spring snowmelt. (*a*) April 15, 1973. (*b*) May 21, 1973. (*c*) June 8, 1973. (*d*) August 6, 1973.

scarce water resources for consumption, industrial uses, irrigation, power generation, and recreation. In times of excess, flood control may become the primary task; in times of drought, irrigation and power generation may be the primary concerns. The perspective gained by satellite remote sensing adds the areal dimension to the conventional hydrologic data collected at point measurement stations. Estimates of the occurrence and distribution of water are greatly facilitated with medium-resolution satellite data, and the repetitive coverage provides a first step toward assessing the rapid changes associated with the continuous regional-scale processes of the hydrologic cycle.

It is fortunate that many of the hydrologic features of interest for improved water resource management are easily detected and measured with remote sensors. Although water sometimes has a light reflectivity similar to other surface features in the visible wavelengths, it strongly absorbs light in the near-infrared region. This effect is easily identified by the near-infrared bands on Landsat. As a result, standing water is very dark in the near infrared, contrasting sharply with dry soil or vegetation, both of which appear bright. Additionally, in the visible region, snow is extremely reflective and provides a marked contrast with non-snow-covered surfaces. Thus, the liquid and solid forms of water are easily distinguished and can be readily monitored with Landsat. Because these liquid and solid forms change rapidly with time, the 18-day repetitive coverage from Landsat (9-day coverage during the period when Landsats 1 and 2 are operating simultaneously) provides an important tool for observing significant areal changes in water. The observed changes can thus be used to characterize the distribution of water throughout drainage basins of various sizes. Results from Landsat water resource investigators indicate that important contributions to understanding the hydrologic cycle are possible in snow and ice mapping, surface water inventories, flood assessment, and water quality monitoring.

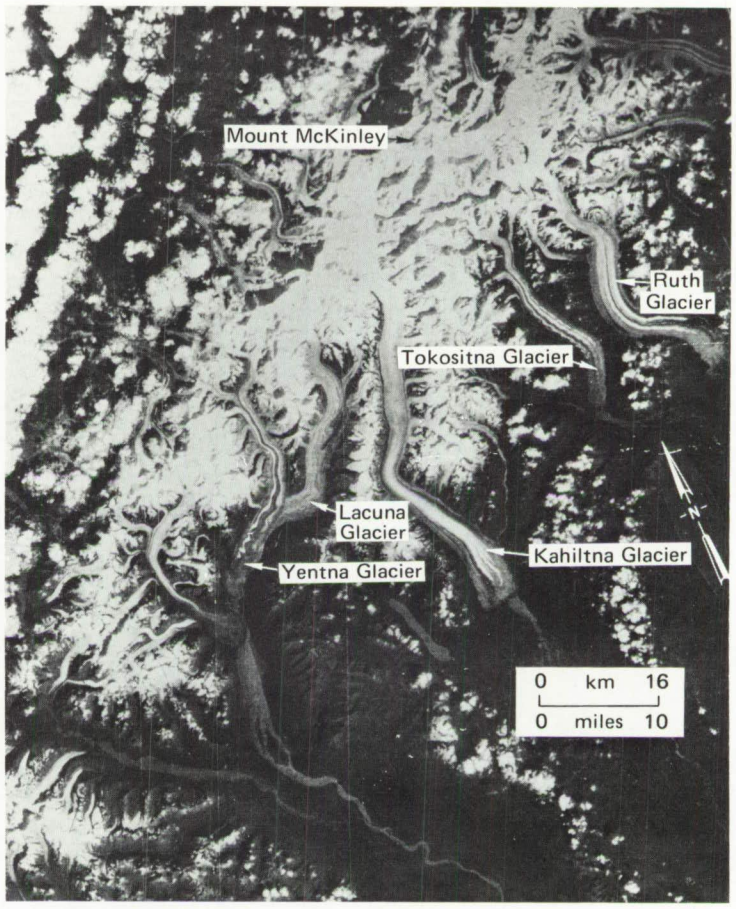


FIGURE 21.—Alaskan glaciers.

Examples of Applications

Landsat investigators have measured snow-covered areas of drainage basins to accuracies within a few percent and have estimated snowline altitudes to ±60 m (200 ft) in optimum situations. The location of snowlines can many times be extracted from Landsat imagery in more detail than is normally obtained from operational aircraft surveys. In many areas of the world, such as the western United States, snowmelt provides a major part of the annual water runoff that can be used for man's needs. Landsat sequential snow-cover images, as shown in figure 20, supply information on the rate of melting and the subsequent volume of water released. This figure shows the entire Wind River Mountain watershed area during the 1973 spring/summer snowmelt period. For ungaged, inaccessible, and remote watersheds, Landsat snow-cover data can be usefully related to seasonal runoff to provide early season water supply estimates. In areas with conventional snowpack monitoring networks, Landsat snow-cover data can be more profitably used as an additional parameter to reduce existing errors in seasonal runoff forecasts and thus make better use of our water resources. The employment of Landsat data for snow-cover surveys appears to be a way to obtain needed hydrologic information from the increasing number of restricted access wilderness areas of the West.

Landsat imagery has proved effective in identifying surging glaciers and monitoring the areal extent of their change. Figure 21 shows a family of glaciers in the vicinity of Mount McKinley in central Alaska. It includes both normal slow-moving glaciers, such as Ruth, Kahiltna, and Lacuna, and surging glaciers such as Tokositna and Yentna, which can advance several kilometers in a few years. A surging glacier can be distinguished from a nonsurging glacier on Landsat imagery by the presence of movement-induced crenulations (zig-zag patterns) in the morainal deposits carried on the surface. Lacuna glacier has been stagnant for 40 yr and its dark surface shows the results of severe melting. Tokositna, however, has just completed a rapid advance that began in 1970 and exhibits the characteristic wiggly folded moraines. This Landsat image of Yentna showed that its folded moraines have been displaced 2000 m (6000 ft) down the valley from their position on recent maps and 1970 aerial photographs. The other two glaciers shown, Ruth and Kahiltna, flow at slow uniform rates and their medial moraines—the dark stripes down the ice centers—are straight and uniform. The causes of glacier surges and why some glaciers surge and others do not are questions of great scientific interest that also have practical aspects. Surging glaciers can advance very rapidly over large land areas and can cause devastating flooding by blocking and then suddenly releasing large quantities of melt waters. Continuous, repetitive imagery from Landsat aids glaciologists in observing glacial movement throughout the world.

Surface water area has been estimated to within a few percent accuracy over large regions such as the playa lake region of the southern High Plains of Texas and New Mexico. Lakes as small as 10 000 m^2 (2.5 acres) can be recognized and located accurately on map scales as large as 1:250 000. Landsat has also proven useful for assessing changes in areal extent for larger water bodies. The Landsat mosaic of the United States has been used to produce a computer printout noting the location, surface water area, and relative dimensions of the 128 surface water bodies in the United States that cover more than 100 km^2 (40 sq miles). Other hydrologically significant land use features, such as impervious area, vegetation, and bare soil are being mapped on many watersheds across the United States. Changes in land use on watersheds resulting from forest fires, clear cutting, or strip mining can be rapidly noted and the information incorporated into watershed management operations.

The two Landsat images in figure 22 show the Mississippi River at St. Louis, Mo. The image on the left shows the St. Louis area with the river at normal levels, while the one at the right at the same scale shows the same area during the extensive flooding that took place in the Mississippi Valley during the spring of 1973. Point *A* on the figure locates the confluence of the Missouri and Mississippi Rivers; point *B*

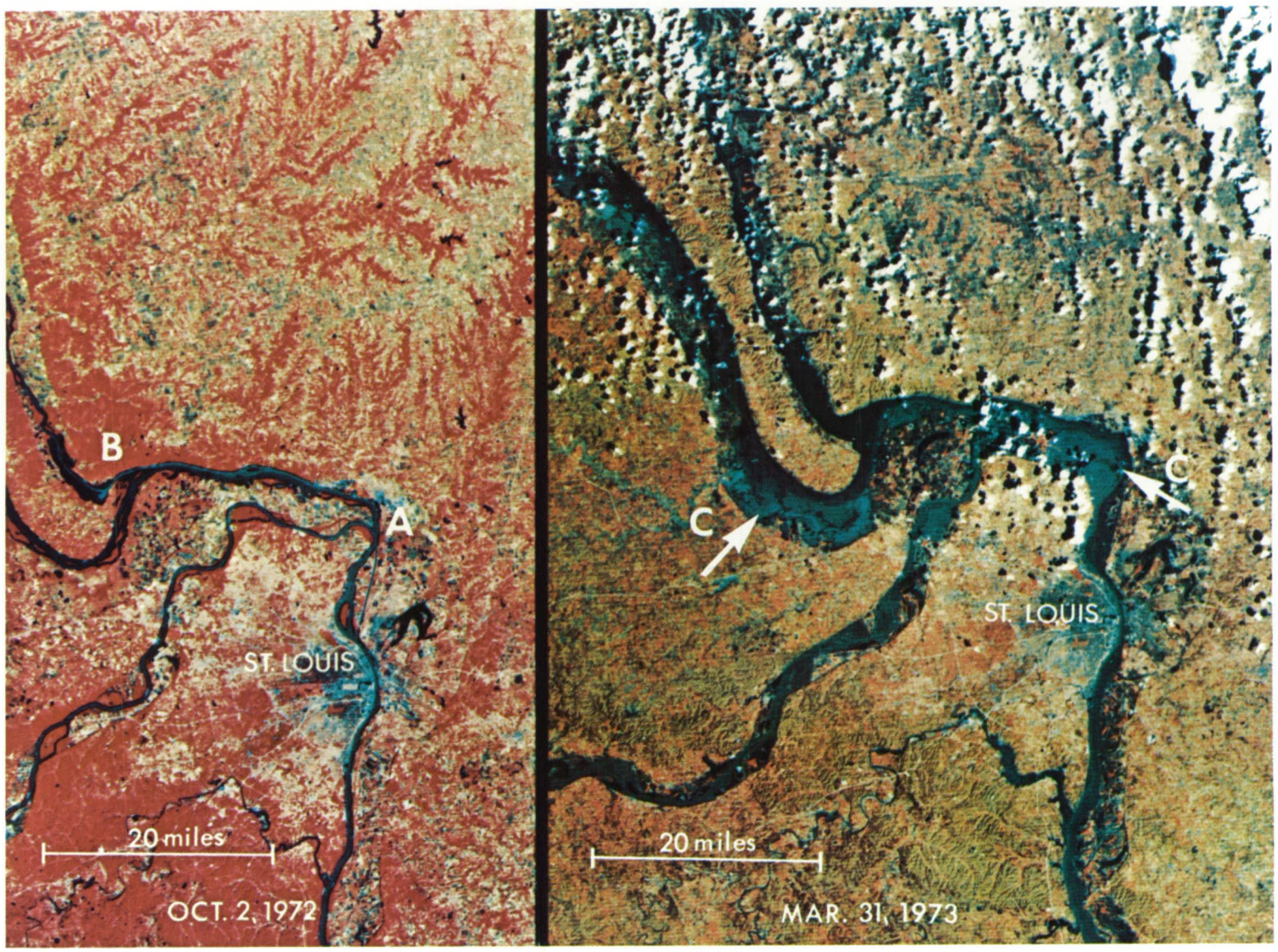


FIGURE 22.—Before and after Landsat scenes of the St. Louis area showing the extent of the spring 1973 flood.

locates the confluence of the Illinois and Mississippi Rivers. The two places labeled *C* are large areas that were inundated during the flood. These and other images were used by Landsat investigators to map the flood area along almost the entire length of the Mississippi. Such data are not only valuable for assessing up-to-date regional flood conditions but also for the planning of additional flood protection systems.

Figure 23 shows three scenes of Utah Lake, south of Salt Lake City, Utah, imaged at three different times of the year: midsummer, late summer, and spring. It exemplifies the ability of Landsat to monitor lake processes. In the first scene (*a*), the lake contains only a small amount of sediment (light blue) in the near surface layers and parts of it are clear (dark blue-black). By late summer (*b*), however, huge algal mattes (red) resulting from nutrient concentration cover a significant portion of the lake's surface. In spring (*c*), large amounts of sediment-laden water have entered the lake in response to snowmelt in the mountains, and it has become a milky blue color.

Landsat data collection system platforms (DCP's) have performed a significant role in several water resource experiments. In southern Florida, for example, water-stage information from DCP's installed in the Everglades (fig. 24) was used in conjunction with water-area information from Landsat imagery to provide water volume estimates in near real time. This information was needed to make management decisions concerning the redistribution of water in the area. The DCP capability when combined with Landsat imagery provides a way to extrapolate conventional point measurements over large normally data-sparse areas.

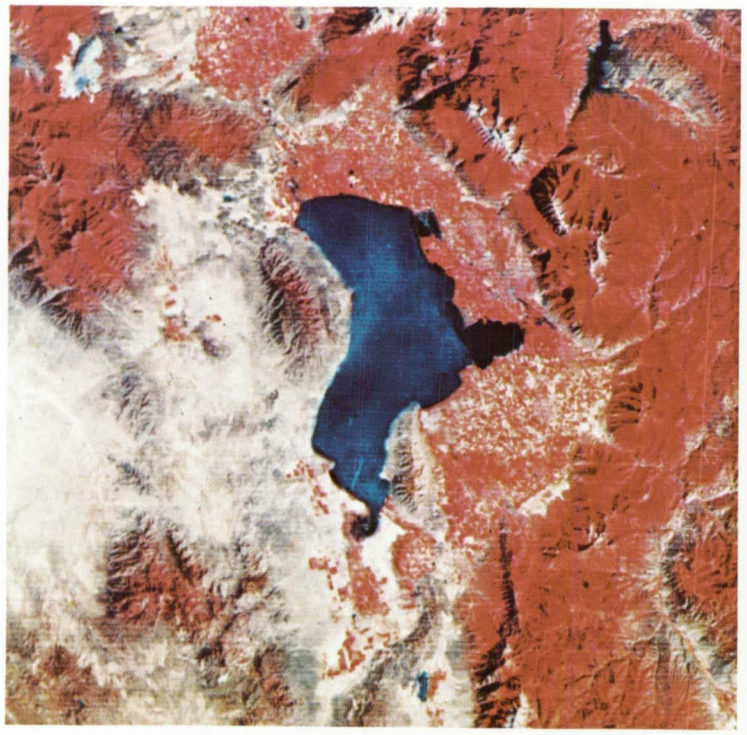
OCEANOGRAPHY AND MARINE RESOURCES

Basis for Remote Sensing Applications

The oceanography and marine resources discipline is concerned with the productivity of the oceans and coastal zones and with natural phenomena and man's activities that directly or indirectly preserve, alter, destroy, or enhance the resources of the open ocean or coastal areas. It also is concerned with the physical properties of the oceans such as depth, temperature, and physical state (i.e., ice or water). The major goal within NASA's Oceanography and Marine Resources Program is to develop remote sensing technology to assist in accomplishing the following goals:

(1) Efficient management of living marine resources
(2) Efficient and effective management of activities within the coastal zone regions
(3) Effective use of the oceans as transportation routes
(4) Meaningful contributions toward the advancement of marine biology and oceanography

Successful accomplishment of these goals is dependent upon the ability to identify, measure, and analyze a number of parameters or processes that operate or react together in a highly dynamic environment. Involved are the observation or measure-



(a)



(b)



(c)

FIGURE 23.—Three Landsat scenes of Utah Lake showing variation in lake processes. (*a*) August 7, 1972. (*b*) September 12, 1972. (*c*) May 22, 1973.



FIGURE 24.—Landsat DCP setup in Florida's Everglades.

ment of the physical, chemical, geometrical, and optical features of the coastal and open zones of the oceans, including such parameters and features as sea ice, temperature, current, suspended sediments, sea state/ocean surface topography, salinity and other chemical properties, plants and animals, land/sea interface, bathymetry, and water and bottom color.

Within this discipline, two main subdisciplines can be defined: coastal and ocean. These are more or less divided by the fundamental temporal and geometric dynamic range of the processes that take place in each. Within these two subdisciplines, a total of 7 application areas and 14 (active and potential) measurement techniques can be defined as shown in table 2.

These application areas and their related problems may be served by remote sensing information systems developed from one or a combination of measurement techniques for which at least some remote sensing capability exists. The information system required for each application can be defined in general, but in most cases the specifics are yet to be developed. Detailing the specifics requires close cooperation with the user, and in many cases requires research by the user. The techniques that can be measured wholly or at least in part from Landsat data have been identified. Platforms and sensor systems outside of Landsat capability must be used to achieve full discipline coverage.

Examples of Applications

A majority of the Landsat investigations in the marine resources discipline deal with coastal processes. Techniques have been developed for defining coastal circulation patterns using sediment as a natural tracer, allowing the formulation of new circulation concepts in some geographical areas and, in general, providing an improved capability for defining the seasonal characteristics of coastal circulation. An analytical technique for measuring absolute water depth (bathymetry), based upon the ratios of two MSS channels, has also been developed. The technique requires some knowledge of bottom reflectivity, water

TABLE 2.—*Marine Resource Application Areas and Related Measurement Techniques*

Measurement techniques	Marine resources							Potential information from Landsat
	Coastal			Ocean				
	Living marine resources	Coastal zone management	Marine biology, oceanography, meteorology	Living marine resources	Transportation	Maritime law	Marine biology, oceanography, meteorology	
Physical:								
Ice	X	X	X	X	X	X	X	Yes
Temperature	X	X	X	X			X	No
Current	X	X	X	X	X	X	X	Yes
Suspended sediment	X	X	X					Yes
Sea state	X	X	X	X	X		X	Yes
Chemical:								
Salinity	X	X	X				X	No
Other chemical properties	X	X	X				X	No
Biological:								
Plants	X	X	X	X			X	Yes
Animals	X	X	X	X			X	Yes
Geometric:								
Ocean surface topography							X	No
Land/sea interface	X	X	X					Yes
Bathymetry	X	X	X					Yes
Optical:								
Water color	X	X	X	X			X	Yes
Bottom color	X	X	X					Yes

transparency, and surface characteristics. Initial evaluation of the technique indicates that it is useful in coastal areas of low to moderate turbidity for depth measurement up to 20 m (65 feet) and for updating the locations of reefs and shoals.

Investigators also report that significant progress has been made in developing techniques for using Landsat data to locate, identify, and monitor sea and lake ice. Ice features greater than 70 m (230 ft) in width can be detected, and both arctic and antarctic icebergs have been identified. Because of the large daily sidelap of Landsat coverage at high latitudes, some tracking and quantitative measurements of ice movement are possible. The substitution of Landsat imagery to replace some present aircraft surveys of arctic sea ice appears both technically feasible and cost effective.

Accurate identification of lake ice and classification of ice types would provide invaluable information for shipping in the Great Lakes and would allow more efficient routing of shipping through ice-covered waters and the possible extension of the shipping season. As shown in figure 25, Landsat 1 provides relatively highly detailed synoptic views of the ice cover on the Great Lakes. Although its 18-day cycle prevents acquisition of imagery often enough to be of operational use in a lake- or sea-ice surveillance system, Landsat 1 has demonstrated the feasibility of using satellite imagery for this purpose.

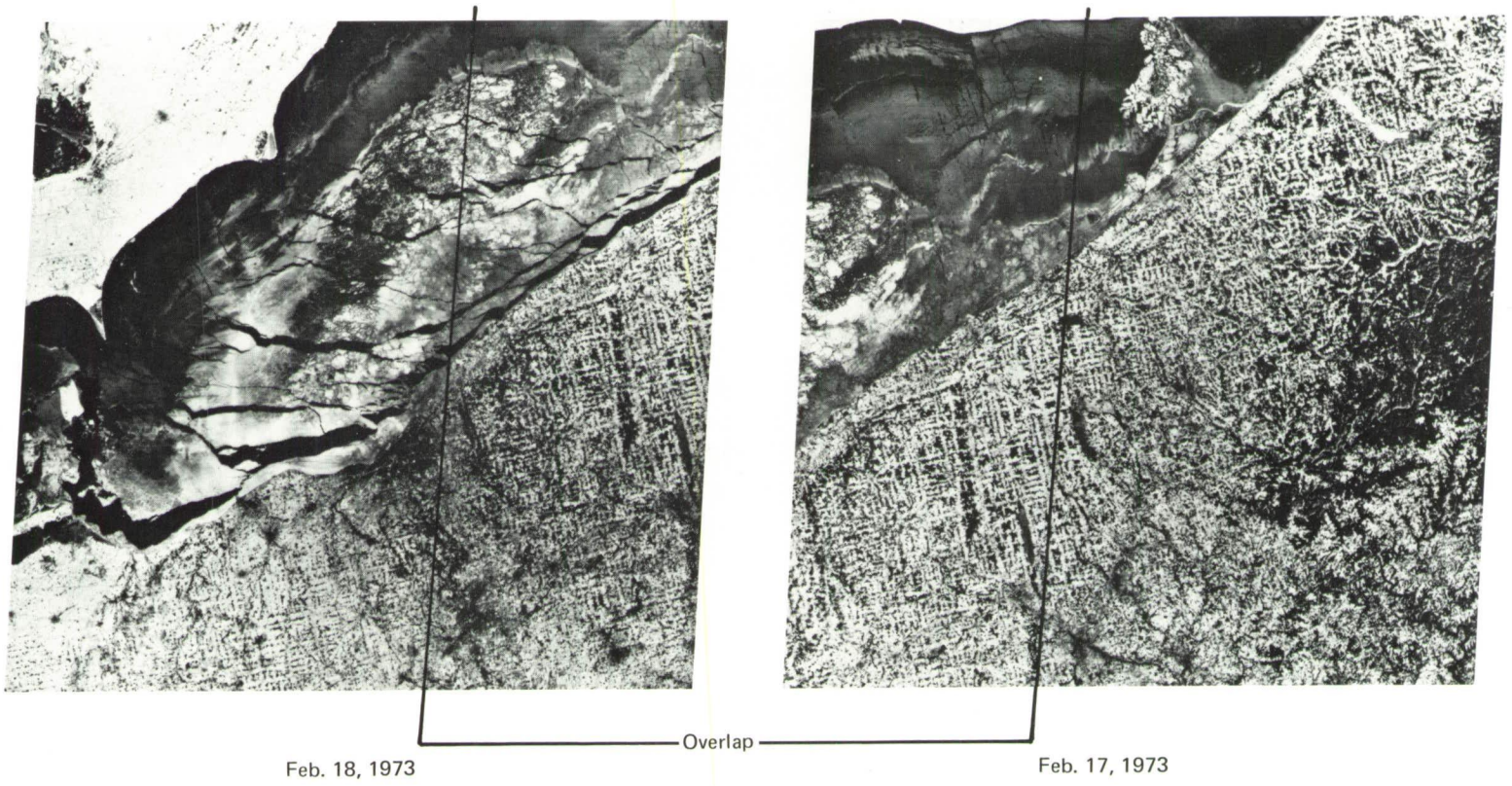


FIGURE 25.—24-hour breakup of ice on Lake Erie as imaged by Landsat 1 MSS band 7.

In the application area of living marine resources, the use of Landsat image-density patterns as a potential indicator of fish school location has been demonstrated for one coastal commercial resource, the menhaden. Further development of these satellite techniques may yield the only practical method of monitoring and assessing living marine resources on a large scale.

Ocean dynamics is another area where large-scale synoptic coverage is required. Landsat data have been used to locate ocean current boundaries using image-density enhancement, and some techniques are under development for measurement of suspended particle concentration and chlorophyll concentration.

Figure 26 shows an example from one Landsat 1 investigation in this discipline, a study of upwelling and plankton patterns off the northwest coast of Africa, which used research ships to collect ground-truth data. Investigations such as this are aimed at detecting the real distribution structure of plankton better with Landsat imagery than could be detected using multiple ship cruises.

An excellent example of Landsat's ability to portray sediment is shown in figure 27, an MSS red-band image of Delaware Bay. Investigators used sediment as a natural tracer to delineate currents and aquatic interfaces or frontal features between areas of water with differing turbidity.

The bathymetry investigation previously referred to has developed a technique for measuring water depth from Landsat data that could be used to quickly and inexpensively update shipping charts throughout much of the world's clear water coastal regions. Figure 28 shows all four MSS bands of a Landsat 1 frame imaged over the Little Bahama Bank. Band 4 (the green band) clearly shows underwater features in the bank north of Grand Bahama Island. Most of these were identified on the International Hydrographic Office depth chart, but there are a number of underwater features in the center of



FIGURE 27.—Sediment distribution in Delaware Bay.

the frame that are not on the published chart. Band 5 (the red band) shows some of the shallower areas of the bank, but bands 6 and 7 (the infrared bands) show no underwater features. Bands 6 and 7 do, however, accurately delineate land/water boundaries. The investigator demonstrated that depths can be calculated by ratio processing for those depths that return a signal in both bands 4 and 5. If additional control

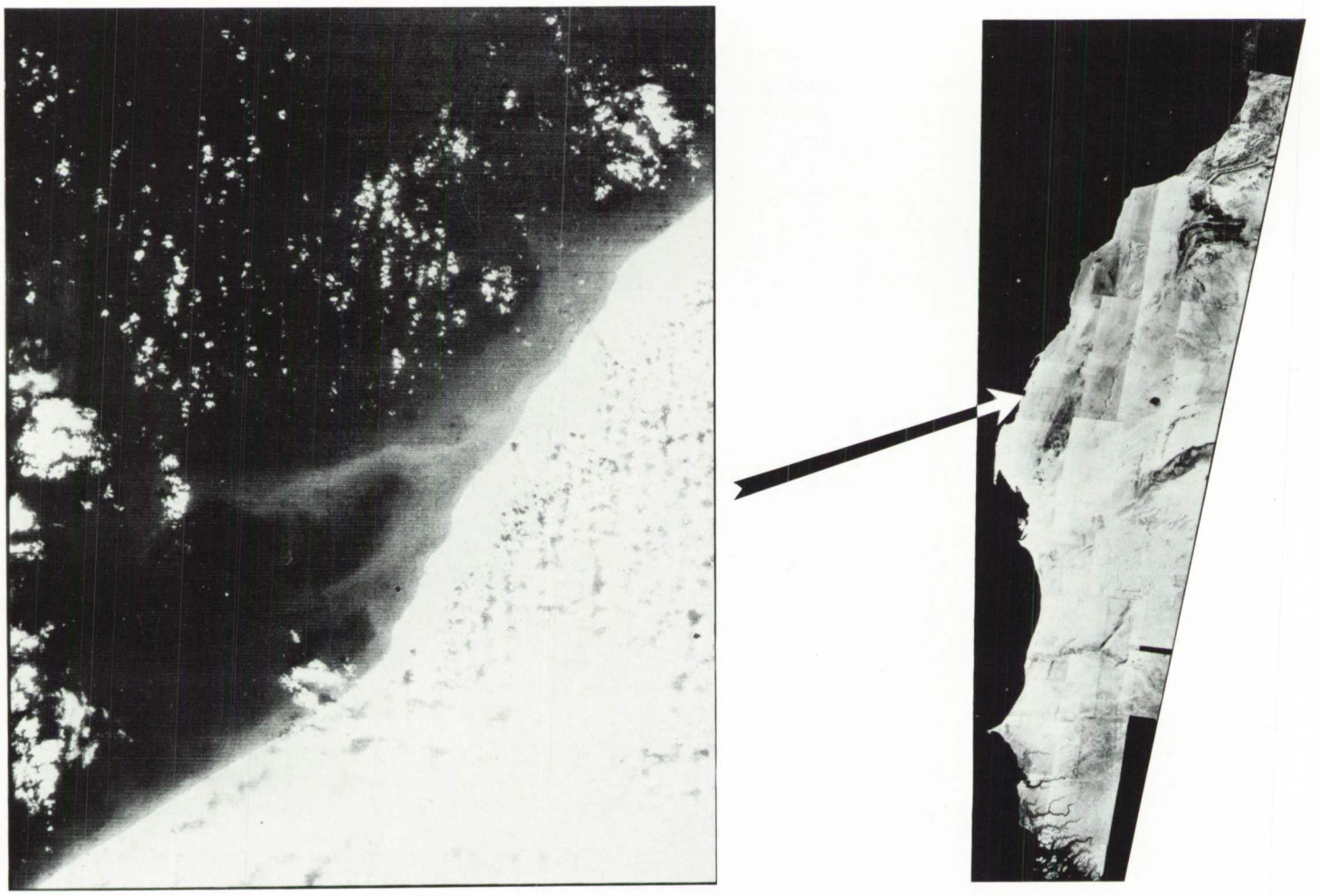


FIGURE 26.—Upwelling and plankton patterns off the northwest coast of Africa. Landsat 1 MSS band 4 image of November 4, 1972.

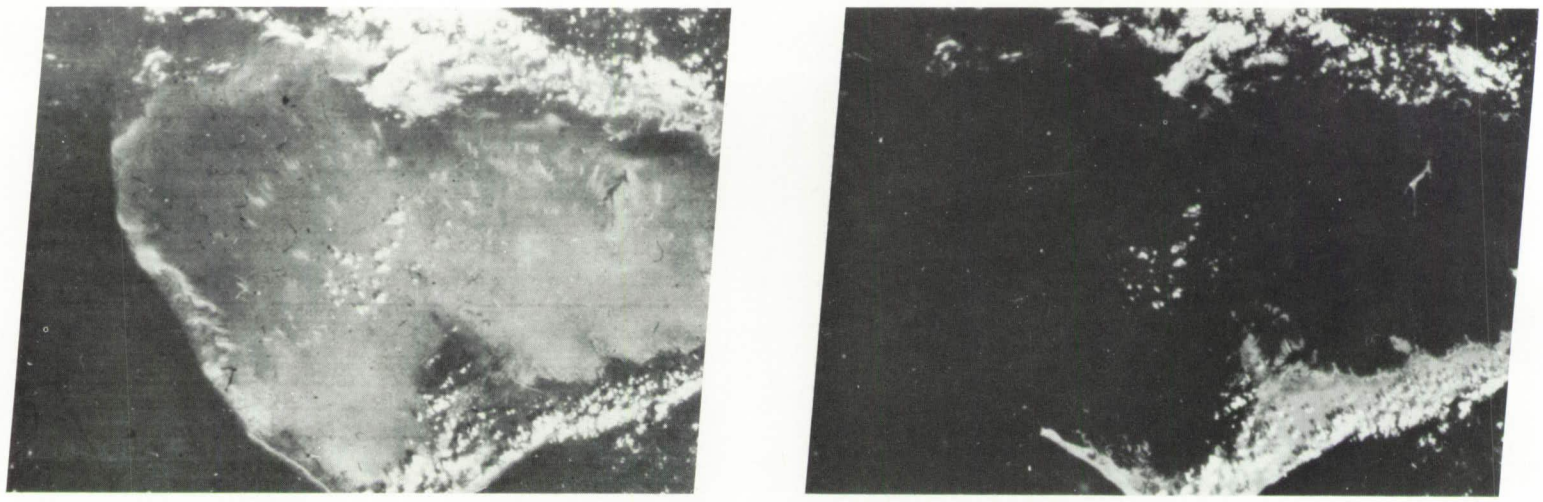


FIGURE 28.—Four-band Landsat MSS data of Little Bahama Bank.

points are known, and if the reflectances of bottom materials are taken into account, an absolute depth map can be made for depths up to 20 m (65 ft).

ENVIRONMENT

Basis for Remote Sensing Applications

As applied to man's environment, remote sensing is concerned with gathering information related to the quality, protection, and improvement of our land, water, and air resources. Of special interest are the detection of changes in the environment brought about by natural and manmade phenomena and the measurement of pollution of these resources. In the simplest sense, remote sensing techniques from satellites (manned and unmanned) and aircraft are directed toward answering these basic questions about the environment:

(1) What can be sensed in the environment that affects man's world?
(2) What are the environmental impacts of man's activities?
(3) How do the changes imposed on the environment affect our way of life?
(4) How can we fix or improve a weakened environment?
(5) Are the things we are doing to repair the environment actually working?

Landsat can effectively address these questions because of two of its attributes. First, the satellite gives a regional or synoptic overview of the total environment: a perspective of the land, water, and air seen as parts of an integrated system. Second, the satellite can provide a repetitive or seasonal look at certain types of steady, persistent pollution or slow changes in a degrading environment or abrupt alterations owing to a disaster.

Varying degrees of success have been achieved from Landsat in the following pursuits involving land and vegetation quality:

(1) Monitoring strip mining and reclamation
(2) Assessment of changes in urban quality
(3) Measurement of damage by pipeline construction
(4) Monitoring effects of construction at major land developments
(5) Classification of vegetation in different ecosystems
(6) Delineation of permafrost zones and tundra scars
(7) Detection of changes in the coastal zone

Applications to problems concerning water quality include the following:

(1) Measurements of suspended solids and chemical wastes
(2) Indirect determination of chlorophyll
(3) Detection of acid and iron wastes and oil spills
(4) Determination of dispersal patterns in turbid waters
(5) Definition of surface circulation patterns
(6) Detection of large-scale ocean dumping
(7) Location of water intake pipes
(8) Monitoring lake eutrophication and algal blooms

It should be pointed out that quantitative chemical measurements of water pollution cannot be conducted from Landsat imagery.

Another application area from Landsat seeks data used in

managing wildlife. Among achievements already shown to be feasible are the following:

(1) Delineation and assessment of wildlife habitats
(2) Management of waterfowl
(3) Measurement of available water and food supplies
(4) Determination of carrying capacity of an ecosystem
(5) Assessment of damage from logging operations

Landsat has demonstrated that it can contribute important knowledge about our atmosphere:

(1) Sources and dispersion of smoke plumes
(2) Influence of air pollution on climate and weather
(3) Detection of urban haze and global and regional atmospheric aerosols

Finally, Landsat is capable of recognizing to varying extents the occurrence and adverse effects of some kinds of short-lived events, including volcanic eruptions, earthquakes, hurricanes and tornadoes, and forest fires.

Examples of Applications

Figure 29 shows an inventory map of strip-mined land in parts of Pike, Gibson, and Warrick Counties in southeastern Indiana. Both strip-mined areas previously mapped from the ground or air and areas newly mapped from the Landsat imagery are located. Landsat's utility for this purpose has been demonstrated by several investigators in coal-mining regions of the Northeast, and the accuracy of the mapping has been verified by ground-truth checking. Landsat's repetitive coverage allows State officials to map newly stripped areas and to check periodically on reclamation progress.

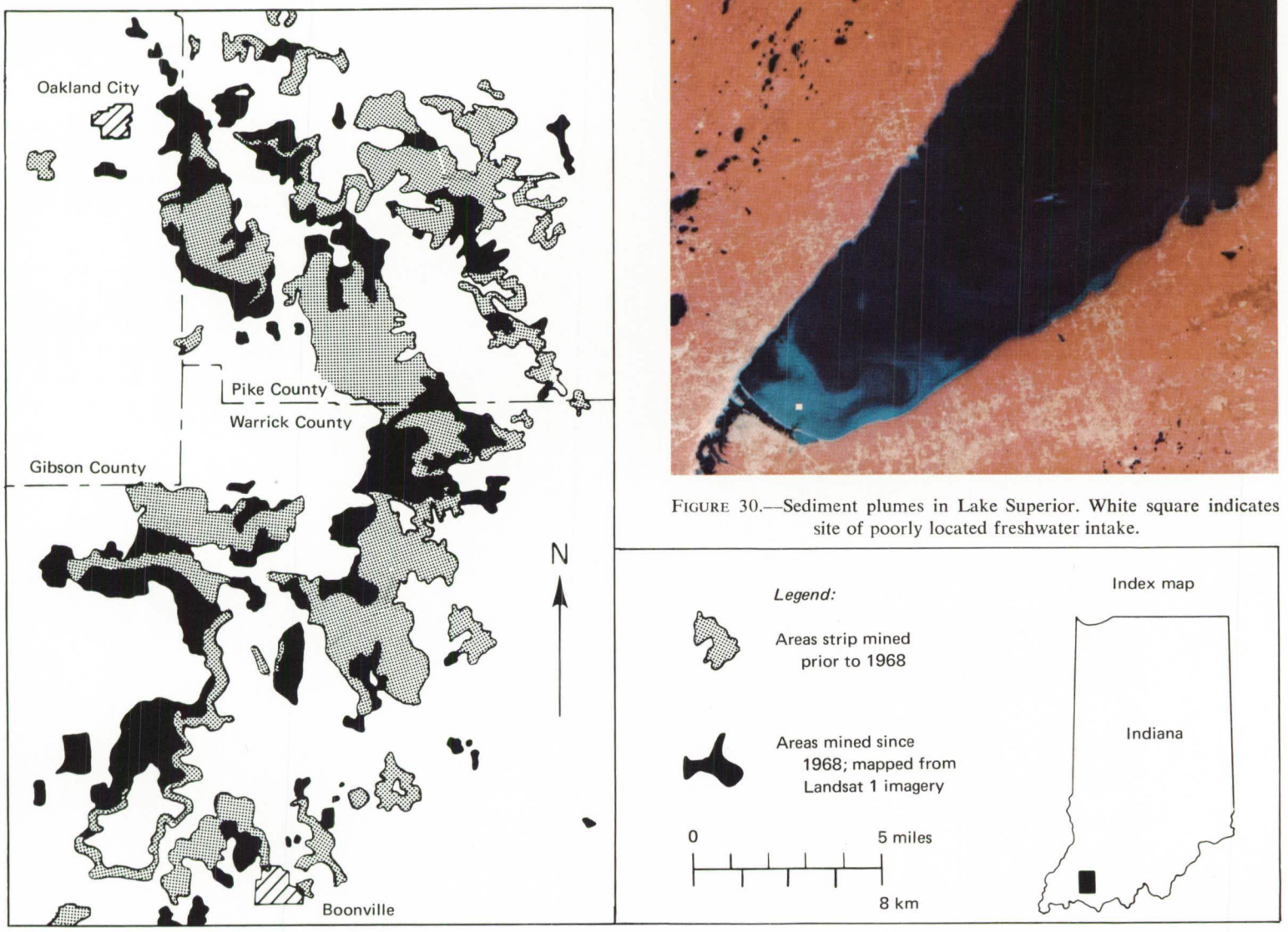


FIGURE 29.—Strip-mine inventory map of southeastern Indiana compiled from analysis of Landsat imagery.

Turbidity swirls in Lake Superior (fig. 30) have provided dramatic evidence of how Landsat data can be of practical use to city and State governments. The light-toned sediment patterns along the lake's shoreline stand out in the Landsat image. The white square in the bottom-middle portion of the lake marks the spot where a freshwater intake line was placed by a local municipality, at a cost of $8 million. High sedimentation at the intake point makes the entire operation unusable. Had Landsat imagery been available to guide the placement of the water intake point, this very costly error could have been avoided.

Meteorologists have suspected for years that air pollution causes weather modifications. Figure 31 provides excellent evidence to back up this hypothesis. This late fall Landsat image of the Chicago, Ill.-Gary, Ind., area shows plumes from seven steel mills and power plants (indicated by arrows) flowing out over Lake Michigan and feeding directly into the cumulus clouds over the lake. The clouds forming out of the plumes begin noticeably closer to the Indiana-Illinois shore and become denser and more developed as they approach the Michigan shore than do the clouds outside the direct lines of the smoke plumes. Because snow and rain form around the particles contained in the plumes, the clouds influenced by them are more likely to produce precipitation than the other clouds. This is believed to be the first clearly observable example of inadvertent weather modification caused by man's activities.

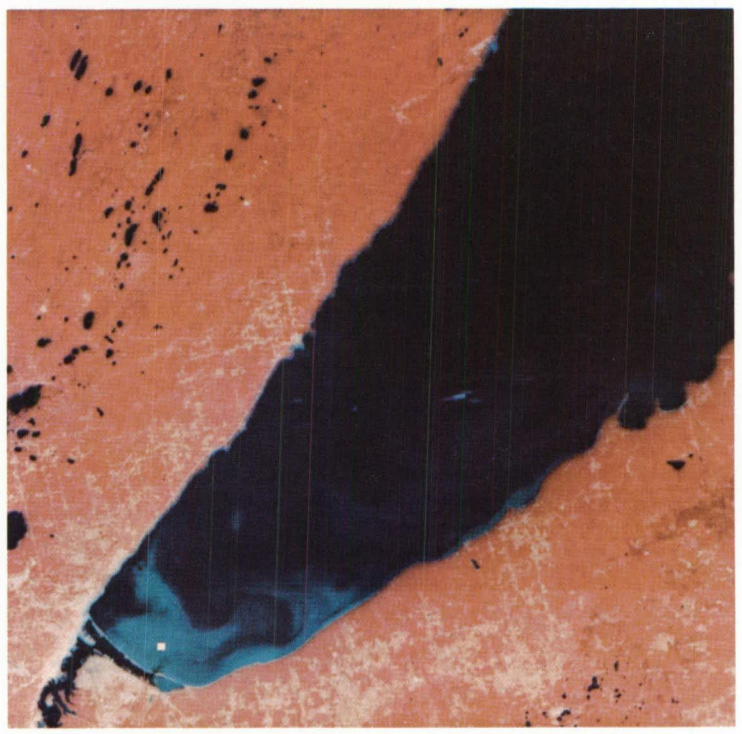


FIGURE 30.—Sediment plumes in Lake Superior. White square indicates site of poorly located freshwater intake.

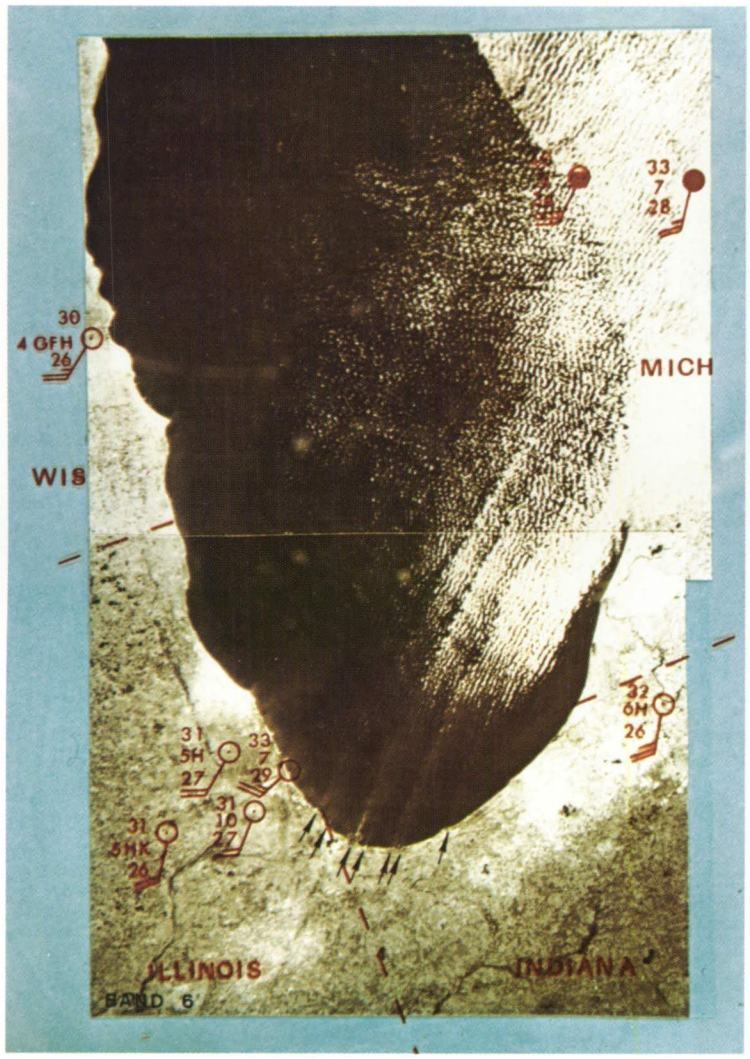


FIGURE 31.—Weather modification over Lake Michigan caused by air pollution.

SUMMARY OF APPLICATIONS/RESULTS

After 3½ years of operation, the Landsat 1 spacecraft had completed over 18 000 orbits and acquired more than 200 000 scenes, resulting in over 5 million products; it had photographed 100 percent of the United States and 78 percent of the remainder of the world's land masses under "cloud-free" conditions (defined as less than 30 percent cloud cover).

There were 217 active DCP's transmitting data through the spacecraft to ground stations. Nearly 1 million useful messages have been transmitted.

In spite of the spacecraft's many accomplishments, there were some problems. Wideband video tape recorder no. 2 failed about 10 days after launch. The RBV power switching relay failed a few days later; however, there are techniques available to reactivate the RBV system by other relay command systems. Wideband video tape recorder no. 1 also failed after over 2 yr of operation, eliminating the spacecraft's recording capacity.

What has been achieved with these millions of data products going to hundreds of scientific investigators throughout the world? Conceding the technical and scientific success of the Landsat 1 system, what has been the payoff for the time and tax dollars spent on developing and building it? What benefits will be derived from Landsat that are of real, everyday, practical use to mankind?

To answer these questions, NASA has held four symposiums where scientific investigators working with Landsat data, including some not funded directly by NASA, were invited to present findings and possible applications of their investigations. The papers given at these symposiums have been compiled and published as the following NASA documents:

(1) *First ERTS Symposium,* September 29, 1972, see NASA TM X–66193

(2) *Symposium on Significant Results Obtained From ERTS–1,* March 5–9, 1973, see NASA SP–327 (vol. I, Technical Presentations), NASA TM X–66283 (vol. II, Summary of Results), and NASA TM X–66284 (vol. III, Discipline Summary Reports)

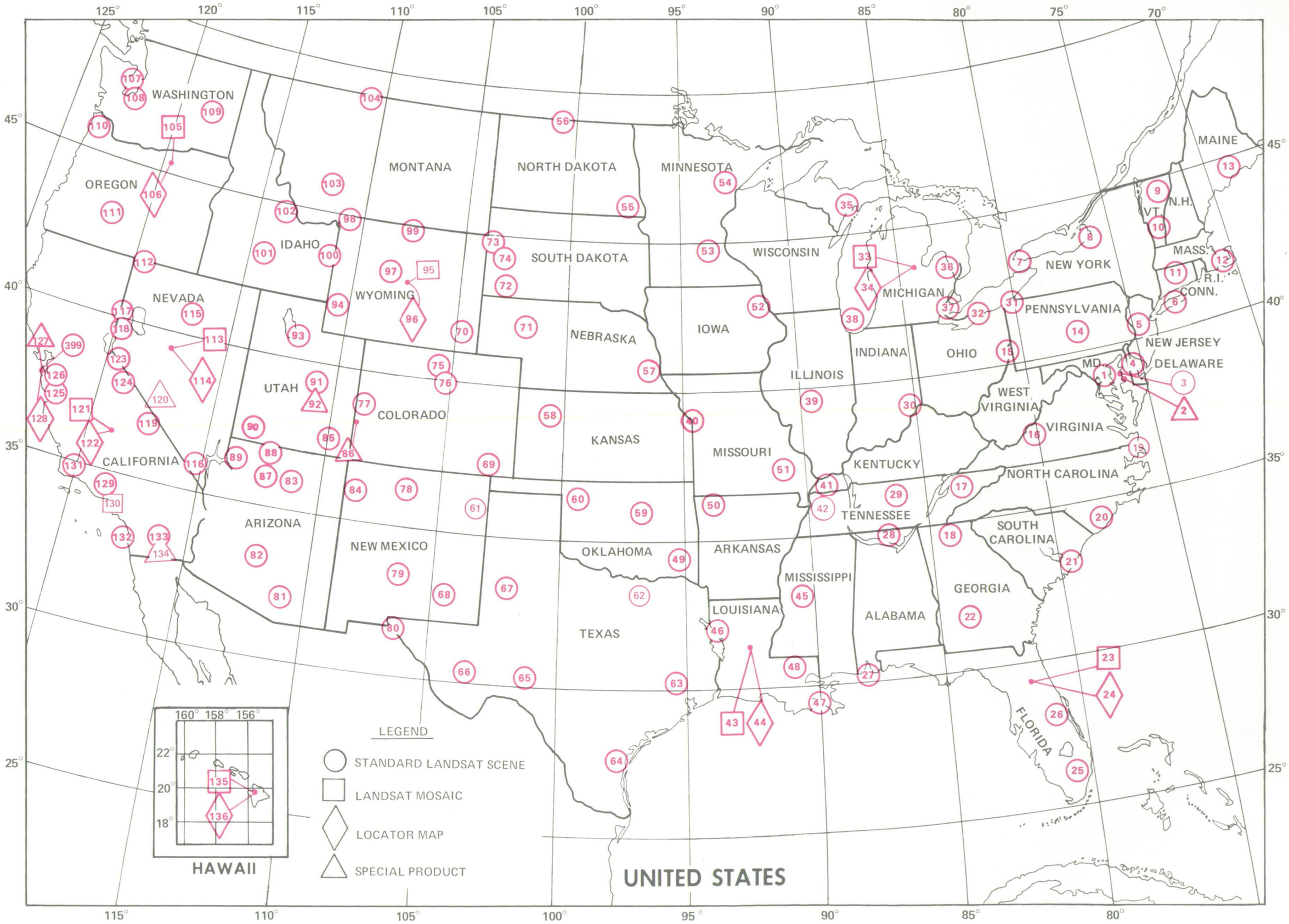
(3) *Third ERTS Symposium,* December 10–14, 1973, see NASA SP–351 (vol. I, Technical Presentations), NASA SP–356 (vol. II, Summary of Results), and NASA SP–357 (vol. III, Discipline Summary Reports)

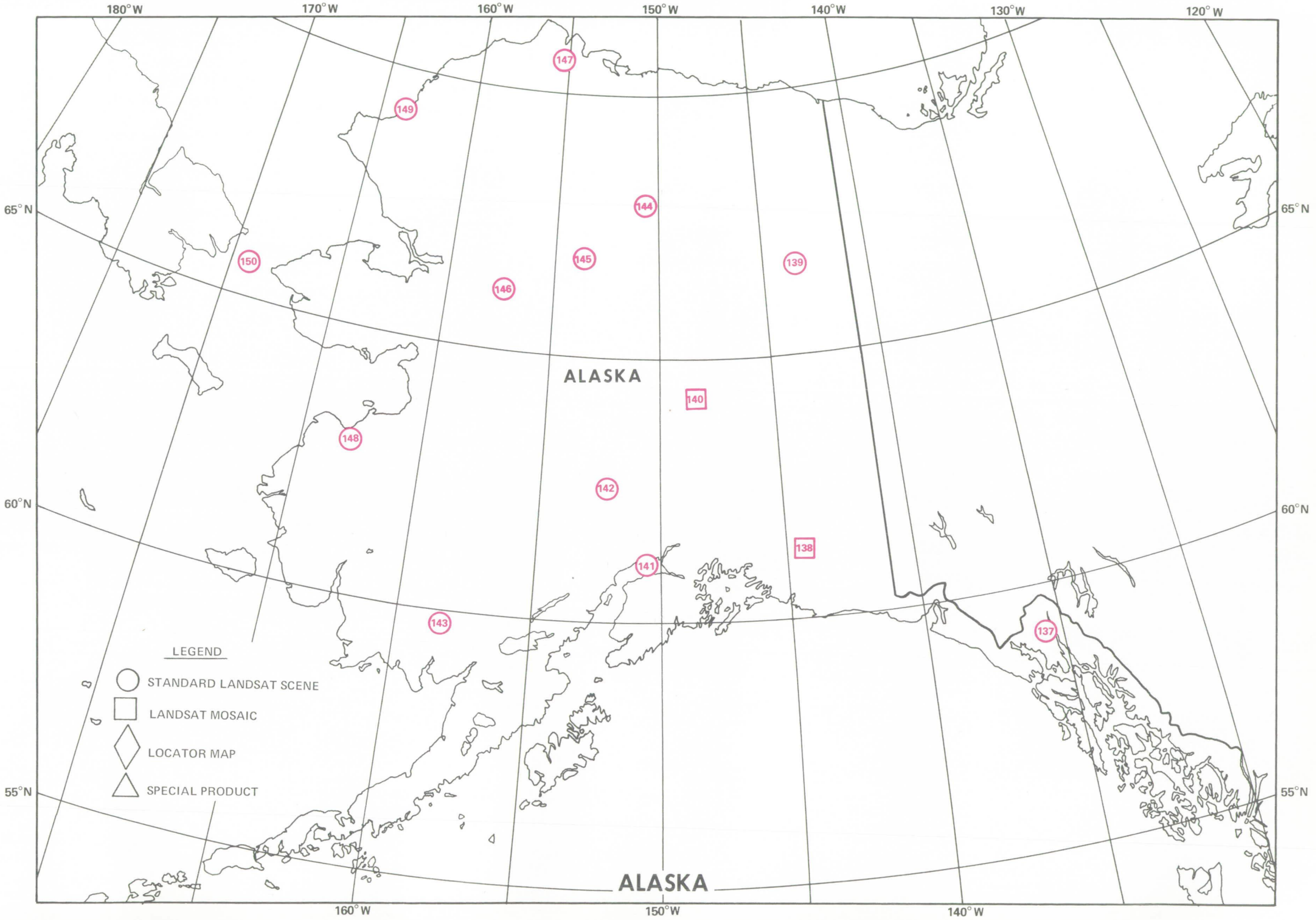
(4) *Proceedings of the NASA Earth Resources Survey Symposium,* Houston, Tex., June 1975, see NASA TM X–48168 (vol. I, Technical Session Presentations) (vol. II, Special Session Reports) (vol. III, Summary Reports)

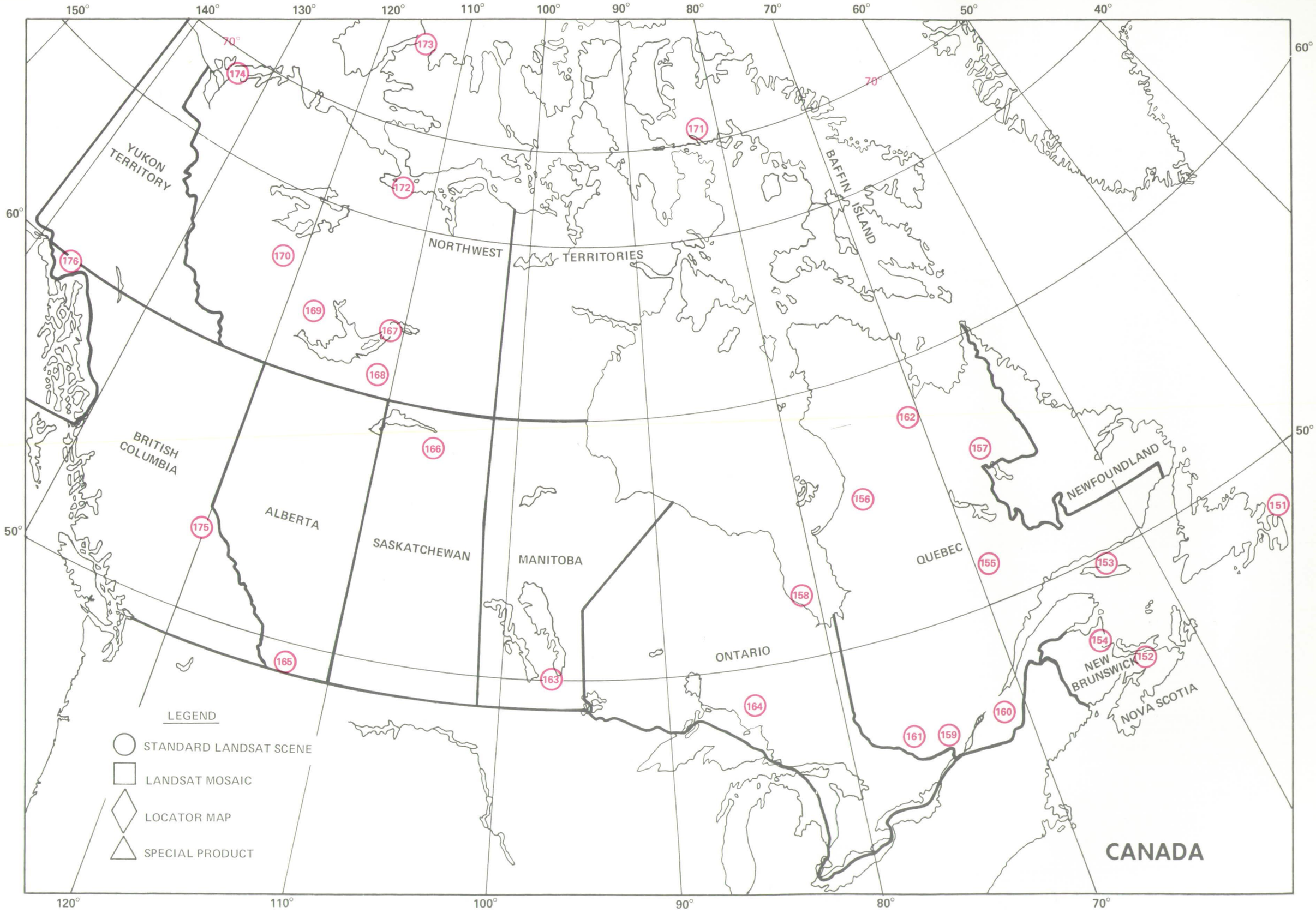
Based on the reports of these investigators (from 44 States, the District of Columbia, and 36 foreign countries), Landsat has been remarkably successful in achieving its mission of demonstrating the utility of multispectral remote sensing from space in practical Earth resource management applications.

Plates of Landsat Images

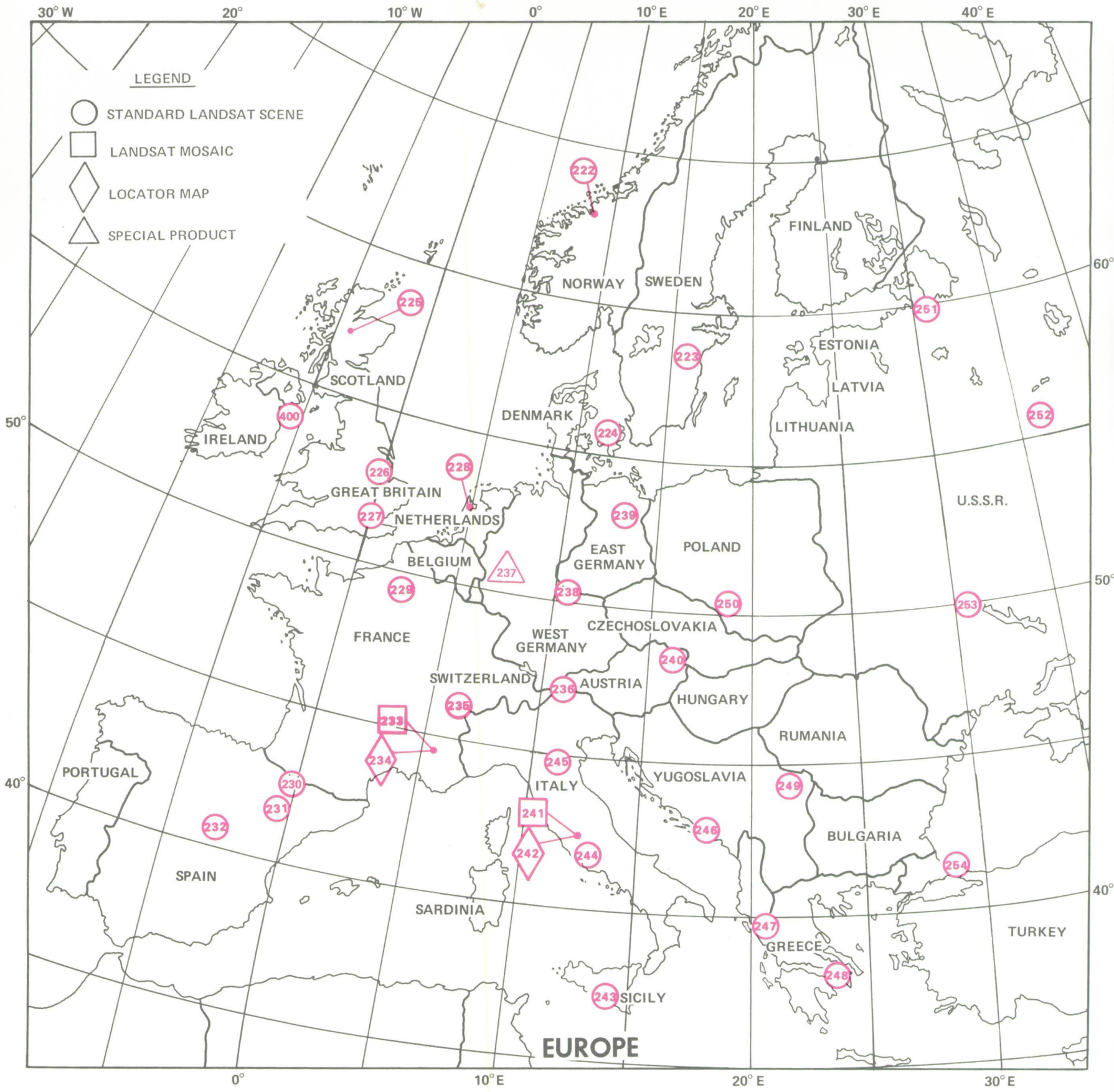
The images in this book are arranged in a predominantly geographic sequence by continent. They are preceded by eight index maps on which the Landsat frames are plotted by plate number according to the center coordinates of each image. Geographic boundaries on the index maps permit ready location of the scene within a familiar context. In most images, the direction of north is indicated by an arrow in the upper left-hand corner.

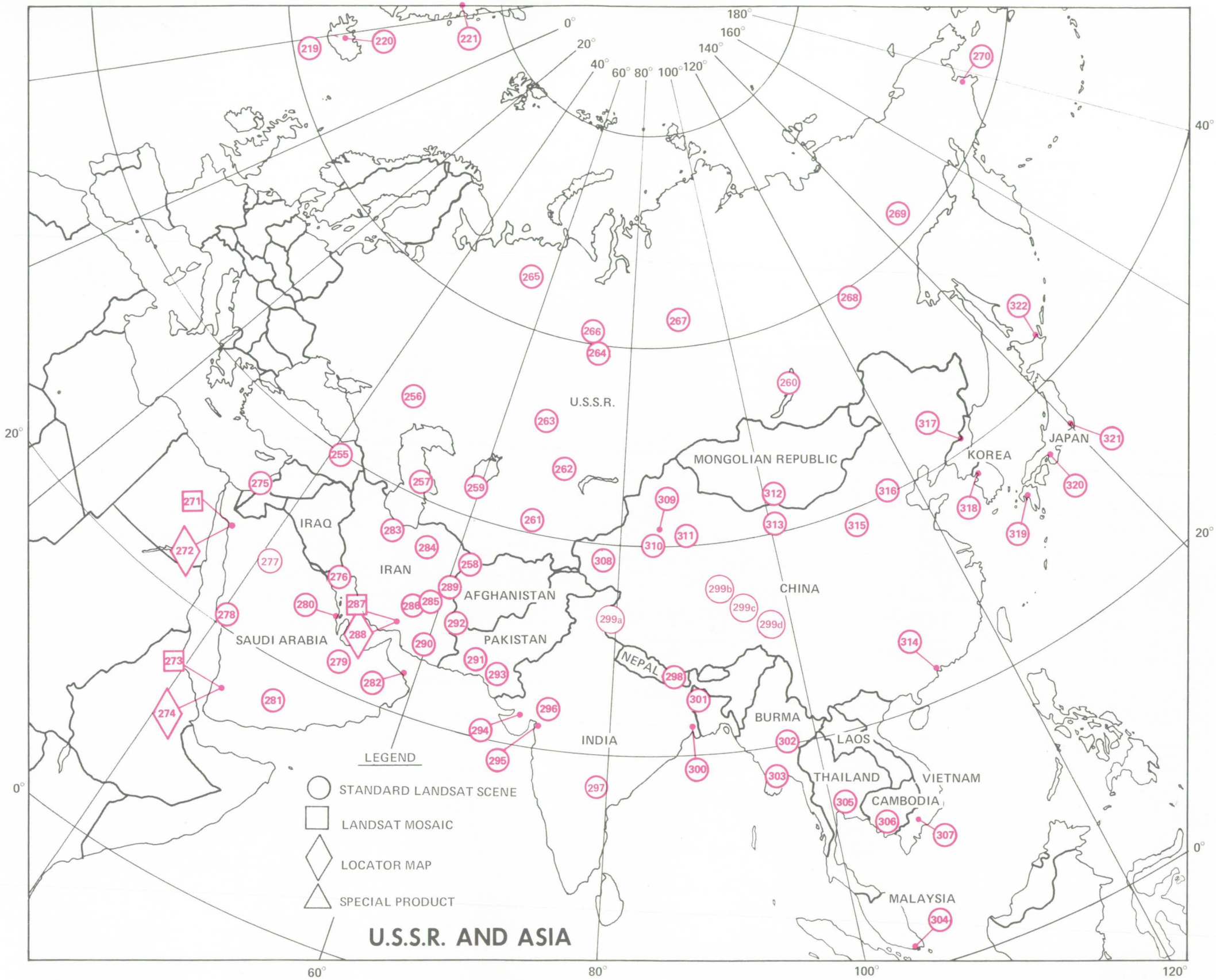

125°
120°
115°
110°
105°
100°
95°
90°
85°
80°
75°
70°
45°
40°
35°
30°
25°
WASHINGTON
OREGON
CALIFORNIA
NEVADA
IDAHO
MONTANA
WYOMING
UTAH
ARIZONA
COLORADO
NEW MEXICO
NORTH DAKOTA
SOUTH DAKOTA
NEBRASKA
KANSAS
OKLAHOMA
TEXAS
MINNESOTA
IOWA
MISSOURI
ARKANSAS
LOUISIANA
WISCONSIN
ILLINOIS
MICHIGAN
INDIANA
OHIO
KENTUCKY
TENNESSEE
MISSISSIPPI
ALABAMA
GEORGIA
FLORIDA
SOUTH CAROLINA
NORTH CAROLINA
VIRGINIA
WEST VIRGINIA
PENNSYLVANIA
NEW YORK
MAINE
VT.
N.H.
MASS.
R.I.
CONN.
NEW JERSEY
DELAWARE
MD.
HAWAII
160° 158° 156°
22°
20°
18°
LEGEND
STANDARD LANDSAT SCENE
LANDSAT MOSAIC
LOCATOR MAP
SPECIAL PRODUCT
UNITED STATES

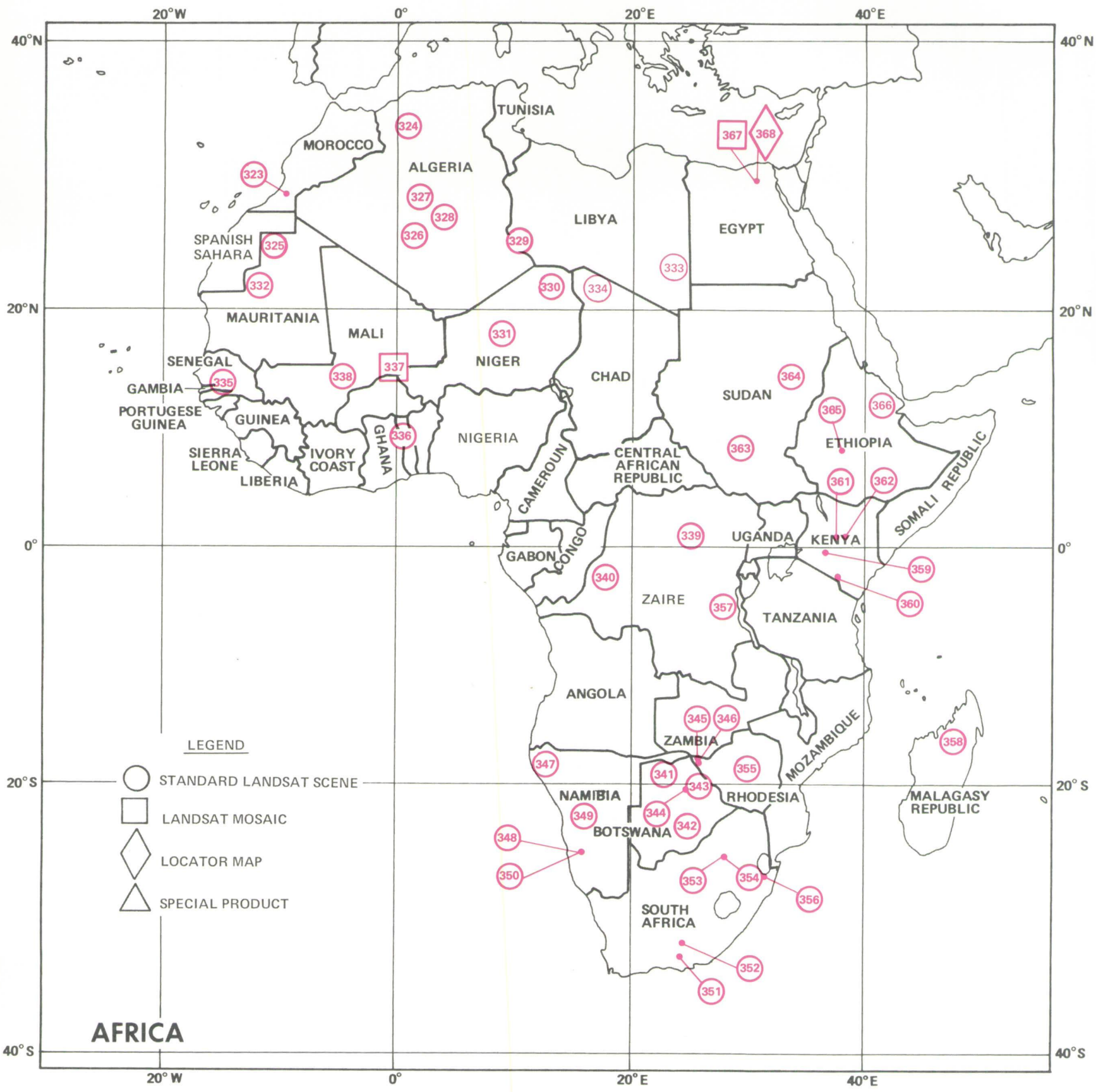

180° W
170° W
160° W
150° W
140° W
130° W
120° W
65° N
60° N
55° N
147
149
144
150
145
139
146
ALASKA
140
148
142
138
141
143
137
LEGEND
STANDARD LANDSAT SCENE
LANDSAT MOSAIC
LOCATOR MAP
SPECIAL PRODUCT
ALASKA


150°
140°
130°
120°
110°
100°
90°
80°
70°
60°
50°
40°
70°
60°
50°
YUKON TERRITORY
NORTHWEST TERRITORIES
BAFFIN ISLAND
BRITISH COLUMBIA
ALBERTA
SASKATCHEWAN
MANITOBA
ONTARIO
QUEBEC
NEWFOUNDLAND
NEW BRUNSWICK
NOVA SCOTIA
CANADA
LEGEND
STANDARD LANDSAT SCENE
LANDSAT MOSAIC
LOCATOR MAP
SPECIAL PRODUCT


120° W
100° W
80° W
60° W
40° W
20° N
0°
20° S
40° S
MEXICO
CUBA
DOMINICAN REPUBLIC
HAITI
PUERTO RICO
HONDURAS
GUATEMALA
NICARAGUA
COSTA RICA
PANAMA
VENEZUELA
GUYANA
FRENCH GUYANA
SURINAM
COLOMBIA
EQUADOR
PERU
BRAZIL
BOLIVIA
PARAGUAY
ARGENTINA
URUGUAY
CHILE
177
178
179
180
181
182
183
184
185
186
187
188
189
190
191
192
193
194
195
196
197
198
199
200
201
202
203
204
205
206
207
208
209
210
211
212
213
214
215
216
217
218
LEGEND
STANDARD LANDSAT SCENE
LANDSAT MOSAIC
LOCATOR MAP
SPECIAL PRODUCT
LATIN AMERICA


30° W
20°
10° W
0°
10° E
20° E
30° E
40° E
LEGEND
STANDARD LANDSAT SCENE
LANDSAT MOSAIC
LOCATOR MAP
SPECIAL PRODUCT
222
226
400
223
251
252
224
228
226
227
239
237
229
238
250
253
233
234
235
236
240
245
230
231
232
241
242
244
246
249
254
247
248
243
NORWAY
SWEDEN
FINLAND
ESTONIA
LATVIA
LITHUANIA
SCOTLAND
IRELAND
DENMARK
GREAT BRITAIN
NETHERLANDS
BELGIUM
EAST GERMANY
POLAND
U.S.S.R.
FRANCE
WEST GERMANY
CZECHOSLOVAKIA
SWITZERLAND
AUSTRIA
HUNGARY
RUMANIA
PORTUGAL
ITALY
YUGOSLAVIA
BULGARIA
SPAIN
SARDINIA
GREECE
TURKEY
SICILY
EUROPE
60°
50°
40°
0°
10° E
20° E
30° E


0°
20°
40°
60°
80°
100°
120°
140°
160°
180°
U.S.S.R.
MONGOLIAN REPUBLIC
KOREA
JAPAN
CHINA
IRAQ
IRAN
AFGHANISTAN
PAKISTAN
SAUDI ARABIA
NEPAL
INDIA
BURMA
LAOS
THAILAND
VIETNAM
CAMBODIA
MALAYSIA
LEGEND
STANDARD LANDSAT SCENE
LANDSAT MOSAIC
LOCATOR MAP
SPECIAL PRODUCT
U.S.S.R. AND ASIA


20°W
0°
20°E
40°E
40°N
20°N
0°
20°S
40°S
TUNISIA
MOROCCO
ALGERIA
LIBYA
EGYPT
SPANISH SAHARA
MAURITANIA
MALI
NIGER
CHAD
SUDAN
SENEGAL
GAMBIA
PORTUGESE GUINEA
GUINEA
SIERRA LEONE
LIBERIA
IVORY COAST
GHANA
NIGERIA
CAMEROUN
CENTRAL AFRICAN REPUBLIC
ETHIOPIA
SOMALI REPUBLIC
GABON
CONGO
ZAIRE
UGANDA
KENYA
TANZANIA
ANGOLA
ZAMBIA
MOZAMBIQUE
NAMIBIA
BOTSWANA
RHODESIA
SOUTH AFRICA
MALAGASY REPUBLIC
323
324
325
326
327
328
329
330
331
332
333
334
335
336
337
338
339
340
341
342
343
344
345
346
347
348
349
350
351
352
353
354
355
356
357
358
359
360
361
362
363
364
365
366
367
368
LEGEND
STANDARD LANDSAT SCENE
LANDSAT MOSAIC
LOCATOR MAP
SPECIAL PRODUCT
AFRICA

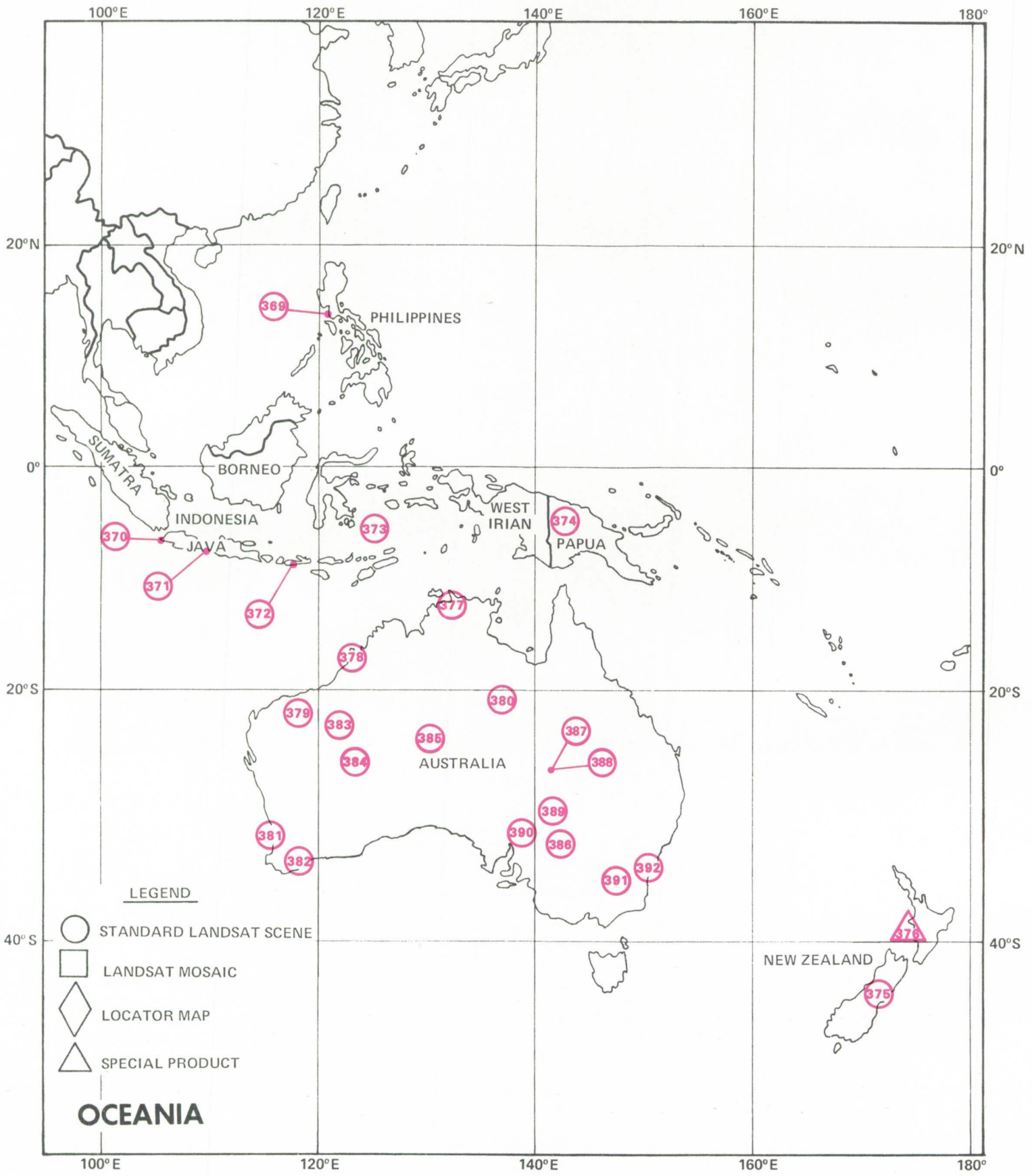
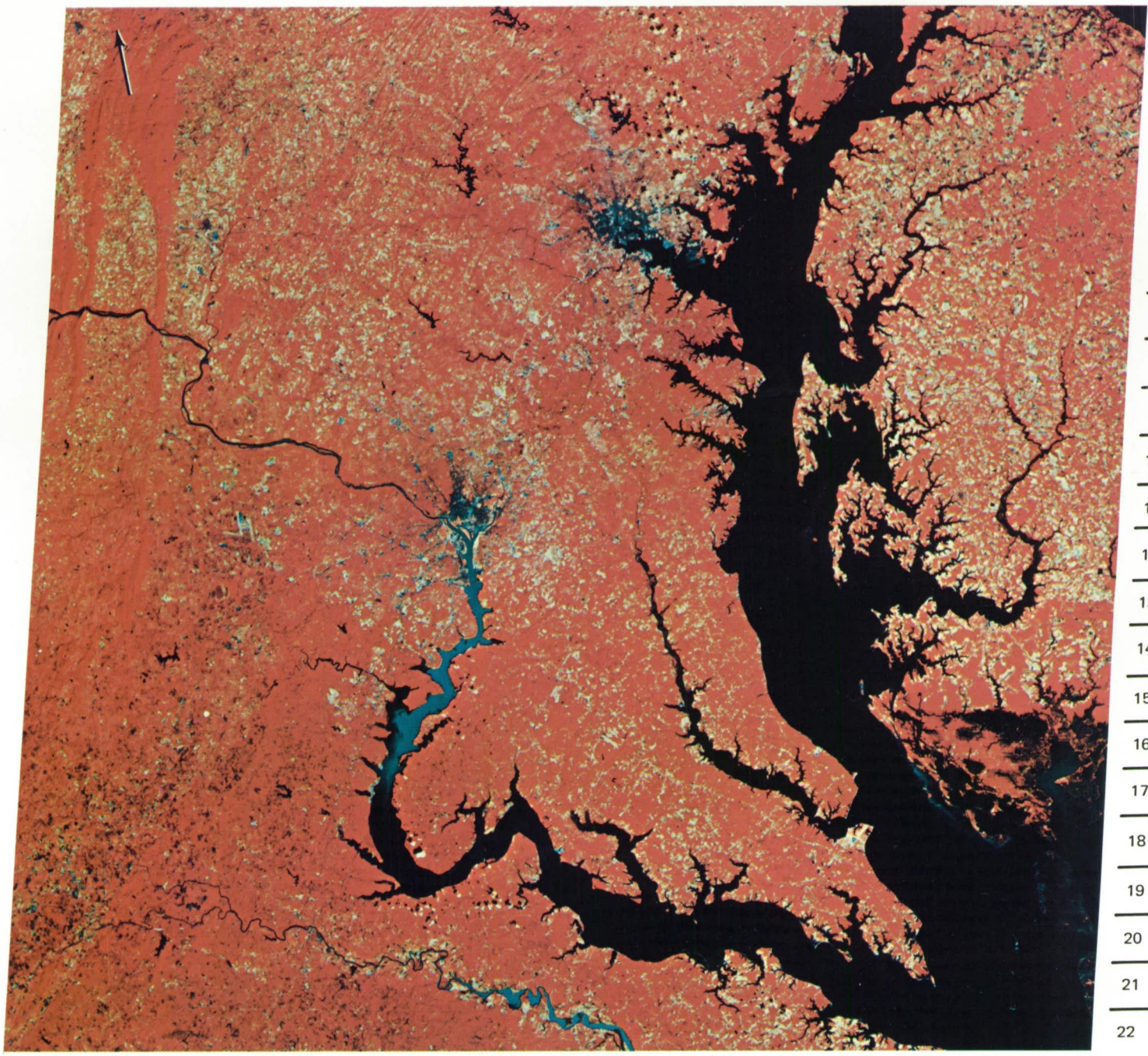

100°E
120°E
140°E
160°E
180°
20°N
0°
20°S
40°S
PHILIPPINES
SUMATRA
BORNEO
INDONESIA
JAVA
WEST IRIAN
PAPUA
AUSTRALIA
NEW ZEALAND
369
370
371
372
373
374
375
376
377
378
379
380
381
382
383
384
385
386
387
388
389
390
391
392
LEGEND
STANDARD LANDSAT SCENE
LANDSAT MOSAIC
LOCATOR MAP
SPECIAL PRODUCT
OCEANIA

PLATE 1



THE WASHINGTON-BALTIMORE AREA: The Nation's Capital (*I*–11) lies astride the Potomac River (*G*–10) at the head of the Potomac estuary (*H*–17) that leads to the Chesapeake Bay. This popular view of Washington, D.C. (taken by Landsat through exceptionally clear air); shows amazing details. The Mall, the Capitol Building area, and the White House grounds are easily picked out (*I*–11). Dulles Airport (*E*–11) and Andrews Air Force Base (*K*–12) stand out; NASA's Goddard Space Flight Center, where the Landsat program is managed, is found at *K*–9 (individual parking lots there are distinguishable in the computer display).

Baltimore, Md. (*L*–15), on the Baltimore Harbor (*N*–6) is connected to Washington by the Baltimore-Washington Parkway (*K*–7) and Interstate 95 (*J*–8). The suburbs of both cities tend to cluster around the Washington (*K*–11) and Baltimore (*K*–5) Beltways. Other cities in the scene are Annapolis (*N*–9), Bowie (*L*–9), and Frederick (*D*–5), Md., and Fredericksburg, Va. (*G*–20).

The light blue tones (*I*–15) in the Potomac represent a surge of sediments washed into the river following a rain the day before this Landsat pass. Similar sediments are seen in the Rappahannock River (*L*–21). Other drowned rivers (estuaries) along the Chesapeake Bay include the Patuxent (*O*–16), the Choptank (*T*–13), the Chester (*R*–6), the Sassafras (*R*–3), and the Elk (*R*–1) Rivers on the Maryland Eastern Shore section of the Delmarva Peninsula (*S*–9). Most of the countryside in the eastern two-thirds of this image is either heavily forested (oak, hickory, and pine) or is given to farming of crops such as wheat, barley, soybeans, watermelon, tomatoes, peas, and tobacco or to raising of dairy cattle and poultry *1080–15192;* October 11, 1972.

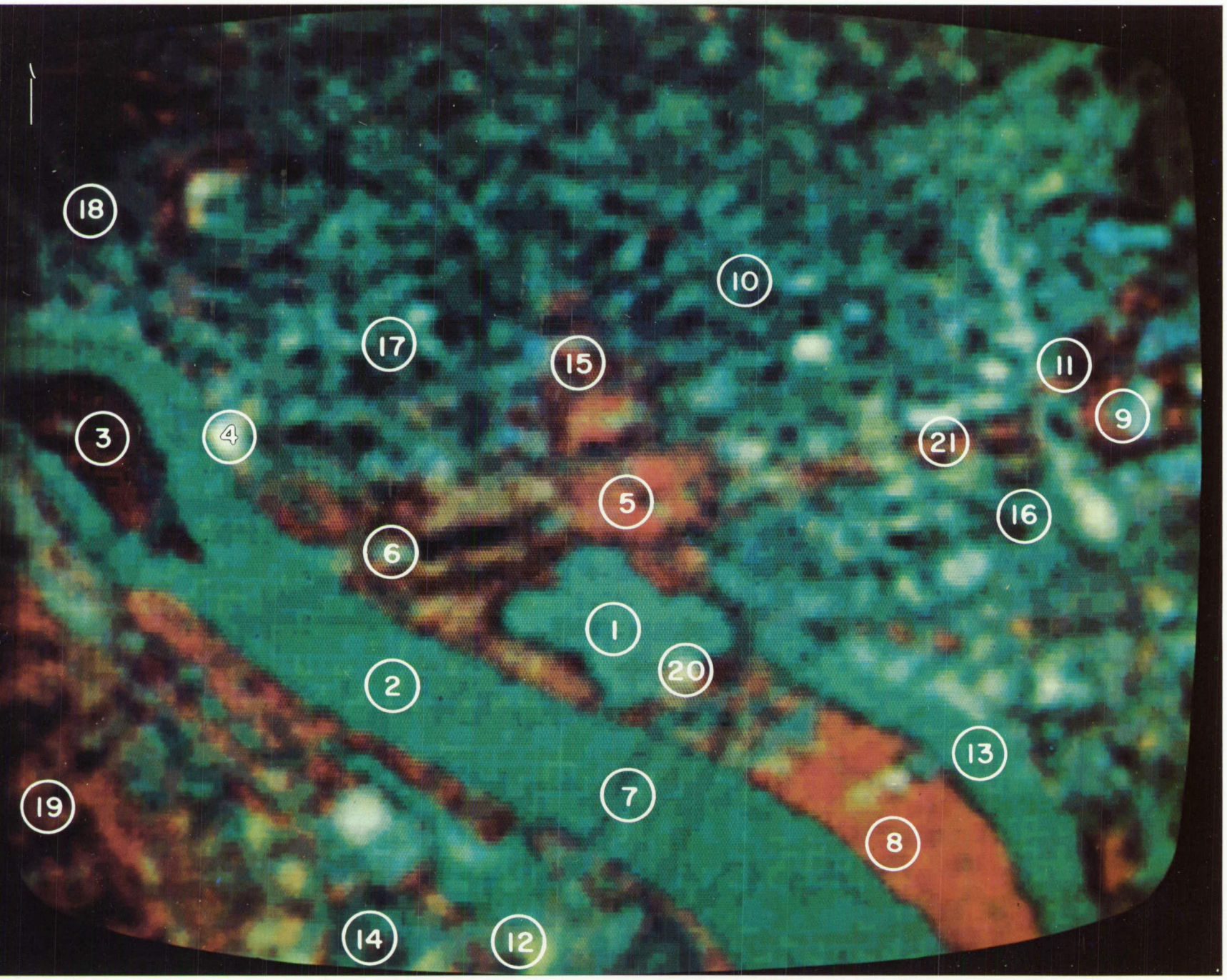
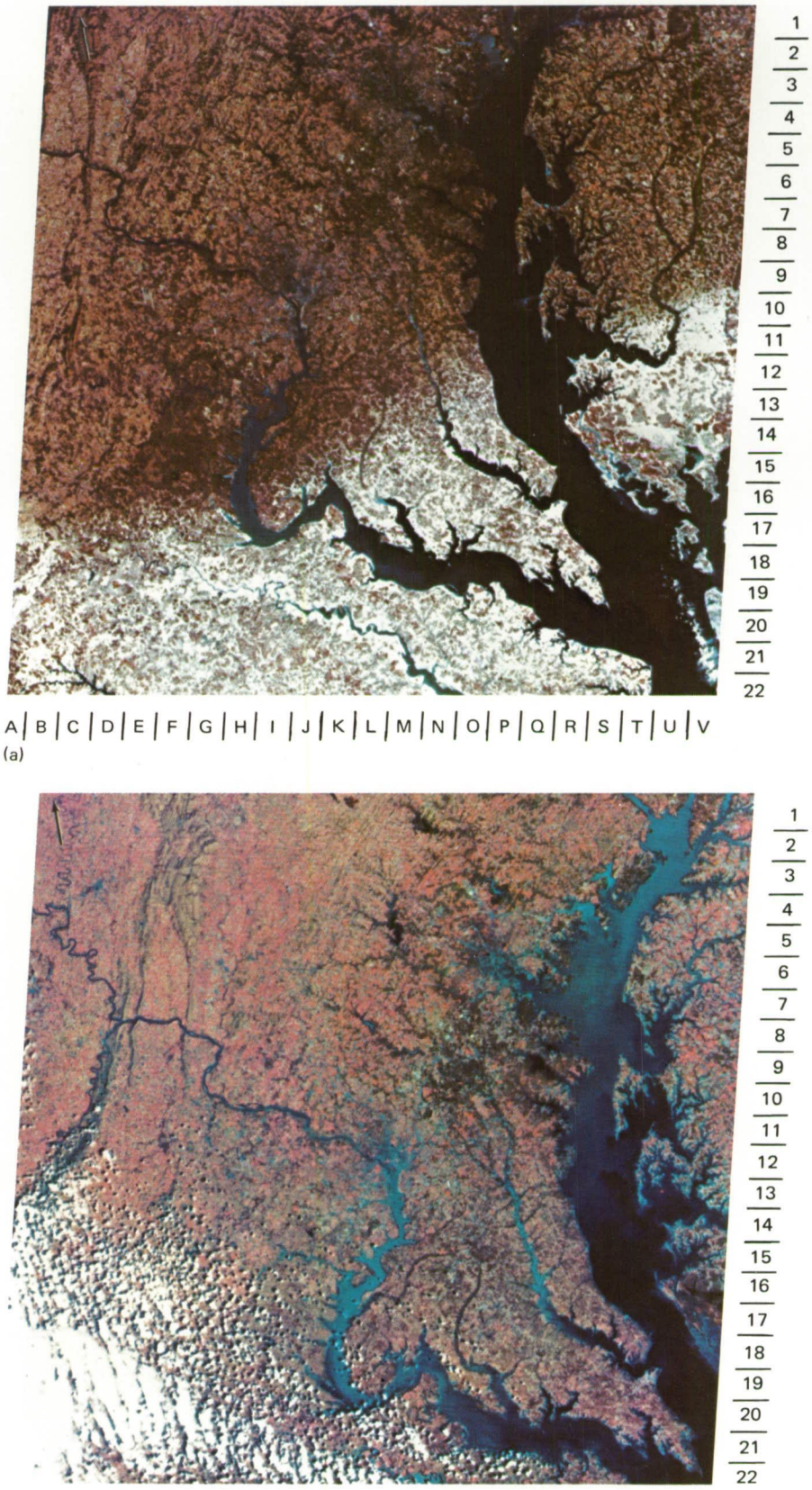


PLATE 2

DOWNTOWN WASHINGTON, D.C.: This illustration shows a computer-generated image of the downtown area of Washington, D.C., made from the digital tape produced for the October 11, 1972, multispectral scanner (MSS) pass over the Capital region (see color composite on the opposite page). This is a photograph taken off the TV screen of the image dissection and manipulation system (IDAMS), a computer-graphics interactive display developed at Goddard Space Flight Center. The individual phosphor elements of the TV screen are visible under a magnifying glass as minisquares. Three minisquares in a row correspond approximately to an individual pixel or resolution cell in an MSS scan line. Reflectance values for each band are modified by interpolation within a 3-by-3 array of pixels. The image for each band is projected through a color gun in the TV display—superposition of equivalent pixel arrays gives the resulting color composite. The scale of this image is 1:30 000 in the rendition on this page.

Landmark sites located in this image are as follows: (1) Tidal Basin, (2) Potomac River, (3) Roosevelt Island, (4) Kennedy Center, (5) Washington Monument (its shadow is barely discernible in a further enlargement), (6) Lincoln Memorial, (7) 14th Street Bridge, (8) Potomac Park, (9) Capitol Building, (10) downtown shopping area, (11) the new FBI building construction, (12) Interstate 95 construction, (13) Washington Channel, (14) Pentagon, (15) White House, (16) NASA Headquarters, (17) business district, (18) Georgetown, (19) National Cemetery, (20) Jefferson Memorial, and (21) National Gallery of Art.

PLATE 3

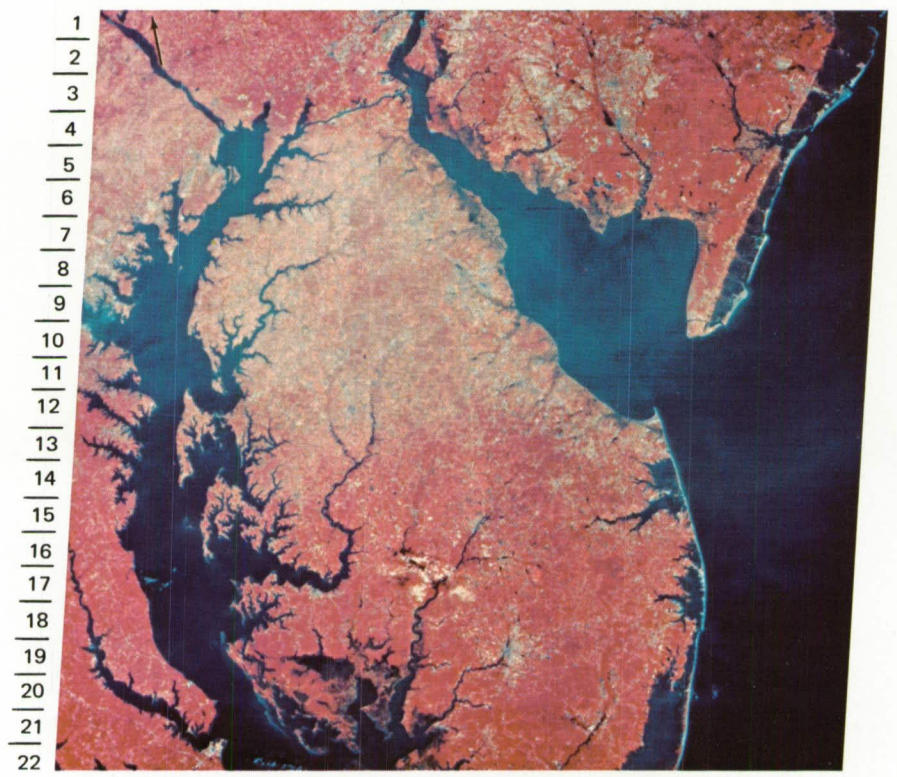


SEASONAL EFFECTS AROUND WASHINGTON, D.C.: This pair of Landsat images shows the Washington area and neighboring Virginia (*G*–14) and Maryland (*L*–8) at the height of winter (*a*) and in early spring (*b*). In the winter scene, grass is dormant and deciduous trees are bare; the darker browns mark the forests, some of which contain a high proportion of coniferous trees. A blanket of snow lines the southern area beginning about 50 kilometers (30 miles) south of Washington. This storm had been forecast to hit Washington and Baltimore but was deflected southward by changing winds. In the spring scene, many of the agricultural fields and some of the natural meadows or grassy hillslopes have responded to early rains by greening.

In both views, the geology of the region is better outlined because of lack of foliage and lower Sun angles. The rocks east of the fall line (*K*–2; *N*–7; *Q*–4), where streams may require an adjustment in gradient, often marked by waterfalls or rapids, after crossing from crystalline rocks into "soft" sediments, are Cretaceous and Tertiary sedimentary units that dip slightly toward the southeast. The rocks of the Piedmont (*I*–6) west of the fall line are mostly Precambrian crystalline complexes such as gneisses and schists. Several "mantled gneiss domes" (*M*–3) can be discerned around Baltimore. The northeast structural grain (*K*–1) of these metamorphic rocks is evident in both views. A block of the Triassic Lowlands (*F*–7; *G*–13) lies further west. Quartzites, metabasalt sills, and granitic intrusives make up the Catoctin Mountain Ridge (*E*–5) and adjacent valleys (*E*–7) west of Frederick. South Mountain (*D*–5) east of the Shenandoah River (*C*–9) and Hagerstown (*C*–4) at the north end of the Shenandoah Valley consist of lower Paleozoic sedimentary units. These ridges are about on line with the Blue Ridge—a crystalline block that represents the first extended high mountains along the east side of the Appalachian belt. (*a*) *1170–15193*; January 9, 1973; (*b*) *1260–15201*; April 9. 1973.



(a)



(b)

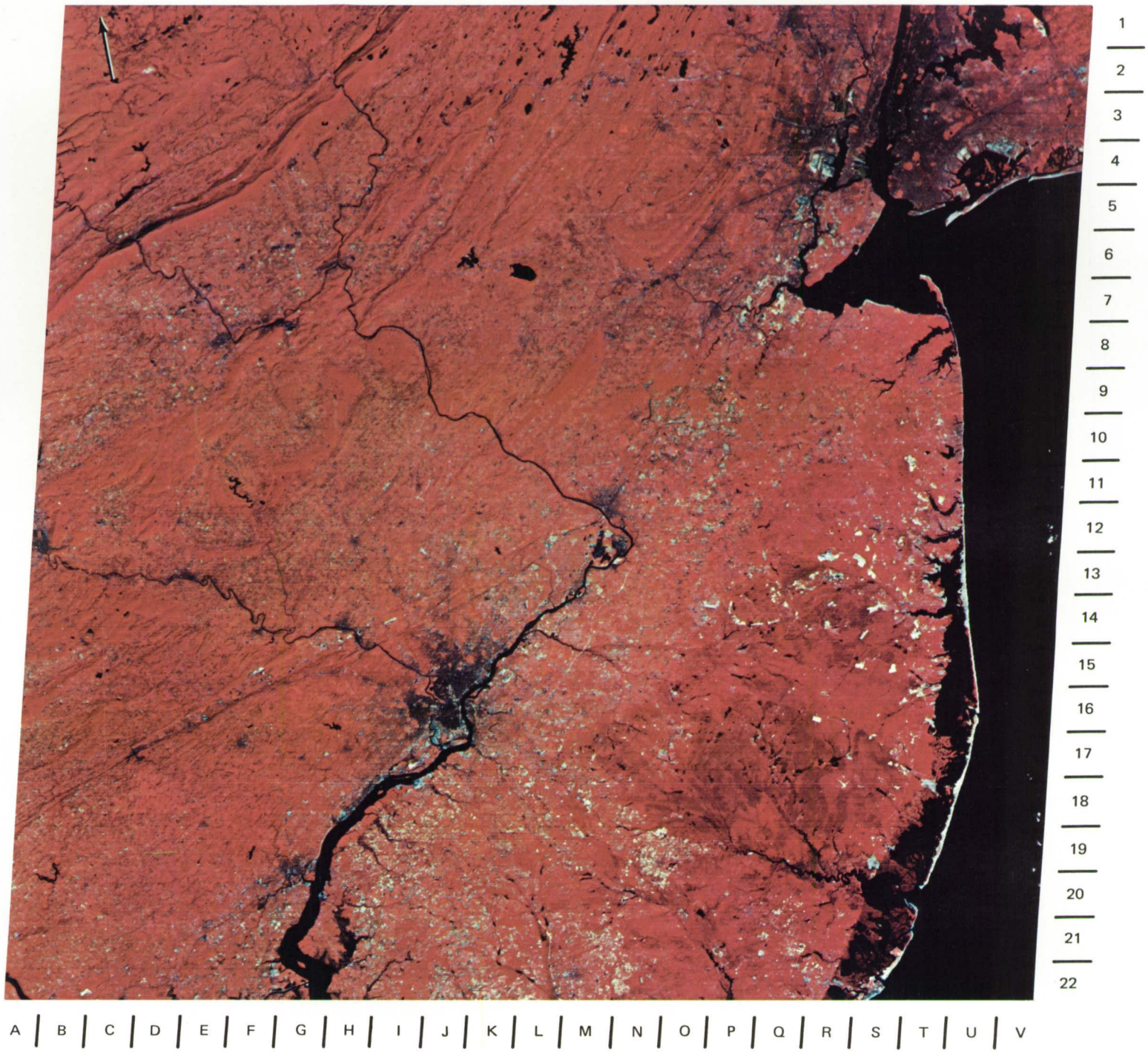
PLATE 4

DELMARVA PENINSULA: This great extension of land, shared by Delaware (*I*–10) and Maryland (*M*–18) here in this scene and by Virginia to the south, is bounded by the Chesapeake Bay on the west, the Atlantic Ocean on the east, and Delaware Bay (*O*–10) on the northeast. The Susquehanna River empties into the Chesapeake and the Delaware River into the bay of its name. Other important rivers not already identified in plate 1 are the Nanticoke (*J*–8), the Wicomico (*L*–19), and Pocomoke (*O*–20) Rivers in Maryland and the Maurice (*N*–4), Great Egg Harbor (*Q*–3), and Mullica (*S*–1) Rivers in southern New Jersey (*O*–3). The manmade Chesapeake and Delaware Canal (*G*–4) is also easily picked out. The Blackwater (*H*–20) and Bombay Hook (*K*–7) National Wildlife Refuges have been set up in coastal marshlands.

Salisbury, Md. (*L*–19), and Dover, Del. (*J*–8), are small cities within the peninsula (which contains the entire State of Delaware shown here up to Wilmington (*I*–1). Several famous Atlantic Ocean resorts—Ocean City, Md. (*R*–18), Rehoboth Beach, Del. (*P*–13), and Atlantic City, N.J. (*T*–4)—lie on the offshore bar beaches that extend from south of Assateague Island (*Q*–20) on the south, past Indian River inlet (*Q*–18), to Cape Henlopen (*P*–12) at the mouth of Delaware Bay and from Cape May (*Q*–9) northward to Great Bay (*T*–2). Behind these bar islands are great lagoons, which are a composite of open shallow water, tidal flats, and salt marshes.

In the winter scene (*a*), ice has formed in many of these lagoons and in some of the bays and marshlands, especially along the New Jersey coast. In the summer scene (*b*), an unusual phenomenon was detected. A large "gray" zone, which converts the false color reds to pinks, is developed over the northern end of the Delmarva Peninsula. Inspection of weather records revealed this to be the effect of a thick smog belt that presumably spread eastward from Washington and Baltimore to the west. Both cities experienced a pollution alert on the day this image was taken. (*a*) *1205–15141;* February 13, 1973; (*b*) *1403–15125*; August 30, 1973.

PLATE 5



NEW YORK CITY AND PHILADELPHIA: Metropolitan complexes (metroplexes) and a diversity of geologic and topographic conditions characterize this image. The metroplexes of New York City (*S*–3); Trenton (*M*–12), Philadelphia (*J*–15), Wilmington (*G*–19), Reading (*A*–12), and Allentown-Bethlehem (*E*–7) constitute the major urban concentrations shown.

The detail that can be observed in urban areas is exemplified in the New York City metroplex. Park areas with their distinctive vegetative signatures are usually identifiable; for examples, Prospect Park and the Botanic Gardens in Brooklyn (*S*–4), Forest Park and Flushing Meadow (*T*–3), and Central Park and its lake in Manhattan (*S*–2). Water features are readily recognizable; for examples, the Hudson River (*R*–3), East River and a part of Long Island Sound (*T*–2), Newark Bay (*Q*–4), Raritan Bay (*Q*–7), and Jamaica Bay with its numerous islands (*T*–4). The piers and terminal facilities in the Upper Bay at Bayonne, N.J., are visible (*R*–4).

The Coastal Plain (*Q*–14), Piedmont (*N*–7), New England (*I*–6), Valley and Ridge (*B*–5), and Appalachian Plateau (*C*–1) geologic provinces are all presented in this image. The Coastal Plain is typified by offshore bar or barrier beach development with associated inner lagoonal area and coastal wetlands (*T*–18) and a classic example of spit growth at Sandy Hook (*S*–6). Large areas of the coastal plain in southeastern New Jersey known as the Pine Barrens (*Q*–16) are developed on infertile sandy soils that support only a scrubby growth of oak and pine trees.

Trenton and Wilmington are considered fall line cities and as such are located at the juncture of the Piedmont and the Coastal Plain. The Piedmont in this area is characterized by the Triassic Lowlands (*N*–7) of younger sedimentary rocks down-faulted between older crystalline masses, one of which, the Reading Prong, is easily recognizable (*H*–7). The Watchung Ridges (*N*–6) are made up of a series of extrusive basalt flows, the eroded scarps of which stand as much as 130 meters (400 feet) above the surrounding area.

The Valley and Ridge folded linear ridges (*D*–4) and the Great Valley (*E*–6) are traversed by the Lehigh (*C*–6) and Delaware Rivers (*G*–3). The Appalachian Plateau province represented by the Pocono Mountains (*D*–1) is an area of maturely dissected essentially horizontal sedimentary strata that has been subsequently glaciated. *1079–15131*; October 10, 1972.

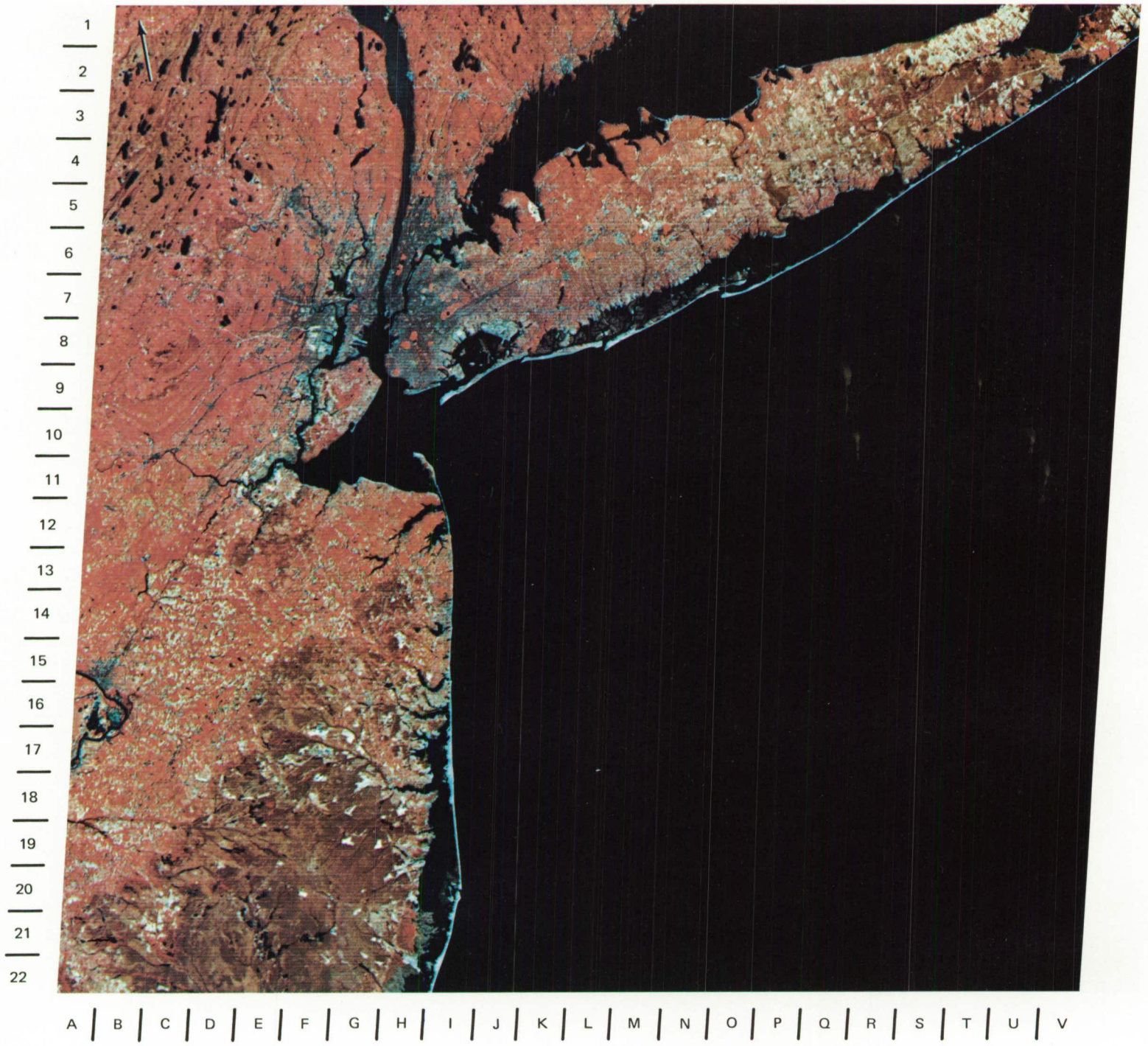
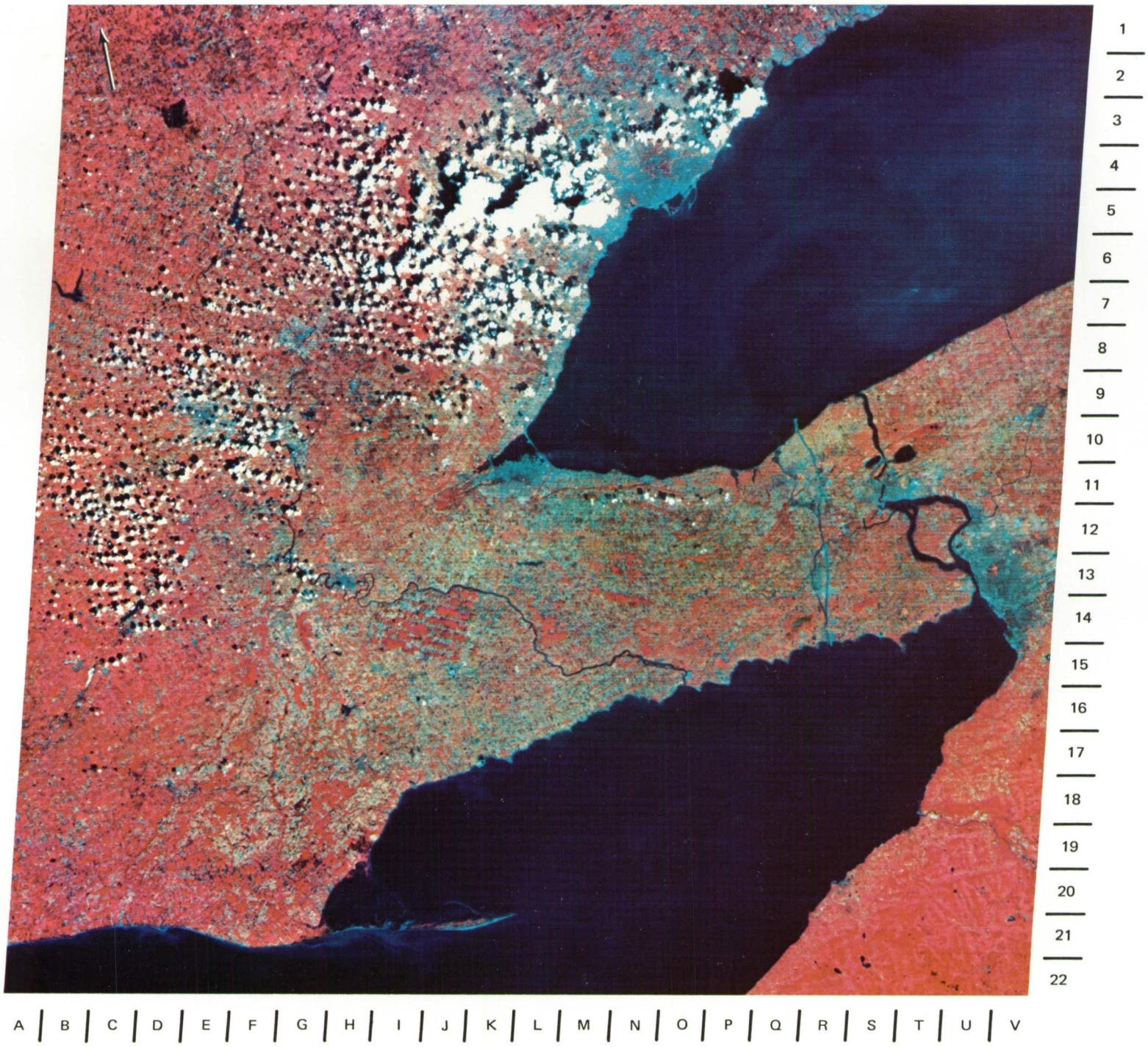


PLATE 6

NEW YORK CITY AND LONG ISLAND: This early spring scene covers much of the same area shown on the opposite page. Well-known localities on Long Island include Oyster Bay (*L*–3), Great South Bay (*P*–6), Jones Beach (*L*–8), Fire Island (*N*–7), and Great Peconic Bay (*U*–1).

Long Island is a slightly upraised section of metamorphosed Paleozoic rocks, with some overlying Cretaceous sediments, now largely covered by glacial materials from an early Wisconsin ice advance near the close of the Pleistocene. A pair of somewhat eroded end moraines line the north shore and interior east to the south shore of Long Island. Ocean currents have reworked sands derived from the outwash plains along the south coast into several offshore bars. Long Island Sound is an eroded lowland that lies along the extension of the fall line. (See plate 3.) Paleozoic schists and gneisses from the New England metamorphic province extend south from White Plains to the north shore of the Sound and into Manhattan. The Hudson Highlands (*B*–2), the northern end of Reading Prong, is a long block of Precambrian gneisses eroded into a landscape of rolling, tree-covered hills and intervening lakes that serve as a principal recreation area for metropolitan New York. The northern end of the Triassic Lowlands, a fault-bounded and down-dropped block of reddish continental sediments and basaltic extrusives, extends from across the Hudson River (*G*–2) at Ossining, N.Y. (*G*–1), southward along a line from western Staten Island (*F*–9) to Trenton, N.J. (*B*–15), and beyond into the central Appalachians. A large basaltic sill, inclined to the west, forms the Palisades (*G*–6) of New Jersey where exposed along the Hudson. Westward, resistant basaltic flows stand up as ridges and scarps 70 to 130 meters (200 to 400 feet) above their surroundings in the Watchung Mountains (*C*–9). The coastal plains of New Jersey consist of Cretaceous sediments inland, Miocene sediments through much of the Pine Barrens (*G*–19), and Pleistocene sediments along the coast around Barnegat Bay (*I*–19). *1654–15013;* May 8, 1974.

PLATE 7



BUFFALO, N.Y., AND TORONTO, CANADA: The Niagara River (*R*–9) descending some 60 meters (190 feet) over a cap of Lockport dolomite at the crest of the Niagara escarpment joins two of the Great Lakes: Erie (*L*–19) and Ontario (*Q*–6). Niagara Falls (*S*–11) was created as the river descended the escarpment following glacial times. The cuesta (escarpment created by dipping sedimentary rocks) trends east to west along the southern shore of Lake Ontario (*M*–11; *S*–10). The falls have now retreated 11 kilometers (7 miles) upstream from the cuesta front near Lewiston, N.Y. The present rate of retreat is estimated to be about 1½ meters (4 or 5 feet) per year. Grand Island (*T*–12) bifurcates the Niagara River a few kilometers (miles) above the falls. Close inspection reveals the much smaller Goat Island (*S*–11), which separates the American and Canadian Falls. The Welland Canal (*Q*–11) was constructed to bypass the falls and the rapids in the gorge below the falls and allow oceangoing vessels to traverse the St. Lawrence Seaway inland beyond Lake Ontario.

The city of Buffalo is located on the northeastern tip of Lake Erie (*U*–13). Delaware Park and the Buffalo Zoo can be located within the metropolitan area due to the characteristic (red) signature resulting from the greater amount of vegetation present in these locations (*U*–13). Canada's "Golden Horseshoe" industrial-agricultural area loops around the southwestern end of Lake Ontario from Toronto (*M*–4) in the north, through Hamilton (*K*–10), to the international border along the Niagara River. Both Toronto and Hamilton have protected natural harbors (visible in the image) as a result of sand bar deposition by the currents of Lake Ontario.

The checkered agricultural pattern (*D*–16 and *H*–11) of rural Ontario results from the essentially geometric layout of the secondary road network and the fact that trees are left along the margins of agricultural fields as windbreaks. Cumulus clouds cover much of the area west of Hamilton and Toronto. *1407–15343*; September 3, 1973.

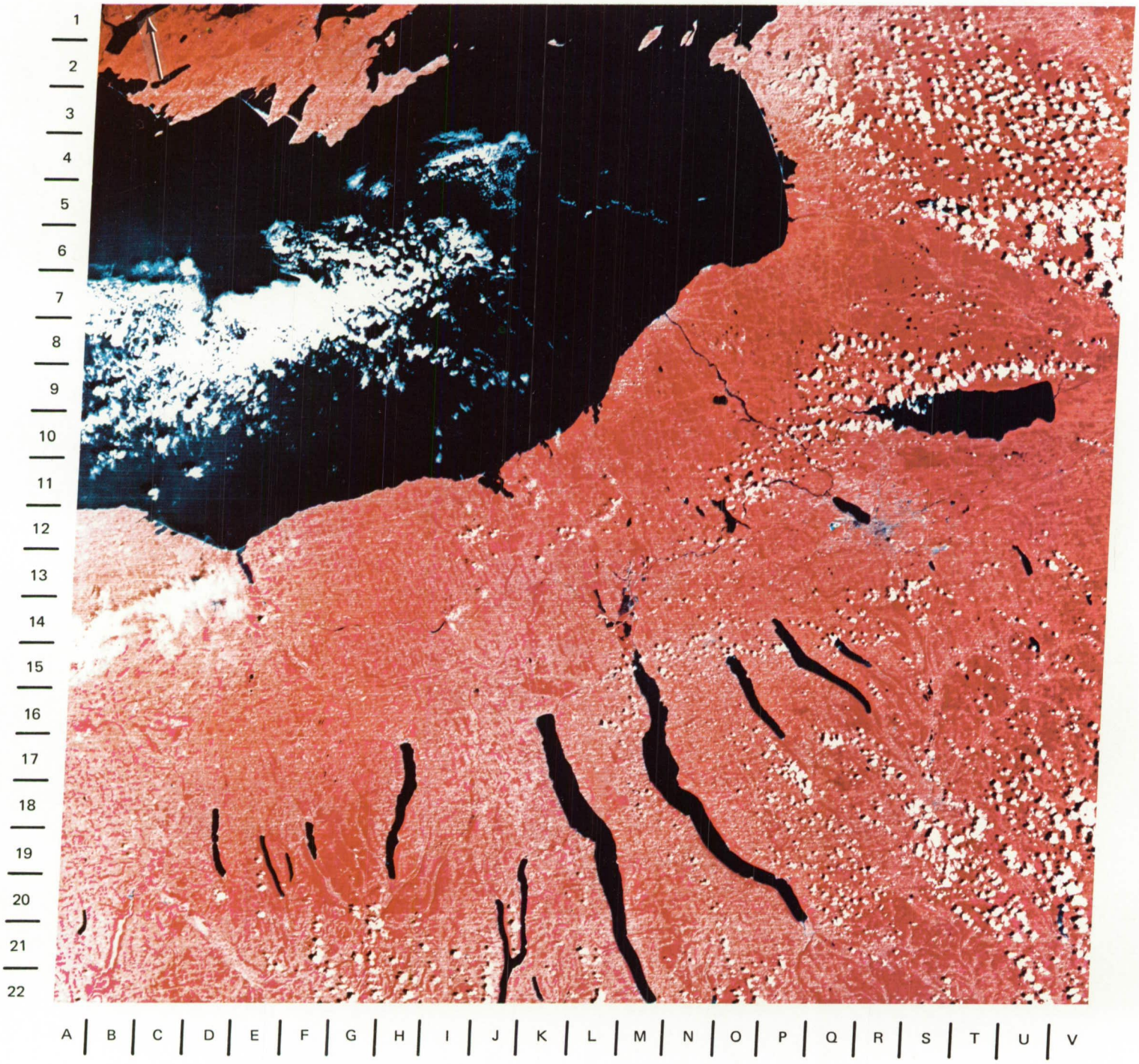


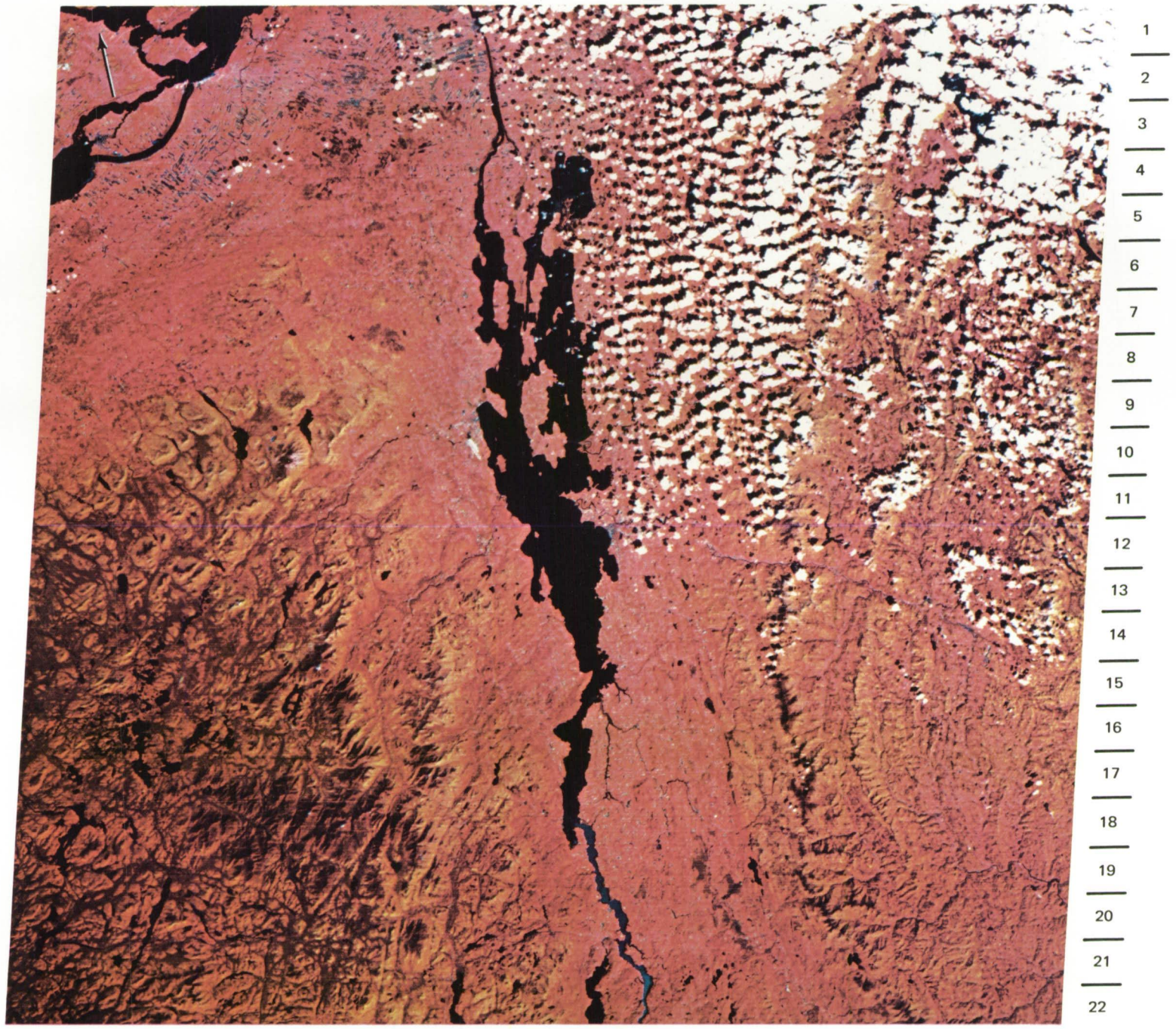
PLATE 8

THE FINGER LAKES, N.Y.: Most of this image covers a physiographic section known as the glaciated Allegheny Plateau. This part of west-central upper New York State is bounded on the north by Lake Erie. A segment of Ontario around Prince Edward Point (*G*–2) is seen across the lake. Principal cities shown here are Syracuse (*R*–12), Oswego (*M*–17) on the Oswego River, and Rochester (*D*–13; largely cloud covered).

The major physical features present in this scene owe much to the geological character of the surface units. The bedrock geology is relatively simple: from Lake Erie southward, progressively younger Silurian and Devonian sedimentary rocks (mainly shales and limestones) dip gently southward. The Allegheny Plateau escarpment, a subdued north-facing ridge, trends east to west from just south of Rochester to south of Syracuse where it grades into the Helderberg escarpment. This entire region was overrun by at least three glacial advances—Illinoian, Kansan, and Wisconsin—during the Pleistocene ice age. Many preexisting stream valleys were further widened and enlarged by erosion from the ice and from melt waters. This produced a series of interconnected "through valleys" south of the limit of the main glacial drift that carve the terrain into rolling hills with relief of 60 to 150 meters (200 to 500 feet). Later, additional thick ice masses occupied some of these valleys and deepened them. The resulting Finger Lakes are troughs cut primarily out of Devonian shales. The principal lakes are an eastern group consisting of the Seneca (*L*–18) and Cayuga (*N*–18), both excavated to below present sea level; and the Owasco (*O*–15), Skaneateles (*Q*–15), and Otisco (*Q*–14), all draining into the Seneca River (*N*–12); and a western group consisting of the Keuka (*J*–21), Canandaigua (*H*–17), Honeoye (*F*–18), Canadice (*E*–19), Hemlock (*E*–19), and Conesus (*D*–19), with outlets flowing into the Genesee River (*B*–20). Oneida Lake (*T*–9) near Syracuse is also glacial in origin. The glacial plains north of these lakes are covered with till. Many drumlins are present in these plains but cannot be clearly defined in the image.

The famous Erie Canal (*H*–14) stands out in sharp contrast to surrounding vegetation. The nearby farmlands produce winter wheat, oats, corn, seed, snap beans, potatoes, and hay; wine and table grapes are also raised in the area, along with apples. Isolated elm, ash, and cottonwood groves are found in parts of the glacial plains. Oak and hickory woodlands occur around parts of the Finger Lakes. Elsewhere, forests are mostly birch, beech, and maple. *1027–15233*; August 19, 1972.

PLATE 9



THE ADIRONDACK MOUNTAINS, N.Y., AND GREEN MOUNTAINS, VT.: The northeast corner of New York State is dominated by the broad uplift of the Adirondack Mountains (*B*–17). The most rugged part of these mountains is seen here. Mount Marcy (*G*–18) rises to 1629 meters (534 feet) above sea level and Whiteface Mountain (*G*–14) reaches to 1483 meters (4867 feet). Popular ski resorts are located around Saranac Lake (*C*–16), Lake Placid (*F*–15), and Tupper Lake (*B*–18). The bulk of the Adirondacks consists of Precambrian igneous and metamorphic rocks. Schists, gneisses, and quartzites of Grenville age occur in isolated bands and patches (*K*–19) surrounded by younger granitic intrusives (*P*–12). A large area centered around *F*–19 was invaded by intrusive gabbro and anorthosite—the latter is a rock type similar to the crust of the lunar highlands. This crystalline complex has been extensively fractured—many new faults and lineaments have been detected for the first time from the Landsat imagery. These linear zones of weakness have been enlarged by water erosion and glaciation to produce a series of interconnecting valleys that stand out as sharp "gashes" (*C*–20; *G*–19) on the Landsat imagery. North-dipping Cambrian sandstones form cuestas (*C*–10) on the north flank of the Adirondacks. These give way to Ordovician limestones and shales in the St. Lawrence Lowlands (*D*–6) around the St. Lawrence River (*A*–3) on both the New York and Quebec, Canada (*F*–3), sides.

The Champlain Lowlands occupies a great structural trough filled with Cambrian and Ordovician sedimentary rocks. Lake Champlain (*L*–12) developed in the Pleistocene through scouring by a lobe of ice during a Wisconsin glacial advance. The area subsequently was invaded briefly by marine waters from the Gulf of St. Lawrence. The present-day lake, the southern tip of which is just below Ticonderoga (*M*–20) near Lake George (*M*–21) and east of Schroon Lake (*J*–21), now drains out of the Richelieu River (*J*–3) into the St. Lawrence northeast of Montreal. The Champlain Valley is bounded on the east, beginning near Burlington, Vt. (*M*–12), by blocks of Precambrian rock carried westward along thrust faults. The lines of ridges of this strongly folded and metamorphosed complex make up the Green Mountains of Vermont (*Q*–10). They are breached here by the Winooski River, which flows past Montpelier (*T*–14) into Lake Champlain just south of Grand Isle (*K*–9).

The mountains of the region are covered with hardwoods mixed with spruce and some fir at higher elevations. These hardwoods (maple, beech, and birch) extend into the lowlands. Farming is limited mainly to corn, hay, and alfalfa. *1079–15115*; October 10, 1972.

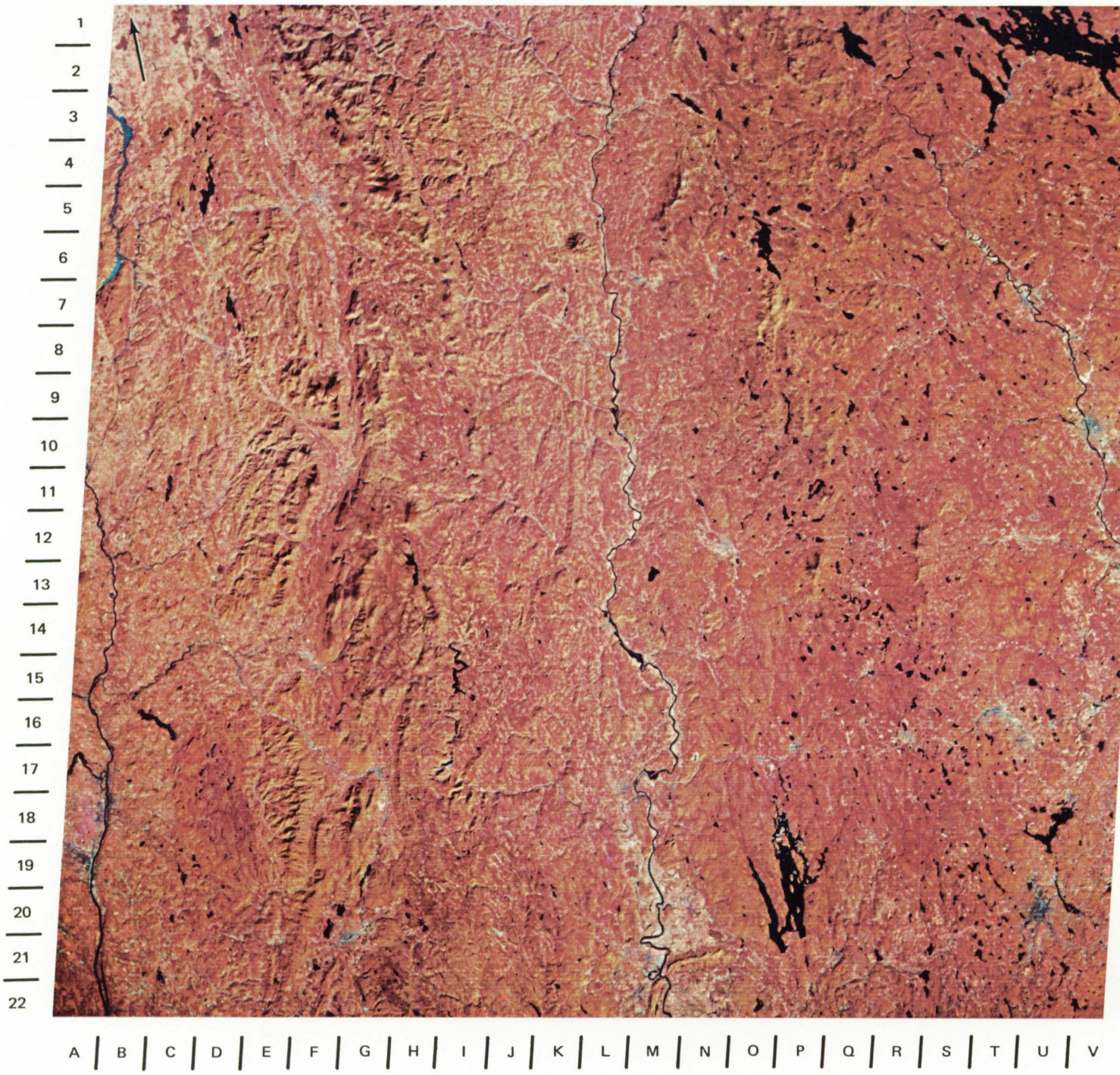
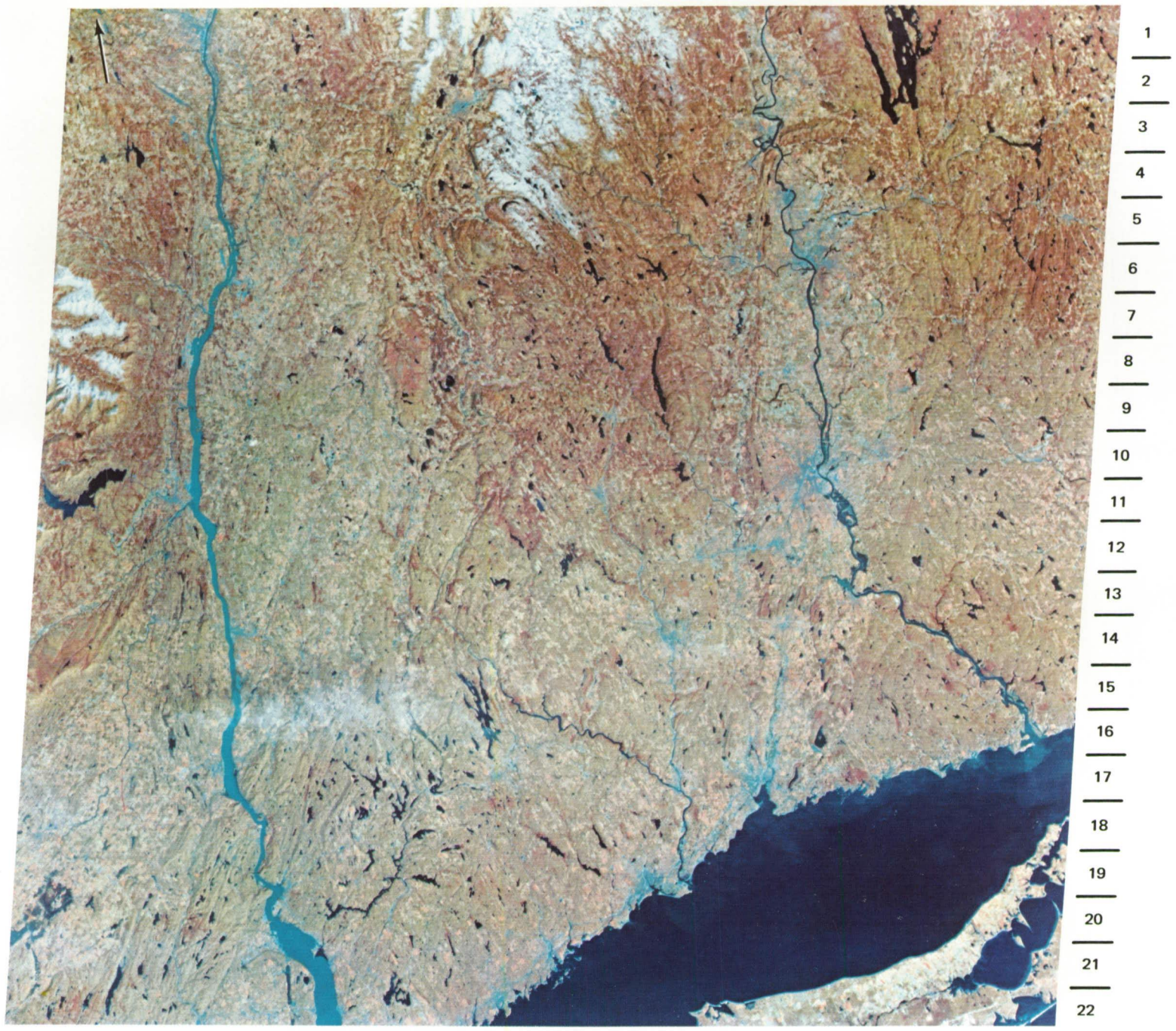


PLATE 10

WESTERN NEW ENGLAND: This part of New England includes most of southern New Hampshire (*Q*–7) and Vermont (*C*–8), divided by the Connecticut River (*L*–1), and much of western Massachusetts (*R*–17). The Hudson River (*A*–11) and its valley lie along the west side and the Merrimack River (*S*–6) and Lake Winnipesaukee (*T*–1) are found to the east. Many towns and cities are scattered throughout the scene: New York State: Albany (*A*–19) and Troy (*A*–17); Massachusetts: Pittsfield (*G*–20), Northampton (*M*–21), Amherst (*N*–20) (west of the Quabbin Reservoir (*P*–19)), and Worcester (*U*–20); Vermont: Rutland (*E*–5) and Brattleboro (*L*–14); and New Hampshire: Keene (*N*–12), Hanover (*K*–3), Concord (*T*–7), Manchester (*U*–8), and Nashua (*V*–12). This midfall scene catches the New England foliage—largely maple, beech, and birch hardwoods or oak and hickory in central Massachusetts, and fir and spruce in the higher ranges—past its climax. The relatively few farms (mostly corn, hay, and truck farming) are mainly confined to the large valleys.

The geology of the region is complicated in detail. The New England province is an extension of the northern Appalachians—a segment of the vast geosyncline whose sediments here became folded, metamorphosed, melted, intruded by magmas, and thrust westward by the middle of the Paleozoic. The Green Mountains (*G*–10) of Vermont and the Taconic Mountains of New York (*E*–19), separated by the Hoosic River (*F*–16), are parts of thrust sheets of Archean gneisses and younger Precambrian schists and slates carried over Cambrian quartzites onto the Rensselaer Plateau (*C*–17). The Berkshire Hills (*J*–21) of Massachusetts and the Hoosic Mountains (*I*–17) are an extension of the Green Mountains that lie just east of the elongate ridges of the Taconics. A long band (*K*–8) of late Precambrian phyllites extends along the western Connecticut River valley to Greenfield, Mass. (*L*–17), on the Deerfield River (*J*–17). Further south, this valley is underlain by arkosic sands and reddish shales that occupy the northernmost segment of the Triassic Lowlands—a fault graben developed along the eastern side of the Appalachians after the main compressive uplifts in the Permian. Trap (basalt flows) mountains of Triassic age hold up the Mount Tom and Holyoke Ranges (*N*–21). East of the Connecticut River, the New England Plateau is a section of rolling hills of Proterozoic schists (*P*–6) or late Paleozoic intrusives (*T*–13). The entire region was subjected to extensive glaciation in the Pleistocene. *1096–15065*; October 27, 1972.

PLATE 11



SOUTHERN NEW ENGLAND: This scene extends the coverage of western New England shown in plate 10 through the lower Hudson River valley (*D*–12) and the lower Connecticut River valley (*Q*–9) to the Long Island Sound (*Q*–20). Cities in New York along the Hudson include Peekskill (*F*–19), Poughkeepsie (*E*–14), Kingston (*D*–11), and Albany (*C*–1); Connecticut River urban areas are Hartford (*Q*–10) in Connecticut and Springfield (*P*–6), Holyoke (*P*–5), and Northampton (*O*–3) in Massachusetts. New Haven (*P*–17), Bridgeport (*N*–19), Norwalk (*L*–20), and Greenwich (*K*–21), Connecticut, are built along the Sound across from Long Island (*T*–21). Danbury (*K*–17) near the Housatonic River (*L*–16) and Torrington (*L*–11) on the Naugatuck River (*N*–16) are other principal inland towns. Most urban centers are concerned with manufacturing as the principal industry. Tobacco is a special crop grown in the lower Connecticut valley. Hay, alfalfa, and corn are also grown there and in the Hudson valley. The forests are primarily oak and hickory.

The regional geology is strikingly revealed in this scene taken in early spring before leafing. The eastern end of the Catskill Mountains (*A*–10)—made up of deltaic sediments of Devonian age folded into a broad syncline—has a steep scarp (*B*–8) in front of a 1200-plus-meter (4000-plus-foot) high dissected plateau (*A*–7). The Shawangunk Mountains (*B*–14) consist of Silurian sandstone overlooking a valley (*B*–16) of Ordovician limestones and bordering Cambrian sandstone that continues up the Hudson valley (*F*–7). The Hudson River passes through the "narrows" (*F*–18) in the Hudson Highlands—part of the Reading prong of metamorphic rocks. Across the river, the south end of the New England prong of similar rocks extends from White Plains, N.Y. (*I*–22), northward through rolling hills and ridges, dotted with lakes, until joining with the Hudson Highlands east of Poughkeepsie. These prongs then connect with the Green Mountains (*H*–2) and the Berkshire Hills (*K*–7) further east. Most of the terrain to the east—the New England Uplands (*T*–7)—is a mature dissected plateau with relief of 60 to 120 meters (200 to 400 feet) or less. Scattered patches of mid-Paleozoic granites occur west of the Connecticut River and in much of the higher areas to the east or along the coast. The Connecticut Lowlands (*Q*–7) here are part of a down-dropped fault block filled with Triassic continental sediments derived from erosion of Paleozoic crystalline rocks. A conspicuous ridge (*O*–4 to *O*–9) along the west side of the valley consists of basalt intruded as sills into tilted Triassic strata. This entire region experienced peneplanation followed by several invasions of the ocean to produce marine terraces (seen as faint color differences running northeast). Pleistocene glaciation further modified the surface by erosional smoothing and deposition of tills and scattered drift. *1258–15080*; April 7, 1973.

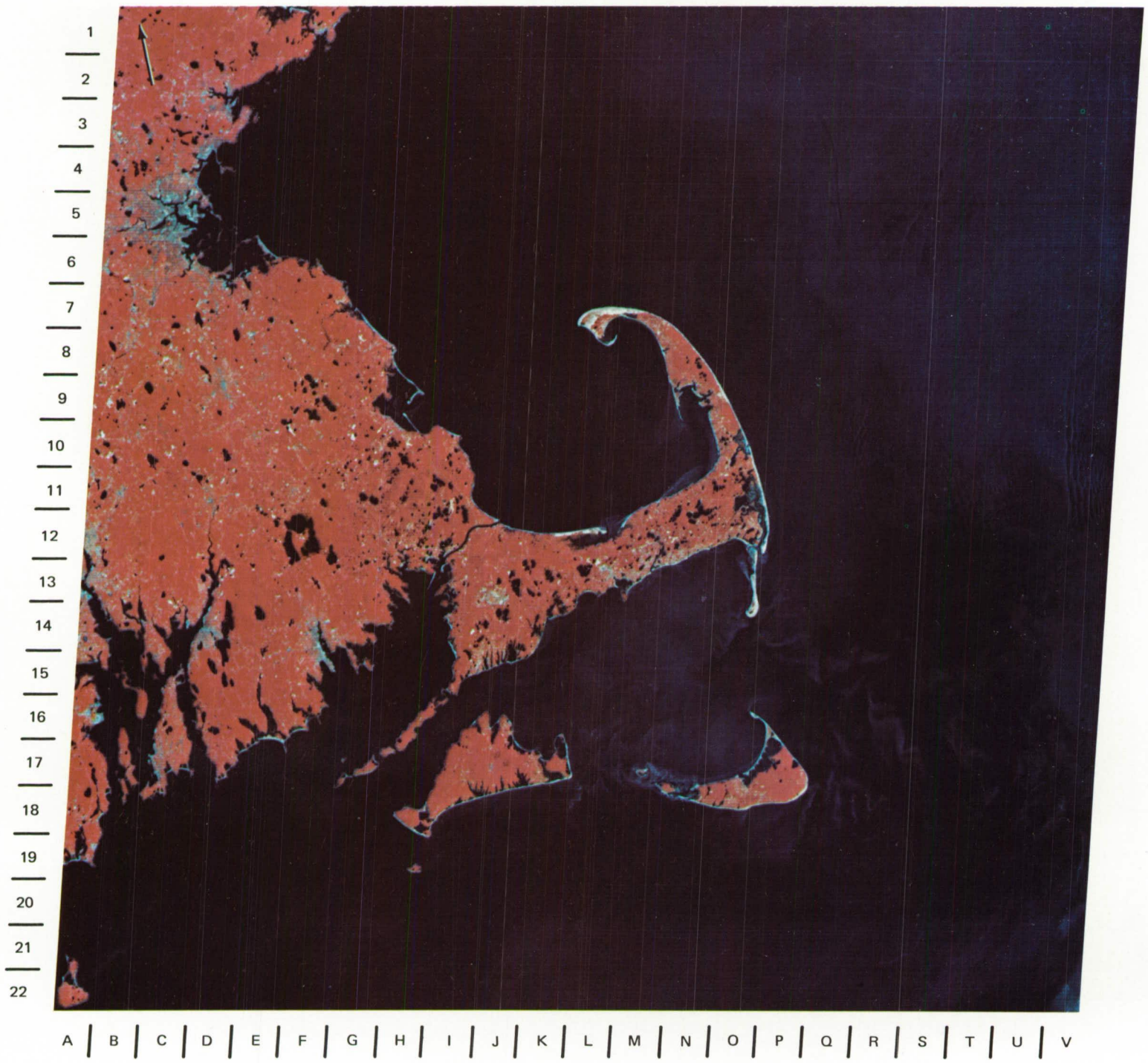


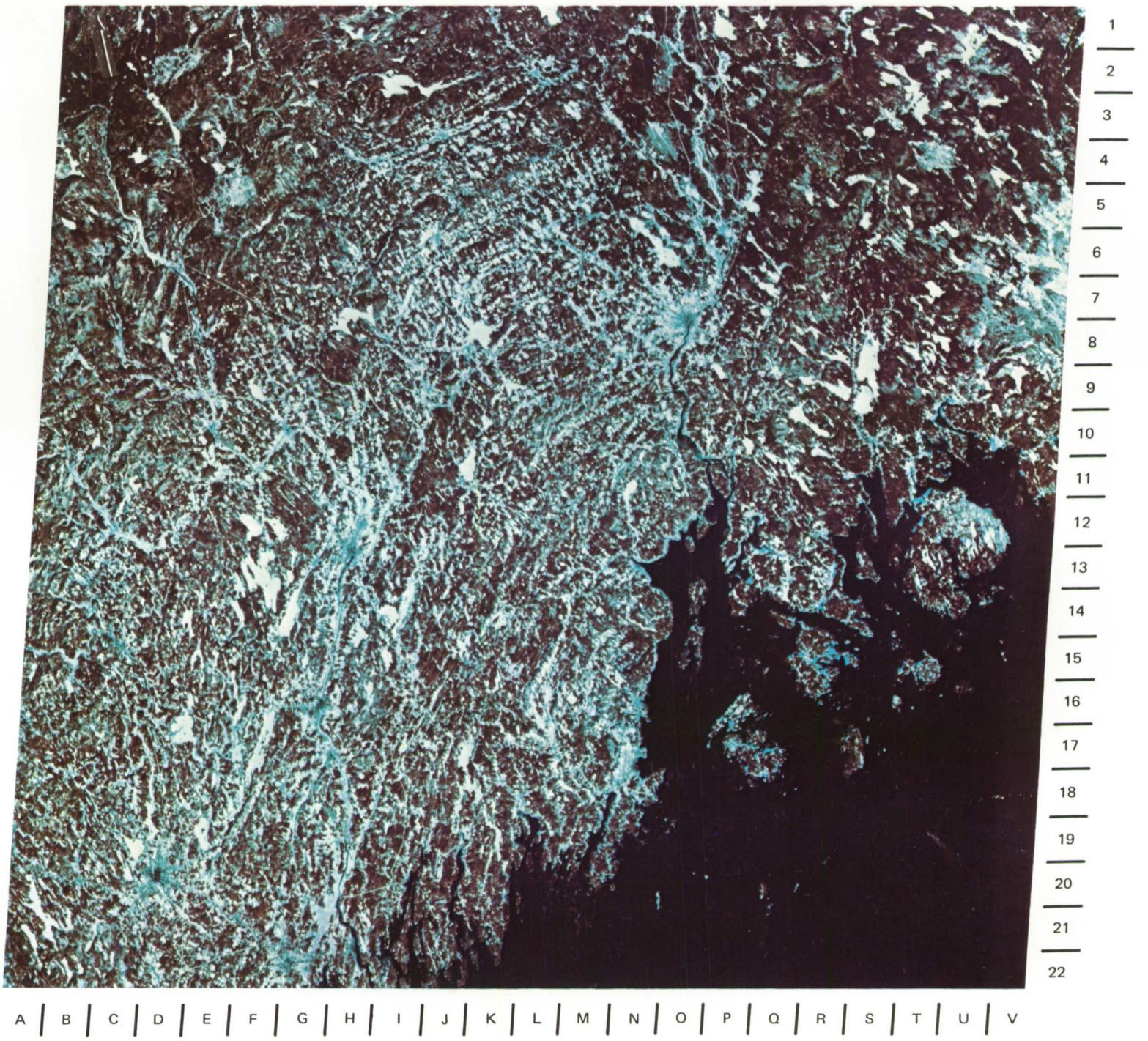
PLATE 12

BOSTON AND CAPE COD: The entire extension of Cape Cod, formed as a series of glacial moraines with some additional growth of sandy hooks, spits, and bars by offshore marine currents, dominates this scene. Provincetown (*L*–7) and Race Point lie at the north end; Monomoy Island (*O*–13), a national wildlife refuge, is situated at the southeast end; and the string of Elizabeth Islands between Buzzards Bay (*H*–14) and Vineyard Sound (*H*–17) marks the southwest end. Martha's Vineyard (*I*–17) and Nantucket Island (*O*–17) enclose Nantucket Sound. The Cape appears cut off as an "island" by the Welland Canal (*I*–12).

Much of the metropolitan area of Boston (*B*–5) is seen along Boston Harbor (*C*–5). The coastal towns of Gloucester (*E*–1), Salem (*C*–3), and Plymouth (*G*–10) are well-known historical sites in eastern Massachusetts. To the west are parts of the New England Uplands (*D*–10), a hilly region covered by oak and hickory in the south. These uplands are underlain by Precambrian metamorphics, mid-Paleozoic intrusives, and Carboniferous slates and volcanics—all sporadically covered by Pleistocene glacial deposits.

The eastern half of Rhode Island falls within this image. The capital of Providence (*A*–12) is located on the Seekonk River at the head of Narragansett Bay (*A*–14). Fall River (*C*–14) and Newport (*B*–17) are also sited on the Bay. Block Island (*A*–22) lies at the entrance to Long Island Sound. *1724–14472*; July 17, 1974.

PLATE 13



THE ROCKY COAST OF MAINE: All of Maine lies within the New England section of the Appalachian Mountains. This section, which extends into the Maritime Provinces of Canada, consists of somewhat metamorphosed Cambrian to Silurian sedimentary rocks (*J*–5) that were involved in the orogenies of the mid-Paleozoic that converted much of the northern Appalachian geosyncline into high mountains. During that activity, schists and slates of Precambrian age were also shoved up and some of the Paleozoic rocks were melted and then intruded into the uplifts. Most of the present coastal strip of Maine is cut from schists (*J*–17) and younger granites (*Q*–10). Subsequent erosion has reduced much of Maine to low rolling hills and ridges but higher elevations occur around the eastern end of the White Mountains (*B*–2) and northeastward through the Katahdin Range in central Maine. Maine was involved in extensive glaciation during the Pleistocene, so that till deposits are now present in most of the valleys. Marine sediments were laid in the lower reaches of the rivers when these became estuaries during high water phases of the oceans. At present, the rise of sea level since the Wisconsin ice advance has again inundated most of the coastal area, producing the rocky cliffs, jagged spurs of land, and islands that characterize Maine's sea coast.

This midwinter scene, with natural enhancement afforded by the snow cover and low Sun angle (31°), brings out considerable detail of structural grain in the terrain (*J*–15). Most of the open country is covered by spruce and fir, except where stretches of maple, birch, and beech prevail. A number of urban areas—Lewiston (*D*–20) and Brunswick (*G*–21) on the Androscoggin River (*E*–21). Augusta (*G*–16) and Waterville (*H*–12) on the Kennebec River (*H*–19), and Bangor (*N*–7) on the Penobscot River (*N*–9)—stand out in sharp contrast to their surroundings because of melting or removal of snow from their streets. Bar Harbor (*T*–11) on Mount Desert Island is a well-known resort area. *1220–14553*; February 28, 1973.

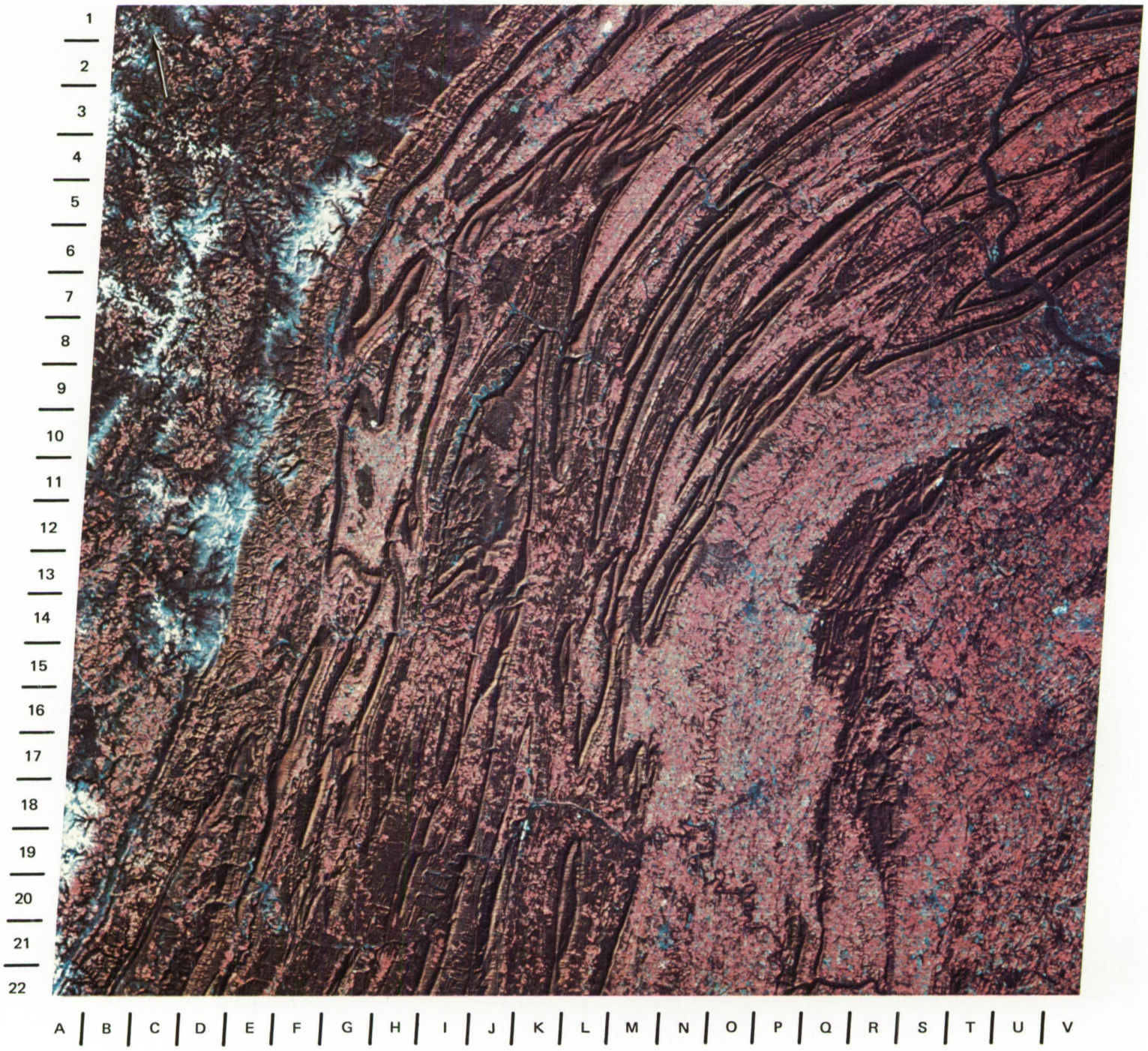


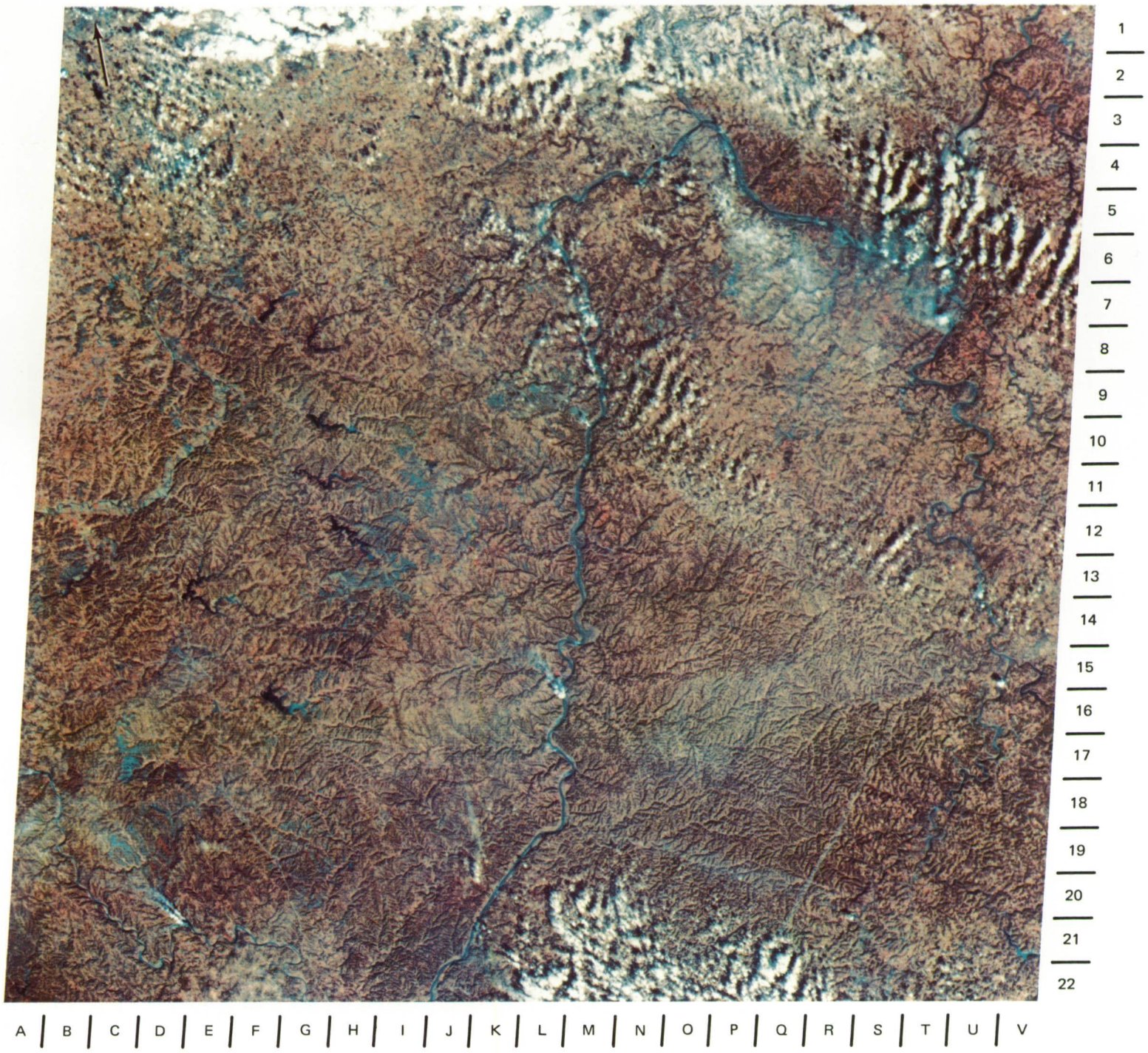
PLATE 14

HARRISBURG, PA.: Suggestive of a giant waterfall, the Appalachians of central Pennsylvania are a classic example of folded mountains. The entire width of the Valley and Ridge province, a physiographic region characterized by doubly plunging anticlines and synclines, is covered here. Some landmarks to help orient the viewer include the Potomac River (*K*–18), the Susquehanna River (*J*–3), the Juniata River (*P*–5), Harrisburg (*U*–7) and Carlisle (*Q*–12), Altoona (*F*–8), State College (*J*–3), Chambersburg (*O*–13), and Gettysburg (*S*–7) in Pennsylvania, and Hagerstown (*O*–7) in Maryland.

Parts of several geologic provinces are visible here. Starting in the northwest (*upper left*), they can be described as follows. The Allegheny Plateau (*C*–4) is a region generally between 300 and 900 meters (1000 and 3000 feet) high consisting of gently folded Paleozoic sedimentary rocks. The east boundary of the Plateau, the Allegheny Front, is an eastward-facing ridge running from *A*–21 to *H*–1. Next are the folded mountains of the Valley and Ridge province, a section of the great Appalachian chain. The folding increases in intensity toward the southeast, a fact evident in this image from the increasing narrowness of the valleys in the eastern part of the Valley and Ridge province. Many of the folds are overturned toward the northwest, and there are many thrust and reverse faults indicating compression in this direction.

An important geologic relationship that should be mentioned is that the present topography of the Valley and Ridge province was not produced directly by folding, which took place in the Paleozoic Era, but by much later differential erosion on the folds. Resistant rocks, in particular sandstones, tend to form ridges, while shales and limestones tend to form valleys. In the drier climate of the far western United States, limestones tend to form ridges. The Great Valley of Pennsylvania (the northward extension of the Shenandoah Valley of Virginia), was formed by the more rapid erosion of Paleozoic limestones; despite its appearance, it is structurally part of the Valley and Ridge fold system. Southeast of the Great Valley is the Blue Ridge anticlinorium (*Q*–17 to *R*–12), a range of Precambrian igneous and metamorphic rock. Beyond that are the Triassic basins and the Piedmont of Pennsylvania and Maryland, the latter underlain by Paleozoic metamorphic and igneous rock. The Appalachians were the site of a Paleozoic geosyncline, and the Piedmont is thought to have also been part of this geosyncline now metamorphosed and tightly folded. *1495–15222;* November 30, 1973.

PLATE 15



WESTERN APPALACHIAN PLATEAU: The terrain imaged in this scene is typical of the intricate dendritic drainage that develops in a region underlain mostly by soft, easily dissected sediments. The area shown encompasses southwestern Pennsylvania, eastern Ohio, and a segment of West Virginia. The principal city is Pittsburgh (*R*–6), situated where the Monongahela (*T*–9; *T*–18) and the Allegheny (*T*–3) Rivers join to form the Ohio (*P*–5). The cities of Steubenville (*L*–9) and Wheeling (*L*–14) lie on the Ohio as it heads south. Other towns include Canton (*C*–4), Cambridge (*D*–15), and Zanesville (*A*–17) in Ohio and Morgantown (*U*–16) and Clarksburg (*S*–21) in West Virginia. The Muskingum River (*B*–19) winds its way to the Ohio while the meandering Tuscarawas River (*B*–11) eventually joins the Muskingum. A line of reservoirs, Atwood (*D*–7), Leesville (*F*–8), Tappan (*G*–10), Clendenin (*G*–11), Piedmont (*G*–12), Wills Creek (*D*–13), and Senecaville (*F*–15), straddle small rivers that flow west of a divide (*I*–12) into the Muskingum drainage system.

The topography of this region, well displayed in this low Sun angle winter scene, is characteristic of the unglaciated Allegheny Plateau. Almost all of the rocks are shales and siltstones, with some thin sandstones. The youngest rocks are part of the Permian Dunkard Series extending from Washington, Pa. (*P*–10), southward along and east of the Ohio. Beyond are successively older flat-lying rocks of Pennsylvania age; many of the individual stratigraphic units contain coal beds.

Note the smoke plumes (*D*–20) on the Muskingum River, presumably emitted from a factory or power plant. Their rise to the northwest indicates a southeast wind. *1137–15364;* December 7, 1972.

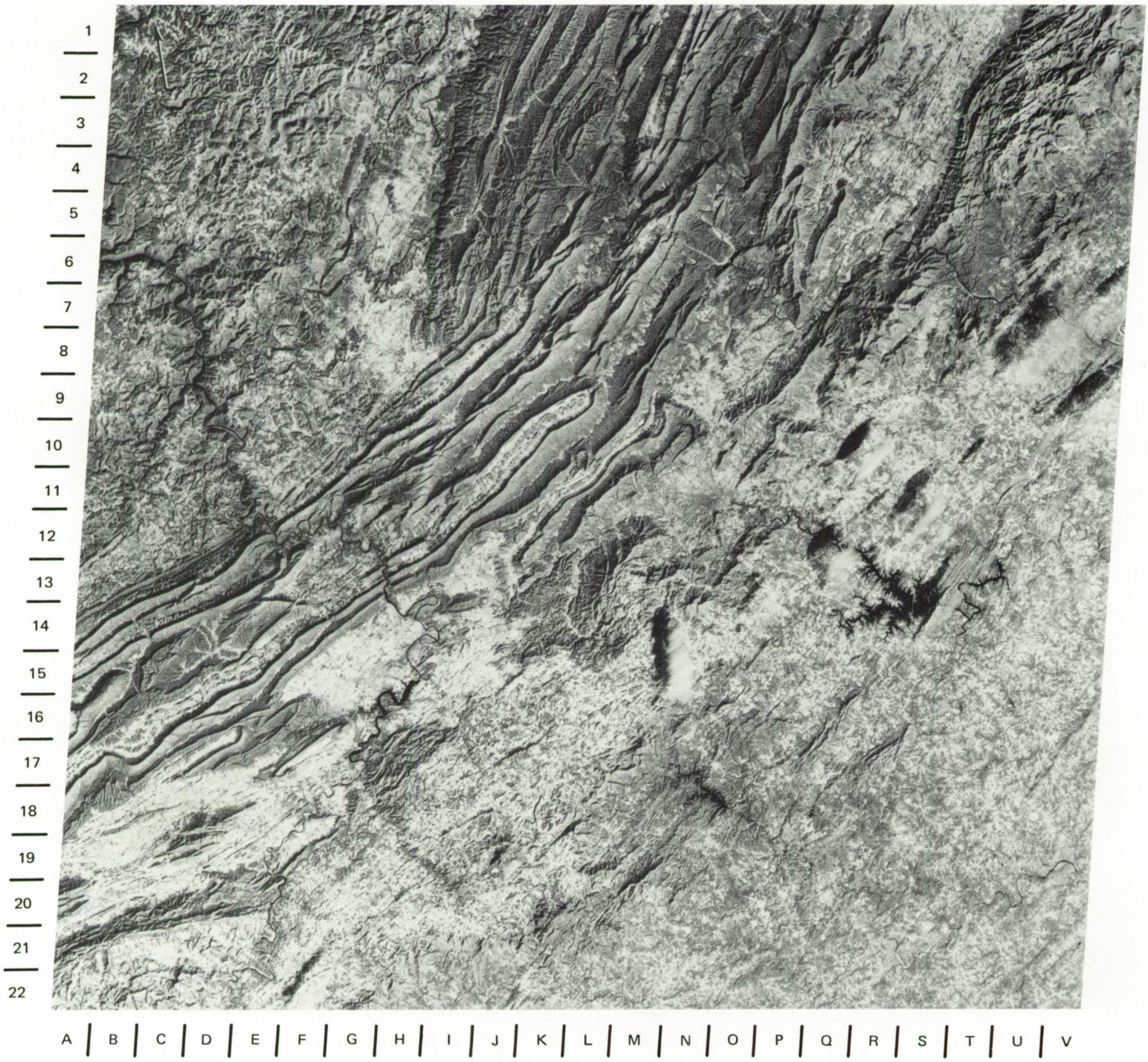


PLATE 16

ROANOKE, VA.: Portions of three States and four physiographic provinces are represented in this image. Danville (*V*–18) and Martinsville (*S*–20), Va., in the southeastern portion of the image are located near the Virginia-North Carolina border, and the dissected plateau country of eastern West Virginia appears in the northwest corner of the image. A light snow cover creates several areas of high reflectance throughout this scene; for example (*F*–15). Thin clouds (*N*–15; *Q*–10) occur in a few places over the Blue Ridge.

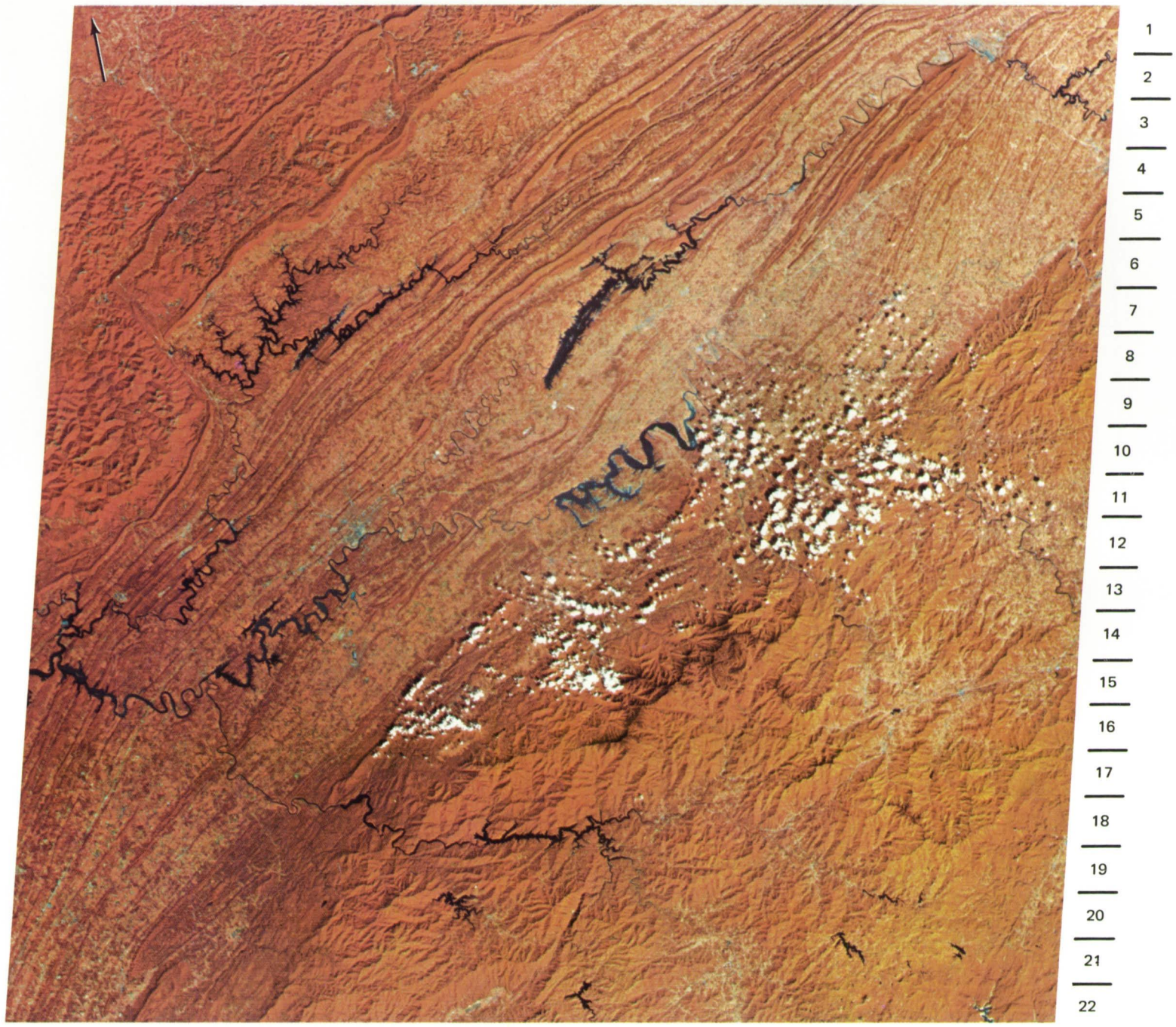
The Piedmont Upland east of the mountainous area (*T*–18) is developed on ancient crystalline rocks and represents an area of moderate relief. Adjoining the Piedmont on the west, the Blue Ridge province (*S*–4; *D*–20) is mostly an upthrust complex of single ridges in places, and closely spaced multiple ridges in others, made up mainly of Precambrian metamorphic rocks, particularly metabasalts. The city of Lynchburg, Va. (*U*–8), is located on the James River in a valley on the margin of the Blue Ridge. In this image Lynchburg is obscured by atmospheric interferences.

The upwarped anticlinal ridges and downwarped synclinal valleys trending northeast to southwest are characteristic of the folded Appalachian country (*I*–9). The Valley and Ridge province, as it is also known, borders the Blue Ridge to the west, in some places quite abruptly along sharply defined fault zones. The city of Roanoke (*N*–11) is located on the eastern margin in a transition zone between the Valley and Ridge and the Blue Ridge.

The fine texture of the maturely dissected Appalachian Plateau province (*C*–5) dominates the northwest corner of the image. The degree of dissection gives rise to a rolling, hilly landscape with few flat areas suitable for agriculture. The New River (*C*–9) traverses the plateau after it has breeched the linear ridges and valleys to the east (*G*–13). The southern end of the Allegheny Mountains (*I*–3) marks the transition between the folded strata of the Valley and Ridge and the essentially horizontal dissected strata of the plateaus—a relationship similar to that shown in the Knoxville, Tenn., image (plate 17) between the Cumberland Plateau and the Valley and Ridge.

Three reservoirs are readily recognizable: Philpott (*N*–7), Smith Mountain (*R*–13), and Clayton (*H*–15). *1172–15312;* January 11, 1973.

PLATE 17



KNOXVILLE, TENN.: Three contrasting types of topography are shown in this image. The mountainous knot of the Great Smoky Mountains topped by Clingman's Dome (*N*–14) rising above 2000 meters (6600 feet) occupies the southeastern portion of the image. Appalachian Valley and Ridge topography, developed upon faulted and eroded elongate synclinal and anticlinal structures, trends northeast to southwest across the image. The dissected horizontal sedimentary strata of the Cumberland Plateau (*B*–2) occupy the northwestern portion of the image.

The eastern boundary of the plateau country lies in a disturbed zone known as the Cumberland Overthrust Block (*G*–4). Here a wedge of sedimentary rocks some 200 kilometers (125 miles) long by 40 kilometers (25 miles) wide has been thrust northwestward. The southwestern margin of this thrust is marked by the Jacksboro fault, readily recognizable in this image (*C*–7). Southeast facing Cumberland Mountain (*F*–5), a homoclinal ridge, marks the boundary between the Cumberland Plateau and the Appalachian Valley and Ridge province.

Numerous reservoirs on the Tennessee and its tributaries signal the activities of the Tennessee Valley Authority in developing this portion of Appalachia. Some of the more obvious multipurpose reservoirs are Fontana (*K*–18), Douglas (*L*–11), Cherokee (*L*–7), and Norris (*F*–7).

The city of Knoxville (*G*–11) is located in the Valley and Ridge area. Coal is strip mined from the Pennsylvanian shale and coal formations, especially in the Middlesboro synclinal basin (*H*–2) in Kentucky. The bluish signature of the mines in that area is characteristic of strip mining activity.

In this heavily vegetated area, the Appalachian oak forest dominates most of the scene with the exception of the higher portions of the Great Smoky Mountains where greater elevation permits the northern hardwood forests (maple, beech, and fir) and the southeastern spruce and fir forests to thrive. Portions of the valley floors in the Valley and Ridge province have been cleared for agricultural purposes as is evidenced by the patterned network of fields in some areas. *1084–15431;* October 15, 1972.

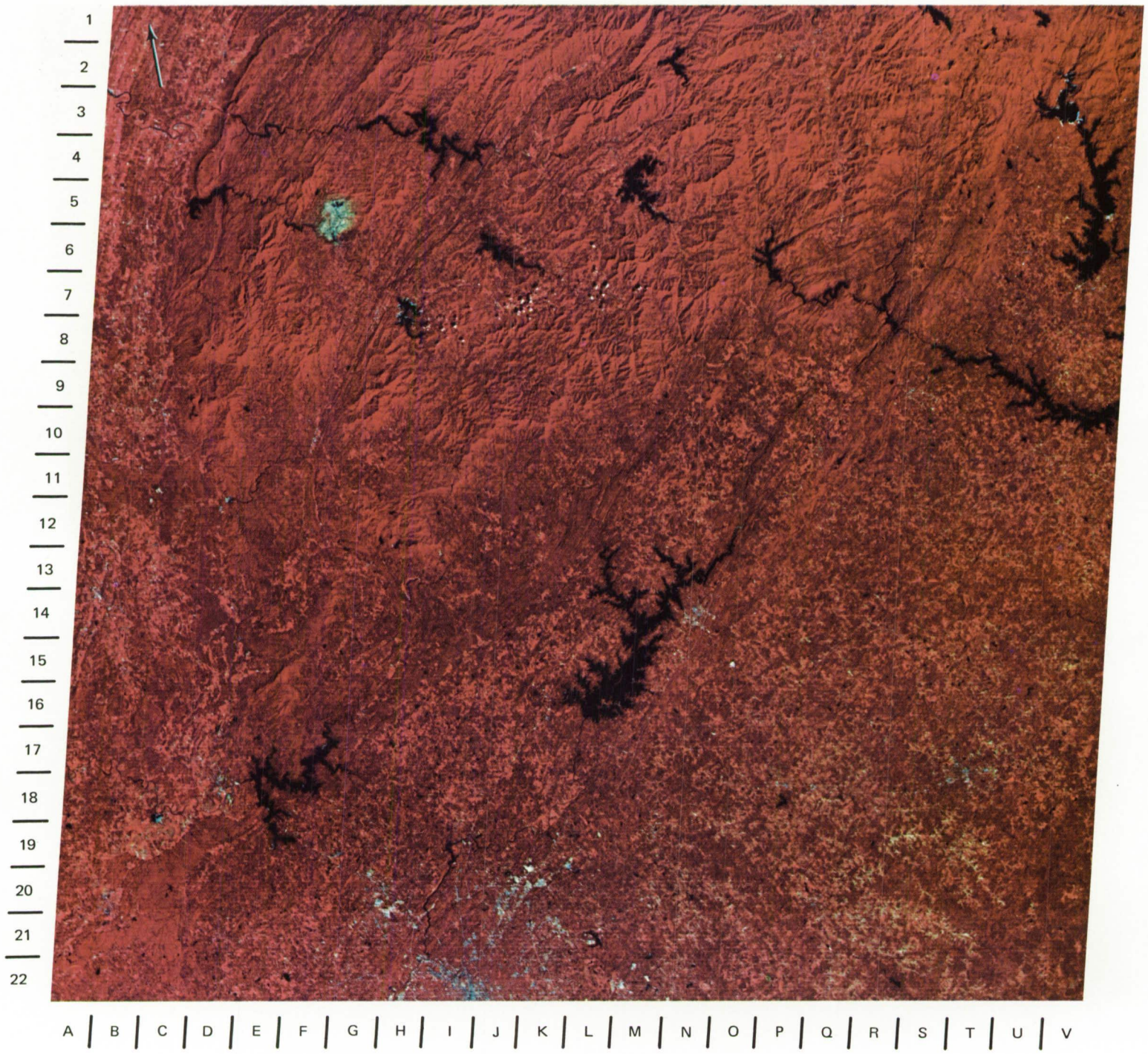


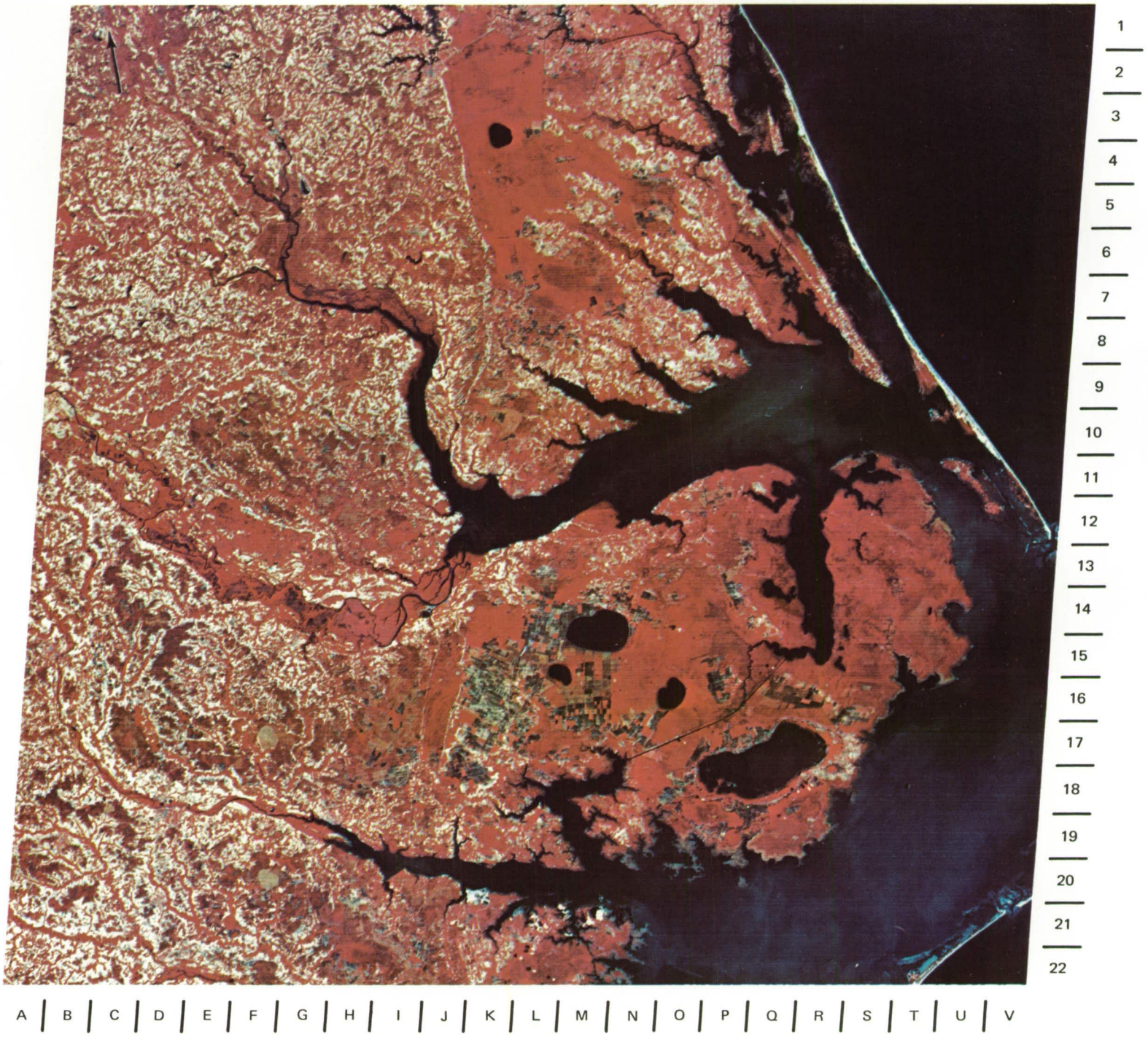
PLATE 18

ATLANTA, GA.: Geologic structure is reflected in the topography of three Appalachian provinces in this scene north of Atlanta, Ga. (*J*–22). The linear ridges on the west near Etowah, Tenn. (*C*–2), are thrust-faulted belts of Cambrian sediments in the Valley and Ridge. The Blue Ridge Mountains to the east, known locally as the Unakas, are divided into rugged mountains on the north, composed of thick Precambrian Ocoee clastic sediments, and the Dahlonega plateau, west of Gainesville (*N*–14) and Toccoa (*R*–9). This lowland, formed on rocks of the Talladega series, is structurally part of the Blue Ridge, but physiographically part of the Piedmont to the east. The two provinces are separated along the Brevard fault zone, which extends from the Chattahootchee River west of Atlanta past Lake Keowee in South Carolina (*U*–3). The Piedmont is a peneplain surface that truncates a wide variety of metamorphosed rocks east of the fault. The topography of the Dahlonega plateau, however, is much more varied, with numerous ridges (*K*–12), monadnocks (*M*–9), and low wooded hills where the Piedmont overlaps the Valley and Ridge south of Cartersville (*C*–17).

The large white scar in the mountains (*F*–5) marks the copper mining district of Ducktown, Tenn., where fumes from open roasting of ore have destroyed the vegetation, causing severe erosion. Parts of the area are being reclaimed with trees and grass. Residual deposits of iron and manganese have been mined near Cartersville, and barite and ocher are mined at present. Gold lodes and placers were worked throughout the Dahlonega plateau.

Interstate 285 circles the Atlanta metropolitan area near Marietta and Dobbins Air Force Base (*H*–20). Stone Mountain (*L*–20), a large granite dome rising 200 meters (650 feet) above the Piedmont, has a large memorial to the Confederacy carved on its side. Athens (*T*–17) is the home of the University of Georgia. Large lakes present include Allatoona Reservoir (*E*–17) and Lake Sidney Lanier (*L*–15). The long string of lakes from Hartwell Reservoir (*U*–19) to Chatuge Lake (*L*–5) on the Hiwassee River suggest linear fault control of the stream courses. *1084–15433;* October 15, 1972.

PLATE 19



THE OUTER BANKS, NORTH CAROLINA: The coastline in this part of North Carolina is perhaps the most distinctive physical feature along the entire Atlantic Seaboard. Offshore, the sandy bottom shoals are notorious for their treacherous effect upon navigation. Stretching all the way from Cape Henry near Norfolk, Va., to Cape Fear, at Wilmington, N.C. (see plate 20), the Outer Banks is made up of sediments brought seaward by the rivers draining across the coastal plain, reworked by wave action, and sculptured into a long, narrow sandy barrier beach that fringes the mainland. In places, the barrier beach is as much as 50 kilometers (30 miles) from the mainland, but along much of the coast the offshore sand beaches are separated from this mainland by only a few kilometers (miles). Tidal and storm actions have produced numerous inlets that interrupt the continuity of the barrier beach while allowing access to the lagoonlike sounds. The long-term geomorphic changes of such a coast configuration will lead to a prograding shoreline, whereby the present sounds will become filled with sediments and vegetation allowing the mainland to extend seaward to the present position of the barrier beaches.

This scene displays some noted landmarks and historical sites. Kitty Hawk (*S*–9), just north of the resort area of Nags Head, is the spot where the Wright Brothers made their first successful flight of an airplane in 1903. To the south is Roanoke Island (*T*–11), on which the first English settlement in North America was established in 1584 only to disappear a few years later. Ocracoke Island (*T*–22) was the land base of the infamous pirate, Captain Bluebeard. The tip of Hatteras Island (*V*–20), part of the Cape Hatteras National Seashore, lies just to the east.

These banks are separated from swampy lowlands (*S*–14) and salt marshes (*O*–19) on the mainland by Pamlico Sound (*T*–19), fed by the Pamlico (*G*–19) and Neuse (*D*–22) Rivers on the south and Alligator Bay (*Q*–12) and Albemarle Sound (*O*–10), the latter ending at the Roanoke (*I*–14) and Chowan (*G*–7) Rivers, on the north. West of Currituck Sound (*Q*–5) is the Great Dismal Swamp (*J*–4) of southeast Virginia near Norfolk. The coastal plains region to the west is dotted with numerous farms growing tobacco, corn, and other crops. *1637–15085*; April 21, 1974.

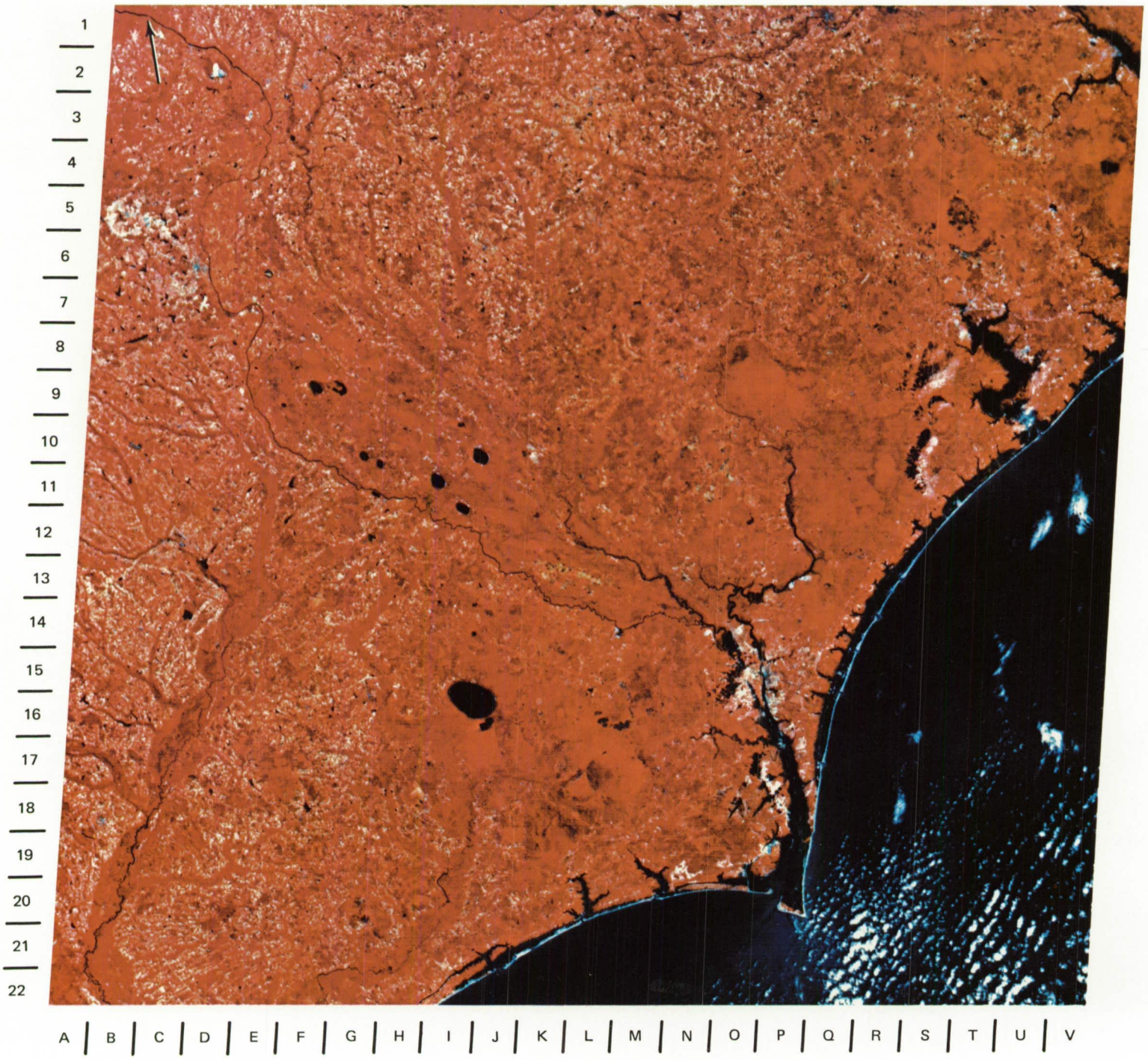


PLATE 20

CAPE FEAR, N.C.: This section of the North and South Carolina coast near Cape Fear shows typical Atlantic Coastal Plain development. The inland portion comprises dissected, terraced hills developed on Cretaceous sands. Crystalline rocks of the Piedmont are indicated by the large quarry near Lillington (*C*–2). The fall line is indistinct here, occurring as a zone of rapids along the Cape Fear River. East of the Suffolk Scarp near Kinston (*P*–1), low terraces are developed on Tertiary sediments and large swamps abound, including Wolf (*S*–5), Angola (*O*–9), Holly Shelter (*Q*–11), and Green (*L*–17). Elliptical Lake Waccamaw (*I*–15), White (*I*–11), Black (*I*–10), and several smaller lakes between the Cape Fear River (*G*–11) and South River (*I*–9) are good examples of the Carolina Bays, discussed in plate 21. The Atlantic coastline here is a compound cuspate foreland. Shore currents have built the cuspate bar at Cape Fear (*P*–20). The area behind the offshore bars along Long Bay (*M*–21) and Onslow Bay (*R*–15) will eventually fill in, and the entire coastland will be prograded to the present bar line.

The city of Wilmington (*O*–15) has been an important harbor throughout North Carolina history, serving as headquarters for the British during the Revolution, and site of a major campaign in the Civil War to shut off supplies to the Confederacy. The area along the New River east of Jacksonville (*S*–6) is the Marine Corps training base at Camp Lejeune. New Bern (*V*–2) lies along the Tidewater section of the Neuse River. Further upstream Seymour Johnson Air Force Base (*K*–1) can be seen south of Goldsboro, as can the extensive training areas around Fort Bragg (*A*–5) near Fayetteville (*C*–6). East of Lumberton (*C*–12) the Lumber and Big Swamp Rivers turn sharply southwestward, joining the Little Pee Dee River in South Carolina. Numerous beach lines can be seen throughout this part of the coast (*D*–21). *1080–15203;* October 11, 1972.

PLATE 21



CHARLESTON, S.C.: Nearly the entire South Carolina coast is shown here, from Beaufort (*G*–21) and Charleston (*N*–15) to Myrtle Beach (*V*–1). The inland part of this Atlantic Coastal Plain area is a dissected upland known as the Sand Hills. The numerous small ellipses scattered throughout the hills near Orangeburg (*B*–7) and Sumter (*F*–1) mark shallow depressions called Carolina Bays, the origin of which has been variously attributed to meteorite impacts or to the geologic processes of solution and subsidence or eddy currents. Traces of old coastal terraces parallel the coast about 50 to 65 kilometers (30 to 40 miles) inland and younger terraces can be seen as long beach lines between Charleston and Georgetown (*S*–6). A chain of sea islands, developed in place of offshore sandbars, extends from Cape Island (*S*–10) south along the entire coast, and includes the large islands of Edisto (*K*–19), St. Helena (*H*–21), and Port Royal (*F*–21). As part of the Santee-Cooper project completed in 1942, the water of the Santee River is dammed at Lake Marion (*I*–6), diverted by canal to Lake Moultrie (*K*–8), and fed through a powerhouse and Tailrace Canal to the Cooper River (*L*–9).

The urban development around Charleston covers most of the peninsula between the Cooper and Ashley Rivers. The 14-kilometer (9-mile) waterfront provides an important Atlantic seaport. Fort Sumter, site of the attack that began the Civil War, is located at the entrance to the harbor. Charleston is noted for its preservation of many Old South buildings, plantations, and gardens.

Interstate 26, going west from Charleston past a large cement plant (*G*–10), intersects I–95, the main north-to-south route (*F*–9). The Intracoastal Waterway enters the Waccamacaw River (*T*–1) and can be traced across the mouth of the Santee River (*T*–8) and through the coastal marshes around Bulls Bay (*O*–12). *1081–15264;* October 12, 1972.

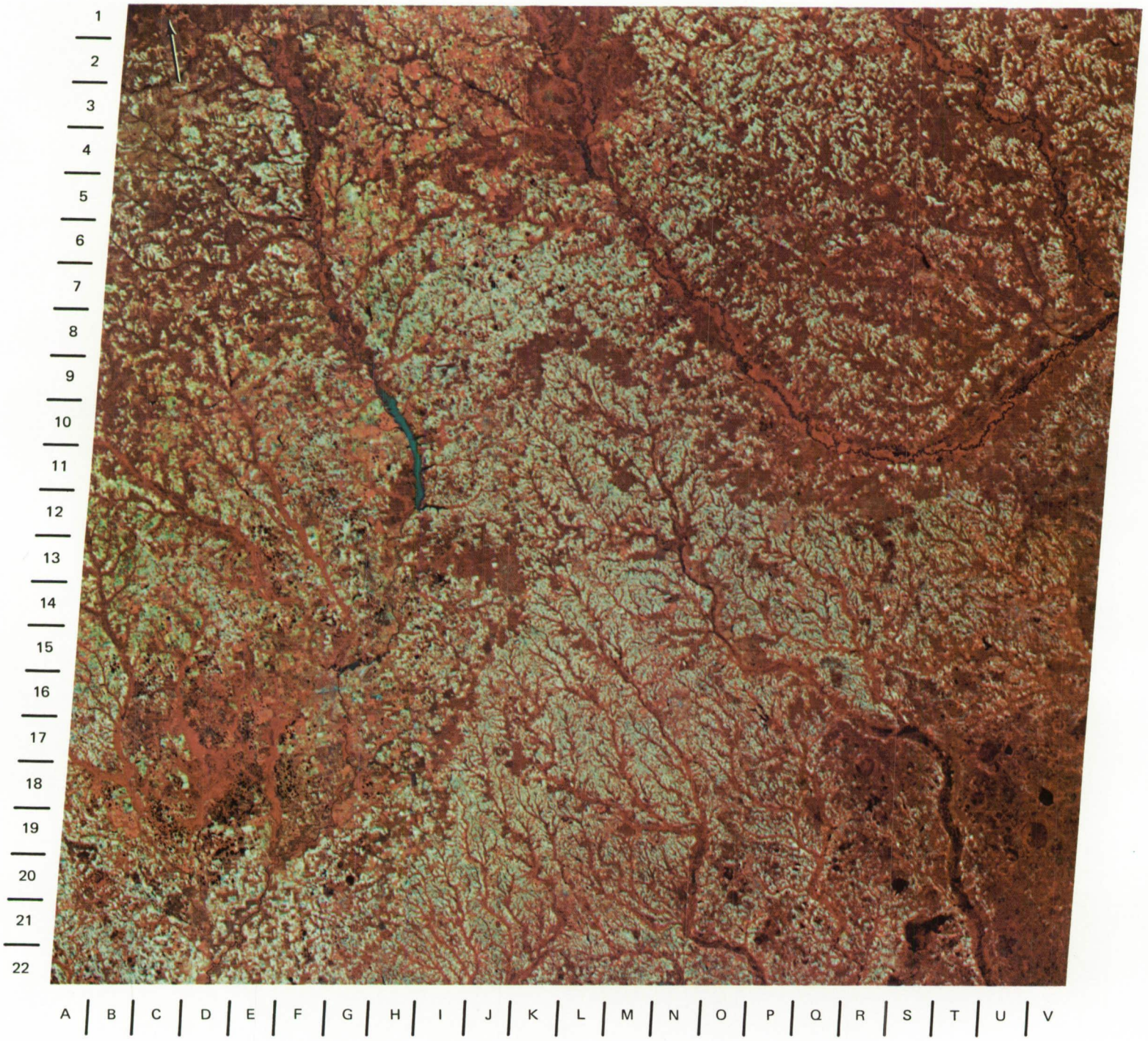


PLATE 22

SOUTH-CENTRAL GEORGIA: This scene is typical of the southern coastal plains of the Carolinas westward through Alabama and Mississippi. Tertiary and Quaternary marine sediments are deposited in nearly flat (slightly coastward dip) units that become progressively older away from the Atlantic Ocean. The oldest formations are Cretaceous units south of the fall line (see plate 3) around Columbus and Macon (both just off the upper left corner of the image). The low country there changes southward to a more hilly uplands around Americus (*D*–9) underlain by the Oligocene Vicksburg Formation. The Dougherty Plains (*C*–13) drained by the Flint River (*E*–6; *E*–20) consists of Miocene beds. East of Albany, Ga. (*F*–15), and the Blackshear Lake Reservoir (*G*–10) are the Tifton (*K*–17) and Altamaha (*O*–4) uplands capped by Oligocene units and bounded in places by a low scarp (*I*–15) on the northwestern side. Miocene and younger sediments continue the sequence over most of the eastern half of the image.

The Flint, Little (*N*–20), Alapaha (*N*–14), Ocmulgee (*O*–9), Oconee (*T*–3), and other rivers in the scene are essentially consequent streams or their tributaries. They flow over rich farmlands that yield tobacco, cotton, corn, soybeans, peanuts, and such specialty crops as watermelons and pecan trees. The remainder of this area is given to pasture, with scattered woodlands and occasional forests. Oak is found northwest of Americus while loblolly pine and slash pine characterize the northwest and southeast sections, respectively, of the plains seen here. The flood plains of many larger streams, particularly along the Flint and Ocmulgee Rivers, support an oak-gum-cypress assemblage. This same forest community begins to increase in areal extent as the edge of the Okefenokee Swamp (*V*–21) is approached. The numerous oval lakes and swampy (peat-filled) depressions visible in the lower right corner are part of the vast swarm of Carolina Bays (see plate 21) found throughout much of the Atlantic Coastal Plains from Virginia to Florida. Those shown here may be part of a lime sink area. *1263–15393;* April 12, 1973.

PLATE 23



THE STATE OF FLORIDA: This mosaic consists of 16 color composite images acquired by Landsat 1 between October 1972 and April 1973. Among the many features of interest in this State (see plate 24 for letter identifications) are the Florida Panhandle (*A*), Pensacola (*B*), Panama City (*C*), Apalachicola River (*D*), Apalachicola National Forest (*E*), Tallahassee (*F*), Suwannee River (*G*), Jacksonville (*H*), St. Johns River (*I*), St. Augustine (*J*), Lake George (*K*), Daytona Beach (*L*), Merritt Island and Cape Canaveral (*M*), Orlando (*N*), old beach ridges (*O*), Tampa Bay (*P*), Tampa (*Q*), St. Petersburg (*R*), Peace River (*S*), Charlotte Harbor (*T*), Lake Okeechobee (*U*), Caloosahatchee River (*V*), Loxahatchee National Wildlife Refuge (*W*), Big Cypress Swamp (*X*), The Everglades (*Y*), Fort Lauderdale (*Z*), Miami (*AA*), Florida Keys (*BB*), and Key West (*CC*).

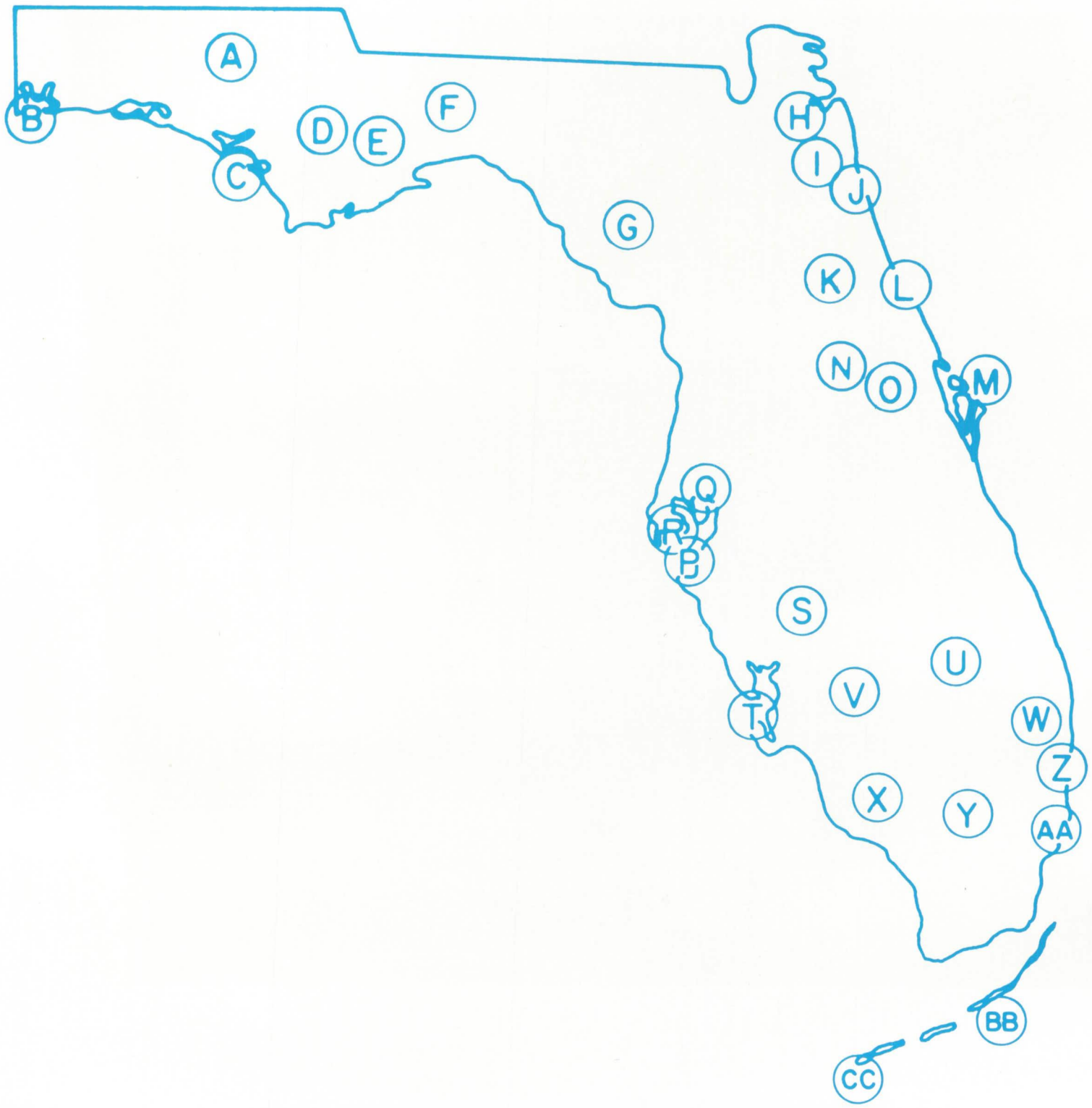
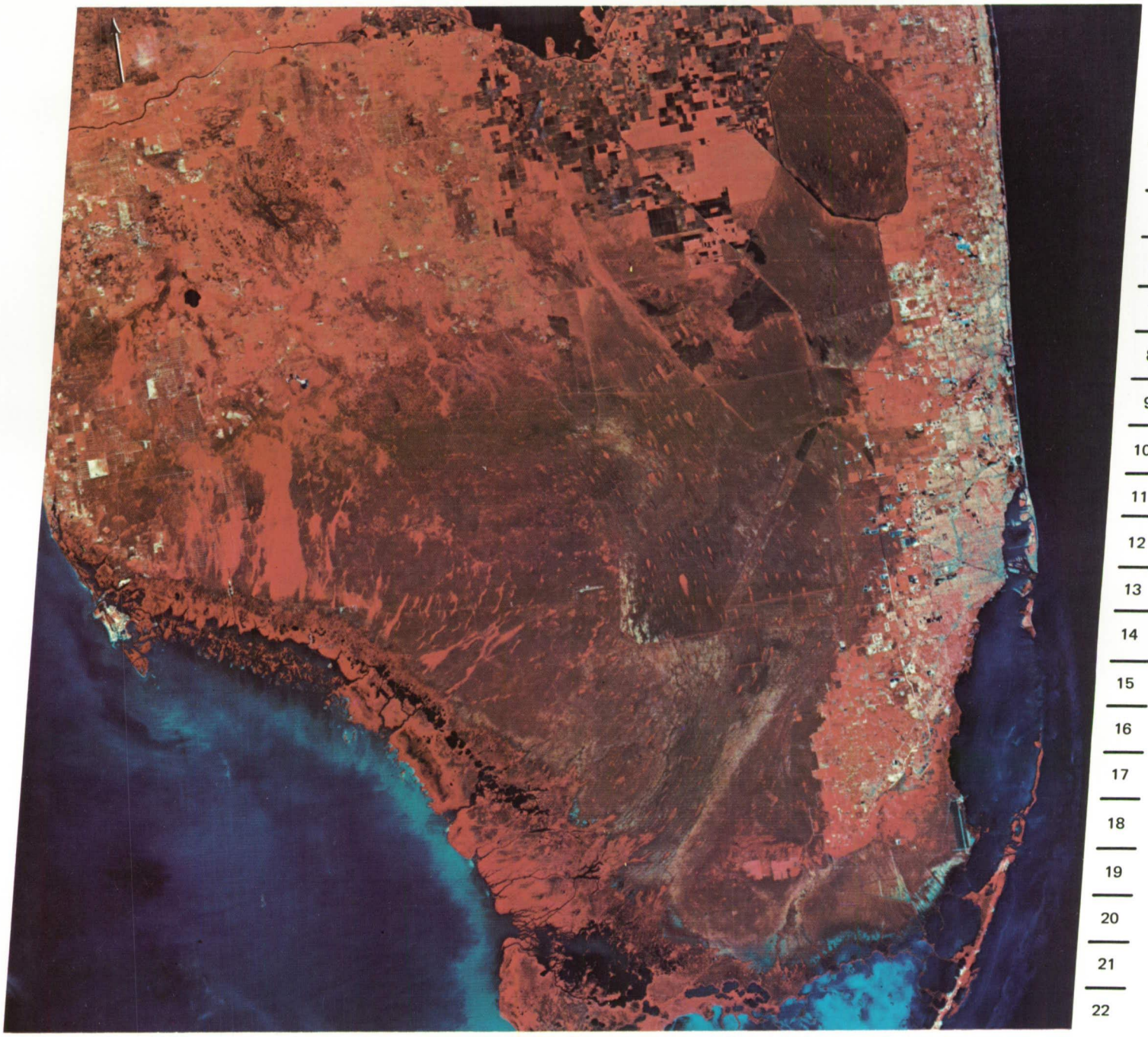


PLATE 24

PLATE 25



SOUTHERN FLORIDA: The southern third of the peninsula of Florida encompasses climates, vegetative habitats, and economic pursuits not found elsewhere in the continental United States. Most of the land surface is near, or only a few tens of meters (feet) above sea level, reflecting its fairly youthful age in terms of emergence from seas that once covered all of mainland Florida. Most of the land area seen in this image consists of sluggishly drained marshes and swamps: the Big Cypress Swamp (*H*–12), the Everglades (*O*–13), and the coastal marshes and mangrove swamps (*D*–13; *P*–21).

Some areas with slightly higher elevations and better drained soils known as Sandy Flatlands occur along the eastern, northern, and western margins of Big Cypress Swamp and the Everglades. Florida's tourism-oriented "gold coast" stretches from the Palm Beach area (*S*–1) to Miami and the shores of Biscayne Bay (*T*–13). Along Florida's west coast, the rectangular grid of street patterns visible east of Fort Myers (*A*–4) and Naples (*C*–8; *D*–11) is evidence of the State's building boom. Along the east coast, inland from the urbanized areas, the eastern margin of the Everglades has been drained for agricultural purposes (*R*–3; *Q*–16). Around the southern margin of Lake Okeechobee, the largest of Florida's thousands of lakes, large acreages are devoted to the production of sugarcane, citrus, and dozens of truck gardening crops (*K*–2). Numerous canals and drainageways (*O*–6; *Q*–5) have been constructed in this area to drain the low northern end of the Everglades.

The Everglades consists of some 12 500 square kilometers (5000 square miles) made up primarily of vast expanses of tall sawgrass (the darker colored signature in the image). Interspersed within the sawgrass are "tree islands" or hammocks, slightly higher rises covered with hardwood trees. The splotches of intense red occurring in a long, arcuate pattern through the Everglades represent hammock areas. The long, gentle curve of the hammock pattern within the Everglades delineates the natural flow of the drainage in the Everglades (*M*–10; *N*–18). Like the Everglades, the Big Cypress Swamp contains areas of both swampland and hammocks. The mangrove swamp area is confined to a well-defined coastal zone stretching from Naples through Ten Thousand Islands (*E*–14), Whitewater Bay (*M*–21), into the Florida Bay area (*R*–21). Florida Bay is a shallow, shoal-filled, sediment-laden body of water between the Florida Keys (*T*–21) and the mainland. *1242–15240;* March 22, 1973.

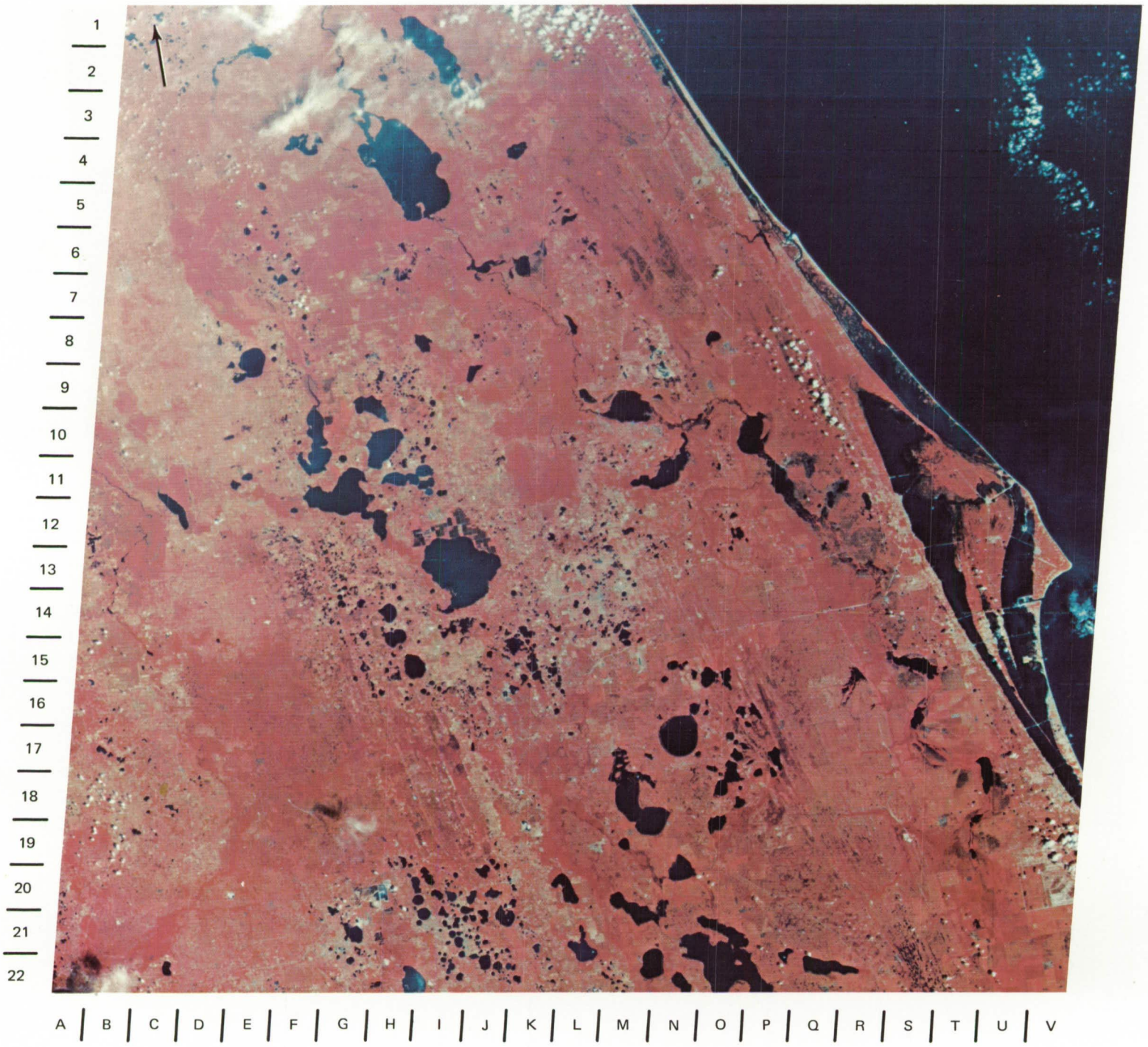
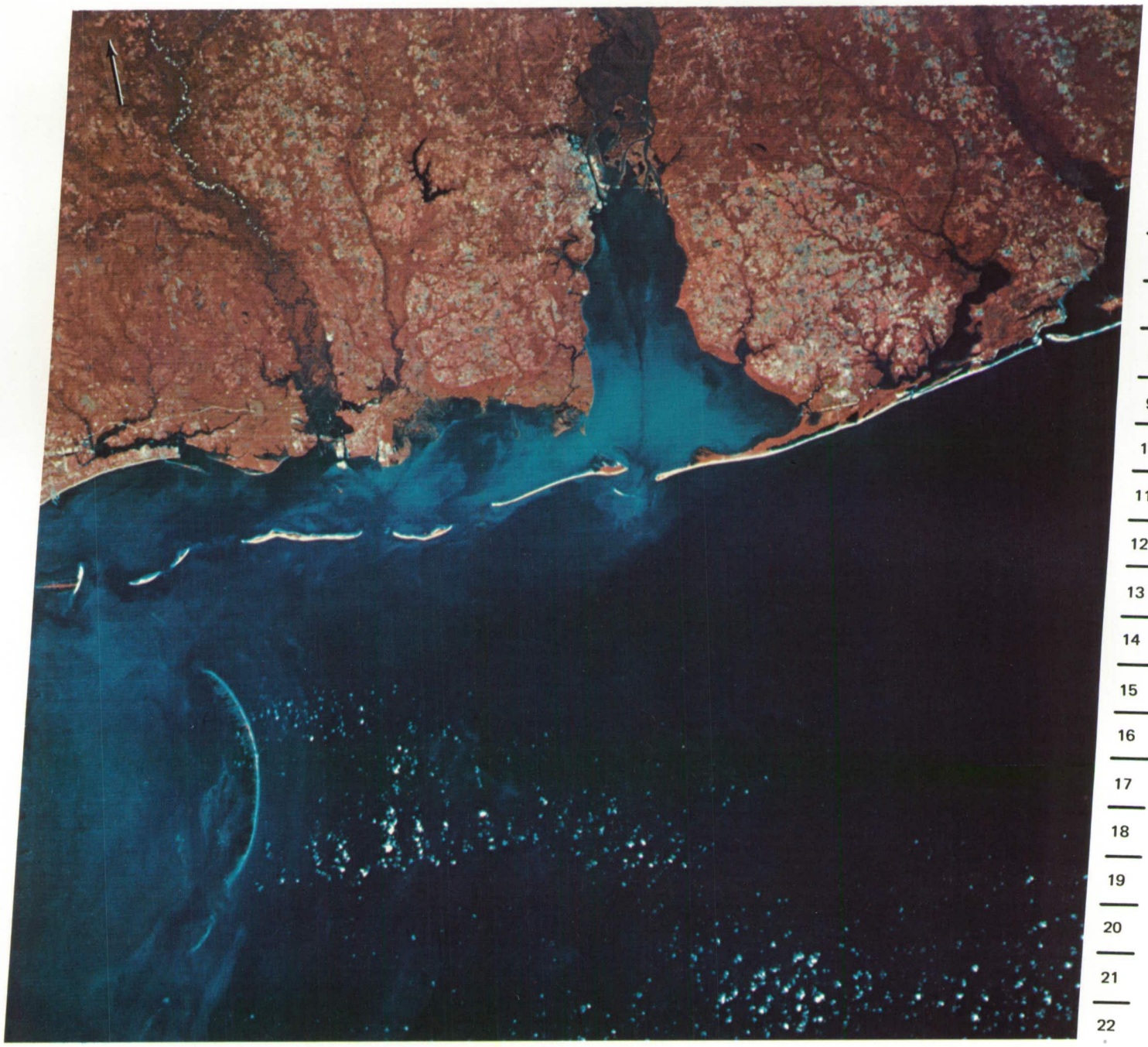


PLATE 26

CAPE CANAVERAL, FLA.: Two contrasting geomorphic landscapes are depicted in this image. The hundreds of lakes shown here occupy solution-weathered sinkholes, now filled with water, creating a pock-marked surface known as karst topography. Three of the larger lakes are Lake George in the north (*G*–4), Lake Apopka in the center (*I*–13), and Lake Kissimmee in the south (*O*–21). Much of the limestone rock material underlying this portion of central Florida is honeycombed with water-filled subterranean passageways, some of which are associated with artesian springs. Silver Springs near Ocala (*A*–6) is said to have a daily discharge of some 22 cubic meters of water per second (500 million gallons of water per day). The linear features trending northwest to southeast (parallel to the coast) are emerged beaches produced as the sea retreated from central Florida, which it covered until fairly recent times.

The second distinctive landform environment in the image is represented by the offshore bar and island complex that fringes Florida's central Atlantic coast. Such development, in addition to the linear marine terraces (*H*–7; *O*–15) in the lake district, attest to Florida's geologic youth. The offshore complex consists of a narrow, sandy beach strip (*Q*–7) bordered inland by the Indian River Lagoon (*R*–9) and a series of islands including Merritt Island (*T*–12). The offshore island and beach area houses the John F. Kennedy Space Center. Individual launchpads are visible (*U*–11) on the crescent-shaped cuspate bar the easternmost point of which is Cape Canaveral (*V*–13). The network of causeways connecting the offshore development with the mainland is readily visible in this image (*S*–12; *T*–14). In addition, the Bee Line Expressway, the central artery linking Orlando (*L*–14) and the coastal area, follows a straight traverse across the St. Johns River lowland (*P*–14). The course of the St. Johns and its tributaries is clearly marked by the brighter red vegetation signature that outlines the denser gallery forest associated with the river course (*P*–13; *N*–12). The location of Ocala National Forest is similarly marked (*C*–6; *H*–6). Cumulus clouds occur in several places over the mainland (*P*–9; *J*–1) as well as out over the open water (*T*–3). *1045–15275:* September 6, 1972.

PLATE 27



MOBILE, ALA.: This scene shows the Gulf Coast from Pensacola, Fla. (*U*–6), to Biloxi, Miss. (*B*–10). Protected by a large natural harbor, Mobile, Ala. (*L*–5), is a large port providing the Gulf Coast with modern shipping, ship building, and repair facilities. Woodpulp is a major industry here, the surrounding pine forests supplying raw materials for many paper and rayon plants. Brookley Air Force Base is located south of the city (*K*–6).

This part of the Gulf Coast features numerous offshore bars, built by wave and current action. These sandy islands and spits provide a wide variety of resort beaches and recreation areas. A National Seashore Park and Wildlife Refuge are established on Horn Island (*E*–12), and wildlife refuges are located on Petit Bois Island (*H*–12) and the Chandeluer Islands (*E*–17). Fort Gaines, on the east end of Dauphin Island (*L*–10), protected Mobile Bay during the Civil War.

The bright white of the sandy soil outlines extensive areas of cleared land east of Mobile Bay. Other evidences of human activity are the narrow strip of manmade beach at Biloxi, an industrial park marked by the white square on Biloxi Bay (*C*–10), and the large shipyard opposite Pascagoula, Miss. (*G*–10). Sections of Interstate 10 are seen north of Biloxi, and from Mobile east to Pensacola and across Escambia Bay (*U*–5). U.S. 98 crosses Pensacola Bay on the south (*U*–7). Pensacola Naval Air Station is located near the inlet (*T*–8). The Intracoastal Waterway canal connects Bon Secour Bay with Perdido Bay (*Q*–9). The belts of vegetation to the east mark low coastal terraces. *1482–15541;* November 17, 1973.

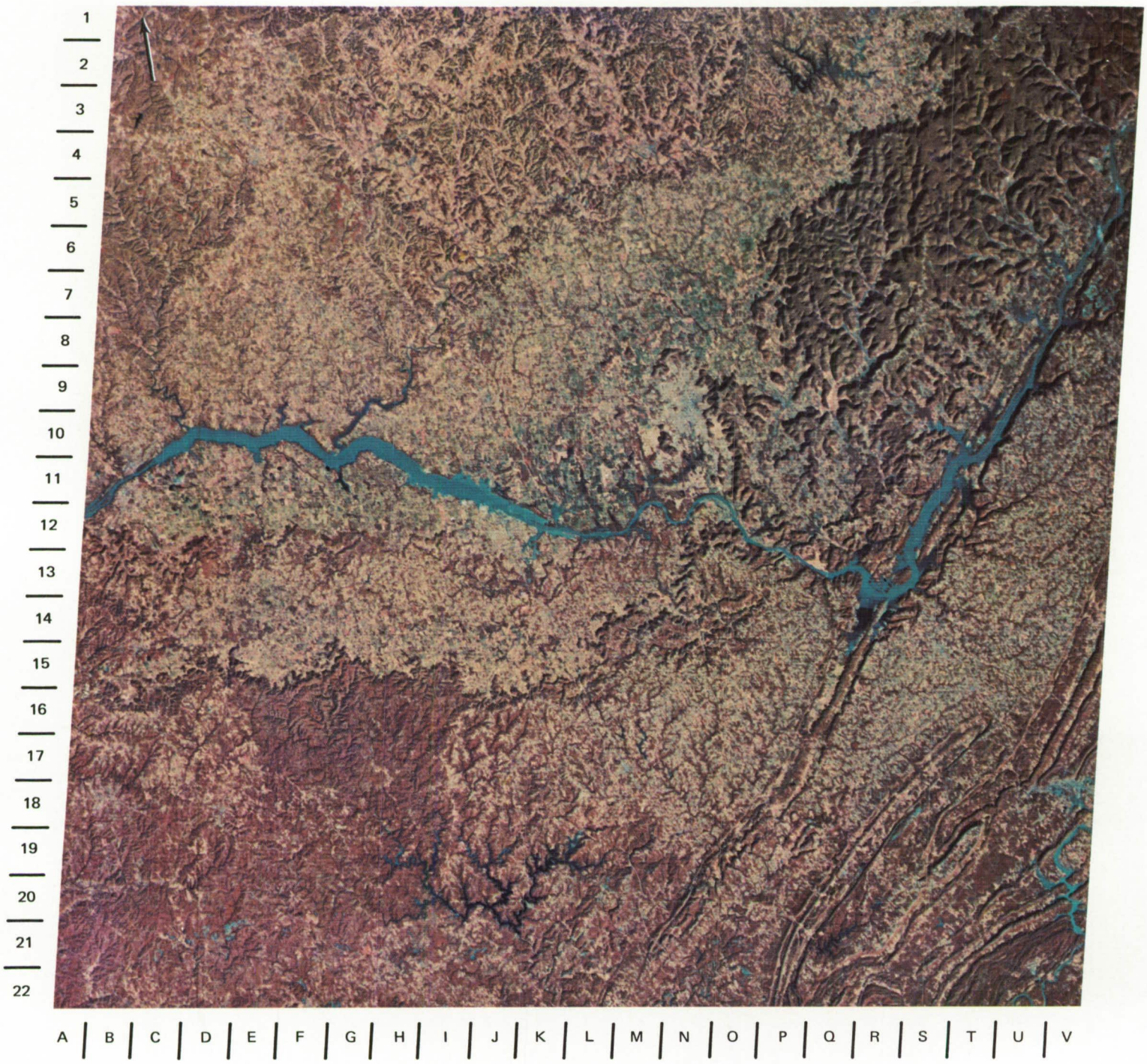
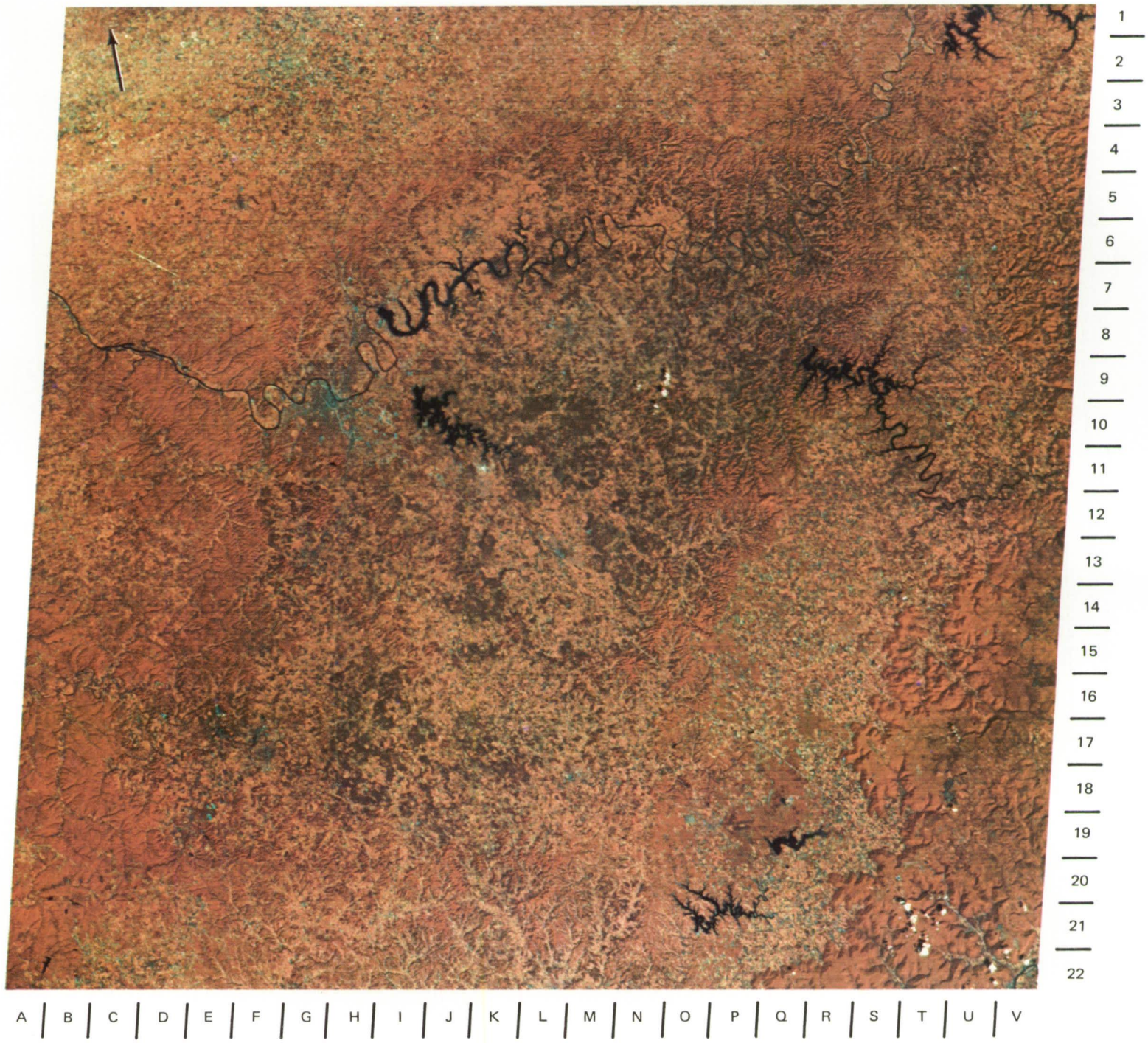


PLATE 28

HUNTSVILLE, ALA.: Two prodigous engineering projects are represented by this image: the Apollo program and the Tennessee Valley Authority. Huntsville, Ala. (*M*–9), just south of the Tennessee border, is the location of Marshall Space Flight Center, where many of the rockets, including the great Saturn V used in the Apollo program and other space projects, were developed. The Center itself is barely visible just southwest of Huntsville. The other engineering project is represented by the Tennessee River, bisecting the image which under the Tennessee Valley Authority has been harnessed by some 27 major dams. Visible here are Lakes Wilson (*D*–10), Wheeler (*I*–11), and Guntersville (*R*–13; *U*–8), all formed by dams on the Tennessee River. As a result of this project, the river is navigable all the way from the Ohio River to Knoxville, Tenn., a distance of 1050 kilometers (650 miles). In addition, the project produces billions of kilowatt hours of electricity, controls floods, and provides many kilometers of recreational waterways and waterfront.

The image covers parts of two physiographic provinces. The linear ridges at lower right, in Alabama, are in the southern part of the Valley and Ridge province of the Appalachians, sections of which are shown in other images. These are folded and overthrust Paleozoic sedimentary rocks the structure of which has been etched into mountains by differential erosion. Guntersville Lake occupies a fold axis on the edge of the Valley and Ridge province. To its northwest are the Gunter Mountains (*S*–9), part of the Cumberland Plateau (*P*–8; *V*–1). This plateau is in turn the southern end of the Appalachian Plateau, underlain by gently folded Paleozoic sedimentary rocks. Much of it is intensively farmed, although this image, transmitted in December, does not show field patterns clearly. A few cities are visible: Florence, Ala. (*B*–10), and Fayetteville, Tenn. (*L*–4), are two; Chattanooga is just off the upper right corner. Two reservoirs shown are Lewis Smith Lake (*J*–19) and Tims Ford Reservoir (*P*–2). *1158–15552;* December 28, 1972.

PLATE 29



THE NASHVILLE DOME AND BASIN: A broad domal uplift centered southeast of Nashville, Tenn. (*G*–9), has brought Ordovician limestones and shales to the present surface. These lower Paleozoic rocks are overlain unconformably by Mississippian carbonates. Erosion has breached the dome to expose the Ordovician rocks, which have outward dips generally less than 1°, in a wide basin whose elevations are 150 to 210 meters (500 to 700 feet) above sea level. The surrounding Highlands Rim Uplands stand at altitudes of 300 to 340 meters (1000 to 1100 feet). This plateaulike terrain is capped by the resistant chert-bearing Fort Payne Formation, which weathers to release cherty terrace gravels that further assist in keeping the uplands from being lowered as fast as the central Ordovician strata. Overall, this uplands is much dissected to produce rolling hills and narrow glens. Some of the Mississippian limestones are susceptible to sink-hole development so that karst topography is common (*B*–12; *R*–14). The boundary between basin and uplands is outlined by the Western (*E*–11) and Eastern (*N*–16) Highland Rim Escarpment, which locally has a relief of 30 to 60 meters (100 to 200 feet) or so. Isolated outliers of Mississippian rocks rise some hundred meters (several hundred feet) above the otherwise gently rolling surface of the basin. Beyond the karst terrain on the east side of the basin, Pennsylvanian rocks constitute the western margin of the Cumberland Plateau (*T*–17), a dissected flatlands rising 150 or more meters (500 or more feet) above the basin floor.

The Cumberland River (*N*–6) crosses the northern part of the basin while the Duck River (*B*–15) traverses the southern end. The Old Hickory (*I*–7) and Center Hill (*Q*–8) Reservoirs result from damming of the Cumberland. Percy Priest Lake (*I*–9) is another dammed water body now in the eastern suburbs of Nashville. The Elk River Reservoir (*P*–20) is on the Elk River. The towns of Columbia (*F*–16), Shelbyville (*L*–17), Tullahoma (*O*–18), and Murfreesboro (*L*–12) all lie within the Nashville basin.

The forests around the basin are mainly oak and hickory while those of the Cumberland Plateau are a mixed assemblage of oak, basswood, maple, and beech. Within the basin, bare rocky areas of limestone (*J*–13), known as glades, are characterized by cedar growth, with some oak. Farm crops include oats, soybeans, corn, hay, and tobacco. *1086–15544;* October 17, 1972.

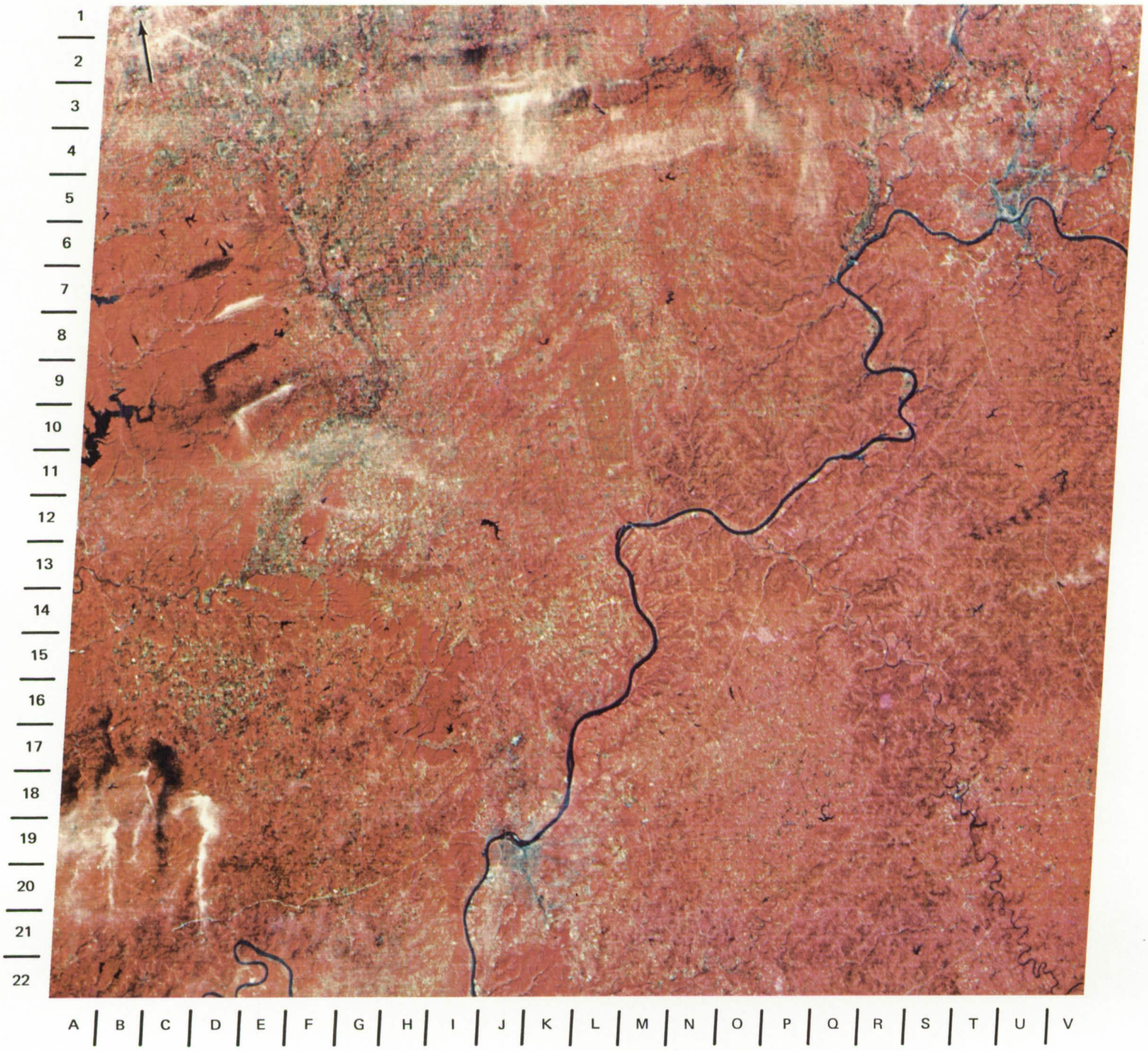


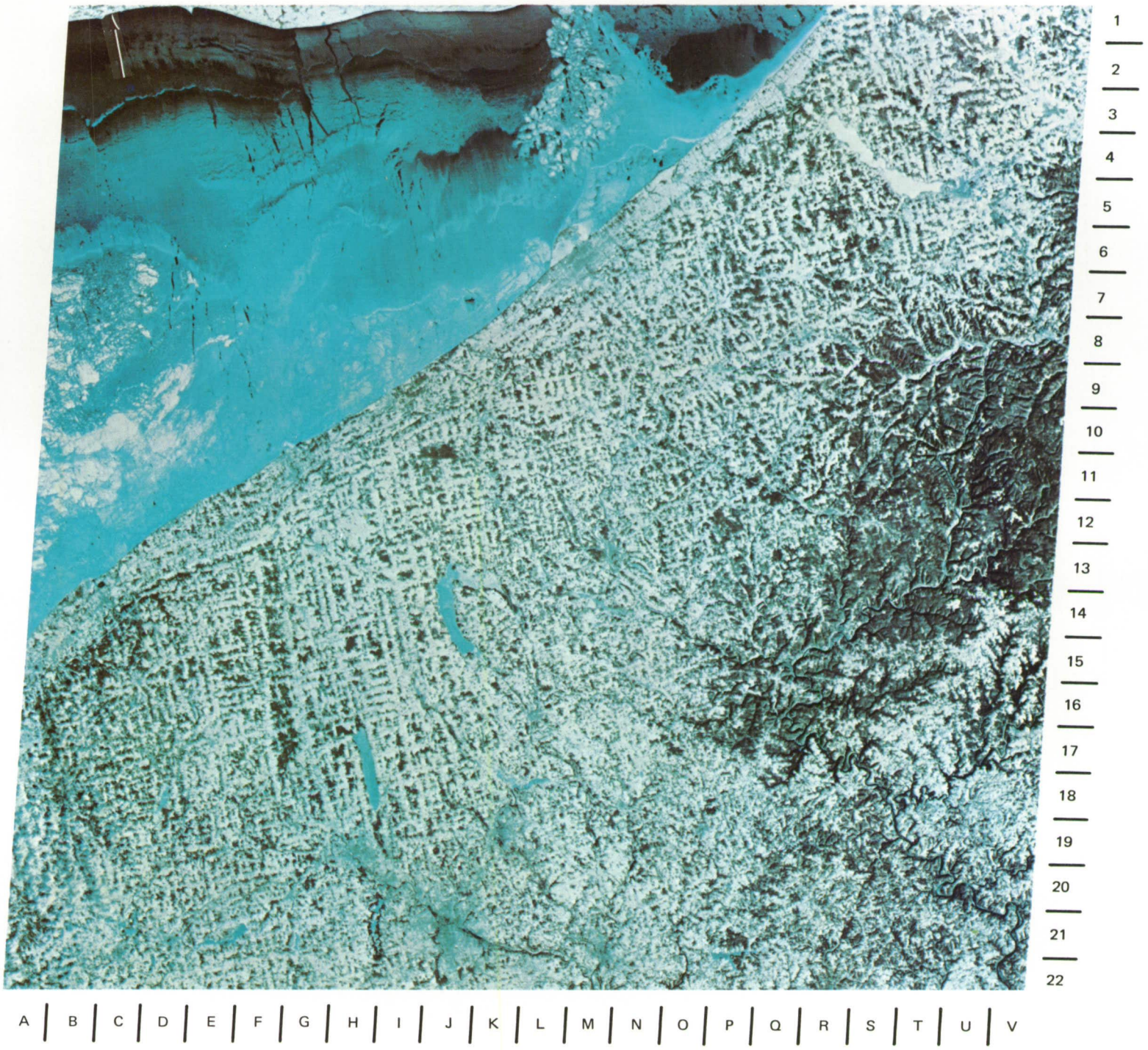
PLATE 30

LOUISVILLE AND CINCINNATI: The Ohio River is the dominant drainage in this scene. After flowing slightly to the north past Cincinnati (*T*–5), it turns southwestward at the Ohio-Indiana line (*Q*–6), where it is joined by the Great Miami River (*R*–3) and continues past Louisville, Ky. (*J*–19). The terrain on either side of the river is influenced by the regional geology. The northern end of the broad Cincinnati arch continues beyond the top of the image. At the Jessamine structural high near Frankfort, Ky. (*T*–17), the Kentucky River has cut into middle Ordovician limestones. A subdued scarp runs northward (*Q*–16) into Ohio west of this river, and hollows and narrow valleys slice into the gently rolling uplands of the Inner Bluegrass region above the flood plains of the Kentucky and Ohio Rivers. To the west, successively younger north-trending sedimentary units outcrop along the eastern flank of the Illinois Basin. The Knobstone escarpment (*G*–13; *I*–16) in Indiana and northern Kentucky, composed of lower Mississippian strata, rises as much as 180 meters (600 feet) above the glacial plains in Indiana (*J*–10) and the Outer Bluegrass region in Kentucky (*M*–20) to the east and in places is broken into isolated hills called "The Knobs." West of the scarp, the Mississippian rocks underlie the Mitchell plains—a subdued hilly terrain pockmarked here and there with sinkholes. Most of southeastern Indiana east of the scarp is covered by drift from the Illinoian glacial advance.

Wheat, corn, and soybeans are the main crops planted in the glacial soils of Indiana. Farming in Kentucky bluegrass country is devoted mostly to tobacco, with some corn and alfalfa. Oak and hickory constitute much of the forest lands of Kentucky and are dominant in the Hoosier National Forest south of the White River (*B*–13) and around the Monroe Reservoir (*A*–9) further north. Oak-gum-cypress occur in a belt in Indiana north of the Ohio from Louisville eastward. Maple and beech are common in the glacial plains.

Interstate 75 between Frankfort and Cincinnati, Interstate 71 between Cincinnati and Louisville, and Interstate 64 between Frankfort and Louisville stand out; the extension of Interstate 64 west of Louisville is particularly conspicuous. The long faint rectangle at *L*–10 outlines the U.S. Army's Jefferson Proving Ground. *1086–15535;* October 17, 1972.

PLATE 31



ERIE, PA.: The rural, agricultural, urban, industrial aspect of the northeastern United States is succinctly shown in this snow-covered scene of portions of three States (Ohio, Pennsylvania, and New York) and a small portion of the coastal fringe of Ontario, Canada, on the northern shore of frozen Lake Erie (*E*–1).

The industrial cities of Erie, Pa. (*L*–6), and Ashtabula, Ohio (*F*–10), border Lake Erie while Warren (*H*–19) and Youngstown, Ohio (*J*–20), and New Castle, Pa. (*M*–21), are situated on interior river valleys. Jamestown, N.Y. (*T*–4), is located on the southeastern end of frozen Lake Chautauqua (*R*–4).

The rectangular grid pattern typical of midwestern U.S. township and section survey is reflected in the agricultural area on the glacial and lake plains that border and extend southward from Lake Erie in the western half of the scene. The snow cover enhances the grid pattern considerably. Mosquito Creek Reservoir (*H*–17) and Pymatuning Reservoir (*I*–13) are located within the glacial plains of this agricultural area.

The Allegheny National Forest (*T*–12) through which flows the Allegheny River (*T*–10) is situated on the stream-dissected sedimentary rocks of the unglaciated western portion of the Appalachian Plateau. The intricate dissection of the plateau has created a rough, rolling hill landscape not suitable for corn belt or other extensive agricultural practices, hence the lack of evidences of intensive land use. The Allegheny National Forest area is primarily a region of Appalachian oak forest with its western boundary serving approximately as the dividing line between oak forest and the northern hardwood forest, most of which has been cleared for agricultural purposes. *1209–15362;* February 17, 1973.

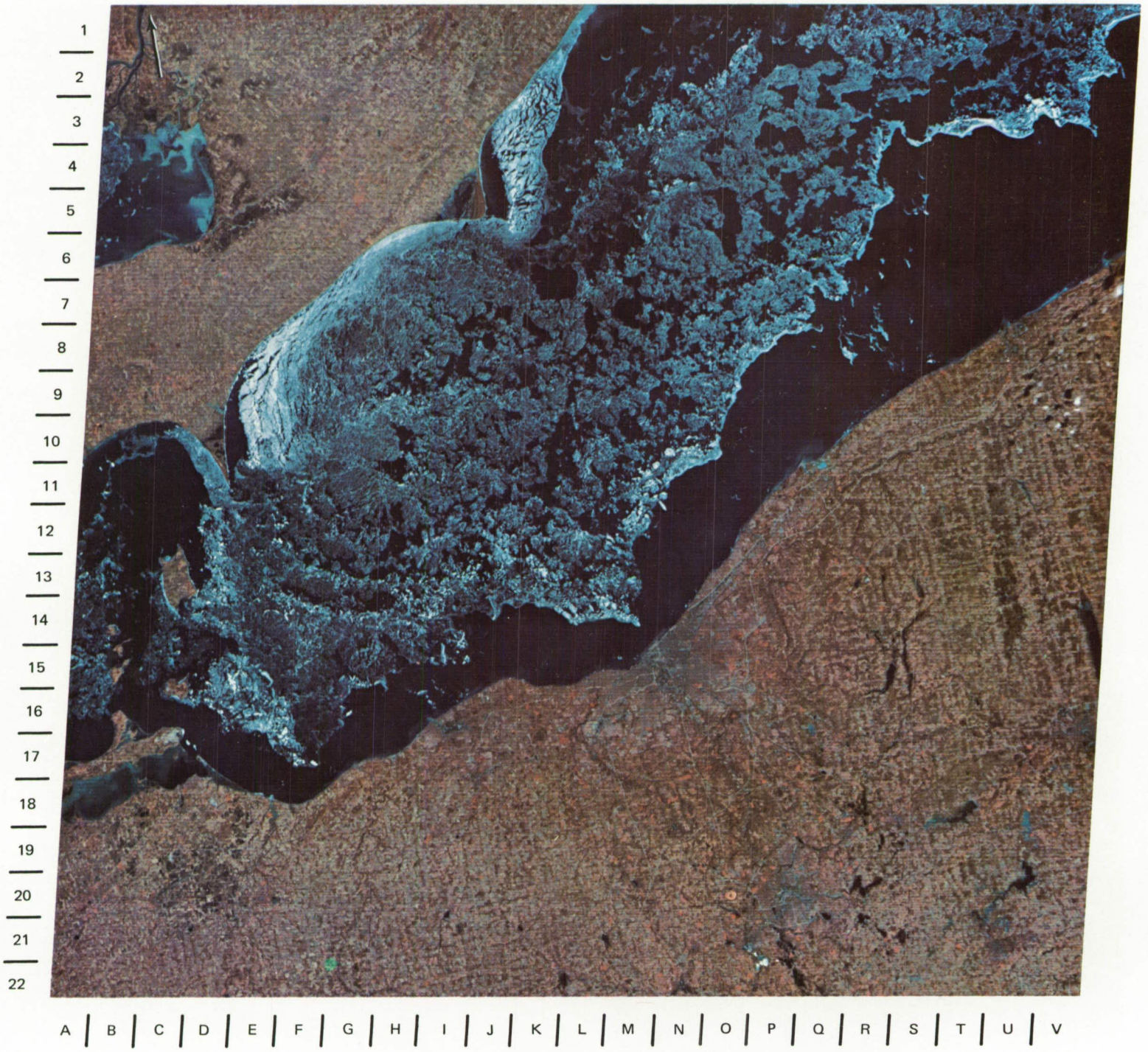


PLATE 32

WESTERN LAKE ERIE: Northern Ohio (*K*–19) and the southernmost part of Canada (*F*–2) (in the Province of Ontario) surround Lake Erie—the shallowest of the Great Lakes (average depth of 18 meters (58 feet)) and the only one whose bottom is above sea level (~110 meters (~360 feet)). In early March 1973, the lake ice that typically extends over all this body of water and prevents iron ore shipment from the Minnesota-Michigan iron ranges to the Ohio and Pennsylvanian steel mills has begun to break up. The shore areas on the U.S. side are now free of ice because of shallow water and wind-driven choppiness. Much of the central ice is partly melted and is fragmenting into individual slabs.

The metropolis of Cleveland (*M*–15) lies near the southern end of the lake. This city and the nearby towns of Sandusky (*D*–10), Lorain (*J*–16), and Ashtabula (*P*–11) are built on lacustrine deposits from Lake Maumee, ancestral to the present Lake Erie. Eight to 16 kilometers (5 to 10 miles) inland, wave-cut cliffs 30 to 60 meters (100 to 200 feet) higher than the lake level line parts of the lowlands. The uplands consist of Illinoian and Wisconsin glacial drift overlying Devonian shales near the lake and Mississippian and Pennsylvanian bedrock further south. The Cuyahoga River (*R*–16) begins almost due east of Cleveland, flows southwestward past Akron (*P*–20), and then turns abruptly northward through Cleveland as it empties into the lake. The Grand River (*S*–10) starts near Warren (*V*–16) west of the Mosquito Creek Reservoir (*V*–14) heading northward until it deflects almost due west after crossing over the bluffs along Lake Erie. Because of the dormant stage of growth in late winter, the regional pattern of farming—that of general alinement of individual farm property lines along township and range section lines—stands out particularly where beech, maple, oak, or ash trees have been left in narrow bands along borders between adjacent properties. In summer these farms produce mostly corn, barley, soybeans, and sorghum; winter wheat is grown on many plots. Pointe aux Pins (*I*–5) and Point Pelee (*C*–10) extend into the lake from the Ontario shore. The Thames River (*F*–2) empties into Lake St. Clair east of Detroit. *1228–15422*; March 8, 1973.

PLATE 33



THE STATE OF MICHIGAN: This mosaic was prepared by the General Electric Photographic Laboratory from parts of 43 Landsat color composite images. Of particular interest are these landmarks and geographic features (see plate 34 for letter identifications): Detroit (*A*), Lake Erie (*B*), Lake St. Claire (*C*), Lansing (*D*), Grand Rapids (*E*), Saginaw (*F*), Bay City (*G*), farmlands of central Michigan (*H*) with characteristic tree-lined boundaries, Saginaw Bay (*I*), Lake Huron (*J*), West Branch moraine (*K*), drumlin swarm (*L*), Grand Traverse Bay (*M*), Lake Michigan (*N*), Grand River (*O*), Muskegon River (*P*), Manistee River (*Q*), Straits of Mackinac (*R*), Upper Michigan (*S*) northwoods, Marquette (*T*), Sault Ste. Marie (*U*), Keweenaw peninsula (*V*), Lake Superior (*W*), and Isle Royale (*X*).

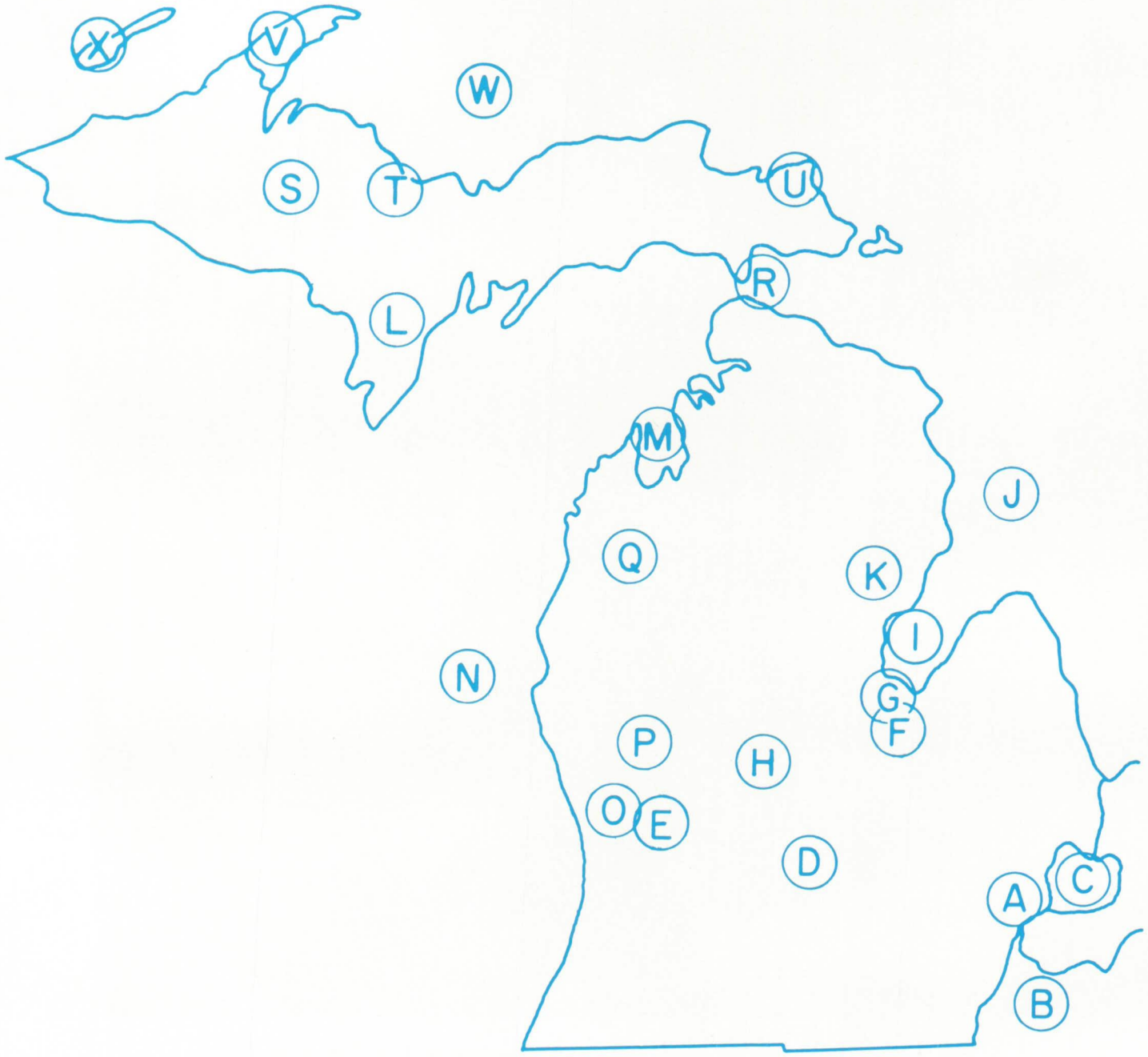
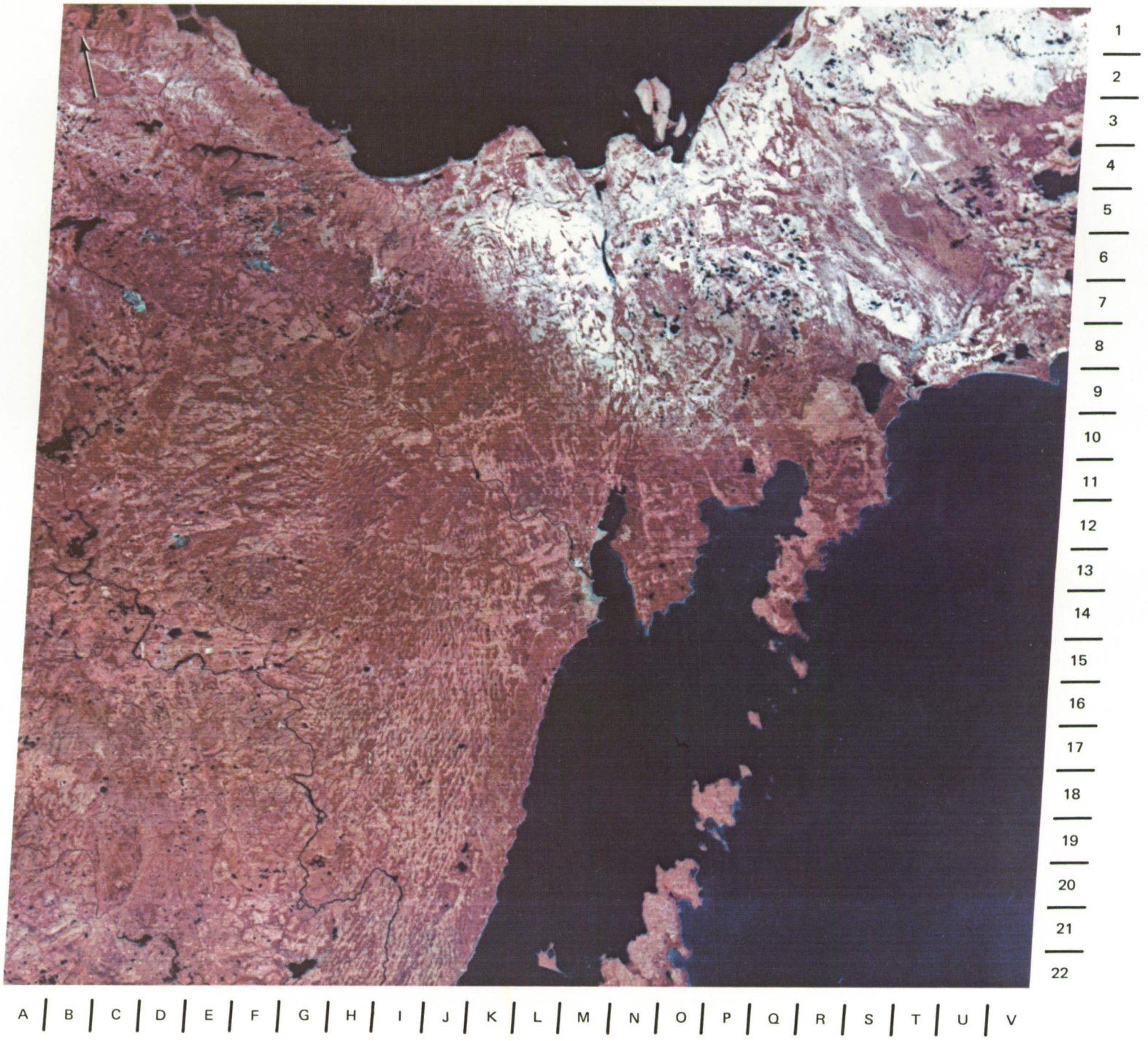


PLATE 34

PLATE 35



UPPER MICHIGAN: This part of the State consists of a long neck of land bounded by Lakes Superior (*H*–2) and Michigan (*T*–17) that extends from the Menominee River (*G*–20) and northern Wisconsin (*C*–19) on the west to the Sault Ste. Marie area to the east. The region is generally covered with northern hardwoods (maple, birch, and beech) and spruce-fir forests along with scattered pinewoods. Conifer bogs (*T*–5) occupy some of the lower areas drained by the Ford (*J*–13), Escanaba (*J*–11), Whitefish (*M*–9), and Sturgeon (*O*–8) Rivers that flow into the Little (*M*–12) and Big (*P*–12) Bays de Noc or by the Manistique River (*T*–7) and its tributaries further east between Indian (*R*–9) and Manistique (*V*–4) Lakes.

The northwest edge of the Interior Lowlands extends beyond the shores of Lake Michigan. A bedrock sequence of lower Paleozoic sedimentary strata generally runs northeast subparallel to the shorelines along both lakes. Silurian dolomites make up the Door Peninsula (*N*–21) of Wisconsin, which bounds Green Bay (*L*–20), and the Garden Peninsula (*Q*–12); these form part of the same Niagara escarpment found at Niagara Falls near Buffalo far to the east. Successively older units recur to the west, with the gentle Magnesian escarpment of lower Ordovician age just east of Cambrian sandstones that run north to a point on Lake Superior (*H*–5) and thence eastward along its snow-covered shores. The Superior Uplands Province (*B*–8)—a part of the Laurentian or Canadian shield of Precambrian rocks—occupies the remainder of the image to the west. Most of the metasedimentary rocks exposed here are Huronian in age. Crystalline intrusive rocks and Archean Keewatin greenstones underlie most of the Marquette Range (*C*–7) and the Huron Mountains (*B*–1) (up to 300 meters (1000 feet) relief) west of the port town of Marquette (*G*–4). Hematitic iron ores are mined near that town, around Lake Michigamme (*A*–5), the Michigamme Reservoir (*A*–10), and at Iron Mountain (C–14).

This region was extensively glaciated during the Pleistocene. Lake Superior itself—the world's largest freshwater lake in terms of surface area, with depths reaching to 210 meters (700 feet)—was probably produced from scouring by the Superior ice lobe of Wisconsin age. Although older glacial deposits are everywhere present, those of the Wisconsin dominate the surface topography. One of the best-developed large drumlin fields (*I*–16) in North America is found west and south of Escanaba (*L*–13). *1089–16090;* October 20, 1972.

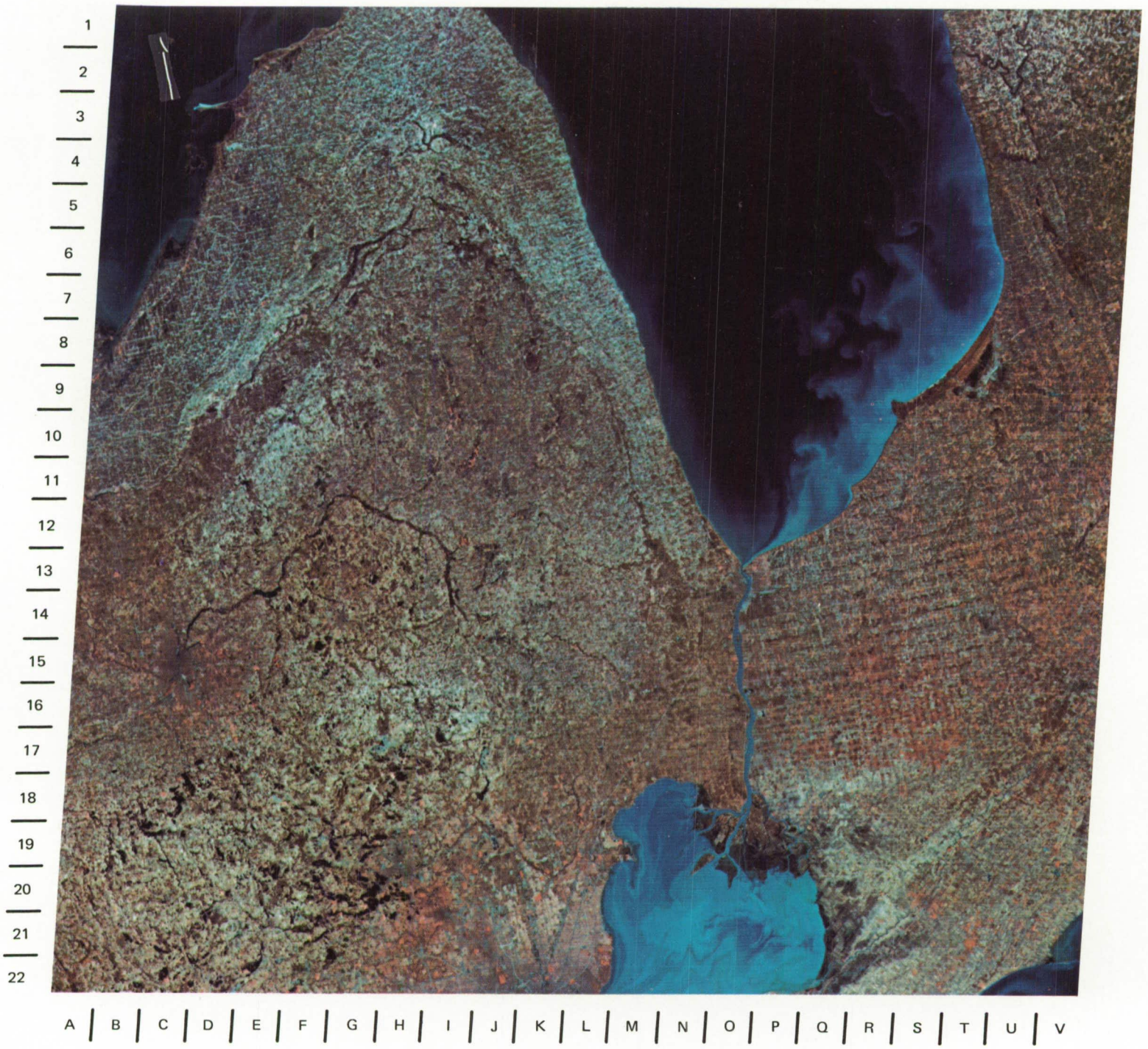


PLATE 36

THE LOWER PENINSULA OF MICHIGAN: This scene displays the southeastern part of Michigan's Lower Peninsula and adjacent Ontario. Part of Detroit (*K*–22) is recognized by its dark gray-blue pattern. A brighter blue linear marking (*L*–20) is caused by road construction associated with a new interstate highway. Golf courses and cemeteries stand out as bright red at this time of year. Other prominent Michigan cities in this image are Flint (*C*–14) and Pontiac (*G*–17). The neighboring cities (*O*–13) of Sarnia, Ontario, and Port Huron, Mich., are located at the southern extremity of Lake Huron (*P*–7) where it discharges southward into the St. Clair River (*O*–15). Sediment plumes are quite evident in both lakes. The discharge point of the St. Clair River into Lake St. Clair (*N*–20) is marked by a classic example of a freshwater delta.

The area pockmarked by lakes northwest of Detroit essentially outlines the limits of the Defiance Moraine (*G*–18) caused by the stagnation and melting of Pleistocene glaciers about 12 000 years ago. This rolling countryside dotted with kettle lakes (*H*–20) is both the prime recreational region for Detroit and a principal source of glacial sand and gravel for building. Subsurface drilling also indicates that the area is underlain by the highest bedrock elevations in southeastern Michigan, evidenced at the surface by the deflections of the Flint River (*H*–12) around the buried bedrock topography. The Cass River (*D*–8), which flows into Saginaw Bay (*A*–3), and the Black River (*L*–10), which meets the St. Clair River at Port Huron, are deflected in opposite directions by the lobate arc of the Port Huron Moraine (*D*–9; *J*–7). The lines subparallel to the shoreline of Lake Huron (*K*–6) are old beaches formed by ancestral Lake Huron during the past glacial period. On the peninsula, the land grid system, which divides the land into sections each 1.6 kilometers (1 mile) square, is made readily apparent by the network of roads (*D*–5) that follow the section boundaries. *1247–15474;* March 27, 1973.

PLATE 37



DETROIT, MICH.: Greater Detroit (*K*–5), the auto capital of the world, is located at the southeastern border of Michigan on the Detroit River (*K*–6) across from Windsor (*L*–5), Ontario, Canada. This river is part of the connection between Lake Erie (*S*–11) and Lake Huron further north; the river passes into Lake St. Clair (*O*–2), which in turn is joined to Huron by the St. Clair River. This channel system is inherited from the glacial age when the present Great Lakes were larger. Lake Maumee was the ancestral Lake Erie.

Much of this scene consists of gray-brown soils derived from lacustrine sediment deposited by Lake Maumee (roughly coincident with the blue-gray open areas around the Maumee River (*G*–18); the old shoreline is particularly evident at *P*–17. Glacial tills from Kansan, Illinoian, and Wisconsin ice advances in the Pleistocene cover almost all the remaining surfaces. End moraines occur northwest of Detroit and Ann Arbor (*E*–7), behind which are numerous kettle lakes (*B*–6). The few rock outcrops and drilling data indicate a bedrock geology defined by northwest-dipping Silurian, Devonian, and Mississippian strata along the southeast flank of the Michigan Basin. Older Silurian rocks underlie much of northwest Ohio (*D*–17) from the city of Toledo (*I*–14) southward, but Devonian rocks reappear around Sandusky (*R*–15) at the head of Sandusky Bay (*P*–15).

The land use pattern in this scene is typical of this part of the upper midwest. The once extensive forests have been cleared to farmland, but narrow strips of trees line farm boundaries (*F*–14) or entire rectangular blocks of forest have been preserved. Elm-ash-cottonwoods are the dominant tree communities around or just north of the Maumee River. A maple-beech-birch assemblage develops south of Sandusky. Oak and hickory are the principal tree types west of Detroit and in a strip (*G*–15) to the south. Farms produce a diversity of crops including winter wheat, corn, oats, soybeans, sugar beets, and tomatoes, plus hay and grazing fodder for dairy cattle. Apple and peach orchards are also planted in the region.

Admiral Perry's naval victory in Lake Erie during the War of 1812 was won at the Bass Islands (*P*–13) south of Pelee Island (*Q*–11) in Canadian waters. *1319–15474;* June 7, 1973.

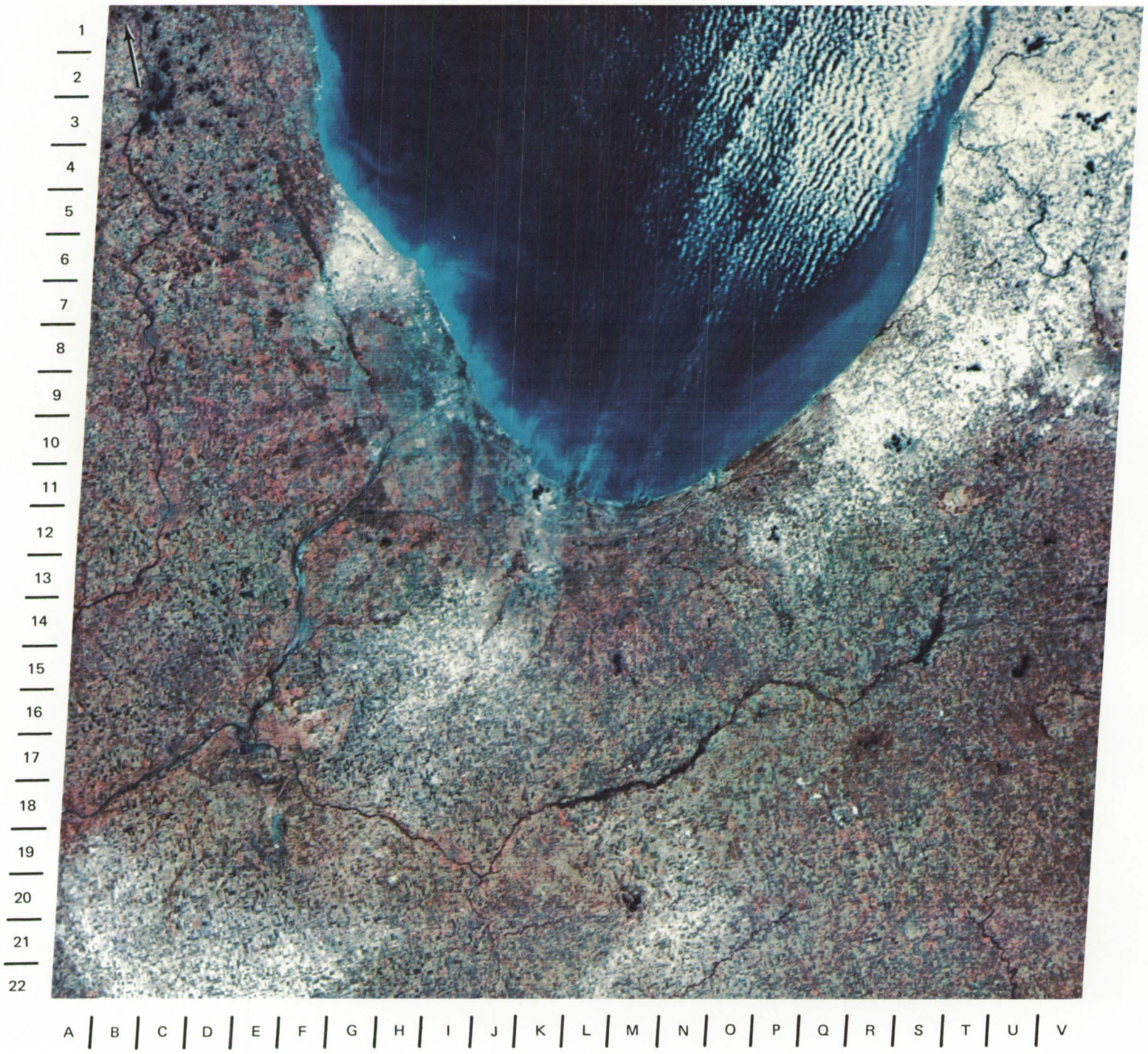
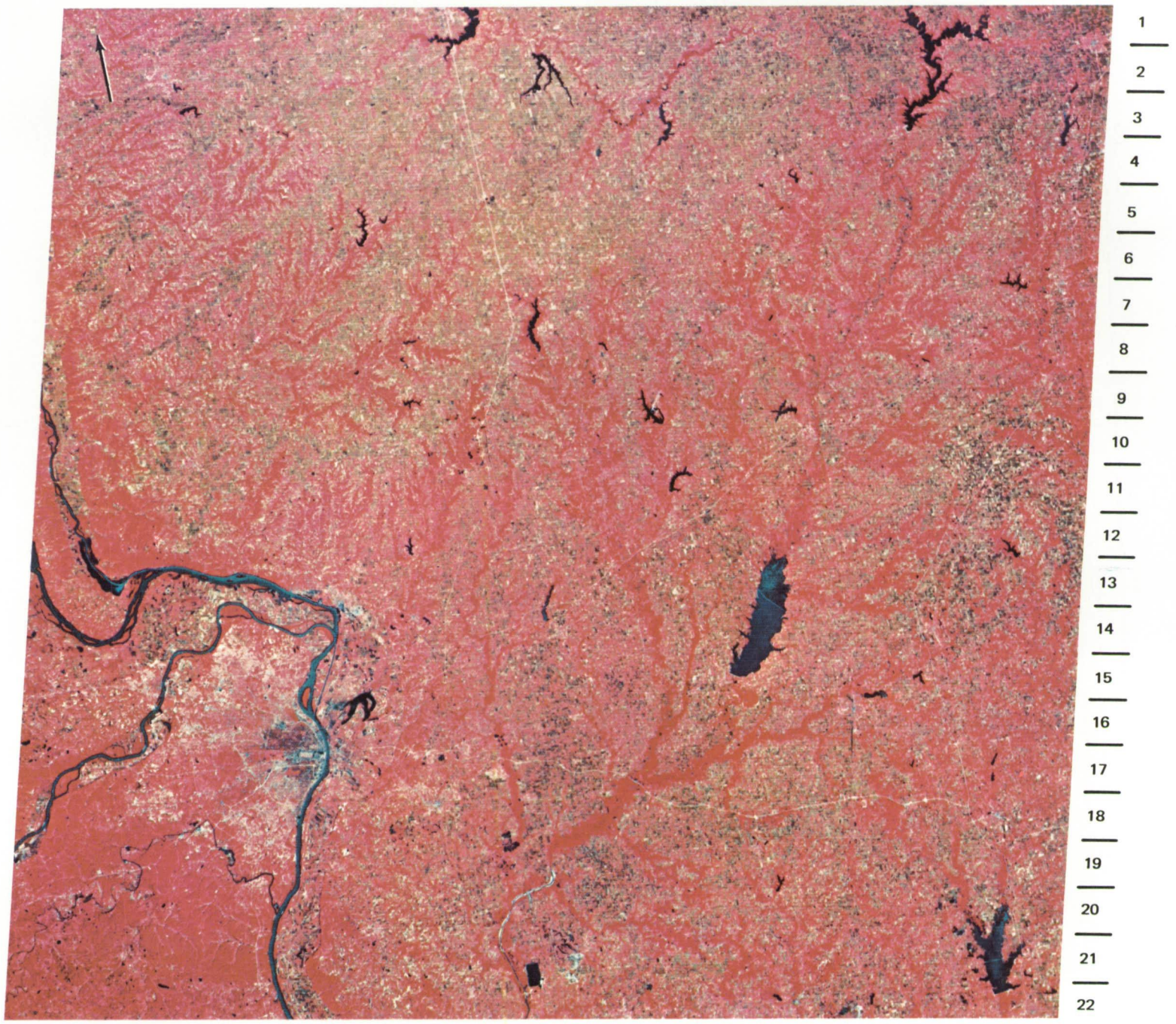


PLATE 38

CHICAGO, ILL.: The area covered by this image includes the second largest city of the United States, Chicago (*H*–9), thousands of factories, rich farmland, and an extensive network of railroads, highways, air routes, and pipelines. Other cities include Waukegan (*E*–3), Joliet (*E*–13), and, in Indiana, Gary (*L*–12) and Hammond (*K*–12). Chicago is the hub of the midcontinent area, and many of the individual highways and railroads are visible; some 40 railroads serve the city. Other landmarks include the Des Plaines River (*D*–3; *G*–9; *A*–18) and the Kankakee River (*J*–19; *O*–15).

The area lies in the northern part of the midwestern corn belt; other major crops include soybeans, oats, and wheat. Cattle raising is also important, and the great dairy region of the midcontinent lies just to the northwest of Chicago. Much of the industry of Chicago is, of course, related to agriculture: meatpacking is typical. The Hammond-Gary area is one of the great steelmaking centers of the country (indeed, of the world); Gary essentially formed around the huge steel plant built by U.S. Steel in 1906. This great concentration of industry has given rise to many environmental problems; for example, the weather around Gary has been significantly altered by the pollution and added heat from the factory area, with more cloudy days than the surroundings. This image may illustrate the effects of air pollution directly. Note the smoke plumes heading northeast across Lake Michigan from the Chicago-Hammond-Gary area. These appear to lead into the lines of clouds over the lake west of St. Joseph and Benton Harbor (*S*–3), Mich. It has been suggested that the smoke particles serve as condensation nuclei, promoting cloud formation. This interpretation is not necesarily certain, for the Great Lakes in general promote cloud formation simply by supplying water vapor to the atmosphere. It is for this reason that the areas southeast (i.e., to leeward) of the lakes generally have much more snow than those to the northwest. A suggestion of this enhanced snowfall is seen in southwest Michigan (*upper right*), although, of course, the snow distribution on this day was notably erratic. *1124–16050;* November 24, 1972.

PLATE 39



ST. LOUIS, MO.: The city of St. Louis (*F*–16) is situated about 32 kilometers (20 miles) below the "meeting of the waters"—the confluence (*G*–14) of the Missouri River (*C*–16) with the Mississippi River (*A*–13; *F*–20). A second junction of the Mississippi with the Illinois River (*A*–10) occurs another 32 kilometers (20 miles) to the west. The Meramec River (*D*–18), flowing east across the Salem Plateau (*C*–20), with rolling hills and narrow valleys of Ordovician carbonate rocks capped in places by Mississippian chert-bearing limestones, joins the Mississippi south of St. Louis. The Mississippi River flood plain is broad around St. Louis but narrows somewhat to the south as it passes through the more resistant carbonates. Carbonate rocks of similar age occur in a narrow zone (*B*–10) along the Illinois River where uplifted along a fault. Oak and hickory forests develop extensively on soils from these carbonate rocks. Where the bluffs of these three rivers are steep, thick beds of wind-deposited loess derived from glacial materials to the north have accumulated.

The State of Illinois occupies this scene east of the Mississippi River. Almost all the gently rolling terrain in this part of Illinois is underlain by coal-bearing shales of Pennsylvanian age, easily dissected to form distinctive dendritic drainage patterns (*F*–6), but much of the uplands has been covered with thin deposits of glacial till from the Illinoian ice advance. The Shelbyville (*S*–1) and Carlyle (*P*–13) Reservoirs were created by the damming of the Kaskaskia River (*K*–19). Lake Rend (*U*–21) is another dammed reservoir. Interstates 64 (*R*–17), 70 (*M*–12), and U.S. Highway 66 (*J*–7) feed into and out of St. Louis. Where these cross the Illinois prairies, farmers cultivate mostly corn, soybeans, and winter wheat. Trees along the river courses are mainly oak and hickory and open fields consist of bluestem prairie shortgrass. Strip mining has been applied to coal removal from parts of western Illinois, as indicated by the blue-toned scars (*G*–13; *L*–21). *1071–16104;* October 2, 1972.

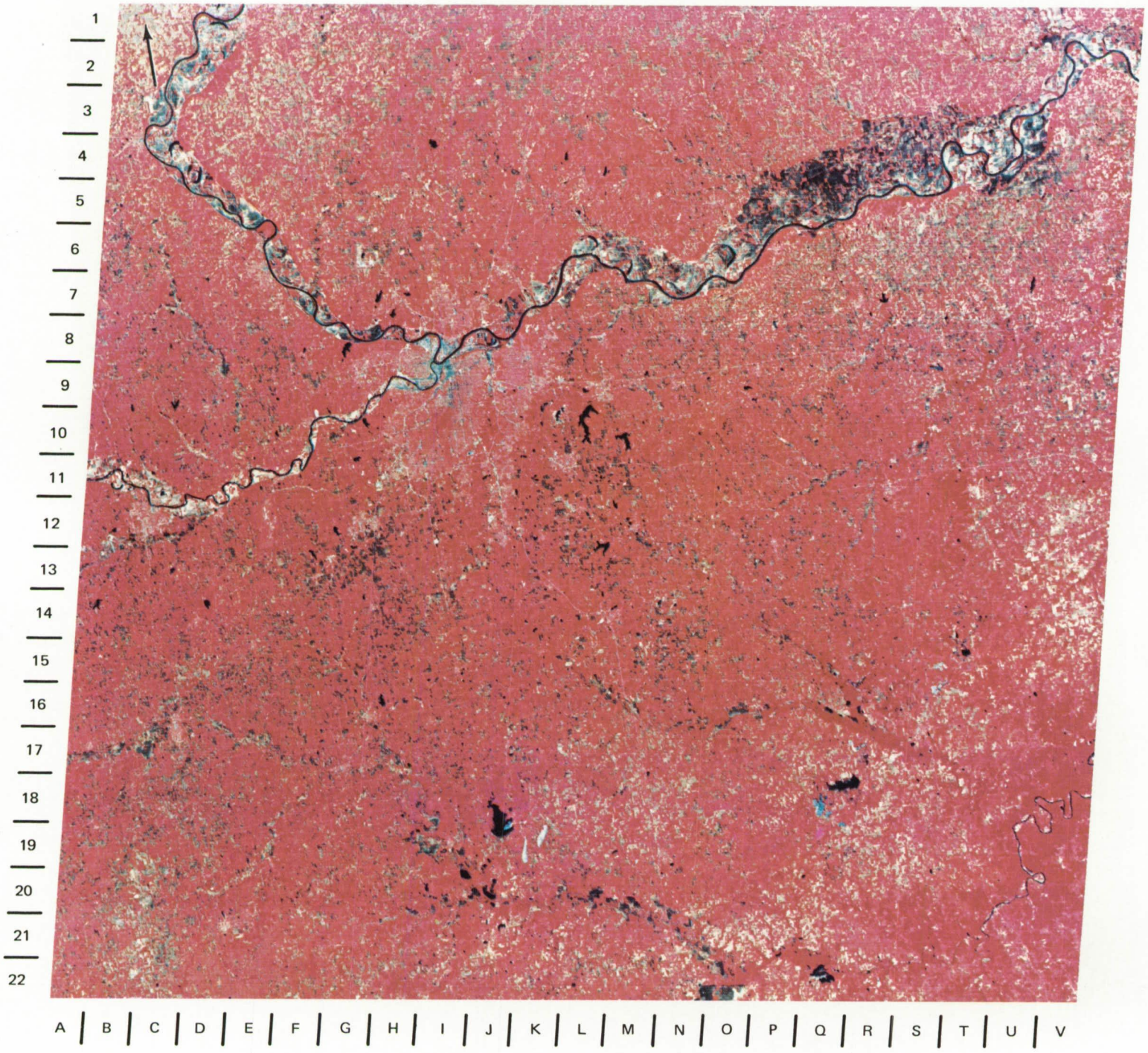


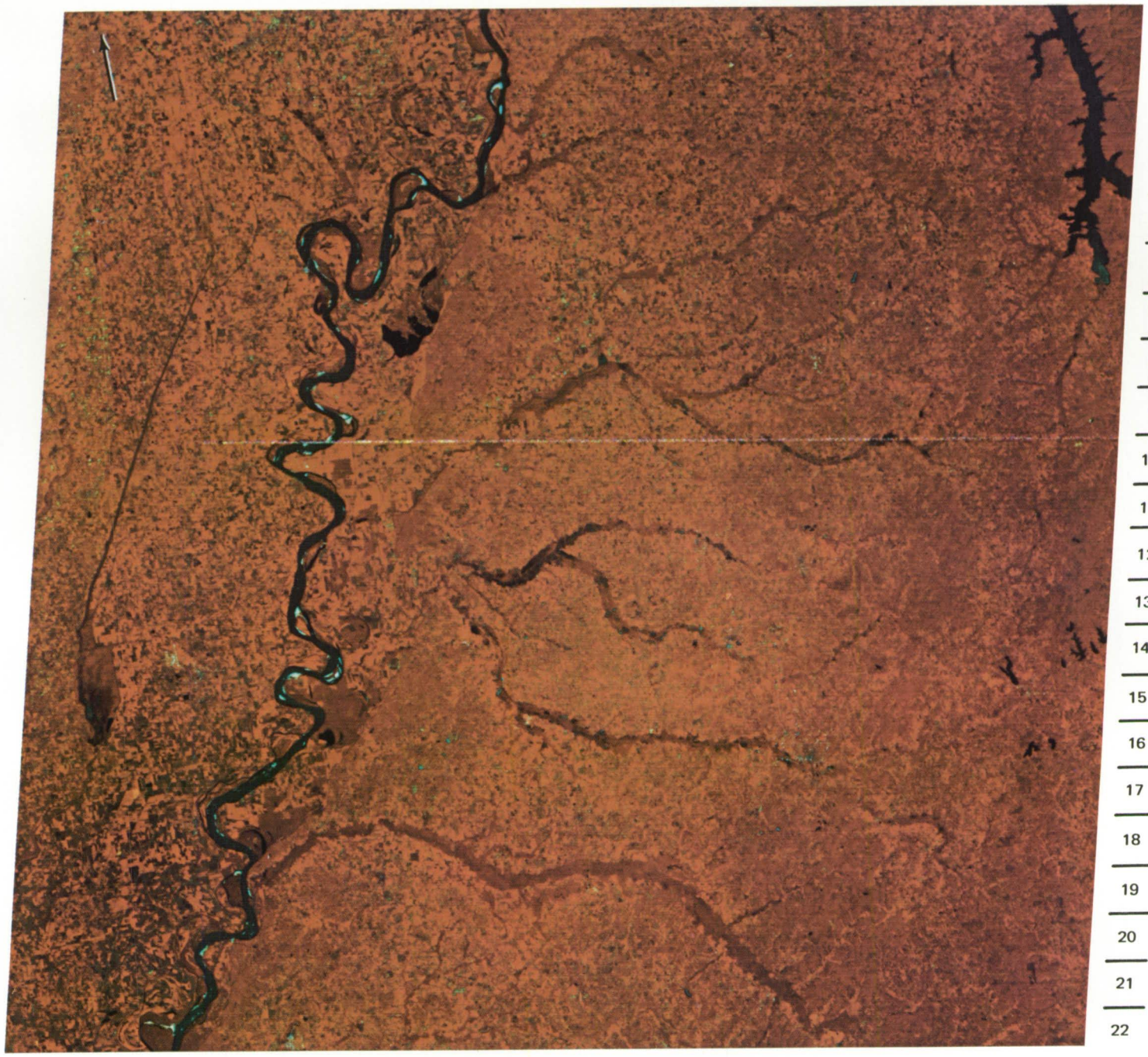
PLATE 40

KANSAS CITY: The twin cities of Kansas City, Mo. (*H*–9), and Kansas City, Kan., lie at the conjunction of the Kansas River (*D*–11) with the great Missouri River (*O*–6). The State boundary of eastern Kansas runs west of the Missouri at *B*–5 and thence through a line extending due south from Kansas City. Other larger towns in the scene include St. Joseph, Mo. (*C*–1), and the Whiteman Air Force Base (*S*–11), Interstates 29 (*D*–4), 35 (*B*–17; *I*–3), and 70 (*N*–9) and U.S. Highways 50 (*M*–11) and 71 (*L*–17) can be traced.

Most of the image covers part of the Osage Plains, a generally featureless, gently undulating surface. Bedrock (seldom exposed) consists of shales and thin sandstones, mixed with coalbeds, of Pennsylvanian age. Coal is mined by stripping (*P*–18; *R*–16) in some parts of the area and appears as blue in this image. The units trend northeast and become progressively older to the southeast. Low, almost imperceptible scarps mark the contacts between several stratigraphic units. The boundary with the Springfield Plateau section of the Ozark Plateau lies near the Osage River (*U*–18). Mississippian and Ordovician rocks underlie the plateau there. Soils from these rocks support oak and hickory forests but tributaries such as the South Grand (*Q*–6) and Blackwater (*S*–9) Rivers are lined with elm, ash, and cottonwood. Pleistocene morainal deposits from the Kansan ice advance cover the region north of the Missouri River and extend south of its present flood plain for 16 to 32 kilometers (10 to 20 miles).

Farming is the principal activity outside the metropolitan area of Kansas City. Winter wheat is the main crop, especially in Kansas, but corn, hay, oats, barley, and soybeans are also grown. *5028–16075;* May 17, 1975.

PLATE 41

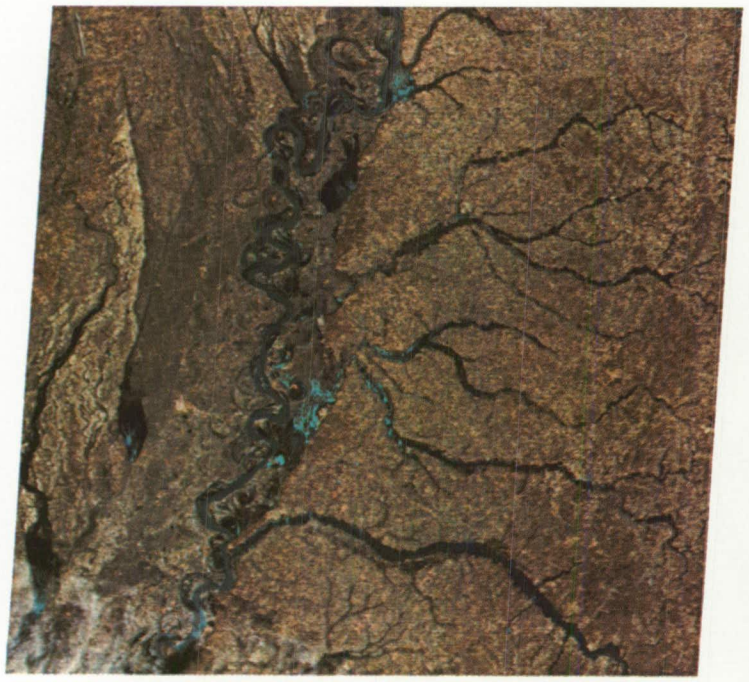


MISSISSIPPI RIVER FLOOD SEQUENCE: The same section of the middle Mississippi River is examined over almost a year on this and the next page to demonstrate the temporal changes associated with the great Mississippi River flood of 1973.

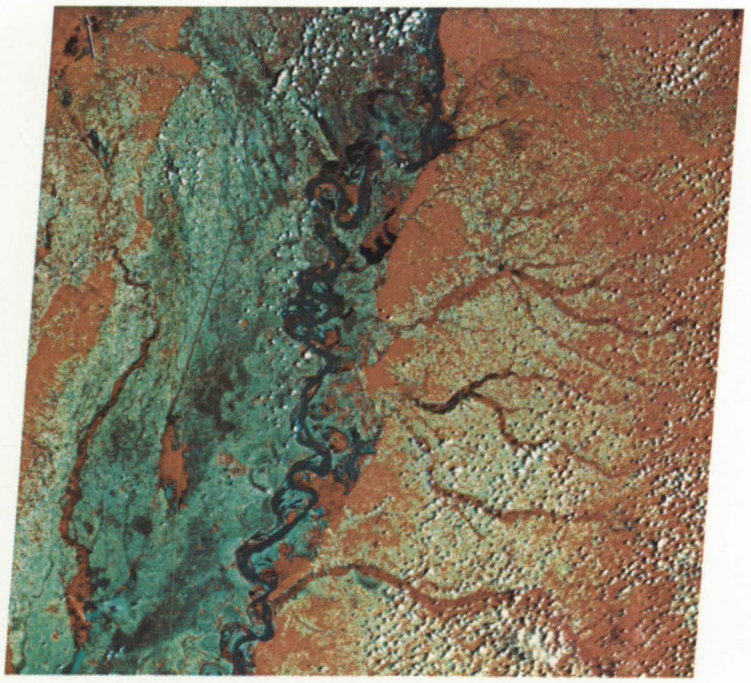
This image shows parts of the States of Missouri (*C*–5), Arkansas (*B*–19), Kentucky (*N*–2), and Tennessee (*R*–15) in the early fall of 1972 prior to the flood period. The region is just north of Memphis (off the image at *E*–22). The Mississippi River flood plain (*D*–13) extends well to the west of the present course of the river (*F*–12) but terminates sharply against loess-covered bluffs only a few kilometers (miles) to the east (*H*–8). The uplands area further east is the Jackson plain (*Q*–12), named from the town of Jackson, Tenn. (*P*–16), which represents the northeastern segment of the Mississippi Embayment. The section of the plain defined by these tree-lined rivers—Hatchie (*J*–18), Forked Deer (*H*–14), Obion (*I*–10) (three forks), and Obion Creek (*K*–3)—is underlain by the Eocene Wilcox and Midway Formations. The Ripley and Eutaw Formations of Cretaceous age are expressed as somewhat more dissected terrain that supports a higher density of the oak-hickory forest covering part of the uplands. Part of Kentucky Lake (*U*–1) along the Tennessee River appears at the upper right.

The section of flood plain shown in the image includes the Big Lake National Wildlife Refuge (*B*–14) into which drains a series of close-spaced irrigation ditches (*C*–8) that run northeastward through the Missouri panhandle. The panhandle itself is bounded on the west by the St. Francis River (*A*–10), which borders Arkansas (best seen in plate 42(*c*)). To the west of that river is the oak-hickory covered Crowley's Ridge, an elevated (relief of about 60 meters (200 feet)) remnant of Eocene Wilcox sedimentary rocks. This ridge was once the east edge of the uplands at the time when the Mississippi River flowed to the west in the valley now occupied by the Black River, tributary to the White River of Arkansas further south.

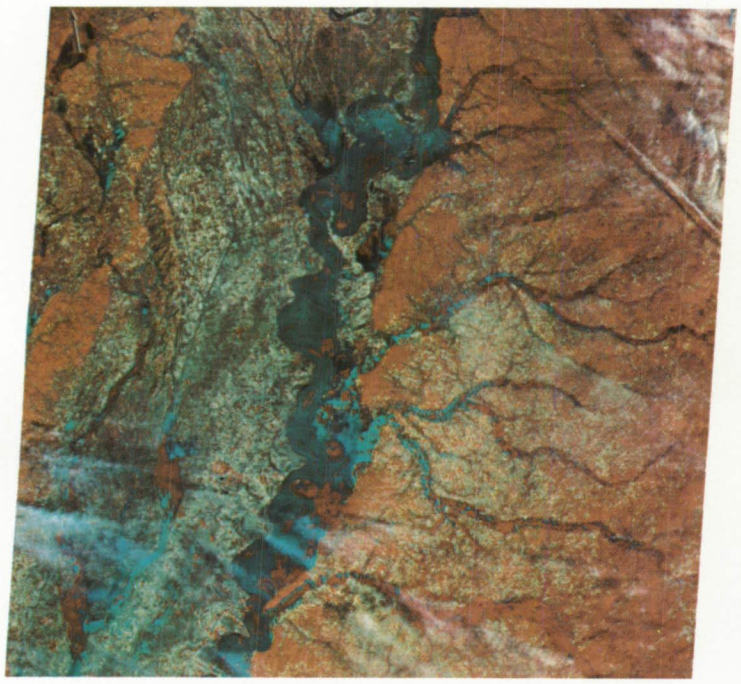
The town of New Madrid appears at *F*–5. This was the site in 1811–1812 of two of the strongest earthquakes ever to occur in the United States. The down-dropping of a block crust and river plains to the southeast produced Reelfoot Lake (*H*–7) by diversion of the Mississippi River. *1070–16055;* October 1, 1972.



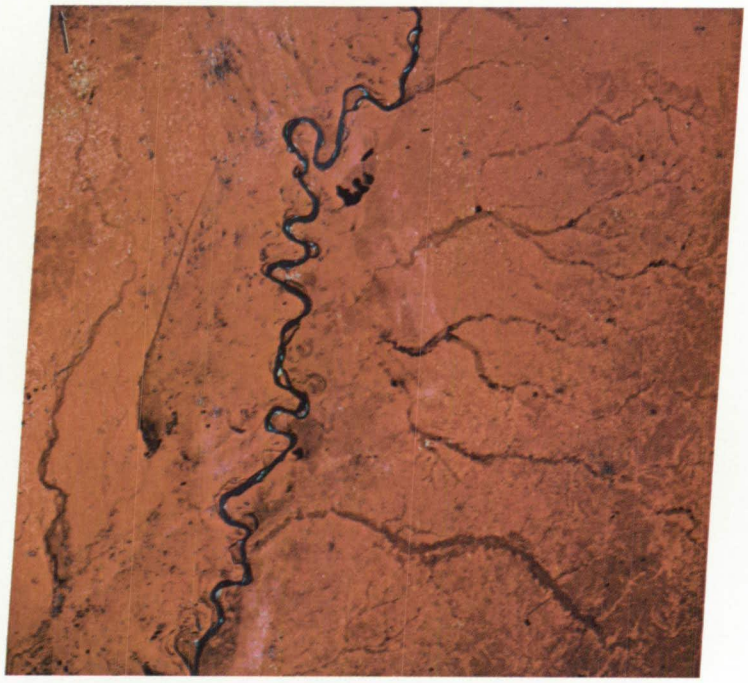
(a)



(c)



(b)

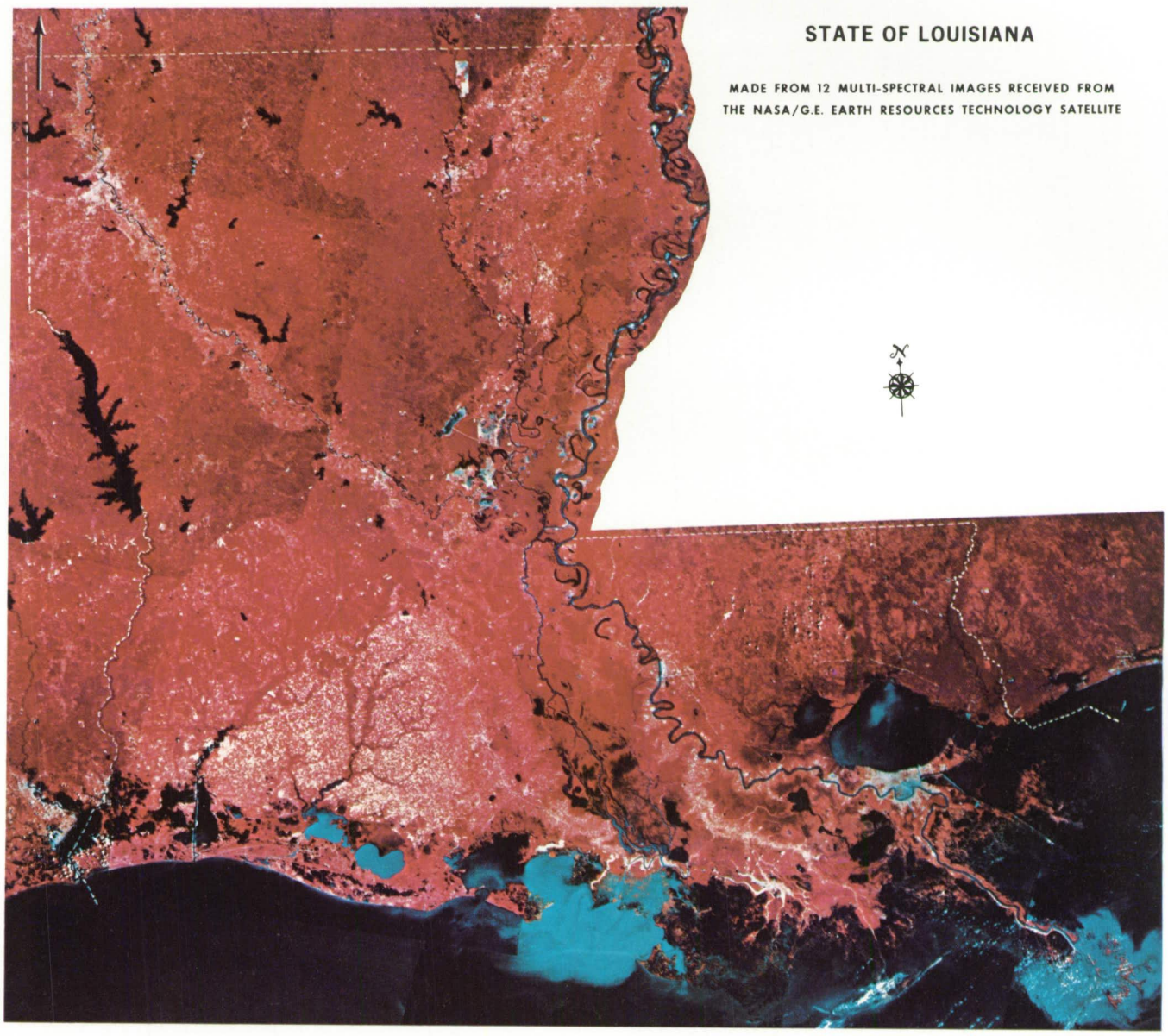


(d)

PLATE 42

MISSISSIPPI RIVER FLOOD SEQUENCE: The four panels shown here depict important stages of flooding and recovery of the flood plains of the Mississippi and St. Francis Rivers during the spring of 1973. (*a*) This scene shows the region in late winter when foliage is minimal. Moderate floodwaters affect both rivers as well as the tributaries to the Mississippi River flowing from the Jackson plains. The contrast between the older, more dissected and terraced St. Francis flood plain and the flatter Mississippi flood plain is sharply defined in this view. *1214–16065;* February 22, 1973. (*b*) This image represents the flooding near its maximum. Water has spread over an 8- to 16-kilometer (5- to 10-mile) wide belt around the Mississippi River channel. Some flooding of the St. Francis River is evident, but flooding appears more extensive along the Little River, which connects the Big Lake Refuge (now marked by bright red from marsh and tree foliage) with the St. Francis just below the Hatchee Coon Island marshlands (also red). Some of the bottom land farms have growing crops at this stage. The upland forests have also begun to leaf. *1286–16065;* May 5, 1973. (*c*) This image reveals the extent of flood damage to the lowlands. Most of the farms (wheat, cotton, soybeans, corn, rice, and watermelons) are not in the normal stages of planting and are "fallow" in the sense of still consisting of water-logged ground. Uplands farms that produce cotton, corn, and soybeans are in a more advanced stage of growth but east of the bluff many still are not in crop. *1322–16063;* June 10, 1973. (*d*) This scene demonstrates the remarkable recovery achieved in this region by late summer. However, some of the flood plain farms are covered by grass and weeds rather than crops. The boundaries of individual farm plots are considerably obscured in both bottom lands and uplands (compare with the October 1, 1972, scene in plate 41). *1394–16053;* August 21, 1973.

PLATE 43



THE STATE OF LOUISIANA: This mosaic of Louisiana, and small segments of adjacent Texas, Arkansas, and Mississippi, was prepared from 12 Landsat images by the General Electric Photographic Laboratories. Some of the major geographic landmarks are more fully described in plates 46 to 48. Some features of interest include (see plate 44 for letter identifications) the present (birdsfoot) delta of the Mississippi River (*A*) and the sediment plume from the discharge on May 21, 1973; the sediment plume from the Atchafalaya River (*B*); White Lake (*C*); Grand Lake (*D*); Calcasieu Lake (*E*); Sabine Lake (*F*); Catahoula Lake (*G*); Bayou D'Arbonne Lake (*H*); the lower Red River (*I*); the Ouachita River (*J*); Lake Charles (*K*); Alexandria (*L*); and Monroe (*M*).

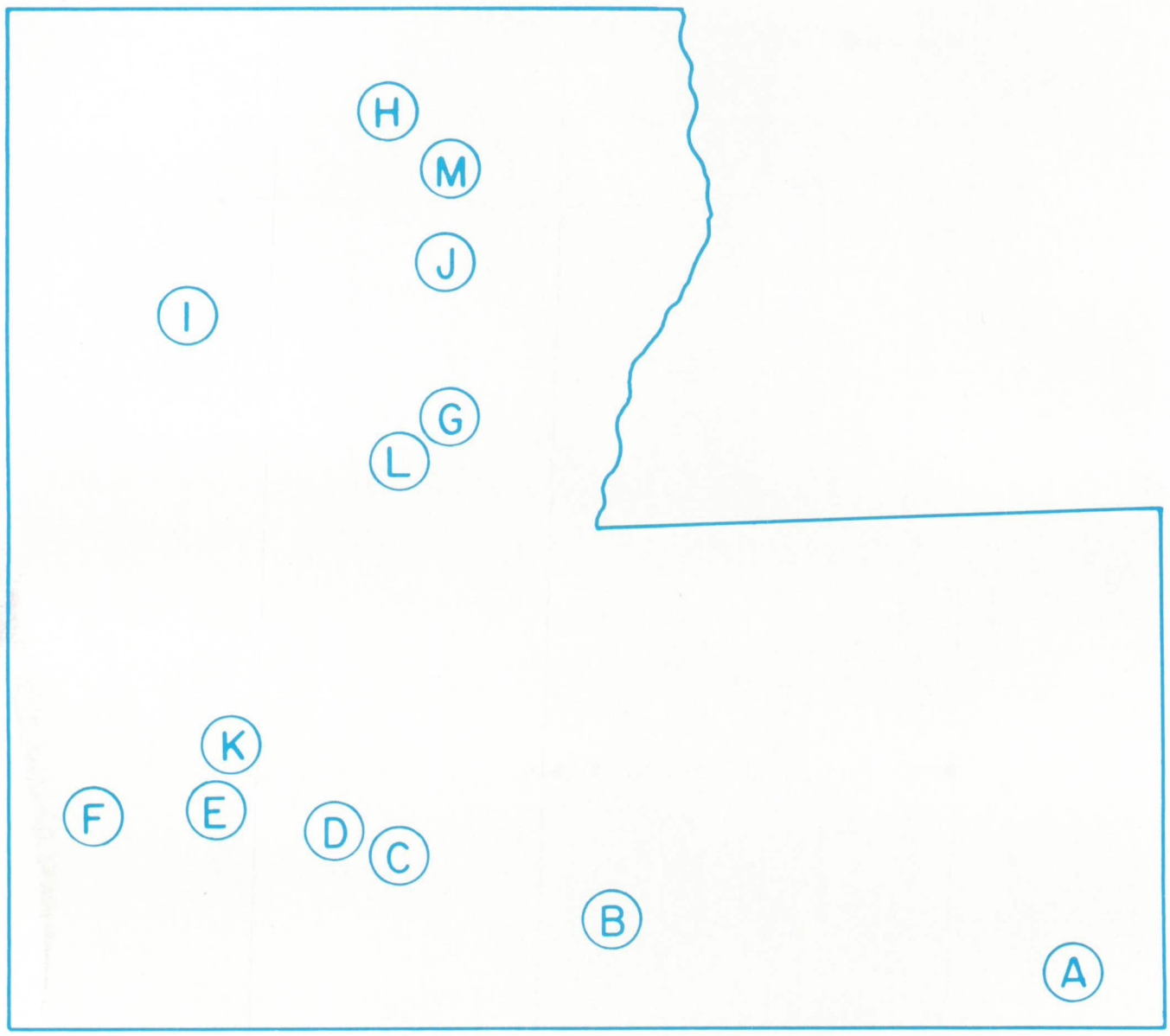
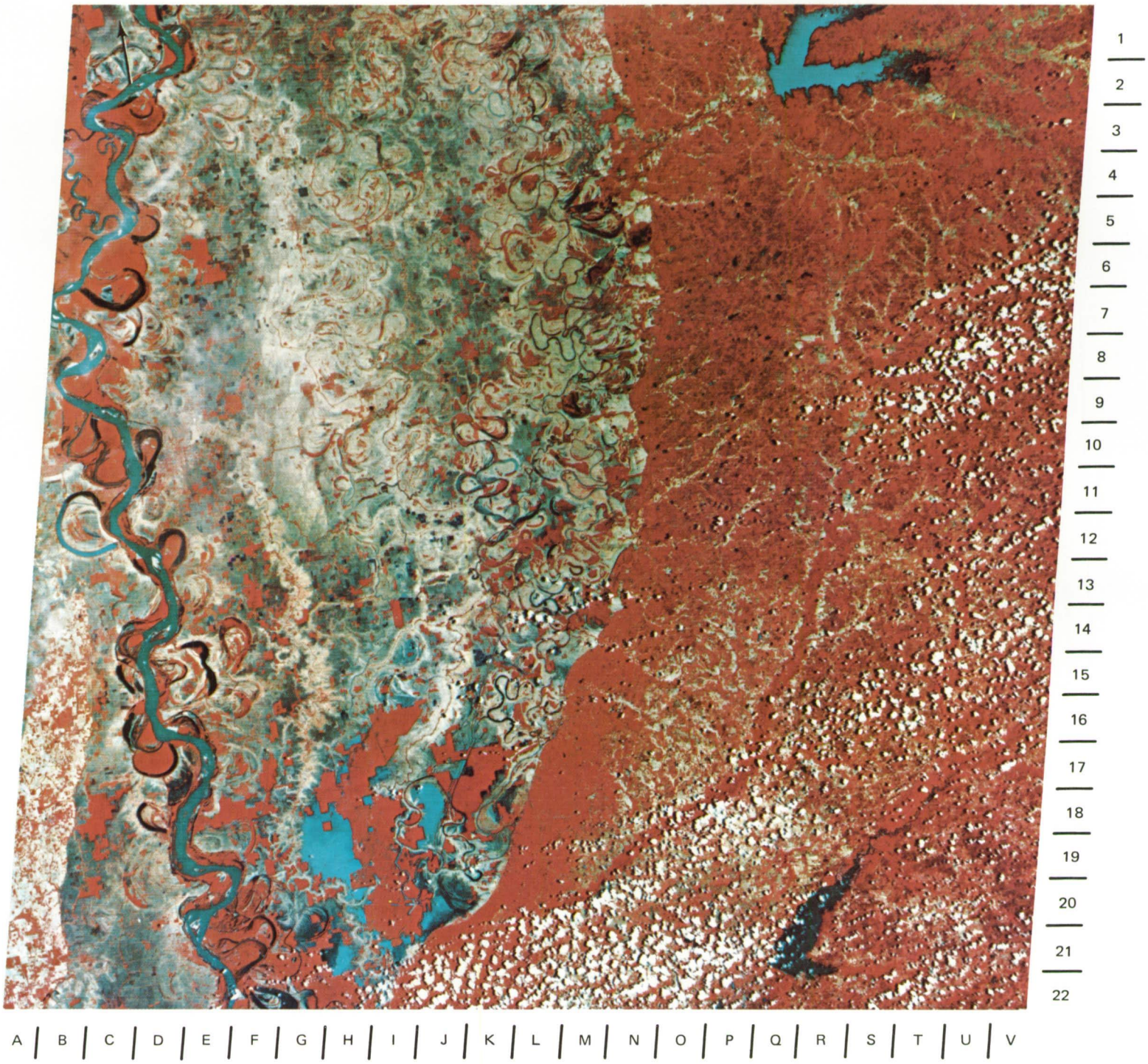


PLATE 44

PLATE 45



THE YAZOO BASIN, MISS.: This section of the lower Mississippi River (*B*–4) dividing the State of Mississippi (*R*–10) from Louisiana (*B*–19) and Arkansas (*A*–4) is characterized by an unusual history of drainage from the Pleistocene to the present. The region is part of the Mississippi Embayment, when marine waters more than 75 million years ago invaded the continent to as far north as southern Missouri. The forest-covered terrain east of the broad flood plain (*G*–12) of the Mississippi River is a dissected uplands underlain by Eocene marine sediments and capped by loess that is thickest along the river bluffs from the Vicksburg area (*H*–22) northward. The Big Black River (*Q*–15) and the Pearl River (*T*–18), with its Ross Barnett Reservoir (*R*–20) north of Jackson, Miss. (*P*–22), are deflected southeastward from these bluffs before joining the Mississippi River. The Yalobusha River (*N*–3), including the dammed Grenada Lake (*P*–2), flows more directly into the flood plain.

This flood plain widens to nearly 80 kilometers (50 miles) east of the present course of the Mississippi. The entire flood plain has been filled with Pleistocene alluvium carried in by the Mississippi, the Arkansas, and the Ohio Rivers, all bearing large loads in the past from glacial melt waters. For a considerable time, the Ohio River occupied the eastern part of the flood plain, cutting its own valley until it joined the Mississippi near Vicksburg. That valley is now being traversed by the Yazoo River (*K*–16) and the parallel Sunflower River (*H*–13), both of which chose this lower area; natural levees along the Mississippi also prevent these other rivers from joining it further upstream.

The entire flood plain in this scene is unusually bare for this time of year because of earlier partial submergence during the spring 1973 floods. Flood backwaters still remain around the Delta National Forest (*H*–18). Without the usual crop cover, it is possible to see the innumerable oxbow lakes and abandoned cutoff meanders produced by earlier wanderings of the rivers. Crops in these bottom lands in other years are cotton, soybeans, rice, wheat, and oats. Uplands forests consist of oak and hickory near the bluffs and also pine further east. *1340–16070;* June 28, 1973.

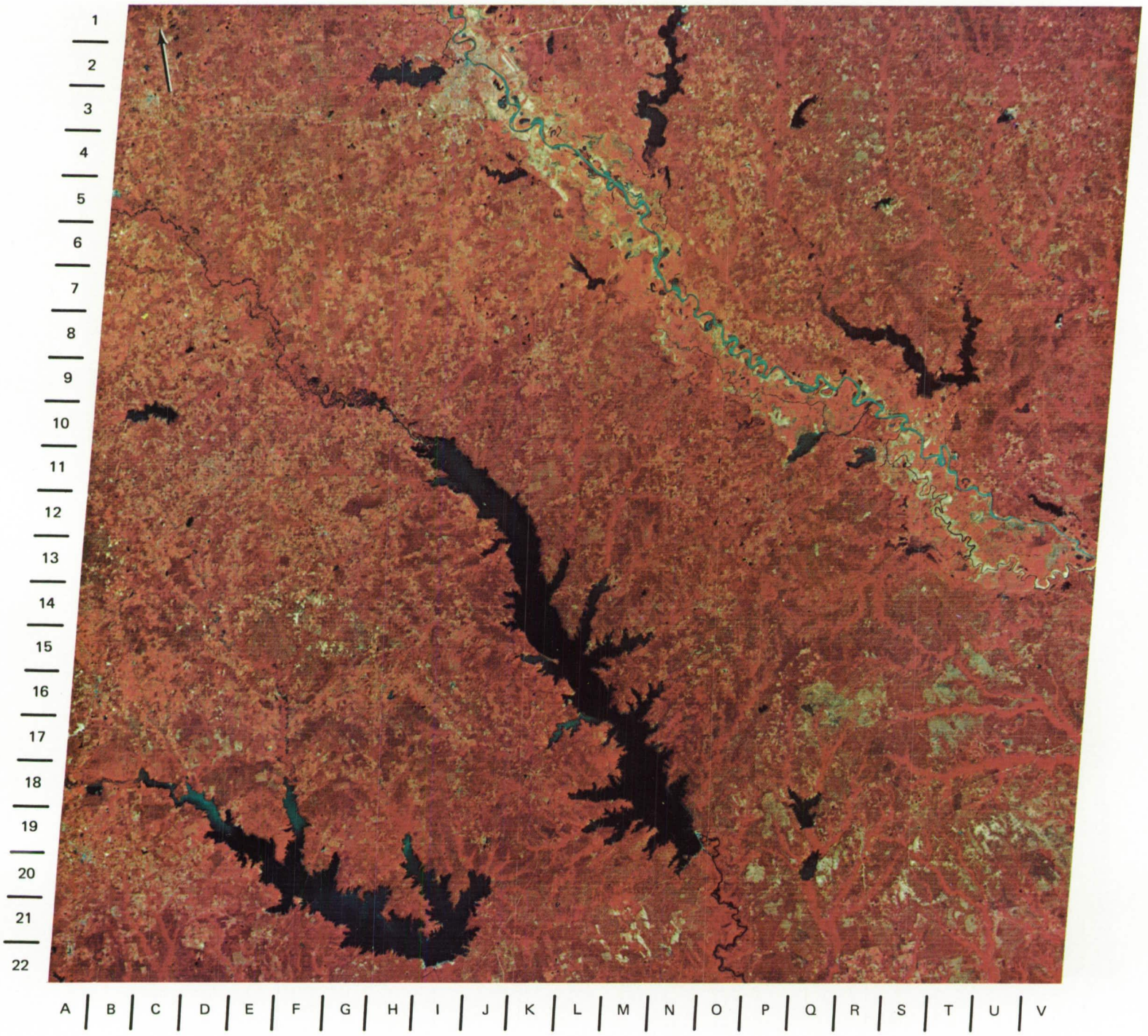
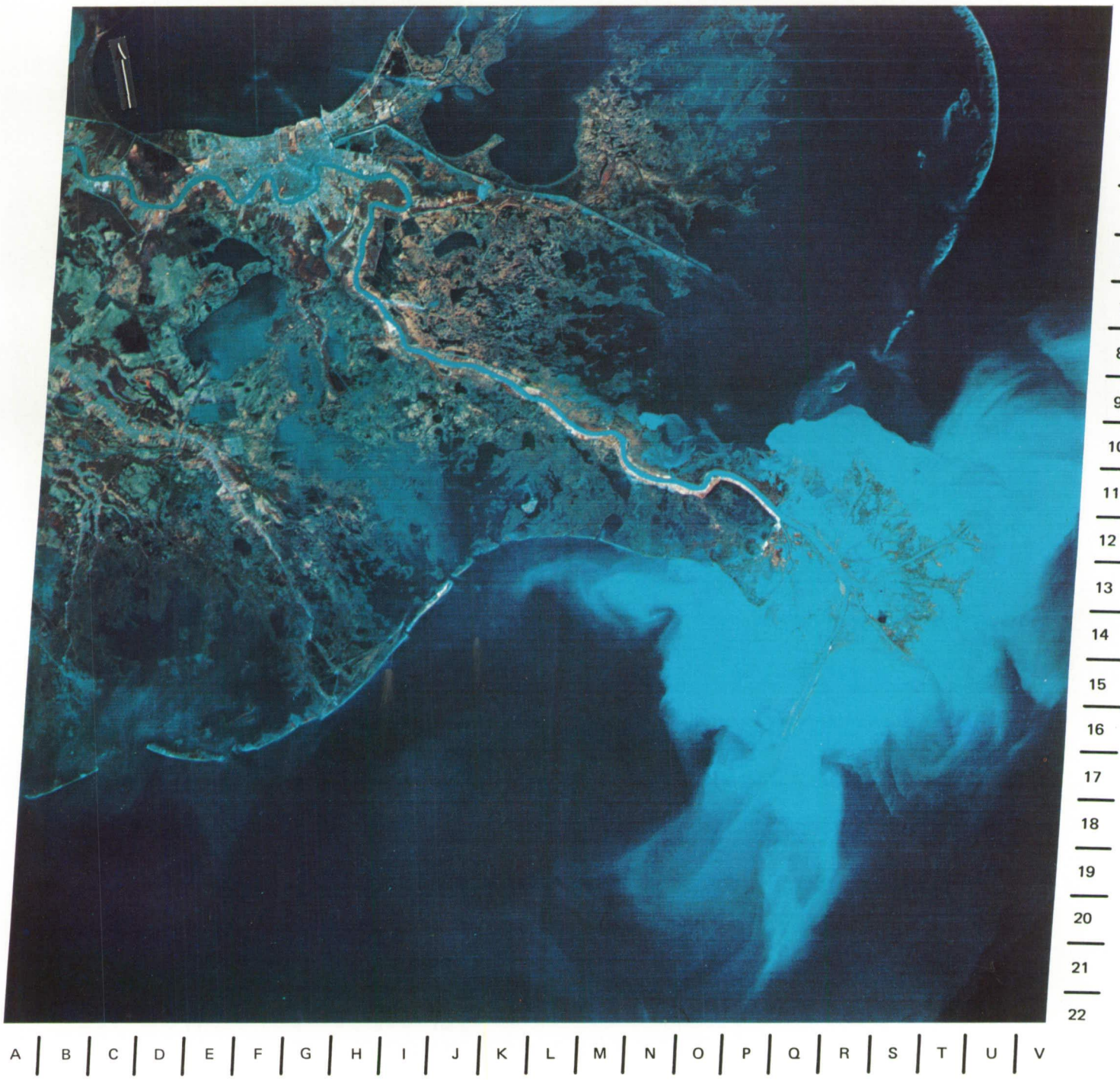


PLATE 46

TEXAS-LOUISIANA TIMBERLANDS: The border between eastern Texas and western Louisiana runs along the Sabine River (*D*–8), here dammed to produce the Toledo Bend Reservoir (*K*–14). To the west, the Angelina River (*A*–18) is backed up in the Sam Rayburn Reservoir (*H*–22). However, the principal drainage in this scene is the Red River (*Q*–9), whose broad flood plain has been largely cleared for cotton farming (soybeans, watermelons, and pecans are the other major crops). The city of Shreveport (*H*–2) is located on this river, which begins its course far to the west in the Texas Panhandle. Lake Bistineau (*L*–3) and Black (*R*–6) and Saline (*S*–6) Lakes lie to the southeast of Shreveport.

Oil fields are found southeast of Shreveport in association with a swarm of subsurface salt domes. Surface expressions of several domes can be seen at *Q*–4. The geology of this region is comparatively simple. Most of the terrain shown here is underlain by Eocene marine sediments. The contact between the Wilcox Group and the younger Claiborne Group to the east approximately coincides with the west-facing Nacogdoches Escarpment (*G*–15). The contact between the Claiborne and the overlying Jackson Group gives rise to the Kisatchie Scarp (*T*–14). Because soils derived from this latter group retain water better than those to the northwest, they are more suited to farming and the land is thus more completely cleared of forestation. The remaining trees are part of the Southern mixed forest community (typified by scattered magnolias) while the remainder of the area further north is a mixture of pine, oak, and hickory. National forest preserves are associated with the reservoirs between the Sabine and Angelina Rivers. *1252–16194;* April 1, 1973.

PLATE 47



MISSISSIPPI DELTA: The Mississippi River winds toward the Gulf of Mexico past New Orleans, La. (*E*–4). The cloud of mud and silt coloring the water around the river mouth graphically illustrates the process of delta building. The Mississippi pours more than a million tons of sediment into the gulf each day, extending banks of mud, sand, and clay out over the Continental Shelf. The Chandeleur Islands (*T*–3), site of Breton National Wildlife Refuge, are remnants of the old St. Bernard delta, built when Bayou la Loutre (*I*–5) was the main channel. The sand islands were formed by wave and current action as the landward sediments compacted and subsided. The overlapping relationship of sandbars, channels, and mudflats at Bay Marchand (*G*–15) indicates the complexity of the sedimentary processes taking place here. The presently active "bird's foot" delta (*R*–13) is advancing rapidly. The subdelta at Main Pass (*R*–11) has grown nearly 20 kilometers (12 miles) in the past 100 years. The small cloud of sediment at California Point (*M*–9) shows leakage through crevasses in the levee.

New Orleans, nicknamed the "Crescent City," is a major port, doing a multibillion dollar business annually, and handling much of America's trade with Latin America. Urban development in the city contrasts with the French land system of long lots extending across the wide natural levees along the Mississippi (*C*–5). Interstate 10 skirts the south edge of Lake Pontchartrain (*C*–2), passing NASA's assembly facility at Michoud (*G*–3). The Pontchartrain Causeway crosses the center of the lake (*D*–1). The Mississippi River Gulf Outlet provides a shortcut for shipping south of Lake Borgne (*I*–4). The Intracoastal Waterway joins the outlet at Michoud and continues south past Lake Salvador (*E*–18), crossing Bayou Lafourche near a large area of flooded farmland (*E*–9). Color contrasts mark the sulfur mining area at Grande Ecaille (*K*–11) and an oil dike at the Garden Island Bay field (*R*–13). *1177–16023;* January 16, 1973.

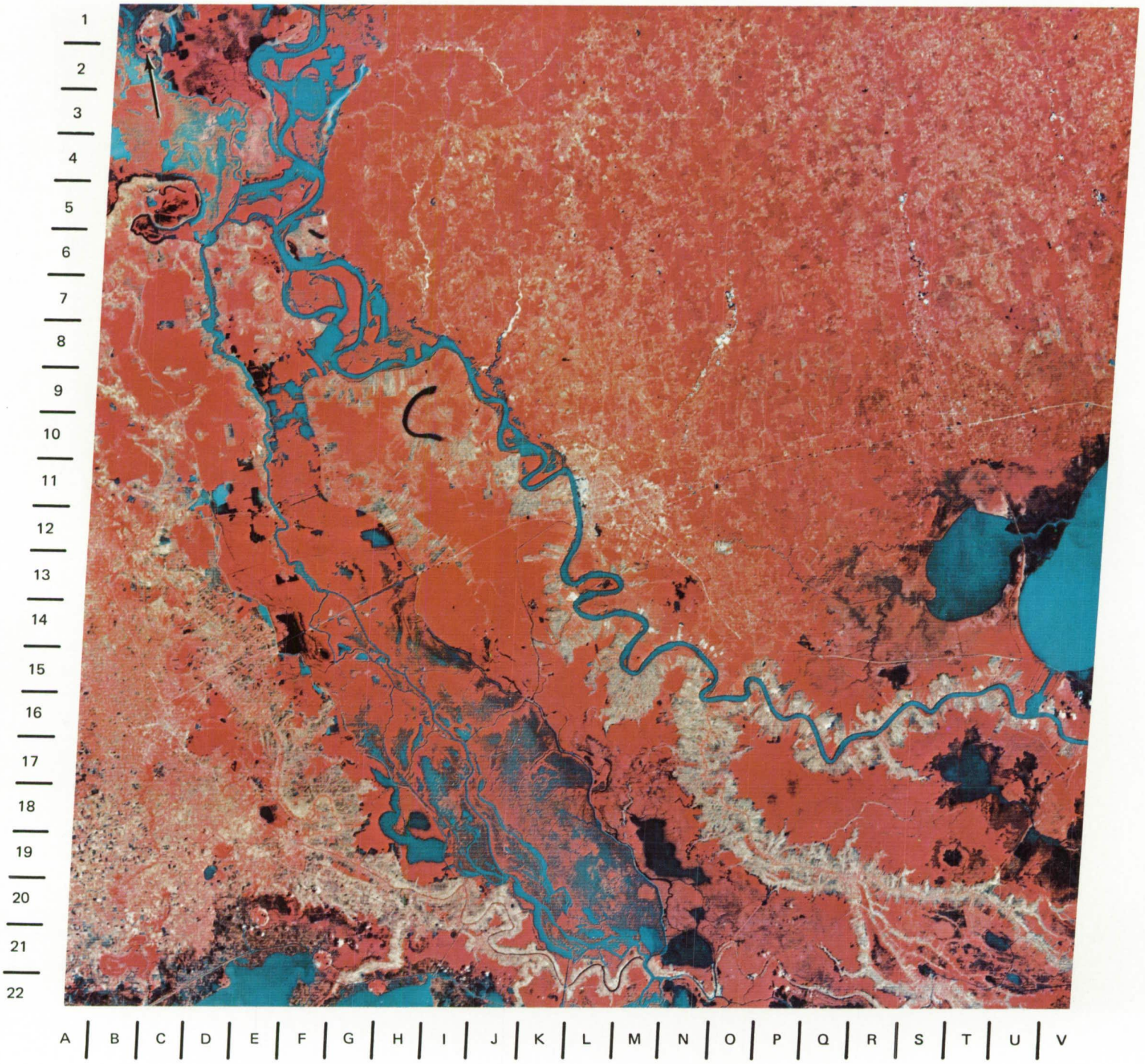


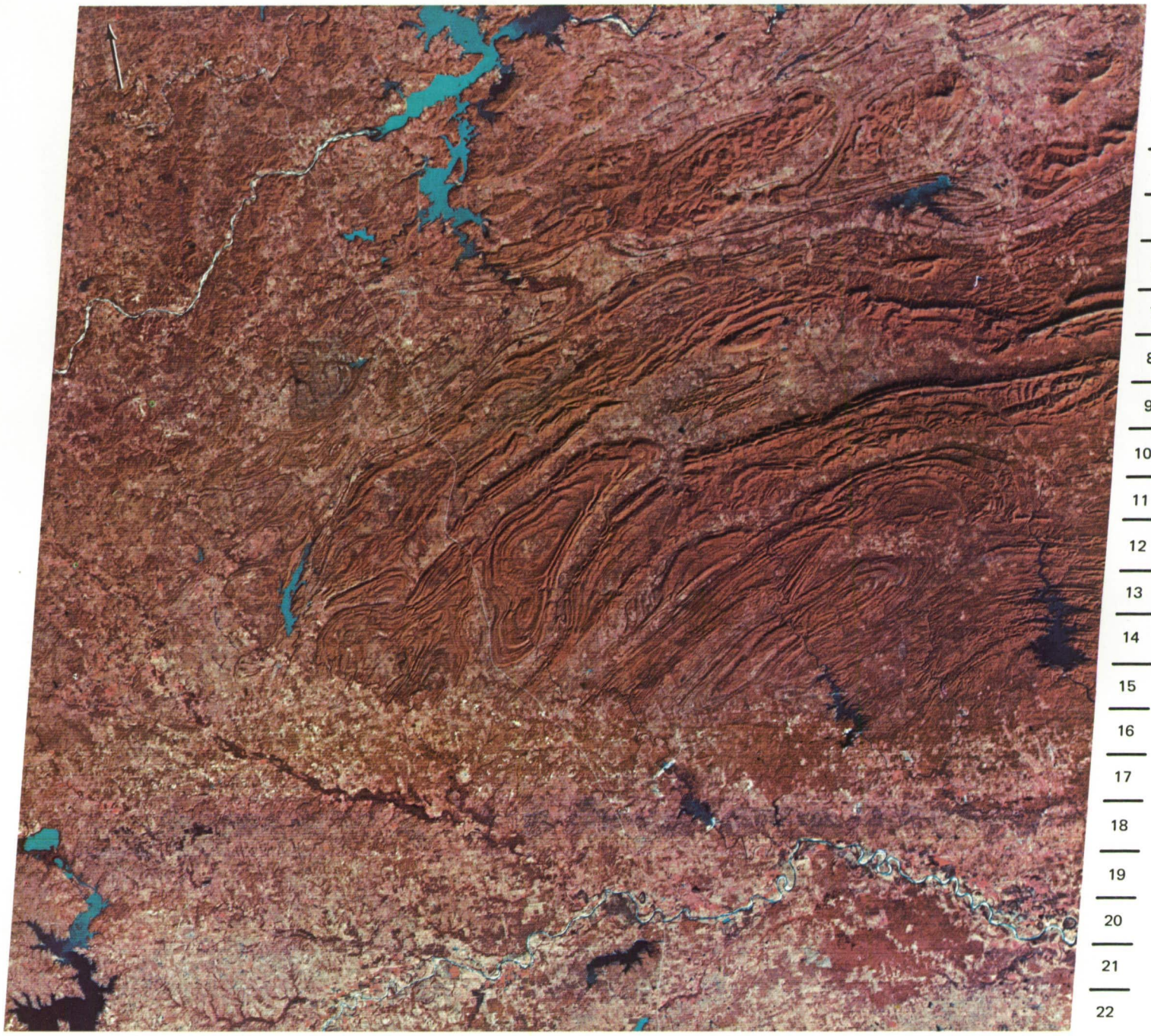
PLATE 48

SOUTHERN LOUISIANA: This scene shows the Mississippi River (*H*–9) north of New Orleans during high water in the 1973 spring flood. The Atchafalaya River (*F*–13; *K*–20) begins as an offshoot of the Mississippi near the Louisiana-Mississippi State line (*E*–5) and continues through the Atchafalaya Basin for 225 kilometers (140 miles) until reaching the Gulf of Mexico at Atchafalaya Bay (*M*–22). The river carries almost one quarter of the total discharge of the Mississippi in the delta region and is thus the largest single distributary. The Atchafalaya Basin was previously used by the Mississippi in the last 1000 to 2000 years as the main route to the gulf; it is predicted that it may be used again as the principal channel because the present course past New Orleans is more than twice as long over a lower gradient. The Atchafalaya Basin is thus part of several older deltas and is still largely a swampy forest with several large lakes (Grand Lake (*H*–18), Lake Verret (*M*–18), and Six Mile Lake (*N*–21)). Other lakes in the area include Lake Ponchartrain (*U*–13) (note the filled Bonnet Carre Floodway (*U*–15) carrying overflow into the lake) connected to the smaller Lake Maurepas (*T*–12) and Lac Des Allemands (T–17).

The regional geology is quite simple. Pleistocene and Recent deltaic and flood plain deposits occupy all the bottom lands. Uplands north of Baton Rouge (*K*–11), the State capital, and into Mississippi State (*L*–2) are capped by the Citronelle Formation, a sequence of continental estuarine and river deposits. However, the lower delta has been pierced by numerous salt domes from 1½ to 8 kilometers (1 to 5 miles) in width. Conspicuous circular domes include Cote Blanche (*G*–21) on West Cote Blanche Bay (*G*–22), Weeks (*F*–21) on Vermilion Bay (*F*–22), and Avery Island (*E*–20) further inland. Most of these domes are oil producers, tapping petroleum along their flanks. The towns of Lafayette (*C*–16), New Iberia (*E*–18), and Houma (*S*–21) are centers for field production.

Cotton, sugarcane, rice, corn, and sweet potatoes are grown around Lafayette and in the bottom lands of the Mississippi River and the Bayou Lafourche (*O*–18). Most of the farms are notably elongated perpendicular to their river frontage—this is the "long lot" system of agriculture brought in by the French settlers before 1800. *1286–16083;* May 5, 1973.

PLATE 49



OUACHITA MOUNTAINS: Low November Sun shadows accentuate the bold relief of the Ouachita Mountains in southeastern Oklahoma. These mountains contain strongly folded and faulted Paleozoic strata, much like the Appalachians, and are thought to be part of a continuous structural province linking the Appalachians with the Marathon Basin in Texas. The Ouachita province is readily divisible into zones of contrasting topography and structure. In the Arkansas valley section, from McAlester (*H*–6) to Poteau (*S*–2), the convoluted folding in Pennsylvanian strata dies out northward, merging with the gentle folds of the Ozark Plateau. Along the northern front of the mountains imbricate thrust faulting has created a belt of long, parallel, steeply dipping sandstone ridges, extending from the Atoka Reservoir (*D*–12) to Rich Mountain (V–7). The Jackfork sandstone is the prominent ridge maker here. To the south, where folding is dominant, broad synclines are interrupted by widely spaced thrust faults. Around Broken Bow Reservoir (*V*–14), folded Cambrian to Devonian strata form a subdued topography of narrow parallel ridges. The sharp cutoff of structure along the southern edge of the mountains marks the overlap of unconsolidated Gulf Coastal Plain sediments. One of the more resistant of these Cretaceous units forms a low escarpment, the Eastern Cross Timbers, whose characteristic vegetation pattern shows up as a grayish belt extending across the entire photo (*B*–18 to *V*–18).

Forest and range control projects are seen in the cleared areas on Signal Mountain (*R*–12) and in the large basin near center (*K*–12). A small patch of gray near Redden (*H*–12) marks vegetation killed by herbicide spraying earlier in the year. A wide range of sediment content is reflected in the colors of the reservoirs, particularly Lake Texoma (*B*–20) on the Red River and Eufaula Reservoir (*I*–2) on the Canadian River. The Indian Nation Turnpike shows prominently across the mountains (*I*–11). The white scars east of Hugo (*M*–18) mark the Lake Hugo dam on the Kiamichi River (*O*–17) and the relocation of Oklahoma Highway 93 (*N*–16). *1128–16300;* November 28, 1972.

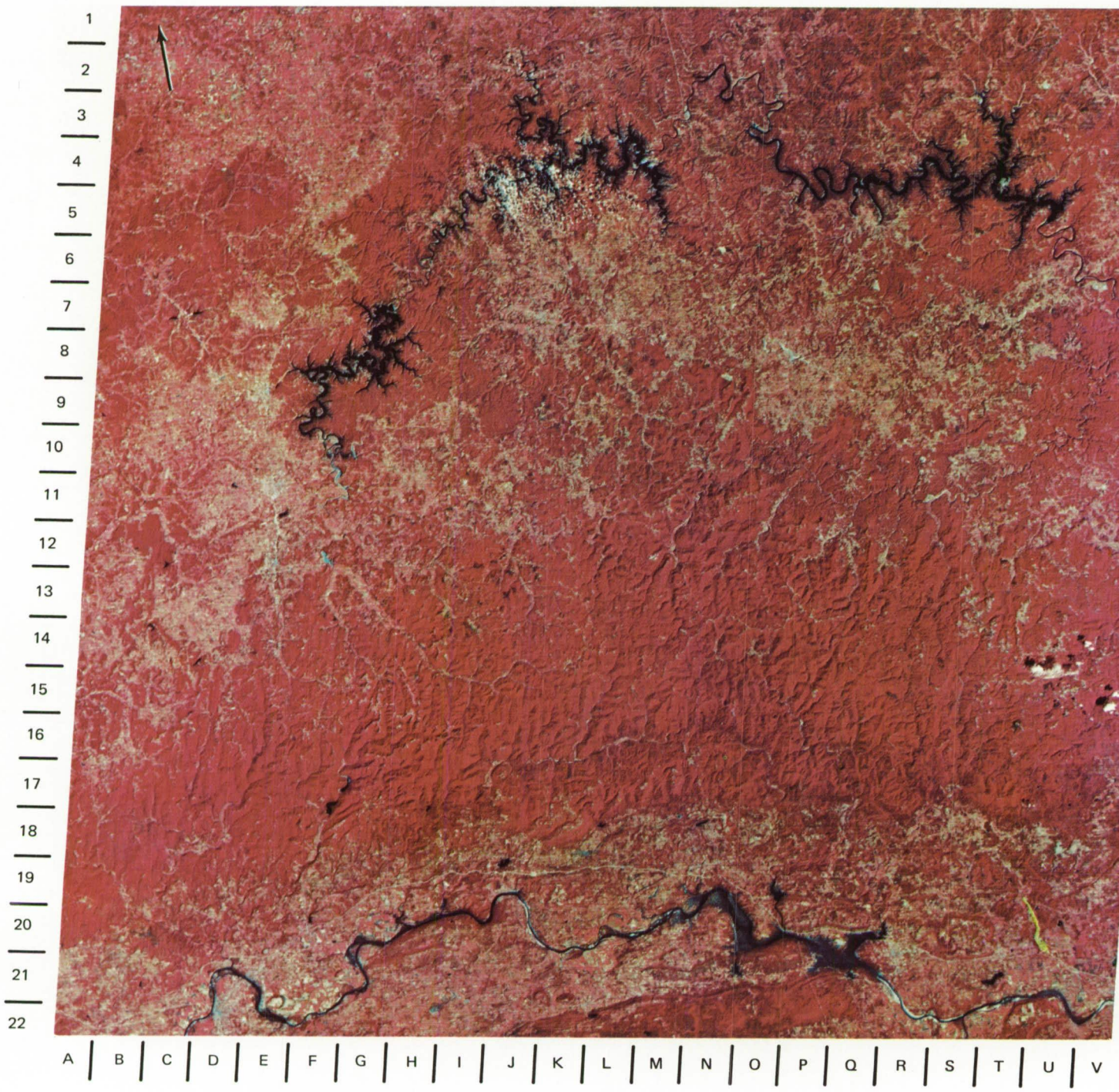
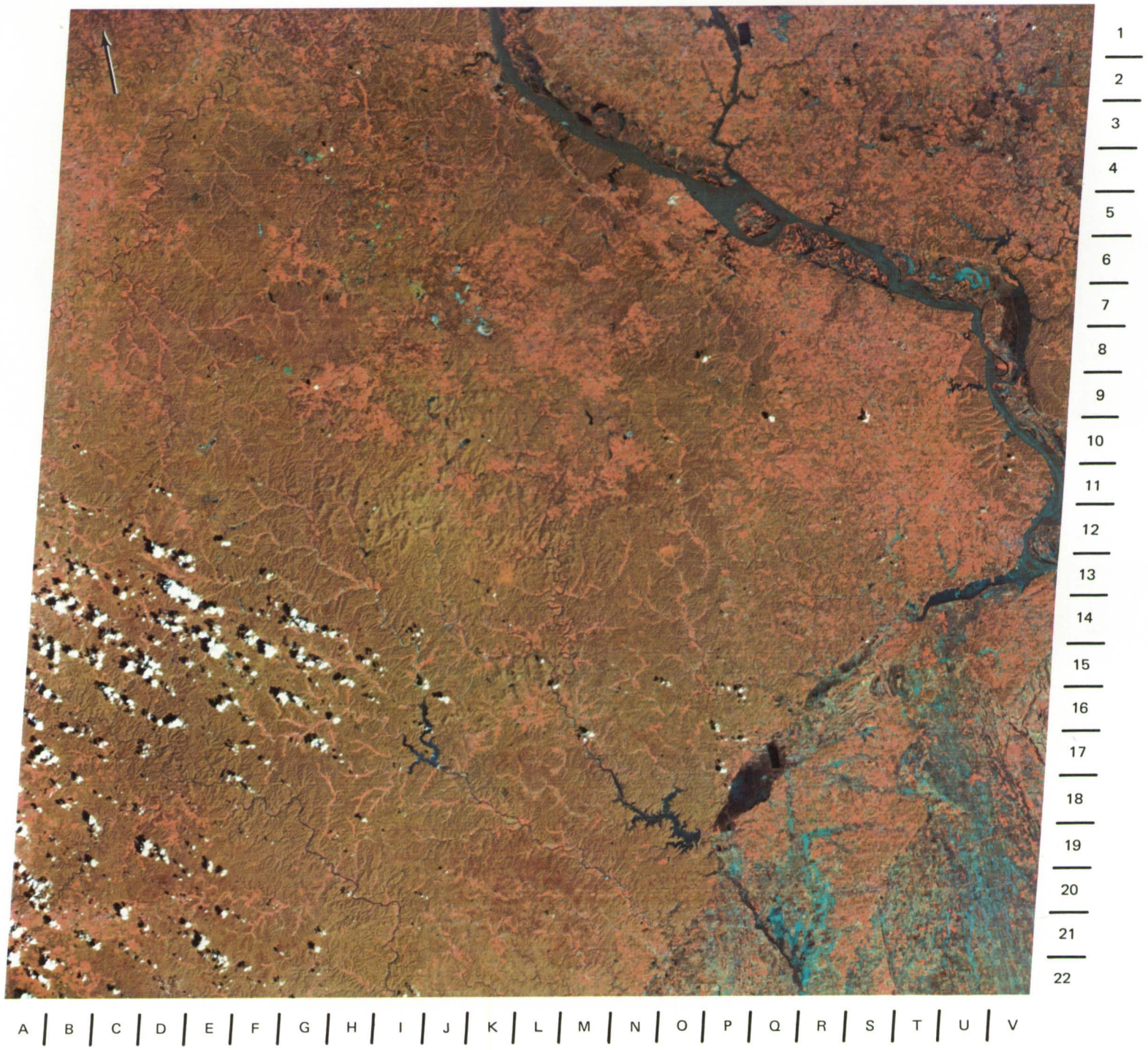


PLATE 50

THE BOSTON MOUNTAINS, ARK.: Several physiographic subprovinces of the Ozark Plateau appear in this scene. The south end of the Springfield Plateau subprovince extends across much of the lower terrain around the White River (*G*–6). This plateau is underlain almost entirely by Mississippian carbonate rocks that weather further north to rolling "prairie" country and hills of 30- to 90-meter (100- to 300-foot) relief. An east-facing ridge, the Eureka Springs escarpment (*F*–4), is capped by the chert-bearing Boone Formation of Mississippian age. This scarp "wanders" erratically above forested lowlands built on a bedrock of Ordovician limestones. These Ordovician rocks form the southwestern tip of the Salem Plateau subprovince, characterized over much of southeastern Missouri by rolling hills of 30- to 45-meter (100- to 150-foot) relief. The third subprovince, almost entirely included in this scene, is the strongly dissected Boston Plateau (*N*–15), with elevations up to 300 meters (1000 feet) or more above the more northern plateaus. Rocks of this unit are sandstones and shales exclusively Pennsylvanian in age. Streams have cut through the capping Atoka Formation, a resistant sandstone, to produce a relief of 150 to 300 meters (500 to 1000 feet). Topographically, then, this east to west feature appears to be that of subdued mountainous terrain, but, structurally, the flat-lying nature of the strata do not fit the geomorphologist's definition of a mountain range. A steep scarp separates the northern edge of the Boston "Mountains" from the adjacent plateaus. Along the southern margins, the strata begin to dip southward into the synclinal belt of the Arkansas Valley (*H*–21).

The Arkansas River (*J*–19) flows through this valley past Fort Smith (*D*–21). It has been dammed to form the Dardanelle Reservoir (*N*–19) near Russellville (*R*–20). The White River has been dammed near the university town of Fayetteville (*D*–10) to make the Beaver Reservoir (*F*–8), dammed again in Missouri at the Table Rock Reservoir (*K*–4), and at the Bull Shoals Reservoir (*S*–4) on the Missouri-Arkansas border. Cedars abound in this region around the Missouri reservoirs; elsewhere oak and hickory make up the forests with some pine in the higher parts of the Boston Mountains. Agricultural production is limited in this part of Arkansas and Missouri mainly to soybeans, sorghum, hay, snap beans, and peaches. *1073–16230;* October 4, 1972.

PLATE 51



MISSOURI OZARKS: One of the few exposures of Precambrian crystalline rocks in the midcontinental United States south of the Superior shield occupies the heart of the dissected Ozark Plateau. Granitic and metamorphic rocks make up hills, ridges, and steep-walled gorges (locally called "shut-ins") around Ironton, Mo. (*I*–11). In this part of the Ozarks, known as the St. Francois Mountains, relief may reach 300 meters (1000 feet). Taum Sauk Mountain (*H*–12), at 540 meters (1772 feet) above sea level, is the highest point in Missouri. These igneous rocks are the exhumed part of an ancient buried terrain, with relief of 610 meters (2000 feet) or more, that was covered by Paleozoic rocks of various ages. The region was subsequently upwarped to produce the broad Ozark "dome," and erosion has since stripped off the sedimentary rocks over a 260-square-kilometer (100-square-mile) area to expose the crystalline basement. In the Salem Plateau section of the Ozarks, Cambrian sandstones and dolomites lie next to the crystalline core or occupy segments of stream valleys. Some of the largest lead sulfide deposits in the world are mined around Farmington (*J*–8) and Bonne Terre (*I*–7); the waste rock or gangue is piled up in huge "chat" piles (blue patches in image) 60 to 90 meters (200 to 300 feet) high and more than 610 meters (2000 feet) at their base. Ordovician carbonates form a wider belt that extends over most of the plateau. Barite (barium sulfate), called "tiff" by the miners, is extracted from red residual soils north (*G*–6) of Potosi. Silica sand, used in glassmaking, is obtained from the Ordovician St. Peter sandstone that holds up the Crystal City Escarpment (*H*–1). Silurian and Devonian rocks occupy a fault block wedge (*O*–7) near Ste. Genevieve (*M*–4) on the Mississippi River (*N*–8). Mississippian rocks make up the bluffs near that town and across the river in Illinois around Chester (*Q*–5). Pennsylvanian coal-bearing rocks underlie the uplands on the Illinois side. In the lower right is the northern tip of the Mississippi Embayment consisting in this image of Pleistocene alluvial plains (*V*–20) and Eocene deposits that make up Crowley's Ridge (*R*–18); see plate 41. The towns of Cape Girardeau (*V*–12) and Poplar Bluff (*N*–21) are situated along the edge of the embayment flatland where it meets the Ozark Plateau.

The Mississippi flood plain, with its 10- to 13-kilometer (6- to 8-mile) wide meander belt confined by steep bluffs, is partially inundated by the early stage of the 1973 floods. None of the tributaries—the Meramec River (*C*–3) southwest of St. Louis, the St. Francis River (*L*–15), Lake Wappapello (*O*–18), the Black River (*M*–19), Clearwater Lake (*I*–17), and the Current River (*G*–19)—show evidence of this flooding. *1251–16122;* March 31, 1973.

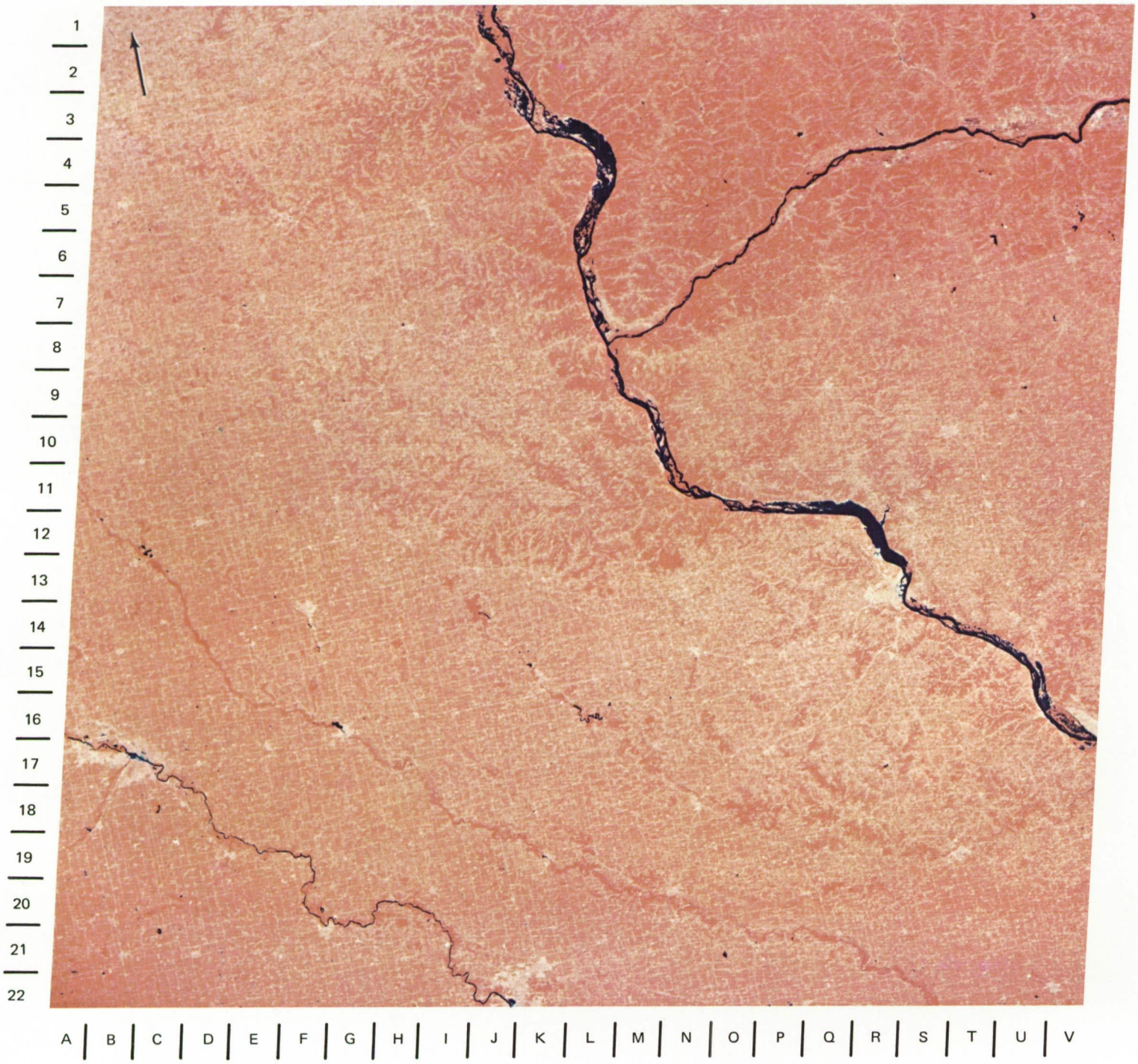


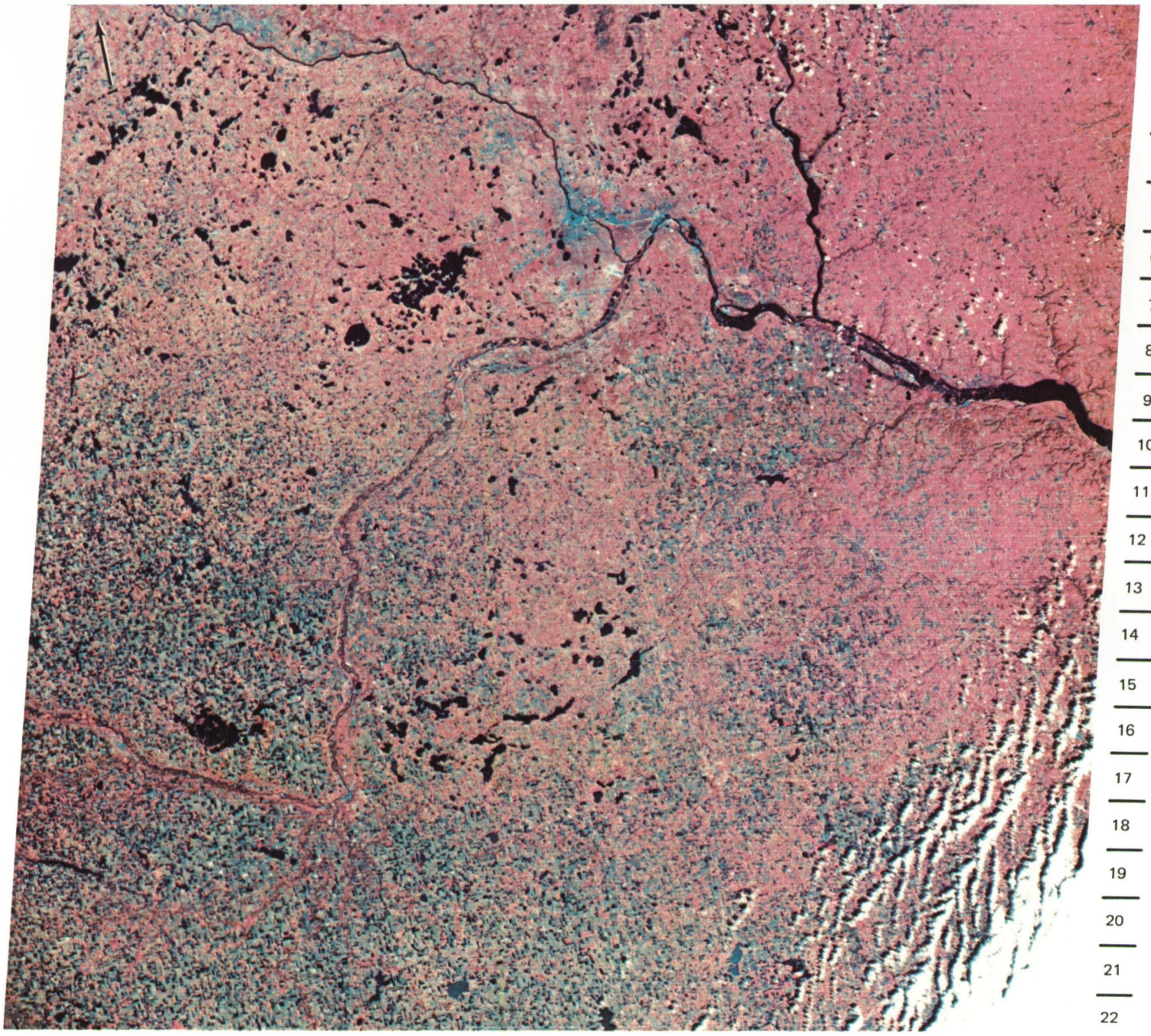
PLATE 52

THE UPPER MISSISSIPPI RIVER: The States of Wisconsin (*R*–8) and Illinois (*V*–14) meet Iowa (west of the Mississippi River) just above the city of Dubuque, Iowa (*R*–13). Waterloo (*B*–16) and Cedar Rapids (*K*–22) are located along the Cedar River (*D*–18), which parallels the Wapsipinicon River (*D*–15) to the east as they wend southeastward toward the Mississippi. The Wisconsin River (*P*–4) cuts through the Driftless area (*O*–3)—a section of the upper midwest supposedly void of glacial deposits—to meet the Mississippi at Prairie du Chien (*L*–7). The flood plains of both rivers are narrow; their meander belts are confined to a bottom land contained between steep bluffs. The several wide areas of the Mississippi itself result from flood control locks.

Much of the region is covered with glacial till from all four of the major ice advances of the Pleistocene. Beneath these drift deposits in Iowa and Illinois are found rocks of Ordovician age near the Mississippi, Silurian in the Dubuque Hills (*S*–17) up to the Wapsipinicon, and Devonian around the Cedar River. The limit of the overlying Kansan drift roughly coincides with the Niagaran escarpment (*H*–11) of Silurian age. To the northeast, the Driftless area (probably once covered by some thin glacial deposits) is a mature topography of gently dipping cuestas and isolated outliers of Cambrian sandstones and Ordovician carbonate rocks. Its southern edge is set at the Military Ridge (*T*–6), a part of the Prairie du Chien cuesta.

This region lies in the heart of the great corn belt of the upper midwest. Most of the farms occupy 1.6-kilometer (1-mile) squares bounded by roads that coincide with the section lines used in the township and range system of surveying followed in the United States. Other crops grown here include oats, soybeans, hay, and alfalfa. *1037–16210;* August 29, 1972.

PLATE 53



LAKE COUNTRY, MINNESOTA: The twin cities of Minneapolis (*L*–5) and St. Paul (*K*–5) on the upper Mississippi River (*F*–2; *N*–6) stand within a heavily glaciated area containing hundreds of lakes in low rolling countryside. Among the largest seen here are Lake Minnetonka (*H*–6) and Swan Lake (*D*–16). The scene lies just to the south of the Lake Superior physiographic province—a densely wooded (conifer) section of the Precambrian Canadian shield. Basal sandstones of Cambrian age are exposed northwest of Minneapolis, in the bluffs of the Mississippi around Lake Pepin (*V*–9), along the St. Croix River (*O*–3), and adjacent to much of the Minnesota River (*G*–13). Lower Ordovician rocks occur at higher elevations and a discontinuous band of middle Ordovician St. Peter sandstone outcrops around Minneapolis and the cluster of lakes (*L*–17) connected by the Cannon River (*N*–12) to the southeast. Cretaceous rocks lap onto these lower Paleozoic units west of the Minnesota River as far east as Mankato (*G*–17). However, most of these rock units are now covered by glacial drift and moraines except where exposed in stream valleys. Outcrops of Ordovician rocks in the State of Wisconsin (*T*–4) are more common in the hills (relief about 120 meters (400 feet)) east of the St. Croix River. Much of the uplands along the Mississippi are capped by easily eroded layers of windblown loess.

The areas around the Mississippi are an oak-dotted savanna grassland. Further away, forests of basswood and maple appear. South and west of Mankato, the farmlands are interspersed with bluestem prairie grass. Farming is given over mainly to oats, soybeans, corn, green peas, alfalfa, and some spring wheat. *1075–16321;* October 6, 1972.

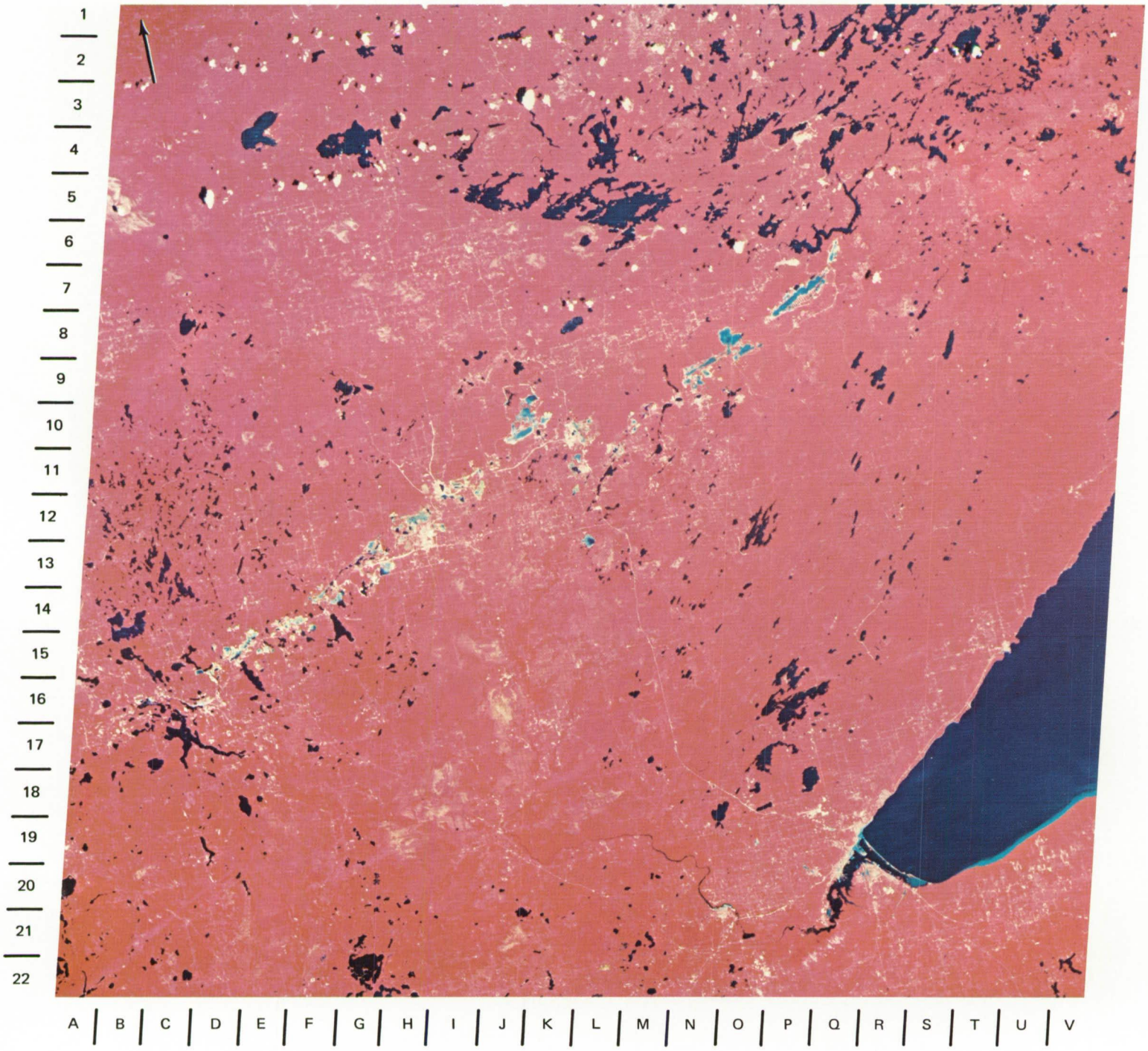
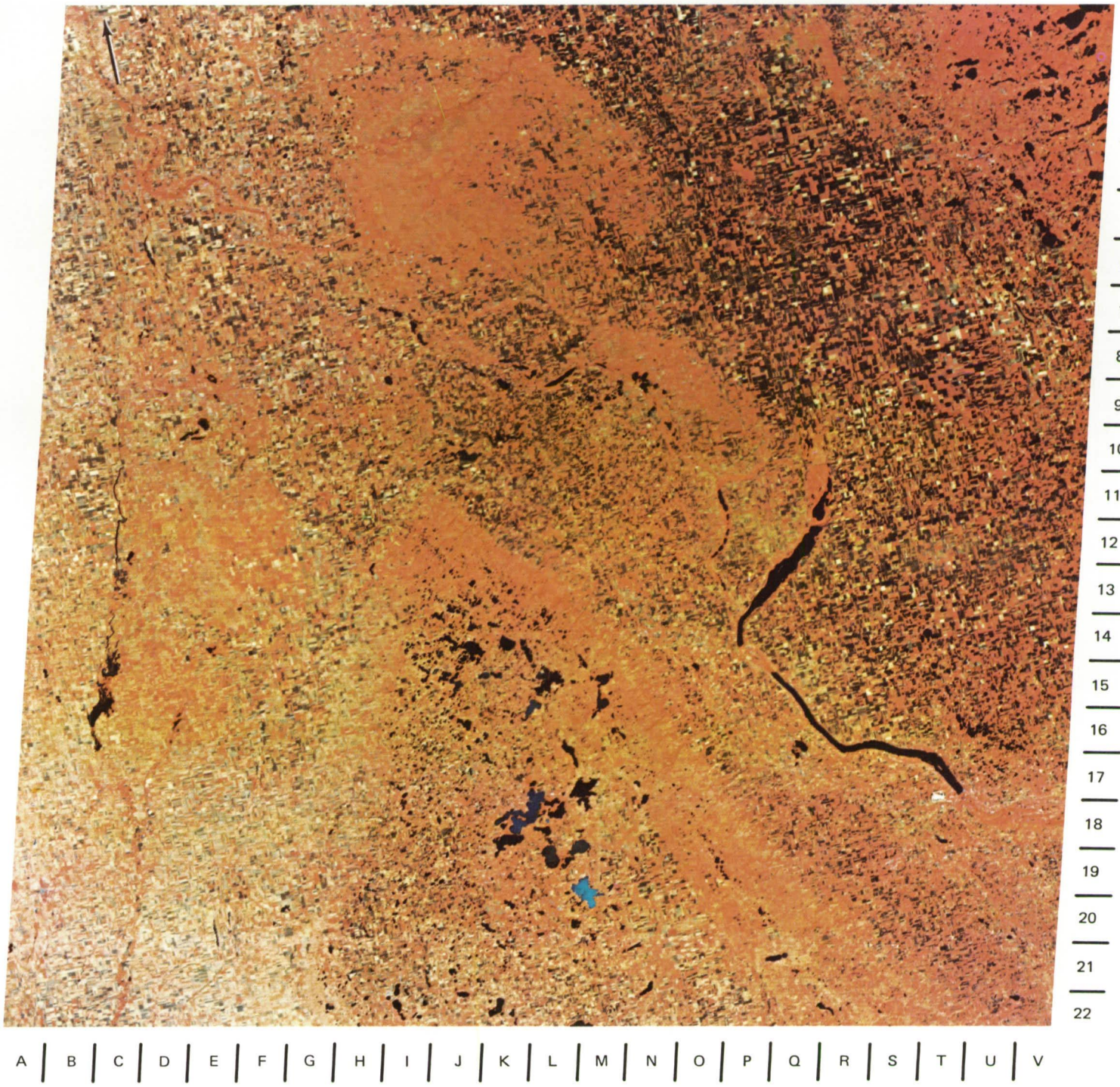


PLATE 54

DULUTH, MINN.: In this scene of iron mining country around the Mesabi Range and Lake Superior in northern Minnesota and Wisconsin, the underlying geology is masked by extensive glacial deposits. The highland belt to the north is underlain by a complex of igneous, sedimentary, and metamorphic rocks in which large rock-basin lakes have been formed by glacial action. The Mesabi Range, a southeast-dipping monocline of Huronian sediments, has produced 3 billion tons of iron ore. Large open pits are seen near Grand Rapids (*D*–15), Hibbing (*H*–12), Virginia and Eveleth (*K*–10), and Birch Lake (*P*–7). Banded iron associated with older greenstones has been mined in the Vermilion Range near Soudan (*L*–6) and Ely (*O*–4), yielding over 100 million tons through 1968. The upper Mississippi River flows south past Grand Rapids and Big Sandy Lake (*G*–21). To the east the St. Louis River drains a large, swampy, drift-filled basin, emptying into Lake Superior at Duluth and Superior (*Q*–19). The upland surrounding Lake Superior is formed on the Duluth gabbro; overlying that igneous body are the drift-covered linear ridges alined with glacial lakes. Wave-cut benches notch the lake bluffs, marking the former extent of the level of Lake Superior. This lake occupies a synclinal lowland eroded on sedimentary rocks. The lowland was deepened by Pleistocene glacial scour and formed the western end of the Great Lakes chain following postglacial drainage realinements.

Superior Bay, the harbor at Duluth-Superior, is protected by a long natural sandbar. Canals are maintained at either end, the canal at Duluth surmounted by a large electric-lift bridge. Numerous ore docks and large grain elevators make the harbor one of the Nation's busiest ports, with railroads, blast furnaces, steel and iron works, and flour mills contributing to the large industrial complex. U.S. Highway 61 follows the picturesque North Shore through Two Harbors (*T*–15). Numerous other roads and railroads can be seen connecting the mining areas with the lake ports. *1345–16313;* July 3, 1973.

PLATE 55



NORTH AND SOUTH DAKOTA AND MINNESOTA: These three States share a common junction at *Q*–9. Lake Traverse (*P*–13) and Big Stone Lake (*R*–16) divide South Dakota from Minnesota. The entire region presents a landscape that was greatly affected by glacial activity in the Pleistocene. Ice from the Nebraskan, Kansan, and Wisconsin glacial advances covered this region, leaving behind a variety of deposits. The preglacial terrain consisted of rolling plains underlain by Cretaceous rocks, except for a large inlier (*U*–2) of the Canadian shield composed of Precambrian crystalline intrusives. After earlier glaciation, two lobes of Wisconsin ice spread southwestward: one, the Dakota lobe, extended westward through the present James River (*C*–20) region toward the Missouri River, and the other, the Des Moines lobe, invaded Iowa to the southeast. These lobes were deflected by the Cretaceous-capped Coteau des Prairies (*K*–16), although the ice eventually overrode this flatiron-shaped plateau (upraised as part of the Sioux uplift) to form morainal mounds and kettle lakes (*H*–14). In late Wisconsin time, the largest ice-margin lake in North America—glacial Lake Agassiz (covering approximately 260 000 square kilometers (100 000 square miles))—developed in the present Red River (*P*–5) Valley, extending from the till plain moraines (*U*–17) around Big Stone Lake (*Q*–16) and Lake Traverse (*P*–12), now connected by the Bois de Sioux River, northward into Canada near Winnipeg. Lake deposits from Agassiz gave rise to the dark chernozem soils (*O*–6) of the valley northward past Fargo (just off the image at *L*–1). The Sheyenne River (*C*–4) in North Dakota emptied into the lake producing still visible delta deposits (*H*–4). Glacial Lake Dakota was formed at this time in the James River Valley east of Aberdeen, S. Dak., between a westward escarpment and the receding ice. Lake Agassiz drained out through the present course of the Minnesota River (*V*–18). The glacial plains in this region are extensively farmed, with principal crops being spring wheat, barley, oats, soybeans, corn, beets, hay, and flax. *1060–16485;* September 21, 1972.

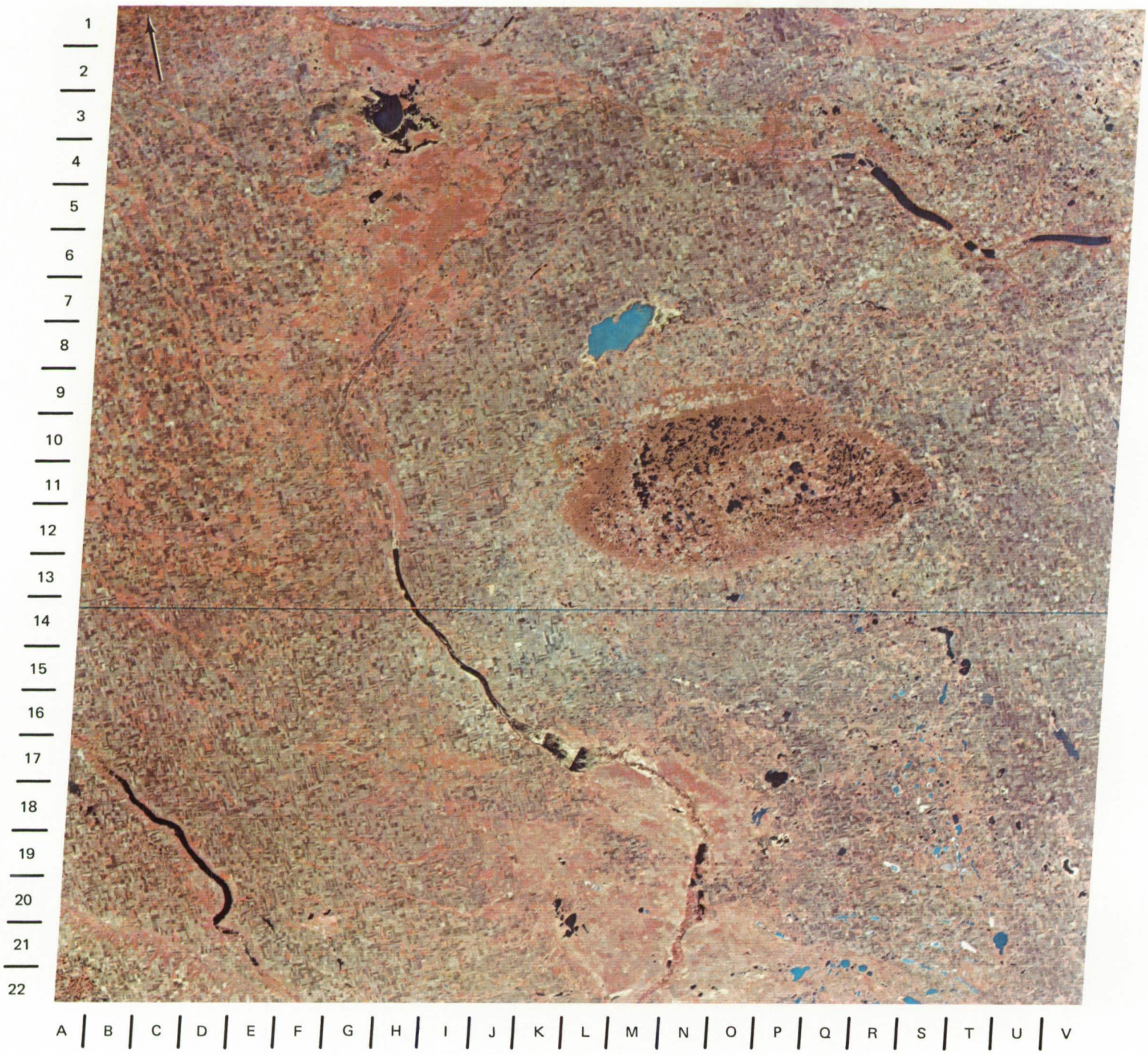
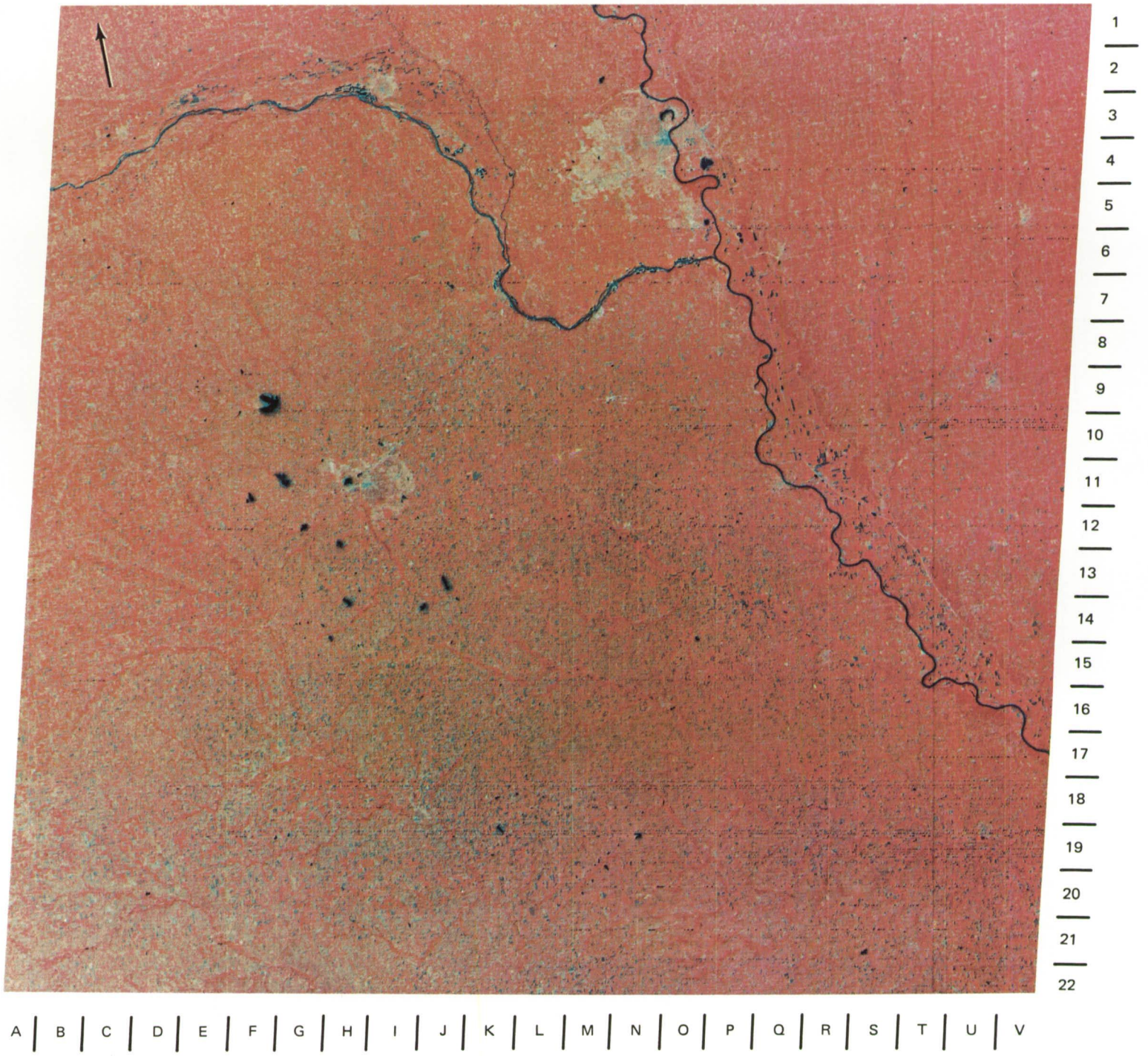


PLATE 56

GLACIAL PLAINS, NORTH DAKOTA: This region, part of the long-grass Second Prairie Plain of eastern Saskatchewan (*A*–8), western Manitoba (*O*–5), and northern North Dakota (*L*–14), is underlain largely by Cretaceous Morrison dark shales. The entire area was covered by Nebraskan, Kansan, and Wisconsin glacial tills during the Pleistocene ice advances. This cover, however, was thin over the Turtle Mountains (*N*–11), a "mesa" of basal Eocene rocks (Fort Union Formation) that rises almost 210 meters (700 feet) about its surroundings; similar Eocene units are present beneath the morainal deposits around Minot, N. Dak. (just below *G*–22), and Lake Darling (*C*–18). That lake, part of the Upper Souris Reservoir, and the J. Clark Salyer Reservoir (*H*–14; *K*–17) lie astride the Souris River (*G*–7; *N*–20), which rises in Saskatchewan, flows into North Dakota, and returns northward into Manitoba to join the Assiniboine River (*Q*–1). The Pembina River (*M*–3) and its Pelican Lake Reservoir (*R*–5) meet the Souris north of Whitewater Lake (*K*–8) in a forested area near Oak Lake (*F*–3). Most of the plains within the big bend (*F*–16) of the Souris River are topped by lacustrine sediments laid down by glacial Lake Souris, which coexisted with Lakes Agassiz and Dakota (see plate 55). A sandy stretch of plains (*M*–20) marks the southern end of this ancient lake. Of interest is the Minot Air Force Base (*F*–20), whose runways are visible in the image. This part of North Dakota is dedicated almost exclusively to agriculture, with spring wheat dominating the plantings along with some barley, oats, hay, alfalfa, and flax. The thin horizontal blue line is a "dropout" or failure to record one of the scan lines monitored in band 5. *1297–17060;* May 16, 1973.

PLATE 57



OMAHA, NEBR., AND COUNCIL BLUFFS, IOWA: Township and range roads grid this view of cornbelt country along the Missouri River. The course of the Missouri, here separating Nebraska from Iowa and Missouri, was determined during the Pleistocene, when large rivers, blocked to the north and east by glaciers, joined to form one master system flowing south along the edge of the great ice sheet. All of the Missouri's major tributaries enter from the west, including the Platte River, shown here curving past Fremont (*H*–2). This cornbelt area derives its loamy soil from a thick blanket of loess, windblown sand and silt, that covers the flat glacial till plains. The white and blue colors of plowed and fallow fields among red squares of growing crops can be seen around Beatrice (*H*–18) and Fairbury (*E*–20). The few forests present in the area show as dark red patches concentrated along the edges of the wide-terraced Missouri flood plain.

Omaha (*N*–3) is one of the Nation's largest grain and cattle markets, a leader in the production of butter, and has one of the world's largest lead refineries. A wide variety of food processing; paper, chemical, plastic, and textile manufacturing; and a major rail center make Omaha the wholesale capital of the west-central States. Offutt Air Force Base, headquarters for the Strategic Air Command, is located south of the city (*N*–5). Council Bluffs, on the Iowa side of the Missouri, is a major center for the manufacture of agricultural implements. The city was named for a council Lewis and Clark held with the Indians in 1804. Lincoln (*H*–11) began as the small town of Lancaster in 1859, exploiting salt deposits around Salt Lake (*G*–11). Established as the capital in 1867, the city became a railroad hub in the late 1800's. The trade center for southeastern Nebraska, Lincoln experienced considerable manufacturing and industrial development after World War II. The University of Nebraska is located here, and Lincoln Air Force Base is north of the city (*G*–10). *1022–16385;* August 14, 1972.

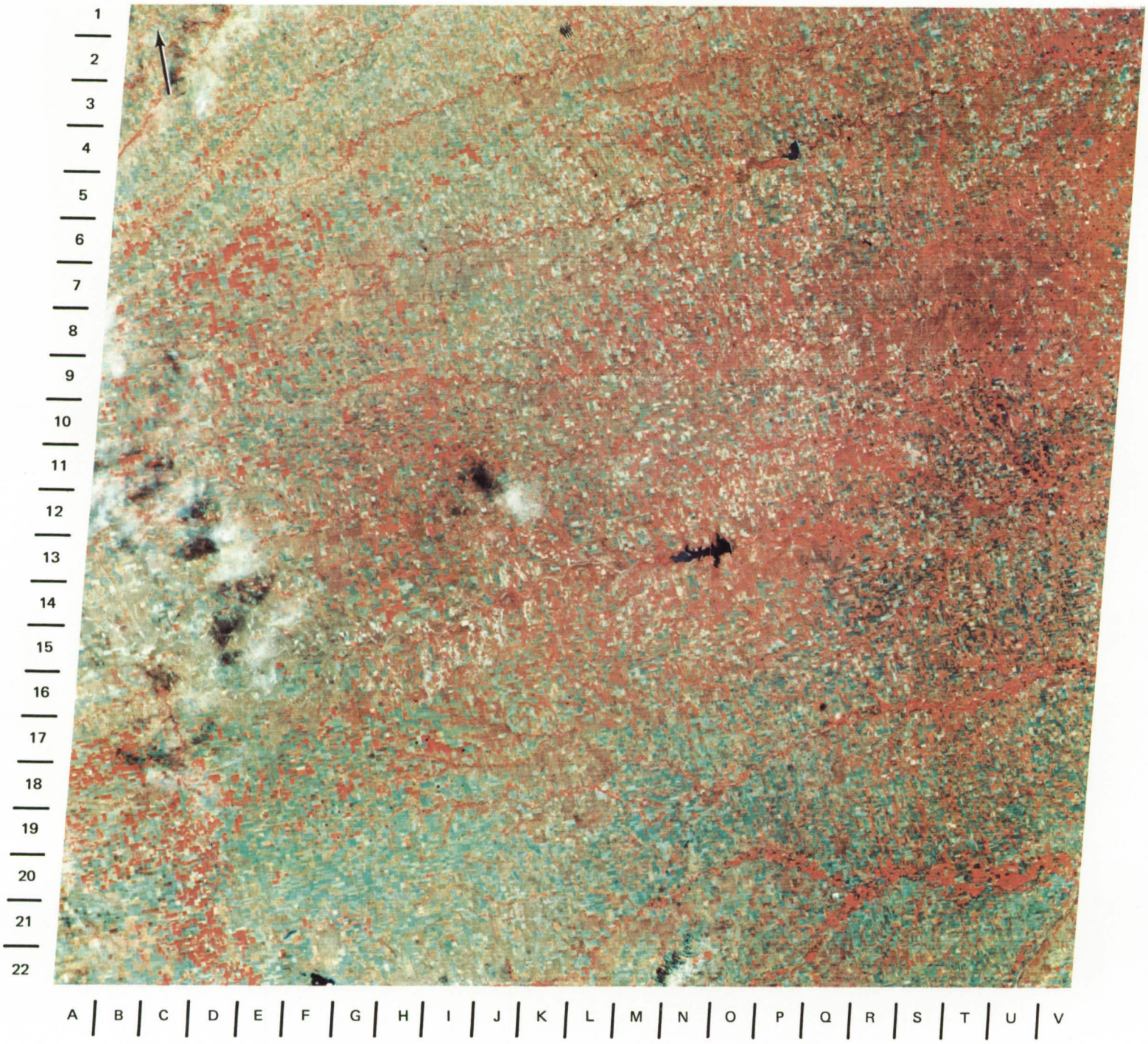
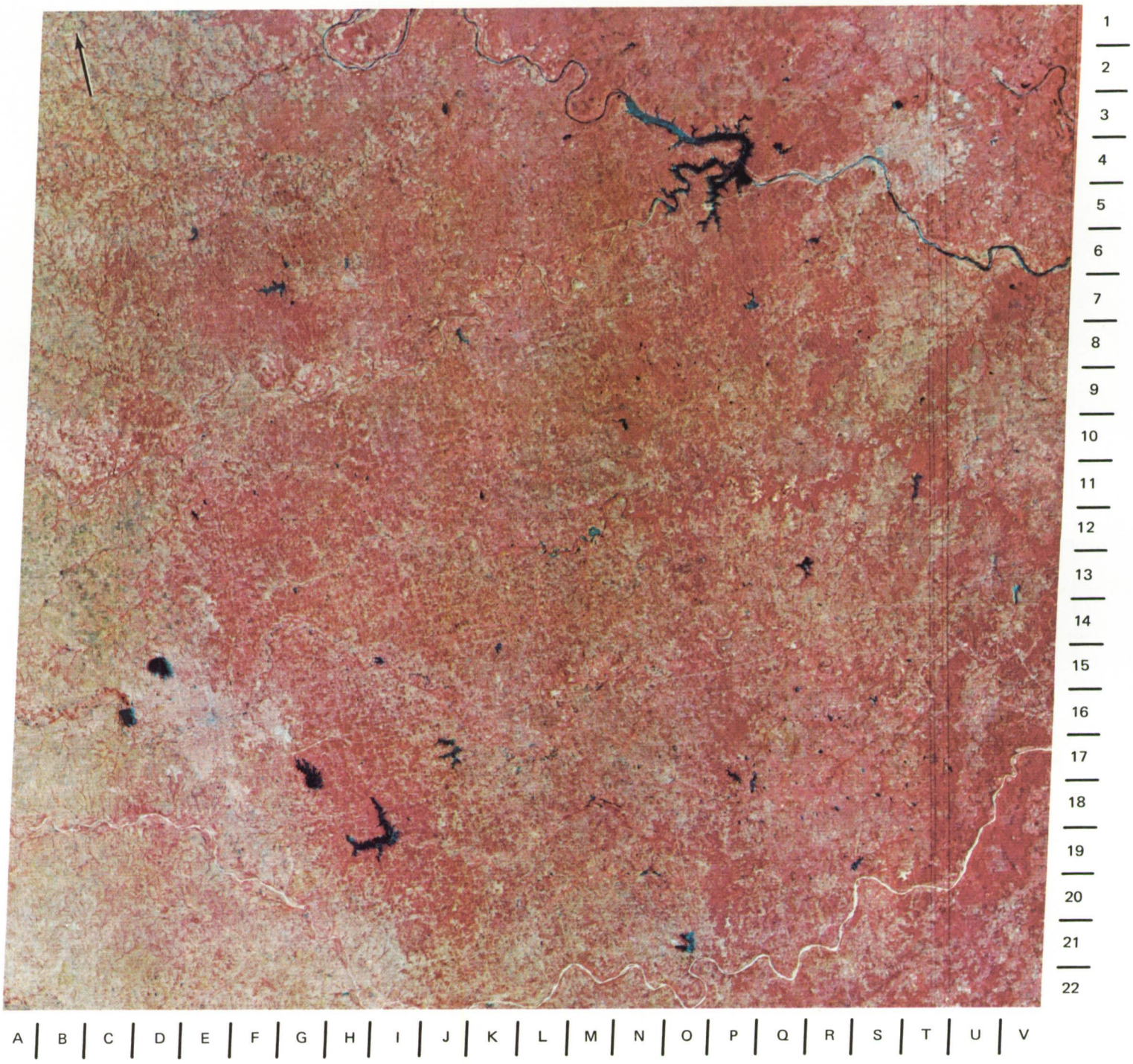


PLATE 58

WESTERN KANSAS: This part of the central Great Plains can be subdivided into the eastern edge of the High Plains (*D*–10), a relatively flat surface covered mainly by the Miocene Ogallala Formation, and the Plains Border Section (*S*–10), a more dissected lower surface underlain by Cretaceous shales (*N*–17) and sandstones (*U*–20). Reentrants of these Cretaceous units extend westward upstream along the Smoky Hill River (*J*–13), the Saline River (*P*–8), and the South (*K*–5) and North (*I*–2) forks of the Solomon River. Other rivers to the south are Walnut Creek (*Q*–16) and Pawnee River (*S*–19), which joins the Arkansas River (*V*–20) around Great Bend, Kans. Water is stored by damming along several of the rivers such as at the Cedar Bluff Reservoir (*N*–12). The area shown lies in the middle of the winter wheat belt (most of the gray-green plots) of the Great Plains, where the grain is sown in autumn and harvested by the following June. Sorghum, barley, and alfalfa are also cultivated in about a fourth of the farmlands. Some cattle grazing is practiced in the Smoky Hills. *1402–16503;* August 29, 1973.

PLATE 59



OKLAHOMA CITY AND TULSA: The two largest cities in Oklahoma are Oklahoma City (*F*–16), on the North Canadian River (*G*–14), and Tulsa (*S*–4), on the Arkansas River (*H*–1; *S*–5) just east of the Keystone Reservoir (*N*–3). The university town of Norman (*F*–19) is a few kilometers (miles) north of the Canadian River (*D*–18; *U*–19), a braided, silt-filled stream that is usually at low water by midsummer. Stillwater (*G*–6), another university town, is located near the Cimarron River (*D*–9).

The geology of central Oklahoma is characteristic of the Central Lowlands physiographic province of the eastern Great Plains geographic unit. This scene is centered about 160 kilometers (100 miles) east of the "Break of the Plains" escarpment—the unconformable juncture between the Tertiary Ogallala Formation (see plate 67) and late Paleozoic sedimentary rocks. The strata all dip very gently eastward, forming broad outcrop bands of Permian (*G*–11), and Pennsylvanian units (*P*–10). The surface is broadly rolling to nearly flat, interrupted only by several very subdued scarps following stratigraphic contacts. The region—part of the Osage section of the Lowlands—has not been glaciated.

A band of dark, blackish chernozem soils, a light blue-gray color (*A*–13) in this image, roughly follows Permian rock units west of Oklahoma City. These soils support bluestem and grama prairie long grasses. Further east, in lime-rich prairie soils, the bluestem, needle, and bunch grasses are mixed with scattered stands of oak and hickory, which increase proportionately toward eastern Oklahoma. The entire region is heavily committed to agriculture. The principal crop is winter wheat, but many farms grow barley, sorghum, corn, hay, alfalfa, peanuts, or watermelons. Pecan orchards are also common in the area. *1003–16352;* July 26, 1972.

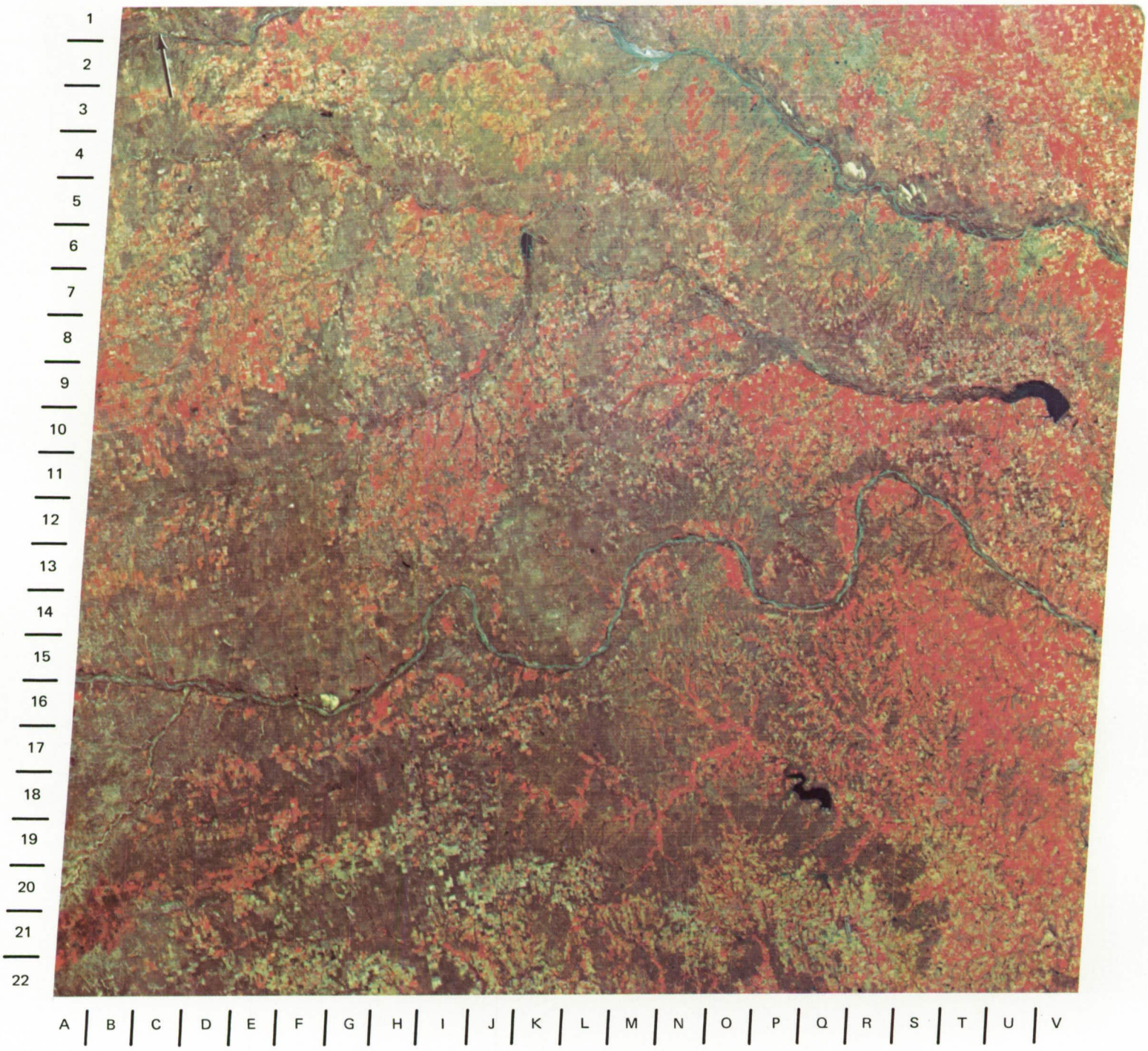


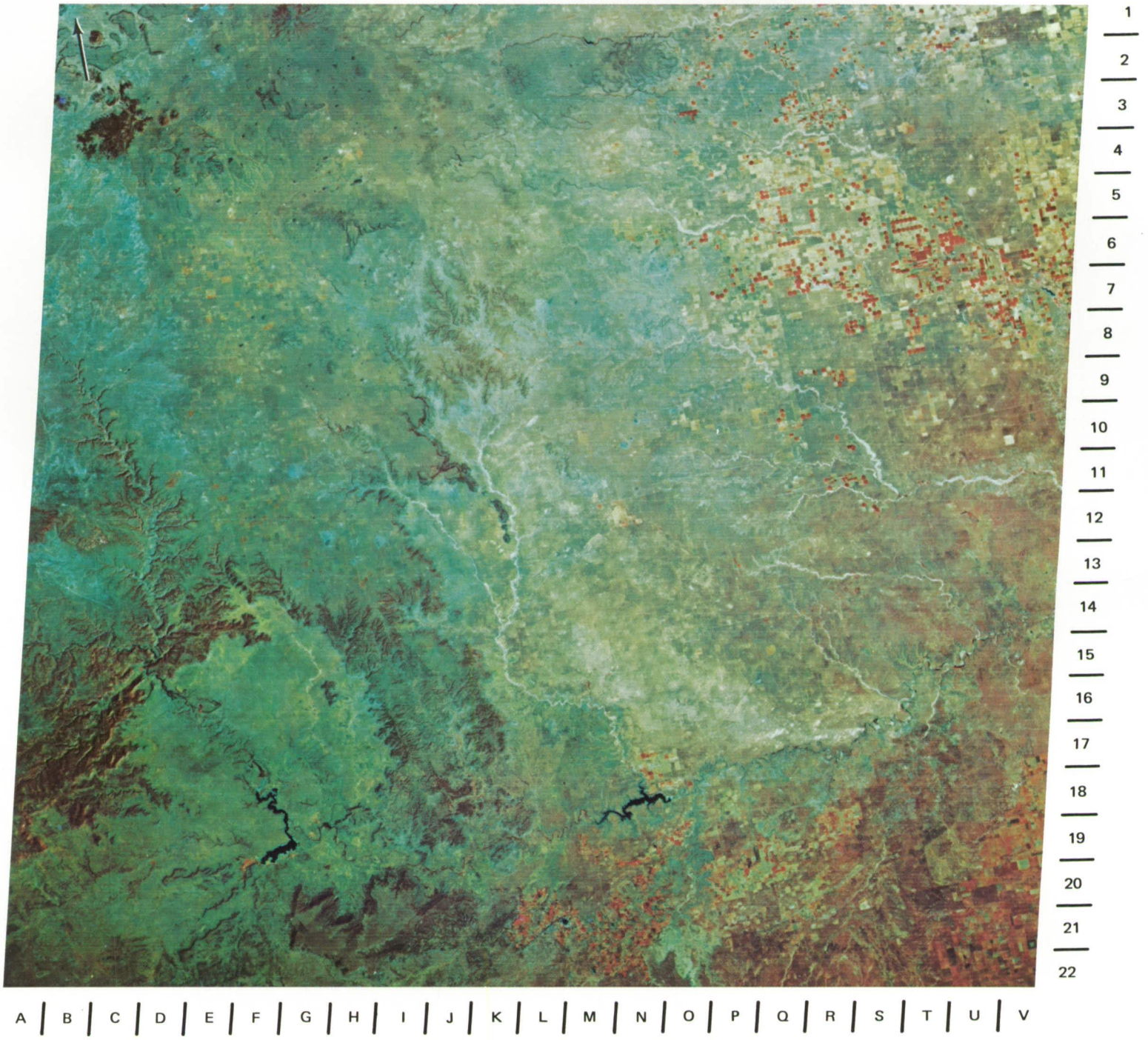
PLATE 60

OKLAHOMA OIL COUNTRY: The Anadarko Basin is one of the oldest oil- and natural-gas-producing regions in North America. Pumping fields extend over much of west-central Oklahoma (*K*–11) and part of the eastern panhandle of Texas (*C*–19). Weatherford (*V*–17) and Clinton (*S*–18), Okla., in the south and Woodward (*K*–7) in the north are among the larger towns in the area. Major rivers that flow eastward include the Cimarron (*R*–5), North Canadian (*Q*–9), and Canadian (*Q*–12); their braided channels generally follow the strike of underlying Permian sedimentary rocks.

The Township-Range pattern of land ownership and usage imposes a pervasive north-to-south and east-to-west grid on the area. Spring wheat shows as bright red in much of the scene; other crops grown seasonally include barley, sorghum, and oats. Freshly tilled fields on sandy soils show as whites and pale yellows. The brown areas are bluestem and grama grasslands dotted with blackjack oaks in the east and juniper in the west. Oaks, cottonwoods, and salt cedars line the drainage channels.

This image exhibits several types of features useful for geologic mapping and regional petroleum exploration. The outcrop patterns of the Elk City (*P*–20) and Doxy (*P*–18) members of the Permian Quartermaster Formation parallel the west-northwest trend of the structural axis of the Anadarko Basin just to the south of the image. Several naturally produced linear features (*E*–8; *G*–7; *L*–16) are important to petroleum exploration because they reflect fractures that either limit production from structural or stratigraphic traps or have produced porosity in deeply buried units. Many closed geomorphic anomalies, including curved or circular drainage patterns (*N*–15; *U*–16), reflect shallow to deeply buried structures that trap hydrocarbons, such as the Aledo field (*Q*–14), Elk City field (*O*–21), Buffalo Wallow field (*H*–20), and the Washita Creek field (*G*–18). Still other closed anomalies defined by apparent degradation or blurring of image detail (so-called "haze" anomalies) correlate closely with areas (*A*–14; *D*–15; *K*–14) of hydrocarbon production. The large elliptical feature (*C*–6; *I*–8) in the North Canadian drainage system is not yet explained. *1257–16471;* April 6, 1973.

PLATE 61



THE HIGH PLAINS: This scene covers the northwest corner of the Texas Panhandle (*U*–12), a small segment of the Oklahoma Panhandle (*T*–1), and much of the northeast corner of New Mexico (*F*–10). Dalhart, Tex. (*V*–6), is a crossroads town through which pass U.S. Highways 54 and 64 and the Southern Pacific rail line. This line continues through Tucumcari, N. Mex. (*L*–19), en route to El Paso.

Two striking examples of agricultural practice are brought out in this spring image. First, much of the farmland around Dalhart is given to winter wheat and many of the fields have been harvested. However, there are still large numbers of red dots—circular fields each irrigated by a long sprinkler free to rotate around a fixed end at the center—that represent growing crops including wheat and sorghum. These fields are conspicuous curiosities to air travelers passing over the Great Plains and parts of the West. Second, a faint tonal difference defines a boundary running from *P*–7 to *R*–13 and beyond. This boundary coincides with the State line between Texas and New Mexico. The cause of the difference may relate to watering practices by the farmers of the two States. An Apollo 9 space photograph revealed a similar feature further to the south and was interpreted then as an indication of greater withdrawal of subsurface (well) waters by the Texans.

The principal stream flowing eastward is the Canadian River (*C*–13; *R*–17), along which the Conchas (*F*–19) and Ute (*N*–18) Reservoirs have been established. The plains rise from about 1400 meters (4500 feet) near Dalhart to 1700 meters (5500 feet) west of Ute Creek (*K*–4). The highest point in the scene is Laughlin Peak (*B*–3), a basaltic mountain that reaches to 2688 meters (8818 feet). Basalt-capped mesas (*A*–2) and plugs (such as Capulin Mountain (*E*–1); see plate 69) of late Tertiary and Quaternary age occur in the vicinity. The Cretaceous Dakota sandstone caps a dissected plateau (*B*–14; *I*–20). The Canadian escarpment (*E*–14; *H*–16) is formed where the overlying Dakota has been stripped to reveal older Triassic rocks (*F*–15). The Ogallala Formation (see plate 67) covers most of the plains in the Texas-Oklahoma Panhandles. *2112–16515;* May 14, 1975.

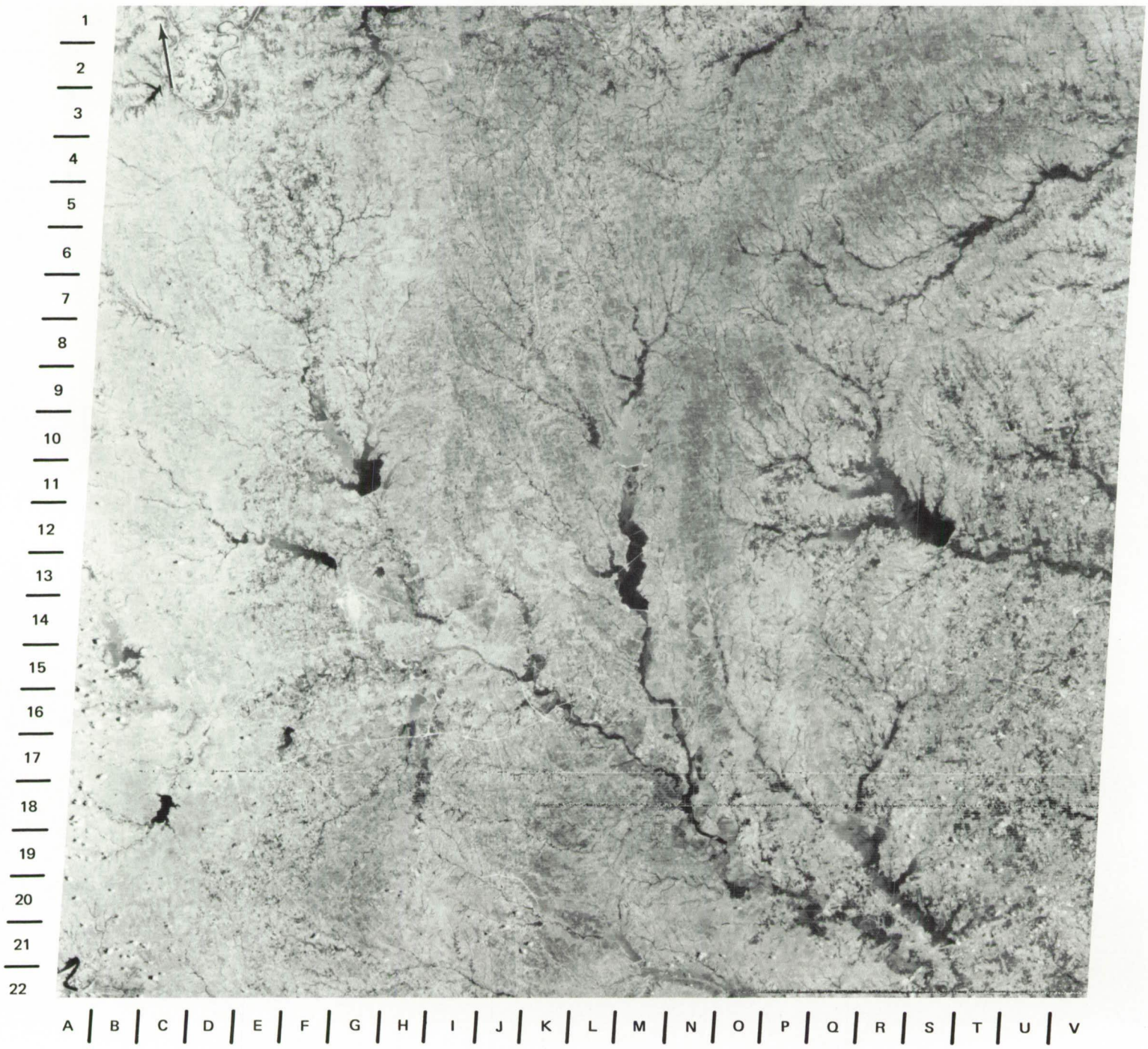


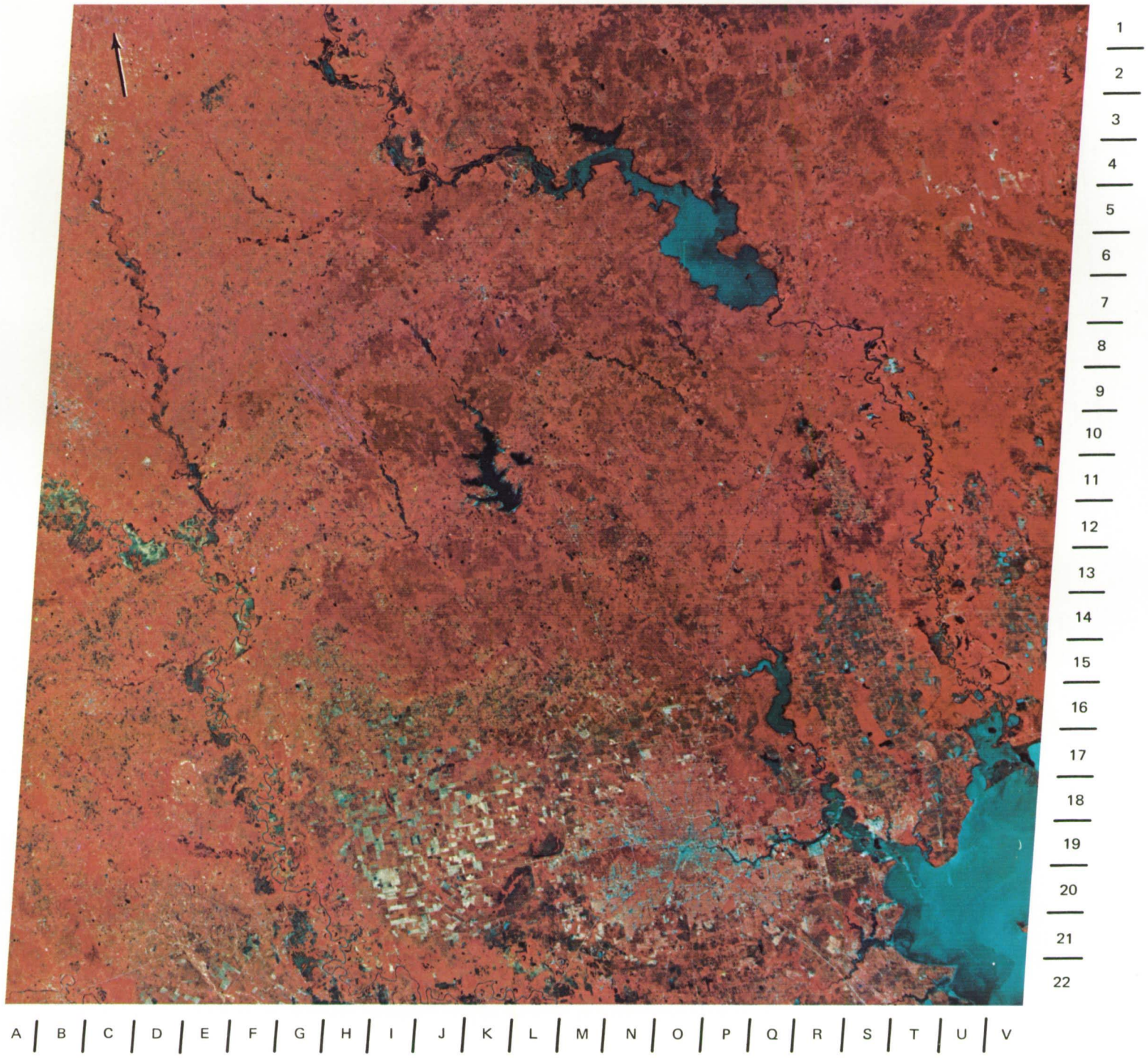
PLATE 62

DALLAS-FORT WORTH, TEX.: This image of northern Texas has considerable historic interest as being the first of those acquired by Landsat 1 to be actually identified as to specific scene location. Its date is July 25, 1972, just 2 days after launch. Its obvious quality was gratifying to the engineers and scientists responsible for the project. The potential value of Landsat imagery in map revision was immediately demonstrated by the fact that several major roads and reservoirs visible in the image could not be identified from available maps because they had been constructed since the maps had been printed.

The area covered has its top margin on the Oklahoma-Texas border, delineated by Lake Texoma (*F*–1) on the Red River (*L*–1). Dallas (*I*–14) and Fort Worth (*D*–16) can be identified even in this early rendition. The large feature at *F*–13 between the two cities is the Dallas-Fort Worth International Airport, then in the final stages of construction. The Texas road network, one of the best in the country, is easily resolved. Several large reservoirs near Dallas are conspicuous, including Lavon (*L*–12), Grapevine (*E*–12), and the Garza-Little Elm (*F*–10) Reservoirs. Further east are Lake Tawanoki (*R*–11) on the Sabine River (*T*–12) and Cedar Creek Reservoir (*S*–20) on a tributary to the Trinity River (*Q*–20).

The area to the east of Dallas illustrates the interrelation between rock strata distribution and associated vegetation. Outcrop zones of gently dipping late Mesozoic and early Tertiary sedimentary units show up here as different gray tones. These units form the western margins of regressing marine seas that gradually retreated over the last 75 million years. They now make up a series of broad valleys and low cuestas in this part of the Coastal Plains. The oldest Cretaceous strata, largely sandy beds of the Eagle Ford and Woodbine Formations, support a mixture of forest and grasslands (*G*–9) just west of Dallas. The broad lowlands underlain by the Taylor and Navarro Formations constitute the Black Prairie physiographic unit (*T*–9), which derives its name from the rich, dark organic soils resulting from weathering of calcareous rocks. Prairie grass is the predominant natural vegetation on that soil. The Sandy Hills (*V*–10), somewhat more rolling topography to the east, support patchy oak and hickory forests, mixed with Southern pine, on soils formed from the younger Wilcox and Claiborne groups. *1002–16314;* July 25, 1972.

PLATE 63



HOUSTON, TEX.: The east Texas Gulf Coast is a broad lowlands consisting of wide outcrop bands of late Tertiary marine sediments north of Houston (*O*–18) and an extensive Quaternary sediment plains near sea level to the south. Downtown Houston (*O*–19) is the hub of a radiating road network that includes Interstates 10 (*K*–19; *S*–17) and 45 (*M*–14; *R*–21) and U.S. Highway 59 (*O*–16). The new Intercontinental Airport (*N*–16) and NASA's Johnson Space Center (*R*–21) are easily picked out in this scene. A small stream, Braes Bayou, has been dredged out east of Houston to form the "Ship Channel" (*Q*–19) that, by accommodating ocean vessels, makes this city one of America's largest ports. The channel opens into Galveston Bay (*U*–20). Lake Houston (*Q*–15) is a large reservoir and recreational area in the pinewoods north of the city. The Trinity River (*R*–8) has been dammed to form Lake Livingstone (*O*–6), where it passes through the Big Thicket Country (*U*–7), a primitive pine, hardwoods, and cypress forest containing abundant wild game. Lake Conroe (Honea Reservoir) (*J*–11) lies at the western edge of a vast loblolly pine forest (dark red) extending to the west. The westernmost forests lie along the Oakville Escarpment (*G*–7). Oak and hickory make up scattered forests and groves elsewhere. The entire region is dotted with hundreds of small lakes, most of which are used as stock ponds. In the region drained by the Brazos River (*E*–14), farms grow cotton, corn, livestock fodder, and pecans. Much of the area around Houston is either pastureland (for the more than 1 million cattle in the vicinity), feed meadows, or rice (dark red associated with blackish tones from water). The Barker (*K*–20) and Addicks (*L*–19) Dams block drainage west of Houston to form paddylike rice-growing fields. *1289–16254;* May 8, 1973.

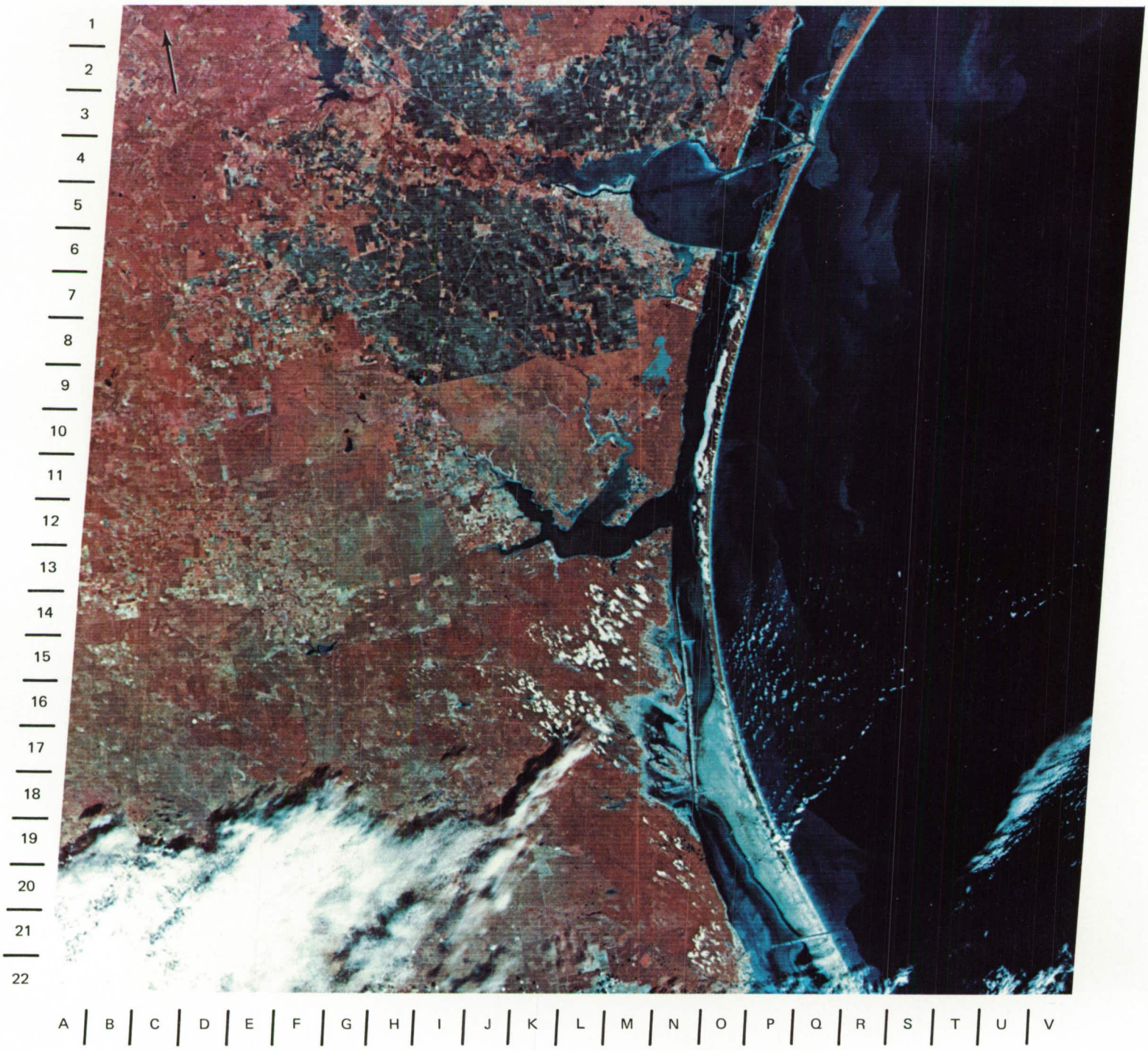
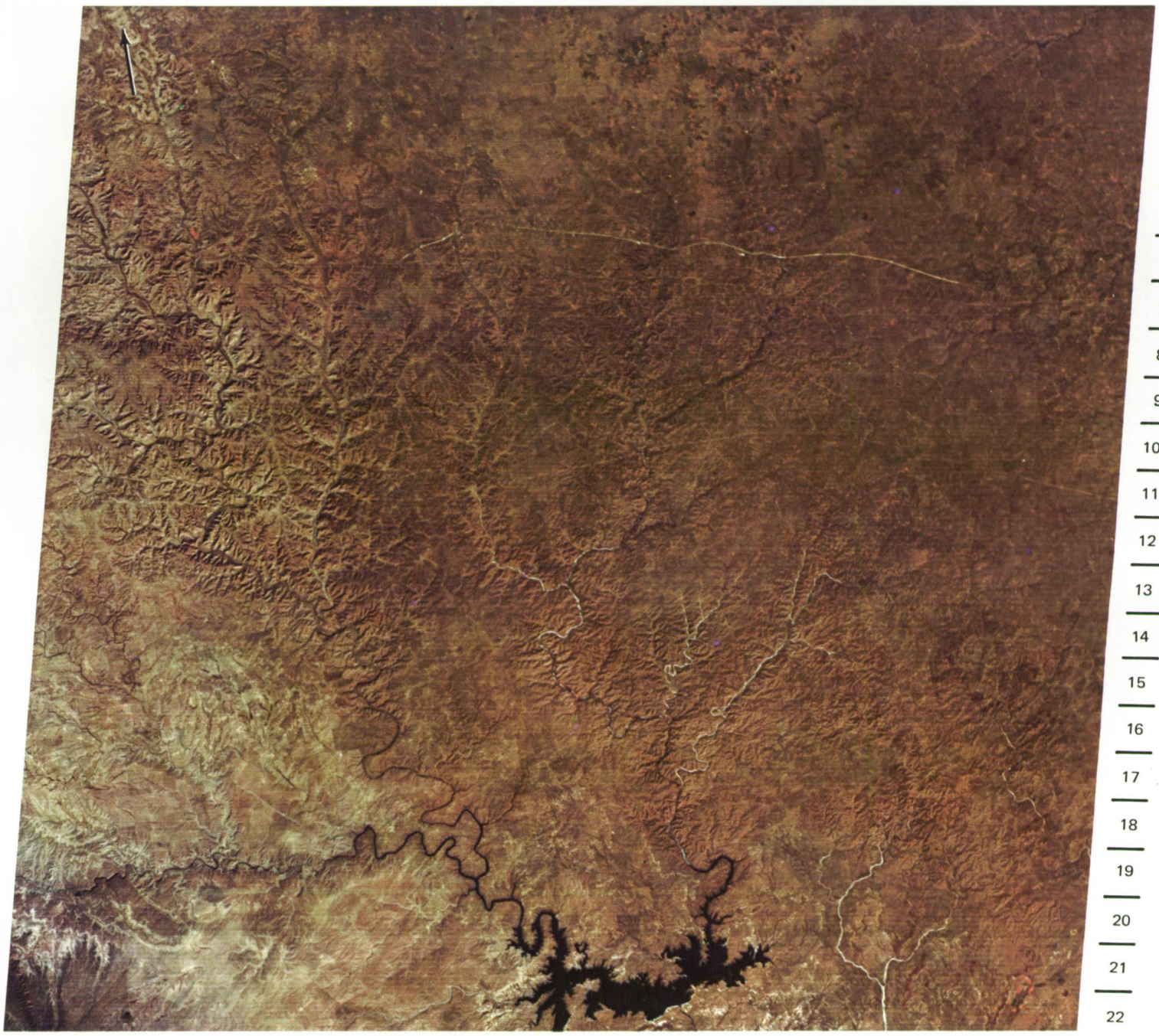


PLATE 64

THE SOUTH TEXAS COAST: The plains of south Texas seen here consist of a flat surface near sea level underlain by Pleistocene sediments (except for Pliocene sediments in the upper left corner). The city of Corpus Christi (*K*–5; *L*–6) lies along the south shore of Corpus Christi Bay protected by Mustang Island (*O*–5). Shipping enters this bay through Aransas Pass (*O*–3) at the south tip of St. Joseph Island (*P*–2). Southward from Corpus Christi is the great concave arc of Padre Island (*N*–8; *Q*–21), a 177-kilometer (110-mile) long offshore bar built by wave deposition of sands along a shoreline of emergence. This barrier island has sheltered the waters off the land coast to form a broad lagoon known as Laguna Madre (*O*–20). Dredging keeps open a channel in the shallow basins gradually being filled by sand and mud that serves as part of the Intracoastal Waterway of the Gulf Coast. Faint beach ridges can be seen on the gulf side of Padre Island whose surface also is covered by elongate dunes rising to 15 meters (50 feet) above the strand line. This scenic island is now protected as a national seashore.

The Nueces River (*H*–4) enters Corpus Christi Bay west of the city. Corpus Christi Reservoir (*E*–2) is impounded along this river. Several small streams, including Los Olmos Creek (*I*–12), flow into Baffin Bay (*K*–12) to the south. The inland area west of the coast is a dry savanna supporting mesquite and acacia; also live oak is seen south of Baffin Bay. The area around Corpus Christi is covered with bluestem prairie grass while the immediate coastal and barrier bar zones support cordgrass. Farming concentrates on cotton, sorghum, and watermelon. The famed King cattle ranch occupies much of the land south of Corpus Christi almost to the Mexican border. *1092–16314;* October 23, 1972.

PLATE 65



THE EDWARDS PLATEAU, TEX.: A broad plateau made up of flat-lying Cretaceous carbonates and shales rises from altitudes of 600 to 900 meters (2000 to 3000 feet) over much of south-central Texas. Austin and San Antonio lie just off the eastern limits of the plateau where the Balcones fault zone is expressed as a well-defined escarpment. On the north the Edwards Plateau laps onto the Llano uplift with its Precambrian core. The plateau passes into the Staked Plains of west Texas (see plate 67) along its western edge. Much of the plateau is capped by the resistant Edwards limestone. In many places streams cutting through this formation occupy small but scenic canyons that give the region a "western" look. Most of the region is devoted to cattle and sheep raising, with very little crop farming.

The southern part of the Edwards Plateau, shown here in late fall, is bounded by the western end of the Balcones escarpment (*T*–19) and the Rio Grande River (*H*–18). Maximum relief occurs along the Pecos River (*H*–16) and its tributaries; the Pecos Canyon (*D*–11) best shows the extent of dissection in this area. To the west, the Cretaceous limestones continue as the Stockton Plateau (*C*–15). This is an area of scrub savanna mixed with junipers that favor a limestone-derived soil. Scattered live oaks appear further to the north and east while the lowlands (less than 275-meter (900-foot) elevation) south of the scarp support mesquite and acacia. The Devils Creek (*N*–17) was dammed to form Devils Lake (*O*–19) while, more recently, the Rio Grande has been dammed to produce the Amistad Reservoir (*M*–21), an important water supply for Del Rio (just off the image at *P*–22) and agricultural activity in this segment of the Rio Grande Valley. The most recent stretch of Interstate 10 (*Q*–6) stands out in sharp contrast to the plateau vegetation. *1131–16483;* December 1, 1972.

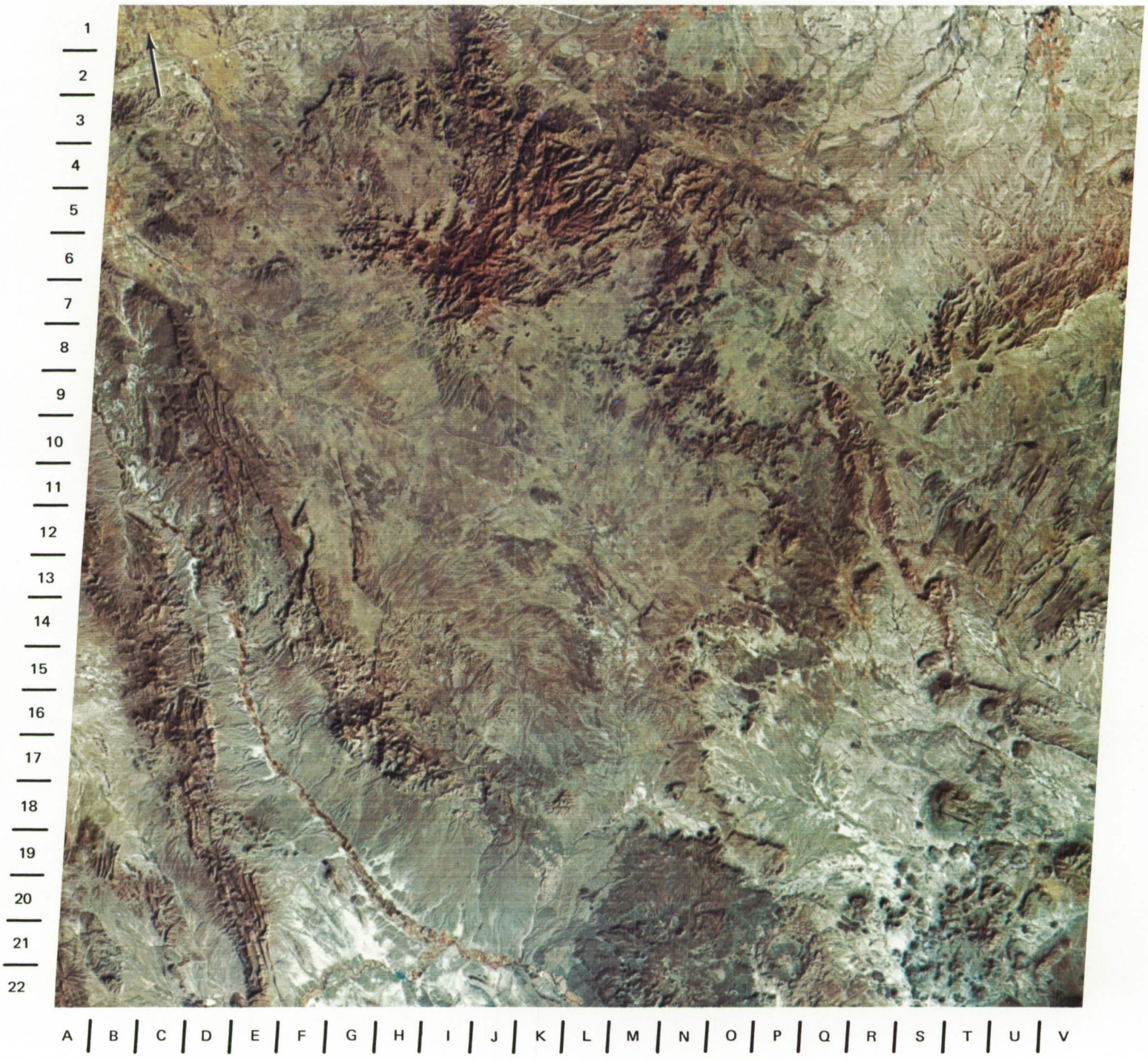


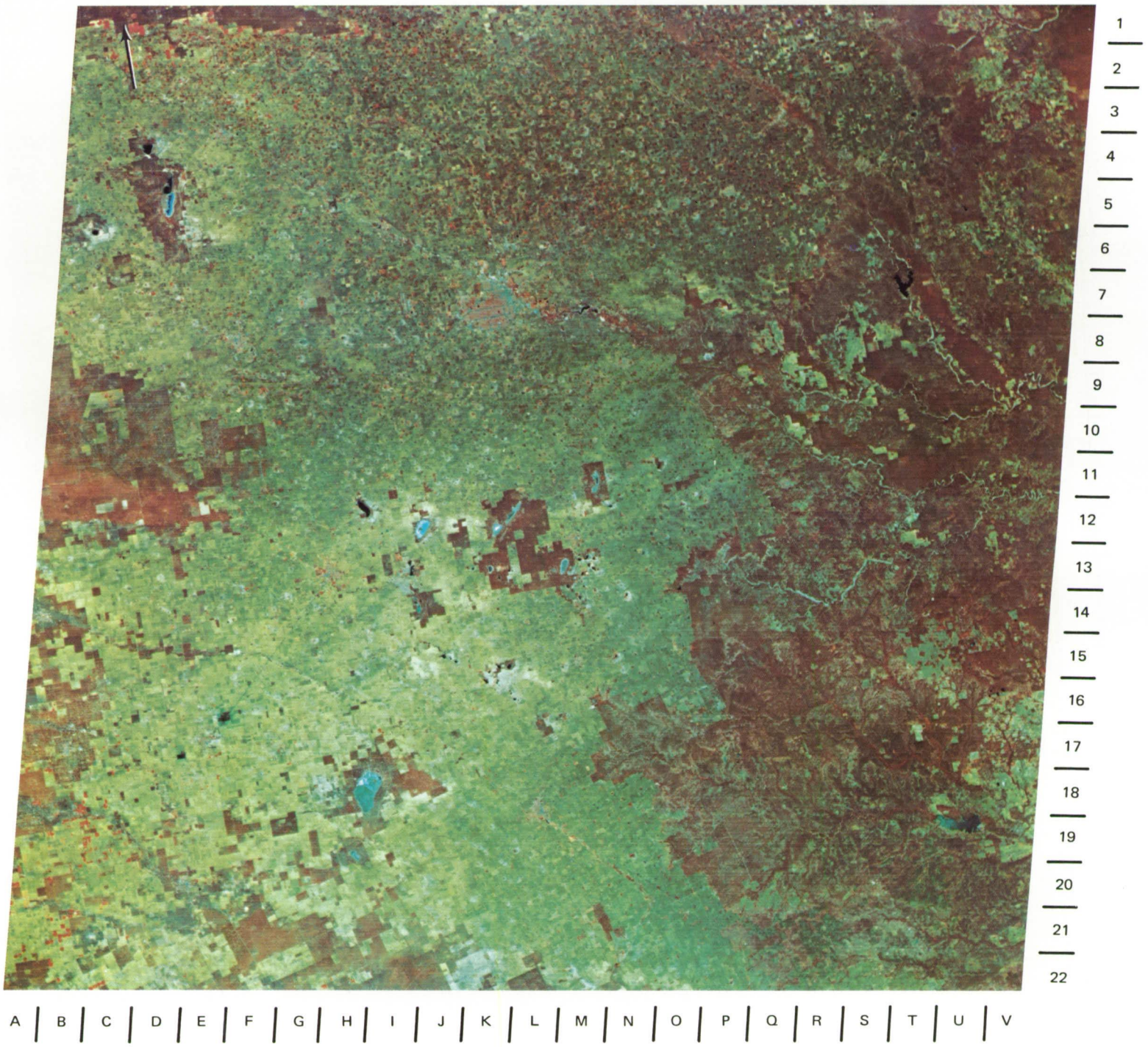
PLATE 66

BIG BEND COUNTRY, WEST TEXAS: The Rio Grande River (*J*–21) makes a northward bend just to the east of this scene, the only major deviation from its continuous southeastward 1900-kilometer (1200-mile) journey to the Gulf of Mexico. Here it passes through some of the most rugged and geologically interesting terrain in Texas. The Mexican mountains south of the river and the Sierra Vieja (*C*–9) and Chinati (*H*–17) Mountains on the Texas side consist of fault-bounded Cretaceous sedimentary rocks, as are most of the older rocks in the Big Bend National Park area (*U*–22). These structures along the river form the eastern edge of the Chihuahua tectonic belt that joins the Sierra Orientale section of the Rocky Mountain extension into Mexico. The Santiago (*S*–13) and Del Norte (*Q*–10) Mountains are narrow fault-controlled ridges lying along a north-trending fault zone. To their east are a series of northeast folds exposing Cambrian and Ordovician rocks and younger Pennsylvanian rocks in the Marathon uplift (*U*–11). This uplift is bounded on the north by Permian rocks of the Glass Mountains (*T*–7).

Most of the remainder of the mountains seen here are part of a vast outpouring of Tertiary lavas accompanied by intrusions to form the only distinct volcanic province in Texas. The Chisos (*V*–21) and Bofecillos (*N*–20) Mountains dominate the Big Bend area but many small stocks and surficial cinder cones (*R*–20) also dot the landscape. The Solitario (*P*–21) is a large, almost perfectly circular dome consisting of Paleozoic and Mesozoic sedimentary units but underlain by igneous intrusives. The Davis (*J*–4) and Puertacitas (*M*–8) Mountains, and part of the Chinati Mountains, are also carved largely out of Tertiary volcanic rocks. This region contains some distinctive minerals found mainly in volcanic deposits, such as mercury sulfide (cinnabar) around Terlingua (*R*–21).

South of Fort Stockton (*T*–1) is a small central peak surrounded by a ringed drainage pattern (*V*–4). This is the Sierra Madera uplift, which has now been identified as the remnant of a giant meteorite impact. *1511–16565;* December 16, 1973.

PLATE 67



LLANO ESTACADO, TEX.: The Staked Plains, which dominate the Texas Panhandle, are made up of the Ogallala Formation of Miocene age. This formation consists of stream-deposited alluvial sediments that filled older valleys to coalesce into a vast continual sheet by late Tertiary time. The Ogallala presently is topped by a 3- to 9-meter (10- to 30-foot) zone of caliche (calcium carbonate), which acts as a more resistant surface capping. Where eroded at its margins, this unit forms the Caprock escarpment (*Q*–6; *Q*–12). The land to the east consists of gullies and rolling swells of Triassic red beds (*Q*–17) and Permian gypsum-bearing rocks (*U*–8). An outlier of the Ogallala is also evident (*V*–17). The contact between the overlying Ogallala and these older formations is readily apparent because of the presence of mesquite east of the escarpment in addition to the more widely distributed buffalo grass.

A vast number of depressions (*K*–3) (some filled with water, others with sand or playa clays, still others enriched with vegetation) occur over most of this image. These depressions have been variously explained as deflation basins, solution and subsidence basins (sinkholes), compaction basins, or even old buffalo wallows. Among larger water-filled depressions are Cedar (*H*–17) and J. B. Thomas (*U*–18) Lakes. Drainage channels include Double Mountain Fork (*Q*–10), the White River (*T*–8), and Sulphur Springs Creek (*M*–19).

The main city in this region is Lubbock, Tex. (*J*–7); other towns are Brownfield (*G*–13) and Lamesa (*L*–18). In addition to cattle grazing, there is farming centered on the growth of cotton, sorghum, and winter wheat, with some pecan and peach orchards. In places, much of the farmland has been occupied by networks of drilling sites and oil pumps (*B*–17) located over some of the West Texas oil fields. *1330–16531;* June 18, 1973.

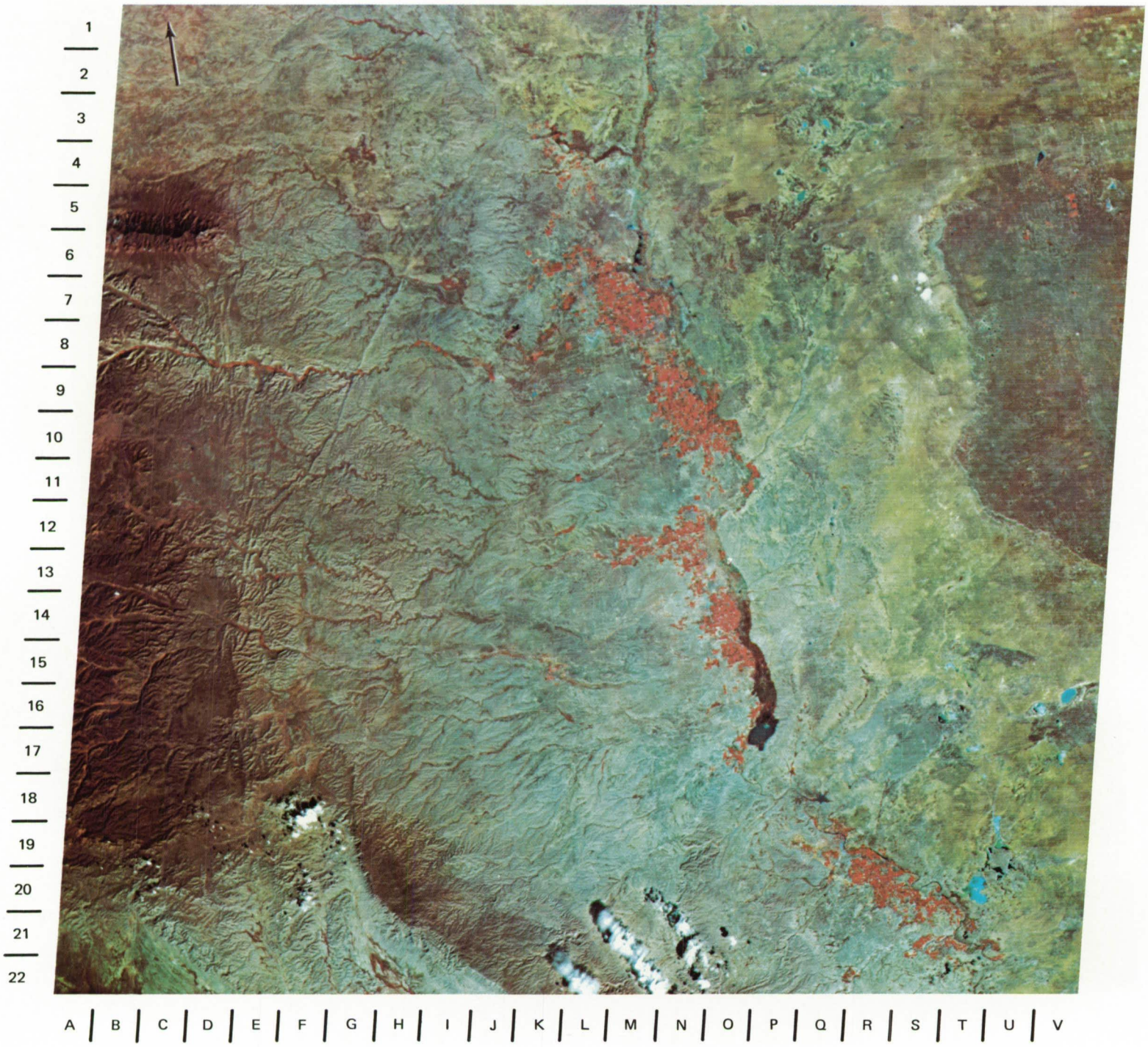


PLATE 68

PECOS RIVER, N. MEX.: After beginning far to the north near Santa Fe, this river flows southward across the Pecos Plains past Roswell (*J*–7) and Artesia (*M*–13) until it turns southeast at Carlsbad (*Q*–19). Much of this valley is filled with Quaternary alluvial deposits that support a shrub steppe vegetation in the open spaces and cotton and hay farms west of the river. Southeast of Carlsbad, Permian gypsum beds and red beds are present. Below these units are the potash-rich salt deposits mined in this region; water used in salt processing accumulates at Salt Lake (*S*–20) and elsewhere. To the west, the country rises to a series of mountain chains including the tilted blocks of the Sacramento Mountains uplift (*A*–12) and the Guadalupe Mountains (*H*–19)—both containing broadly arched Permian limestones, except where these are involved in a series of folds and normal faults (*C*–13). Among these limestones are the Capitan Formation, an ancient organic barrier reef now exposed, possibly by faulting, as a resistant unit along the Rim (*F*–19) and culminating in El Capitan, to the south, the highest point (2669 meters (8757 feet)) in Texas (below *K*–22; this should not be confused with Capitan Peak (3073 meters (10 083 feet)) in the Capitan Mountains (*A*–5)). Near the contact between Permian limestone and gypsum units, the fabulous Carlsbad Caverns (*N*–22) have formed from subsurface water solution to a depth greater than 300 meters (1000 feet). These mountain chains drain to the east along Rio Hondo (*F*–8) and Rio Peñasco (*G*–14). With decreasing elevation, the vegetation communities change from pine through piñon, juniper, and oak.

East of the Pecos, the western end of the Llano Estacado rises abruptly along the Mescalero escarpment (*R*–7). The capping Ogallala Formation is here covered by thick buffalo grass. Note the grid pattern (*T*–5) produced by the removal of vegetation around oil drill and pumping sites laid out in many cases along section lines. *1098–17043;* October 29, 1972.

PLATE 69



SOUTHEASTERN COLORADO: This scene shows parts of three physiographic subunits of the Great Plains: (1) the Colorado Piedmont (*F*–5), underlain by mainly Cretaceous rocks including the Dakota sandstones and shales exposed in canyons and draws along the Purgatoire River (*G*–7), and the Cody shales westward along the Arkansas River (*B*–2) near La Junta (*F*–3); (2) the High Plains (*U*–6; *U*–17), consisting of fluviatile sediments of the Miocene Ogallala Formation, where farms produce winter wheat, sorghum, hay, beans, tomatoes, and beets; and (3) the Raton section (*D*–9), both a series of lava-capped large and small mesas rimmed by steep escarpments—some rising 2100 to 2400 meters (7000 to 8000 feet) above sea level—including Raton (*A*–17) and Johnson (*B*–19) mesas and Mesa de Maya (*J*–15) and a region of dissected canyons around the Cimarron River (*L*–16). This region also includes Tertiary intrusive plugs like Sierra Grande (*G*–20) and the Spanish Peaks just off the image northwest of the gateway (*A*–19) to the Raton Pass in New Mexico through which passes the Sante Fe Railroad (*A*–12). The western end of the Oklahoma Panhandle lies along the North Canadian River (*T*–19). *1098–17032;* October 29, 1972.

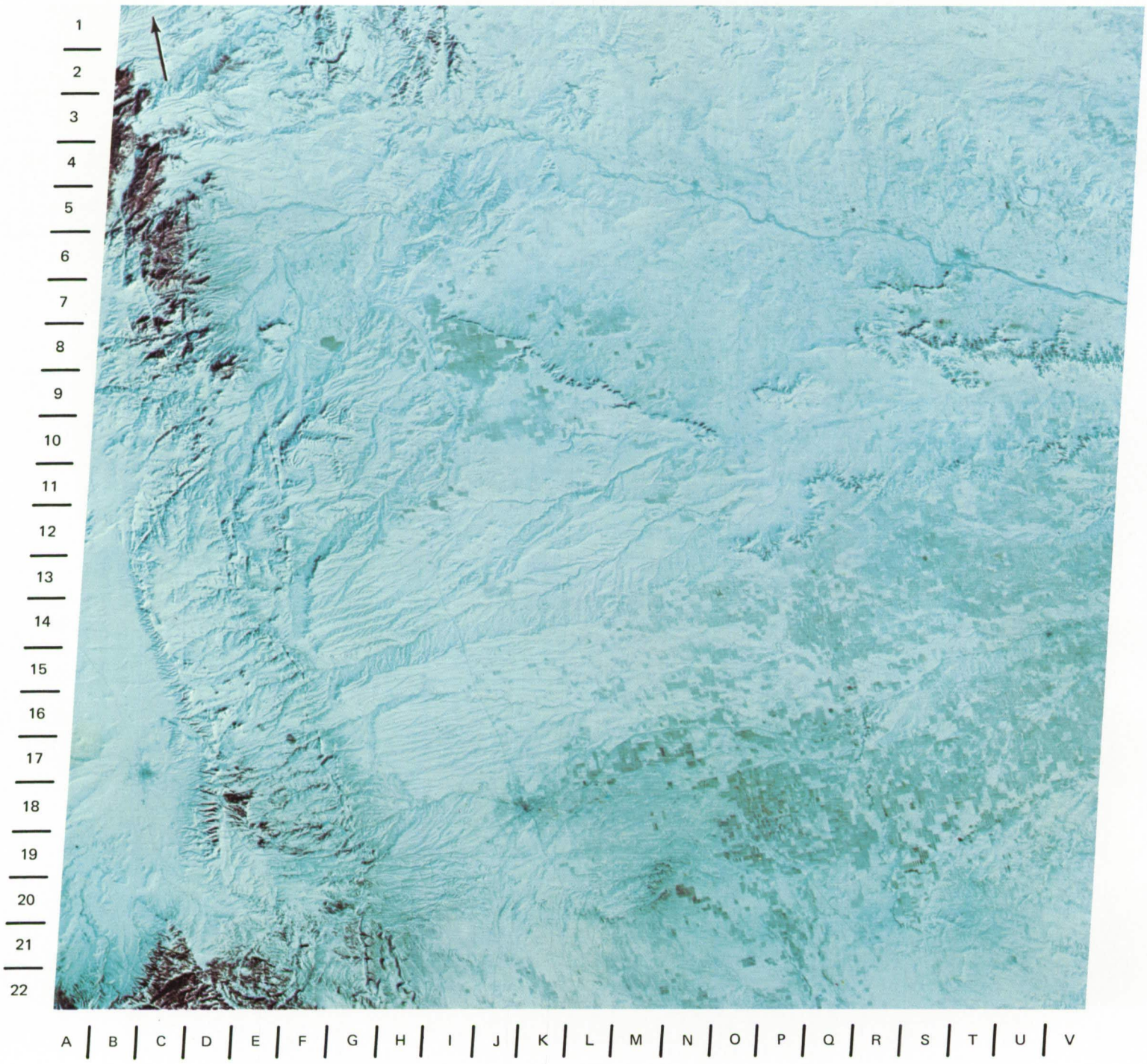


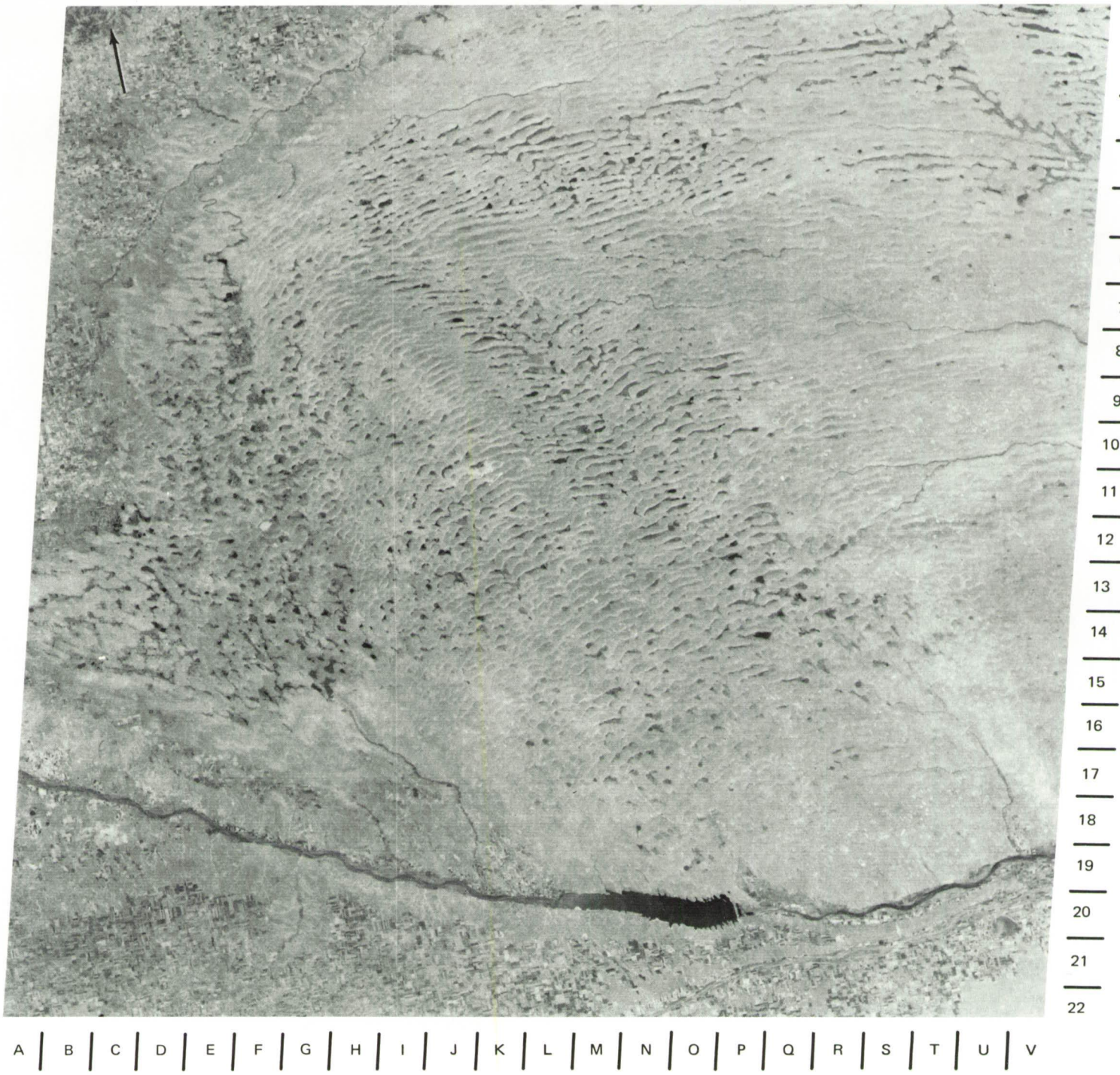
PLATE 70

CHEYENNE, WYO.: A blanket of snow highlights the landforms of the Great Plains and Rocky Mountains in this scene. The Laramie Range, trending north between Laramie (*B*–17) and Cheyenne (*J*–17), Wyo., is a broad, asymmetrical upwarp of Precambrian crystalline rocks. Pennsylvanian and Mesozoic sediments dip steeply off the east flank of the range, more gently to the west beneath the Laramie basin. Folding is outlined by the contorted bedding near the headwaters of Chugwater Creek (*E*–12). South and west of Wheatland (*F*–6), large faults and fractures line the exposed crystalline core. The Hartville uplift (*G*–2), a low domed structure, connects the Laramie Range with the Black Hills. The circular fractures (*E*–21) in the northern end of the Colorado Front Range outline a large granite pluton. Big Hollow (*A*–17) west of Laramie is a 14-kilometer (9-mile) long "blowout" depression produced by wind erosion.

The eastward-sloping Great Plains are the remnants of an extensive alluvial plain laid down during the Tertiary. Near Cheyenne the flat plains surface is formed on the Ogallala Formation. The merging of this erosional surface with the peneplain on the Sherman Granite at the "gangplank" (*G*–19) is probably indicative of conditions near the close of the Tertiary. The continuity of the Ogallala surface is interrupted by the Goshen Hole Lowland, where extensive erosion has widened the valley of the North Platte River to nearly 50 kilometers (30 miles) at Torrington, Wyo. (*M*–4). Sharp bluffs (*L*–9; *U*–10) mark the edge of the retreating Ogallala beds. North of Scottsbluff, Nebr. (*S*–6), the surface of the plains is much hillier, and is covered with extensive areas of sand dunes (*O*–1).

Main roads are widely spaced in this area. Interstate 25 can be seen coming north out of Colorado, past Cheyenne and Wheatland, toward Douglas; and Interstate 80 heads west from Nebraska past Pine Bluff (*Q*–16) and Cheyenne, through Granite Canyon (*F*–19), to Laramie. *1172–17132;* January 11, 1973.

PLATE 71



THE SAND HILLS, NEBR.: In west-central Nebraska, the landscape is dominated by the sand dunes of the Sand Hills (*L*–10) region. These are mainly a series of elongate ridges and mounds with interdune areas occupied by ephemeral to persistent lakes (*C*–12; *G*–5; *P*–14) or silty soils on which flourish a genus of prairie grass peculiar to this region. The Sand Hills—the largest continuous dune field in the United States—formed in Quaternary times from sand left behind by the winnowing out of the finer particles in the Ogallala Formation. Some particles were redeposited as loess to the southeast. Prevailing winds have since reorganized the lag sands into dunes. The northern part of the Sand Hills is crossed by the Niobrara River (*E*–3). The southern part is bounded by the North Platte River (*B*–17), here dammed to form Lake McConaughy (*O*–20). The South Platte River (*P*–21), flowing northeastward from the Denver area, follows and then meets the North Platte east of the Sutherland Reservoir (*U*–20). The farms in the flood plains of these three rivers produce extensive hay for fodder; winter wheat; and some barley, oats, and corn. *1296–17023;* May 15, 1973.

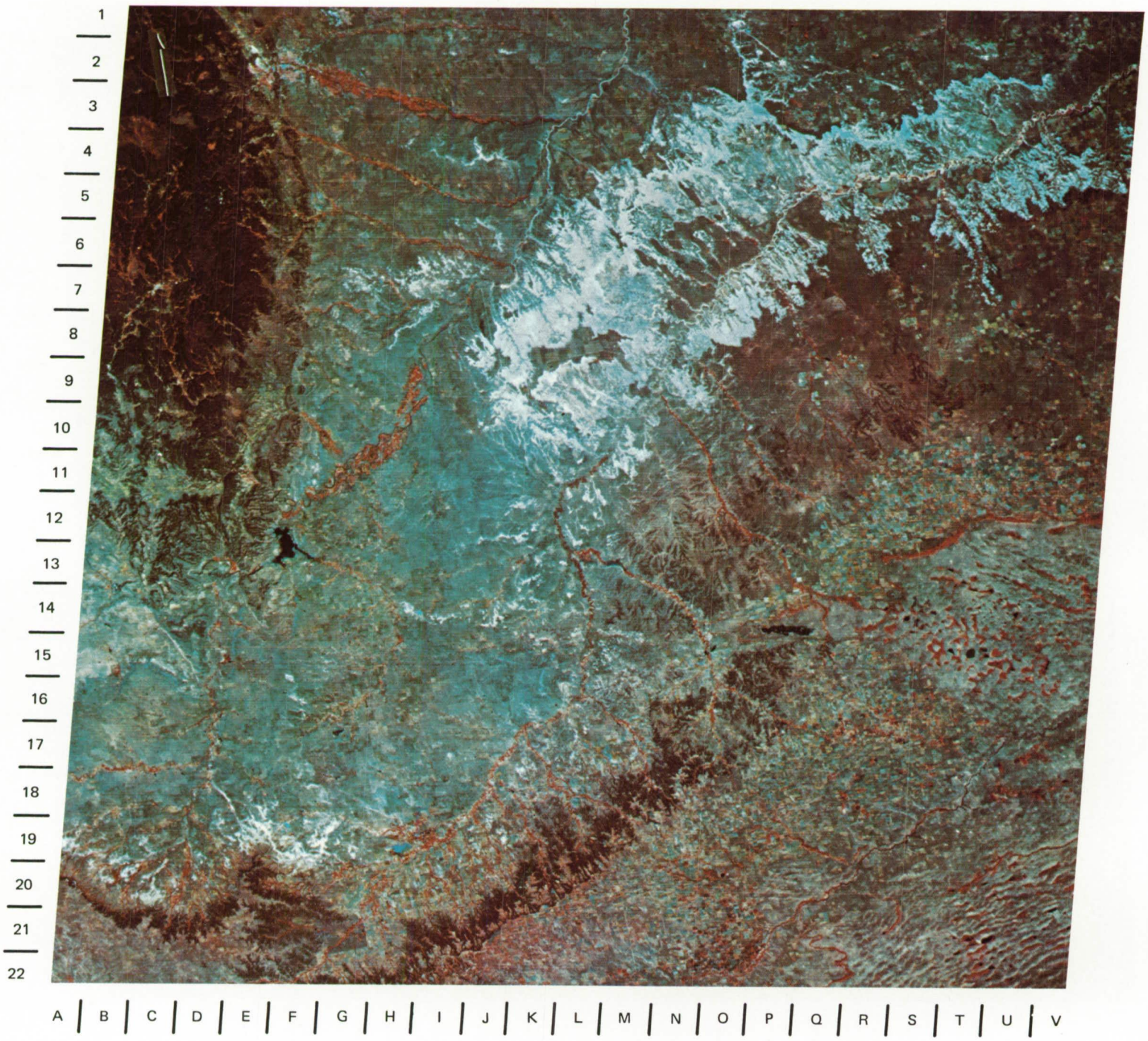
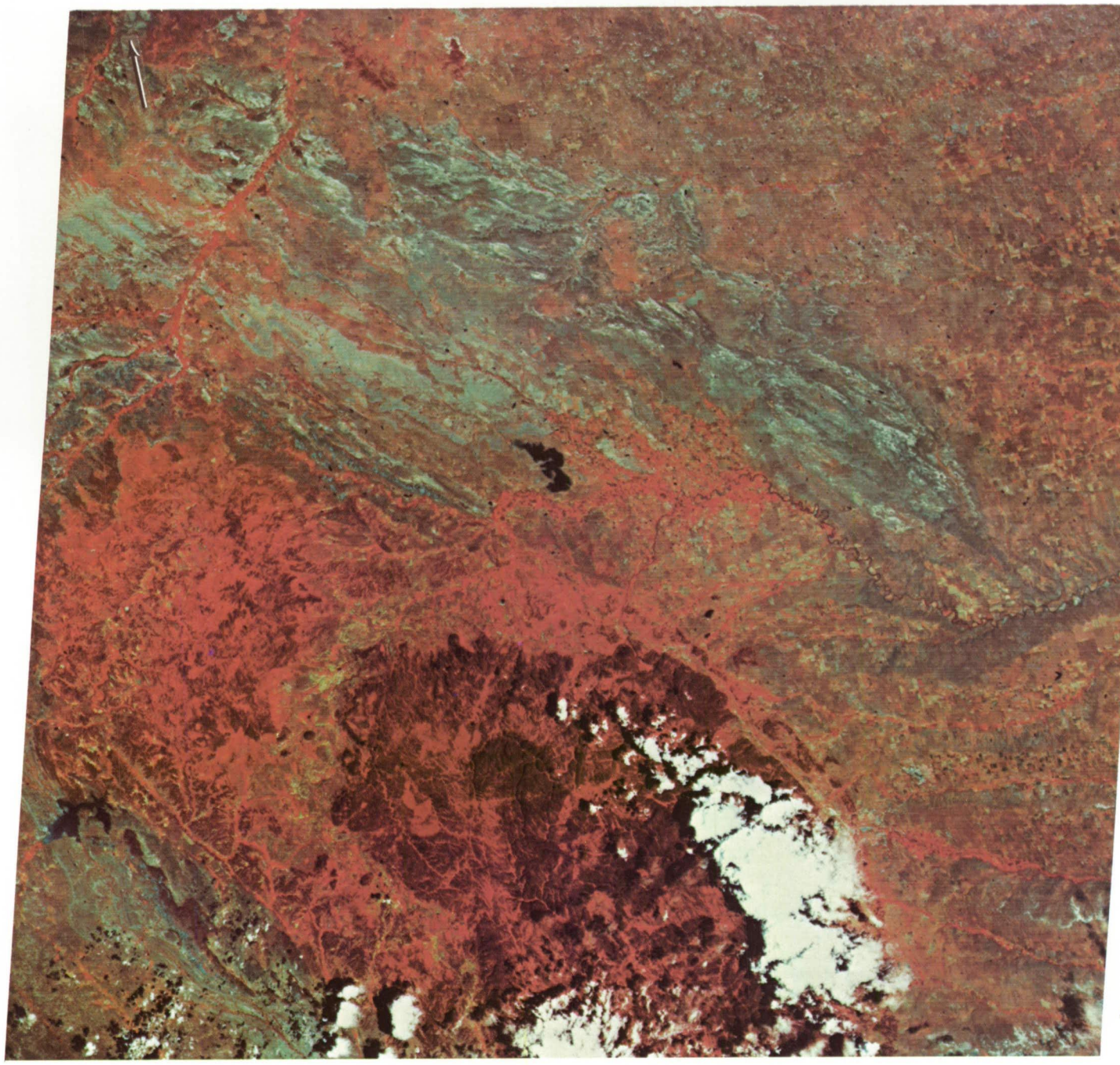


PLATE 72

THE WESTERN GREAT PLAINS: This part of the Missouri River Plateau includes four distinct geomorphic landscapes. The southeastern side of the Black Hills in South Dakota, from Rapid City (*D*–2) south to Hot Springs (*D*–11), is seen in the upper left. The edge of the evergreen-covered central core (*C*–6) of Precambrian rocks is flanked by a Paleozoic limestone ridge and then the Red Valley (*E*–6), cut out of Triassic red beds, and is rimmed farther east by the prominent hogback (*C*–1; *E*–5) of the Dakota sandstone. The headwaters of the Cheyenne River (*J*–4) north of Angostura Reservoir (*E*–12) begin just south of the Black Hills. Also in South Dakota (upper half of the image), the White River (*P*–5) has carved a typical badlands topography (steep gullies, irregular winding ridges, and isolated buttes) into the soft White River Formation of Oligocene age. The Badlands National Monument occupies the area around *K*–7. The plains to the north consist of Cretaceous Pierre shales. To the south in Nebraska in a segment of the High Plains are the breaks (spurs and valleys along the dissected edge of a tablelands) of the Pine Ridge Escarpment (*K*–20). This mesalike landform is held up by more resistant (caliche-cemented) layers of the Miocene Ogallala Formation. (See plate 67.) Much of the Pine Ridge area is assigned to two Indian reservations, one of which includes the town of Wounded Knee (*N*–15), known as the site of the last major encounter between the American Indians and the U.S. Cavalry. In northwest Nebraska (lower right), the landscape is dominated by the sand dunes of the Sand Hills (*U*–21) region. (See facing page.) The northern part of these hills is crossed by the Niobrara River (*S*–18).

Wheatgrass is dominant around the Badlands region, grama buffalo grass prevails in the Pine Ridge area, and a prairie grass peculiar to the Sand Hills occurs further east. The farms produce mostly winter wheat, with some barley, oats, and corn, plus extensive hay for fodder. *1711–16592;* July 4, 1974.

PLATE 73



BLACK HILLS REGION, S. DAK.: The paired scenes in plates 73 and 74 show the massive uplift of the Black Hills—the first western-type mountains encountered after crossing the Great Plains. This classic structural dome consists of a broad core (*M*–20) of Precambrian granites flanked by a ring of outward-dipping sedimentary rocks of Paleozoic and Mesozoic age—the eastern segment (*P*–16) being especially evident in the snow-covered winter scene. The broad bluish areas in the summer scene are dissected, vegetation-sparse exposures of late Cretaceous dark shales and sandstones (*P*–9). The Black Hills earn their name from the thick cover of Ponderosa pine, which remains particularly dark in the low Sun angle illumination of winter. To the northwest, the Bear Lodge Mountains in Wyoming (*E*–13) are carved out of early Mesozoic sedimentary rocks. Several Tertiary volcanic plugs (*F*–15) are

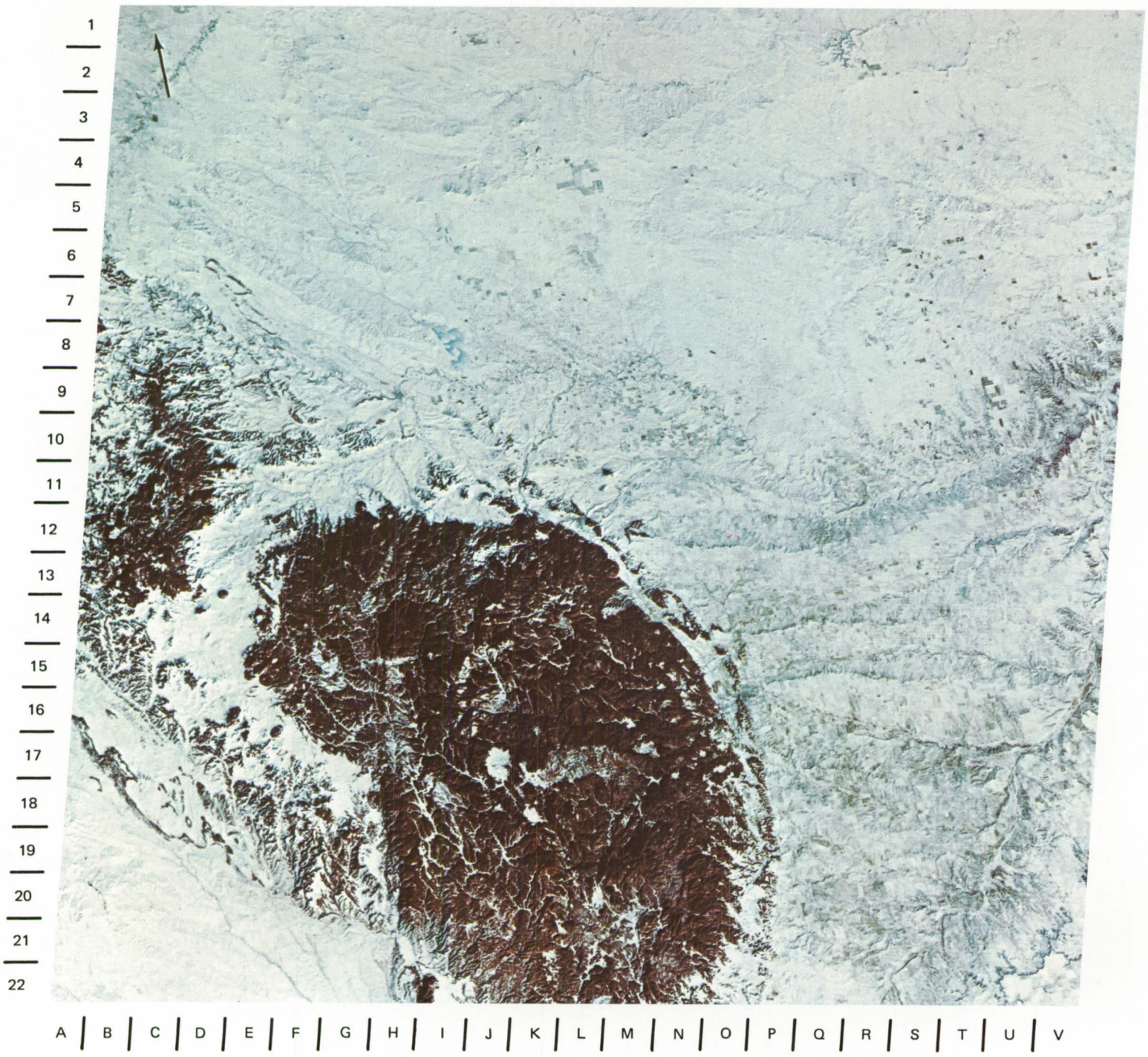


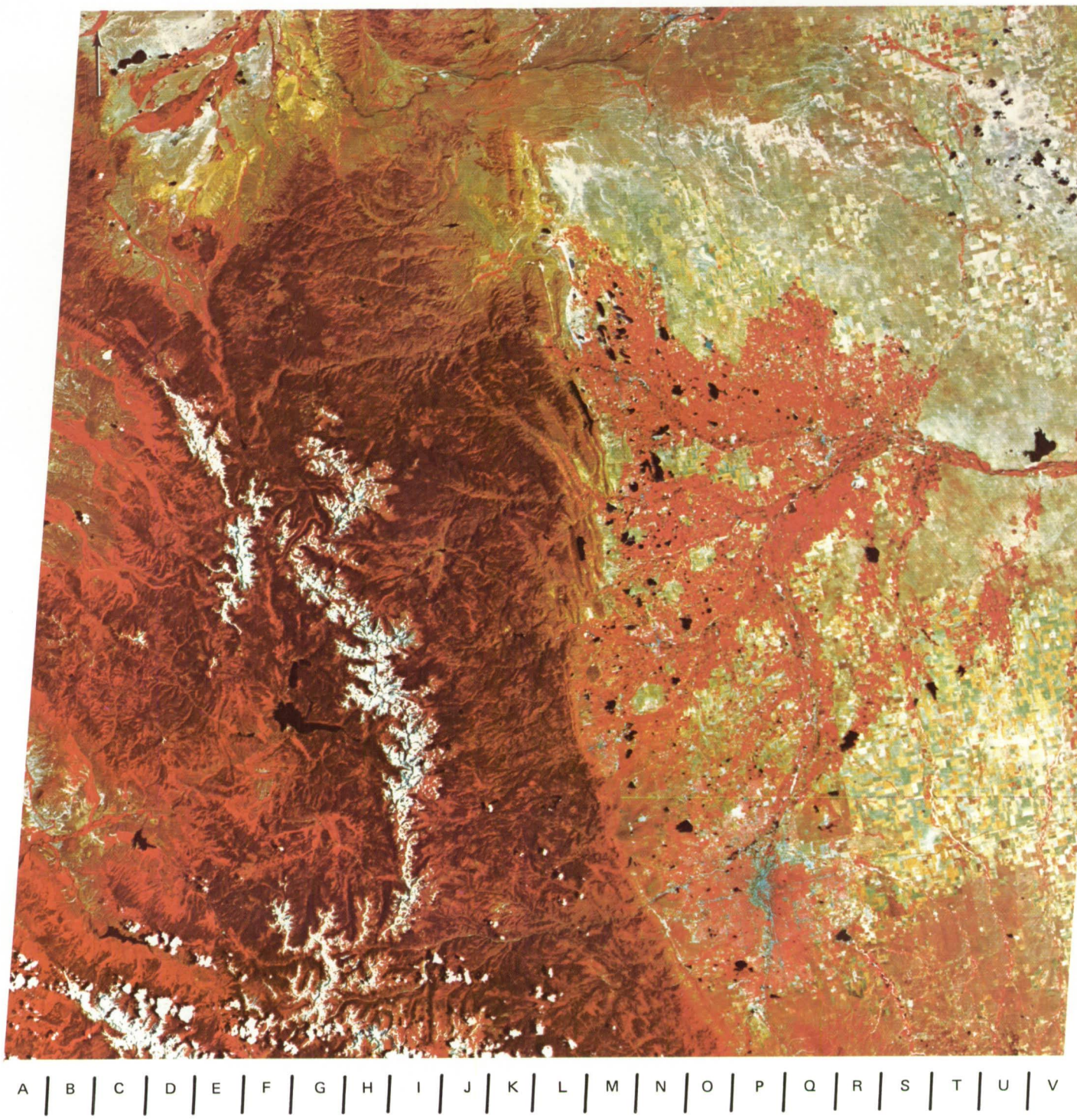
PLATE 74

evident, although the most famous of these—Devils Tower—is too small to be distinct on the image. Southeast of Rapid City (*Q*–18), the granite-hewn faces of Presidents Washington, Jefferson, Lincoln, and Theodore Roosevelt at Mount Rushmore (*N*–19) are a popular tourist landmark.

The Belle Fourche River (*O*–10; *T*–13) and the Little Missouri River (*D*–5) make up the principal drainage; numerous cattle ponds dot the image, along with the Belle Fourche (*K*–9) and Key Hole (*B*–17) Reservoirs. Numerous fields to the east produce mainly wheat, alfalfa, and hay.

A broad swath (*J*–17) within the heavy forests south of Deadwood represents the track of a tornado that cut across that area some years ago. *1352–17123;* July 10, 1973. *1172–17123;* January 11, 1973.

PLATE 75



COLORADO ROCKY MOUNTAINS: The above scene is a computer-processed version made by IBM without producing a negative. It displays the maximum resolution attainable in Landsat imagery. The images in plates 75 and 76 cover the Front Range (*I*–10; *K*–18) of the Colorado Rockies and the high plains-piedmont (*S*–11) to the east. The winter scene graphically emphasizes the urban areas of Denver (*M*–17) and the smaller cities of Boulder (*J*–14), Longmont (*K*–11), Fort Collins (*J*–6), and Greeley (*N*–7), where street clearing and the "heat island" effect remove the snow in contrast to the surrounding plains. The Interstates 70 (*Q*–16), 80S (*P*–11), and 25 (*L*–11) and many other roads also stand out. The summer scene shows the extent to which these plains have been converted to farmlands: the blue-gray areas (*T*–16) support mainly winter wheat while the South Platte River (*I*–10) and its tributaries irrigate a variety of crops such as barley, oats, hay and alfalfa, corn, beets, beans, and potatoes. Uncultivated areas are covered by grama and buffalo grasses.

The gently dipping Eocene and Cretaceous units of the plains give way abruptly to steep-dipping Mesozoic and late Paleozoic sedimentary rocks that rise as hogbacks (*N*–20) along the east edge of the Front Range—itself a complex of Precambrian granites and metamorphic rocks. Steep-walled canyons (e.g., Big Thompson

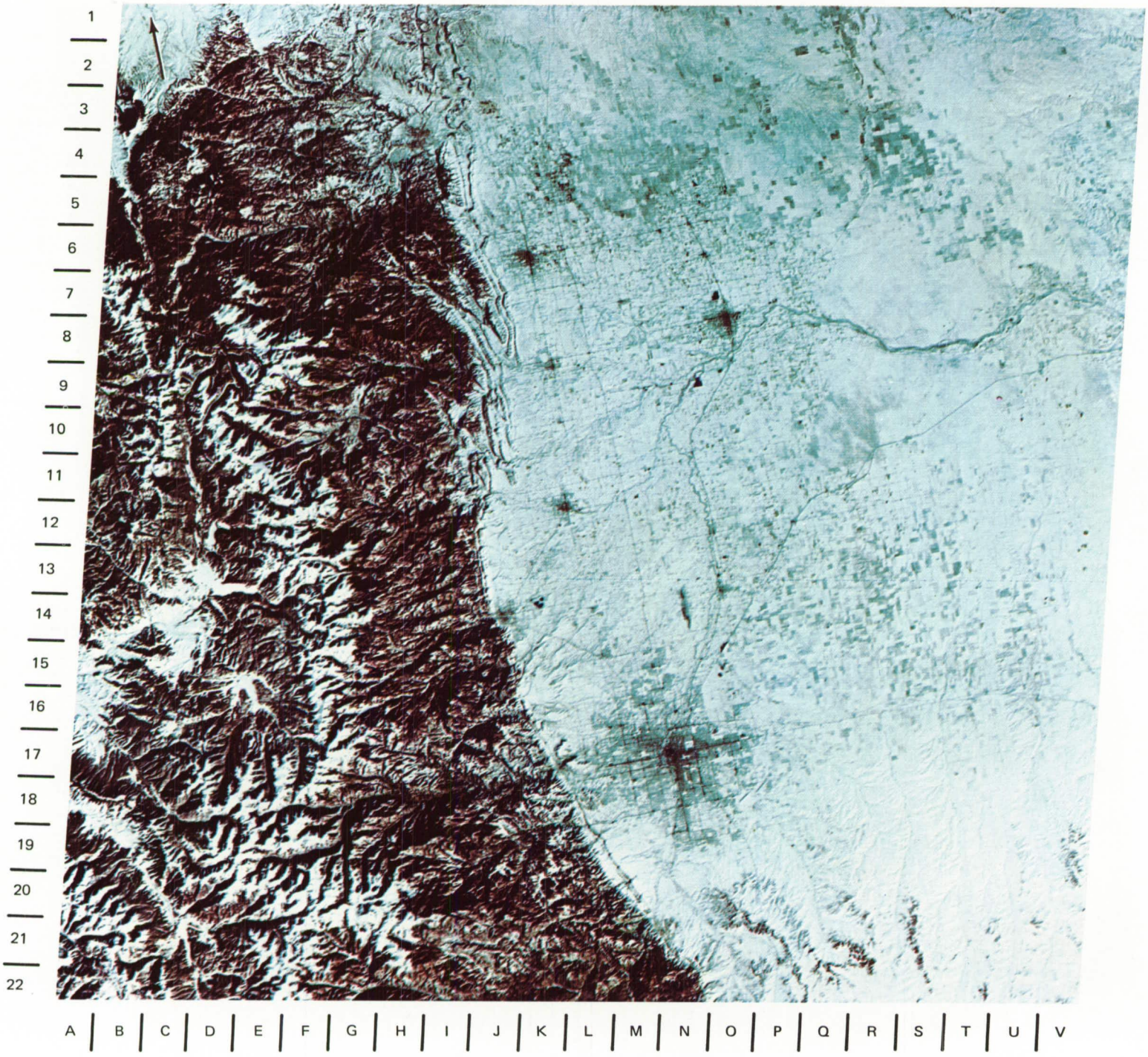


PLATE 76

Canyon (*J*–11) leading to Rocky Mountain National Park (*G*–10)) are carved from these rocks by rushing mountain streams like Poudre River (*G*–8) and Clear Creek (*K*–20). Clear Creek forms a valley used by Highways 40 and 91 as they climb over the continental divide at Berthoud (*H*–20) and Loveland (*G*–22) Passes, the latter being the highest (over 4200 meters (14 000 feet)) auto road pass in North America. The Front Range, the Gore Mountains (*A*–21), and the southern end of the Medicine Bow Range (*B*–7) are forested with pines, Douglas fir, spruce, and aspen except above elevations of about 3300 meters (11 000 feet), where alpine meadows and bare rock (*H*–15) take over. The highest promontory in this scene is Long's Peak (*H*–15), rising to 4345 meters (14 255 feet) above sea level. The headwaters of the Colorado River (*A*–18) form just to the west, passing through Grand and Granby Lakes (*F*–14; *F*–15) and across Rabbit Ears Range (*G*–14). Part of the Laramie Basin (*C*–5) in Wyoming, including an area of red Pennsylvanian sedimentary rocks (*E*–2), is visible in the upper left corner northwest of Virginia Dale, a small mining area that seems in the Landsat view to lie within a series of concentric fractures (*G*–4) around a domal igneous intrusion. *1352–17134;* July 10, 1973. *1172–17135;* January 11, 1973.

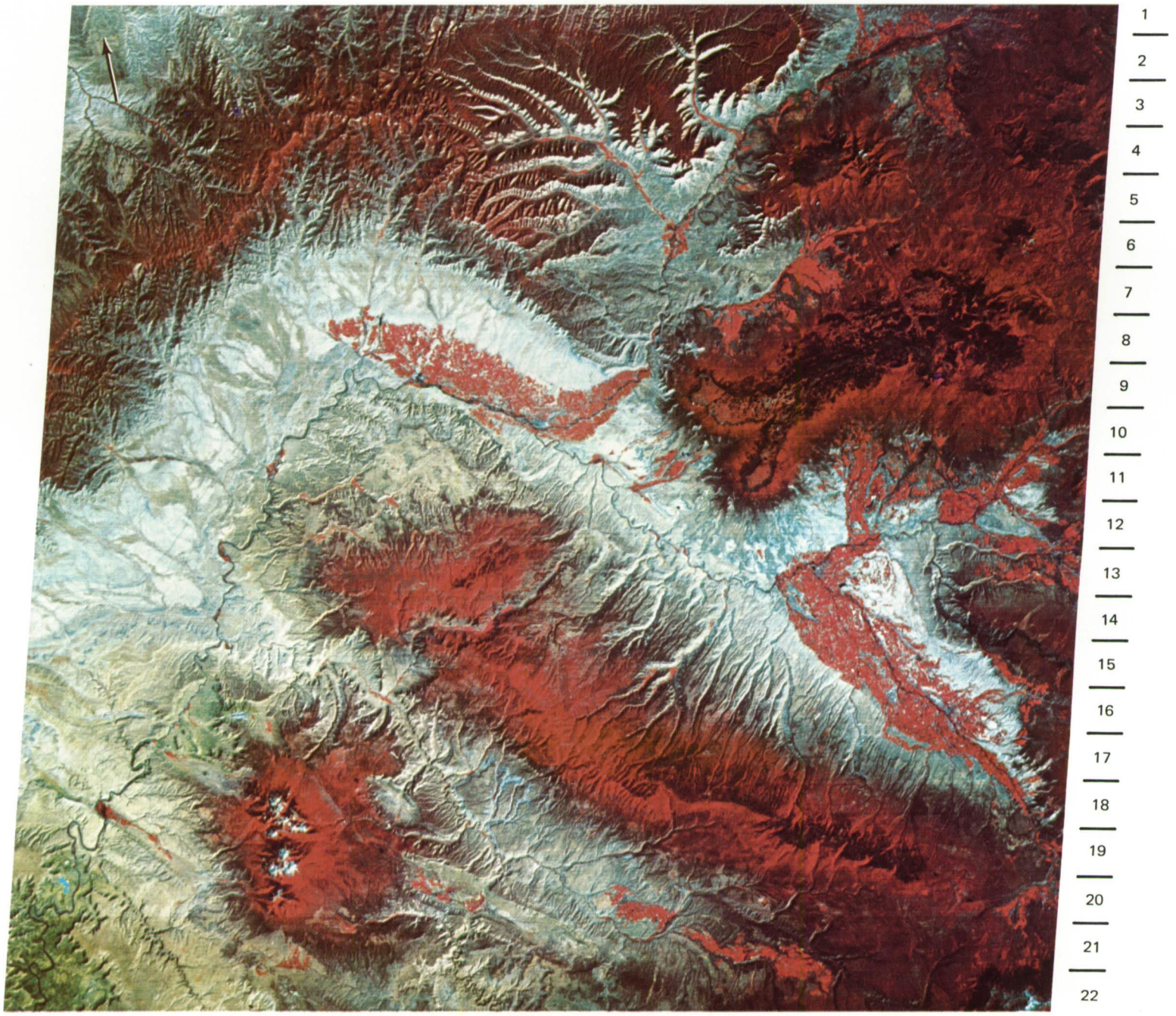


PLATE 77

URANIUM COUNTRY, UTAH-COLORADO: Since the late 1940's, Grand Junction, Colo. (*K*–9), and Moab, Utah (*B*–18), have been centers of uranium exploration in the Colorado Plateau. Both lie along the Colorado River (*D*–15; *N*–5); Grand Junction itself is at the confluence of the Gunnison River, which flows westward past Delta (*Q*–12) into the Colorado after cutting deeply into Precambrian rock at Black Canyon (*U*–14). North and west of the valley of the Colorado, underlain by Jurassic and Cretaceous shales, are the Roan Cliffs (*K*–7), held up by the Mesaverde sandstone, and the Roan Plateau (*C*–3; *J*–2), topped by Eocene sedimentary rocks. Piñon and cedars cover much of that area. Pine, fir, and spruce dominate the higher elevations (up to 3300 meters (11 000 feet)) around Grand Mesa (*O*–9) and Battlement Mesa (*Q*–3)—both late Tertiary basalt lava-capped plateaus. The San Juan Mountains to the southeast, the edge of which appears at *V*–21, are constituted of older Tertiary rocks. The Colorado and Gunnison River valleys receive enough water to foster farming of corn, barley, oats, hay, alfalfa, sugar beets, and apple and peach orchards.

These valleys are bounded on the south by the Uncompahgre Plateau (*K*–14; *Q*–18), a broad uplift that exposes large areas of Precambrian granites overlain unconformably by Jurassic strata. Unaweep Canyon (*J*–14), formed by West Creek, cuts across the northern end. The south end of this plateau is cut by the San Miguel River, which then joins the Dolores River (*G*–15) after passing through San Miguel Canyon (*R*–21). The La Sal Mountains (*G*–18), reaching to 3877 meters (12 720 feet) at Mount Peale, are part of an exposed granitic laccolith of Tertiary Age. At their eastern end lies Paradox Valley (*K*–20), where an anticlinal structure has been breached to expose Pennsylvanian rocks flanked by Permian gypsum and salt beds. This, and similar structures such as Salt Valley (*B*–16) just north of the Arches National Monument (*B*–17) are actually elongated "salt domes" pushed up by intrusion of plastically deformed bedded salt. *1408–17244;* September 4, 1973.

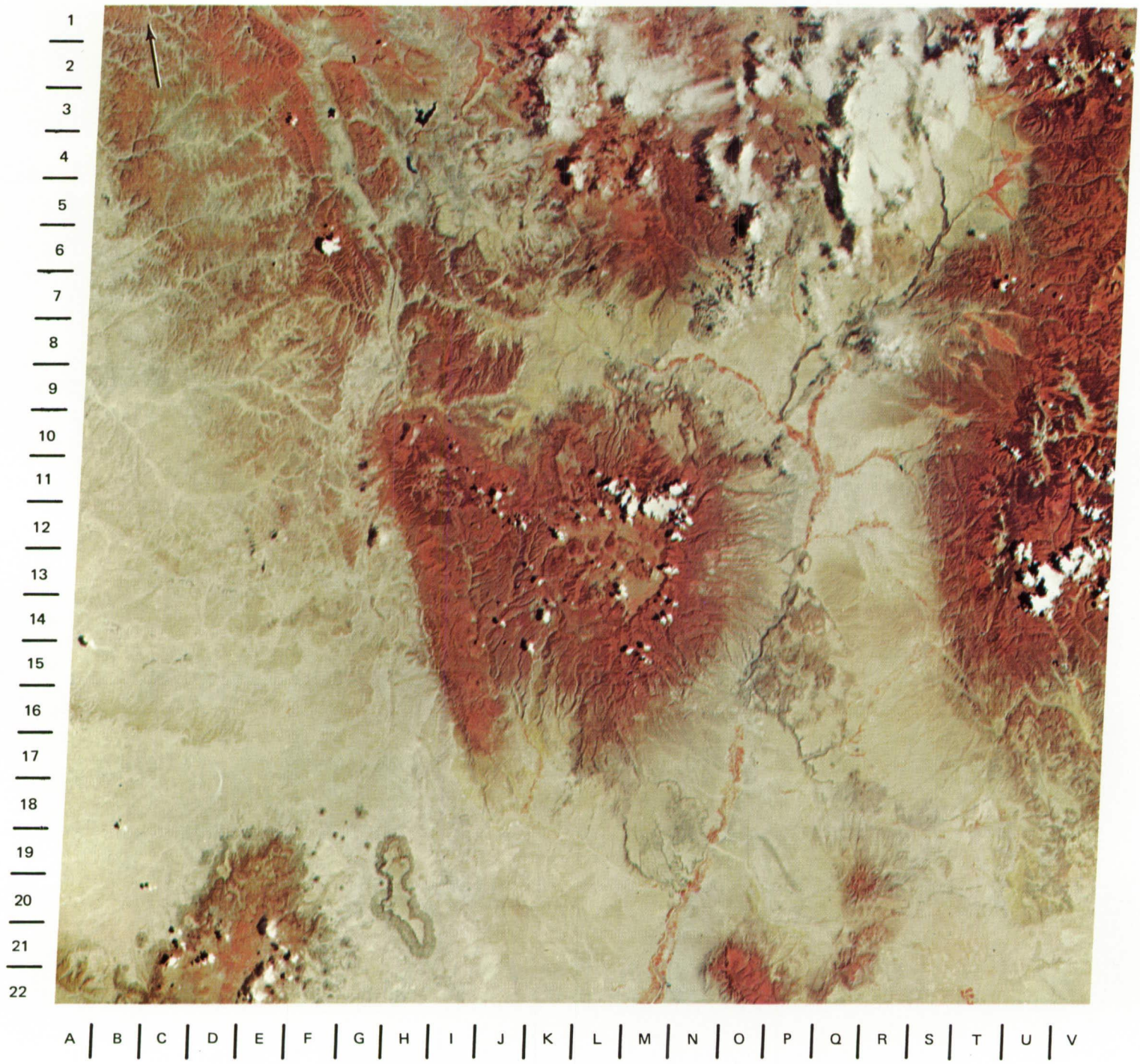


PLATE 78

NORTH-CENTRAL NEW MEXICO: The southeastern edge of the Colorado Plateau (upper left) meets the south end of the Sangre de Cristo Range (*U*–12) block of the Southern Rocky Mountains at the Rio Grande depression (*Q*–14), a series of downfaulted grabens occupied by the present Rio Grande River (*N*–19). This depression is part of the eastern edge of the basin and range province; Ortiz Mountains (*R*–19) and the Sandia Mountains (*O*–21) north of Albuquerque (just off the image at *M*–22) are also fault blocks. Truchas Peak (*U*–10), a Precambrian granitic mountain, is the high point 5384 meters (13 301 feet) of the Sangre de Cristos—here a central granitic core overlain by Permian rocks. Santa Fe (*S*–14) and Taos (*S*–5) are nestled near the base of this towering range.

The Nacimiento Mountains (*H*–12), bounded on the west by the Nacimiento fault (*H*–14), are steeply folded Paleozoic and Mesozoic sedimentary rocks that extend northward around the Chama River valley (*M*–8) and Mesa de los Viejos (*H*–8). Northwestward on the Colorado Plateau, dissected uplands are underlain by the Eocene Wasatch Formation—the youngest units in the San Juan Basin (*D*–1).

The region also displays a variety of volcanic features. Mount Taylor Mesa and the San Mateo Mountains (*E*–20) are made up of Tertiary lavas from eruptions that formed the Mount Taylor lava field of late Tertiary Age, and Mesa Prieta (*H*–20) is a lava-capped plateau left as an outlier of this field. Volcanic rocks (*G*–18) are exposed nearby. In the center of the Jemez Mountains (*L*–14), composed mostly of late Tertiary volcanic rocks, is the large (21- to 24-kilometer (13- to 15-mile) diameter) Valles Caldera (*L*–12), a craterlike volcanic feature produced in Pleistocene times by catastrophic blowouts and subsidence and then subjected to resurgence by upwelling of more lavas to form a ring of domes (*L*–12) and cones. Los Alamos, the nuclear research center, lies just to the east (*N*–13). Lava spilled out from other eruptive centers west of Taos. The Rio Grande has cut a deep canyon (*R*–6) through these flows.

The higher elevations are mantled by pine and fir and some spruce. Much of the lower slopes support piñon and cedar. Sparse grama grasses occupy vast stretches of the lowlands. Alfalfa and apple trees are among the few crops grown along this stretch of the Rio Grande. *1010–17143;* August 2, 1972.

PLATE 79



WHITE SANDS, N. MEX.: The White Sands flats (*L*–16), west of Alamogordo (*O*–15), N. Mex., is famous as the site of the detonation of the first atomic device in 1945 and, later, as the first launching site for rockets in the United States. The large sand field is made up of grains of gypsum (hydrous calcium sulfate) transported eastward by the wind from Permian beds exposed in the San Andres Mountains (*G*–14; *I*–19)—a fault block of Paleozoic rocks that is part of an uplift extending northward as the Oscura (*H*–6) and Chapadera (*I*–3) Mountains. The Tularosa Basin (*K*–11; *N*–19) is a Quaternary alluvium-filled depression lying west of the Sacramento Mountains uplift (*R*–13)—a broad upwarp of Permian carbonate rocks now covered by pine and fir trees. Mesozoic sedimentary rocks and Tertiary intrusive rocks make up the northwest corner of these mountains, as well as the Sierra Blanca (*O*–4) and Capitan (*S*–4) Mountains. Another alluvium-filled structural basin, the Jornada del Muerto (*D*–16; *E*–5) lies to the west of the San Andres uplift. The present Rio Grande (*B*–5; *B*–21) may once have occupied this depression east of the Caballo Mountains (*A*–17) uplift. The Malpais (*J*–10; *L*–5) is a Quaternary lava flow that carried more than 64 kilometers (40 miles) from its northern vent (*L*–3). Another basalt field (*C*–9) and a swarm of older Tertiary intrusives at Point of Rocks (*D*–18) are also evident.

Several interesting manmade features appear in the image. The Southern Pacific railroad tracks (*O*–19) can be followed through the Tularosa Basin. Airstrips around Holloman Air Force Base (*M*–16) can be discerned. A large white circle (*F*–7 and *F*–8) is a gypsum-covered launchpad for weather balloons. Part of the Elephant Butte Reservoir (*A*–13) is visible at the left edge of the image. *1333–17102;* June 21, 1973.

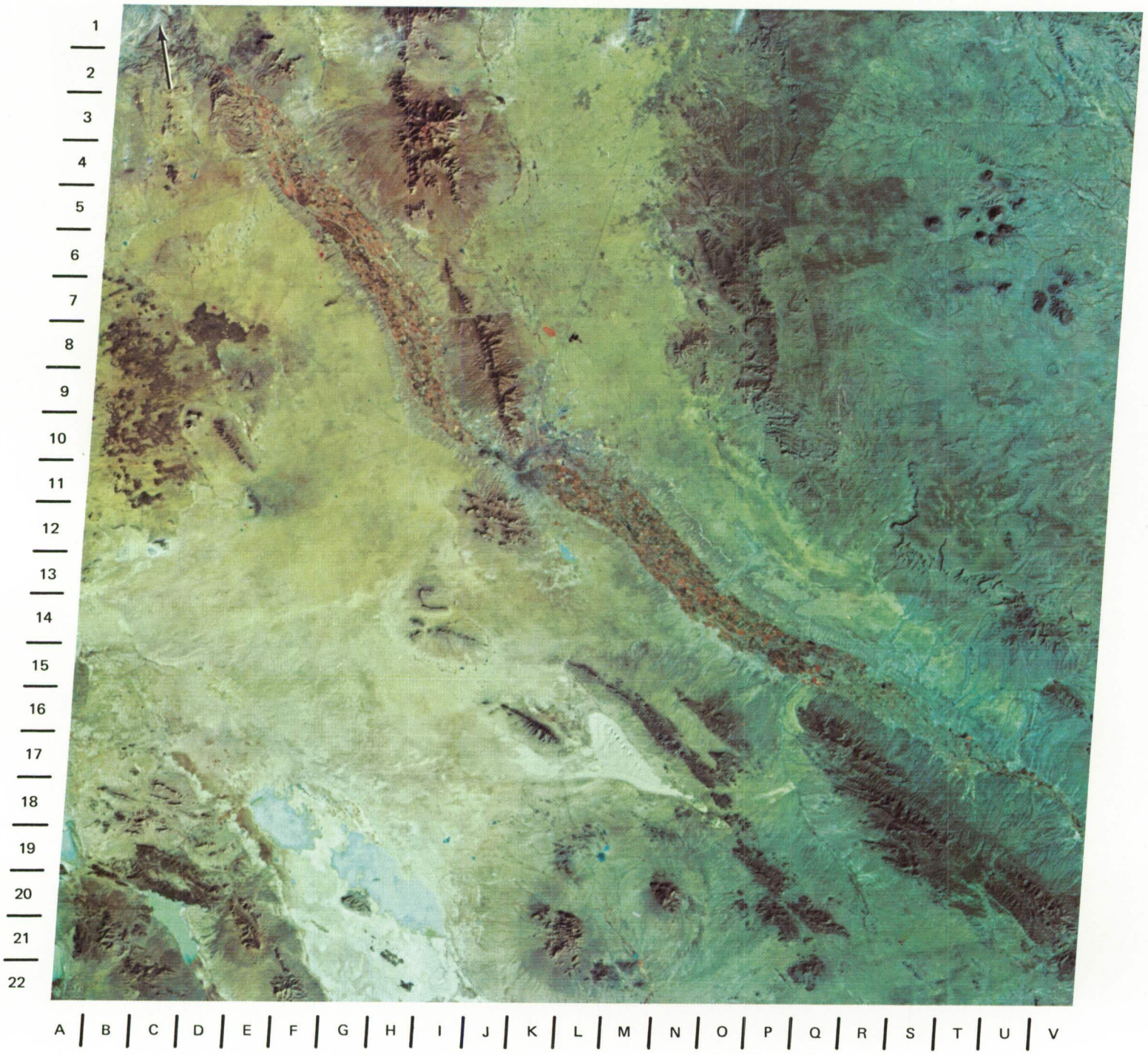


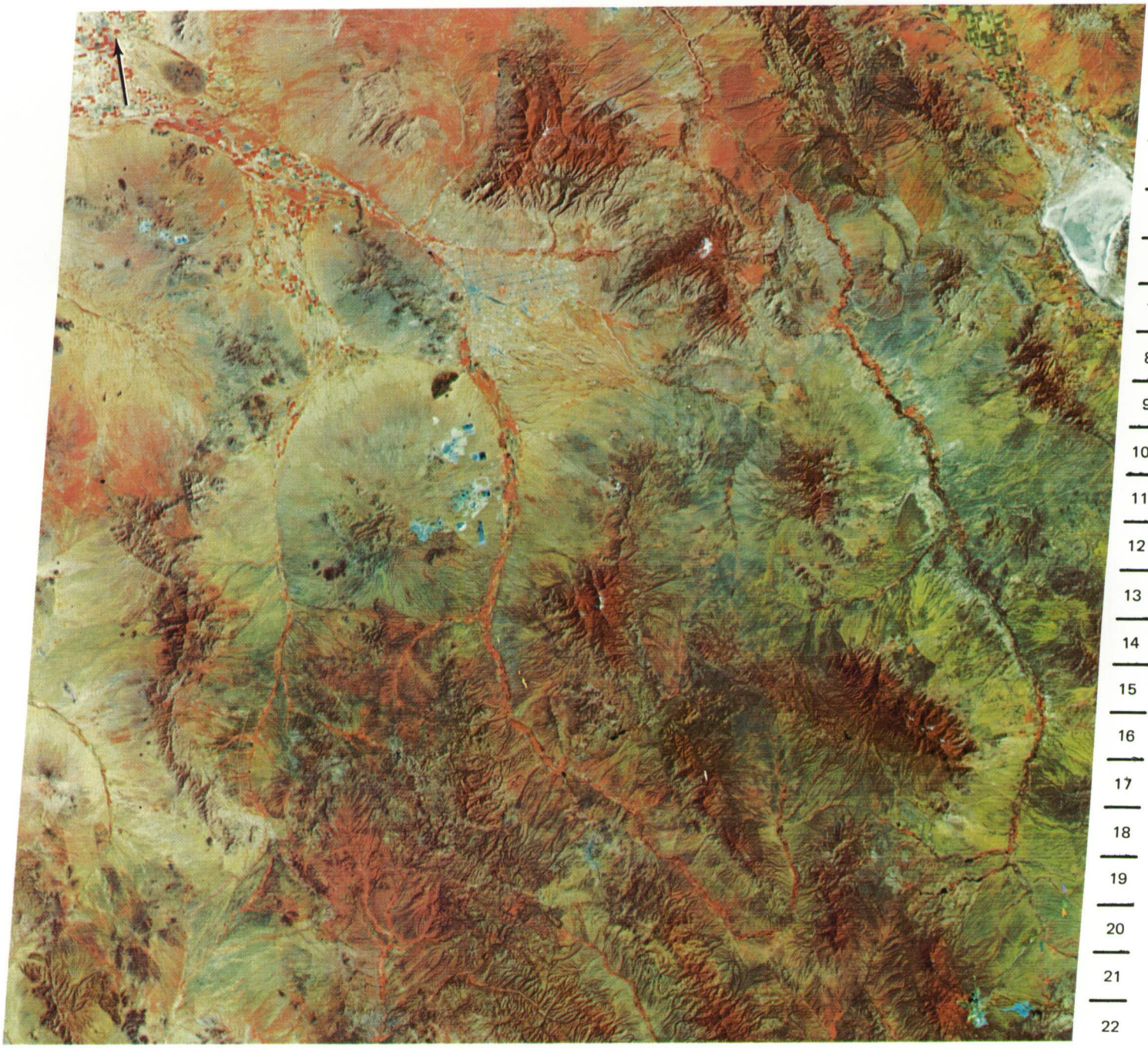
PLATE 80

EL PASO, TEX.: This westernmost city (*J*–10) in Texas and its companion, Ciudad Juarez (*J*–11) in Mexico, both lie along the Rio Grande as it cuts through Paseo del Norte. The Franklin Mountains (*I*–8), a fault block of Paleozoic sedimentary rocks, and the Organ Mountains (*G*–3), a Tertiary intrusive mass, form the southern end of the San Andres uplift. The Hueco Mountains (*N*–6), consisting mostly of late Paleozoic folded rocks, grade southward into the Finlay Mountains (*R*–12), made up of flat-lying Mesozoic sandstones. Between these pairs of mountains are the Tularosa (*K*–1) and Hueco (*O*–12) Basins. Broad, Quaternary alluvium-filled basins and occasional fault-uplifted ranges appear in the Mexican province of Chihuahua, shown here over most of the lower left of the image south of the Rio Grande (*O*–14). Among the mountain chains are Sierra Amargosa (*S*–18), Sierra de Presidio (*N*–17), and Sierra de Sabinal (*B*–21). Other Mexican landmarks include dune fields (*G*–17; *L*–16) and shallow, intermittent playa lakes (Laguna de Guzman (*E*–18); Laguna de Santa Maria (*H*–20)).

In west Texas, a series of Tertiary volcanic intrusives have cut into the Diablo Plateau (*U*–4). These include the Cornudas Mountains (*T*–5), Sierra Tinaja Pinta (*U*–7), and Cerro Diablo (*U*–6). West of El Paso, a cluster of younger (Quaternary) cinder cones makes up the West (*A*–10) and East (*C*–10) Potrillo Mountains. Kilbourne Hole (*D*–9) is one of several explosion craters or maars formed during the eruptive sequence.

The Rio Grande, from Las Cruces (*D*–4) southeastward, is an important agricultural area specializing in cotton growing, with some field crops, hay, and pecan orchards. *1153–17105;* December 23, 1972.

PLATE 81



TUCSON, ARIZ.: The southern Arizona desert appears here in the midst of springtime bloom. The higher slopes of the uplifts are largely covered by Ponderosa pine, grading through successively lower ecozones into chaparral scrubland such as oak and juniper, then creosote and saltbush, and cactus. Peculiar to this region in the United States are the giant Saguaro Cacti, best preserved in the Saguaro National Monument (*L*–7) east of Tucson (*J*–6). Farming is confined to narrow strips along the San Pedro River (*Q*–6; *U*–16), the Santa Cruz River (*D*–3; *J*–11), and the Brawley Wash (*F*–8); crops are mainly barley, sorghum, and cotton. The fields at *S*–1 are fallow at this time and appear yellow in this rendition, the color expected from a soil that is actually a dark red. Yellow coloration elsewhere in the image (e.g., *E*–12; *S*–13) relates to reddish iron surface staining that coats alluvial fans.

Geologically, the region is part of the Great Basin, marked by block fault mountains separated by broad alluvium-filled valleys. The Santa Catalina Mountains (*M*–3), rising to 2800 meters (9100 feet), the Rincon (*M*–6) and Tanque Verde (*J*–6) Mountains, and the Baboquivari Mountains (*D*–13; *E*–17), more than 2200 meters (7400 feet) high, have cores of Precambrian crystalline rocks. The Tucson Mountains (*H*–7) and other ranges, such as the Galiuro (*P*–1) and Winchester (*K*–2) Mountains; the Santa Rita Range (*L*–13); the Huachuca Mountains (*R*–15); the Patagonia Range (*N*–16); and the Tumacacori (*J*–15), Atasco (*J*–16), and Pajarita (*K*–18) Mountains are composed of folded Carboniferous to Cretaceous sedimentary rocks, frequently overlain by Tertiary volcanics. The basins and stream valleys presently are uniformly topped by Quaternary sediment debris, derived by erosion of the uplands. The Willcox playa (*V*–6), a young deposit of alluvial clays and salts, commonly fills with water in the brief spring rainy season.

The region contains several of the largest porphyry copper mining districts in the west, such as at the Pima Mission (*I*–10), Twin Buttes (*I*–11), and Esperanza (*H*–11) open pit mines in the Sierrita Mountains—a complex of old granites, sedimentary rocks, and metamorphic rocks surrounded by a broad alluvial fan (*G*–9; *I*–12). Copper is also extracted on the Mexican side (*T*–21) of the border (*N*–17), southeast of the town of Nogales, Mexico (*L*–18). *1264–17283;* April 13, 1973.

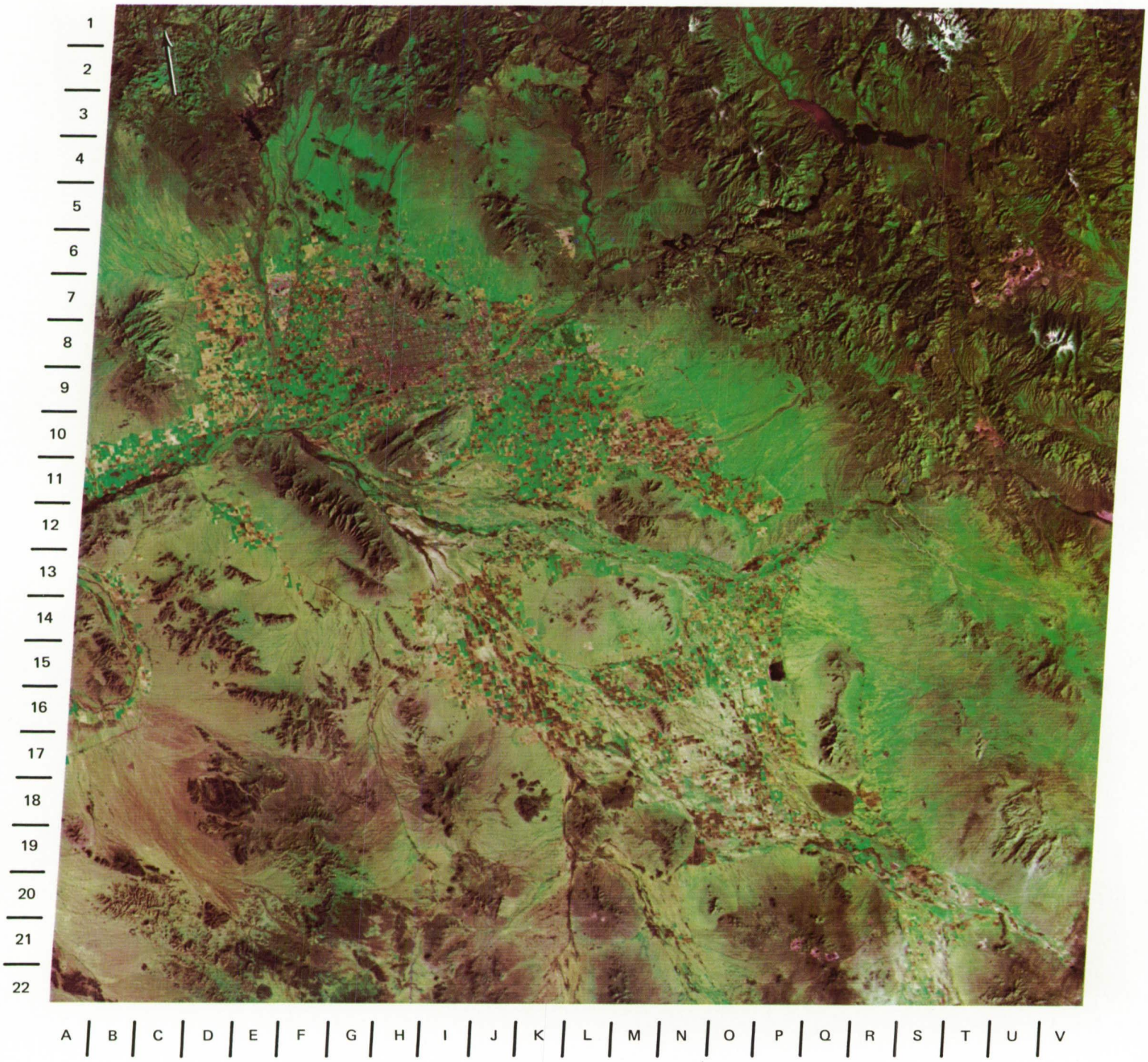


PLATE 82

PHOENIX, ARIZ.: This is an experimental product produced by the NASA Data Processing Facility attempting to display natural vegetation and agricultural crops in various hues of green.

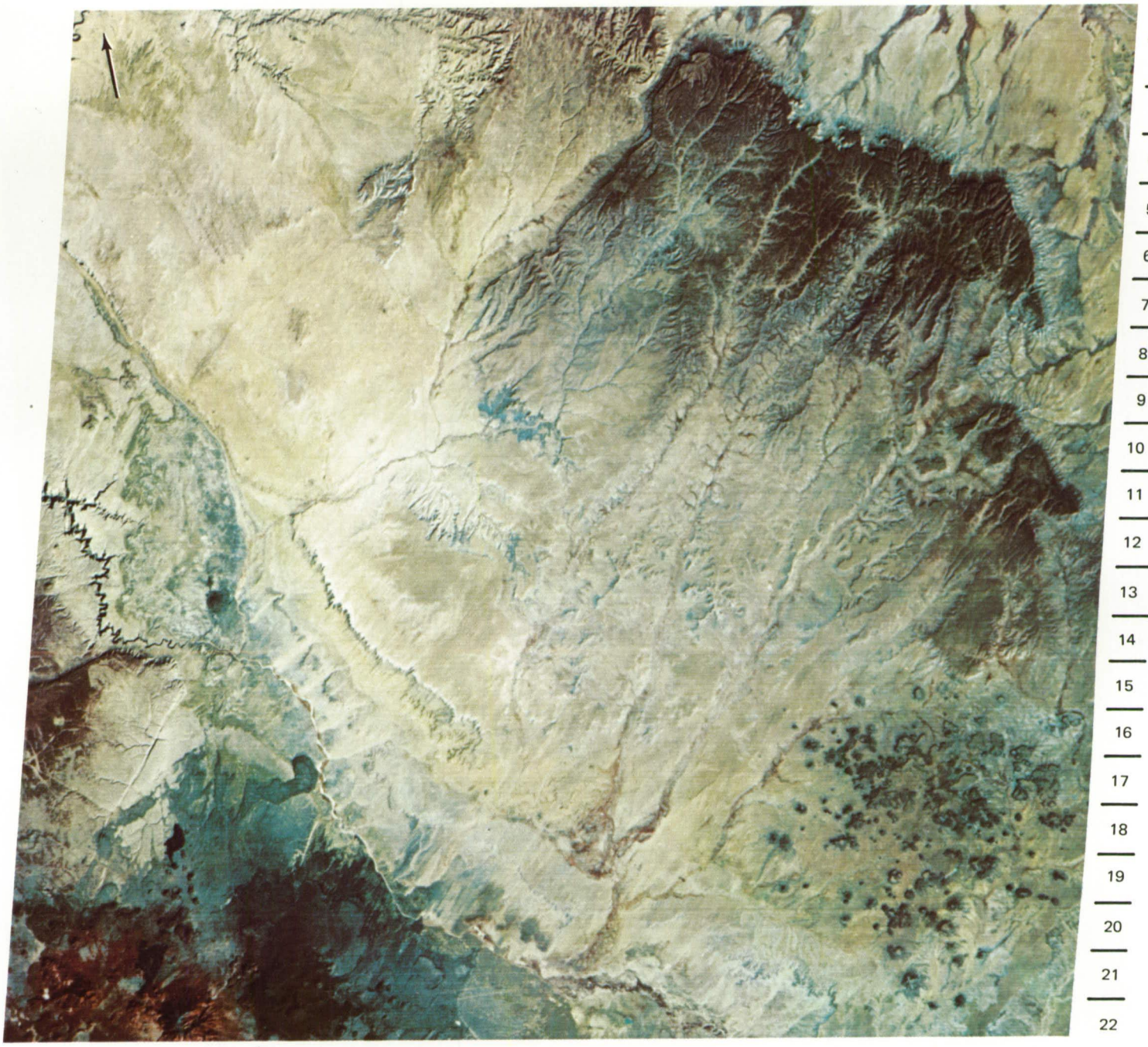
Approximately one-half of Arizona's population and a predominant proportion of the State's agricultural and extractive mineral industries are contained within the boundaries of this image. The rectangular grid pattern of the Phoenix metropolitan area street system abuts abruptly against the dark-colored metamorphic and volcanic rocks of the Phoenix Mountains, the northeast margin of the city (*G*–7).

Four major river systems and their associated irrigated agricultural patterns are evident in this image: the Verde (*K*–5), the Salt (*L*–6), the Gila (*K*–12), and the Agua Fria (*D*–6). Several reservoirs control flow and storage on these rivers. The largest, Theodore Roosevelt Lake on the upper Salt River, lies east of the Mazatzal Mountains (*N*–3). Three lesser reservoirs occupy the Salt River course between Roosevelt Reservoir and Phoenix. The Gila River descends from the Dripping Spring Mountains and flows south of Phoenix, marked by the field patterns and vegetation along its course. As the Gila continues westward, its course describes a long arcuate swing (*B*–14) in the vicinity of Gila Bend, Ariz. Lake Pleasant reservoir (*D*–3) controls flow and usage on the Agua Fria River.

Concentrations of pinkish colorations appear in several places within this image. A notable one is the Superior-Miami-Globe copper mining district in the Pinal Mountains (*T*–6). The distinctive signature is caused by the extensive tailing deposits resulting from mining activities.

Past volcanic activity is evidenced by such features as Picacho Peak (*Q*–17) and other nearby volcanic landscapes. *1211–17334;* February 19, 1973.

PLATE 83



NORTH CENTRAL ARIZONA: This scene is dominated by geologic features, many highlighted here by the low Sun illumination in the late fall. The area lies just to the east of the Grand Canyon. A series of steplike plateaus result from erosional recession of cliffs of successively higher (and progressively younger) flat-lying resistant rocks. The lowest levels include Permian sandstones and shales (*B*–16) to the west and Triassic red sandstones in the Painted Desert (*D*–11; *J*–9) around the Little Colorado River (*B*–12). The Moenkopi Plateau (*I*–14), bordered by the Ward Terrace (*H*–14), and, further north, the Kaibab Plateau (*D*–7; *G*–7), bounded by the Echo Cliffs (*B*–7), are underlain by Jurassic and lower Cretaceous sandstones and shale units; these in turn are overlain by successively higher units of Cretaceous rocks, stream-dissected to form numerous mesas and spurs (*S*–8).

Volcanism was extensive in late Tertiary and Quaternary times. North of Flagstaff, Ariz., the stratovolcano topped by Humphreys Peak (*D*–21) at 3851 meters (12 633 feet) forms the center of the San Francisco volcanic field (*A*–23; *D*–19; *G*–21), consisting mostly of cinder cones such as Sunset Crater (*F*–21) and SP Crater (*D*–19), both less than 1000 years old, and associated lava flows (*G*–17; *J*–21). To the east are the Hopi Buttes (*S*–17), a swarm of cones and eroded volcanic pipes of Tertiary age.

Other features of particular interest are a fault graben (*C*–17), and large, northeast-trending wind markings (*I*–13; *K*–19).

The area around the San Francisco Mountains is extensively covered with pine at higher elevations and juniper and piñon at lower levels. The juniper-piñon association appears again at Black Mesa (*U*–6) and elsewhere (*V*–11). Sagebrush dominates in the lower reaches of the Colorado Plateau but gives way to grama grass at higher elevations.

Most of the upper two-thirds of the image encompasses part of the Navajo Indian Reservation. The Hopi Indian tribe occupies the first, second, and third Mesa area (*O*–12) within this largest of reservation lands in the conterminous United States. *1463–17300;* October 29, 1973.

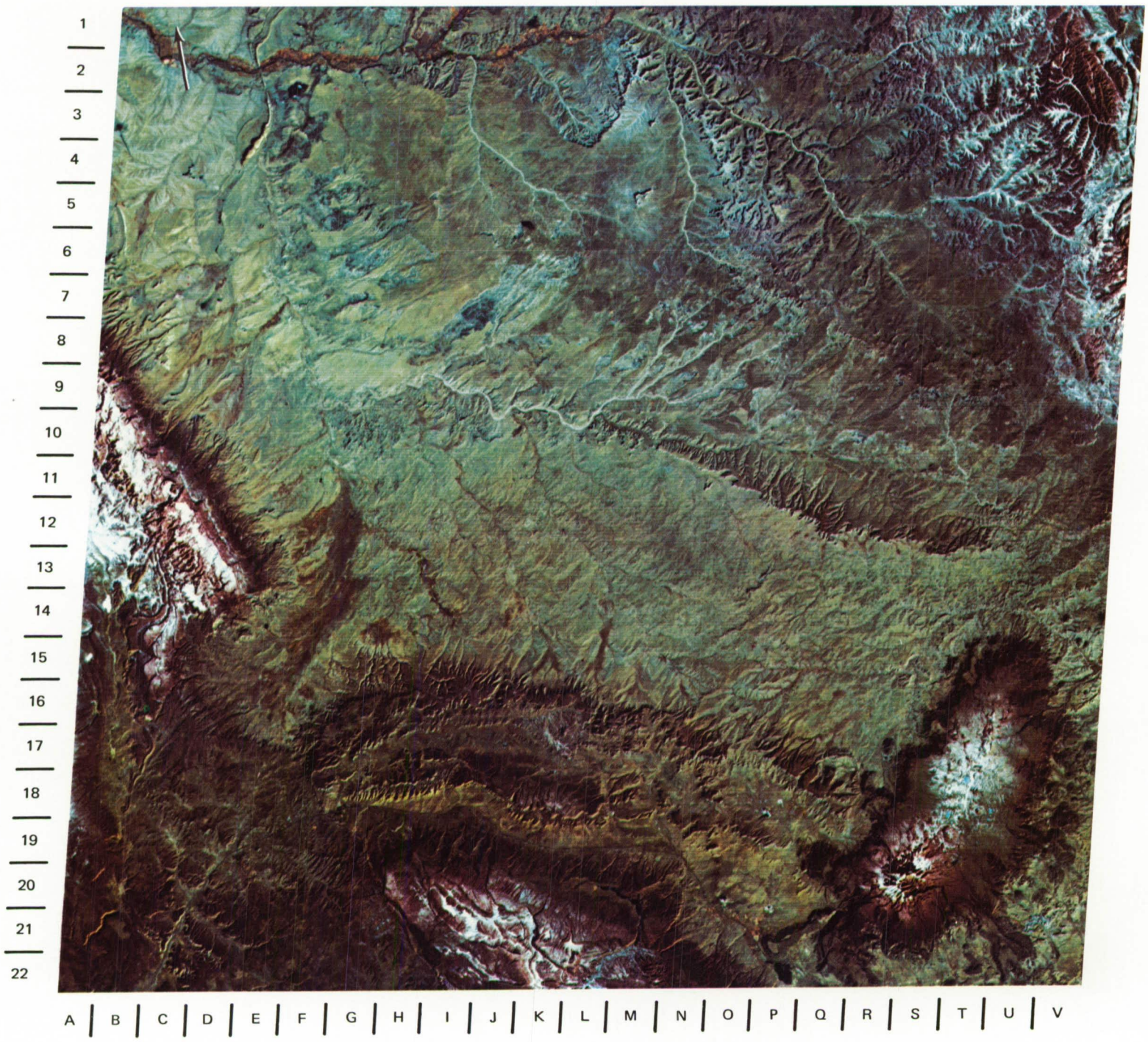


PLATE 84

NORTHWEST NEW MEXICO: The southeastern section of the Colorado Plateau includes thick deposits of Cretaceous and Tertiary sediments that fill the San Juan Basin (*T*–3). The Wasatch Formation of Eocene age is dissected by headwaters of the San Juan River (*P*–5). Cretaceous sandstones (*I*–5) and shales (*E*–5) form a broad flatlands to the southwest. Its surface is carved into scenic channels and tablelands, such as exposed in the Chaco Canyon National Monument (*L*–10). Northeast-trending streaks along this part of the plateau are partly produced by prevailing winds but also represent stream and eolian erosion along numerous joints, as evidenced by the gullies in the Chaco Cliff (*O*–11), a sandstone-capped cuesta. Where it dips sharply to the east, the Cretaceous Mesa Verde Formation makes up a conspicuous ridge at Hogback Mountain (*D*–3). Further east, Farmington, N. Mex. (*G*–1), an important center for natural gas production, uranium exploration, and farming lies at the confluence of the Animas (*H*–1) and San Juan Rivers. Westward, the central plug and radiating dikes of the old volcano (*A*–3) at Ship Rock are graphically displayed.

The eastern edge of the Defiance Plateau (*A*–16) is bounded by the Defiance monocline (*B*–17) while its northeast flank abuts against the Wasatch Formation capping the Chuska Mountains (*A*–10), which also contain more than 30 volcanic explosion pipes (diatremes). One pipe—Buell Park (*A*–14)—forms a calderalike basin eroded from soft volcanic tuffs.

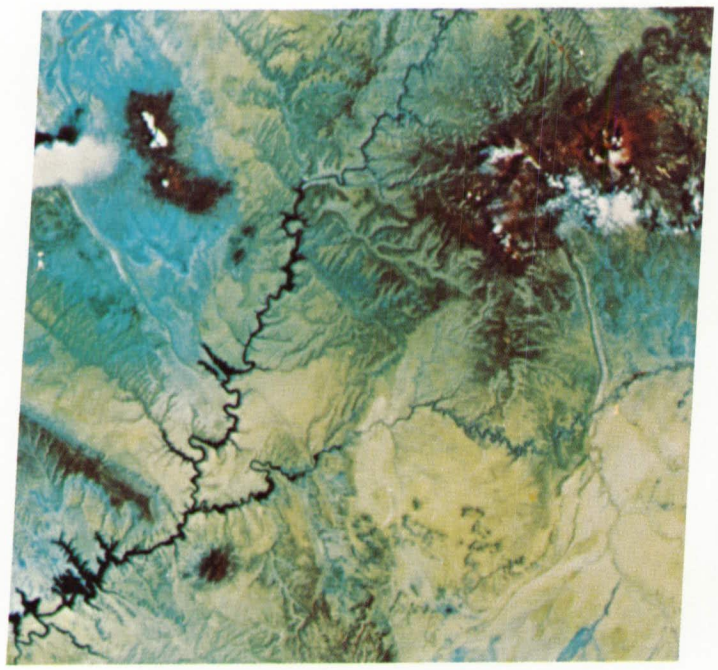
Much of the Zuni Uplift (*I*–19) appears near the bottom of the image. Jurassic and Cretaceous rocks dip northeast along its northern flank. An intervening valley (*L*–17) gives access to extensive mining of uranium minerals from this sequence. Reddish Triassic sediments (*H*–18) form cliffs overlooking the valley drained by the Puero (*D*–19) and San Jose (*N*–19) Rivers. Famed Highway 66 (now Interstate 40) passes through the valley between Grants (*E*–18) and Gallup (*O*–20), N. Mex. Permian rocks outcrop near the core of the uplift in the pine-forested mountains (*J*–21) that reach above 2700 meters (9000 feet). A basalt-capped mesa (*T*–17) constitutes the volcanic field named from the 3340-meter (11 300-foot) high stratocone of Mount Taylor (*S*–19). Many eroded volcanic necks (*U*–14) mark the vents supplying the eruptive materials. *1515–17180;* December 20, 1973.

PLATE 85

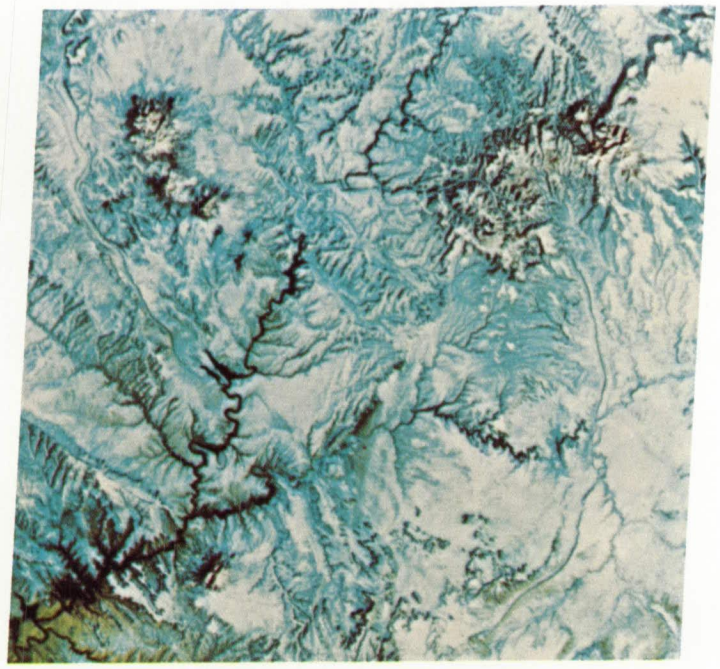


CANYON LANDS, SOUTHEAST UTAH: This desolate region includes some of the most photogenic scenery in the Colorado Plateau. The view on the left shows the varied topography highlighted by a low Sun illumination in late February. The six scene panel on the opposite page presents much the same region imaged at different seasons, with varying Sun angle and changes in vegetation and snow cover at the surface.

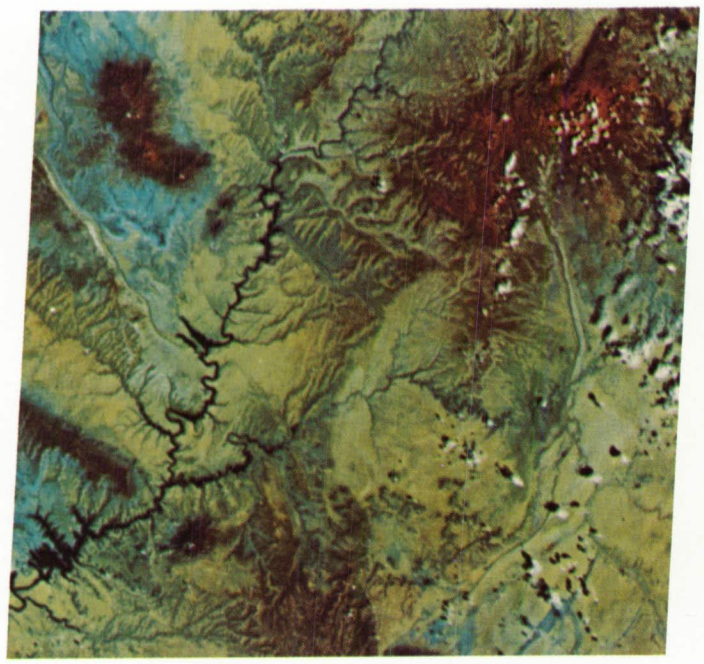
The confluence (*G*–16) of the San Juan (*M*–13) and Colorado (*I*–11) Rivers lies upstream from Lake Powell (*D*–18), a canyon-filling body of water backed up from the Glen Canyon Dam (*B*–20). Old abandoned meanders (*H*–14) are evident in this area. Directly to the west is the Kaiparowitz Plateau (*A*–15), edged by the sandstone-capped Straight Cliffs (*C*–13), the Valley of the Escalante River (*D*–11), and the Triassic Circle Cliffs (*B*–9) bounded on the north by the Waterpocket monocline (*C*–5). The Monument Valley region (*O*–17) is carved into richly colored Permian and Triassic sandstones and shales. To the south is Navajo country, including piñon- and cedar-covered Black Mesa (*O*–22) and the Chinle Valley (*U*–19). Comb Ridge (*Q*–19; *T*–12), part of a strong monoclinal flexure that exposes Triassic shales, runs northward to the Abajo Mountains (*S*–4). These are among several uplifts underlain by igneous intrusions. The most famous of these is the Henry Mountain (*F*–4), a classic locality at which the concept of updoming of sedimentary rocks by laccoliths was developed. Modern studies show such peaks as Mount Ellsworth (*G*–6), Mount Hillers (*F*–5), and Mount Pennell (*E*–3) to be laccolithic domes connected to a much larger stock responsible for the entire uplift. Navajo Mountain (*H*–18) is another example of an intrusive stock which, in this case, has not yet been exposed by erosion through the covering Jurassic sedimentary rocks. *1211–17323;* February 19, 1973.



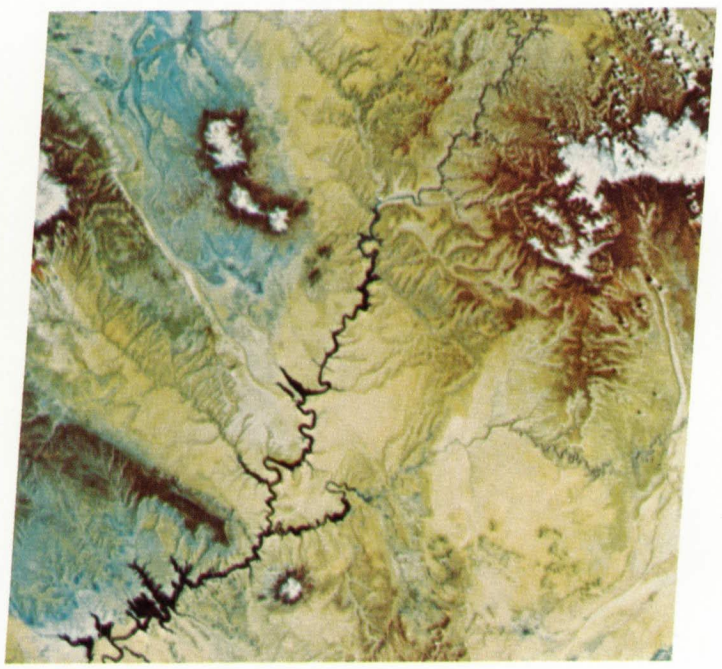
August 5, 1972



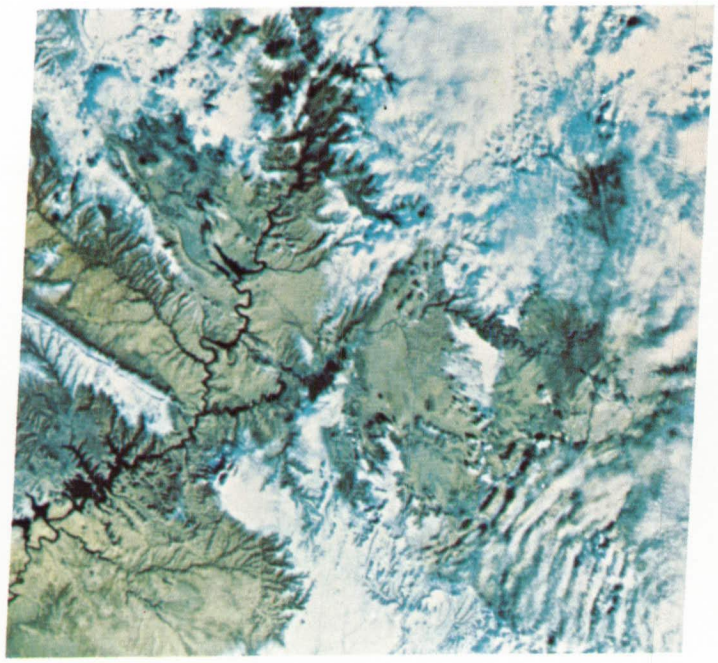
February 1, 1973



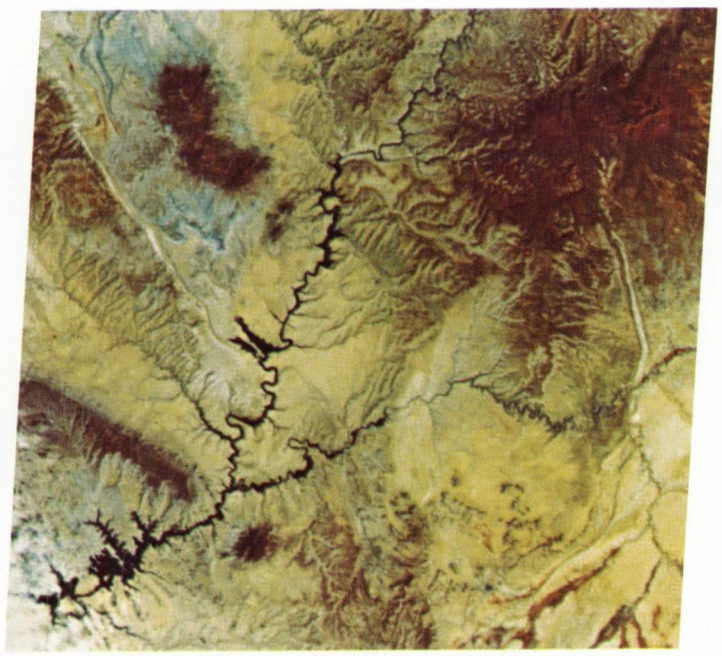
September 1, 1972



May 2, 1973



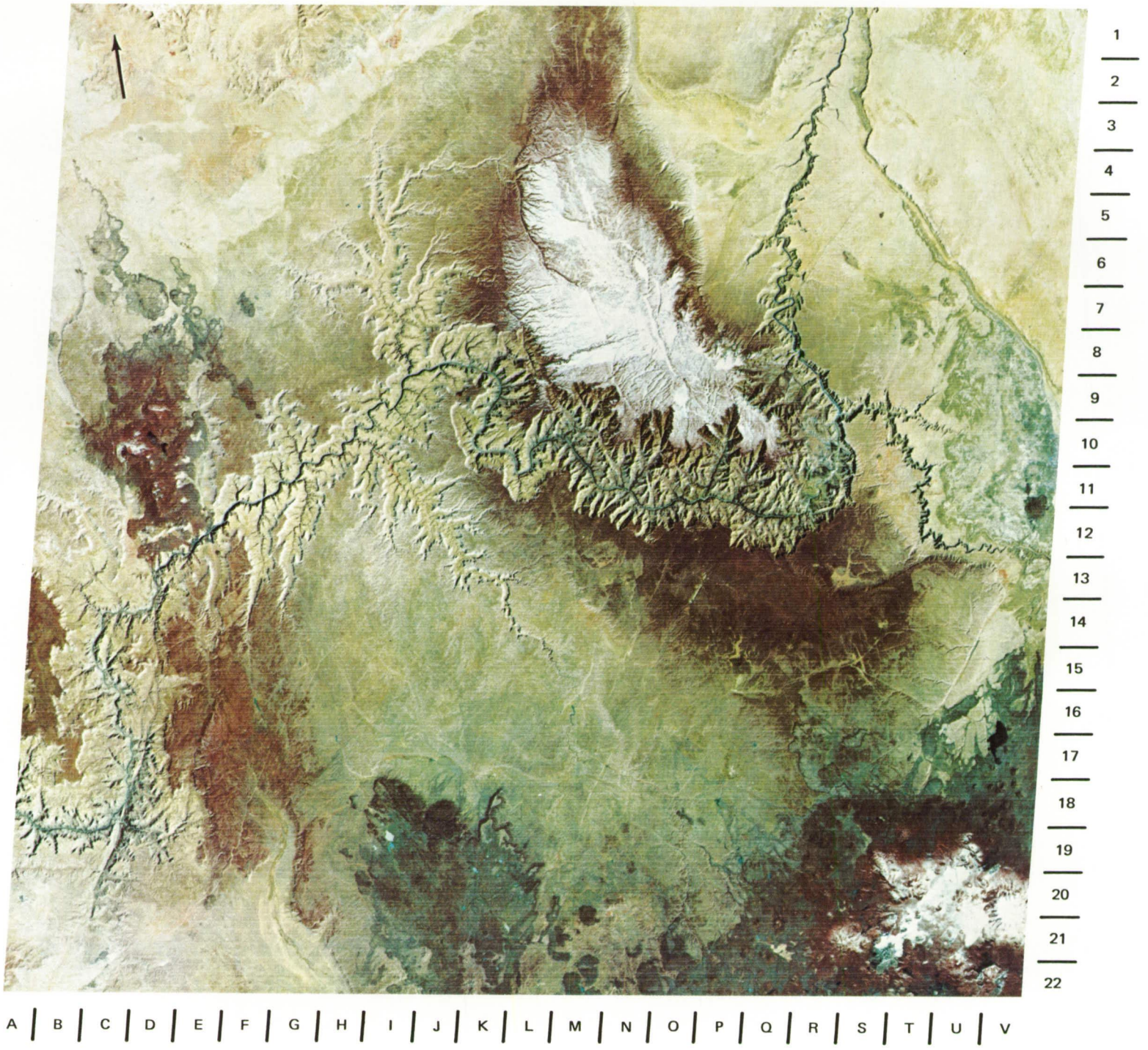
November 21, 1972



September 5, 1973

PLATE 86

PLATE 87



GRAND CANYON, ARIZ.: One of the most conspicuous features on this image is the Grand Canyon of the Colorado River (*O*–11). At this point the Colorado River flows in a canyon almost 1.6 kilometers (1 mile) deep and roughly 19 kilometers (12 miles) from rim to rim. The canyon is incised in essentially horizontal Paleozoic sedimentary rocks exposing a relatively undisturbed stratigraphic cross section unequaled elsewhere in the world. In the innermost gorge of the canyon the river has cut into ancient metamorphic schists and gneisses representing the remnants of an ancient land mass that once occupied this area.

A second noticeable feature is the Kaibab Plateau (*M*–7) shown here with a snow cover. The plateau is a broad upwarped area of the Paleozoic sedimentaries exposed in the Grand Canyon reaching elevations in excess of 2700 meters (9000 feet). The higher elevations result in orographically induced precipitation, which in turn supports a substantial vegetative cover, primarily of spruce and fir, bordered by pine. Along the lower south rim pine, juniper, and scrub oak are the dominant vegetation.

The well-defined canyon of the Little Colorado joins the Colorado River west of Cameron, Ariz. (*R*–9), as the Colorado emerges from its Marble Canyon section (*Q*–4).

Other large plateau areas shown are the Coconino (*P*–14), the Paria (*N*–2), and the Kaibito (*T*–3). The western margin of the Kaibito Plateau is marked by the trend of the Echo Cliffs monocline (*S*–5).

Two sizable volcanic fields are shown in this image. The 3700-meter (12 000-foot) high snow-covered San Francisco Peaks surrounded by lava flows and cinder cone volcanoes appear around *V*–20, which stand out in this scene because of snow enhancement. The Mount Trumbull volcanic field centered about Mount Trumbull (*C*–10) lies north of the river in the western portion of the image.

Numerous faults, mostly with a northeast-southwest trend, cut across the image. An outstanding example is the fault-bounded graben (*U*–14) on the eastern margin of the Coconino Plateau. *1284–17384;* May 3, 1973.

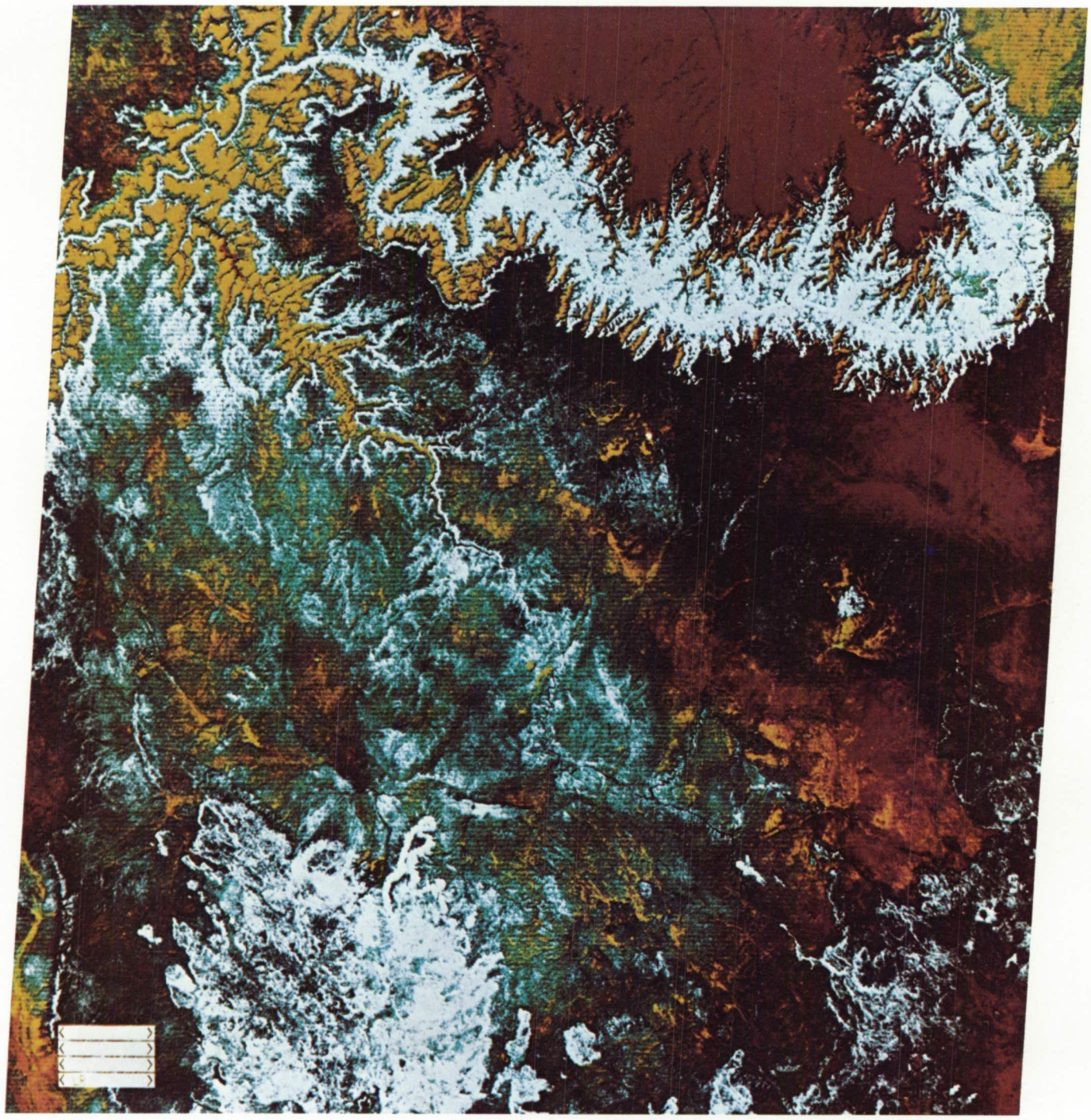
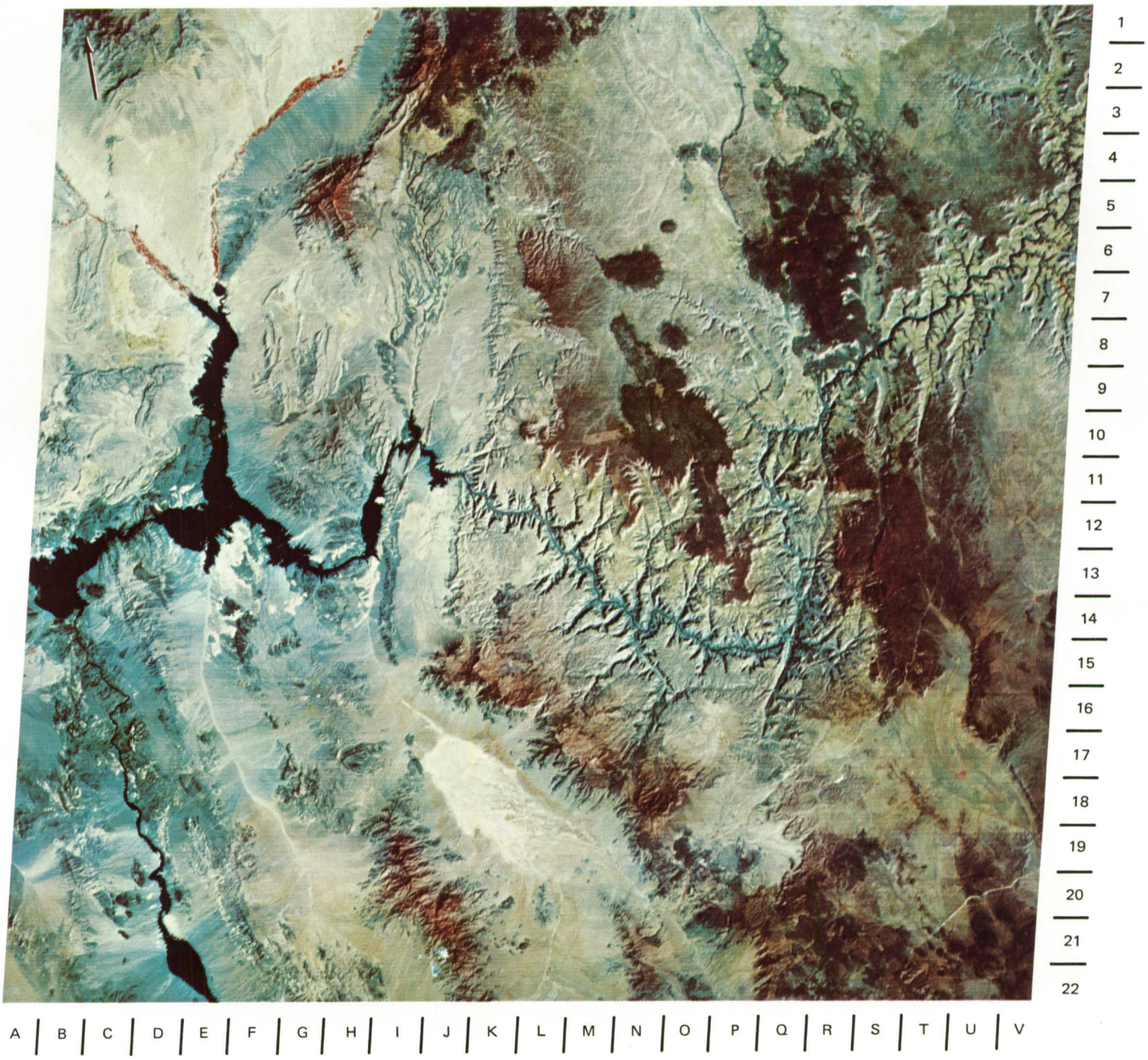


PLATE 88

ROCK UNITS IN ARIZONA: A. F. H. Goetz of the California Institute of Technology's Jet Propulsion Laboratory has applied digital techniques using Landsat computer-compatible tapes to enhance and discriminate different rock types. This technique consists of preparing several black and white positive images from the pixel to pixel variations of ratio values of selected pairings for any two of the four multispectral scanner band signals (e.g., bands 4/6 or 7/5). Each new ratio image (which resembles a typical black and white single band image but shows different gray tone distribution and higher contrast) is projected through a color filter. A color composite is then produced by combining three ratio images each of a different color. In the image seen here, log ratios of multispectral scanner bands 5/4, 7/4, and 4/7 have been printed as green, red, and white, respectively.

This composite image is a combination of parts of Landsat frames *1032–17373* and *1032–17375*. The area covered contains a section of the Coconino Plateau and a stretch of the Grand Canyon enclosed between the points located in the Landsat frame reproduced in plate 87. The green and white areas in the scene correspond to limestone units within the Kaibab Formation and the yellow areas coincide with reddish sandstones and conglomerates exposed on the plateau or in the canyon. Some of those sandstone units within the Kaibab Formation have proved to be shallow perched aquifers from which groundwater has since been extracted after drilling into the units defined in this image. The red tone in this ratio color composite characterizes vegetation. *1032–17373;* August 24, 1972.

PLATE 89



SHIVWITS PLATEAU, ARIZ.: The plateau country west of the Grand Canyon is capped by the resistant Permian-aged Kaibab limestone and underlain by the same horizontally bedded formations seen in the Grand Canyon. The Colorado River (*R*–7; *M*–13) has incised its course across the Coconino Plateau (*S*–13) and the Shivwits Plateau (*N*–9) as it flows westward into Lake Mead (*E*–12), created by Hoover Dam east of Las Vegas, Nev. Lake Mojave (*E*–22), another of the manmade lakes on the Colorado River, lies west of Arizona's Black Mountains (*J*–20).

The boundary between the Colorado Plateau and the basin and range physiographic provinces is marked by the north-south trending, Grand Wash fault (*V*–7). A second major system, the Hurricane-Toroweap (*O*–5), parallels the western margin of the Mount Trumbull volcanic field (*P*–6) and further south separates the Shivwits and Coconino Plateaus. Cliffs developed in association with these fault systems are readily visible west of Lake Mead and in the Hurricane Cliffs or Ledge area west of Mount Trumbull.

Considerable vegetative contrast exists between the xerophytic creosote bush scrublands in the more arid areas of the basin and range province, and the juniper-piñon woodland forests occupying the more elevated portions of the plateaus. Areas such as the saline Red Lake playa (*J*–17) are almost devoid of vegetation while stringlike gallery forests and irrigated agriculture along river valleys such as the Virgin River (*F*–2) yield vivid reddish signatures. *1411–17424;* September 7, 1973.

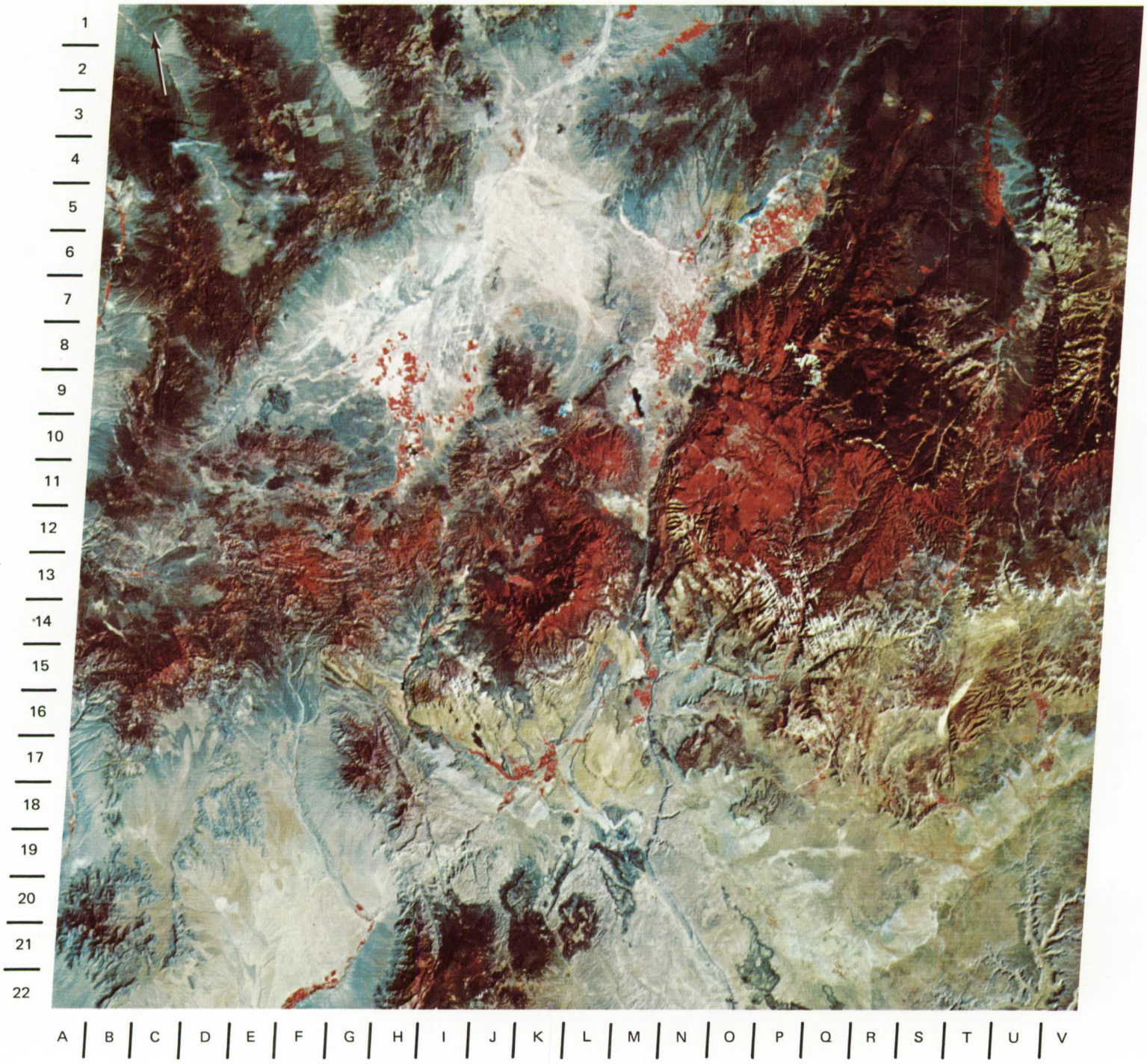
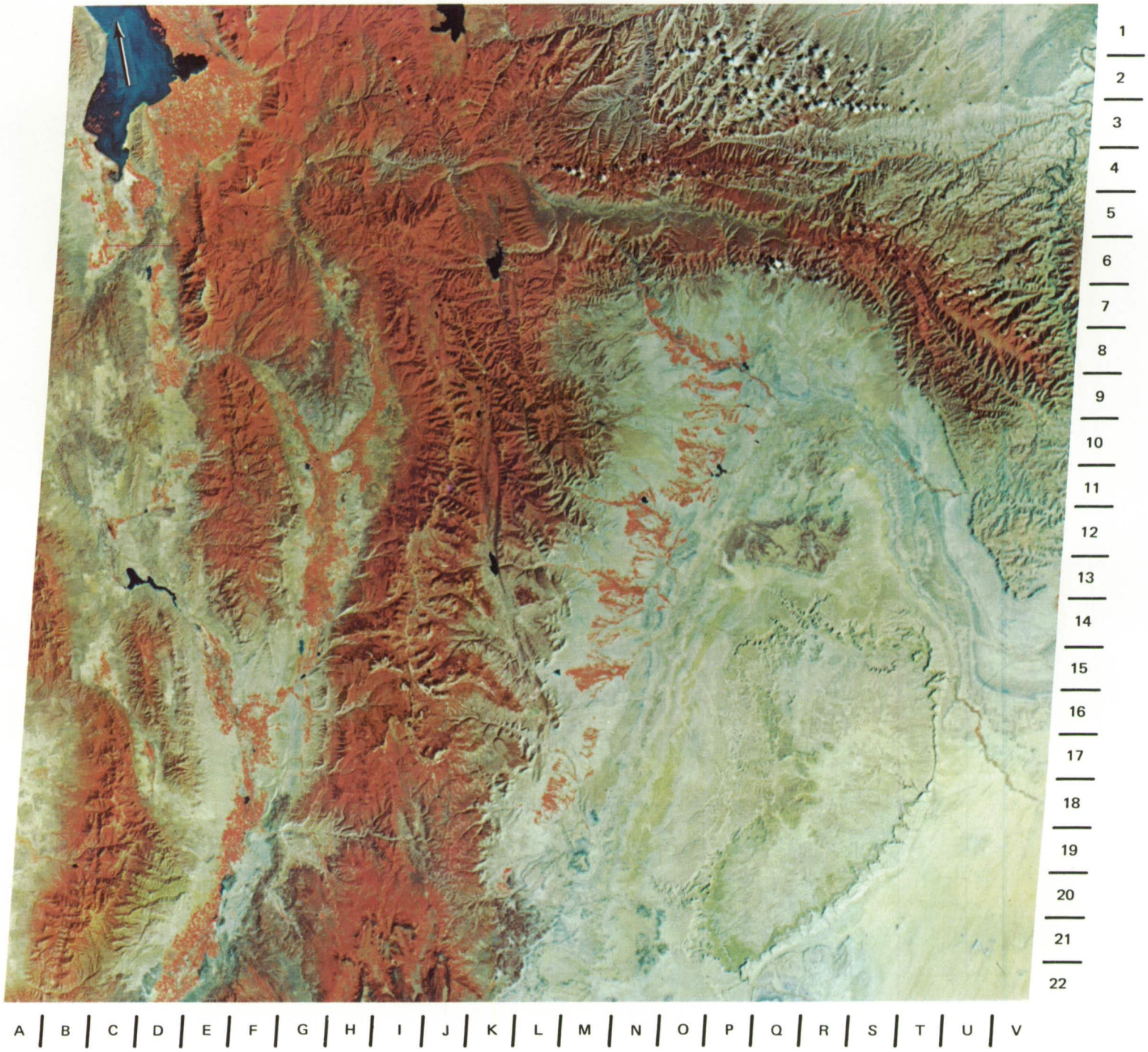


PLATE 90

HIGH PLATEAU, UTAH: This section of the Colorado Plateau near its western limit is marked by a pronounced "cliff and bench" topography consisting of a terracelike stack of tablelands separated by steep escarpments usually topped by resistant rock units. Prominent examples are the Markagunt (*P*–11), Paunsugunt (*T*–4), and Table Mountain (*T*–11) Plateaus. These, the Tushar Range (*P*–1), and the Pine Valley Mountains (*I*–15) are made up of Tertiary lava flow caps that overlie the Eocene Wasatch Formation and Cretaceous and Jurassic sedimentary rocks. A series of steep cliffs made up of less easily eroded sedimentary beds are arranged in the following order (oldest units at the lowest elevations): Chocolate Cliffs (*T*–19) (Triassic Shinarump Formation); Vermillion Cliffs (*O*–19; *T*–17) (Jurassic Wingate Formation); White Cliffs (*T*–15) (Jurassic Navajo Formation); Gray Cliffs (*T*–14) (Cretaceous sandstones); and the Pink Cliffs (*P*–13; *T*–12) (Eocene Wasatch Formation). The spectacular Zion National Park (*N*–16) highlights exposures of Navajo and Wingate sandstones in deep stream-cut canyons; extensive joints that control many cliff faces in the park can be seen in this image. The fantastic columns and spires in Bryce Canyon National Park (*U*–9) and Cedar Breaks National Monument (*N*–11) are carved out of the easily eroded, multicolored Wasatch Formation. Triassic red sandstones appear as yellowish areas (*K*–19) around the town of St. George (*I*–19) on the Virgin River (*K*–17). To the east are the Hurricane Cliffs (*L*–20). The Hurricane fault runs northward past the small town (*K*–17) of that name and continues beyond Cedar City (*L*–10). A broad alluvial valley (*G*–9), making up the Escalante Desert, runs northeast past the Wah Wah Mountains (*B*–5). The southernmost finger of the now dry Lake Bonneville—the vast Pleistocene lake that has receded to the present Great Salt Lake well to the north—reached to the upper part of this valley (*I*–4). The several areas of farmland evident in the image were originally developed by Mormon settlers in the last century. *1411–17422;* September 7, 1973.

PLATE 91



SAN RAFAEL SWELL, UTAH: This broad structural dome or uplift (*R*–17) is shown on these two pages first as a false color Landsat view, at 1:1 000 000 scale, and then in a higher resolution (1:500 000 scale) view taken in "true" color on June 5, 1973, by the S–190B terrain camera on the Skylab 2 mission. It is evident at a glance that most of the details on major rock units, fractures, topography, and vegetation present in the Skylab photo can also be picked out adequately in the Landsat coverage of the corresponding area.

The center of the Swell, known locally as the Sinbad (*S*–17), consists of Pennsylvanian and Permian sandstones and carbonates. The Reef (inner reddish (Skylab) or yellowish (Landsat) unit) is an escarpment (*P*–18; *T*–16) of dipping Triassic and Jurassic rocks capped by the Navajo sandstone; the steep-dipping flatirons (*R*–20) on the southeast are called the Goblins. The outer red (yellow) units (*N*–8) are outcrops of Cretaceous sandstones. Beyond are the Coal Cliffs (*N*–14), made up of Cretaceous shales, and the Castle Valley (*L*–18; *O*–8), where hay and other crops are grown along canals (*N*–12) connected to the San Rafael River (*O*–14; *U*–16) below Price, Utah (*N*–8). The high country to the west is



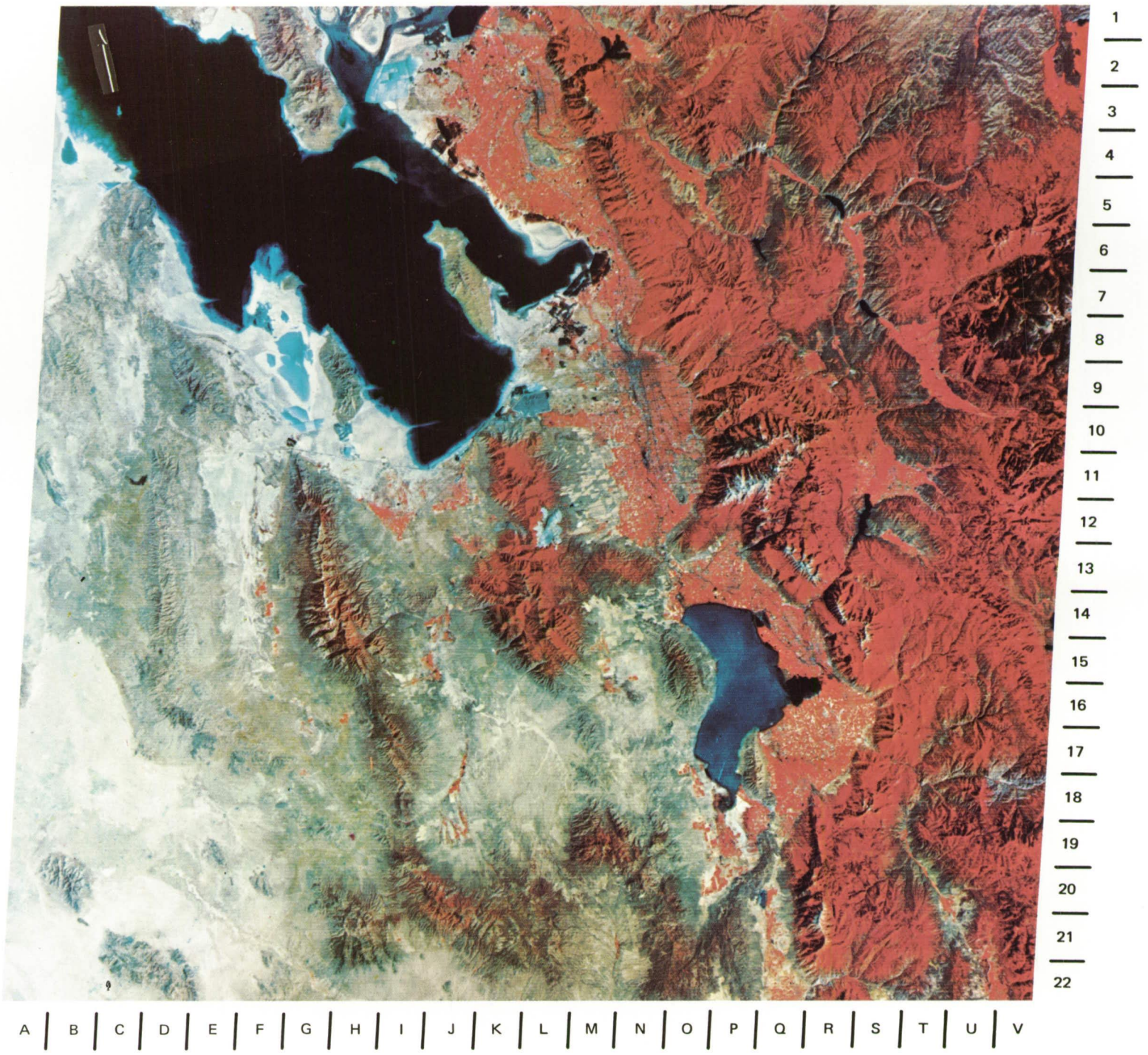
PLATE 92

part of the Wasatch Plateau (*I*–17; *I*–8), underlain by gently dipping Cretaceous shales and sands and the Eocene Wasatch Formation. This physiographic unit wraps around the Swell to form the Book Cliffs (*O*–6; *U*–13) comprised of the Mesa Verde sandstone; the Roan Cliffs (*O*–5; *U*–8), capped by the Wasatch Formation; and the Tavaputs Plateau (*P*–2). These units dip northward into the Uinta Basin (*U*–2) drained by the Green River (*V*–2) before it passes through Desolation Canyon (*V*–4).

Provo, Utah (*C*–1), lies between the southern end of the Wasatch Range (*D*–7) and Lake Utah (*B*–2) (containing large patches of algae—red blotches in the Landsat view—that "bloom" at this time of year). The San Pitch Mountains (*D*–11) stand between the Juab (*C*–8) and San Pete (*G*–11) Valleys that merge east of the Pavant Mountains (*C*–19) where the Sevier River (*S*–19) flows to the north through hay, alfalfa, sugar beets, and wheat farms.

The highest ranges and uplands support spruce, fir, and scrub oak-mahogany hardwoods. Piñon pine and juniper coat the lower slopes extending into the basin, which contains rather sparse greasewood and sagebrush. *1032–17364;* August 24, 1972.

PLATE 93



GREAT SALT LAKE, UTAH: This saline body of water (*G*–5) is the remnant of Lake Bonneville, a late Ice Age freshwater lake that once covered much of northern Utah. Deposits from this ancestral lake cover most of the lowlands, as at the edge of the Great Salt Lake Desert (*A*–21) and the Dugway Proving Ground (*C*–19). Many of the block fault mountains—Cedar (*C*–12), Stansbury (*G*–13), Onaqui (*H*–15), and Oquirrh (*K*–13)—were isolated islands when Bonneville was filled to elevations of 300 or more meters (1000 or more feet) above the present level of the much smaller Great Salt Lake. Salt flats (*A*–4; *H*–10), commercial salt evaporating ponds (*F*–9; *H*–2), and tule marshes (*K*–7) lie beyond its shoreline. Owing to the interruption of circulation by the causeway (*D*–4) of the Southern Pacific railroad, the lake has developed a more saline phase in the north that fosters production of brine shrimp and algae, which produce a uniformly turbid appearance best seen in black and white bands 4 and 5. Antelope Island (*I*–6) and the Promontory Range (*F*–3) are Precambrian crystalline outliers. Lake Utah (*P*–15) is another remnant of Lake Bonneville.

The valley, containing Salt Lake City (*M*–8), Ogden (*K*–3), and Provo (*Q*–15), has borne out the hopes of the early Mormon settlers as fertile ground for agricultural production. Irrigated farms (checkered red patterns) growing barley, alfalfa, potatoes, sugar beets, tomatoes, lettuce, corn, peas, and dry wheat (yellow tones), as well as apple and peach groves produce abundantly in the alluvial and lake bed soils of the region.

To the east lie the Wasatch Mountains (*Q*–6), rising abruptly at the Wasatch Front (*M*–6; *G*–13)—developed from a great normal fault—to elevations as high as 3700 meters (12 000 feet) at Mount Timpanogos (*Q*–12). This block consists largely of Devonian and Carboniferous sedimentary rocks overlapped on the east by the Eocene Wasatch Formation. Much of these mountains is covered by chaparral (mostly scrub oak and mahogany), but fir and some spruce abound at higher elevations. The mountains west of the Front are populated mainly by piñon and juniper.

One of the world's largest copper mines is at Bingham Canyon (*L*–12), where ore is extracted from a great terraced open pit (light blue). Smelters at Magna reduce the ore, leaving a residue dumped into a huge tailing pond (*K*–9). To the south in the Tintic Mountains (*M*–18) other mines produce silver and lead. *1015–17415;* August 7, 1972.

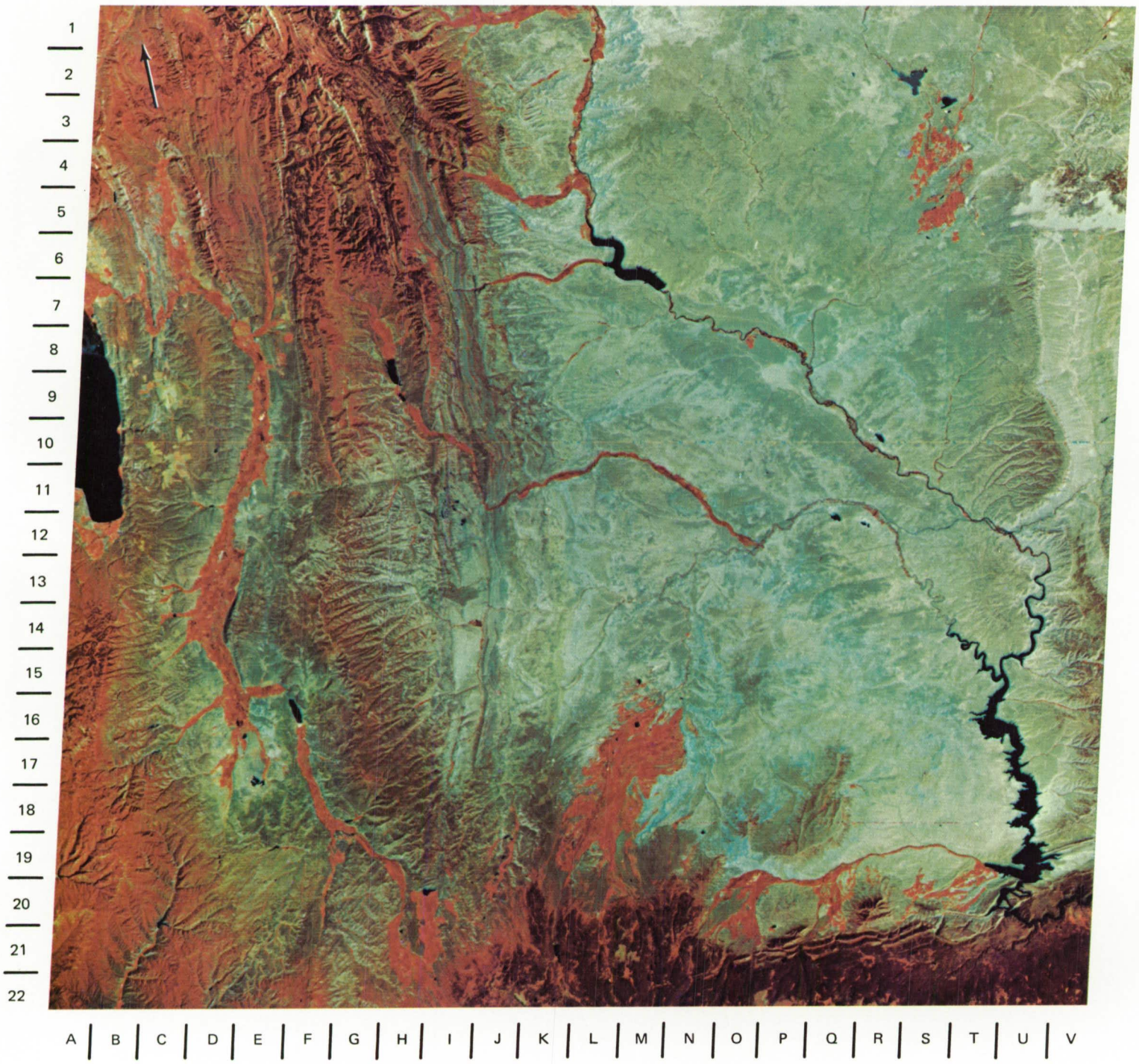


PLATE 94

SOUTHWESTERN WYOMING: The Green River Basin (*O*–14; *R*–6), lying between the Wind River uplift (off upper right corner), the Rock Springs uplift (*V*–8), the Uinta Mountains (*N*–21), and the southern extension of the Wyoming (*F*–1) and Salt River (*D*–1) ranges, is a large intermontane depression filled with Tertiary sediments including the Eocene Bridger and Green River Formations at the surface. The basin is drained by the Green River (*Q*–9), dammed up at the Flaming Gorge Reservoir (*U*–19) and again at the Fontenelle Reservoir (*L*–6). Major tributaries from the west include Hams Fork (*L*–10), La Barge Creek (*J*–5), and the forks of Piney Creek (*I*–1).

The Wyoming-Salt River Ranges are composed of tightly folded and thrust faulted sedimentary rocks of Permian through Cretaceous age that structurally resemble parts of the folded Appalachians. The folds die out southward along the Tunp Range (*F*–7), Commissary Ridge (*H*–6), Oyster Ridge (*I*–12; *J*–15), and Mammoth Hollow (*I*–14) segments. Coal is mined near Kemmerer (*I*–11) from Cretaceous beds exposed in the dipping units. As the Wasatch Range (*A*–14; *B*–20) is approached from Evanston, Wyo. (*F*–18), rocks of the Eocene Wasatch Formation are exposed in the dissected valley drained by the Bear River (*D*–9) as it flows northward past Bear Lake (*A*–10) into Idaho near the Sublette Range (*C*–5).

East of Farson (*R*–5) and the Big Sandy Reservoir (*R*–2) is the east end of the Kilpecker dune field (*U*–5), one of the largest windblown sand deposits in the United States. Further south, whitish trona (natural sodium carbonate) is mined from Eocene beds. Coatings of trona at several processing plants (*Q*–11; *R*–9) with small lakes resemble "clouds and their shadows" as though illuminated in this image from the northwest.

The Green River Basin is essentially a sagebrush steppe with some grass. As elevations increase, piñon and juniper appear, followed still higher by oak and aspen, and finally pine and fir in the upper regions of the Wyoming, Wasatch, and Uinta Mountains. The stream valleys support mostly irrigated hay and alfalfa cut as cattle fodder. *1014–17355;* August 6, 1972.

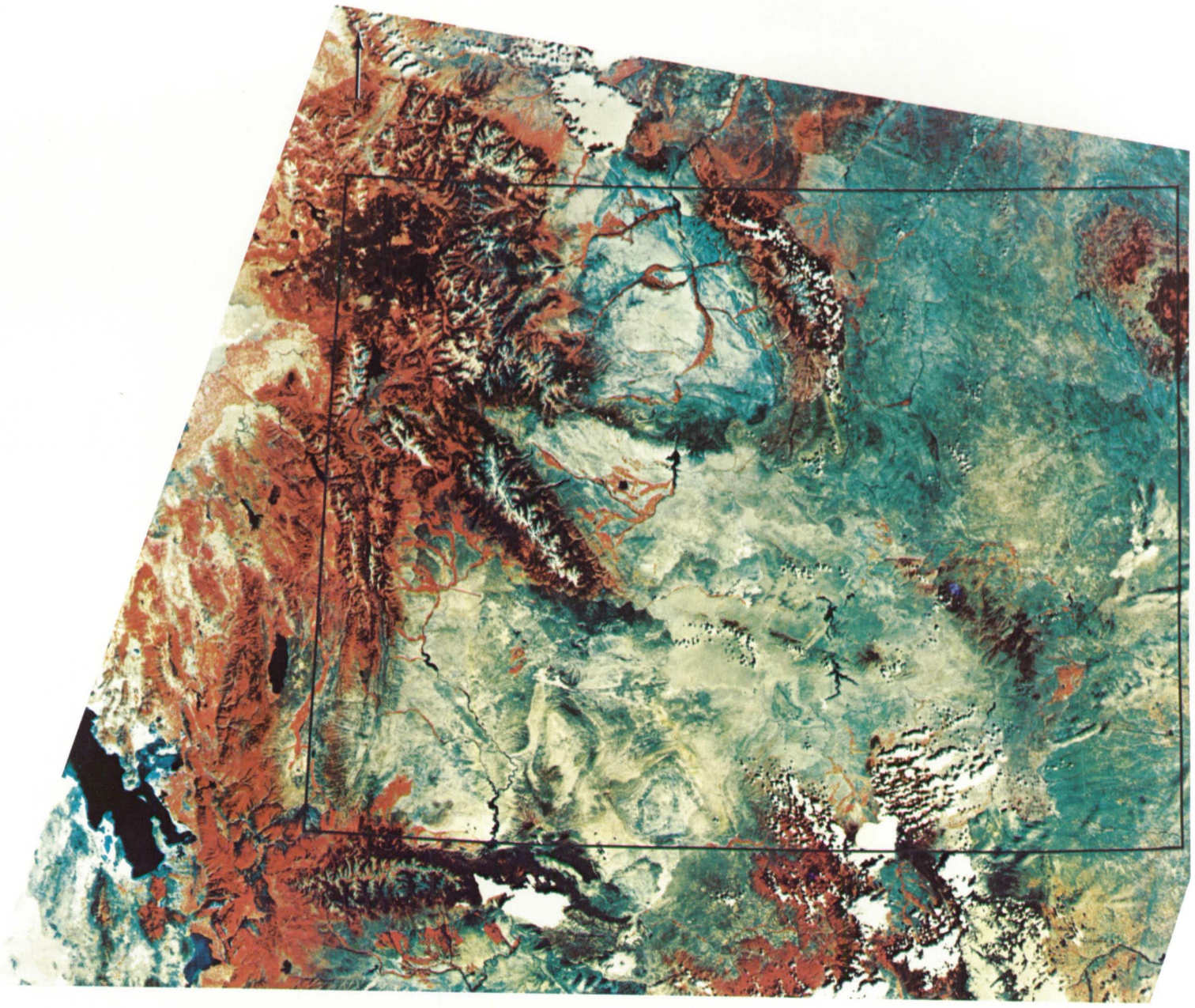


PLATE 95

THE STATE OF WYOMING: This is the first mosaic of a large area of the United States to be produced in false color. The entire State of Wyoming, extending for more than 650 kilometers (400 miles) from corner to corner, is portrayed together with parts of five adjacent States. Twenty-seven individual Landsat image scenes, taken mainly in the months of August and September 1972, were used by specialists at the General Electric Photographic Laboratory in Beltsville, Md., to prepare the mosaic. (See plate 96 for letter identifications.) Major features of interest are as follows: *Wyoming:* Laramie Range (*A*); Cheyenne region (*B*); Medicine Bow Mountains (*C*); Black Hills (*D*); Powder River Basin (*E*); Casper Mountain (*F*); Wind River Basin (*G*); Boysen (*H*), Pathfinder (*I*), Seminoe (*J*), and Flaming Gorge (*K*) Reservoirs; Shirley (*L*), Ferris (*M*), and Green (*N*) Mountains; Rawlins uplift (*O*); Washakie Basin (*P*); Rock Springs uplift (*Q*); Green River Basin (*R*); Green River (*S*); Wind and Bighorn Rivers (*T*); Owl Creek Mountains (*U*); Bighorn Mountains (*V*); Bighorn Basin (*W*); Absaroka Range (*X*); Yellowstone National Park (*Y*); Grand Tetons (*Z*); Gros Ventre Range (*AA*); Wind River Range (*BB*); and Wyoming and Hoback Ranges (*CC*). *Montana:* Pryor Mountains (*DD*); Snowy Mountains (*EE*); Madison Range (*FF*); and Gallatin Range (*GG*); *Idaho:* Snake River Plain (*HH*); Snake River Range (*II*); Bannock Range (*JJ*); Bear Range (*KK*); and Bear Lake (*LL*). *Utah:* Great Salt Lake (*MM*); Salt Lake City (*NN*); Wasatch Range (*OO*); Great Salt Lake Desert (*PP*); Oquirrh Range (*QQ*); Utah Lake (*RR*); Uinta Mountains (*SS*); and Uinta Basin (*TT*). *Colorado:* Elkhead Mountains (*UU*); Park Range (*VV*); North Park (*WW*); Rocky Mountain National Park (*XX*); Front Range (*YY*); and Denver area (*ZZ*).

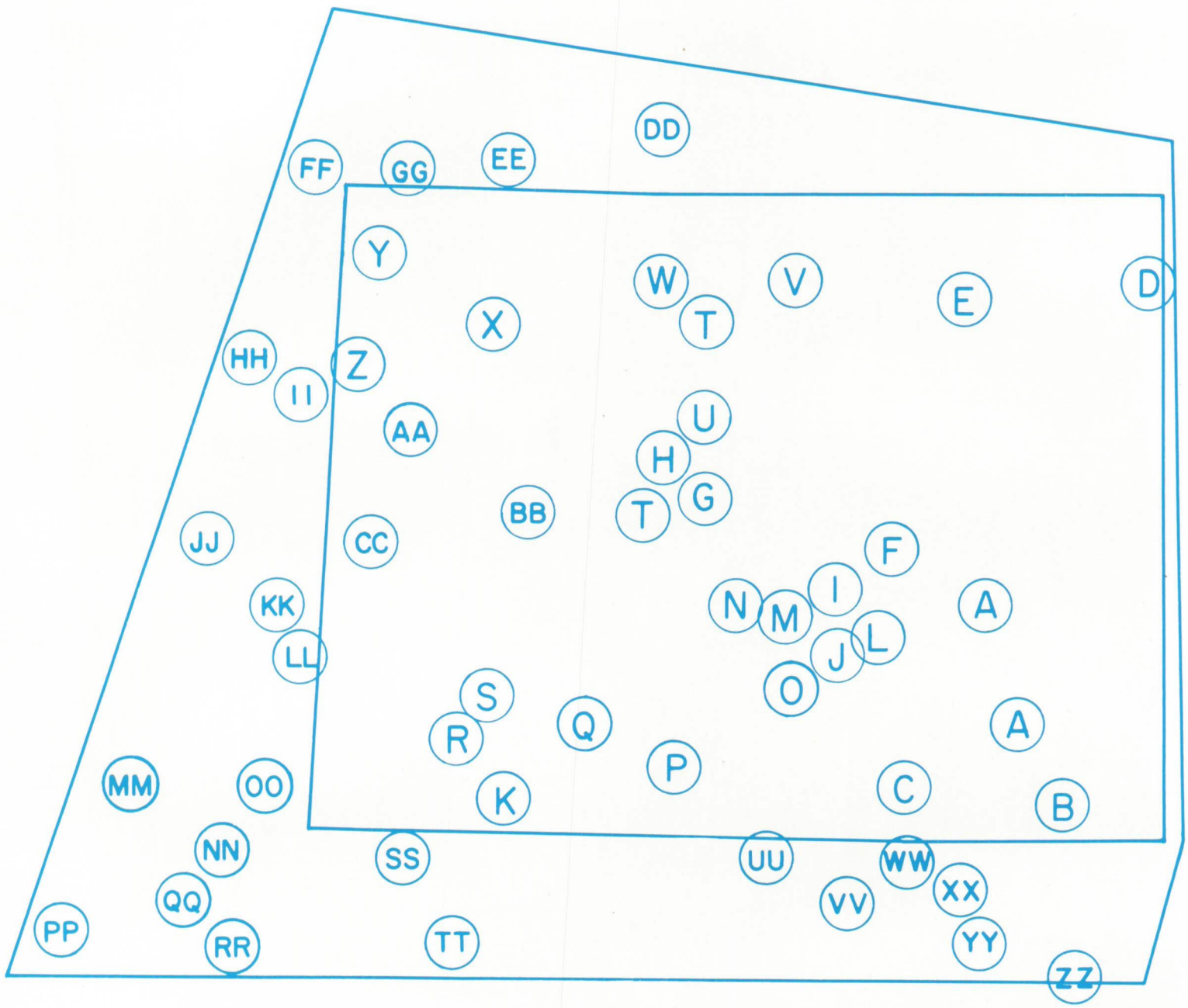
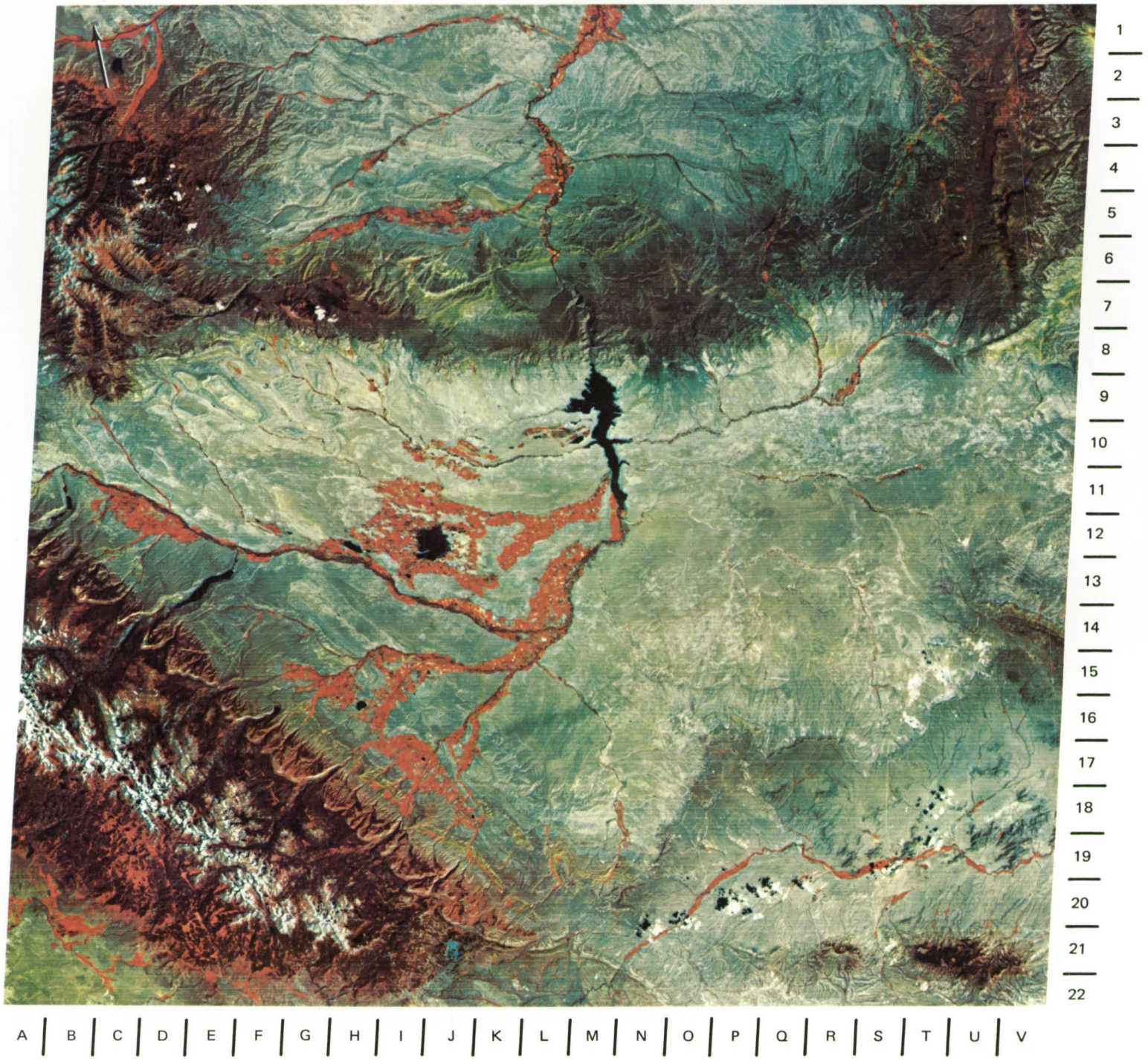

DD
FF
GG
EE
Y
W
V
D
E
T
X
HH
Z
II
U
AA
H
G
BB
T
JJ
CC
F
I
KK
N
M
A
L
LL
J
O
S
A
R
Q
P
MM
OO
C
B
K
NN
SS
UU
WW
XX
VV
QQ
YY
PP
RR
TT
ZZ

PLATE 96

PLATE 97



CENTRAL WYOMING: This view centers on the Wind River Basin—a Tertiary sediment-filled intermontane block surrounded by the high 4000-meter (13 000-foot) Wind River Mountains (*E*–18) on the west, the Absaroka Range (*A*–4), and the Owl Creek-Bridger (*G*–7; *N*–7), and southernmost Bighorn Ranges (*U*–2) that separate this basin from the Bighorn Basin (*U*–2) to the north. The basin joins the Sweetwater Arch (*R*–21) at the Beaver Divide (*U*–15). The Sweetwater River (*S*–19), the Green Mountains (*U*–21), and the Granite Mountains (*V*–18) (including the famous Independence Rock along the Oregon Trail of the mid-1800's) lie along the southern edge of the Wind River Basin. The Wind River (*L*-13) drains off the western high country until it collects at the Boysen Reservoir (*L*–9) at the head of the Wind River Canyon (*L*–7); to the north this river is called the Bighorn. The farming area along this river consists mostly of hay, alfalfa, and other feeds. Ocean Lake (*I*–12) lies in the heart of this irrigated land; elsewhere the basin is dominated by sage and grassland. Among conspicuous oil-producing anticlinal structures are Maverick Springs (*E*–9) and Conant Creek (*P*–16). The deposits of uranium mined from surface pits (*T*–15) in the Gas Hills district are among the largest in the United States. Magnetic iron ore is extracted at Atlantic City leaving a scar in the metamorphic greenstones that appears blue (*J*–21) in this color rendition. Dipping hogbacks of Paleozoic and Mesozoic sedimentary rocks occur along the flanks of several ranges (*D*–15; *I*–7). *1013–17294;* August 5, 1972.

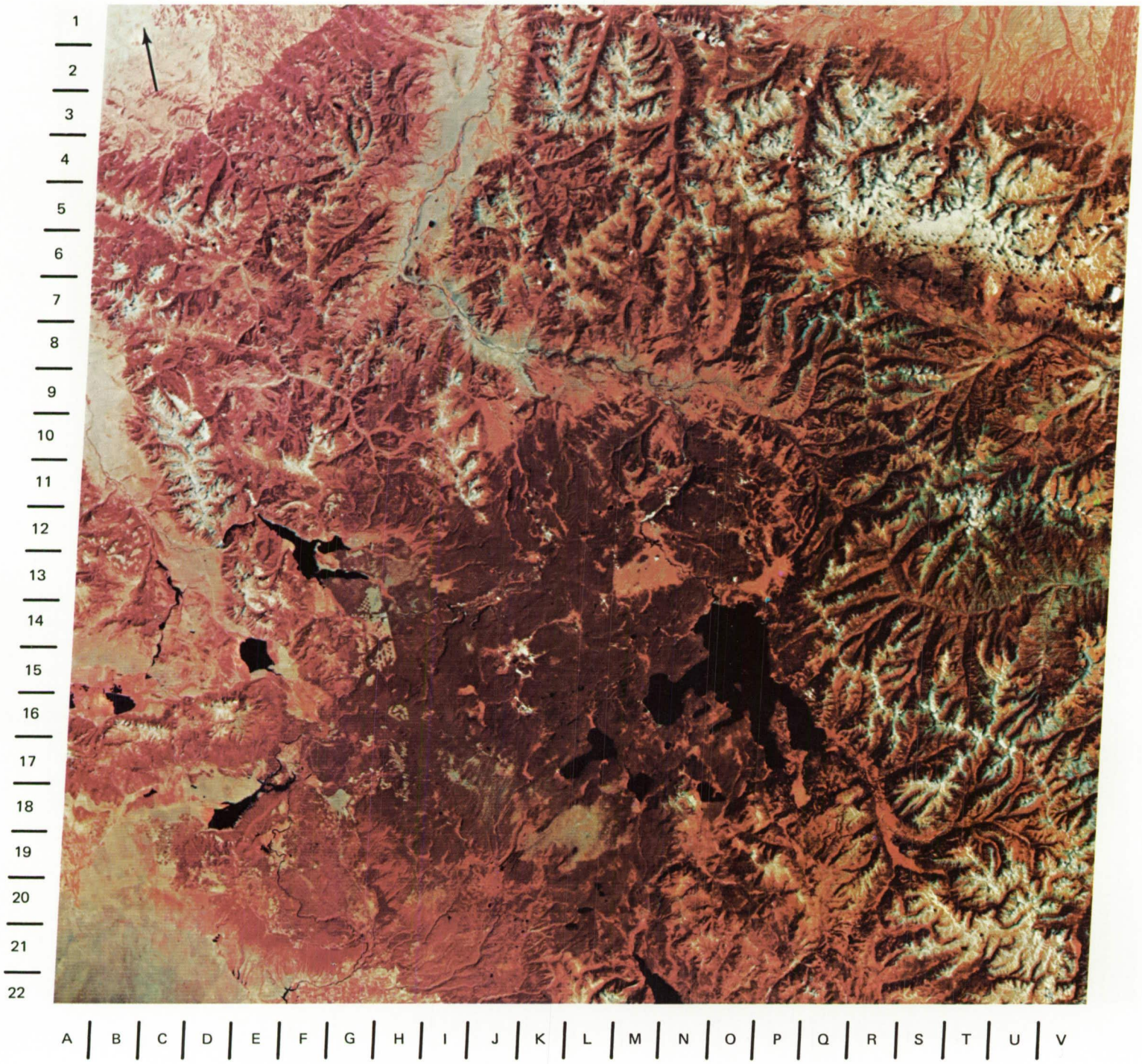
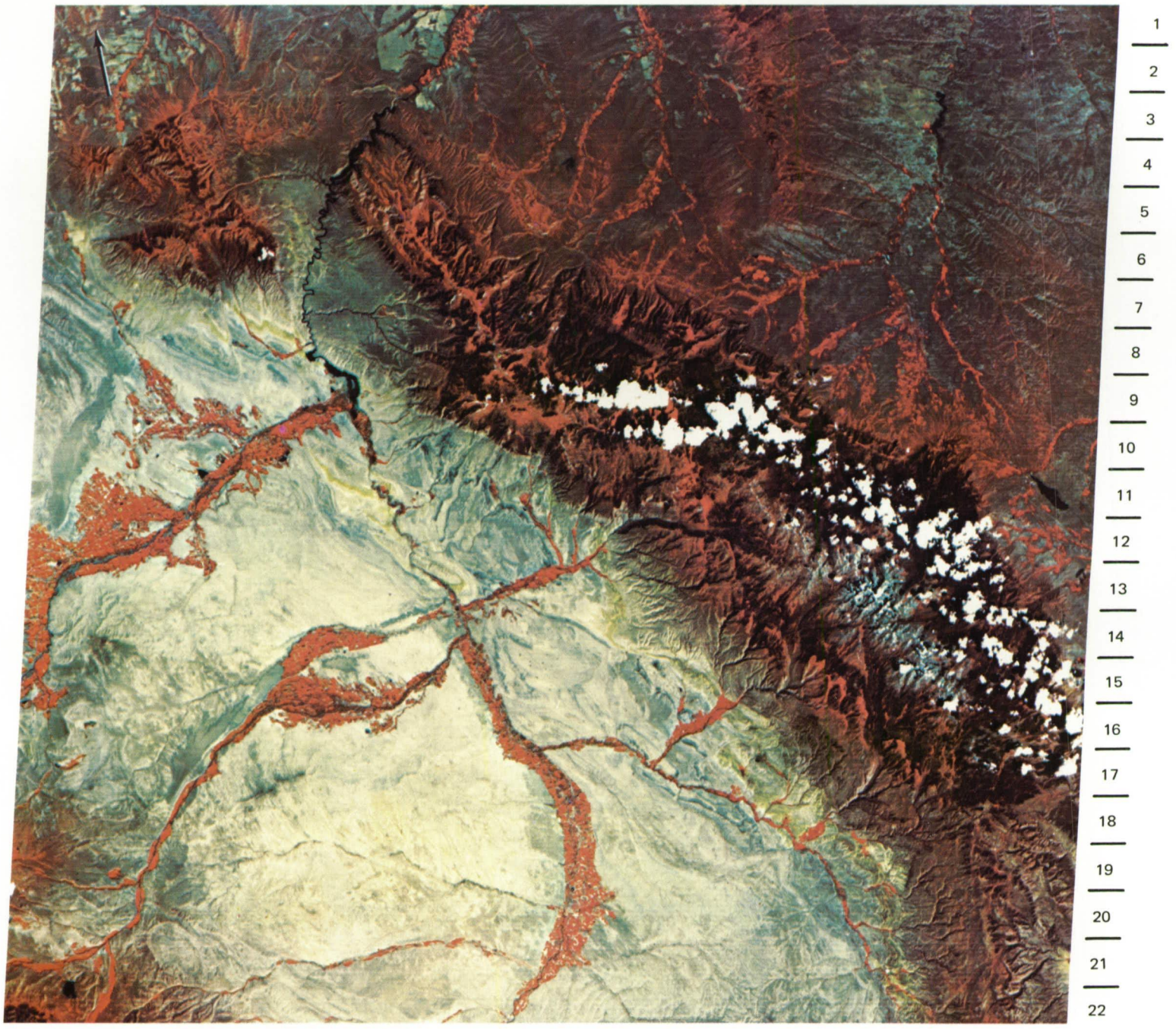


PLATE 98

YELLOWSTONE NATIONAL PARK: All of Yellowstone, the first national park established in the United States, appears in this scene. The Yellowstone River (*S*–18) drains into Yellowstone Lake (*O*–14), thence over Yellowstone Falls and through Yellowstone Canyon (*M*–11), then westward and northward (*G*–5) into Montana. The Old Faithful region (*J*–14) and Mammoth Hot Springs (*H*–8) are two well-known park landmarks; other geyser areas also show up as white patches. These geysers result from steam-driven expulsion of groundwater heated from still hot volcanic flow rocks of late Tertiary and Quaternary ages. Most of the park is covered with lodgepole pine, interspersed with spruce and fir, but open grassy meadows (*I*–9; *M*–13) are favored haunts of elk and moose. The Yellowstone region is bounded by the high Absaroka Range (*T*–15), made up of dissected and glaciated Tertiary volcanic rocks. To the north are the lofty Beartooth Mountains of Montana (*S*–5), parts of which appear as light toned where Precambrian granites are exposed above timber line. The volcanic Gallatin (*E*–5) and folded sedimentary Madison (*C*–8) Ranges, separated by the Gallatin River (*D*–7), tie this region to the eastern edge of the Montana Rocky Mountains. Seismic activity along this trend was responsible for the 1959 earthquake-induced landslide into the Hegben Reservoir (*E*–12), resulting in a number of fatalities among nearby campers and the formation of Earthquake Lake (*O*–12) downstream on the Madison River (*C*–12). The edge of the Snake River Plains in Idaho includes the Island Park caldera (*D*–18), associated with Eocene volcanic flows. Note the forest clear-cutting pattern (*G*–14) that extends up to the boundary of the national park. *1015–17404;* August 7, 1972.

PLATE 99



BIGHORN MOUNTAINS, WYO.: This uplift (*O*–11; *U*–19) is a large block of Precambrian granites, exposed around Cloud Peak (*R*–13) and elsewhere, that is flanked on all sides by outward dipping Paleozoic and Mesozoic rocks (*G*–5; *O*–8; *Q*–15). Carboniferous and younger rocks make up the Pryor Mountains (*C*–4) in Montana. These ranges separate the Bighorn Basin (*F*–17), through which drain the Bighorn River (*F*–5; *L*–18) and its tributaries, the Greybull (*D*–16) and Shoshone (*C*–11) Rivers and Nowood Creek (*P*–17), from the northwestern extension of the Powder River Basin (*U*–3), drained by the Tongue (*S*–3) and Little Bighorn (*M*–3) Rivers (the site of General Custer's famed "last stand" is just off the image at (*L*–1)). Numerous oil-bearing anticlines, including the Sheep Mountain (*I*–12) and Little Sheep Mountain (*H*–12) structures north of Greybull (*J*–13), were produced by folding of basin sediments along the southwestern flank of the Bighorn and Pryor Mountains as these were pushed upward. The yellow-toned units (*E*–7; *M*–13) are outcrops of a distinctive Triassic red bed formation—in general, reddish units are rendered yellowish in the standard Landsat color composites. The dark feature shown at *D*–16 is a pediment of Tertiary gravels representing a remnant of an earlier surface now "stranded" by erosional lowering of surrounding surfaces.

The striking difference in tone between the yellowish Bighorn Basin and the dark bluish-gray Powder River Basin results mainly from differences in natural vegetation—saltbush, sagebrush and wheatgrass in the former and grama and needle grass interspersed with ponderosa pine in the latter—that result from average elevation differences (lower in the Bighorn Basin) and differences in rock types. The uplifts are covered with spruce and fir. Hay and alfalfa used for stock feeding dominate the crops grown along the rivers, along with some sugar beet and bean production. *1013–17291;* August 5, 1972.

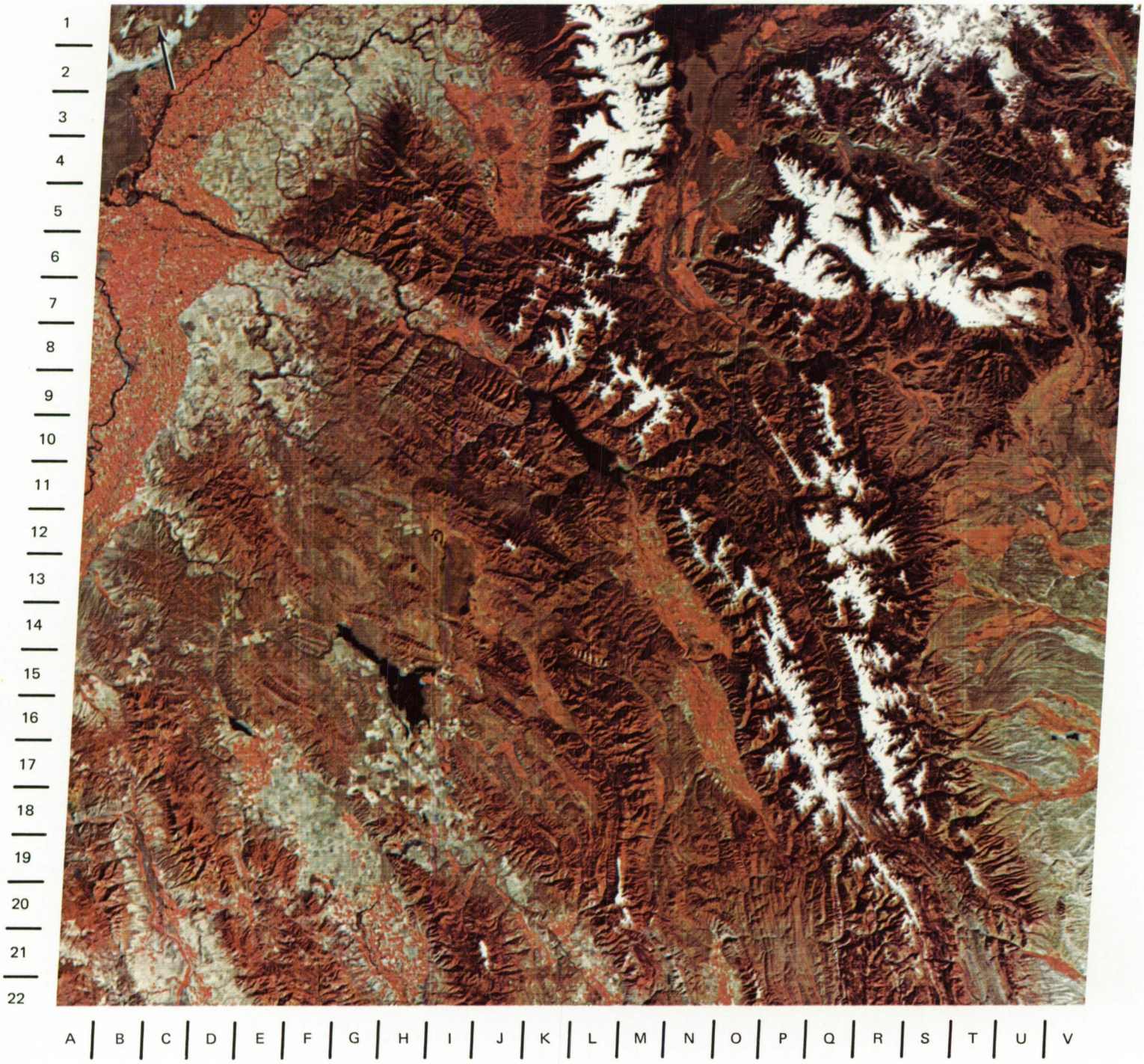
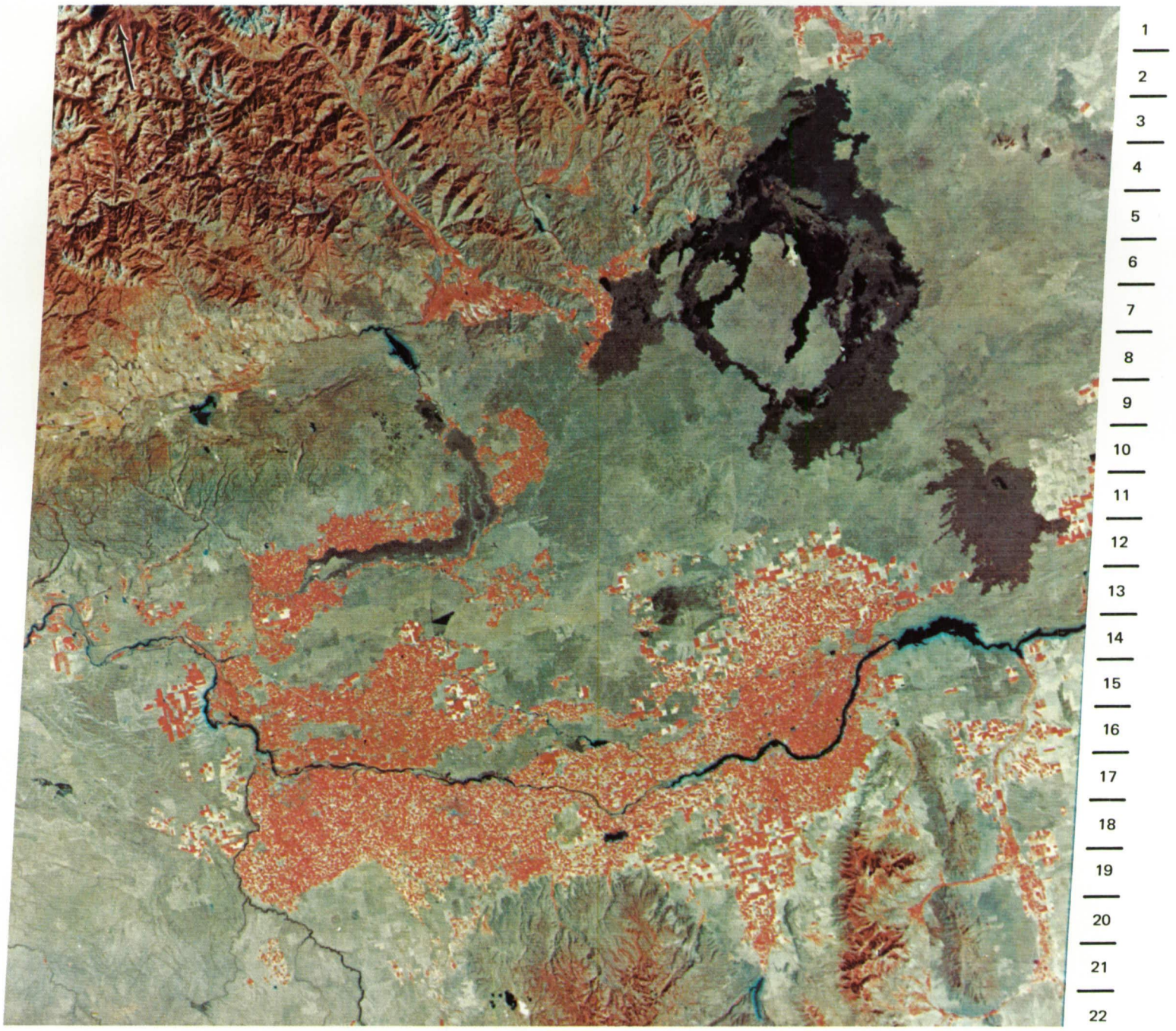


PLATE 100

WESTERN WYOMING AND SOUTHEASTERN IDAHO: This region includes the famed Teton Mountains (*K*–3), a tilted Precambrian fault block, nearby Jackson Hole (*M*–4) and Jackson Lake (*M*–1), and the Gros Ventre Mountains (*Q*–6), exposing mainly Paleozoic sedimentary rocks. To the south, the strongly folded Hoback (*P*–10), Wyoming (*Q*–14), and Salt Ranges—Paleozoic and Mesozoic strata sliced up by several thrust faults including the Bannock overthrust—deflect northwestward into the Snake River Mountains (*G*–5). The Caribou Range (*H*–9) runs into the Preuss Range (*N*–18) to the south, thence into the Aspen Range (*K*–18) that extends from the Wasatch Mountains of Utah. The Bannock thrust lies to the west, passing through Swan Valley (*E*–17) and Grays Lake (*I*–13)—a dried-up depression in this view north of the Blackfoot Reservoir (*H*–15). These northwestward-trending ranges are terminated abruptly by the Tertiary and Quaternary lavas of the Snake River plains, drained by the Snake River (*E*–6).

Idaho Falls (*A*–8) lies in an agricultural region (*B*–6) that specializes in potatoes, along with wheat, sugar beets, and field crops. Stock-feeding crops are grown in the Star Valley (*N*–14), well known for its cheeses, which extends below the Palisades Reservoir (*K*–10). Hay meadows abound along streams in the upper Green River Valley (*U*–12) of Wyoming. Timber products include Douglas fir, spruce, and lodgepole pine, distributed in the higher mountains. *1069–17411;* September 30, 1972.

PLATE 101



SOUTHERN IDAHO: The Snake River (*L*–17), flowing out of western Wyoming, here passes over the Snake River Plains—a vast series of lava flows of Tertiary to Quaternary age. The youngest of these flows (*O*–6; *P*–4; *Q*–6) shows up as varying shades of dark blue—representing basalt lavas—that have yet to form stable soils that can support vegetation such as sagebrush and grass that elsewhere cover most of the plains. Craters of the Moon National Monument (*P*–4) present a spectacular display of recent volcanism once thought to resemble the Moon's landscape (a comparison now largely disregarded after the lunar exploration of the early 1970's). Older volcanic rocks occur to the west of Salmon Falls Creek (*J*–11). South of the Lake Walcott Reservoir (*T*–14), a piñon- and juniper-covered range topped by Cache Peak (*T*–20) consists of late Precambrian metasedimentary rocks. The southern edge of the Idaho Rocky Mountains in the upper left includes the Pioneer Mountains (*J*–3), the Smoky Mountains (*E*–5), and the southern end of the Sawtooth Range (*D*–1), which is underlain by the granitic Idaho batholith. The popular Sun Valley resort (*G*–3) lies along the Big Wood River (*H*–5). Douglas fir, spruce, and ponderosa pine predominate in this high country.

The fertile farmlands along the Snake River are major producers of Idaho potatoes, sugar beets, beans, corn, wheat, barley, and alfalfa. Twin Falls (*N*–17) is the largest town in this agricultural region. *1035–17525*; August 27, 1972.

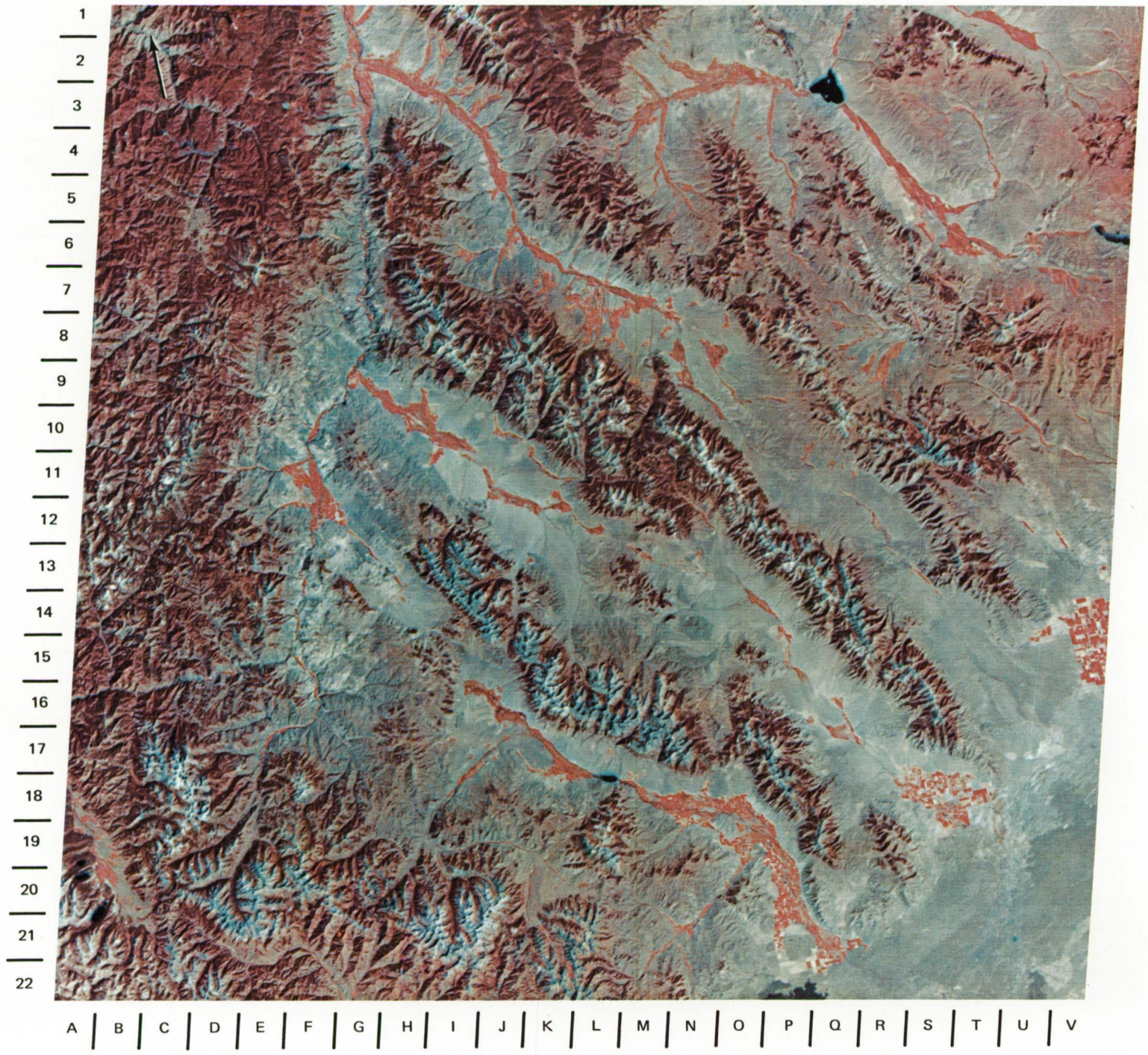
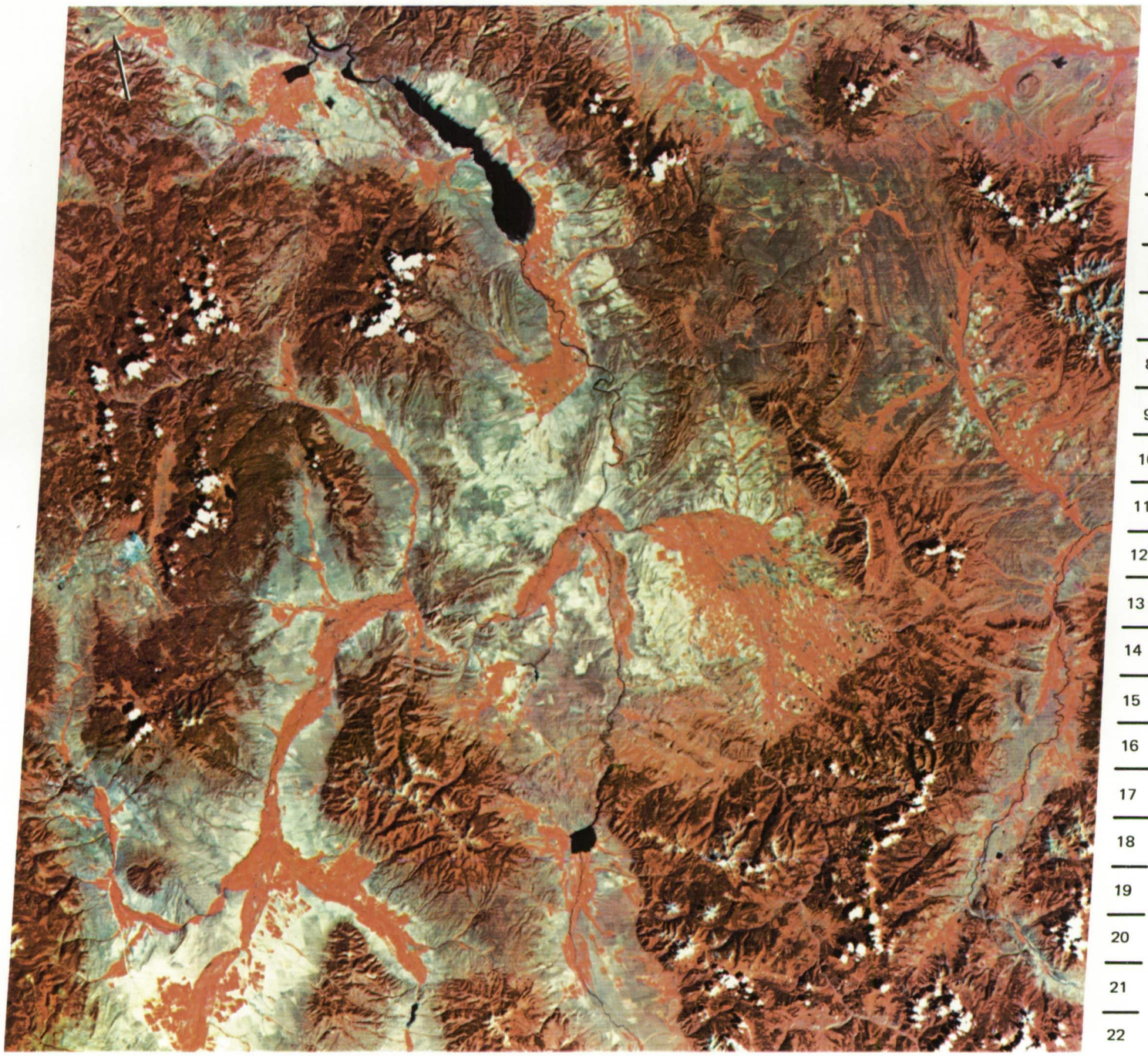


PLATE 102

IDAHO ROCKY MOUNTAINS: The central Rocky Mountains deflect northwestward in Wyoming and follow that trend in south-central Idaho before they swing northward again in western Montana and northern Idaho. This deflection is interrupted by the volcanic flows forming the plains that fill the Snake River downwarp just below the bottom of this image. (See plate 101.) The continuation of the Rocky Mountains in this part of Idaho is expressed in a series of parallel ranges that are bounded by normal and/or thrust faults. Those east of the Salmon River (*F*–9) aline along the northwest trend. Typical of these is the Lemhi Range (*M*–10), whose southeast half (*P*–13) consists of Paleozoic sedimentary rocks that give way to rocks of the Proterozoic belt series on the northwest half (*H*–7). An alluvium-filled valley, through which flow the Lemhi (*H*–3) and Birch (*L*–7) Rivers, separates this range from the elongate Beaverhead Mountains (*K*–5), which also are split into a similar division of belt series (*H*–1) and Carboniferous (*R*–10) rocks. The Tendoy Mountains (*P*–4), also composed of late Paleozoic rocks, and the Centennial Range (*V*–9), made up of Eocene volcanics, straddle the border between Idaho and Montana. The Red Rock River (*Q*–4) flows into the Beaverhead River (*P*–1) at Haphawkins Lake (*P*–2). The continental divide runs along the crest of the Beaverhead Range, eventually diverting the waters of the Beaverhead to the Missouri River and those of the Salmon to the Columbia River. The highest point in Idaho, Borah Peak (*K*–15), reaches to 3860 meters (12 662 feet) in the Lost River Range (*J*–14), a block of Paleozoic sedimentary rocks, which continues southeastward as the Hawley Range (*P*–17).

Challis (*F*–11) and Salmon (*F*–2), Idaho, are mountain communities established on the Salmon River. To their west is the eastern edge of the Salmon River Mountains (*C*–5; *C*–11), the principal group of high peaks in the southern Idaho Rockies. *1035–17522;* August 27, 1972.

PLATE 103



MONTANA ROCKY MOUNTAINS: The towns of Helena (*E*–3), Butte (*B*–12), Bozeman (*Q*–13), and Livingston (*V*–12) in Montana are nestled near high, open ranges of the Rocky Mountain system. The Deer Lodge Mountains (*D*–9) are part of the Boulder batholith; the Madison (*O*–18) and Gallatin (*R*–16) Ranges cut into Tertiary volcanics extending from the Yellowstone Park region. The Big Belt (*N*–6) and Bridger (*Q*–20) Ranges consist of Precambrian metasediments and are bounded by the Lombard thrust fault on the west. The Tobacco Root Range (*I*–16) is formed from Precambrian metamorphic rocks. Crazy Mountains (*U*–6) and Castle Mountains (Elk Peak: *Q*–2) are sculptured out of Tertiary intrusives. Folded Paleozoic and Mesozoic sedimentary units are evident in the basins. Principal rivers include the Yellowstone (*U*–16), Beaverhead-Jefferson (*F*–15), Madison (*L*–19), and Gallatin (*R*–21) which meet at Three Forks (*L*–12) to form the headwaters of the Missouri River. The Canyon Ferry Reservoir (*J*–4) lies to the east of Helena. Douglas fir and lodgepole pine cover the high ranges, with foothill prairie grass extending into the basins. The chief field crops include wheat, barley, and hay. Copper mining near Butte (open pits and tailings appear light blue (*C*–12)) and Anaconda (just off the image at *A*–12) makes up another major industry. *1034–17461;* August 26, 1972.

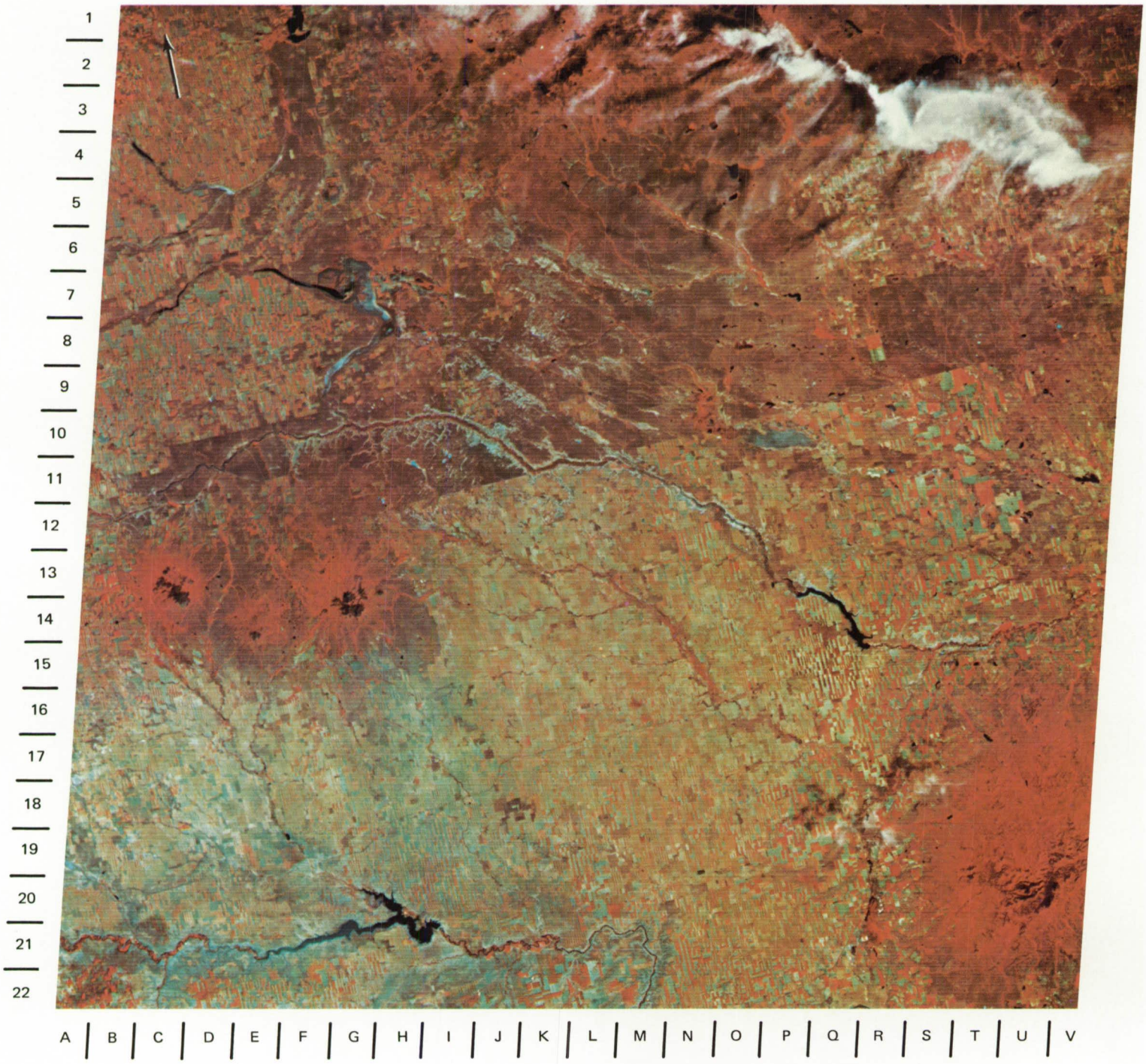
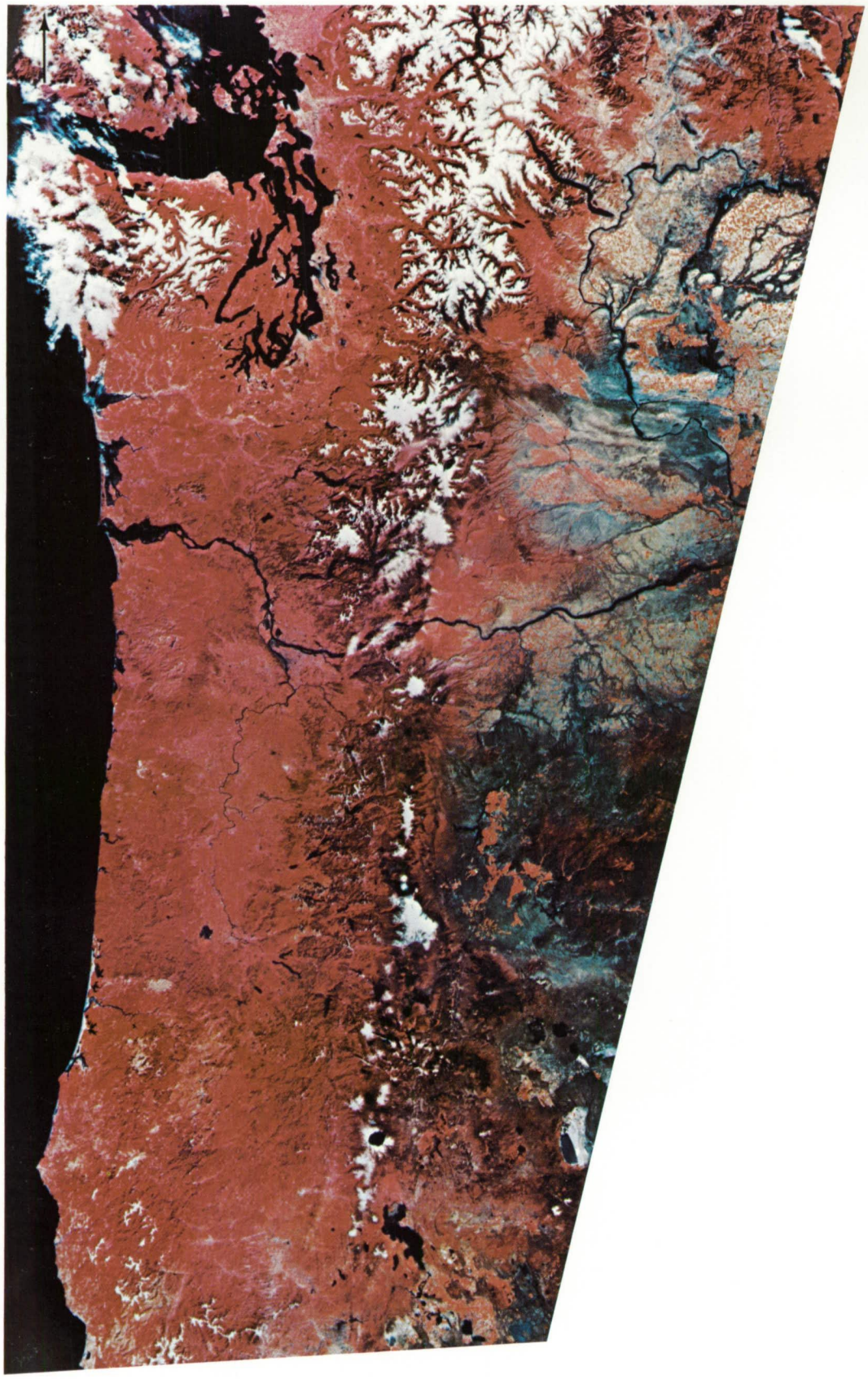


PLATE 104

THE U.S.-CANADIAN BORDER: Land use is responsible for the sharp definition of the border (*I*–11) between the United States and Canada separating the western Great Plains of north-central Montana from the southeastern corner of the province of Alberta. Here the plains form a part of the west edge of the Missouri Plateau where elevations increase westward from about 790 meters (2600 feet) near the town of Havre (*S*–14) to 1000 meters (3400 feet) around the Tiber Reservoir (*H*–20) on the Marias River (*K*–20). This river along with the Milk River (*I*–9) (and its Fresno Reservoir (*Q*–14)) flow into the Missouri River as it moves eastward from Great Falls, Mont. Dark brown and brown soils have been derived from glacial tills of Wisconsin age and/or underlying Cretaceous sedimentary rocks (mostly shales). Short grasses (grama grass, wheatgrass, and needlegrass), developed on these soils, still cover large areas (*J*–4) of the Alberta plains and the area around Havre. Cattle grazing is extensive in such areas. Elsewhere, the natural vegetation has been largely cleared for production of winter and spring wheat (R–12). Barley and hay are the other principal crops.

The Bearpaw Mountains (*U*–19), rising to almost 2100 meters (7000 feet), and the Sweet Grass Hills (*C*–13; *E*–13) further west are outliers of exposed Tertiary intrusive igneous rocks originally emplaced as shallow laccoliths and stocks. These erosional landforms are now covered mainly with ponderosa pine and some Douglas fir. *1700–17381;* June 23, 1974.

PLATE 105



OREGON AND WASHINGTON: This is a continuation of the special color mosaic of the west coast of the United States prepared by the General Electric Photographic Laboratory, Beltsville, Md., showing the western half of the State of Oregon and most of the State of Washington (*at top*), divided by the Columbia River. Among well-known geographic landmarks (see plate 106 for letter identifications), these are cited: Klamath Lake (*A*), Medford and its valley (*B*), the Oregon Coast Ranges (*C*), Summer Lake (*D*), Crater Lake (*E*), Newberry volcano (*F*), the Three Sisters volcanic group (*G*), the Deschutes River farmlands (*H*), the Blue Mountains (*I*), the Cascades (*J*), Mount Jefferson (*K*), Mount Hood (*L*), the Willamette Valley and River (*M*), Eugene (*N*), Portland (*O*), the Snake River plains (*P*), the Columbia River (*Q*), the Dalles Dam (*R*), the Channeled Scablands of Washington (*S*), Mount Adams (*T*), Mount St. Helens (*U*), Willapa Bay (*V*), Mount Rainier (*W*), the Grand Coulee (*X*), the Olympic Range (*Y*), Puget Sound (*Z*), Seattle (*AA*), Mount Baker (*BB*), the Juan de Fuca Straits (*CC*), Vancouver Island (Canada) (*DD*), the Fraser River delta (*EE*), and Lake Chelan (*FF*).

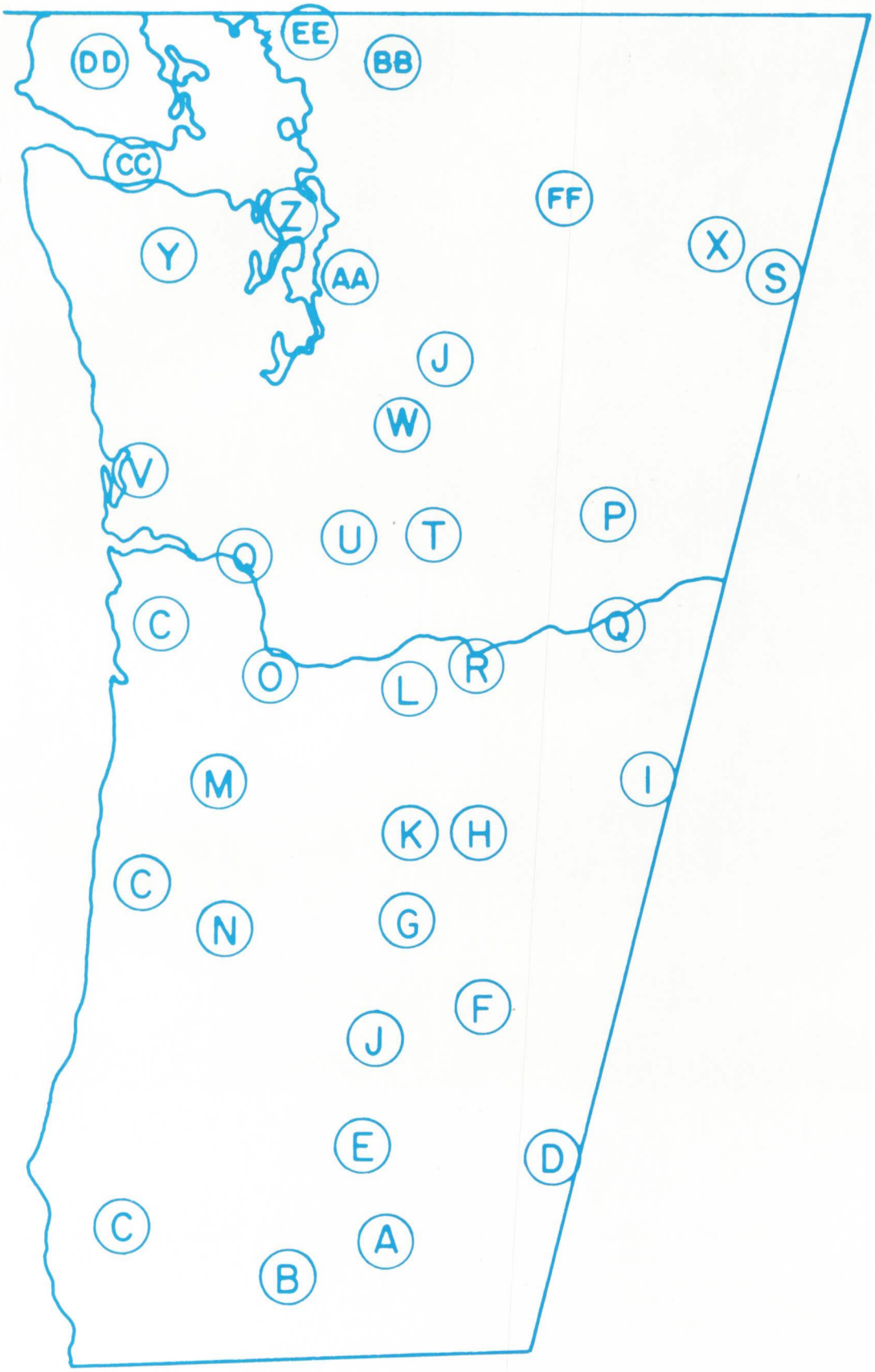
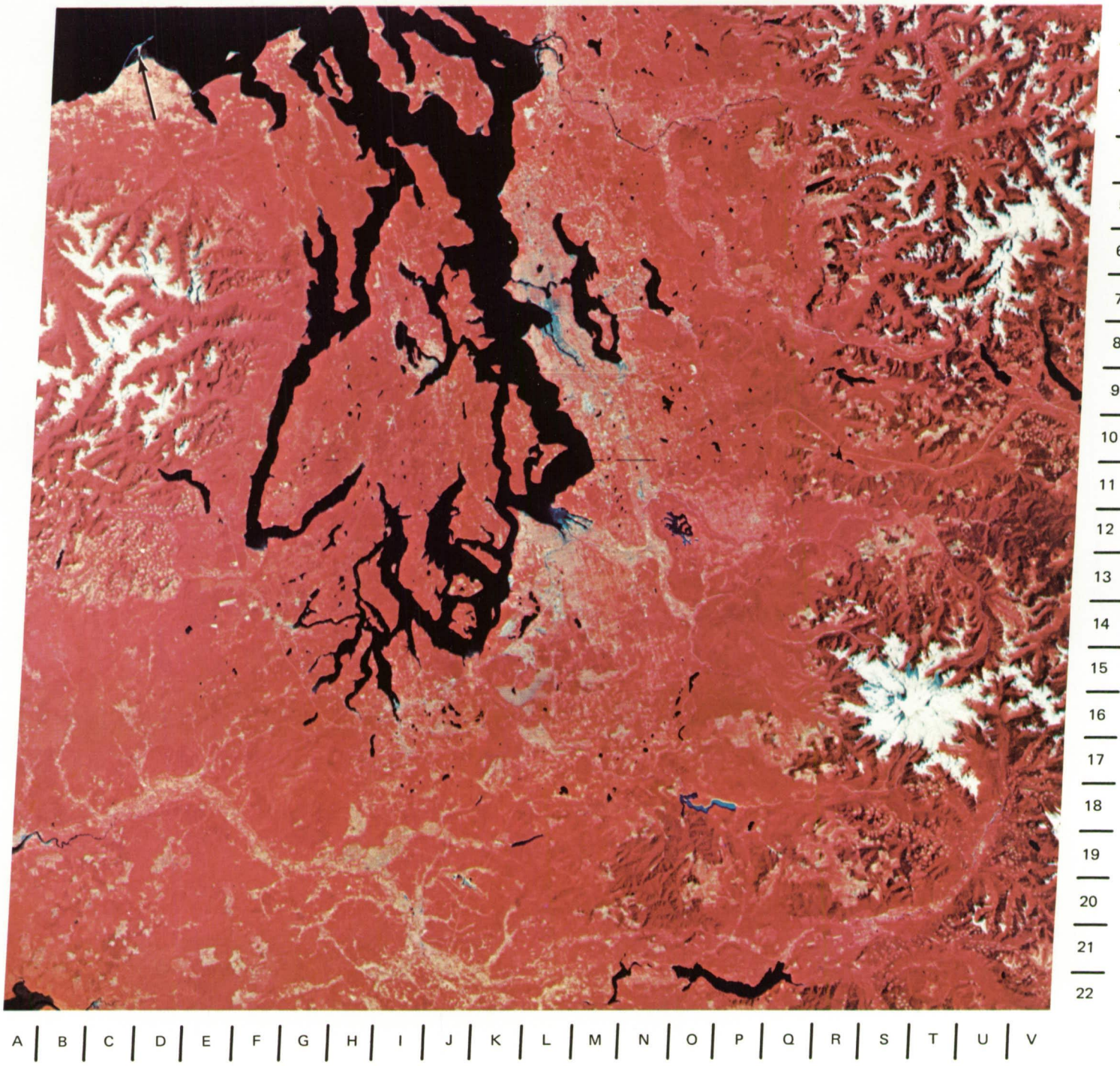


PLATE 106

PLATE 107



NORTHWEST WASHINGTON STATE: The most populated part of the State lies along Puget Sound (*J*–6) and other waterways to the south that open into the Juan de Fuca Straits (*A*–1) between the United States and Canada. Major cities include Seattle (*K*–7) (with Lake Washington (*L*–7) to the east), Takoma (*L*–12), Everett (*K*–2), and the State capital at Olympia (*I*–16). This region occupies a broad valley filled with Eocene continental sediments. Eastward the land rises rapidly into the Cascade Mountains, made up largely of Pliocene and Miocene volcanic rocks. The 4390-meter (14 410-foot) high Mount Rainier (*S*–15), still snow-capped in summer, is one of the most beautiful of the younger (Quaternary) stratovolcanoes in the entire Cascades. North of Snoqualmie Pass (*T*–8), the high country is carved out of older Jurassic intrusives as it is drained by the Skykomish River (*N*–5). West of the Hood Canal (*F*–9), a complex of Eocene igneous and sedimentary rocks make up the scenic Olympic Range (*B*–6) that rises to Mount Olympus (just off the image at *A*–7). Southwestward from the Sound the Coast Range (*B*–15) consists of hills of Eocene and Miocene marine sedimentary rocks that extend to Aberdeen (*A*–18) where the Chehalis River (*F*–18) reaches the Pacific Ocean.

Most of the higher elevations are covered by fir and spruce that have been extensively timbered by clear cutting, forming patchwork patterns (*T*–18) particularly around Mount Rainier and the southern slopes of the Olympic Range (*C*–12). Hemlock forests increase to the west and are found along with cedar in the lower regions along the Sound. Agriculture is limited mainly to hay, and some peas, beans, and corn are grown in the valleys.

Because of the sharp contrasts with the forest cover, many of the major roads and interstate highways stand out in this scene. *1006–18313;* July 29, 1972.

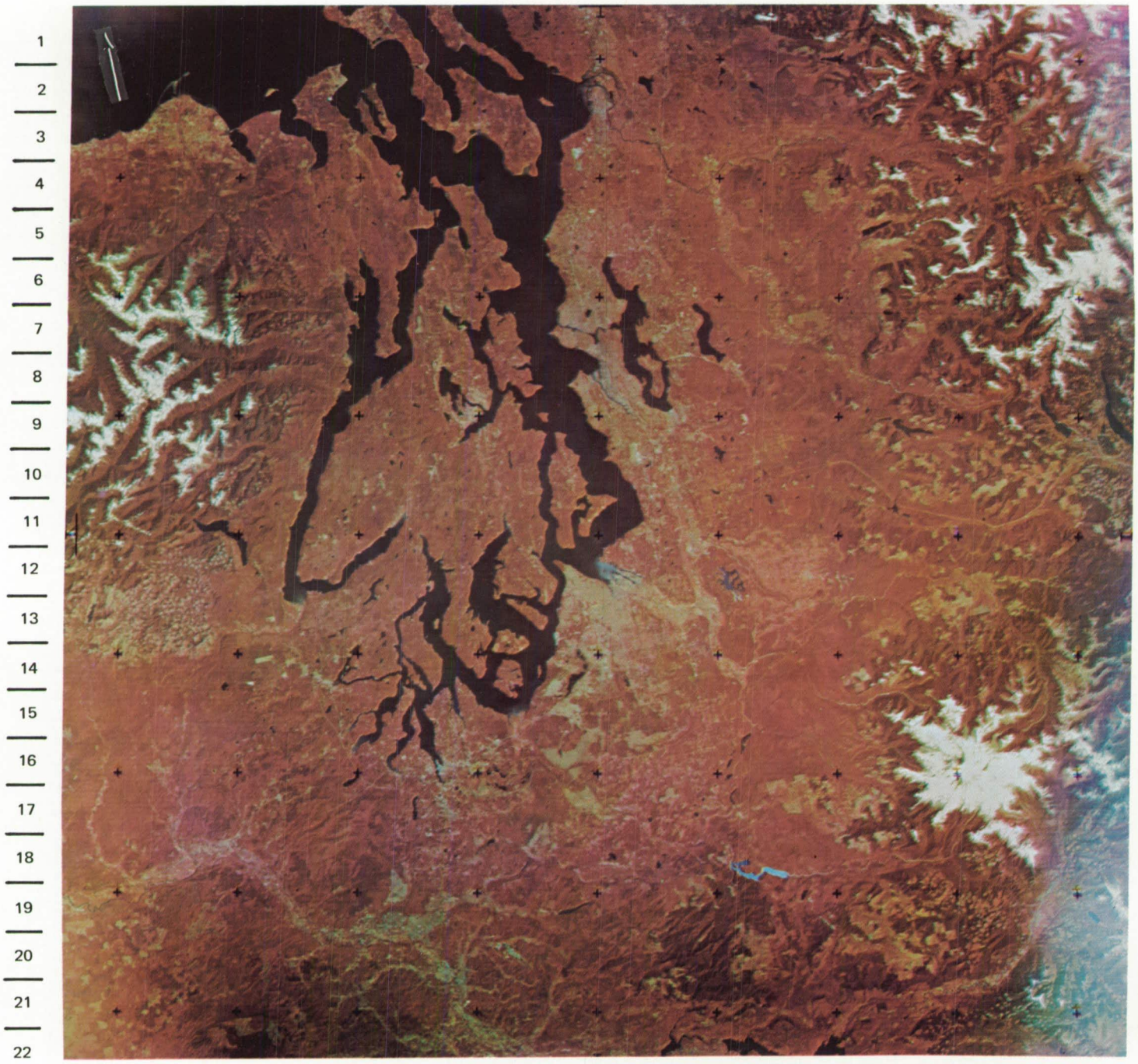
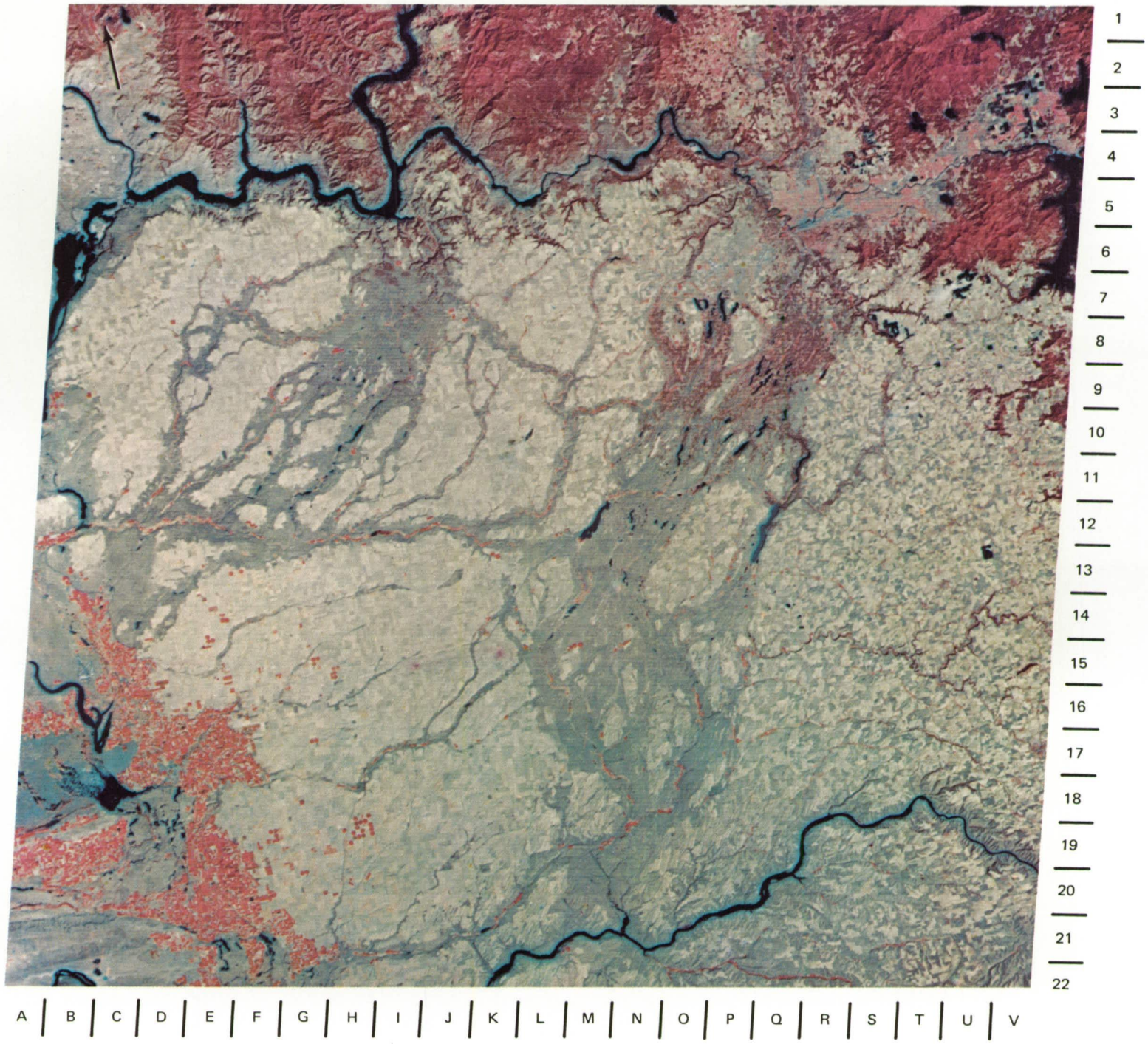


PLATE 108

NORTHWEST WASHINGTON STATE: This is the identical scene as the one appearing on the facing page. In this case, the image is another color composite made from the positive images produced by the three return beam vidicon (RBV) cameras within the same time interval that the multispectral scanner (MSS) was operating over the scene. When the RBV and MSS renditions are compared, the differences in color tones result, for the example shown here, from somewhat different wavelength intervals for the RBV bands, and differences in photoprocessing conditions between the NASA Data Processing Facility RBV version and the General Electric Photographic Laboratory MSS version. The plus signs (+) in the RBV image are reseau marks (used for precise calibration to aid in locating ground points) that were inscribed on the vidicon photocathode plate of each camera. *1006–18313;* July 29, 1972.

PLATE 109



EASTERN WASHINGTON: This portion of the Columbia Plateau, drained by the Columbia (*E*–4) and Snake (*P*–20) Rivers, is underlain by a thick series of Miocene and Pliocene basaltic flows from which rich, dark red soils have been derived. Most of the fields appearing in shades of gray (*R*–12), fallow at this time of year, support extensive winter wheat production. Much of the Palouse River (*R*–14) area is also covered by dissected loess and volcanic ash (*P*–18)—shown here as gashlike markings. The farms around Moses Lake (*B*–16) and Potholes Reservoir (*C*–17) produce sugar beets, potatoes, alfalfa, hay, and peas. Note the red circular fields (*H*–19) that make use of large rotating sprinklers for irrigation.

The city of Spokane (Q–5) lies south of ponderosa pine and Douglas fir-covered mountains including the Kettle River Range (*F*–2), an extension of the Rocky Mountains composed of Jurassic granites (*E*–2) and Silurian sedimentary rocks (*L*–2). Beginning at the Coeur d'Alene Lake (*V*–6) near Coeur d'Alene, Idaho (*V*–4), the Spokane River (*O*–4) flows westward into the Columbia where that river has been backed up by the Grand Coulee Dam (*B*–5) to form the 241-kilometer (150-mile) long Franklin Delano Roosevelt Lake (*H*–2).

The Grand Coulee (*A*–6) contains a dammed equalizing reservoir used to maintain irrigation water supplies for the Columbia Basin reclamation project to the south. This coulee is an abandoned overflow channel from the Columbia River that formed near the end of the Ice Age. It is part of the Channelled Scablands (*G*–9; *L*–10; *M*–14), a strongly dissected terrane consisting of canyons and outliers in basalts overlain by loess. Current opinion holds this incised topography to have formed in just a few weeks as a result of massive flooding. This occurred after a large glacial lake rapidly emptied following failure of a natural "dam" made up of terminal moraines laid down at the edge of a continental glacial ice mass. *1039–18143;* August 31, 1972.

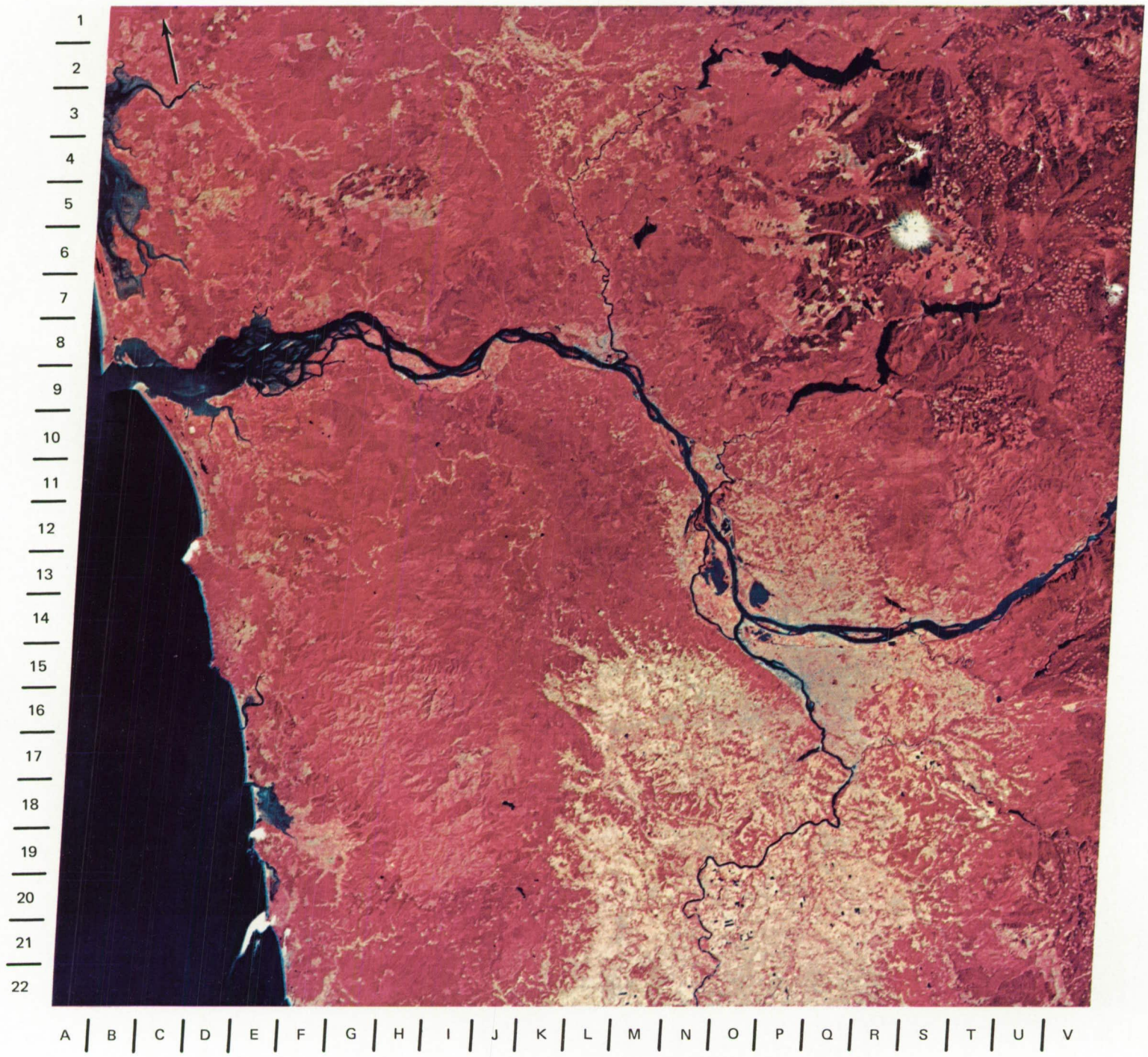


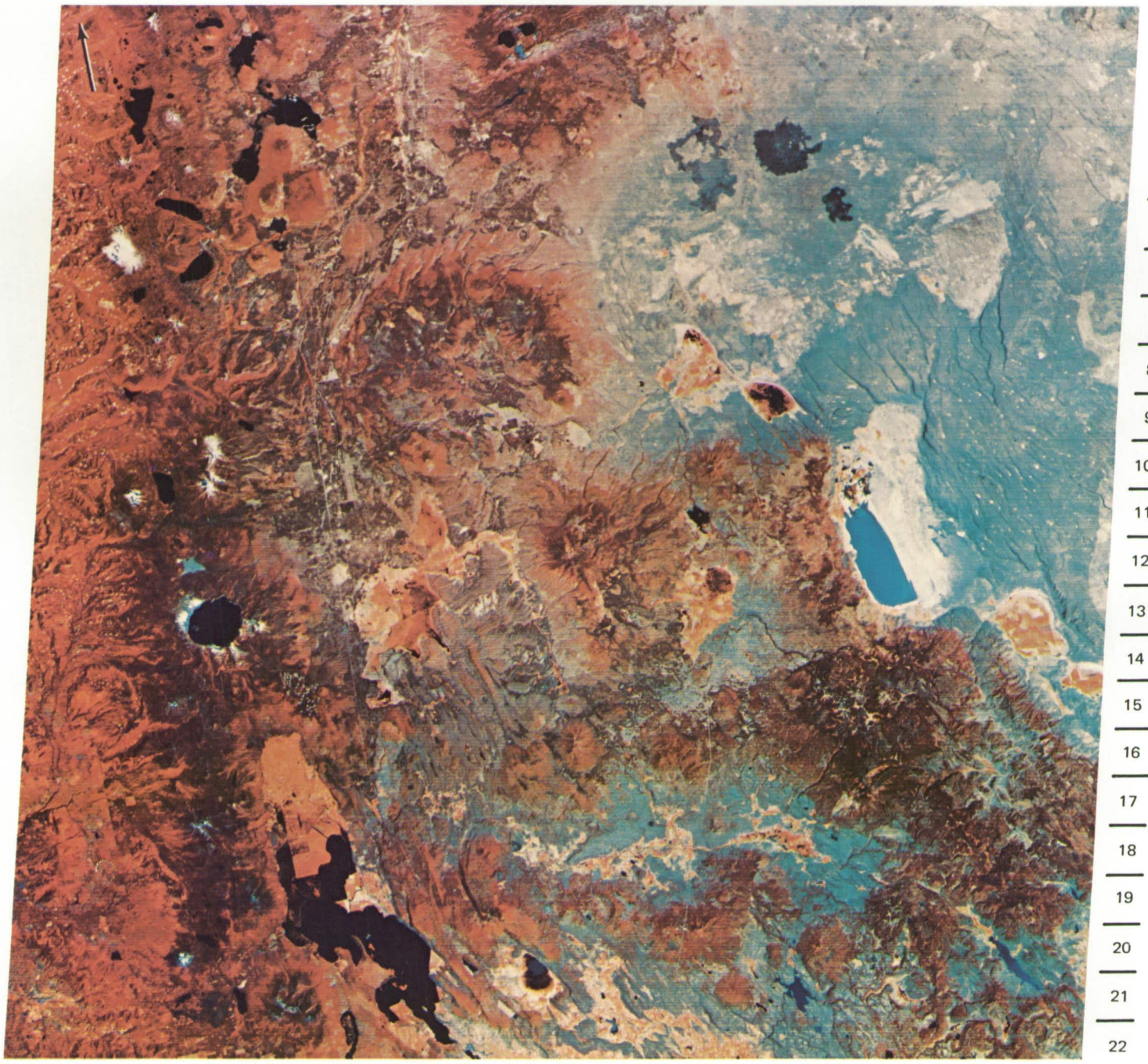
PLATE 110

PORTLAND, OREG.: This city (P–15) of nearly 500 000 people lies on the Columbia River (*K*–8; *S*–14) across from Vancouver, Wash. (*O*–13). Portland is also near the confluence of the Willamette River (*O*–19) at the head of the Willamette Valley (*P*–20). This valley, capping a structural downwarp, was filled in Oligocene times with continental sediments. It now has become one of the great agricultural areas of the northwest, supporting beans, corn, strawberries, winter wheat, oats, barley, hay, alfalfa, and plum, apple, and walnut orchards.

To the east the fir-covered western slopes of the Cascade Mountains rise from the valley toward Mount Hood (just off the image at *V*–17)—a great Quaternary stratovolcano similar to Mount St. Helens (*R*–5) that rises to 2950 meters (9677 feet) in southern Washington. Lake Merwin (*P*–9) and Yale Lake (*R*–8) on the Lewis River (*O*–10) and Mossyrock Lake (*P*–2) on the Cowlitz River (*K*–6) are backwaters from a series of dams.

The Coast Ranges (*I*–14), here made up mostly of Miocene sediments south of the Columbia River plus some Tertiary volcanic rocks to the north, form the forested mountains to the west. These support Douglas fir, hemlock, and, along the coastlands, Sitka Spruce, sporadically timbered for years but now less so than in the clearcut areas (*U*–7) of the Cascades. Narrow beaches (*C*–11; *D*–16) develop along the wavecut coasts. Tillamook Bay (*E*–18) is used as a fishing harbor in Oregon. Willapa Bay (*A*–4), north of Cape Disappointment (*A*–8) at the mouth of the Columbia, has extensive deltaic mud flats (*A*–2; *A*–5; *A*–6) around the mouths of incoming streams. *1006–18315;* July 29, 1972.

PLATE 111



CASCADE RANGE, OREG.: The high Cascades (*D*–8) consist of Tertiary and Quaternary volcanic deposits that include more than 50 well-preserved stratovolcanoes. Among the most famous is the present Crater Lake (*E*–13) formed from the explosive collapse of Mount Mazama less than 10 000 years ago. This scene also includes Mount Thielsen (*D*–10) and Mount McLoughlin (*E*–20), both towering more than 2700 meters (9000 feet) above sea level, and Diamond Peak (*B*–5) at 2665 meters (8744 feet). Part of the Newberry volcanic caldera (*J*–1) with its twin lakes is likewise visible; the blue patch is a recent lava flow and the adjacent white streak is a wind-distributed ash deposit. Most of the Great Sandy Desert country (*U*–3) to the east is covered by Pliocene and Quaternary lava flows and ash. Dark blue patches are recent basalt outpourings at the Devil's Garden (*N*–4), Lava Mountain (*P*–3), and Four Craters (*Q*–5). Faults and erosional gullies (*T*–8) cut these plains and the rolling hills east of Upper Klamath Lake (*G*–19) up to the Klamath Marsh (*H*–13). Volcanic hills, including the Fremont Mountains (*R*–15), extend eastward.

A conspicuous elliptical feature (*J*–6; *K*–8), almost 50 kilometers (30 miles) long bounded by the Walker Rim (*G*–8) on the west, has been recognized for the first time in this Landsat view. Subsequent field studies suggest this feature may be a huge volcanic ring, which is the locus of several small cones and lava flows and is intruded by dikes. If confirmed, this could be one of the most perfectly developed structures of this kind in the world.

Other prominent landmarks are Summer Lake (*R*–12), which undergoes considerable enlargement in the wet season; Wickiup Reservoir (*F*–3); Silver Lake (*P*–8); Fossil Lake (*T*–6), now dry; Paulina Marsh (*N*–8); and the Sprague River (*M*–18). The two linear rights of way (*G*–9) running north from Klamath Falls (*J*–22) are a highway and railroad bed, while the white line to the east (*O*–16) is a power line.

The highest part of the Cascades supports lodgepole pine, with ponderosa pine along the eastern slopes. The western slopes are covered with Douglas fir now being extensively clearcut (light red patches). Agricultural products in the valleys (*M*–21; *P*–18) include barley, sorghum, hay, alfalfa, and potatoes. *1004–18212;* July 27, 1972.

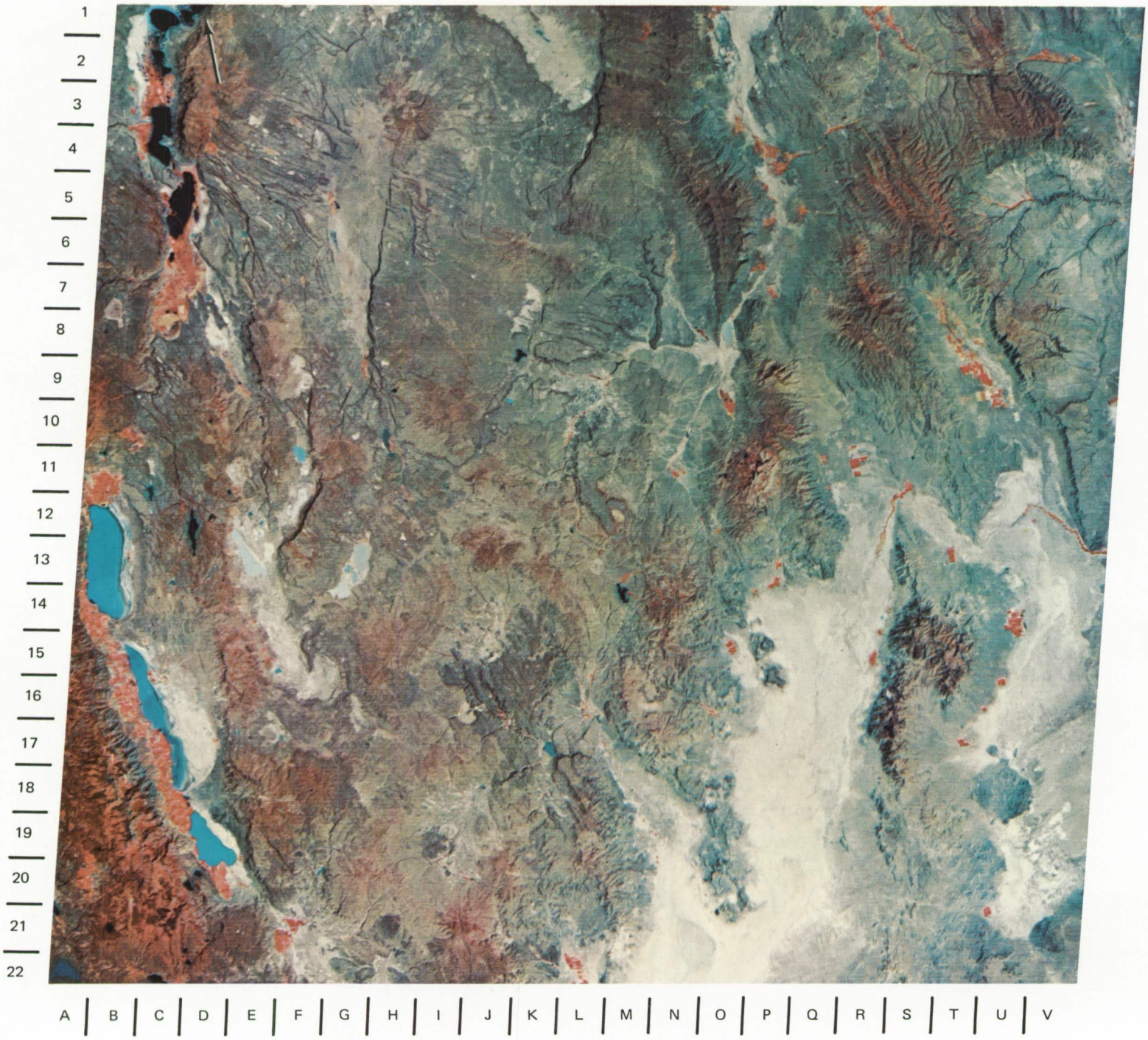


PLATE 112

BASIN AND RANGE COUNTRY, OREGON AND NEVADA: The Basin and Range or Great Basin physiographic province extends over parts of seven western States. The ranges consist of elongated blocks of crystalline, sedimentary, and volcanic rocks that trend generally north to south. These are bounded by high-angle faults along which intervening blocks of crust have downdropped to form basins now largely filled with Quaternary alluvial sediments derived from erosion of the ranges. A widely held view today considers this province to have developed by flexure of the crust as the continental part of the North American plate passed over hot spots in the East Pacific Rise during westward drift; the arching of this crust produced tensional fractures along which uplifts and downdrops occurred.

The northwestern end of the Basin and Range province spills over from Nevada, which lies entirely within it, into northeastern California east of the southern Cascades and into southern Oregon. These States meet Nevada at *B*–8. The southern limit of the Columbia Plateau province ends just north of this scene. Most of the surface here is underlain by Pliocene and Quaternary volcanic rocks, part of a vast outpouring that covers the southeastern third of Oregon in the Owyhee volcanic province. These volcanic rocks have since been involved in younger faulting that produced structural grabens now expressed as valleys. One such graben makes up Surprise Valley (*C*–15) in California, with its Upper, Middle, and Lower Alkali Lakes and its farmlands producing hay, barley, and potatoes, next to the conifer-covered Warner Mountains (*B*–19). Other grabens underlie the Warner Valley Lakes (*B*–3), Guano Valley (*F*–5), Catlow Valley (*J*–3), and Alford Valley (*N*–2) in Oregon. The Pine Forest Range (*O*–11) consists of Jurassic intrusive rocks but the Pueblo Mountains (*N*–5) and the Jackson Mountains (*S*–15) between the north ends of the Black Rock Desert (*P*–17) and Kings River Valley (*V*–16) are composed of young volcanic rocks.

This region, largely a sagebrush steppe with junipers at higher elevations, supports mainly ranching and some mining. Interest has recently centered on a series of shallow subsurface "hot spots" (including *D*–12, *L*–19, *N*–7, and *Q*–11) as potential sources of geothermal energy. *1380–18102;* August 7, 1973.

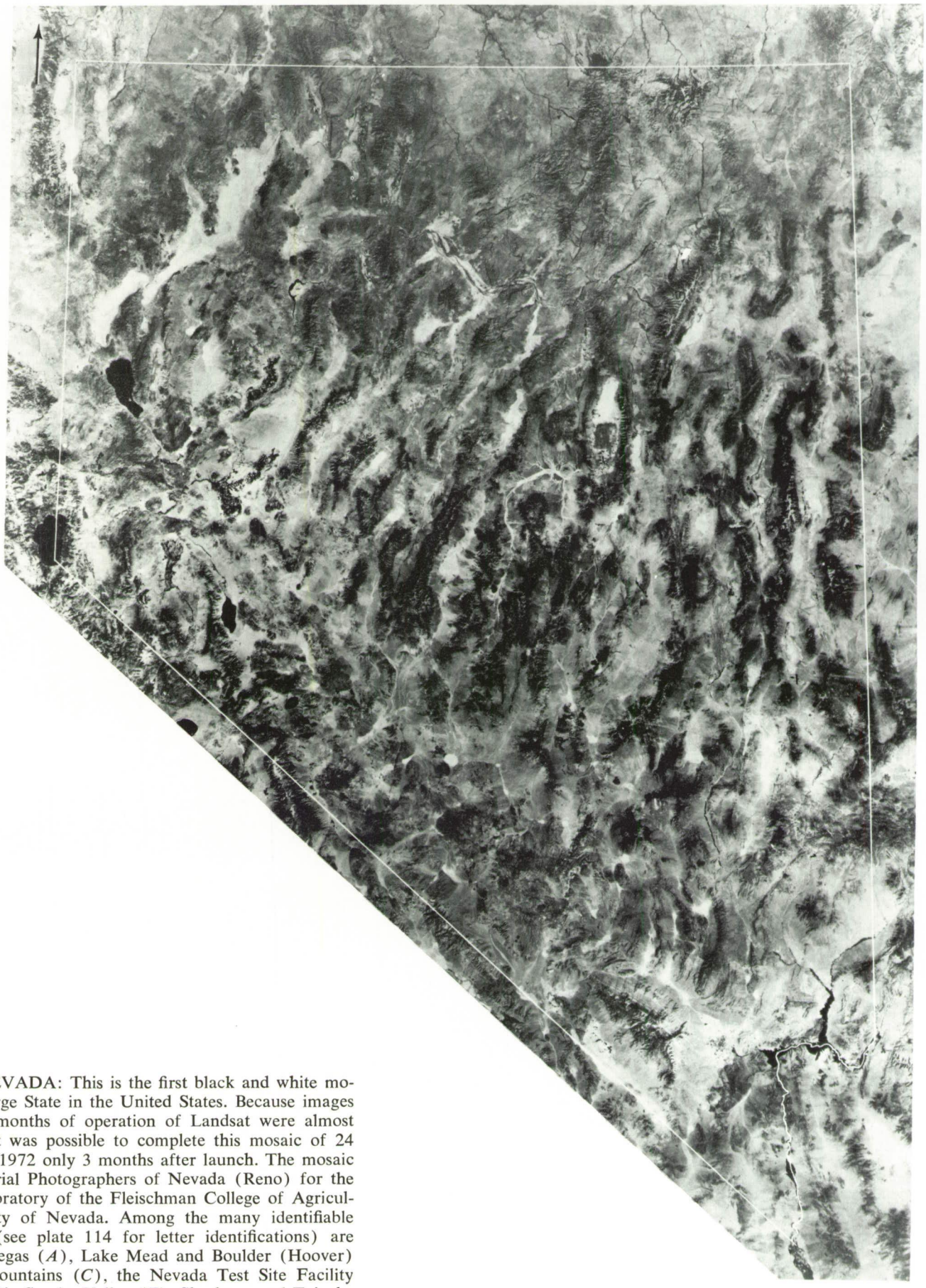


PLATE 113

THE STATE OF NEVADA: This is the first black and white mosaic prepared of a large State in the United States. Because images taken in the first 2 months of operation of Landsat were almost entirely cloud free, it was possible to complete this mosaic of 24 images in September 1972 only 3 months after launch. The mosaic was produced by Aerial Photographers of Nevada (Reno) for the Remote Sensing Laboratory of the Fleischman College of Agriculture of the University of Nevada. Among the many identifiable features of interest (see plate 114 for letter identifications) are the following: Las Vegas (*A*), Lake Mead and Boulder (Hoover) Dam (*B*), Spring Mountains (*C*), the Nevada Test Site Facility (*D*), Tonopah (*E*), Big Smoky Valley (*F*), Shoshone and Toiyabe Ranges (*G*), Wheeler Peak (*H*), Walker Lake (*I*), Lake Tahoe (*J*), Reno (*K*), Carson Sink (*L*), Black Rock Desert (*M*), Pyramid Lake (*N*), Humboldt River (*O*), Stillwater and East Ranges (*P*), and Ruby Mountains (*Q*). Nevada is the classic area of the Basin and Range province of the western United States; almost all the mountains are blocks of Paleozoic and Mesozoic rocks uplifted along steep-angled normal faults. Much of the southern and western parts of the State are now covered by Tertiary volcanic rocks, ashfall deposits coming from volcanoes and calderas such as Timber Mountain (*R*) and flows of mostly basaltic rocks. The basins are downdropped blocks that have been filling up with alluvial materials washed in from the eroding mountains.

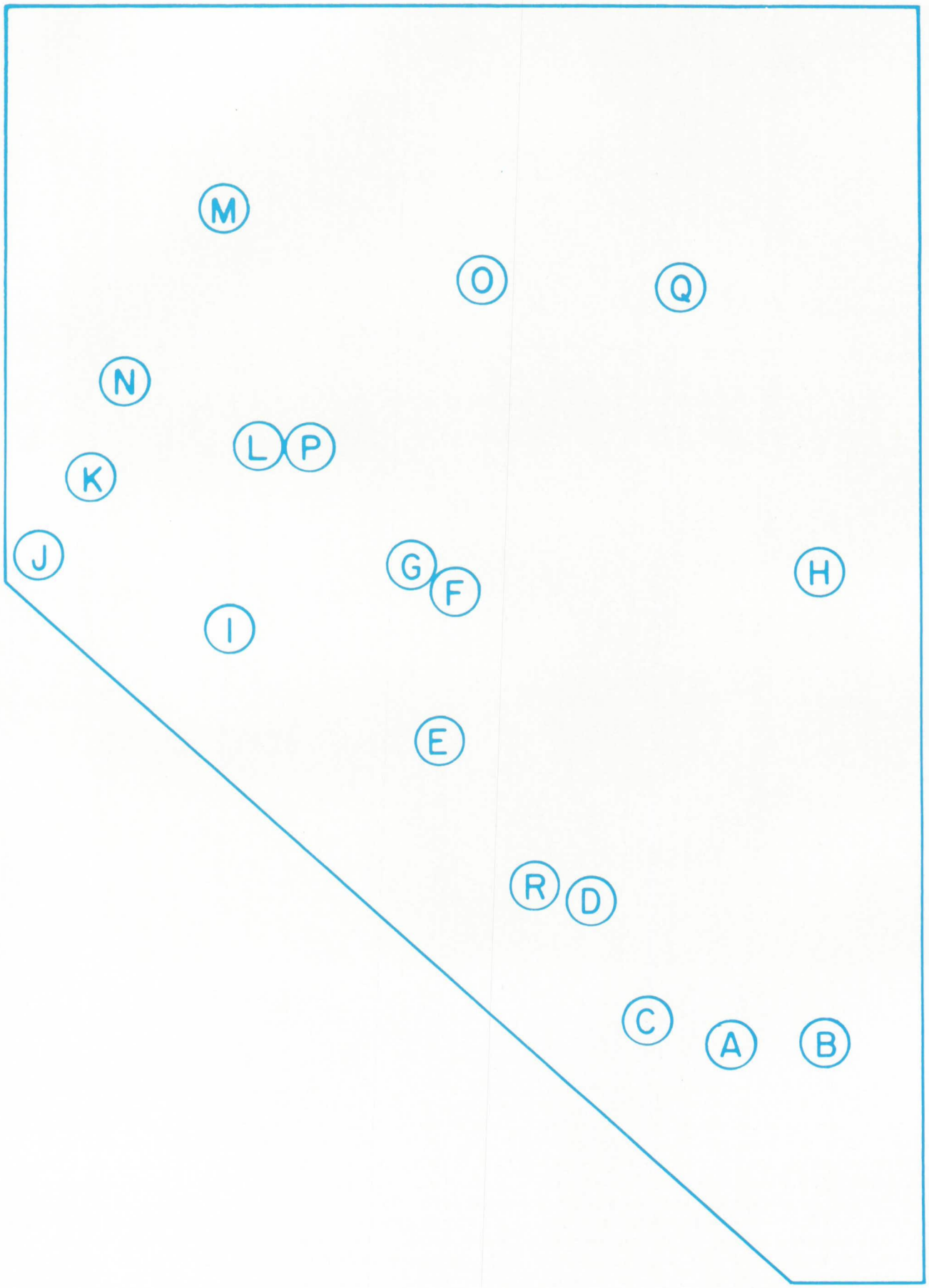
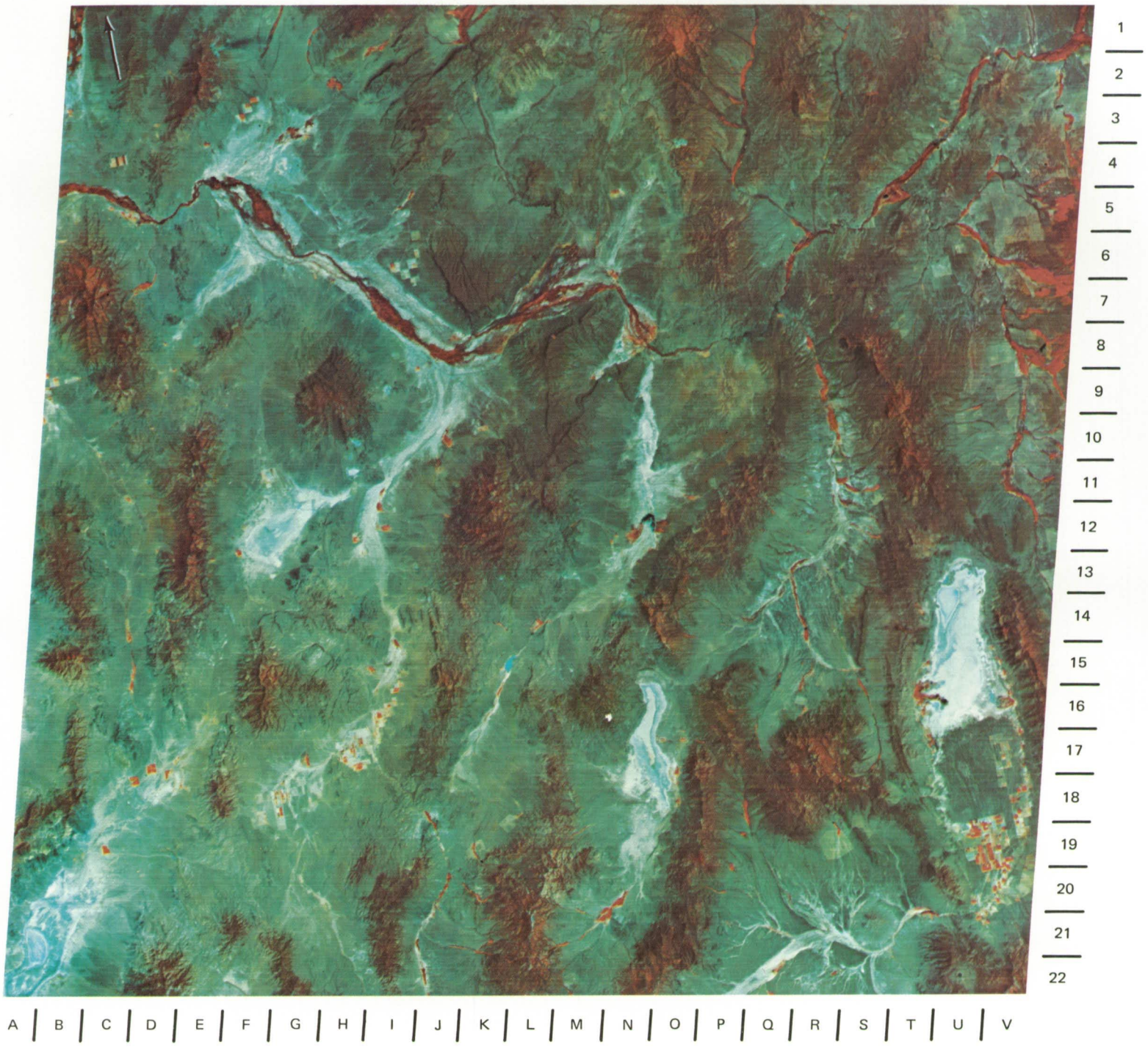


PLATE 114

PLATE 115



ELKO, NEV.: This image of Great Basin country in central Nevada is reminiscent of a remark by Major C. E. Dutton, an early explorer of the American West, who described the mountains appearing on a hachure map of the Basin and Range province as resembling an "army of caterpillars crawling northward out of Mexico." Such characteristic topography is the result of a complex structural history dominated by block faulting. The isolated, subparallel ranges rise abruptly 1000 to 1500 meters (3000 to 5000 feet) above the basin floors. Mount Callaghan (*L*–20) and Roberts Creek Mountain (*R*–17) are slightly over 3000 meters (10 000 feet) in elevation. In this arid region only the higher slopes are wooded, and the infrequent but torrential rains produce sudden, powerful sheetflooding on the bare lower slopes. Great quantities of rock debris are moved downslope, filling the intermontane basins. A good example of the pediments thus formed is seen around Battle Mountain (*G*–9). Internal drainage is the rule in this scene, with many of the closed basins such as Diamond (*T*–15), Grass (*N*–17), Buffalo (*F*–12), and Dixie (*A*–21) Valleys occupied by dry salt flats. Even the Humboldt River (*I*–8), whose extensive valley and headwaters are marked by red patches of irrigated farmland, drains westward to a sink.

The rocks exposed in the mountains, mostly Paleozoic and Mesozoic carbonates and Cenozoic volcanics, are host rocks for many gold and silver mines, including discernible workings at the Getchell (*D*–1), Copper Canyon (*G*–10), and Carlin (*N*–4) mines. Towns in this area, located on U.S. 40-Interstate 80 along the Humboldt River, are Elko (*T*–3), Carlin (*Q*–6), Battle Mountain (*I*–8), and Golconda (*C*–5). *1342–17594;* June 30, 1973.

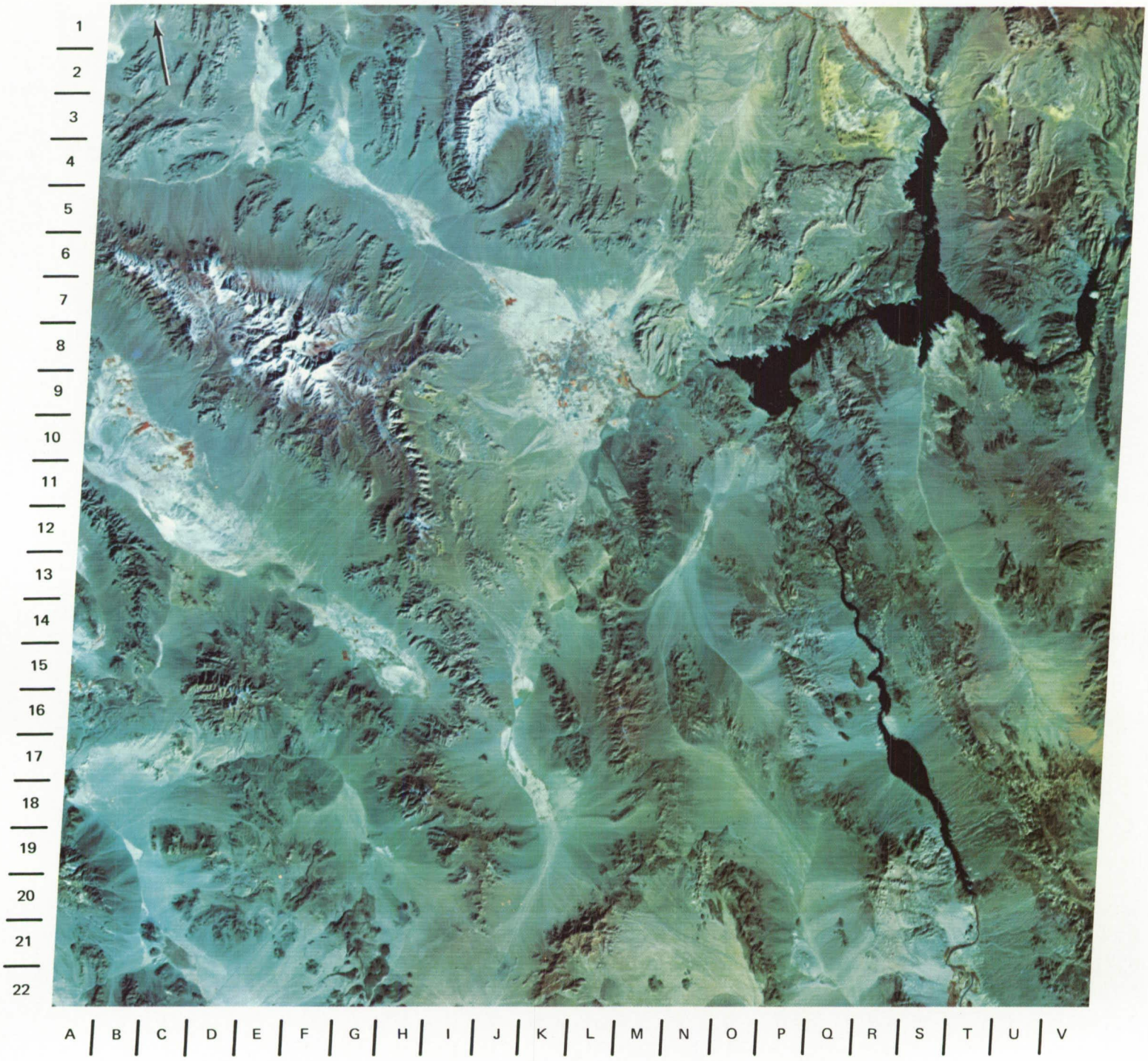


PLATE 116

LAS VEGAS, NEV.: The Basin and Range topography represented here extends from Sonora, Mexico, into southern Oregon. The landscape consists of a series of short, steep-sided, isolated ranges, generally rising to elevations of 1000 to 1500 meters (3000 to 5000 feet), although some reach altitudes of more than 3000 meters (10 000 feet). Individual ranges are usually surrounded by aprons of weathered debris and separated from neighboring ranges by alluvium-filled basins. Most of these ranges are intricately faulted and folded. An example of structural control can be seen in the folded ridges in the southern end of the Las Vegas Range (*J*–5).

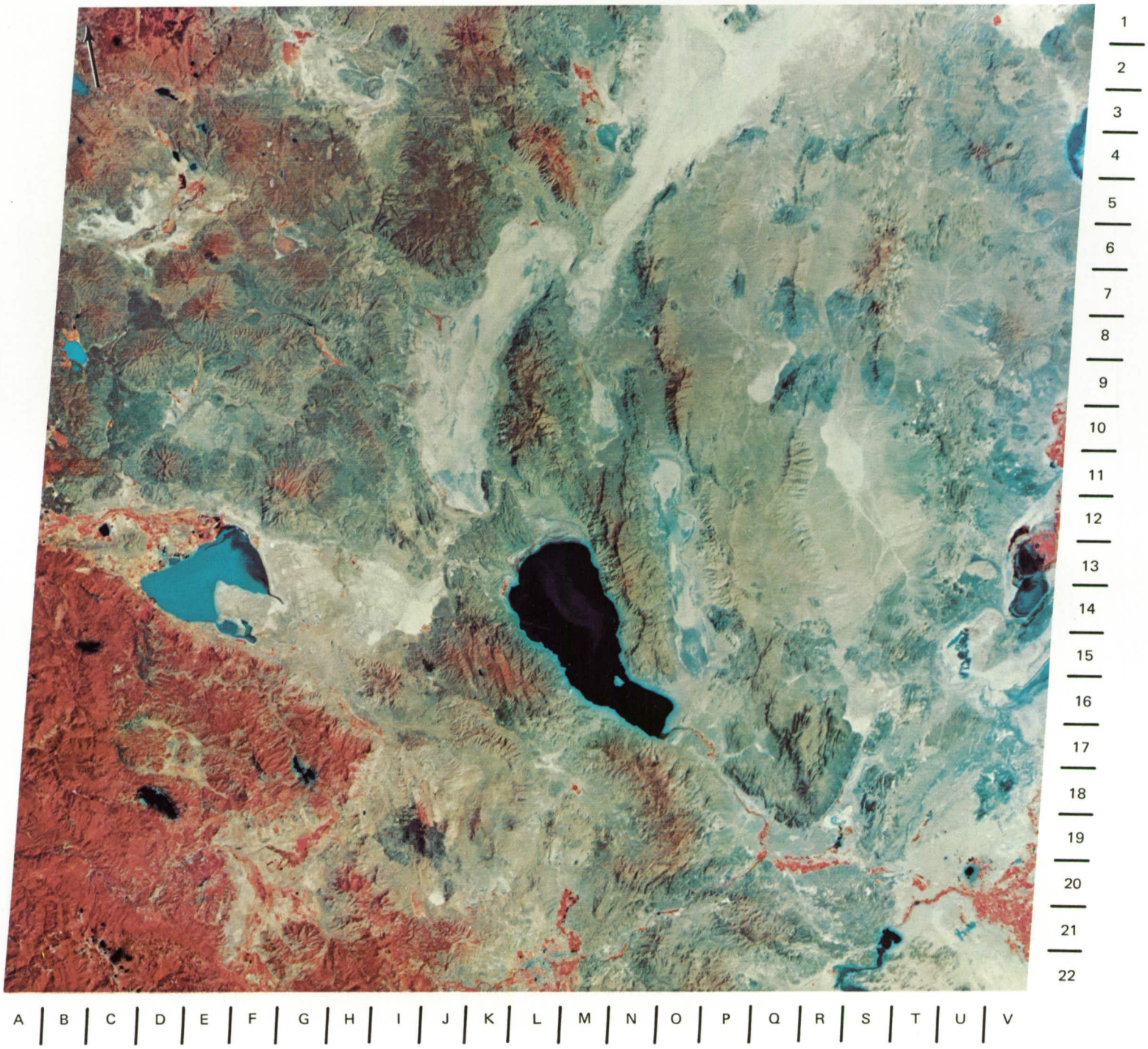
Due to the arid climate, the basins usually contain playa or saline lakes, and consequently have a highly reflective white signature in false color infrared. Las Vegas (Spanish for "the plains") is situated in such a basin (*K*–8). The downtown casino area (more intense blue area) and "the strip" area radiating to the southwest are visible. The red areas are golf courses. The 3000-meter (10 000-foot) runway at McCarran Airport (*K*–9) is visible along the southern boundary of Las Vegas.

Two of the higher mountain areas in this late November image are snow covered. The Spring Mountains with nearly 3700-meter (12 000-foot) high Charleston Peak (*E*–8) are the site of a national forest and a winter resort area. Sheep Peak in the snow-covered Sheep Range to the northeast rises to almost 3000 meters (10 000 feet) (*I*–2).

The 885-kilometer (550-mile) shoreline of Lake Mead (*R*–7), contained by Hoover Dam in the Black Canyon (*P*–9) of the Colorado River, stretches sinuously along the former course of the Colorado through Boulder Canyon (*Q*–7) into the Overton Arm (*R*–4), where the Virgin River empties into Lake Mead, and eastward through the Virgin Canyon (*U*–8) on to the easternmost portion of the lake. The Colorado River flows southward out of Black Canyon into Lake Mojave (*R*–17) created by Davis Dam (*T*–19) located a few kilometers (miles) north of the Fort Mojave Indian Reservation and Needles, Calif. (*T*–21).

Agricultural pursuits are limited to areas where water is available from springs, deep wells in valley alluvium, or perennial streams. Evidence of land being used for agricultural purposes appears in Pahrump Valley (*C*–10), the Virgin River Valley (*R*–1), and in the area centered around the town of Overton (*Q*–2). *1124–17495;* November 24, 1972.

PLATE 117



RENO, NEV.: This famed town (*L*–21) stands at the eastern edge of the Sierra Nevada (*C*–19) as a gateway to the Basin and Range physiographic province (right half of image). Individual block fault mountains visible here include the Lake Range (*M*–11) next to Pyramid Lake (*L*–13), the Nightingale Mountains (*N*–19) just to the east, the Granite Range (*K*–4), Pah-rum Peak (*K*–9), the Truckee Mountains (*Q*–17), and the Virginia Mountains (*J*–14; *P*–21). These ranges are variously composed of Jurassic intrusive rocks and Tertiary to Quaternary volcanic rocks. Many of the intervening valleys contain large playas, such as occupy the Smoke Creek Desert (*H*–9) and Black Rock Desert (*N*–2) and Winnemucca Dry Salt Lake (*N*–14). Several low areas, like the Carson Sink (*V*–15) and the Humboldt Sink (*V*–14), now enclose lakes bordered by tule marshes. The nearby Carson River has been dammed to form the Lahontan Reservoir (*S*–21)—one of the first such Government projects in the United States; the Rye Patch Reservoir (*V*–4) lies along the Humboldt River.

Tertiary volcanic rocks make up the segment of the Sierras shown here, as the Diamond Mountains (*C*–15). Forest cover consists mainly of silver, red, and Douglas fir and some pine. To the north, the shallow Honey Lake (*D*–12) in California has formed in a depression filled with Quaternary sediments. The upper left quadrant of the image shows a topography of furrowed low hills and symmetric cones (e.g., Schaffer Peak (*C*–10)) carved out of Pliocene and Quaternary volcanic ash and flow rocks. McDonald Peak (*B*–1), at the south end of the Warner Range, rises to 2417 meters (7931 feet).

The first Landsat image of the Reno area revealed a hitherto unknown circular structure (centered on *J*–18) about 32 kilometers (20 miles) in diameter formed by the arcuate end of the forested Sierras on the west and low hills on the north and east. This feature, once noticed, could be seen even in very small-scale photos of the western United States taken from Apollo Moon-bound spacecraft more than 32 000 kilometers (20 000 miles) from Earth. Field inspection ruled out an impact origin for the feature; no satisfactory explanation has since been proposed but a volcanic ring structure is suspected. *1380–18104;* August 7, 1973.

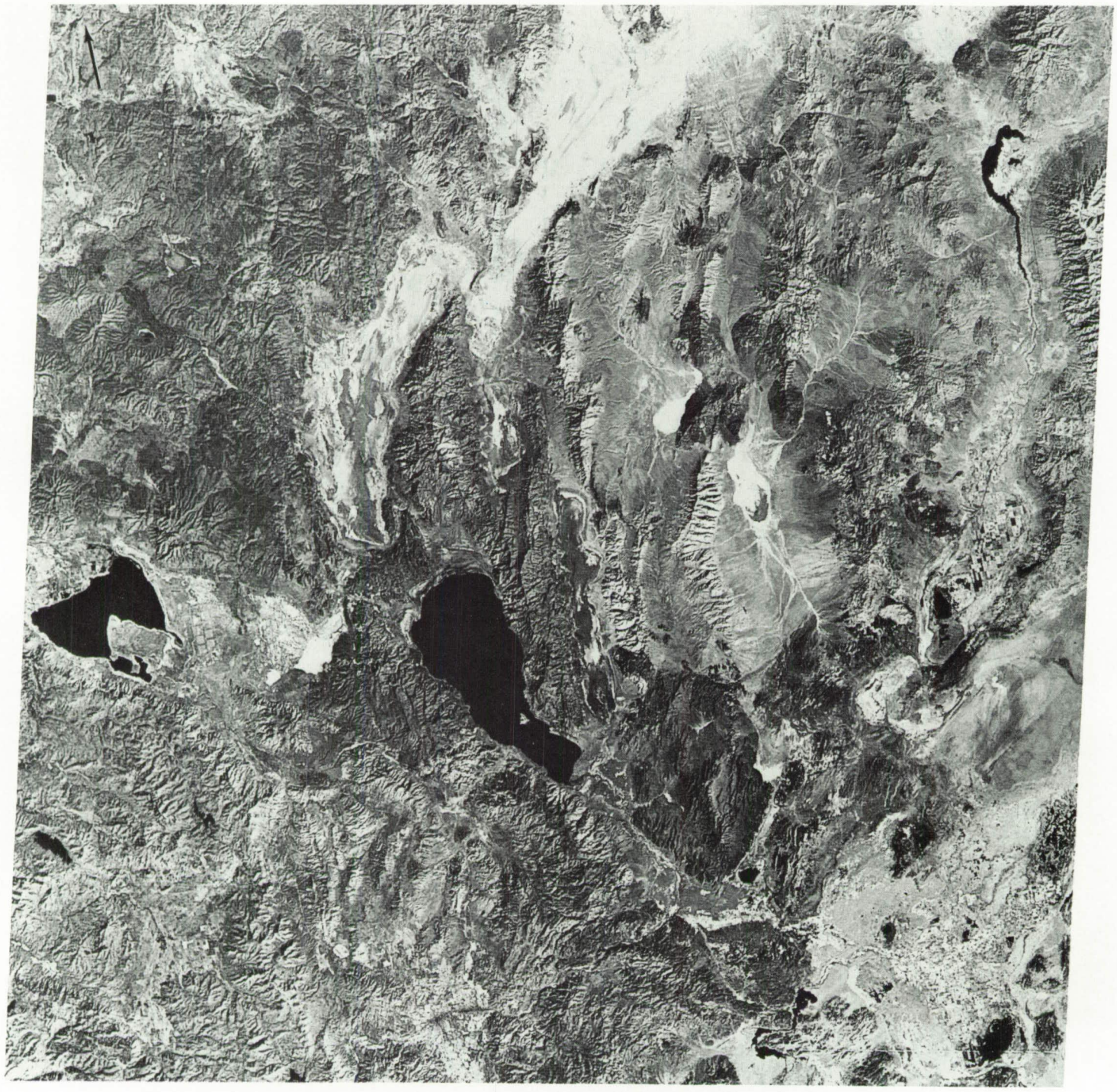
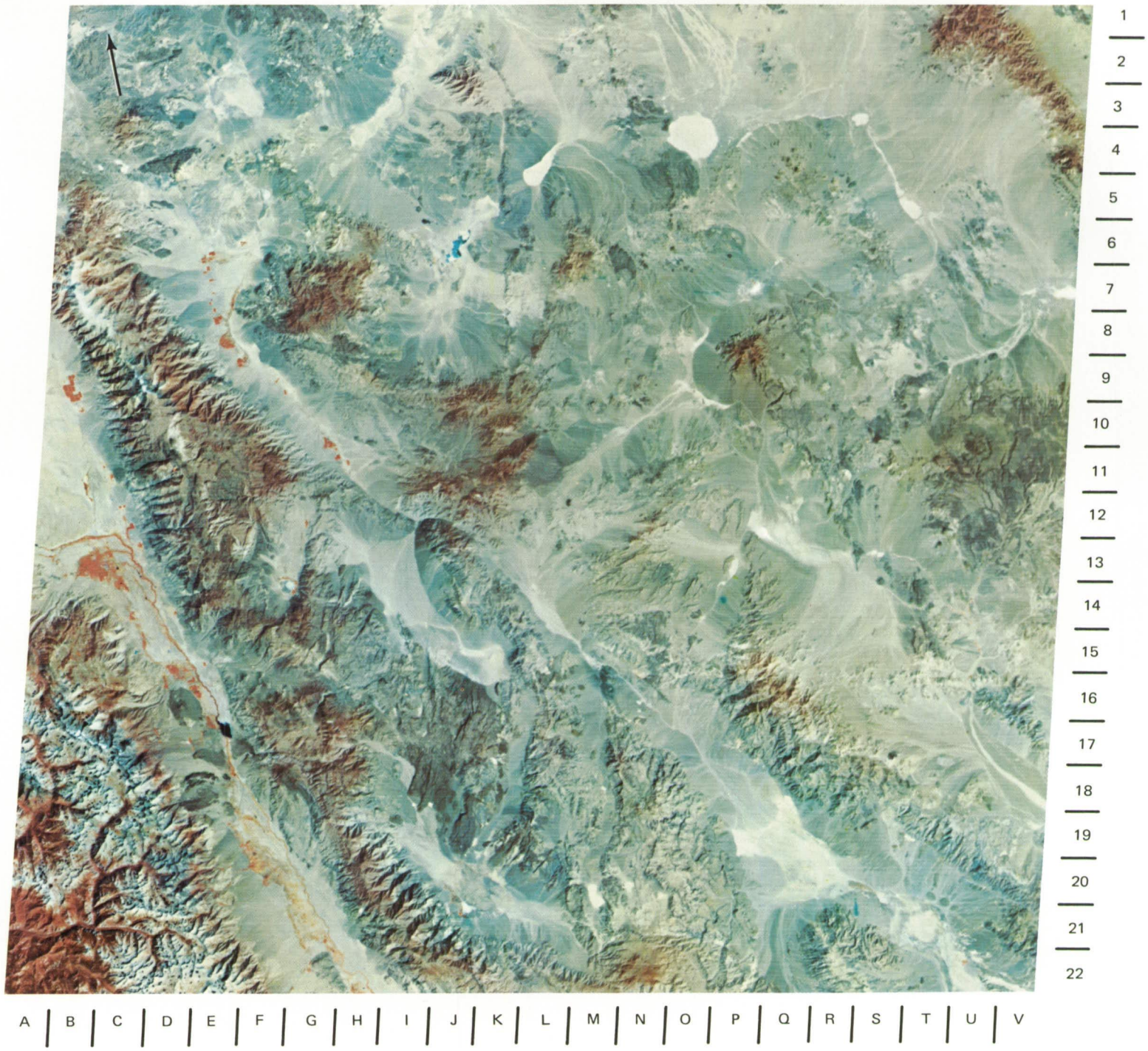


PLATE 118

RENO, NEV.: This scene is a computer-reprocessed version of most of the same area shown in color on the opposite page. In this example, IR band 7 has been subjected to a contrast-stretching operation developed at the U.S. Geological Survey's Remote Sensing Laboratory in Flagstaff, Ariz. The resulting effect is to increase the range of gray tones. Initially dark tones are made even darker and some light tones become lighter. This enhancement tends to produce a pseudo-relief aspect to mountainous terrain, in much the same way as airbrush shading produces a "3–D" effect on a contour map. A similar effect is introduced by low Sun angle illumination of a scene in which the lengthening of shadows helps the mind's eye to see rugged relief in this manner. *Courtesy of L. Soderblom, U.S. Geological Survey. 1380–18104;* August 7, 1973.

PLATE 119



OWENS VALLEY, EASTERN CALIFORNIA: This scene is split by the California-Nevada State line (*D*–8; *Q*–16) as it runs almost due northwest. The eastern front of the Sierra Nevadas (*B*–18) here includes part of the Kings Canyon National Park (*A*–18). The Owens River (*E*–17), a segment of the Los Angeles aqueduct system, occupies a fault valley bounded on the east by two high ranges. The White Mountains (*C*–10) consist of metamorphic and granitic rocks of Jurassic age on their northeast flank (*C*–7) and Ordovician and Silurian sedimentary rocks toward the south (*F*–14). These lower Paleozoic units continue southward into the Inyo Range (*G*–17). The intervening Owens Valley, with the town of Bishop (*B*–13) near its north end, offers some of America's most spectacular scenery resulting from relief westward of up to 3000 meters (10 000 feet) to the lofty Sierras and 1500 to 2100 meters (5000 to 7000 feet) to the eastern ranges. Mount Whitney, the highest peak in the continental United States at 4418 meters (14 494 feet), lies at *D*–20. Behind the Inyo Mountain Range is Saline Valley (*H*–13) and the northern end of the Panamint Range (*N*–18). Between that range and the Amargosa Range (*Q*–15) is the northern end of Death Valley (*P*–18), which to the south drops to an elevation of −86 meters (−282 feet) to rank as the lowest point in the United States. Isolated mountain ranges inside Nevada, such as the Silver Peak Mountains (*J*–9) and the Cactus Range (*O*–8), are a composite of Paleozoic sedimentary rocks and/or Tertiary to Quaternary volcanic rocks. Volcanic rocks and underlying intrusive rocks are the sources of sulfide mineralization in the gold and silver ore deposits around Goldfield (*M*–6). Mud Lake (*N*–3) is a large playa north of Goldfield. *1054–18001;* September 15, 1972.



PLATE 120

GOLDFIELD, NEV.: The image above is a ratio color composite produced in the way described for plate 88. In this version, multispectral scanner ratios 4/5, 5/6, and 6/7 were projected onto blue-, yellow-, and magenta-toned diazo transparencies, respectively.

The area thus enhanced lies within the points *L*–1, *V*–1, *L*–13, and *V*–13 shown in Landsat frame 1054–18001 on the opposite page; the frame chosen for this ratio composite was 1072–18001, which includes slightly different limits.

In this rendition, orange hues represent vegetation and blue hues denote playas. Clouds are pinkish-brown and their shadows white. Volcanic flow rocks of basaltic to andesitic composition appear in dull white tones (arrow at *A*) and intrusive or extrusive igneous rocks with higher silica content appear as brownish-pink tones (*B*). Rocks altered to, or stained by, iron compounds appear in shades of green (*C*) to dark green (*D*). Areas marked by brown (*E*) to red-brown (*F*) colors correspond to rocks altered to iron-poor compounds.

The Goldfield mining district, a source of gold and silver ores, occurs within the green anomaly at the left arrow *C*. Other areas of current or once active mining are associated with some of the green and brown tones brought out in this ratio color composite. By processing Landsat data in this way, enhancement of alteration zones related to surface oxidation and hydration of certain minerals found in ore deposits can be achieved. This technique, especially when combined with definition of ore-localizing fractures in the Landsat imagery, offers promise as a new exploration tool.

PLATE 121

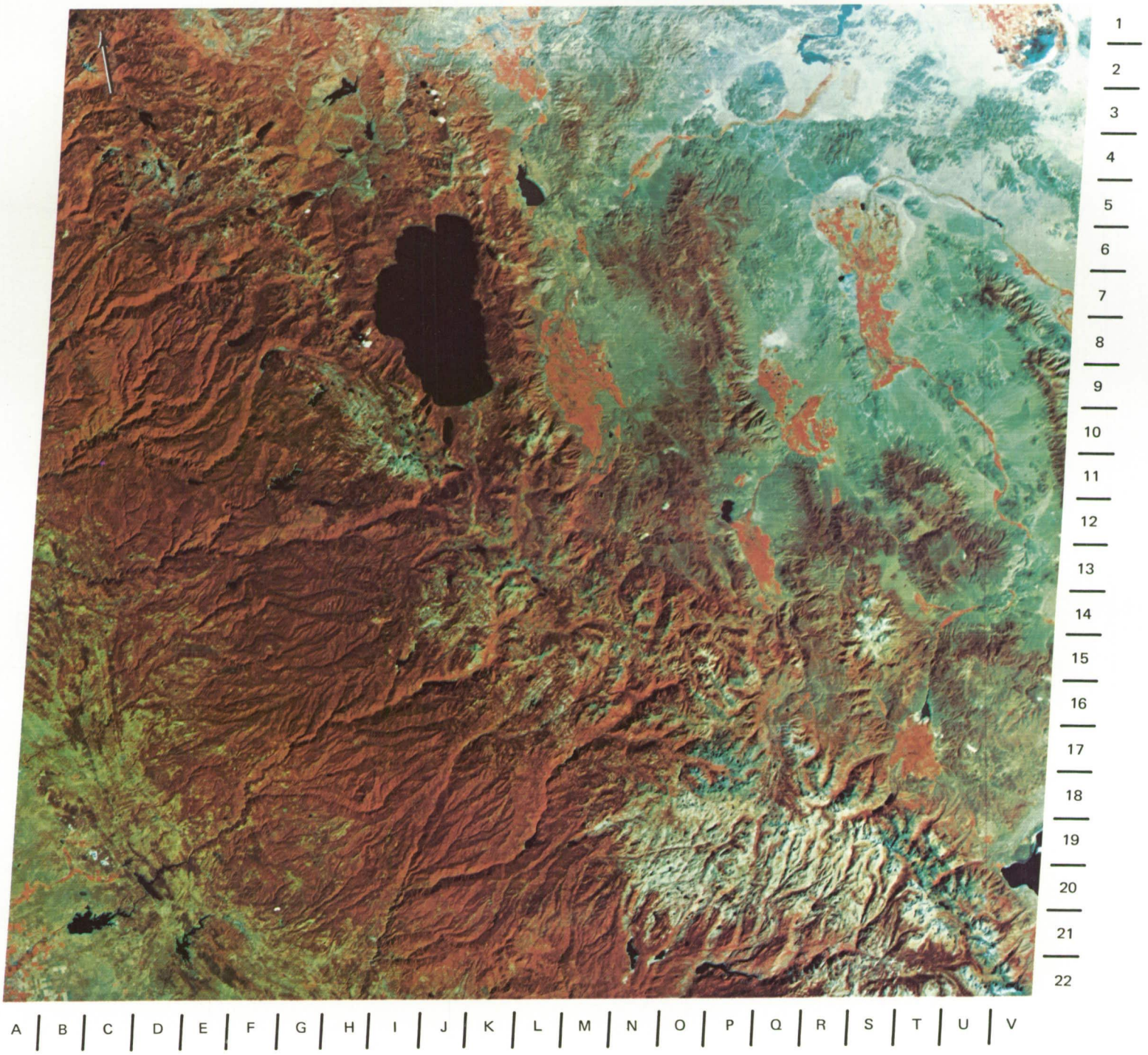


THE STATE OF CALIFORNIA: This color mosaic uses 42 Landsat images to depict the entire State of California—extending in length for more than 1100 kilometers (700 miles) from the Mexican border on the south to the Oregon State line on the north. Among many points of interest (see plate 122 for letter identifications), from south to north, are the Salton Sea and Imperial Valley (*A*), San Diego (*B*), the Peninsular Ranges (*C*), Los Angeles area (*D*), the Channel Islands (*E*), the Transverse Ranges (*F*), the Mojave salient (*G*) bounded by the San Andreas (*H*) and Garlock (*I*) faults, the eastern Mojave Desert (*J*), the Colorado River farmlands (*K*), Death Valley (*L*), the Santa Ynez Mountains and Santa Barbara (*M*), Mount Whitney (*N*), and the southern Sierra Nevada (*O*), the San Joaquin Valley (*P*), Bakersfield (*Q*), the southern Coast Ranges (*R*), the extension of the San Andreas fault (*S*), Monterey Bay (*T*), Yosemite National Park (*U*), Owens Valley (*V*), Mono Lake (*W*), the San Francisco Bay area (*X*), Sacramento (*Y*) and the Sacramento Valley (*Z*), the Marysville (Sutter) Buttes (*AA*), Lake Tahoe (*BB*), the northern Coast Ranges (*CC*), Cape Mendocino (*DD*), the Trinity Alps (*EE*), Mount Shasta (*FF*), Mount Lassen (*GG*), Modoc lava fields (*HH*), and Honey Lake (*II*). Parts of adjacent Nevada are also included in this mosaic, with these major landmarks: Las Vegas (*JJ*), Lake Mead and Hoover Dam (*KK*), Walker Lake (*LL*), Reno (*MM*), and Pyramid Lake (*NN*).


HH
FF
EE
DD
GG
II
NN
Z
MM
CC
AA
BB
Y
LL
X
Z
U
W
T
O
V
S
P
N
L
R
S
JJ
KK
Q
I
G
M
F
H
J
E
D
K
E
C
A
B

PLATE 122

PLATE 123



LAKE TAHOE, CALIF.: The Sierra Nevada was for many decades a major barrier to California; Donner Pass (*E*–5) is named for a party of immigrants who, in 1846, lost several of their number to starvation while marooned in the winter Sierra snows. But from space we can see the entire width of the Sierra Nevada at a glance, from the Great Valley of California (*B*–20) to the sagebrush deserts of Nevada (*upper right*). Lake Tahoe (*I*–7) and the corner of Mono Lake (*V*–19), as well as dozens of smaller lakes, are prominent. Reno, Nev. (*J*–1), is the only city of any size in the area covered. The Truckee (*I*–1), Carson (*M*–4), and Walker (*R*–6) Rivers are barely resolved, but their valleys are conspicuous with the bright red of irrigated farms.

The Landsat image shows many aspects of the Sierra Nevada. The dense red areas are forest, chiefly conifers but including a wide variety of deciduous trees as well. These forests lie between elevations of about 1200 and 2750 meters (4000 and 9000 feet). Below that we see the chaparral and grass of the foothills (*lower left*) in California and sagebrush in Nevada. At elevations above 2750 meters (9000 feet), timberline in this area, are the meadows or bare rock of the Alpine zone. The white areas (*O*–19; *R*–19) in particular are exposed granite, not snow, although this part of the Sierra receives up to 1800 centimeters (700 inches) of snow in the winter. The granite is intensely jointed in many areas (*L*–14; *H*–9).

To American geologists, "Sierra Nevada" is nearly synonymous with "batholith," because it consists largely of an immense mass of granite, granodiorite, and more mafic igneous rocks. The term "batholith" implies a single body, but in fact the rocks of the Sierra Nevada were intruded in many separate episodes during the Mesozoic Era; the vague curvilinear patterns visible in the drainage may be the expression of individual intrusions. Structurally, the Sierra Nevada can be described as a large block, uplifted in the northeast along a series of faults and dipping toward the southwest. Many of the linear valleys, such as that of the Stanislaus River (*H*–21; *J*–17), were probably eroded along faults or joints. *1056–18111;* September 17, 1972.

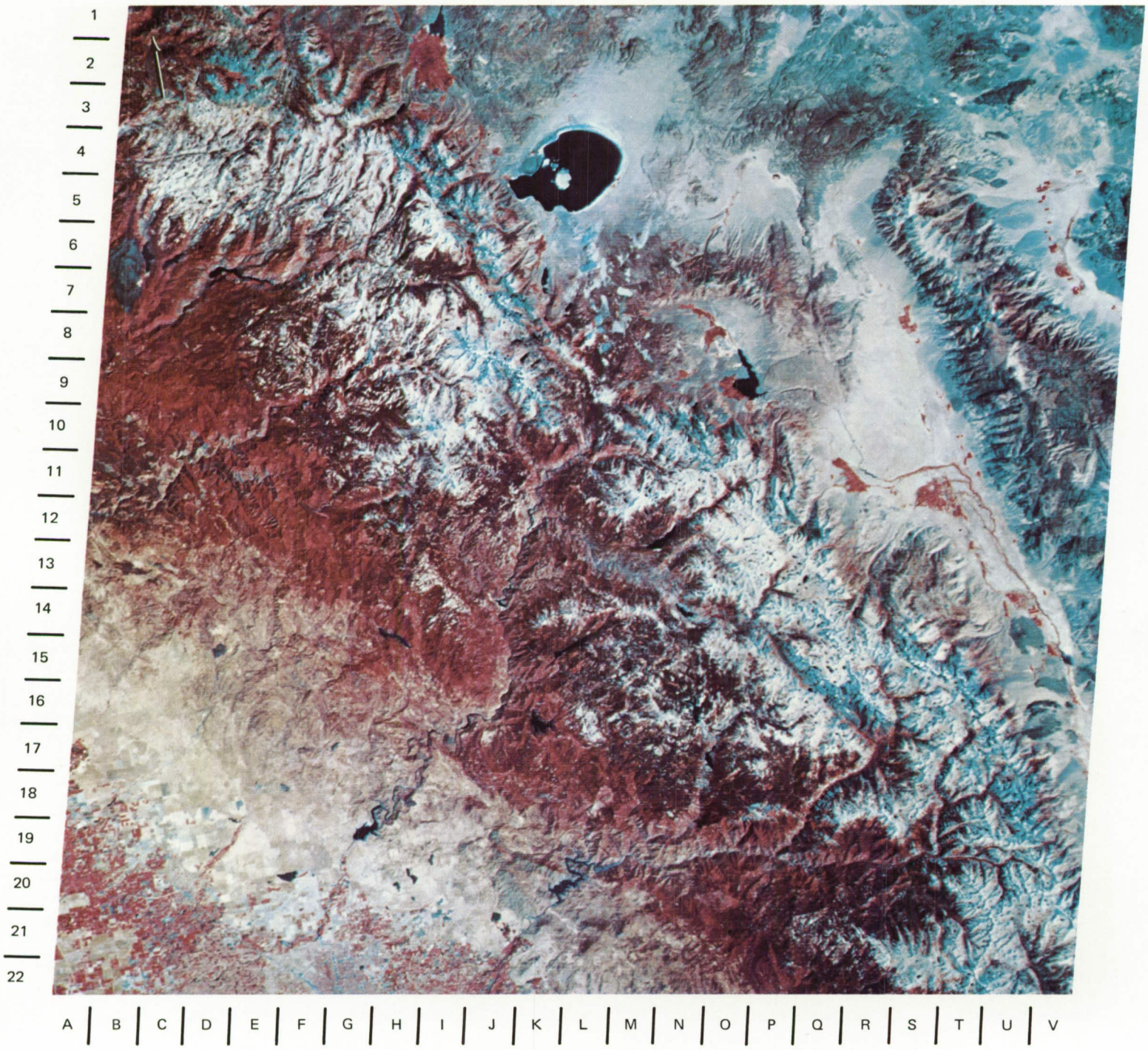


PLATE 124

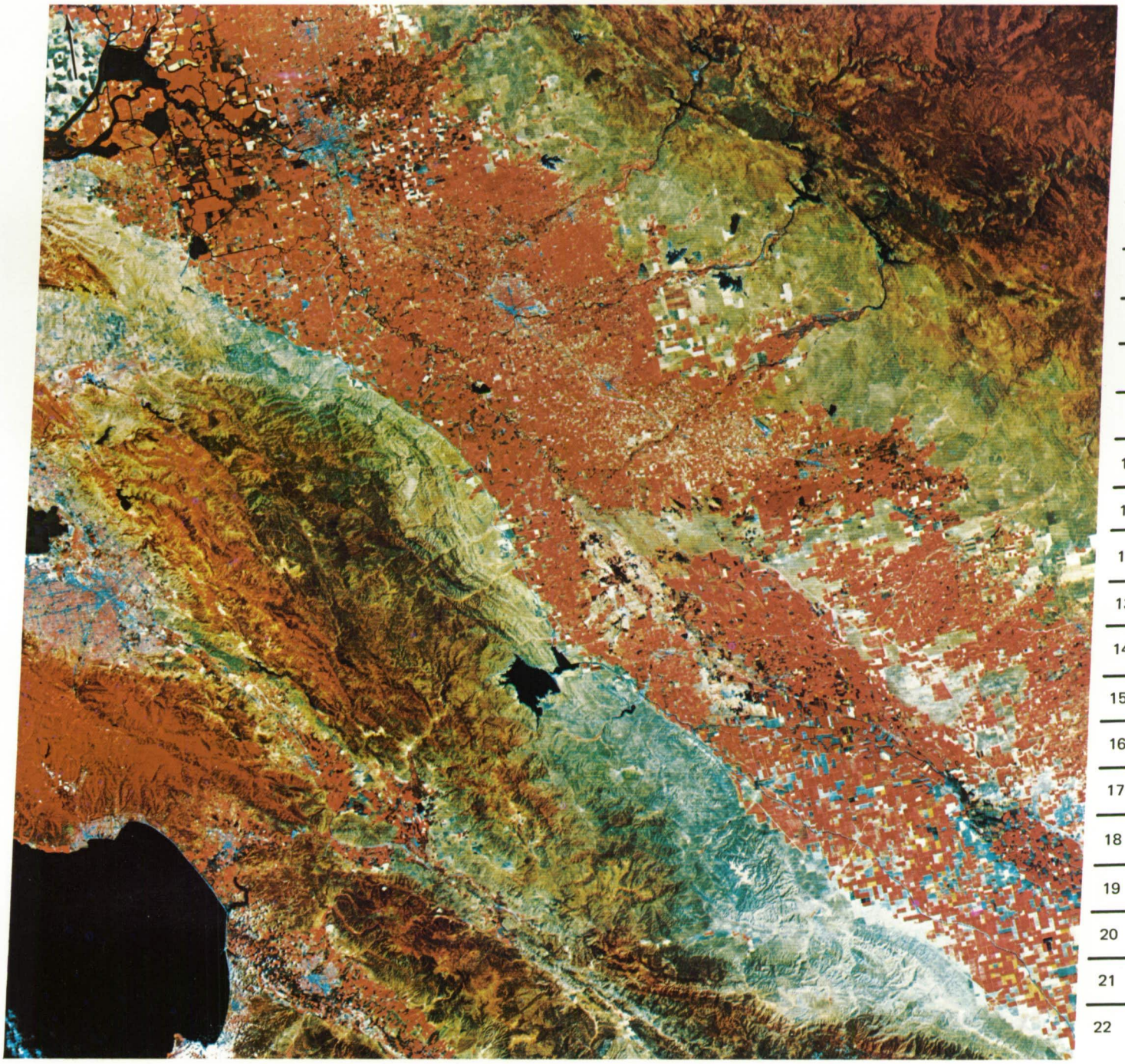
MONO LAKE, CALIF.: Three major physiographic regions are represented in this image: the Great Valley of California (*B*–21), the snow-covered Sierra Nevada trending northwest to southeast across the image (*C*–4; *P*–16), and the Basin and Range region (*L*–1; *V*–12). The checkerboard pattern shown in the San Joaquin Valley subdivision of the Great Valley depicts the Fresno, Calif., agricultural district (*C*–20). Two large reservoirs east of Fresno, Millerton Lake (*G*–19) on the San Joaquin River and Pine Flat Reservoir (*K*–20) on the Kings River, provide water for the irrigated fields on the valley floor.

The Sierra Nevada is a giant, uplifted block descending gently on its westward side from elevations of more than 3900 meters (13 000 feet) through a foothill zone to the floor of the Great Valley. Mixed coniferous forests occupy the higher elevations of the Sierra while California oaks dominate the lower elevations of the western foothill zone. The Tuolumne (*D*–7) and the Merced (*F*–9) Rivers occupy deep canyons incised into the western flank of the Sierras in the Yosemite National Park area. The Hetch Hetchy Reservoir (*C*–6) on the Tuolumne provides water via aqueduct to the San Francisco metropolitan area.

The northeast flank of the Sierra Nevadas descends abruptly to the third physiographic region depicted in this image: the Basin and Range. This area consists of a series of uplifted mountain blocks with steep-sided downfaulted valley troughs lying between the mountain blocks. Sands and saline materials accumulate in these intermontane troughs yielding highly reflectant signatures such as is seen in the Columbus Salt Marsh near the California-Nevada border (*U*–1). Two valleys are clearly delineated within the Basin and Range by the elongated patches of red indicating gallery vegetation and irrigated agriculture.

Mono Lake (*K*–4) and Mono Craters (*K*–5) represent a volcanic area superposed upon the Basin and Range landscape. The lake occupies a nearly circular downfaulted depression. The brighter areas within the lake are islands consisting mostly of pyroclastic rocks and lava flows. The row of brighter spots extending southward from the lake shore is a series of volcanic domes and steep-sided lava flows known as Mono Craters. *1397–18053;* August 24, 1973.

PLATE 125



MONTEREY BAY: This view of Monterey Bay (*B*–19) and the California Coast Ranges was the first color composite made from an individual Landsat image, and one of the first images received. The image shown here is a computer-processed version produced later by IBM. It covers an area extending from the foothills of the Sierra Nevada (*upper right corner*), across the San Joaquin Valley and the Coast Ranges to the Pacific coast. Several cities are visible: San Jose (*B*–13), Santa Cruz (*B*–18), Monterey (*D*–22), and Salinas (*G*–21). The prominent lake at *K*–15 is San Luis Reservoir in the Diablo Range. The picture immediately verified the potential value of Landsat color composites in vegetation discrimination; compare the sharp field pattern of the San Joaquin and Salinas Valley farming areas with the dense coastal forests of the Santa Cruz (*B*–16) and Santa Lucia (*F*–22) Mountains. The Diablo (*G*–12) and Gabilan (*J*–21) Ranges are covered with grass and chaparral and are used chiefly for cattle raising.

To a geologist, this picture is virtually a textbook in structural geology. One of the world's greatest (and most dangerous) faults, the San Andreas, bisects the area. This fault is moving continuously in this area at a rate of about a centimeter (one-half inch) a year, with the west side going northward. This right-lateral movement, as it is termed technically, is thought to have produced great drag folds by compression along the San Andreas fault. Some of these are visible at lower right. One (*Q*–22) is occupied by the New Idria diapir, a plug of serpentine that has been intruded into the sandstones of the anticline. This is the site of the most productive mercury mine in the United States, the mercury occurring as a low-temperature hydrothermal cinnabar deposit.

Covering as it does such a geologically interesting region, this image was closely studied when it was received. A number of drainage anomalies, such as unusually straight or angular valleys, were noted in the Gabilan, Santa Lucia, and Diablo Ranges, and it is likely that at least some of them are major unmapped faults. A preliminary geologic map (see fig. 15 of the introductory chapter) of the area was finished only 1 week after Landsat 1 was launched, demonstrating the great time saving possible with orbital imagery. *1002–18134;* July 25, 1972.

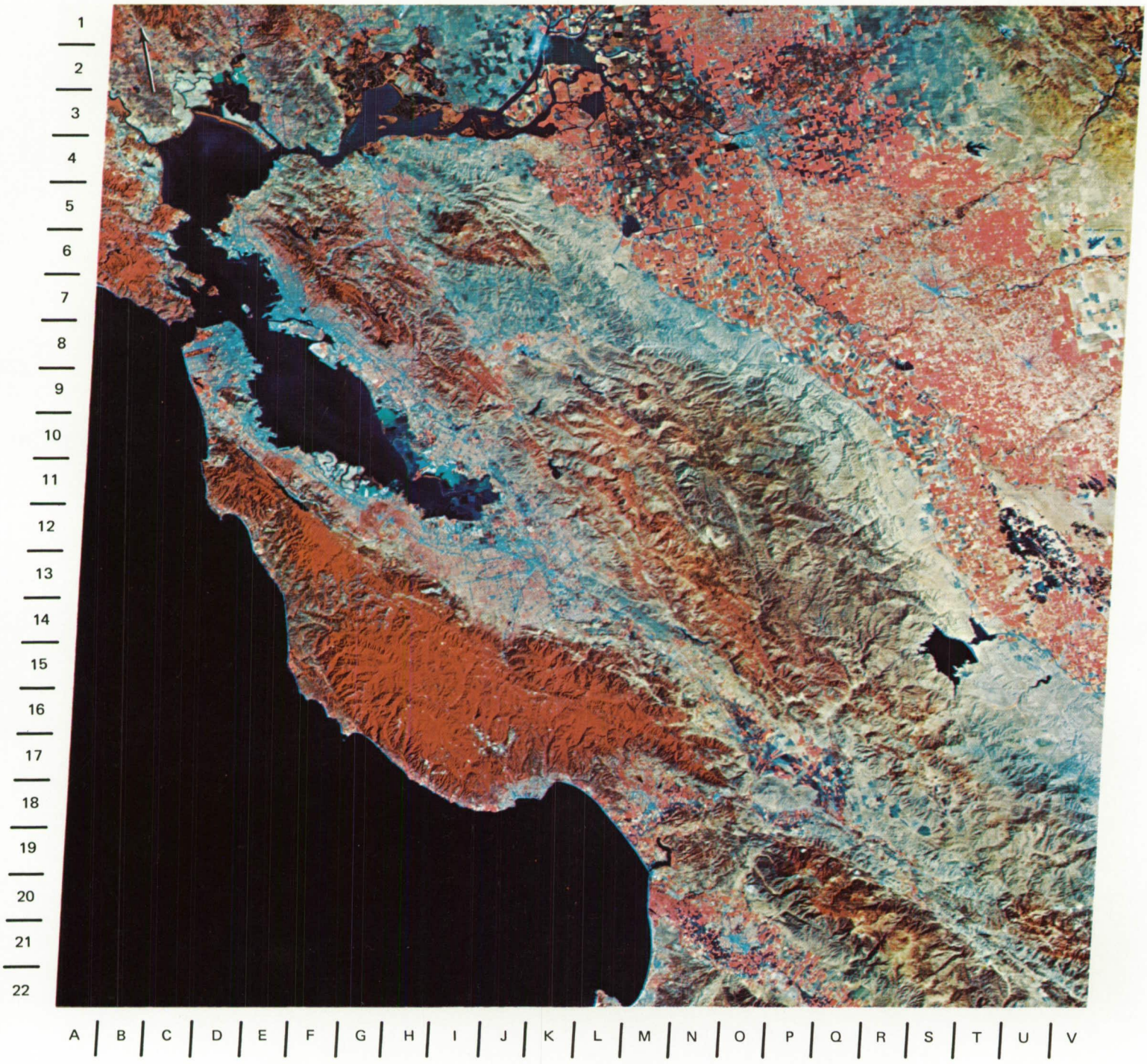


PLATE 126

THE BAY AREA, CALIFORNIA: This spectacular view of northern California shows many well-known cities: San Francisco (*C*–8), Oakland (*E*–7), San Jose (*J*–12), and others clustered around San Francisco Bay (*E*–9) and San Pablo Bay (*C*–4), Santa Cruz (*J*–17), Salinas (*O*–20), and Monterey (*M*–22) to the south, and Stockton (*O*–3) and Modesto (*R*–7) in the Great (Sacramento) Valley (*Q*–5) of central California. Recent landfill (*F*–10) and salt evaporation basins (*I*–1) are evident in the southern part of the Bay.

Geologically, the area west of the Sacramento Valley includes the intricately folded Coast Ranges (*O*–12) composed of Mesozoic metamorphic rocks and Cretaceous and Tertiary marine sediments. Several active faults include the famed San Andreas (whose trace is emphasized by Crystal Springs Lake (*E*–11), which occupies the fault valley west of San Mateo) and the Hayward (*H*–9) and Calaveras (*J*–10) faults in the East Bay region. Mount Diablo (*H*–6), the highest (1173 meters (3849 feet)) peak in the Bay area, is a fault-bounded piercement structure made up of greenstone and serpentine. The edge of the Sierra Nevada foothills (*U*–1) appears to the east of the Quaternary sediment-filled Great Valley.

The Santa Cruz Mountains (*H*–15) contain the southernmost Redwood forest—indicated by the deep reds—along the California coast. The hills to the north and east of the Bay area and southward support California Oaks and evergreens (such as the imported Eucalyptus trees) mixed with chaparral in places. The eastern slopes (*R*–3) of the Coast Ranges are covered with grasses that turn a distinctive golden brown in summer. Tule marshes dominate the delta country (*H*–3) near the mouth of the Sacramento River.

The region includes a diversity of farm products, including truck crops in the Salinas Valley (*P*–21) and grapes in the Santa Clara (*O*–16) and Great Valleys. The Sacramento Valley is used almost entirely to farm such cash crops as rice, cotton, barley, sunflower, sugar beets, beans, and tomatoes. Some fields have been burned after harvest (*I*–2). Peach trees are also common in the valley and walnut groves abound in the warm climates of the valleys east of the ranges near the fog zone of the coast. *1075–18173;* October 6, 1972.

PLATE 127



SAN FRANCISCO, CALIF.: This enlargement of part of Landsat image *1255–18183* taken on April 4, 1973, to a scale of 1:400 000 shows the Bay area (see plate 128 for letter identifications) around San Francisco (*A*), Oakland (*B*), and San Jose (*C*) in considerable detail. The Golden Gate Bridge (*D*) leads to the Presidio (*E*) in San Francisco. Alcatraz (*F*), Angel Island (*G*), and Treasure Island (*H*) are readily discerned. Golden Gate Park (*I*) lies west of the downtown section (*J*). Lake Merced (*K*) is near the Pacific coastline. Twin Peaks (*L*) and the San Bruno hills (*M*) stand out. The San Francisco International Airport (*N*) with its runways is clearly seen as is the newly developed Foster City (*O*)—a residential community built by landfill into the Bay. Other communities along the Bayshore include San Mateo (*P*), Palo Alto (*Q*), Sunnyvale (*R*), and Santa Clara (*S*). The Upper and Lower Crystal Springs (*T*) and San Andreas (*U*) Reservoirs are built in a narrow valley in the eastern coast ranges; this valley marks the line of the famous San Andreas fault (*V*). The 3.2-kilometer (2-mile) long Stanford Linear Accelerator is plainly seen (*W*) in this view. Other well-known places in the East Bay are Fremont (*X*), Hayward (*Y*), Berkeley (*Z*), and Richmond (*AA*). Salt evaporating basins (*BB*) can be picked out in the south half of the Bay. East of the Berkeley Hills (*CC*) are the towns of Concord (*DD*), Walnut Creek (*EE*), and San Ramon (*FF*). Highway 50 crosses the Livermore Valley (*GG*) south of Mount Diablo (*HH*). Vallejo (*II*) lies at the head of San Pablo Bay (*JJ*). Clusters of World War II Liberty ships in the "mothball" fleet (*KK*) lie at anchor in Suisun Bay (*LL*) into which flows the Sacramento River (*MM*).

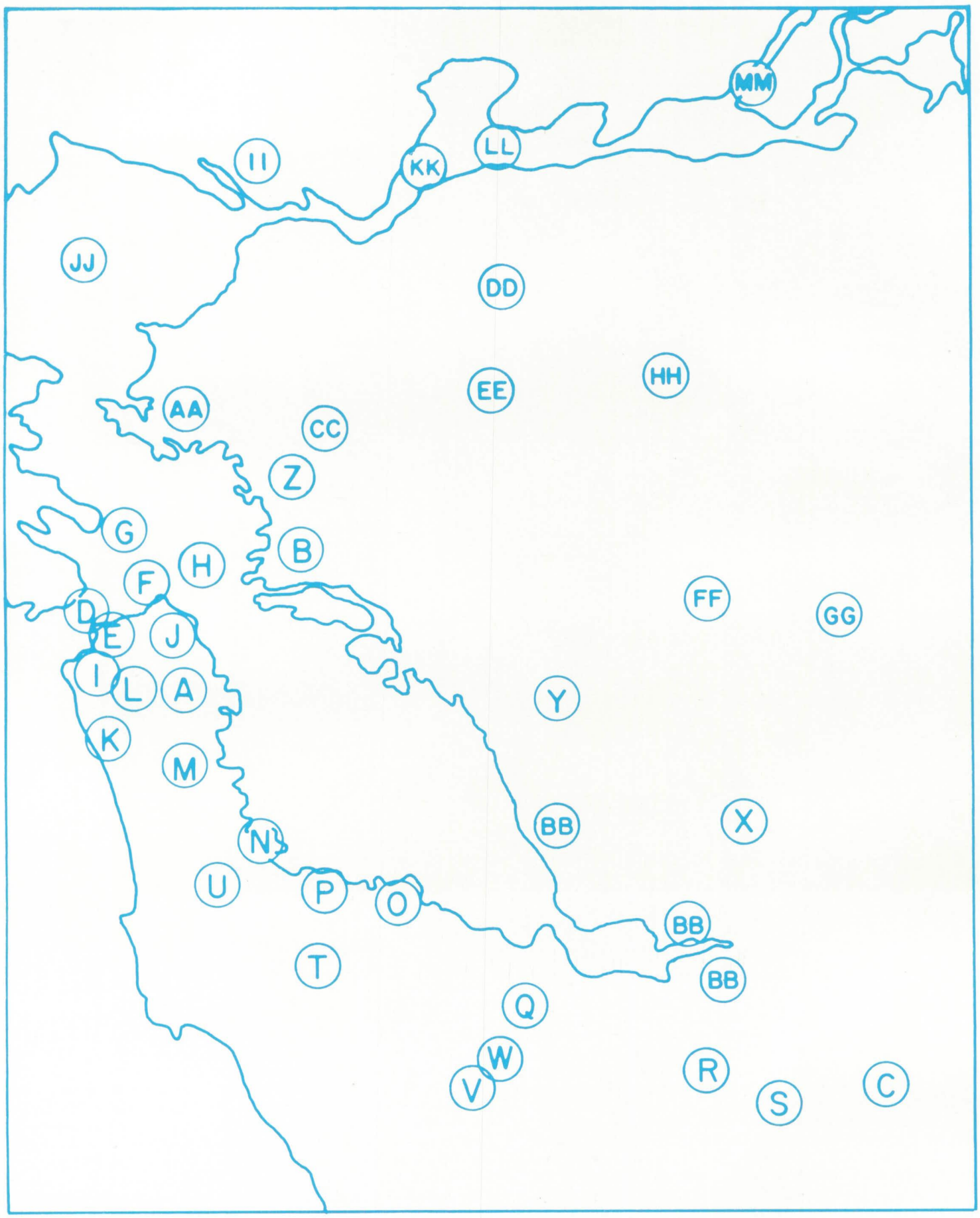
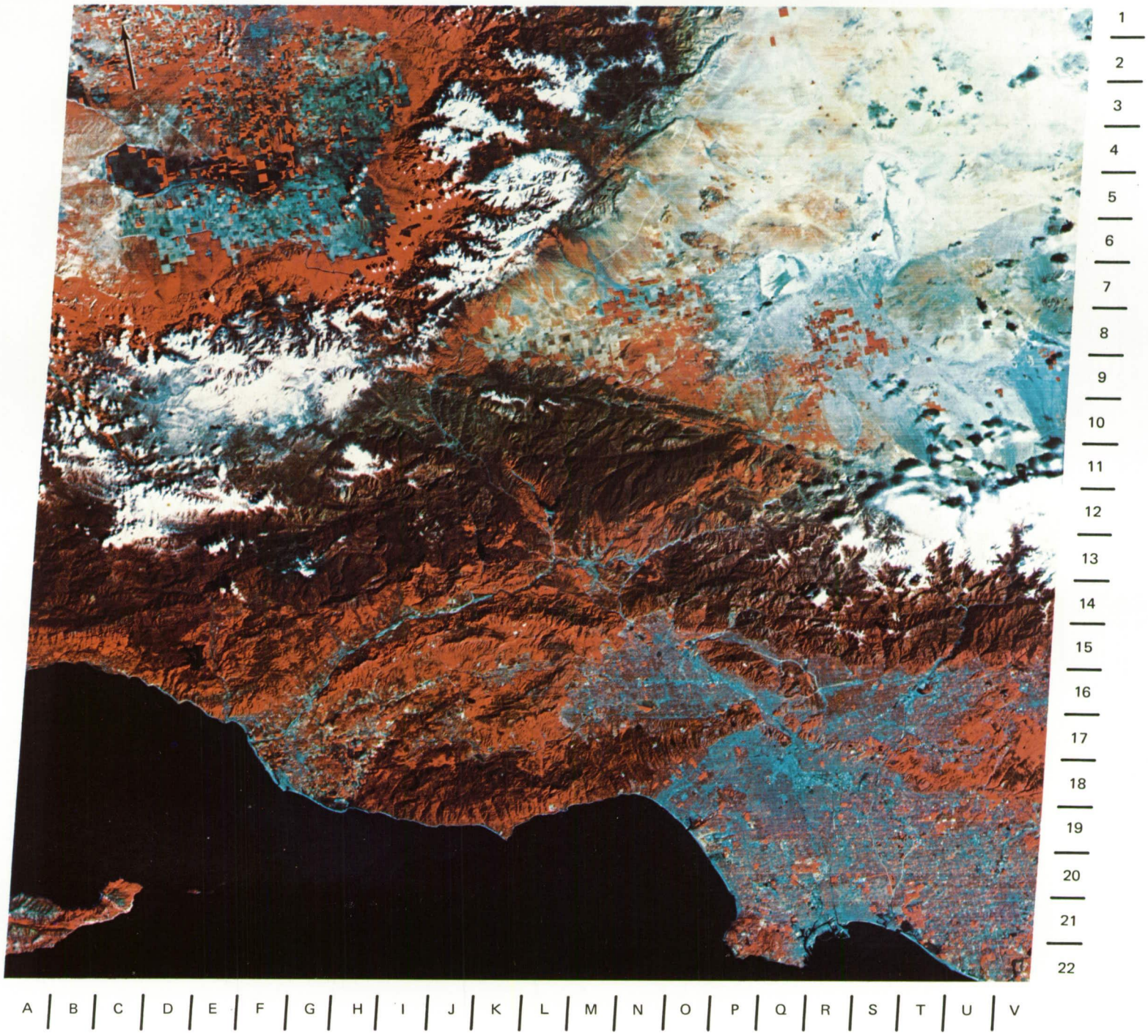

MM
LL
KK
II
JJ
DD
HH
EE
AA
CC
Z
G
B
H
F
FF
GG
D
E
J
I
L
A
Y
K
M
BB
X
N
U
P
O
BB
T
BB
Q
W
V
R
S
C

PLATE 128

PLATE 129



LOS ANGELES, CALIF.: The Los Angeles metropolitan complex prominent in this image (*Q*–17) is situated in a series of basins and valleys containing over 9 million people distributed in a multiplicity of communities. Topographically the lowland is ringed by mountains of the Transverse and Peninsula Ranges of southern California. The east to west trending Santa Monica (*N*–17), Santa Susana (*L*–14), and San Gabriel (*P*–13) Mountains flank the north rim of the lowland and delineate the San Fernando Valley (*N*–15). The Santa Ana Mountains (*V*–17) partly mark the southern boundary. Isolated hill areas outcrop throughout the lowland, often alined with fault zones and petroleum-producing areas. The Whittier fault (*S*–17) is an example, and to some degree also the Newport-Englewood fault zone (*P*–18; *Q*–19).

One of the more obvious features in this image is the intersection of the linear patterns produced by the San Andreas (*K*–8; *P*–10) and the Garlock (*L*–5) fault zones. Lakes, ridges, minor scarps, and displacement of various features attest to the crustal activity taking place in both these zones. At least a dozen major fault systems are shown in this image and only four are mentioned by name; the reader has only to look for obvious linearity, then refer to the geologic map for confirmation. See, for example, the lineation along the backbone of Santa Cruz Island (*A*–20).

Other landmarks include the coastal communities of Ventura (*E*–16) and Oxnard (*F*–17) in the Ventura structural basin, the Santa Clara River Valley (*G*–15), and the Casitas Reservoir (*D*–15). The Los Angeles lowland littoral includes Santa Monica (*N*–18), Playa del Rey (*O*–19), the Palos Verdes Hills (*Q*–21), and the San Pedro-Long Beach harbor area (*R*–21).

Northwest of Los Angeles in the snow-covered mountainous knot which marks the meeting point of the California Coast Ranges, the Transverse Ranges, and the southern end of the Sierra Nevada Mountains (*G*–7), the landscape descends abruptly into the southern end of the San Joaquin Valley and the irrigated field patterns surrounding Bakersfield (*E*–1). Here in the arid interior, the fertile alluvial soils, including old lake beds such as Buena Vista Lake (*B*–4), are being irrigated from rivers whose headwaters reach into the high Sierra Nevadas to the east. A similar transition marks the boundaries of the Mojave Desert northeast of Los Angeles. Since the 1950's, irrigated agriculture and electronic and aerospace industrial development have combined to produce a population boom in the once barren high desert country. The need for space and the priorities of land use as the Los Angeles area mushroomed, forced producers of field crops, truck crops, and poultry to establish in areas like the Antelope Valley (*N*–8) and in urban centers such as Lancaster (*P*–8) and Palmdale (*Q*–10). The test facilities of Edwards Air Force Base occupy the dry lake bed of Rogers Lake (*R*–6). *1234–18021;* March 14, 1973.



PLATE 130

LOS ANGELES AERIAL MOSAIC: This aerial photomosaic of a large area roughly comparable to the 34 000 square kilometers (13 000 square miles) of a Landsat frame shows Los Angeles, the Transverse Ranges, and a part of the Mojave. The mosaic was constructed from more than 8000 individual aerial photos taken from a series of low-flying flights during the 1950's. Only the central interior of each overlapping photo was used in the final product to minimize image distortion and displacement effects and vignetting (change in gray tones toward the outer edges). As reproduced on this page, the effective resolution in this photomosaic is estimated to be approximately 40 to 50 meters (130 to 160 feet). This image can be compared with that of Landsat on the opposite page, although the scales are slightly different, to judge the quality and information content inherent to the Landsat scanner-produced images. The aerial mosaic was made by Aero Service, Inc., of Philadelphia, Pa., and is reproduced here with their permission.

PLATE 131



SANTA BARBARA, CALIF.: The phrase "North American Riviera" has been applied to the roughly 16-kilometer (10-mile) wide and 80-kilometer (50-mile) long coastal zone bordering the city of Santa Barbara (*P*–15). While the climatic allegory is essentially correct, the geologic situation is dissimilar. Unlike its European counterpart, the Santa Barbara coastal zone has an abrupt fault-bounded mountain range immediately inland. Most of the coast has the Santa Ynez Mountains and fault zone as a backdrop (*T*–5; *O*–14). Structural control is the dominant topographic determinant within the entire image. The convergence of three major California physiographic regions is shown: the northwest to southeast trending Coast Ranges (*J*–10), the east to west trending Transverse Ranges (*L*–14), and the Great Central Valley (*Q*–2).

Rugged terrain has restricted concentrated settlement to the valleys. Likewise, large-scale agriculture is restricted to valleys where water is available from deep wells, or reservoirs supplied from the mountainous surroundings. The coastal valleys of Santa Maria (*D*–8), San Antonio (*E*–9), Santa Ynez (*E*–12), and Santa Clara (*T*–13) are well known for their production of vegetable and field crops, orchards, lemons, and avocados. Interior areas like Cuyama Valley (*O*–7) and the San Joaquin Valley (*S*–3), here centered around Bakersfield (*U*–1), lend themselves to large-scale "factory farm" production of grains, cattle, citrus, grapes, cotton, and vegetables. Availability of irrigation water from the neighboring Sierras aided development in the San Joaquin Valley around Bakersfield. Agricultural expansion now includes intermittent lake beds whose circular nature is visible in this image (*Q*–3).

Numerous reservoirs have been built in the mountainous interior to alleviate water supply problems in the more densely populated coastal areas. Casitas Reservoir (*S*–14), upstream from Ventura, and Lake Cachuma (*L*–13), supplying Santa Barbara, are examples.

Tiny Anacapa Island's Channel Island National Monument (*T*–19) stands in contrast across the Santa Barbara Channel (*M*–17) to its companion islands. The linearity of the fault system on Santa Cruz Island (*P*–20) resembles those on the mainland.

The reflective white areas along the coast at the mouth of the Santa Maria Valley represent sand dunes. A similar signature occurs further south along the coast opposite Vandenberg Air Force Base (*E*–12), the launch site of the Landsat satellites. *1307–18073;* May 26, 1973.

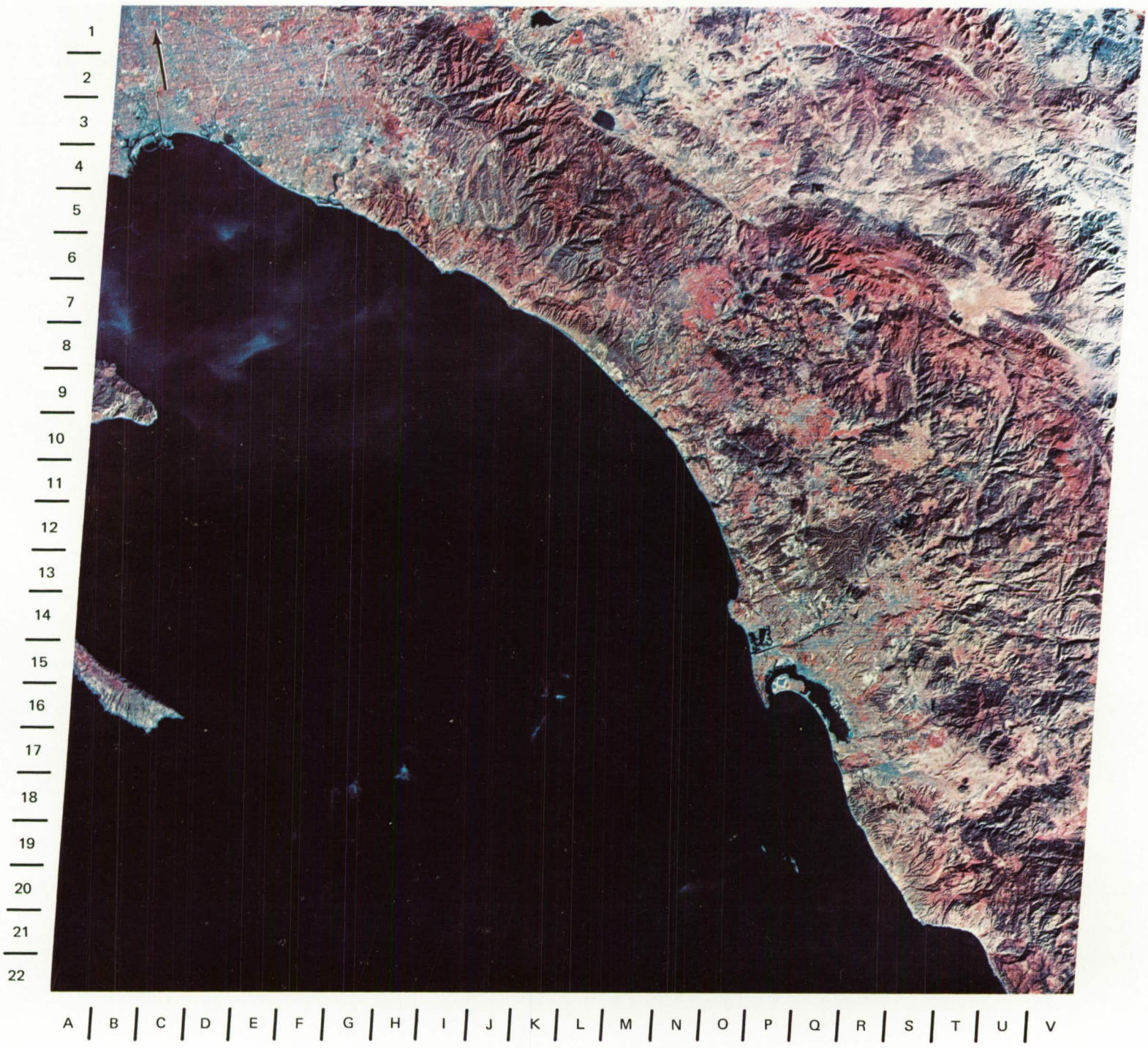


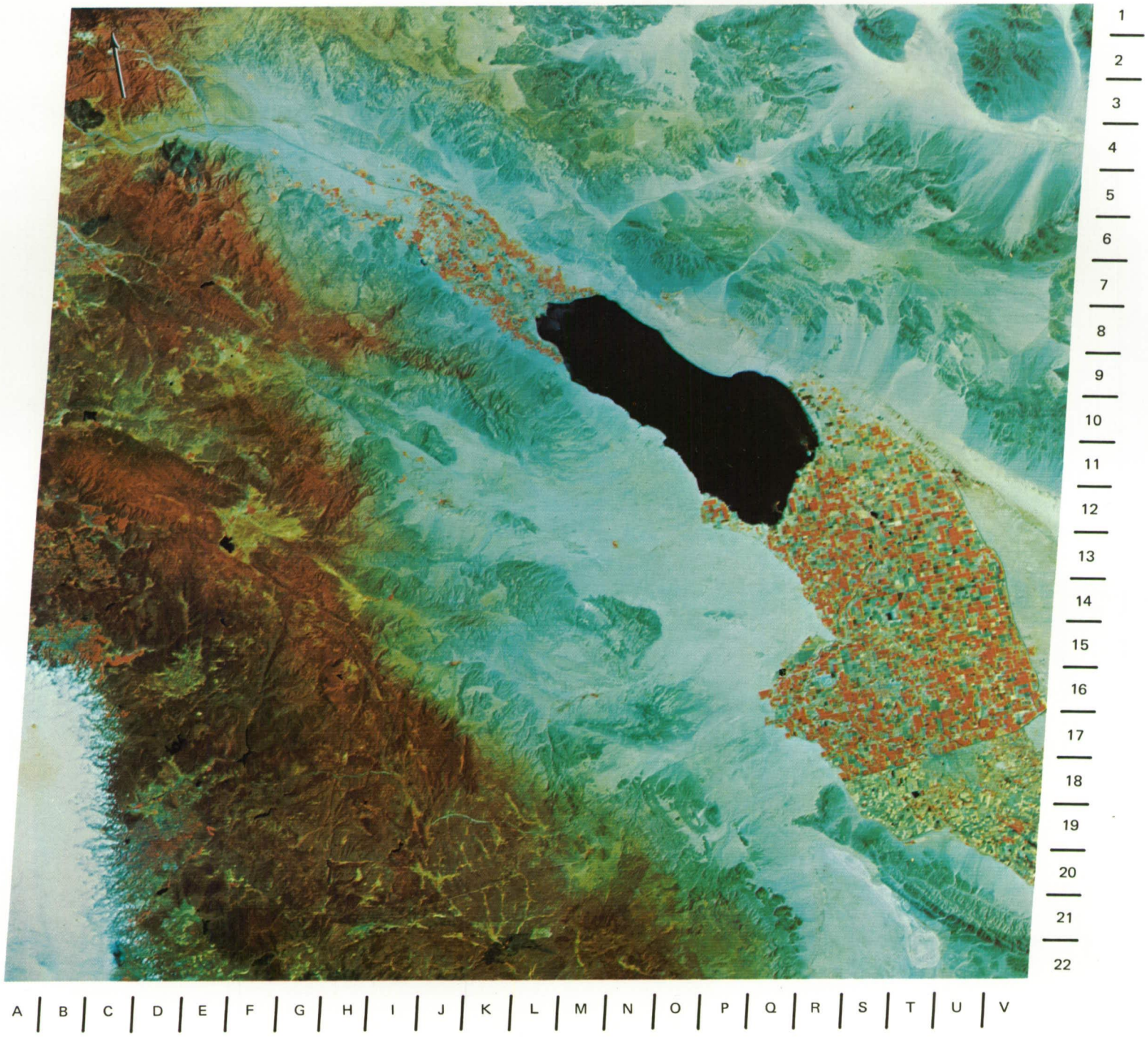
PLATE 132

SAN DIEGO, CALIF.: The natural harbor in San Diego Bay is formed partly by a narrow strip of coastal sand dunes (*Q*–16) connecting to the mainland the city of Coronado. The North Island Naval Air Station, whose darker bluish signature results from large asphalt-covered areas (*P*–16), lies at this strip. The westernmost margin of the bay is formed by the Point Loma peninsula (*P*–16). San Diego's central business district (light bluish tone) and Balboa Park and Zoo (red signature) are near the northeast margin of the bay (*P*–16). Islands and peninsulas mark the aquatic recreation area of Mission Bay north of San Diego Bay (*O*–15). Tijuana, Mexico (*R*–18), is adjacent to the international border a few kilometers (miles) south of San Diego Bay. Numerous coastal lagoons indent the shoreline between San Diego and the Long Beach-Santa Ana metropolitan complex (*C*–3) in the northwestern part of the image.

The Long Beach harbor facilities (*A*–4); the rectangular grid of the metropolitan area (*C*–2); the concrete-lined channels of the Los Angeles (*A*–2), San Gabriel (*C*–2), and Santa Ana (*E*–2) river systems; and the citrus and agricultural areas surrounding Orange, Tustin, and Irvine (*G*–3) are clearly shown in this image. The structural depression often referred to as the San Jacinto Basin (*M*–2) lies between two of southern California's best known fault systems: the Elsinore (*L*–4) and the San Jacinto (*R*–2). Both fault zones consist of individual faults alined in a northwest to southeast fashion along the flanks of the Santa Ana Mountains (*J*–4) west of the basin and the San Jacinto Mountains to the east (*R*–1). Note also the conspicuous linear valley (*T*–11; *V*–12) trending northeast; these may be unmapped faults or eroded close-spaced joint sets. Numerous reservoirs dot the basin floor. Two of the largest are Lake Mathews (*J*–1), a major storage point along the Colorado River Aqueduct into Los Angeles, and Lake Elsinore (*K*–3). The distinctive red signature northwest of the San Jacinto Basin (*H*–1) is the dairying and citrus area centered around Corona and Chino in the flood control basin of the upper Santa Ana River.

Like the Santa Ana and San Jacinto Mountains to the north, the Agua Tibia (*Q*–6) and Volcan (*U*–8) Mountains, and other members of the Peninsular Ranges, rise high enough to support coniferous forests; hence the characteristic bright red signature of the higher mountain areas. The famed Palomar Observatory (*Q*–6) at the southeastern end of the Agua Tibia Mountains is located at an elevation of 1670 meters (5470 feet). Southeast of Palomar Mountain a distinctive signature marks the grass-covered Warner Basin and the Lake Henshaw reservoir (*S*–7). The San Diego River gorge (*T*–10), cut into the western flank of San Diego County's mountain block, trends southwestward toward the metropolitan area. In the foothill zone the avocado- and citrus-producing areas centered around Fallbrook (*N*–7) and Escondido (*P*–10) yield characteristic color patterns. *1125–17563;* November 25, 1972.

PLATE 133



IMPERIAL VALLEY, CALIF.: The Salton Sea (*P*–10) was created during the early part of this century when the Colorado River flooded its right bank and, aided by ditches and canals dug in an early attempt at irrigation, spilled over through two dry washes and filled the lowest portion of the trough some 82 meters (270 feet) below sea level, forming the Salton Sea. The deltas of both the flood courses can be seen projecting from the southeastern shore of the sea (*P*–11; *Q*–10). Subsequent evaporation in the hot desert climate produced a saline sea, and groundwater input resulting from modern day irrigation in the valley maintains the sea.

The checkerboard pattern on both the northwestern and southeastern margins of the sea represents irrigated agriculture in the Coachella Valley, centered about the town of Indio (*K*–7) in the northwest, and in the Imperial Valley, centered about the town of El Centro (*S*–15) in the southeast. Irrigation is made possible by the All American Canal (*V*–16) leading from the Colorado River near Yuma, Ariz. Subsidiaries of the main canal such as the East Highline Canal along the eastern fringe of the irrigated El Centro area (*U*–13) and the Coachella Canal (*U*–11) have greatly extended the limits of the irrigated areas. Mild winters permit year-round cultivation of a variety of agricultural products. A multiplicity of vegetable crops and feed and grain crops are grown in conjunction with sugar beets, cotton, and citrus fruits. Differences in seasonal planting and harvesting practices combined with variations in the intensity of land use are vividly shown in the line of demarcation delineating the U.S.-Mexico boundary south of El Centro. The hub of the Mexican irrigated area is the city of Mexicali located adjacent to the border (*T*–17).

The need for irrigation to sustain the intense agriculture of the Salton Trough is evidenced by the numerous indicators of the basic dryness of the region. Saline playas and alluvial fans are scattered throughout the area. Laguna Salada (*R*–20), the highly reflective area southwest of Mexicali, lies at the northern end of the Gulf of California. Several sizable alluvial fans (*O*–7; *T*–9) blanket the west flanks of the Chocolate Mountains (*Q*–7). The Algodones sand dunes, built from beach materials of an ancient lake that occupied the Salton Trough, extend southeastward along the flank of the Chocolate Mountains (*U*–11).

In the northwestern end of the Salton Trough Interstate 10 threads its way through San Gorgonio Pass (*C*–3) into the Los Angeles Basin to the west. The resort area of Palm Springs (*E*–4) lies in the shadow of 3000-meter (10 000-foot) high San Jacinto Peak (*D*–5) south of Interstate 10. *1358–17501;* July 16, 1973.

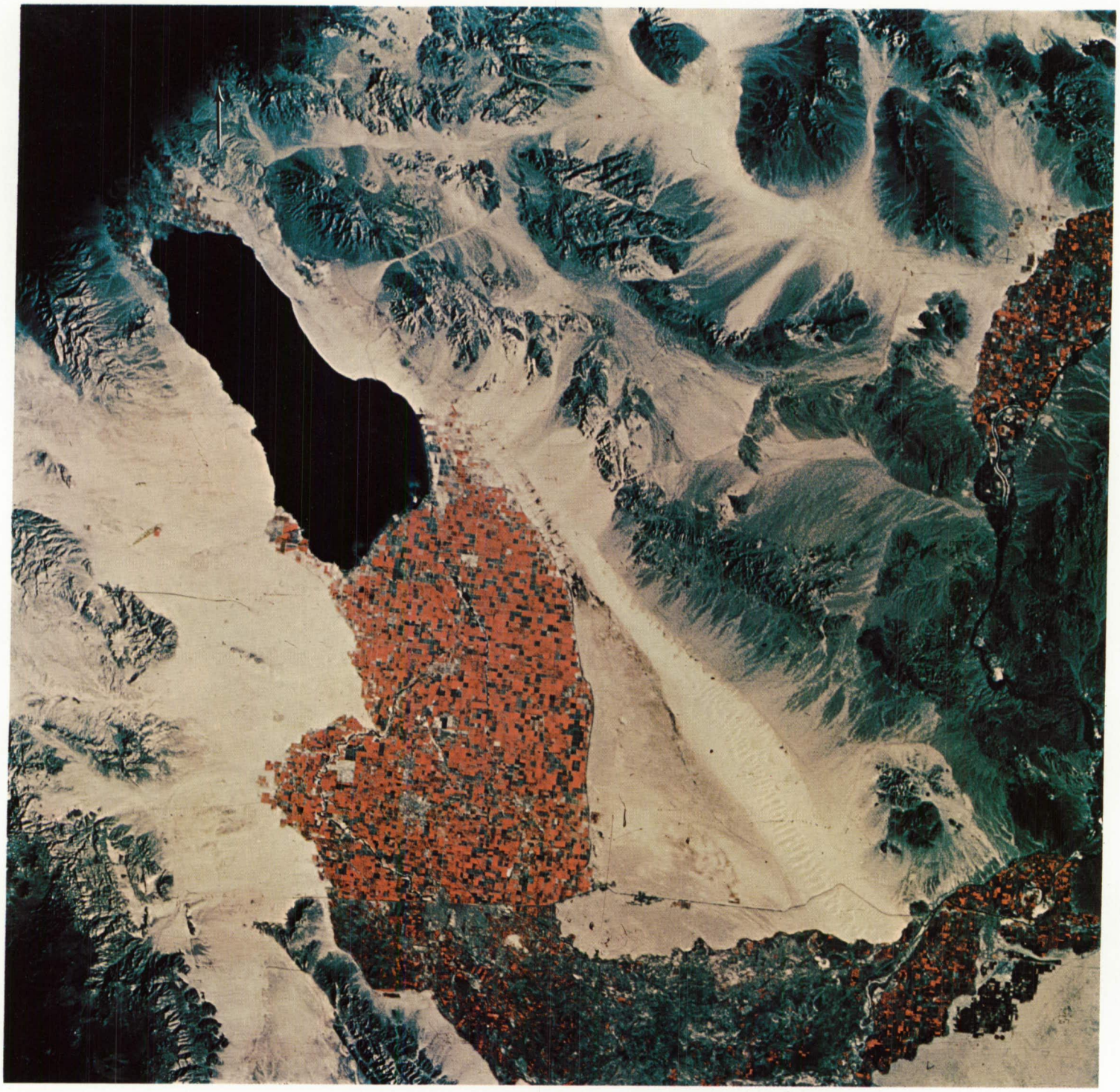


PLATE 134

SALTON SEA, CALIF.: The Apollo 9 Earth-orbital mission in 1969 carried a multispectral photography experiment (S065), using four 70-millimeter cameras, that was essentially a rehearsal for Landsat. This view of the Salton Sea was taken with color infrared film, which reproduces the colors of the now-familiar Landsat composites of multispectral scanner bands 4, 5, and 7. The resolution of the picture is strikingly good, and in places clearly better than that of the Landsat image. But because the Apollo picture was taken from an altitude of only 193 kilometers (120 miles), this fact serves to emphasize the remarkably high quality of Landsat imagery. The Apollo photograph was extensively used before Landsat was launched to test image interpretation techniques. It is of permanent value as a record of the appearance of the area in March 1969; Apollo photography (and in fact even Gemini photography) can be considered the beginning of repetitive coverage from space. This photograph clearly shows the All American Canal crossing the Sandy Desert bringing fresh water from the Colorado River to the Imperial Valley. Also, the U.S.-Mexican border is notably visible due to differences in land use. March 1969.



PLATE 135

THE ISLAND OF HAWAII: This mosaic made from two images depicts the largest and southernmost of the principal Hawaiian Islands. (See plate 136 for letter identifications.) The island is also one of the youngest in this chain of volcanic shields that began to build up from submarine outpourings of basaltic lavas on to the Pacific Ocean floor in the late Tertiary period. The pile of successive lava flows rises from a water depth of more than 4500 meters (15 000 feet) well offshore to a height of 4170 meters (13 680 feet) above sea level at the summit of Mauna Loa (*A*). This great volcano, last erupting in 1950, is topped by the 5-kilometer (3-mile) long Mokuaweoweo Caldera. Dark lavas have frequently spewed out along a major north-northeast fissure and several auxiliary fissures. Another set of fissures, the East Rift, runs eastward to form the currently active zone of pit craters, lava fountains, and Kilauea caldera and its adjacent pit crater at Kilauea Iki. These all can be viewed from the nearby Hawaiian Volcano Observatory (*B*). The older, inactive Mauna Kea Volcano (*C*) reaches to 4205 meters (13 796 feet). Haulalai (*D*) last erupted in 1801; the cloud-masked Kohala volcano (*E*) is no longer active.

Almost all the towns and villages on this island are located along rocky beaches set against high to low cliffs along the coast. Hilo (*F*), the largest town on the island, lies at the head of Hilo Bay (*G*). In addition to tourism, the chief industry of the local residents centers on production of sugarcane, some peas, tomatoes, and pineapple and on the raising of cattle in coastland farms (*H, I,* and *J*). Much of the rest of the island is given to grassland (*K*) or forest. The forests tend to stratify with elevation: guava mixed forest occurs near the coast (*L*), ohia (*M*) and koa (*N*) forests further up the slopes, and koa-mamani parkland (*O*) at higher elevations up to the lower limits of the more recent basalt flows.

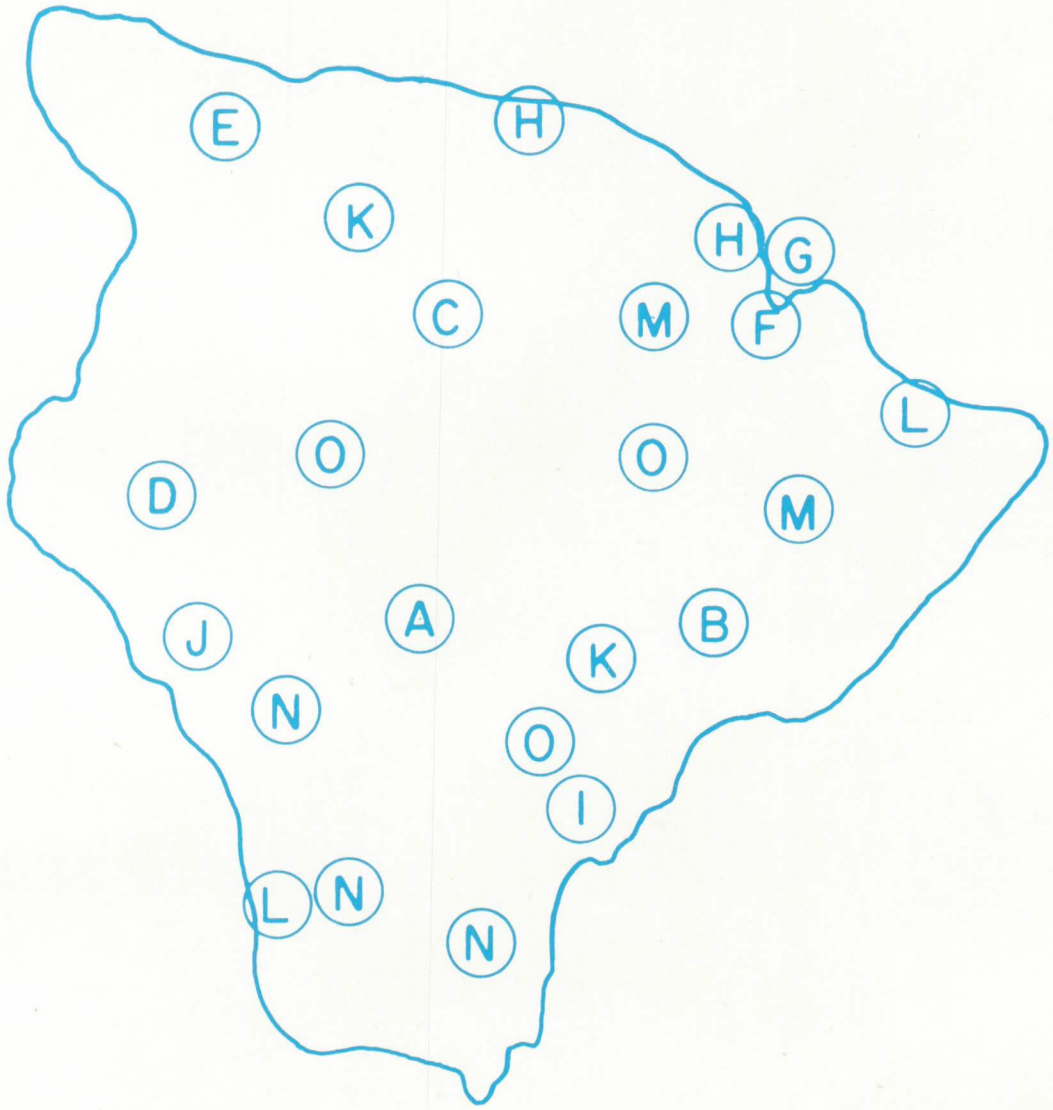
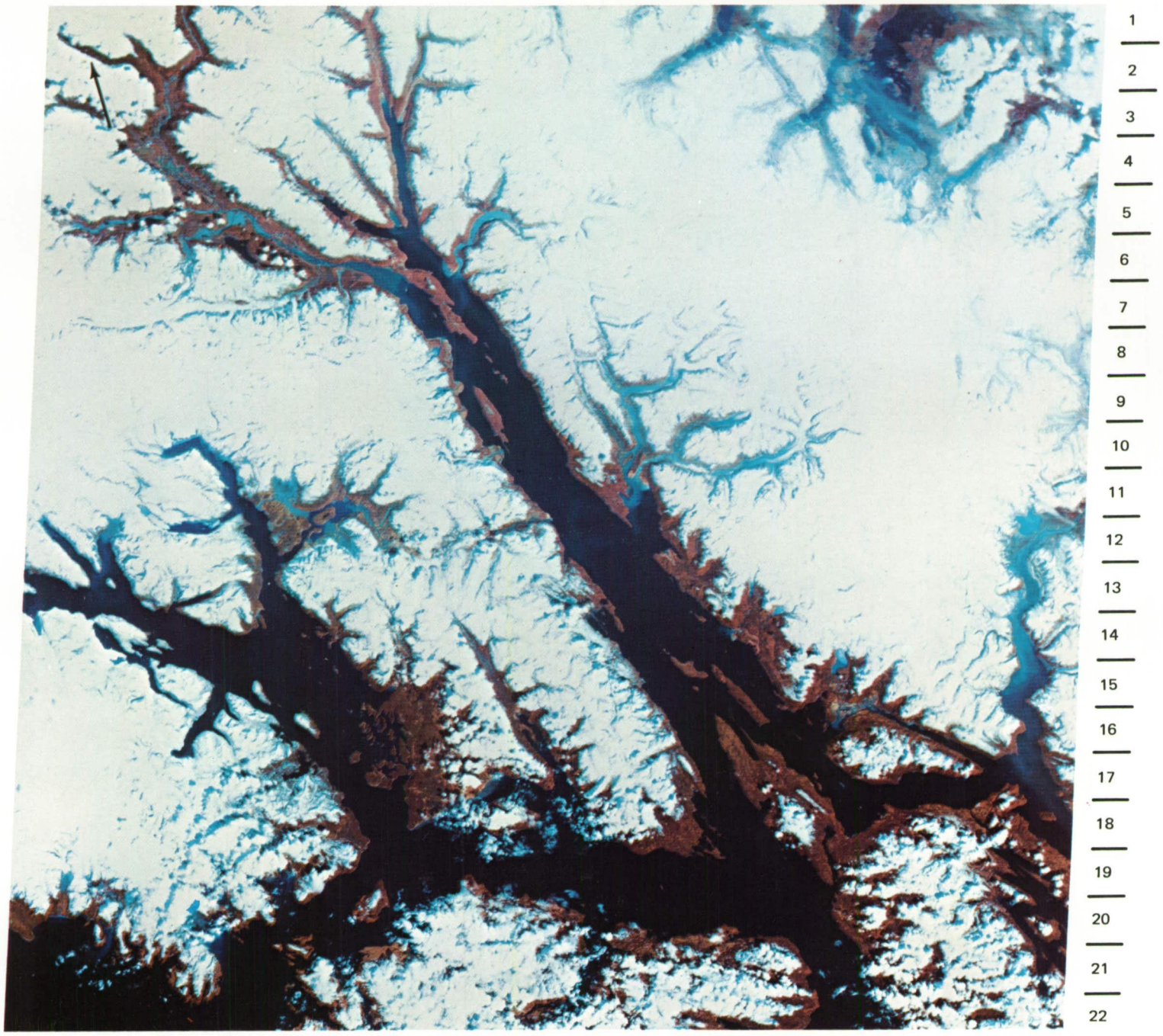
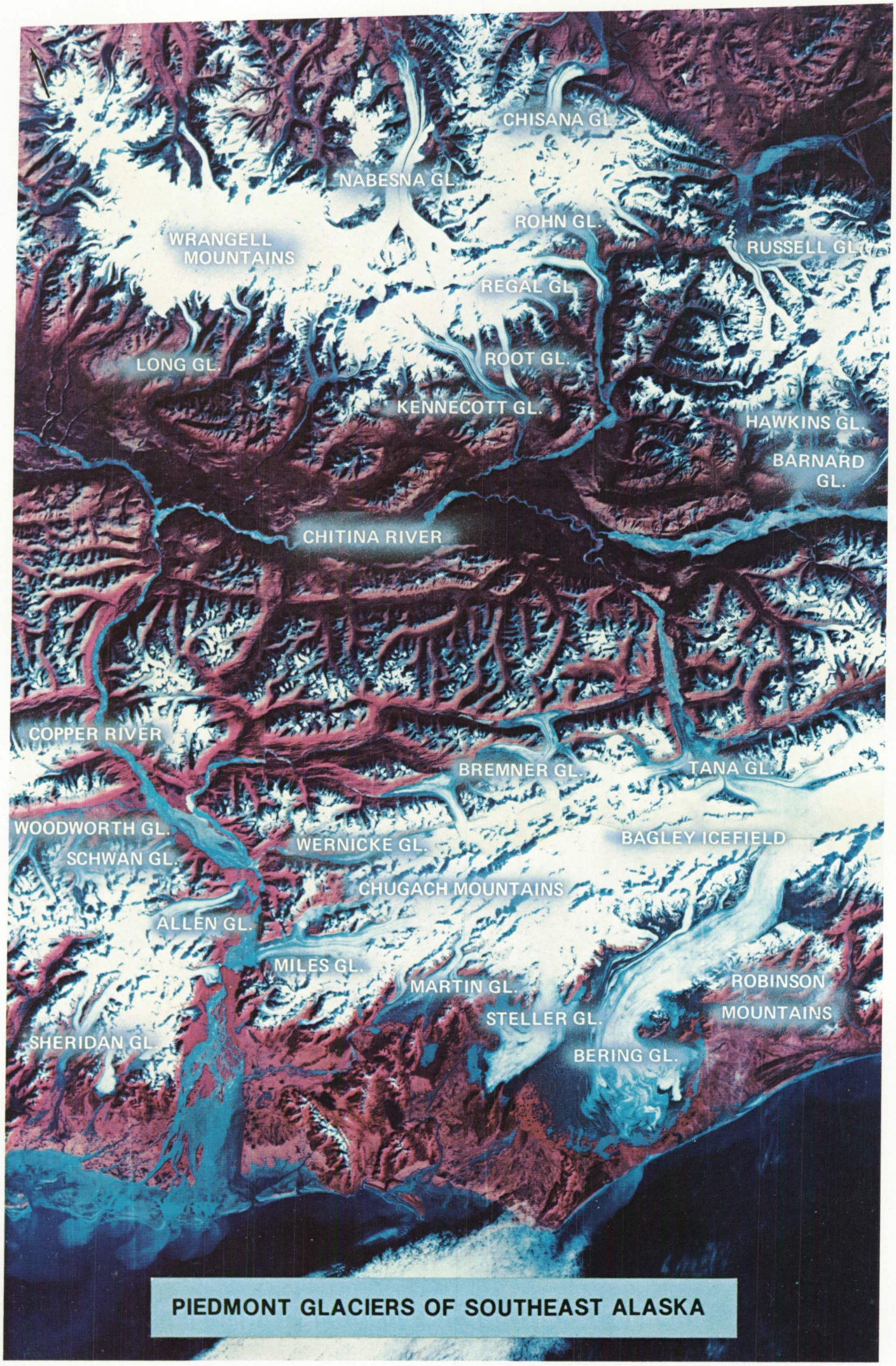


PLATE 136

PLATE 137



JUNEAU AND GLACIER BAY, ALASKA: Juneau (*S*–16), the capital of Alaska, is located on Gastineau Channel (*T*–16) in the southeastern panhandle. Across and slightly south is the town of Douglas (*S*–16) on Douglas Island (*R*–16). The area north of Juneau around Auke Bay (*Q*–15) and Mendenhall Glacier (*Q*–14) is highly developed; Juneau airport (*R*–15) and the proglacial lake (*Q*–14) at the terminus of the glacier are apparent. This region was glaciated throughout the Pleistocene and valley glaciers (e.g., Herbert (*P*–13), Gilkey (*P*–10), Antler (*O*–9), Muir (*C*–10), and Taku (*T*–13) Glaciers), and mountain icefields (e.g., Juneau Icefield (*S*–10)) are common today. Most of the area is snow covered above approximately 760-meter (2500-foot) elevation, but differentiating clouds (*T*–20) from the snow is difficult here (cloud shadows (*T*–19) aid in defining the clouds). Lynn Canal (*L*–11), Glacier Bay (*F*–14), and Chatham Strait (*Q*–20) are the largest glacial fjords in the image, although many of the smaller embayments are also fjords (e.g., Gastineau Channel (*T*–16) and Excursion Inlet (*L*–16)). Many of the valley glaciers discharge large volumes of glacial flour directly into the sea and the resulting suspended sediment plumes (*I*–6) act as natural tracers for viewing surface circulation patterns. The semidiurnal tides (two high-water and two low-water stages per tidal day) and the high tidal range (typically 5 meters (16 feet)) characteristic of this region produce very complex currents. The repetitive Landsat imagery provides a very convenient method of analyzing the circulation patterns of this area. In many locations the water is too shallow for navigation at low tide and extensive tidal flats (*U*–12) are exposed. On close inspection, extensive outwash plains (*M*–8; *O*–10; *C*–11; *B*–11) are evident at the terminal points of several glaciers. Additional features: proglacial lakes (*O*–9); town of Gustavus (*V*–7), below the clouds; Icy Strait (*M*–19); Admiralty Island (*T*–20); town of Haines (*H*–6); Atlin Lake (*R*–1), Canada; and Taku Arm (*N*–1), Canada. *1307–19434;* May 26, 1973.



PIEDMONT GLACIERS OF SOUTHEAST ALASKA

PLATE 138

PLATE 139



THE BEND OF THE YUKON: The Yukon, Alaska's principal river, begins in the northwest corner of British Columbia not far from Juneau in the Alaskan Panhandle (see plate 137) and passes through the Yukon Territory of western Canada. It then flows northwest to west for more than 1900 kilometers (1200 miles) through plateaus and lowlands between the Alaska and Brooks Ranges, before emptying through a growing delta (see plate 148) into the Norton Sound along Alaska's west coast. At its northernmost point (66°50′ N) as it flows into a lowlands of Quaternary sediments, the Yukon (*K*–15) is joined by the Porcupine River (*H*–7), which drains upland to the northeast. Fort Yukon (*E*–11), the oldest non-Eskimo settlement in Alaska, is built at the confluence of these two rivers. In the segment seen here, the Yukon has a broad flood plain as the river becomes braided owing to extensive deposition of the sediment load collected upstream. The Porcupine River and its tributary, the Black River (*L*–6), are conspicuously meandering through the lowlands. A Yazoo-type river (see plate 45), the Birch Creek (*L*–17), roughly parallels the Yukon to its south because of inability to cut through higher flood plain sediments around the larger stream.

The northern edge of the White Mountains (*J*–21) reaches elevations close to 1200 meters (4000 feet). Rocks in the vicinity range from Devonian sedimentary strata to Cenozoic volcanics. A dissected plain to the east (*O*–12) is underlain by Mesozoic sedimentary rocks.

Although the many lakes in the region are now frozen, most of the surface is devoid of heavy snow cover typical of this time of year. The low Sun angle (8°) helps to emphasize many subtle topographic features. *1102–20441;* November 2, 1972.

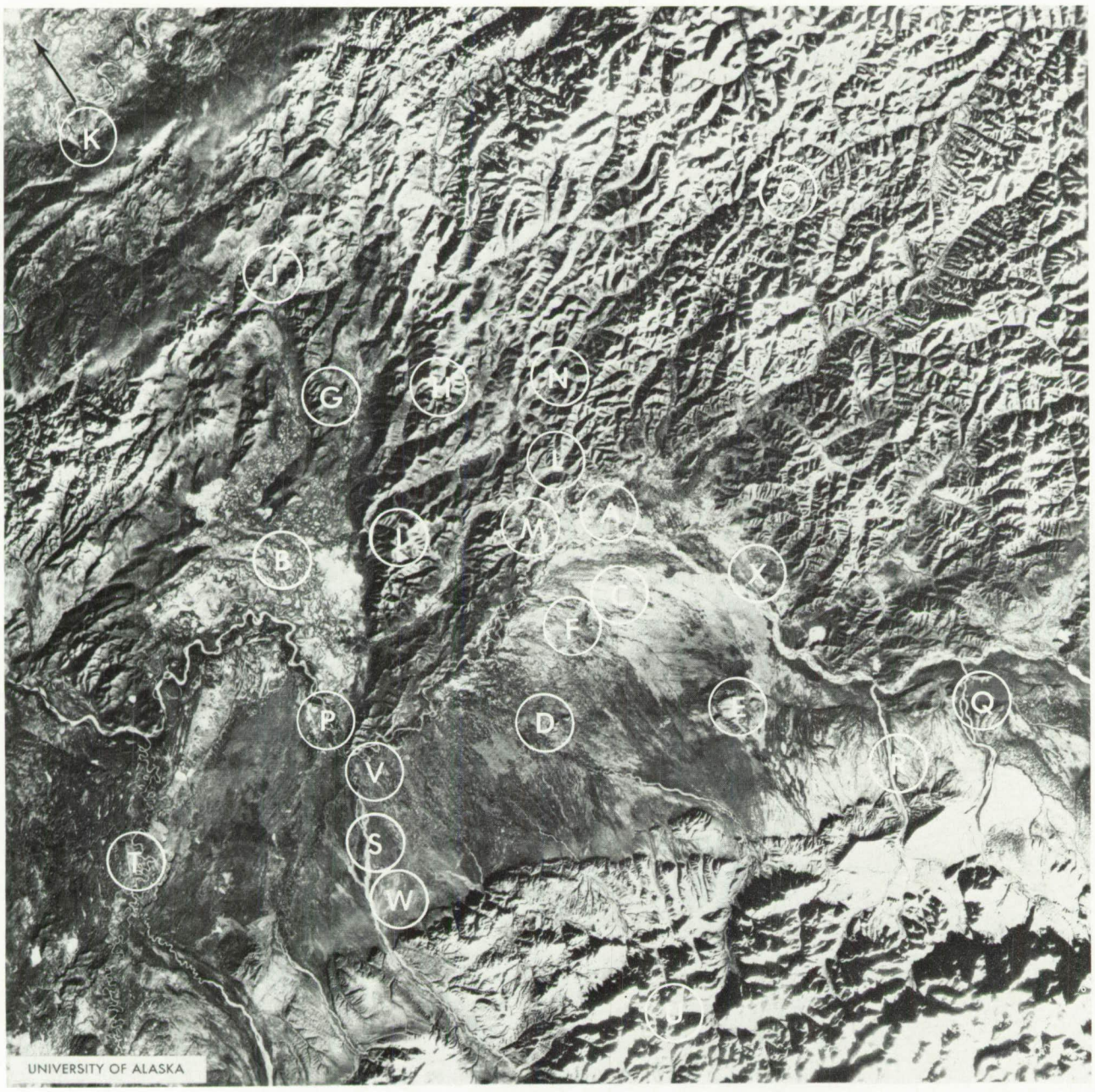
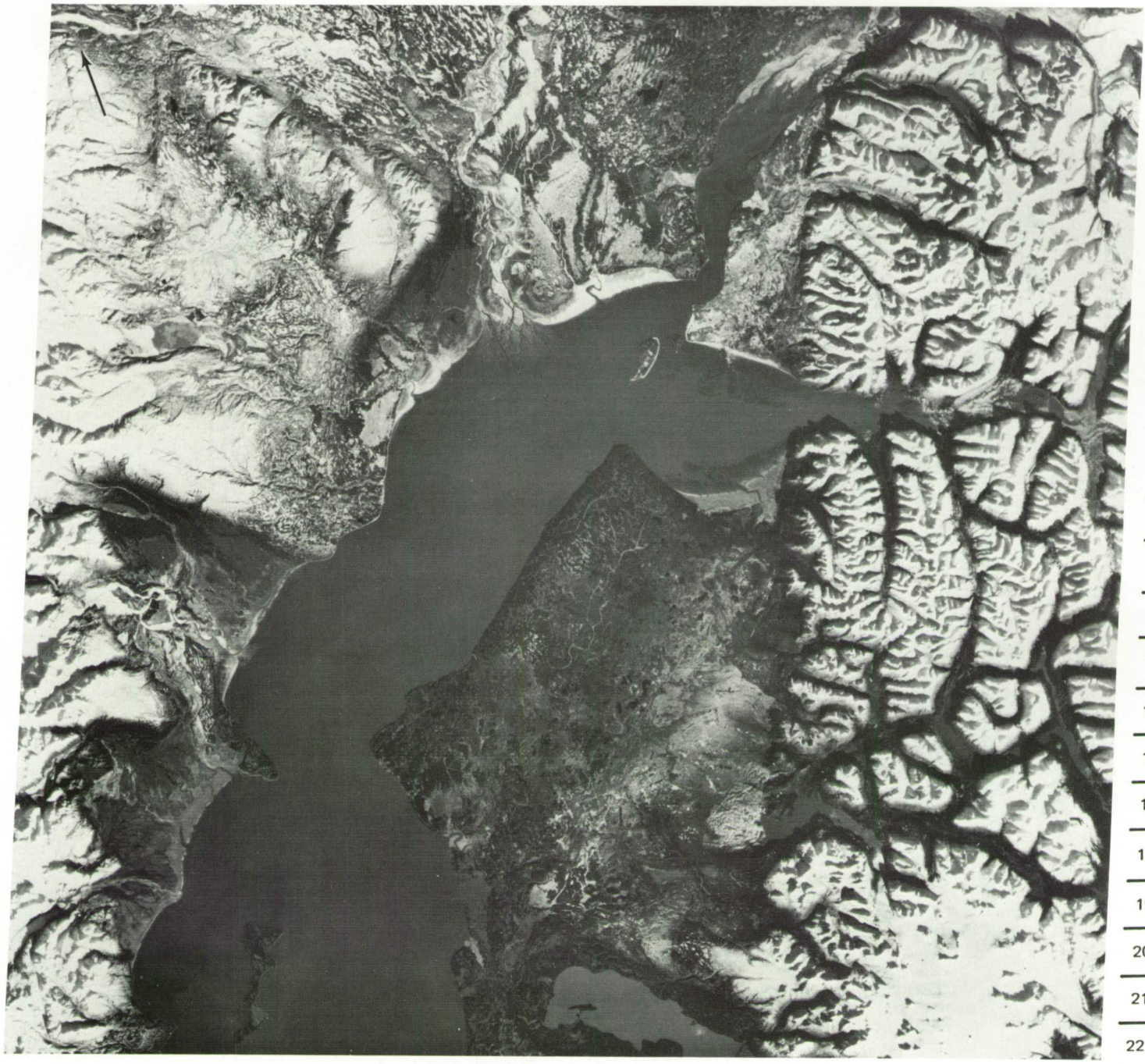


PLATE 140

FAIRBANKS AREA, ALASKA: This scene of central Alaska is a mosaic of four Landsat images made by the University of Alaska. West of Fairbanks (*A*) Minto Flats (*B*) is covered by low brush muskeg interspersed with stunted black spruce, birch, and aspen that border the numerous small thaw lakes (light ice or snow covered) and meandering stream courses. Thick ground cover includes sedges, mosses and floating mats of aquatic vegetation on many of the lakes. Permafrost usually occurs near the surface except in the immediate vicinity of larger lakes and active stream courses. The extensive flat area south of Fairbanks is locally known as the Bombing Range (*C*). Vegetation in this area is primarily low brush muskeg, with linear developments of black spruce, birch, and aspen. (The linearity is caused by locally better drained areas near active or abandoned stream courses.) Wood River Buttes (*D*), Blair Lake Buttes (*E*), and Clear Creek Buttes (*F*) are well-drained and have a well-developed mixed spruce, aspen, and birch forest. Shallow, continuous permafrost occurs throughout the area except for the buttes and areas adjacent to large streams or lakes. Closely spaced white spruce forest (*G*) covers most of the moderately to well-drained upland portions of this scene. The timberline ranges from 700-meter (2300-foot) elevation in the western part of the scene to about 940 meters (3100 feet) in the eastern part. The alpine tundra appears white due to snow cover. This tundra association grades from willows and alders 2 to 4 meters (8 to 13 feet) high near the timberline to dwarf willows and alders, herbs, and lichens at higher elevations. The alpine zone is barren above about 1100 meters (3700 feet). Wickersham (*H*), Murphy (*I*), and Livengood (*J*) Domes are identified.

The Yukon River and Rampart Canyon (*K*) are located in the north corner of the image. Evidence of gold dredging can be seen in the Goldstream valley near Fox (*L*) and at Ester Creek (*M*). The "tailings" left by the dredges cover the flood plains of streams and for the most part are unvegetated and highly reflective. Permafrost is absent in these areas. Extensive tailing piles near Chatanika (*N*) have been overgrown with vegetation and are distinguishable only on very close examination. The Yukon-Tanana Uplands (*O*) were not modified by continental glaciation but local valley glaciers eroded cirques on some of the highest peaks in the uplands. The Tanana (*P*) River and several large tributaries, Delta Creek (*Q*), Little Delta River (*R*), Nenana River (*S*), and Kantishna River (*T*) (note the extreme meandering), drain a large portion of the uplands and the Alaska Range (*U*). Several towns and roads are visible throughout the scene: Nenana (*V*), Rex and Browne (*W*), and the Alaska Highway (*X*).

PLATE 141



COOK INLET AND ANCHORAGE AREA: Anchorage (*N*–6) is situated between Knit (*N*–5) and Turnagain (*P*–9) Arms in the northern portion of the inlet. Fire Island (*M*–8) is located approximately 8 kilometers (5 miles) off the coast west of Point Campbell. The Susitna River (*J*–5) is a major contributor of sediment to the inlet. Note the well-defined tidal channels that have formed at the river mouth on the tidal delta. Chickaloon Bay (*N*–10) and other areas around the border of the northern inlet have extensive tidal flats (*N*–3) that are exposed during low tide. McArthur River (*D*–13), a glacial stream originating in the Chigmit Mountains to the west, drains into the inlet in Trading Bay (*F*–13). Trading Bay has 14 oil-producing platforms around Middle Ground Shoal and is the major site of active petroleum production in the Cook Inlet area. There is an oil refinery and a tanker terminal located in Nikishka (*H*–16).

Kenai (*I*–17), at the mouth of the Kenai River, is a fishing and oil and gas processing center. The Kenai Lowland (*L*–14) is a flat, glaciated plain marked by numerous lakes and swampy areas. The Kasilof River (*J*–20) begins at Tustumena Lake (*M*–21) and discharges into the inlet approximately 4 kilometers (13 miles) northeast of the lake. Kalgin Island (*E*–19) is located in the central portion of the inlet and separates the two deep submarine channels found between Harriet Point and Kasilof. Near the mouth of the Drift River is an offshore tanker terminal, an oil storage area, and a landing strip (*C*–18). Sediment patterns and a tongue of oceanic water (*H*–21) with a lower suspended sediment concentration than the surrounding water are discernible in the inlet. Kenai Mountains (*S*–12) border the inlet on the east and the Aleutian Range (*A*–13) is the western border. Recessional moraines (*N*–15) on the Kenai Lowlands mark the terminal positions of Pleistocene glaciers that advanced from the Kenai Mountains.

Additional features are Harding Icefield (*T*–20); Skilak Lake (*Q*–17), with clouds over the western portion; snow-covered Capps Glacier (*B*–8); Triumvirate Glacier (*A*–7); and Beluga Lake (*C*–7), partially frozen. *1103–20513;* November 3, 1972.

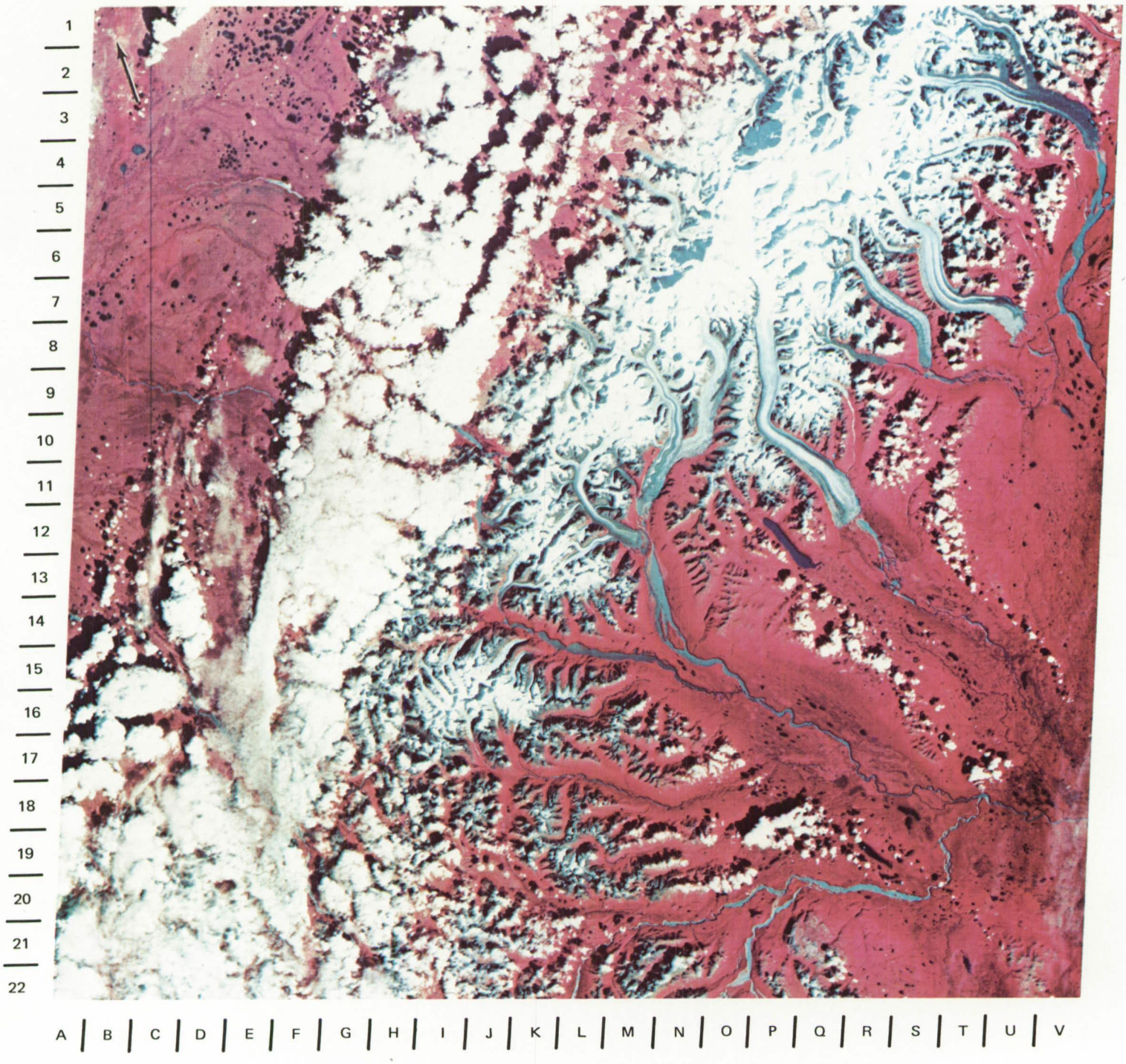


PLATE 142

ALASKA RANGE: The area shown is situated approximately 225 kilometers (140 miles) north of Anchorage. Mount McKinley, 6194 meters (20 320 feet) (*P*–4), the highest mountain in North America, and the surrounding high peaks in Mount McKinley National Park are snow covered and glaciated. Eldridge (*S*–3), Buckskin (*T*–4), Ruth (*S*–5), Tokichitna (*R*–7), and Kahiltna (*Q*–11) glaciers flow into the Susitna River valley (*V*–13) on the east. Notice the well-developed medial, lateral, and terminal moraines in most of the glaciers. The wavy appearance (*R*–7) in the medial moraines is indicative of a surging (rapidly moving) glacier. The different colors in the glaciers are a result of the amount of debris within or on the ice: deep blue is clean ice and the brown or black color is dirty ice (*T*–3). Altocumulus (*C*–15) and stratus (*G*–11) clouds cover a portion of the area west of the range, and scattered cumulus (*S*–15) clouds top many of the highlands on the east. The valleys (*S*–13) on the southeast were glaciated during the Pleistocene and are now blanketed with glacial outwash and till.

The Denali fault, one of the great series of faults paralleling the southern coast of Alaska, is visible at *J*–10 and *N*–5. The fault appears to have offset a number of valleys to the right, and is believed to have undergone right-lateral movement. However, its history is complex, and vertical movement has also occurred along it. The Denali and other faults of southern Alaska are presently active, producing frequent earthquakes. This activity is thought to be the result of sea-floor spreading in which the Pacific crust is being thrust under the North American plate beneath southern Alaska and the Aleutian Islands. *1033–21020;* August 25, 1972.

PLATE 143



THE "FINGER LAKES" OF ALASKA: This part of southwestern Alaska is just north of Bristol Bay on the coast. The western half of the area shown is a complex of folded Jurassic and Cretaceous rocks intruded here and there by granitic stocks of Tertiary age. These make up the Tikchik Mountains (*G*–14), which rise to more than 1500 meters (5000 feet) at Mount Waskey (*H*–13). This range is the eastern front of the Kilbuck Mountains (*A*–3), an extension of the Kuskokwim Mountains that is parallel to and northwest of the Alaska Range. Near the crest of the Tikchiks is a linear valley (*F*–12) expressing the trace of a large strike-slip fault that may be the westernmost extension of the great Denali fault system. (See plate 142.)

A few small active glaciers persist in the Kilbuck Mountains. Late Pleistocene alpine glaciation in the Tilchik Mountains produced a series of elongated valleys extending eastward into the piedmont. Most of the valleys are now occupied by fjordlike lakes (cut below sea level), including Nuyakuk (*J*–11), Nerka (*L*–15), and Nunavaugaluk (*A*–20) Lakes. Glacial erosion also enlarged the fault valley where Togiak Lake (*F*–17) and its draining Togiak River (*E*–20) are developed. This band 6 (IR) image also reveals some of the outwash plain deposits (*P*–15) in the Quaternary lowlands east of the "Finger Lakes." This lowlands is drained by the Nushagak River (*U*–16) and tributaries from the piedmont lakes.

The higher mountains tend to be barren or covered with alpine meadows in summertime. Spruce and birch cover the eastern slopes of the Tikchik Range and the Nushagak River valley with much of the remaining lower areas covered by tundra. *1018–21200;* August 10, 1972.

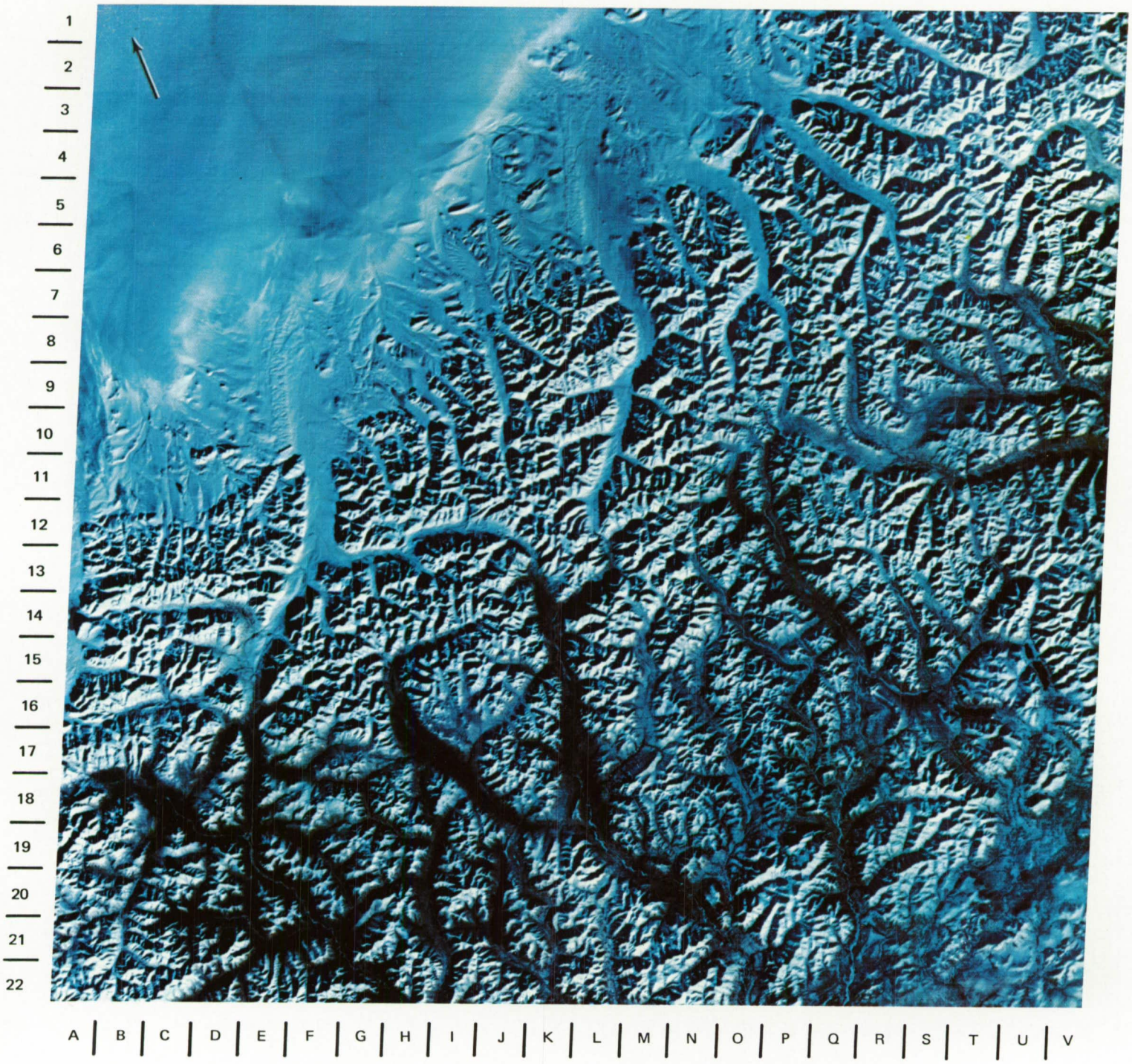
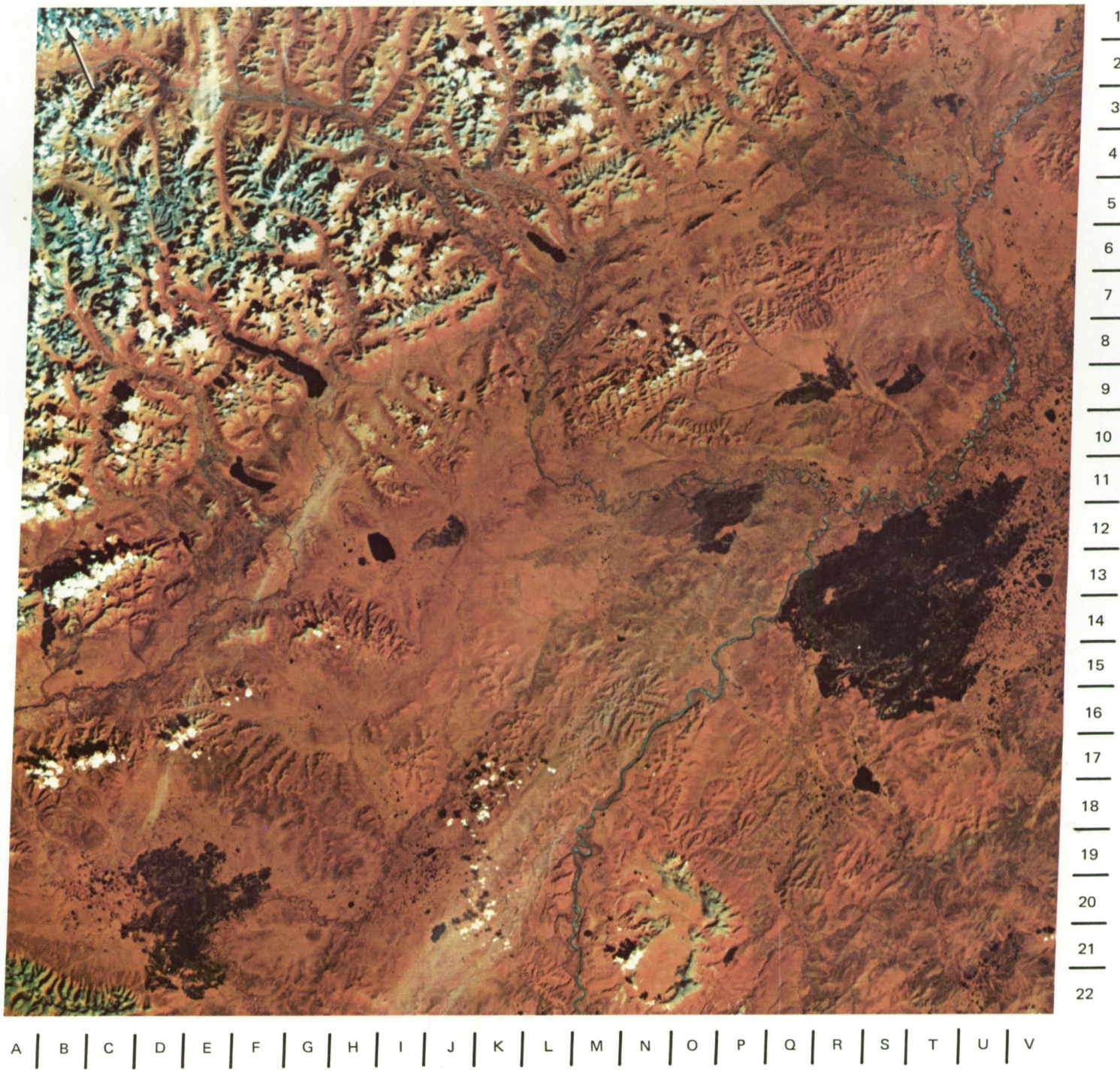


PLATE 144

BROOKS RANGE: The proposed route for the oil pipeline through the Brooks Range (*M*–14) follows the valleys identified by *O*–6, *P*–12, and *Q*–18. The route primarily follows U-shaped valleys glaciated during the Pleistocene. These valleys generally have wide, gently sloping floors and provide the best access through the mountains within this image. The route parallels these rivers going northward: Middle Fork Koyukuk River (*O*–6) from Cathedral Mountain (*R*–21) past Wiseman (*Q*–18) to Sukakpak Mountain (*R*–15; *R*–20), where the Bettles River (*S*–15) joins to form the Dietrich River (*Q*–14), then along the Dietrich River past Snowden Mountain (*Q*–12), then it passes over a narrow divide to the North Fork River (*Q*–10) and crosses the Continental Divide (*N*–9; *T*–3) over a narrow spur (*P*–8) (⌐1400 meters (⌐4700 feet) elevation) into the Atigun River (*O*–6) valley; then it runs along this river to Galbraith Lake (*N*–4) (frozen and snow-covered on the image) and shifts east through a narrow tributary valley to the Sagavanirktok River (*O*–2), which it follows to the Prudhoe Bay field on the Arctic Coastal Plain. Note the faint red tone (*E*–14; *U*–7) of the vegetation showing through the light dusting of snow in many of the valleys and lowlands. The snow enhances the topography of many terminal and recessional moraines (*E*–7; *K*–4; *L*–2 on the Southern Foothills Province (*C*–9) of the Brooks Range. U-shaped valleys (*H*–14; *M*–19; *U*–10) and sharp Alpine mountains with numerous cirques (bowl-shaped valley heads) (*C*–14; *T*–18; *V*–12) and aretes (sharp ridges) (*E*–15; *K*–9; *T*–6) dominate the landscape of this area. Clouds (*C*–2) obscure the topography in the northern part of the image. *1072–21173;* October 3, 1972.

PLATE 145



WALKER LAKE AREA, ALASKA: Seven burn scars (*T*–3; *S*–9; *Q*–9; *P*–11; *S*–14; *V*–12; *E*–20) dominate this image of a portion of the Intermontane Plateau province in western Alaska. The large burn scar (*E*–20) in the eastern part of the scene shows the extent of the Pah River flats fire that was burning during the Landsat overpass on July 26, 1972 (1003–21355). Considerably more area was charred since the July 26 image was acquired. The largest fire (*S*–14) in the area burned approximately 1600 square kilometers (600 square miles) in and around the Kanuti Flats (*V*–11) south of the Koyukuk River (*N*–17). The burn scar (*S*–9) in the uplands east of Allakaket (*R*–11) superficially resembles a large lake but reference to topographic maps confirms that no lake exists at this location. Walker Lake (*G*–8), Iniakuk Lake (*L*–6), and Nutuvukti Lake (*F*–10) occupy abandoned glacial valleys that were covered with ice from the early to late Pleistocene. Multiple glaciations throughout the Pleistocene sculptured the present topography of the Brooks Range (*F*–2).

Note the complex meandering and braided character of the Kobuk (*E*–13), Alatna (*L*–10), John (*S*–4), and Koyukuk (*N*–17) Rivers. Oxbow lakes (*N*–11; *G*–13) and point bars (*T*–10) are numerous along these rivers. Vegetation associations on the uplands and the low lying areas are very evident based on the tonal differences. Bedrock exposures (lighter gray tones) occur on the mountain crests. The Kobuk Fault Zone (*P*–4; *G*–10; *T*–6; *L*–10) and related northeast-trending fractures (previously unknown) have been identified in the Landsat imagery. The fractures are probably shears formed during strike-slip movement along the fault zone. Other points of interest are the Hughes landing strip and Hughes village (*M*–21), Indian River Placer mine and landing area (*O*–20), Zane Hills (*B*–21), Hogatza River (*H*–20), Lockwood Hills (*E*–16), Bettles Field (*U*–5), and Bettles (*T*–5). *1037–21234;* August 29, 1972.

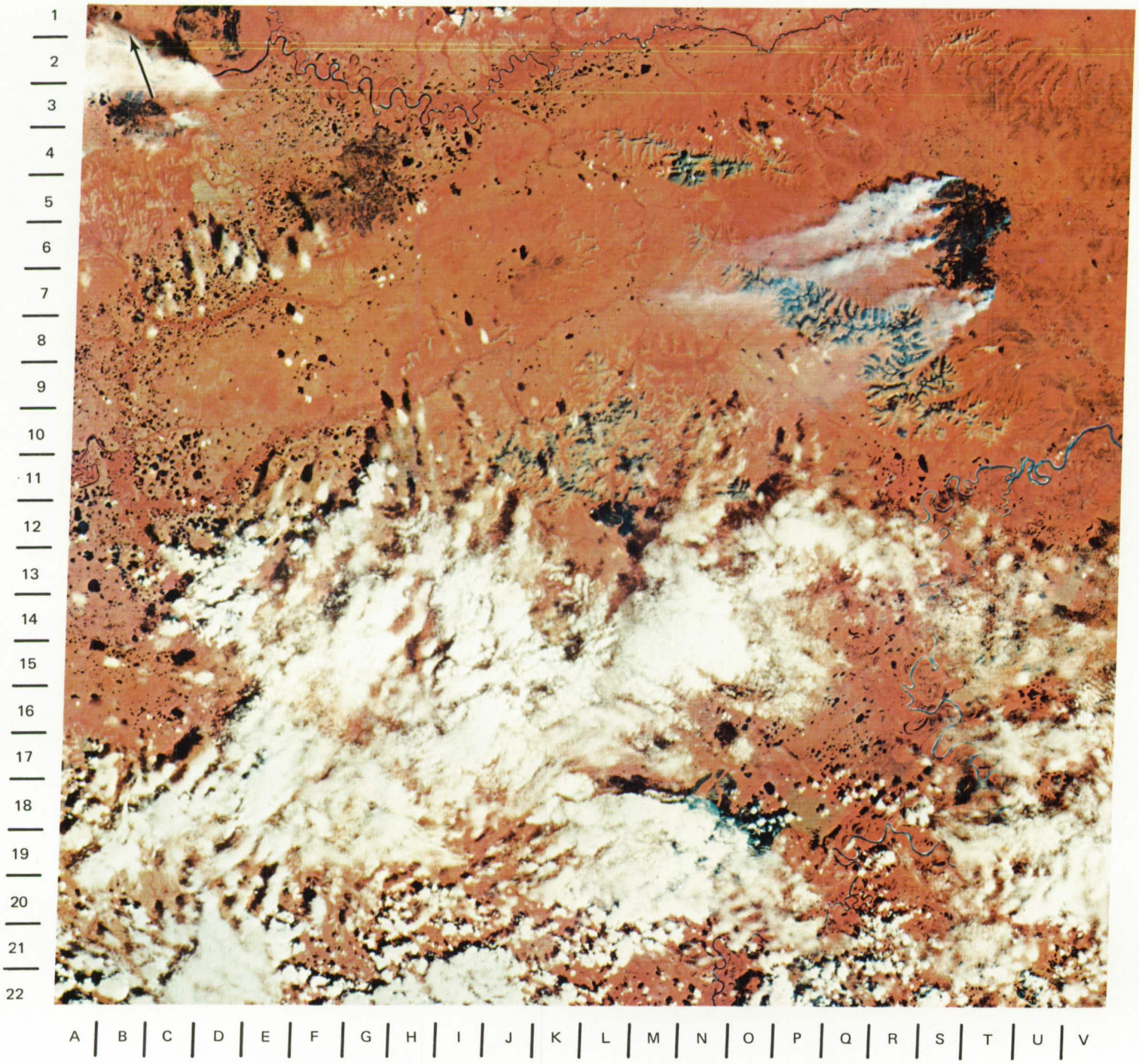


PLATE 146

UPPER KOYUKUK-KOBUK RIVER AREA, ALASKA: This scene is located about 390 kilometers (240 miles) northwest of Fairbanks. A forest fire (*S*–7) was burning in the Pah River flats area and had burned approximately 330 square kilometers (81 000 acres) when this image was acquired. Recently burned areas (*S*–5) appear black while old burn scars (*F*–4) show a lighter tone due to revegetation. Clouds (*A*–17; *V*–17) cover the southern portion of the image and cloud shadows (*N*–16) may be confused with the many lakes (*Q*–16). Dahl Creek Airstrip (*I*–1) and Shungnak (*H*–2) and Kobuk (*V*–2) villages along the Kobuk River (*N*–1) are the only indications of human activity. Kugarak River (*C*–7), its tributaries, and several other rivers are well defined by a dark red tone. This tone is related to vegetation density and species composition along the river bank. It is distributed in a gallery forest pattern (of closed spruce hardwoods) along several streams. The Kobuk and Koyukuk (*U*–10) Rivers are characterized by abundant meander scars and oxbow lakes (*F*–2); e.g., Pitlik Lake (*E*–2). Point bars (*J*–2) and midchannel islands (*U*–10) (light blue color) also occur along the rivers. A clearly defined dendritic drainage pattern (*A*–5) occurs on the south side of the Waring Mountains. The alternating dark and light red tones reflect vegetation differences along the streams and on the interstream areas, respectively. Vegetation tones differ on mountain slopes and wet lowlands with numerous lakes. Extensive bedrock exposures (dark areas) occur on the peaks and crest lines of the Lockwood Hills (*M*–4), Zane Hills (*P*–7), and the Purcell Mountain area (*J*–10). Eolian deposition was active in this area during the Pleistocene when winds swept across extensive periglacial outwash plains. Dunes (irregular-shaped, light-colored features) are found in several locations: Little Kobuk Sand Dunes (*C*–3), eastern portion of Great Kobuk Sand Dunes (*A*–3), and Nogahabara Sand Dunes (*N*–17) (somewhat hidden by clouds). Other features include Selawik River (*D*–10), Hogatza River (*U*–18), and Cutoff slough (*T*–11). *1003–21355;* July 26, 1972.

PLATE 147



POINT BARROW, ALASKA: Point Barrow (*C*–3), the northernmost spot in the United States, is just under the clouds. Frazil ice and ice floes (*E*–2) border the offshore islands (*F*–3; *G*–3) east of Barrow. Nearly the entire land area is part of the Arctic Coastal Plain province (*S*–10). The Northern Foothills province (*V*–21) of the Brooks Range is just at the lower edge of the image. Note the varied shapes and sizes of the thaw lakes. Some appear to be partially frozen (*C*–9) (light gray cover) even in late July. Cloud shadows (*F*–16) in the southern portion of the scene produce confusing patterns on the ground, and thaw lake outlines are more difficult to define. Note the meandering patterns and braided nature of the Meade (*E*–12) and the Ikpikpuk (*P*–12) Rivers. A large delta (*O*–5) has formed where the Ikpikpuk River discharges into Smith Bay (*N*–4) on the Arctic Ocean (*M*–1). Many oxbow lakes (*S*–17) and meander scars (*H*–18) are present along the river courses. Other features are Teshekpuk Lake (*S*–6), and Dease Inlet (*I*–5). *1006–21510;* July 29, 1972.

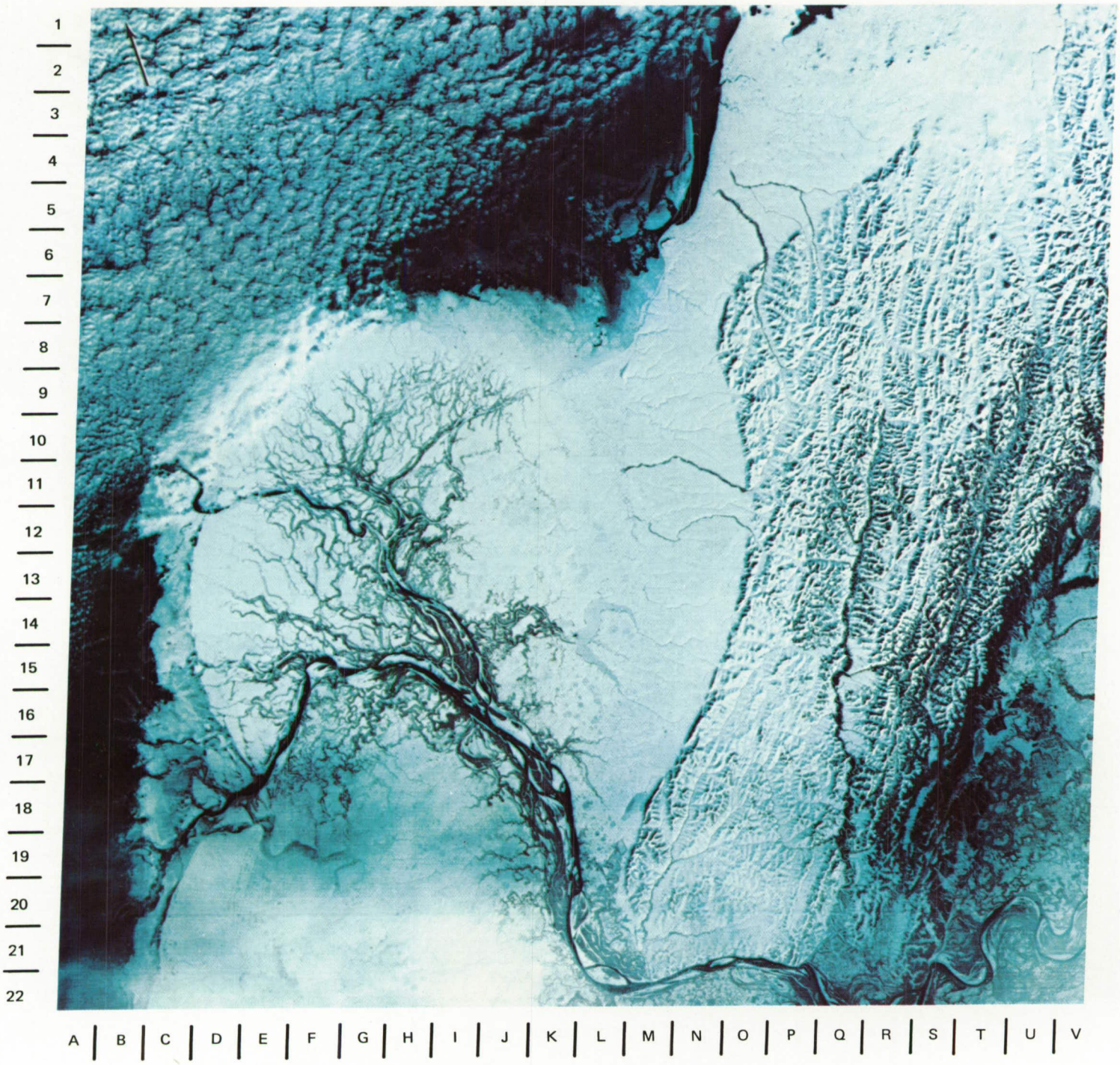


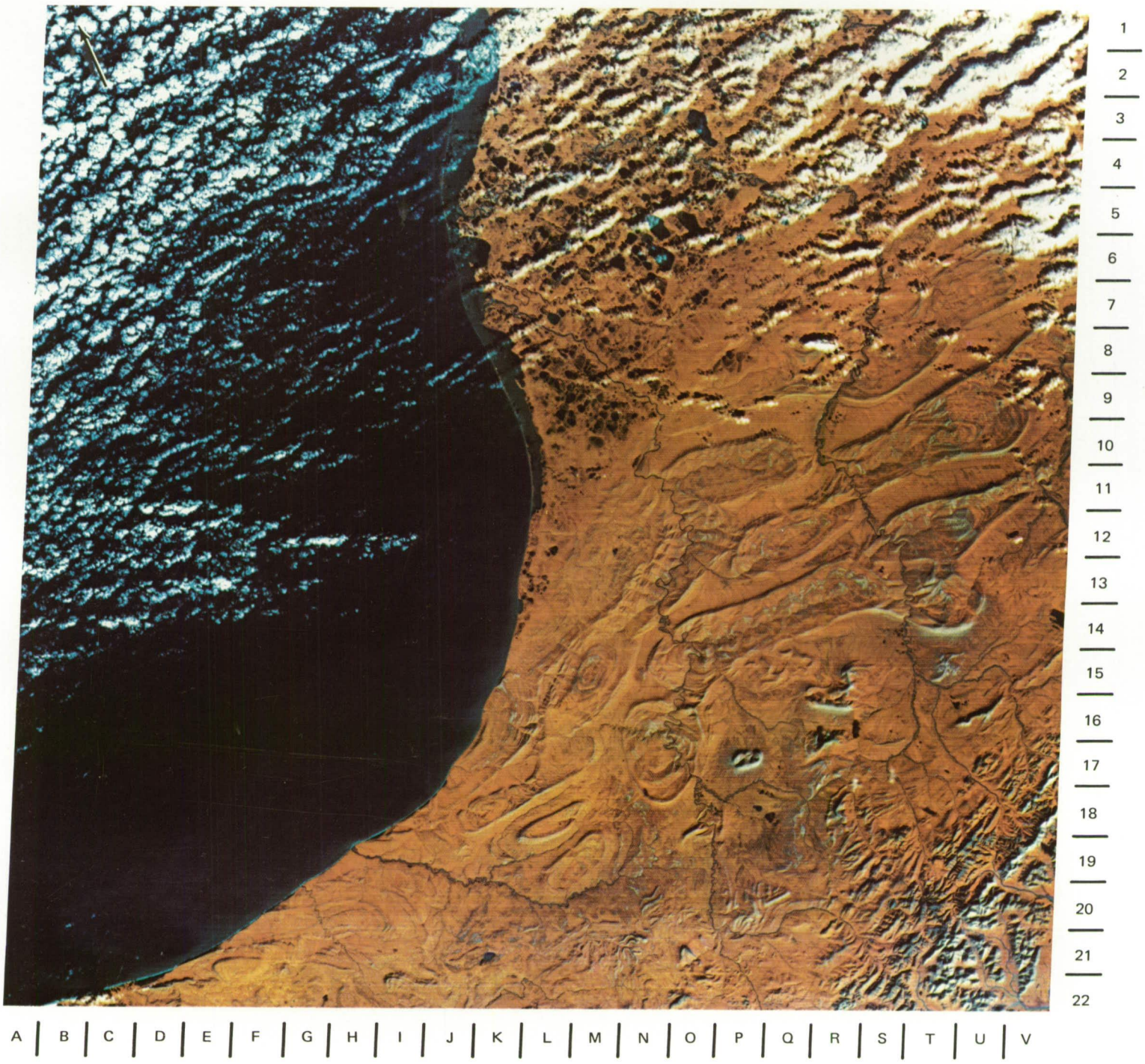
PLATE 148

THE YUKON DELTA, ALASKA: This remarkable image illustrates the effect of a "dusting" by snow on the flatlands delta (*I*–12) of the Yukon River as it enters the Norton Sound off the Bering Sea. The many anastomosing channels or distributaries of the river are graphically enhanced by the sharp contrast between snow and river banks and water. This delta appears to have an almost perfect semicircular outline here but the perimeter has been extended by sea ice through which several large channels have been cut beyond the summer land/sea interface.

This part of western Alaska is a broad lowlands consisting of late Tertiary and Quaternary marine and continental deposits brought in by the Yukon, Kuskokwim, and other rivers. In this scene, the Yukon passes through hills and ridges (300 to 900 meters (1000 to 3000 feet) above sea level) of folded Cretaceous sedimentary rocks crossed by valleys drained by the Andreafsky (*Q*–16) and Atchueelinguk (*T*–17) Rivers. Spruce and birch forests occur within the meander-cut valleys of these rivers, but tundra covers most of the lowlands elsewhere.

The region was not covered by glaciers during the Pleistocene. Much of it was submerged during interglacial warm periods when sea level was higher than at present. However, today and in recent times this region has lain in the broad discontinuous permafrost belt that runs across central Alaska. The lowlands area contains thousands of thaw lakes formed from melting of the permafrost. *1455–21460;* October 21, 1973.

PLATE 149



CAPE BEAUFORT, ALASKA: A striking example of inverted topography, with anticlinal valleys and synclinal hills, is located east of Cape Beaufort (*R*–15). The bedding planes in most of these structures between Cape Beaufort on the Chukchi Sea (*E*–11) and the De Long Mountains (*U*–20) have an east to west orientation. The Kulpowruk (*N*–11) and Kokolik (*R*–9) Rivers, eroding across the geological structures, are probably superimposed streams. The thaw lakes (*M*–7) in the north-central portion of the scene are indicative of an area of low topographic relief, fine-grained sediment, and a high ground-ice volume. The nearly black water in the lakes is very clear, while more turbid or shallow water would appear to be a lighter blue owing to reflectance from suspended sediment. The approximate locations of the axes of some previously recognized synclines are illustrated on the image. These include Howard Syncline (*O*–9; *T*–7), Meat Mountain Syncline (*U*–11), Poko Mountain Syncline (*R*–15), and many unnamed synclines (*P*–10; *Q*–12; *S*–10; *P*–14; *S*–13; *O*–16). Three additional folds (*L*–17; *L*–18; *M*–19) were recognized but not identified as synclines or anticlines; they appear to be synclines. The synclinal folds are composed of undifferentiated sediments from the Nanushuk group (Lower Cretaceous) and the Colville group (Upper Cretaceous). The major anticlinal folds (*O*–13) occupy the valleys and are composed of Lower Cretaceous, undifferentiated Okpikruak, and Torok formations. Additional features and points of interest are Point Lay (*J*–5), Pitmegea River (*I*–19), and altocumulus clouds (*U*–2). *1046–22143;* September 7, 1972.

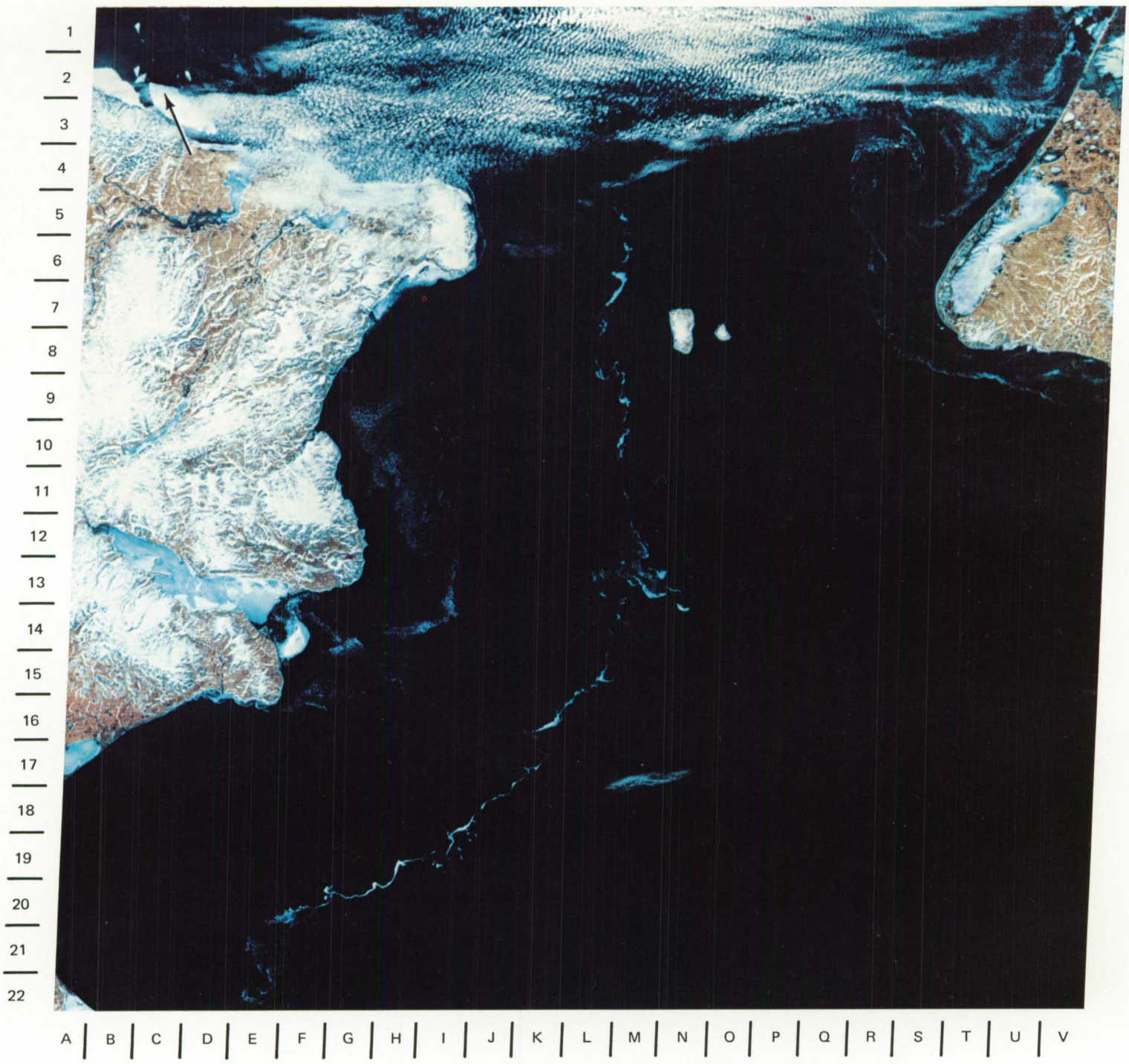


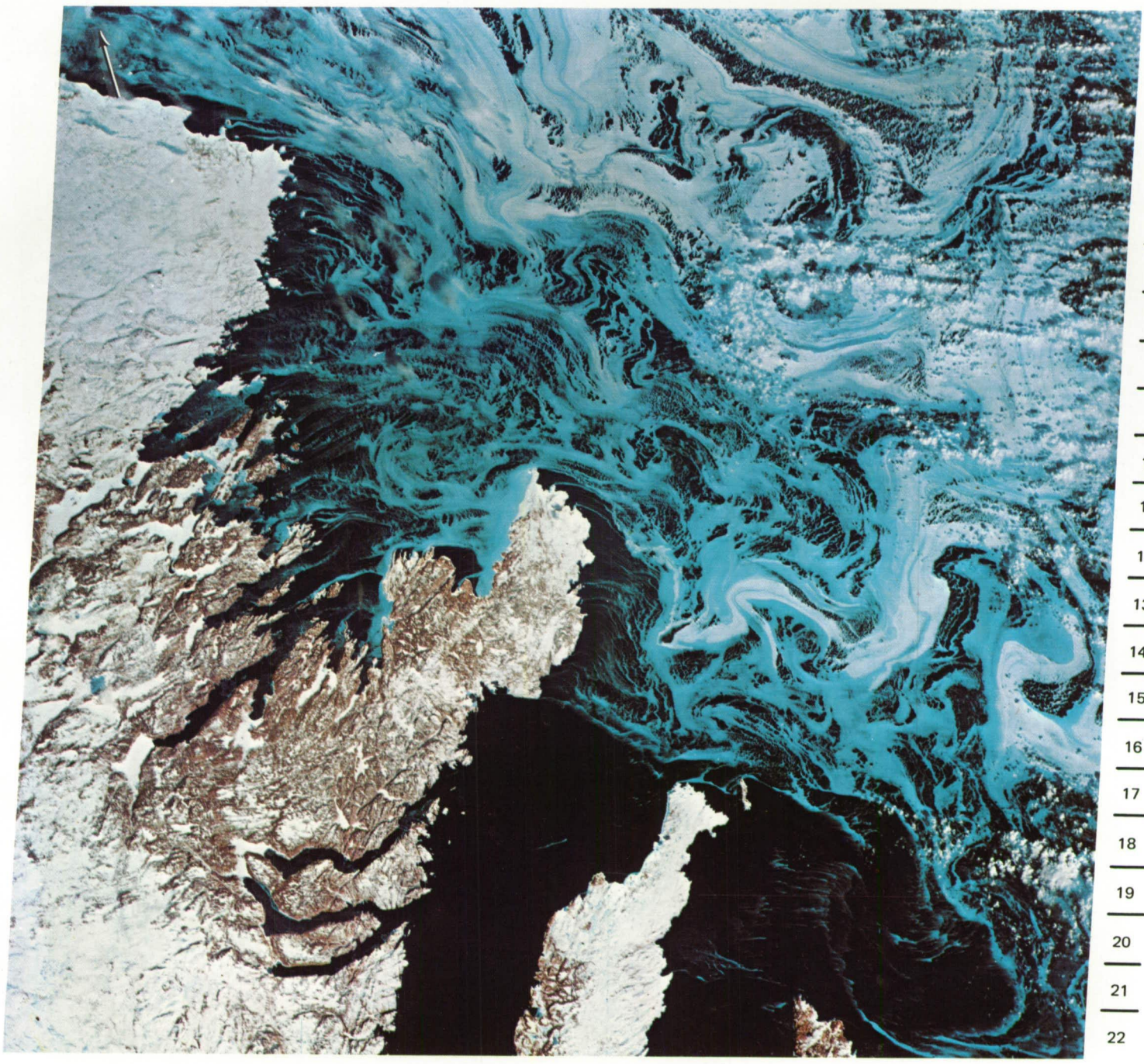
PLATE 150

THE U.S.-SOVIET BORDER: Following the sale of Alaska to the United States by the Imperial Russian Government, the border between eastern Siberia and the western tip of Alaska (at 168° W) was formally set in 1867 to pass through the Bering Straits between the islands of Ratmanova (*M*–7) on the Soviet side and Little Diomede (*N*–8) on the U.S. side. This boundary also coincides with the international dateline, which then runs southwest past the west end of the Aleutians 1600 kilometers (1000 miles) away.

The Soviet territory lies at the tip of the Ckukotskiy Peninsula (*C*–10). This snow- and tundra-covered land consists of mid-Paleozoic rocks along the north shore where drained by the Chegitun River (*B*–5) and granitic intrusives further south inland from the ice-locked bay (*D*–13). The U.S. segment shows Cape Prince of Wales (*S*–7) at the west end of the Seward Peninsula. Rocks there are Ordovician sediments to the east and mid-Paleozoic strata along the cloud-covered lagoons.

The irregular arc of bluish-white segments in the Bering Strait is probably a line of piled-up sea ice. *1335–22215;* June 23, 1973.

PLATE 151



SEA ICE OFF THE EASTERN COAST OF NEWFOUNDLAND: This swirling mass of brash and drift ice occurred in the Atlantic Ocean off the east coast of Newfoundland. The prevailing wind at the time of observation was westerly as can be seen from the streamlines of ice flowing around the north-trending peninsulas (*K*–13). The bay ice (*D*–16) appears to be thicker and more solid than the sea ice, probably because of decreased salinity from the influx of freshwater streams and because of the shelter in the lee of the shores. Scattered, low cumulus clouds (*R*–6) occur over the main ice mass.

The coastal area of Newfoundland shown here includes Cape Freels (*C*–5), Bonavista Bay (*H*–7), Cape Bonavista (*K*–12), Trinity Bay (*K*–17), and Grates Point (*M*–20) and Cape Saint Francis (*Q*–22), two northward extensions of land separated by Conception Bay (*O*–21) on the Avalon Peninsula. Saint John's, the capital of Newfoundland, lies just off the image on Cape St. Francis. Note the road and power transmission line to fishing outports along the coast (*D*–13). Late Precambrian rocks underlie most of the land surfaces in the scene except for metamorphosed Paleozoic sedimentary rocks and associated intrusives around Cape Freels. *1570–13520;* February 13, 1974.

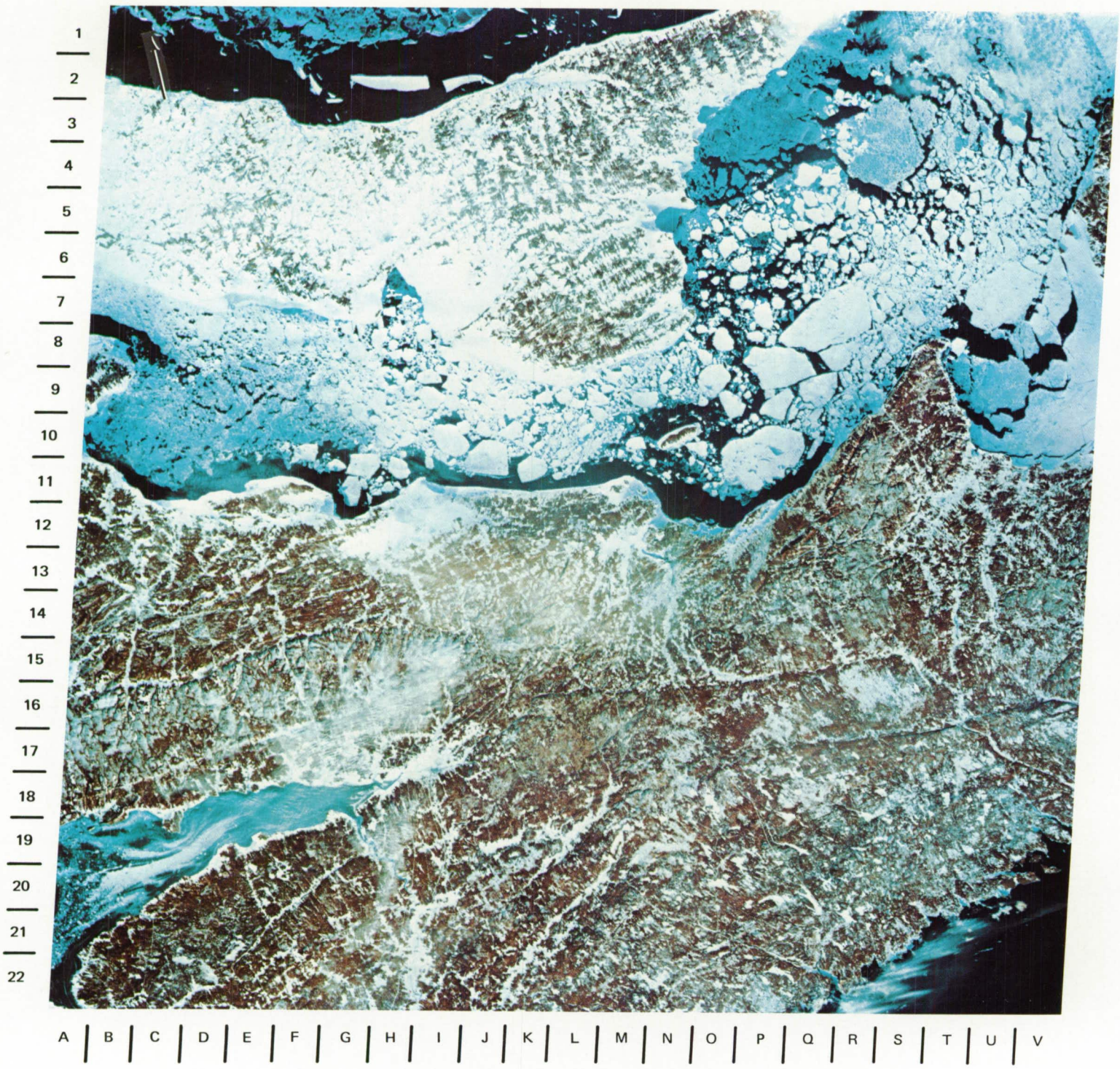
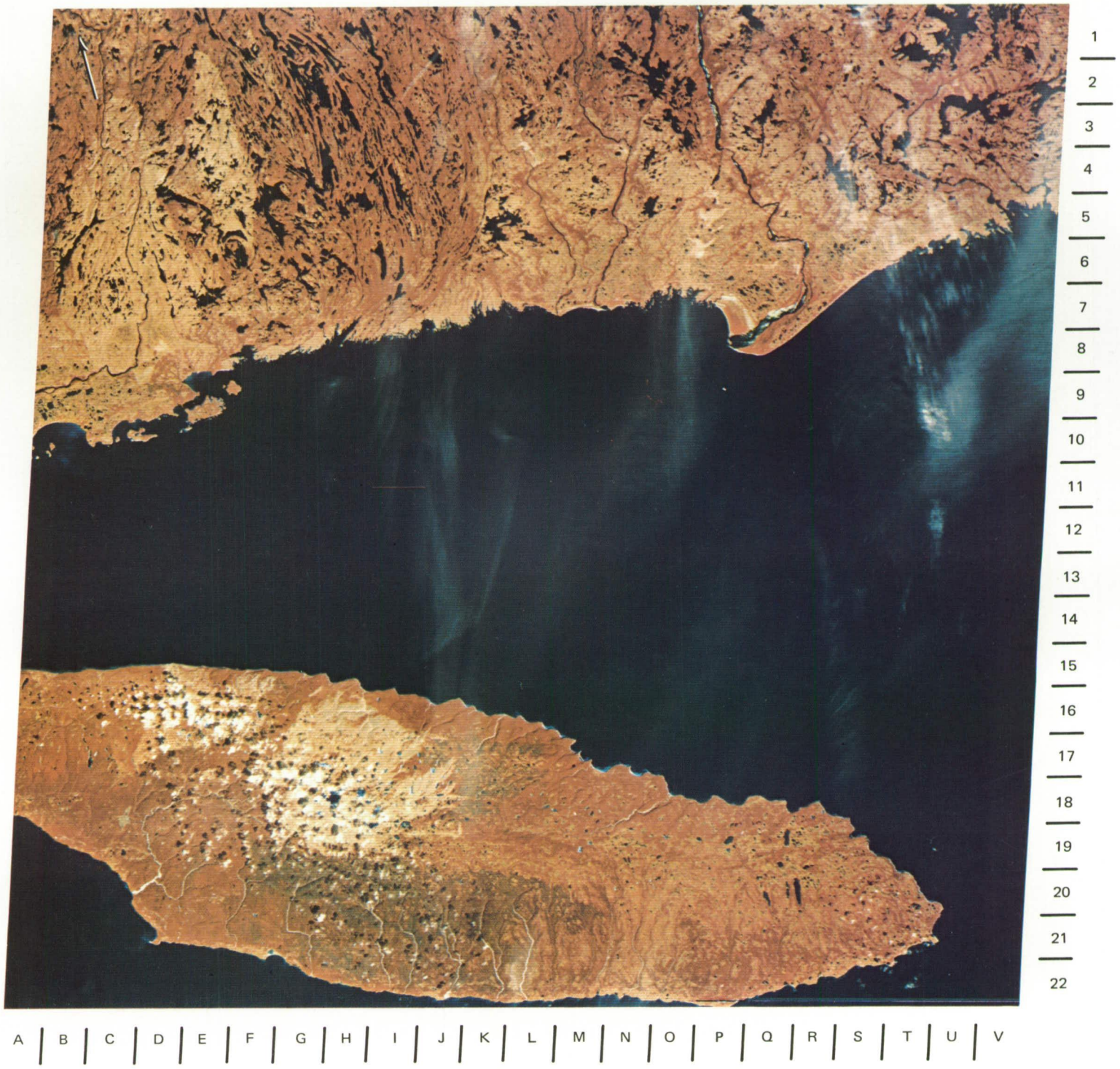


PLATE 152

PRINCE EDWARD ISLAND, NOVA SCOTIA: This winter scene shows the eastern half of Prince Edward Island (*I*–2) and north-central Nova Scotia. A daily ferry service to Charlottetown is maintained despite the floe-congested waters of Northumberland Strait (*E*–8). The strong currents resulting from the constricted tidal flow of Minas Basin (*E*–18) are revealed by the flow patterns in brash ice. Snow-covered clearings and field patterns show that farming is more intensive on Prince Edward Island than in this part of Nova Scotia. Networks of transportation and powerlines converge on Truro (*I*–18), located at the head of Cobequid Bay (*B*–10), which itself connects to the Bay of Fundy.

This part of eastern Canada is actually part of the Appalachian fold belt system that extends southwestward from the eastern United States into Texas and Mexico and northeastward through the Scottish Highlands and the Hercynian Mountain groups of Scandinavia. Rocks in the Atlantic Uplands from the Atlantic Ocean (*U*–20) inland are largely lower Paleozoic in age and were involved in the Acadian orogeny during the Devonian. Rocks of Carboniferous age dominate the area north of Cobequid Bay, including those of Prince Edward Island. These were folded and intruded during the maritime orogenic disturbance near the close of the Paleozoic. Lineaments (*D*–17; *P*–15; *Q*–10) representing several major faults are sharply expressed at the surface. The escarpment (*E*–13) of the Cobequid Mountains, a mass of Devonian granites reaching heights of 500 meters (1600 feet), marks a clear boundary with the maritime plain to the north. *1180–14314;* January 19, 1973.

PLATE 153



ANTICOSTI ISLAND: This scene of sparsely populated Anticosti Island (*N*–19) and the north shore of the Gulf of St. Lawrence illustrates the effect of insect and fire damage on the forests of an area where logging and tourism are important industries. The large light-colored area (*H*–17) is a scar from a forest fire in 1955. An adjacent light-colored area has been cut over by logging operations. In 1972, the trees on Anticosti Island were subjected to a major infestation by an insect called Hemlock looper. Large areas of damage are indicated by the dark purplish-red color (*J*–20; *K*–17; *R*–21), in marked contrast to the bright red (*F*–20) of healthy forest that was protected by spraying in 1972. Old fire scars show as contrasts in forest cover. Note the linear lakes in the folded metasedimentary rocks (*G*–4) of Middle Precambrian age and the irregular lakes in the granites (*B*–6) of the Precambrian terrain along the North Shore. Anticosti Island, consisting of Ordovician rocks on the north and Silurian rocks to the south, is a remnant of the sedimentary cover that forms part of the St. Lawrence platform between the shield on the north and the Appalachian fold belt (bounded by the Logan's Line fault) to the south. Thin cloud and haze introduce a bluish tint to the upper right corner of the scene. *1073–14354;* October 4, 1972.

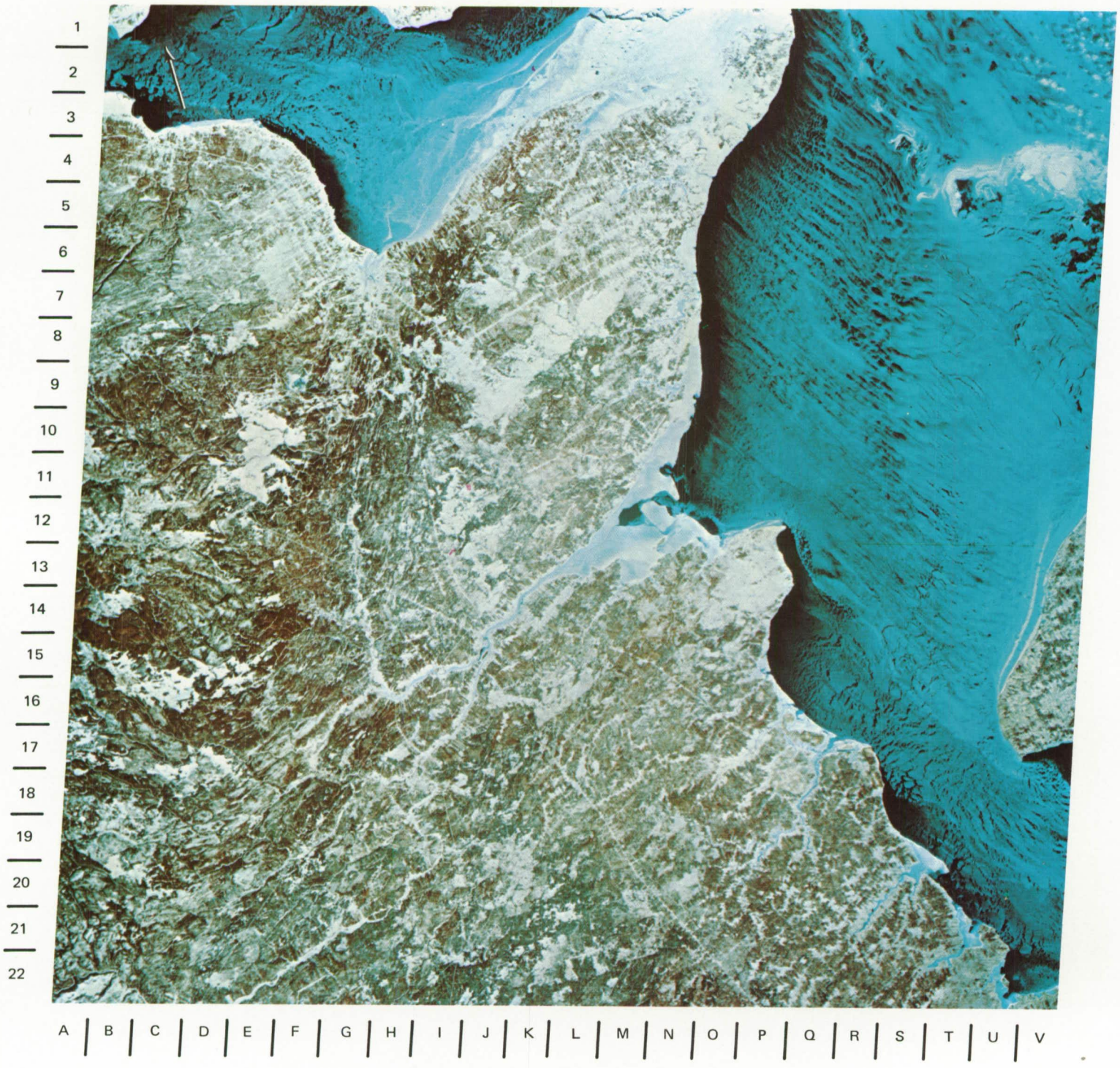
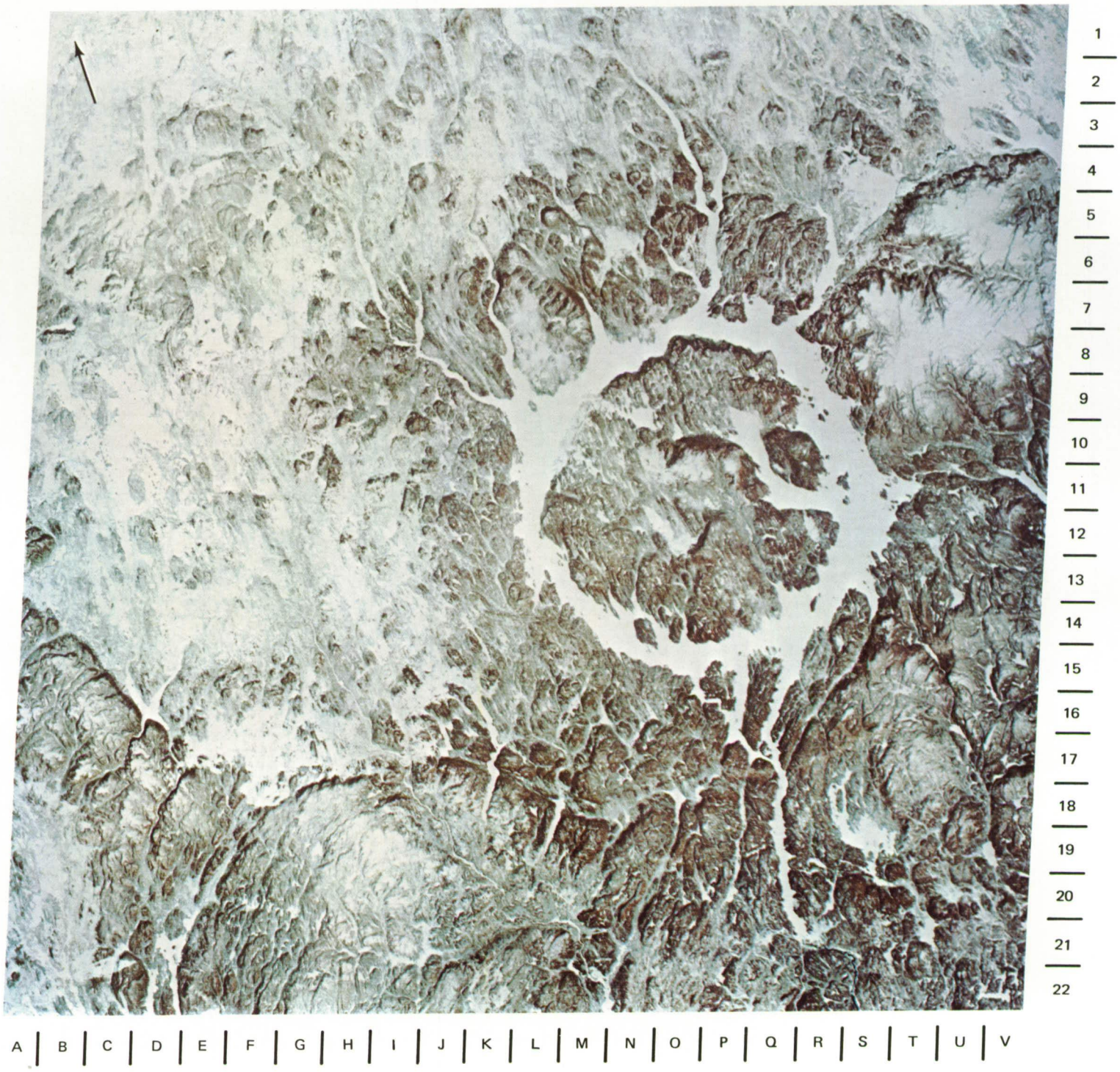


PLATE 154

NEW BRUNSWICK: This late winter scene of northeastern New Brunswick covers the Gulf of St. Lawrence (*T*–2), Northumberland Strait (*T*–17), Chaleur Bay (*G*–2), the western tip of Prince Edward Island (*V*–15), and the towns of Bathurst (*G*–7) and Chatham (*K*–14). Much of the sea is covered with brash and pack ice, which has been trailed into a streaky pattern by strong northwesterly winds. The ice has moved from the lee shores and has piled up against the northwest coast of Prince Edward Island and against Shippegan and Miscou Islands (*O*–2).

The snow cover enhances many details of the terrain. The area is heavily forested, and the economy of New Brunswick is heavily dependent on logging; this activity can easily be inferred from the conspicuous cut-over areas such as those at *E*–10 and *C*–15. Two base metal mines, Brunswick No. 12 (*E*–9) and Brunswick No. 6 (*F*–9), are visible. The lines crisscrossing the area, also enhanced by snow, are powerlines, railroads, logging roads, and highways. The main road south to Moncton, route 11, is especially noticeable (*L*–17; *P*–21). The area is geologically complex, most bedrock consisting of Paleozoic volcanics of the former eugeosyncline. However, glacial features such as the linear patterns at *G*–10 tend to obscure the bedrock geology. *1614–14373;* March 29, 1974

PLATE 155



MANICOUAGAN LAKE, QUEBEC: Manicouagan Reservoir occupies a circular depression some 66 kilometers (41 miles) wide located in east-central Quebec. Precambrian crystalline rocks constitute most of the higher central core but these are overlapped by Mesozoic volcanic rocks within this depression. This geological feature is believed by some to be a volcano-tectonic structure but the probability that it is a meteorite crater scar has recently gained wide acceptance. The circular depression serves as a water reservoir, here covered with ice, for the hydroelectric power station located at the dam (*R*–21), below which open water can be seen. Adjacent hills display prominent crag-and-tail morphology (*K*–3) resulting from Pleistocene glaciation. Such scouring also emphasized the contrasts between the major classes of Precambrian rocks, as represented by the rugged landforms developed on crystalline igneous and metamorphic rocks (*G*–19) and the subdued relief of the gneisses and schists (*D*–10).

The theory that the Manicouagan structure is the result of a great meteoritic impact will have major implications if verified, for it is as big (some 66 kilometers (41 miles)) as many of the large lunar craters. Because the Apollo program was curtailed before astronauts could visit one of these large craters, the study of terrestrial analogs may be the only way to learn in detail how they were formed. Proof of a volcanic origin for the Manicouagan structure would be of equal interest, because there are few if any volcanoes this large anywhere on Earth, especially not in Precambrian shield areas. *1636–14584;* April 20, 1974.

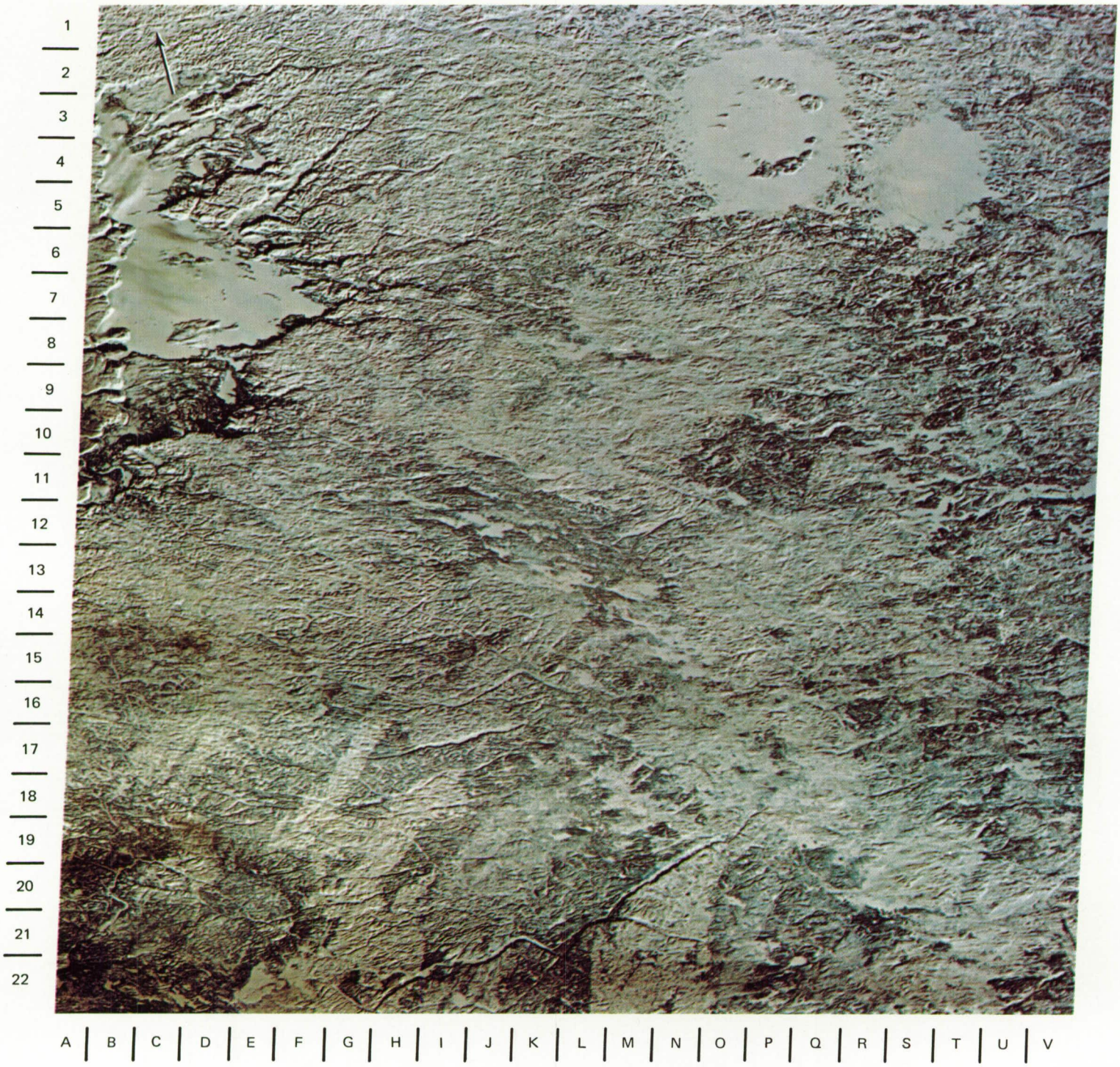


PLATE 156

CLEARWATER LAKES, QUEBEC: The two conjoined circular lakes in the upper right corner of this winter image are the east and west basins of Clearwater Lake in northern Quebec, near the shore of Hudson Bay. Both basins are located in massive to foliated Precambrian granitic rocks and have associated shock metamorphic features indicating an explosive origin. They are believed to be craters resulting from the impact of meteorites or, less likely, from the collapses of a pair of volcanic calderas. The crater constituting West Clearwater Lake is about 30 kilometers (20 miles) across and includes a central ring of islands composed of lavalike rock. The East Clearwater crater is about 20 kilometers (12 miles) across but its central uplift does not extend above the water. The large body of ice-covered water on the left side of the image is Richmond Gulf, indented along the great semicircular Nastapoka arc at the eastern end of Hudson Bay. The inlet from Hudson Bay is not frozen. The hills west of Richmond Gulf are formed by flat-lying volcanic flows. An interesting pattern is centered here on Richmond Gulf. The textures show that surficial deposits are thin and that the topography is rugged though subdued. A mosaic of Landsat images taken at low Sun angles over this region reveals a tendency for the fractures and related patterns to aline along a divergent fan of orientations pointed generally east to west. One hypothesis for the origin of the Nastapoka arc holds it to be the trace of a rim of an ancient basin produced by the impact of a giant meteorite. The fracture pattern does bear some resemblance to the radial lineations around the Mare Orientale Basin on the Moon. *1552–15333;* January 26, 1974.

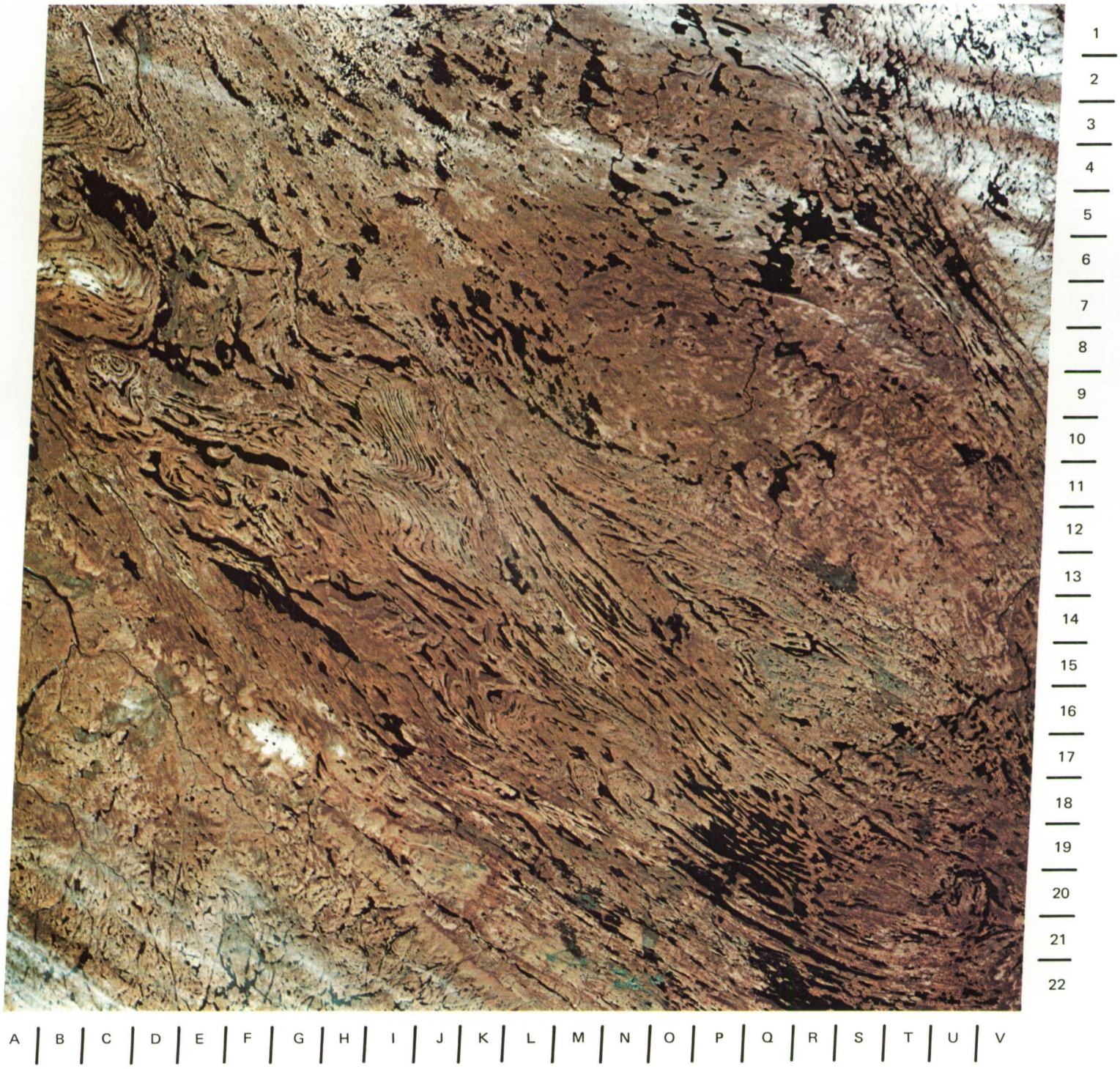


PLATE 157

LABRADOR FOLD BELT: The Labrador fold belt in Quebec and Newfoundland is a major source of Canadian iron ore. The Precambrian fold belt resulted from the deformation of sedimentary strata between two granitic complexes (*C*–19; *U*–2). Many folds (*E*–11) of different sizes and styles are obvious in the metasedimentary rocks and some of the numerous faults (*I*–11) can be seen also. An area of flat-lying metamorphic rocks is obscured by an extensive cover of glacial moraine (*M*–8) with boulder plains, drumlins, and muskeg. The first signs of the imminent winter are revealed by snowcaps on high ground (*G*–16) and by long swaths of snow (*T*–3) along the path of local storms. Prominent ribbed and hummocky moraine (*G*–1) occurs in the northwest part of the area. The major iron mines are located at Schefferville just to the south of this image although large deposits of soft hematitic ores occur also along the west edge of the fold belt (*N*–19) in this area.

The Labrador fold belt represents a former mountain chain similar to the Alps, the Appalachians, and the McDonnell Ranges of Australia. The origin of such mountains, and thus of the Labrador fold belt, is controversial. Proponents of the new global tectonics consider them to form by continental collisions, in which an ocean is closed. But field work by Erich Dimroth in Labrador indicates that the geosyncline that eventually gave rise to the fold belt was formed on continental granitic crust rather than oceanic crust. Which concept is correct remains to be seen; perhaps this image, acquired on the 16th anniversary of the launching of Sputnik 1, the world's first artificial satellite, will help settle the controversy. *1483–15013;* October 4, 1973.

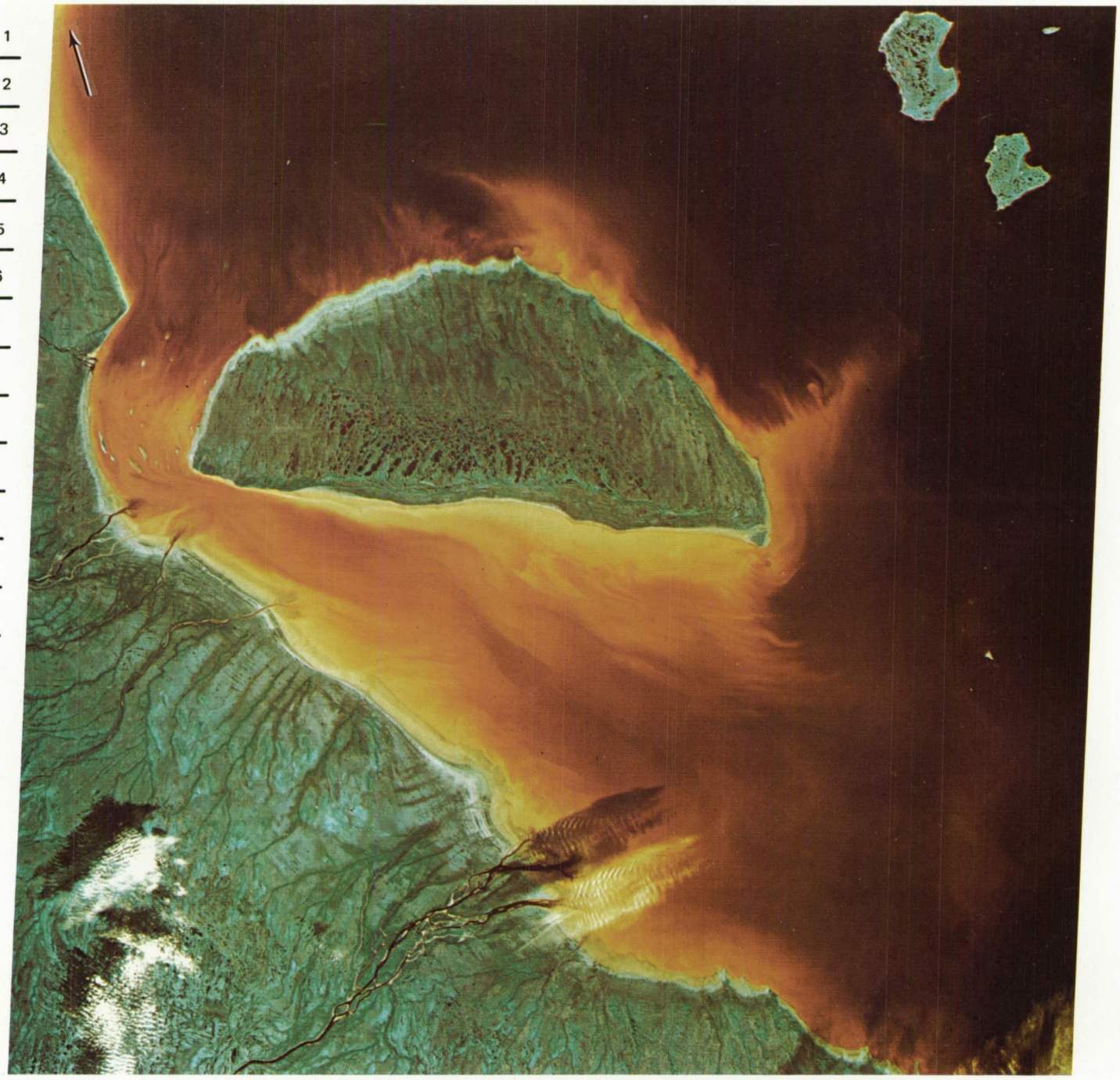
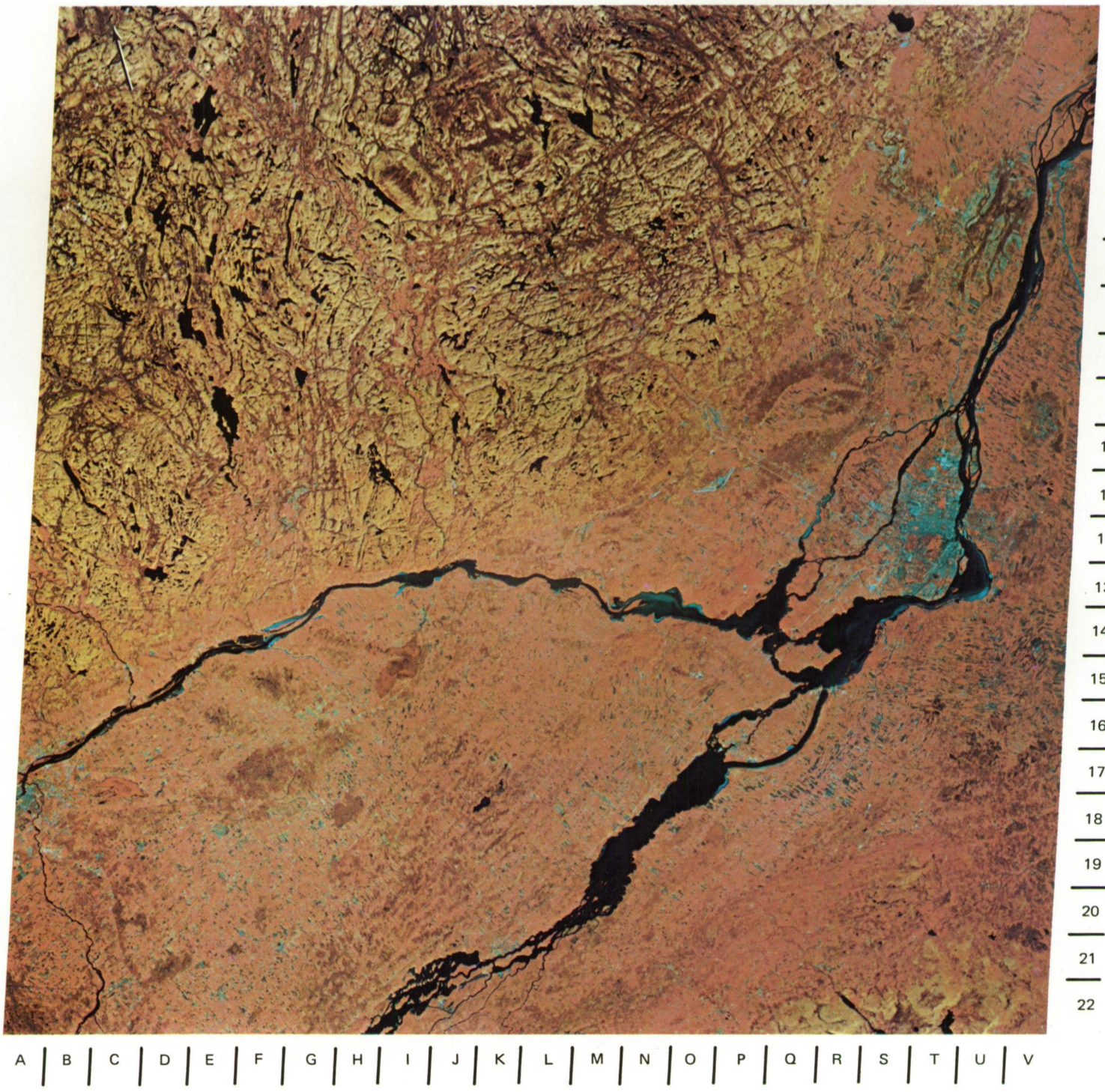


PLATE 158

AKIMISKI ISLAND, JAMES BAY: This color composite was produced by projecting multispectral scanner band 5 through a red, band 6 through a green, and band 7 through a blue filter. The large yellow-orange halo around Akimiski Island (*J*–8) on the west side of James Bay, a southward extension of Hudson Bay, is caused by fine sediment suspended in the water as a result of strong wave action on the silty shores. The sediment load serves to define current patterns (*H*–12) in this part of the bay. The discharge from the Albany (*L*–18) and Attawapiskat (*C*–11) Rivers is clearer than the agitated coastal waters. Numerous raised beaches (*E*–14) parallel the present shorelines of the island and the mainland and indicate the location of former submergence following Pleistocene glaciation. Vegetation is concentrated along the drainage channels and string bogs. The rocks of both the islands and the mainland are Paleozoic in age, being part of the Hudson platform built up by deposition in a depression largely underlying the present Hudson Bay. *1447–15534;* October 13, 1973.

PLATE 159



MONTREAL: This view of the Montreal area was recorded in the early fall. However, there is a marked change in the spectral reflectance of the hardwood trees, with the most notable result being the change in the overall color of the forest cover on the Laurentian Highlands. The dominant hardwoods (*J*–8), which appear red on the summer image, are yellow on the fall image. They have lost their chlorophyll with the onset of seasonal change to fall colors. The evergreens (*M*–1) retain their dark red color on the fall image. Hardwood and evergreen bush can also easily be separated on the St. Lawrence Lowlands. Harvested fields (*R*–17) have a greenish color rather than the red indicative of chlorophyll in fallow and grassland. The low Sun angle and the high contrast between hardwoods and evergreens, which tend to occur in poorly drained valleys, serve to enhance geological structures, especially in the Precambrian rocks of the Laurentian Highlands.

The area shown includes two strikingly different geologic provinces. The Laurentian Highlands are part of the Canadian shield, an immense area of Precambrian rocks, chiefly igneous and metamorphic, making up much of northern North America. The Adirondack Mountains, whose northwest corner is just visible in the lower right corner (*T*–22), are an outlier of the shield. The St. Lawrence Lowlands are a structural depression, bounded partly by faults and filled with Paleozoic sedimentary rocks. Some of these faults are evidently active at great intervals because occasional earthquakes occur along the St. Lawrence River.

Montreal (*S*–11) is located on the St. Lawrence River (*U*–4), which flows out of Lake Ontario off the image to the south. *1440–15155;* October 6, 1973.

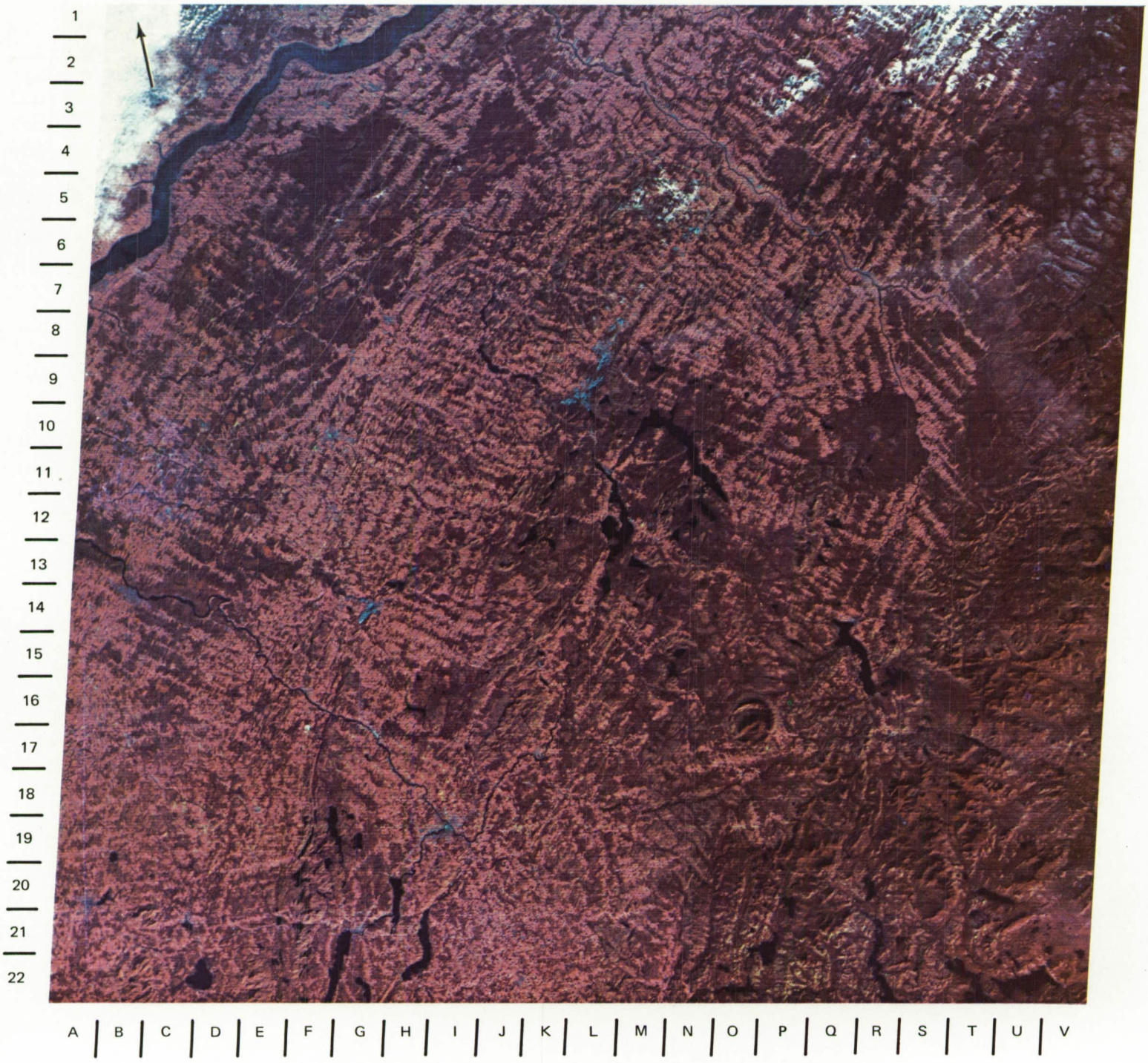
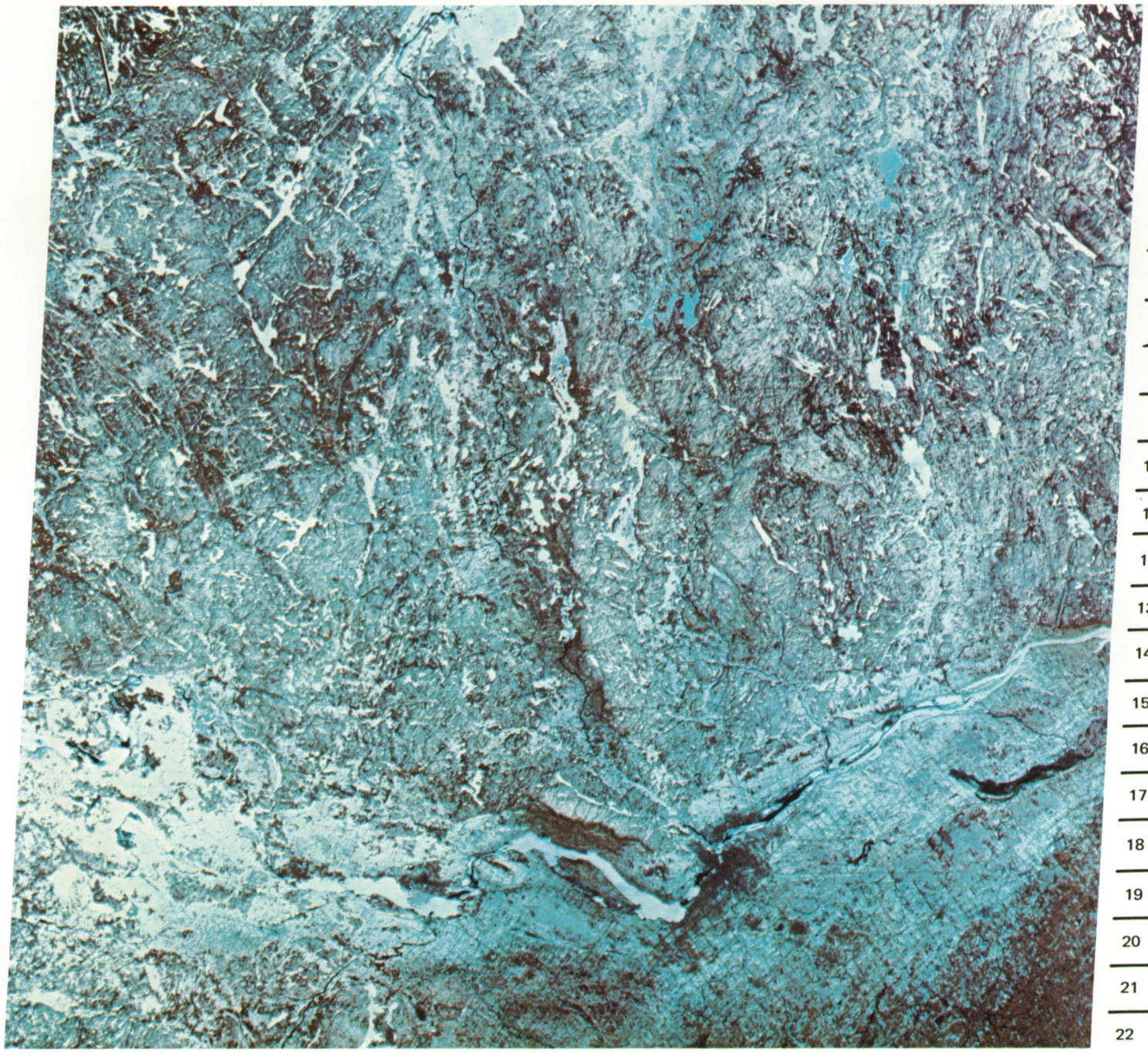


PLATE 160

EASTERN TOWNSHIPS, QUEBEC: This section of the Laurentian Lowlands east of Montreal and just south of Quebec City (near *K*–1) strikingly displays the effects of the seigneurie land system of farm development from the once nearly continuous virgin forests. In this system, French settlers cleared the land granted to these landlords (seigneurs) in long strips perpendicular to river fronts and roads (see plate 48 for an example of this system introduced during the French colonization of southern Louisiana). Although boundaries of the strips were generally regular along river bottomlands, they appear to be much more irregular ("ragged edged") in this scene (e.g., *E*–9; *N*–6). Close inspection with a magnifying glass reveals, however, that the strips extend to different lengths (and sometimes widths) into the forests, which here consist mostly of spruce, fir, pine, and tamarack, with some maple, birch, and beech. Some of the cleared strips result from timbering but others were opened for farming, particularly of hay for dairy cattle but with oats, barley, and buckwheat as other crops. This land practice ends abruptly in the border region (*P*–17; *S*–13) between Quebec and Maine.

The area near the St. Lawrence River (*C*–3) is a lowlands dominated by farming. The country to the southeast becomes a hilly uplands that is part of the extension of the Appalachians into the Maritime Provinces of Canada. Upper Ordovician rocks underlying the lowlands are separated from Cambrian and Lower Ordovician rocks to the east by a great thrust fault whose surface expression is poorly defined here. Younger rocks, through the Devonian, outcrop further east. A series of ultrabasic rocks were intruded as stocks, sills, and dikes in a belt running north of Sherbrooke (*I*–18) on the St. François River (*E*–15) to the town of Thetford Mines (*L*–8) northwest of Lake St. François (*N*–11), then almost to the Chaudiere River (*O*–5). In the Devonian, these ultrabasics and some of the sedimentary units were intruded by granitic plutons, such as those making up Mégantic Mountain (*O*–16). The ultrabasics were converted to serpentine, which contains extensive deposits of asbestos. Open pits and waste piles are evident (as blue patches) around Thetford Mines and the town of Asbestos (*G*–14). *1096–15060;* October 27, 1972.

PLATE 161



OTTAWA, ONTARIO: This image of the Ottawa-Hull region is a late winter scene with snow covering most of the area. However, a snow-free region (*V*–21) can be seen south of the snow line (*T*–20). The Gatineau (*L*–16) and Lievre (*P*–15) Rivers are largely free of ice while the Ottawa River (*M*–18) still has large areas of ice cover. An area of flooding in the valley of the South Nation River (*U*–17) is obvious, and the extent of flood can be readily mapped. Other smaller areas of flooding can also be seen. The large stands (*D*–10; *G*–7; *R*–7) of predominantly coniferous forest are emphasized by the dark greenish color while hardwood forest (*S*–12) shows as snow-covered ground because of seasonal defoliation. The snow enhances the network of county roads (*S*–19) in the Ottawa valley agricultural area. The color of the ice indicates stages in breakup from the light tan tones of solid ice (*R*–10) to the yellowish tone of melting ice (*Q*–4).

The boundary between the central St. Lawrence lowland (*R*–16) and the Laurentian Highlands (*B*–18; *F*–7; *O*–11) is generally evident in this scene. The lowland is here occupied by Ordovician sedimentary rocks. The uplands to the north and west are composed of Precambrian crystalline rocks of Grenville age. Those near Ottawa are a complex assemblage of rocks somewhat younger than the granites and gneisses farther north.

This color composite has been produced by projecting band 4 through a red filter, band 6 through green, and band 7 through blue. *1243–15235;* March 23, 1973.

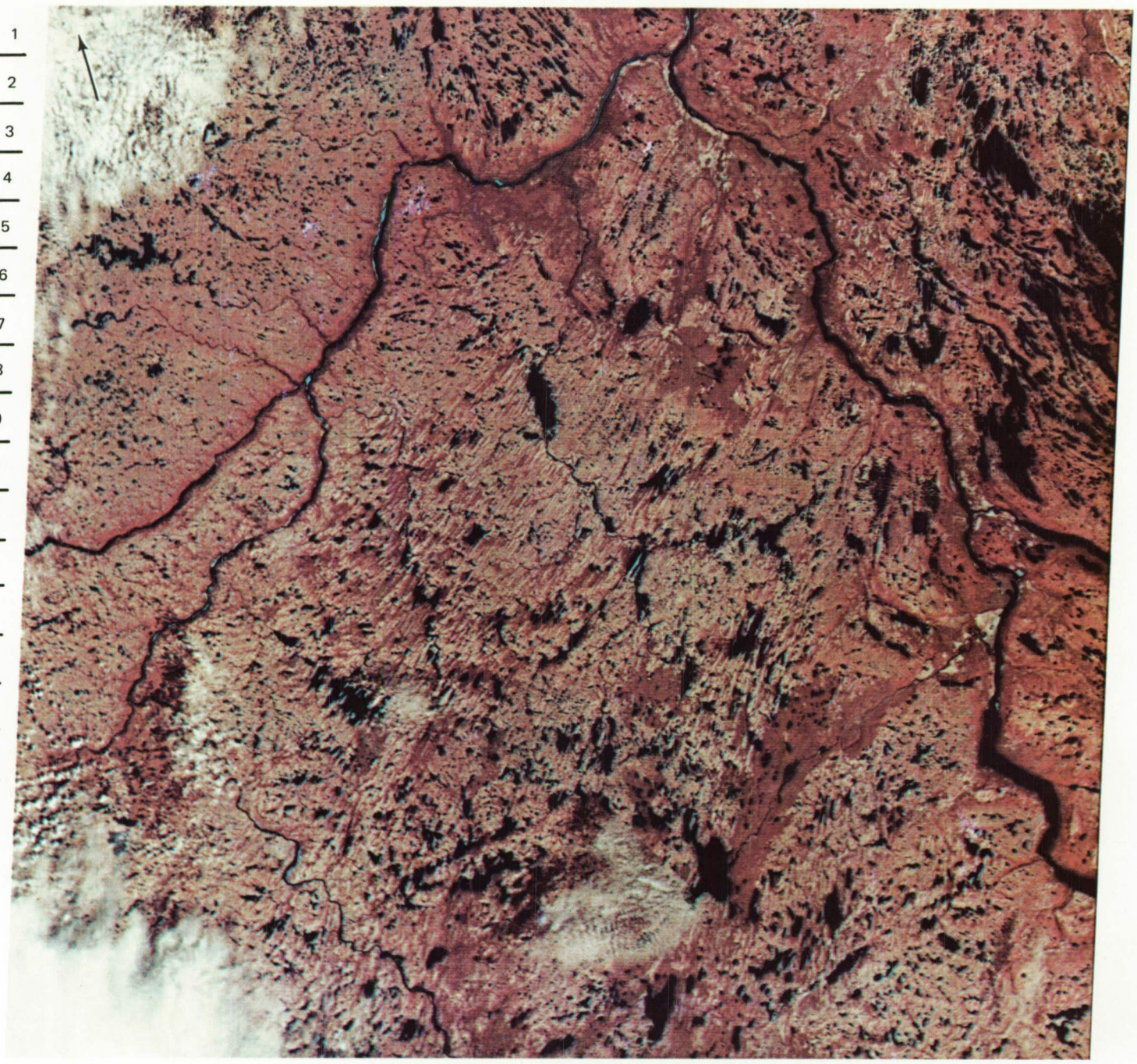


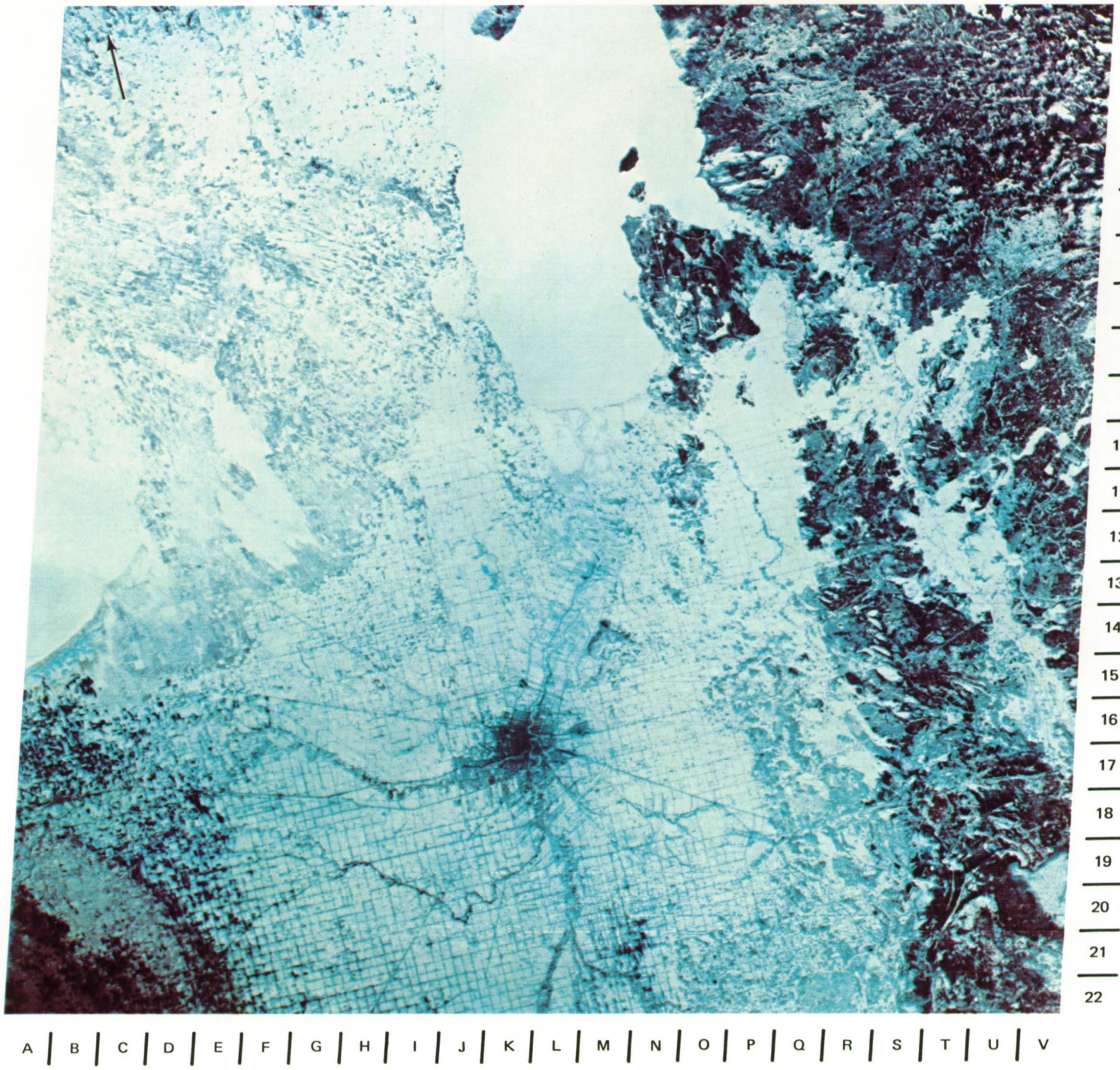
PLATE 162

UNGAVA BAY REGION, QUEBEC: The top edge of this scene lies about 100 kilometers (60 miles) south of Ungava Bay, an indentation into northern Quebec from the Hudson Strait. The Mélèzes (or Larch) River (*C*–11), joined by the Du Gué River (*F*–11), meets the Caniapiscau River (*R*–8) to form the Koksoak River (*N*–1), which empties into the bay. The area on either side of the Caniapiscau is part of the Labrador Hills (*T*–5), here a low range (maximum elevation ~370 meters (~1200 feet)) with relief less than 90 meters (300 feet). These hills are the northern continuation of the great fold belt of lower Proterozoic igneous and metamorphic rocks derived from sediments deposited in the ancient Labrador or Ungava fold belt. (See plate 157.) Other Proterozoic rocks, mostly granites and gneisses, are exposed in the Larch Plateau, an undulating surface within the Canadian Shield that is generally less than 300 meters (1000 feet) above sea level.

The entire region was extremely glaciated during the Pleistocene. Overall, moraines and till deposits are thin in this area. Prominent features made by the retreat of the last ice sheet toward a center around Ungava Bay are particularly evident in this scene. Glacial lakes have been produced by scouring into the crystalline rocks and by damming behind moraines. Ice flow features responsible for the elongate patterns that converge radially toward the northeast included fluted and ribbed moraines and crag-and-tail hills. Eskers are also developed in places.

The region is situated just south of the northern tree line—the boundary between forests and tundra. The darker red patches seen here are part of the woodlands of the subarctic or transitional boreal forest. In this belt, these woodlands consist of spruce, tamarack (larch), jack pine, dwarf birch, willow, and aspen that are interspersed with muskegs and marshes in wet areas and in areas of lichen-covered rock surfaces elsewhere. *1027–15193;* August 19, 1972.

PLATE 163



WINNIPEG, MANITOBA: This late winter image of the city of Winnipeg (*K*–15) and the surrounding agricultural community graphically illustrates the effects of snow enhancement of surficial features. Snow has melted or been cleared from the immediate metropolitan areas, the major highways, and the farm roads that bound the 1.6-kilometer (1-mile) wide sections in the plains. The Trans-Canada Highway (*F*–17; *N*–16) passes through this part of the Province of Manitoba.

Winnipeg developed at the confluence of two major rivers, the Assiniboine (*H*–16) from the west and the Red River (*L*–19) from the south. The Red River floodway (*L*–14) was built to divert spring floodwaters around the city. The Sandilands Forest Reserve to the southeast, within the western edge of the Precambrian Canadian Shield (*T*–10), provided much of the lumber for the early settlement of the Winnipeg region. Stands of jack pine, black spruce with tamarack, and hardwoods are interspersed with sedge wetlands.

The entire region was extensively glaciated in the Pleistocene. Characteristic flutings (*C*–6) show the trend of ice movement. Ice-covered Lakes Manitoba (*A*–12) and Winnipeg (*K*–6) are remnants of a larger system of glacial lakes, including the once vast Lake Agassiz, which cut raised beaches into moraine deposits (*R*–21) along its shorelines. *1223–16542;* March 3, 1973.

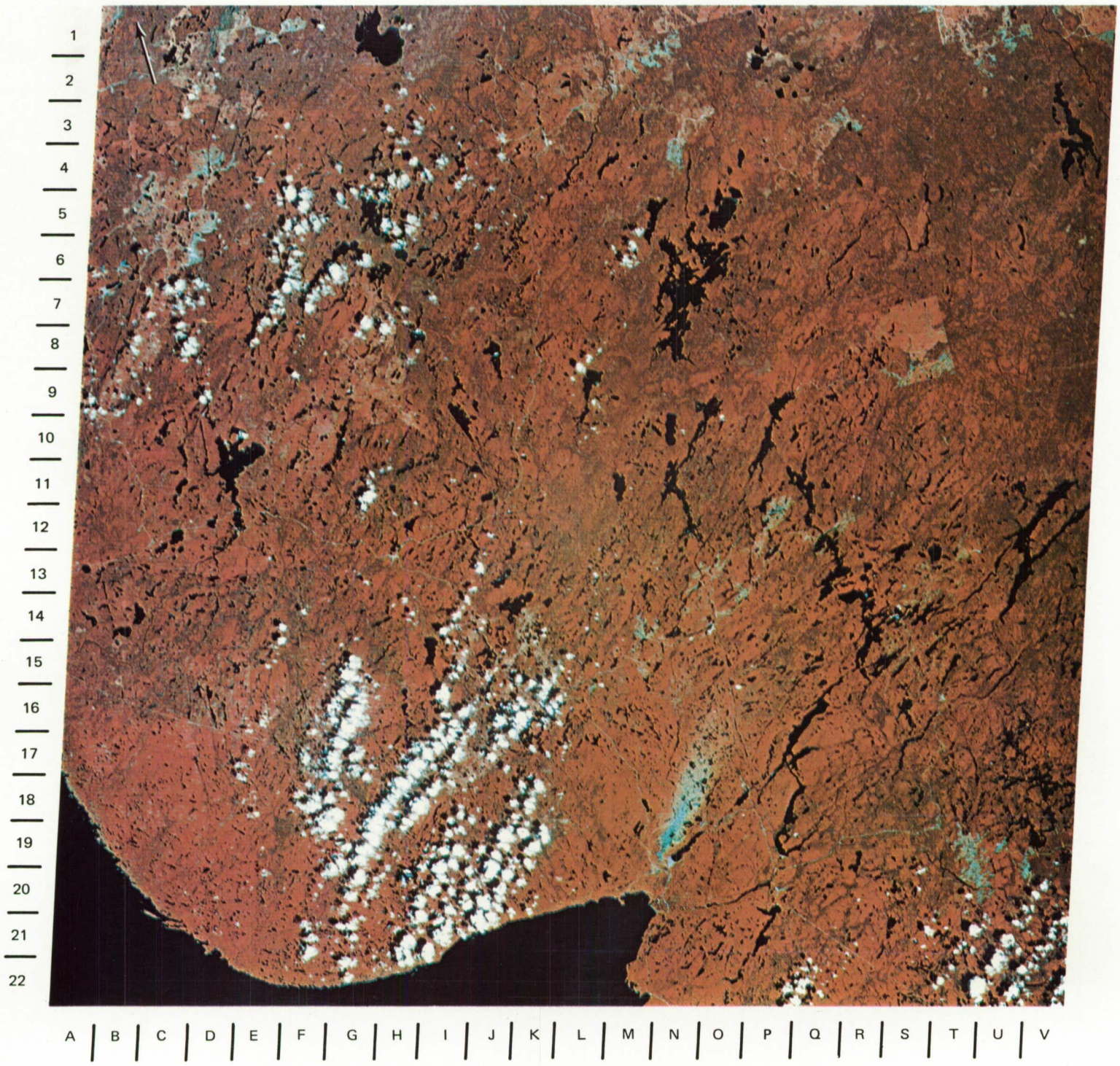
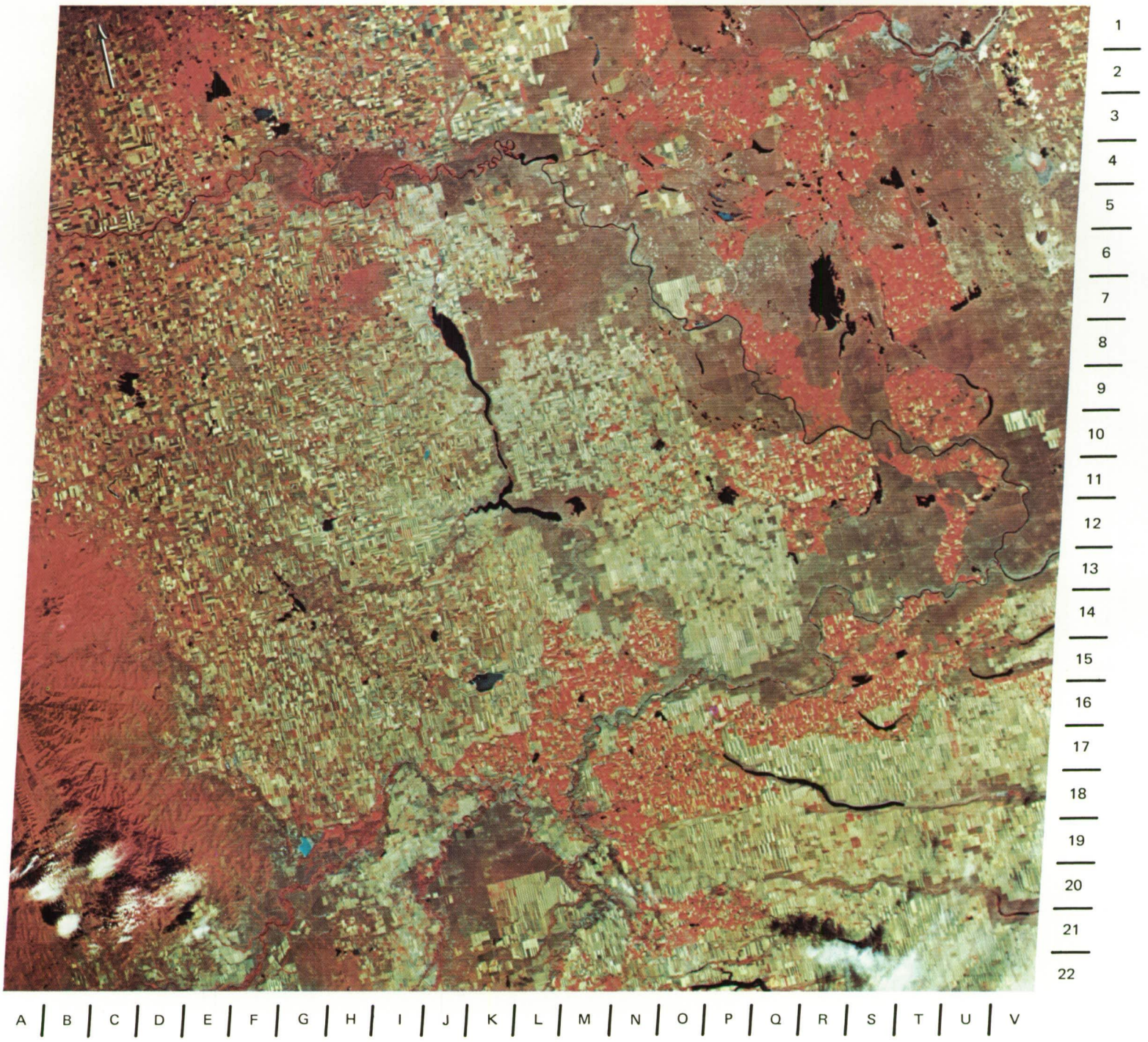


PLATE 164

WAWA, ONTARIO: This image clearly reveals man's modification of the natural environment in north-central Ontario. The town of Wawa (*N*–19) lies just north of the east end of Lake Superior (*L*–21). The Trans-Canada Highway follows Lake Superior south of Wawa (*N*–21) before moving inland (*F*–12) past White Lake (*D*–10). The main industry in Wawa is an iron mine with an associated sintering plant. Over the years, large quantities of sulfur dioxide have been emitted into the atmosphere from the sintering plant. These fumes were carried by the prevailing wind and caused a plume of vegetation damage (*N*–18). The central blue area of the plume represents total kill while the pinkish envelope defines the bounding areas of severe stress. The area of damage is about 900 square kilometers (350 square miles). The sharply delineated areas (*N*–1) toward the top of the image are major logging operations within the conifer-broadleaf forests. New timber cutting shows as blue or greenish color while older cuttings are various shades of pink because of new growth.

The region shown lies within the Canadian Shield. The glaciated surface is underlain by lower Precambrian granites, gneisses, and metasedimentary rocks. Long fractures within these crystalline rocks have, in places, been carved out by glacial action. The resulting depressions are often water filled (bogs and lakes) and, because of the low reflectance of water, are delineated by dark tones. Several larger lakes, such as Esnagi (*N*–10), Missinaibi (*V*–13), and Manitowik (*Q*–16), are excellent examples of this scouring along zones of weakness. *1376–16021;* August 3, 1973.

PLATE 165



LETHBRIDGE, ALBERTA: This scene of the Lethbridge (*M*–18) area in southern Alberta shows several prominent patterns representing different land uses. The large expanse of pasture and rangeland (*M*–6) is used for livestock production. Within this region there are irrigated areas (*Q*–3) in which corn, sugar beets, potatoes and other green crops (bright red on image) are raised. Dryland farming, largely wheat and other cereals, is carried out in the region within long narrow fields (*P*–19) that have a light tan to brown color. Mixed farming is conducted in the darker fields of more rectangular shape just east of the foothills. The Porcupine Hills (*B*–17) are covered with forest (red). Several of the rivers have been dammed to form reservoirs for irrigation (*R*–18). *1396–17560;* August 23, 1973.

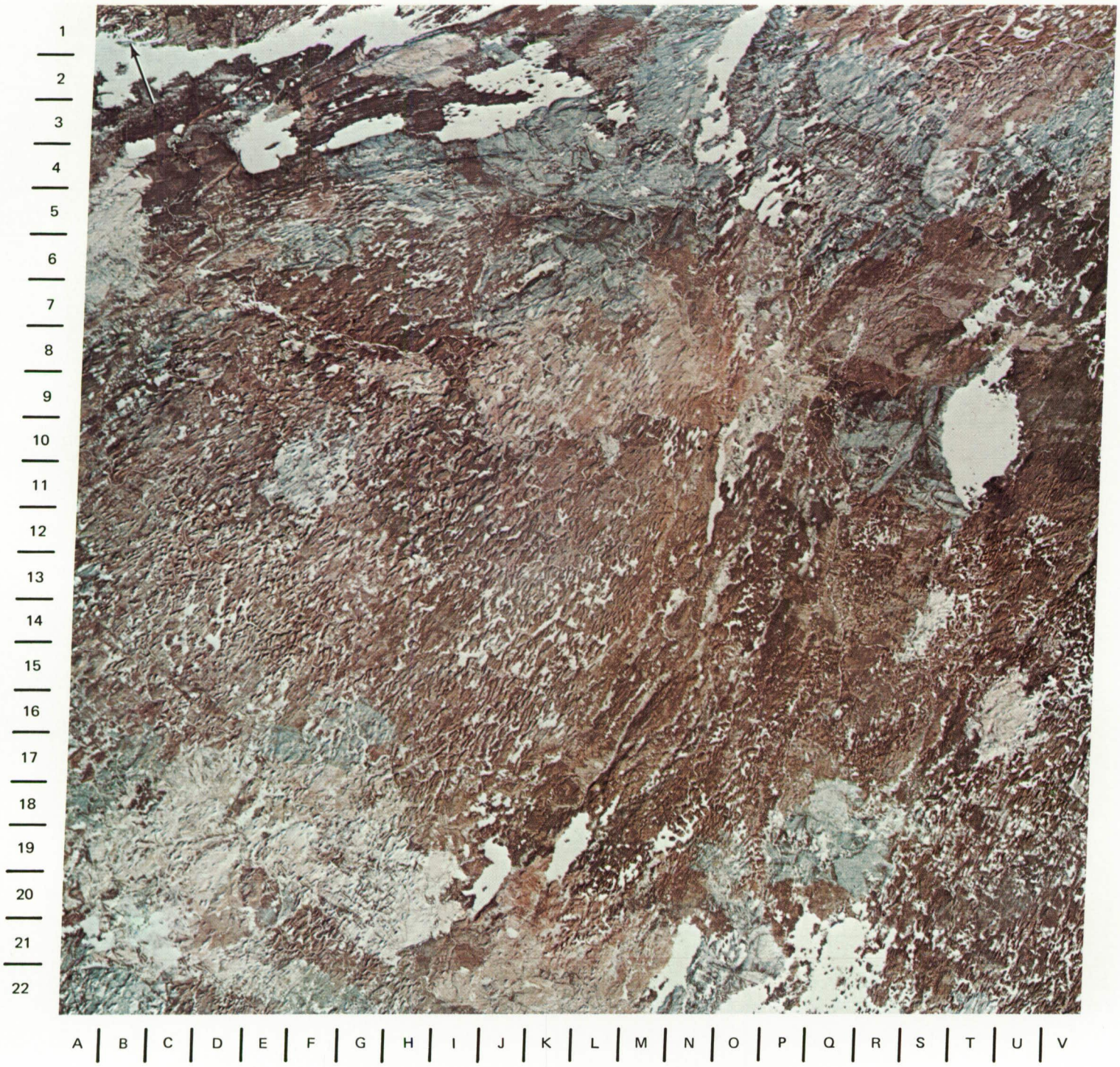
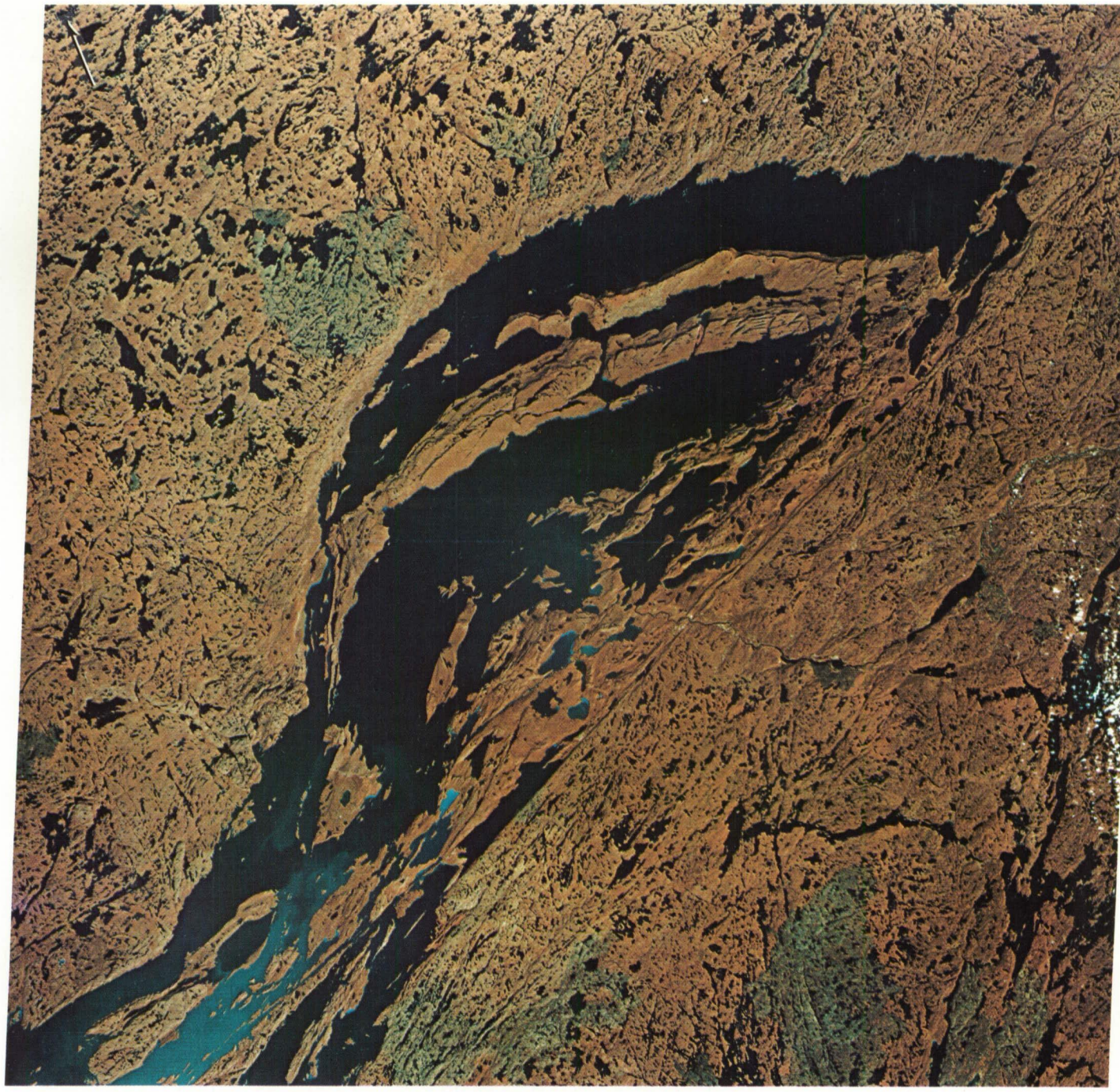


PLATE 166

DRUMLIN FIELD, NORTH SASKATCHEWAN: Drumlins are streamlined hills of glacial drift with a rounded nose pointing in the direction from which the ice came and an elongated tail in the direction of glacial flow. Drumlins are easily identified in this scene as short, elongate hills oriented northeast to southwest because of a light-dark highlighting of a sunlit slope next to a shadow resulting from the low (12°) Sun angle. These extensive drumlin fields were developed by Pleistocene glaciers passing over Precambrian bedrock of northern Saskatchewan. The Wisconsin ice sheet forming these drumlins thus moved southwestward from top right to lower left. Kames and eskers are also present in this glaciated terrain. Lake Athabasca (*B*–2) lies along the contact between Proterozoic (*D*–8) and Archean crystalline rocks (*D*–1). The region has been heavily scarred by forest fires. More recent burns have a bluish color (*M*–3) while older scars are whiter (*Q*–8). *1557–17443;* January 31, 1974.

PLATE 167



GREAT SLAVE LAKE: This pair of two Landsat images taken in succession along a single orbital strip depicts the east arm of Great Slave Lake in the Northwest Territories of Canada. The load of sediment discharged by the Slave River (plate 168, *D*–16) into Great Slave Lake shows as a light blue color. Four different geological regions are shown: the Canadian Shield (plate 168, *S*–6) with folded and faulted crystalline rocks, a Proterozoic basin (plate 167, *K*–8) with flat-lying sedimentary rocks and igneous sills, Paleozoic sedimentary rocks of the Interior Platform (plate 168, *B*–19), and Quaternary river deposits (plate 168, *E*–15). Several scars from recent (1973) forest fires are visible as black patches (plate 167, *A*–15) in the red background of the forest. Large greenish scars (plate 168, *P*–9) represent older fires (circa 1971), while light-colored scars may be still older. The McDonald fault system (plate 167, *Q*–13; plate 168, *H*–5) is one of the major structures of the Canadian Shield, having been mapped over a total length of 560 kilometers (350 miles). It is believed to extend southwest under the Paleozoic cover for an even greater distance.

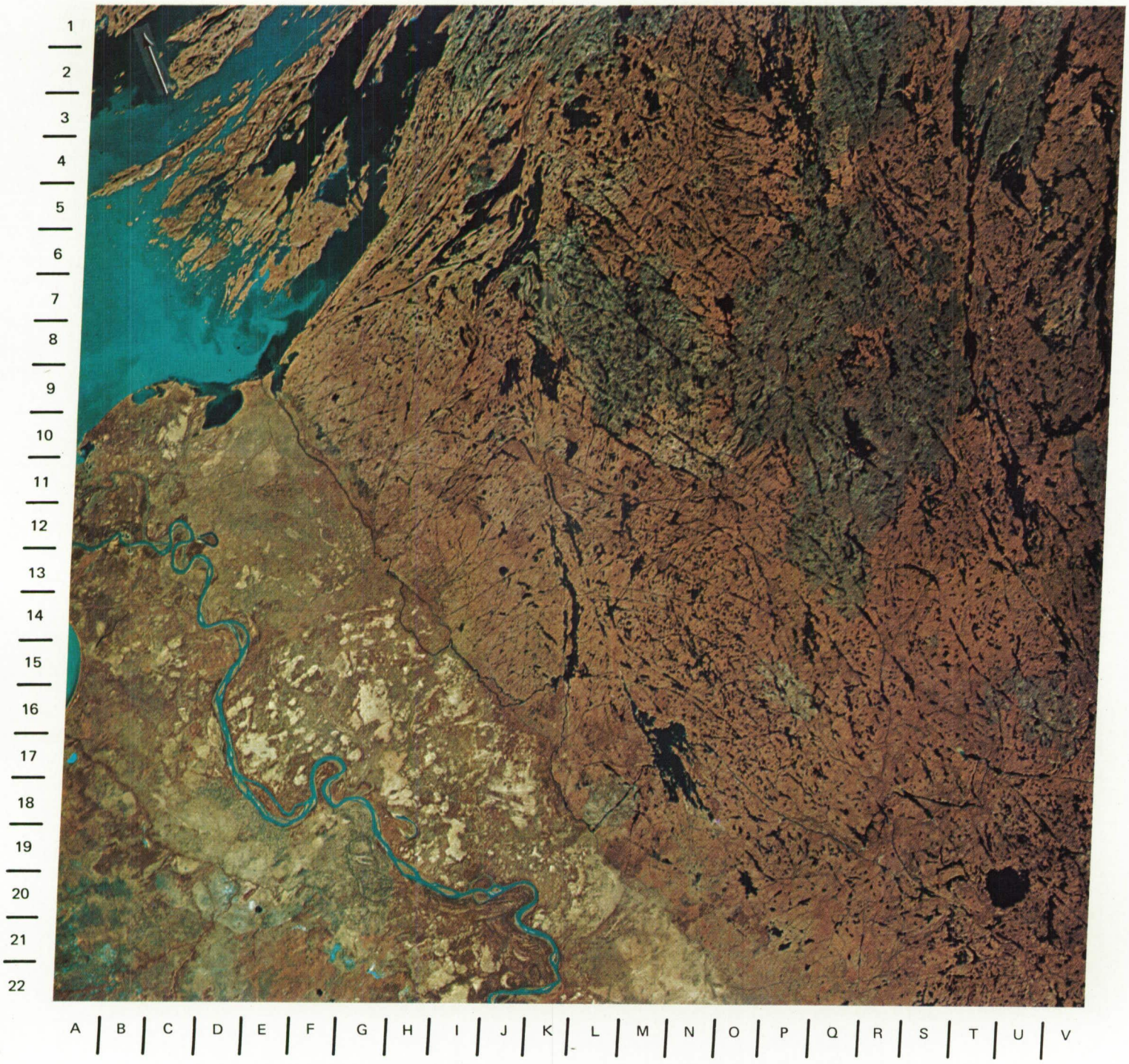
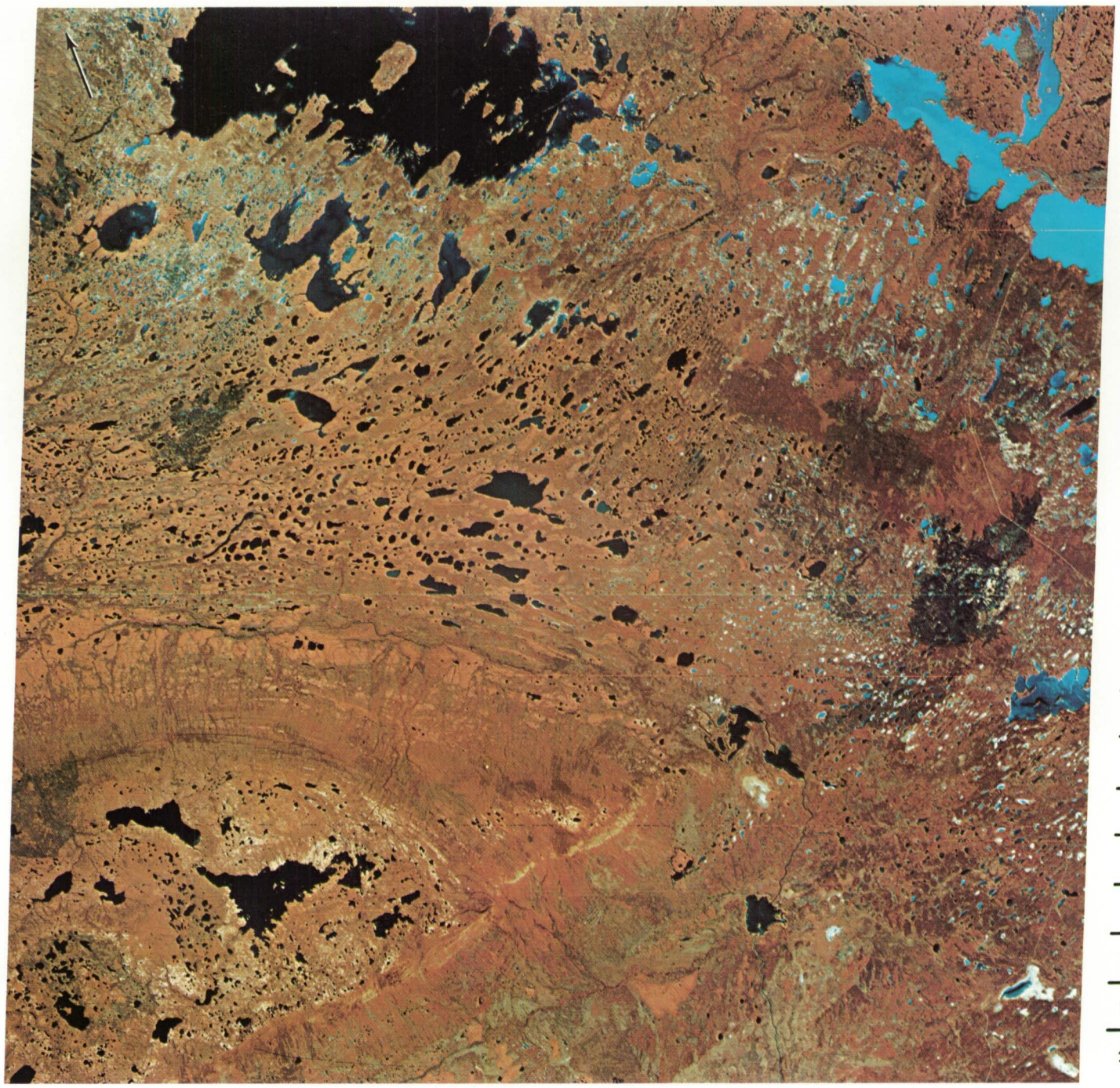


PLATE 168

Some granitic (plate 167, *D*–15 and *D*–18) and gabbroic (plate 167, *C*–19) intrusions are revealed by spectral contrasts of good exposures, but such distinctions cannot be consistently made in this area.

The conspicuous straight northeast edge of the Slave River valley is essentially of tectonic origin, being the trace of a major fault separating the very old (1.6 billion year) rocks of the Churchill province (plate 168) from the Devonian sedimentary rocks to the west (plate 167). The boundary is partly covered by the light-colored alluvial sediments of the Slave River. Note the intricate pattern of cutoff meanders and oxbow lakes along the river's course, typical of mature rivers with very low gradients. A final feature of geologic interest is the family of northwest-trending linear features east of Great Slave Lake. These appear to be part of an immense family of gabbro dikes covering many thousands of square kilometers (miles) of the Northwest Territories. *1436–18143, 1436–18145;* October 2, 1973.

PLATE 169



HORN PLATEAU, NORTHWEST TERRITORIES: A heavily glaciated part of the Northwest Territories is seen in this image of the Horn Plateau (*D*–18), Lac la Martre (*G*–2), and Marian Lake (*S*–4) near the tip of the north arm of Great Slave Lake (*U*–5). A wide range of lake colors occurs in the scene, including almost white, dry to shallow lakes, milky blue lakes with variable silt loads or shallow depths, and dark blue lakes that are relatively deep and free of suspended sediments. A northwest-trending belt of Paleozoic sedimentary rocks, ranging from Cambrian (*O*–8) (adjacent to Precambrian rocks (*S*–2) at the edge of the Canadian Shield) through Middle (*H*–8) and Upper (*L*–21) Devonian, lies beneath the glacial cover. Cretaceous strata distributed in a broad oval pattern (*G*–15) make up the raised Horn Plateau, an outlier of the extensive Alberta Plateau to the south. Complex trends of glaciation resulted from the deflection of Pleistocene glaciers by the Horn Plateau. The flutings and drumlin ridges (*I*–12) reveal the directions of flow. Pitted moraines extend southeasterly from Lac la Martre. The heaviest (dark red) vegetation is found on the ridges (*J*–8) while wetlands (*I*–12) and lakes occupy the intervening areas. Scars from recent (*T*–12) and older (*S*–16) forest fires are evident. The highway (*T*–10) from Hay River swings around the north arm and turns south to Yellowknife. *1423–18433;* September 19, 1973.

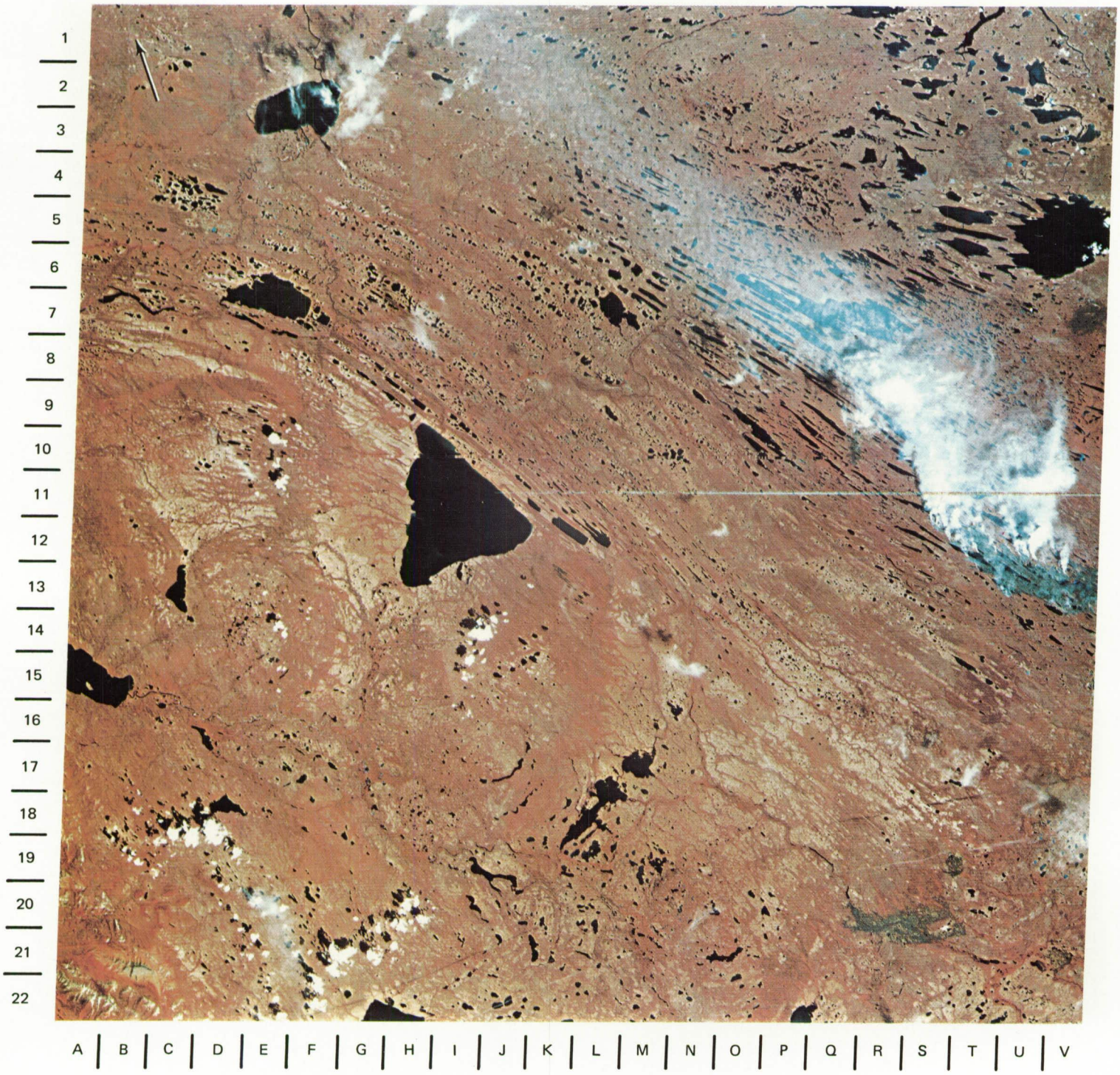
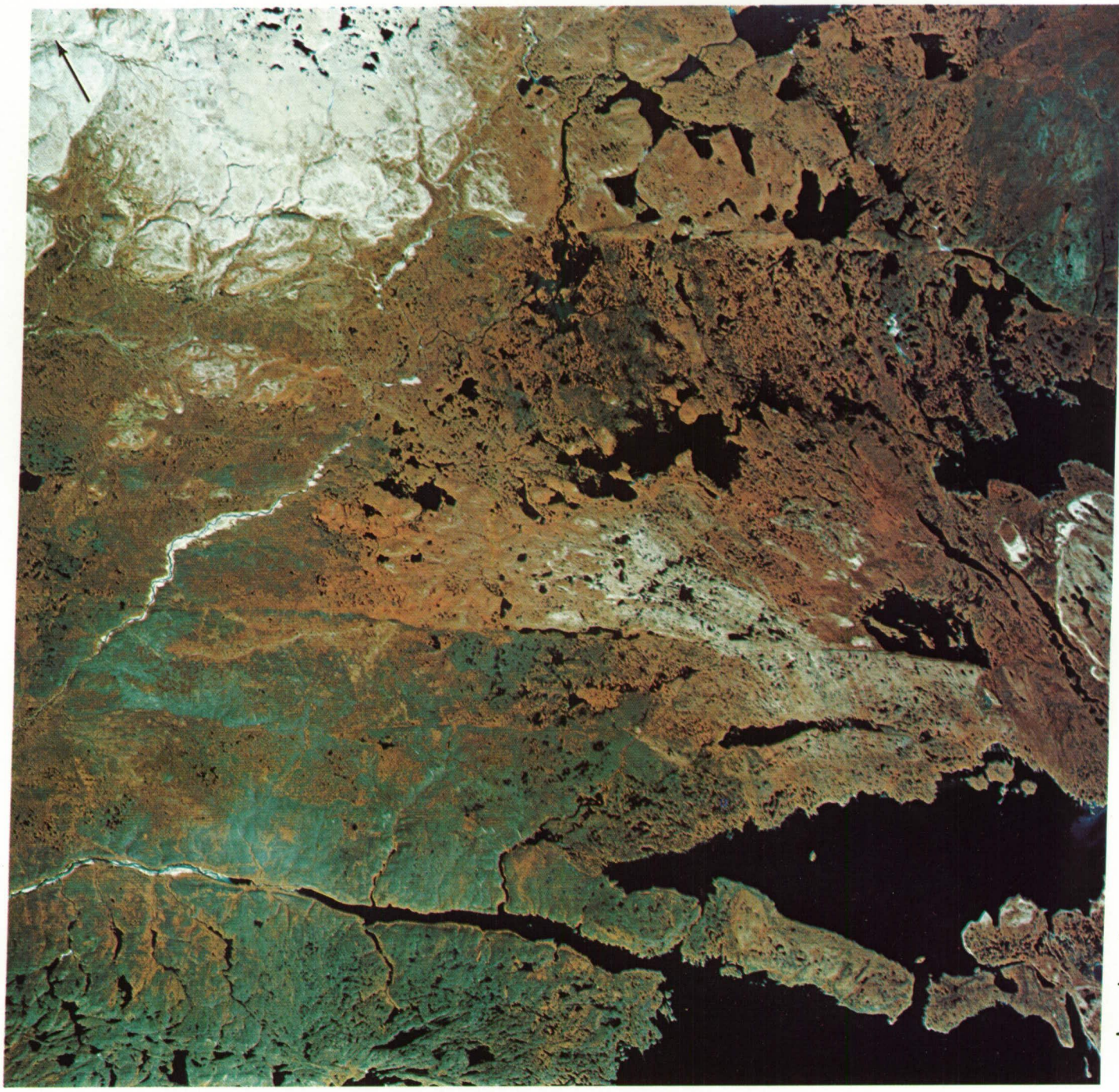


PLATE 170

FOREST FIRE SOUTH OF GREAT BEAR LAKE: The forest fire (*U*–13) shown on this image in the glaciated plains of the Northwest Territories is only one of hundreds that destroy millions of square kilometers of virgin boreal forest in Canada each year. The burned-over area (*U*–14) can be very easily and rapidly mapped from these images. The way in which the forest fire spread is also recorded. Note the northward advance fanned by winds from the south. The advancing front consists of a number of hot spots indicated by plumes of smoke while the back edge is inactive because the wind is blowing the flames into the burnt area. Glacial fluting (*O*–8) and drumlinoid ridges (*K*–11) produced by northwestward movements of a Pleistocene ice sheet orient the lakes and vegetation patterns and accordingly also influence the direction of advance of the fire. This particular fire is located east of Keller Lake (*I*–12), near Great Bear Lake in the Northwest Territories. A part of the McConnell Range, at the eastern edge of the folded Mackenzie Mountains, is seen at the lower left corner, in terrain underlain mainly by Cretaceous rocks. Note the jet contrail (*K*–21; *S*–19) and shadow (*I*–21; *S*–13) at lower right. From the Sun elevation and shadow geometry, the altitude of the jet was calculated as 10 000 meters (34 000 feet). *1372–19011;* July 30, 1973.

PLATE 171



BAFFIN ISLAND NORTHWEST TERRITORIES: This impressive summer image depicts Arctic terrain north of Murray Maxwell Bay (*S*–18) on Baffin Island. The highly reflective area in the northern corner is a barren Paleozoic plateau with deeply incised river valleys. Two dolomitic formations, which cap this high plateau, can be separated by slight differences in color despite the heavy cover of glacial rubble. Thus the light tan of the Baillarge Formation (*E*–2) defines the extent of that formation relative to the underlying, cream-colored Ship Point Formation (*E*–4). At lower elevations (less than 240 meters (800 feet)), vegetation tends to obscure these and other contacts. Two major soil-vegetation associations are represented by greenish-blue and reddish-brown colors. The greenish-blue association has low infrared reflectance (possible lichens) and is developed on Precambrian silicic rocks (granites and sandstones) and adjacent glacial drift. The reddish-brown association has high infrared reflectance (chlorophyll from grasses, shrubs, etc.) and is developed on Paleozoic sedimentary rocks at low elevations, derived glacial drift, and low swampy areas resulting from marine submergence. Fluvial sand deposits along the Gifford River (*E*–11) are highly reflective as are windblown sands in the moraines and drumlin fields (*N*–13) west of Neergaard Lake and along the raised beaches (*U*–11) bounding the fluted moraine. Ribbed moraine and patterned ground with numerous small lakes and ponds dominate the terrain at the head of Steensby Inlet (*Q*–8). Several striking southeasterly faults cut across the region. One of these leaves small horsts of Precambrian rock (*B*–5) within the flat-lying Paleozoic rocks. *1404–16522;* August 31, 1973.

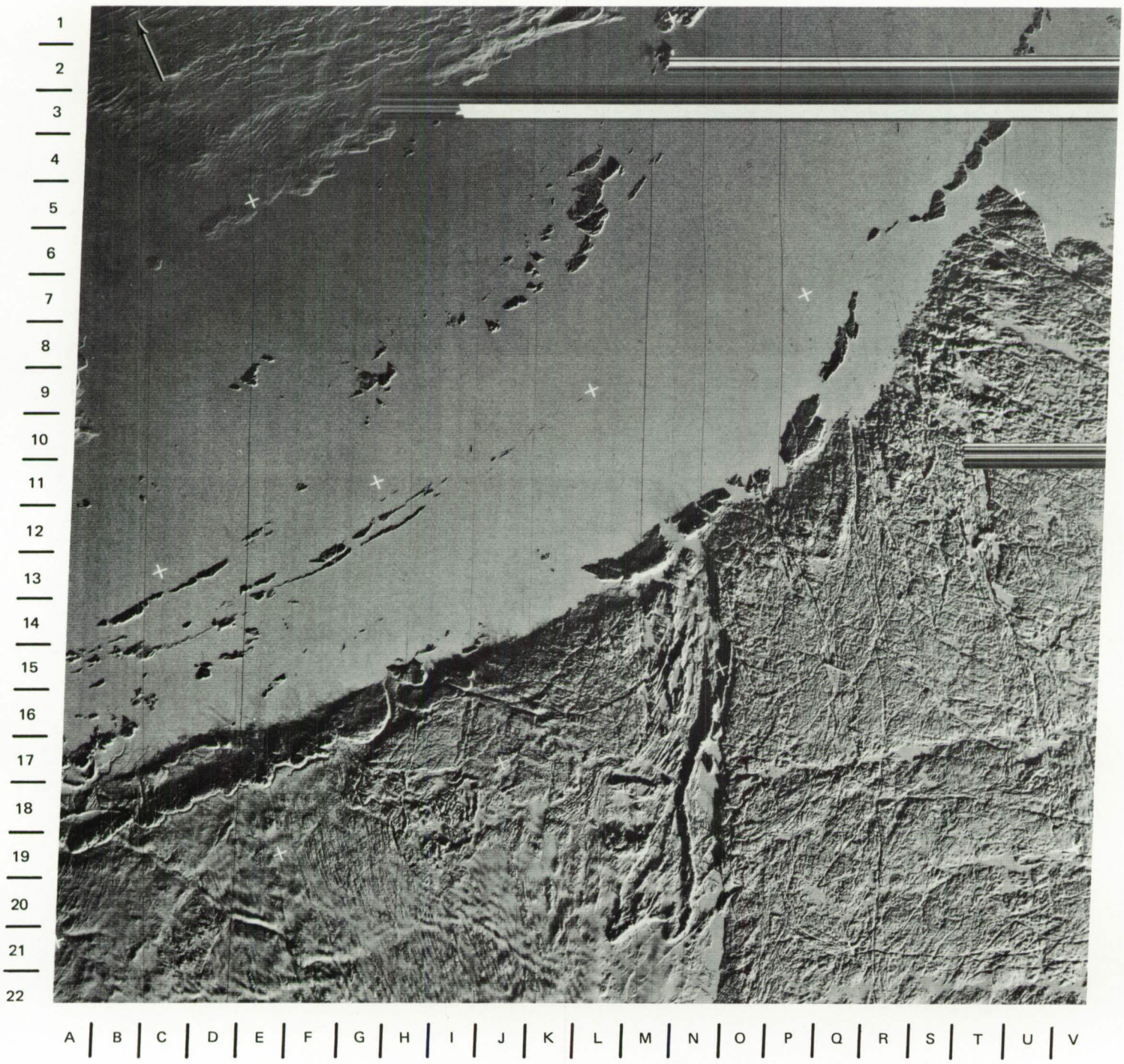
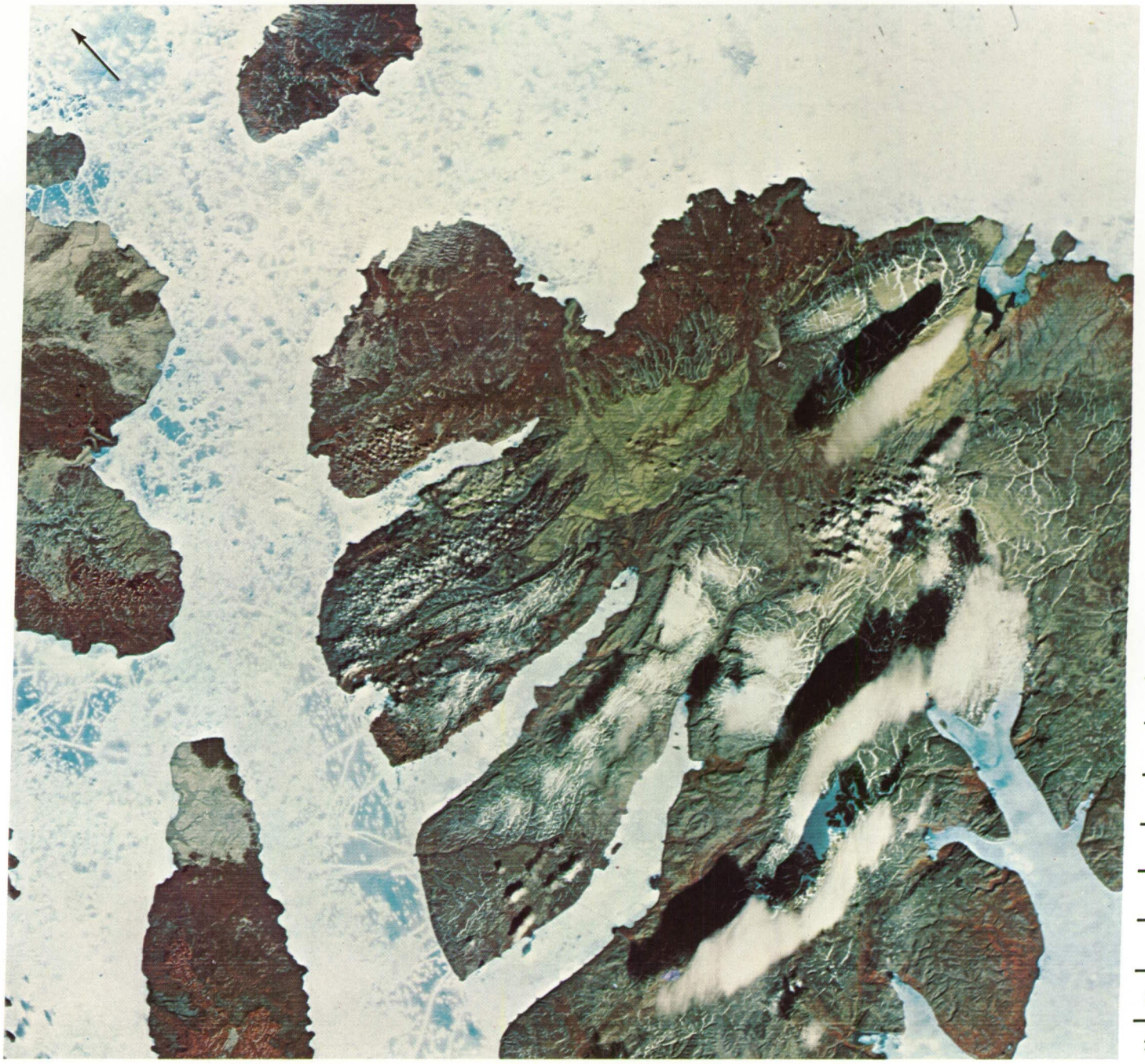


PLATE 172

CORONATION GULF, NORTHWEST TERRITORIES: The extremely low Sun angle (3°) in this image is characteristic of illumination preceding and following the lengthy period of darkness that accompanies midwinter in the Arctic. This image depicts the Tree River valley and vicinity on the south shore of Coronation Gulf in the Northwest Territories. A prominent enhancement of structural and textural detail results from the low solar elevation, especially with the presence of a uniform snow cover and the absence of tall vegetation. On this image, one can see textural details that have topographic relief of about 9 to 15 meters (30 to 50 feet). Such features are not portrayed on the 1:250 000 scale maps that are standard for this part of Canada. A distinct change in textural patterns occurs across the Tree River valley and represents the boundary between the Bear and Slave geological provinces. The large gabbro dike along this boundary is enhanced by the low Sun angle. Similarly enhanced are flat-lying gabbro sills, granitic intrusions, Proterozoic sedimentary rocks, and numerous faults and fractures. Thin clouds overlie part of the area in the lower left corner of the image. The light and dark horizontal bars near the top and right side of the image are dropout lines caused by loss of data from the multispectral scanner or from later processing. *1189–18432;* January 28, 1973.

PLATE 173



MELVILLE ISLAND, NORTHWEST TERRITORIES: This image of the western part of the Canadian Arctic Archipelago shows summer pack ice between Melville (*N*–10), Prince Patrick (*B*–8), Eglinton (*E*–20), and Emerald (*G*–1) Islands. A well-developed network of pressure ridges (*B*–15) can be seen as white lines on the ice. Snow remains only in the sheltered river valleys (*S*–6).

Devonian strata underlie most of the terrain in the southern two-thirds of Melville Island. Ordovician and Silurian rocks are strongly folded in one arm (*I*–13) of the land. The irregular yellow-gray surfaces (*M*–10) generally coincide with Pennsylvanian sediments. Mesozoic rocks occur along the northern edge (*I*–7) of Melville Island and on the islands to the west. Tundra vegetation develops more profusely on the thin rocky soils derived from these Mesozoic units.

Clouds on the image are of two types as shown by the relative positions of their shadows; i.e., high-altitude cirrus clouds (*R*–8) and small cumulus clouds (*R*–11) much closer to the ground. *1005–20000;* July 28, 1972.

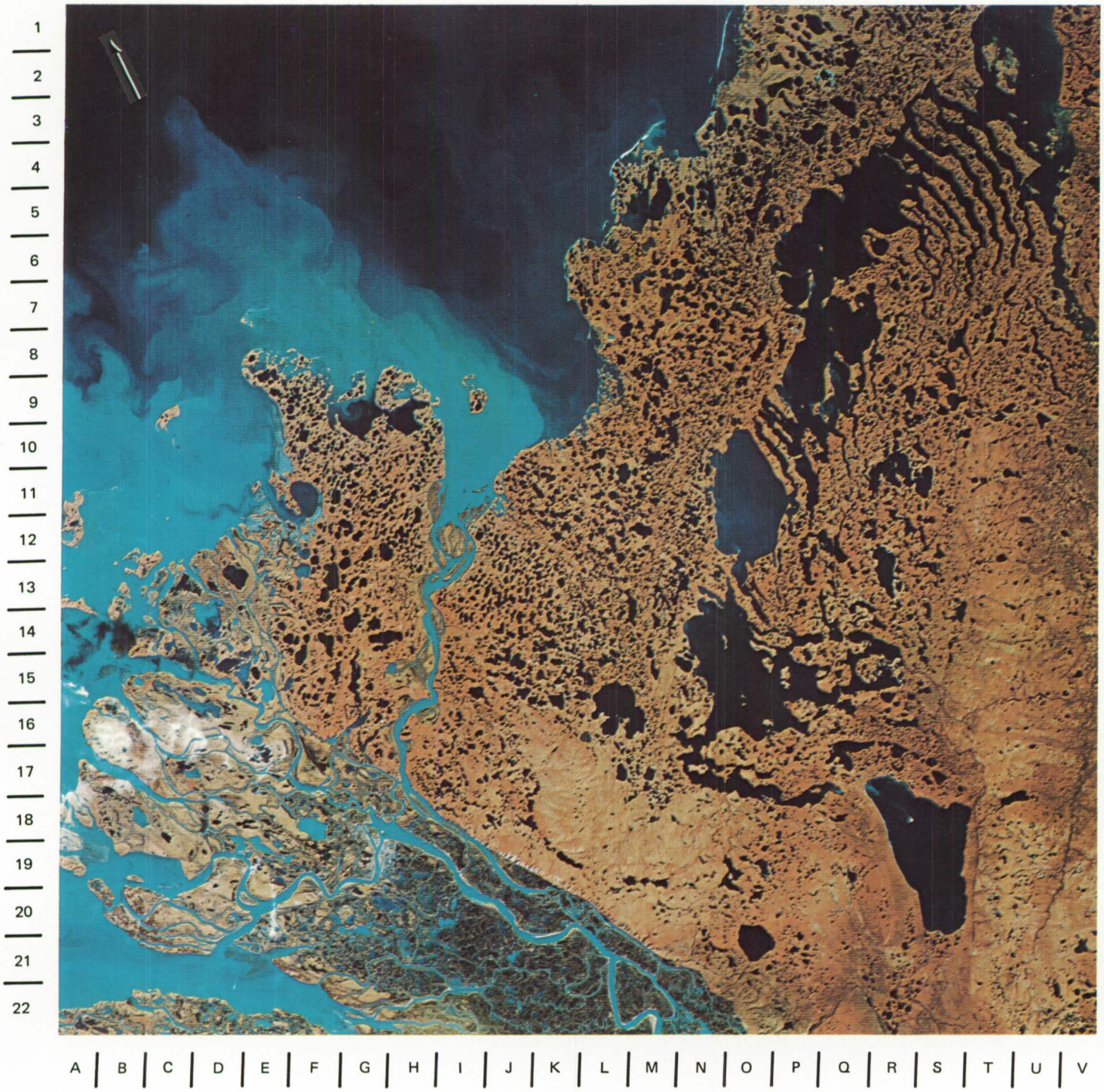


PLATE 174

TUKTOYAKTUK PENINSULA: This scene includes the delta of the Mackenzie River and morainal topography of Tuktoyaktuk Peninsula, District of Mackenzie, Northwest Territories, Canada. The Mackenzie River empties into the Beaufort Sea through a series of distributaries of which the East (*I*–13), Middle (*E*–19), and Napoiak (*H*–21) Channels are most prominent. Note that the vegetative cover on the deltaic sediments changes from sedges and willows (light pink) along the coast (*D*–16), through a willow-alder-poplar community (mauve) farther up the delta (*G*–18), to a spruce-willow-alder-poplar community (dark purple) in the older parts of the delta (*J*–20). The milky blue silt-laden waters of the Mackenzie River show marked contrast with the myriad clear lakes (dark blue) in the upper delta, as does the sediment plume intruding into the Beaufort Sea. Scattered light clouds (white) and accompanying shadows occur over the lower delta.

A multitude of small lakes and ponds dot the hummocky moraine of Tuktoyaktuk Peninsula (*N*–7) and the region east of the Eskimo Lakes (*T*–8). Note the ice pushed ridges (*S*–4). An area of oriented lakes (*P*–2) and outwash extends to the eastern end of the peninsula. The vegetation in these areas is largely tundra with local development of scrub in the transition zone beyond the tree line. Open woodland (darker red) occurs near Sitidgi Lake (*S*–19) and in the lower parts of the Eastern Uplands (*U*–17). Note scarps (*T*–20) bounding the Cretaceous sediments of the Caribou Hills and east of Sitidgi Lake. There is no evidence of man's activities in this scene although it includes several small settlements. *1421–20131;* September 17, 1973.

PLATE 175



ROCKY MOUNTAIN TRENCH, BRITISH COLUMBIA: Some of the most impressive geologic and topographic features in all Canada and, for that matter, in all North America are included in this view of British Columbia, Alberta, and the Canadian Rockies. The Fraser River (*H*–11; *O*–14) bisects the picture. It flows into Moose Lake (*S*–13) just west of Jasper, Alberta, which is off the image. The area receives heavy precipitation, especially as snow; in fact it still covers the higher mountains in this image and thus is able to support many glaciers such as those around Mount Sir Wilfrid Laurier (*M*–17), one of several mountains over 3300 meters (11 000 feet) high in this area. This image includes part of the continental divide between drainage to the Pacific Ocean (including the Fraser River) and the Arctic Ocean (the rivers northeast of the Fraser, which flow into the Peace River).

The valley occupied by the Fraser River is a small part of the Rocky Mountain Trench (*E*–10; *R*–16), a great fault zone over 2400 kilometers (1500 miles) long, that extends from Alaska to Montana. The trench is conspicuous because the snow-covered mountains on either side contrast with the valley floor, and it can be seen on photographs taken from Apollo spacecraft thousands of kilometers from Earth. Its nature and origin are, to say the least, not well understood. There is some geologic evidence that it is a strike-slip fault, with the northeast block moving to the south, and some geologists suggest considerable total displacement. However, its physiography resembles that of valleys formed by downfaulting; the roughly triangular slopes on the northeast side of the trench are especially characteristic of block-fault valleys. The origin of the Rocky Mountain Trench is one of many regional geologic problems that Landsat images will perhaps help to solve. *2182–18183;* July 23, 1975.

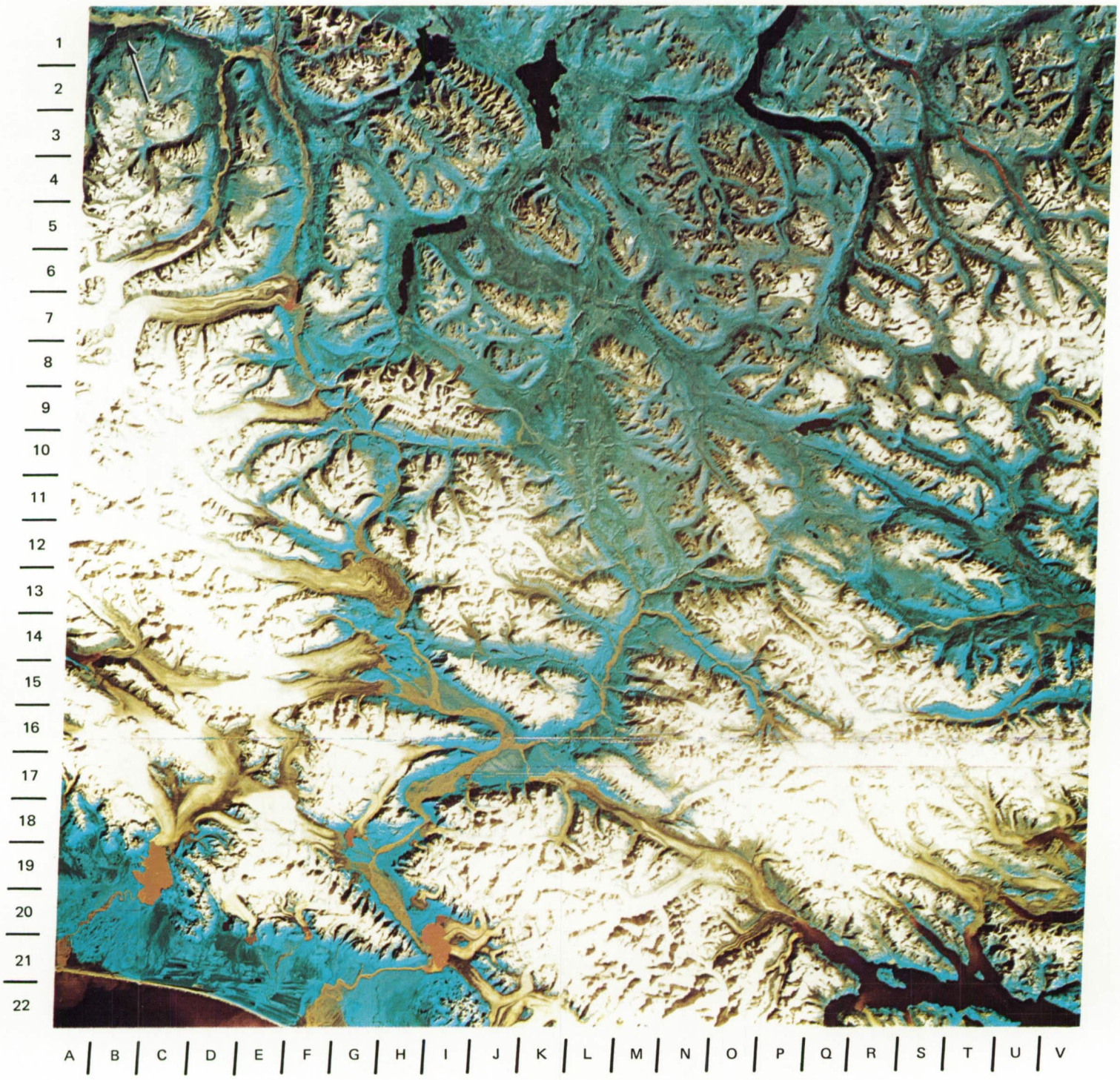


PLATE 176

SURGING GLACIERS IN NORTHERN BRITISH COLUMBIA: Alpine glaciers and their consequences are depicted on this image of the St. Elias Mountains in the Coast Mountains of northwestern British Columbia, southern Yukon, and the Alaskan panhandle. These mountains, a complex of older Paleozoic metamorphic rocks, Triassic volcanic rocks, and younger Mesozoic sedimentary rocks and intrusives, reach elevations of 2400 meters (8000 feet) near Lake Kusawa (*P*–3) and up to 4500 meters (15 000 feet) westward near the Malaspina and other glaciers. Both surging and flowing glaciers are present in the area. Surging glaciers such as the Lowell glacier (*D*–7) have characteristic convoluted moraines, whereas flowing glaciers (*K*–21) have streamlined or relatively straight moraines. In the winter of 1973, Tweedsmuir glacier (*F*–13) surged forward, advancing at an estimated rate of 88 meters (288 feet) per day. The glacial lakes (*C*–19) contain a high silt load as shown by their red color in this rendition (band 5: red; 6: green; 7: blue), while coarser sediment is being deposited in the braided river channels (*I*–17). Broad U-shaped valleys (*L*–5) to the north of the active glaciers were carved out by earlier alpine glaciers that have since melted. Forest cover has a distinctive blue color (*G*–8) associated with vegetation in this false color composite. *1417–19532;* September 13, 1973.

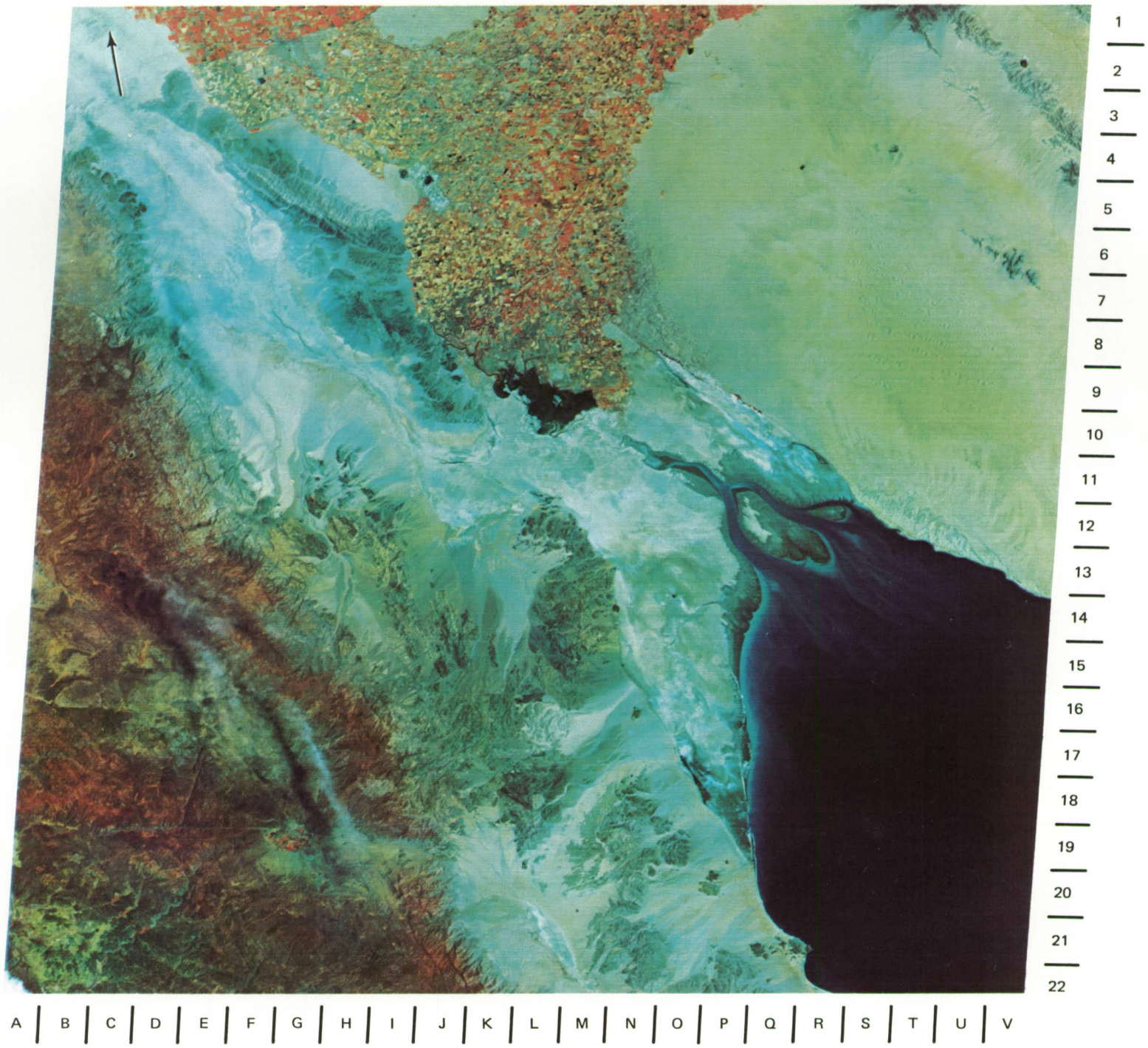


PLATE 177

COLORADO RIVER DELTA, MEXICO: The Colorado River terminates its 2330-kilometer (1450-mile) traverse, from Rocky Mountain National Park across the arid southwestern United States, in an expansive delta deposited at the head of the Gulf of California (*N*–10). The last 150 kilometers (90 miles) of its course crosses the U.S.-Mexico boundary at Yuma, Ariz., and continues southwestward in a series of distributaries across the older portions of the upper delta (*K*–6) until it reaches its present day, marshy, island-filled junction with the Gulf of California (*P*–12). The high tidal ranges, more than 7 meters (24 feet), occasioned by the tapering configuration of the upper portion of the gulf, create considerable areas of salt marsh tidal flats around islands at the head of the gulf, such as Isla Montague (*P*–11) and Isla Gore (*R*–11). The tonal variations in the water signature near these islands and along the western shore (*P*–14) are produced by differences in water depth and sediment content.

Similar to practices established in the Imperial and Coachella Valleys in California, a series of canals has been constructed to channel the river's water for purposes of irrigation (*K*–5). The international boundary near the Mexican city of Mexicali (*F*–1) reflects differences in cultivation, harvesting, and land use practices on either side of the border. The northward continuation of this area is shown in the Salton Sea image in plate 133.

The inherent desert nature of this region is exemplified by the presence of huge salt flats such as the Laguna Salada (*D*–5). Dozens of salt- and sand-filled basins occur on the lowlands associated with the river mouth (*E*–10; *O*–9). Extensive sand dune fields cover the surface southeast of the irrigated region (*S*–8). This area is known as the Gran Desierto and in one portion (*T*–4) includes dunes that represent a southeastward extension of the Algodones dunes shown on the Salton Sea image (plate 133). The small fishing village of San Felipe on the western shore of the gulf (*Q*–21) is the only settlement of consequence south of the irrigated region.

While this area is tectonically active and several offshoots of California's San Andreas fault system are mapped as being buried beneath the alluvial fill within the Salton trough, there are only a few places within the lowland area of this image showing sufficient linearity to warrant possible fault association (*E*–4; *U*–2).

The southwestern margin of this image is dominated by the more humid and better vegetated highlands of the Sierra San Pedro Martir (*C*–11; *D*–19). *1321–17451;* June 9, 1973.

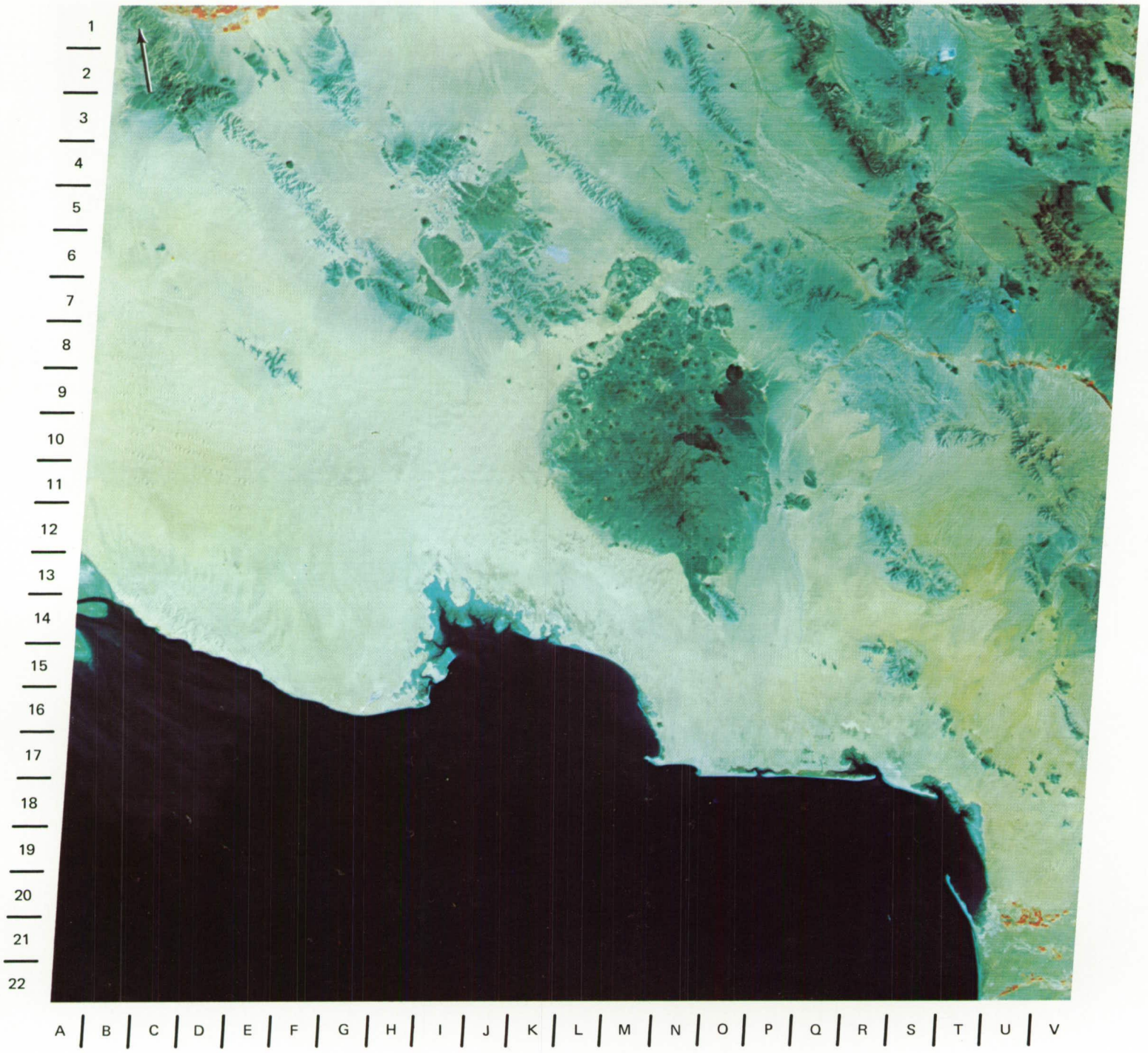


PLATE 178

PINACATE VOLCANIC FIELD: A portion of the Sonora Desert, at the north end of the Gulf of California, lying in both Sonora, Mexico, and Yuma County, Ariz., is shown in this view; the border between the United States and Mexico runs from *A*–4 to *U*–8. The Gran Desierto of Sonora, a barren area of sand dunes, is at the left (*A*–8 to *G*–14). The area is sparsely settled on both sides of the border. The only visible evidence of human activity are the farms on the delta of the Magdalena River in Sonora (*U*–20) and in the Gila River valley of Arizona (*B*–1), and the copper mines and tailings ponds at Ajo, Ariz. (*R*–2). The Organ Pipe Cactus National Monument occupies a section of the Arizona side of the border at *T*–6.

The most prominent feature in this image is the Pinacate volcanic field (*M*–10), a large family of Recent volcanoes, some of which have erupted within the last thousand years. The lavas and pyroclastics are chiefly basalt, as the dark color suggests. A number of the individual craters are "maars," deep-seated volcanoes characterized by very gaseous, violent eruptions. Such volcanoes frequently bring up fragments of mantle material, such as peridotite and eclogite. Other areas of Recent basaltic volcanism are visible in the Gila (*D*–4) and Coyote (*I*–5) Mountains northwest of the Pinacate volcanic field.

The pronounced northwest-southeast alinement of the mountains of both Arizona and Sonora suggests that they are related to the processes that created the Gulf of California. This region of North America is generally considered part of the Basin and Range province, an area of block faulting in which the valleys are alluvium-filled grabens. The Gulf of California was formerly considered a graben, but most geologists now believe it to be an area of sea-floor spreading underlain, at least in the south, by oceanic crust. This Landsat picture may throw light on its origin by showing the relation between the gulf and the structure of surrounding areas such as this. *1410–17382;* September 6, 1973.

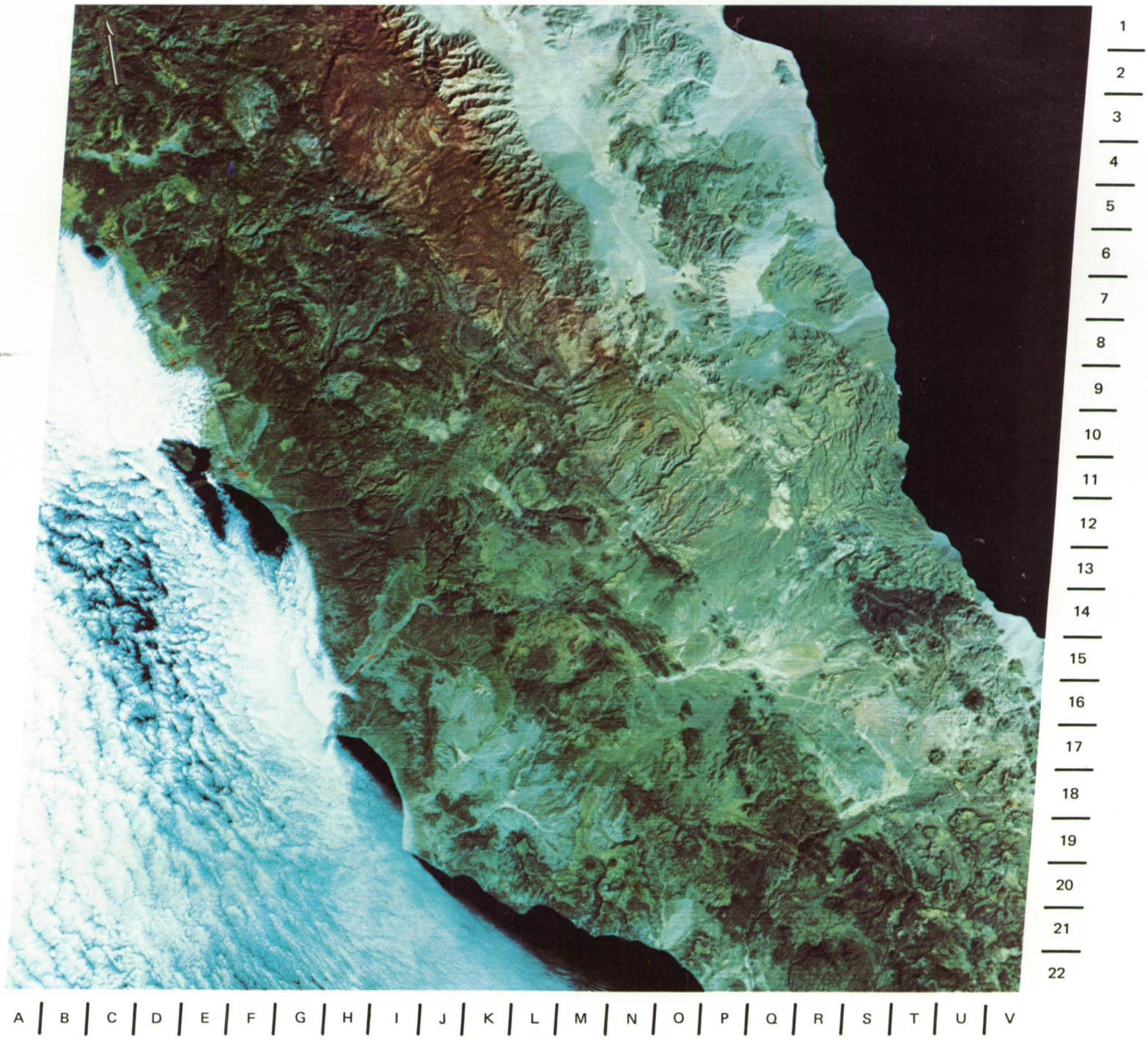


PLATE 179

NORTHERN BAJA CALIFORNIA PENINSULA, MEXICO: The Baja California Peninsula has traditionally been one of the most remote regions in the Republic. It is isolated by virtue of its peninsular nature, as well as by distance and difficulty of communication, from the populated heartland on the plateau. It was only in the early 1970's that a paved road was completed to connect the northern and southern extremities of the peninsula. These factors, coupled with the fact that the majority of the peninsula is a tropical desert receiving less than 25 centimeters (10 inches) of rainfall per year, have kept the peninsula sparsely populated and without an agricultural base.

Geologically, the peninsula is a southward extension of the Southern California batholith which forms the core of the mountainous backbone of the land surface protruding between the depression occupied by the Gulf of California (*R*–5) and the Pacific Ocean (*D*–19). The tectonically active peninsula is flanked by coastal terraces (*C*–8) and in many places covered by lava flows. Many of the terraces now stand a hundred meters (several hundred feet) above the shoreline and the lava flows cap the top of eroded mesas. A volcanic landscape occurs in the southeastern corner of this scene (*T*–18).

The most imposing landscape feature in this image is the Sierra San Pedro Martir (*I*–4). Rising to elevations of more than 3000 meters (10 000 feet), this range is sufficiently high to produce precipitation from marine air masses moving from the west. The more abundant precipitation, not only in the Sierra but also in the foothill region (*F*–7) on the Pacific Ocean side, is evidenced by comparing the vegetative signatures across the peninsula from the Pacific to the gulf. On the leeward side, the Sierra and the adjoining lowland (*L*–3) show highly reflective signatures, indicative of little or no vegetative cover. The strongest red vegetative signatures are produced by the forests along the higher elevations of the Sierra.

The stratus cloud pattern along the Pacific coastal margin (*B*–9) is typical for the entire southwestern coastal zone at this time of year. It is this cloud pattern that gives rise to the night and morning low clouds and fog along much of the Pacific southwest coast.

Several small patches of irrigated agriculture are visible at places where water is available from wells or in stream valleys. From north to south, these small enclaves are the Colonia Camaliu and Mision de Santo Domingo (*B*–5), San Quintin (*D*–10), and Rosario (*G*–15). *1069–17450;* September 30, 1972.

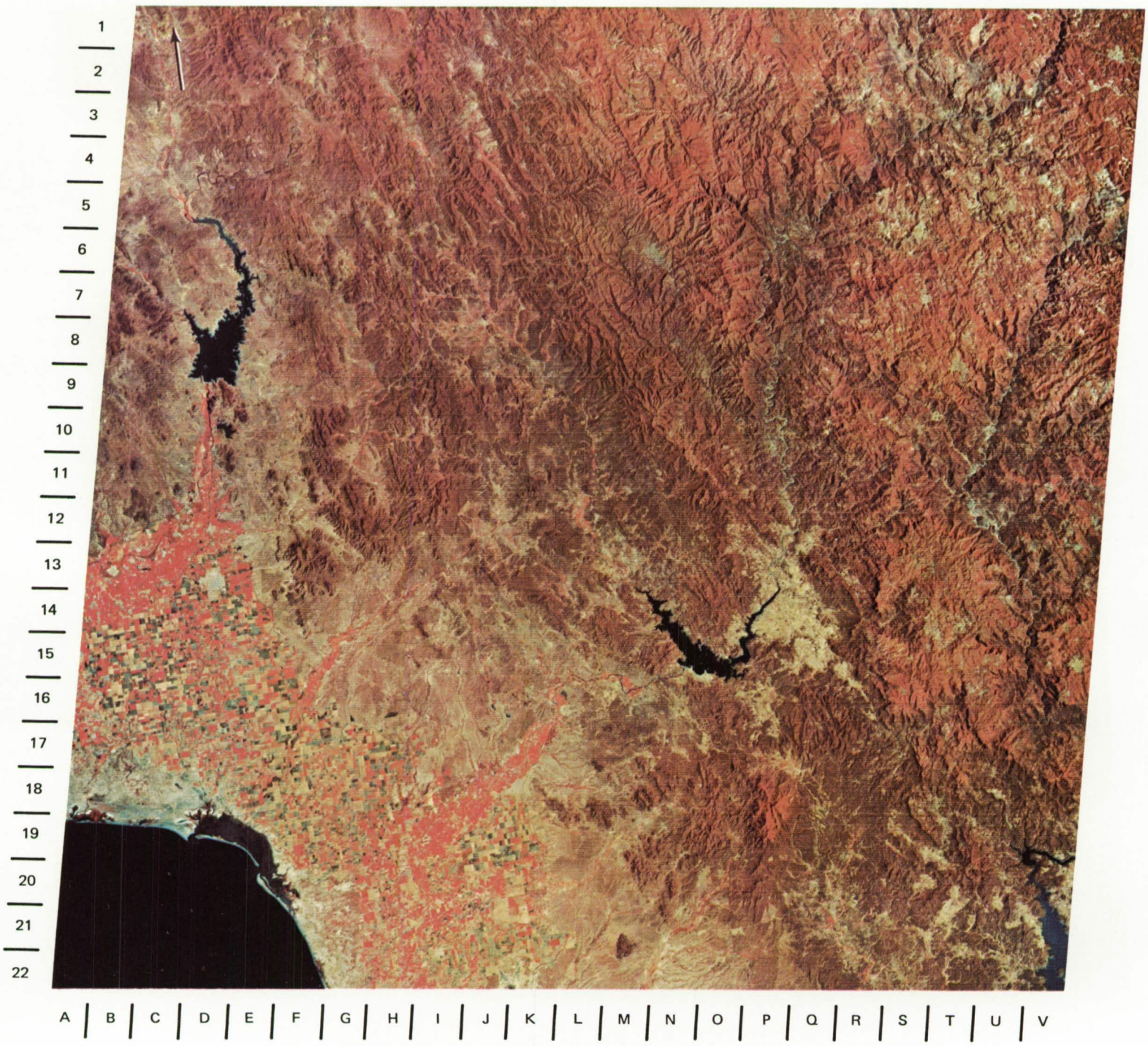


PLATE 180

CIUDAD OBREGÓN, MEXICO: The width of this tropical desert coastal plain is restricted due to the fact that the Sierra Madre Occidental (*S*–13; *H*–4) extends westward almost to the shores of the Gulf of California (*B*–20) at this latitude. The climate along this coast becomes progressively drier as one proceeds north.

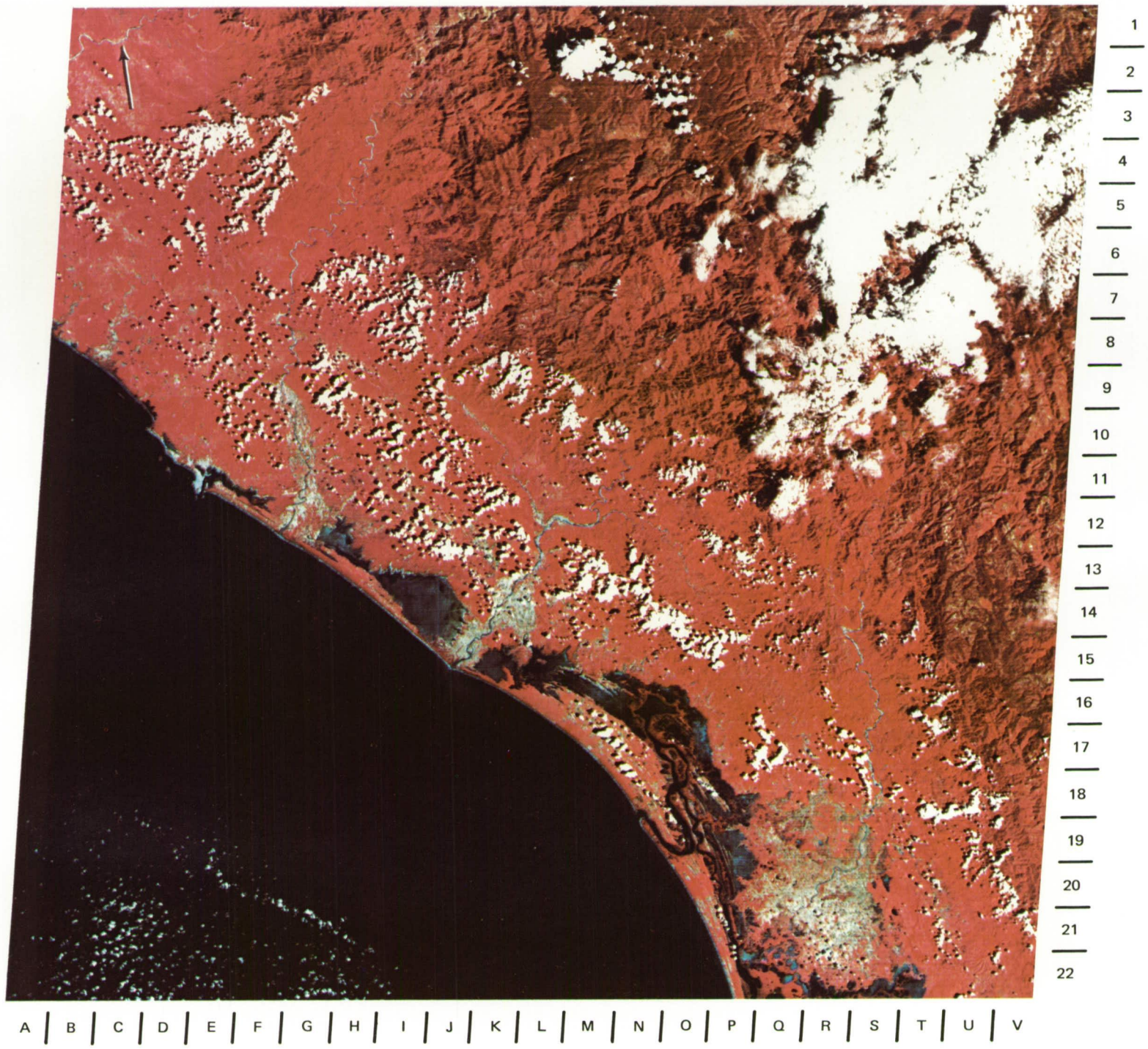
Mazatlán (see plate 181), about 23° N latitude, receives about 75 centimeters (30 inches) of rain per year. The amount decreases to less than 25 centimeters (10 inches) in the State of Sonora at the head of the Gulf of California.

Commercial agriculture, as seen in this image centered about Ciudad Obregón (*C*–13) and Navajoa (*J*–17), requires irrigation. Fortunately, the high west-facing slopes of the Sierras receive ample rainfall to supply perennial streams that cross the coastal deserts. Reservoirs have been built in the Sierra foothills above the coastal plain to provide a regulated supply of irrigation water. Obregón Reservoir (*C*–8) on the Yaqui River upstream from Ciudad Obregón, and Macuzari Reservoir (*N*–15) on the Mayo River northeast of Navajoa, supply the large irrigated region seen in this image (*B*–14; *H*–19). The third reservoir is Miguel Hidalgo (*V*–21), which serves the Los Mochis area farther south along the coast. The chief crops in this area are wheat, sugarcane, rice, and vegetables, especially tomatoes. Ciudad Obregón is one of the principal rice-producing areas in Mexico. In addition to the commercial crops, there is considerable subsistence farming in numerous ejidos (communally operated farms) along this coast.

Much of the immediate coastal zone is not used for agriculture due to its low, swampy nature. Some of the shoreline of Santa Barbara Bay (*E*–19) south of Navajoa is farmed, but sizable coastal flats west of the bay are not used.

As is true farther south, the higher slopes of the Sierra support coniferous forests, areas of more intense red (*P*–18; *L*–4), whereas the lower west-facing slopes support stands of mixed forests, areas of duller red (*N*–13; *E*–2). The natural vegetation on the dry coastal plain is xerophytic shrub (*L*–21). *1262–17182;* April 11, 1973.

PLATE 181



MAZATLÁN, MEXICO: The town of Mazatlán (*D*–11) is located on Mexico's tropical western coastal lowland in the State of Sinaloa almost astride the Tropic of Cancer (*E*–8). Mazatlán is the principal port for western mainland Mexico and an orange-growing and meat-packing center.

The shoreline is characterized by a series of coastal lagoons lying behind offshore sandbars (*H*–13; *N*–17). Inlets mark the mouths of streams draining across the coastal plain. Several river valleys are discernible: the Quelite (*B*–7), the Presidio (*I*–11), the Baluarte (*K*–13), and the Acaponeta (*R*–19). The town of Tecuala and its surrounding agricultural area is located in the valley of the Acaponeta. Cumulus clouds cover much of the coastal lowland (*H*–10; *T*–18). The tropical climate and well-watered stream valleys permit commercial agricultural crop production such as oranges, sugarcane, and tomatoes. Considerable acreage is devoted to subsistence crops also. Maize and numerous other vegetables are produced for local consumption.

A significant contrast exists between the natural vegetation on the tropical coastal lowland and that of the higher, cooler Sierra Madre Occidental (*O*–2). A distinct line of demarcation is visible along the foothills of the Sierra (*K*–10). The coastal zone with its tropical wet-dry season regime supports a broadleaf evergreen shrub woodland, whereas the darker red vegetative signature of the highlands results from a needleleaf evergreen forest.

The volcanic Sierra Madre Occidental rises to elevations of almost 2800 meters (9000 feet) above the coastal lowland. Much of the higher surface of the Sierra is obscured by cloud cover. *1079–17012;* October 10, 1972.

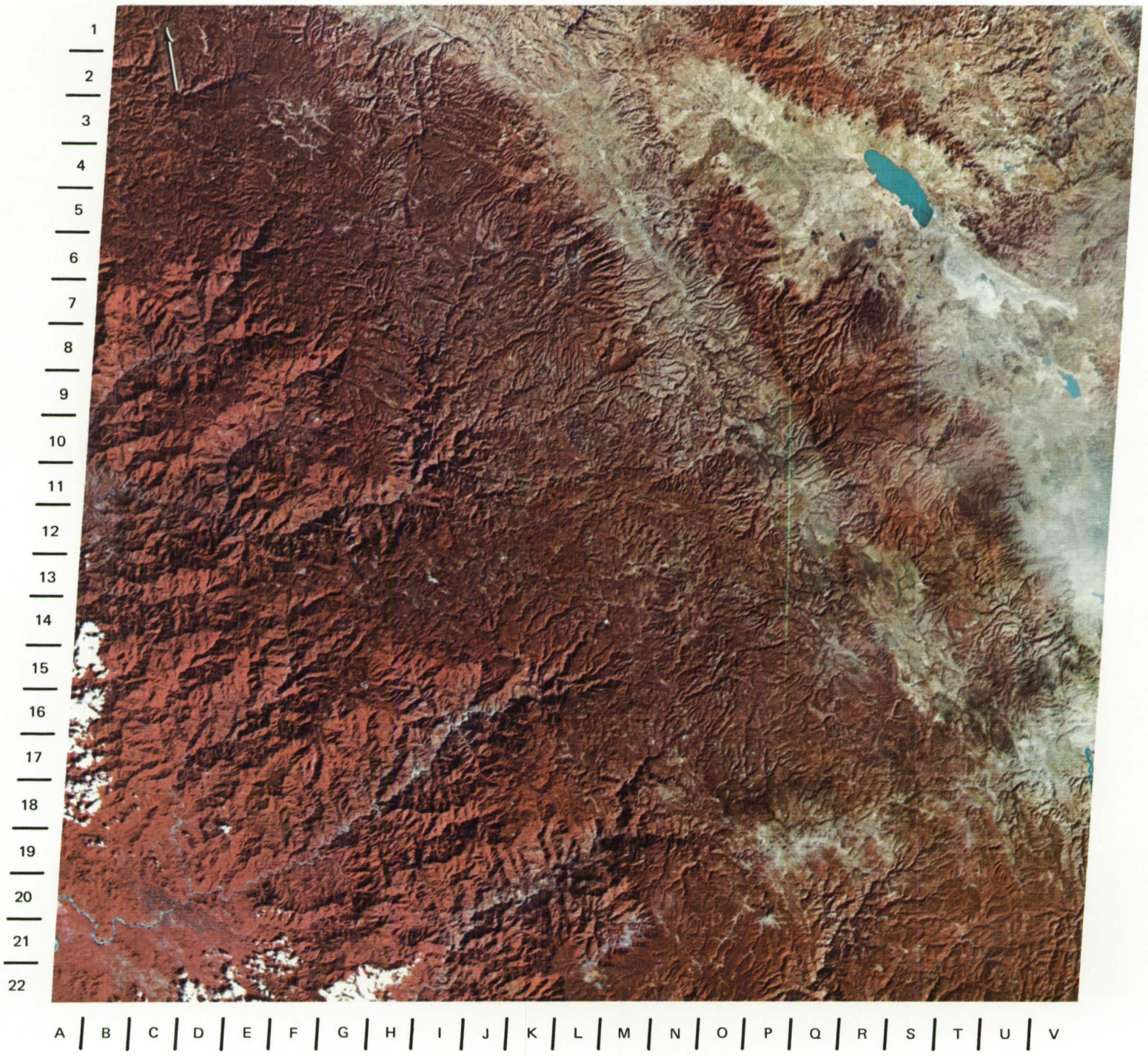


PLATE 182

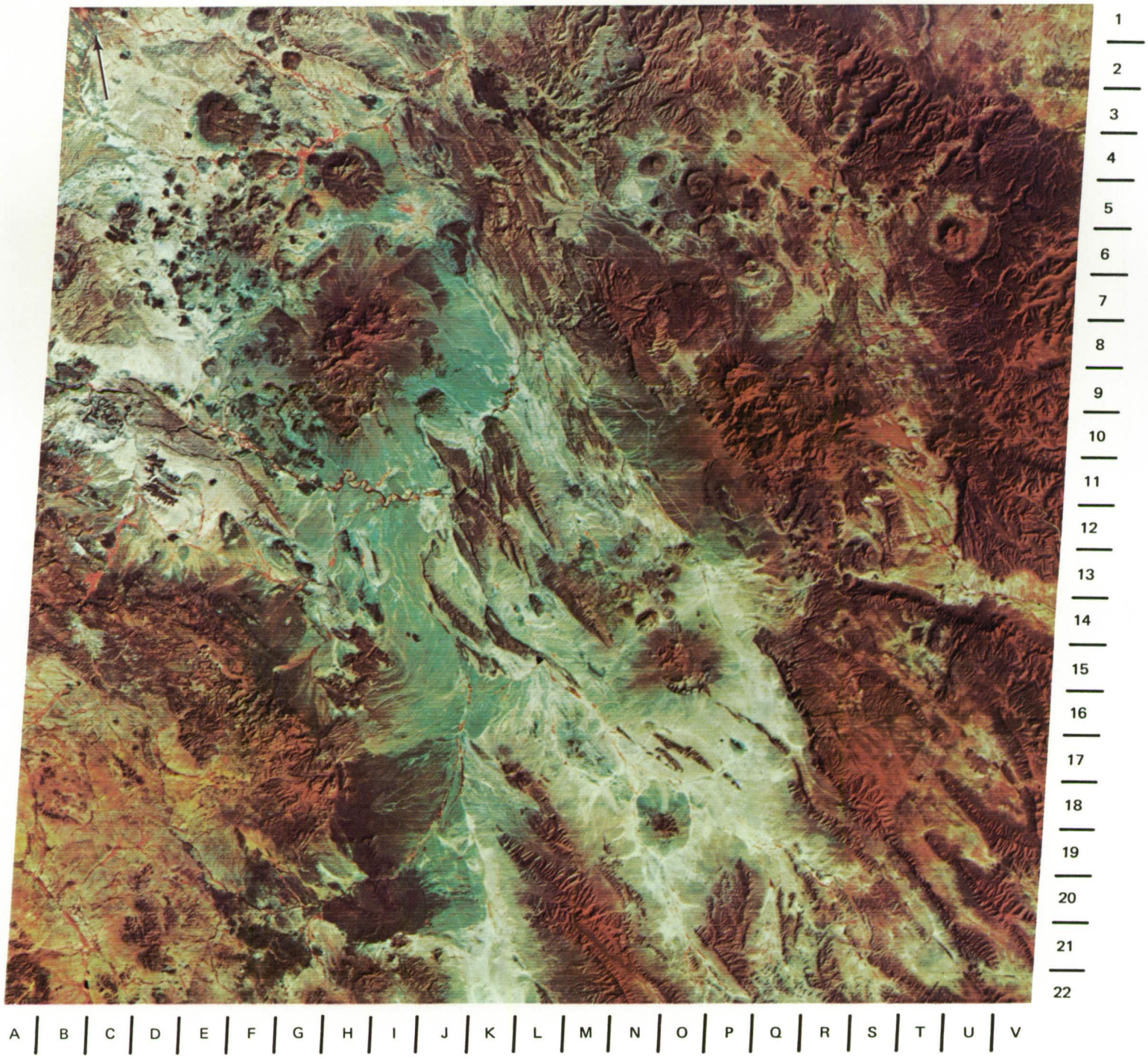
SIERRA MADRE OCCIDENTAL, MEXICO: The topography of northern Mexico is dominated by two mountain ranges extending northwest to southeast, enclosing a large basin between them, with fringing coastal plains on the Pacific Ocean and the Gulf of Mexico. The westernmost of these ranges, the Sierra Madre Occidental (*E*–6; *K*–17), extends for some 1300 kilometers (800 miles) from the U.S. border. The easternmost range, the Sierra Madre Oriental, is discussed in plate 184. The area between the two ranges represents a southern extension of the Basin and Range topography of the western United States.

This image depicts the contrasting environments between the Sierra and the adjoining basin and range west of the city of Durango in northwestern Mexico. The Sierra is a volcanic range with downthrown faulted areas along its eastern flank (*P*–10). The western side of the Sierra received enough precipitation to support the well-watered streams that have dissected the Pacific slope. Four sizable river systems seen in this image drain to the Pacific: the De Los Lobos (*D*–3), the San Lorenzo (*B*–8), the De Los Remedios (*G*–11), and the Piaxtla (*B*–20).

Conversely, the eastern slopes of the Sierra (*N*–13; *R*–9) are drier, steeper, and lack the deeply incised river canyons seen on the western slope. The eastern margin of the Sierra consists of a series of fault-controlled blocks with intervening basins. These basins, lying as much as 1500 meters (5000 feet) below the crest of the Sierra, usually have no external drainage and contain playas and saline accumulations in their lower portions. The Laguna de Santiaguillo (*R*–5; *T*–7) represents such a basin.

Vegetative differences also result from the contrasting climatic environments. The cool, well-watered, higher slopes of the Sierra support a coniferous forest, while the warmer, lower, western slopes support mixed deciduous and evergreen forests. The drier east-facing slopes are more sparsely vegetated, and the lower basin country has a sparse, xerophytic shrub cover. The western slope forests contain some of Mexico's largest forest reserves. Agriculture, other than subsistence levels, is not important in this area; however, the Sierra contains valuable deposits of gold, silver, lead, zinc, and copper. Nearby Durango is an important regional mining center. *1115–17013;* November 15, 1972.

PLATE 183



BIG BEND, TEX., AND CHIHUAHUA: The Rio Grande winds around the Big Bend National Park and the Chisos Mountains (*G*–8) in western Texas, where dozens of Tertiary igneous plugs dot the wide, alluviated valleys. Some of the larger plugs form prominent mountains, and at El Solitario (*A*–6) the overlying sedimentary rocks are domed into a nearly perfect circle. In Mexico, a similar feature in the Sierra del Burro (*T*–5) is appropriately named El Sombrero. South of the Rio Grande, in Coahuila, the mountains are dominantly Cretaceous sediments, and many mines are located throughout the folded ranges east of the Alamo River (*J*–11), in the Sierra del Carmen (*O*–8), and in the Sierra Encantada (*S*–17). To the west, in Chihuahua, where Tertiary volcanic rocks are spread out over a large, mountain-rimmed plateau, the local name "Llano de los Ranchos" is evidenced by grassland and ranch boundaries and signs of agriculture along the streams. *1816–16430;* October 17, 1974.

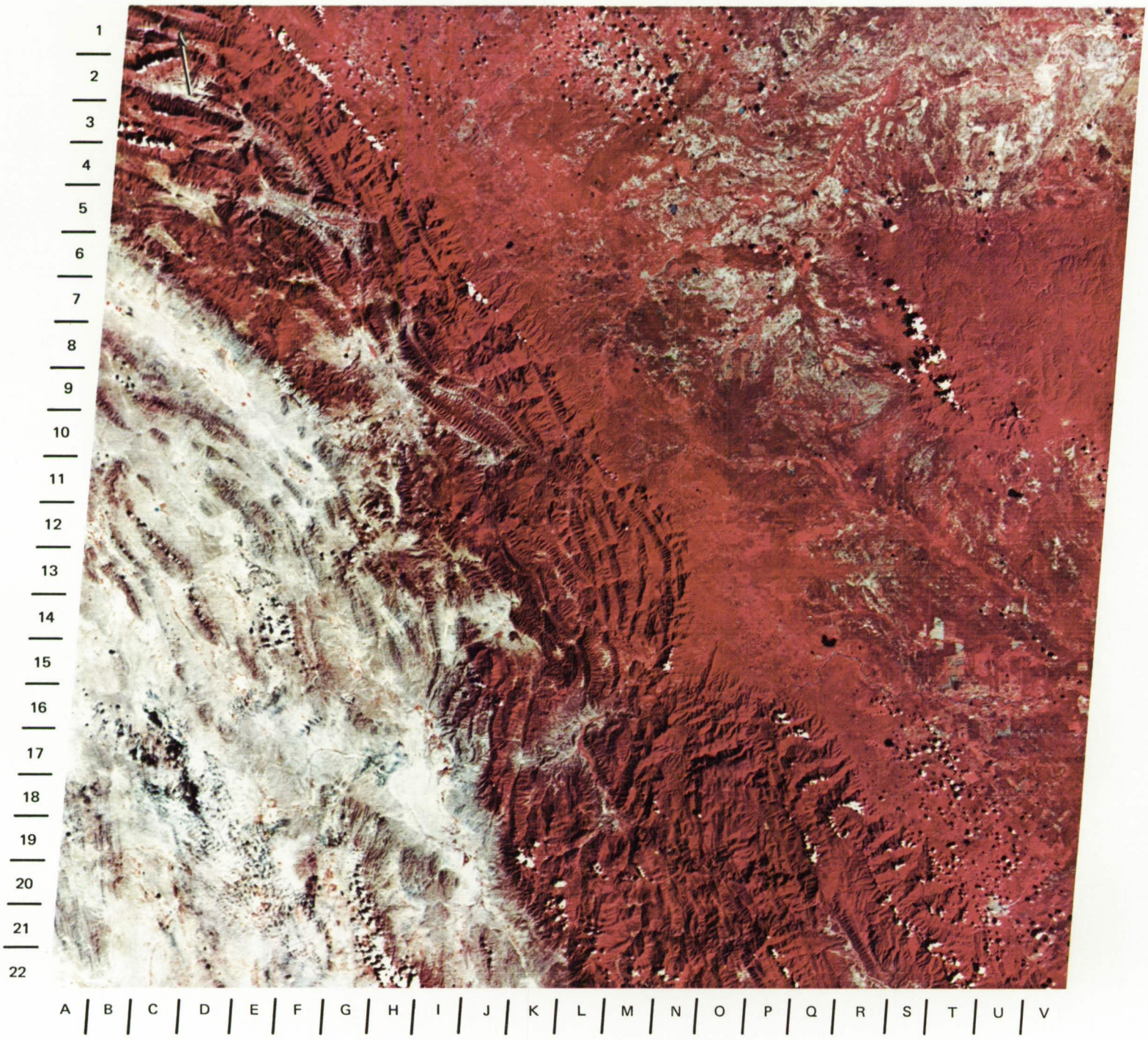


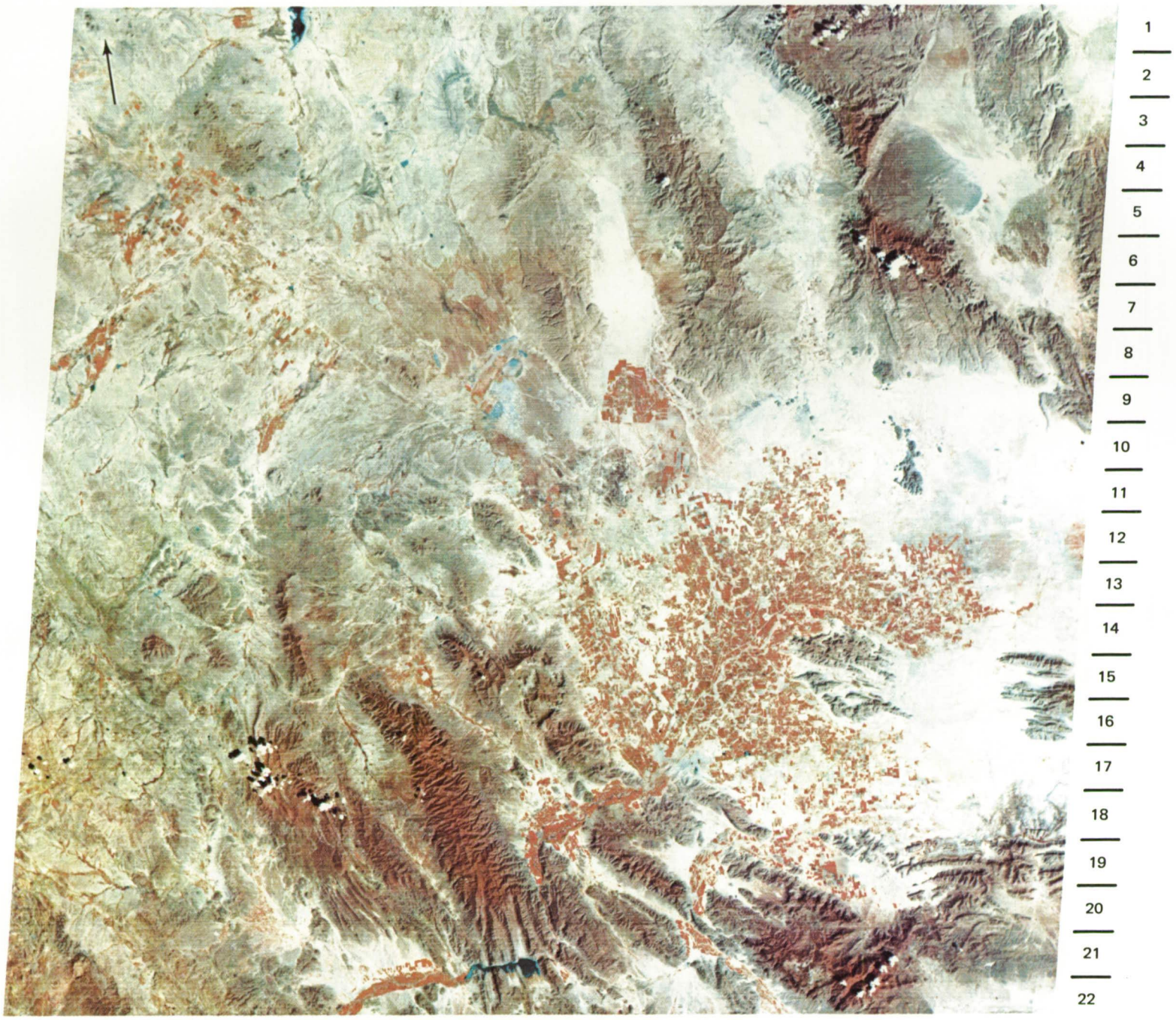
PLATE 184

SIERRA MADRE ORIENTAL, MEXICO: This scene spreads just to the south and east of the Landsat image shown as figure 13 in the introductory chapter. Color tone differences result in part from processing by different photo labs and from the 15° higher Sun angle when this view was taken nearly 2 months earlier.

The drastic difference in vegetation cover between the high desert in the Mexican States of Nuevo Laredo (*A*–10) and San Luis Potosi (*L*–21) west of the Sierra Madre Oriental (*L*–13) and the lower coastal plains of the State of Tamaulipas (*R*–3) to the east is mainly the effect of the greater rainfall in the coastal region affected by moisture from the Gulf of Mexico. Annual precipitation in this humid belt is greater than 750 millimeters (30 inches). This region has a temperate monsoon climate, with rainy hot summers and dry winters. Moisture-laden winds moving inland off the gulf must pass over the mountains, which reach elevations of 2600 meters (8500 feet) just below Monterrey to more than 4000 meters (13 000 feet) near the south border of this scene. As a result, the arid interior receives far too little rain to support other than typical desert flora, such as the palm cactus—a source of istle, a fiber used as a curly filling in upholstery and in shoebrushes.

The Sierra Madre Oriental, a tightly folded belt of Cretaceous sedimentary rocks, is mantled with both broadleaf and coniferous trees. The plains to the east are semidesert savanna that gradually becomes more tropical southward. Livestock ranching is the main agricultural pursuit, along with the raising of cotton and other crops and growth of oranges and other citrus fruits. The Pan American Highway passes south from Monterrey through the town of Linares (*L*–6) on the Rio Conchos, thence across the Rio Purificación (*Q*–15), and through the State capital of Ciudad Victoria (*U*–20). This latter town is a center for production of sisal—extracted from henequen, one of the agave plants—a tough fibrous leaf used in making baskets and hammocks. *1075–16380;* October 6, 1972.

PLATE 185



TORREÓN, MEXICO: Torreón (*N*–16) is located in a basin lying between the westernmost ridges of the Sierra Madre Oriental (*U*–19) and the easternmost outliers of the Sierra Madre Occidental (*J*–16). At this point, northern Mexico's two great mountain ranges almost meet. Its strategic location between the two Sierras has caused Torreón to become the major rail and highway communication center for this part of Mexico.

A second factor has also contributed to the rapid growth of Torreón and its hinterland during the last quarter century. During colonial times this area was held by a few owners under original Spanish land grants. The hacienda system of large land holdings devoted mostly to wheat production persisted in the Torreón area until the mid-1930's. A series of land reforms imposed by the Mexican Government divided the area into several hundred smaller, communal units known as ejidos. The ejido system necessarily called for more intense usage of the land. Dams were built on perennial rivers flowing from the Sierra Madre Occidental into the dry basin country. The largest of these dams, El Palmito, is located immediately west of this image. A smaller reservoir is located on the Nazas River near the southern margin of the image (*K*–21).

Torreón, and its satellite agricultural areas, have subsequently become the showplace for the ejido land reform program in Mexico. The large agricultural district north of Torreón known as the Laguna District (*P*–13) was developed upon the dry bed of a basin known as Bolson de Mapimi. Other smaller areas have been developed (*D*–5; *L*–18) and many other dry basins in the area await future development (*M*–7; *U*–16). Today the area is devoted primarily to wheat and cotton production—roughly one-half of Mexico's cotton crop is produced in the Torreón area. *1078–16545;* October 9, 1972.

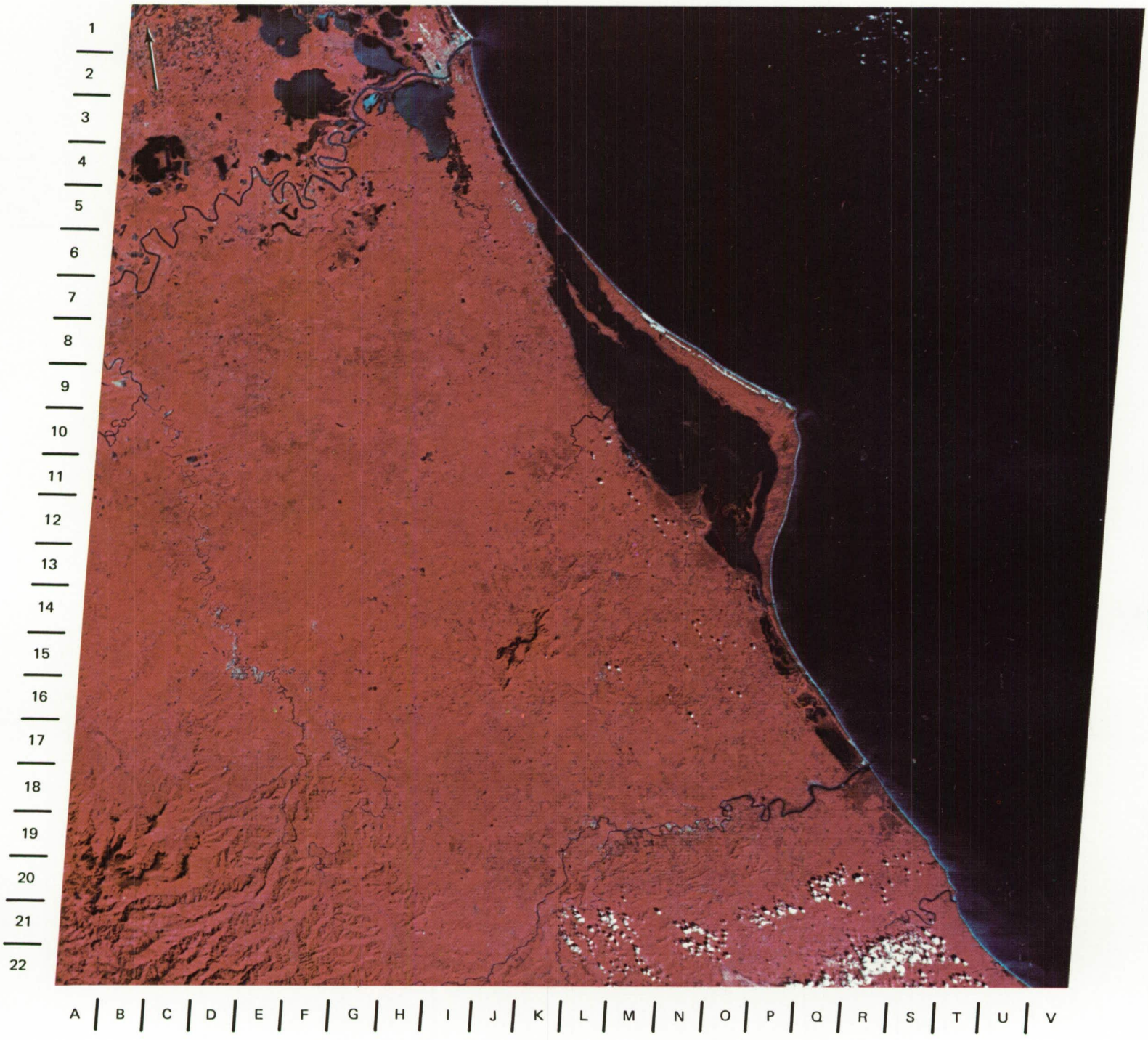


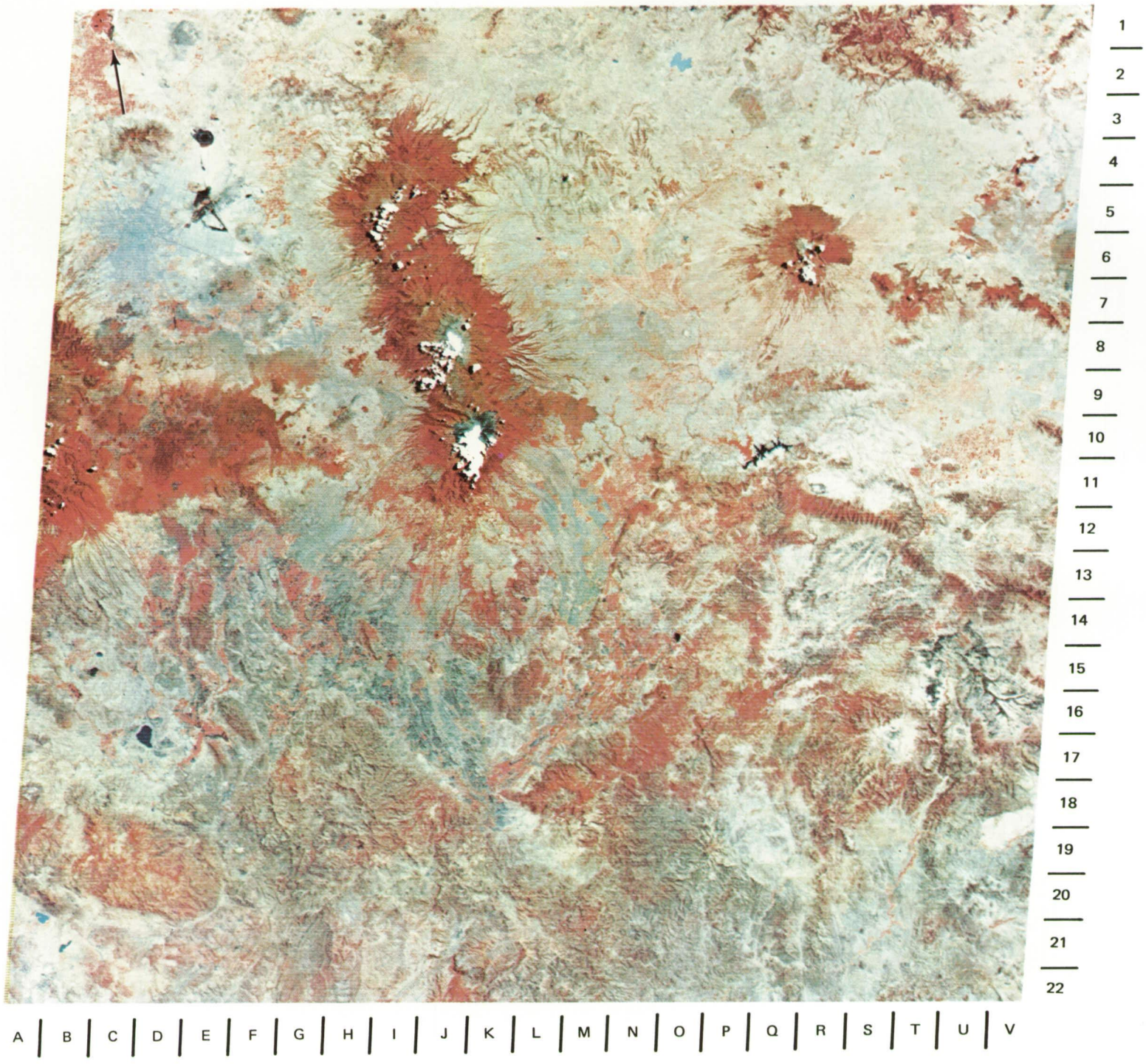
PLATE 186

TAMPICO, MEXICO: Tampico (*G*–1), a major population, petroleum, and port center, is located at the mouth of the Pánuco River (*E*–4) on the Gulf of Mexico coastal plain. The coastal plain, usually no more than 32 kilometers (20 miles) wide in this region, is a complex of lakes, offshore sandbars, lagoons, mangrove swamps, streams draining from the foothills of the Sierra Madre Oriental, and fringing coral reefs. Five sizable lakes occupy the Pánuco River lowland west of Tampico (*A*–4; *F*–2). A classic example of offshore bar development occurs south of Tampico. Cabo Rojo marks the easternmost point of this bar (*P*–9). Local longshore currents have molded the bar into its arcuate shape. The Laguna de Tamiahua (*N*–10) occupies the low, swampy area inland from the outer bar. Several islands of vegetated higher ground dot the surface of the lagoon (*K*–7; *M*–11). Coral reefs appear as whitish islands offshore (*R*–15; *S*–16).

In addition to the Pánuco River in the northern portion of this image, the Tempoal River (*C*–12) and the Tuxpan River (*Q*–17) traverse the coastal plain south of Tampico. The drainage network incised into the flank of the Sierra by tributaries of the Tempoal River is readily visible (*B*–20). Sediment plumes, formed as rivers empty their transported loads into the gulf, can be seen at the mouth of the Tuxpan and several lesser rivers in the vicinity. Because the summer into November is rainy, the streams would be carrying maximum loads and creating large sediment plumes during this time of year.

Two of Mexico's major oil-producing areas are shown in this image. The Pánuco Valley fields, west of Tampico (*C*–4), is the oldest producing region in Mexico. The first well was developed in 1901. Ciudad Madero, located in the northern outskirts of Tampico, is the major refining and transport center in this part of Mexico. Road and rail connections link Ciudad Madero with the major mining and industrial centers in the Sierra Madre Oriental and on the interior plateau. The second oil-producing area along this coast occurs in a valley near the town of Cerro Azul (*L*–15). *1109–16275;* November 9, 1972.

PLATE 187



MEXICO CITY, MEXICO: The oldest city still inhabited in the Western Hemisphere was founded in 1324 under the name Tenochtitlán; today, as Mexico (or Mexico City) (*B*–5), it is the leading city of Latin America, with a population of over 7 million. The Distrito Federal, the national capital, has a population of more than 8½ million (including that of Mexico City itself). The geographic setting of Mexico's capital is well exhibited in this Landsat image. Lying at an altitude of 2800 meters (7500 feet) in the Valley of Mexico, surrounded by volcanic mountains, the city was originally located on an island in Lake Texcoco, whose mostly drained remnant is visible at *D*–5. The most famous volcanoes of Mexico are Iztaccihuatl (*I*–8) and Popocatépetl (*J*–10); these are the highest peaks (over 5100 meters (17 000 feet)) in a major northwest to southeast trending volcanic range. Note the strong control of vegetation by height; this range has dense forest cover above 2700 to 3000 meters (9000 to 10 000 feet), but the upper timberline is visible still higher, at about 4300 meters (14 000 feet). Similar vegetation zones can be seen around La Malinche (*P*–6), another great volcano nearly 4600 meters (15 000 feet) high just northeast of Puebla (*O*–8), Mexico's fourth city. Cuernavaca is just visible at *B*–16 south of Mexico City.

The Valley of Mexico and the many volcanoes visible here are part of the Neo-Volcanic Plateau, a great zone of seismic and volcanic activity running east to west across Mexico. It appears to be the continental continuation of the Clarion Fracture Zone, one of the immense east-west transform fault zones of the Pacific Basin; if North America has drifted to the west as believed by proponents of continental drift, the continent may have overridden the Clarion Fracture Zone. South of the Neo-Volcanic Plateau we see the Oaxaca Upland, a mountainous region composed largely of intensely folded Mesozoic sedimentary and igneous rock. The folds trend roughly north to south (note the one at *G*–21), and their orientation may control that of the volcanoes within the Neo-Volcanic Plateau, which tend to occur in clusters crossing the plateau as shown here. Landsat 1 imagery is valuable for showing such regional relationships. *1307–16285;* May 26, 1973.

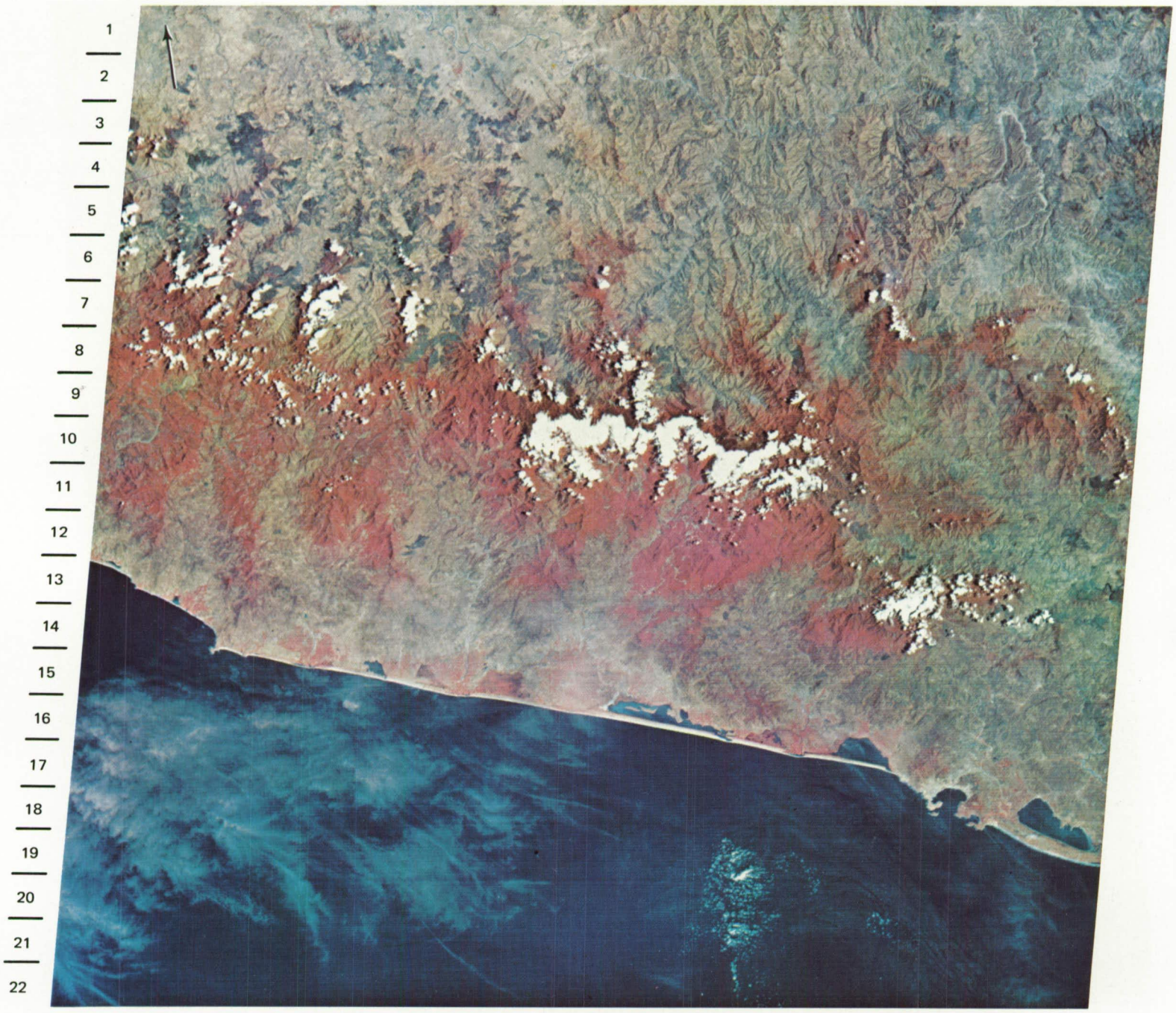


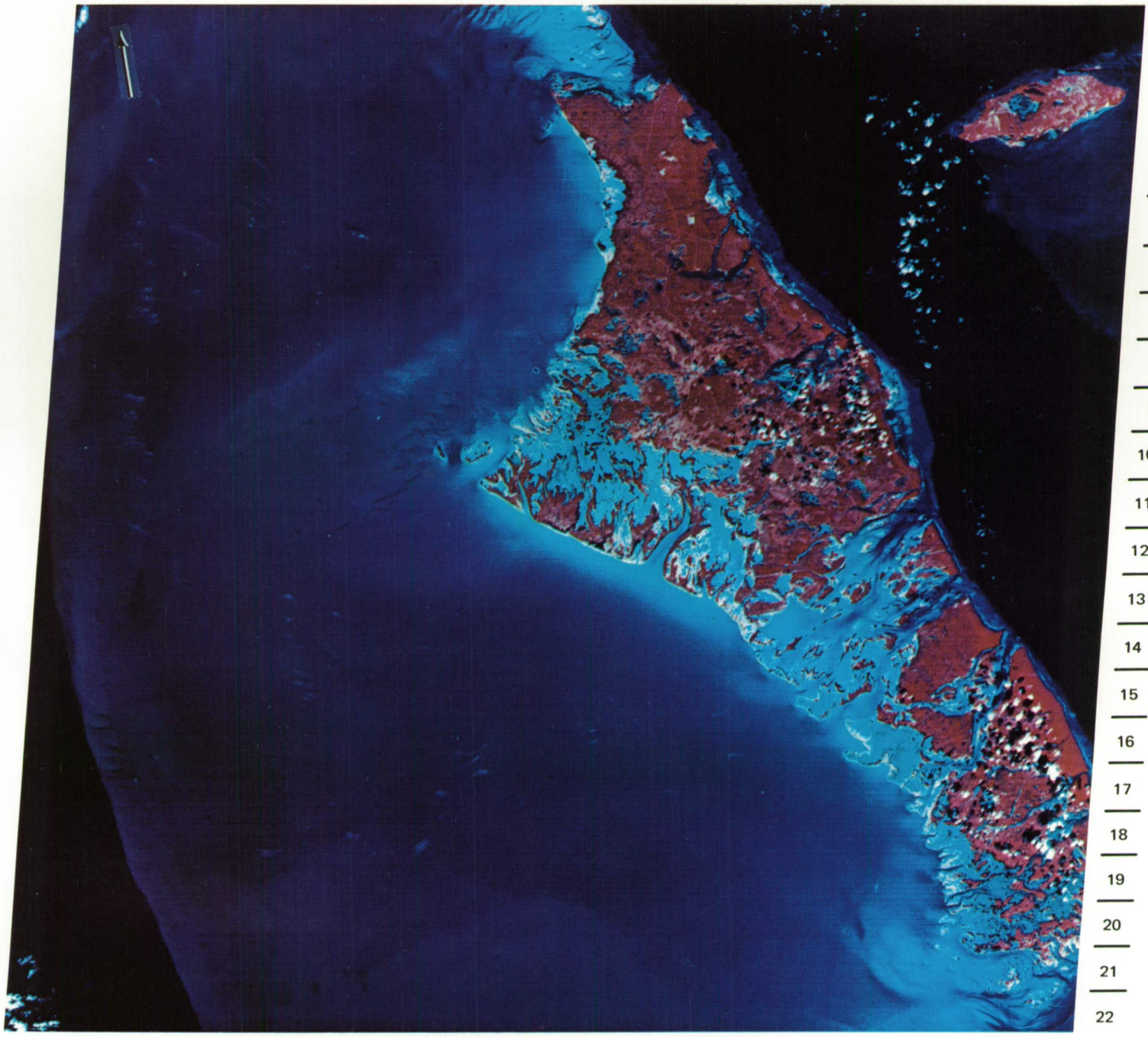
PLATE 188

ACAPULCO: This famed resort town (*S*–17) in the Mexican State of Guerrero is set in a small natural bay against a backdrop of steep mountains. Elsewhere along the coast, longshore currents have built up sandbars that enclose freshwater lagoons such as Laguna de Coyuca (*Q*–16) and Laguna Papagayo (*V*–18). There, white sand beaches are dotted with coconut palms. This part of Mexico is a tropical savanna, with some scrub woodlands at higher elevations. Annual rainfall averages about 125 centimeters (50 inches).

The Sierra Madre del Sur (*F*–9) is a northern segment of the Central American Ranges that extend to Panama. These mountains rise abruptly from the narrow coastlands to elevations above 3000 meters (10 000 feet). The cloud-topped Teotepec Peak (*N*–10), the highest point in this range, reaches to 3703 meters (12 149 feet). At lower to middle elevations, the rocks are mostly Paleozoic metamorphics. The higher, largely forested elevations are covered by volcanic rocks of Tertiary age. The Rio Balsas (*G*–1) cuts through continental sediments (*O*–3) of mid-Tertiary age.

Copra, the dried kernel of the coconut and source of coconut oil, is a major product along the coastal zone. Some coffee is also grown there, and wild rubber trees are found in this region. Sugarcane is cultivated along the northern slopes and valleys of the Sierra Madre del Sur, as indicated by many large dark patches (*C*–3; *I*–6) that result from burning of the stubble in the fields after harvesting. *1254–16352;* April 3, 1973.

PLATE 189



THE BAHAMAS PLATFORM: One of the few modern day sites of extensive deposition of carbonate sediments is found in the group of hundreds of large and small islands in the Bahamas centered about the resort town of Nassau (*U*–2) some 320 kilometers (200 miles) southeast of Miami, Fla. Much of the carbonate material is produced by marine organisms, which incorporate calcium carbonate into their hard parts or cause it to be precipitated as a sediment. Essential to carbonate production in this environment are conditions that allow prolific growth of these organisms—warm, shallow water clear enough for light to penetrate to bottom dwellers.

The Bahamas Platform extends over about 160 000 square kilometers (60 000 square miles) from Bimini on the west to Long Island on the east. The platform rises abruptly from depths of 460 meters (1500 feet) or more in the Florida Straits (*B*–22) and descends rapidly to depths below 3700 meters (12 000 feet) on the Atlantic Ocean side. For considerable distances offshore around subaerial islands such as the mangrove-covered Andros Island (*O*–9), the largest of the group, and New Providence (*U*–3), to the east, water depths are from less than 15 meters (50 feet), to about a hundred meters (several hundred feet) at most. These islands are built from coral and algae reefs that normally face the open ocean (mainly to the east) on the windward side. Behind the reefs are lime muds and sands (indicated by lighter blue tones) composed of skeletal fragments of the organisms and oolitic or pelletoidal (rounded accretionary grains) sands. Ocean and tidal currents distribute these sands further to the west along the Great Bahama Bank (*C*–1; *M*–21). Between the islands are deeper channels (generally below 300 to 600 meters (1000 to 2000 feet) and as deep as 2400 meters (8000 feet) in parts of the "Tongue of the Ocean" (*Q*–5)). Carbonate sedimentation has continued in the Bahamas at least since Cretaceous times, so in places more than 4600 meters (15 000 feet) of limestone and dolomite have accumulated. The platform itself has been periodically sinking to accommodate the new materials. *1510–15093;* December 15, 1973.

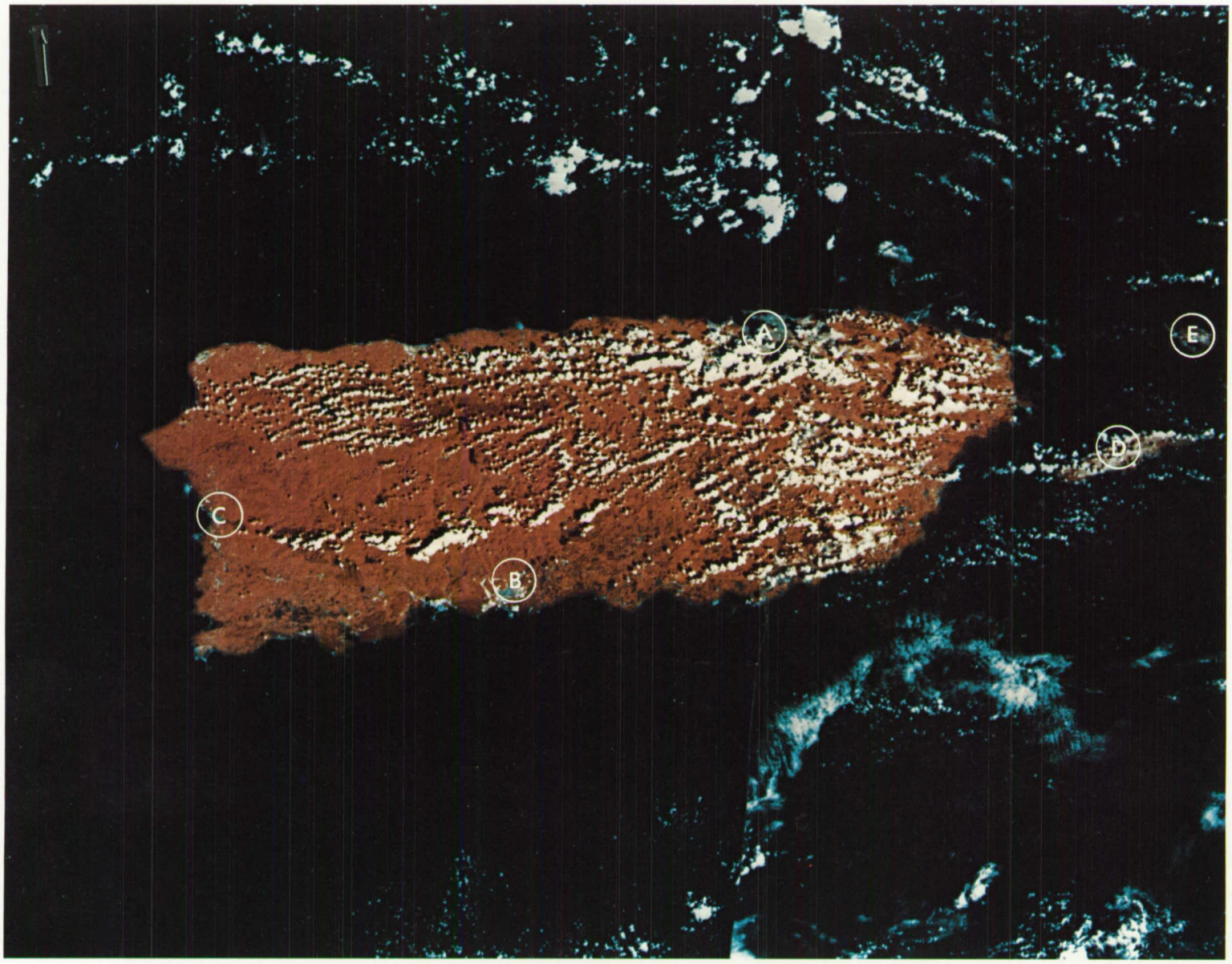
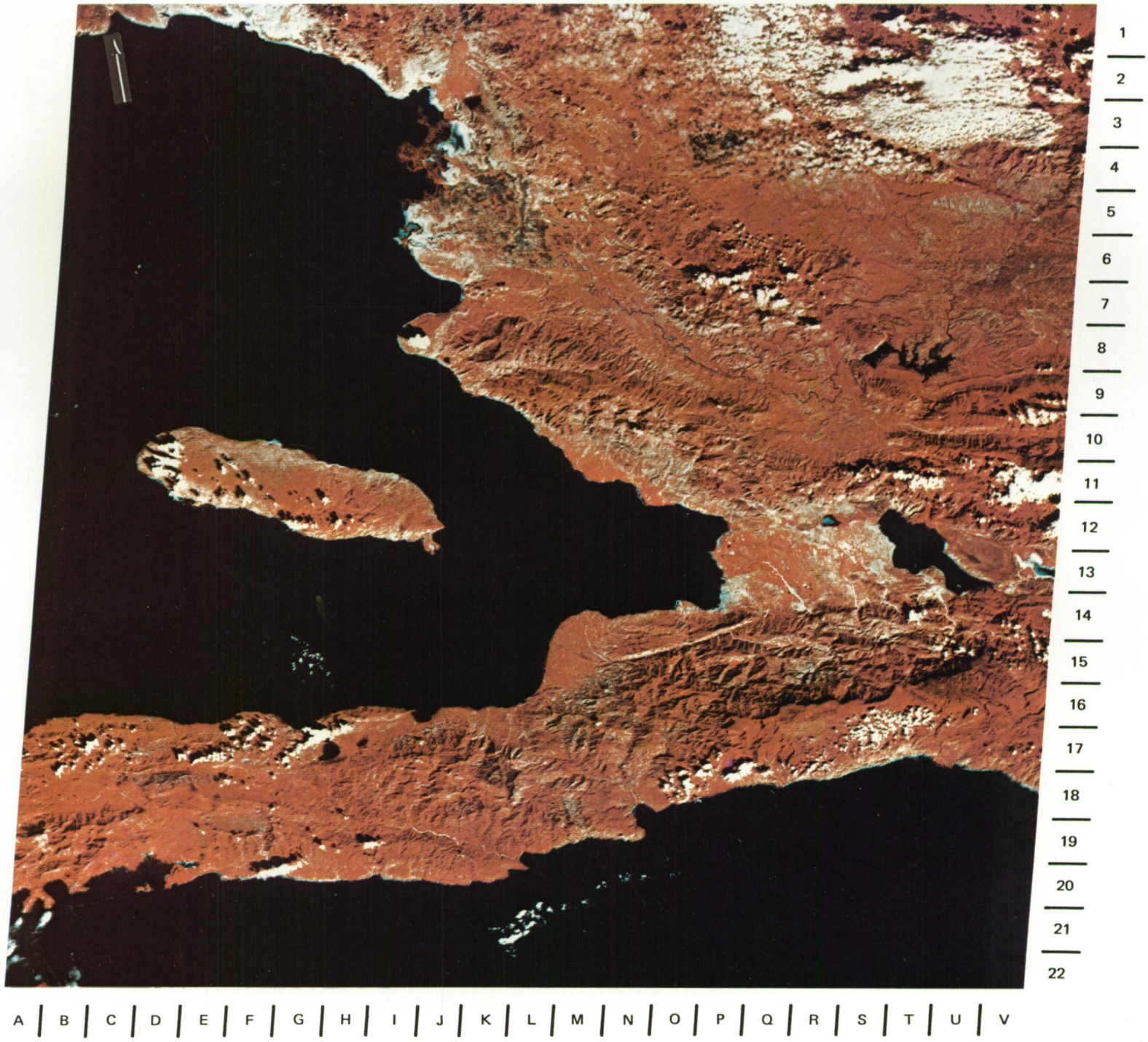


PLATE 190

PUERTO RICO: This mosaic of Puerto Rico was made from imagery obtained on two successive days. The island, about 160 kilometers (100 miles) long and 56 kilometers (35 miles) wide, is located in the Caribbean some 1553 kilometers (965 miles) southeast of Miami, Fla., and about 710 kilometers (440 miles) north of the Venezuelan coast of South America. Puerto Rico is freely associated with the United States, having been given Commonwealth status in 1952. The more than 2.7 million people living there are nonvoting citizens of the United States. The capital, San Juan (*A*), presently has a population of nearly half a million. Other large cities include Ponce (*B*) and Mayagüez (*C*). The population density of the main island is one of the highest in the world. The small islands of Vieques (*D*) and Culebra (*E*), part of this territory, are more sparsely settled.

Puerto Rico was discovered by Columbus during his second voyage to the New World. It is richly vegetated with many tropical species, including a variety of palms. Sugarcane is a major crop in the lower coastal regions, along with bananas and pineapples. Tobacco and coffee are grown in the highlands which in places reach above 1200 meters (4000 feet).

PLATE 191



HISPANIOLA: This large island, part of the Greater Antilles group, lies between Cuba and Jamaica on the west and Puerto Rico and the Virgin Islands to the east. It is subdivided into the French-speaking country of Haiti on the west, much of which appears in this view, and the Spanish-speaking Dominican Republic on the east. The border is located on an irregular line passing near the right edge of the frame.

A long east-west peninsula (*H*–18) less than 32 kilometers (20 miles) wide is capped by rugged mountains reaching 1200 to 1500 meters (4000 to 5000 feet) above sea level. Elevations up to 1786 meters (5860 feet) occur north of the Artibonite River (*N*–8) west of Lac de Peligre (*S*–8). This range consists mostly of strongly folded Tertiary marine sediments of Paleocene, Eocene, and Oligocene age interspersed with volcanic rocks.

Port au Prince (*O*–13), the capital of Haiti, occupies a strip of flood plain at the juncture of the Canal du Sud (*G*–14) and Canal de St. Marc (*I*–10) separated by the Ile de la Gonâve (*F*–11). St. Marc (*I*–7) and Gonaïves (*H*–3) are two of the larger coastal towns in this part of the island. Lush tropical forests and grasslands cover much of Haiti and mangroves (*H*–4) develop at the mouth of the Artibonite River. *1523–14421;* December 28, 1973.

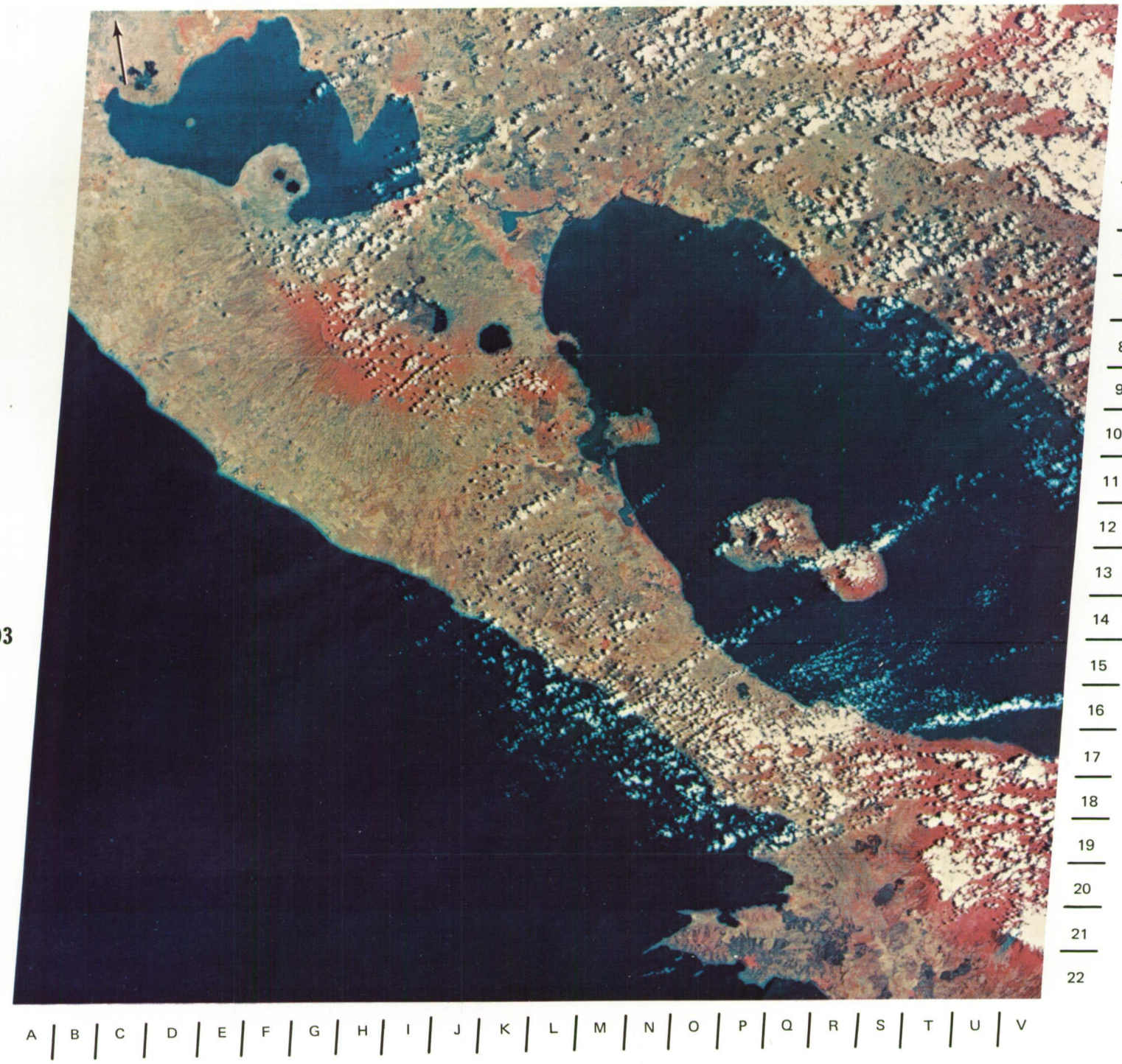


PLATE 192

HAVANA, CUBA: The capital city (*Q*–8) of the island of Cuba lies along the northern coast approximately 180 kilometers (110 miles) southwest of Key West in the Florida Keys. To the west is the Pinar del Rio district (*E*–19) in the westernmost section of the island. The Sierra de los Organos (*F*–14) is a folded sequence of Cretaceous sedimentary rocks (locally invaded by serpentinized basic intrusives) that form a range rising to about 760 meters (2500 feet). Oligocene and Miocene marine sediments extend south (*D*–18) and east (*L*–13) of these mountains. Older Paleocene and Eocene sedimentary rocks have been folded southeast of Havana (*T*–9). Quaternary coastal terrace and beach deposits (*Q*–14) line most of the southern shore region here around the Gulf of Batabano (*Q*–18).

The red clay soils derived from limestones south and east of Havana have proved to be among the most fertile in the world for cultivation of sugarcane. This has long been the major agricultural activity in Cuba. Tobacco is grown in the Vuelta Abajo region (*E*–17)—a long lowlands south of the Organos Mountains. Various vegetables and fruits (including pineapple) are produced around Havana. Other parts of the lowlands are given to grazing. *1171–15295;* January 10, 1973.

PLATE 193



MANAGUA, NICARAGUA: This image covers the southwestern part of Nicaragua from near Puerto Somoza (*B*–8) on the north to the northern sector of Costa Rica around Cabo Santa Elena (*P*–20) on the Pacific coast. Most of Lake Nicaragua (*R*–10) lies in the eastern half of the scene. Ometepe Island (*P*–12) and the smaller Zapatera Island (*M*–10) to the northwest are of volcanic origin and form a segment of the chain of volcanic centers that extend northwestward and southeastward beyond the image. On the south shore of Lake Managua (*D*–2), the city of Managua, devastated by a series of catastrophic earthquakes on December 23, 1972, lies beneath scattered clouds. The Chiltepe Peninsula (*E*–4), marked by the two crater lakes Apoyegue and Jiloa and the small island of Motombito (*C*–3), a volcanic cone, also form part of the above-mentioned volcanic chain. Older dark volcanic flows (*R*–21) are particularly evident around Cabo Santa Elena.

Another Landsat image taken the day after the Managua earthquakes (covering mostly the area to the northwest of the city) was studied to determine the pattern of linear features that could have been active faults during the seismic events. After relating major linear patterns to the known fault zone patterns, detailed ground work by Nicaraguan and U.S. Geological Survey geologists showed that lateral and vertical movements did take place along fracture zones trending northeast through the city. This demonstrated that useful regional geologic knowledge could be acquired in a short time from Landsat imagery which, when coupled with aircraft data and field investigations, would help in the analysis of causative factors in earthquakes.

Darker red tones relate to natural forest vegetation generally found at the higher elevations. Most of the area, however, is semi-arid as indicated by the faint pinkish tones. Light and dark gray tones are mainly bare soils, largely of volcanic origin. Some of those areas may have been burned recently to control weeds and prepare the land for planting. Other areas appear to be swampy where soil moisture is high. *1243–15335;* March 23, 1973.

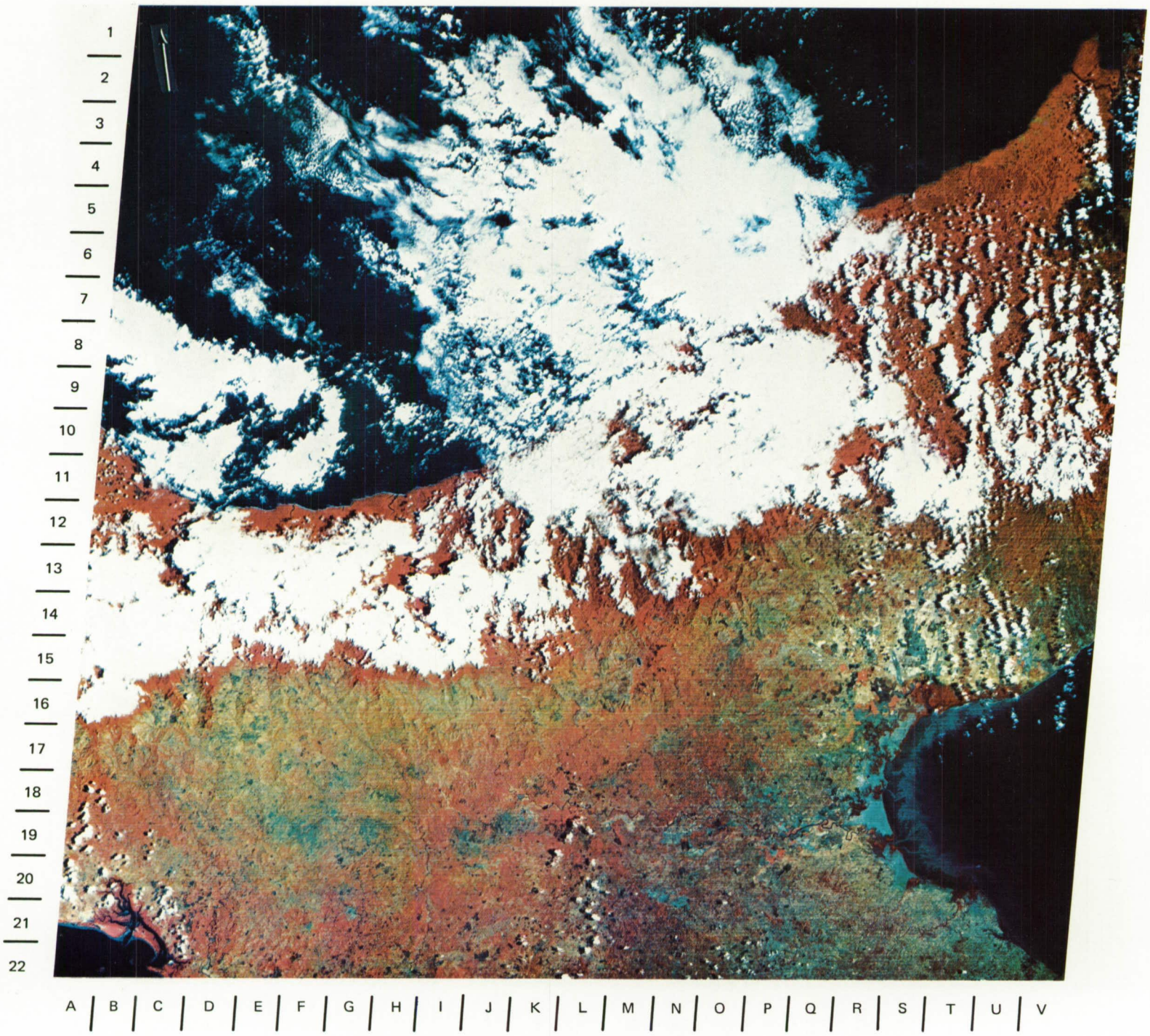


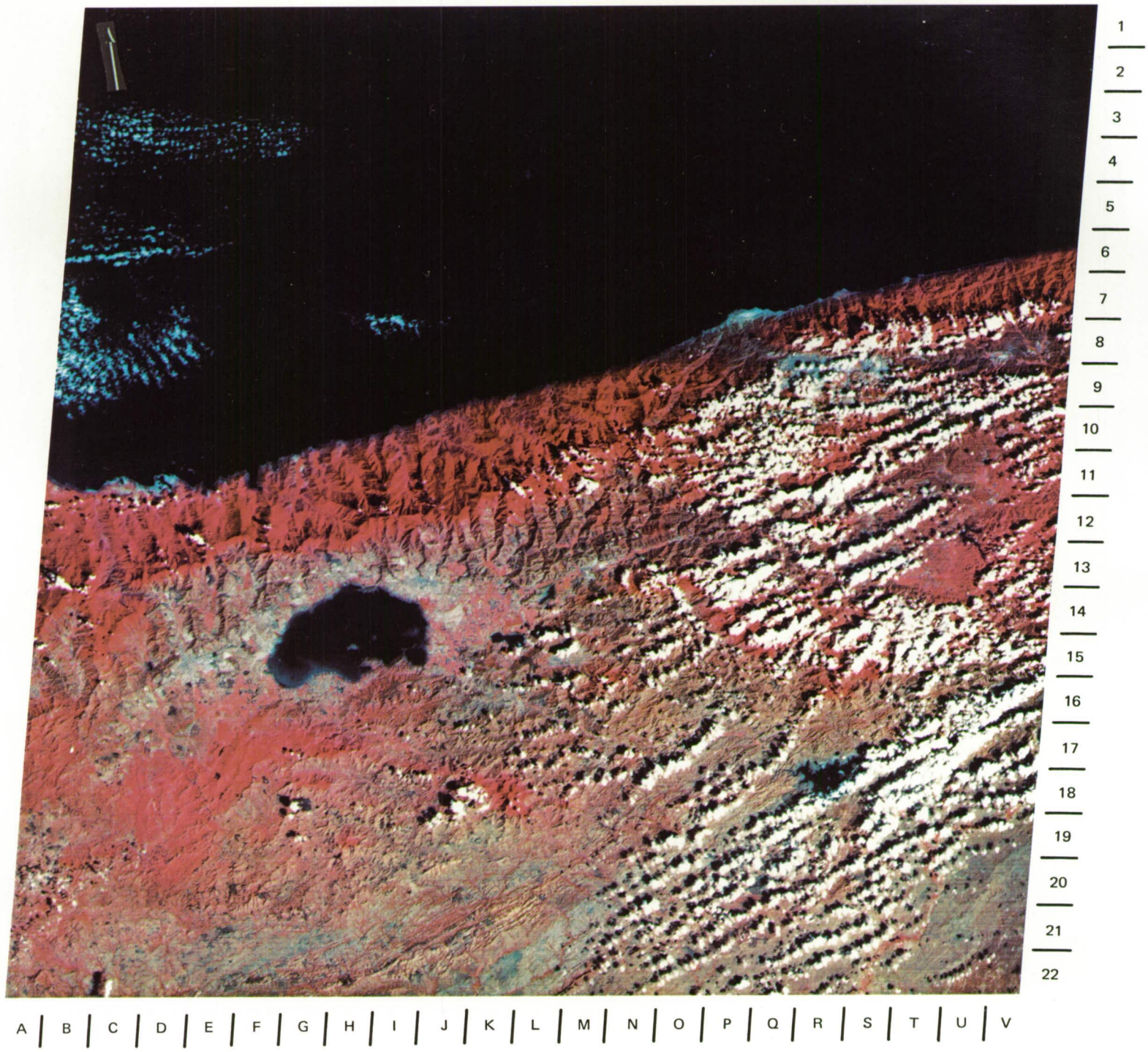
PLATE 194

THE ISTHMUS OF PANAMA: Much of the western half of the Panamanian isthmus, which trends east to west, is imaged here under nearly cloud-free conditions. Clouds have built up over the Serrania de Tabasará (*G*–13), which rises to elevations of 1200 to 1500 meters (4000 to 5000 feet) above the Caribbean coast (*H*–11). This coastal region normally receives up to 305 to 380 centimeters (120 to 150 inches) of rain each year; a tropical rain forest similar to that of Darien to the east develops in these northern heights. The land is considerably lower around Santiago (*L*–20) at the top of the Azuero Peninsula (*J*–21). Vegetation there is characteristic of the semideciduous dry tropical forest. Savanna occurs in places around the Santa Maria River (*P*–19), which empties through swampland (*S*–16) into Parita Bay (*T*–18) at the Gulf of Panama on the Pacific Ocean side. The Pan-American Highway crosses the peninsula in this area after passing south of the mountains at the Gulf of Chiriquí (*A*–21).

A segment of the Panama Canal Zone appears in the upper right corner. Part of the natural Gatun Lake (*V*–5) and its outlet along the Chagres River (*U*–2) are shown, together with the Gatun Locks (*V*–2), a section of the dug canal, which joins the lake (that makes up about 40 percent of the canal waterway) with Limon Bay (*V*–1).

The high Tabasará mountains are composed mostly of Cretaceous sedimentary rocks. Tertiary volcanic rocks constitute the uplands south of the Canal Zone. The Azuero Peninsula is underlain by Oligocene marine sediments. Some soils are derived from volcanic ash carried in by winds after eruptions of volcanoes in Costa Rica. *1239–15115;* March 19, 1973.

PLATE 195



CARACAS, VENEZUELA: The capital (*Q*–8) of Venezuela is situated about 8 kilometers (5 miles) inland from the coastal town of La Guaira (*P*–7), the country's leading port. This city is built in a river valley some 900 meters (3000 feet) above sea level but is surrounded by the high coastal range (*J*–11) of the Central Highlands. This range, made up of metamorphic rocks of Mesozoic age, rises abruptly from the sea to elevations of 2100 to 2400 meters (7000 to 8000 feet) (one peak just northeast of Caracas reaches 2765 meters (9072 feet)). Southward is a structural trough in which Lake Valencia (*G*–14), some 460 meters (1500 feet) above sea level, has formed in an intermontane basin. Mountains to the east have been breached by the River Tuy (*L*–13), which cuts a deep valley en route to the Caribbean further east. South of the Tuy is a mountainous belt of Mesozoic volcanic rocks (*N*–15) juxtaposed against a Cretaceous and Paleozoic sequence (*J*–21) of folded sedimentary rocks. Quaternary sediments are found in the Llanos Lowlands drained here by the Guarico River (*T*–20), tributary to the Orinoco, whose headwaters have been dammed (*R*–17) at the edge of the Central Highlands.

The Valencia Basin is an important agricultural area. Cotton and sugarcane are the chief crops, with maize, beans, and rice also produced. Both cacao and coffee are also grown there and in the highlands around Caracas and the Tuy River. The coastlands are hot and dry and support scrub savanna vegetation. However, rainfall increases notably only a few kilometers inland, producing a dense rain forest. *1176–14185;* January 15, 1973.

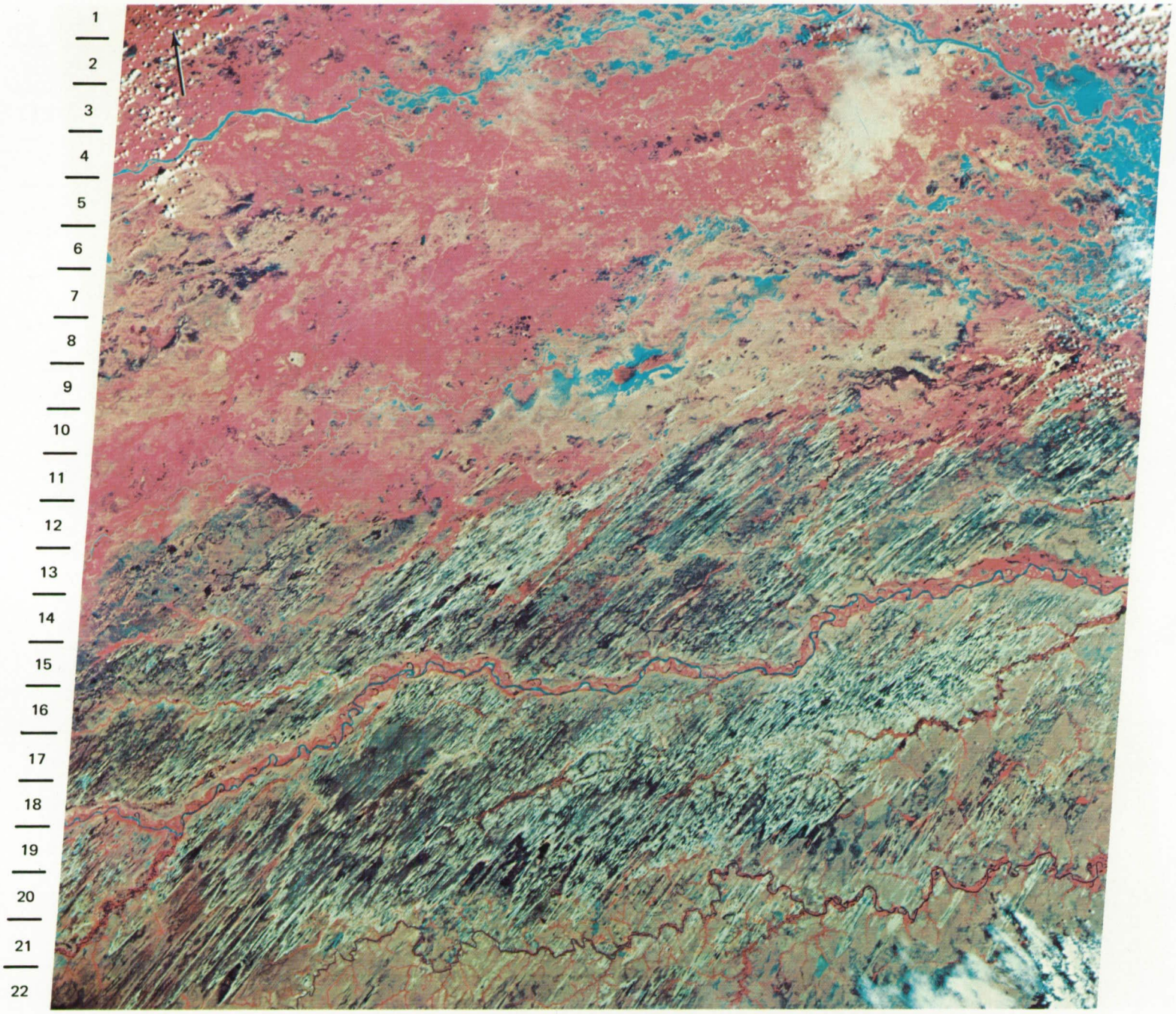
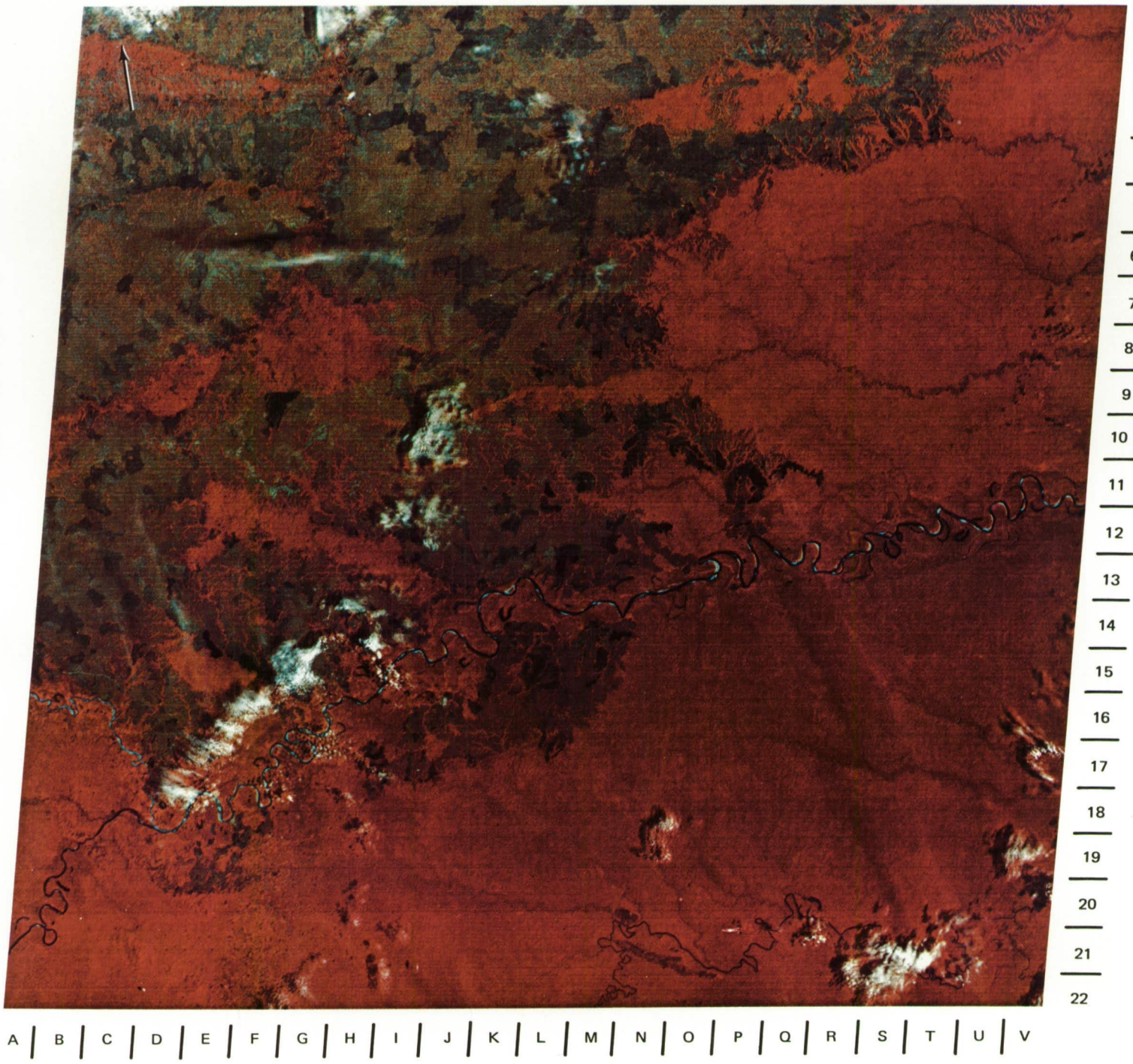


PLATE 196

ORINOCO BASIN, VENEZUELA: This image is located some 560 kilometers (350 miles) upstream roughly near the center of one of the three large drainage basins in South America. The Orinoco Basin is an immense expanse of savanna grassland and scrub woodland, known as the Llanos, extending from the Guiana Highlands on the south to the Venezuelan Andes on the north and west. Four of the major tributaries of the Orinoco River are shown in this scene. From north to south they are the Apure River (*T*–3), the largest; Arauca River (*R*–6); Capanaparo River (*R*–13); and Cinaruco River (*R*–19). A small part of the course of the master stream, the Orinoco, is obscured by clouds near the southeastern corner of the image (*V*–21). This section of the Llanos is an extremely remote area subject to drastic seasonal fluctuations of climatic regimes. The only settlement of any consequence is the town of San Fernando de Apure (*Q*–1) on the Apure River. The Llanos is subject to a tropical savanna climate causing it to experience a wet season during the period from April to October and a dry season during the remaining portion of the year. During the rainy season, much of the area is flooded and impassible; in the dry months from November to March the area is parched and waterless. This mid-October scene toward the close of the wet season shows many seasonal lakes occupying the shallow basins of this gently undulating surface (*V*–3; *L*–8). Hundreds of smaller lakes and swamps are visible especially in the northern half of the image.

In several places along the course of the Orinoco, fingerlike prongs of the ancient crystalline rocks of the Guiana Highlands protrude northward and outcrop above the surrounding recent sediments of the river basin. Where this occurs, an area of low hills with slight relief, usually less than 60 meters (200 feet), may result. During the rainy season the lower areas in such hill lands will be flooded, creating large swampy areas. Such appears to be the case both north (*N*–13) and south (*J*–19) of the Capanaparo River where extensive swamps cover much of the southern region of this scene. *1086–14194;* October 17, 1972.

PLATE 197



THE COLOMBIAN INTERIOR: A broad basin in eastern Colombia drained by tributaries to the Orinoco River of Venezuela is situated to the east of the northern extension of the Andes. Bogota, high in the Eastern Cordillera, lies about 160 kilometers (100 miles) northwest of the upper left corner of this image. The northern half of the terrain here is an extension of the Llanos of Venezuela, a flat lowlands covered by a woodland savanna vegetation. The area drained by the Rio Manacacias (*F*–3), which flows into the Rio Meta to the north, is given to limited cattle grazing. This area, and the lands to the southeast, are sparsely settled by Indians who still engage in cultivating maize, potatoes, and other staples. During the winter dry season the savanna grasses become brown, leading the natives to burn vast tracts (*E*–9; *K*–5), a land practice carried out in primitive regions of South America, Africa, and parts of Asia to remove weeds, destroy insects, and add ash to the soil.

The savanna gives way to a selva or rain forest in the watersheds of the Rio Guaviare (*R*–12), the Rio Ariari (*A*–15), and the Rio Inirida (*O*–21). A few rubber plantations occur in these areas, but production is severely hindered by an almost complete lack of roads. Much of the eastern plains of Colombia is being explored for petroleum under the Cenozoic surface deposits. One large oil field has been brought in near the Ecuadorian border some 320 kilometers (200 miles) to the south. *1196–14325;* February 4, 1973.

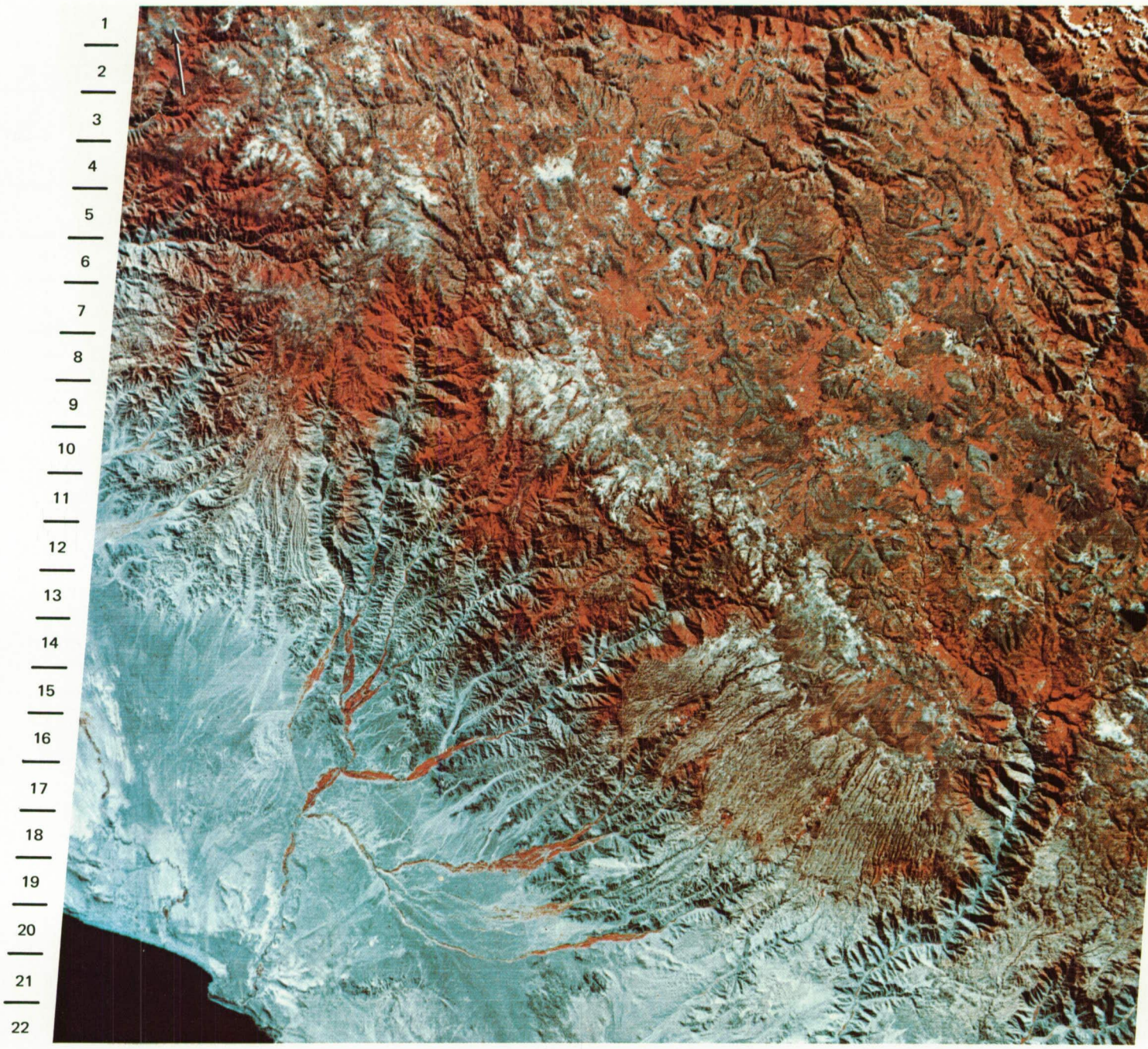
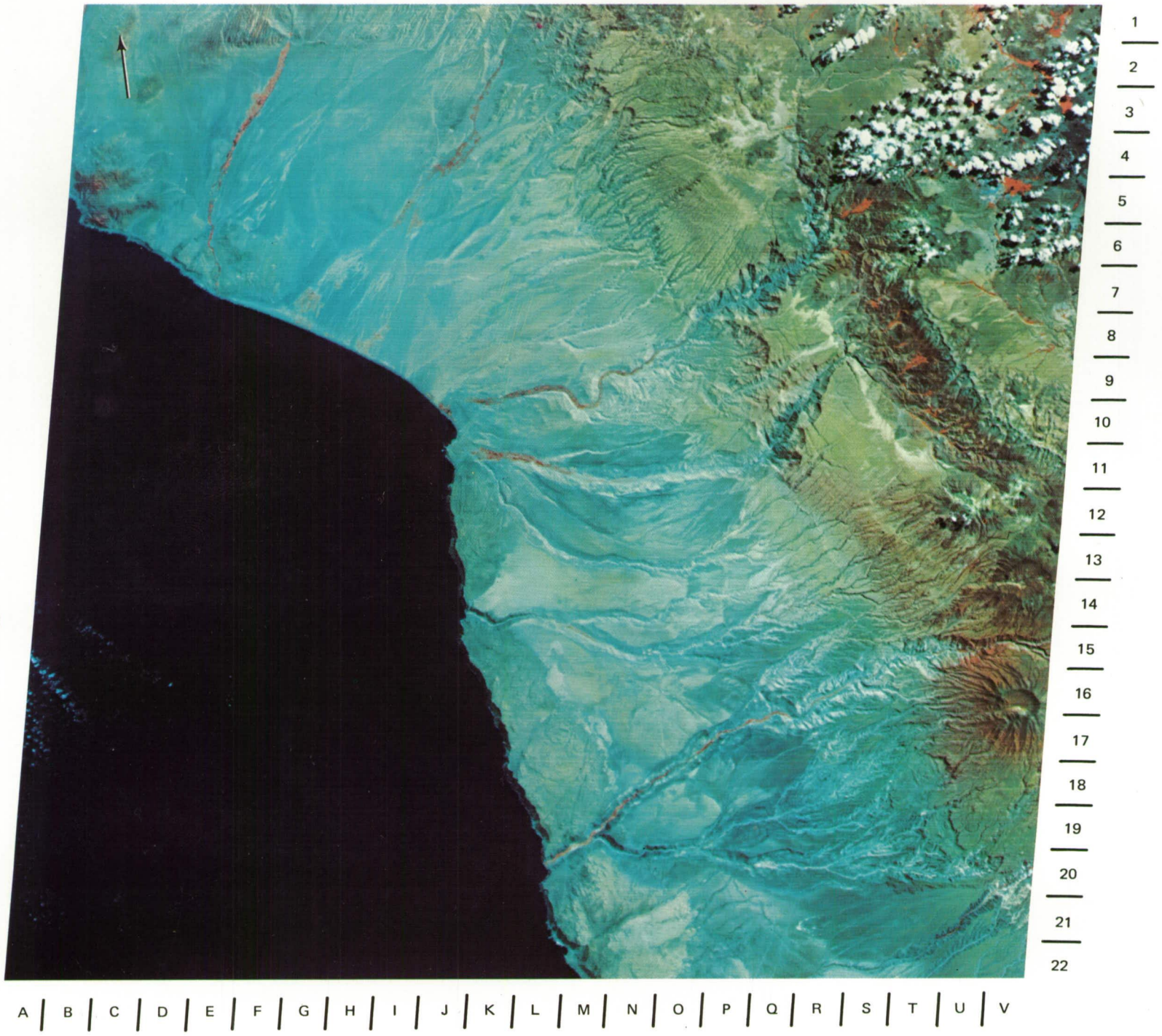


PLATE 198

SOUTHERN PERU: The upper left corner of this scene lies about 320 kilometers (200 miles) southeast of Lima on the Pacific Ocean coast. The coastal region here is part of the Sechura Desert, a lowlands consisting of Tertiary and Pleistocene sediments in alluvial deposits carried down from the eastern highlands. The Rio de Icá (*A*–17), Rio Grande (*E*–10), and Rio Acarí (*Q*–20) are perennial streams draining across the desert from the highlands. Cotton, alfalfa, and fruits are grown along these rivers. Low coastal hills, composed of Mesozoic sedimentary rocks, contain iron ore mined in open pits (just below the bottom of the image). The land rises abruptly to altitudes of 4300 to 5200 meters (14 000 to 17 000 feet) in a dissected range made up of Jurassic and Cretaceous sediments (*H*–14) and Mesozoic to Cenozoic intrusive rocks (*I*–9). Vegetation along these mountains is mainly tussocky clumps of grasses, deciduous scrub, thorny trees, and other drought-resistant species collectively known as monte vegetation. The light areas (*J*–8) along the east side of the mountains are barren rock, much of which is above the snowline and is largely devoid of vegetation.

The terrain to the northeast is part of the Peruvian Altiplano, a dissected uplands ranging from 4300 to 5500 meters (14 000 to 18 000 feet) in the Cordillera Occidental, or High Andes. Rocks in this section are primarily volcanic extrusive ash and flows of Cenozoic age. Sparse mountain grasses and low shrubs of the puna type develop on the thin soils derived from these volcanic rocks. The Rio Pampas (*R*–1) cuts sharply into the terrain to form a deep canyon. *1645–14255;* April 29, 1974.

PLATE 199



ATACAMA DESERT, PERU AND CHILE: The Atacama coastal desert shown here in portions of the Republics of Peru and Chile is truly one of the world's most arid areas. To simply say that it is desert is an understatement indeed as is evidenced by the lack of a characteristic red vegetation signature over tens of square kilometers seen in this image. The coastal city of Arica has an average annual rainfall of less than 3 millimeters (0.1 inch). Habitation in this parched area is restricted to the better watered upland valleys of the volcanic Cordillera Occidental (*O*–3; *S*–9) or to the narrow ribbons of oases stretching along the few rivers draining westward from the cordillera.

Only two towns of any size are located in this image: Tacna, Peru (*I*–3), located inland near the head of a large alluvial fan, and Arica, Chile (*I*–10), a seaport located between two river oases. Arica, connected by rail and road across the cordillera, serves as a major port outlet for landlocked Bolivia. Other oasis belts are centered upon the Sama River (*D*–6) in the north and the Camarones River (*L*–19) in the south. Some vine crops are grown but agriculture is oriented primarily to serving the local inhabitants.

Huge alluvial fans have accumulated in many places between the coast and the western flank of the cordillera. The fan descending from Tacna is a good example (*G*–7). The distributary stream network yields the braided pattern typical of alluvial fans as this fan stretches to the seacoast. In other coastal locations, especially south of Arica (*J*–12; *K*–17), low hills developed upon Jurassic volcanic materials mark the land-water contact.

The volcanic origin of the cordillera is exemplified by the 4600-meter (15 000-foot) high volcanic cone and caldera in the southeastern portion of the scene (*V*–16). As elevation increases along the highly dissected flank of the cordillera, increased moisture, especially in the form of fog, permits vegetative growth, mostly in the form of tufted and bunched grasses and other scrubby drought resistant plants. *1245–14105;* March 25, 1973.

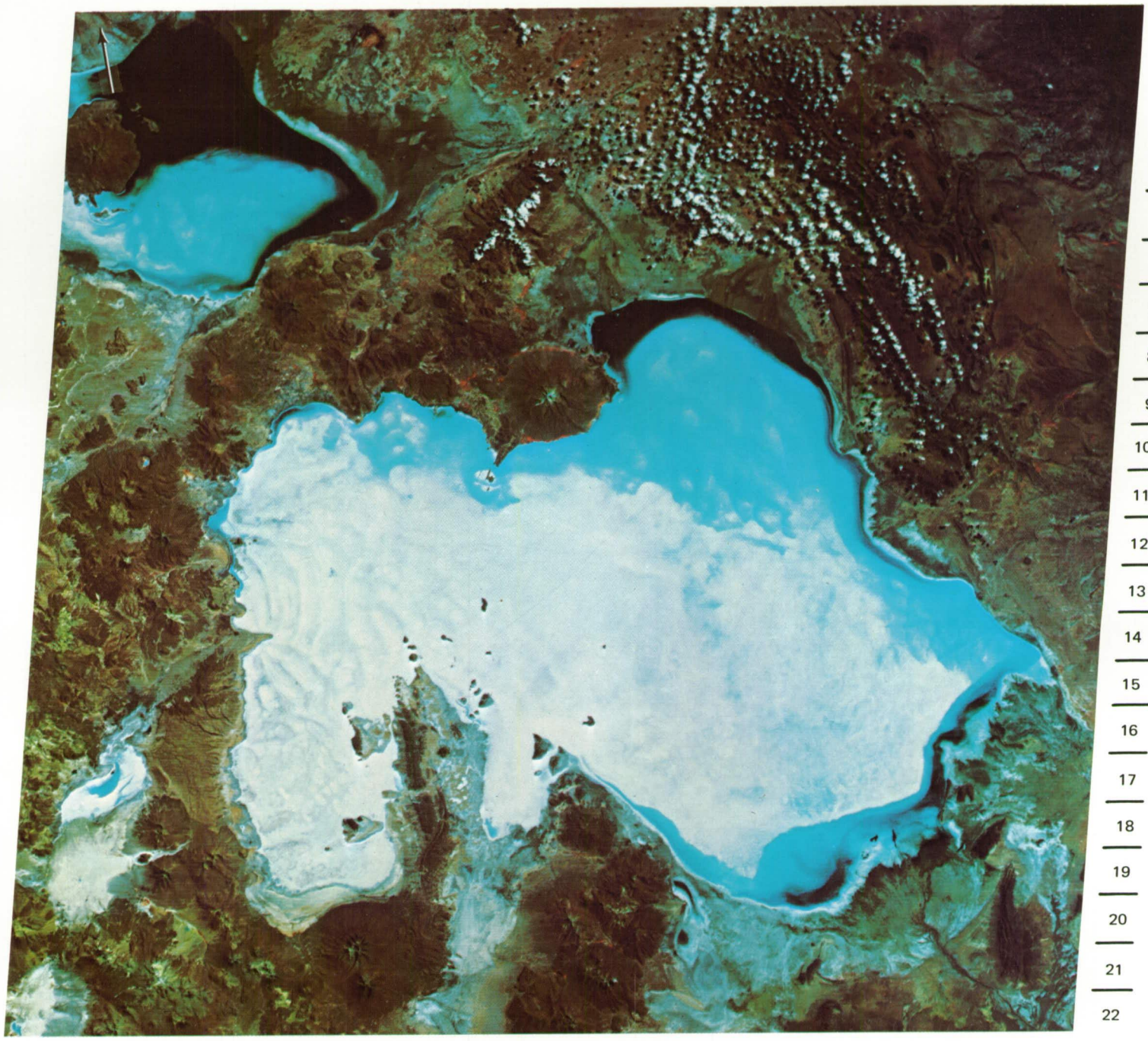


PLATE 200

CHUQUICAMATA AND CALAMA, CHILE: Aridity, with characteristic lack of vegetation, which in turn displays geologic conditions graphically, typifies this scene. This is a southward continuation of the Atacama Desert, coastal lowlands, and Andean cordillera, depicted so succinctly in plate 199, except that at this latitude the Andes converge to form more or less a single chain, with few high basins as found northward. It is, however, a tectonically active region of fault zones and volcanoes. Volcanic landforms are typified by snow-covered cones such as those seen in the northeastern part of the image (*T*–3; *T*–5).

Two contrasting mining operations in this scene help to emphasize the geologic diversity. Evaporite deposits, typical of dry climatic regimes, containing various chlorides, nitrates, and iodine, occur in the vicinity of Maria Elena (*J*–18) and Pedro de Valdivia (*J*–22) on the Salar Del Miraje. These and similar deposits have played a considerable part in the economic and military history of Chile, Peru, and Bolivia. Considerable effort has been expended to mine and ship this natural resource. An aqueduct (*H*–17) has been built from the Loa River to support the port city of Tocopilla (*A*–15), mostly obscured by the typical (for this season) coastal pattern of stratus clouds. Tocopilla serves as the port city, not only for the nitrate fields, but also for Chuquicamata, one of Chile's largest open pit porphyry copper mines (*S*–16). Calama, the support town for the mine, is located nearby in the upper Loa River valley (*R*–17). *1010–14044;* August 2, 1972.

PLATE 201



THE SALARS OF BOLIVIA: Two contrasting landforms dominate this image. On the west, the Cordillera Occidental consists essentially of a massive igneous plateau dotted with huge volcanic cones and lava flows. To the east lies the Altiplano, the largest basin of interior drainage in South America.

The Andes mountain system bifurcates in southern Peru, sending two prongs southward into Bolivia. The volcanic Cordillera Occidental represents the western prong. Many volcanic peaks along the spine of the cordillera rise above 5200 meters (17 000 feet). A few streams flow eastward from the cordillera, providing water for the dry Altiplano. Numerous individual symmetrical volcanic cones occur on the Altiplano floor near the edge of the cordillera; the high Volcan Tagua (*K*–9) rises to 5348 meters (17 457 feet).

The Altiplano is a structurally depressed basin lying between the Andean prongs in Bolivia. The basin is partially filled with alluvial material, glacial debris, and volcanic ash derived from the surrounding mountains. The porous soils developed upon these materials combined with the arid and cold climate (less than 25 centimeters (10 inches)) of rainfall per year, and most of the Altiplano surface is above 3000 meters (10 000 feet) elevation) create an extremely hostile environment. Only in the protected river valleys where some water is available does one find agriculture. Even then it is a subsistence form with a low yield of crops such as hay and potatoes. Vast salt flats such as the Salar de Coipasa (*C*–5) and the Salar de Uyuni (*L*–13), one of the largest playa-type ephemeral lakes in the world, represent the remnants of a drainage and lake network dating from more pluvial glacial periods. Today Coipasa occasionally receives overflow from the Lake Titicaca drainage system to the north during periods of flooding. Coipasa does retain some of this freshwater input as is indicated by the darker colored Lake Coipasa (*C*–2) on the north side of the salar. Another conspicuous feature on the Altiplano surface is the tilted, linear sedimentary strata in the northeast corner of the image (*S*–6). *1243–13595;* March 23, 1973.

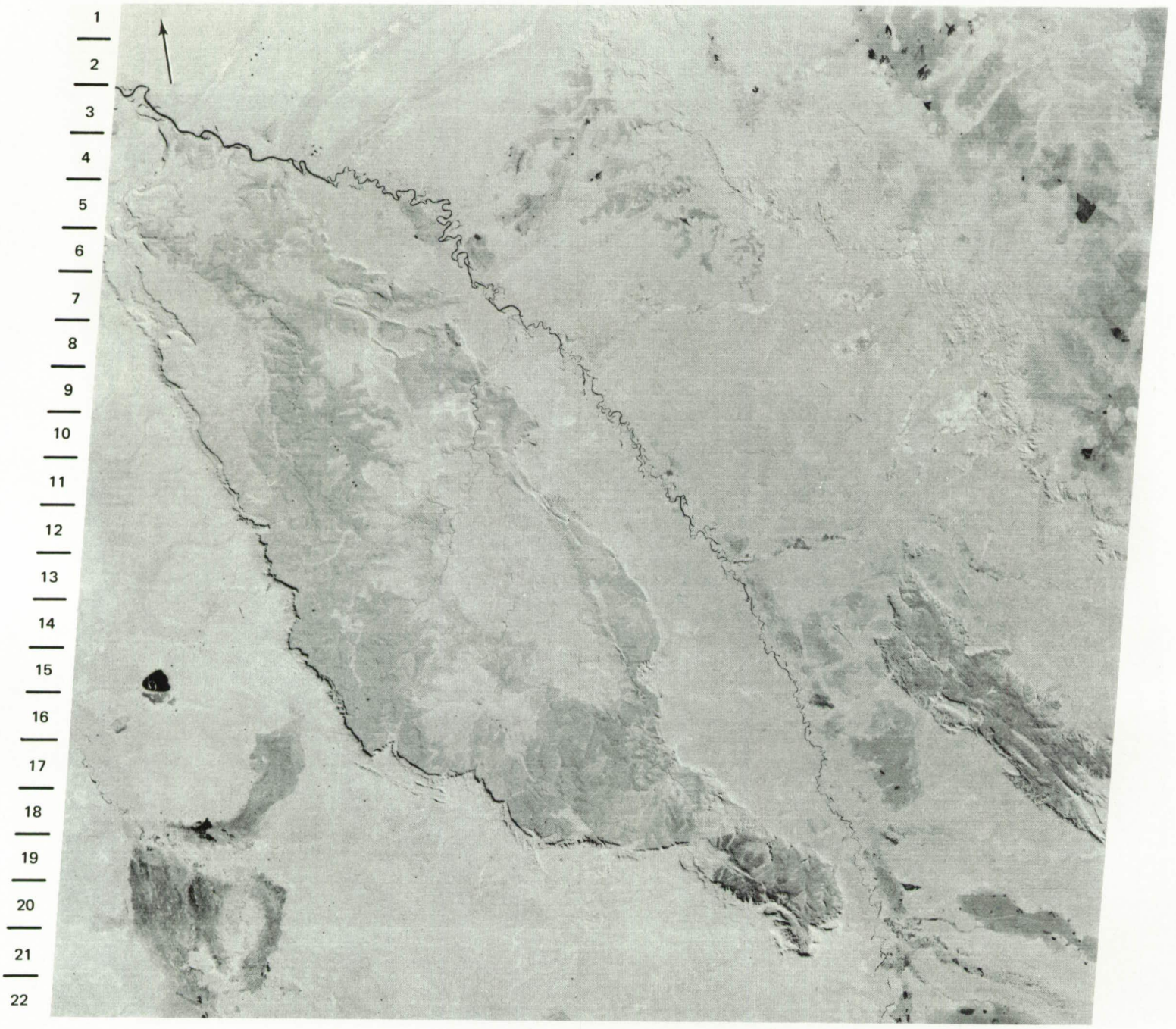


PLATE 202

SERRANIA DE HUANCHACA, BRAZIL-BOLIVIA: The disputed Brazilian-Bolivian boundary follows a stream course cut into the immense plateau surface shown in this image (*O*–9). The Serrania Huanchaca (*I*–13) is an outlier of a much larger highland to the northeast, the Serra dos Parecis. Only a small portion of the western margin of the Serra dos Parecis is shown in this image. When observing erosional surfaces of this magnitude and uniformity, one is clearly reminded of Lester King's discussions of cyclic land surfaces in Gondwanaland. Topographically the Serrania is similar to the chapada (mesa) surfaces seen on the Chapada das Mangabeiras on plate 207. Much of the surface of the Serrania is somewhat below 7600-meter (2500-foot) elevation, but it rises to an elevation above 2000 meters (6500 feet) on its southeastern end (*O*–19). The scarp-bounded plateau surface capped by resistant sedimentary strata rises abruptly above the Guaporé River (*M*–11) lowland on its northeastern flank.

The meandering course of the Guaporé, strongly outlined in this band 7 rendition, is indicative of the flatness of the lowland. Indeed much of the lowland is filled with swamps, especially during the wet season. This is typical of much of this general area of South America because of the fact that the headwaters of many Amazon tributaries and tributaries to the Parana-Paraguay River system originate along a flat drainage divide centered immediately south of this image. The area shown in this image is part of the Amazon watershed.

This remote portion of Brazil and Bolivia is very sparsely settled. Two small towns are located within the image: La Bahia (*C*–18) with its nearby reservoir and Mato Grosso (*S*–20). The telegraph line right of way can be seen east of Mato Grosso (*U*–20). This is truly an agricultural frontier where the tropical grasslands and tropical scrub woodland are given to extensive cattle raising. *1005–13335;* July 28, 1972.

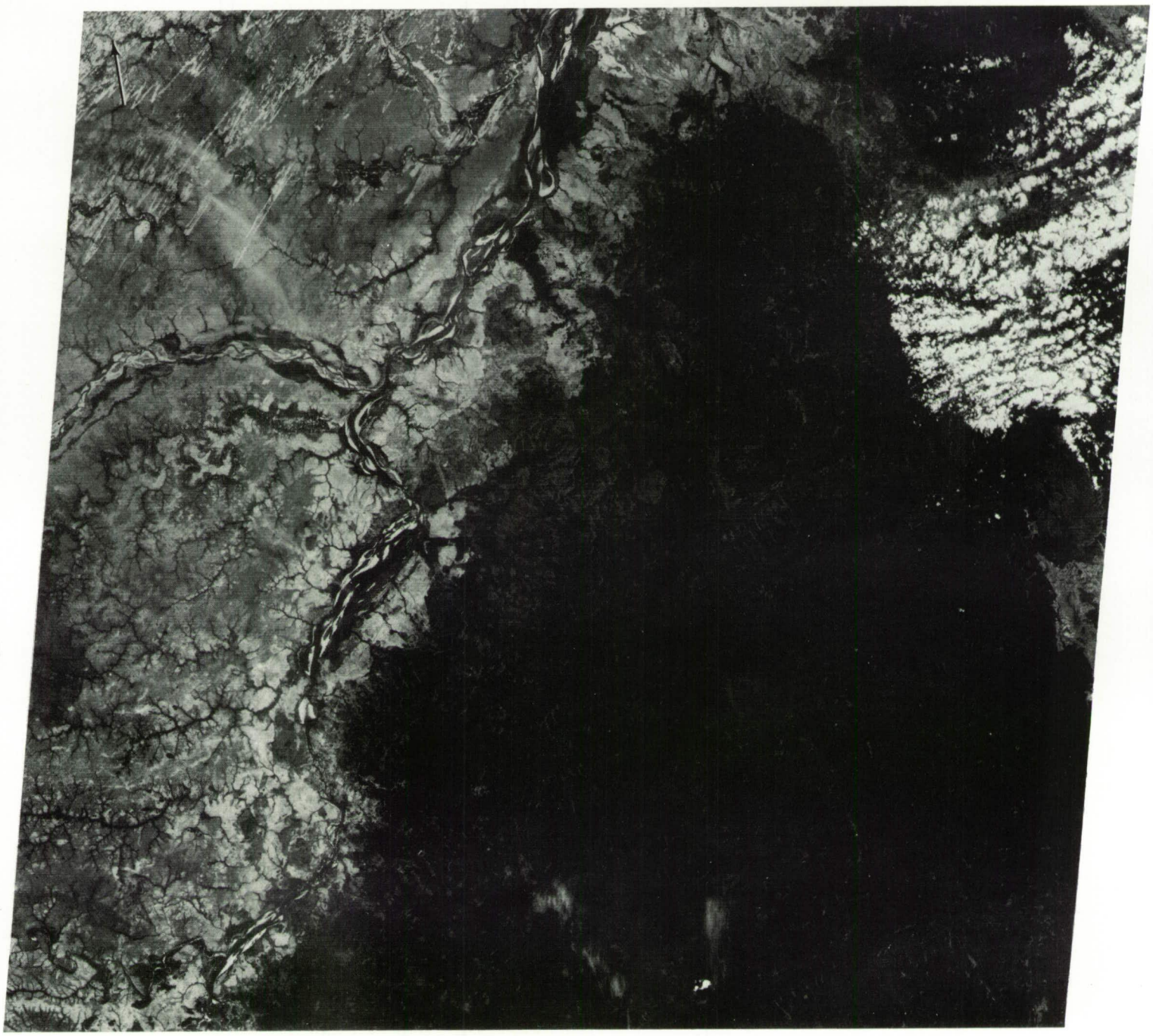


PLATE 203

ORINOCO BASIN: Radar as a remote sensing instrument has a seemingly distinct advantage over aerial photography and multispectral scanning within visible and near-infrared wavelengths. It is generally an "all-weather" device, being capable of imaging the ground through clouds.

Under certain conditions, bands 6 and 7, representing the reflective near-infrared in the wavelength interval between 0.7 and 1.1 micrometers, can image the ground surface through thin clouds. Again, in thick jungles or rain forests, these bands produce images that appear to show the ground itself; actually, they show the top of the tree canopy, but where trees are on irregular slopes (such as mountainous terrain), the variations of topography are "mirrored" by the general variations of the canopy surface.

This effect is dramatically exemplified by the pair of images on

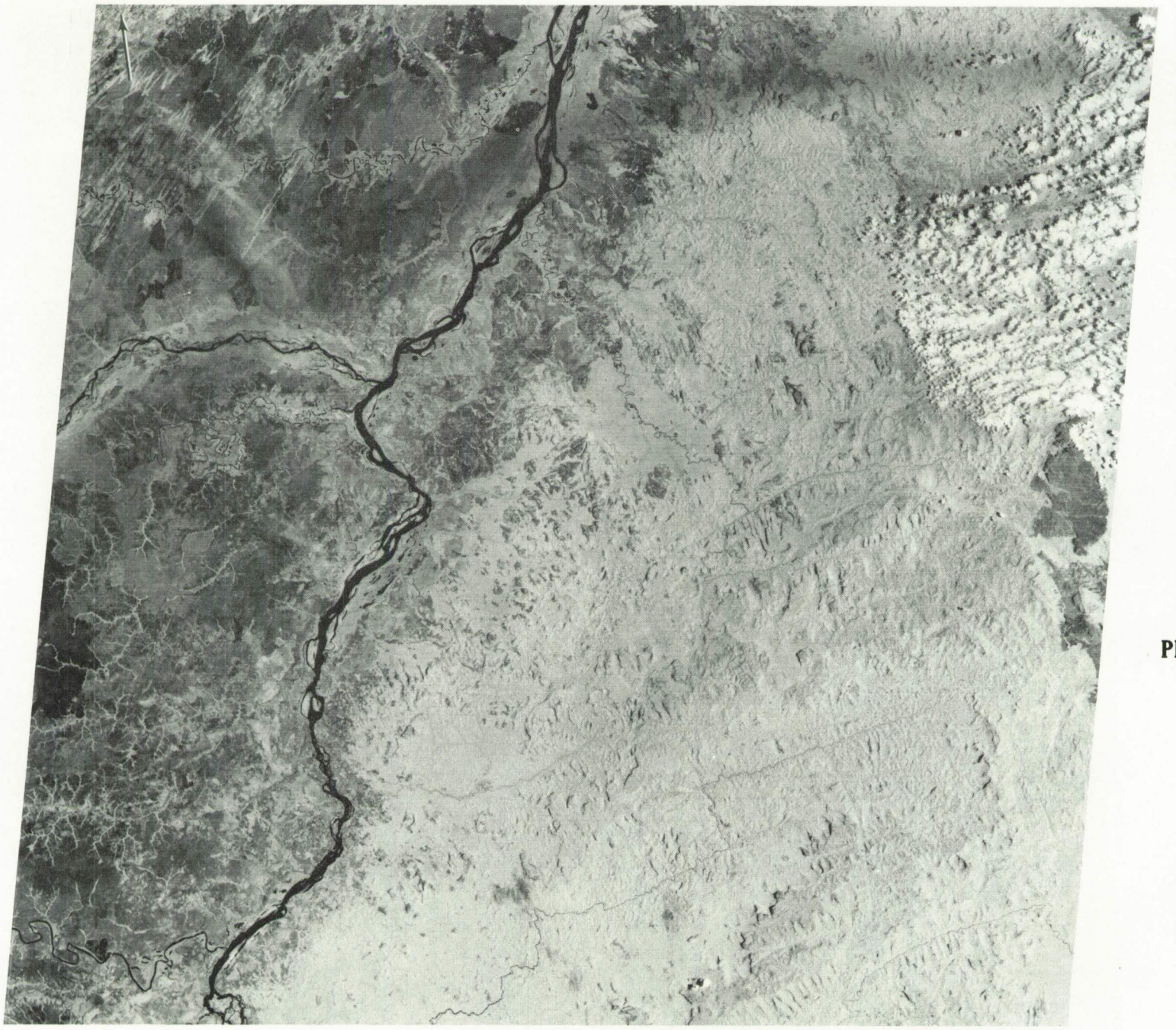
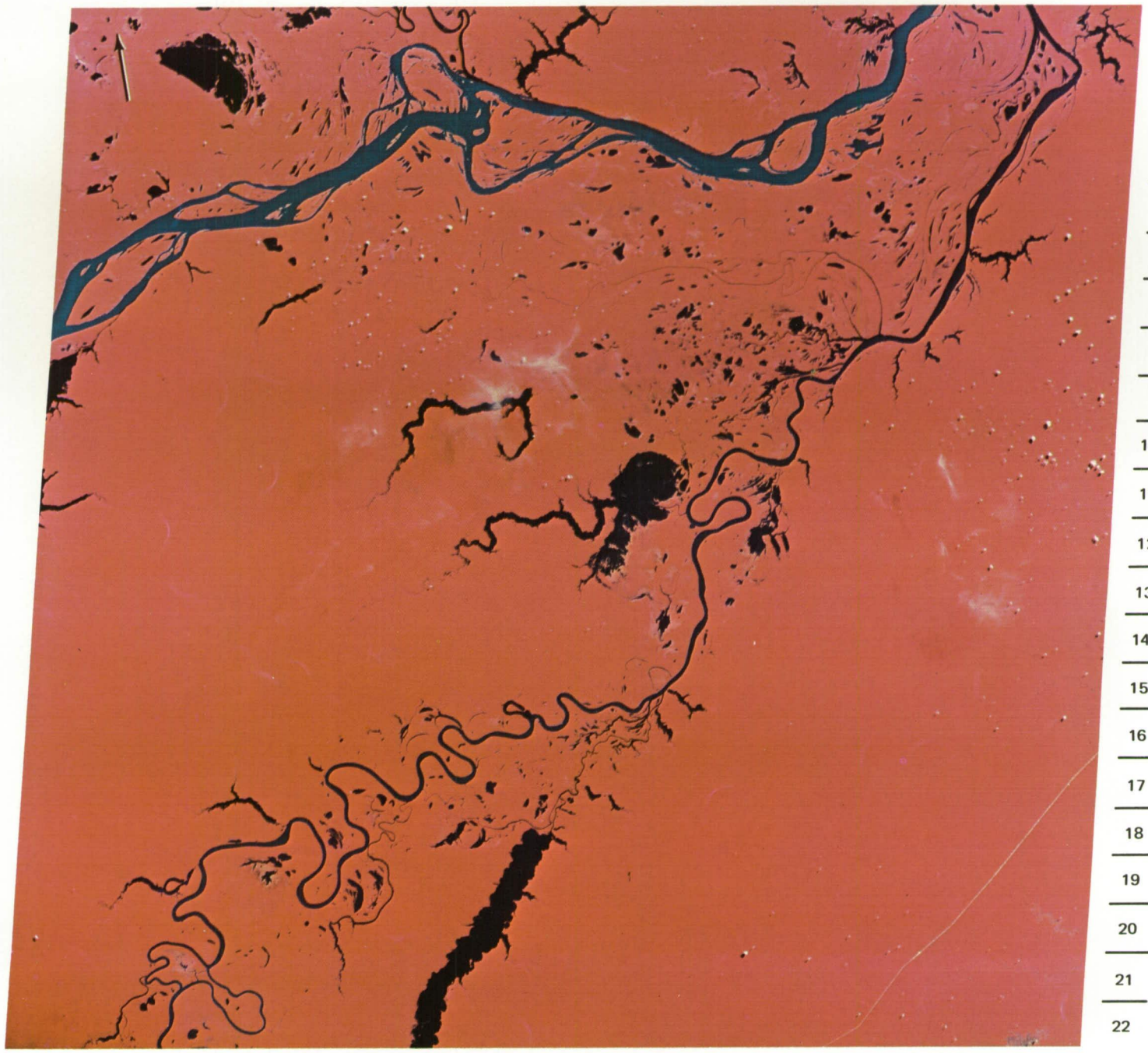


PLATE 204

these two pages. The region shown is in southern Venezuela. The Orinoco River flows northward here near the edge of the Llanos (see plate 196), a savanna grassland, where it abruptly changes into a thick rain forest that continues southward into the upper Amazon Basin. In the band 5 image, plate 203, details of the Llanos are evidenced by tonal contrasts, but the jungle terrain is obscured by the uniform dark tones of the continuous vegetation. In band 7, plate 204, however, much of the regional topography of the jungle, developed here out of Proterozoic granitic rocks and Archean metamorphic rocks at the west end of the Guinea Highlands, seems to be made visible as though imaged by a radar beam. *1229–14151;* March 9, 1973.

PLATE 205



AMAZON RIVER, BRAZIL: This portion of the Amazon River (*D*–6; *Q*–2), known as the Solimões to the Brazilians, is in the State of Amazonas about midcourse along the 2820-kilometer (1750-mile) length of the river. The world's largest river system occupies a drainage basin of some 6.0 square megameters (2.3 million square miles) in the Republic of Brazil and countries hosting its headwater tributaries. The area depicted here is truly a remote world of water and vegetation. The only evidence of man's activities is the road cutting diagonally across the southeastern corner of the image (*S*–20).

The Amazon and its tributary, the Purus (*T*–3; *G*–18), flow upon a low basin filled mainly with unconsolidated gravels, sands, clays, and silts. These sediments may be the residue of a once extensive freshwater lake that covered the entire basin in the Cenozoic era. The river flood plains are filled with thousands of lakes, swamps, and old channels. Several large lakes are included in this scene. One of the largest, Lake Aiapuá, is located near the center of the image (*M*–11). Even though this area is more than 1600 kilometers (1000 miles) inland, elevations are quite low. Most of the area is little more than 30 meters (100 feet) above sea level.

Slight tonal variations between the bluish-colored Amazon and its darker colored tributary, the Purus, attest to the greater sediment load carried by the Amazon. The Amazon and its tributaries are not greatly affected by flooding due to seasonal variations in flow, mainly because of the storage capacity of the numerous backwater areas along the flood plains.

The ubiquitous red vegetative signature in this image is a result of the nature of the tropical rain forest tree growth. The hundreds of different species of predominantly hardwood evergreen trees have a crown of dense foliage that overlaps to form a continuous vegetative canopy. This rain forest is more than 480 kilometers (300 miles) wide in this region but gradually merges with open forest and savanna at distances farther from its banks. *1008–13481;* July 31, 1972.

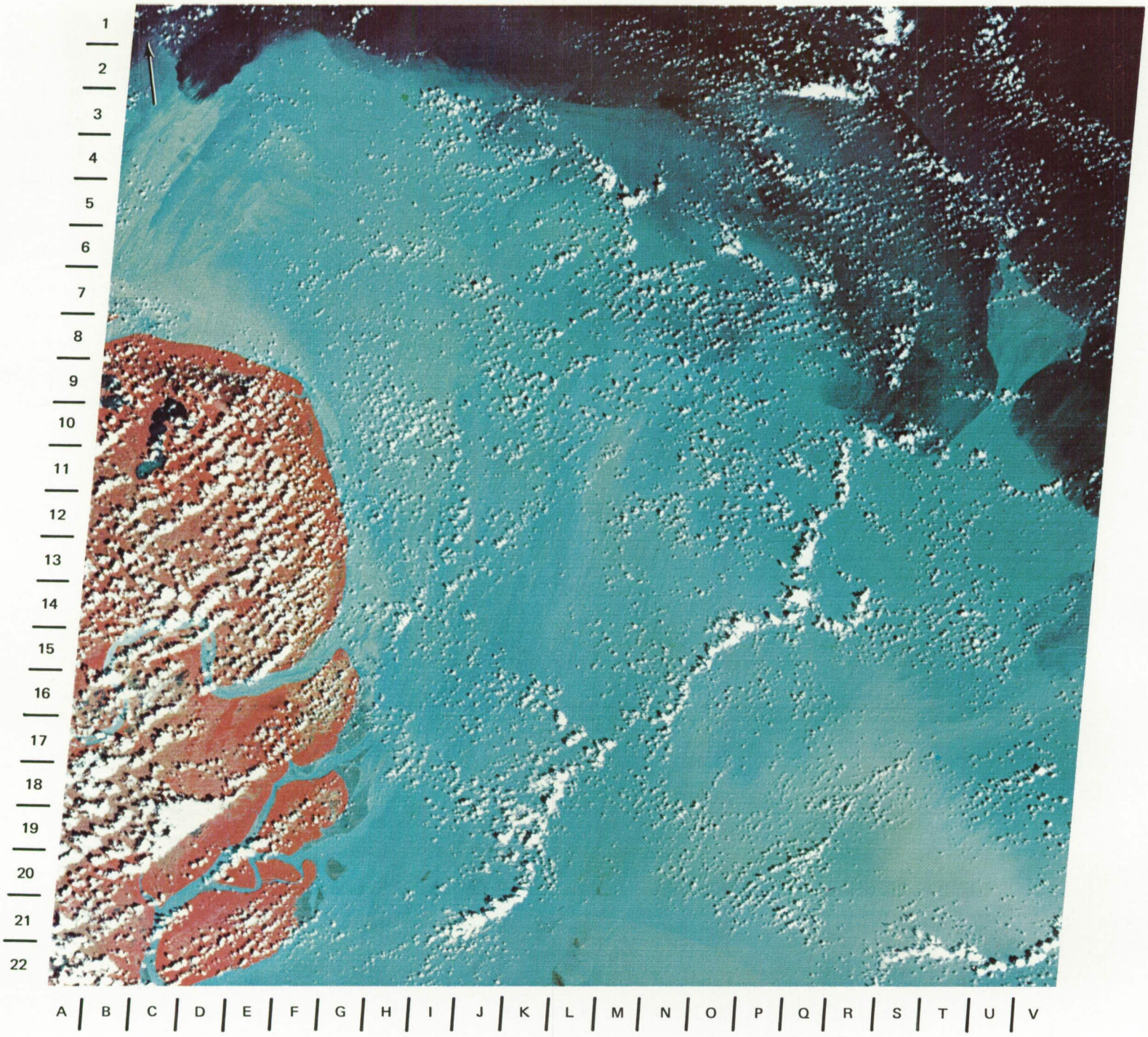


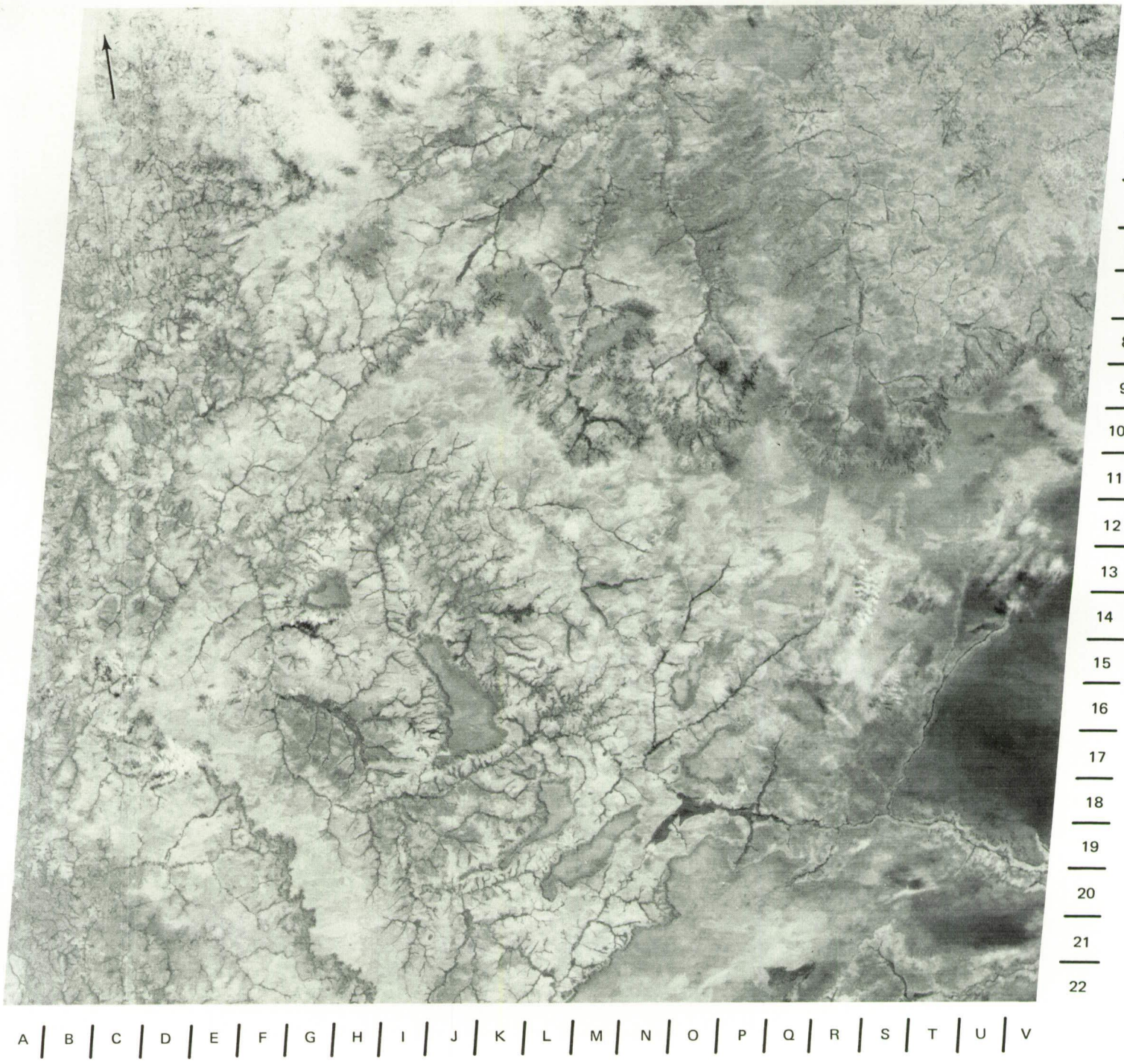
PLATE 206

MOUTH OF THE AMAZON: The Amazon is the greatest river in the world in terms of water discharge. Its daily flow amounts to about 15 teraliters (4 trillion gallons) of water. This accounts for nearly 15 percent of all freshwater introduced into the oceans by all the rivers on the Earth. The discharge rate exceeds that of the Congo River by a factor of 4 and is almost 10 times that of the Mississippi River. Water is carried into the Amazon from more than 200 tributaries, many running for 1600 kilometers (1000 miles) or longer.

Over millions of years, the soils in the Amazon Basin have been leached of their mineral content, leaving them infertile over vast areas. The water now reaching and flowing through the Amazon is thus exceptionally pure, with a dissolved salt content equivalent to that of distilled water. The sediment load is relatively small for the size of this river (in its lower stretches the Amazon is 3 to 8 kilometers (2 to 5 miles) wide and in places 60 to 90 meters (200 to 300 feet) deep). This load is, on the average, 1.4 gigagrams (1 500 000 tons) of sediment per day.

This image shows a vast plume of sediment discharged into the Atlantic Ocean from the north channel of the Amazon. The landmass on the left (west) margin is Cabo Norte (North Cape). The meandering Araguari River cuts across this tropical forest terrain. The sediments carried into the ocean are transported northward along the Guiana coast by the South Equatorial Current. *1126–13013;* November 26, 1972.

PLATE 207



CHAPADA DAS MANGABEIRAS, BRAZIL: Parts of four Brazilian States are shown in this image: Bahia (*U*–16), Goias (*L*–16), Piaui (*T*–7), and Maranhao (*N*–6). This area is located in the Brazilian Highlands some 560 kilometers (350 miles) north of Brasília, the capital city of Brazil.

The Brazilian Highlands are underlain by the oldest rocks of the continent. These ancient crystalline rocks were covered by essentially horizontal sheets of younger sedimentary strata. Subsequent erosion has partially stripped away the sedimentary cover exposing the older basement rocks in places and leaving flat, scarp-bounded plateau surfaces in others. Such plateau surfaces in Brazil are referred to as "chapadas," corresponding to the Spanish term "mesa." As the processes of weathering and erosion proceed, the more resistant sedimentary strata form a cap layer that gives rise to the steep-sided chapadas seen in this image (*J*–7; *J*–16). The Chapada das Mangabeiras reaches elevations above 900 meters (3000 feet) in several places. Several of the flat-topped chapadas stand as much as 450 meters (1500 feet) above the surrounding lowland.

This area serves as the drainage divide for streams tributary to three of the major river systems of northern and eastern Brazil. River systems in the northwest portion of the image, such as the Perdida (*C*–4), drain into the Tocantins River, a major tributary of the Amazon. Systems flowing northeastward, as does the Riozinho (*M*–2), join the Parnaiba River in its journey to the Atlantic Ocean. Many of the stream courses are forested (*N*–16), but most of the interfluvial areas are covered by grass or a low bushy tropical scrub woodland. Much of central Brazil is sparsely inhabited as is seen in this image. It is the Brazilian frontier, referred to as the "sertão." Rivers draining southeastward are a part of the Rio Prêto (*V*–19) system, which joins the São Francisco, the largest and most important river in northeast Brazil. *1050–12411;* September 11, 1972.

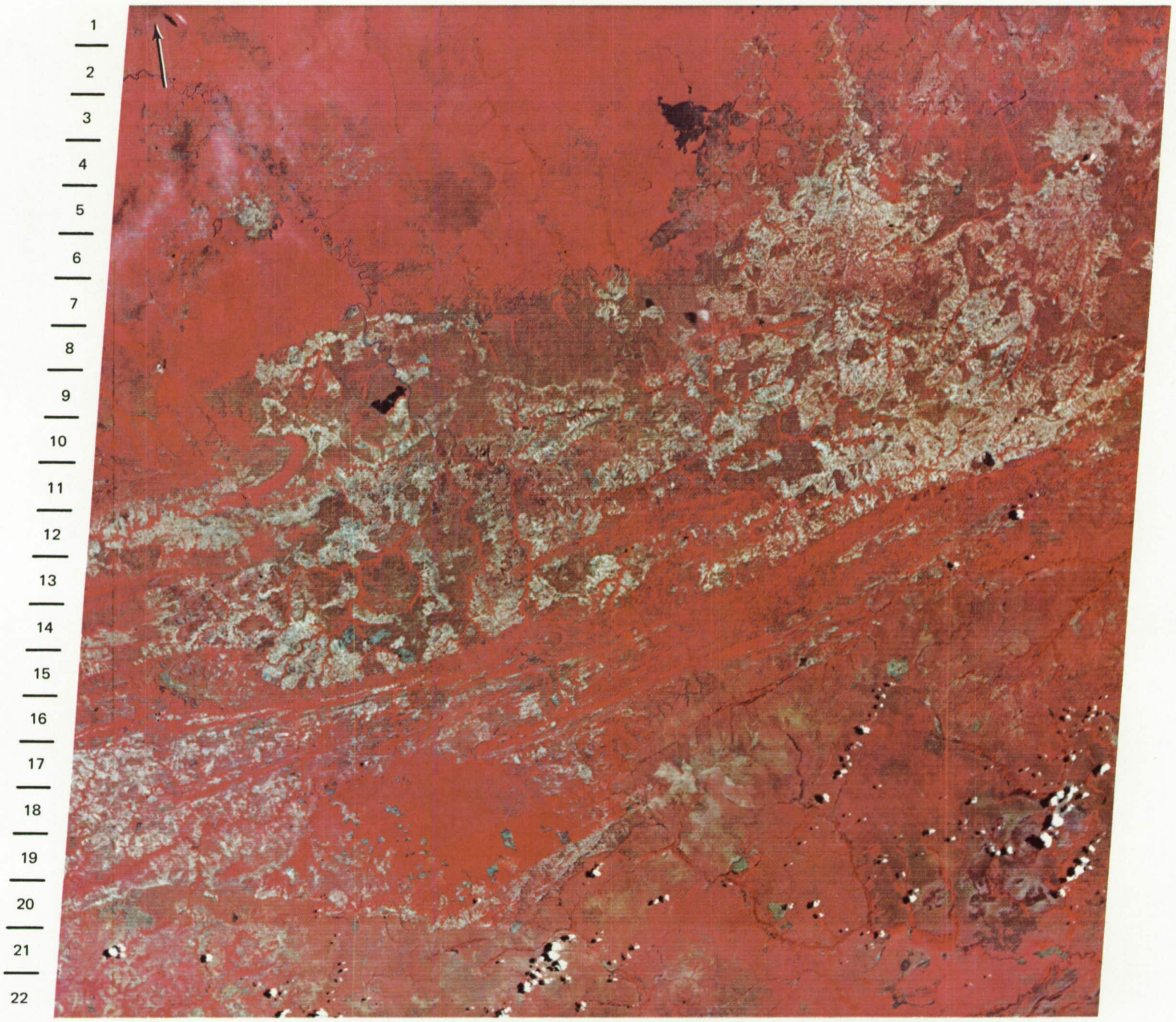


PLATE 208

MATO GROSSO PLATEAU, BRAZIL: The spawning ground of portions of two of the major river systems of South America is depicted in this image. The dominant landform shown is the Serra Azul (*J*–15; *Q*–12), an area of deformed Cretaceous strata rising some 1000 meters (3300 feet) above a flatter, plateaulike area around its flanks. A series of northward- and eastward-draining streams, the Teles Pires River (*B*–2), the Ronuro River (*J*–6), the Tamitatoala River (*P*–3), and the Culuene River (*V*–12), form the headwaters of three of the major tributaries of the Amazon River. The Manso River (*C*–20), draining westward from Serra Azul, eventually swings southeastward to become a part of the huge Parana-Paraguay drainage network draining southward to the Atlantic.

This image was recorded near the beginning of the wet season as is evidenced by the fact that the rivers appear to be well watered. The tropical savanna climate of this area has a distinct wet-dry season regime permitting periods of overabundance of water and periods of near drought.

The lack of field patterns, roads, or other evidence of man's activity attests to the remoteness and undeveloped nature of the plateau country shown in this scene.

Scattered cumulus clouds dot the southern margin of this image (*K*–21; *U*–18). *1091–13113;* October 22, 1972.

PLATE 209



A NEW METEORITE CRATER IN BRAZIL: The Araguainha Dome in Brazil is situated in the State of Mato Grosso some 650 kilometers (400 miles) west of Brasilia. Its center point lies near latitude 17° S and longitude 53° W. It takes its name from the town of Araguainha on the Araguaia River, a major tributary to the Amazon. The region is part of the "campos," or tropical savanna, a grasslands with scrub, bush, and scattered woodlands.

This dome was considered to be an igneous intrusion that arched the surrounding Paleozoic sedimentary units. It was drilled in 1962 as a possible oil trap, but no producing zones were found. In 1973, Dr. R. S. Dietz, a U.S. scientist renowned for his identifications of astroblemes (the surficial scars of ancient meteorite impacts), visited the structure and discovered shatter cones (conical features indicative of shock wave action) in the central uplift of Precambrian crystalline rocks. This clue to an impact event was reinforced by recognition, by use of the microscope, of shock damage by Dr. B. M. French of the National Science Foundation. On the same day as this further verification, a circular ring pattern in a Landsat image being considered for inclusion in this publication was noted and shown to Dr. French. Upon checking its geographic coordinates it was determined that the Araguainha Dome coincided with the ring. The Landsat image clearly revealed, however, that the structure was at least 40 kilometers (25 miles) in diameter, almost twice as wide as earlier field evidence had indicated.

This picture is an enlargement to a scale of 1:400 000 of that portion of Landsat image *1089–13005,* taken on October 20, 1972, which contains the surface expression of the dome. The dome itself is located at the center of an interior bull's-eye—actually a central mountain of Precambrian rock. The dark part of the bull's-eye represents vegetation lining the lower slopes of the peak. The main ring surrounding the core consists of sandstones and shales on which grow mostly grasses. One unit near the outer edge produces a soil that supports trees and other thicker vegetation. Thus, the presence of the two dark annular bands gives the impression that the Araguainha Dome is a double-ringed astrobleme while, in fact, it is not.

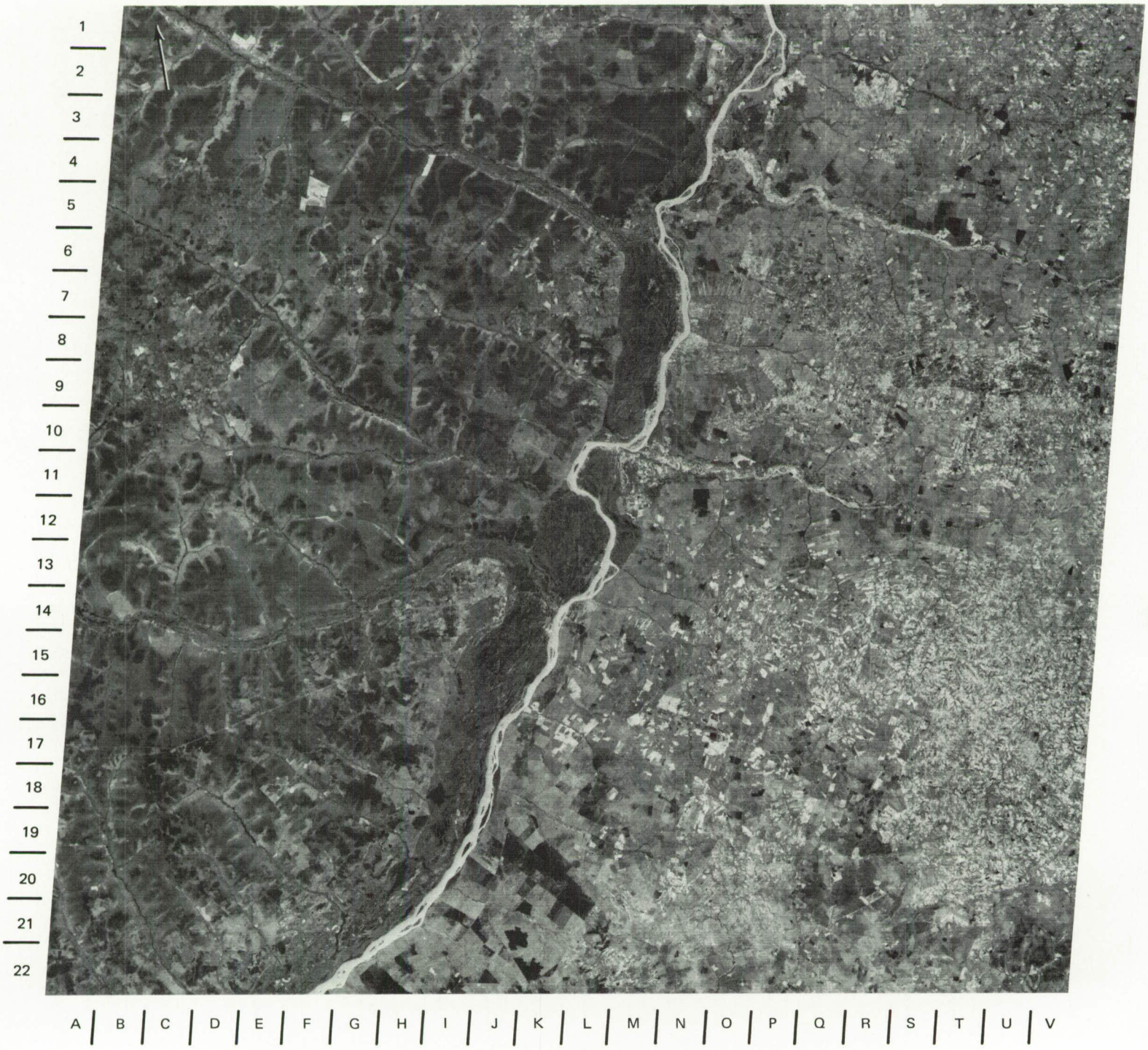


PLATE 210

PARÁNA RIVER, BRAZIL: Two contrasting land use practices and vegetative patterns mark the eastern and western banks of the Parána River (*M*–5; *J*–17) in this scene. The river serves as the boundary between two Brazilian States: São Paulo on the east and Mato Grosso on the west.

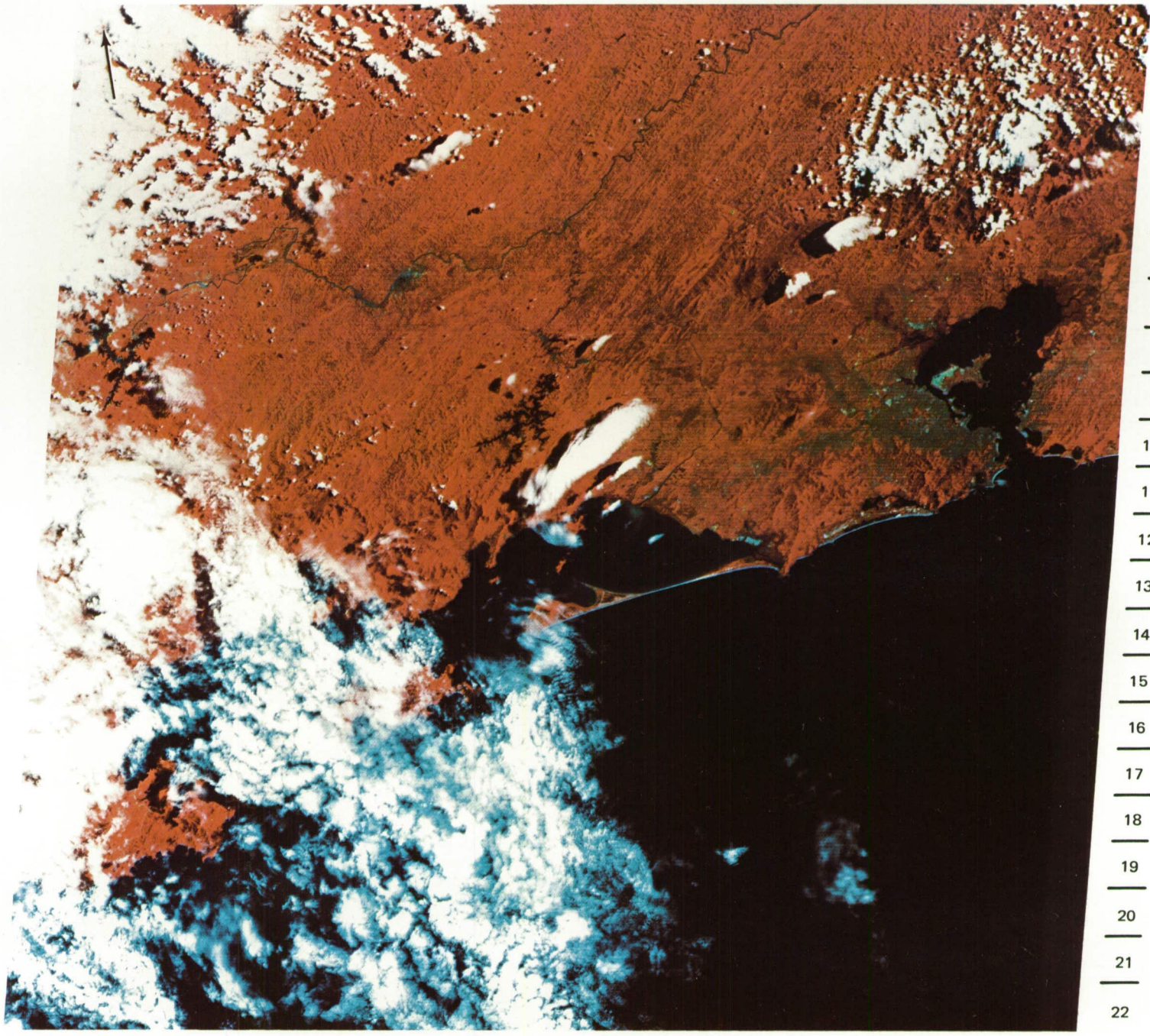
In Mato Grosso the vegetation is a scrubby deciduous woodland with open patches of savanna grasses, a vegetative association known locally as campo cerrado, or a closed grassland. On this side of the river livestock ranching with little agriculture is the dominant economic activity.

On the east side of the river in the State of São Paulo the natural vegetation consists of tropical semideciduous forests of mainly broadleaf evergreen species. During the past quarter century, coffee production and associated roads, rail, and powerline networks have spread westward in São Paulo to the Parána River. Dozens of small towns and coffee plantation complexes dot the landscape east of the river.

Due to the scrub-grassland nature of the vegetation and the lack of widespread economic development on the west margin of the Parána, the drainage networks are easily recognizable, beginning with the Verde River (*J*–4) in the north, the Taquari River (*F*–9), and the Pardo River (*E*–14). The drainage divides between these three river systems are sharply defined; for example, an area on the divide between the Verde and the Taquari may be seen at *F*–6. The denser gallery forests typical of river flood plains are visible along each of these rivers as well as in the broad, flat flood plain of the Parána (*K*–4; *K*–12).

Conversely, the patterned nature of agricultural activities and the greater cover provided by the semideciduous forest on the eastern side of the Parána tend to subdue the nature of the terrain. Two sizable rivers enter the Parána from the east in this image: the Feio Aquapei River (*Q*–5) and the Peixe River (*M*–10). *1088–12562;* October 19, 1972.

PLATE 211



RIO DE JANEIRO, BRAZIL: This city (*S*–9) of 4 000 000 is located along the southwest edge of Guanabara Bay (*T*–8), where the sea has penetrated through a rocky inlet (*T*–10) into the Baixada Fluminense open lowlands (*S*–6). Part of the Serra do Mar mountain range passes through the Rio area, rising to elevations between 300 and 760 meters (1000 and 2500 feet). In places, wave erosion has cut into the Precambrian crystalline rocks near the bay, isolating several peaks within the city, such as the knobby Sugar Loaf peak (*T*–10) at the entrance to the bay and Corcovado (*S*–10) to the west. The residential city of Niteroi (*V*–9) occupies a harbor area across the bay.

The land rises abruptly at the great escarpment inland from the lowlands where the Serra dos Orgãos (*N*–6) consists of northeast-running ridges that reach to 1000 meters (3000 feet). Beyond is the valley of the middle Paraiba River (*K*–5). This river runs northeastward parallel to the coastline through a structural trough that separates the coast ranges from the Serra da Mantiqueira (*F*–1), an even higher (1500 meters (5000 feet)) chain of Precambrian crystalline rocks, with one peak near 2700 meters (9000 feet)). The steel-producing city of Volta Redonda (*H*–6) is situated along the Paraiba; it receives its raw iron from Minas Gerais to the north. The steel is shipped from Sepetiba (*M*–11) on the Bay of Sepetiba (*L*–12), part of the coast sheltered by a long spit (*L*–13). Power for the region is supplied by hydroelectric facilities at the reservoir dam (*K*–8) near Lages.

An evergreen rain forest lines the coast but mixes with semideciduous and mountain vegetation further inland. Bananas and oranges grow in the lowlands around Rio de Janeiro. *1208–12225;* February 16, 1973.

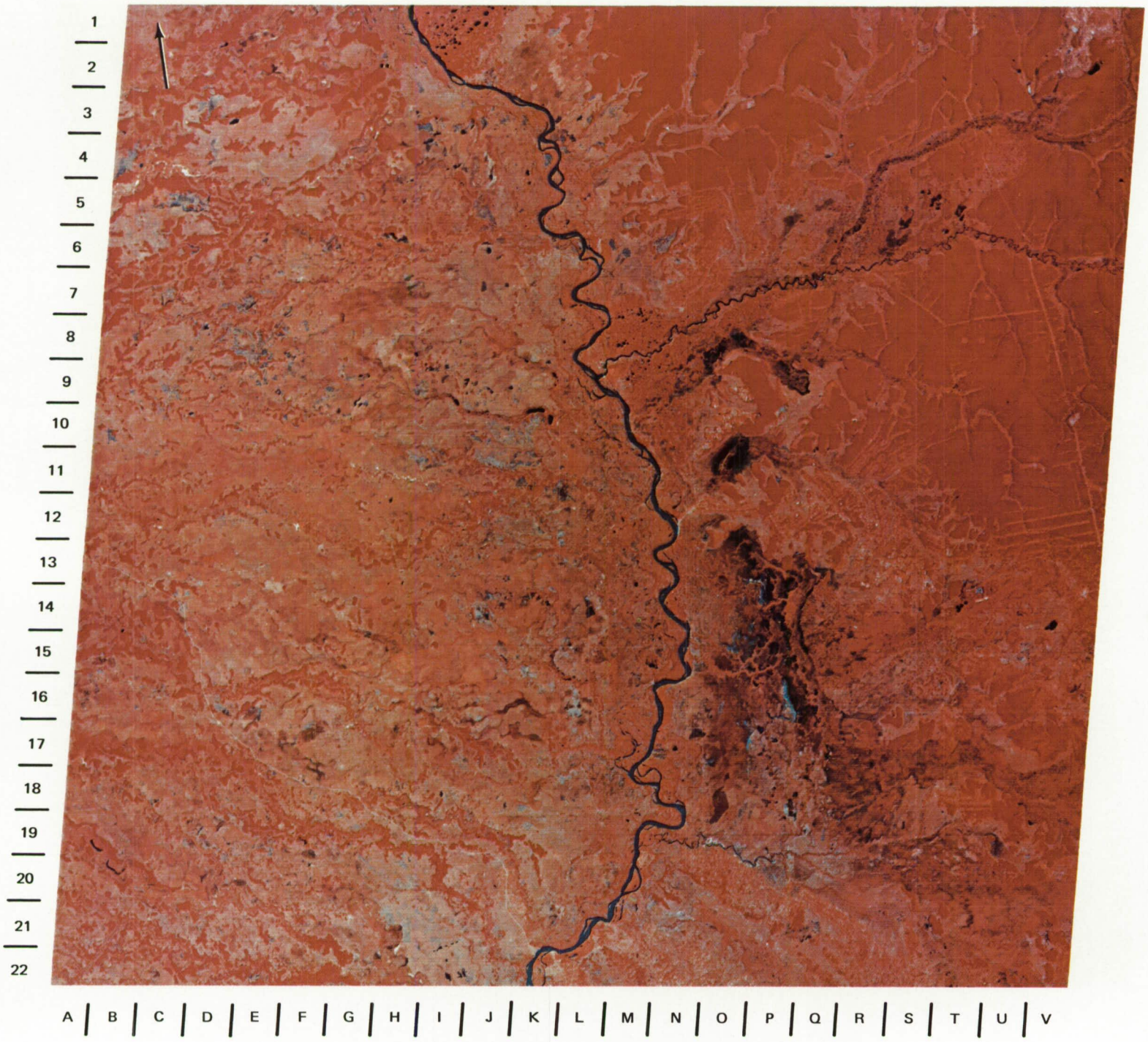
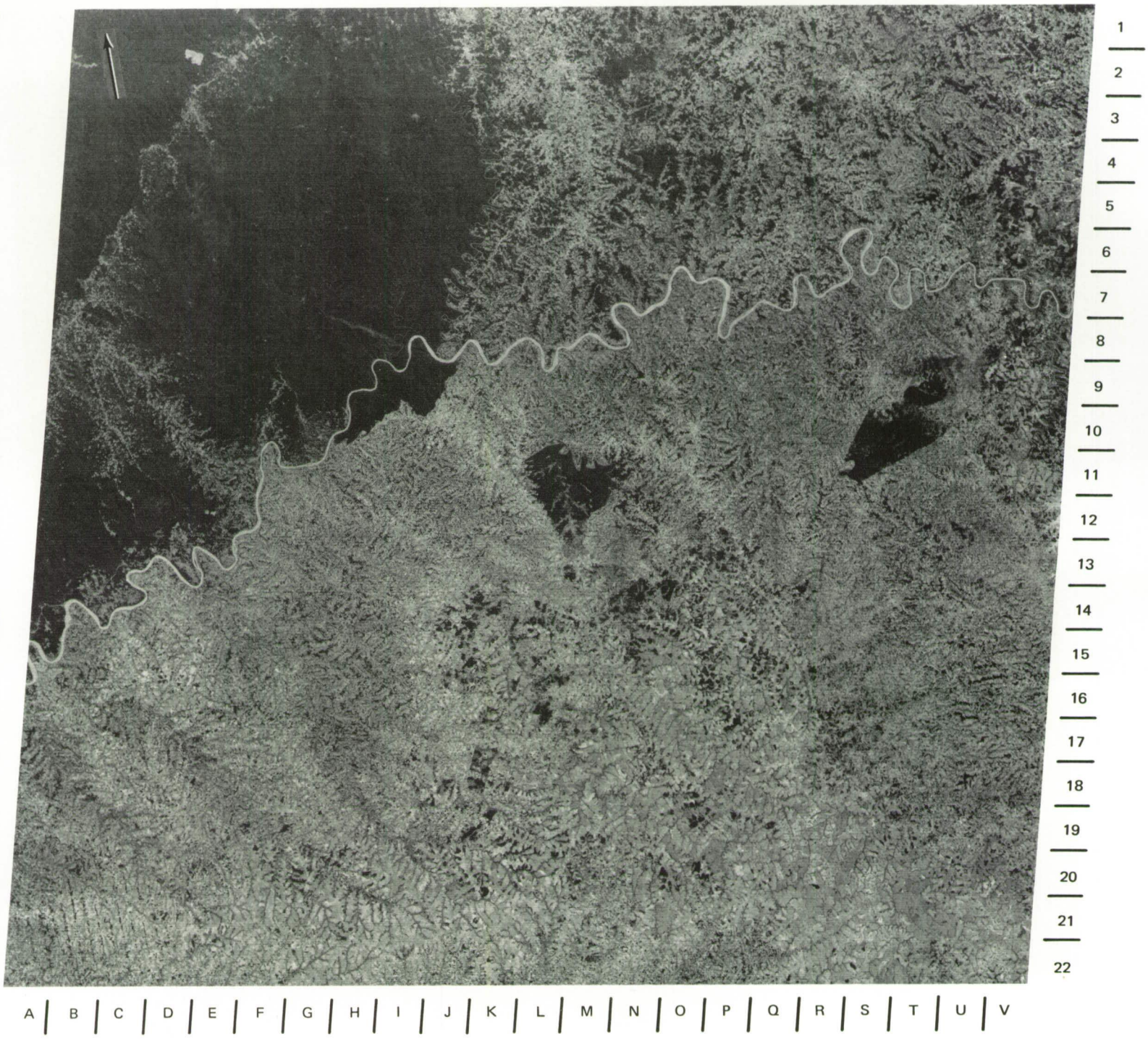


PLATE 212

PARAGUAY: Much of the central lowlands of this small, landlocked nation appears in this image. This area lies along the Rio Paraguay (*M*–13) just north of the capital at Asunción. The town of Concepción (*J*–5) is the largest settlement (~40 000 people) in the northern two-thirds of the country. The swampy lowlands west of the Rio Paraguay are drained by such tributaries as the Rio Confuso (*I*–20), next to the highway (*J*–19) leading to the northwest. Rio Monte Linda (*K*–11), and Rio Verde (*G*–6), are part of the plains of the Gran Chaco. The Chaco is a vast series of Cenozoic alluvial deposits built up of sediments carried by rivers from the Andes. Vegetation characteristic of the Chaco includes palm savanna, tall grasses, thorny shrubs and forests of quebracho (a source of tannin) and other trees. East of the Paraguay River is a series of low rolling hills underlain by late Paleozoic sandstones and other sedimentary rocks. The land around the Rio Guazú (*N*–7) is a moist savanna interspersed with scrub forests and palm groves and areas of marshy ground (*O*–13). Much of this region is devoted to cattle raising. Further east are extensive tropical semideciduous forests given in places to lumbering along networks (*U*–12) of logging roads. *1235–13151;* March 15, 1973.

PLATE 213



URUGUAY RIVER, BRAZIL AND ARGENTINA: For part of its course the Uruguay serves as the international boundary between the Argentine Province of Misiones (*F*–7) and the Brazilian States of Santa Catarina (*P*–5) and Rio Grande do Sul (*I*–11).

The entire area is part of the western margin of the Parana basaltic lava plateau. The striking tonal differences between the area north of the river in Argentina and the lighter area in Brazil results from a vegetative change. The darker area north of the river (*E*–6) is a tropical semideciduous forest consisting essentially of broadleaf evergreen species, some of which lose their leaves during the dry season. South of the river (*P*–9) and in the eastern one-half of the scene the vegetative cover is a middle latitude mixed forest consisting of broadleafed species mixed with needleleaf species, especially the Araucaria pine. Further southward in Rio Grande do Sul, the mixed forest grades into the grass prairies common to southern Brazil and Uruguay.

There is also a contrasting land use pattern on either side of the international border. Misiones Province represents a remote, primarily undeveloped region of Argentina where cultivation of a native tea, yerba maté, is a primary agricultural practice. The western areas of Rio Grande do Sul and Santa Catarina are pioneer farming communities consisting of both large coffee plantations and regions of small farms peopled primarily by European immigrants encouraged to settle in this developing belt by various government support schemes. Evidence of agricultural activity can be seen in various places, particularly south of the river; for example, in the darker areas surrounding the settlements of Tenente Portela (*L*–11) and Frederico Westphalen (*S*–10) and in the patterning in the lower left of the image (*B*–20). *1106–12582;* November 6, 1972.

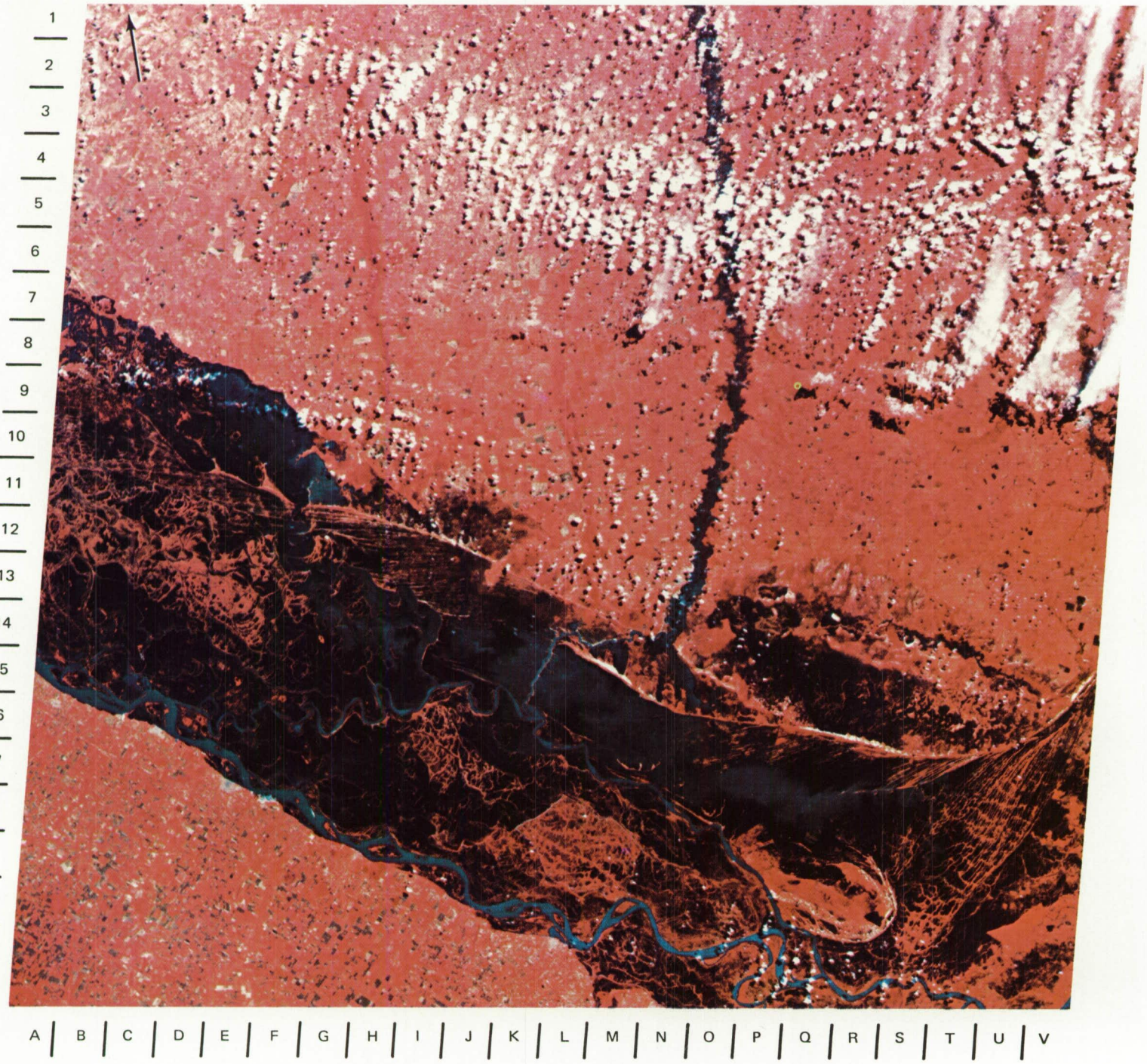
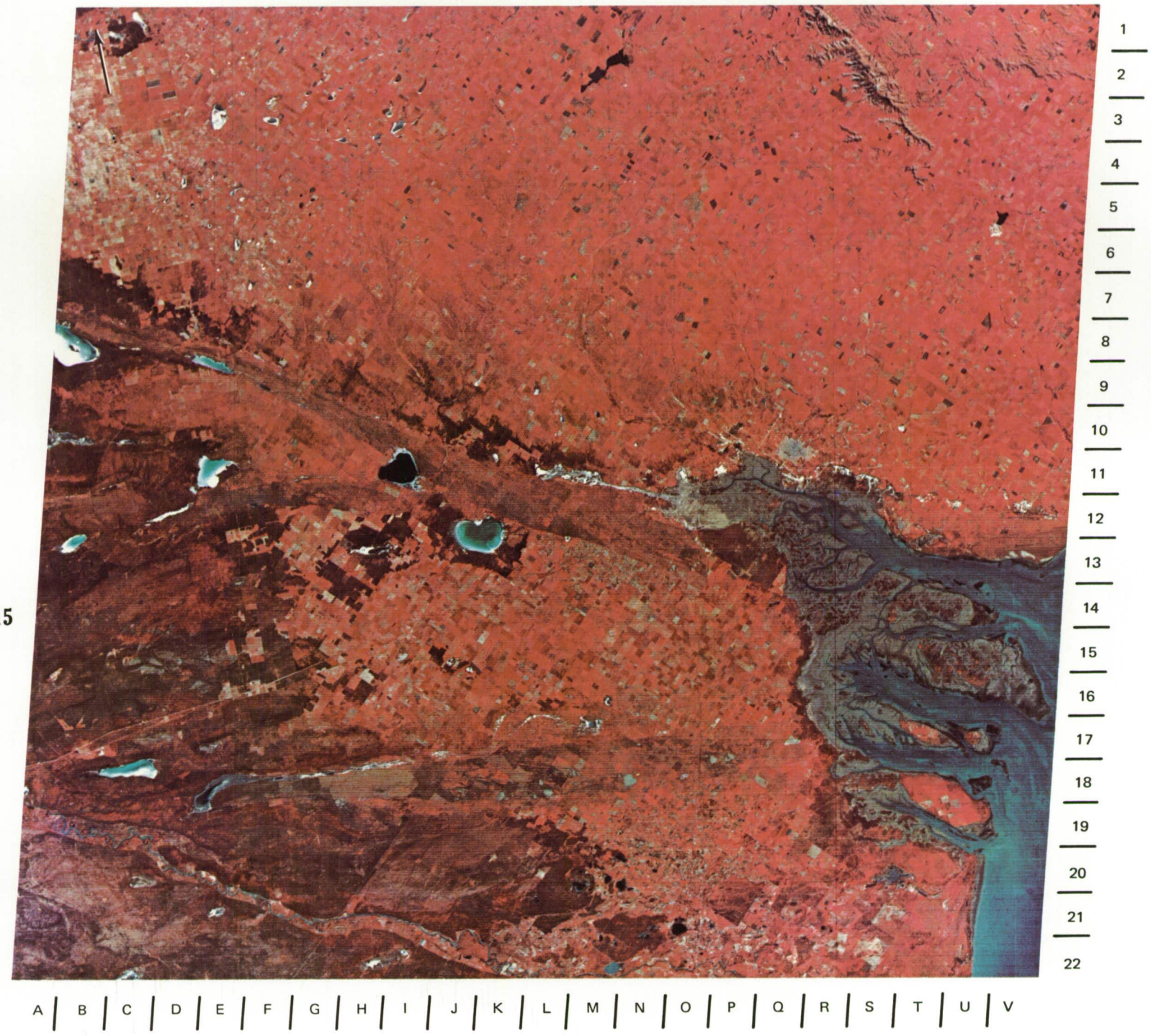


PLATE 214

THE HUMID PAMPA, ARGENTINA: A vast low plains, one of the pampas of northeastern Argentina, was once covered before Spanish settlement by extensive tall prairie grasses. Rainfalls of 80 to 130 centimeters (30 to 50 inches) per year provide this region with excellent growing conditions so that most of the land has been converted to pastoral farming (grazing of cattle and sheep) and cultivation of maize, wheat, flax, and alfalfa. The fertile soils supporting this growth are derived from thick deposits of Quaternary alluvial muds and sands that have buried much older crystalline rocks.

The Paraná River (*N*–20) forms a broad swampy flood plain between the plains of Entre Rios (*S*–10) (i.e., between the Paraná and the Uruguay River further east) on the north and the northeast pampa rim section (*O*–20) to the south. A bluff about 30 to 45 meters (100 to 150 feet) high, known as the Barranca (*K*–20), lines the river along the south side. This segment of the Paraná falls between Rosario (just off the scene on the left) and Buenos Aires (off the scene in the lower right). The lower part of the Paraná has formed a delta extending into the Rio de la Plata estuary where the Uruguay and Paraná Rivers meet. Buenos Aires lies at the head of this estuary. The Paraná here splits into a second channel, the Paranibicuy (*M*–17), into which empties the Guateguay tributary (*N*–12). The Paraná appears to be in flood at this time, spilling over into the marshy bottom lands. Distinctive patterns are produced by old meander channels (*E*–14) and by elongate (*H*–12) to reticulated (*U*–18) linear features, which seem to be shifting sandbars characteristic of a braided river. *1073–13163;* October 4, 1972.

PLATE 215



BAHÍA BLANCA, ARGENTINA: Bahía Blanca (*Q*–10) is located on the north bank of the Sauce Chico River (*P*–11), a relatively small river draining out of the Southern Pampa into a sizable coastal bay area also known as Bahía Blanca (*V*–17). The inner portions of the bay are quite marshy and distributary streams have divided several areas into large islands. A steep cliff, known locally as the Barranca, borders the coastal zone east of Bahía Blanca (*U*–12).

The gently undulating pampa surface seen in this image is pockmarked with small marsh- or lake-filled depressions. A fine, wind-transported material known as loess covers most of the pampa. In a few places older rocks protrude above the sediments forming low ranges of hills such as the Sierra de la Ventana (*R*–2), rising to elevations above 1200 meters (4000 feet). The fertile soils developed upon the loess contribute toward making the Argentina pampa one of the world's most productive agricultural areas. In the Bahía Blanca portion of the Southern Pampa, alfalfa, wheat, maize, and barley are the major crops.

South and west of Bahía Blanca, in the vicinity of the Colorado River (*E*–20), the humid subtropical climate characteristic of much of the pampa phases into a drier semiarid climate. In the drier areas, agricultural emphasis shifts from crops to pastoral activities centered about livestock ranching. This shift in agricultural emphasis accounts for the lack of large field patterns in the southwestern portion of the image (*B*–16). *1074–13240;* October 5, 1972.

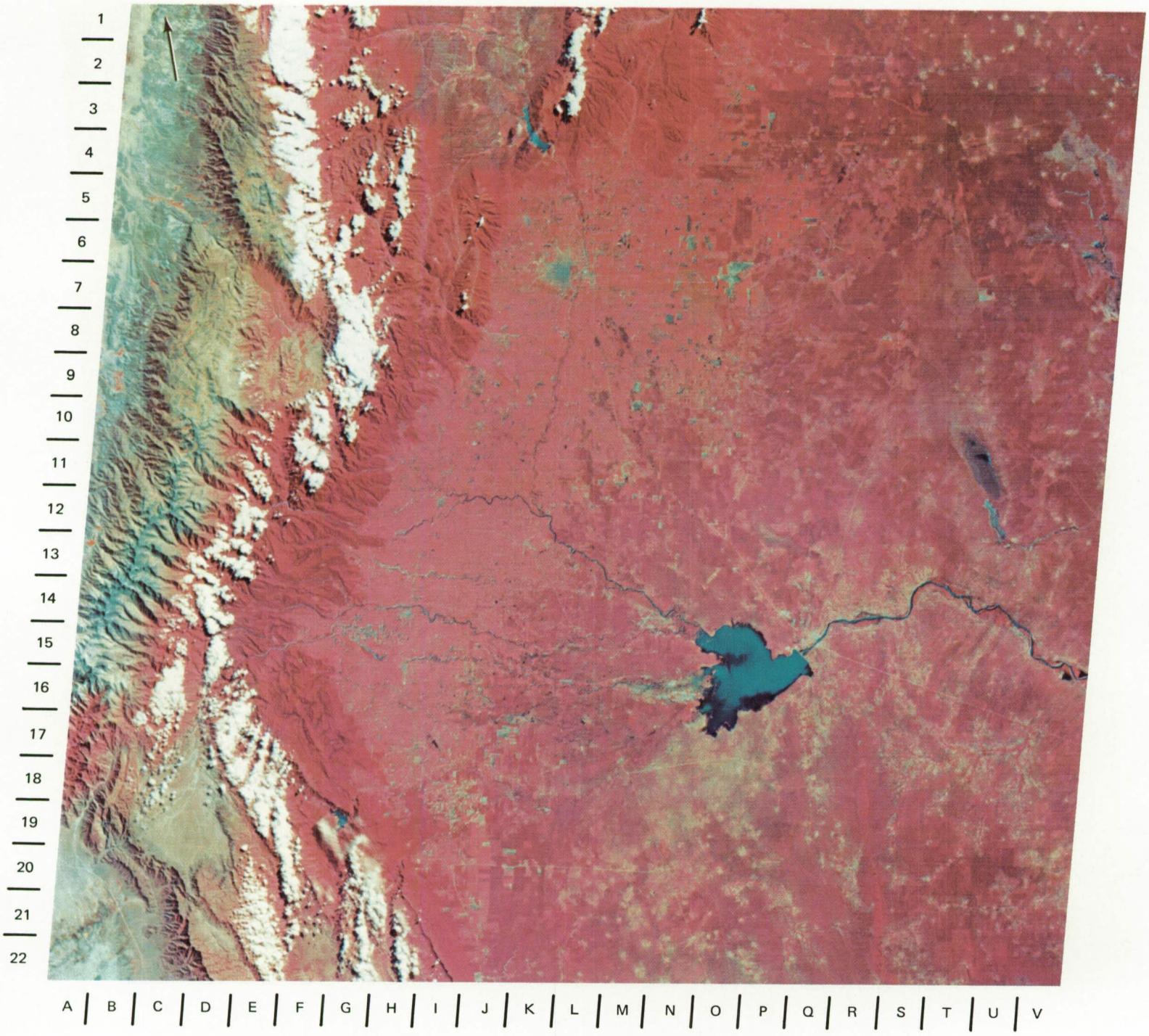
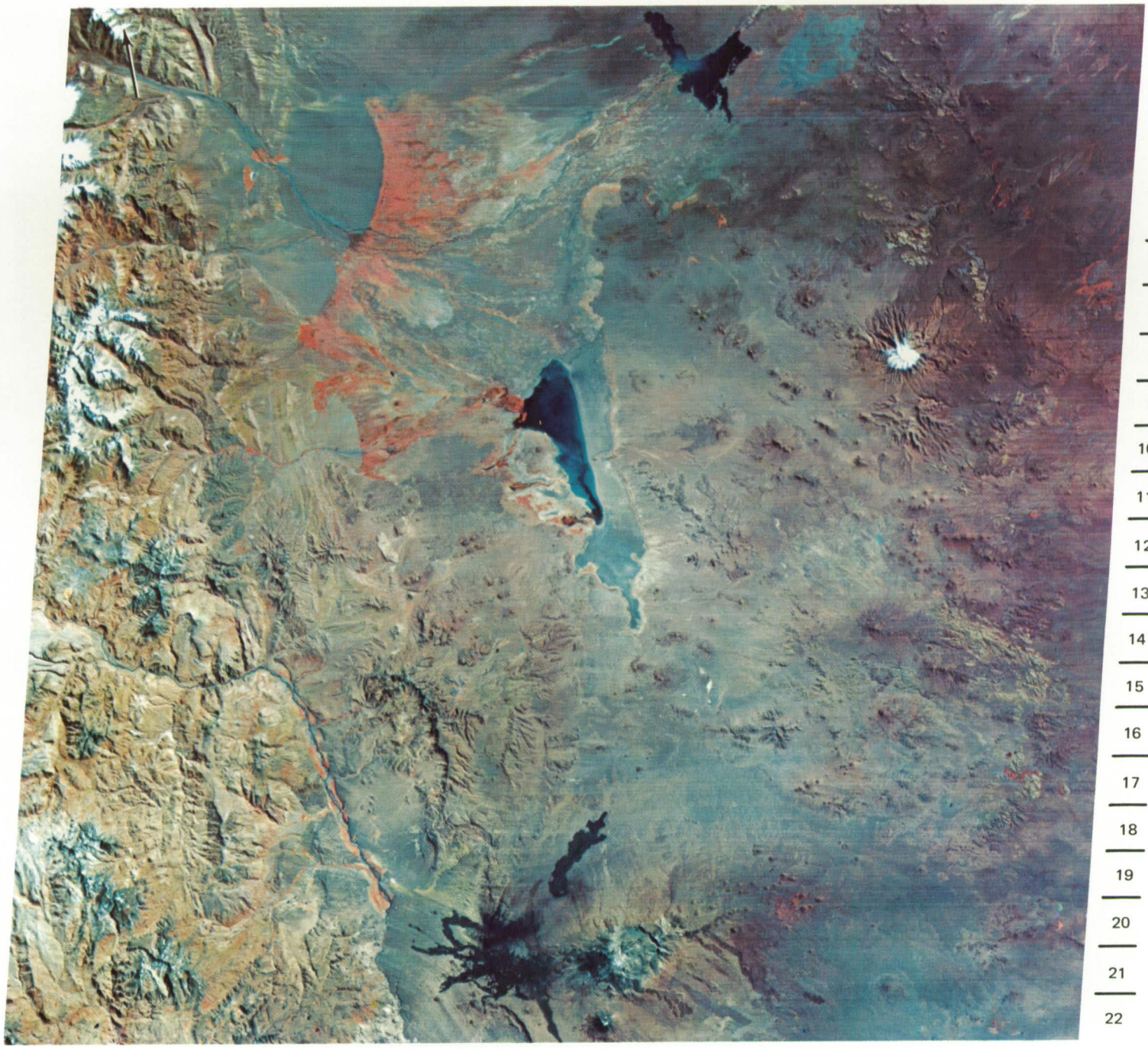


PLATE 216

TUCUMÁN, ARGENTINA: Tucumán (*J*–6), the largest city in the Argentine northwest, and a colonial trade center during the Spanish era, is a leading sugarcane producing area. An opportune combination of physical conditions exists along the flank of the Sierra de Aconquija (*I*–5), which restricts sugarcane production to the Tucumán area. Streams fed by snowmelt and rainfall from surrounding mountains serve as a source of power and irrigation water. A reservoir impounded by the El Cadillal dam on the Sali River, north of Tucumán, serves this purpose (*J*–3). Additionally, westward flowing air masses rise up the flanks of the Sierra de Aconquija, producing either rainfall or cloud banks that retard radiation and prevent frosts. Clouds banked against the eastward facing slopes (*J*–2; *D*–17) signify cloud alinements dictated by elevation. Eastward, onto the gently undulating drier plain surface known as the chaco, frosts and rainfall deficiency prevent sugarcane production. Instead, the drier areas, centered about regional foci such as Las Cejas (*Q*–8), are devoted to the production of cotton, wheat, and maize. Irrigated agriculture is spreading to the chaco as is evidenced by the fairly new reservoir (*O*–15) west of Las Termas (*P*–14), a regional transportation center. A road network can be seen converging upon Las Termas (*R*–15).

Significant vegetative changes mark the transit from the lowland chaco surface (*P*–8) to the alluvial fans on the flank of the Sierra de Aconquija (*H*–5), then upward into the higher elevations of the Andes (*D*–4), and onto the high plateau surface (*A*–5) above the tree line. The natural vegetation of the chaco is a deciduous scrub woodland reflecting the lesser rainfall. The more abundant rainfall on the eastward facing mountains supports a semitropical humid forest of broadleaf trees. The higher, drier, and colder elevation of the interior plateau is sufficient to support only xerophytic plants of a desert scrub nature. *1240–13444;* March 20, 1973.

PLATE 217



LAKE NIHUIL, ARGENTINA: This remote region of Argentina is located southwest of the oasis city of San Rafael and north of the Colorado River. One of the more conspicuous features in the image, Lake Nihuil (*N*–2), is located approximately 56 kilometers (35 miles) from San Rafael on a tributary of the Salado River system. A second lake, Ilancanelo (*K*–9), exhibits characteristics indicative of the dry climatic regime in this section of Argentina. The lake is subject to seasonal fluctuations, and saline deposits resulting from evaporation rim the lake margin.

The Andes Mountains (*A*–3; *B*–18), with snow-covered peaks rising above 4800 meters (16 000 feet), dominate the western portion of the image. Rivers draining eastward from the Andes have deposited huge alluvial fans along the flank of the mountains. In one case (*G*–4) the fan appears to be capped by an impervious layer in its upper section with water issuing from an aquifer exposed along the margin of the cap layer. Availability of water in this zone is responsible for the vegetated area along the margin of the fan.

The Rio Grande (*G*–17), in segments of its course, exhibits the characteristics of an underfit stream. During the Pleistocene, when glaciers capping the Andes began to recede, the large volume of glacial melt water was channeled into streams draining eastward, creating wide, deep valleys. Today, the Rio Grande, with a lesser volume, flows in such a course.

Volcanic activity is evidenced in the lower center of the image. Cerro Payún (*M*–20), a volcanic peak, rises 3700 meters (12 000 feet) above a series of dark-colored lava flows (*L*–18). Snow-covered Cerro Nevado (*R*–8) stands above a surrounding volcanic field in the northeastern part of the image. *1241–13525;* March, 21, 1973.

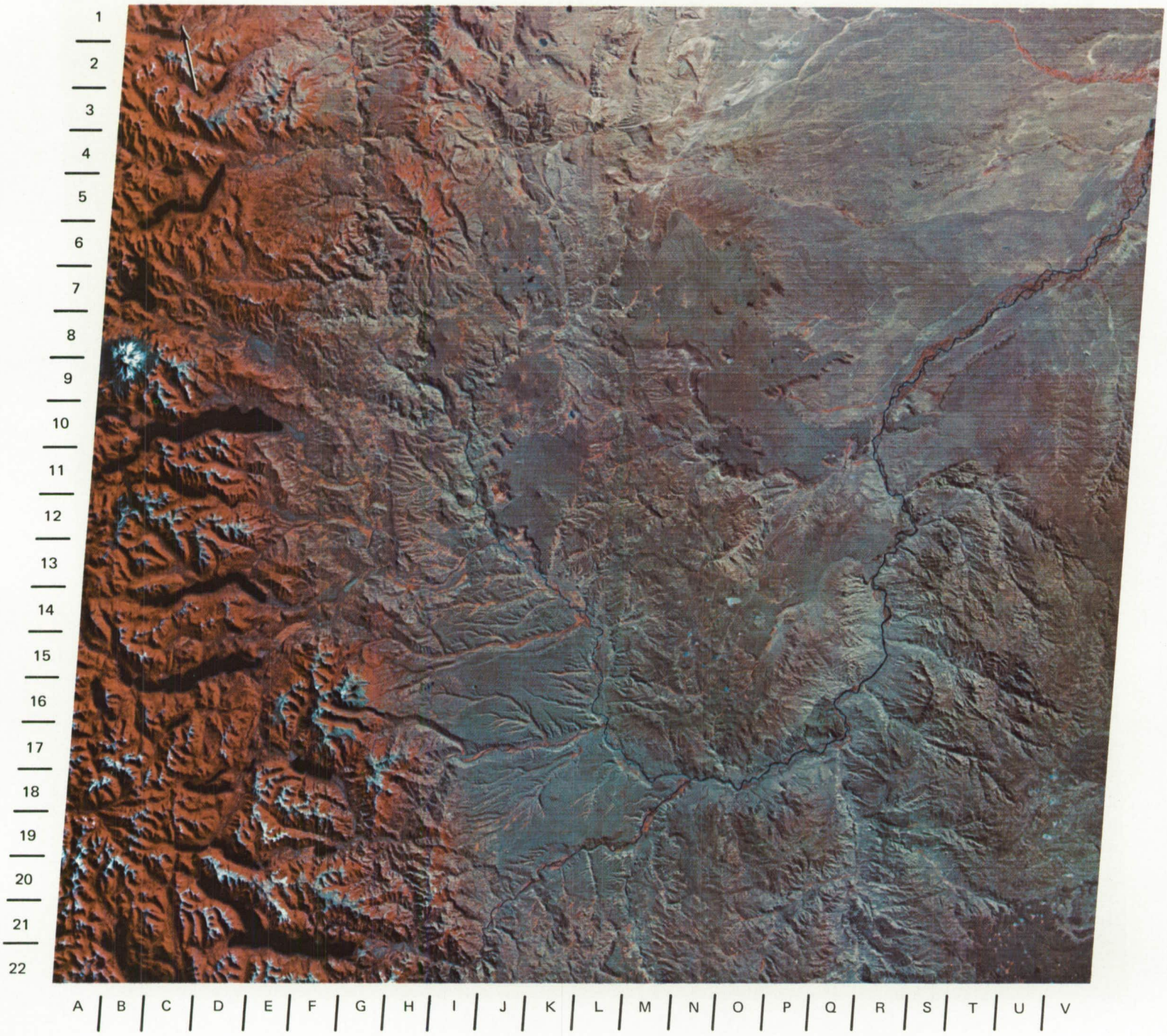


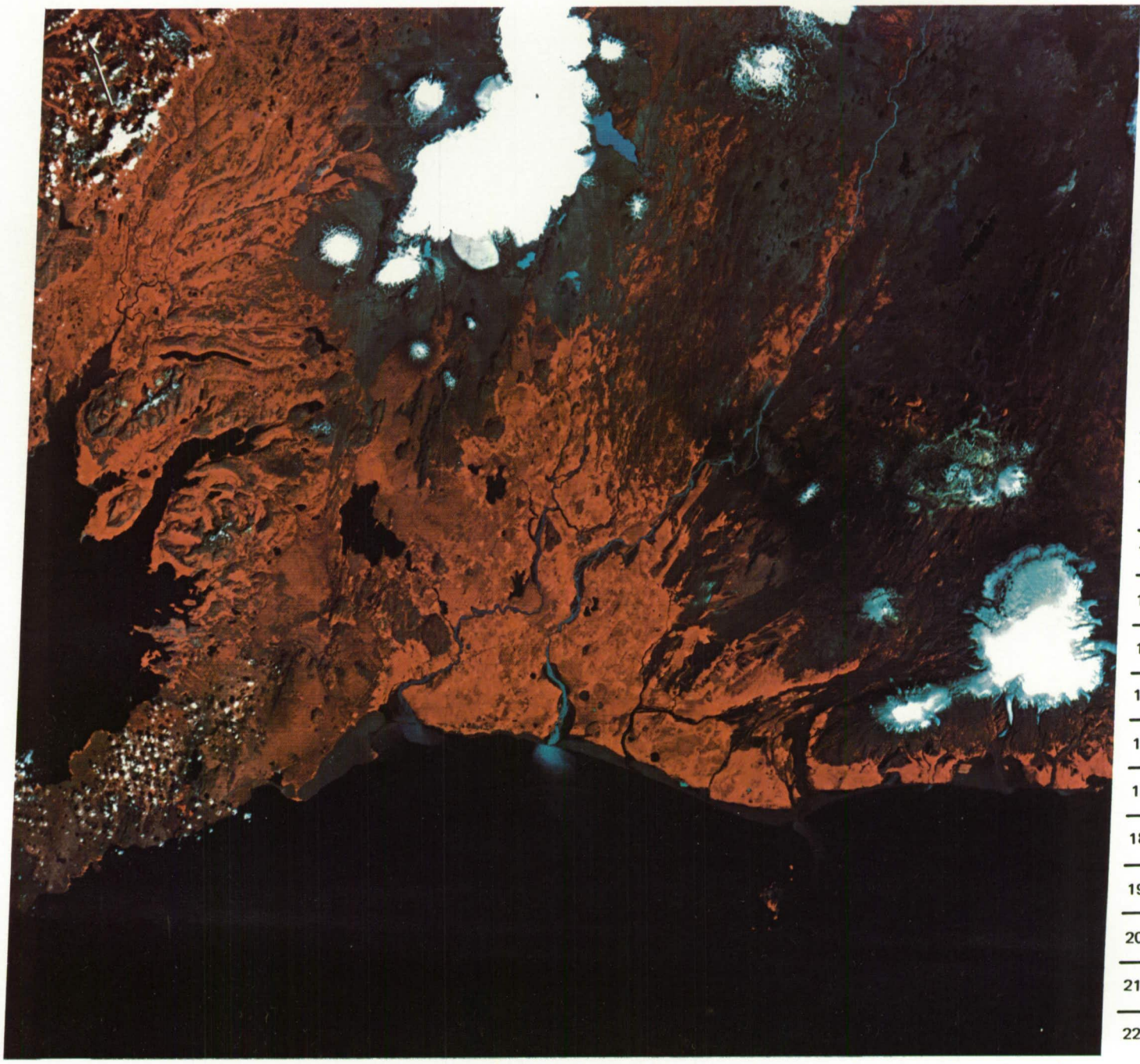
PLATE 218

PATAGONIA, ARGENTINA: Patagonia refers to the physical region constituting the southernmost section of Argentina from the Rio Colorado on the north to Tierra del Fuego in the south. Its western edge runs along the crest of the Andes at the border with Chile (*B*–18). The mountains in this scene rise only to about 2100 to 2400 meters (7000 to 8000 feet), being much lower than the central and northern Andes. However, the peak of Volcano Lanín (*A*–8) reaches to approximately 3600 meters (12 000 feet). The Andes here consist of mid-Cenozoic intrusive rocks and Tertiary-Quaternary volcanic effusives. These mountains were extensively glaciated during the Pleistocene, with the streams widened and deepened by scour. Many valleys contain elongate lakes (*C*–13) dammed by glacial moraines at their lower ends. This region is part of the lake country of Argentina. Lake Nahuel Huapi (*E*–21) is a popular resort spot, with visitors staying in nearby San Carlos de Bariloche (*F*–21).

The country to the east of the Andes slopes is a flat, high tablelands consisting of horizontal Jurassic, Cretaceous, and Tertiary sedimentary rocks (*K*–15) in stepped mesas overlying ancient Archean crystalline rocks (*R*–18). Recent basalt flows form distinct flat mesas in several places (*J*–10; *N*–9; *U*–21). The Rio Limay (*Q*–15) and its tributary, the Rio Aluminé (*L*–16), have cut narrow canyons through this highlands terrain.

In contrast to the arid, almost barren slopes of the Andes to the north (see plate 201), the lower Andes here is covered with conifers and deciduous (principally beech) trees typical of a cool temperate climate. The tablelands are a semidesert environment, supporting shrubs and coarse grass. Some cattle and sheep graze in this desolate wilderness. Wheat, vegetables, and fodder crops are grown in the narrow valleys (*M*–18; *U*–2) by the natives of this sparsely settled region. *1241–13541;* March 21, 1973.

PLATE 219



ICELAND: The red, white, and blue of the Icelandic flag stand for molten lava, ice, and ocean. This Landsat image coincidentally reproduces them, although the red here represents green meadows. This image may give a misleading idea of the island's vegetation; there are practically no trees. Only one city, Reykjavik (*C*–13), the capital, is clearly visible. The site of the world's first parliament, which met in an open field in the year 930 A.D., is at Thingvellir (*G*–10). Most of the visible landmarks are natural: Mýrdalsjökull (*U*–14) and Langjökull (*J*–4) are snow-covered mountains with active valley glaciers. The U-shaped valleys (*D*–7) were carved by former glaciers from Langjökull. Mount Hekla (*P*–10), an active volcano, is 1491 meters (4892 feet) high. Thingvallavatn (*G*–11) is Iceland's largest lake.

Geologically, Iceland is a remarkable land. To begin with, it shows us new crust in the process of formation. It is located on the Mid-Atlantic Ridge, which is the site of repeated basaltic dike intrusions and eruptions. The crust along the ridge is fractured, as is this main valley, and is eventually moved slowly away from the ridge by sea-floor spreading. Studies in Iceland have thrown much light on the process, which is here taking place on land. The southwest-trending features in the Thingvellir depression (*G*–10) follow the structural trends in this part of Iceland; the spreading is at roughly right angles to these trends. This valley is thus the central rift of the Mid-Atlantic Ridge. All the land area shown here is either lava; volcanic ash; or glacial, fluvial, or eolian sediments derived from them.

Dramatic examples of new land forming have been provided in the island of Surtsey (*O*–21), southwest of Heimaey. This tiny island was produced by a volcanic eruption from the sea floor in 1963, continued erupting intermittently until 1967, and has since been an invaluable natural laboratory. An example of geologic hazards was the 1973 eruption of a new volcano, Eldfell, on the island of Heimaey, in the Westmann Islands (*P*–19) (Vestmannaeyjar in Icelandic). Lava and ash buried more than a third of the fishing town of Vestmannaeyjar, although there were no casualties. There was at least one potential fossil formed to puzzle geologists of the distant future: the July 1973 *National Geographic* illustrated a 1958 Chevrolet being slowly buried by volcanic ash. *1392–12191;* August 19, 1973.

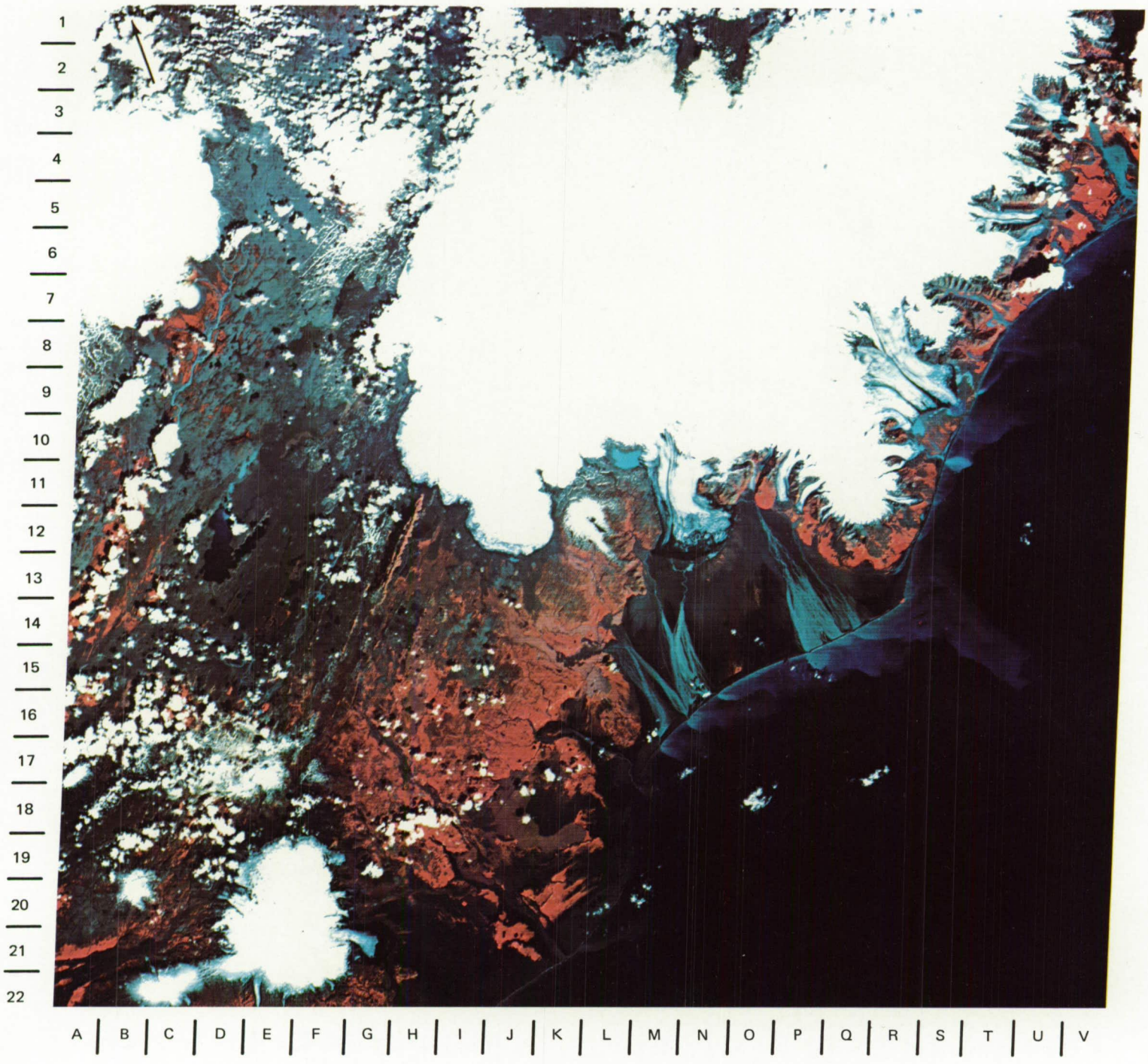


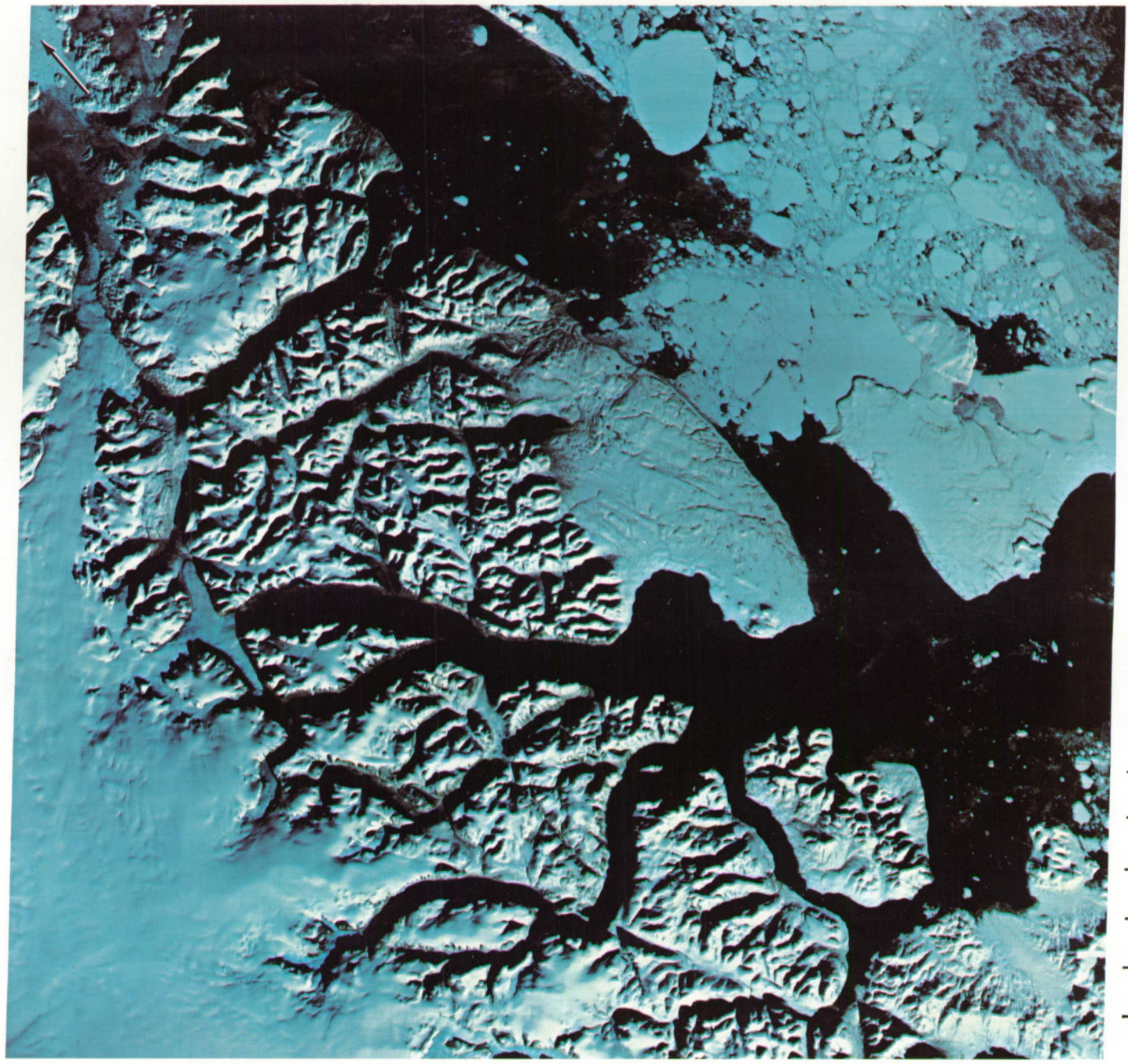
PLATE 220

NORTHERN ICELAND: The classic geology text *Principles of Physical Geology* by Arthur Holmes, has 23 index references to Iceland; this image, with a wealth of geologic features, shows the reason. It overlaps the previous view at the bottom, but was acquired 3 weeks earlier in the summer. There are practically no manmade features visible, except for a road (*J*–17).

The dominant feature is, of course, the great ice cap of Vatnajökull (*H*–10; *T*–1), over 80 kilometers (50 miles) wide in places, which encloses Iceland's highest mountain, Oræfajökull, with a height of 2119 meters (6950 feet). To the west is Hofsjökull (*A*–4) and to the south is Mýrdalsjökull (*E*–20). These icecaps are small versions of the continental glaciers that covered much of North America and Europe during the Pleistocene. Iceland is not especially cold, because of the moderating influence of the ocean, but it has the one overriding requirement for glacier formation: enough snow. The icecaps feed several outlet glaciers, most of which surge from time to time. Note the excellent moraines on these glaciers; they are ribbons of rock debris on the surface of the ice. Between Vatnajökull and the coast are low-lying outwash plains, locally called "sandur." They are formed by braided streams issuing from the glaciers. Such streams form when there is too much material for the stream to carry; those shown here are loaded with debris from the glaciers.

The central depression at left is, as explained previously, the exposed median rift of the Mid-Atlantic Ridge, which intersects Iceland. The dark rock in the center (not to be confused with the lake, Thorisvatn (*D*–12)) is ground moraine and eolian material. There have been very few fissure eruptions in historic times, but one of them, the Laki eruption, occurred here in 1783, producing 12 cubic kilometers (3 cubic miles) of basaltic lava in a short time. The pink ridge (*H*–12), trending southwest from Vatnajökull, is a hyaloclastic (rocks consisting of glassy fragments) ridge, according to Dr. R. S. Williams, Jr., of the U.S. Geological Survey. It was formed by a fissure eruption under the ice. The pink color on the southeast-facing slope reflects a different microclimate, which is more favorable for growth of vegetation. *1372–12080;* July 30, 1973.

PLATE 221



GREENLAND: The low September Sun brings out the rugged topography of the northeast coast of Greenland, with the ice-filled Greenland Sea at upper right. Part of the immense Greenland ice sheet, King Wilhelms Land, is visible at lower left. The islands of Shannon (*T*–10) and Kuhn (*R*–17), and the tip of Store Koldewey (*J*–1), are easily identifiable. The large peninsula at *I*–6 to *O*–11 is Hochstetters Forland.

The Greenland ice sheet is an immense iceberg factory, the icebergs being formed when glaciers enter the ocean or fjords and break off. The process is visible here; note the glacier at *B*–7. This glacier, impressive as it would be on the ground, is but one of many valley glaciers providing outlets for the ice sheet. Others can be seen at *E*–13 and *F*–17. The sea ice appears to include both large floes, or tabular icebergs, up to several kilometers long, and newer ice in the process of formation. Much of this ice will eventually drift south, menacing shipping; satellite coverage of this sort may be of use in directing low-altitude iceberg patrols.

The bedrock geology is difficult to interpret, even where exposed, because of the intricate glacial sculpturing. Most of the area, except for the southern section, is composed of Precambrian rock related to those of the Canadian shield. Those in this area were part of the Carolinidian fold belt, according to P. B. King. This fold belt, the roots of a former mountain chain, has been tectonically overprinted by a later orogeny in the Lower Paleozoic Era that produced the East Greenland fold belt. This superposition of fold belts tends to contradict the theory that continents grow by concentric accretion of such belts; the East Greenland fold belt, for example, evidently formed on preexisting continental crust, not on oceanic crust, as would be implied by the lateral accretion concept.

The relatively level areas on Hochstetters Forland and Shannon Island are underlain by Permian and Triassic sedimentary rock. Small areas of Tertiary plateau basalt also occur on Shannon Island; these are part of the immense volcanic field extending from Scotland to Baffin Island (west of Greenland). Much of Greenland now covered by ice probably belongs to this province. Proponents of continental drift consider the now-separated segments to have been dismembered by crustal fragmentation and sea-floor spreading. *1064–13360;* September 25, 1972.

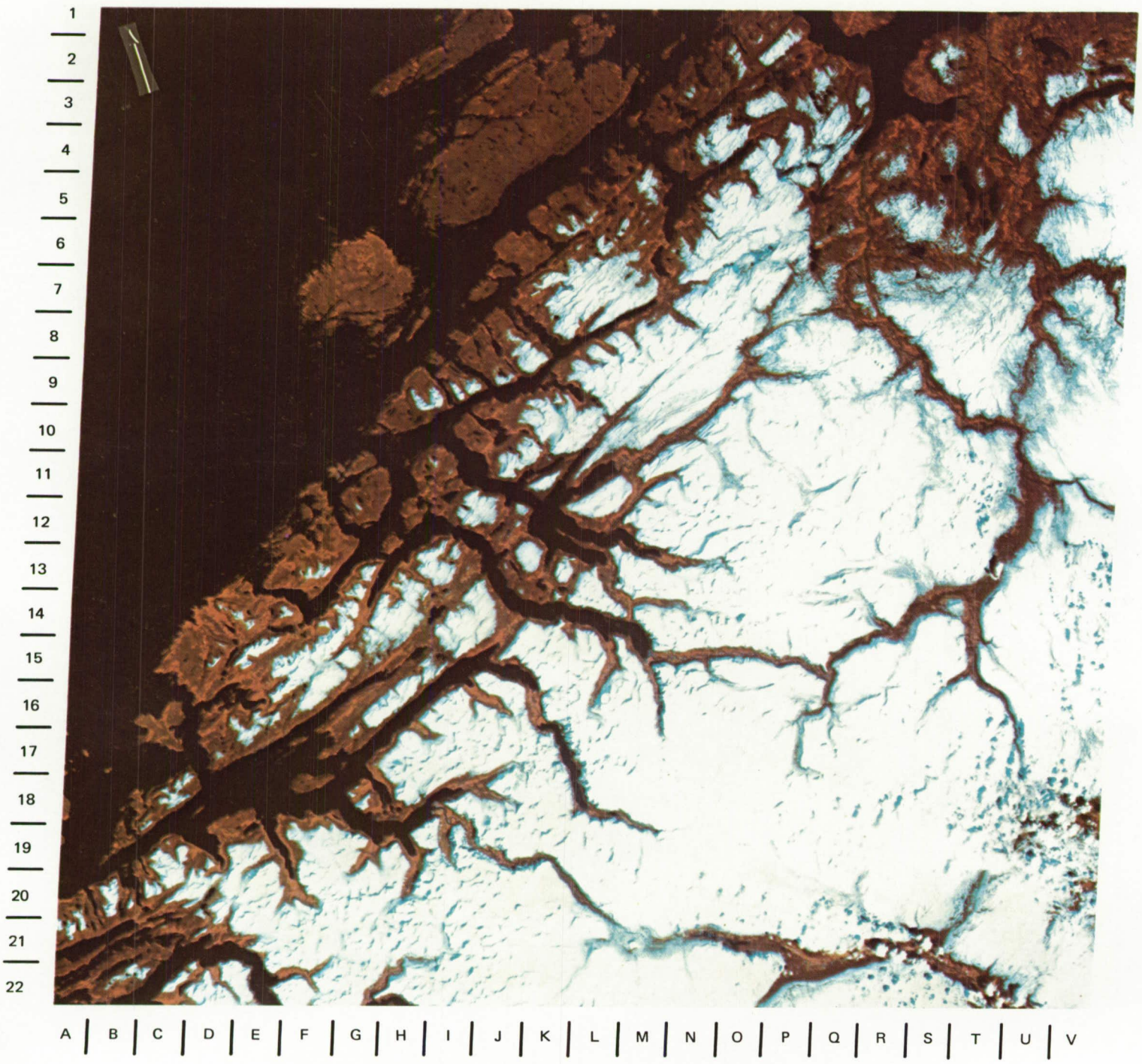


PLATE 222

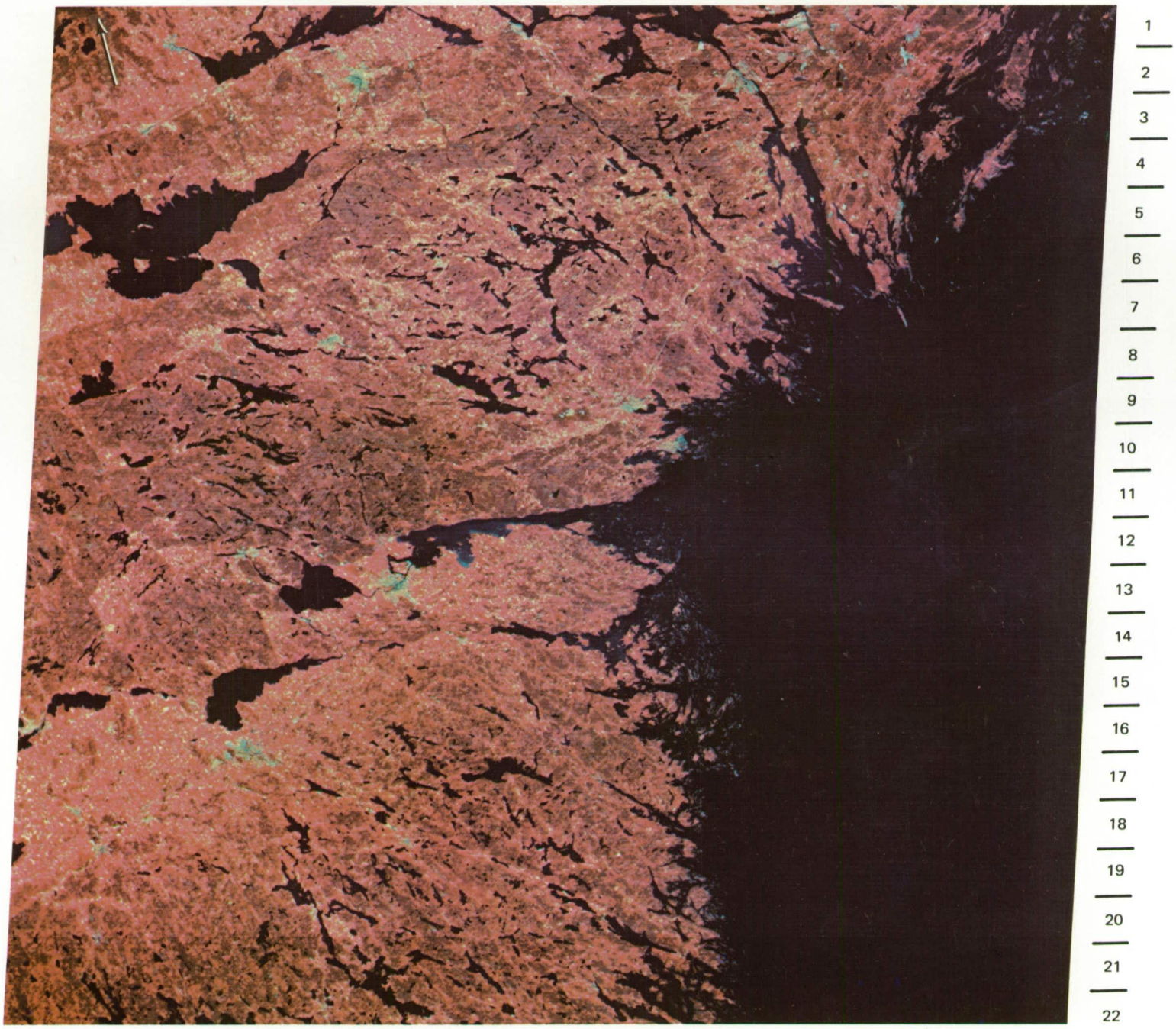
NORWAY: Norway's physiography is epitomized in this image: snow-covered mountains (even in May); an intricate, glacier-carved coast; and very little level terrain. The area gives the impression of being uninhabited, but it includes Norway's third largest city, Trondheim (*S*–1), with a population exceeding 100 000, and the cities of Molde (*E*–17) and Åndalsnes (*I*–17). There are, of course, innumerable small villages in the valleys and fjords. Other landmarks include the islands of Hitra (*I*–3) and Smøla (*F*–6); Trondheim and Molde are located on fjords of the same names.

This image also shows two of Norway's main resources: hydroelectric power and the sea. Norway has the greatest hydroelectric potential of northern Europe for reasons apparent here, namely the abundant precipitation (snow and rain) and the steep gradients of many streams. The high precipitation is due, of course, to the influence of the ocean; Sweden, at the same latitude, has a much drier (and colder) climate.

All of Scandinavia was covered by the Pleistocene ice sheets, whose glaciers carved the many fjords visible here. The ocean itself is a Norwegian resource in several ways. Fishing is a major industry; the herring catch is about 1½ teragrams (1½ million tons) each year. In addition, Norway has the third largest merchant marine fleet in the world.

The mountains visible here, ranging up to some 2400 meters (8000 feet) in height, are part of the great Caledonian chain, the Kjolen Mountains. This chain corresponds in age (Lower Paleozoic) to the southern Appalachians and continues in Scotland. Proponents of continental drift suggest, in fact, that the Appalachians are the North American continuation of the Scottish chain. The Norwegian part of the chain is composed of intensely folded sedimentary rocks whose fold axes trend in this picture northeast to southwest. The folded structure is not as obvious here as in the Appalachians, largely because of the extensive peneplanation and glaciation that have exposed the very deep crystalline roots of the chain. *1299–10202;* May 18, 1973.

PLATE 223



SWEDEN: The corrugated landscape and coastline of southern Sweden is shown in this cloud-free image. This region is called the lake belt, for obvious reasons. The great abundance of lakes is due to the Pleistocene glaciation, a major center of which was in Scandinavia, and which has excavated the lakes by ice plucking. The rocks of this area are extremely complex, being Precambrian igneous and metamorphic types of the Fennoscandian shield; this has added to the effects of glaciation to produce the unusually intricate lake network. The reader may find it interesting to compare this area to the Canadian shield.

The lake belt, also called the Central Lowlands, is the heartland of Sweden. Stockholm is barely off the image at *Q*–1, but several other major cities are easily visible as gray areas: Sodertalje (*O*–2), Eskilstuna (*G*–2), Norrköping (*H*–12), Linköping (*F*–16), Katrineholm (*G*–7), Nyköping (*M*–9), and Söderköping (*J*–14). Some of the more prominent lakes include Mälaren (*M*–1), Hjälmaren (*C*–5), and Roxen (*E*–15). The Gotha Canal, which crosses Sweden from Göteborg to the Baltic Sea, goes through Lake Roxen, reaching the coast at Söderköping.

Much of this region is forested, as the image clearly shows. However, the area is also heavily cultivated, with oats, potatoes, sugar beets, and hay being major crops. Dairy farming is extremely important in this area, producing enough dairy products for export as well as for domestic use. The area has numerous industries using wood for such purposes as furniture, paper, matches, and chemicals. *1345–0935;* July 3, 1973.

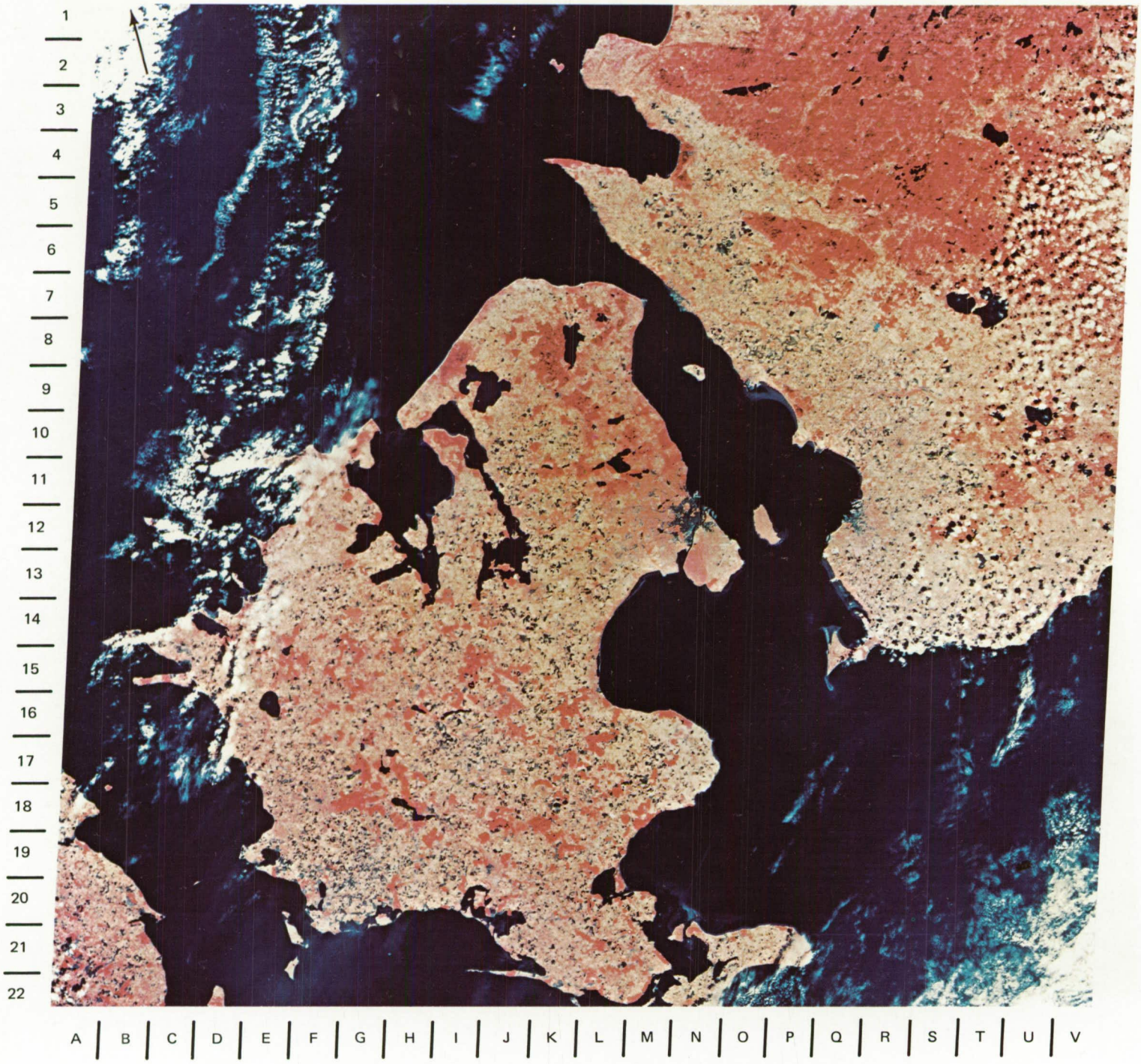


PLATE 224

DENMARK: This scene is part of one physiographic area: the North European Plain. Sections of two countries are included, with Sweden at upper right and Denmark at left. The chief landmarks, for orientation, include Copenhagen (Kobenhavn) (*N*–11) and Naestred (*J*–19), both in Denmark, and Malmö (*Q*–11) and Hälsingborg (*M*–7) in Sweden. The island of Zealand (Sjaelland), largest in the Danish Archipelago, dominates the image.

Most of the land area shown here, with the exception of the forested region in Sweden at upper right, is relatively low, flat terrain consisting of glacial moraine and outwash deposits. The climate is mild, as far as Scandinavian climates go, due to the latitude and the moderating influence of the ocean. Terrain and climate have combined to make this one of the most intensely farmed areas in Europe; the Skane lowland (*M*–5; *U*–12) is known as "the granary of Sweden." An interesting regional characteristic brought out by the Landsat image is the small size of the farms, typically one-quarter square kilometers (60 to 70 acres) in Denmark. It is instructive to compare this scene with farming areas in the United States, or, even better, with the immense collective farms of the Soviet Union. Danish farming is notably efficient; wheat yields are, in fact, the highest in the world. However, the main products of Danish farms are used for animal fodder—potatoes are especially important. Animal products are accordingly predominant in Denmark: meat, dairy products, and eggs.

Although there are few bedrock exposures in most of this region, the Landsat image does show part of one major structure. The linear boundary (*M*–3; *S*–7) between the south end of the Smaland Plateau and the Skane lowlands is the east edge of a great graben, or down-faulted block. This graben extends northward, forming the Oslo Fjord, and southward, forming (in part) the Rhine Valley. Some geologists have suggested that this great fault zone extends all the way to the Mediterranean Sea. *1041–09471;* September 2, 1972.

PLATE 225



SCOTLAND: The rugged terrain of the Scottish Highlands occupies most of this scene, except for the lower right corner, which is a small section of the Lowlands. The city of Perth (*U*–19) is barely visible at the mouth of the Tay River. This image was acquired in March when the highest peaks of the Grampian Mountains (*H*–21; *P*–4) and the Northern Highlands (*B*–20; *E*–1) are snow covered. The area was covered by glaciers during the Pleistocene, some 10 000 years ago; low-hanging clouds in the valleys at lower left suggest what the Highlands might have looked like then from space.

It is well known that the Highlands are a harsh region, with thin soils and a short growing season. They are sparsely inhabited, in fact, essentially uninhabited in many areas, with sheep raising being the only substantial agriculture. About one-fourth of the Highlands is timber, and the rest moor of heath and brush. The Lowlands are much more suitable for agriculture and manufacturing; the great cities of Glasgow and Edinburgh are just south of the area shown here.

The scene includes many famous landmarks. The highest point in the British Isles, Ben Nevis (1343 meters (4406 feet) high), is at *H*–17. Loch Ness, home of the legendary monster, is at *I*–9; the monster is not visible. Loch Ness lies in the Great Glen, the unusually straight valley reaching from the North Sea to the Atlantic. As might be suspected from its shape, this valley was formed by erosion along a fault. The Great Glen fault was demonstrated by W. Q. Kennedy to have undergone about 105 kilometers (65 miles) of left-lateral horizontal movement in which the north side moved southwest relative to the south side. Most of the movement took place in the Paleozoic Era, but minor earthquakes still occur along it. Several other similar faults cut the highlands, appearing as alined valleys parallel to the Great Glen. The Highland boundary fault (*P*–21; *V*–13) separates the Dalradian metamorphic rocks of the Highlands from the old red sandstone of the Lowlands; both are Paleozoic in age. *1233–10564;* March 13, 1973.

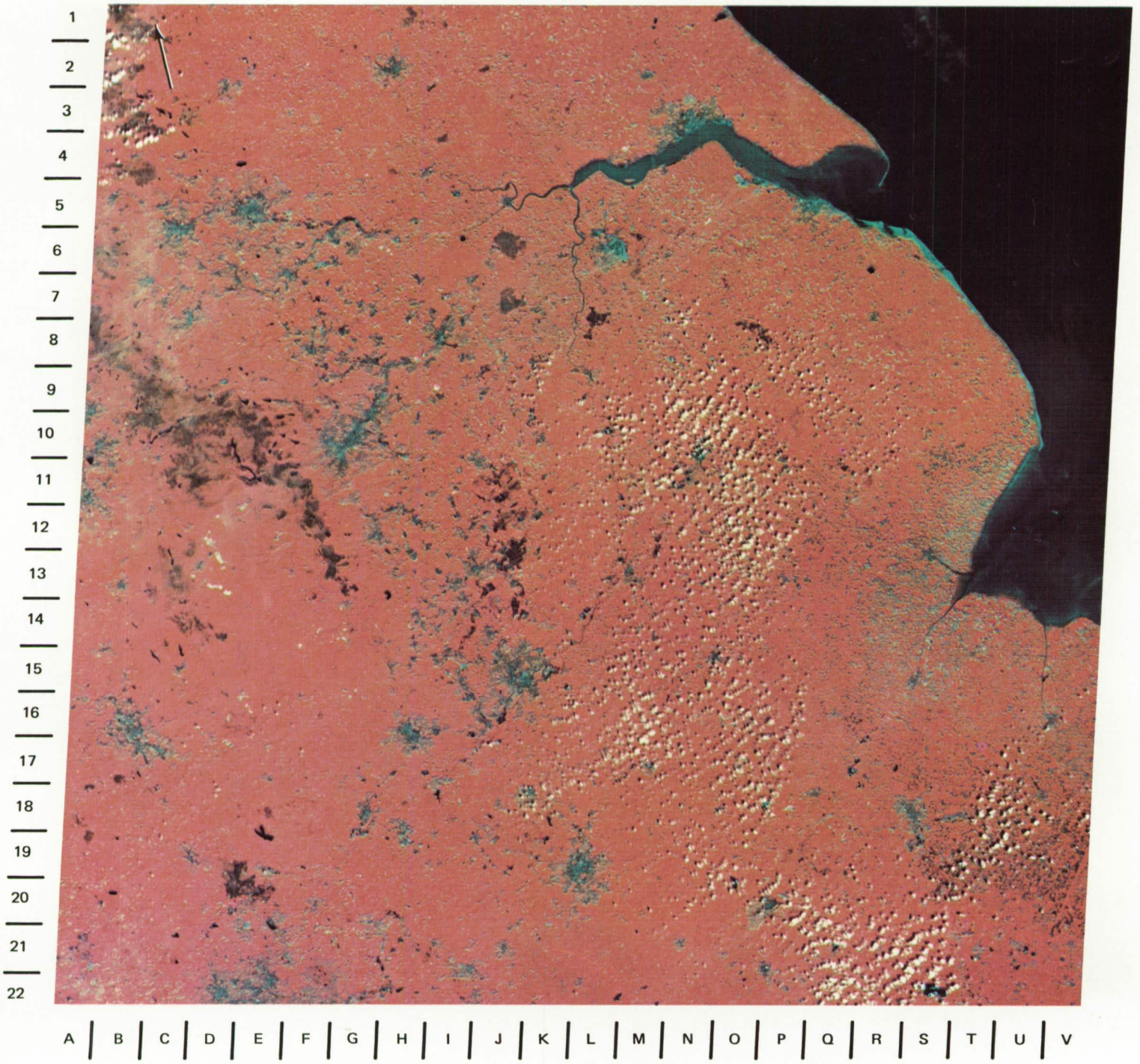


PLATE 226

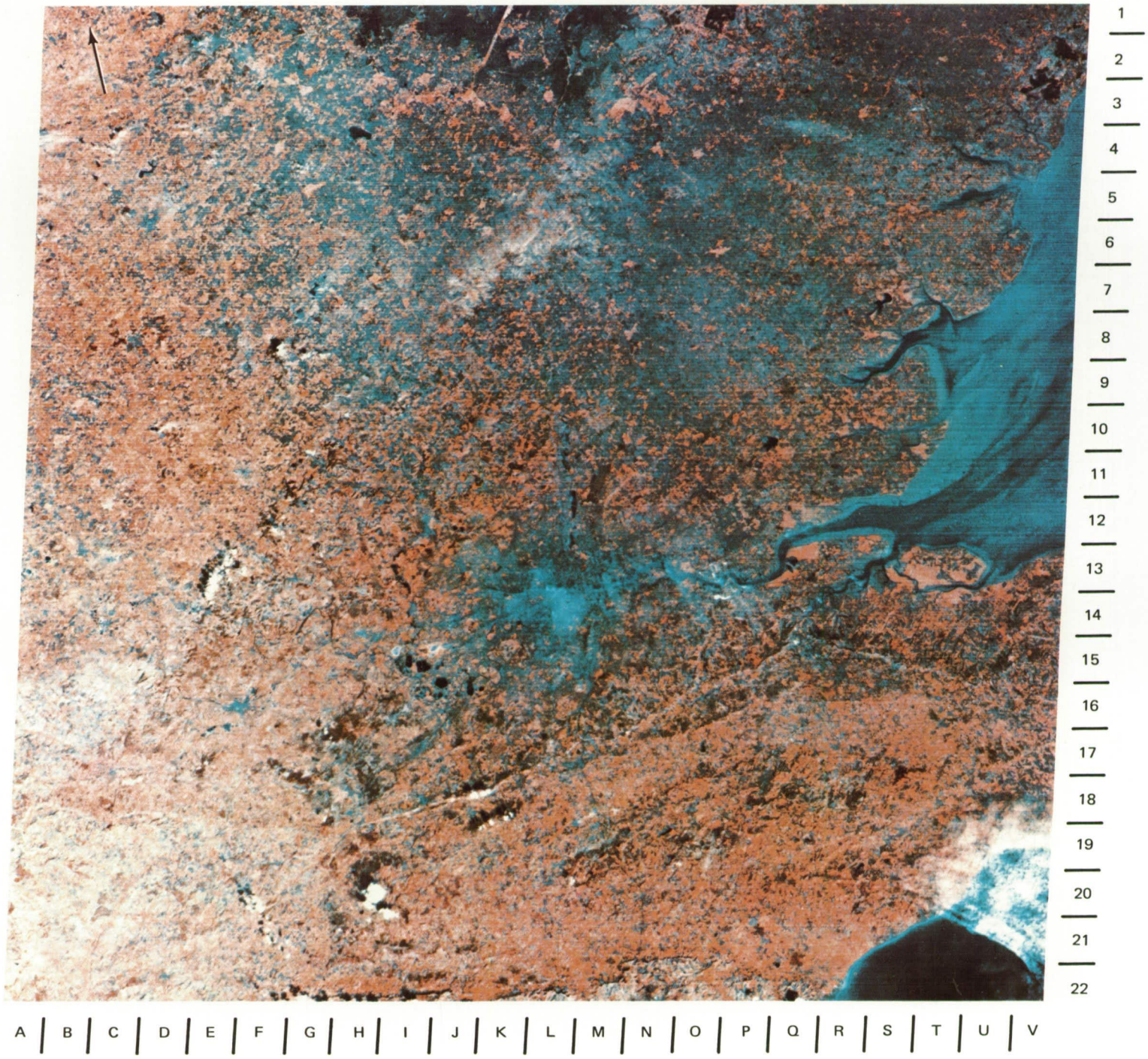
NOTTINGHAM—ROBIN HOOD COUNTRY: This part of the Midlands in north-central England is rich in lore of the past. Many well-known cities and towns stand out in the scene because their large central sections (dark blue) are surrounded by tree-shaded residential areas that blend into the rolling hills of the countryside. In this late spring scene, the plentiful broadleaf forests and open fields appear bright red from the rich foliage. Most famed of these woods is Sherwood Forest (*K*–13) north of Nottingham (*J*–15) where the legendary Robin Hood frequently challenged the Sheriff and others of King John's men in the late Middle Ages.

The two largest cities in this section of England each lie just at the margins of the scene. The suburbs of Birmingham appear at *E*–22 while the east side of Manchester is seen at *A*–10. Other centers include Leicester (*L*–19), Derby (*H*–16), Stoke-on-Trent (*B*–16), Peterborough (*S*–18), Sheffield (*J*–15), Lincoln (*N*–10), Boston (*S*–12), Doncaster (*H*–8), Bradford (*B*–6), Leeds (*D*–5), Scunthorpe (*K*–6), Kingston-upon-Hull (*M*–3), and York (*F*–2).

Yorkshire (*J*–2) and Lincolnshire (*O*–9) are two of the counties that straddle the Humber (*N*–4), a drowned estuary fed by the Ouse (*I*–5) and Trent (*K*–7; *L*–14) Rivers. The Wash (*U*–12) is a large inlet from the North Sea (*F*–3).

Manufacturing and agriculture are the two main activities in the region. Coal is mined at the surface (*F*–12) and in shallow mines in Derbyshire (*G*–13), Nottinghamshire (*J*–12), and elsewhere. Some sedimentary iron deposits are mined in this area. Together, coal and iron are used with limestone rock in steelmaking at many of the towns in the Midlands. Much of the open country is given to dairy farming or to wheat, barley, oats, and soybean fields. *1319–10343;* June 7, 1973.

PLATE 227



LONDON: The ancient Roman settlement of Londinium lies buried beneath today's London (*L*–13), the capital of the United Kingdom, having a population in 1971 of 7.6 million. London is in many ways the capital of the English-speaking world, and as a minor curiosity, is geographically at one center of the world in that the Prime Meridian goes through Greenwich (*L*–13); the longitude of the image center is 6′ W. The clouds and smoke on this particular day unfortunately mask landmarks in London itself, except for the red area of Hyde Park (*K*–13). Other cities visible include Ipswich (*T*–4), Southend on Sea (*R*–11), and Reading (*E*–15). Eastbourne is barely off the image at *R*–22. Hastings, landing site of the Norman invasion of 1066, is at *S*–20.

Taken on March 8, 1973, the image shows the characteristic pink of early spring vegetation in southern England, where some 2000 years of agriculture have largely removed what was once dense forest. The blue-gray areas at upper right are the southern end of the East Anglian Heights, which are much less farmed. The very dark areas (*G*–1; *L*–1) are marshes of the Fen Country surrounding The Wash (off the image to the north).

The image appears nearly featureless geologically but, in fact, does show regional structure. London lies in a syncline, the London Basin, filled with Tertiary sediments. The axis of the syncline roughly follows the Thames (*L*–13; *T*–11). To the south lies the North Downs (*Q*–15; *J*–17), south-facing cuestas of Cretaceous chalk. The broad elliptical feature at *R*–17 to *M*–19 is The Weald, an anticline exposing older clays and sands. These are relatively infertile, and hence The Weald is sparsely populated. At the very bottom edge of the image (*P*–22; *I*–22) are the South Downs, north-facing chalk cuestas corresponding to those of the North Downs. Charles Darwin lived on the North Downs (the village of Down, in fact), and William Smith, the founder of modern geology, came from Oxford (*E*–11). *1228–10293;* March 8, 1973.

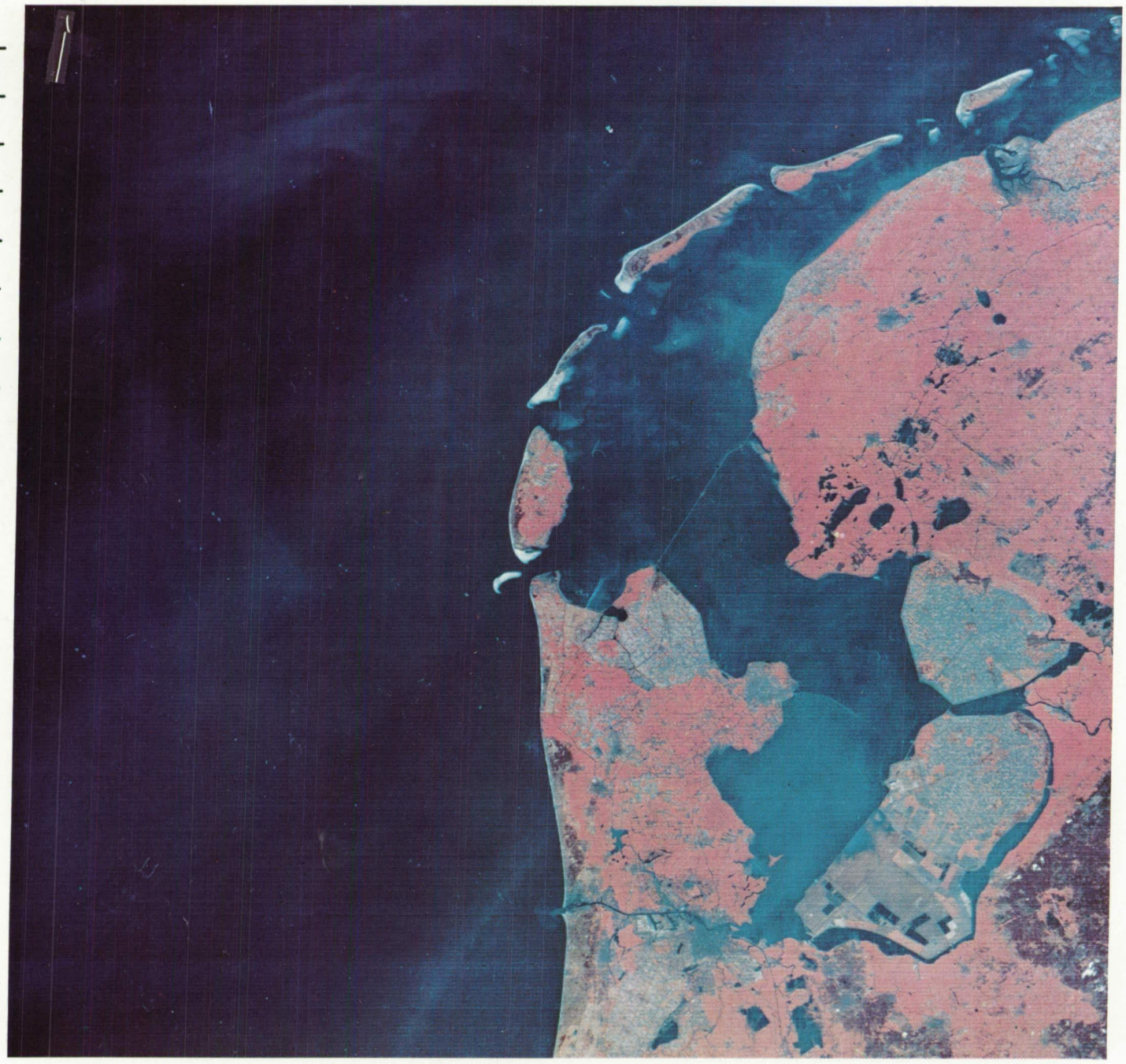
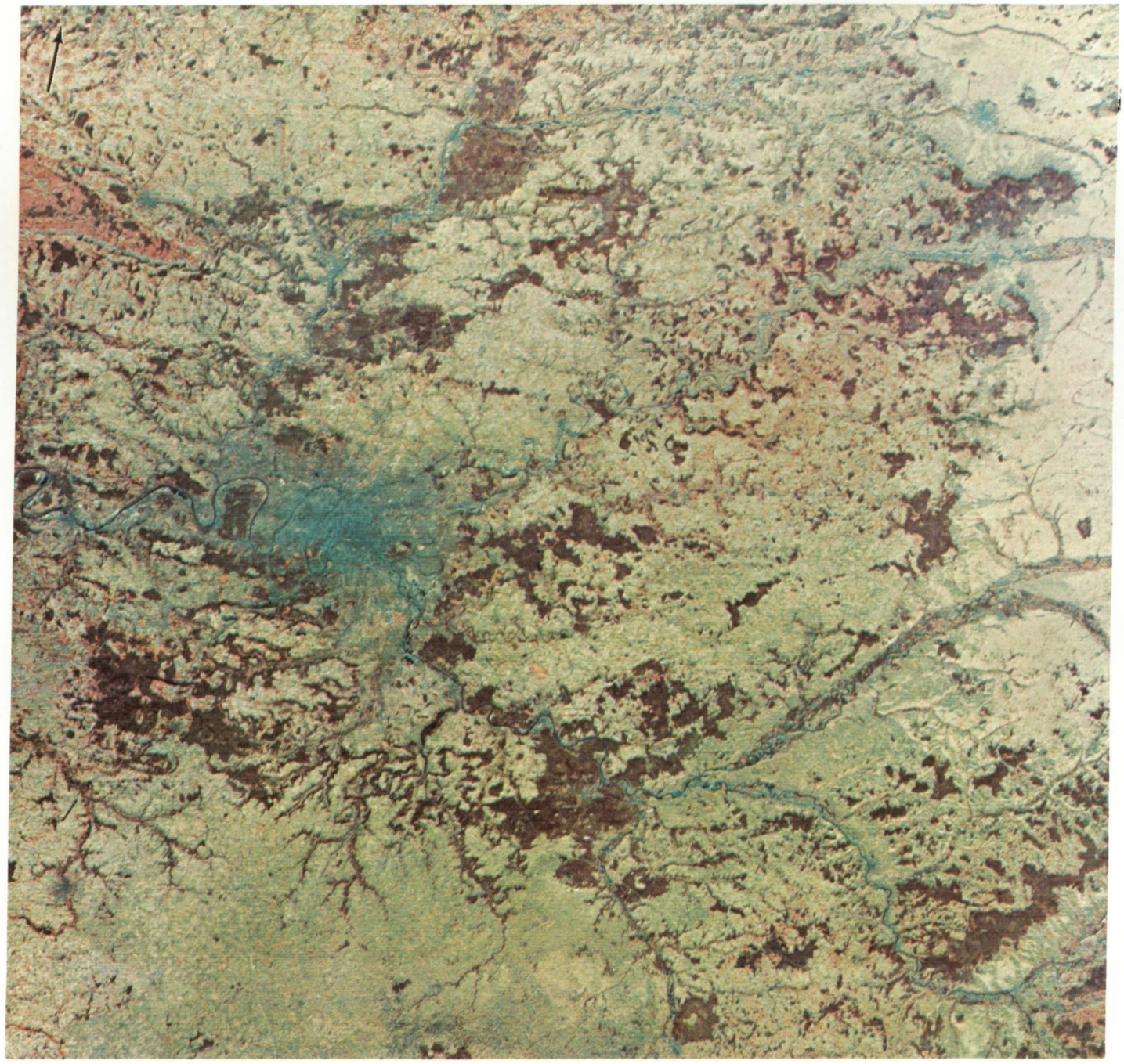


PLATE 228

THE NETHERLANDS: The term "planetary engineering" is sometimes encountered in science fiction; but this Landsat image shows an example of what can surely be considered planetary engineering in progress today: the immense project of reclaiming land from the North Sea to form The Netherlands. This work began as a defensive measure against flooding as early as 1000 A.D., but it developed into a full-scale reclamation effort beginning in the 15th century. Oddly enough, the Zuider Zee (IJssel Meer in Dutch) (*Q*–13) was formed only in the 13th century, when the sea breached an offshore sandbar to form the West Frisian Islands (*K*–11; *Q*–4) and flood low-lying marshes and fields. Since then, reclamation work by diking and pumping has gone on continuously; the Zuider Zee was changed from a sea to a lake at 1 p.m. on May 28, 1932, when the great causeway (*N*–11) was finished. Modern technology has, of course, greatly accelerated the work of reclamation. The northeast polder (*T*–13) was drained from 1927 to 1942; the east polder (*T*–16) from 1950 to 1957; and the northwest polder (*N*–13) from 1927 to 1930. The south polder (*S*–18) is shown as open water on the 1966 National Geographic Society map of western Europe. The west polder is being drained as this is written; and as the Landsat image shows, the water is getting steadily shallower. This process has, incidentally, uncovered a fascinating assortment of ancient and modern ships, as well as aircraft shot down during World Wars I and II.

There is obviously no difficulty in locating the works of man in this space image. Some individual landmarks include Amsterdam (*O*–19), the North Sea Canal (*M*–19), Haarlem (*M*–20), Leeuwarden (*R*–7), and the Wadden Zee (*M*–10; *P*–5). Most of the area shown is below sea level and must be drained continuously; the network of ditches and canals is easily visible. Holland, of course, depends heavily on these canals for transportation. The land is intensively farmed, with the farms having the highest yield in Europe. Amsterdam has always been a major shipping and shipbuilding center, although ship repair work has become more important recently. *1243–10120;* March 23, 1973.

PLATE 229



PARIS: Paris, the political, cultural, and industrial center of France, is the most prominent landmark in this spring view (*G*–11). The Seine River can be easily traced (*A*–10; *K*–15; *R*–14), as can the Marne (*O*–8; *R*–6) and the Oise (*F*–7; *I*–3). The most easily visible cities are Epernay (*T*–6); Compiegne, the site of the French armistice in 1940 (*I*–3); Reims (*S*–3); and Chartres (*B*–19).

The physiography of central France, specifically the Paris Basin, is strikingly visible here. Paris itself is at the center of a smaller basin filled with Tertiary sands, clays, and limestones, called the Ile de France. This basin is surrounded by concentric belts of Cretaceous limestone, or chalk, equivalent to the chalk deposits of southeastern England. These belts dip inward, toward Paris, forming outward-facing cuestas. The broad, light-colored area at right (*U*–15; *I*–1) is the Champagne region. This is a relatively dry chalk plateau, called "Champagne Pouilleuse," or dry champagne, in contrast to "Champagne Humide" lying to the east (out of the image). The area is not well-suited for agriculture, being used primarily for sheep grazing. It also produces, of course, the sparkling wine named for the region, although wine production is more important in other parts of France. Physiographically, much of the Ile de France appears youthful, the Tertiary sediments being only partially dissected by streams. This is especially noticeable in the lower left (*G*–17 and surroundings), where there are broad interstream areas. The drainage pattern is dendritic in most of the image area.

France as a whole is, of course, a major manufacturing country, and Paris is a major industrial city. However, the Paris Basin is predominantly rural, as the land pattern visible here suggests. The dark red patches are forest and the lighter areas are open country used for various forms of agriculture or cattle and sheep raising. The tones in this image are farmland still fallow in the early spring; one later in the year would undoubtedly show a more uniform pink or red. *1243–10132;* March 23, 1973.

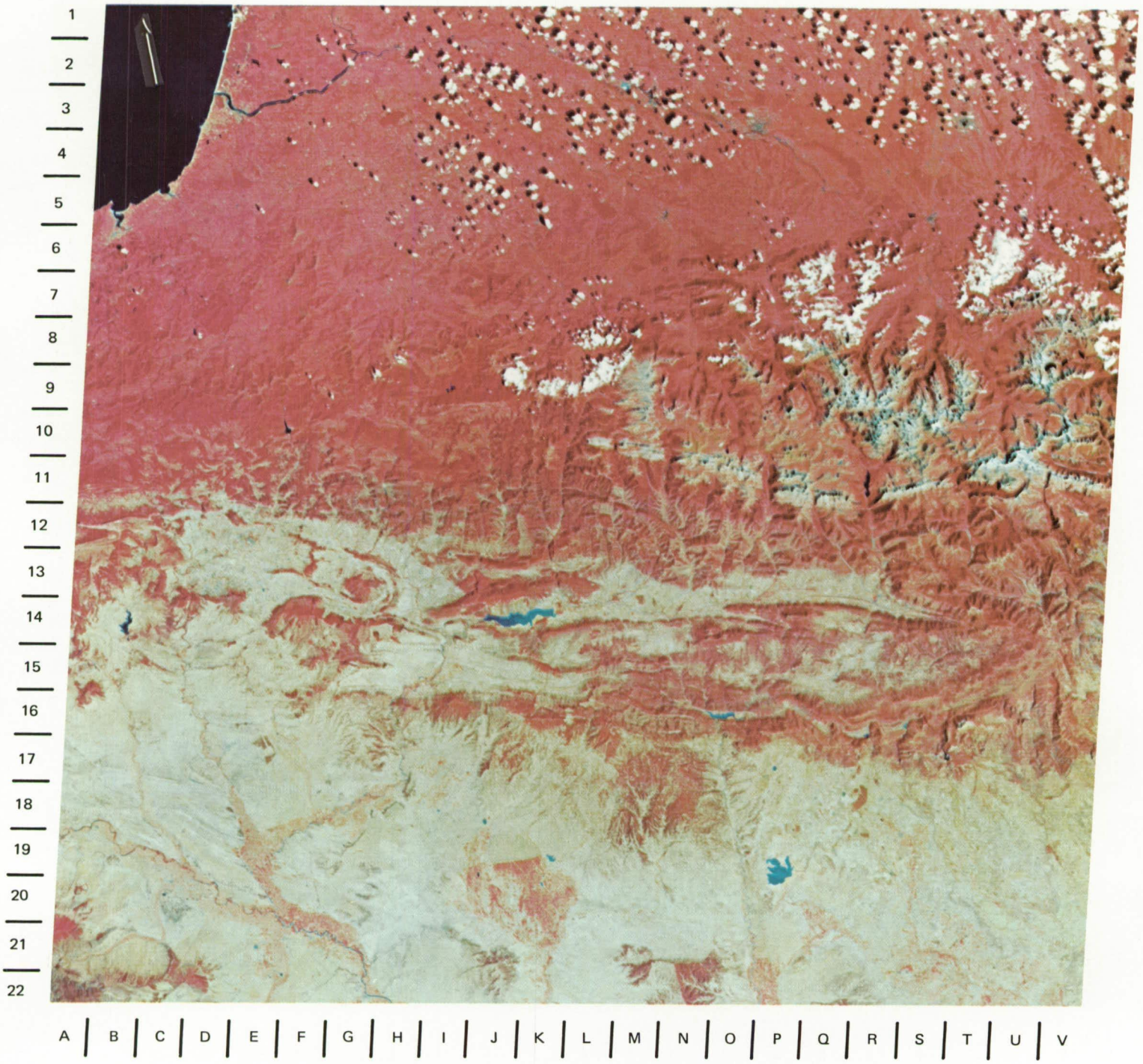


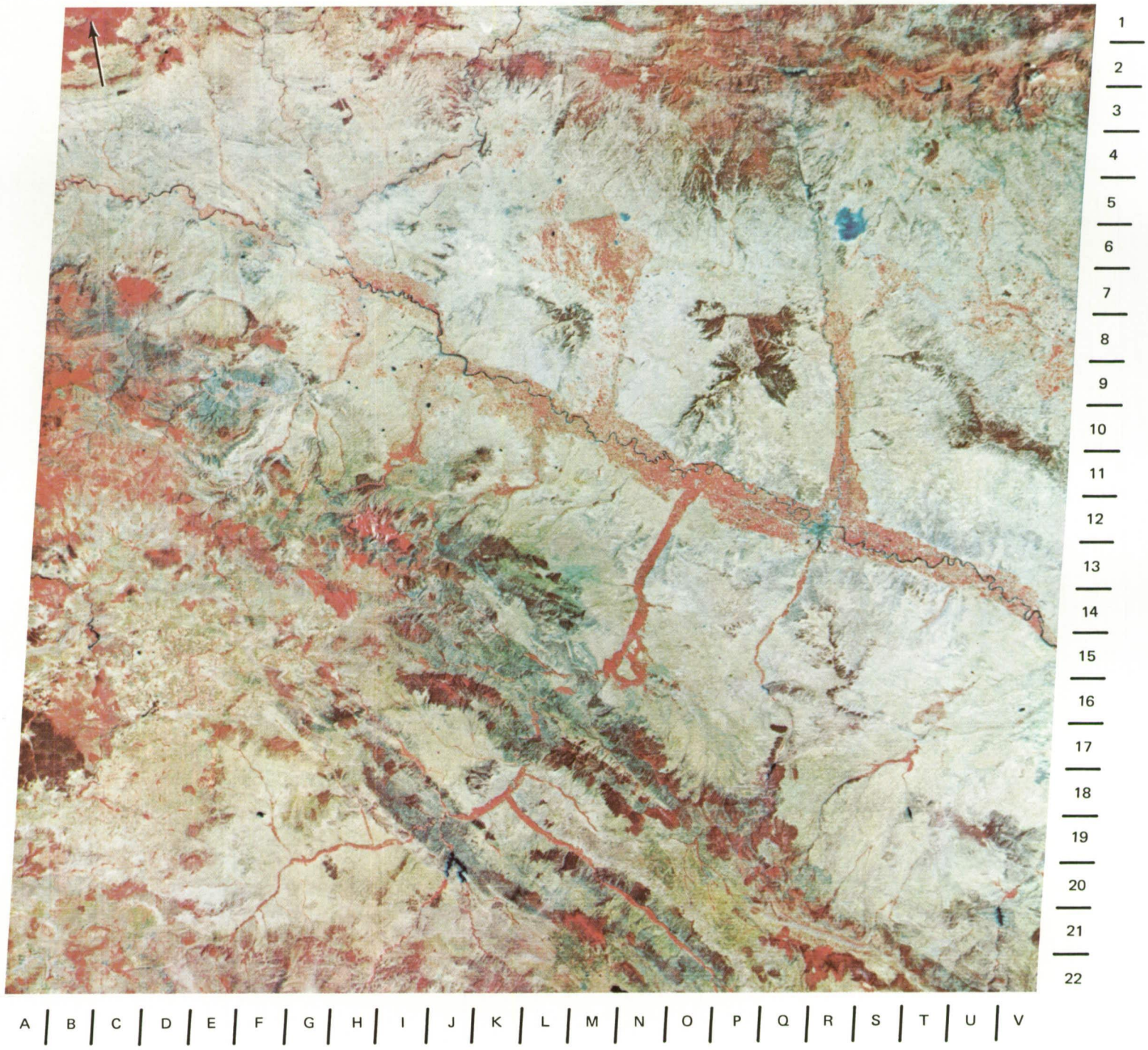
PLATE 230

PYRENEES: The saying "Africa begins at the Pyrenees" is illustrated by this image of the western Pyrenees and adjacent France (north) and Spain (south). The political border runs from Cabo Higuer (*A*–5) on the Bay of Biscay to the right edge of the image at *V*–10. However, the Pyrenees are a major natural barrier as well. Especially noticeable is the contrast between the dark, relatively humid French terrain north of the mountains and the light-colored, dry Spanish terrain of the Ebro valley (the Ebro River itself being visible at *A*–18 to *H*–21). Climatically, much of the Iberian Peninsula is more like North Africa than Europe, which is one reason the Moorish conquerors were attracted to it from the 6th century onward.

The Pyrenees themselves, crossing the image from left to right, are of course the dominant landmark. The Sierra de la Peña (*J*–14 to *S*–14) are also conspicuous; note the characteristic sinuous pattern typical of folded mountains. Relatively few cities are visible; these include Biarritz (*C*–3), Pau (*N*–3), and Pamplona (*D*–3). The north-trending river (*P*–21 to *O*–17) is the Gállego; it and several others are tributaries of the Ebro, which is largely off the image to the south. The Pyrenees are generally considered by geologists to be part of the Cenozoic Alpine system. However, only their most recent orogenic and metamorphic episodes are Cenozoic; the chain actually is Paleozoic in age, and has been rejuvenated. Structurally, they are folded mountains, with the axes running east to west. In modern plate tectonic theory, the Pyrenees are considered by some to be the former boundary between two plates, one now France and the other the Iberian Peninsula. This Landsat image may throw some light on this possibility.

Economically, neither the French nor Spanish sections of this area are especially productive. North of the Pyrenees is the Landes region, a low-lying coastal plain whose main resource is timber. Natural gas has been discovered in the foothills of the Pyrenees about 50 kilometers (30 miles) west of Pau. In Spain, the Ebro valley is farmed only by means of extensive irrigation because it receives only about 60 centimeters (24 inches) of rain per year. *1028–10193;* August 20, 1972.

PLATE 231



ZARAGOZA, SPAIN: A question sometimes asked is whether the works of man are visible from space. This Landsat view of the Ebro River valley of northern Spain shows a striking irrigation pattern that outlines the rivers and dominates the scene. Much of Spain is very dry; the Ebro valley is especially so, having only about 30 centimeters (12 inches) of rainfall per year, because the surrounding mountains cut off the moisture-bearing winds. Cereals, sugar beets, and a wide variety of other crops are now grown in irrigated areas. Elsewhere the barren land is suitable only for sheep raising. The sheep must be moved into the mountains during the hot, dry summers.

The Ebro valley is sparsely inhabited, as the image suggests. The chief city is Zaragoza (*Q*–12) with a population of 380 000; it is a major manufacturing and food processing center. Also visible are Tudela (*I*–8) and Huesca (*T*–5). Other rivers visible include the Jalón, joining the Ebro at *N*–11, and the Gállego, joining the Ebro at *R*–11.

This image suggests that the valley of the Ebro is of tectonic, rather than erosional, origin. The evidence is primarily that the Ebro River is far too small for its valley and shows little evidence of lateral erosion such as in extensive meanders. The valley, in fact, occupies the Ebro Basin, known to be of structural origin for other reasons. It is bordered on the north by folded mountains of the Alpine system satellitic to the Pyrenees, such as the Sierra de Guara (*N*–2 to *U*–2). Older folded mountains border the basin on the south; these consist of Paleozoic and Mesozoic sedimentary rocks, with fold axes trending roughly parallel to the Ebro River. *1352–10201;* July 10, 1973.

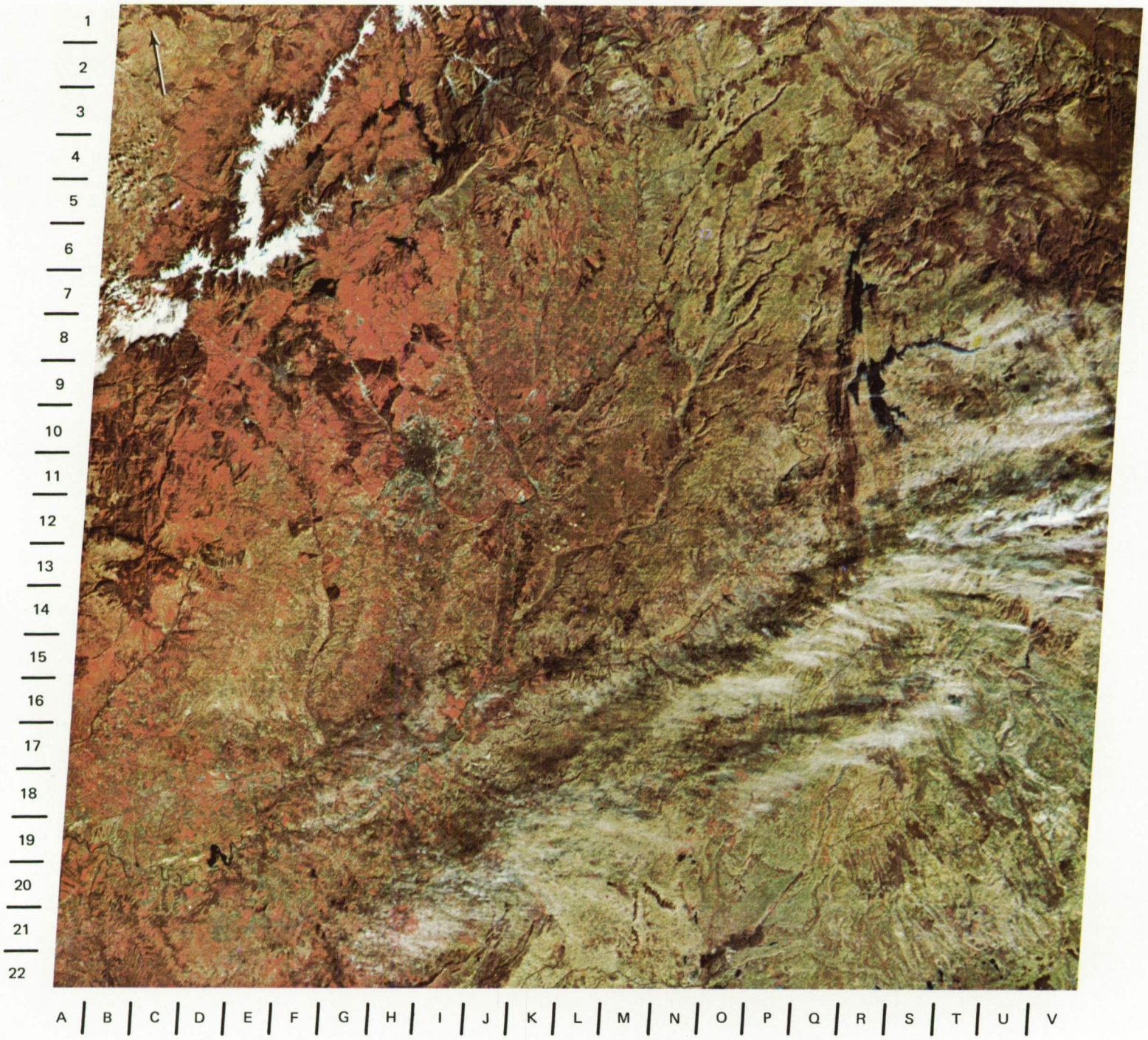


PLATE 232

MADRID: Madrid, the capital of Spain, is conspicuous in this image (*H*–10). It was founded by Philip II in the 16th century and located at the center of his kingdom; therefore, we are seeing the geographic center of Spain. Physiographically this area is in the southern Meseta, part of the great interior plateau of the Iberian Peninsula. The main topographic features shown here include the snow-capped Sierra de Guadarrama cutting the upper left corner of the image. This is one of several Hercynian mountain belts of the peninsula and is composed of Paleozoic rocks. The highest peaks are about 2400 meters (8000 feet) in altitude. To the east (right) of the Sierra de Guadarrama is the broad valley occupied by the Tagus River (Tajo in Spanish) (*A*–18; *J*–15; *P*–9) and its tributaries, some dammed to make large reservoirs. At far right are the western parts of the Serrania de Cuenca, whose greatest altitudes are about 1500 meters (5000 feet). An interesting physiographic feature is the dendritic pattern of the Henares River at (*N*–7), where the river has dissected relatively young, flat-lying sediments.

The Meseta is a very dry area, except for high mountains; Madrid, for example, receives only 43 centimeters (17 inches) of rain per year. This Landsat image gives a good idea of this dryness; the only areas with much natural vegetation are the foothills of the Sierra de Guadarrama west of Madrid. Irrigated areas along the rivers are also visible. Extensive irrigation is a necessity in much of Spain because of the great seasonal variation in rainfall and river flow; irrigation was introduced to Spain by the Moors over 1000 years ago.

It is clear from the image that the location of Madrid was chosen for political reasons, not for its favorable environment. There are few other cities in the area shown here: Alcala (*K*–9) and Toledo (*F*–18) are the main ones of importance. *1227–10271;* March 7, 1973.

PLATE 233



RHONE VALLEY, FRANCE: This mosaic covers most of southeastern France, including parts of the provinces of Languedoc *(lower left),* Dauphine *(upper right),* and Provence *(lower right).* The area is divided into two sections by the valley of the Rhone River at left; the Rhone enters the Golfe du Lion (part of the Mediterranean) at lower left. Most of the population is concentrated in various river valleys in cities (see plate 234 for letter identifications) such as Grenoble (*A*) on the Isère River, Valence (*B*) near the junction of the Isère and Rhone, and Avignon (*C*) at the junction of the Durance and Rhone. Other major cities include Marseille (*D*) and Toulon (*E*). As the mosaic shows, the area covered is climatically a transition zone, ranging from Alpine to Mediterranean conditions—literally from peaks to palms. Agriculture in the northern part of the Rhone valley produces wheat, corn, sugar beets, and potatoes, while in the south fruits, olives, and similar warm climate crops predominate. The Rhone River and its tributaries are exten-

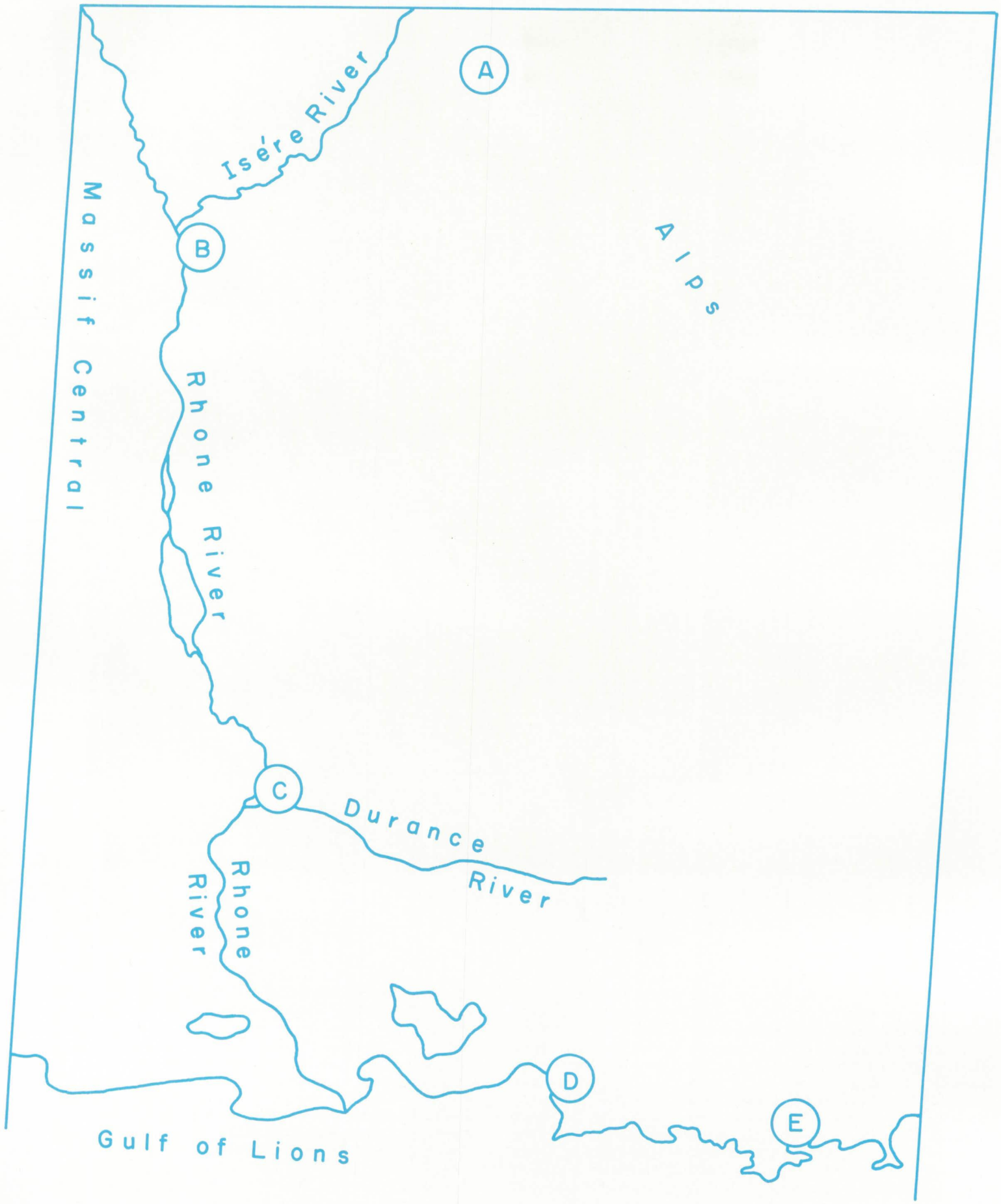
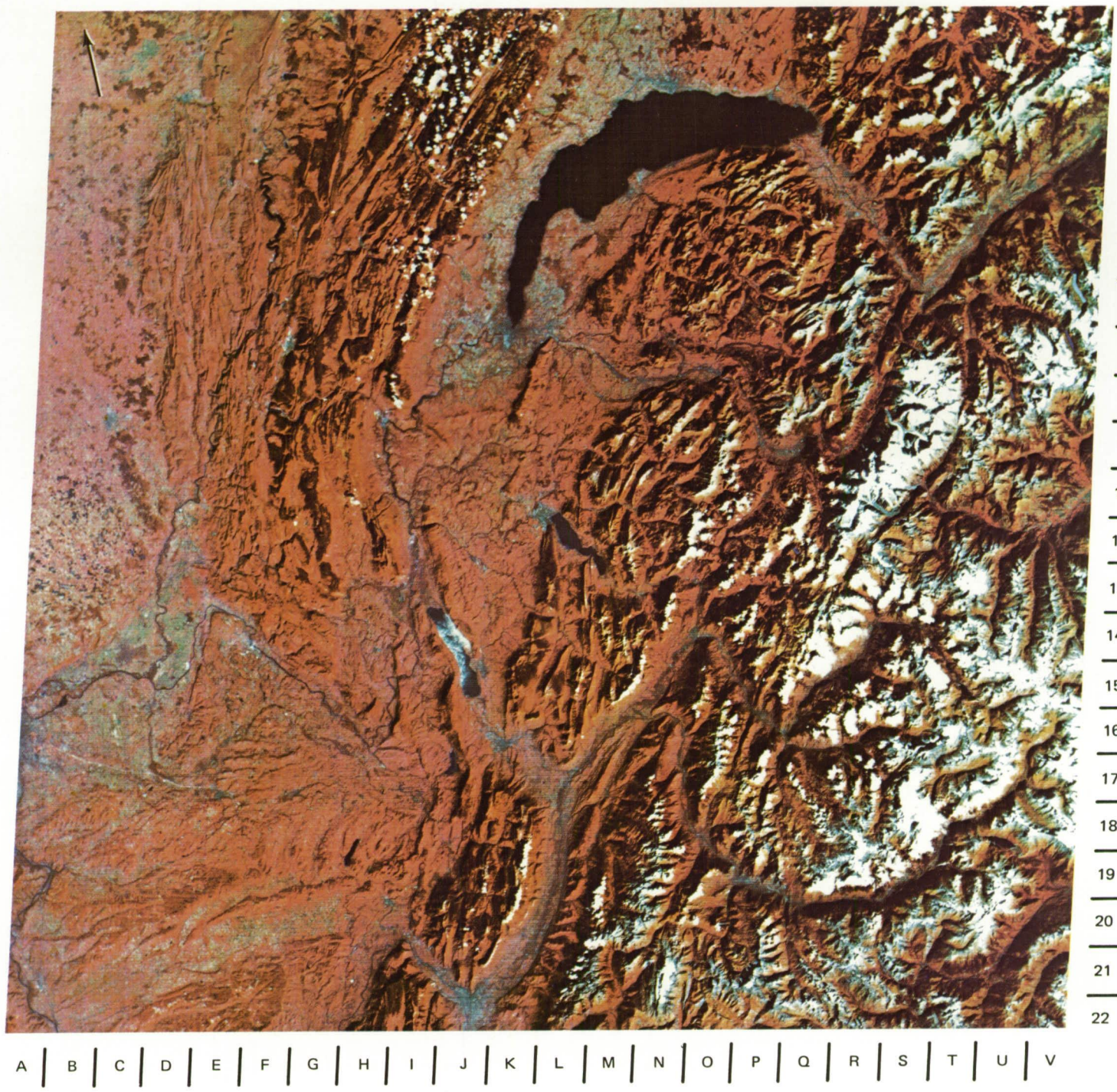


PLATE 234

sively harnessed by a number of dams for water storage, flood control, and power. The Rhone is not a good waterway for navigation, for the rugged topography of its source areas, especially the French Alps *(upper right),* make the flow swift and variable. However, as the mosaic shows, the Rhone valley itself offers the only easy route from the Mediterranean coast to central France, and has historically been a major travel route. In World War II, Allied forces invaded southern France in Operation Anvil, the southern counterpart of the Normandy invasion, and advanced up the Rhone valley.

The city of Marseille, France's greatest port, has been a port for thousands of years because of its critical location; its name in fact is derived from the Greek Massilia. The Mediterranean coast at lower right, east of the Rhone delta, is a typical submerged coast, having rugged, embayed topography. Toulon, the main French naval base, occupies one such bay. *1078–09562;* October 9, 1972.

PLATE 235



LAKE GENEVA: We see here one of the most spectacular parts of Europe: the extreme western corner of Switzerland and the highest part of the Alps, divided among Switzerland, France, and Italy. The Lake of Geneva (*L*–4) is the most prominent landmark, lying between the Jura Mountains (*F*–8; *J*–1) and the Alps. The cities of Geneva (*J*–7) and Lausanne (*L*–2) are on the lake, part of which is in Switzerland and part in France. Several other cities are visible, all in France: Annécy, on the lake of that name (*K*–11); Chambéry (*K*–16); Grenoble (*J*–21); and the outskirts of Lyon (*A*–16). The Lake of Bourget (*J*–14) is marked by low-lying morning clouds (not ice). The mountains are still covered by Alpine vegetation and are therefore a bright red. Crops were presumably harvested in the lower areas when the image was transmitted; therefore, the image there is a pale pink.

The snow-covered Alps, of course, dominate the picture. Prominent peaks include Mont Blanc (*R*–10) and Gran Paradiso (*U*–15). Areas above timberline are distinguished by their blue-gray color. This Landsat image provides a good cross-sectional view of the structure of the Alps, as seen from above. Starting at the upper left are the Jura Mountains, a belt of folded mountains formed by "thin-skinned" deformation, specifically gravity sliding on lubricating layers. Next comes the Swiss Plain (in which is located the Lake of Geneva), a trough filled with Tertiary sediments derived from the growing Alps. To the southeast are the Pre-Alps (*O*–6), which have been overthrust to the northwest. Next, still farther southeast, we see the high calcareous Alps, great nappes, or overturned folds, of limestone. They are succeeded by the older crystalline rocks making up, for example, Mont Blanc. Finally, the innermost Alpine zone shown here consists of the Pennine Alps, intensely deformed limestones and schists. The origin of these structures has taken many decades to understand; it will be discussed further in the caption of plate 236. *1078–09555;* October 9, 1972.

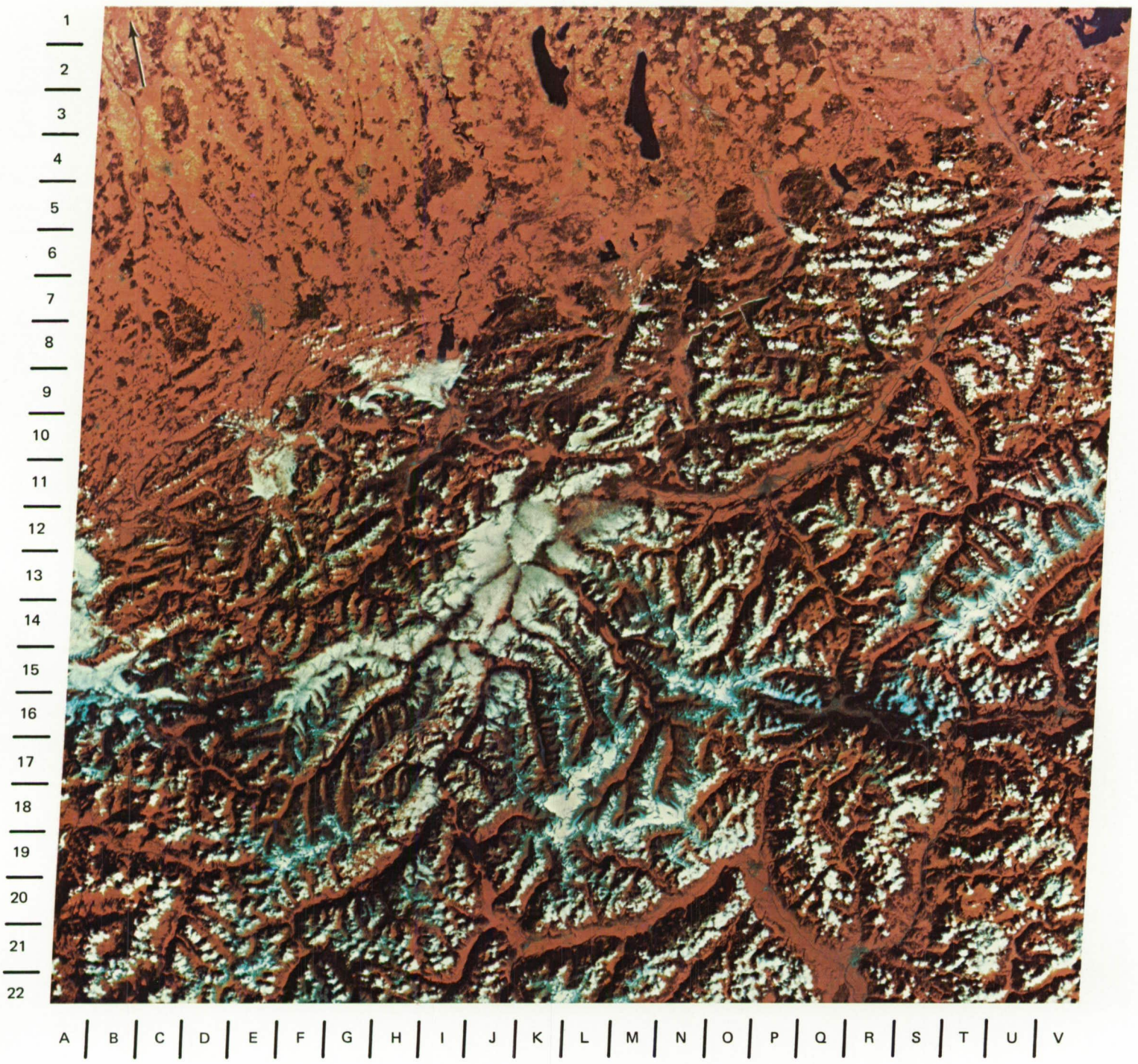


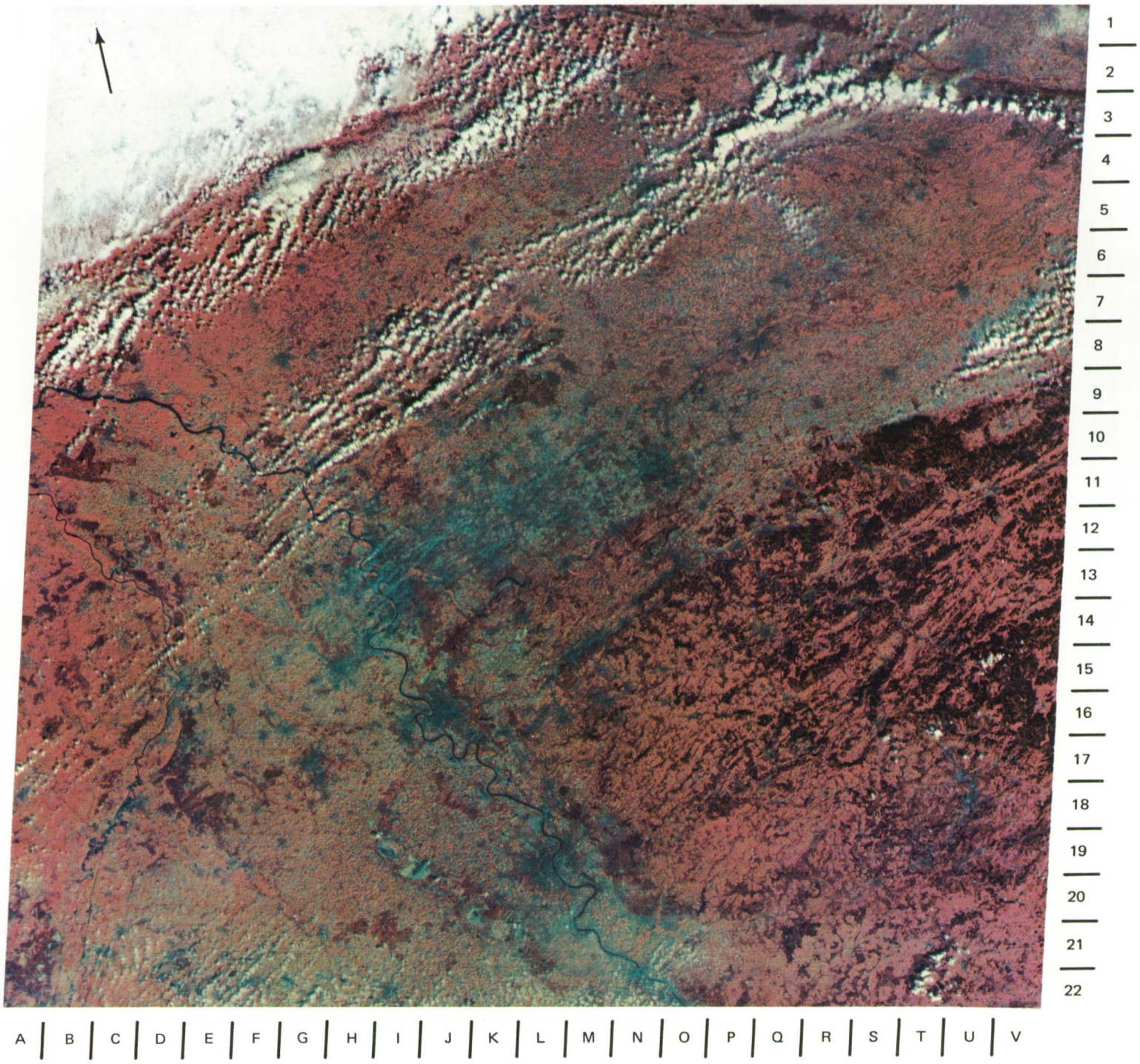
PLATE 236

CENTRAL ALPS: Parts of three countries are covered in this view of the Alps: to the north, southern Germany (Bavaria); at center, western Austria; and to the south, northern Italy. Cities can be easily distinguished by their contrasting blue-gray color against the red countryside: in Bavaria, Rosenheim (*S*–2) and Kempten (*D*–7); in Austria, Innsbruck (*O*–11); and in Italy, Merano (*O*–19) and Bolzano (*R*–21). The Brenner Pass (*Q*–14) was the site of a famous meeting between Mussolini and Hitler in 1940. The two lakes at top center are the Ammer See (*J*–2) and the Starnberger See (*L*–3). Southern Germany is generally sparsely populated, with the main agriculture being dairying, although the city of Munich (population 1.2 million) is just northeast of the Starnberger See off the image.

The Eastern Alps are somewhat lower than the western Alps, having maximum elevations on the order of 3000 meters (10 000 feet). They are bordered on the north by what is known geologically as the molasse trough, an area of thick deposits of coarse sediments derived from the Alps to the south. It is equivalent to the Swiss Plain pictured in plate 235. The Alps in this area are unusually complex, being deformed into immense overturned folds (nappes) and overthrust sheets. The origin of these structures is still not fully understood, but it now appears that the deformation has been largely gravity driven. The large thrust sheets are too weak to have sustained compressive stress; instead, high fluid pressure in the rock is believed to have permitted them to slide primarily by internal buoyancy. The direction of folding and overthrusting was largely from south to north in the area covered by this image. The Alps have of course since been sculptured by glaciation and other kinds of erosion.

The dark bluish feature crossing the lower part of the picture (*A*–15; *V*–16) is not understood, but it may be the track of a thunderstorm that had passed over the area several hours before the image was acquired. Similar "rain prints" have been seen along the paths of rain storms in parts of the American Great Plains; what they would look like in a mountainous area is not evident. *1039–09381;* August 31, 1972.

PLATE 237



THE RHINE AND RUHR VALLEYS: The heartland of West Germany's industrial base lies along the banks of the Rhine (*C*–9; *K*–19) and the Valley of the Ruhr (*L*–11). Here the Rhine flows northwest after passing through the gorges cut into the Rhenish uplands southeast of the nation's capital at Bonn (*N*–21) and then by the forested westernmost edge of the Central Uplands (*U*–15) east of the great cathedral city of Cologne (*L*–19). Thereafter, the Rhine spills onto the North German Plains (*I*–9) as it swings westward through The Netherlands (*A*–9; *G*–3). The South Limburg region (*B*–15) of Holland is crossed by the River Maas (*B*–12) (the Meuse in France and Belgium) and its companion canal (*B*–20). The German border town of Aachen (*E*–22) (or Aix-la-Chapelle, the capital of Charlemagne's Frankish Empire) straddles a main road into Belgium (*A*–15; *A*–20).

Düsseldorf (*J*–16), the gateway to the Ruhr from the upper Rhine and the capital of the North Rhine-Westphalia State, is a center of commerce where textiles and chemicals are also produced. Farming around that city and the plains to the west concentrates on sugar beets, vegetables, and cereals. Textiles are the principal product of Wuppertal (*M*–14) on the Wupper River to the east. Silk, woolen, and rayon goods are also manufactured in Mönchen-Gladbach (*G*–17) and Krefeld (*H*–15) to the west in a region devoted to dairy farming.

Most of the industrial cities of the Ruhr valley cluster between the Ruhr (*J*–13) and Lippe (*K*–11) Rivers and their interconnecting waterways such as the Dortmund-Ems canal leading past Münster (*M*–4). The city of Duisburg (*H*–13), the largest freshwater river port in Europe, sits at the junction of the Rhine and Ruhr Rivers. Beyond are the large cities of Oberhausen (*I*–12), Essen (*K*–12), Bochum (*L*–11), and Dortmund (*N*–10), here blending their dark blue central sections with those of smaller cities. Essen, the largest, is the site of the great Krupp steelworks. Iron and steel are the chief output of this region. Iron ore from Lorraine, Sweden, and elsewhere is shipped by barge and rail to the Ruhr where vast coal deposits from more than 100 mines provide the fuel for smelting this metal. In addition, the Ruhr cities also produce a wide variety of chemicals, textiles, cars, and electrical goods. *1043–09595;* September 4, 1972.

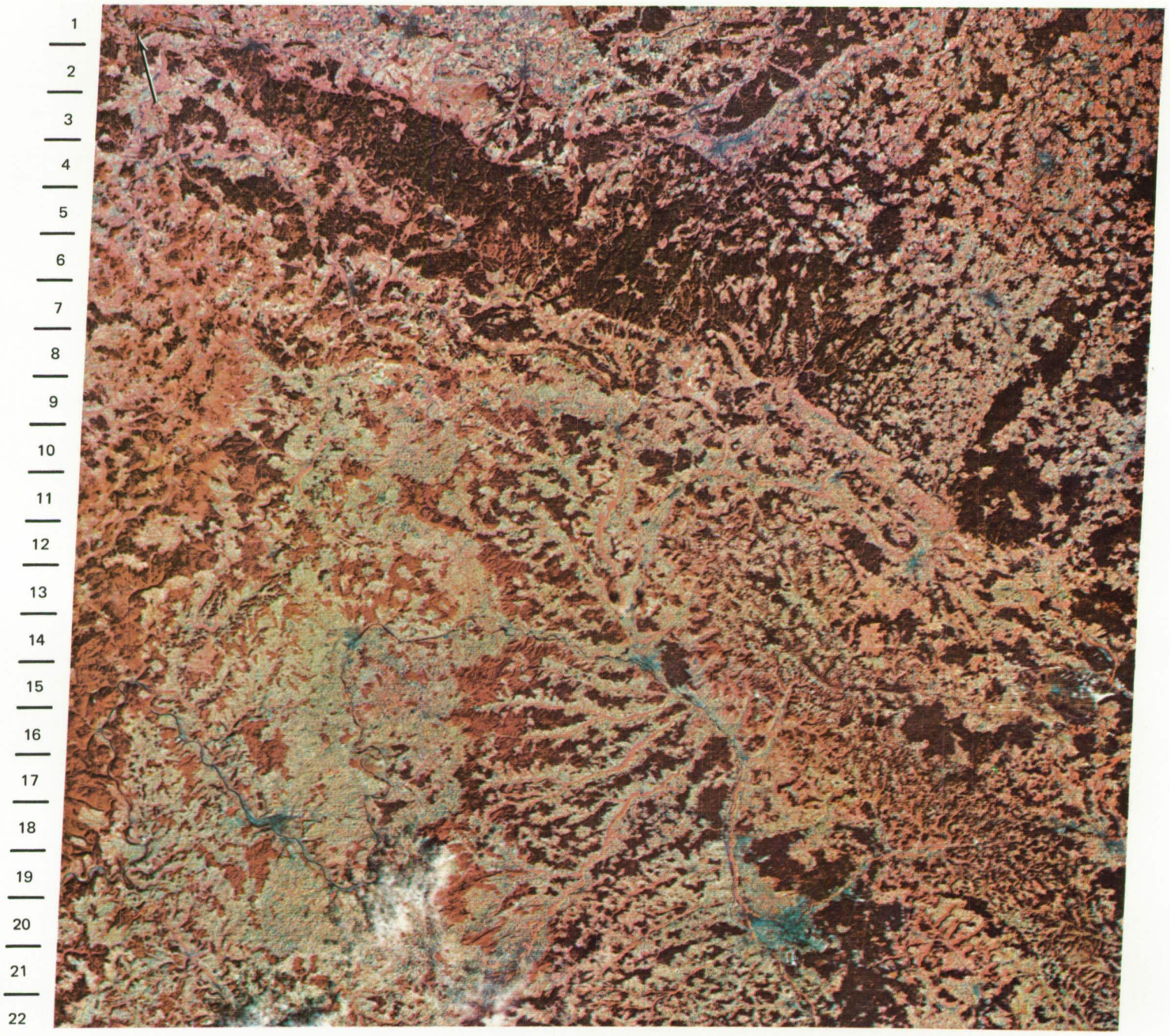
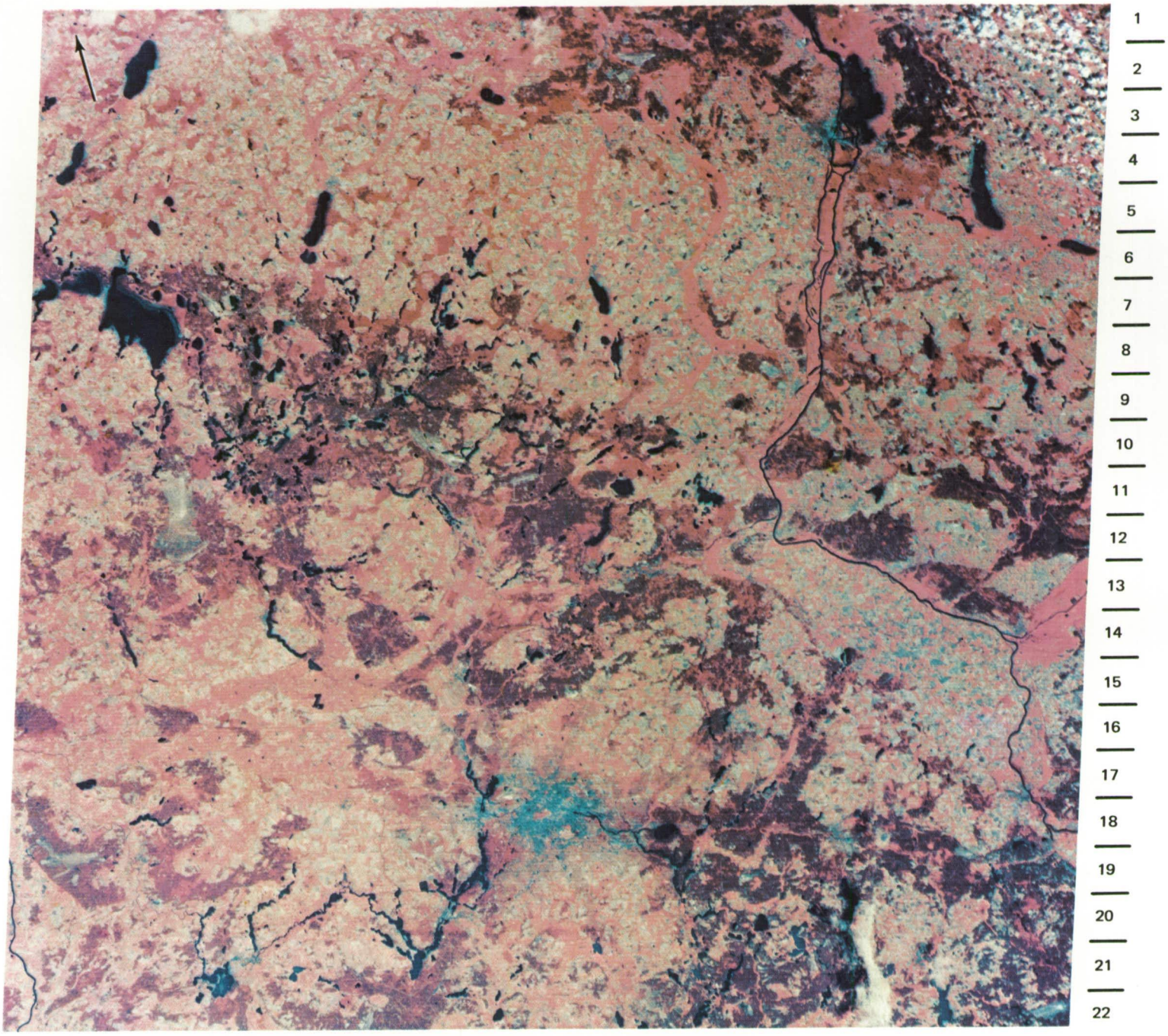


PLATE 238

NÜRNBERG: Germany, like Gaul, can be divided (geologically) into three parts: the North German Plain (bordered by the Baltic and North Seas), the Central Uplands, and the Alpine Mountains and Foreland. This image covers part of the Central Uplands, divided politically into two parts: the Federal Republic (West Germany) and the German Democratic Republic (East Germany). The border is extremely irregular; roughly speaking, the German Democratic Republic is the upper right corner of the image. Many large cities are visible: Nürnberg (*P*–20), Bamberg (*L*–14), Würzburg (*E*–17), and Schweinfurt (*F*–14), all on the Main River. The cities mentioned are manufacturing centers, producing various types of high technology machinery. Schweinfurt is the chief ball-bearing source in Germany. Other landmarks include Bayreuth (*R*–12), for many years a music center, and, in the German Democratic Republic, Gotha (*G*–1), Arnstadt (*I*–2), and Rudolstadt (*M*–3). The Fichtel Gebirge are easily recognizable by their dark (forested) color at *T*–11; their maximum heights are about 1000 meters (3400 feet). The dark hills bordering the upper right corner (*D*–2 to *V*–12) are the Thüringer Wald, or Thüringer Forest, with heights around 900 meters (3000 feet).

The land use pattern is markedly irregular, and typical of the Central Uplands. Dark areas are forest, and the lighter areas either farms or pasture. The pattern reflects the nature of the underlying geology and physiography. This area is primarily one of old crystalline rocks, Paleozoic in age. It has undergone no orogeny for perhaps 200 million years or more, and was eroded to a peneplain after the Paleozoic. The effects of the Alpine orogeny, however, were expressed in this area as regional uplift and faulting. The southwest front of the Thüringer Wald follows a fault. Basement structure in the Paleozoic rocks is faintly visible in the Thüringer Wald as northeast to southwest trending drainage. However, the maturity of the landscape, deep weathering, and vegetative cover generally conceal the geologic structure and lithology. *1076–09431;* October 7, 1972.

PLATE 239



BERLIN: The focal point of this image must, of course, be Berlin (*L*–17), the former capital of all Germany. Since 1945 Berlin has been split into sectors: The United States, France, and the United Kingdom have responsibility for the western sector; the Soviet Union has responsibility for the eastern sector. This Landsat image shows another political development resulting from World War II, the Oder River (*Q*–3; *P*–11; *V*–18), now the border between the German Democratic Republic and Poland. This border was shifted westward after the war, with the result that several cities, such as Szczecin (*Q*–3), once German (as Stettin), are now Polish. Chojna (*Q*–9), formerly Königsberg, is another example. A number of other cities in the German Democratic Republic are visible: Frankfurt an der Oder (*U*–17), Brandenburg (*F*–20), and Prenzlau (*L*–6).

The area covered here is in the North German Plain. The dark-colored area centered on *H*–9 is a forested region with many lakes, the Mecklenburg Lake Plateau. It is a terminal moraine of the Pleistocene glaciation, consisting of sand, gravel, boulders, and clay, and is generally infertile. There are also morainal deposits to the south, but they are less obvious on the image. The area is under cultivation, as the land use pattern indicates, but it is not Germany's most productive farming region. The chief crops are rye, potatoes, wheat, oats, barley, and sugar beets. Poland has a similar agricultural pattern.

Szczecin, or Stettin, is a former Hanseatic League city. It is now one of Poland's leading cities, and is its chief port. The Oder River is a major transportation route, and is augmented with a complex network of canals, serving both Poland and the German Democratic Republic. *1021–09362;* August 13, 1972.

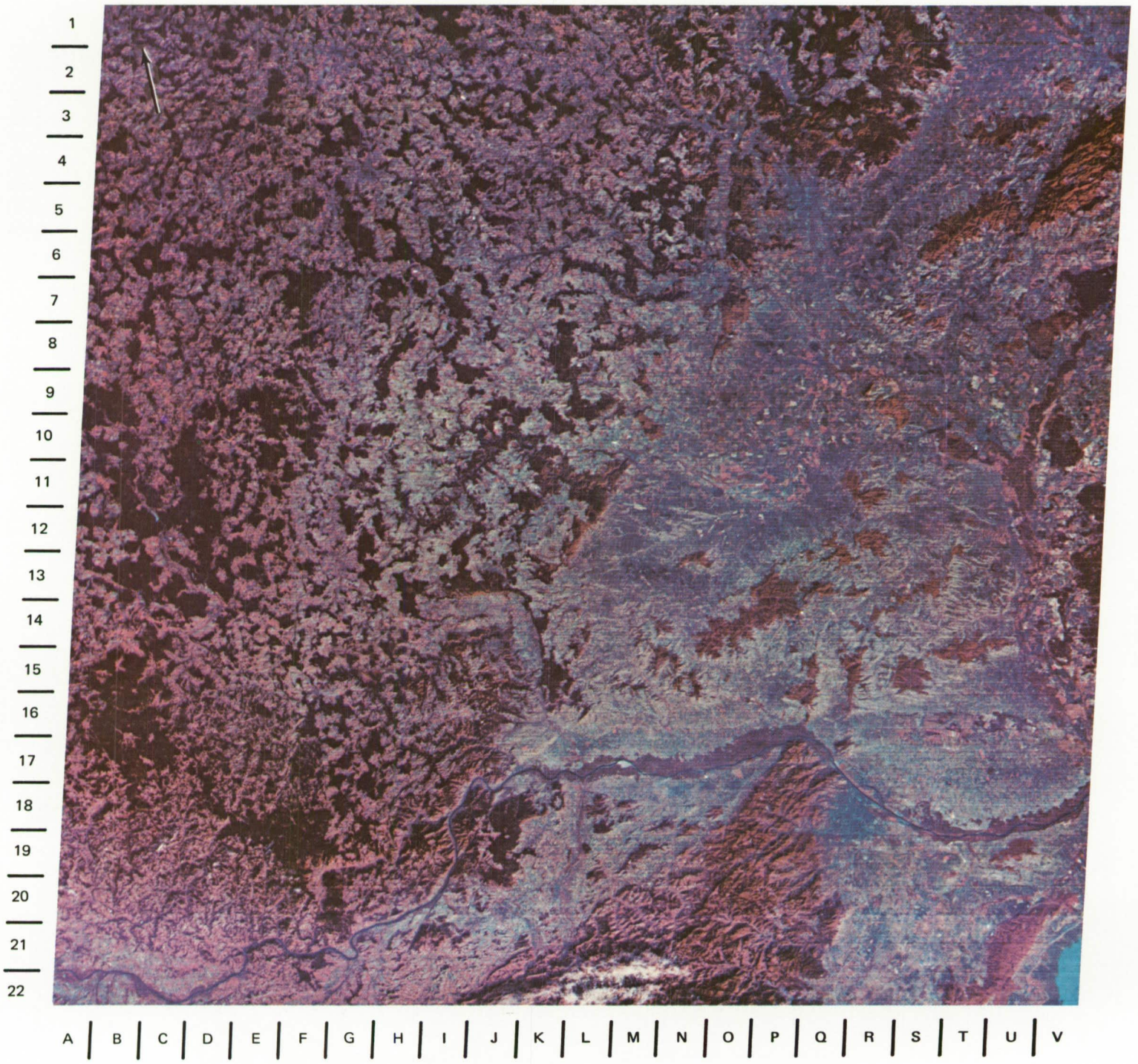


PLATE 240

VIENNA: This city (*Q*–18) has long been the crossroads of Europe and the center of a vanished empire. The strategic location of this famed city of 1 650 000 people led to its founding as a Roman fort some 2000 years ago; since then it has been a political; cultural; and recently, an industrial center. Vienna is built along the Danube River (*A*–21; *M*–17); the part of the Danube covered in this image is entirely in Austria. At Vienna the river has been extensively rechanneled for flood control; the cutoff loop on the east bank, the "Old Danube," is the former channel, now a lake. To the northwest of the city (*Q*–17) are the famed Vienna Woods, covering hills some 450 meters (1500 feet) high. These hills are actually the very eastern end of the Alps. To the north is Czechoslovakia; the border roughly bisects the image (*V*–17; *M*–11). Brno (*P*–5), one of Czechoslovakia's major manufacturing centers, is visible. The broad, low area to its east is the Morava Valley, a wide pass between the Carpathian and Sudeten Mountains, which has been a major migration route for various peoples for thousands of years. It is a major farming area, producing wheat, barley, sugar beets, and corn. The large dark areas are probably deciduous forest areas that have, by November when this image was acquired, lost their leaves.

Geologically, this area is the junction of the Alps (southwest), the Carpathians (northeast), and the Bohemian massif. The massif is the broad, semiforested region in the upper left two-thirds of the image. It is composed of Paleozoic igneous and metamorphic rocks long since eroded into a peneplain, and subsequently uplifted. The Danube has been able to maintain its course, cutting down into these relatively hard rocks and thus producing the many scenic steep-walled valleys for which the river is noted. Soil on the massif is not as fertile as that in the Morava and Danube valleys, and farming is consequently less important; lumber is a major product. *1468–09184;* November 3, 1973.

PLATE 241



ITALY: Despite the intermittent coverage of most areas outside North America, some remarkably scenic mosaics have been constructed; this one of Italy and adjacent areas, made from 46 Landsat images, shows the major physiographic features very well. (See plate 242 for letter identifications.) At the top of the mosaic are the Alps (*A*), and just southward the Po Valley (*B*). The cities of Turin (*C*) and Milan (*D*) are conspicuous even at this reduced scale. The Apennines (*E*) are the geologic backbone of Italy; their structure is locally enhanced by snow. The great volcanic chain (*F*) bordering the Tyrrhenian Sea is well displayed. Vesuvius (*G*) is marked by the recent black deposits of lava and ash on its flanks; Naples lies just left of Vesuvius. Another active volcano, Mount Etna (*H*), is in Sicily. Sardinia (*I*) and Corsica (*J*) (the latter, of course, part of France) are nonvolcanic islands consisting largely of Hercynian (Paleozoic) rocks.

Vegetation patterns can be recognized to some extent; for example, the thinner vegetative cover of southern Italy and Sicily, resulting from their drier climates, is obvious. However, seasonal changes cause confusing patterns because not all the images were acquired at the same time of year. Note the broad red patch trending southwest across the peninsula just north of Rome (*K*). This is not a belt of unusually lush forest, but a series of images acquired during the spring or summer.



PLATE 242

PLATE 243



SICILY: The southern part of the largest island in the Mediterranean is well displayed here. This region of Sicily is underlain chiefly by volcanic rocks, and like the rest of the island, is generally hilly or mountainous, with level terrain found only along the coast; the Plain of Catania (*R*–6) is the largest level area. Snow-covered Mount Etna (*P*–2), 3180 meters (10 958 feet) high, dominates the island topographically. Climatically, the southern part of Sicily is more like North Africa than typical Mediterranean lands, being considerably drier and warmer. Much of the vegetation is desertlike, but irrigated areas make Sicily Italy's main citrus producer. Considerable wheat is also grown in the central part of the island. All the main cities are along the coast; Catania (*R*–6) is the largest one in this view. The city of Syracuse (*U*–10) should also be mentioned for its historical importance. Syracuse was founded by Greeks in the year 733 B.C., and was for some time the greatest city of Sicily. It was during the siege of Sicily by the Romans in 212 B.C. that Archimedes was killed by a soldier, supposedly because he would not leave his mathematical calculations for safety elsewhere.

The geology of Sicily is related to that of northwest Africa and the Italian peninsula, both being part of the great Alpine orogenic belt marked by intense Cenozoic folding, overthrusting, and local volcanic activity. Rocks in the western part of the area shown here are chiefly sedimentary Cenozoic carbonates that have been overthrust toward the south. The southeastern corner *(lower right)* of Sicily, however, is composed largely of volcanic rocks with a distinctive topography. Those of the Iblean Mountains (*P*–11) are the youngest, being Pleistocene. Mount Etna is one of the world's greatest volcanoes and has been extensively studied. It is almost continuously active and, being easily accessible, has served as a working model of still-erupting volcanoes. Innumerable measurements have been made of its escaping gases, lavas, and pyroclastics. The volcanic rocks are intermediate in composition between basalt, andesite, and phonolite. *1106–09130;* November 6, 1972.

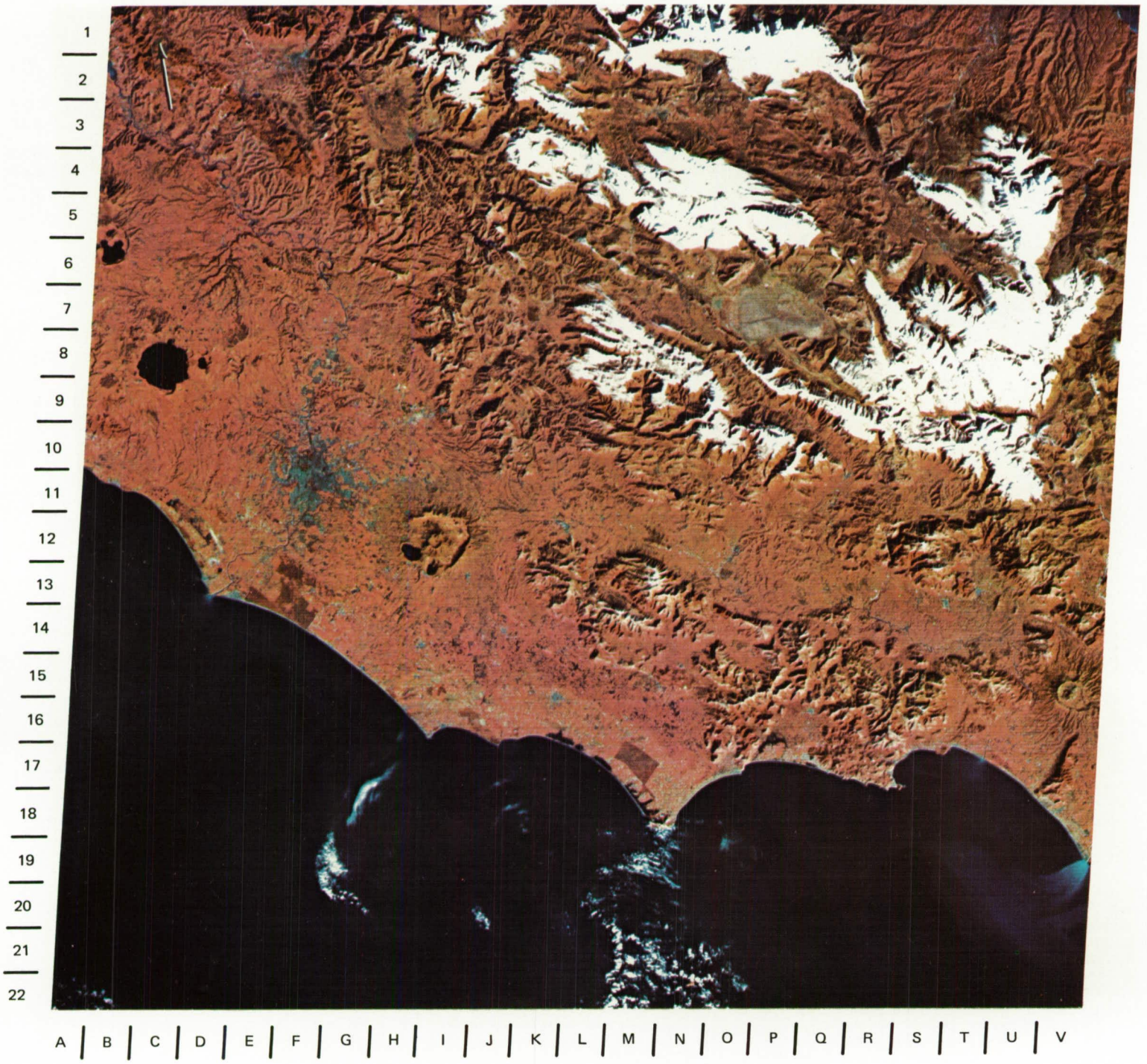


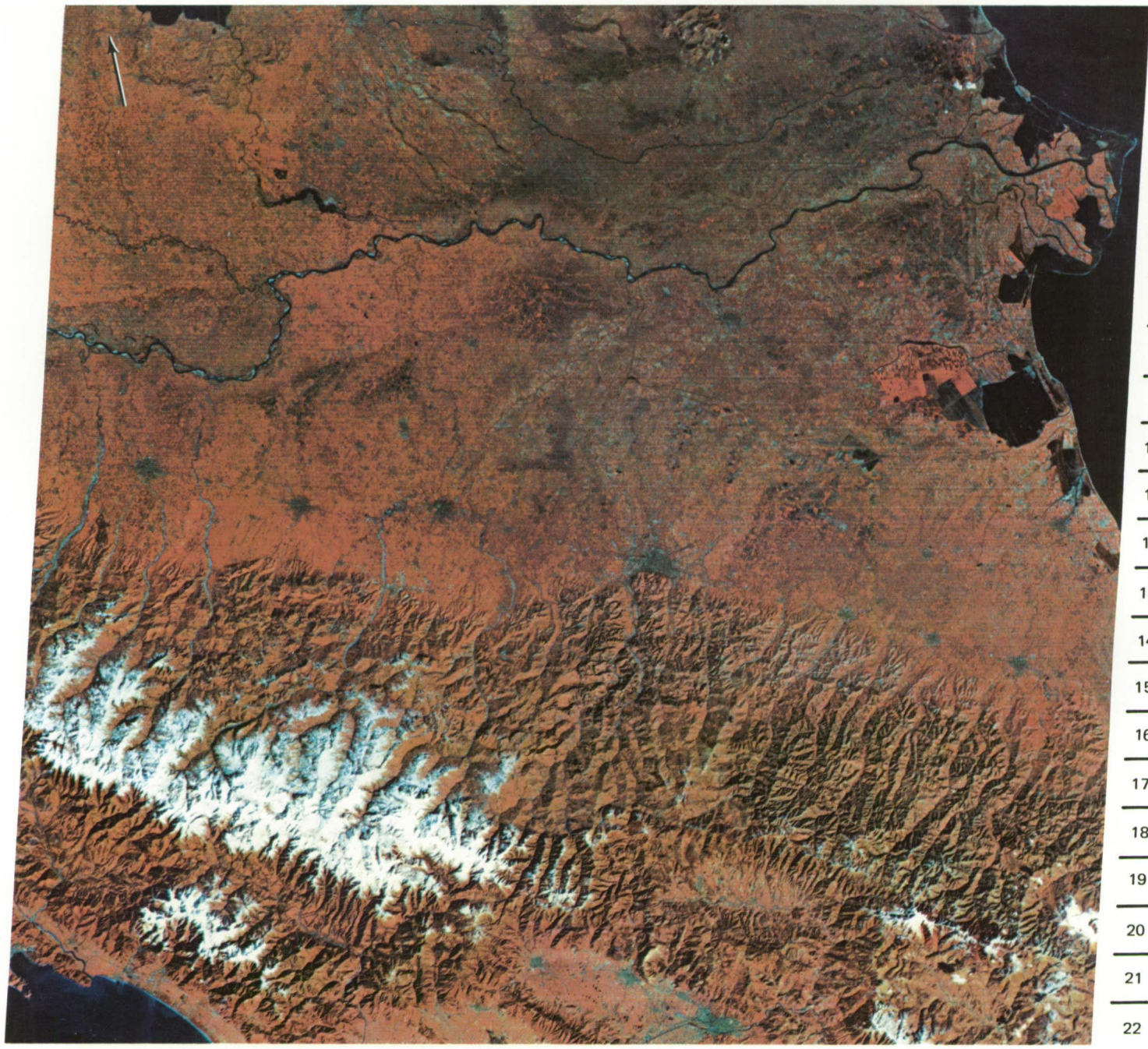
PLATE 244

ROME: The center of western civilization for thousands of years is shown in this view of Rome (*E*–10) and central Italy. The western coast on the Tyrrhenian Sea as far south as the Gulf of Gaeta is depicted, while the upper right corner of the image just reaches the Adriatic Sea. The central Apennine Mountains are partly snow covered in this winter image. Most of the population and farms in this area are in the low-lying coastal plain, which includes well-known landmarks such as the Pontine Marshes (*M*–16); the dark rectangle at *M*–17 is Circeo National Park.

Innumerable historic sites are in this area, though not necessarily evident at this scale; a few include Anzio (*I*–16), the Appian Way (*F*–13), Cassino (*Q*–12), and Castel Gandolfo (*H*–12). The many landmarks in Rome itself cannot be resolved, except for the Tiber River.

Many geological features are strikingly shown. Most prominent are the Apennines, young, active mountains forming a small part of the Alpine chain reaching from Indonesia to the Atlantic Ocean. This chain has many branches in central Europe and the Mediterranean region. All are essentially Cenozoic in age, and are constructed of innumerable folds and faults. The general trend of folding here is northwest to southeast. The most spectacular geologic structures visible in this image are the volcanoes lying between the Apennines and the Tyrrhenian Sea. Some, like the Sabatini volcano, are occupied by lakes such as Lago di Bracciano (*B*–8). All the volcanoes shown here are extinct, although geologically young. Those to the southeast, just out of the image, are more active; Vesuvius is the best known example. These volcanoes are generally in the caldera stage, having very wide craters. The Latian volcano (*H*–12), partly filled by Lago Albano, on whose shore Castel Gandolfo is located, is a classic example. Some of these calderas resemble lunar craters to some extent and have figured in the debate about crater origins over the years. Like many calderas, these tend to have lavas and pyroclastic deposits relatively high in alkali and silica content. Because of the greater viscosity and gas content of such magmas, eruptions from calderas tend to be explosive, producing volcanic ash, rather than the quieter eruptions of basaltic volcanoes. *1198–19232;* February 6, 1973.

PLATE 245



PO VALLEY: The North Italian Plain of Italy, the eastern part of which is covered here, is both the main farming area of the country and its industrial heart. Reasons for this are visible in the image: level terrain and abundant water supply. The Alps, north of this area, feed many rivers, in particular the Po (*A*–7; *U*–4), whose distinctive delta is well shown (*U*–4). The area is dotted with industrial cities; the chain along the foot of the Apennines (at the bottom of the image) is especially prominent: Bologna (*M*–12), Modena (*I*–11), Reggio (*F*–11), and Parma (*C*–10). Textiles are most important, followed by food processing. The area has long been a source bed of western art, especially since the Renaissance.

The northern plains are Italy's most productive farming region because of climate, terrain, and water supply. Corn, wheat, and rice are especially important in this area; the Po delta is a major rice-producing district. Cattle raising is concentrated here because of the availability of good meadowland.

Physiographically, the area covered here is largely alluvial plains, underlain by marine sediments and great thicknesses of sediments derived from the Alps and Apennines. Considerable natural gas is produced from these rocks. The northern Apennines (*A*–15; *V*–21), whose structure was produced by Cenozoic deformation, is composed of eugeosynclinal rocks: dark sandstones, volcanics, and ophiolites (iron-rich volcanic rocks and serpentine found in the core of folded mountains, thought to have originated in oceanic spreading centers). Sea-floor spreading and subduction eventually brought the ophiolites to their present position in some fashion. The main direction of subduction and folding in this area was from lower left to upper right; i.e., from the Ligurian Sea (*B*–21) inland. *1218–09341;* February 26, 1973.

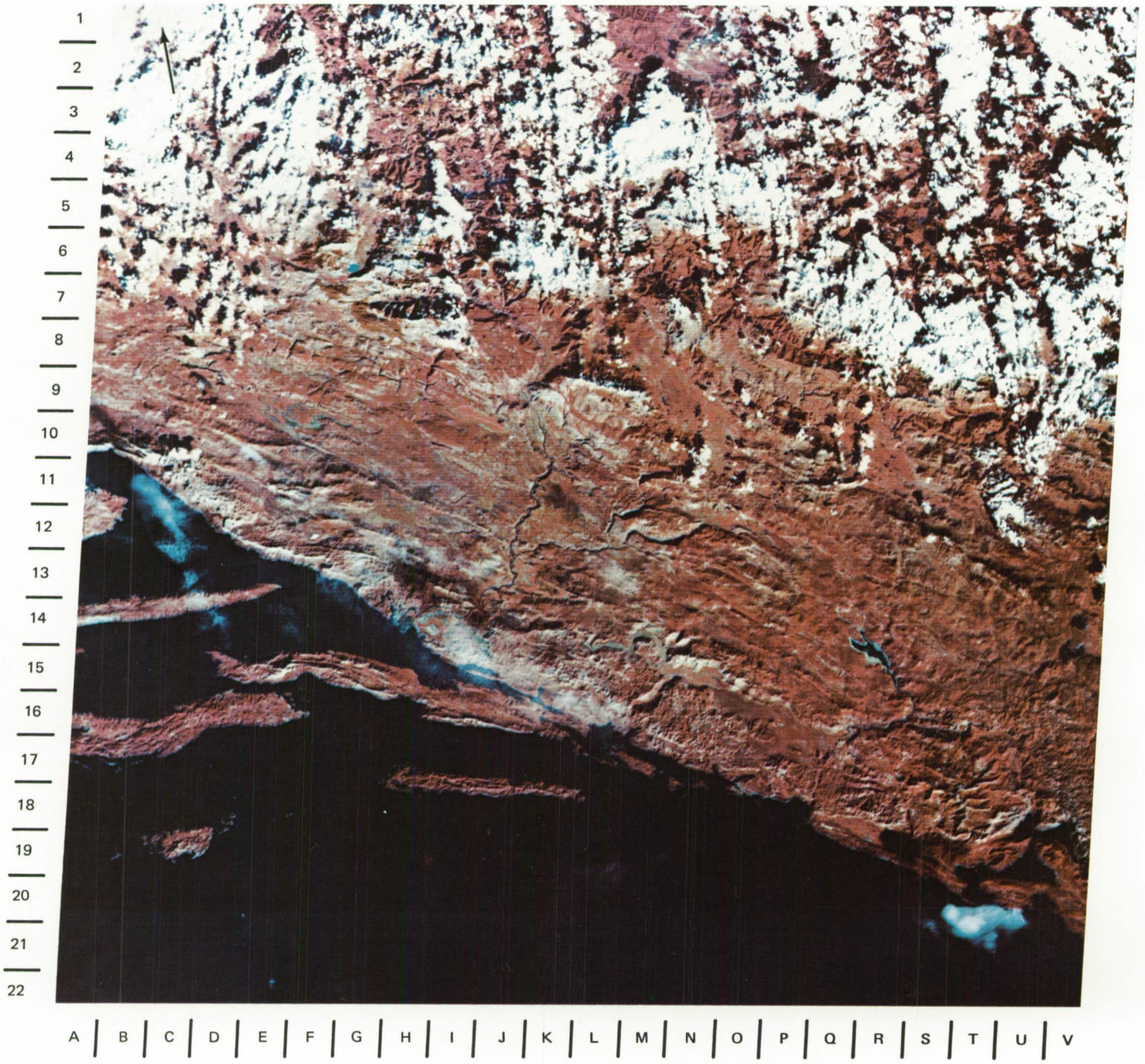


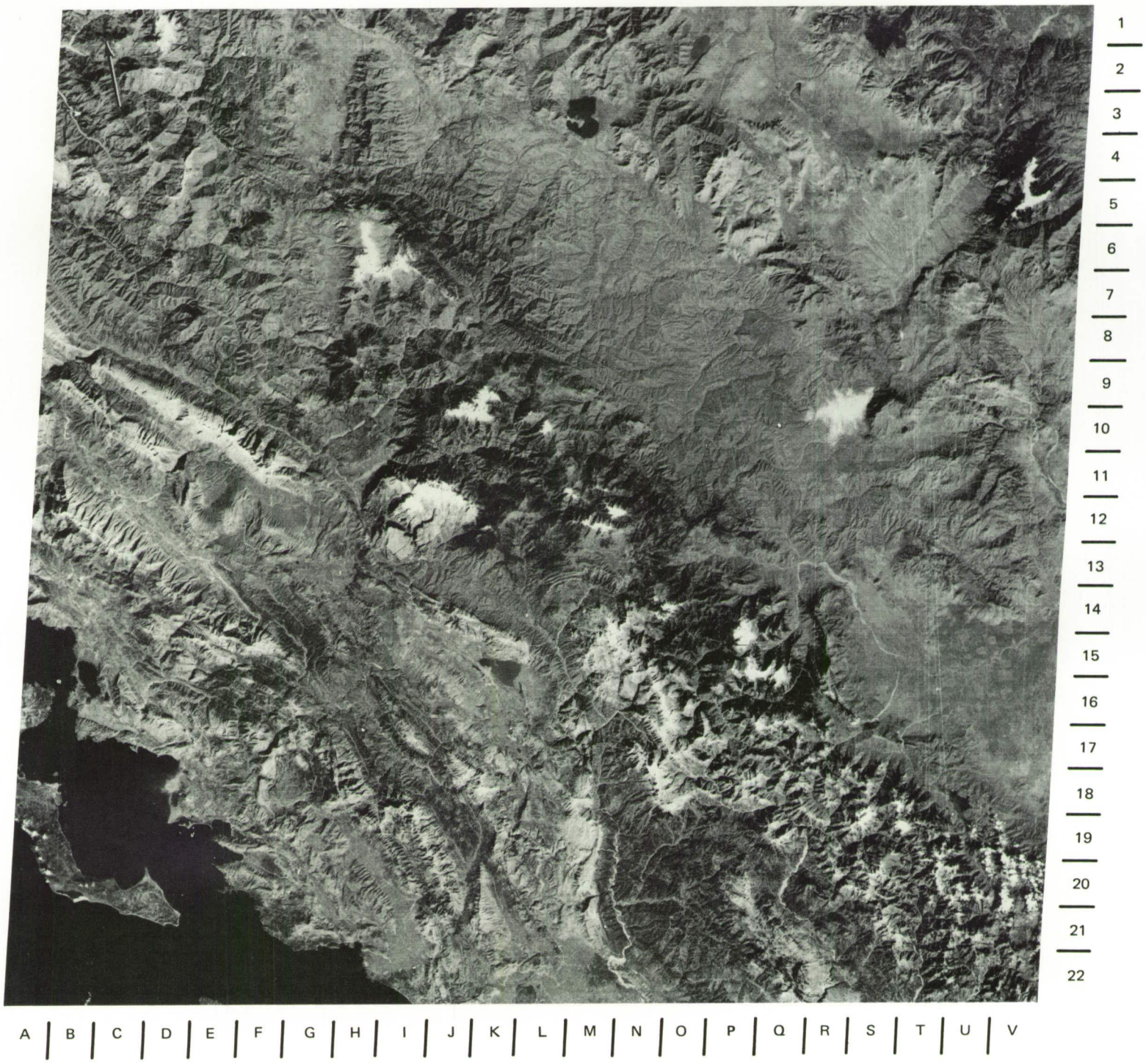
PLATE 246

THE DALMATIAN COAST OF YUGOSLAVIA: This scene includes parts of Bosnia and Hercegovina (*F*–5), Croatia (*Q*–14), and Montenegro (*T*–15), administrative republics of present-day Yugoslavia in the Balkans. The old town of Dubrovnik (*O*–17), now one of the most popular resort spots on the Adriatic Sea (*G*–20), lies midway between the Bay of Kotor (*U*–19) and the Neretva River (*J*–11). The city of Sarajevo, scene of the assassination of Archduke Ferdinand of Austria that triggered World War I, appears at *M*–1.

The narrow coast, with its typical Mediterranean climate, here supports growth of olive, citrus, and fig trees and grape vineyards. Some grain crops are cultivated along the coast and further inland. The mountains, which rise to 1800 to 2400 meters (6000 to 8000 feet), show numerous bare rock ledges and cliffs (*N*–15) where not covered with grasses and scrub vegetation.

These mountains are part of the Dinaric Alps, a southeastern extension of the main Alpine belt, which joins the Pindus Mountains to the south. The segments that trend northwest here are complexly folded sedimentary rocks of Cretaceous and Eocene age near the coast and older Triassic and Jurassic age in the interior. The folding reached its climax in the late Tertiary even as the Adriatic began to sink rapidly as a subsidence basin. During this phase of uplift, sedimentary rocks along the flank of the rising crest broke loose in detached blocks along a series of faults and moved, under gravity, southwestward into the basin. The islands of Brac (*A*–12), Hvar (*B*–13), and Korcula (*B*–16) are examples of this gravity sliding. Limestones are by far the most abundant rock type in the Dinaric Alps. These carbonates are easily attacked by chemical solution, bringing about the distinctive karst topography marked by caves, sinkholes, underground rivers, and valleys formed by roof collapse. *1465–09030;* October 31, 1973.

PLATE 247



ALBANIA AND GREECE: This image portrays the border between Greece *(right)* and Albania *(upper left)* from its beginning in the Adriatic Sea just east of the island of Corfu (*A*–18), itself in Greece. The border trends northeast, leaving the image just north of Kastoria. Most of the area covered by the image is in Greece, but the predominantly mountainous physiography of Albania is well illustrated. These snow-capped mountains, with elevations up to 2600 meters (8600 feet), are part of the Alpine system of Cenozoic age; the local names in Greece are the Pindus Mountains and in Albania, the Albanian Epirus region. The main rock type is limestone. Structurally, the area is one of intense folding and overthrusting, the direction of compression being from the northeast toward the Adriatic Sea. The ranges at extreme upper right include iron and magnesium-rich volcanic assemblages (ophiolite complexes) typically found in the cores of folded mountain belts. These complexes have been interpreted as the beginning of oceanization (i.e., crustal foundering) or as relics of sea-floor spreading centers now incorporated in mountain chains.

The mountains of the Epirus region are still well forested, unlike most Greek mountains. The area is chiefly used for livestock raising, in particular goats and sheep. In addition to being mountainous, the area is poorly suited for farming because the widespread limestone bedrock permits immediate infiltration of rainwater. The region is thus sparsely settled and somewhat isolated.

The recent history of the Albania-Greece border has been a turbulent one, with the area shown by this image being the scene of heavy fighting early in World War II, and of irregular warfare in the early postwar years. *1102–08491;* November 2, 1972.

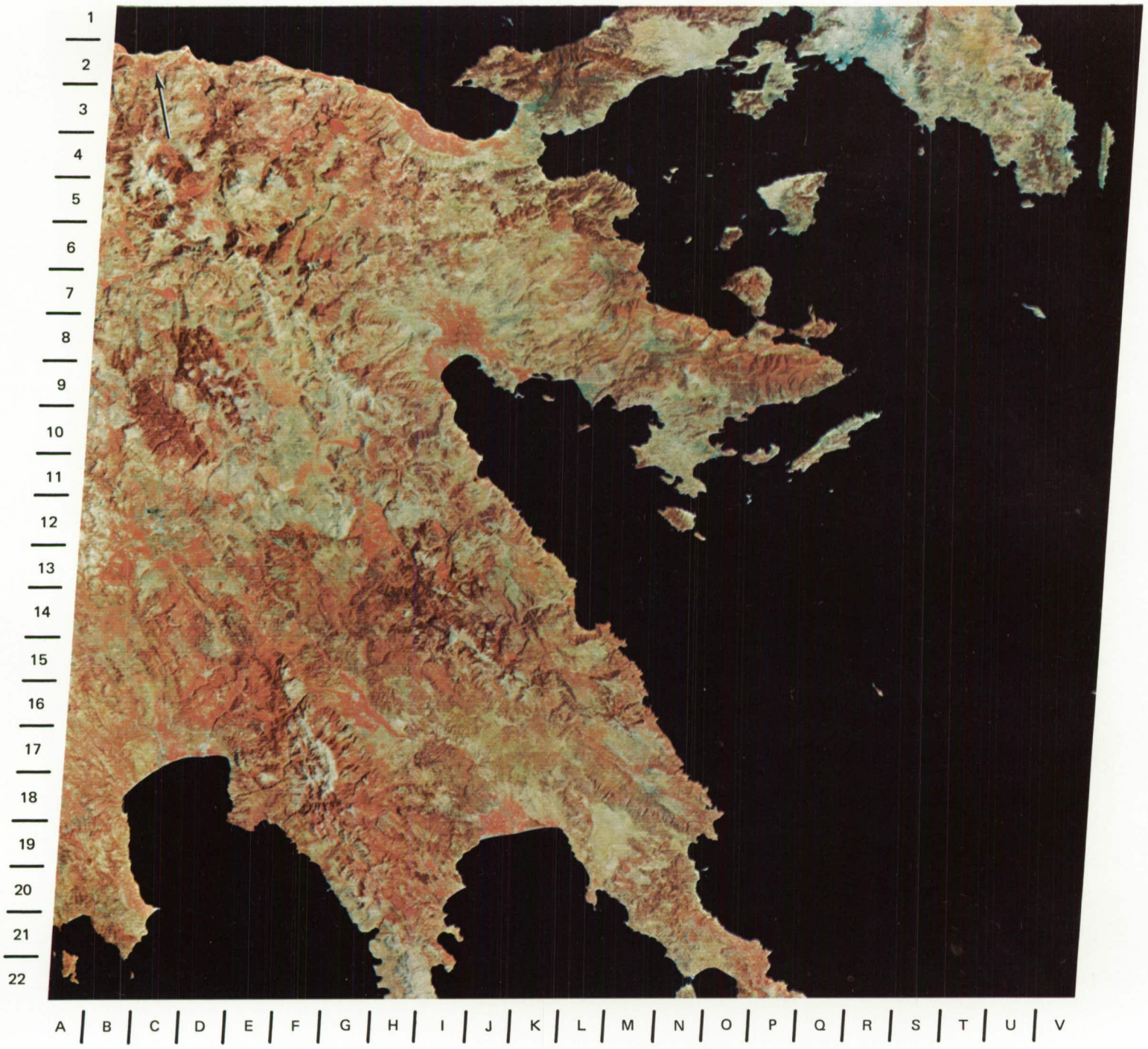


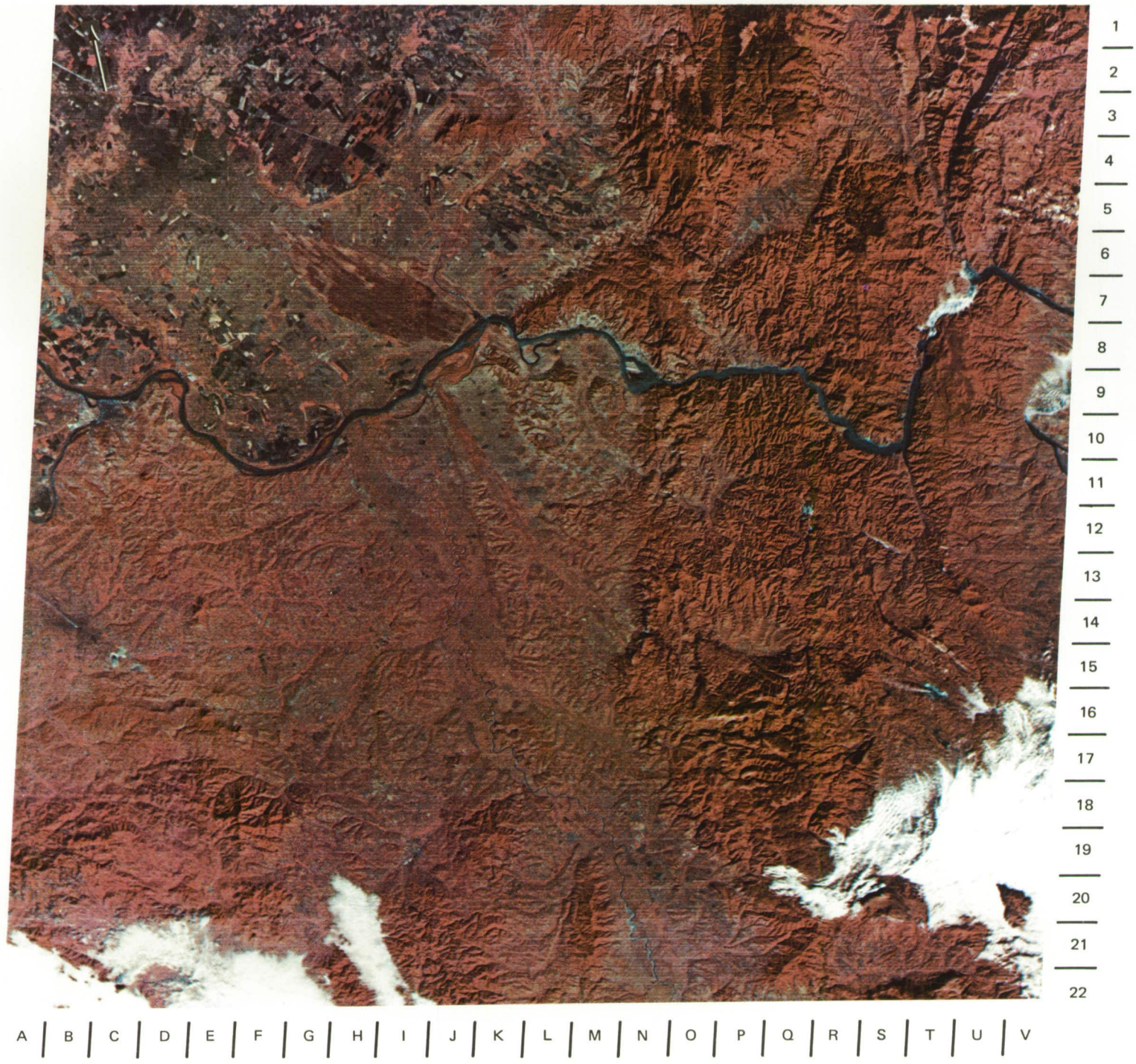
PLATE 248

ATHENS: The Peloponnesus of Greece was once thought to be an island, and as this Landsat image shows, nearly is, being connected to the mainland only by a narrow isthmus (*I*–3). This isthmus is now breached by the Corinth Canal; before the canal was built, ships were actually hauled across the isthmus to avoid the much longer sea route around the Peloponnesean Peninsula. Attica is partly included in the picture at upper right; Athens (*Q*–1) and its port, Piraeus, are visible (*P*–2). The island of Hydra is at *P*–10.

The natural scenery of Greece is well illustrated here. The land is mountainous, being part of the Alpine chain, with very little of the area included in this view being level enough for easy cultivation. What farming areas there are can be seen along the shores of the Gulf of Corinth (*A*–1 to *H*–3), a major currant raising region (the word "currant" is in fact derived from "Corinth"), and in a few coastal strips. The climate in this part of Greece is typically Mediterranean, and the crops mirror this fact, consisting largely of fruits (oranges, figs, and grapes). The mountains have largely been deforested by man and are now largely covered with scrub. These areas are useful chiefly for raising sheep and goats. One of the main problems faced by agriculture in southern Greece is lack of dependable, year-round rain. This is aggravated by a geologic factor, the predominance of limestone, in that the porous rock permits rain to sink in quickly.

The northwest to southeast trend of the coast visible here reflects the trend of the Alpine fold axes. This area is one of Cenozoic folding. It is undergoing active tectonism today, as indicated by the many earthquakes. The coastline is mostly one of submergence, and the region (especially the Aegean Sea to the northeast) is generally considered to be one of crustal subsidence. *1010–08375;* August 2, 1972.

PLATE 249



YUGOSLAVIA AND RUMANIA: The strategic position of Belgrade (*B*–9), Yugoslavia's capital, at the junction of the Danube and Sava Rivers is well shown in this image. The Danube itself, flowing eastward, dominates the image and forms the border between Yugoslavia and Rumania east of *L*–8. The sinuous Morava River is visible at *H*–10. Although the area covered here (especially the northwest part) is well populated, other cities are difficult to resolve.

This Landsat image gives some idea of the diversity of Yugoslavia's topography. Most of the country is mountainous, lying in the Dinaric Alps (a branch of the Alpine chain paralleling the Adriatic Sea). The area shown here includes three main physiographic divisions. The lower left section, with altitudes of 3000 to 4600 meters (1000 to 1500 feet), is part of the Dinaric Alps. Separated from them by the valley of the Morava River are the Hellenides, a branch of the Alpine chain trending northwest from Greece and grading into the Carpathian Mountains, whose western end is at the extreme upper right. These mountains also are not very high, despite their geologic youth, with altitudes of 370 to 600 meters (1200 to 2000 feet) in this area. Some of the physiographic features are obviously of tectonic origin, or at least show tectonic influence; note the linear valley at *P*–7; *Q*–4, almost certainly eroded along a fault. At upper left is the southern end of the Danube plain, a large basin shared by Yugoslavia, Rumania, and Hungary. As the field pattern suggests, this is Yugoslavia's main granary, producing corn, wheat, sugar beets, tobacco, and grapes from chernozem loessal soils.

The climate and vegetation of the area covered here are essentially European rather than Mediterranean, although Yugoslavia is geographically a Mediterranean country. High areas are covered with mixed deciduous and evergreen forest, and winters are like those of central Europe. As the image suggests, Yugoslavia is a composite country physiographically, a fact that helps to account for its broad cultural diversity. It consists of six republics, unified after World War I, with two alphabets and several languages and religions. The area of Yugoslavia covered here is in Serbia. *1463–08511;* October 29, 1973.

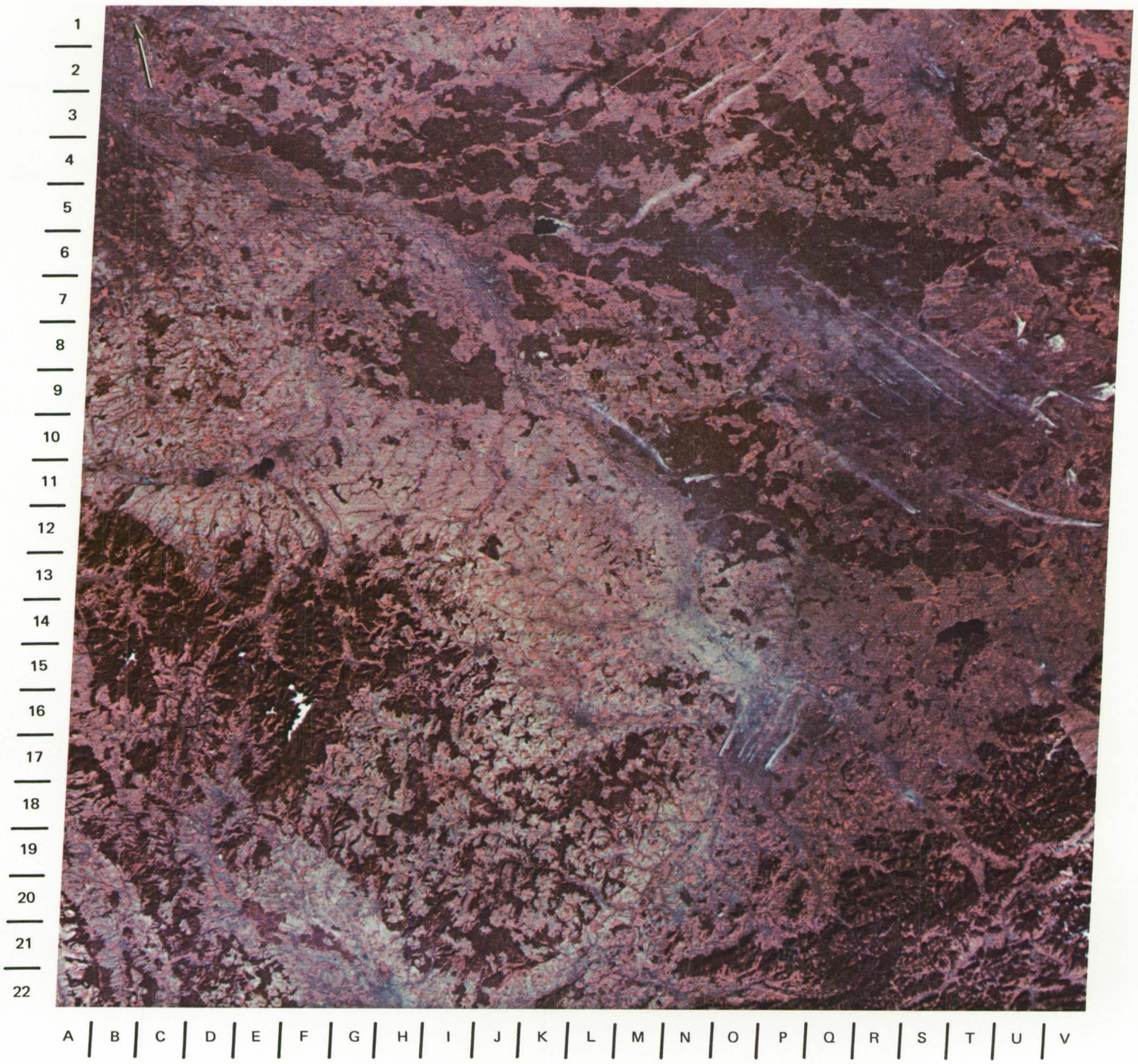
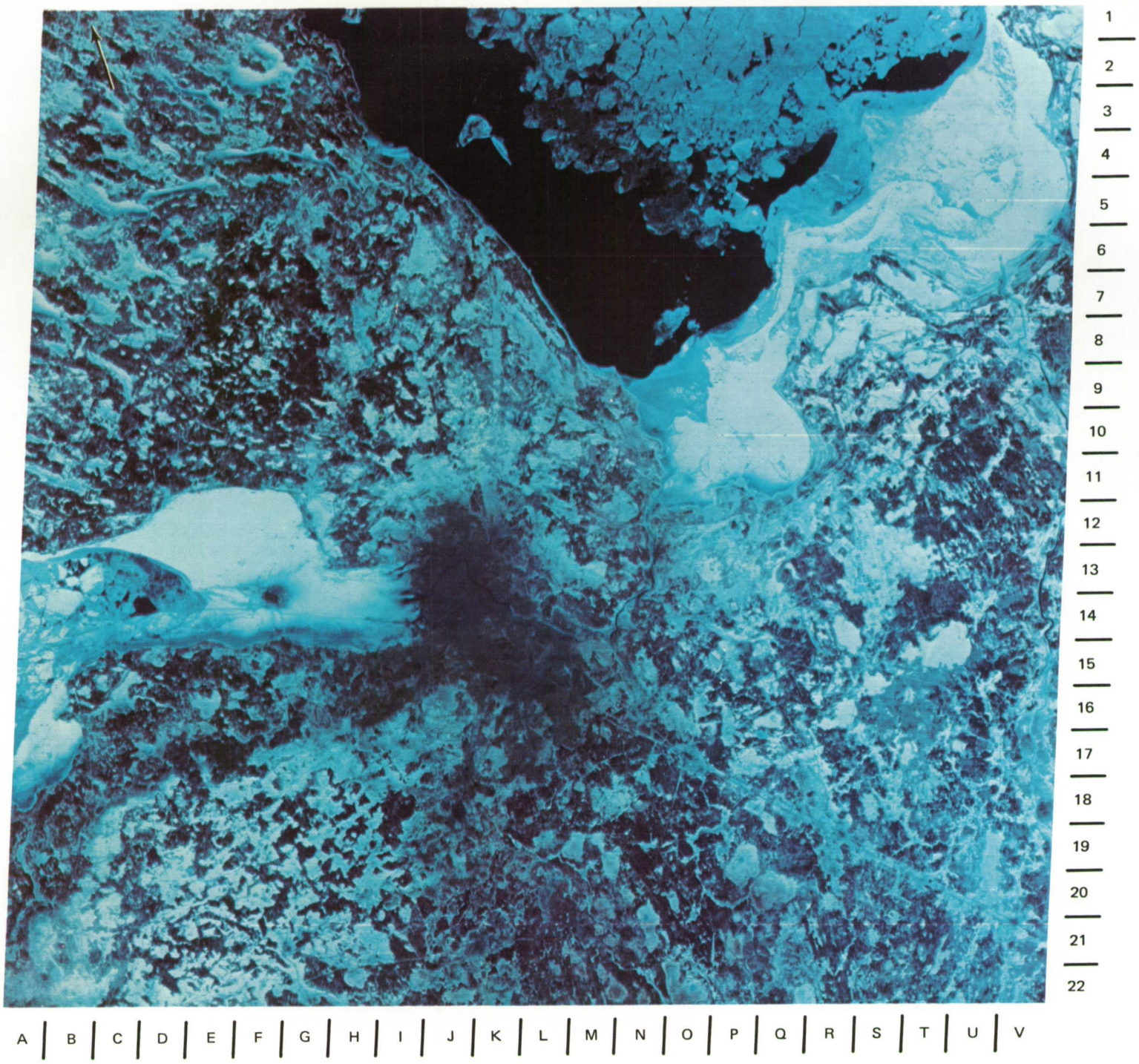


PLATE 250

MIDDLE EUROPE: Part of Bohemia (*C*–18) in central Czechoslovakia and the plains of Silesia (*D*–6) in southern Poland are seen in this image. The Czechoslovakian section is in Moravia east of the city of Brno (off the image at *A*–22). Included here is the northeastern front of the Bohemian Massif, a great block of crystalline basement and infolded sedimentary rocks that was part of the Hercynian belt deformed near the close of the Paleozoic. The present mountains, known locally as the Jesenicky, attain elevations of 1200 to 1500 meters (4000 to 5000 feet) in a section *B*–13 underlain by Archean crystalline rocks. Carboniferous rocks (*C*–20; *I*–18) make up lower hills on either side of the Morava River (*F*–20). To the southeast in Slovakia are the East Beskids (*R*–20), folded Cretaceous rocks that form part of the westernmost Carpathian Mountains. The Odra (or Oder) River, which eventually flows into the Baltic, begins above the valley (*M*–19) between these two mountain groups and swings past the Czech industrial city of Ostrava (*O*–17) and thence northwestward across the plains in Poland past Opole (*I*–6) and Brzeg (*D*–5) toward Wroclaw (Breslau) (off the image near *A*–2). The headwaters of the Wisla (or Vistula) River east of Ostrava are dammed at a reservoir (*T*–14) in Poland; this river flows past Krakow (about 32 kilometers (20 miles) off the image at *V*–13) and eventually Warsaw to the north. Cenozoic and Pleistocene sediments underlie most of the plains along and west of the Odra. East of the river is a broad belt of Carboniferous rocks around the vast industrial complex (*Q*–9; *U*–9) containing the cities of Gliwice, Bytom, Katowice, and Chorzów. This is a major center of coal mining in middle Europe that has fostered production of steel in the same area. Triassic rocks outcrop further to the north and Jurassic rocks are found around the city of Czestochowa (*R*–2).

The scene records a noteworthy phenomenon. Winds from the southwest carry smoke from the stacks at Ostrava northeastward (perhaps controlled by the valley behind it), but a shift in winds on the Polish plains directs smoke from the factories to the northwest (*Q*–9; *U*–9). The white streaks west of Czestochowa appear to be clouds and/or airplane contrails. *1467–09123;* November 2, 1973.

PLATE 251



LENINGRAD: The city of Leningrad (*J*–13) is the focal point of this image; other cities visible include Kronshtadt (*F*–13), on an island in the ice-clogged Gulf of Finland, and Gatchina (*J*–20). The Karelian Isthmus (*A*–1; *J*–10), once part of Finland, is bounded on the east by Lake Ladoga (*M*–4). Leningrad is a major Russian port, but only with difficulty, because the Baltic Sea and the Gulf of Finland (*C*–13) are frozen over several months of the year, as late as April (this image was taken in late March 1973). The Soviets have, therefore, become very proficient at ice breaking, and channels cut in the ice can be seen even from 920 kilometers' (570 miles') altitude (*E*–13; *H*–14).

Turning to the natural features of the scene, which is largely blanketed by snow, the region lies at the east margin of the Fennoscandian shield. The area at upper left is Precambrian rock, mantled by glacial debris, and at lower right (southeast of Leningrad) is the edge of the Russian platform, covered by relatively thin, flat-lying lower Paleozoic rock. The entire area was glaciated during the Pleistocene, accounting for the complex land pattern and the many lakes. An interesting postglacial effect can be seen in the linear features concentric with the shore of Lake Ladoga at *Q*–6 and *U*–10. These may be emerged beaches or abandoned shorelines caused by the isostatic rebound of the crust following disappearance of the glaciers some 12 000 years ago. *1246–08435;* March 26, 1973.

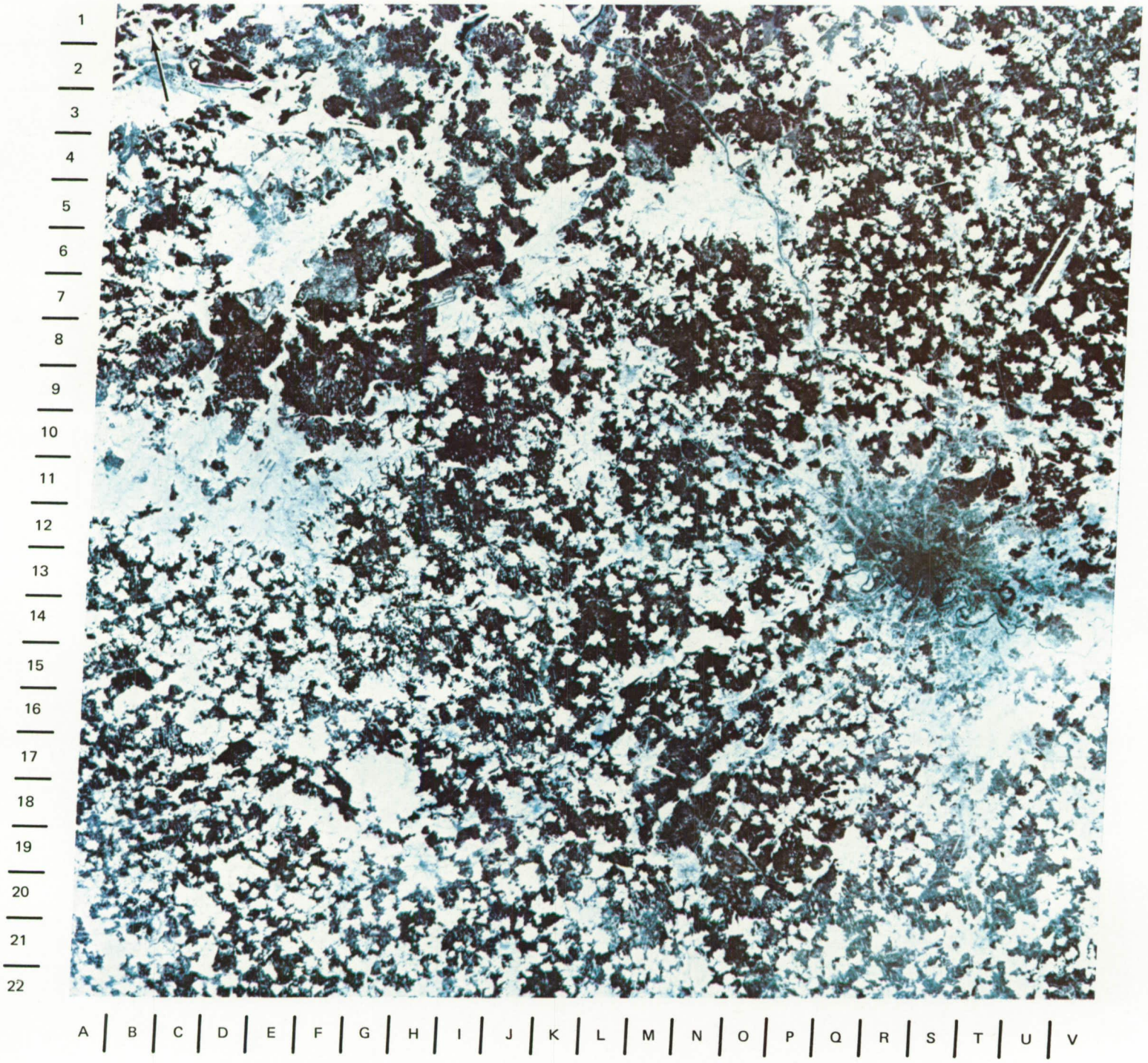


PLATE 252

MOSCOW: This striking midwinter scene shows the modern capital of the Soviet Union surrounded by heavy snows in much the same way as Napoleon must have witnessed it during his ill-fated attack in 1812. The many dark patches spread across the countryside are copses of evergreen forests intermixed with deciduous trees. Elsewhere, snow covers open fields cleared for agriculture that includes cultivation of oats and rye for food, flax for fabric, and feed for dairy cattle.

Moscow itself stands out in dark tones because it is a "heat island" in which man's activities have removed or melted the snow. This great city of 6½ million people is now the political, financial, cultural, and manufacturing center of the Soviet Union. The Moskva (Moscow) River (*U*–14) flows eastward through the heart of Moscow. To the north, the manmade Moscow Canal (*O*–5) runs for 130 kilometers (80 miles) before connecting with one of the lakes along the headwaters of the Volga River (*C*–2). This great stream continues for hundreds of kilometers to the east and then swings southward to empty into the Caspian Sea. *1582–08052;* February 25, 1974.

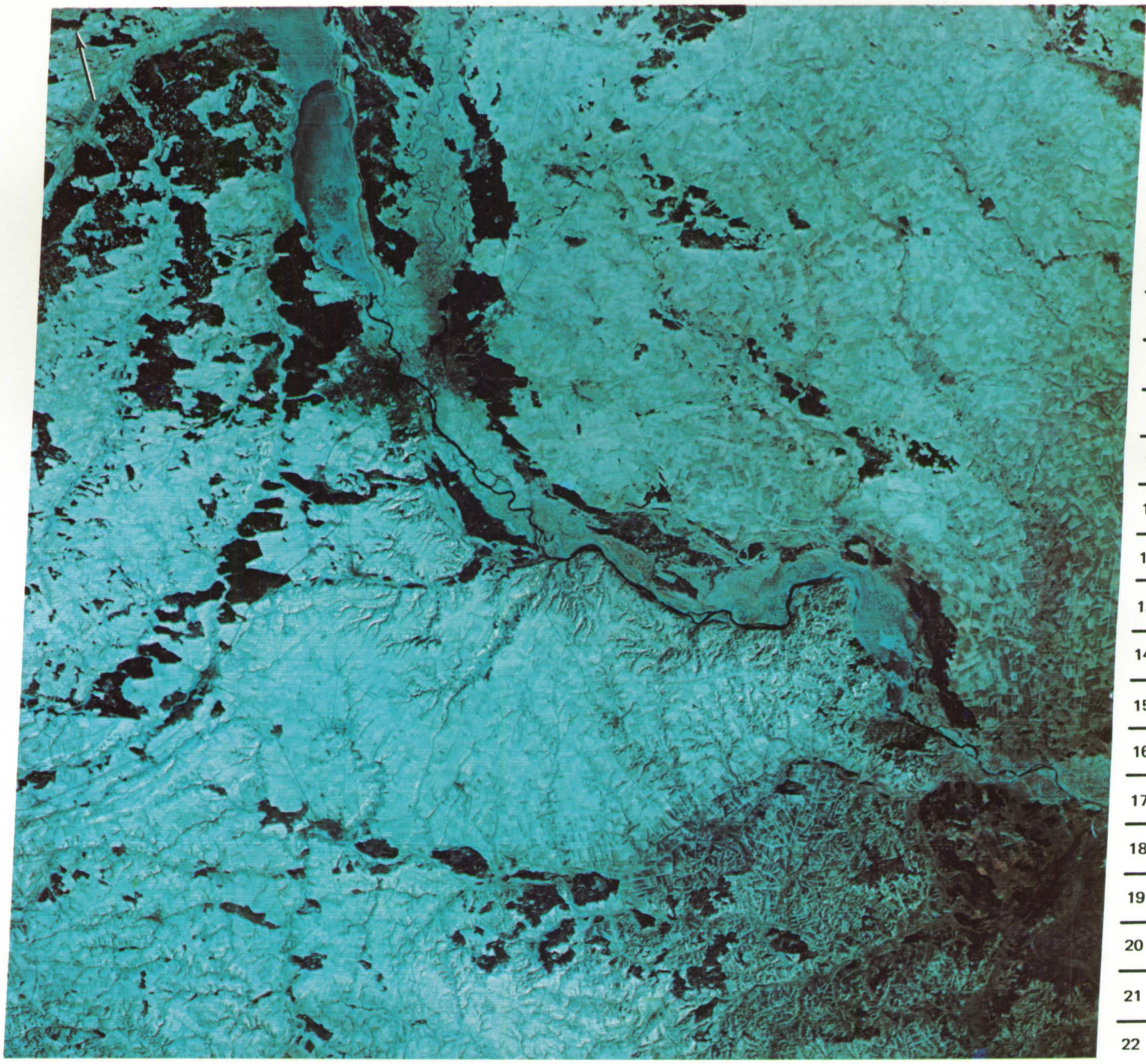


PLATE 253

THE UKRAINE: This view of the Soviet Ukraine around the Dnieper River (*J*–10) shows the remarkable detail possible in Landsat imagery obtainable because of the dual enhancement effects of low Sun angle (13°) and a broad "dusting" by snowfall. Especially notable are the many roads and farm boundaries in the rural areas and the intricate gulleying done by right bank tributaries to the Dnieper.

The region is subdivided into the Dnieper Lowlands (*R*–4), northeast of the river (underlain by Oligocene sedimentary rocks), the Dnieper flood plain (with terraced Quaternary alluvium and occasional outcrops of Paleocene and Eocene rocks along the bluffs), and the Dnieper Uplands or Plateau (*I*–16), southwest of the river (whose bedrock is mostly Miocene sediments but with older Tertiary sediments exposed by streams near the Dnieper and scattered exhumed Precambrian crystalline rocks (eastern edge of the Bug Massif) revealed further upstream in the Ross (*I*–18), Rostovitso (*E*–18), and Irpen (*B*–16) tributaries). During the Pleistocene, the southernmost ice lobe in Europe extended approximately to the present course of the Dnieper in this image. The Desna (*H*–3) and Supoy (*T*–10) Rivers now flow over thin glacial tills in the lowlands. Loess deposits mantle this area and the uplands to the south.

Kiev (*H*–8) is the capital of the Ukraine and a major transportation hub, as indicated by the radiating network of roads and rail lines emanating from it. Smaller urban areas also stand out as dark patches in the snow: Fastov (*D*–14), Belaya Tserkov (*G*–17), and Borispol (*L*–8). Water for the region is stored in the Kievskoye (*F*–4) and Kanevskoye (*R*–14) Reservoirs along the Dnieper. Agriculture is the principal activity of the Ukraine, with wheat as the main crop, along with rye, barley, oats, millet, corn, sugar beets, flax, and hemp. The region falls within the forest steppe zone of the European Soviet Union; the dark patches are groves of hornbeam (a member of the birch family) and oak, with maple, ash, and spruce also present. *1530–08200;* January 4, 1974.

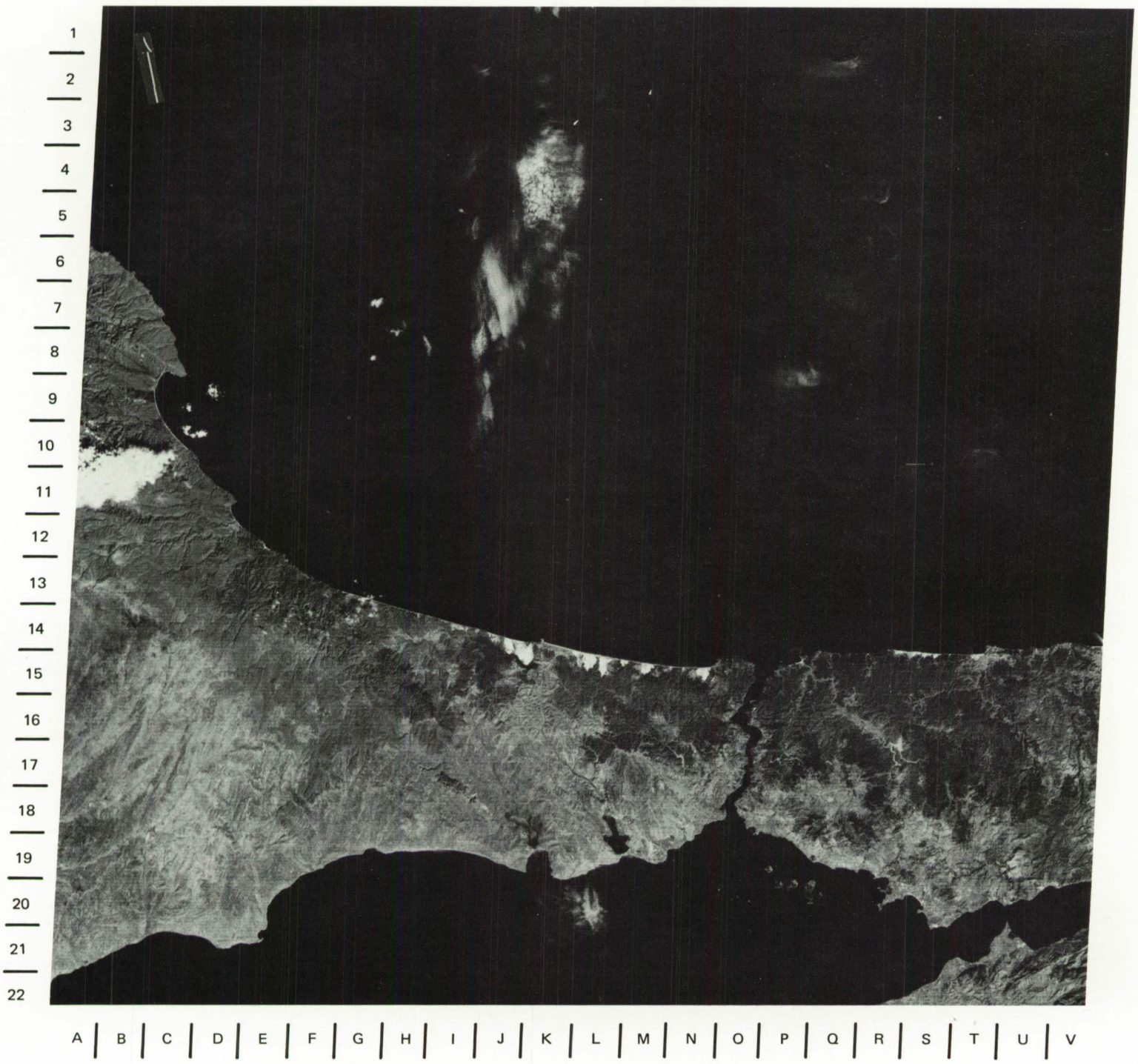


PLATE 254

BOSPORUS, TURKEY: Few Landsat images show the junction of two continents, as does this one of the Bosporus, which is the traditional boundary between Europe *(left)* and Asia *(right)*. The boundary is obviously a human one only, the physiographic continuity of the region being evident. The Black Sea is to the north; the Bosporus (*Q*–15) connects it to the Sea of Marmara to the south. Istanbul is at the south end of the Bosporus (*O*–18). The narrow body of water at right (*U*–20) is the Gulf of Izmit.

The Bosporus is the only water outlet to the Black Sea; the strategic importance of it and the Dardanelles (at the other end of the Sea of Marmara) is strongly suggested by this image. The central location of Istanbul, formerly Constantinople, at the junction of two continents and two seas is also shown. The border with Bulgaria is at the extreme upper left, at *A*–5.

This part of Turkey (the Marmara Lowlands) has a mild though not truly Mediterranean climate, with moderate rain. Consequently, it is an important farming area, unlike much of the Anatolian Plateau, which is in many places too dry for reliable farming. The basin of the Ergene River (*D*–17) is especially productive; tobacco, corn, hemp, sunflowers, and plums are raised. The dark areas fringing the Black Sea are forested hills, between 300 and 600 meters (1000 and 2000 feet) in height on the average. The white areas at *J*–14 and *L*–14 are sand dunes along the Black Sea coast. *1115–08201;* November 15, 1972.

PLATE 255



ARMENIA, TURKEY: The Armenian Highlands in eastern Turkey are a central plateau of rugged dissected mountains that represent an eastward extension of the Taurus Mountains. The Taurus Mountains form part of a vast belt connecting the Mediterranean Alpine zone with the mountains in eastern Asia Minor, to the west grading into the Pontus Mountains along the Black Sea and into the Pindus Mountains and Dinaric Alps of Greece and Yugoslavia. To the east the two Turkish systems join near Mount Ararat in eastern Armenia and then southeastward into Iran along the Zagros and Elburz chains. The physiography of the Taurus Mountains reflects their complex history. That history is still in the making, as evidenced by the shallow and deep focus earthquakes occurring in a zone parallel to the trend of the mountains. A prominent southwest-trending fault is visible between *Q*–13 and *H*–21, passing through Lake Hazar (*N*–15). A strong earthquake occurred along this fault in 1971, with 20 centimeters (8 inches) of left-lateral displacement.

Because of the rugged terrain, this part of Turkey is relatively inaccessible and lightly populated. The only major city in this scene is Malatya (*C*–18) (population about 110 000), situated at the edge of a plain south of the Firat River, which becomes the Euphrates after entering Syria. The headwaters include the Peri and Murat (*I*–10) Rivers. Melt waters are also introduced from the snow-covered Munzur Silsilesi Range (*A*–3), which reaches elevations above 3400 meters (11 000 feet). Seminomadic herding is practiced throughout the region. Rice, cotton, and fruit are grown around Malatya and Elazig (*M*–13) north of Lake Hazar. *1485–07323;* November 20, 1973.

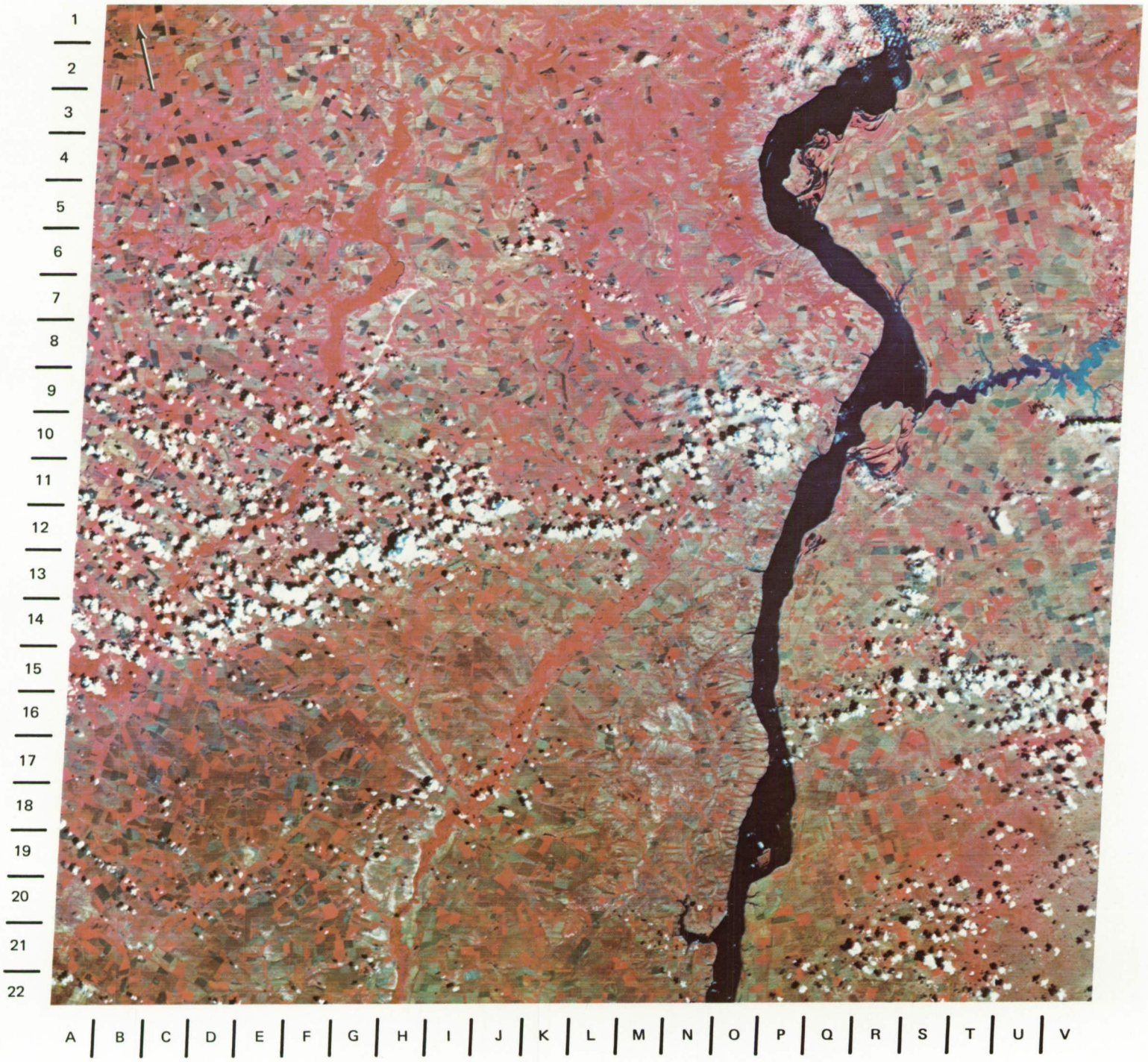


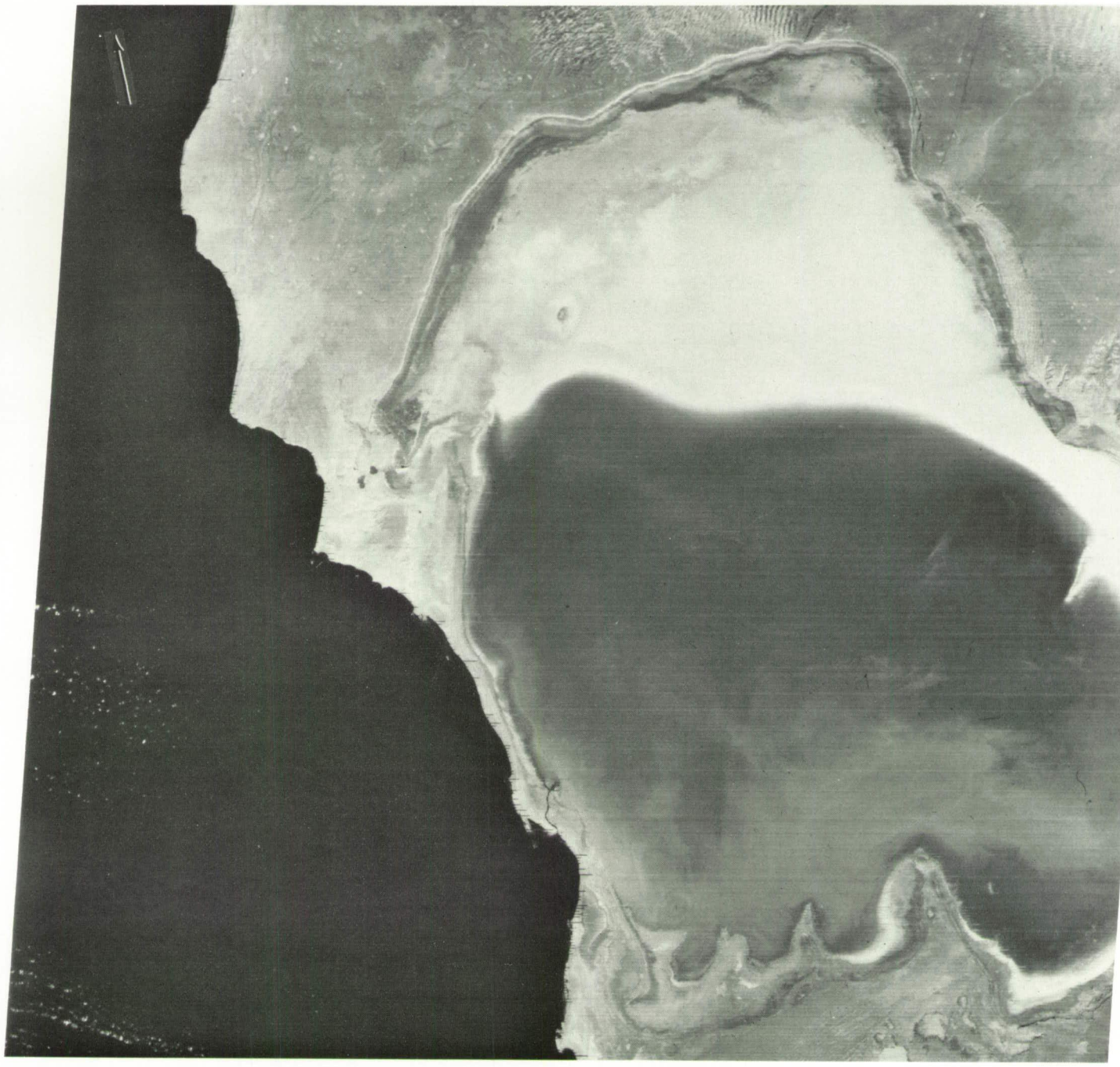
PLATE 256

THE LOWER VOLGA: This great river, which begins west of Moscow, flows southwestward for more than 1600 kilometers (1000 miles) before turning southeast at a bend just below the famed city of Volgograd (formerly Stalingrad). The Volga has been dammed at Volgograd to form the Volgograd Reservoir, a broad backwater "lake" (*R*–8) that extends 320 kilometers (200 miles) upstream past the city of Saratov. The stretch of river-reservoir seen here lies between these two cities. Few large towns are within the scene; Kamyshin and Nikolayevski (*P*–10) on the Volga are of moderate size.

The terrain east of the Volga is mainly a smooth plain only about 15 meters (50 feet) above sea level. The immediate flood plain of the Volga is actually below sea level here. During the Pleistocene, the Caspian Sea, a large saltwater lake, transgressed as far north as the Yeruslan River (*V*–8); therefore, lacustrine sediments now cover the low areas. Somewhat higher, more dissected country is found to the west where the Ilovlya (*H*–20) and Medveditsa (*G*–6) Rivers flow southwestward to meet the Don River as it swings to within 64 kilometers (40 miles) of the Volga just below this scene. The region near the Volga is known as the Privolzhskaya Heights (*M*–17) on the Volga Plateau; the west bank of the river, dissected by many small consequent streams (*O*–18), shows a relief in excess of 30 meters (100 feet). Bedrock here and to the west consists of Cretaceous and early Tertiary sediments.

The natural vegetation of the region is classified as that of a semidesert steppe zone. Fescue short grasses and Artemisia are the prevailing types. Light chestnut soils are the rule west of the Volga, grading into solonchak (salinized clay loams) to the east. The region is given almost exclusively to agriculture, with many large fields being part of the communal system. Wheat is the principal crop, but rye, oats, barley, millet, sugar beets, hemp, and flax are also grown. *1358–07253;* July 16, 1973.

PLATE 257



KARA BOGAZ GOL GULF, U.S.S.R.: This nearly 18 000-square-kilometer (7000-square-mile) indentation of the Caspian Sea, located in Turkmen S.S.R., is one of the world's largest natural evaporation basins. Once an open free-flowing gulf of the Caspian (*D*–16), the Kara Bogaz Gol Gulf (*P*–14) has almost been sealed off from the main water body due to sandbar deposition across its mouth (*J*–15; *L*–18). Its remaining link to the Caspian is a narrow north to south trending strait (*K*–17). The strait, which is approximately 13 kilometers (8 miles) long, up to 3 kilometers (2 miles) wide, and everywhere less than 6 meters (20 feet) deep, must be kept open artificially to provide water from the Caspian for the evaporation process, which provides vital chemical products.

The gulf occupies a natural basin, a synclinal structure, and is surrounded by highlands on all but its Caspian margin. The plateau-like southern end of the Mangyshlak Mountains (*L*–1) and the southwestern margin of the Ustyurt Plateau (*T*–3) form a cliffed bank (*M*–2) rising some 300 meters (1000 feet) along the northern and eastern margin of the gulf. Sand dunes dot the plateau surfaces north of the gulf (*J*–1; *T*–1). Salt lakes also occur on this surface (*F*–4; *U*–7). The Krasnovodskiy Plateau (*Q*–21) reaches nearly to the southern shores of the gulf, but it also forms a cliffed boundary below which lies a series of spits, lagoons, and salt lakes (*N*–20; *S*–19). The prevailing depth of the gulf is around 10 meters (33 feet), but along the shore margins the depth is much less, usually about 1½ meters (5 feet). The shallow shore margins account for the highly reflective white areas of the gulf (*O*–6).

It has been estimated that a depth of over 130 centimeters (50 inches) of water is evaporated from the gulf's surface annually. The dry climate, about 10 centimeters (4 inches) of rainfall per year, permits strong solar evaporation to concentrate salts. In addition to the common chloride evaporite minerals yielded, additional processing of these salts yields industrially valuable products such as soda, sodium sulfate, and sulfuric acid. *1134–06425;* December 4, 1972.



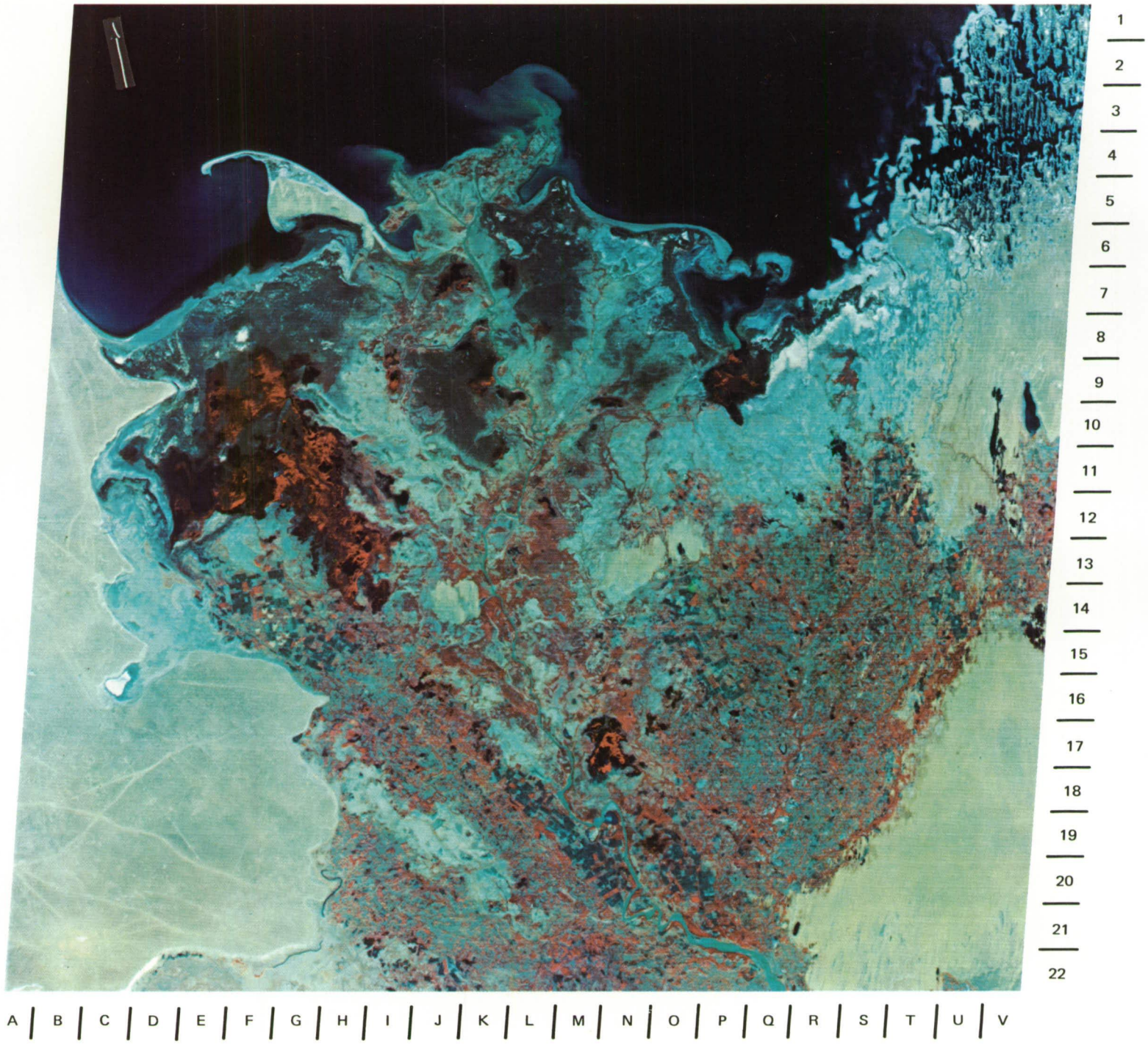
PLATE 258

THE MEETING OF THREE COUNTRIES: The common border point for Iran (*E*–16), Afghanistan (*S*–19), and the Turkmen S.S.R. (*N*–8) is located approximately at *K*–14. The Iranian city of Mashhad lies just to the west of *A*–11; the Afghanistan city of Herat is near *U*–22 off the image; and the Turkmen town of Mary is situated beyond *O*–1. The two conspicuous mountain belts are the Kuh-Hajar-Masjid (*F*–11), consisting of Jurassic, Cretaceous, and Paleocene sedimentary rocks, and the Kuh-i-Aleh (*J*–17), a central core of mid-Cenozoic intrusive granites surrounded by metamorphosed Cretaceous and Paleocene rocks. These ranges are part of the eastern end of the Kopet Dagh chain separating eastern Iran from the Soviet Union; they continue as the Paropamisus Range in Afghanistan. The Quaternary deposits along the south edge of the Kara Kum desert encroach over much of the lower terrain in Turkmen and Afghanistan. Oscillatory sand dunes (*S*–3) have developed in parts of the area.

The Tedzhen River flows into Turkmen from the border area. Cultivated "oasis" bottom lands (*I*–7) are the result of offshoot irrigation canals. The Kashaf River (*D*–11) flows past Mashhad into the Tedzhen. The Tedzhen is renamed the Hari River where it forms the boundary between Iran and Afghanistan (*L*–21). The Obeh Hari (or Jam) River (*C*–19), a major branch, provides water for wheat and barley farming.

The lower areas are covered by cold steppe grasses in Iran and Afghanistan and by desert steppe vegetation in Turkmen. The slopes of the ranges support some almond and pistachio trees. The higher elevations (up to 1800 meters (6000 feet)) have scattered juniper and oak trees. *1091–06035;* October 22, 1972.

PLATE 259



SOUTHERN ARAL SEA, U.S.S.R.: The Aral "Sea" is actually a large, presently evaporating saline lake less than 25 meters (80 feet) deep at its center located in the southwest Soviet Union. It receives a daily inflow of water from the Syr Dar'ya River on the east and the Amu Dar'ya River on the south. Both rivers originate in the high mountains of the Tyan Shan chain between the city of Tashkent and the Afghanistan border. The south half of the Aral Sea is located in the northwest part of Uzbek S.S.R. The area here is subdivided into a tablelands upland (*B*–18) on the west, with a barren surface of clay alluvium and into a lower alluvial plains on the east, now degrading by wind deflation to form sand massifs (*T*–20) that mark the edge of the Kyzyl Kum Desert. Most of the scene is dominated by the actively building delta (*I*–5) of the Amu Dar'ya (*P*–21). This river, with its headwaters in the glacial- and snow-fed mountains of northern Afghanistan, is the longest (2300 kilometers (1400 miles)) in central Asia and is noted for having the highest suspension load of sediments of any major river on Earth. The delta is terraced, reflecting the effects of the lowering of the Aral Sea on the course of the river. Cane thickets and woody brushland are scattered throughout the delta, along with a few tugai forests and marshy areas, especially east of Lake Shile Kol (*D*–11). Farming is limited because of frequent flooding, but controlled irrigation has allowed development of some new sections. The two principal towns on the delta are Nukus (*O*–20) and Muynak (*G*–6) at the base of Tomak'Aty, a sandy spit being built into the Aral Sea. The sandy islands (*T*–3) to the east are being dissected by recent rises in water level in this part of the sea. *1310–06192;* May 29, 1973.

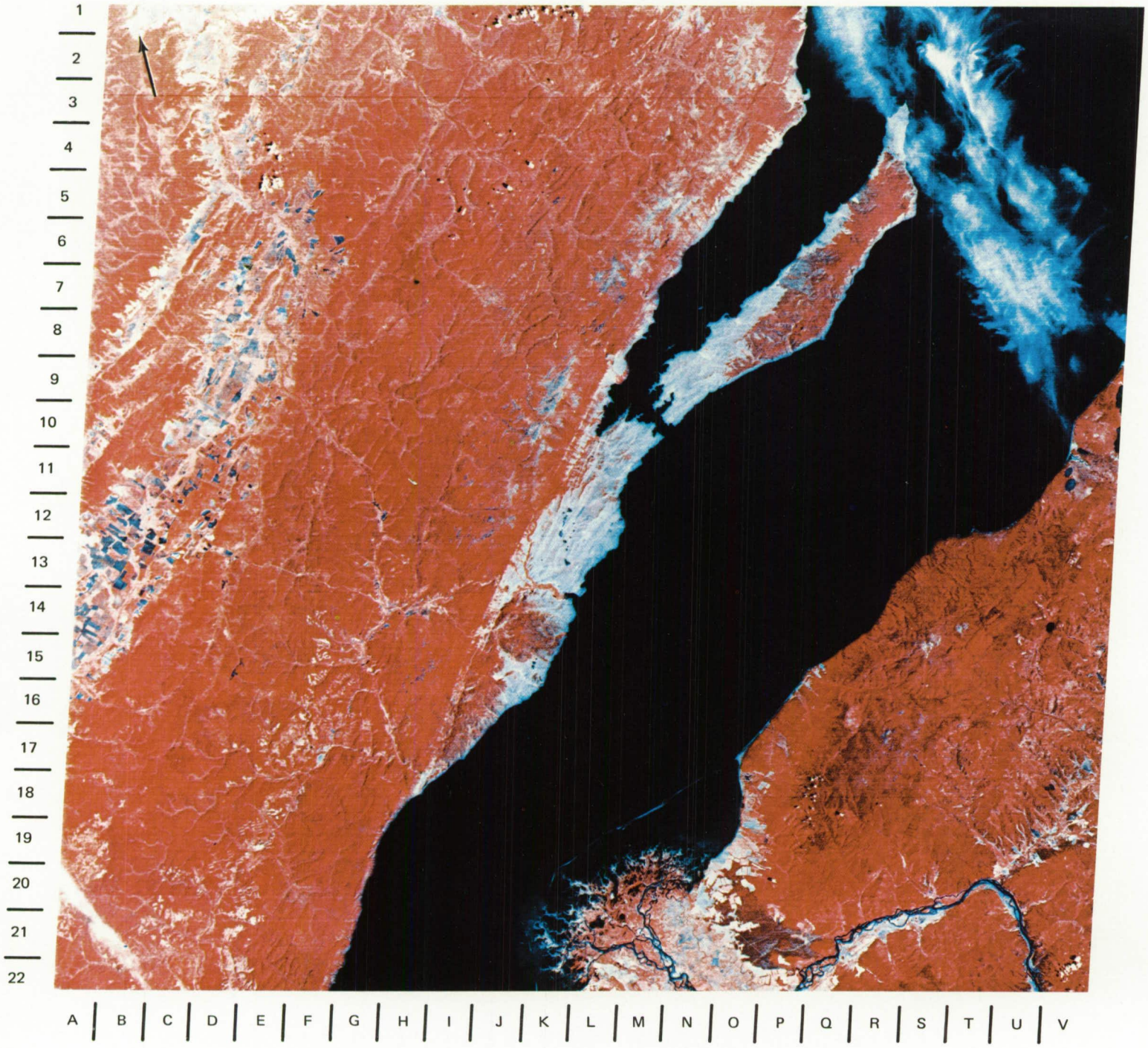


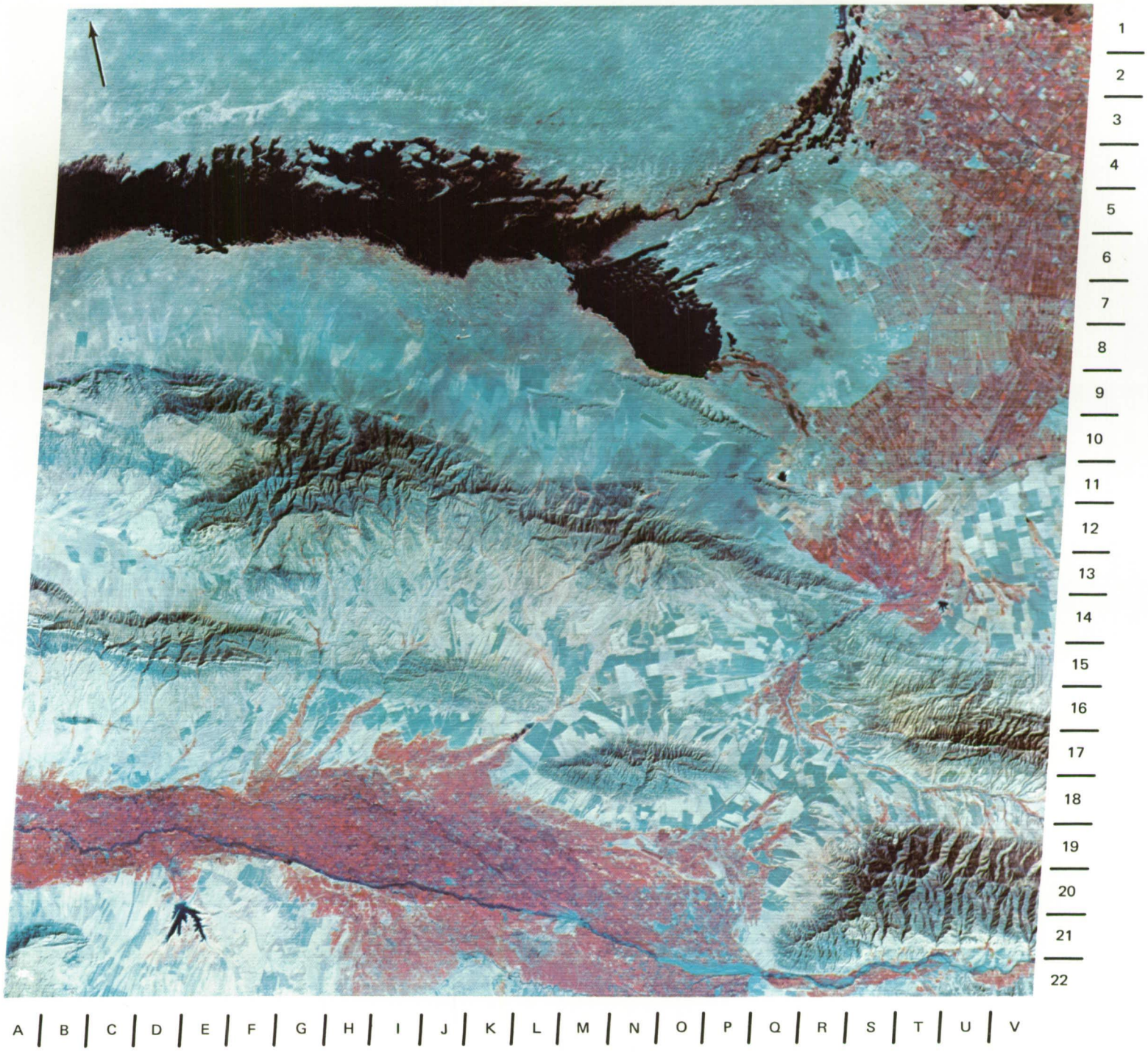
PLATE 260

THE WORLD'S LARGEST LAKE: This is Lake Baykal (*O*–13) in southern Siberia not far from the Mongolian border. In area (30 710 square kilometers (11 780 square miles)) it is the ninth largest lake in the world. Baykal runs northeast for almost 640 kilometers (400 miles) and in places is up to 80 kilometers (50 miles) wide. Parts of the lake are more than 600 meters (2000 feet) deep and at one place the depth reaches 1620 meters (5310 feet), making Baykal the deepest landlocked lake on any continent. Its total volume of 23 000 cubic kilometers (5520 cubic miles) places Baykal first as the largest nonsaline water body on Earth; in fact, this lake contains approximately 20 percent of all surface freshwater on the planet. Lake Baykal, composed of exceptionally pure, clear, oxygen-rich water, is also an effective heat sink capable of modifying the surrounding regional weather to a more temperate climate than occurs in the nearby mountains.

These mountains are part of the Yablanoy chain, which trends northeast and reaches to more than 3000 meters (10 000 feet) in places. The Primorskiy Range (*H*–9) on the west side of Lake Baykal and the Ulan Burkassy Range (*R*–18) on the east both have peaks near 2200 meters (7200 feet). Although many of these ranges and the intervening basins are underlain by Precambrian rocks of the ancient Siberian shield, the region is nevertheless now tectonically active. Lake Baykal itself is a fault trench or graben that bears a strong structural resemblance to Lake Tanganyika in the East African rift zone (see plate 357). One postulate holds the Baykal region to be undergoing active rupture or splitting in an incipient stage of breakup analogous to that leading to the drift of continents atop crustal plates. A disastrous earthquake (1300 killed) in 1861 caused a block of land (*P*–7) now called Ostrov Ol'Khon (Gypsy Steppe) to split along a fault (*J*–13) and slide into the Baykal trench, producing the deep Prolivy More (Proval Bay) (*O*–5).

More than 330 streams feed into Lake Baykal; it is drained, however, by a single river, the Angara, to the west. The largest feeder river, the Selenga (*T*–20), is building a delta (*L*–20) into the lake. The city of Ulan Ude lies along this river just off the image. This city, together with Irkutsk and others, is part of the growing industrial complex of the Trans-Baykal region. *2150–03123;* June 21, 1975.

PLATE 261



UZBEK S.S.R.: This small Soviet republic stretches from the Aral Sea on the northwest through much of the Kyzyl Kum Desert (*K*–1) to the western end of the Tien Shan Ranges at the Afghanistan border well to the south. The largest city, Samarkand (*M*–20), lies in the fertile valley of the Zeravshan River (*F*–19), which eventually joins the Amu Dar'ya to the west. Cotton and wheat are the major products from the farmlands around this river. The river emerges onto these plains past the Turkestansky Range (*T*–19), made up mainly of Silurian sedimentary rocks, which runs parallel to the much higher (up to 4900 meters (16 000 feet) to the east) Zeravshanskiy Range just to the south. The Nuratau Ranges (*G*–10) to the northwest are composed of Silurian and Devonian rocks intruded at several places (*A*–10; *N*–12) by mid-Paleozoic granitic rocks. All these mountains lie along an active earthquake zone.

Extensive farming is carried out in the bottom lands of the Syr Dar'ya River (*U*–1) southwest of Tashkent (off right corner). Most of those farms are elongate parallel to drainage ditches but larger wheat farms (*N*–15) elsewhere in the region are more equant in shape. The large blackish area at the edge of the desert is the Aydar salt marsh (*H*–5) in flood and the enlarged Lake Tuzkan (*N*–8). *1070–05445;* October 1, 1972.

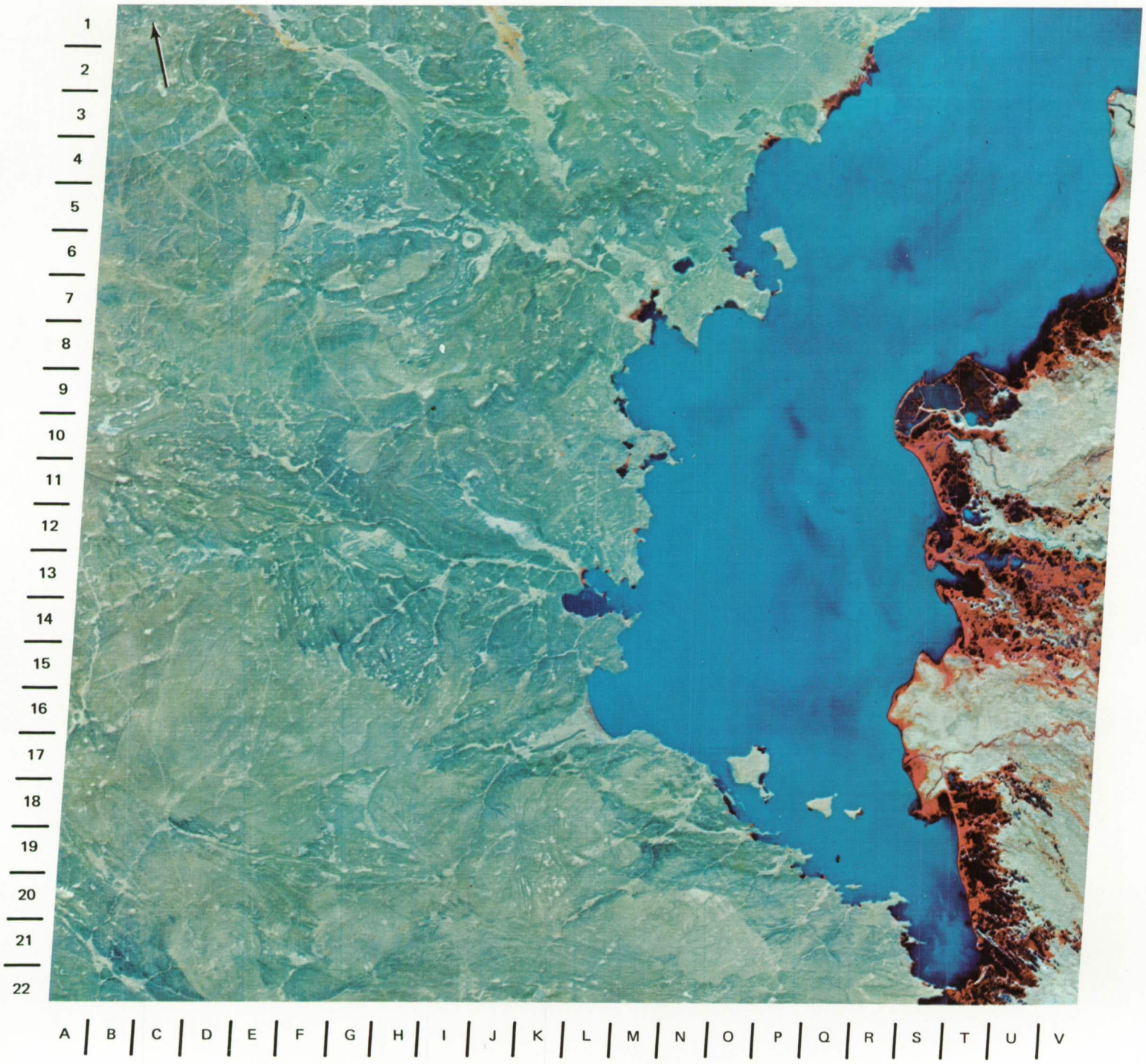
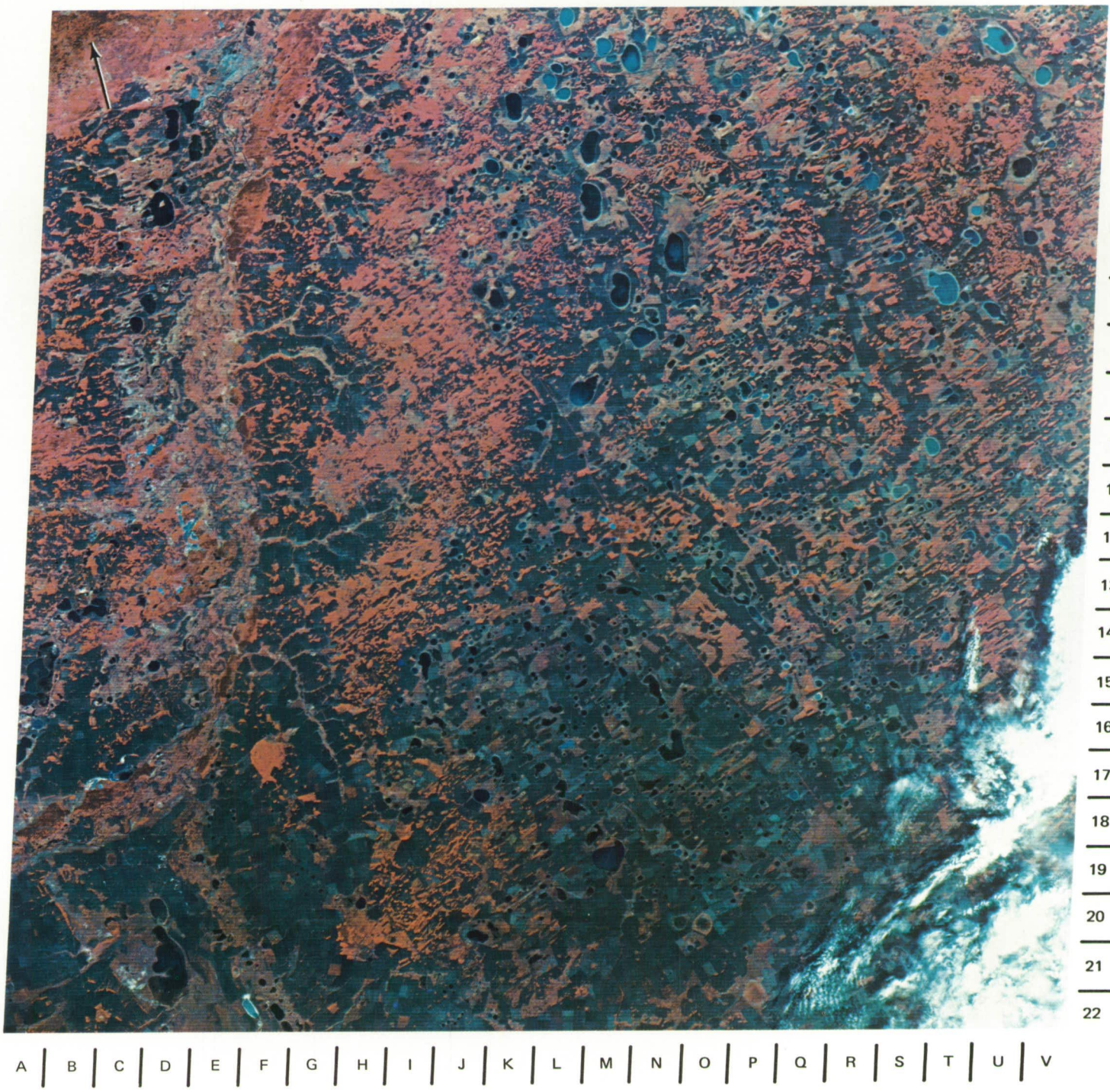


PLATE 262

LAKE BALKHASH, U.S.S.R.: Ozero (Lake) Balkhash (*P*–10) is a 320-kilometer (200-mile) long slightly brackish water body in the southeastern section of Kazakh S.S.R. The lake is slowly losing water, especially in the east-west segment to the east of this image; depths in the segment shown are still as great as 100 meters (340 feet). The Bet Pak Dala Plateau (*D*–10), west of the lake, consists of gently rolling foothills (about 30 meters (100 feet) of relief) developed on folded Paleozoic sandstones and shales and granitic rocks to the south. The western shore of the lake is lined with rocky cliffs. Depressions (*B*–11) in this terrain are filled with salts and fine soil. Drainage within the plateau is almost entirely internal. The southern and eastern shores are surrounded by the sandy plains of the Sary-Ishikotrau Desert. The Ili River flows across this desert to empty through several distributaries (*S*–10; *S*–17) that form a delta westward into the lake. Vegetation on this side of the lake includes artemisia, salt trees, and reed thickets. Salt marshes, hemp, and shrubs (in groves) occur in the swampy backwaters from river floods. Numerous bays (*T*–20) alternate with sandy ridges and mounds along the shore. *1049–05260;* September 10, 1972.

PLATE 263



WESTERN SIBERIAN STEPPES, U.S.S.R.: The region seen here is about 400 kilometers (250 miles) southeast of Sverdlovsk in the Urals and 480 kilometers (300 miles) west of Omsk. The city of Kurgan (*D*–2) on the Tobol River (*B*–18; *D*–5) is a stop on the Trans-Siberian railway. The border between the Kazakh S.S.R. and this part of the Russian Soviet Federated Socialist Republic to the west, the most populated and by far the largest of the Russian States, runs approximately through *B*–17 to *L*–11.

The scene shows the Kustanay Plains (150 to 210 meters (500 to 700 feet) above sea level) in the western Siberian Lowlands. This is a flat to undulating surface developed on stratified alluvium; the surface is slowly being stripped off by eluviation (stream erosion of top layers). Dark, fertile residual soils (*F*–19) are underlain by Paleocene marine and Recent continental sediments. Numerous small lake basins contain fresh to slightly brackish water although some saucer-shaped depressions remain unfilled during most of the year. The Tobol River here passes through the Tobol-Ubagan structural trough; the flood plain is terraced within the river meander zone defined by low slopes (*C*–11; *E*–11) rising to the uplands plains.

Because the water table is close to the surface, grassy marshes, wet meadows, and bogs are found over much of the plains. Where feather grass abounds on the steppe plains, the land is used for pasture; where farming in cleared land takes place, cereals are the principal crops. Some birch and aspen copses are scattered in the area, but these and a few pine woods increase in extent as the wooded steppe zone is reached north of the scene. The river bottoms support meadow grass, reeds, and shrubs. *1309–06102;* May 28, 1973.



PLATE 264

VASYUGAN SWAMP, U.S.S.R.: This vast inland swamp lies near the center of the Western Siberian Lowland, which stretches for roughly 1600 kilometers (1000 miles) from the Ural Mountains on the east to the Yenisey River valley on the west. The lowland is drained northward into the Kara Sea arm of the Arctic Ocean by several river systems, the largest of which are the Ob and the Yenisey. The Vasyugan Swamp lies astride the water divide between the Ob and the Irtysh, a major tributary of the Ob. The image shown here is located about 120 kilometers (75 miles) south of the town of Surgut on the Ob River. (See plate 266.)

In past geologic time this region was inundated by an extension of the Arctic Sea that reached inland to the present-day Aral Sea. Later, continental glaciers extended into the lowland from the Ural Mountains on the east and the Taimyr mountains on the west. Apparently the area south of the Ob River, which includes the Vasyugan Swamp, was not directly affected by glaciation, which could have produced the extensive swamp, marsh, and lake environment.

Following glacial times, the Vasyugan swamps and marshes have been forming as a result of swamping, a condition in which abundant precipitation coupled with very low, flat relief causes areas to become flooded. Poor drainage due to low relief is indicated by the fact that although this region is nearly 1600 kilometers (1000 miles) from the sea, no portion of this image is higher than 180 meters (600 feet) above sea level. Poorly drained conditions are indicated in this late fall image, where the water in the low, swampy areas has frozen (*E*–9; *S*–12), creating the bright, reflective signature while the coniferous forest areas not yet flooded are seen as the darker toned areas (*I*–18; *O*–11). All evidence indicates that swamping is continuing and areas of sphagnum moss and peat are replacing former stands of coniferous trees. *1126–05513;* November 26, 1972.

PLATE 265



NORTHERN URALS: The Ural Mountains run north to south for more than 1800 kilometers (1100 miles), roughly from a position about 480 kilometers (300 miles) northeast of the Caspian Sea on the south to the Gulf of Baydaratskaya in the Kara Sea above the Arctic Circle. These mountains, about 1300 kilometers (800 miles) east of Moscow, are arbitrarily selected as the dividing line between European and Asiatic Russia.

The scene imaged here in midwinter is almost due east of the Arctic port of Archangel. A very low Sun angle (13°) accounts for the extreme darkness of the terrain, except for the snow cover on the higher Urals. The lowlands on the west, drained by the Pechora River (*E*–13) and its tributaries, the Padcherye (*I*–16) and Shehugor (*J*–10) Rivers, is less than 90 meters (300 feet) above sea level. The terrain rises eastward to elevations in excess of 1200 meters (4000 feet), with Mount Telpos-Iz (*O*–13) reaching to almost 1600 meters (5200 feet), and drops abruptly again to little more than 100 meters (a few hundred feet) above the sea on the east. These low areas tend to be swampy whereas the slopes leading to the mountain crests are typical of a "taiga" boreal forest (larch and fir).

The Urals are now considered by many geologists to have formed under compression by a collision of the European plate with the main Asian plate after the close of the Paleozoic Era. Representatives of all time periods of the Paleozoic Era are exposed on the west flanks of the Urals. The snow-capped strata are mostly Cambrian and some Ordovician sedimentary rocks, penetrated here and there by granitic plutons and basic intrusives. (Note how the headwaters of the Shehugor River (*R*–16) follow along the strike of the Cambrian-Ordovician units in this part of the mountains.) Descending toward the Pechora River, folded belts and anticlines of Silurian, Devonian, Carboniferous, and Permian rocks are exposed in hilly terrain. A broad, more gently dipping zone of Permian rocks lies along and to the west of the river (the city of Perm, near the type locality of the Permian system, is about 650 kilometers (400 miles) to the south). On the east side of the Urals, Pleistocene glacial deposits lap onto the flanks of these mountains. *1211–07045;* February 19, 1973.

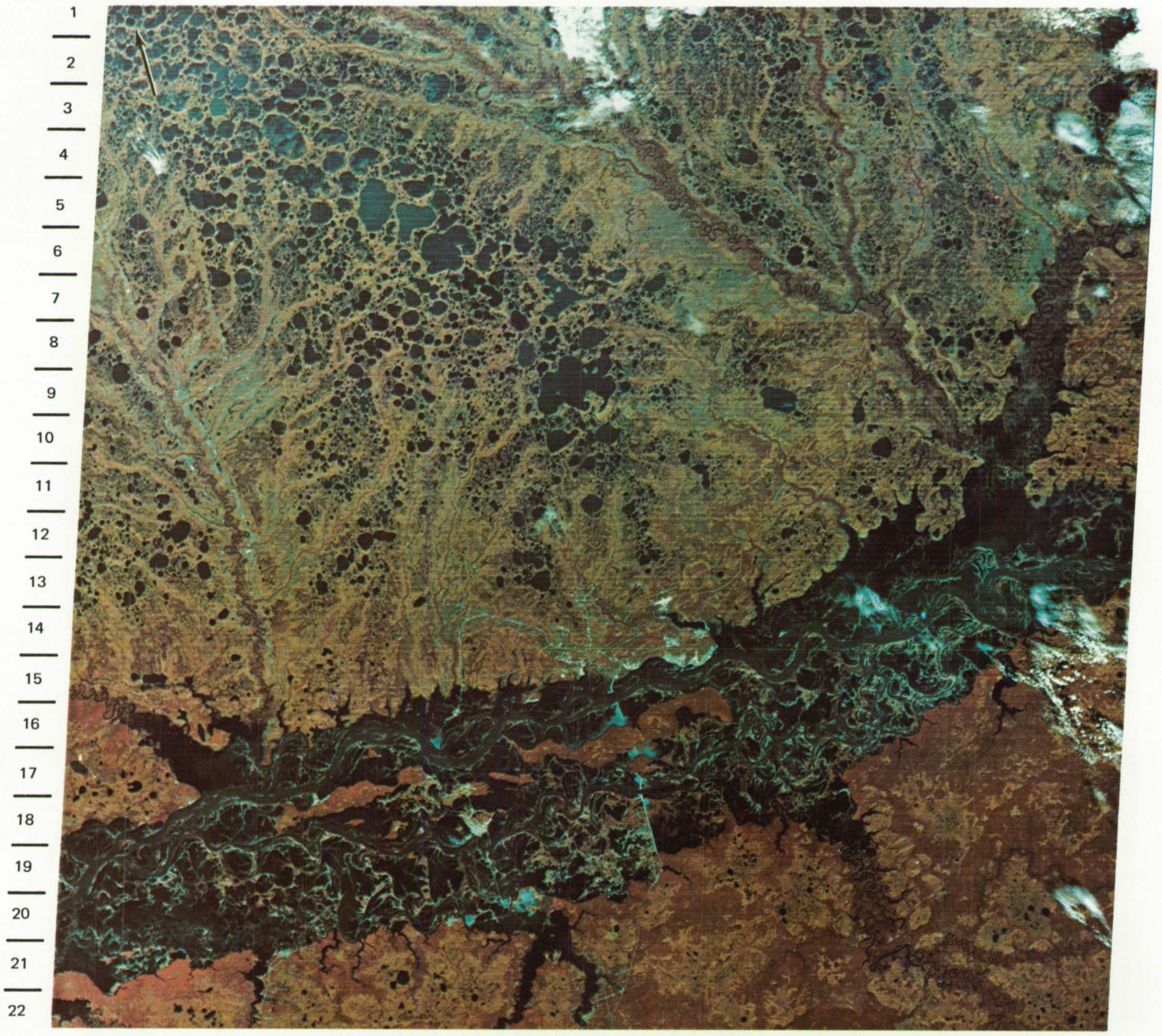


PLATE 266

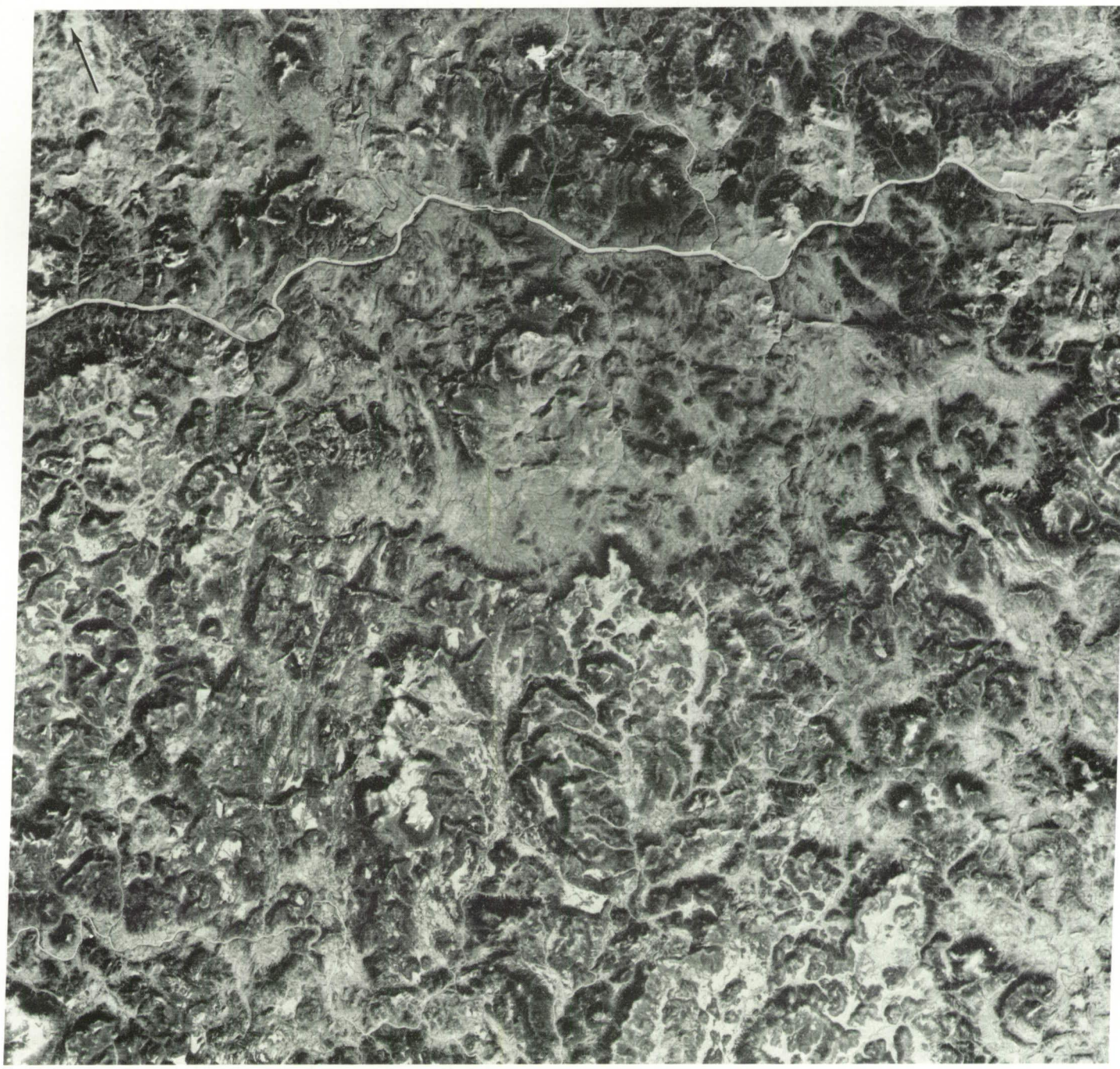
OB RIVER, SIBERIA: One of the world's longest rivers, the Ob (*P*–14), flows for more than 4000 kilometers (2500 miles) westward from the Novosibirsk region of southern Siberia to the Obskaya Gulf extending from the Kara Sea. In the scene shown here, the Ob is crossing the western Siberian Lowlands, a great depression filled with late Mesozoic and Tertiary marine sediments and presently almost everywhere less than 210 meters (700 feet) above sea level.

The nearly east to west course of the Ob in this area reflects the influence of extensive Pleistocene morainal deposits; the southern limits of these deposits coincide approximately with this stretch of river. The river has a broad, alluvium-filled flood plain that is only slightly lower than the glacial terrain of the Ob-Tazov rolling plains (*M*–8) to the north. The very low gradient of the Ob is responsible for its extreme meandering. At this time of year, following the melting of snow and ice, the Ob is in full flood, spilling water into almost the entire flood plain. Its tributaries, the Yamin (*A*–15), Pim (*D*–13), Trom-Yugan (*M*–5), and Agan (*T*–8) on the north side and the Bolshoy Balvik (*L*–21) and Bolshoy Yugan (*T*–21) on the south, show flooding only near their entry onto the Ob flood plain.

The land to the south is part of a vast regional swamp developed in the interfluve between the Ob and Irtysh Rivers. North of the Ob, most of the lakes have formed as sinks owing to poor drainage in the undulating glacial tills. This area is also one of extensive bogs in which sphagnum mosses predominate. The entire region lies within the taiga forest zone of western Siberia. This zone consists of Siberian fir, stone pine, larch, and spruce. Evergreen stands are particularly evident south of the river.

A railroad and road (*M*–19) lead from Tobol'sk some 400 kilometers (250 miles) southwest to the town of Surgut (*L*–14) on the north bluff of the Ob valley. *1325–05563;* June 13, 1973.

PLATE 267



NIZHNYAYA TUNGUSKA RIVER, U.S.S.R.: One of the major tributaries of the Yenisey River, the Nizhnyaya Tunguska, enters the Yenisey at the town of Turukhansk, just south of the Arctic Circle (not shown in this image). The segment of the river course shown here (*R*–4; *B*–6) is flowing across the Siberian platform, a geographic subdivision of Asiatic Russia containing intensely folded and faulted sedimentary rocks topped by lava flows and volcanic peaks. The Chiskova River joins the Tunguska from the North (*N*–4).

The Tunguska here is flowing across the rugged western margin of the upland plateau surface, which rises abruptly above the Yenisey River lowland region of the vast Siberian lowland that stretches eastward from the foothills of the Ural Mountains. The Siberian platform is one of the most remote and inaccessible regions of the Soviet Union.

The low Sun angle (12°) on this late October date gives rise to spectacular shadowing effects in many areas of this image (*M*–12; *D*–9). The north sides of the high peaks and cliffed areas all show this dark shadow effect. A noticeable shadow area occurs along the river course itself, where a large meander has cut into the sedimentary materials outcropping on the southern river bank (*E*–7).

Several mountain peaks rise to elevations of 700 meters (2300 feet) or more above the dissected plateau surface in the southern one half of this image: Avsa (*S*–17), Chipkamakin (*L*–14), and Sulimo (*B*–14). Like other areas of higher elevation throughout the image, they appear to be snow capped, as is indicated by the light-toned reflectance signatures. *1097–04465;* October 28, 1972.



PLATE 268

LENA-ALDAN PLATEAU, U.S.S.R.: This vast plateau extends some 650 kilometers (400 miles) from the flanks of the Stanovoy Mountains to the Lena River flood plain, south of Yakutsk in eastern Siberia. The Precambrian basement of the plateau surface is overlain by limestones and dolomites that have been intensely dissected, especially around the margins of the plateau and in the vicinity of the large rivers crossing the plateau. The intricate dissection patterns are readily visible along the Amga River (*U*–9; *K*–16) and its tributaries. The Amga is tributary to the Aldan River, itself a major tributary of the Lena River, with its confluence just north of the town of Yakutsk. The road and powerline network connecting Yakutsk with the iron mining region centered around the town of Aldan, immediately southwest of this image, can be traced north to south as they traverse the plateau and river basins (*M*–3; *N*–16).

Latitude and elevation combine to make this a region of permafrost. Because solar radiation is more effective on the south-facing slopes, certain physical anomalies result between north- and south-facing slopes within the plateau. Melting of the permafrost proceeds more rapidly on south-facing slopes, thereby providing more water for erosion. This in turn creates steeper south-facing slope areas, establishing microenvironments of differing climate, soil, slope, and vegetation.

The dominant vegetation within the area is taiga forest made up mostly of larch, pine, birch, and aspen. However, the special environment on south-facing slopes produces a wooded steppe, which here are mostly grass-covered areas known as meadow steppes. The lighter toned, more reflective locations (*G*–15; *I*–7) appear to represent such areas. When used for agriculture, these steppe areas produce a variety of agricultural products in the short growing season found at these latitudes. Grain crops such as barley, rye, and wheat are typical, but the long summer days also permit the production of vegetables, and even watermelons on the warmer ridges. *1089–02184;* October 20, 1972.

PLATE 269



INDIGIRKA RIVER SYSTEM, U.S.S.R.: This river system, draining from the great mountainous knot of northeastern Siberia, is yet another of the vast network of Soviet rivers emptying into the Arctic Ocean. The Indigirka (*F*–20; *A*–3) has its headwaters in the Chersogo Mountains south of this image and drains northward across the tundra lowlands of the Arctic coastal plain into the East Siberian Sea.

In this image, two large tributaries of the Indigirka, the Nera (*E*–6) and the Ulakhan (*D*–12), have intricately dissected the folded mountain ranges and rolling plateau surfaces. The pattern of dissection carved by the Nera and the Ulakhan and their numerous tributaries is made even more discernible by two factors. First, the low Sun angle (12°), typical of this time of year at these latitudes, creates a shadowing effect that enhances ridge and valley contours; second, the uniformity of surface reflectivity produced by the snow cover yields a topographic detail not normally readily visible. In fact, this combination of factors often yields a kind of pseudorelief whereby, when the image is viewed from a certain angle, the lower areas, such as stream valleys, appear to be higher than surrounding ridges.

Topographically, the area south of the Nera River (*H*–10) is essentially a rolling plateau surface that has been etched by the effects of past glaciation and more recently by stream erosion. Northeast of the Nera River (*R*–4) is a zone of folded metasedimentary rocks eroded to produce a series of parallel ridges where, in places, streams like the Delyankir River (*T*–6) have established courses that cut across the topographic grain.

Few of man's activities interrupt the starkness of this remote, sparsely settled area. The largest village shown on maps of the area is Oymyakon (*C*–20) in the Indigirka River valley. *1097–01201;* October 28, 1972.

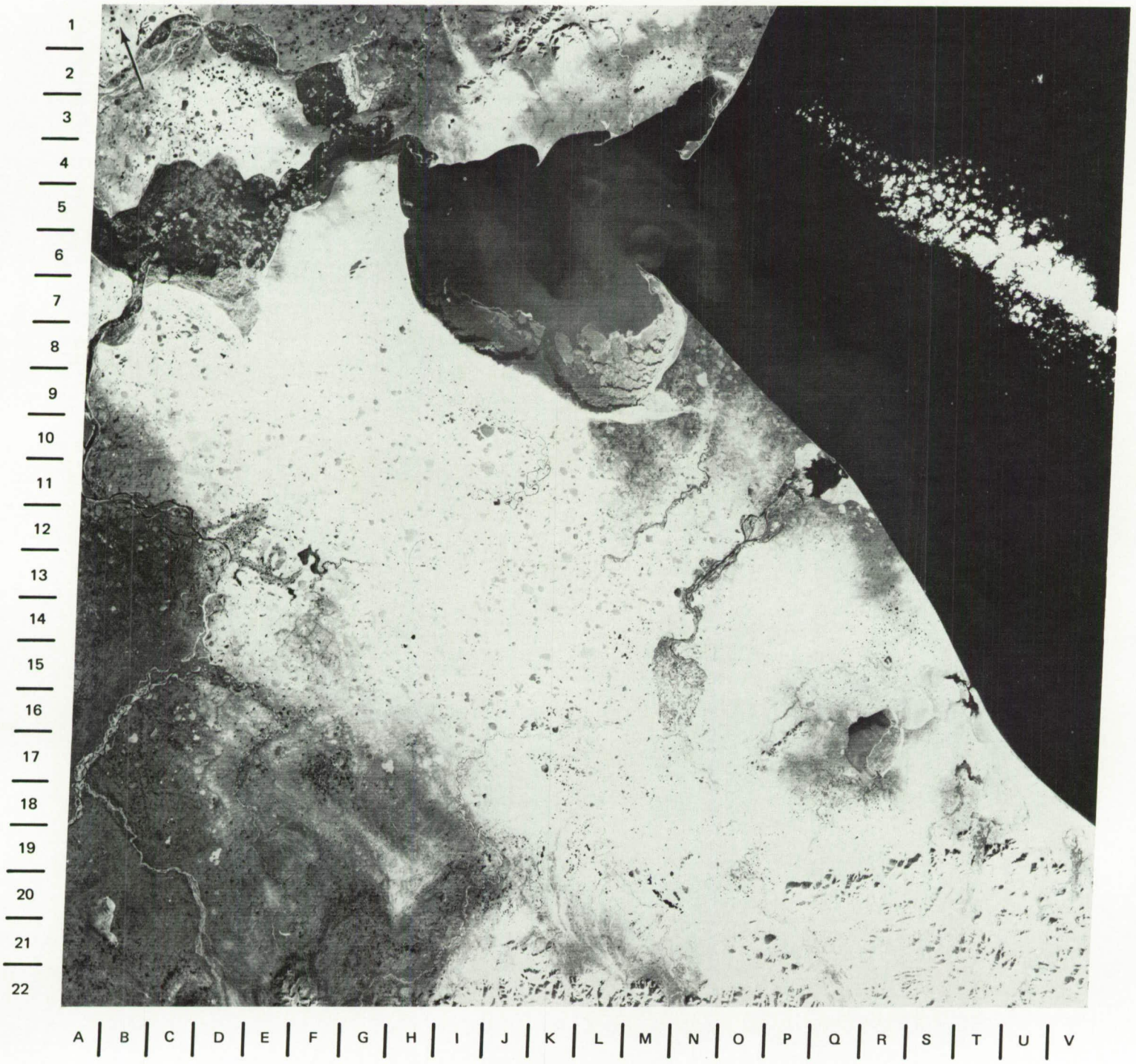


PLATE 270

ANADYR', U.S.S.R.: This early fall image enhanced by snow cover is located in a remote area of eastern Siberia, north of the Kamchatka Peninsula, near the Arctic Circle. The 180° meridian, the basis for the international dateline, cuts across the northeast corner of the image.

The Anadyr' Basin is a region of crustal subsidence and past volcanic activity, lying between the extreme northern end of the Koryakskiy Range (*S*–20) and the Zolotoy Range (*K*–1). This vast lowland contains Lake Anadyr' (*J*–5) and the Gulf of Anadyr' (*R*–7) embayment of the Bering Sea and the deltaic mouth area of the Anadyr' River (*A*–5). The town of Anadyr' (*G*–4) is located on a peninsula east of the mouth of the Anadyr' River.

The glaciated plain south (*H*–10) of the town of Anadyr' is dotted with hundreds of small circular lakes, most resulting from the effects of continental ice sheets. Some lakes are thought to be the result of subsidence caused by the thawing of fossil ice buried in the permafrost cover. The coastal lagoonal lakes (*Q*–10; *T*–15) apparently originated as longshore currents deposited sand and closed them off from the sea.

A line of volcanoes (*J*–1; *G*–6) extend from the Zolotoy Range, southwestward onto the Anadyr' Lowland. A second well-defined tectonic zone (*R*–19) marks the contact between the northern extremity of the Koryakskiy Range and the lowland of the Anadyr' River.

A line of cumulus clouds lies in the Gulf of Anadyr' (*S*–5). *1073–23075;* October 4, 1972.

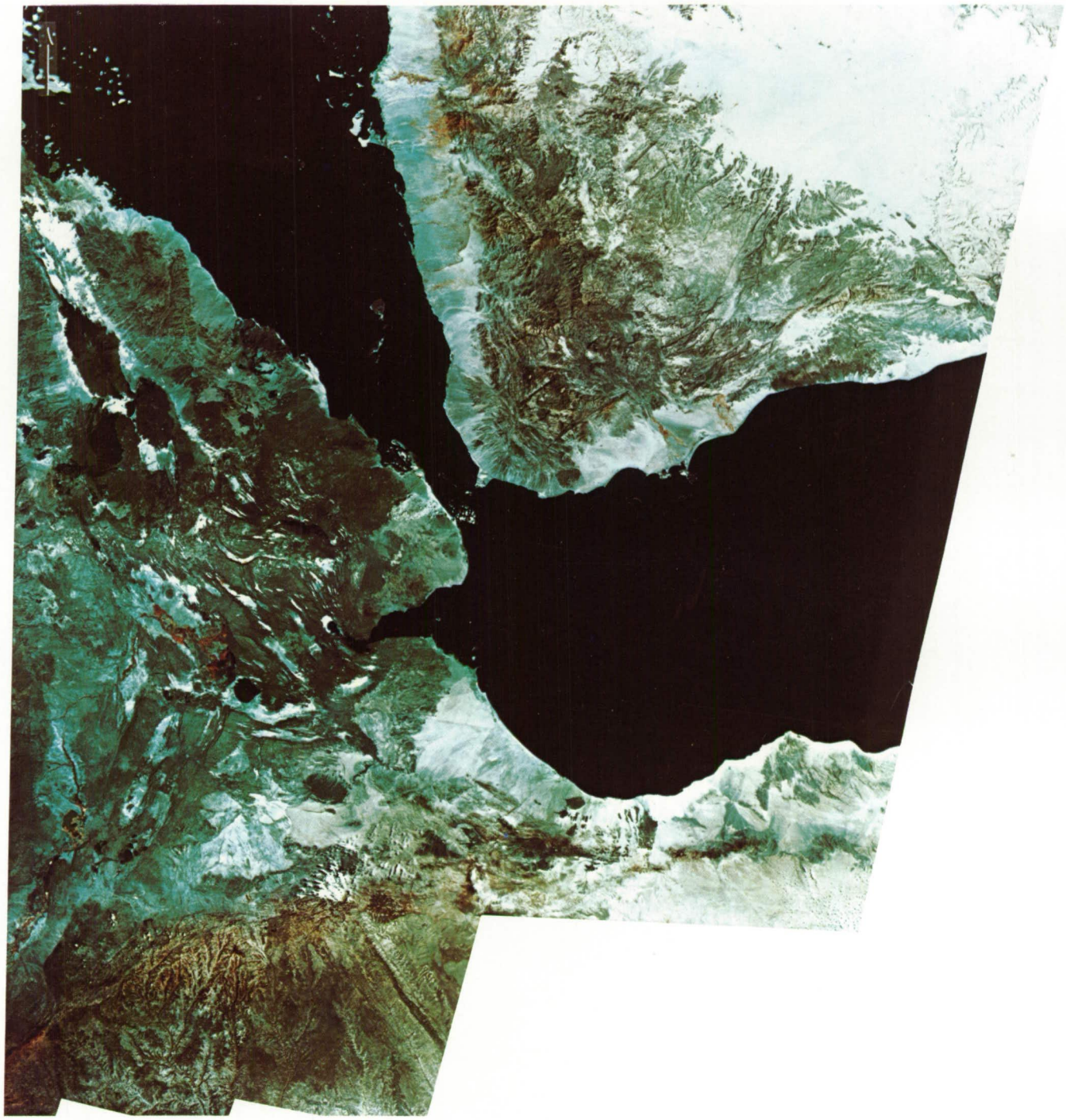


PLATE 271

SOUTHERN RED SEA: The Red Sea, Gulf of Aden, and East African rifts (*A*) (see plate 272 for letter identifications), an important part of the world rift system, meet at the triple junction of the Afar triangle. (See plate 366.) The junction, shown here at a smaller scale, is centered at *B* in the large dark triangular-shaped Afar depression. To the geologist, this scene depicts an area of incipient crustal fragmentation and probable movement of continental plates. That is, the Arabian plate, occupied by Yemen and Southern Yemen on this mosaic, was once a part of Africa. About 35 million years ago, the continental plate ruptured along what is now the approximate axes of the Red Sea and Gulf of Aden, and the Arabian plate moved in a northwesterly direction away from Africa. The Afar thus represents an area in which the process of "sea-floor" spreading is taking place on land; that is, much of the area is exposed "sea floor" and many of the dark volcanic rocks (*C*) are of compositions typical of oceanic basalts. Much of the interior is, in fact, topographically below sea level, with Lake Assale (*D*) in the Danakil depression (*E*) at 116 meters (361 feet) below sea level being the second lowest terrestrial area in the world.

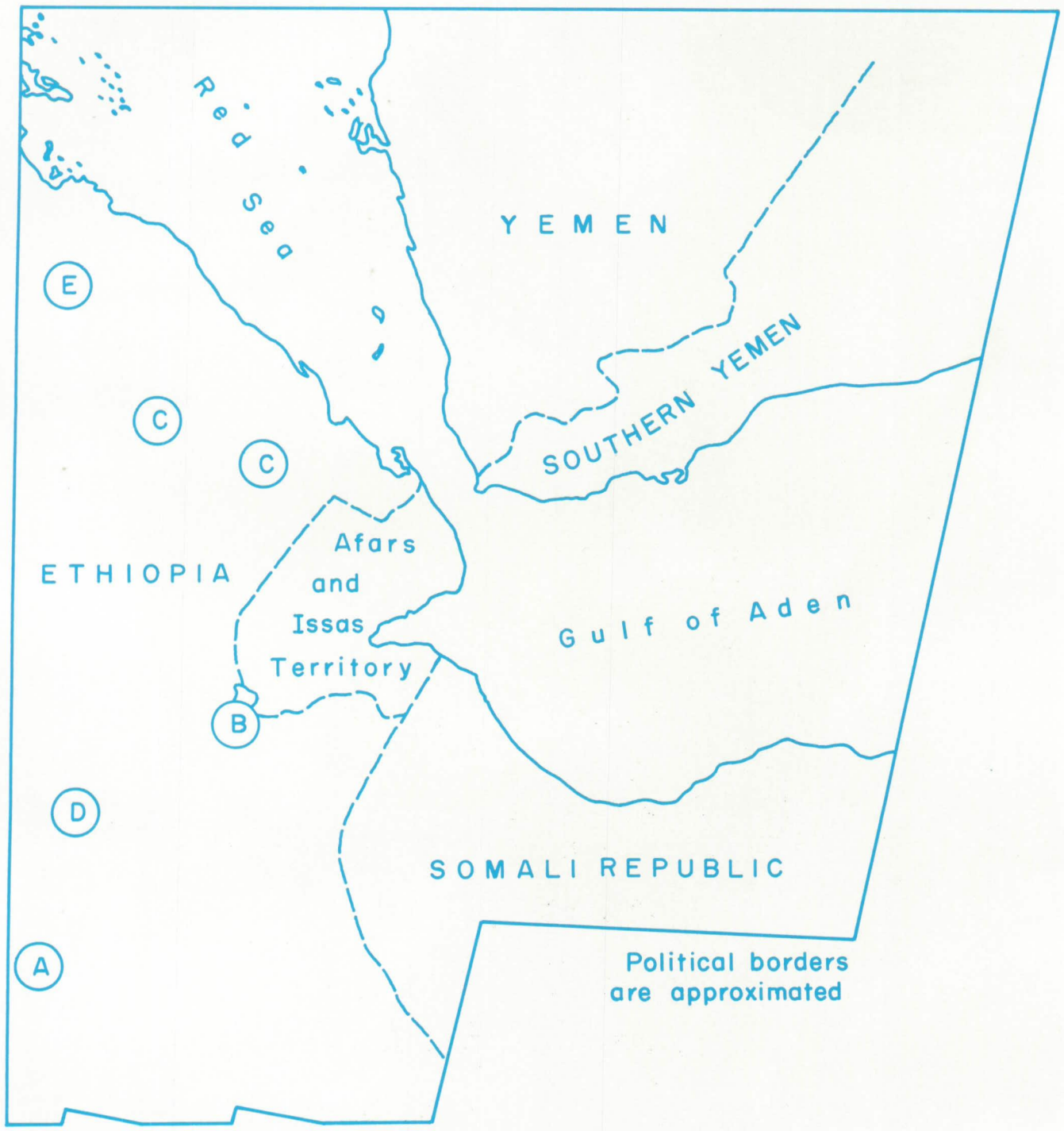

Red Sea
YEMEN
SOUTHERN YEMEN
E
C
C
ETHIOPIA
Afars
and
Issas
Territory
Gulf of Aden
B
D
SOMALI REPUBLIC
A
Political borders
are approximated

PLATE 272

PLATE 273



NORTHERN RED SEA: This mosaic of the northern Red Sea area was constructed using 37 Landsat scenes. The area is of extreme interest to the structural geologist for it shows a zone of incipient plate movement along a line of transcurrent faulting. The separation of the Arabian plate in a northwest direction away from Africa was briefly discussed in the caption for the Southern Red Sea mosaic (plate 271). In this mosaic, the near parallelism of the opposing coastlines is clearly evident. Mountains on both sides reach elevations of 1500 to 2100 meters (5000 to 7000 feet). The northwestward movement of Arabia is alleged to have occurred along the Dead Sea rift system (*A* to *B*), which is recognized by its clear linearity. (See plate 274 for letter identifications.) Relative displacement along this fault has been calculated by several means to be approximately 105 kilometers (65 miles). Large volcanic flow fields are visible at *C*.

The mosaic format provides an excellent base for plotting regional land use development. The northeastern tip of the fertile Nile delta (*D*) is located immediately west of the well-defined Suez Canal that separates the Sinai from the main part of Egypt. The sinuous, dark feature extending from (*E*) to (*F*) is the Nile River and its associated flood plain. Note the patterns of red that mark the areas of agricultural development. A striking difference in land use management is illustrated along the northern border of the Sinai with Israel. Here the more effective Israeli conservation practices, particularly in controlling goat herds in this desert region, are reflected in the darker tone indicative of a greater vegetation density.

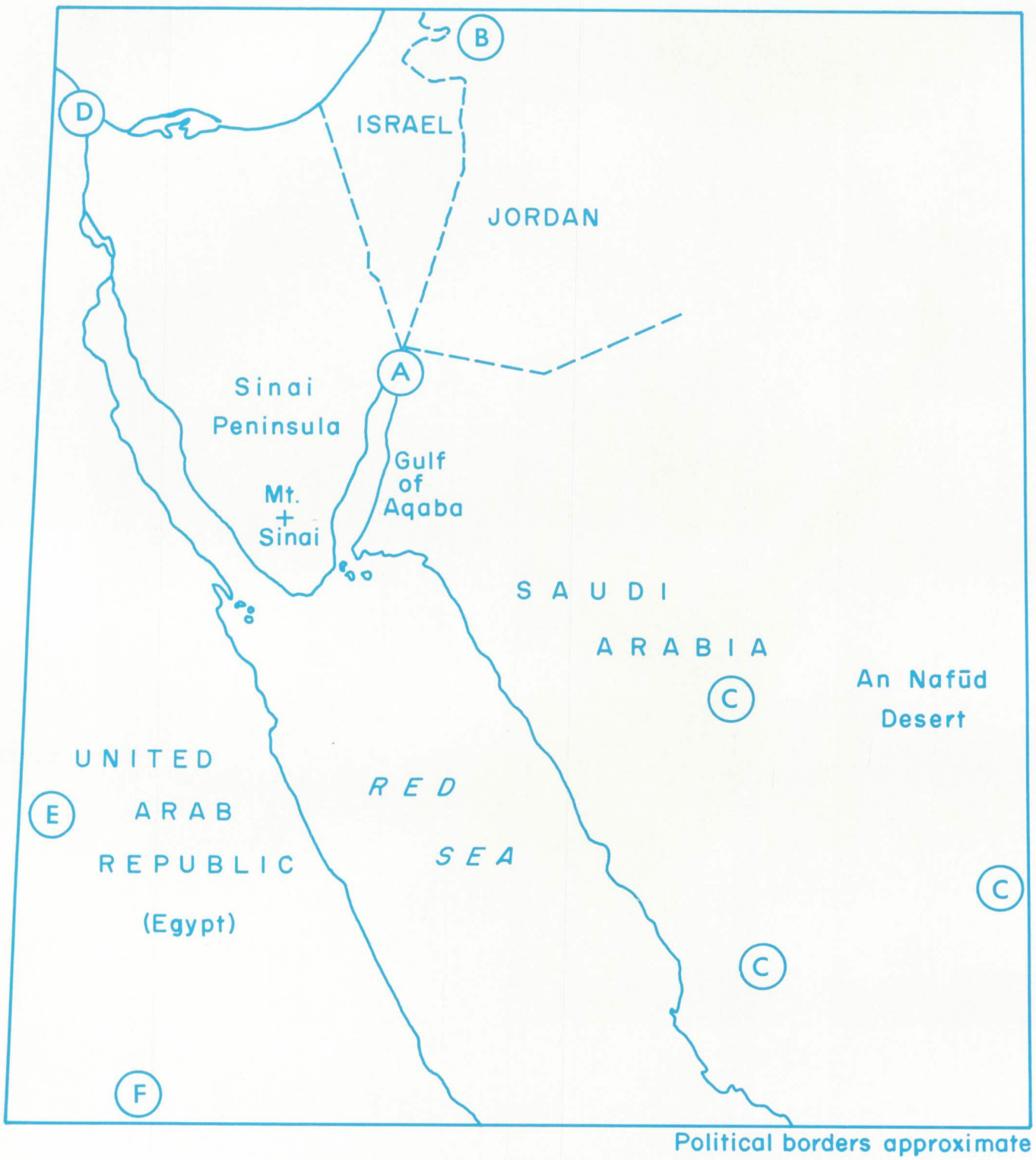
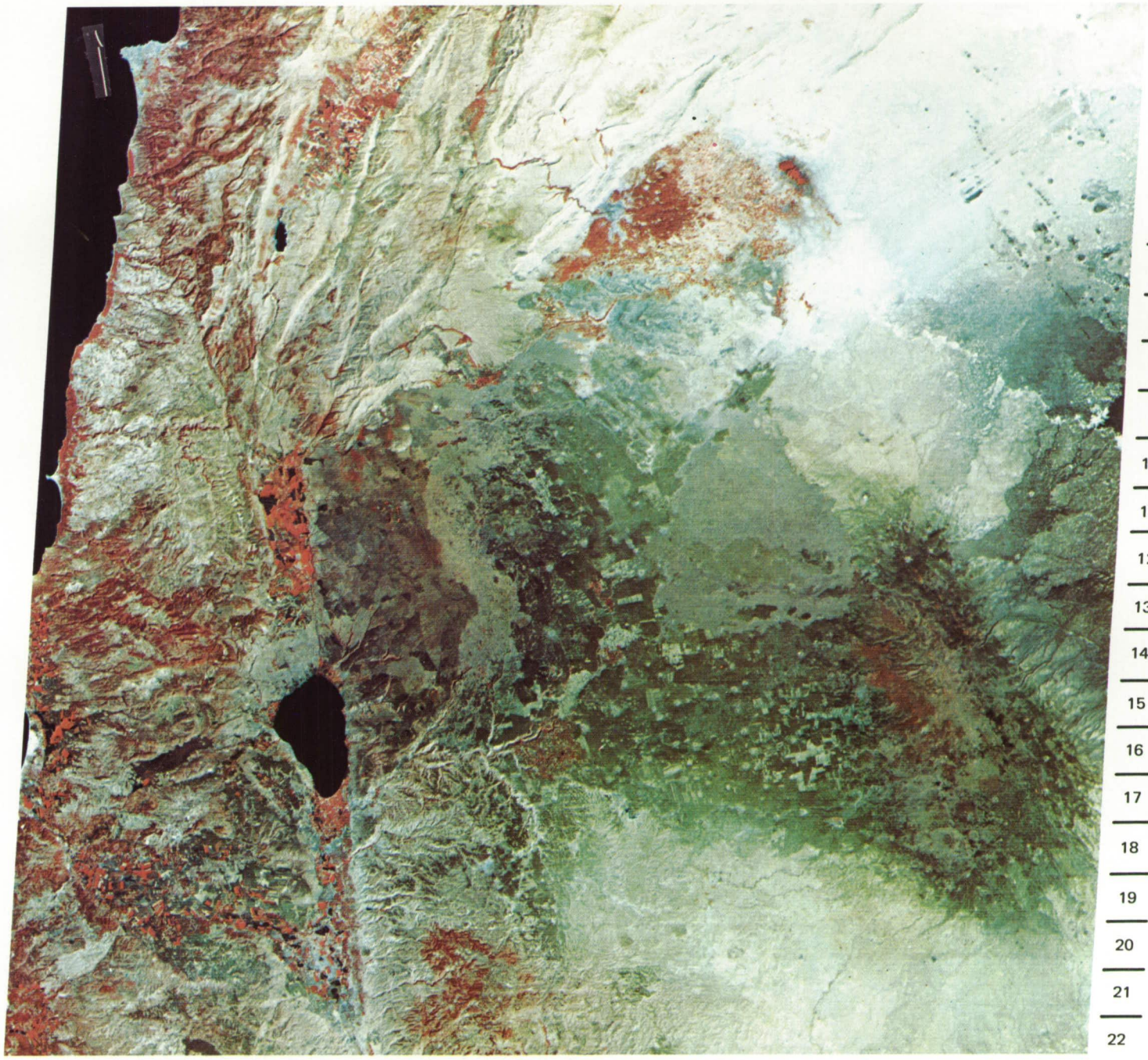

B
D
ISRAEL
JORDAN
A
Sinai
Peninsula
Gulf
of
Aqaba
Mt.
+
Sinai
SAUDI
ARABIA
C
An Nafūd
Desert
UNITED
E
ARAB
REPUBLIC
(Egypt)
RED
SEA
C
C
F
Political borders approximate

PLATE 274

PLATE 275



THE MIDEAST: The three countries of Israel (*D*–18), Syria (*Q*–7), and Lebanon (*C*–8) meet just north of an irrigated valley (*F*–12) settled with kibbutzes. To the northeast is the 858-meter (2814-foot) high Mount Hermon (*G*–8). To the south are the Golan Heights (*G*–13) lying along the approach to Damascus (*L*–5) in Syria. The southern end of these heights is bounded by the Sea of Tiberias (or Galilee) (*F*–15) in northern Israel. Nazareth (*D*–17), the childhood home of Jesus Christ, is situated some 40 kilometers (25 miles) to the west. The northwest corner of Jordan (*J*–18) is roughly outlined by a sharp tonal change in the north and the Jordan River (*G*–20) on the west. Further north Beirut (*B*–2) lies on the Lebanese shores. Inland, the Lebanon Mountains (*D*–3; *H*–5) rise to more than 790 meters (2600 feet). The famed Cedars of Lebanon are part of the foliage of their western slopes.

Part of the great north-trending Levantine fault system (*D*–8; *G*–19) that forms the Jordan-Dead Sea graben to the south continues through the Sea of Galilee into the Mediterranean south of Beirut. Related faults (*E*–4; *F*–6) that trend to the north and northeast have been traced into Syria and Turkey. Jurassic, Cretaceous, and younger sedimentary rocks are found to the west of the fault zone and in the Lebanon Mountains and the folded mountains in Syria (*N*–3). The Golan Heights and the Djeb 'Druze (*P*–14) south of Damascus consist of a series of late Tertiary and Quaternary basaltic flows; cinder cones are evident in places (*K*–14). Older Tertiary sediments, capped by desert sands and soils, are found in the Aneza (*U*–3) to the east. *1054–07415;* September 15, 1972.

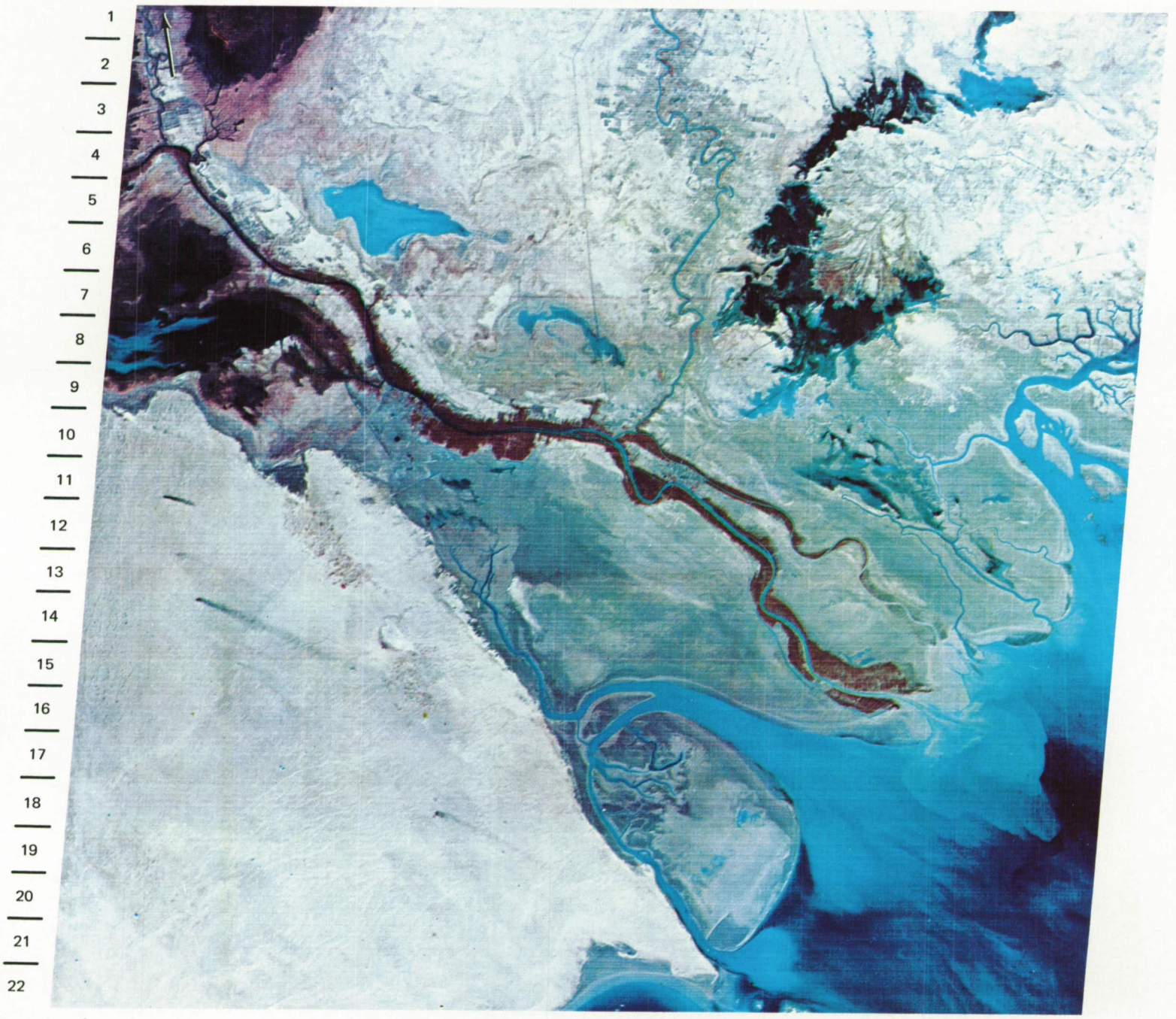
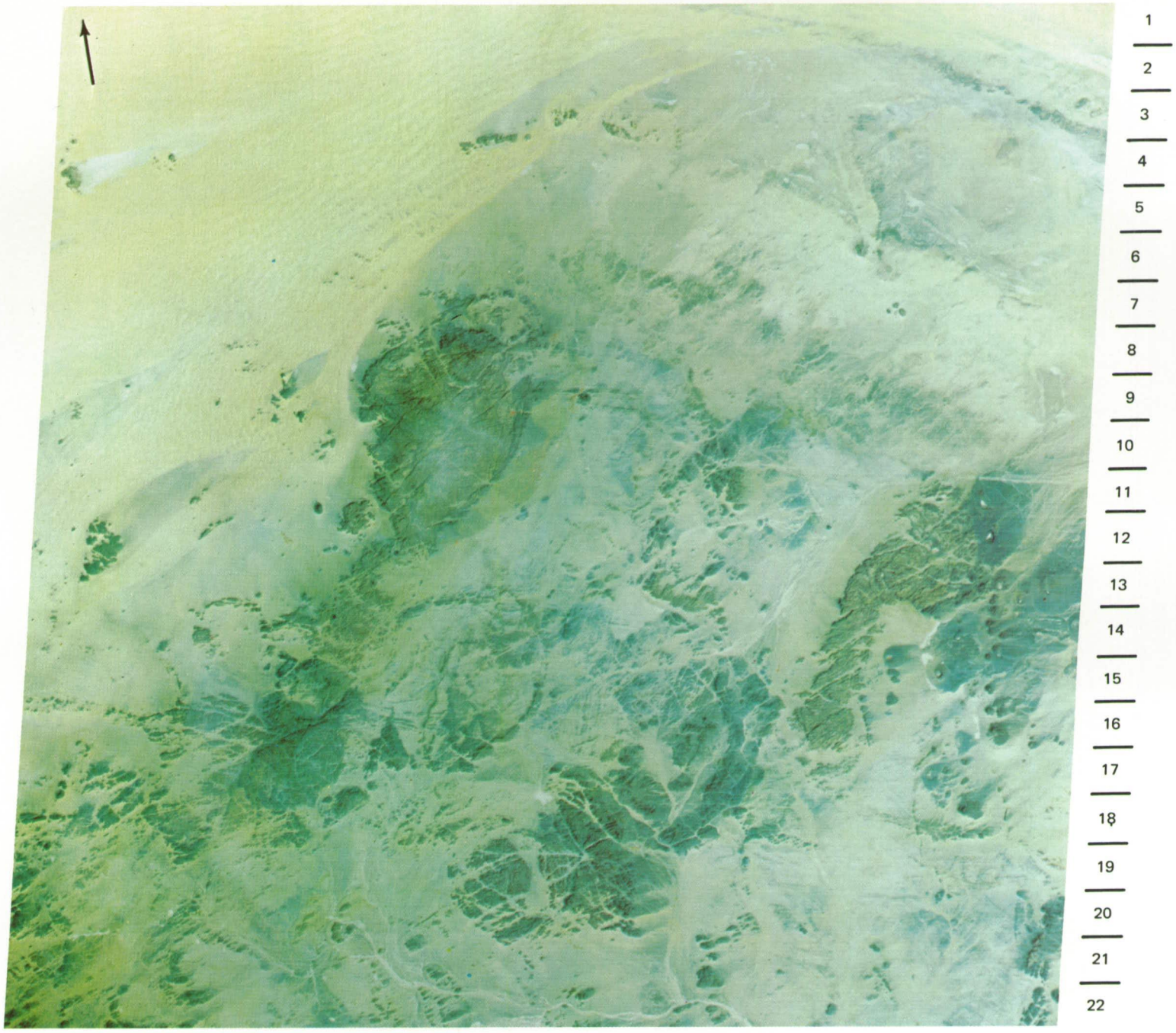


PLATE 276

THE MOUTH OF THE TIGRIS AND EUPHRATES RIVERS: These fabled rivers meet (*B*–4) in Iraq just north of the swamplands around Hawr al Hammar (*A*–8). The single channel, known as al Arab, then flows past Al Basrah (*G*–9) in Iraq and Abadan (*M*–11) in Iran until it empties across a great delta into the Persian Gulf (*S*–18). Crops grown along the riverway consist of wheat, millet, sorghum, cotton, rice, and date palms. The Karūn (*L*–1; *L*–9) and Jarrāhi (*Q*–7) Rivers drain through a swampy region of westernmost Iran.

The entire region here is covered with Quaternary deposits at the surface. Sand dunes, especially, cover barren wastes south of the al Arab. Part of the sheikdom of Kuwait (*F*–17), reputedly underlain by one of the richest concentrations of oil in the world, is shown here, including the "island" of Bubiyān (*N*–19). Plumes of burning gas from oil well heads in both Iraq and Kuwait are visible. *1153–06514;* December 23, 1972.

PLATE 277



NORTHERN SAUDI ARABIA: Hā'il (*K*–8), the largest population center of northern Saudi Arabia, has a special significance in the local history; until 1921 it was the stronghold of the House of Rashid, which had long contested Saudi sovereignty over the central areas of the Arabian peninsula. This great oasis now serves as administrative capital for the northern parts of the central (Najd) province and is the commercial hub for the northern interior territories. Agricultural production, which was originally dominated by date cultivation, has become more diversified in recent years in response to changing dietary habits induced by increased national prosperity; vegetables, melons, and other truck garden crops have become increasingly important with the development of improved irrigation practices. Areas under cultivation are depicted by the pink-tinged areas, which extend up to 16 kilometers (10 miles) from the city.

This area falls within three distinctive physiographic provinces. Northeast from a line extending from *V*–11 to *J*–5, the homogeneous, low-relief, lower Paleozoic sedimentary formations dip gently to the northeast and form a part of the interior homocline. The predominantly yellow-tone area northwest of a line *A*–11 to *N*–1 forms a southeastern part of An Nafūd, the great sand desert of the north. Closely spaced, northeast-trending longitudinal dunes tend to predominate in the immediate area. The remainder of this scene consists of partially sand-covered Precambrian igneous and metamorphic rocks that form the northern part of the Central Plateau; elevations here range from 900 to 1200 meters (3000 to 4000 feet).

During Quaternary time, a volcanic field consisting of more than 30 discrete volcanoes developed along the eastern margin (*U*–10 to *T*–11) of this frame. The distinct alinement strongly suggests that their distribution is controlled by a linear zone of structural weakness. *1049–07145;* September 10, 1972.

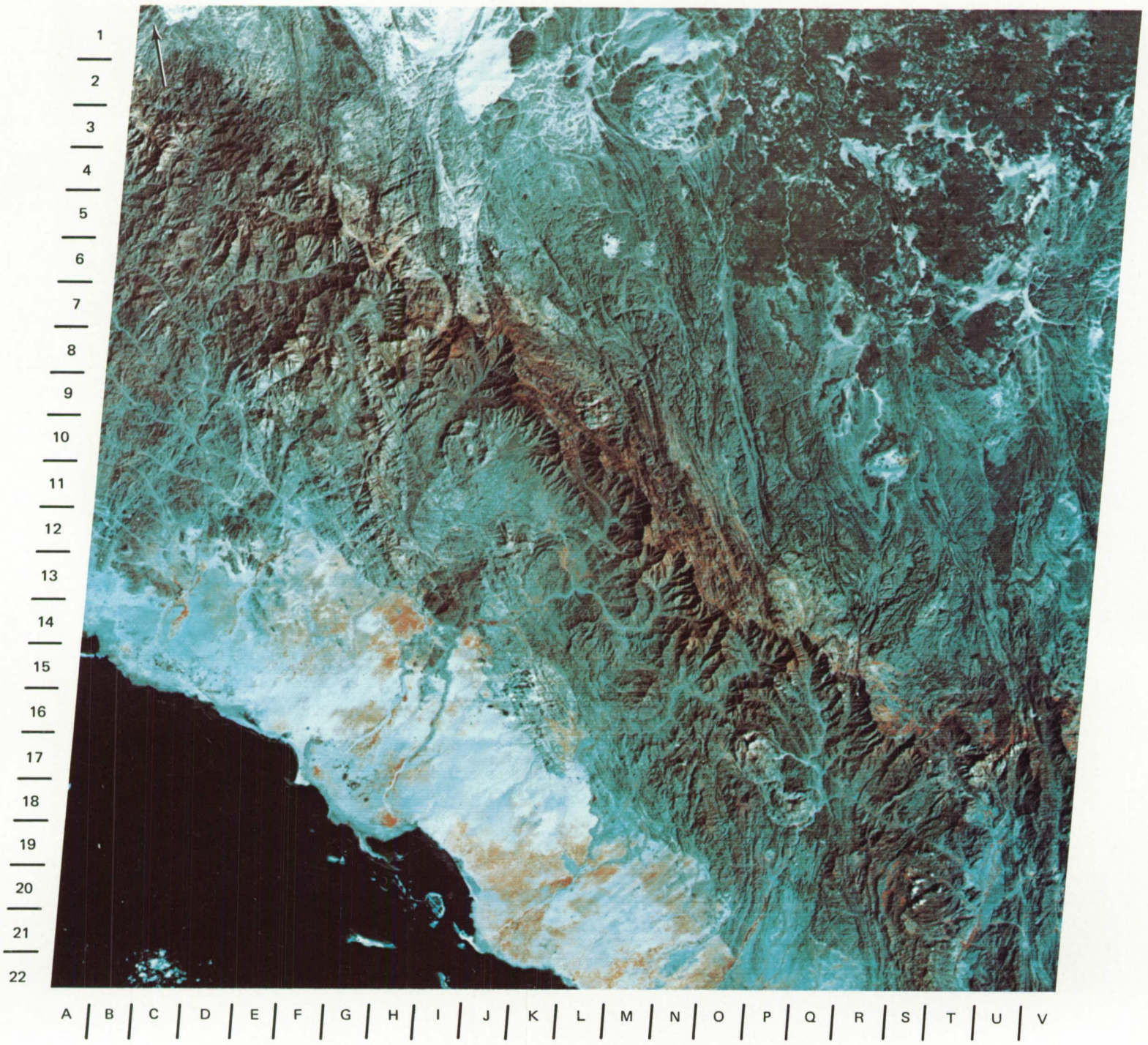


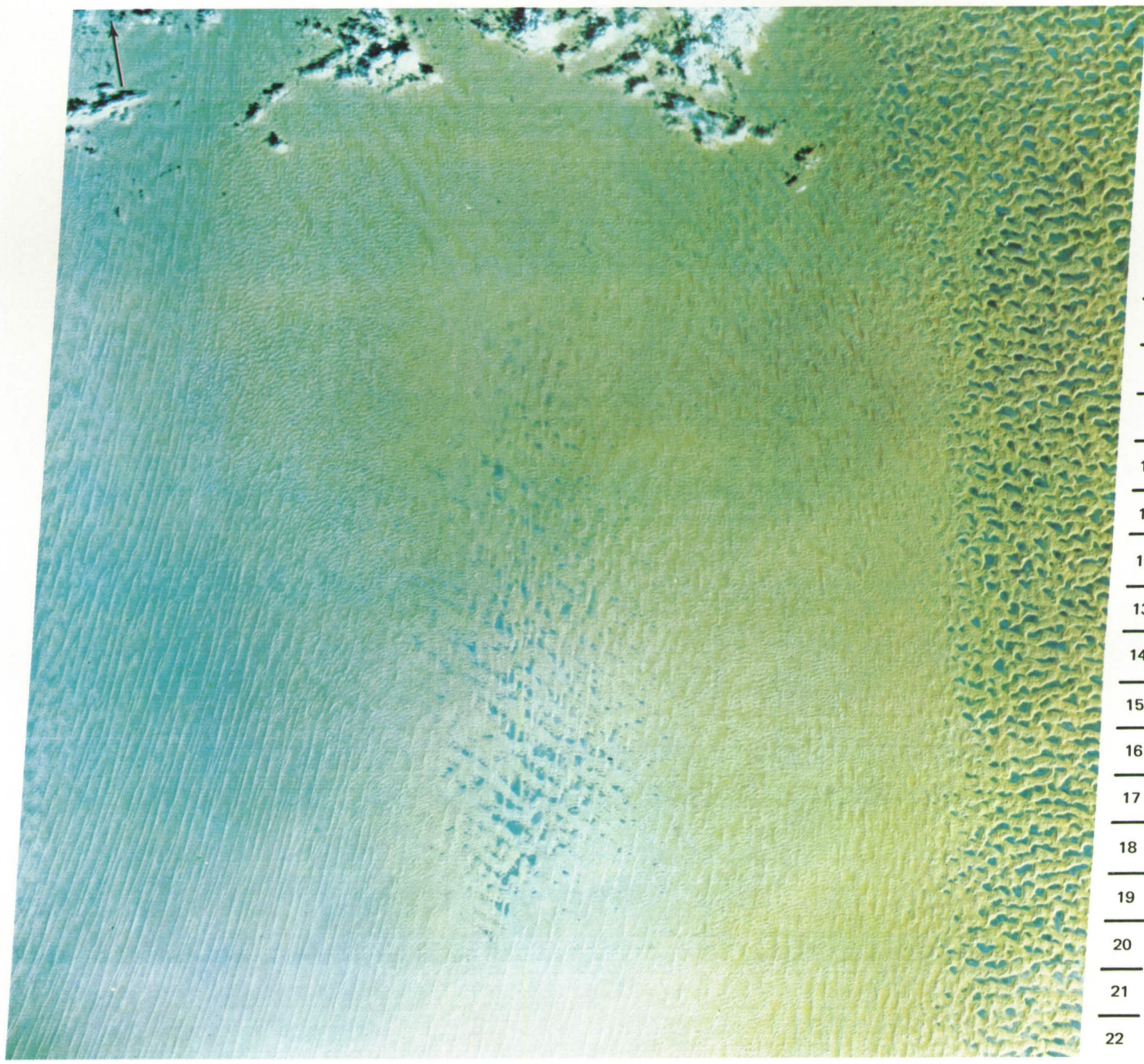
PLATE 278

WESTERN SAUDI ARABIA: The Precambrian basement rocks of western Arabia are generally recognized to have been a part of the African crystalline rock shield until they were separated by Red Sea rifting during early Tertiary time. These lithologically and structurally complex rock assemblages are found a short distance inland from the Red Sea along the entire western peninsula margin.

This scene located about 240 kilometers (150 miles) south of the major port of Juddah provides a good example of the difficulty of mapping rock types even in arid areas where excellent outcrops exist. Regional geologic structure is magnificently displayed, but only a few lithologies can be readily recognized by characteristic hue, shape, or texture. Young sediments, for example, are commonly light colored and develop along the coastal plains and other areas of low relief such as in low-gradient stream valleys. Here, the coastal deposits extend up to 16 kilometers (10 miles) inland; the associated red-tinged areas indicate the abundance of winter vegetation in bloom. Young basalt volcanics, on the other hand, are very dark and, as can be seen in the northeast quadrant (centered about *R*–4), even individual volcanoes and flows can frequently be identified. The complex shield rocks, which dominate this scene, consist largely of various metamorphic rock units that have been locally intruded. Although over a dozen generalized Precambrian rock units have been mapped at small (1:2 000 000) scale from ground surveys, the slight tonal and textural differences of the weathered surfaces do not permit their ready identification from Landsat. Circular intrusions are most easily recognized, and the light ones at *L*–2 and *K*–8 have been mapped as peralkaline granites. A similar feature at *P*–17, however, has been field mapped as a diorite. Computer data enhancement and extraction techniques are currently being researched to improve rock-type discrimination capability.

The single most spectacular feature in this scene is the erosion scarp extending diagonally across the frame from *V*–15 to about *A*–3. This scarp, which does not seem to be controlled by mapped formational units, averages about 1.6 kilometers (1 mile) in height according to published topographic data. *1192–07115;* January 31, 1973.

PLATE 279



EASTERN SAUDI ARABIA: The area shown here overlies the eastern flank of the Ar Rab' al Khālī basin. This immense geologic structure developed largely in response to the separation and movement of the Arabian tectonic plate away from Africa along the Gulf of Aden. The compression that led to the regional down-buckling also formed localized fold structures that now control the accumulation of some of the world's largest known oil deposits. Subsequently, the depression filled with detrital material derived from the basin flanks; the closed nature of the drainage system caused the ground waters within this alluvium to become highly saline. The uppermost strata of the eastern part of the basin thus generally consist of silt, clay, or muddy sands that are commonly saturated with brine and are salt encrusted. These surfaces, locally known as sabkhah deposits, are seen as dark areas visible between sand dunes in the center (*K*–17) and along the eastern margin. The present surface consists primarily of windblown sands deposited above the sabkhah. The configuration of the dune patterns is primarily the result of local wind conditions. Along the eastern edge of this scene a lacelike pattern is developed by a system of closely spaced, compound barchan dunes. The direction of the cusps indicates a dominant northwest wind. On the west, the narrow elongate seif dunes or Urūq parallel the dominant northeast winds. The large complex area between these dune fields is a transitional zone characterized by overlapping sand dunes of several types. *1166–06252;* January 5, 1973.

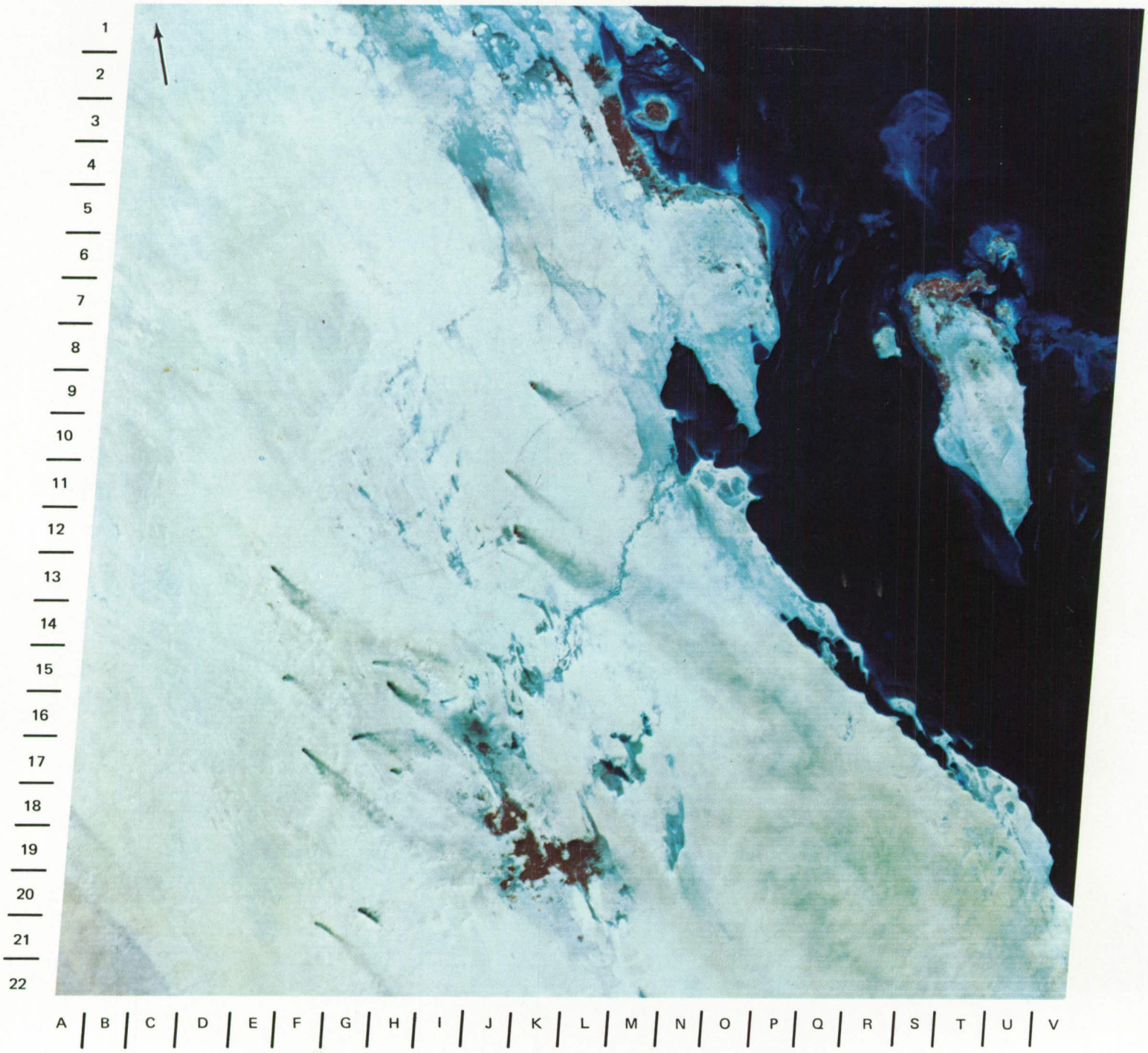


PLATE 280

ARABIAN OIL FIELDS: Beneath the desert sands of eastern Saudi Arabia lie some of the world's largest and most prolific oil-bearing structures. Two of the largest, the Abqaiq (*J*–9 to *J*–12) and Ghawar (south from *D*–13) fields, can be identified here by the huge smoke plumes generated during the burning of residual gas near the gas/oil separation plants; the flames are clearly visible at several of these flaring sites. Headquarters for the giant oil complex is at Dhahran (*M*–6). This community can be identified in the center of the subcircular Damman dome (where the initial discovery of commercial oil was made in 1937) by the red vegetation reflectance of the irrigated lawns.

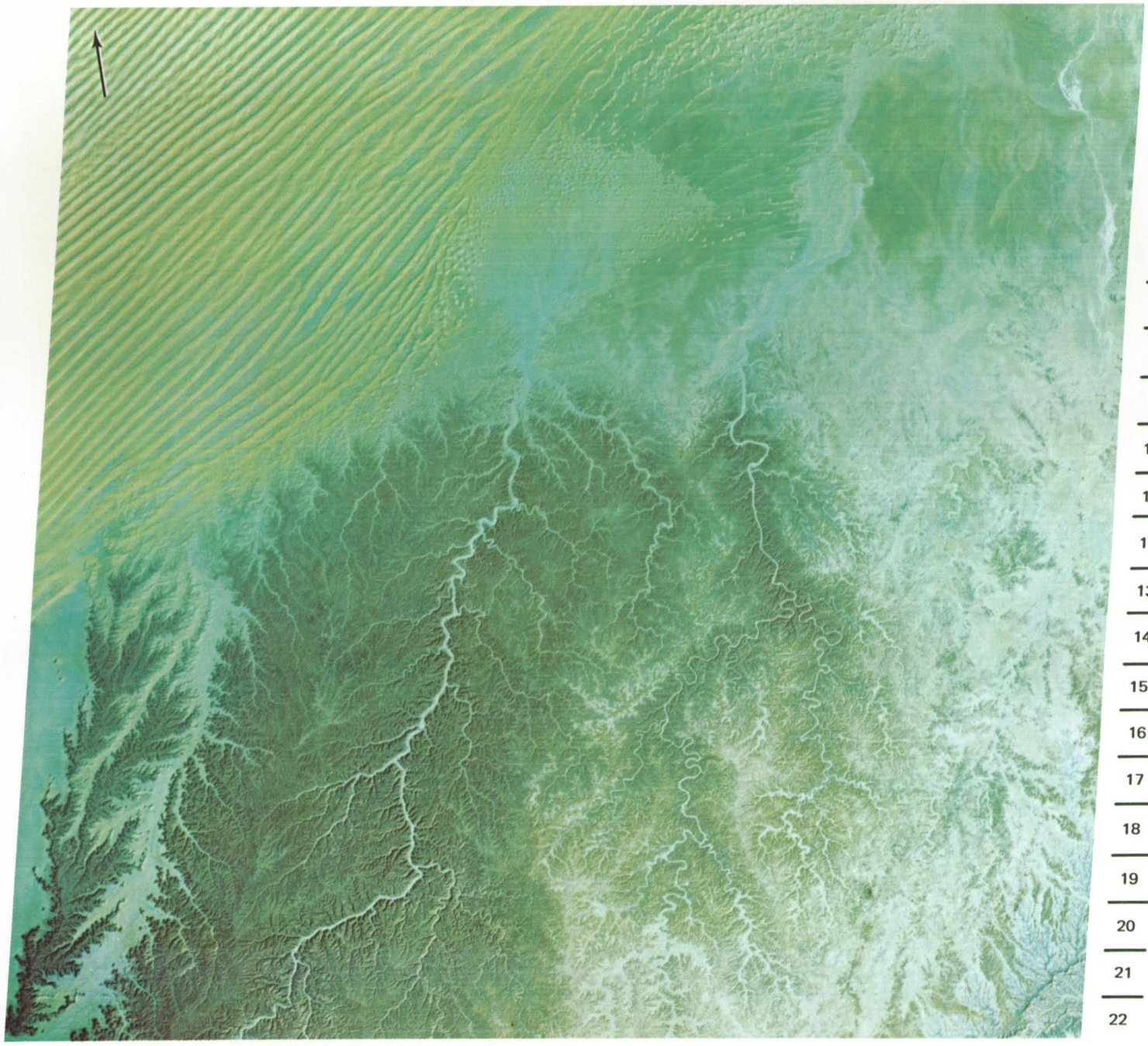
The L-shaped al Hasa oasis (*J*–19) is the largest agricultural center in the Eastern Province, and, until recently, it served as the commercial and governmental center for the area.

In conjunction with the rapid industrial growth, the construction of a modern international airport (*N*–7) southeast of Dhahran and a deep water pier 11 kilometers (7 miles) long (*N*–4) at Damman has made the area an international commercial center. To serve the new needs of the modern community, the provincial government seat was moved to Damman (*M*–5).

The rich agricultural areas of the Al Qatif Oasis (*K*–3; *K*–4) and Tarut Island (*I*–3) are second in size only to those at al Hasa in the Eastern Province. Irrigation waters for these areas are obtained from artesian sources.

The Sheikdom of Bahrain consists of Bahrain Island (*S*–8) and the several smaller islands off the northern east and west coasts. Oil production and refining constitute the main industry of this island country but irrigated agriculture developed near the northern coasts also contributes significantly to the local economy. The lighter blue areas off the coasts indicate shallow coral reefs. *1169–06411;* January 8, 1973.

PLATE 281



SOUTHERN ARABIAN PENINSULA: The Hadramawt plateau is an elevated dissected area located between the southern Arabian Precambrian shield complex, which forms most of the southwestern portion of the Arabian Peninsula, and the sands of the Ar Rab' al Khālī. The formations constituting the plateau are primarily early Tertiary sediments that dip gently northward to form the southern margin of the Ar Rab' al Khālī Basin. The dark strata dominating the southwest quadrant of this scene consist predominantly of calcareous shale and limestone. These grade easterly into dominant massive gypsum deposits. The local drainage systems are strongly influenced by this change in lithology and its related influence on the topography. Note the well-developed dendritic drainage developed in the west (*H*–16) and how it grades to a modified meander pattern in the *P*–13 area and then to a very poorly defined system along the entire eastern margin.

In the northwest quadrant, extensive longitudinal seif dunes or urūq, which are characteristic of large areas of the Ar Rab' al Khālī desert, overlie part of the southern flank of the Ar Rab' al Khālī structural basin. These dunes have formed in response to the dominant northeasterly winds in the area. Note how the dune patterns change east of a line extending from approximately *H*–7 to *L*–1; this is in response to changes in dominant wind circulation cells. Several groups of largely individual dunes have developed near the borders of the light triangular area (*K*–4). Northeast of these (*N*–1), short, compound elongate dunes are distributed along sublinear trends. *1186–06381;* January 25, 1973.

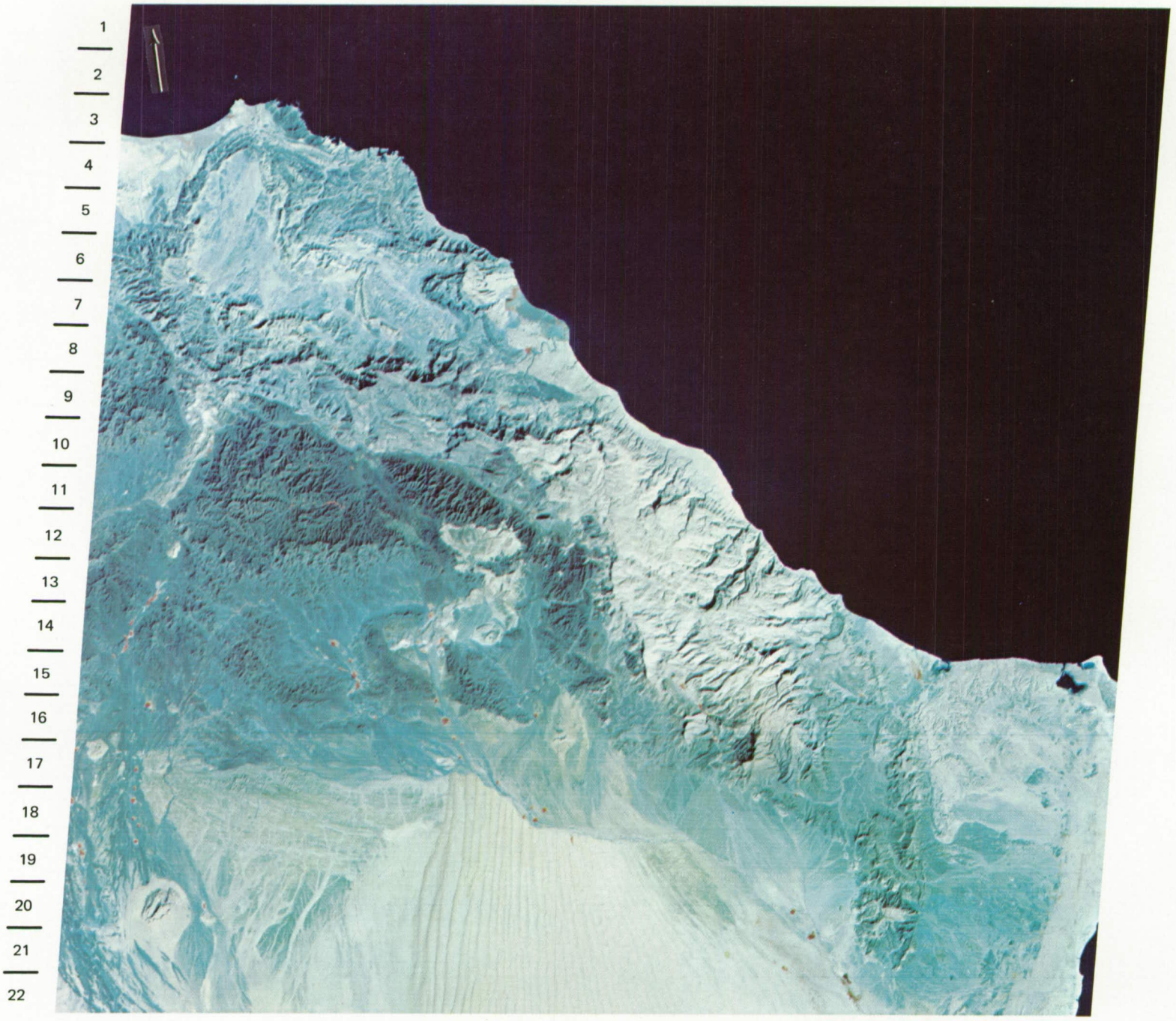


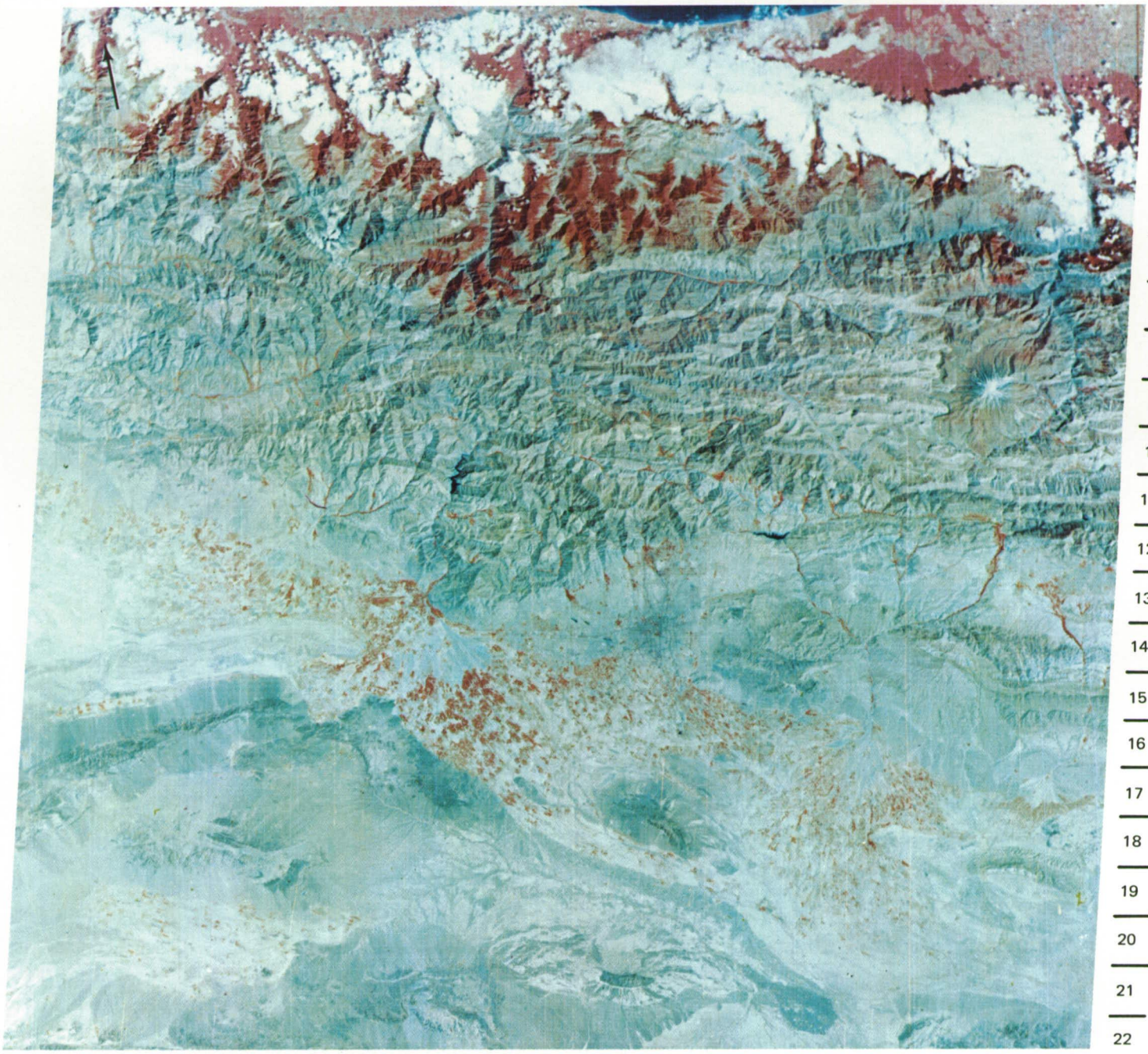
PLATE 282

OMAN MOUNTAINS: This scene centers on one of the more remote parts of the Arabian Peninsula, the Oman Mountains in Muscat and Oman. The area is very sparsely settled; the city of Muscat is at *D*–3, but is not visible. The chief source of income along the coast of the Gulf of Oman *(upper right)* has traditionally been fishing, but here as elsewhere in the Middle East oil exploration is changing this situation. The Oman Mountains are extremely dry, like most of the Arabian Peninsula, but occasional oases and farming areas are visible as red patches.

As other Landsat images demonstrate, the areas best suited for geologic study are frequently the most inhospitable. In the Oman Mountains, the high relief and lack of vegetation combine to expose the geologic structure and lithology unusually well. The Oman arc is an extremely complex area, as the image suggests. Some of the geologic features visible include the Sayh Hatat uplift (*D*–6), a Precambrian area surrounded by Paleozoic and Mesozoic limestones. To the south we see the dark-colored basic and ultrabasic igneous rocks of the Semail igneous complex (*C*–10; *H*–10). These rocks (called "ophiolites" by the petrologist) are poorly understood. H. H. Wilson has suggested that they are the result of eruptions of ultrabasic magma in deep water. He interpreted the structure of the Oman Mountains as resulting from crustal tension associated with formation of the Gulf of Oman. Other geologists, however, feel that compression resulting from the supposed collision of the Arabian Peninsula with Asia has produced the structures shown here.

Other interesting geologic features visible include a salt dome (*B*–19), the Jebel Madar, longitudinal sand dunes (*G*–20; *M*–20), and radiolarian cherts of the Hawasina unit (*E*–18). The northeastern part of the Oman Mountains has been covered by Tertiary limestones (*K*–10; *M*–15). An important geologic relationship widely misunderstood is shown here; the mountains near the tip of the peninsula turn south (*R*–16; *R*–20) instead of striking east into the ocean, as generally illustrated in the geologic literature and textbooks. *1126–06022;* November 26, 1972.

PLATE 283



TEHRAN, IRAN: The capital of Iran (*M*–13) is located at the edge of a long desert basin near the base of the Elburz Mountains (*J*–6). These mountains infringe on the southern end of the Caspian Sea (*M*–1), spanning part of a chain that runs from the Turkish-Armenian S.S.R. border on the west to the Iran-Turkmen S.S.R. border east of the scene. The highest peak in the Elburz range, and in all of Iran, is Mount Damavand (*T*–8), which rises to 5601 meters (18 376 feet).

The Elburz Mountains consist largely of Mesozoic sedimentary rocks on the north surrounding a core of Paleozoic rocks at higher elevations. Folding of the chain began in the Eocene and culminated in Oligocene time with volcanic outpourings that are now part of the range. Volcanic rocks also make up the hills south and west of Tehran and the cultivated plains watered by the Shur (*K*–18), Karaz (*E*–13), and Jaji (*R*–13) Rivers. Vegetation in these lowlands is largely steppe grasses with scattered juniper and pistachio trees. On the side of the mountains facing Tehran, the vegetation gradually changes from one of increased numbers of juniper trees to a series of altitude-dependent zones of grasses and alpine shrubs characteristic of a cold temperate climate. On the Caspian side, Mediterranean-type vegetation covers the slopes. *1044–06434;* September 5, 1972.

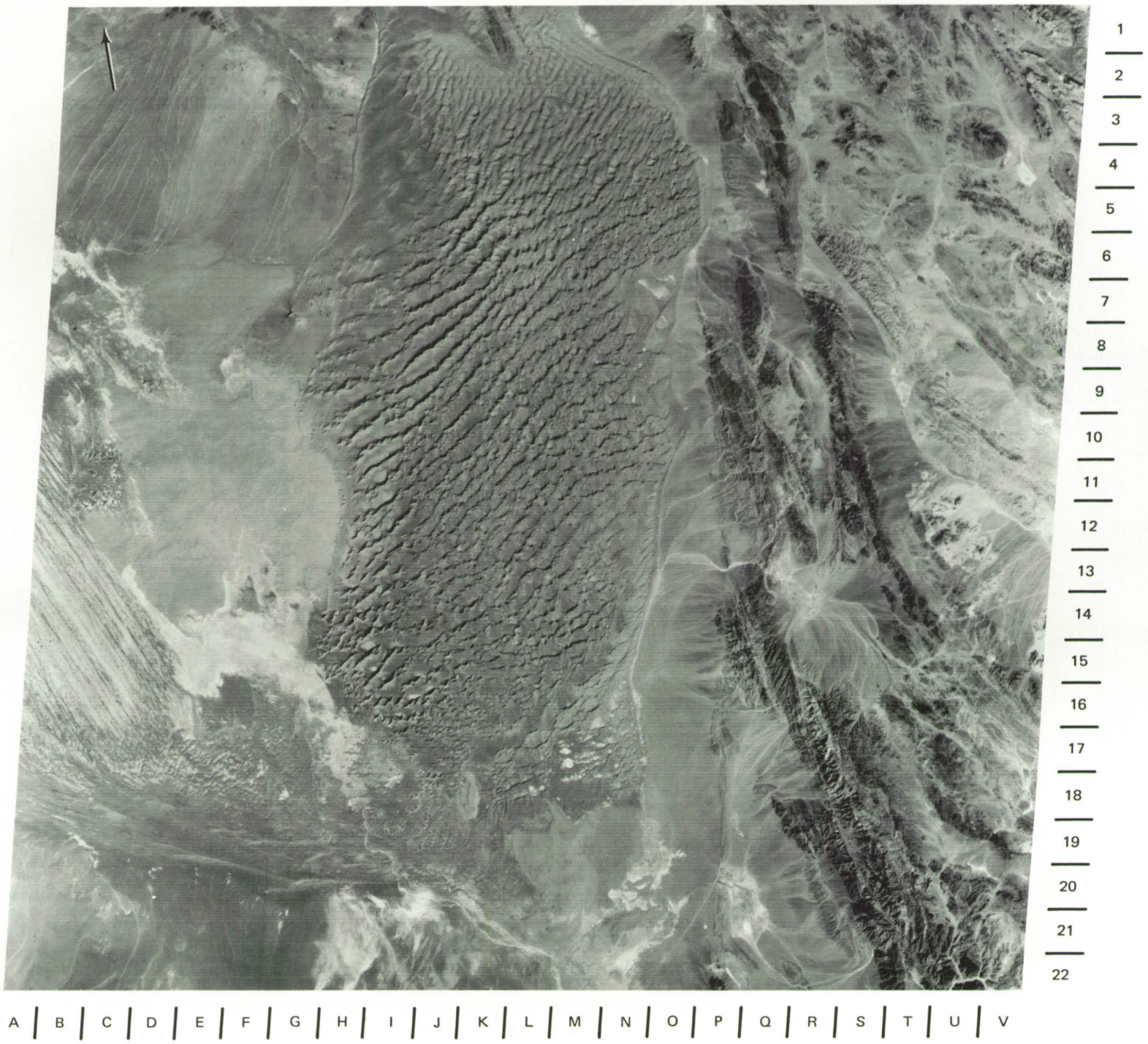


PLATE 284

THE GREAT KAVIR, IRAN: This scene is centered about 320 kilometers (200 miles) southeast of Tehran. The term "kavir" refers to playas or ephemeral lakes that usually contain water during the wet season but are dry salt crusts or clay flats most of the year. Such salt crusts are evident at *B*–14, *Q*–17, and *R*–2, and a typical clay flat appears at *N*–21. Less well-developed salt crusts, without extensive surface saline deposits, occur at *F*–10 and *K*–12. These playas occupy depressions in the regional peneplain surface of the Great Kavir that, in this area, stands about 640 meters (2100 feet) above sea level. Much of the peneplain is developed on intricately folded Miocene and Pliocene sediments. Those exposed in this scene are mainly siltstones, marls, and evaporites of the Miocene Upper Red Formation. In many places, beveling defines a "plan view cross section" of individual folds (*C*–7; *J*–4). Uplifted blocks form higher mountain ridges (*C*–2; *G*–21). The Great Kavir fault is a major rift that cuts across *D*–20 and *O*–17 in this scene.

A road has been proposed for construction through the western *(left)* part of the image, passing on the east side of the playa. Studies of Landsat imagery by D. B. Krinsley of the U.S. Geological Survey indicate favorable conditions here for an all-weather road that would shorten the present road distance between northern and central Iran by almost 725 kilometers (450 miles). *1149–06273;* December 19, 1972.

PLATE 285



DASHT-E-LUT, EASTERN IRAN: These two adjacent frames were selected to show two distinctive types of eolian features formed in a desert terrain. The area is centered on the salt wastes of the southern Dasht-e-Lut desert. This desert is bounded on the west by folds of Mesozoic sedimentary rocks intruded by post-Cretaceous granites. Thrust faults and other fractures cut through this range. On the east are late Cretaceous and Paleocene folded sedimentary rocks (*R*–18), Eocene volcanic rocks, and younger (Miocene-Pliocene) basic intrusives (ophiolites). The western edge of this range is bordered by a large thrust fault (*O*–16).

Quaternary desert deposits occupy the Dasht-e-Lut. The area referenced at *N*–7 is known as the Namakzar, identified on some maps as a salt marsh and others as a dry salt lake. As a geomorphic

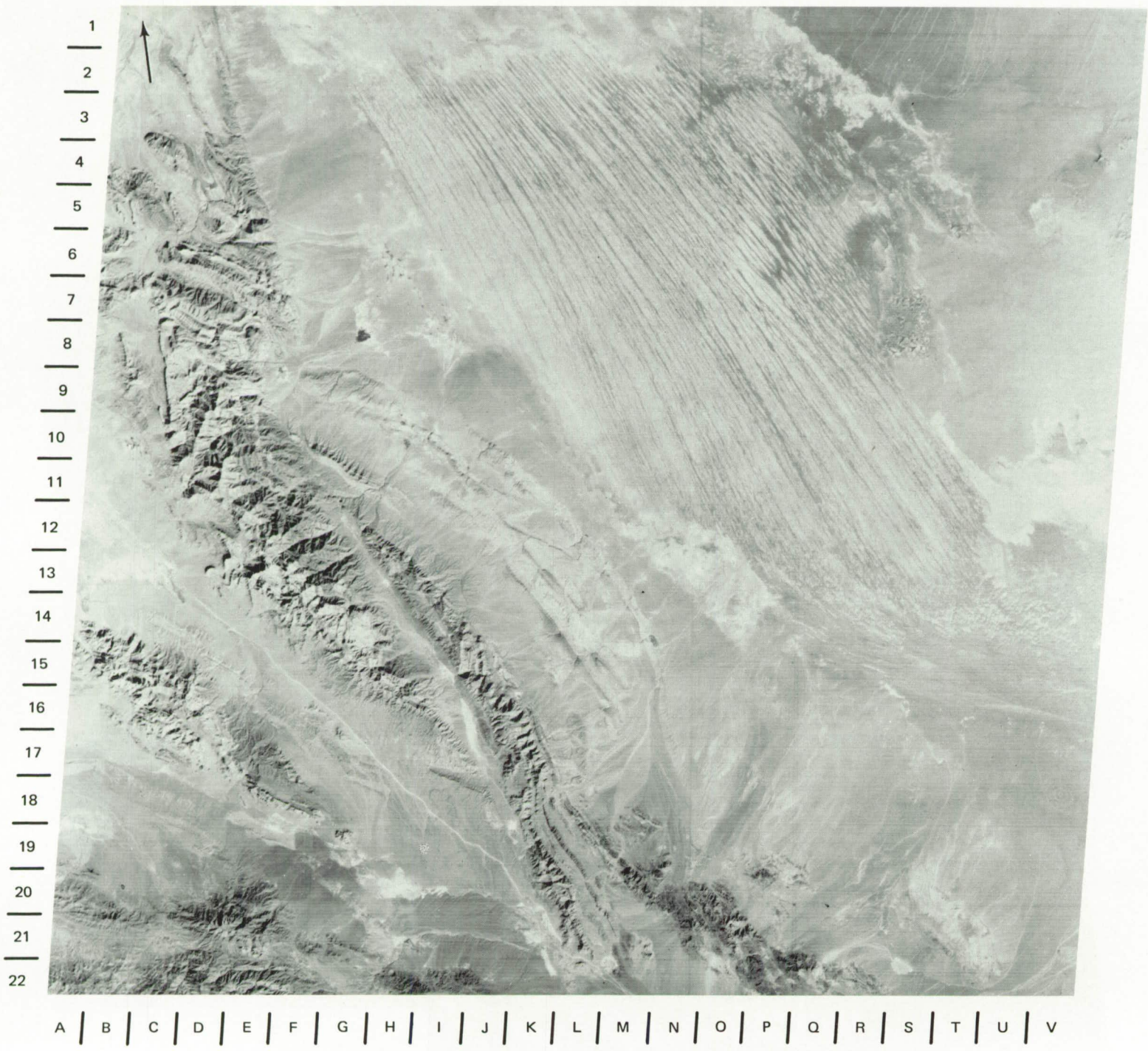
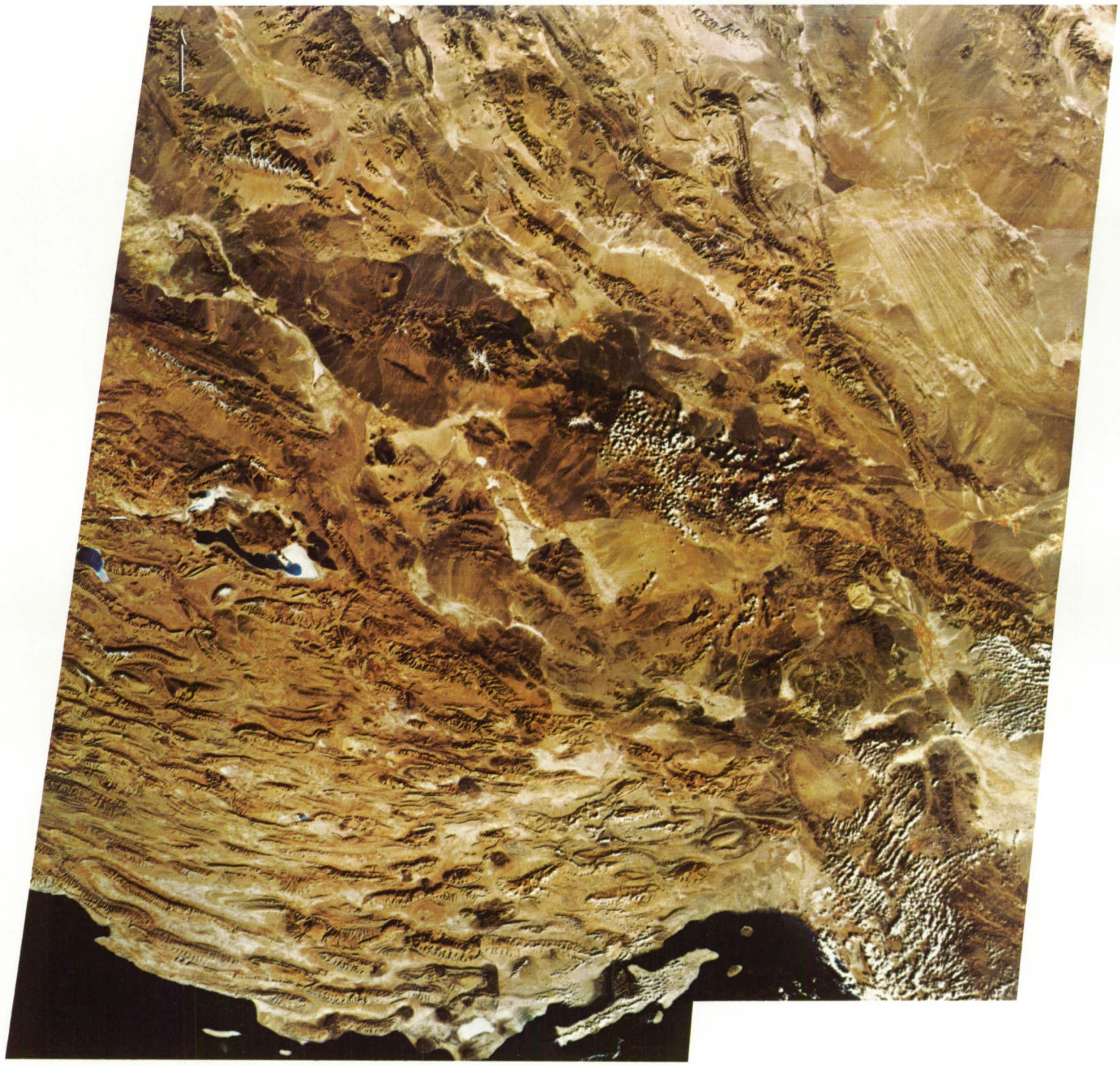


PLATE 286

feature, it is actually a yardang—a series of elongate ridges and depressions formed by eolian erosion of unconsolidated clay sediments. The direction of elongation parallels the direction of prevailing winds. The sand sea deposits to the east (*K*–10) are organized into a large field of transverse dunes oriented roughly at right angles to the wind.

One of the few arterial routes running through the center of Iran from Pakistan and Afghanistan to Tehran stands out in sharp contrast (*I*–18) to the desert surface in this scene. The town of Kermān (*C*–13), the largest in this region, is a junction for several roads in this desolate part of old Persia. *1127–06060;* November 27, 1972 (plate 285). *1128–06114;* November 28, 1972 (plate 286).

PLATE 287



SOUTHERN IRAN: This mosaic of 12 Landsat images illustrates much of the geologic structure of the southern end of Iran. (See plate 288 for letter identifications.) Most of the region was once part of the great Tethys geosyncline that extended northwestward through the present Mediterranean and its surrounding mountains and was intensely deformed in the Cenozoic, with maximum activity in Pliocene times. Activities associated with continuing plate tectonic movements persist today as evidenced by frequent earthquakes.

Quaternary desert features, including yardangs (*A*), appear in the upper right corner. A line of mountains made of Mesozoic rocks extends northwestward east of the arterial junction of Kermān. High mountains (some exceeding 4200 meters (14 000 feet)) to the west (*B*) consist mainly of volcanic rocks. West of the Sirjan depression (*C*) are the High Zagros Mountains (*D*), composed of Mesozoic rocks, some Tertiary sedimentary rocks, metamorphosed Paleozoic rocks, and a core of Archean (Precambrian) crystalline rocks and granites. Ophiolites intrude into this complex. Several major thrust faults (*E*), involving southwestward movements of these blocks, follow the trends of these mountains. The thrust sheets extend into the main belt of the Zagros Mountains (*F*), where Tertiary limestone and sandstone units have been folded into huge anticlines commonly breached by erosion to expose Cretaceous interiors. In addition, this region has been pierced by many immense salt domes, including some that form islands in the Strait of Hormuz (*G*) between the Persian Gulf and the Gulf of Oman. At the lower right is the Bashagird Range (*H*), the westward termination of the Makran Range (see plate 290), which abuts against the Zagros trend along sharp fault lines. This mosaic was prepared by the Earth Satellite Corp., Washington, D.C., for the Government of Iran.

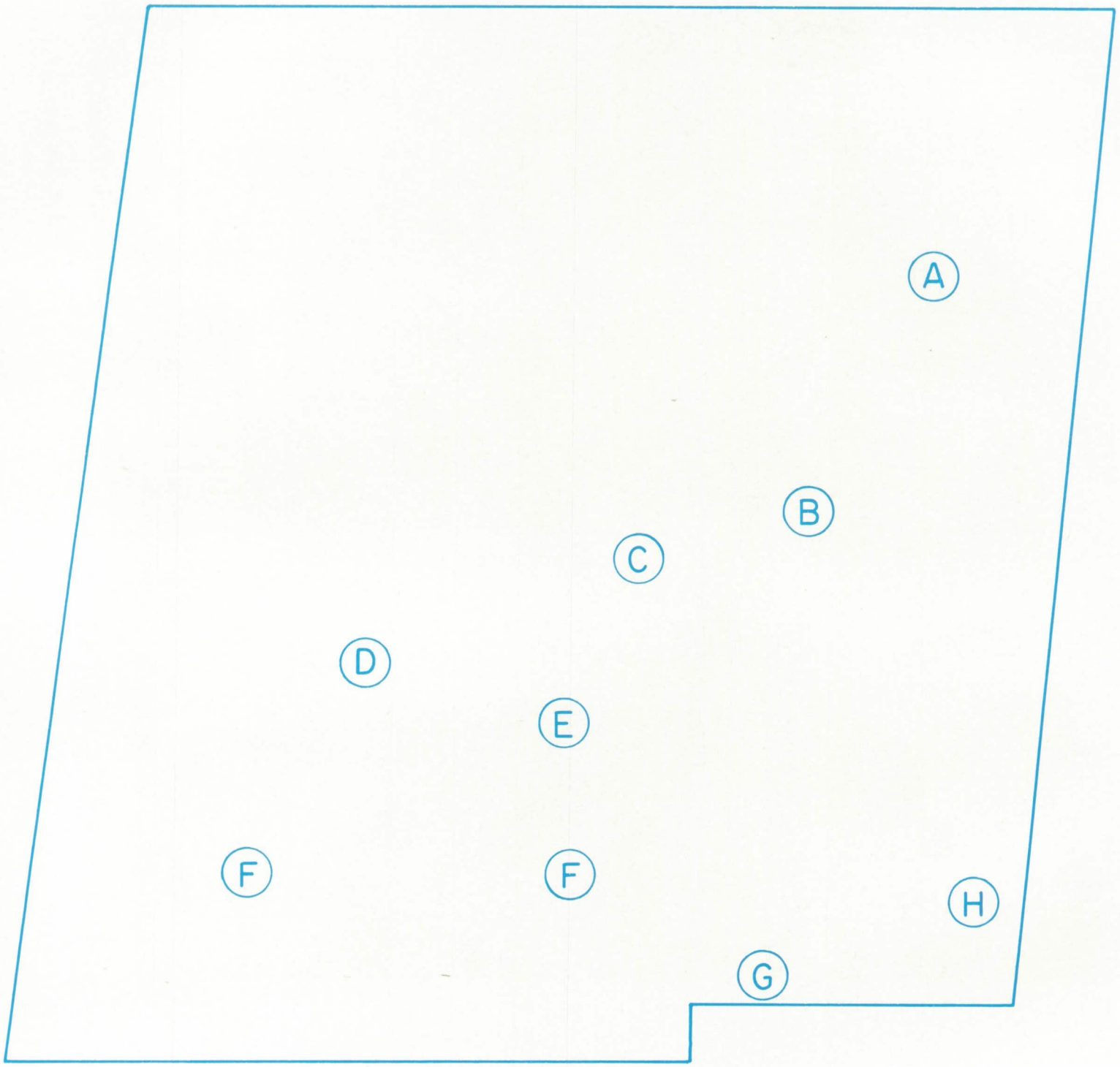
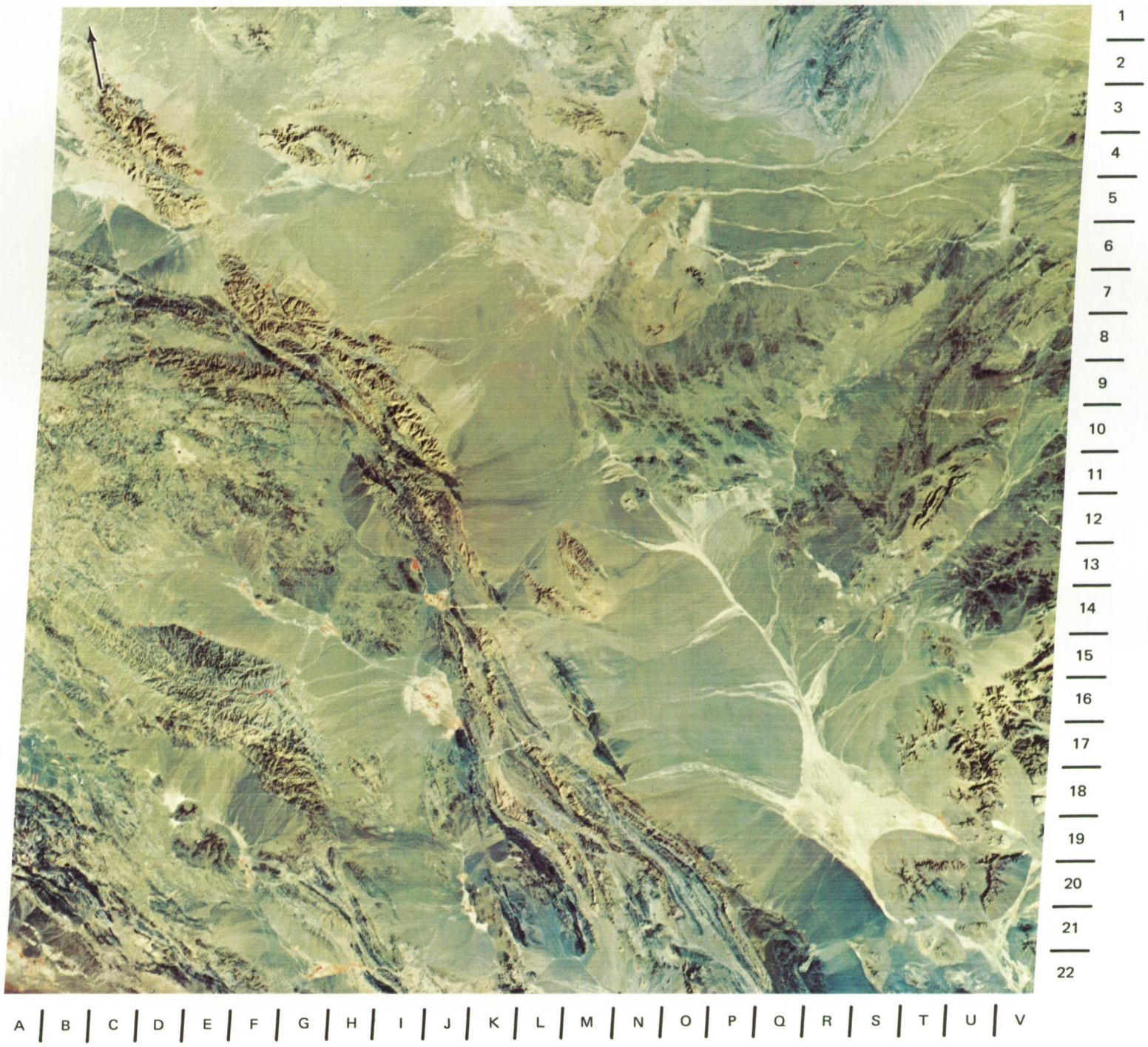


PLATE 288

PLATE 289



THE IRAN-AFGHANISTAN BORDER: A vast belt of rocks folded in an Eocene-Oligocene orogeny lines the eastern uplands border region of Iran from Mashhad in the northeast to the Makran Range of western Pakistan in the south. Tertiary (*O*–19) and Mesozoic (*E*–7) sedimentary rocks, mixed with extensive volcanic rocks (*F*–17), make up the mountains east of Birjand *(west of left margin).* The border runs through the Dasht-e-Naomid Desert (*K*–10), with its playa lakes (*I*–1; *L*–5). The mountains in Afghanistan, south of Herat *(off upper right corner),* here trend to the northeast roughly at right angles to those in Iran. These include volcanic rocks (*U*–13), Paleozoic crystalline rocks (*T*–8), and Mesozoic sedimentary rocks (*U*–17) that were involved in mountain building events from the late Mesozoic through early Tertiary.

The region is sparsely populated, with some permanent settlers and nomadic tribes. Farming is limited to small oasislike areas (*I*–13) around stream channels where water must be extracted from wells. More extensive agriculture is developed around Zabol, just south of the image; around Helmand delta; and around the Hamun-e-Saberi (lake), from which the Harut River flows to the northeast just below the lower right corner. Natural vegetation is confined mostly to steppe grasses and scattered brushland. *1073–06042;* October 21, 1972.

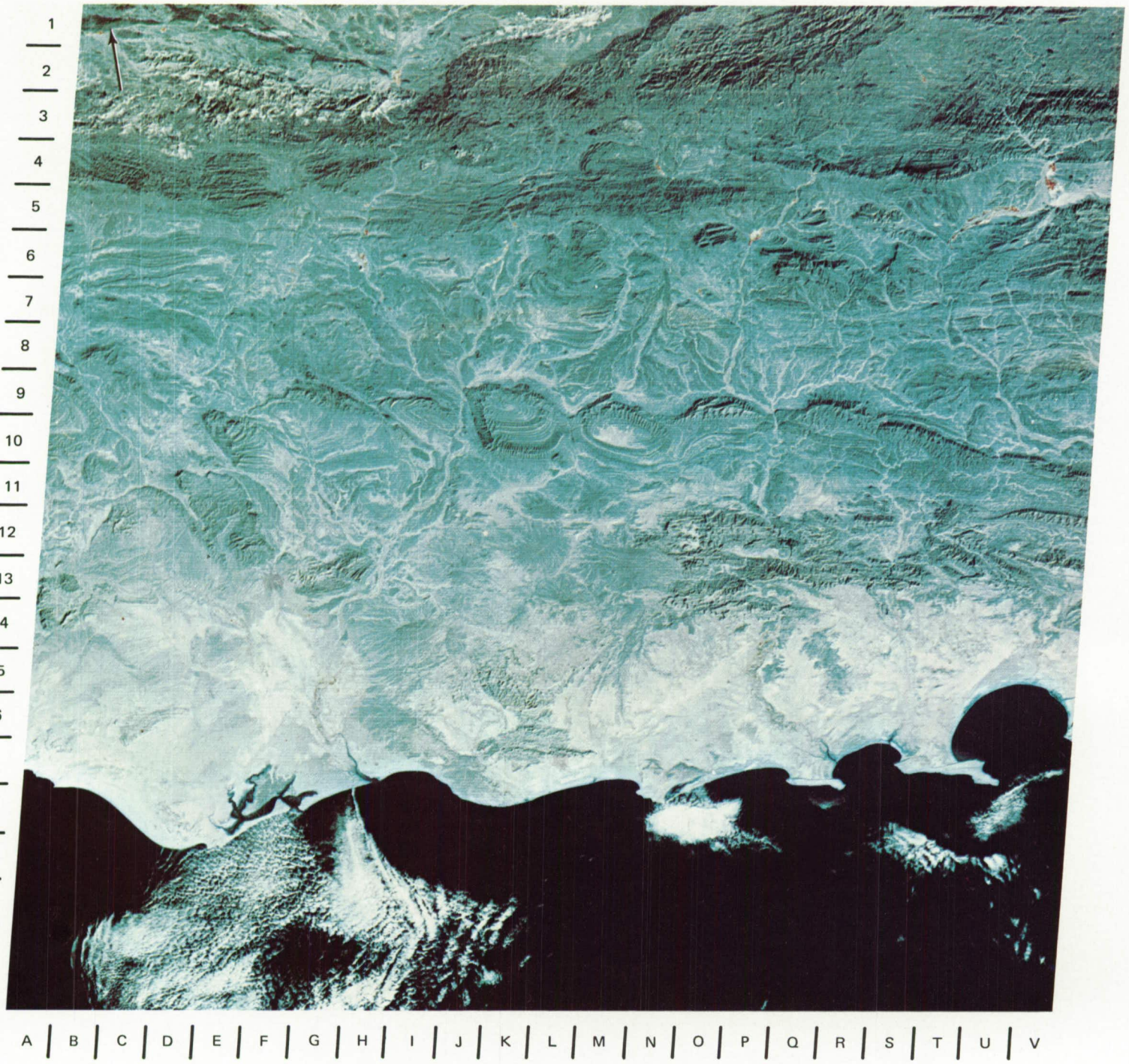
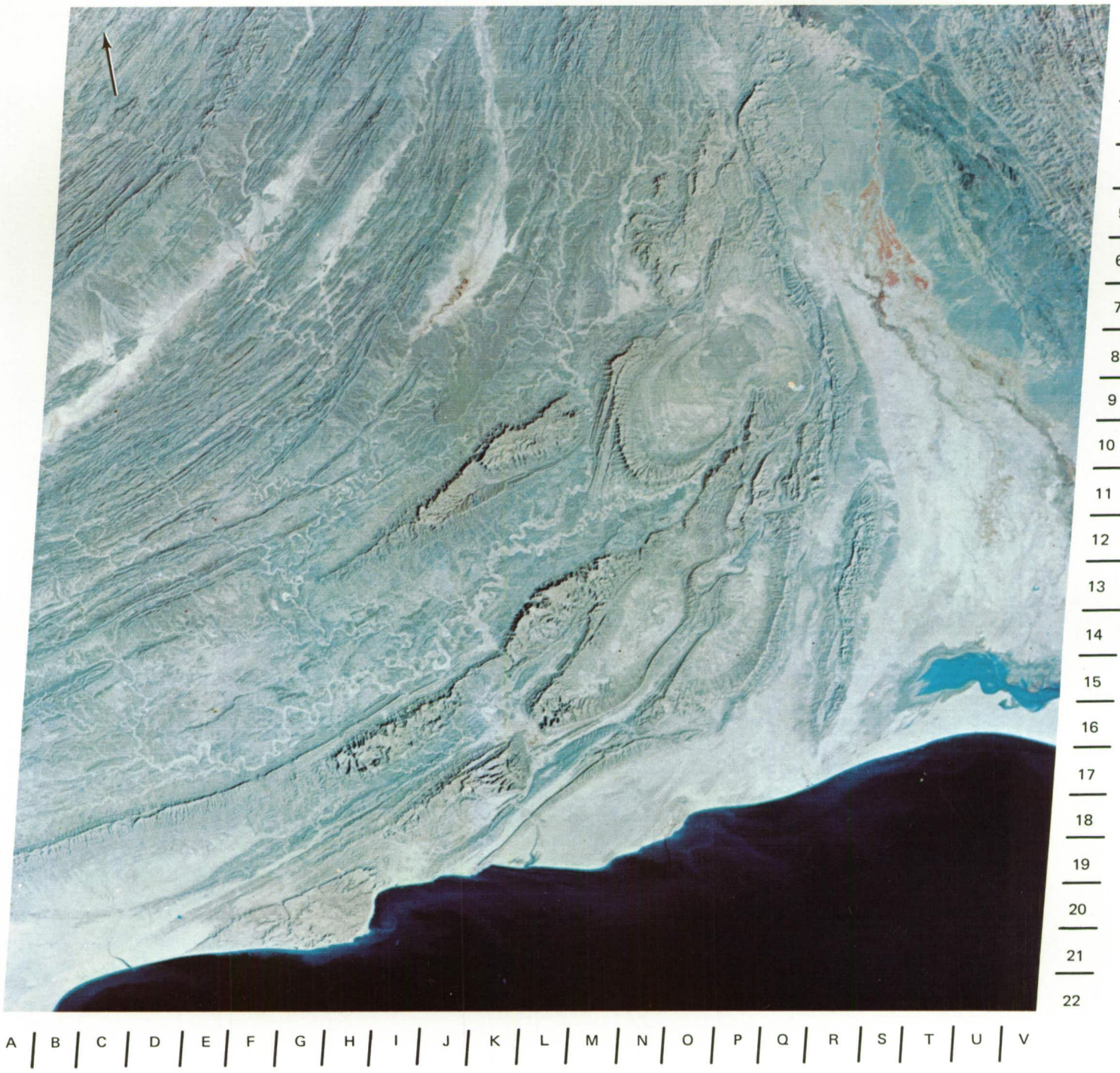


PLATE 290

MAKRAN RANGE, IRAN: This broad band of fold mountains lies between the Zagros Mountains along the Persian Gulf and the Baluchistan Ranges in Pakistan. These mountains can be subdivided into two zones: the coastal zone and the high Makran Range. The coastal zone (*G*–11; *S*–11), along the Gulf of Oman (*L*–20), is made predominantly of Tertiary carbonates and sandstones whose style of folding resembles that of the Zagros anticlines to the northwest. The high Makran Range (*J*–3) further inland consists of late Precambrian and Paleozoic metasedimentary rocks whose style of deformation, into continuous belts of steep-dipping units, is similar to the fold belts in Pakistan. (See plate 291.) Ophiolites (metamorphosed basaltic rocks and greenstones that represent upward intrusions and infolding of deep oceanic crust) are evident at *C*–3 in this part of the range. Note also the pattern of regional jointing—and some faulting—at *U*–3. Most of the deformation that produced the present structures took place in the Miocene and Pliocene epochs. Vegetation is extremely sparse in these mountains except in a few moist areas in the generally dry streambeds. *1090–06010;* October 4, 1972.

PLATE 291



BALUCHISTAN MOUNTAINS, PAKISTAN: Two structural trends come together in this view of the barren mountains of the Baluchistan section of Pakistan. The Central Makran Range (*E*–8) and the Makran Coast Range (*J*–17) consist of tightly folded and extensively faulted Oligocene and Miocene sedimentary rocks. Here they are deflected from their eastward trend along the coast toward a northward trend that continues for another 400 kilometers (250 miles) beyond the upper edge of the image. They abut abruptly against the Pab Range (*U*–2) along a pronounced fault line (*S*–6). The Pab Range contains open folds and steep strata varying in age from Jurassic and Cretaceous rocks through Paleocene and Miocene-Pliocene sediments. These ranges, which here rise 1200 to 1500 meters (4000 to 5000 feet) above sea level, are covered by sparse grasses and dwarf shrubs but are mostly bare rock. Narrow valleys lined by alluvial fans are often occupied by dry rivers, such as the Hingol (*F*–13) and Nal (*I*–7) Rivers. Some farming (mainly wheat and barley) takes place along the Rorali River (*R*–17). This river is building a delta and flood plain into Sonmiani Bay (*T*–15) on the Arabian Sea. Karachi lies off the image on the coast about 100 kilometers (60 miles) to the southeast. In the high mountains few permanent settlements are found; many of these are situated near karez—tunnels into the fans that tap near-surface water. Many peoples are nomadic and engage in raising sheep and goats. *1068–05373;* September 29, 1972.

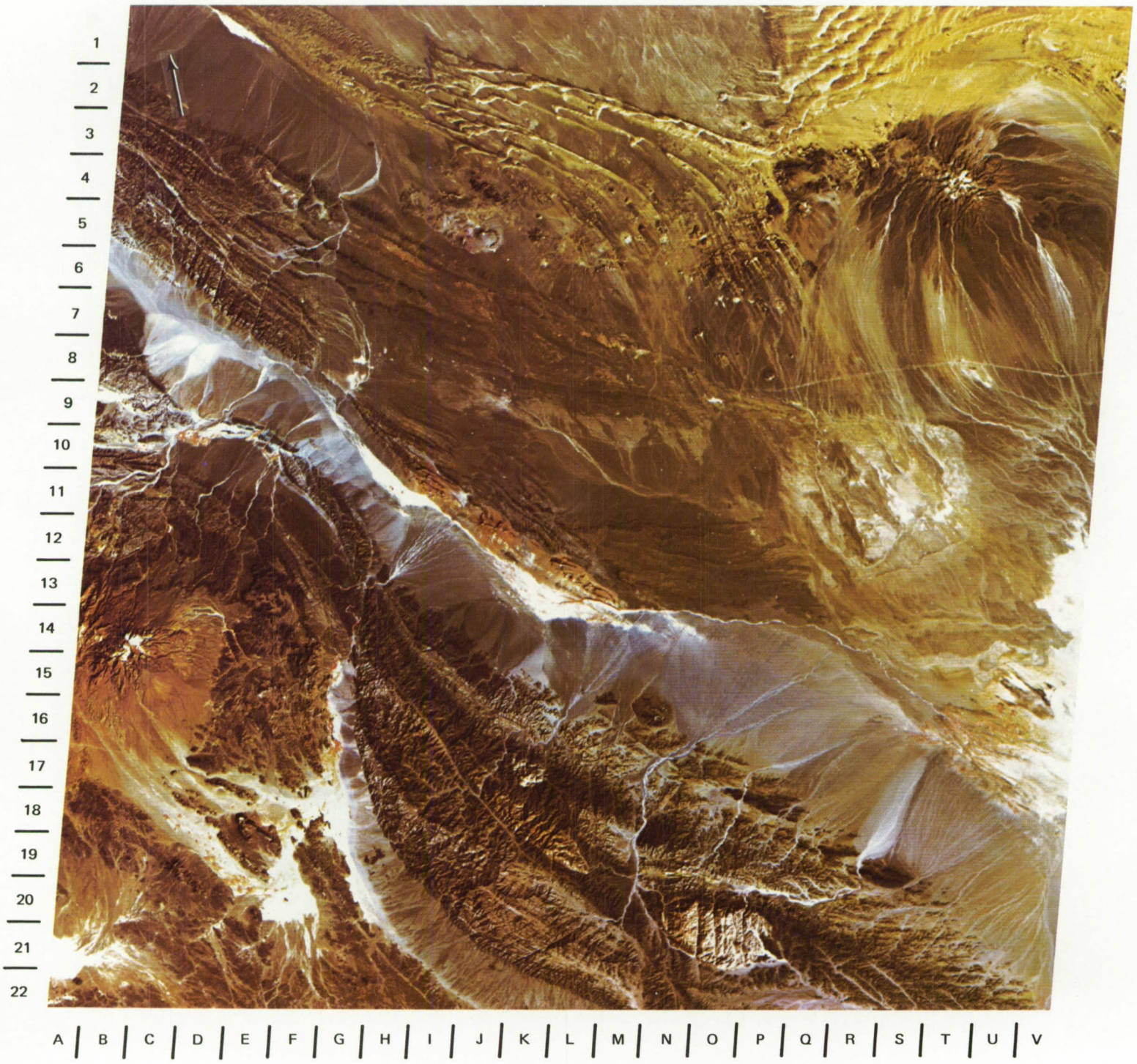
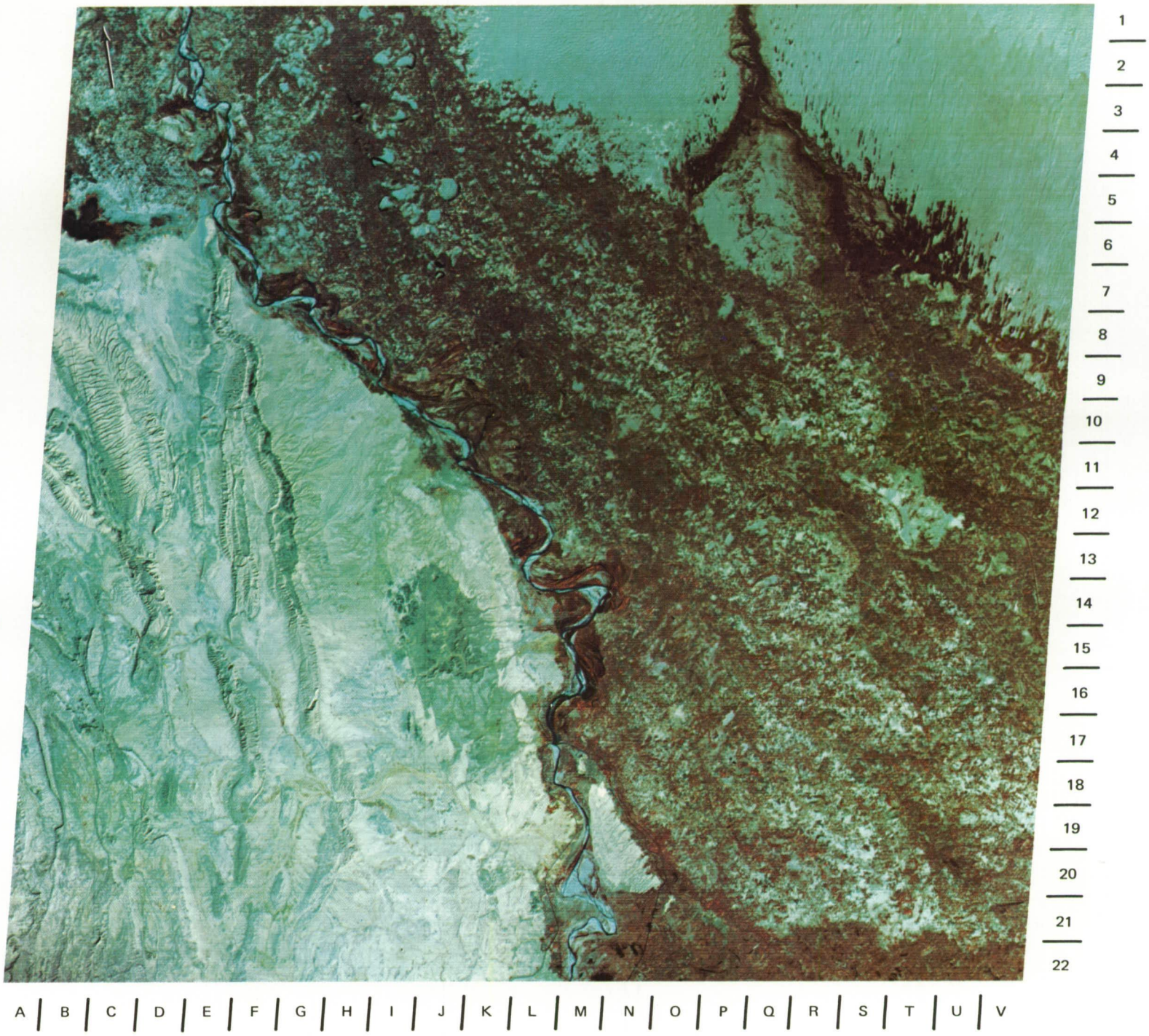


PLATE 292

THE BALUCHISTAN DESERT: This remarkable image is another of the experimental versions made by R. Bernstein of IBM in which the final photo product is made directly from computer tape data without the need to generate an internegative. Most specialists familiar with Landsat imagery consider this view to be an outstanding example of the quality of information (in terms of tonal balance and resolution) inherently extractable from the multispectral scanner data. It is certainly competitive with the best photographs obtained from the Skylab, Apollo, and Gemini missions.

The border between the westernmost end of Pakistan (*P*–7) and the eastern edge of Iran (*D*–27) lies along the Tahlab River (*I*–12). The Mirjawa Range (*K*–19) exposes folded and faulted sedimentary rocks of Cretaceous and Tertiary age. In places these rocks have been intruded by igneous plutons (*N*–21). The large dormant volcano Kuh-i-Taflan (*B*–14) is a dissected cone rising to 4615 meters (13 262 feet). Another volcano, Koh-i-Sultan (*S*–4), just below the Afghanistan border, reaches 2333 meters (7654 feet) in the western Chagai Hills (*P*–4). The edge of a series of longitudinal sand dunes (*D*–1; *K*–3) appears to the north. The main road and rail line (*P*–9) through northern Pakistan into Iran is visible north of the large Hamun-i-Mashkhel Playa (*V*–15). Several other auto roads pass through the junction town of Khāsh (*E*–20). At several localities, such as at Saindak (*D*–4), deposits of porphyry copper ores are associated with the metamorphic rocks around igneous intrusives. R. Schmidt, of the U.S. Geological Survey, has used the Saindak deposit as a reference site for "training" a computer classification program to recognize similar surface reflectance signatures in this Landsat scene. More than 20 other areas in the scene are classified as similar to the altered rock present at Saindak. At least five of these show signs of copper mineralization and are being investigated by Pakistani geologists. *1125–05545;* November 25, 1972.

PLATE 293



THE INDUS RIVER PLAINS, PAKISTAN: The Indus River (*K*–12), beginning far to the north as glacial melt water from the Krakoram Range of the western Himalayas, forms a broad inland delta (*R*–16) in the Sind Province as it approaches the Arabian Sea (about 100 kilometers (60 miles) south of the image bottom). This delta today is topped by flood plain and streambed deposits laid down by numerous now-abandoned channels of the older Indus River. Natural vegetation is composed of a brushland of semidesert subtropical shrubs, thickets, and grasses intermixed with open patches of sand. Rainfall in the region is generally less than 13 centimeters (5 inches). The delta is crossed by many irrigation canals, turning watered areas into "oases" in which paddy rice, wheat, cotton, and millet are grown. The heart of the delta is at Hyderabad (*M*–17), a city of nearly a half million people.

The western end of the Thar desert appears in the upper right of this image. Barchan dunes (*M*–1) develop west of the Nara Canal (*O*–3); longitudinal dunes (*R*–2) occur above the Mithrau Canal (*Q*–5).

West of the Indus River the country changes rapidly as the dry, rocky terrain of the Kirthar Range (*B*–11), part of the Baluchistan mountain system, turns to the north. The conspicuous anticlines and synclines (*E*–12) expose Eocene, Oligocene, and Miocene sandstones and limestones. Younger Miocene and Pliocene sedimentary rocks occur closer to the river except for an outlier of Cretaceous and Paleocene rocks (*J*–15) near Hyderabad. *1120–05270;* November 20, 1972.

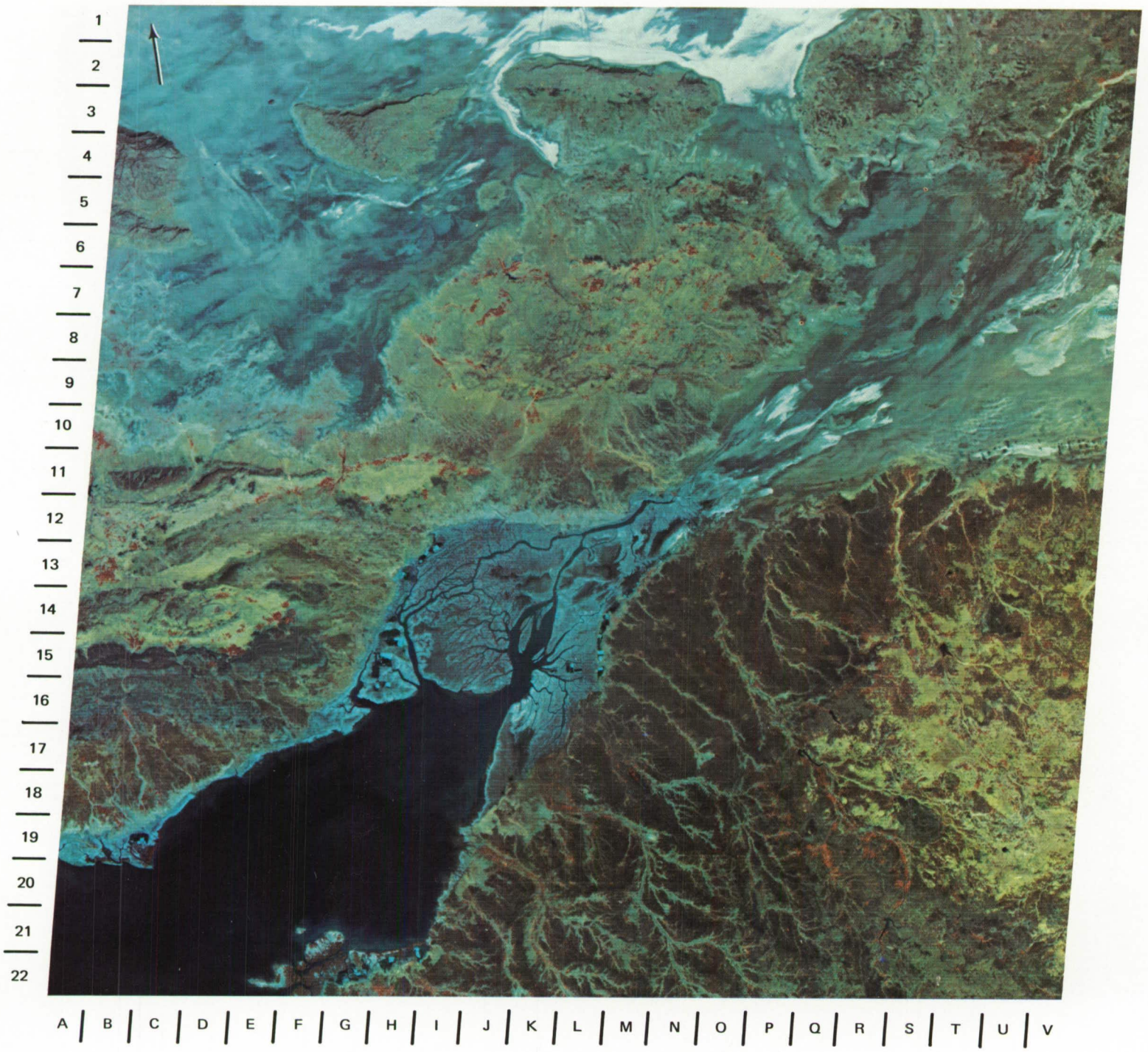


PLATE 294

THE RANN OF KUTCH, INDIA: The Gulf of Kutch (*E*–19) is bounded by the Kutch Lowlands (*E*–7) on the north and the Kathiawar peninsula (*O*–19) on the south. Much of this western part of the State of Gujarat consists of vast tidal salt marshes developed on Quaternary alluvial plains that lie close to sea level. The Kutch marshland has been divided into the Little Rann of Kutch (*I*–13), with its maze of interconnected channels, and the Great Rann of Kutch (*F*–6), both of which partly inundate vast stretches of mud, in places isolating higher ground as "islands" (*G*–3). Older, usually subaerial mudflats with dry saline-encrusted surfaces are visible at *O*–1 and elsewhere. Slightly higher elevations on both sides of the gulf are covered by Deccan basalt flows (*C*–17; *N*–15), which have weathered in places to red soils and elsewhere to regur or black soils deficient in nitrogen and humus. Still higher elevations (*H*–9; *Q*–2; *U*–17) are underlain by sedimentary rocks of Jurassic and Cretaceous age. Just north of this scene, the Sind and Thar deserts are now encroaching upon the Rann. Agricultural activities are confined to clusters of farms growing wheat, cotton, and millet along streams and open areas where soils from the basalts and sedimentary rocks are more favorable. Natural vegetation in these areas consists of savanna thickets and a few dry forests. *1190–05161;* January 29, 1973.

PLATE 295



GULF OF CAMBAY, WESTERN INDIA: This region, in the State of Gujarat, is located along India's west coast some 320 kilometers (200 miles) north of Bombay. The Gulf (*G*–17) forms a major inlet from the Arabian Sea. It is bounded by the Kathiawar peninsula (*B*–14) on the west. The Mahi (*J*–4), Narmada (*N*–11), and Tapti (*N*–17) Rivers on the coastal plains beyond the eastern shore carry heavy loads of sediment from the hinterlands into the gulf for redistribution by tidal flow into the open seas. Most of the lowlands around the gulf consist of Quaternary alluvial and deltaic materials on which marshlands (*D*–5), savanna thickets, and dry tropical rain forests have developed. Agriculture, fairly successful on the coastal lowlands that receive up to 65 centimeters (25 inches) of rain, is concentrated in cotton, wheat, and millet farming. The edge of the western Ghats (*V*–11), a hilly plateau of early Tertiary sedimentary rocks and the widespread Deccan basaltic lavas of Cretaceous age, extends to the coast along the right edge of this view. Spurs and patches of Deccan lavas are visible on the east side of the image (*T*–9; *U*–15) and also in the Kathiawar peninsula (*C*–13). *1242–05054;* March 22, 1973.

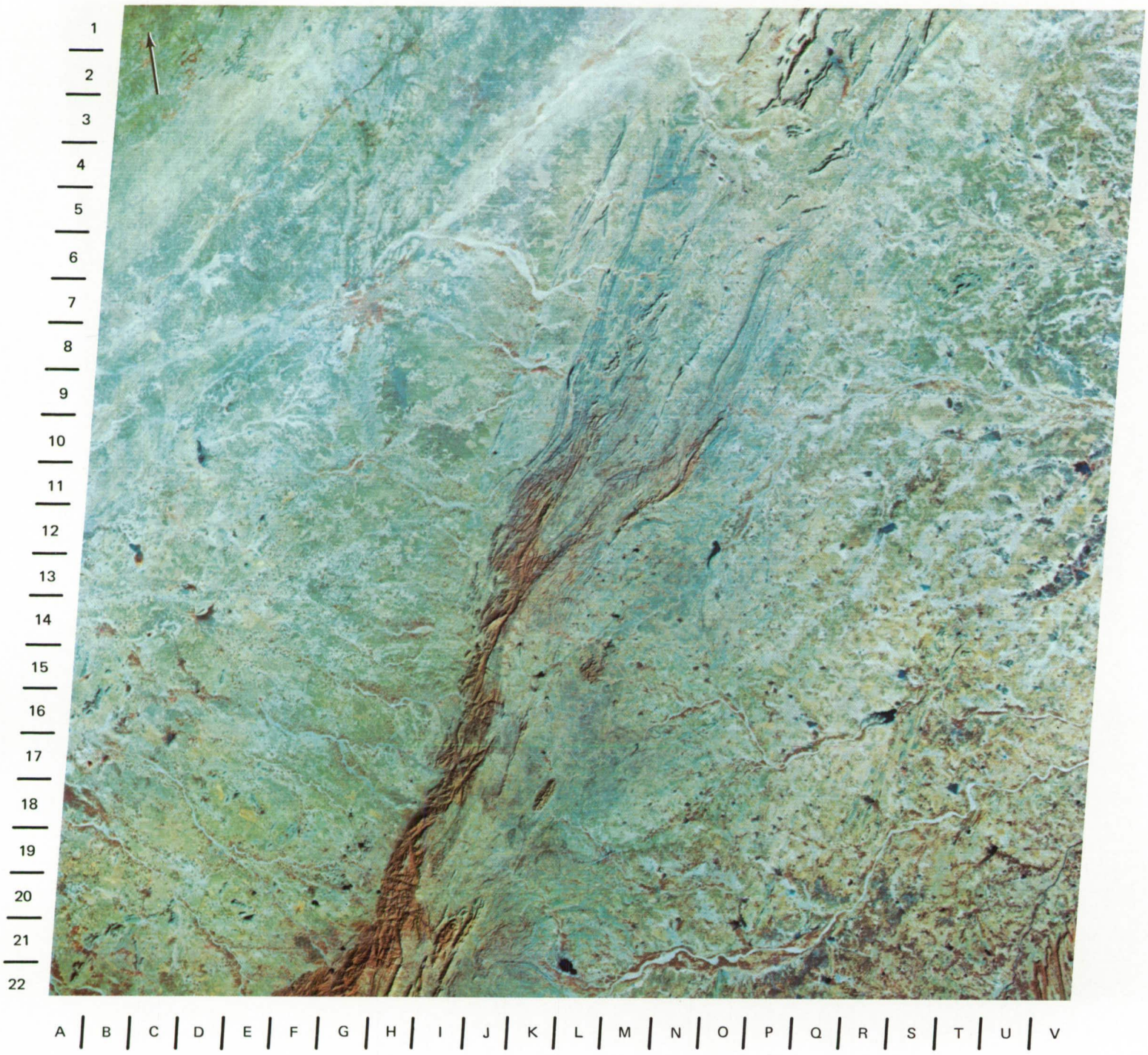
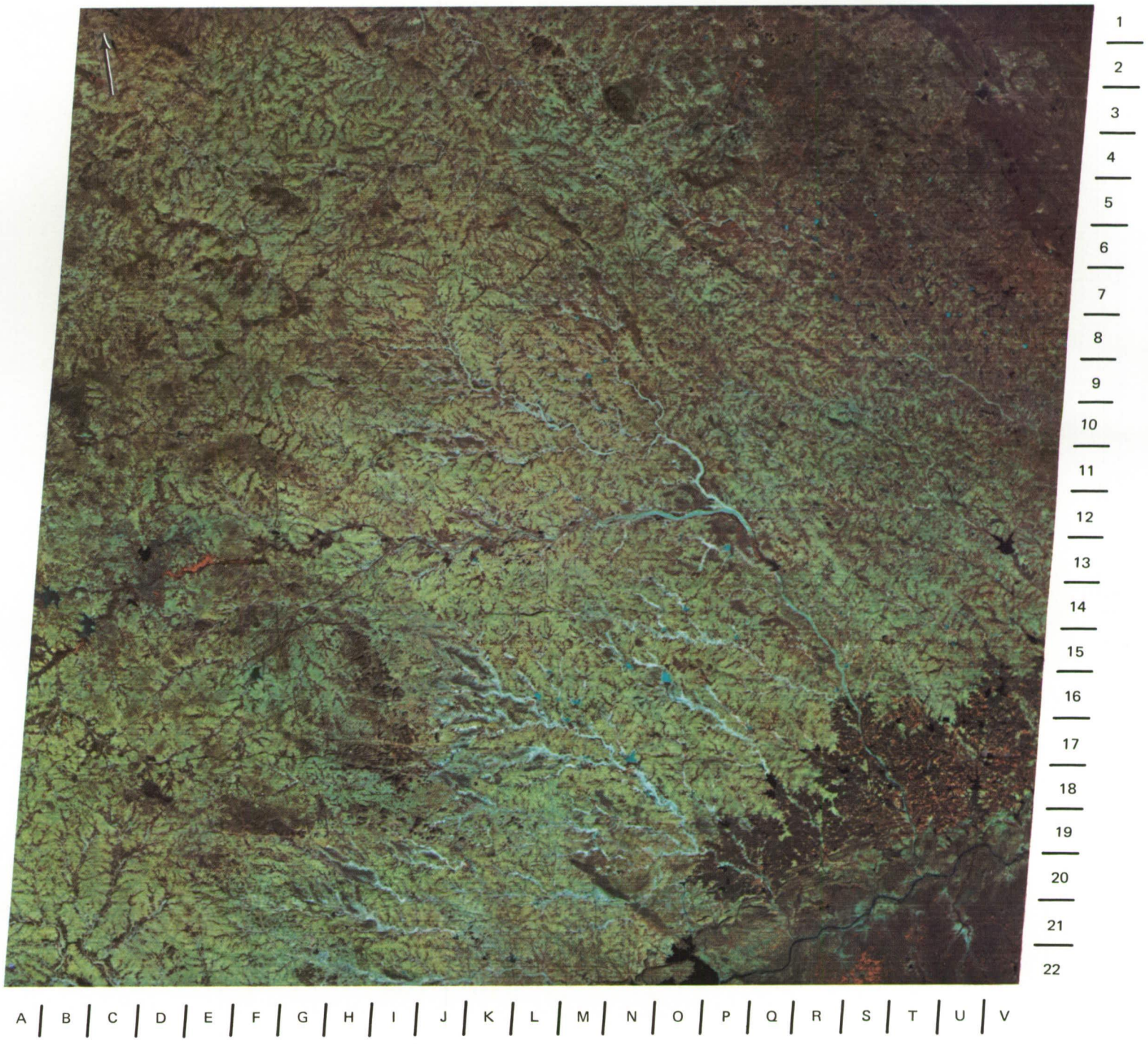


PLATE 296

ARAVALLI RANGE, INDIA: This section of northwestern India, in the State of Rajasthan, lies just to the east of the Great Indian or Thar desert and the city of Jodhpur *(off the image in the upper left)*. Quaternary desert alluvium (*C*–3) gives way to a complex terrain dominated by tightly folded, metamorphosed Precambrian rocks, expressed as low hills in the northeast-trending Aravalli Range (*J*–12). This range consists of a central belt of Proterozoic crystalline rocks (*I*–17), including granites and metabasalts; flanked by older Archean rocks, mainly to the southeast (*L*–17; *R*–20); and younger late Precambrian-early Paleozoic metasediments (*G*–11) interspersed with Quaternary alluvium to the northwest. The entire region is one of desert steppe, savanna thickets, and thorn scrub, with limited wheat and barley farming in areas of higher soil moisture. Limited flowing drainage is confined mainly to the Banas (*N*–21) and Kolari (*Q*–16) Rivers and the Luni River system (*C*–8; *I*–6) and their larger tributaries. The region receives about 25 centimeters (10 inches) of rainfall a year. Large settlements are few—Ajmer (*P*–2) and Beawar (*M*–7) are the principal towns. Gypsum and salt are mined in desert depressions. *1134–05041;* December 4, 1972.

PLATE 297



THE PENINSULAR INTERIOR OF INDIA: This scene is located near the center of the ancient (Archean) shield of crystalline rocks that forms the core of the Indian subcontinent that drifted northward to eventually slam into the main Asian continental mass. The bleak midwinter landscape here consists of isolated hills and knolls (*H*–15) on a plateau less than 650 meters (2000 feet) above the sea that is dissected by broad shallow valleys. The edge of a northwest-trending belt of upper Precambrian rocks appears within the upper right corner of this image, and rocks of similar age also occur along the flood plain of the eastward-flowing Kistna (Krishna) River (*S*–20). This region is covered mainly by poor, infertile sandy red soils (expressed in the image as greenish tones); but some of the regur or black soils more common to the north and west are found locally in the valleys and the Precambrian belt.

The area shown lies entirely within the modern State of Andhra Pradesh. The city of Hyderabad (*C*–13), currently with a population exceeding 1 200 000, is a cultural-administrative center of southern India that dates back to the 16th century. Agriculture is an important activity involving cultivation of paddy rice and jowar millet and some sugar and cotton. A natural savanna vegetation flourishes during the monsoon season when most of the annual rainfall of about 100 centimeters (40 inches) is deposited. Rains are almost absent in the winter, and the scrub around drainage channels becomes brown and dormant. *1183–04373;* January 22, 1973.

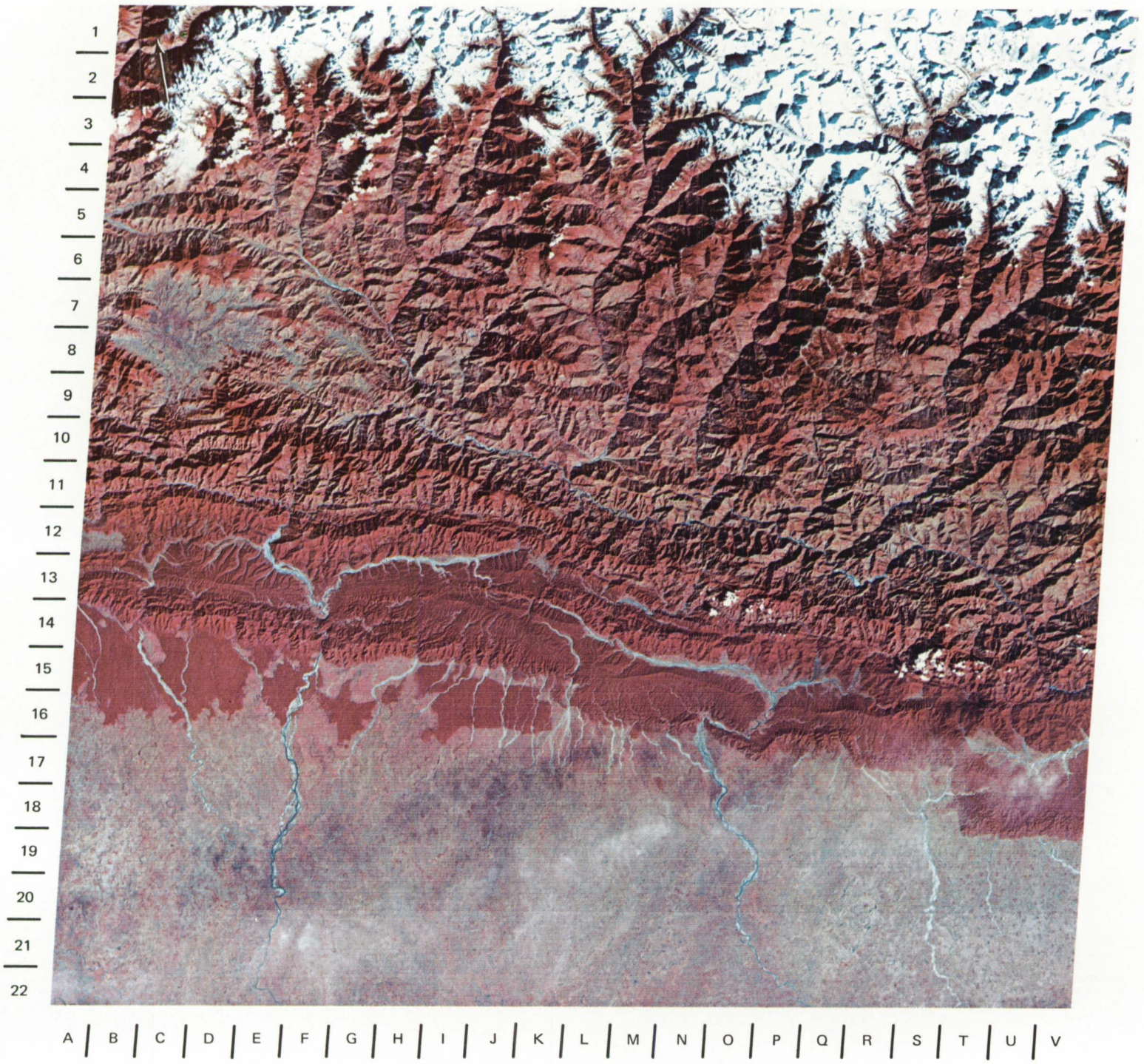


PLATE 298

THE TOP OF THE WORLD: Much of the eastern third of the mountain kingdom of Nepal, a sparsely populated country between India and Tibet, occupies this scene. The high plains (*K*–19) of the Ganges along the Indian border (*O*–20) gives way to the Siwalik Hills (*J*–14) at the base of the Himalaya Mountains (*J*–6), a huge mass of faulted rocks compressed and shoved up when the Indian subcontinent slammed into Asia and then plunged under it along a great thrust fault. These hills are a low (1000 to 1300 meters (3300 to 4300 feet) above sea level) dissected range of Miocene and Pliocene continental sediments deposited as gravels by streams from the high mountains to the north. The Siwalik Hills are mantled by thick, almost tropical forests of bamboo and other vegetation that respond to monsoonal rains.

The relief becomes strikingly rugged in the Lesser Himalayas (*K*–8), a section of the Himalayan system that rises to heights in excess of 3000 meters (10 000 feet). Further north is a crest region containing many peaks of 6000 to 8800 meters (20 000 to 29 000 feet) above sea level. Among these is Mount Everest, at 8848 meters (29 028 feet), the highest point on Earth. This famed peak (*T*–1) lies just at the edge of this image. A shadow marks the precipitous North Col beyond the summit; a ridge can be followed southward to Lhotse I, a peak reaching to 8501 meters (27 890 feet).

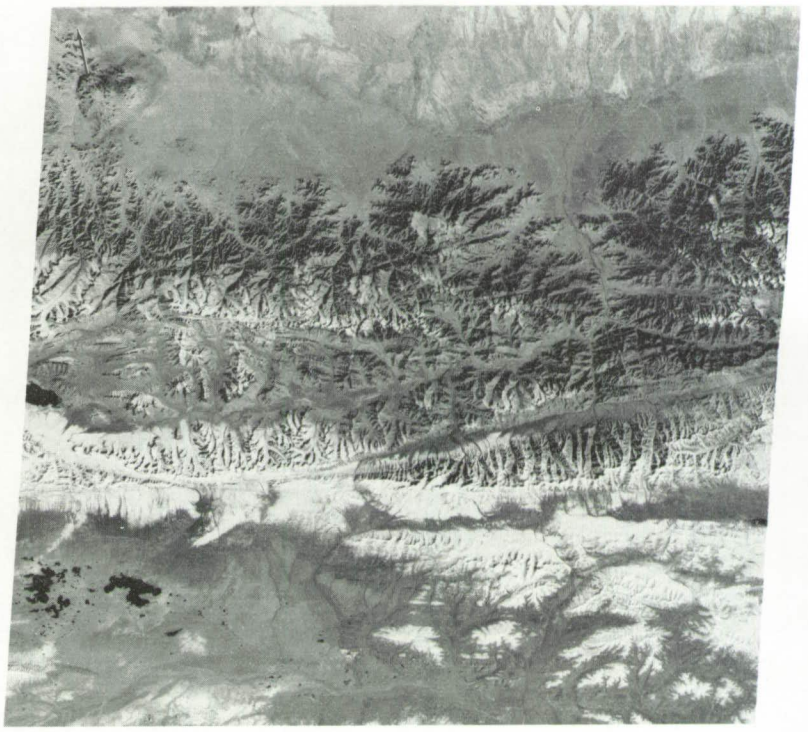
Mount Everest has been a challenge to climbers for many decades. Despite lack of modern equipment—including oxygen—Sir George Leigh-Mallory almost made it to the top in a daring climb in 1924 before losing his life. The first conquest of Everest—since climbed by many parties—occurred on May 29, 1953, when the New Zealander, Sir Edmund Hillary, and his Sherpa guide, Tenzing Norkay, placed the British flag on the summit.

Hillary's expedition followed the customary "shortcut" to the base of Everest. Most climbing parties leave from Nepal's capital, Kathmandu (*B*–7), situated in a mountain-fringed valley. An easier path wends along the Sun Kosi River (*I*–10) but then requires a long trek up the Dudh Kosi River (*R*–11). The more rugged approach moves over high country across the Indrawati (*G*–8) and Bhote Kosi (*K*–7) Rivers to the Dudh Kosi at Jubing (*R*–6) and thence along its valley to a base camp in the monastery town of Thijangboche (*S*–3), nearly 4000 meters (13 000 feet) above the sea. The final assault by Hillary's team followed the Imja Khola river valley and its glacier (*T*–2). *1144–04174;* December 14, 1972.

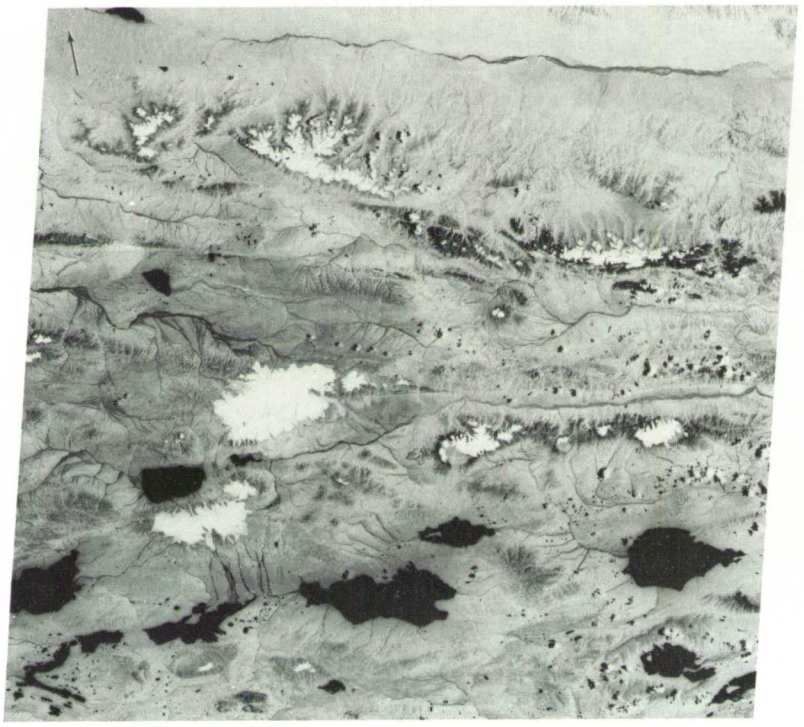
PLATE 299



(a)



(c)



(b)



(d)

THE TIBETAN PLATEAU: This great landmass, part of the People's Republic of China, covers more than 1.2 million square kilometers (about 460 000 square miles) and has an average elevation exceeding 4800 meters (16 000 feet). It is bounded on the south by the Himalayan Front—a high chain of folded sedimentary rocks north of a great thrust fault that were shoved up when India collided with Asia about 40 million years ago. The boundary on the north includes the K'unlun Mountains adjacent to the Tarim Basin (occupied by the Takla Makan Desert). The region is sheltered from the monsoons of the Indian Ocean, so rain or snow is sparse (about 250 millimeters (10 inches) a year) and cloud-free conditions are common. As seen in Landsat imagery, the mountainous areas do not seem any more rugged than the Alps, Andes, or other similar regions in the world; the relief here is comparable to those regions but actual elevations are notably higher. Four typical areas are shown: (*a*) Westernmost Tibet and the Indian State of Kashmir, with the Indus River cut along the northwest-trending Karakoram Fault. *1096-04501;* October 27, 1972. (*b*) A high plateau area with moderate relief, now dotted with lakes, near the north-central edge of Tibet. *1358-04031;* July 16, 1973. (*c*) Further east, the K'unlun Mountains and K'unlun Fault. *1482-03493;* November 17, 1973. (*d*) The Yangtze and Yalung Rivers south of the Bayan Mountains, a region with peaks above 7000 meters (23 000 feet); the headwaters of the Yangtze, Huang (Yellow), and Mekong Rivers all are located in this section of Tibet. *1461-03331;* October 27, 1973.

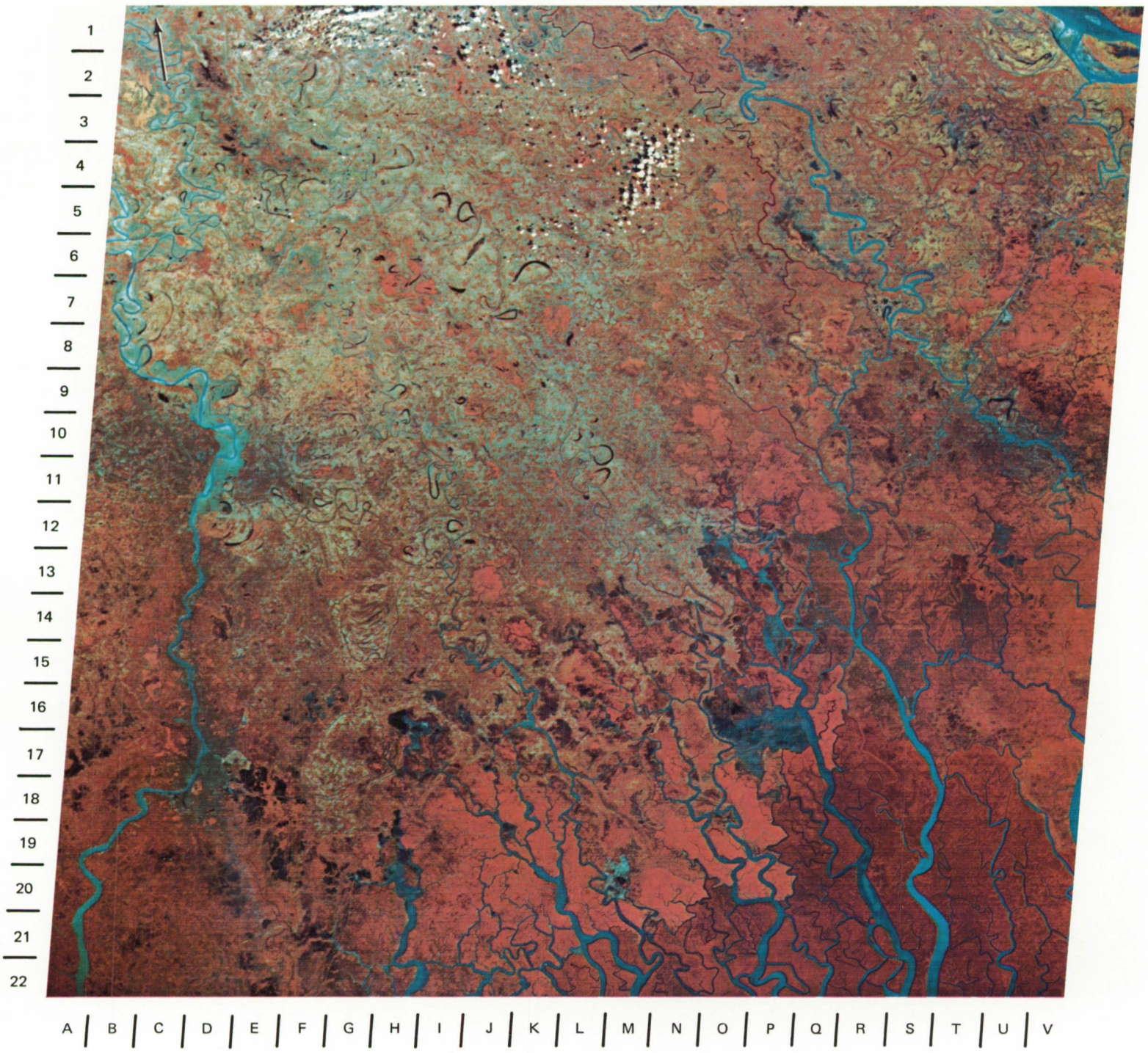


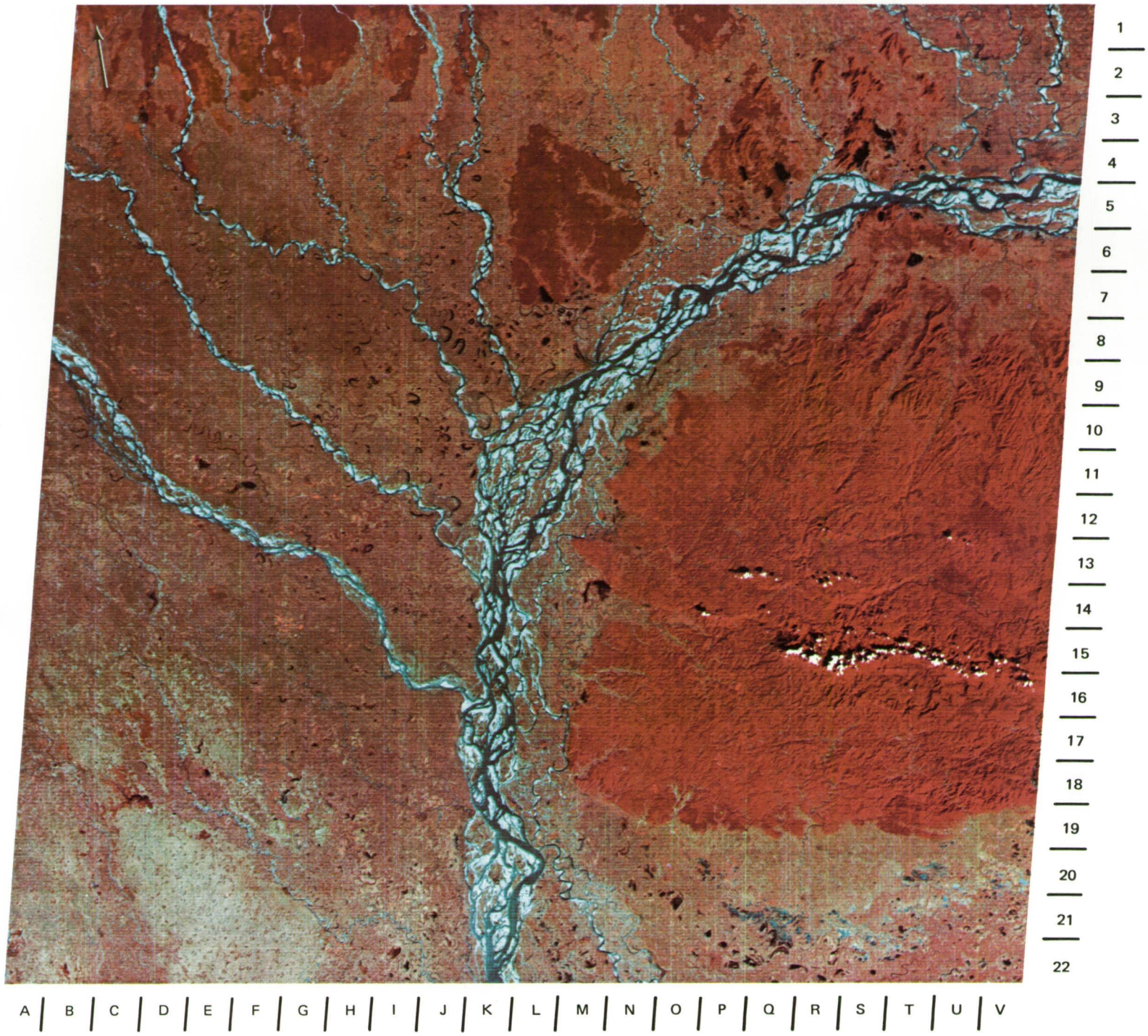
PLATE 300

THE GANGES DELTA: The mighty Ganges River (*U*–1) reaches the Bay of Bengal after flowing through the Ganges valley for more than 1600 kilometers (1000 miles) from the Himalayan slopes. Most of this valley is topped by Recent alluvium. A tremendous delta is being built into the ocean from sediments carried by the Ganges, the Brahmaputra, and other rivers. Owing to heavy monsoon rains and the huge loads transported during floods, the Ganges River system is constantly shifting across this delta. Migration, in general, has been eastward.

Some of the many distributaries of this system, part of the "Mouths of the Ganges," are shown in this image. Many are no longer directly connected to the Ganges itself but hold water accumulated during the monsoon season. The Madhumati River (*P*–4) is an active distributary, as is the Hooghly River (*C*–13) on which Calcutta (*C*–17), the capital of the West Bengal State in India, is situated.

West of the India-Bangladesh border (*J*–13), soils tend to be lateritic; jute, a fiber crop, is the principal vegetation cultivated in that district. Across the border, jute and paddy rice are grown in the "Moribund Delta" region (*H*–5), where myriads of abandoned distributary channels and oxbow lakes prevail. Agriculture is limited there because new alluvial soils are no longer building up. To the south are areas that remain partly inundated year round—homes on stilts and dikes are common. Near the shore are the sparsely inhabited Sundarban areas (*T*–19), which are thickly forested with vegetation adapted to saline waters brought in with the tides. *1105–04014;* November 5, 1972.

PLATE 301



THE BRAHMAPUTRA RIVER: This great river (*K*–11), noted for its huge loads of sediment, begins where several feeder rivers from the mountains of Tibet and Burma meet in eastern Assam, the easternmost state of India. The river then flows through Assam past the forested Shillong Plateau (*V*–11) and Garo Hills (*P*–15), a Precambrian crystalline complex, then into the upper part of Bangladesh, and finally into the Ganges west of Dacca. En route it is joined by several rivers, including the Tista (*E*–12), Jaldhara (*D*–8), and Godadhar (*I*–4), that flow through the northern section of West Bengal (*G*–3) after starting in the foothills of Sikkim and Bhutan. These areas and the Assam Hills are famed for tea such as that grown near Darjeeling *(just off the left side of the image).*

The Brahmaputra during the rainy season can be greater than 8 kilometers (5 miles) in width. The view shown records the river channel a month or so after the end of the monsoons. With the greatly reduced flow, the river has dropped its load, mostly highly reflective sand and silt, and reached a braided condition in which active channels interweave with flood plain and bed deposits. *1123–04010;* November 23, 1972.

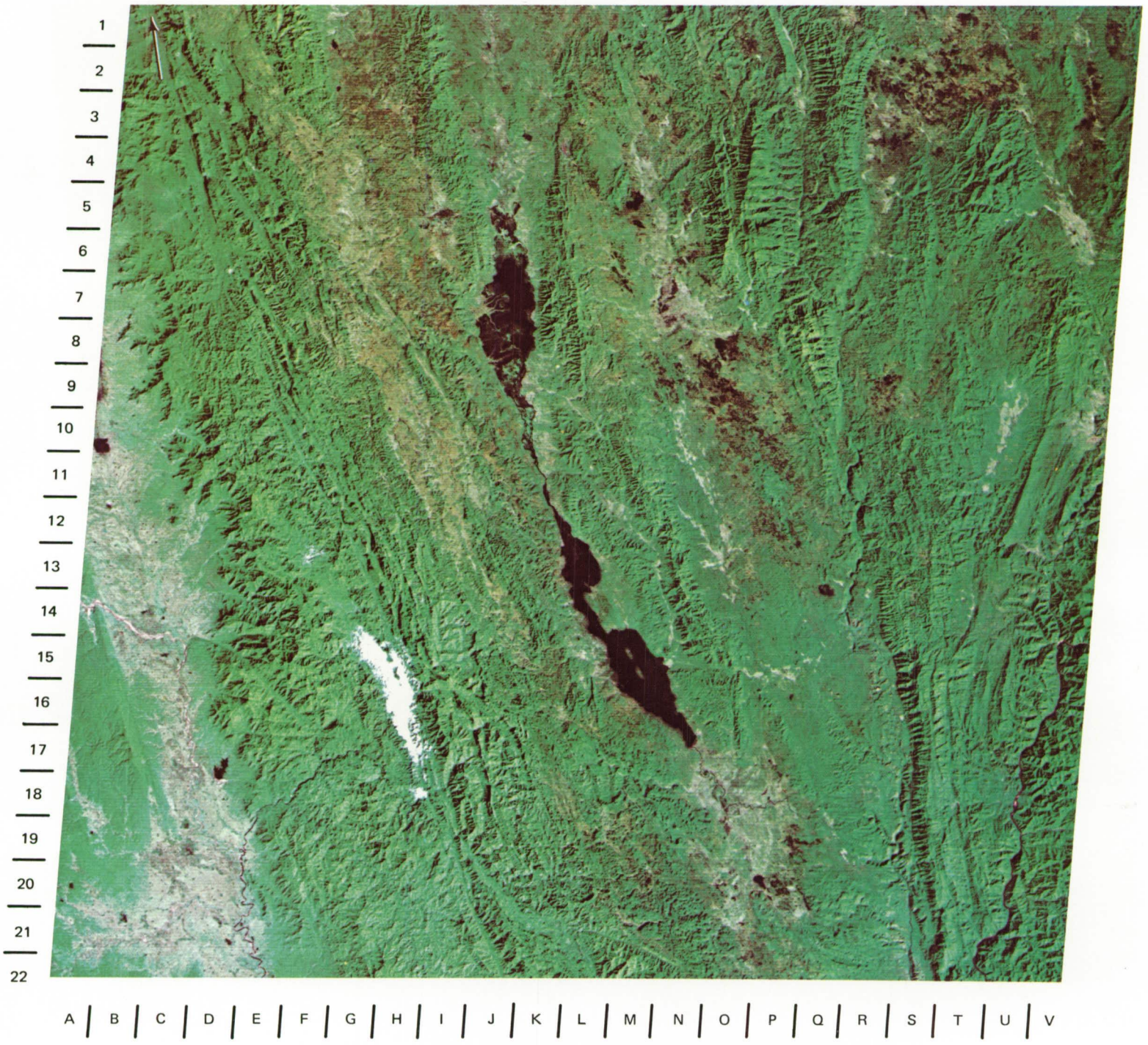
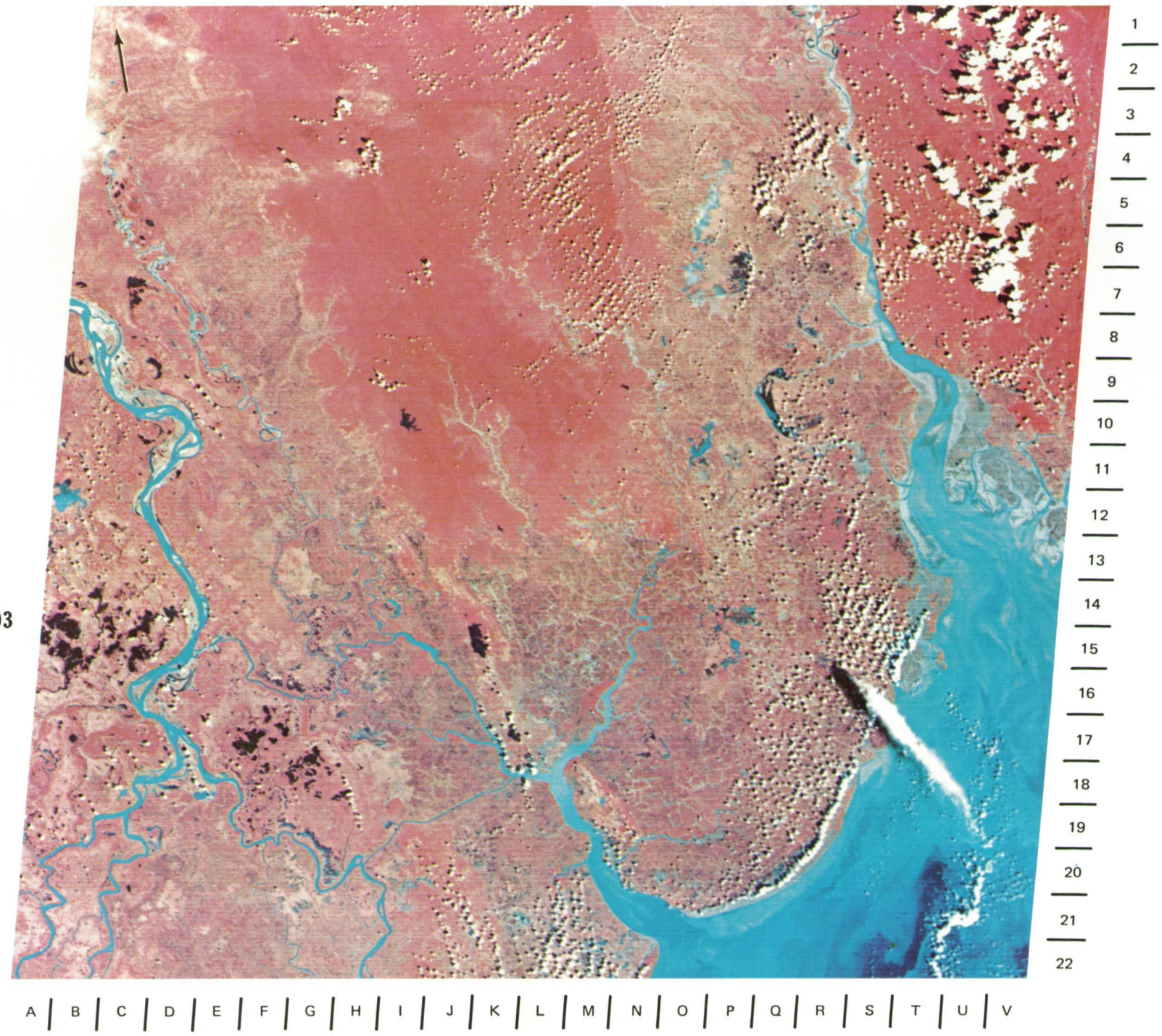


PLATE 302

THE TROPICAL FORESTS OF EASTERN BURMA: This color rendition uses the combination of multispectral scanner bands 4 (through a blue filter), 5 (red), and 7 (green) to emphasize the thick vegetation that clothes the Shan Plateau. The vegetation is largely hardwoods of the monsoon forest, with teak the most important commercial wood, and some rain forests on high slopes where rainfall reaches 150 centimeters (60 inches) or more per year. Savanna growth has taken over where the lands have been cleared. The Shan Plateau in places is a dissected karstland developed on limestones of late Paleozoic age. Along the west front of the plateau, which rises to elevations of 1000 to 2300 meters (3000 to 7000 feet), igneous and metamorphic rocks of early Precambrian age make up the terrain. Tungsten, tin, lead, silver, and gold are mined in this region of the Shan Highlands.

Mandalay, made famous by Rudyard Kipling, lies about 120 kilometers (75 miles) north of the upper left of this scene. The Salween River (*U*–13; *U*–21) cuts through the rugged uplands. It is joined by the Pawn River (*S*–20) and its tributary, the Nam Pilu (*O*–18), along which Lake Inle (*M*–15) and other lakes have formed. The Sittang River (*B*–14; *E*–21) drains the eastern edge of the Irrawaddy Lowlands. *1531–03244;* January 5, 1974.

PLATE 303



SOUTHERN BURMA: The southern end of Burma provides almost all the rice grown in that country. This land, once covered by marsh and forest, was cleared in the 19th century and converted largely to paddy rice fields (*K*–13). Mangrove swamps (*I*–15) and scattered lakes remain over parts of the delta formed by the distributaries (*A*–18; *B*–18; *G*–18) of the Irrawaddy River (*C*–9). One of these separates near Henzada (*A*–7) to flow into an estuary from the Gulf of Martaban (*S*–18). The capital city of Rangoon (*K*–15) lies at the top of this estuary between the Rega (*I*–15) and Hlaing (*L*–15) Rivers. Another larger estuary forms the mouth of the Sittang River (*P*–3), whose headwaters have now been captured by the Irrawaddy far to the north. Pegu Yoma (*I*–7) is a forested range of hills composed of Miocene sedimentary rocks that rise 760 meters (2500 feet) above the Quaternary alluvial lowlands on either side. *1099–03285;* October 30, 1972.

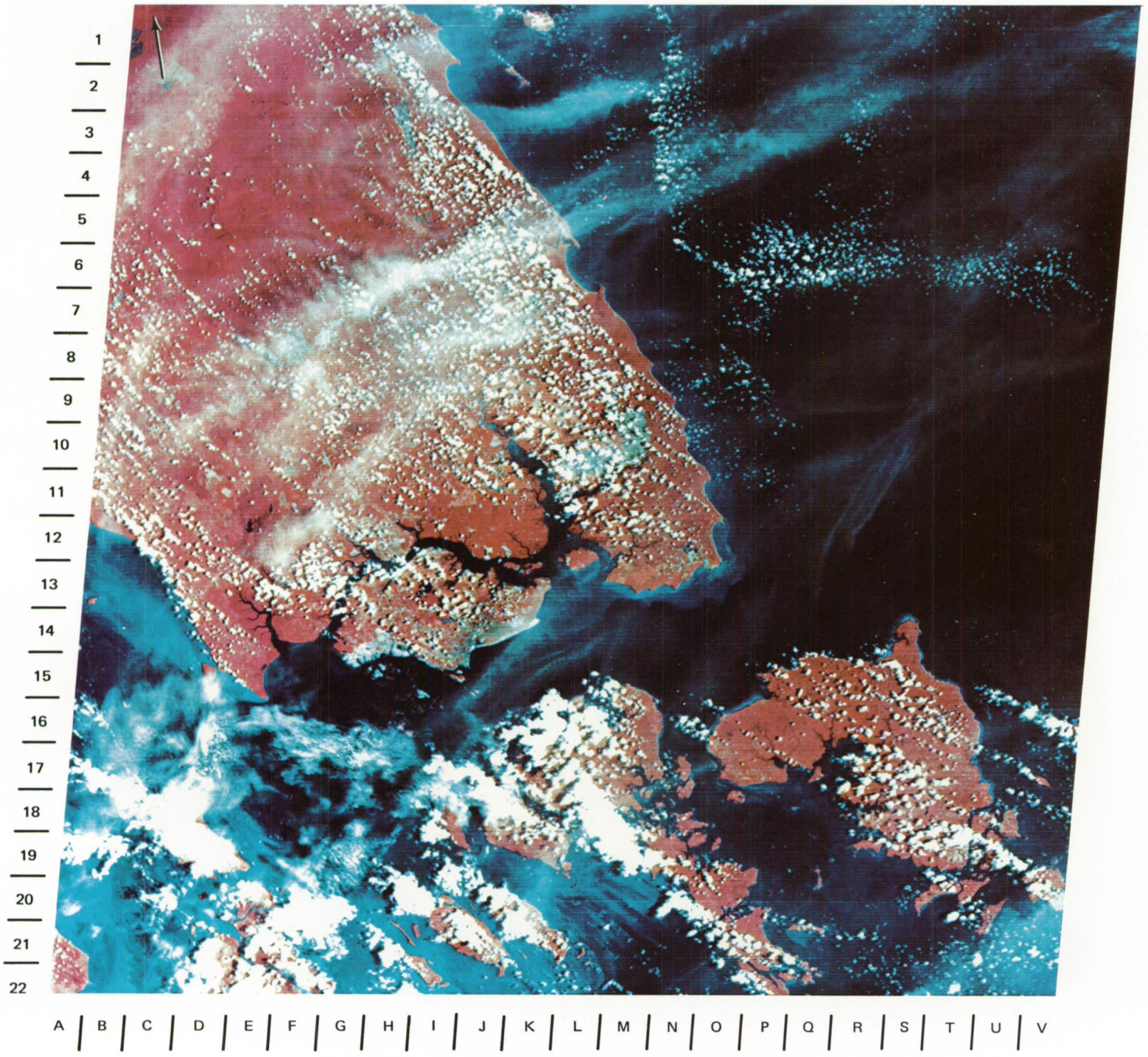
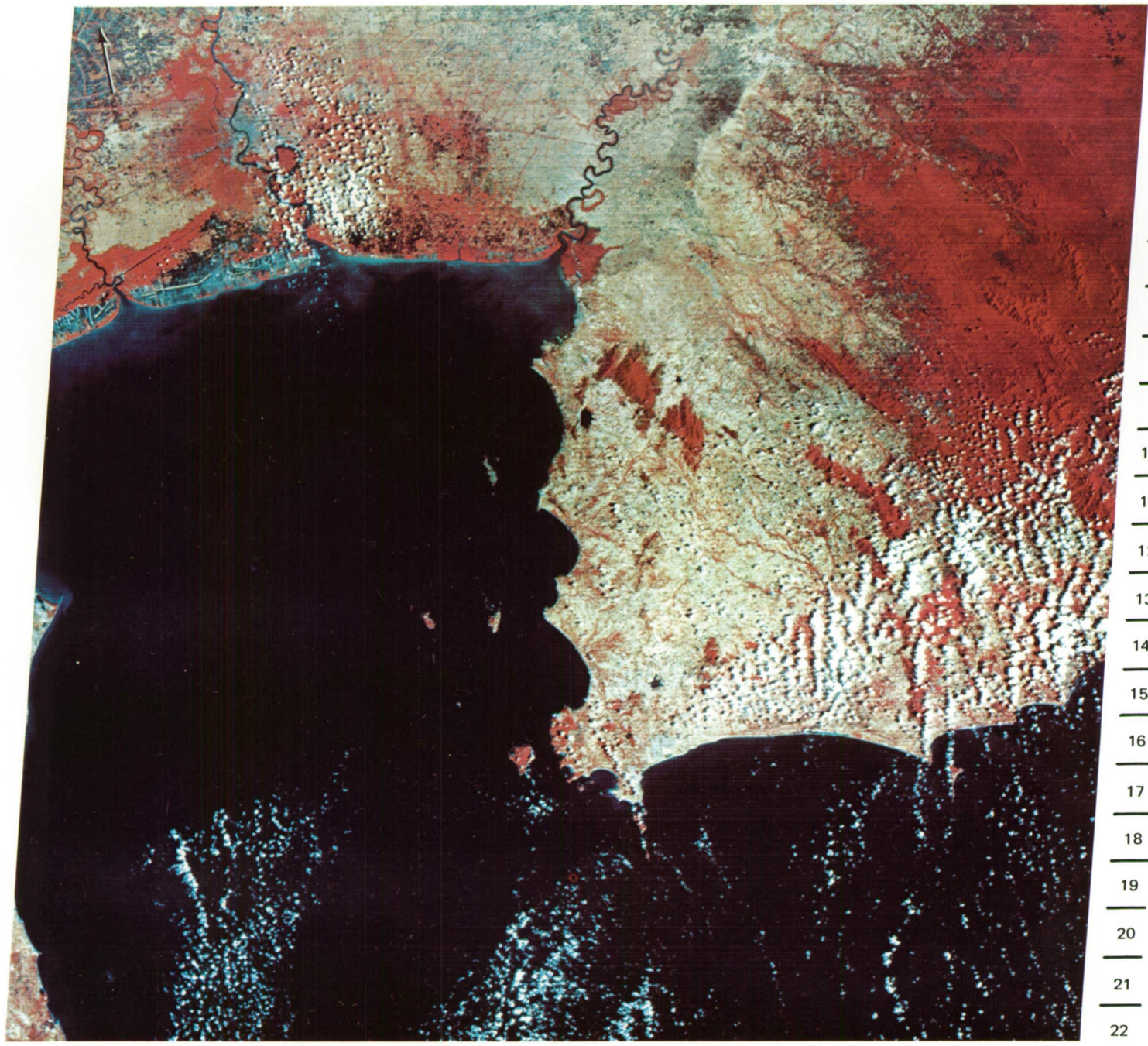


PLATE 304

MALAYA AND SINGAPORE: The southern tip of the Malay peninsula reaches to the Straits of Singapore (*J*–15), which connect the Pacific Ocean to the Indian Ocean via the Straits of Malacca (*A*–15). The city state of Singapore (*H*–13), now a country separated from the Malaysian Union, occupies an island 39 kilometers (24 miles) by about 23 kilometers (14 miles) in dimension. The island is actually growing in size by landfill along the southwest (*G*–14) and southeast (*J*–14) coasts (bluish areas). The "downtown" area of Singapore (*I*–14) is also the harbor area for one of the great shipping ports of the world. Singapore is across the Straits of Johore from the State of Johore (*F*–8) in Malaya. This part of the peninsula consists of swampy lowlands, including mangroves (*D*–13) along the coasts. Inland, thick jungles of bamboo, palm, ferns, and hardwoods cover low hills of Jurassic basalts and Triassic and Jurassic sedimentary rocks. The rocks yield some iron ore and bauxite. The central region contains numerous rubber tree plantations and also oil palm groves. Pineapples and some bananas are grown in the area just north of Singapore while coconut trees are harvested along the southwest coast as the source of copra.

The islands to the southeast of Singapore, including Bintan (*P*–16), belong to Indonesia and are administered from Sumatra (*A*–21). *1451–02451;* October 17, 1973.

PLATE 305



SOUTHERN THAILAND: This scene shows Bangkok (*D*–3) and its environs at the south end of the Menan Plains, east Thailand (*O*–10), and the Gulf of Thailand (*F*–14). Much of the land around the capital city of Bangkok is devoted to rice growing, although many fields (*B*–5; *M*–6) are bare at this time of year during the hot, dry season. The dark area (*A*–1) to the northwest shows the effects of recent burning to prepare the fields for the next crop. This vast agricultural area is interconnected by numerous treelined "klongs" or canals (*J*–3) that join to the Chayo Phraya (*D*–2) and Bang pa Kong (*L*–2) Rivers to provide a transportation network. The bright red area (*D*–4) west of Bangkok is given mainly to fruit orchards. Near the coast, the red-colored region (*B*–6) is mostly mangroves and nipa palm trees. The patterned area (*A*–7) just to the south represents saltpans where this staple is recovered by sea-water evaporation. Along the shore are found shrimp "farms" (*B*–7).

The Cardamon Hills (*U*–6) are a heavily forested area to the east. However, much more of this region had been timbered since the last survey in 1965 than was inventoried by the Government until this drastic reduction was realized after examination of Landsat imagery. The light blue area at *M*–16 is the Utapas Air Base, once used by the U.S. Air Force for B–52 flights.

Two unusual features deserve special mention. The reddish "square" surrounded by a thin dark band (*B*–3) is Wat Buddhamaton, a moated Buddhist temple compound. The curving red strip at *K*–5 is a heavily vegetated oxbow lake cut off from the Bang pa Kong River. *1221–03073;* March 1, 1973.

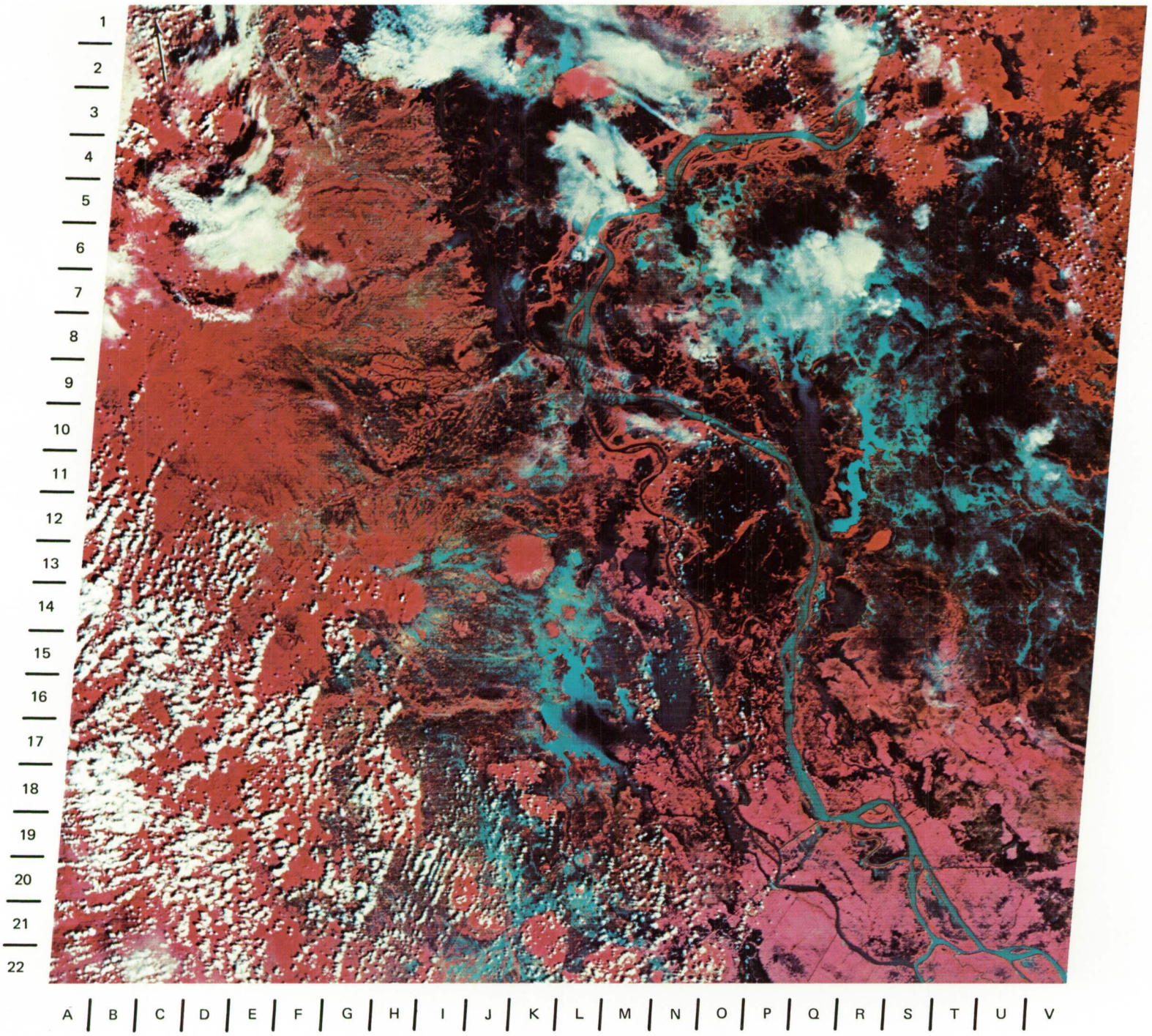
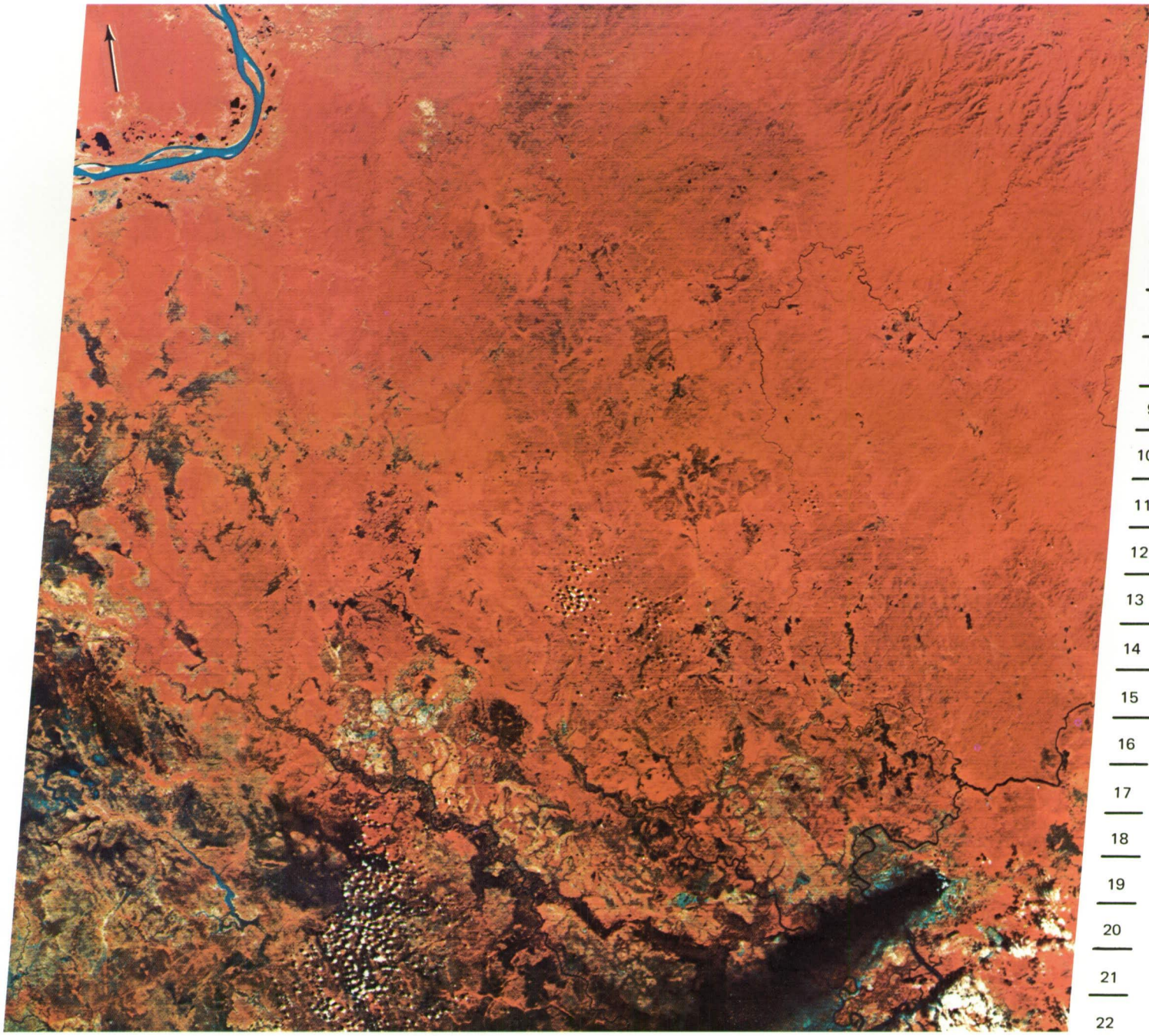


PLATE 306

SOUTHERN CAMBODIA: This scene reveals graphically the extent of flooding in the lowlands of Cambodia along the Mekong River (*N*–3; *P*–16) near the end of the monsoon season. Vast stretches of the flood plains in the Mekong Basin are inundated (*O*–13; *R*–9) from the rains. In the dry season some of these areas remain as ill-drained swamps like the Veal Phoc (*I*–4) or "Plain of Mud." Much of the remaining land is given to rice paddies. Some of the dark areas (*S*–17) may be burned rice fields—a common practice, especially where terraced dry rice is cultivated. Low forested hills stand out when the surrounding areas are covered by water. The capital, Phnom Penh (*K*–9), lies on higher ground at the confluence of the Tonle Sap River (*J*–8) with the Mekong. The high country to the west is a vast rain forest that receives up to 410 centimeters (160 inches) of rain per year. It includes the Cardamon or Elephant Hills (*C*–8), consisting of dissected Mesozoic sedimentary rocks with elevations of 900 to 1800 meters (3000 to 6000 feet). As the Mekong is diverted into a second distributary (*M*–12), it passes onto the broad deltaic plains of South Viet Nam (*U*–2). In these lowlands, numerous canals (*Q*–21) have been dug to facilitate transportation by barge and boat as well as irrigation. *1110–02503;* November 10, 1972.

PLATE 307



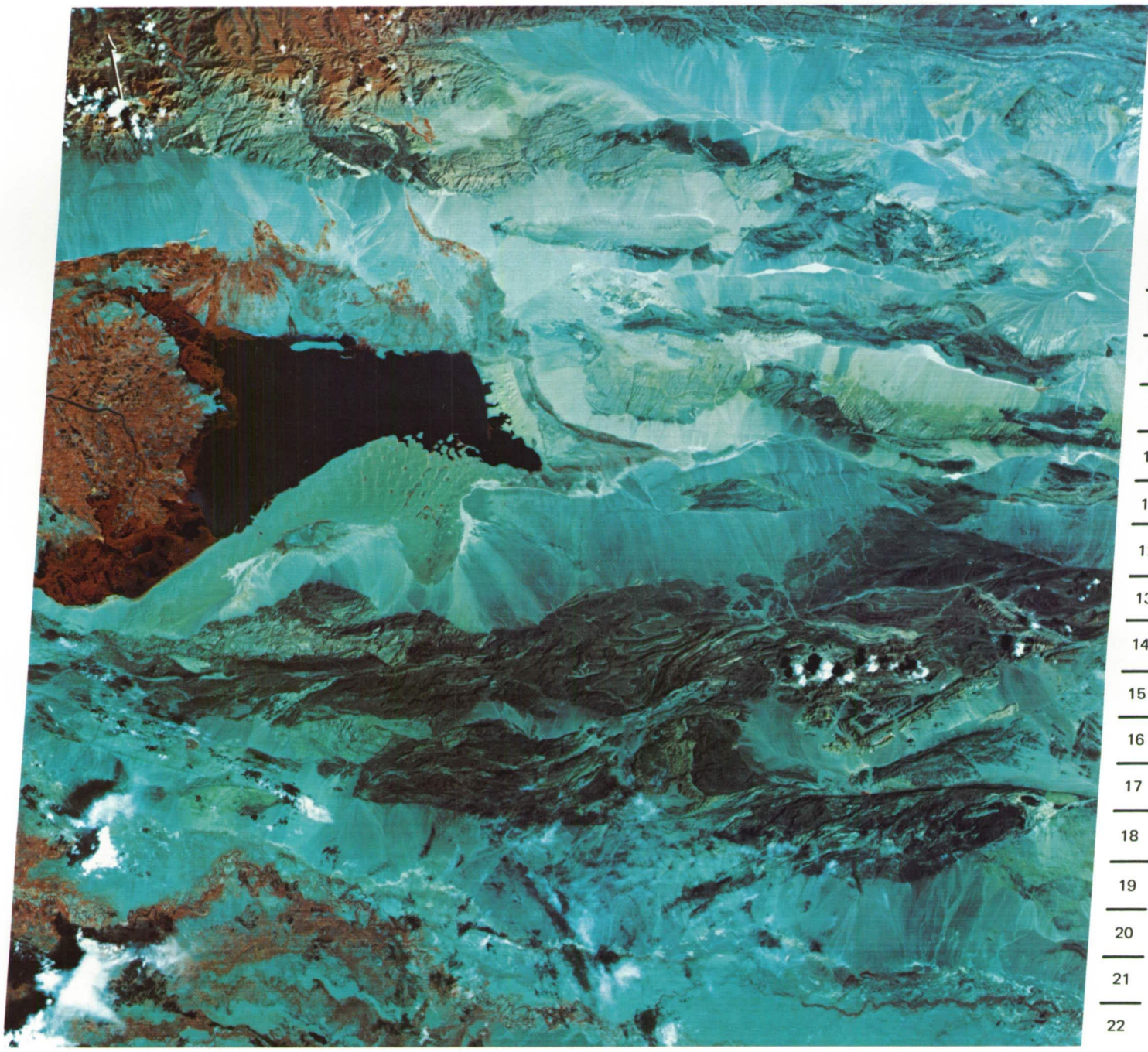
SOUTHERN VIET NAM: Saigon (*Q*–21), the largest city in South Viet Nam, lies along the Saigon or Nha Be River (*S*–17). Nearby, a dark plume of smoke from burning oil tanks marks the location of Bien Hoa (*S*–19). To the west of Saigon is seen the paddy rice fields (*B*–15) and swamps (*F*–19) at the north edge of the Mekong Delta where drained by the Vam Co Dong River (*J*–18). At this time the new crops planted after the end of the monsoon season are beginning to ripen. The Mekong River north of Kampong Cham appears at *D*–3. In the far right (*R*–2) are a cluster of hills reaching 900 meters (3000 feet) that straddle the Cambodian and South Vietnamese frontier. These are made up mostly of Tertiary basaltic lava flows. *1163–02443;* January 2, 1973.



PLATE 308

SOUTHWEST SINKIANG PROVINCE, CHINA: The juncture between the Kunlun Mountains (*K*–18) and the great Takla Makan desert (*K*–4) is sharply defined in this view. These mountains form the northernmost ranges in the Himalayan chain. Peaks reaching up to 5200 to 6000 meters (17 000 to 20 000 feet) are included in this scene. Here they consist of a succession of tightly folded rock units beginning with Mesozoic sedimentary rocks in the north, followed successively by older Paleozoic sedimentary and metasedimentary rocks, Paleozoic granites, and Precambrian crystalline rocks to the south in Kashmir across the border with India. The Takla Makan desert occupies the deep Tarim Basin, topped by Pleistocene sediments in its central section (*R*–3) and Recent alluvium in fans (*C*–9; *I*–11) in piedmont sections and along the Kara Kash River (*U*–5). The regional town of Hot'ien (Khotan) lies just off the image on the Yurung Quish River (*V*–6) at the head of the vegetated alluvial plains (*S*–8). The main road in this part of westernmost China can be seen (*Q*–11) north of the foothills. *1133–04550;* December 3, 1972.

PLATE 309



LAKE BAGHRASH, SINKIANG, CHINA: This area lies at the northern edge of the Tarim Basin where it is bounded by the eastern end of the lofty (4300-meter (14 000-foot)) Tien Mountains (*E*–1). Lake Baghrash Kol (*F*–9) is a perennial feature located in a fault trough that forms a mountain-ringed basin about 900 meters (3000 feet) above sea level. The inflowing Yeke Yuldus River (*B*–9) forms a swampy lowlands (*B*–10) on the west; a small river drains out of this marshland to join a complex river system including the Koniche Darya (*K*–21) and Inchiki (*C*–21) Rivers in the Tarim River Basin that flow entirely within the northern part of the Takla Makan desert (*P*–21) without breaching the encircling mountains.

The Altyn Tagh (or Kulukotako) Range (*L*–14) is a complex of Precambrian metamorphic rocks, granitic intrusions, and infolded Ordovician rocks. The narrow ranges to the north (*O*–7) expose Silurian and Mesozoic rocks. A great wrench or strike-slip fault (*I*–17; *R*–17) carries the southern part of this range eastward for 40 kilometers (25 miles). The trace of the Altyn Tagh fault can be followed in adjacent Landsat images for several hundred kilometers.

Both American and Chinese scientists have interpreted this and several other east to west wrench faults to be zones of fracture in the crust along which adjustments are even now taking place (as evidenced from persistent earthquakes in response to the collision of India with the Asian mainland that resulted in the Himalayan Range to the south). Landsat imagery has been used by these scientists to expand and refine this conclusion. *1398–04235;* August 25, 1973.

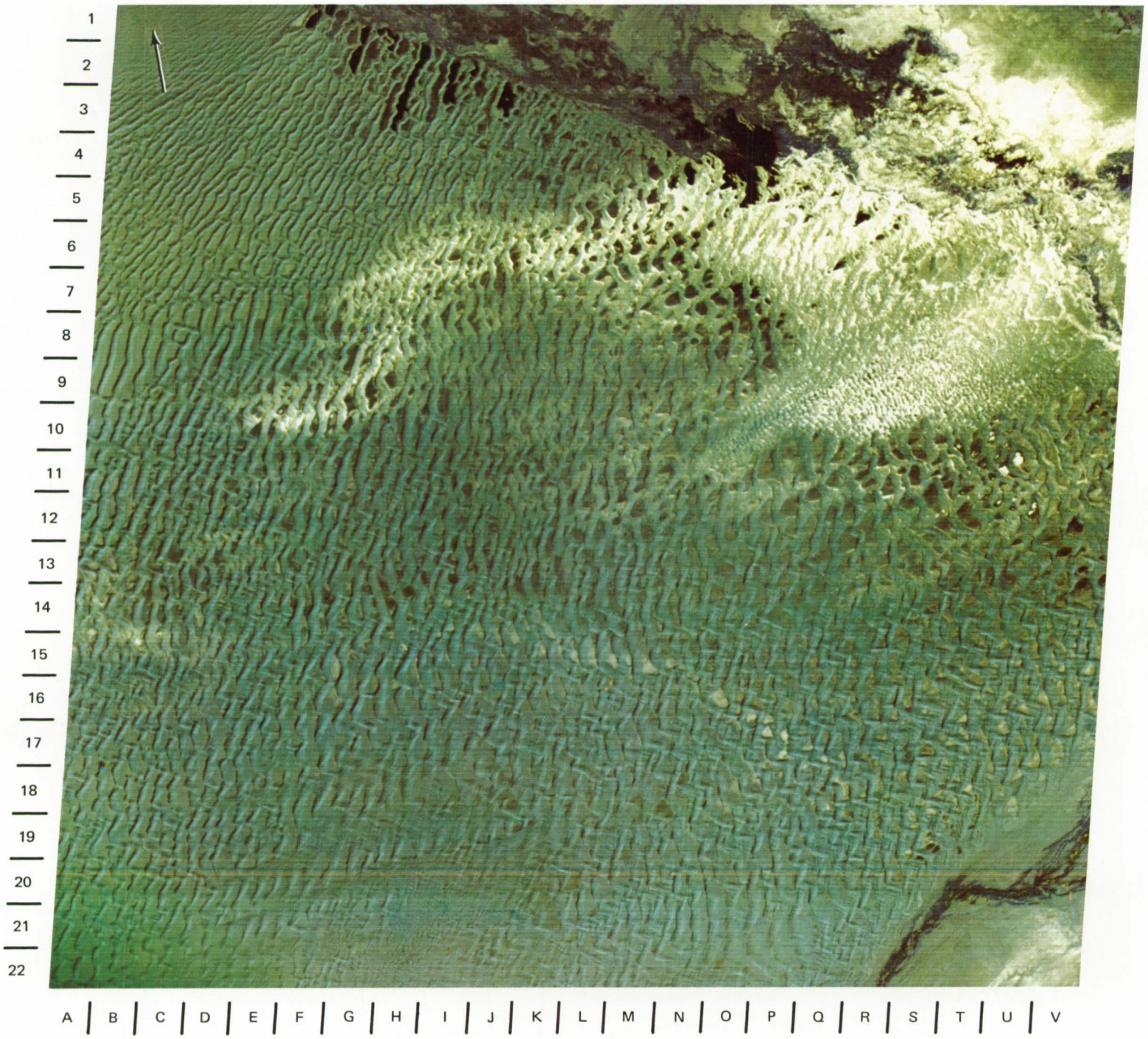


PLATE 310

DESERT DUNES, SINKIANG, CHINA: The area imaged here is in the northern half of the Takla Makan desert in the Tarim Basin. The edge of marshland around the Tarim River appears at the top of this scene. The desert itself contains longitudinal dunes trending north-northeast. Individual dune ridges are 1½ to 3 kilometers (1 to 2 miles) in width and some extend continuously for 8 to 32 kilometers (5 to 20 miles). Many are curved, especially on their leeward (downwind) sides to the west. The effect produces a pattern that superficially resembles a "bamboo curtain." Snow covers a part of the desert on the northeast. *1128–04253;* November 28, 1972.

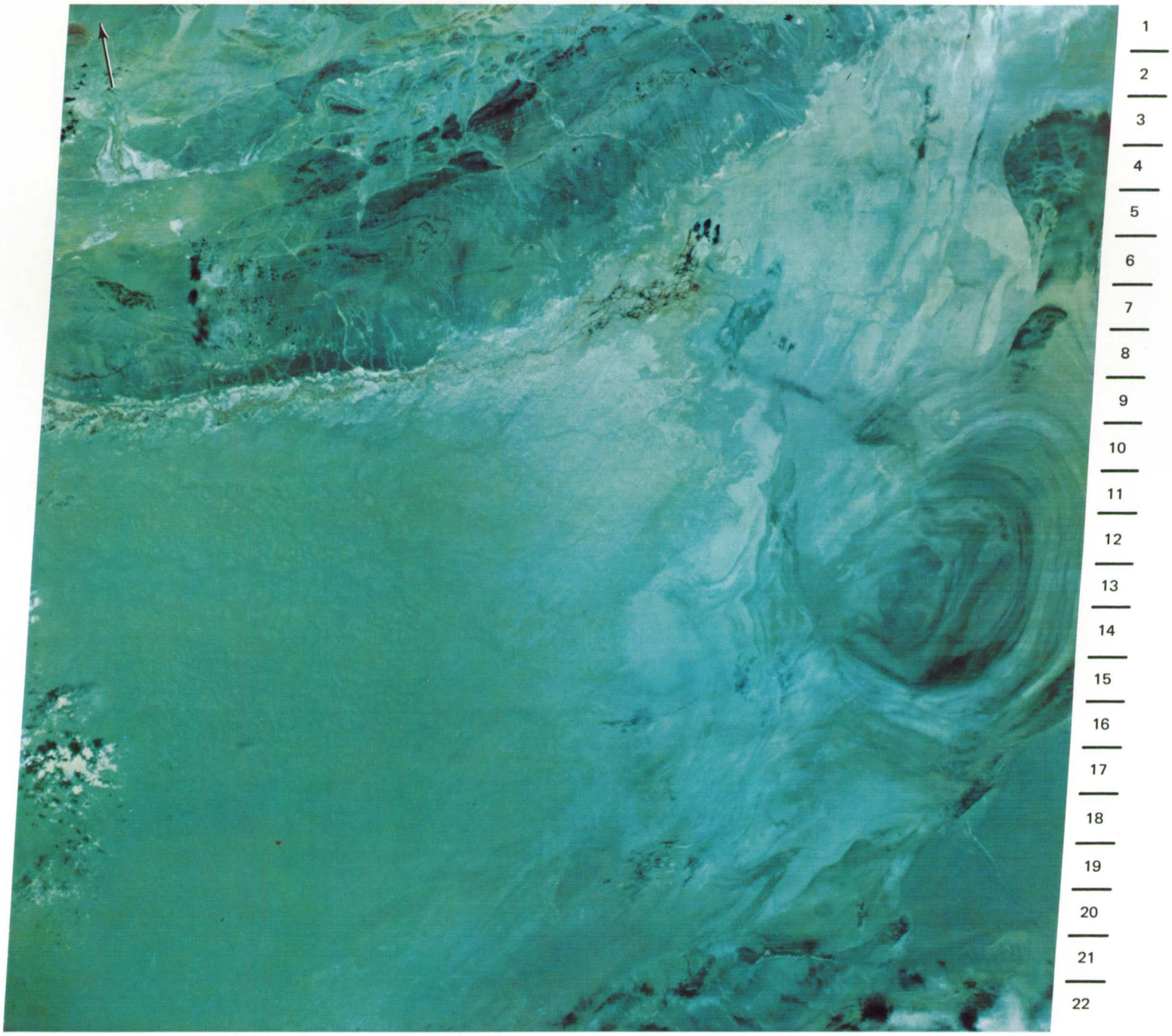


PLATE 311

THE "GREAT EAR" OF CHINA: This scene shows part of the eastern end of the Takla Makan desert (*G*–16) in the Tarim Basin of Sinkiang Province. The large feature at *S*–13 is Lop Nor, an ephemeral playa lake; at this time it is empty, although apparently the sediments contain considerable moisture (darker blue). A series of shorelines attest to frequent filling to different levels during rainy seasons. The feature at this time resembles a giant "ear" in shape. The Kuruk Darya River (*J*–8) (also identified on some maps as the Kum Darya River) taps the overflow from the lake that feeds its swampy headwaters (*M*–7). To the north are the Aerhchin hills (*G*–6), a folded sequence extending from Precambrian metamorphic rocks through Ordovician and younger Paleozoic rocks along the south flanks; these hills are an eastern extension of the Kulukotako Mountains. (See plate 309.)

The area around the Lop Basin has been used by the Chinese as their principal test site for nuclear explosions. *1324–04135;* June 12, 1973.

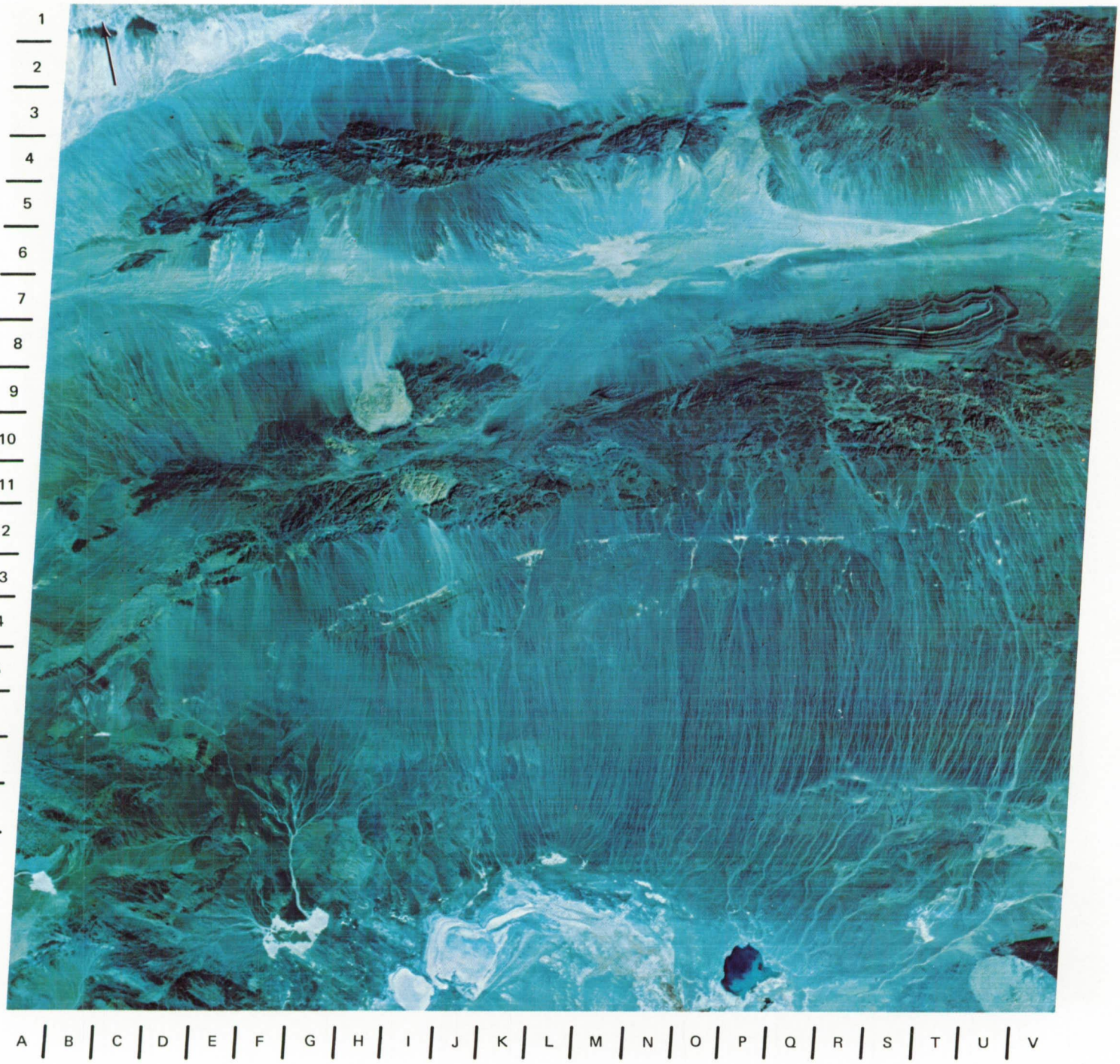
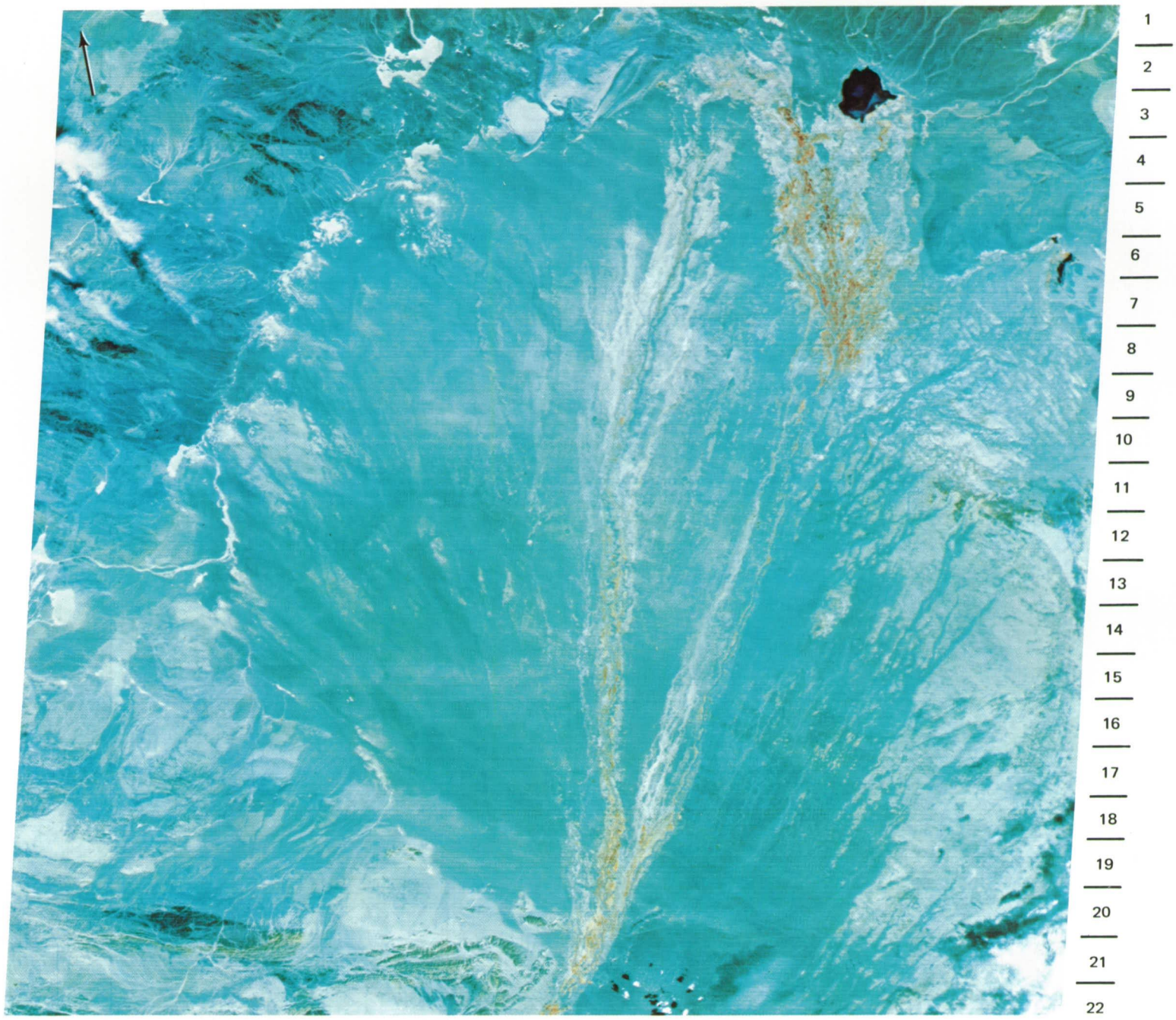


PLATE 312

GOBI DESERT, MONGOLIA: This region is just north of the Chinese border in the western Gobi Desert. The east to west trending Tost-Uul (*P*–9) and Nemest Uul (*H*–4) ranges rise to elevations above 2400 and 2800 meters (8200 and 9200 feet), respectively, while the surrounding basins lie between 1100 and 1400 meters (3500 and 4500 feet) above sea level. The ranges are made up in part of late Precambrian metamorphic rocks, intruded by granites (*G*–9), and, in part, of tightly folded Paleozoic sedimentary rocks (*S*–7). Great alluvial fans (*D*–9; *J*–5) built up from deposits washed down from these mountains have coalesced to form huge bolsans (*L*–15) with numerous ephemeral distributaries (*U*–16). Those to the south flow toward the basin of the Edsin Gol River, whose headwaters begin at the Kashun playa lake (*I*–20) and the usually filled Sokuo Lake (*P*–21). *1083–03323;* October 14, 1972.

PLATE 313



SOUTHERN GOBI DESERT, INNER MONGOLIA: This scene shows a continuation of the area covered on plate 312 although the date of acquisition is nearly a year later. The Edsin River (M–19), which originates in the high (4600 meters (15 000 feet) or more) Nan Shan ranges about 160 kilometers (100 miles) to the south, flows out into the Ala Shan Desert (*U*–14) of Inner Mongolia. The river ends abruptly in the playa lake (*O*–2) and permanent lake (*Q*–2) named in the previous plate. This river carries a large load of sediment down its steep gradient from the mountains. The loss of velocity on emerging into the flatlands causes rapid deposition from the active stream channels. Over time in the Quaternary and Recent, shifting distributaries have aided in building a huge alluvial fan (perimeter along *D*–11; *K*–3; *R*–13)—certainly one of the largest features of this kind in the world. In contrast to the coalesced multiple fans or bolsans just to the north shown on plate 312, the fan here remains a single feature retaining the classic shape best described by analogy to an opened "lady's fan." This fan has spread out over older stream deposits, encroaching on Paleozoic sedimentary rocks (*F*–3; *J*–20) exposed in the structural basin now covered by the Gobi sands. The area is very sparsely populated; a few villages on the Edsin engage in spring wheat farming. *1407–03320;* September 3, 1973.

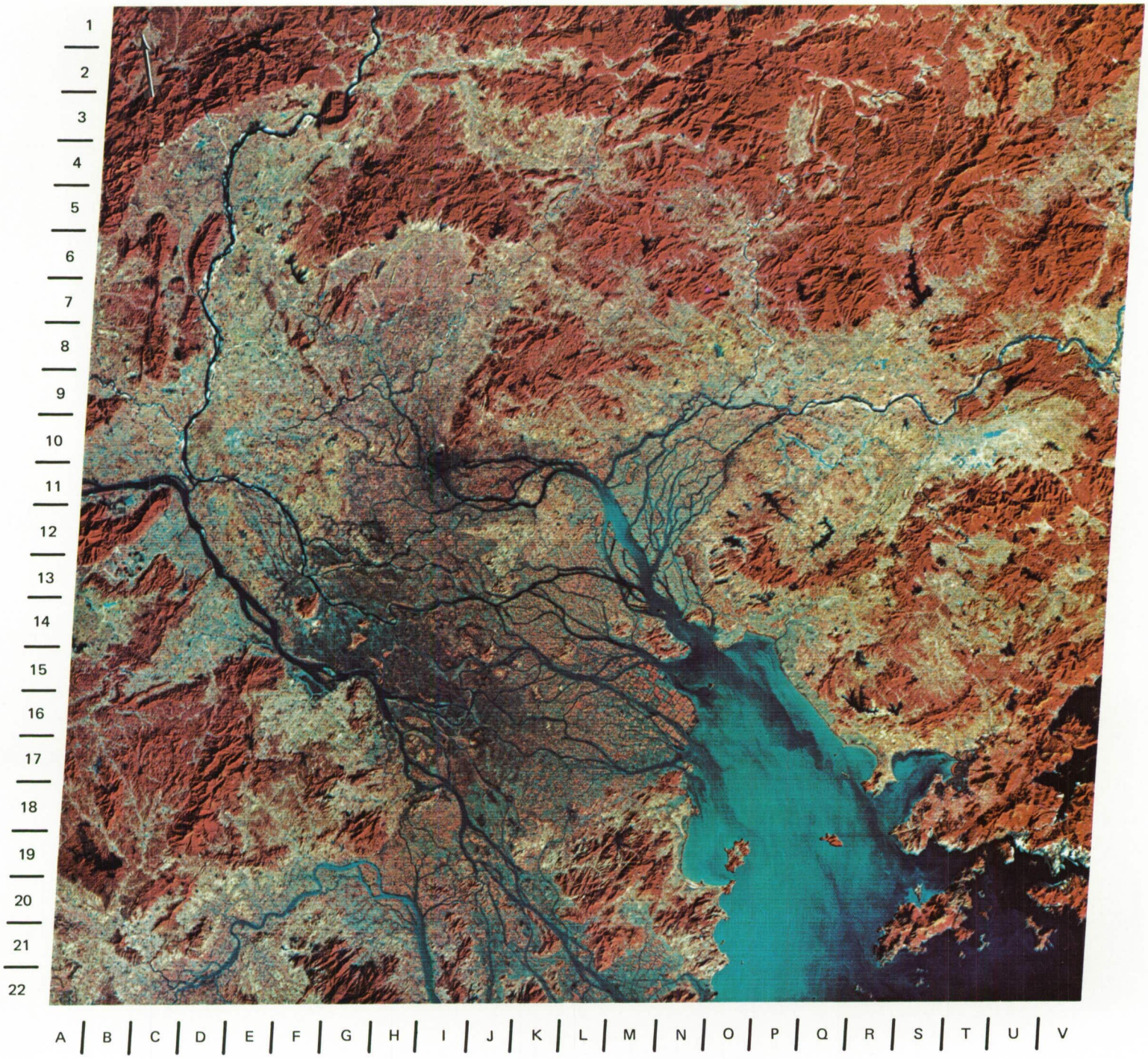
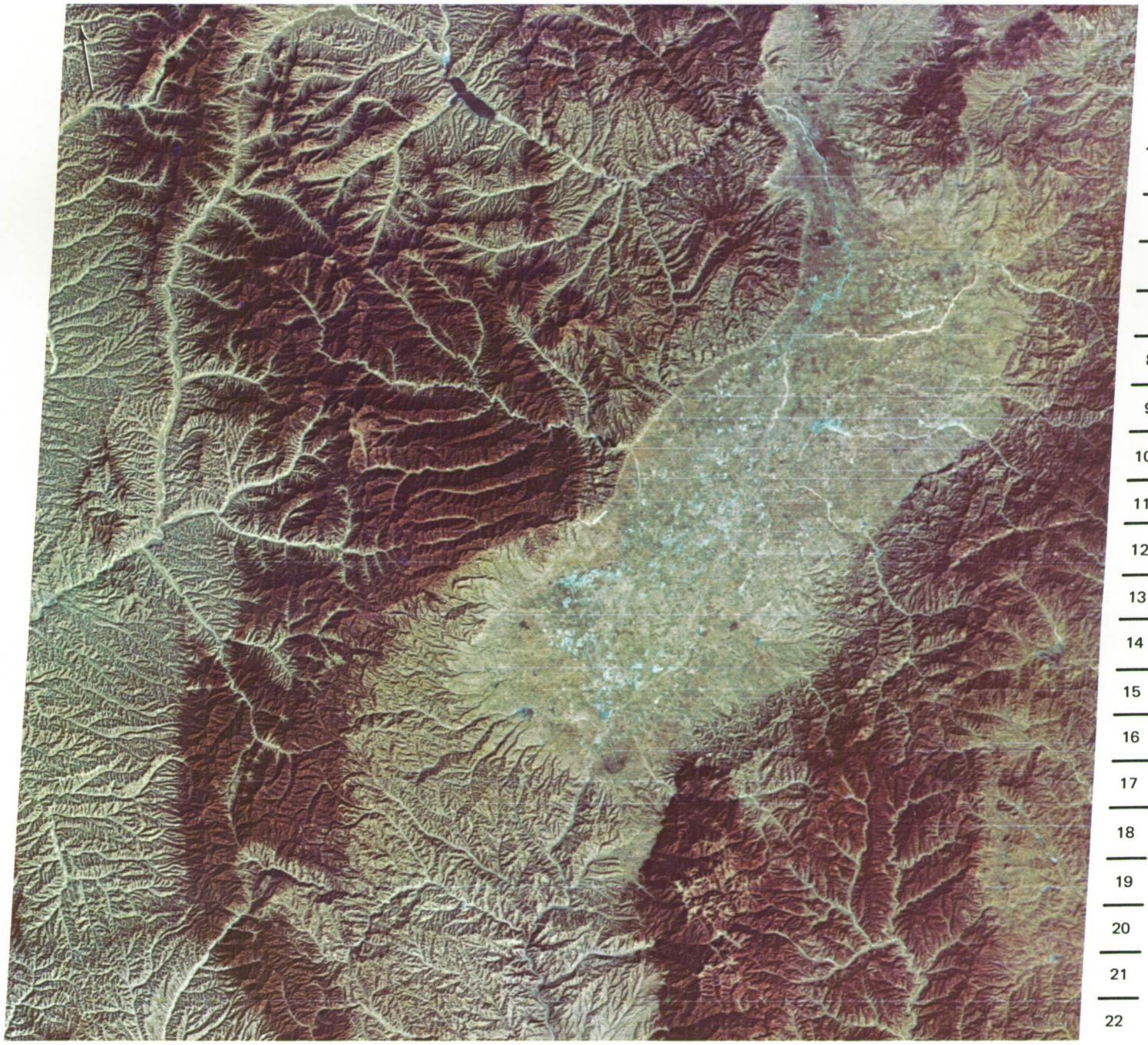


PLATE 314

HONG KONG AND CANTON, SOUTH CHINA COAST: The cities of Kuangchou (formerly Canton) (*H*–10), capital of Kwangtung Province in mainland China, and Hong Kong (*V*–19), the British Crown colony on an island and a peninsular stretch of land (the New Territories) (*U*–17), appear together in this scene. The Portuguese trading port of Macao (*O*–21) is located at the west entrance to the Chu-kiang estuary (*P*–17). This estuary is the submerged portion of the delta of the Kiang River system that spreads out in distributaries at the southern end of the Kwangtung alluvial plains (*J*–12). The principal channel is the Si Kiang (*A*–11) flowing in from the west. The Pei Kiang (*C*–6) drains highlands to the north while the Tung Kiang (*B*–9) reenters from the east. Canton itself, a city of 4 000 000, straddles a beheaded distributary that widens into the estuary. Most of the lowlands from Canton south are subject to frequent flooding, compounded by inundation. The plains, filled with fertile silt and favored by a mild climate, is extensively farmed. Besides the mainstay of rice, vegetables, grains, maize, sugar, tobacco, coffee, bananas, and other fruits are produced in abundance. Mulberry trees are cultivated in large groves to provide leafy food for silkworms. Many of the high hills, once islands when this region was further submerged as a gulf, are composed of Jurassic basalts. Other rocks of late Precambrian to early Paleozoic age were involved in extensive folding in the middle Paleozoic. These hills, rising to 900 meters (3000 feet), are covered with evergreen shrubs, with some bamboo and palm forests. *1520–02210;* December 25, 1973.

PLATE 315



THE YELLOW RIVER, CHINA: In this section of north-central China, in the Shansi Province south of Inner Mongolia, the Huang Ho or Yellow River (*C*–6) runs north to south before turning eastward again in its course toward the Yellow Sea. The region is one of dissected mountains—grass covered with scattered trees—up to 1800 meters (6000 feet) high that form part of the northeast-trending Shansi crustal block. Triassic sedimentary rocks are exposed on both sides of the Yellow River and into the Luliang Mountains (*I*–4). The river also crosses darker Ordovician sedimentary units (*F*–17). Carboniferous beds outcrop at the southern end (*J*–18) of the Taiyuan Basin (*Q*–9), filled with lake beds and younger alluvium and now drained by the Fen River (*N*–13) as it moves southwest toward the Huang Ho. The northern parts of the Luliang Mountains shown here consist of Paleozoic units and late Precambrian crystalline rocks (*L*–1). The Hwo Mountains (*Q*–18) are a tilted block of Paleozoic sedimentary rocks with a long patch of later Tertiary sediments (*O*–19) on their west side and Triassic rocks (*V*–17) to the east. Most of the uplands terrain shown in this scene has been covered with loess, windblown "dust" carried in for countless centuries from the Gobi Desert of Mongolia. Surficial deposits have accumulated to thicknesses of 30 to 90 meters (100 to 300 feet) over vast areas of inland China. Where eroded by many small streams, gullies having a trellis- to dendritic-drainage pattern become the dominant influence on surface topography (*A*–9). The yellowish-brown loess soils added to the Huang Ho are responsible for its distinctive color.

Coal is mined from the hills around the Fen Valley and iron is extracted to the east. The city of Taiyuan (*Q*–4) has become a major center for steelmaking, as suggested by the smoke plumes visible in this image. The broad valley to the south is devoted largely to winter wheat and millet farming. *1524–02394;* December 29, 1973.

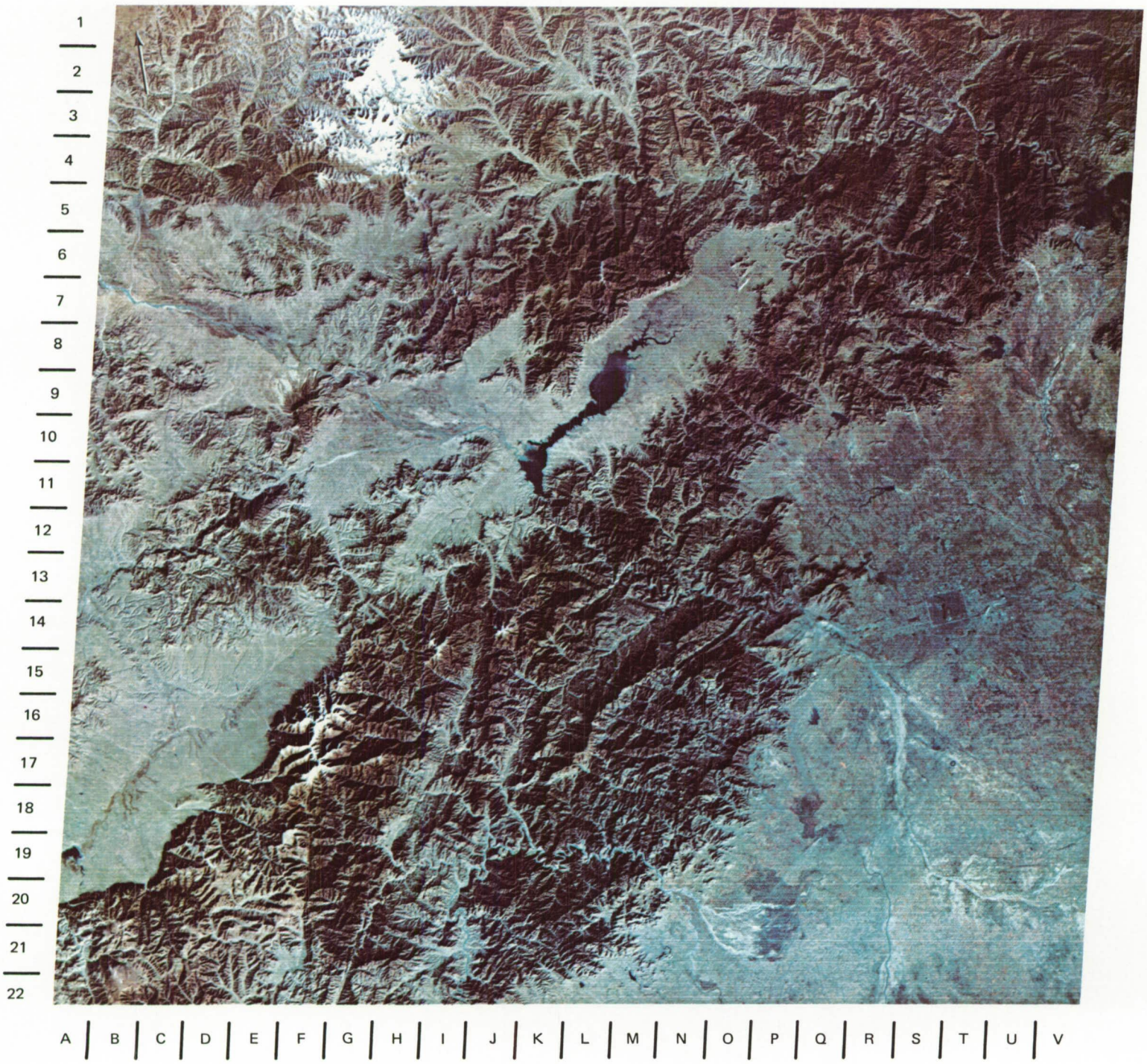
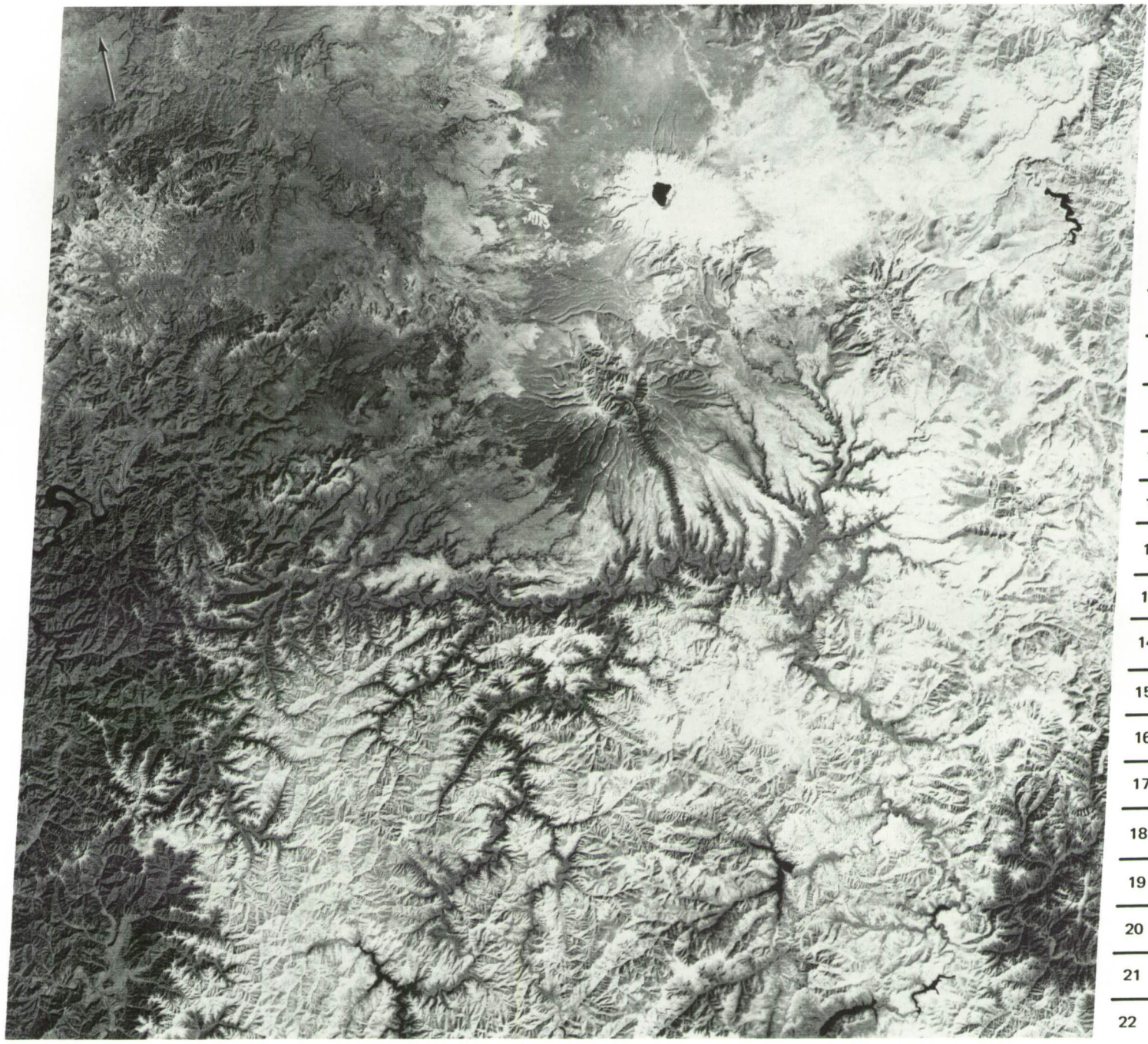


PLATE 316

PEKING: The capital of the People's Republic of China was once known as Peiping when it was then the capital of the Manchu dynasty. In this late fall view, the Great Wall of the old city (*S*–13) is clearly seen. Within it are the lakes near the Imperial Palace. Just to the south, the walled gardens of the Temple of Heaven (*S*–14) are also visible. Peking has now grown to a city of about 7 million people.

Peking lies near the northern end of the Northeastern Plains, mostly covered by Quaternary alluvium. This valley, drained here by the Yunting River (*R*–16), is used for growing wheat, maize, sweet potatoes, and cotton. To the west are the T'Ai-Hang and Wut'ai Mountains, extensions of the Great Khingan Range, here a complex of Precambrian metamorphic rocks, Ordovician and younger Paleozoic sedimentary rocks, granite and diorites, and Jurassic basalts, that rise to 2300 meters (7600 feet) in the region shown. The valley to the north carries the Sangkan River (*H*–9) past the towns of Suanhwa (*D*–7) and Wanchuan (*A*–5). Both that river and the Yunting are connected to the Kuant'ing Reservoir (*L*–8), the main water supply for Peking. The uplands further north include the Tahaito Range (*I*–2) and other high mountains made up of Precambrian metamorphic rocks. The Great Wall of China winds its way for many hundreds of kilometers through the several mountain blocks shown in this image. When a transparency of the scene is viewed under magnification, small segments of the wall can be discerned. *1486–02280;* November 21, 1973.

PLATE 317



YALU RIVER, CHINA AND KOREA: The border between the Kirin Province of Manchuria and North Korea lies along the Yalu River (*D*–10; *K*–13). The Korean side, in particular, consists of rugged terrain, a part of the Nangnim Sanmaek Range (*J*–16), a crystalline complex of Precambrian metamorphic and Cretaceous granitic rocks rising to elevations of 2100 to 2400 meters (7000 to 8000 feet). One mountain (*Q*–7) reaches 2744 meters (9003 feet) on the border near the headwaters of the Yalu. To the north, in the Ch'angpai Range (*D*–4), are several volcanic peaks (*M*–4) surrounded by older (Jurassic) volcanic rocks (*L*–2). The Changjin Reservoir (*H*–21) is developed on the Changjin River. The Pujon Reservoir (*P*–19) lies to the east. *1100–01441;* October 31, 1972.

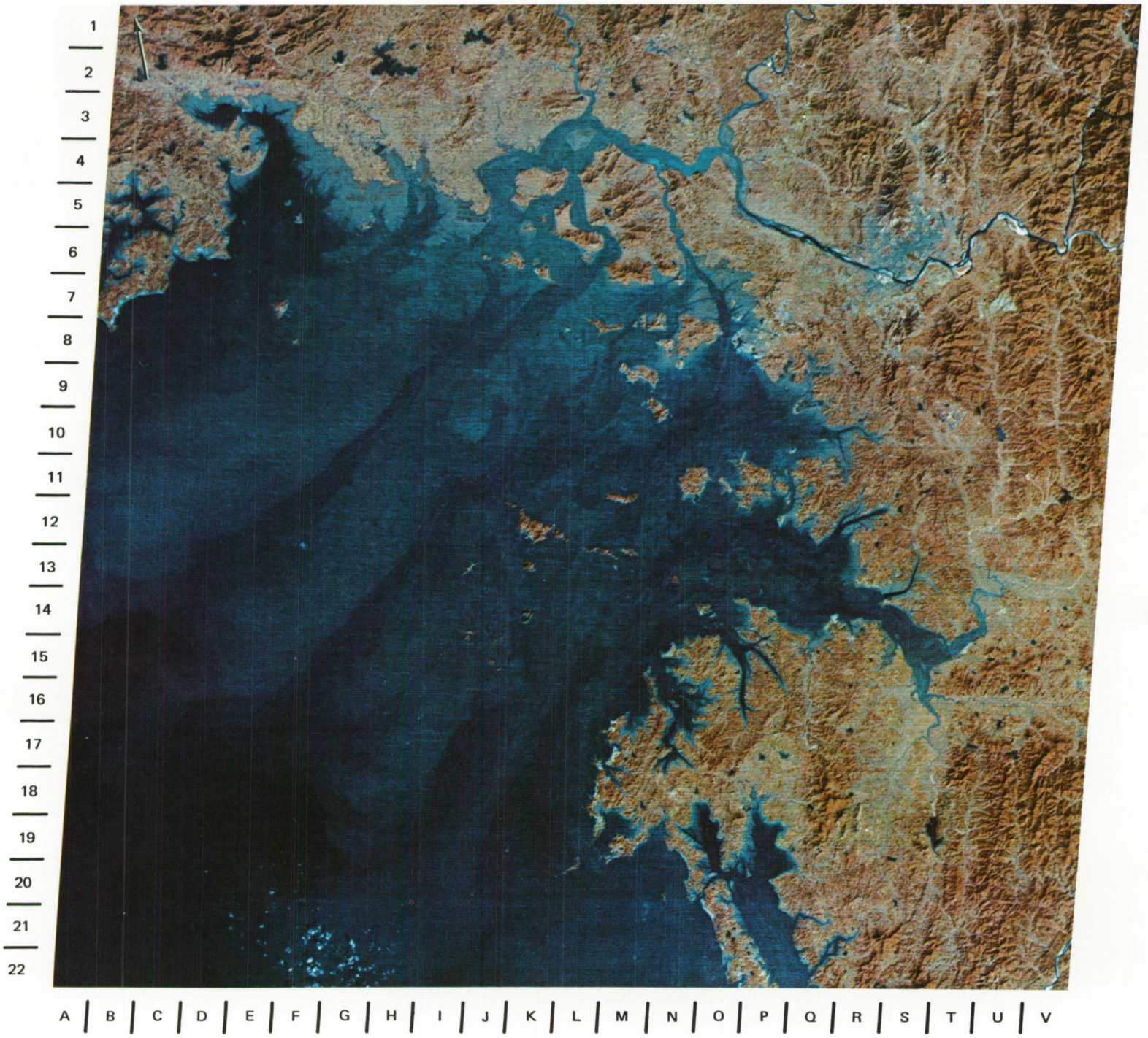
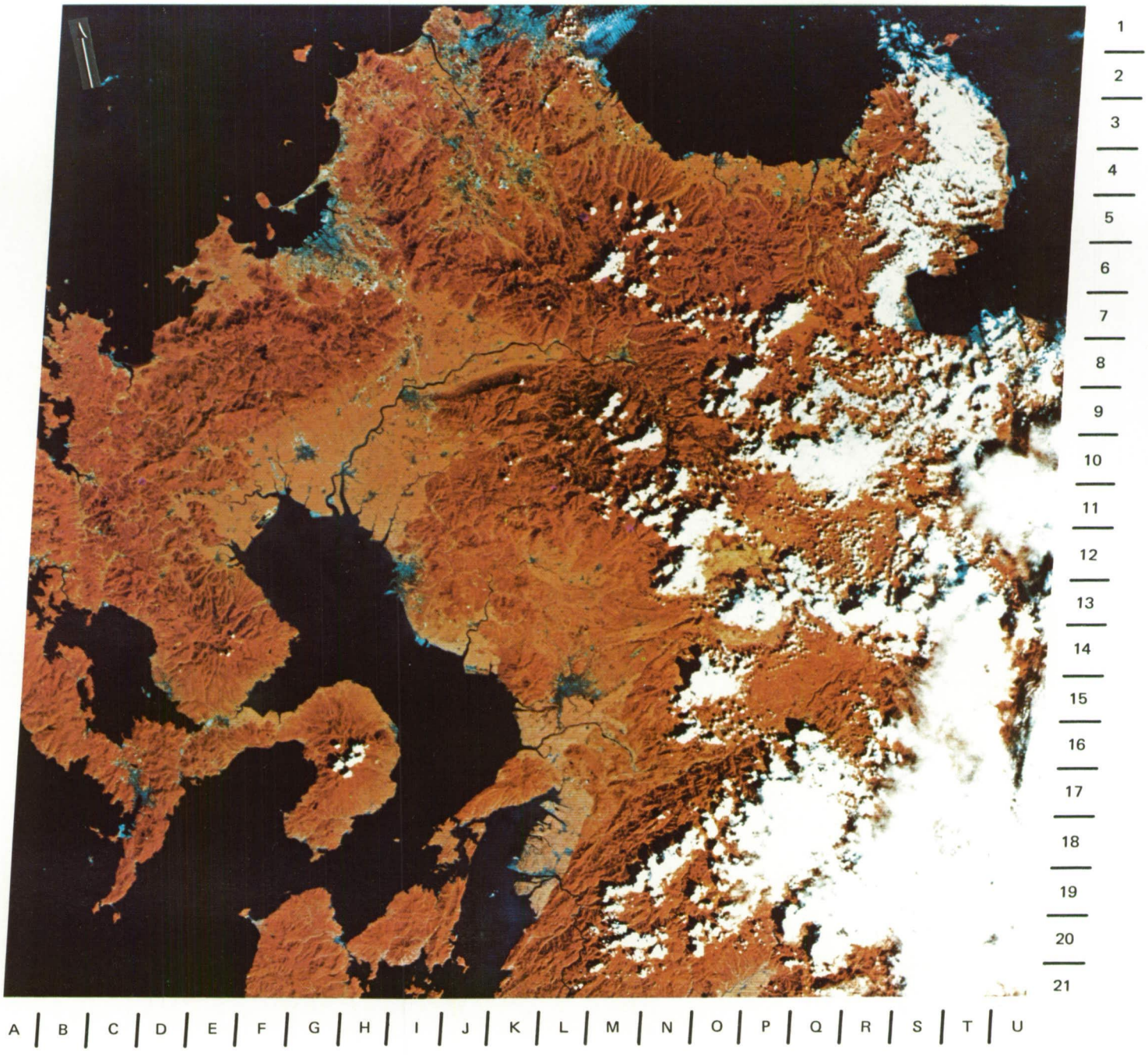


PLATE 318

THE TWO KOREAS: The segment of the Korean peninsula seen in this view is situated just south of the 38th parallel. A small part of North Korea (*F*–3) lies to the west of the Imjin River (*O*–1) where it flows into the Han River (*S*–6). The Han, joined southward by the Pukhan River (*V*–3), discharges a heavy load of sediments through several distributaries and past offshore islands to form a series of sediment plumes (*D*–10) extending more than 80 kilometers (50 miles) into the Yellow Sea. These sediments are derived from mountainous ranges (rising 600 to 900 meters (2000 to 3000 feet) above sea level) of Precambrian schists and gneisses and Cretaceous granitic intrusives to the east. Seoul (*Q*–6), the capital of South Korea, straddles the Han River while Inchon (*O*–11) serves as the seaport. Fishing and rice cultivation along terraces in the lowlands are the main source of income outside the industrial areas around Seoul. *1100–01453;* October 31, 1972.

PLATE 319



NORTHWESTERN KYŪSHŪ ISLAND, JAPAN: This westernmost of the major islands of Japan is that nation's principal producer of coal from mines and some surface pits cut into Cretaceous beds in highly folded strata mixed with Mesozoic granites within mountains of the Saga (*D*–9) and Fukuoka (*I*–4) districts. Most of the other mountainous areas, particularly in the Kyushusanchi Ranges (*Q*–15) in this scene, consist of Tertiary andesitic ash beds and/or Quaternary volcanic flow rocks (*P*–15). The volcanoes Aso (*O*–13) and Unzen Nat (*G*–16) are active; others at *D*–13, *L*–9, and *R*–4 are probably extinct. The lowlands around the Chikugo (*I*–8) and Midori (*L*–15) Rivers are Recent sediment-filled extensions of the Ariakeno Unu (*G*–13) and Yatsushiro (*J*–19) inlets. These and other flat areas are devoted to rice and sweet potatoes. Mandarin oranges and tea and tobacco are also grown in the region. The highlands are covered by natural evergreen oaks, or, where reforested after timbering, by oak and pine. Industry, refining, and manufacturing occur in the larger cities at Fukuoka (*F*–5), Kumamoto (*K*–4), Kurume (*H*–8), Sasebo (*A*–12), and Yawata-Moji (*I*–1)—the last-named city is the principal port on the island. The city of Nagasaki (*C*–17) is located below the Omura inlet (*B*–14). *1078–01232;* October 9, 1972.

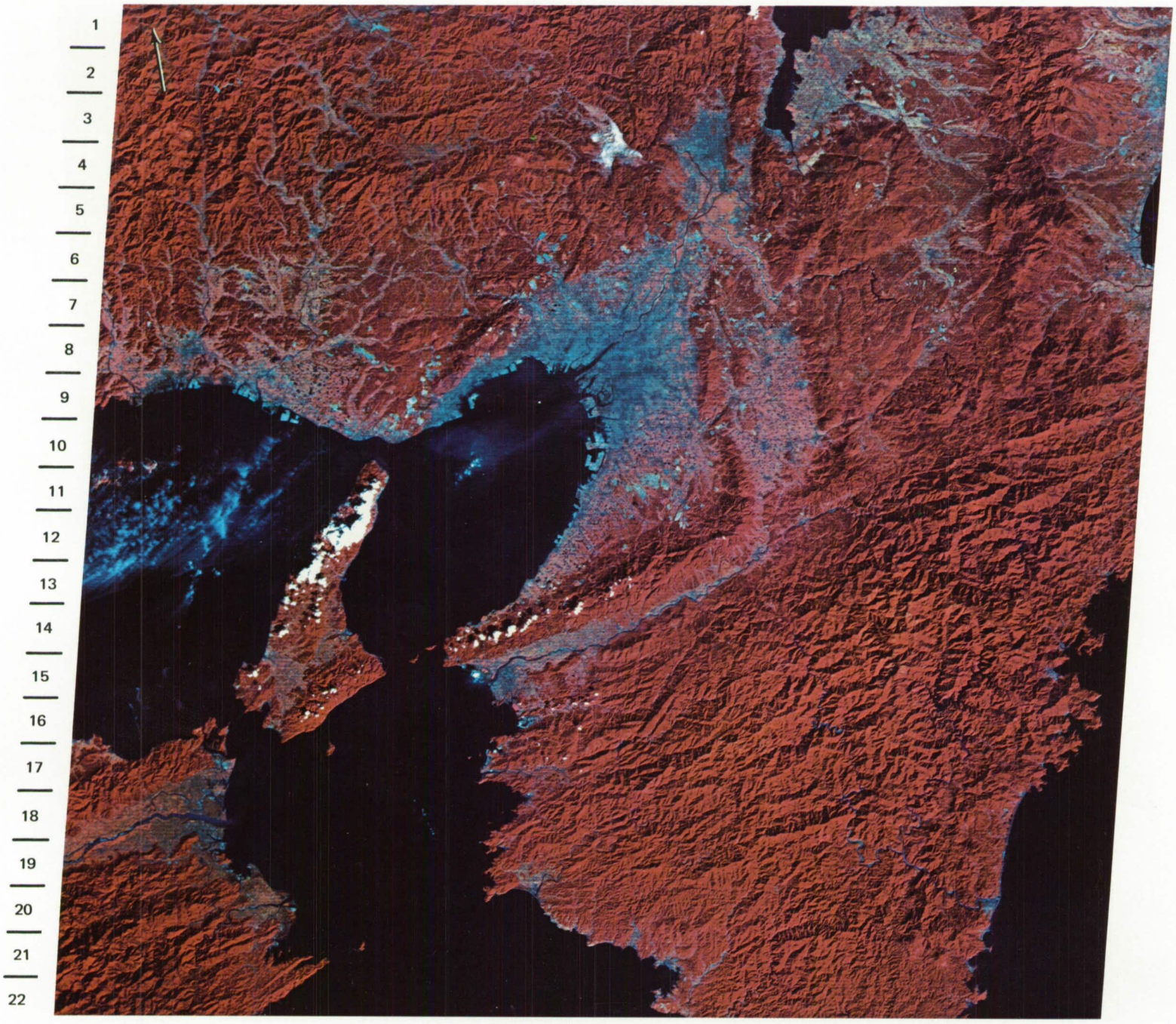


PLATE 320

OSAKA, JAPAN: This region of west-central Honshu Island contains several major metropolitan centers of Japan. Osaka (*K*–8), the second largest city (3 400 000 people), a center for textiles, heavy industry, and electronics, is built on the delta of the Yodo River (*L*–6). Nearby Kobe (*H*–9), with its landfill wharves (*I*–8), is the second largest seaport in Japan. Both cities lie on Osaka Bay (*I*–11), almost completely sheltered by Awaji Shima island (*E*–14), at the east end of Japan's "inland sea." This great marine passage results from partial enclosure by the Nara peninsula (*P*–16) on the east, the island of Kyushu on the west, and the island of Shikoku (*B*–20) in the center at the south. The Kii Suido (*H*–20) is the eastern inlet to this sea.

The geological setting is an important factor in the urbanization of this region. A great strike-slip fault, the longest in the Japanese islands, runs through the Kino River (*K*–14) valley (with the city of Wakayama (*I*–15) at its mouth) on Honshu Island and through the Yoshino River (*B*–18) valley (with the city of Tokushima (*C*–18) at its mouth) on Shikoku Island. Movement along this fault has carried Paleozoic crystalline rocks (*M*–15) into juxtaposition with Cretaceous sedimentary rocks (*K*–13). To the south are a succession of younger Paleozoic (*N*–18) and then Mesozoic (*R*–21) sedimentary rocks in broad bands parallel to the fault. Immediately north of the fault are a series of late Mesozoic volcanic rocks (mostly andesites). Late Paleozoic sedimentary rocks occur northwest (*F*–4) of Osaka and Kyoto (*M*–3) while silicic volcanic rocks of Tertiary age are found to the west (*C*–4). The Kinki Lowlands (*M*–6) between Osaka and Kyoto has developed from northeast-trending faults. Intersecting faults are responsible for the down-dropped block now occupied by Lake Biwa (*O*–1), which is fed by mountain stream drainage.

The Yodo flood plain, those of the Kino and Yoshino Rivers, the enclosed Nara Basin (*O*–9) (site of the oldest capital of Japan), and the coastal plains around Himeji (*B*–8) are Quaternary plains (with numerous small lakes) on which extensive cultivation of paddy rice is carried out. Wheat, vegetables, fruit (particularly mandarin oranges), and tea are all grown in these lowland fields. The rugged mountainous country is covered by deciduous trees and subtropical evergreens. Timbering takes place inland, and fishing is important in the coastal communities. *1093–01060;* October 24, 1972.

PLATE 321



TOKYO, JAPAN: Tokyo (*G*–14), one of the world's largest cities (with a population of more than 10 million people), is built up along the north end of Tokyo Bay (*J*–16). The seaport of Yokohama (*H*–18) is located next to deeper water that provides better access for ocean vessels. Through a system of landfill into the bay and interconnecting canals, a series of manmade extensions (*I*–15; *L*–15) supported by retaining walls, cluster around most of the bay. Some serve as docking areas or industrial sites. The Imperial Palace grounds and nearby parks form red patches at *H*–14.

Tokyo is situated on poorly consolidated materials (making it especially prone to earthquake damage) at the southern end of the Kwanto Plains (*E*–9), formed from Pleistocene and Recent marine sediments and from alluvial deposits of the River Tone (*L*–11) and its tributary, the Kinu (*F*–6). The Tone has built a delta into the Pacific at Choshi (*S*–11). The Chiba peninsula (*M*–19) results from the joining of an island of older Pliocene sediments by a broad spit of land (*N*–15) to form Tokyo Bay. Old beach terraces (*P*–12) are evident on its eastern shore. The mountains north of Lake Kasumiga-Ura (*N*–8) consist of late Paleozoic sedimentary rocks intruded by Mesozoic granites with overlying patches of Pliocene sediments. Those to the west (*B*–16; *C*–4) are even more complex, being made up of strongly folded and faulted rocks of similar age, together with extensive outpourings of Tertiary and Quaternary basic volcanics (Mount Fujiyama, the 3700-meter (12 000-foot) high stratovolcano, lies just off the image at *A*–19).

The Kwanto Plains, once very swampy (*G*–7), have been almost completely drained to allow farming and land development. Many small cities and towns (*C*–9) dot this region. Paddy and terrace rice is the main crop, with sweet potatoes, wheat, and barley also grown. On lower hill slopes, mulberry trees, tea, and tobacco are important staples. The mountains are covered by deciduous trees, including oak, beech, and maple, and by conifers such as pine and hemlock. *1126–00484;* November 26, 1972.



PLATE 322

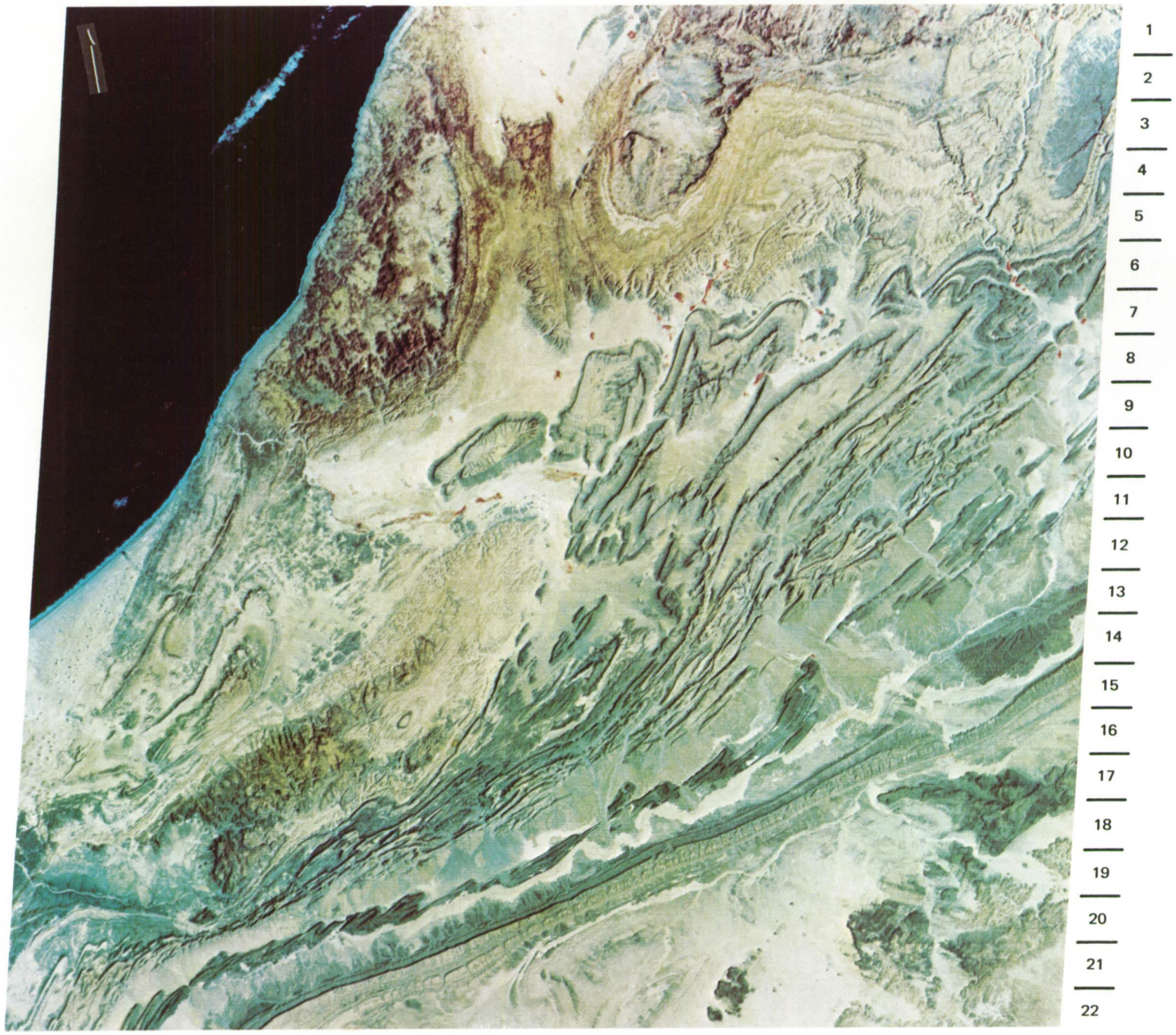
A DORMANT VOLCANO AWAKENS: The volcano Tiatia (*O*–14) lies at the northeastern tip of Kunashir Island, the southernmost of the Kuril Islands, a volcanic chain that runs between the Kamchatka peninsula in far eastern Siberia and the northeastern end (*G*–17) of Hokkaido Island in Japan. This stratovolcano, similar in many characteristics to Mount Vesuvius in Italy, had been quiet for 161 years since its last reported eruption in August of 1812. The volcano rises abruptly from the sea to an elevation of nearly 1800 meters (5900 feet). Its central peak is capped by a large sommatype crater (*O*–14).

Two days before this Landsat image was obtained on July 16, 1973, Tiatia began to erupt in a series of violent explosions audible 50 to 80 kilometers (30 to 50 miles) away in the isolated fishing villages of this Soviet island. A great plume of ash-laden gases, such as seen here (*U*–18) as it crosses Shikotan Island (*U*–21), rose to heights of 4600 meters (15 000 feet) or more as the volcano continued to discharge for weeks after the start of the event. This eruption cloud is emitting from a new vent (*P*–15), a crater developed on the south side of the volcano's flanks. Much of the volcano slopes on the north, east, and south have been covered by dark ash (*P*–14) to depths exceeding 60 to 90 centimeters (2 to 3 feet) in places. The dense scrub vegetation has been damaged or killed off by burial or by fires (*Q*–14) set from the hot ashes. The village of Tyatina (*P*–15) along the south coast has been directly affected by the ash and the smoke.

In the early days of activity, the volcano produced a series of strong explosions, with visible flashes of flame, about every 60 to 90 seconds. It is possible that the distinct semicircular arc (*N*–11; *R*–12) impressed on the low moisture clouds over the sea is the result of the periodic shock pulses accompanying the explosions, although thermal effects may be a factor.

The volcanoes in the Kuril Islands were unusually active in 1973. Several others erupted during the year including volcano Ivan Groznyy on the island of Iturup (*V*–10) north of volcano Rikorda (*U*–11). *1358–00341;* July 16, 1973.

PLATE 323



SOUTHERN MOROCCO: The poorly defined border separating Morocco from the Spanish Sahara to the south trends along the Oued (wadi) Dra (*A*–18 to *D*–19, then south to *D*–20 and east-northeast along the light-toned flood plain to *V*–13). The former Spanish Ifni enclave was essentially confined within the brown-tan mottled area centered at *G*–6.

The spectacular geology in this area includes three major structural styles. The dark mottled area centered at *G*–6, *F*–16, and *M*–3 are Precambrian basement rocks exposed by erosion of broad domal uplifts. Younger sedimentary strata trend in a concentric pattern around the core exposures. The northeasterly trending Jebel Bani Mountains (*G*–18 to *V*–6) are located immediately to the east of the domes and consist of a system of commonly plunging folds. These flexures become more tightly compressed toward the southeast, then terminate abruptly at approximately the Oued Dra. South of the Oued, the continuous outcroppings (*F*–21 to *V*–14) mark the northwest flank of the Tindouf basin.

The average rainfall in this dry area is only 10 to 15 centimeters (4 to 6 inches) per year, but this is adequate to support limited livestock and agriculture. The chief products are sheep, goats, camels, dates, and vegetables, which are produced largely for local consumption. The major agricultural areas are easily recognized on the Landsat color composite imagery by their characteristic bright red color (*N*–6). Here, it should be noted, the agriculture appears to be localized along the drainage patterns, indicating that the crops are dependent for water from the ephemeral streams and shallow irrigation wells dug into an aquifer below the flood plain. *1247–10420;* March 27, 1973.

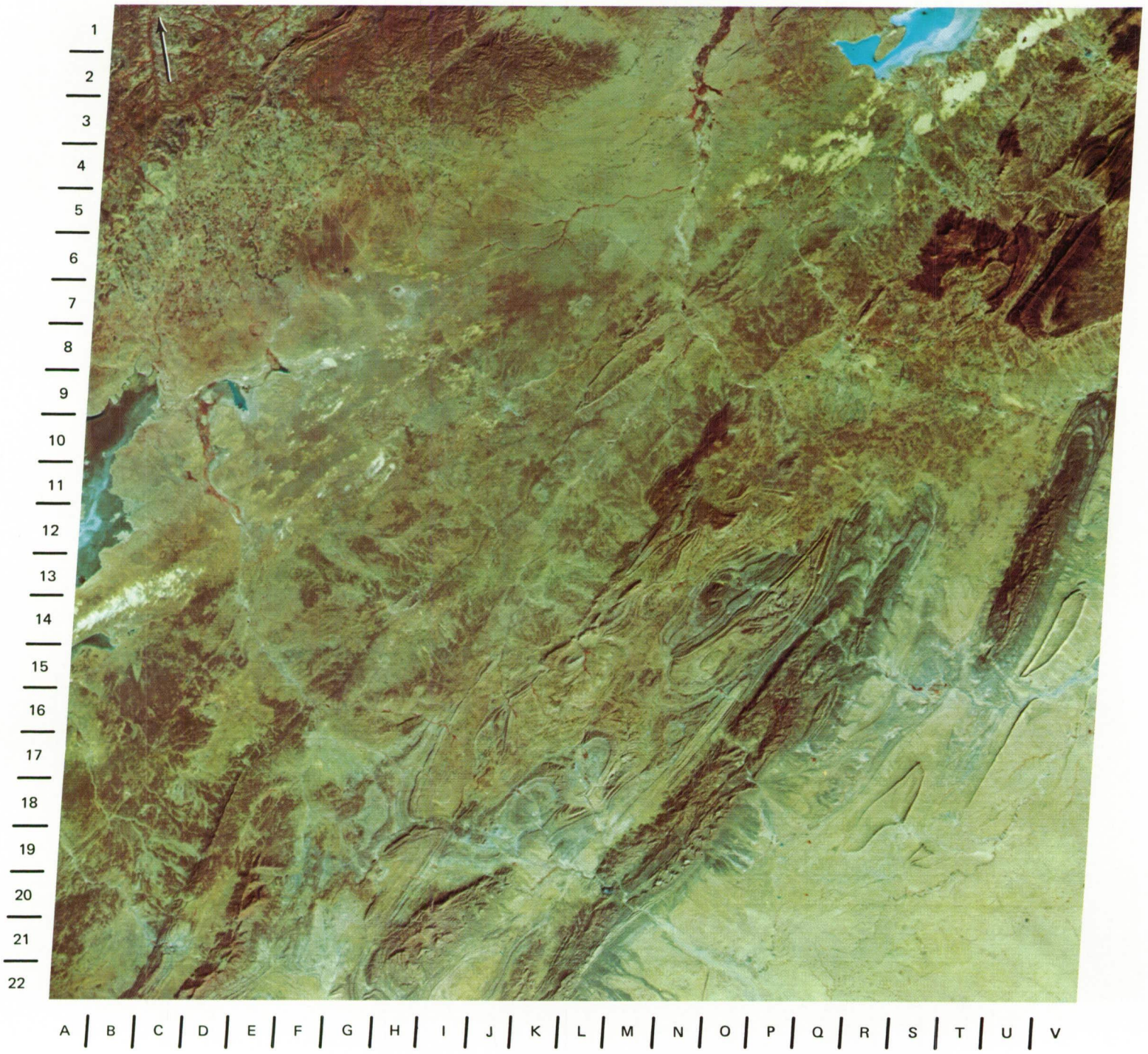
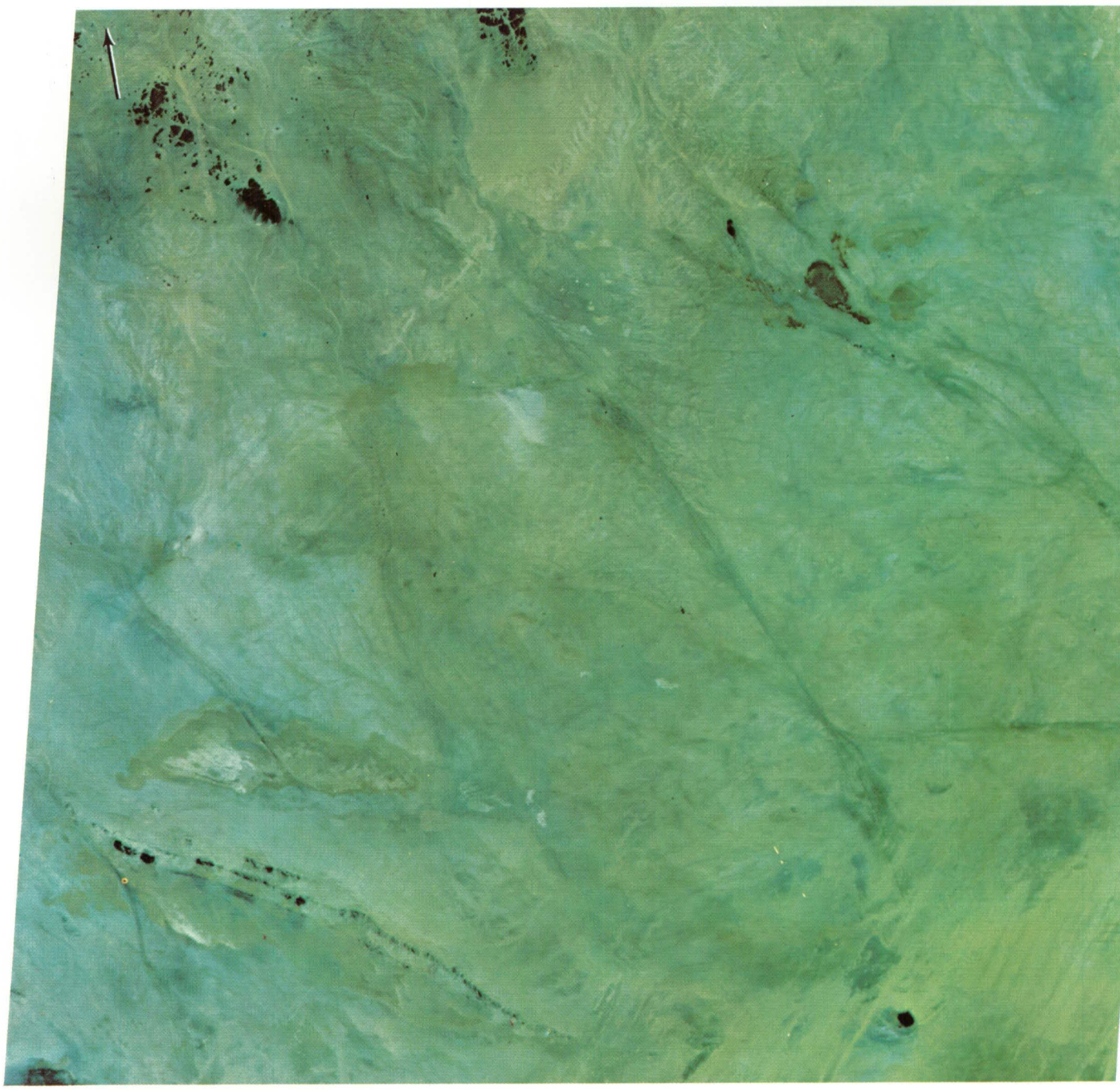


PLATE 324

ATLAS MOUNTAINS: A good cross-sectional view of northern Algeria is provided by this image, covering parts of several major geologic provinces and climatic zones. Regionally, this area is part of the Atlas Mountains, themselves a branch of the great Alpine system reaching one-third of the way around the Earth. The main Algerian subdivisions of the Atlas Mountains are traversed in this image from upper left to lower right as follows: Tell Atlas (*A*–3; *F*–1); High Plateaus (*A*–11; *P*–1); Saharan Atlas (*A*–21; *V*–1); Subatlic Hamadas (*extreme lower right corner*). Climatically, this traverse would encounter successively drier areas; the Landsat image shows this in the vegetation change from reddish-brown in the Tell Atlas to the yellow of the Sahara. Most of the area is very dry by European standards, with only limited agriculture. Sheep and goat-raising are important for the area. Some specific landmarks include Chott ech Chergui (*A*–12), Zahrez Rharbi (*R*–1), and El Ousseukh (*R*–1; barely visible town). Several motor routes are visible.

The Atlas Mountains are one of the world's great folded mountain chains, and their structure is well displayed here. The High Plateaus are sediment-filled valleys 1000 to 2000 meters (3300 to 6600 feet) above sea level; the sediment was derived from the growing mountains north and south of these valleys. Geologically, they are molasse troughs, corresponding to the Swiss Plain shown in plate 235. The Saharan Atlas are a series of open anticlines and synclines whose structure has been emphasized by differential erosion, with the more resistant rocks such as sandstones forming ridges. It should be noted that anticlines *or* synclines may form mountains; examples of this are visible at lower right. The physiography is strikingly similar to that of other folded mountains, such as the Appalachians or the Ouachitas. Many geologists believe such fold belts are formed by plate collisions following continental drift; Landsat images, permitting each geologist to make his own global field trip, may help prove or disprove this theory. *1114–09595;* November 14, 1972.

PLATE 325



MAURITANIA: The northwest corner of Mauritania is covered by this image, which includes no settlements; Fort Trinquet is just off the picture to the northwest. This area is the Yetti Plain, or Dorsale Reguibat, a barren gravel desert covering several tens of thousands of square kilometers in Mauritania and the Spanish Sahara. The only formally named landmarks in the image are the salt lakes, or sebkhas: Oumm ed Drous Telli (*F*–15) and Oumm ed Drous Guebli (*E*–19). The northern edge of an erg (dune field) is just visible at lower right (*T*–20); this is part of the Hammami, a collection of seif dunes.

Geologically, the area is of considerable interest, although little is known about it. The Dorsale Reguibat is an immense uplift of Precambrian rock, mainly granite, trending northeast to southwest, cut by long igneous dikes. One of these, running from *H*–5 to *Q*–16, is over 120 kilometers (75 miles) long. They follow fractures, possibly faults, which have broken the crust locally into a mosaic of blocks. The dark hills at *C*–3 are also igneous intrusions. Most of the rock exposed in this image is apparently granitic, probably forming batholiths or gneiss domes. The Dorsale Reguibat is an erosion surface that provides an unusually good exposure of these ancient rocks, which in most other areas are covered by younger sedimentary rocks, dune fields, or vegetation. *1247–10432;* March 27, 1973.

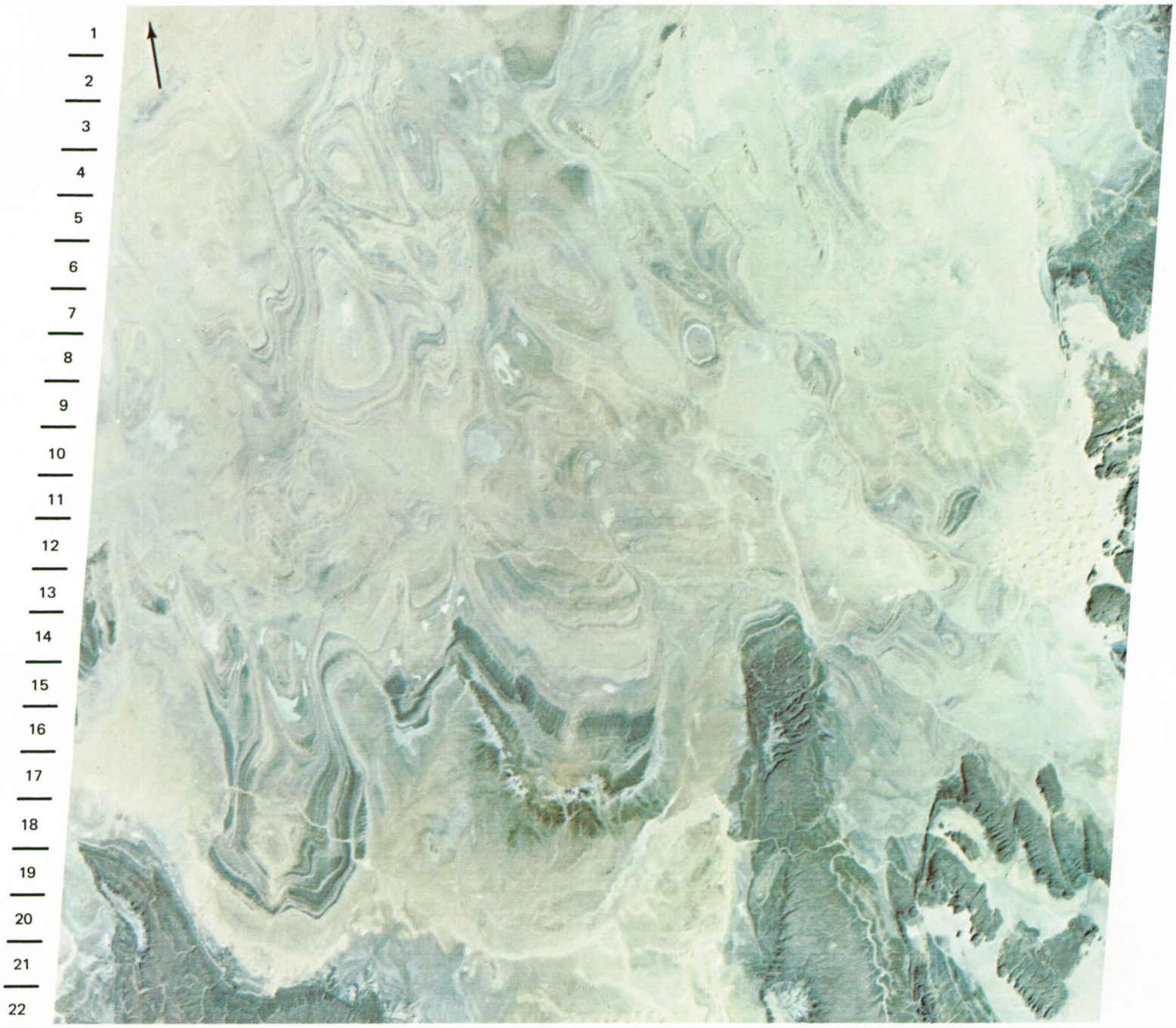


PLATE 326

TANEZROUFT, ALGERIA: This striking outcrop pattern of concentric loops and ellipses is in one of the most desolate parts of the generally desolate Sahara: the Tanezrouft, or "Land of Terror," in southern Algeria. The center of the image lies roughly 160 kilometers (100 miles) south of the In Salah oasis, but there are no visible settlements or, for that matter, no traces of human activity. Maps of the area have descriptive phrases such as "impassable area," "gravel plain devoid of vegetation," and "undrinkable," the last referring to the occasional mineral springs and salt flats (sebkhas). Generally speaking, the area is mainly gravel desert, or "erg," and can be easily driven over; although completely invisible to Landsat, a major motor route south from the In Salah oasis goes along the right edge of the area.

The complex land patterns suggest complex geologic structure, but this is misleading. This is one of the most stable parts of Africa, being underlain by very slightly deformed Paleozoic sedimentary rocks. The concentric patterns are the expression of these strata after erosion by wind, or "deflation," just as the grain of wood appears after sandpapering. This part of the Sahara is nearly free of major topographic barriers and is extremely dry; consequently, wind erosion is much more important here than in other deserts such as the Basin and Range province of North America.

There is a small dune field at *U*–11, consisting of peaked dunes. The dark ridges along the lower part of the picture are "tassilis," or cuestas, consisting of sedimentary rocks dipping, in this scene, very gently to the north. Their structure is also simple, the complex pattern reflecting low-angle erosional beveling rather than intense folding. The prominent ridge at *B*–19 to *G*–22 is the north slope of the Assedjrad escarpment, itself off the image to the south. *1112–09505;* November 12, 1972.

PLATE 327



TADEMAÏT PLATEAU, ALGERIA: Although this part of Algeria is nearly uninhabited, there is evidence of human activity in the form of motor trails across the Sahara (*left,* parallel to the image edge, from *C*–7 to *F*–21). These are actually roads used for scheduled bus service between El Golea (north of this area) through Fort Miribel (*G*–5, not visible) to In Salah to the south. The desert here is mainly gravel and may be crossed with little or no preparation. Other motor routes are visible converging at Fort Miribel.

Physiographically, this area is part of the Tademaït Plateau. This is one of several such areas in this part of Africa between 500 and 1000 meters (1600 and 3300 feet) above sea level, consisting of flat-lying or gently dipping sedimentary rocks of Cretaceous or Tertiary age. They show that considerable parts of North Africa have undergone submergence since the beginning of the Paleozoic Era. In this area, the deformation was of the basin-and-swell type; i.e., primarily vertical, as opposed to folding and faulting indicating horizontal movement. This Landsat image shows a surface of Cretaceous marine sediments youthfully dissected in a dendritic drainage pattern. Most of the drainage is to the northeast, into the Oued Mya (*L*–9), but at the lower left it is to the southwest. An interesting example of stream piracy is visible around *K*–17. The initial drainage was to the southwest here; the dendritic pattern converges in that direction. But a prominent wadi (filled with sand when the image was acquired) that, when filled, flows to the northeast has cut across the older drainage. Evidence of this sort will help physiographers reconstruct the Cenozoic geologic history of the area.

A few relatively small dune fields (ergs) are visible. The one at the extreme right (*U*–6) is the west end of the immense Grand Erg Oriental, which stretches for some 480 kilometers (300 miles) to the northeast off the image. *1022–09491;* August 14, 1972.

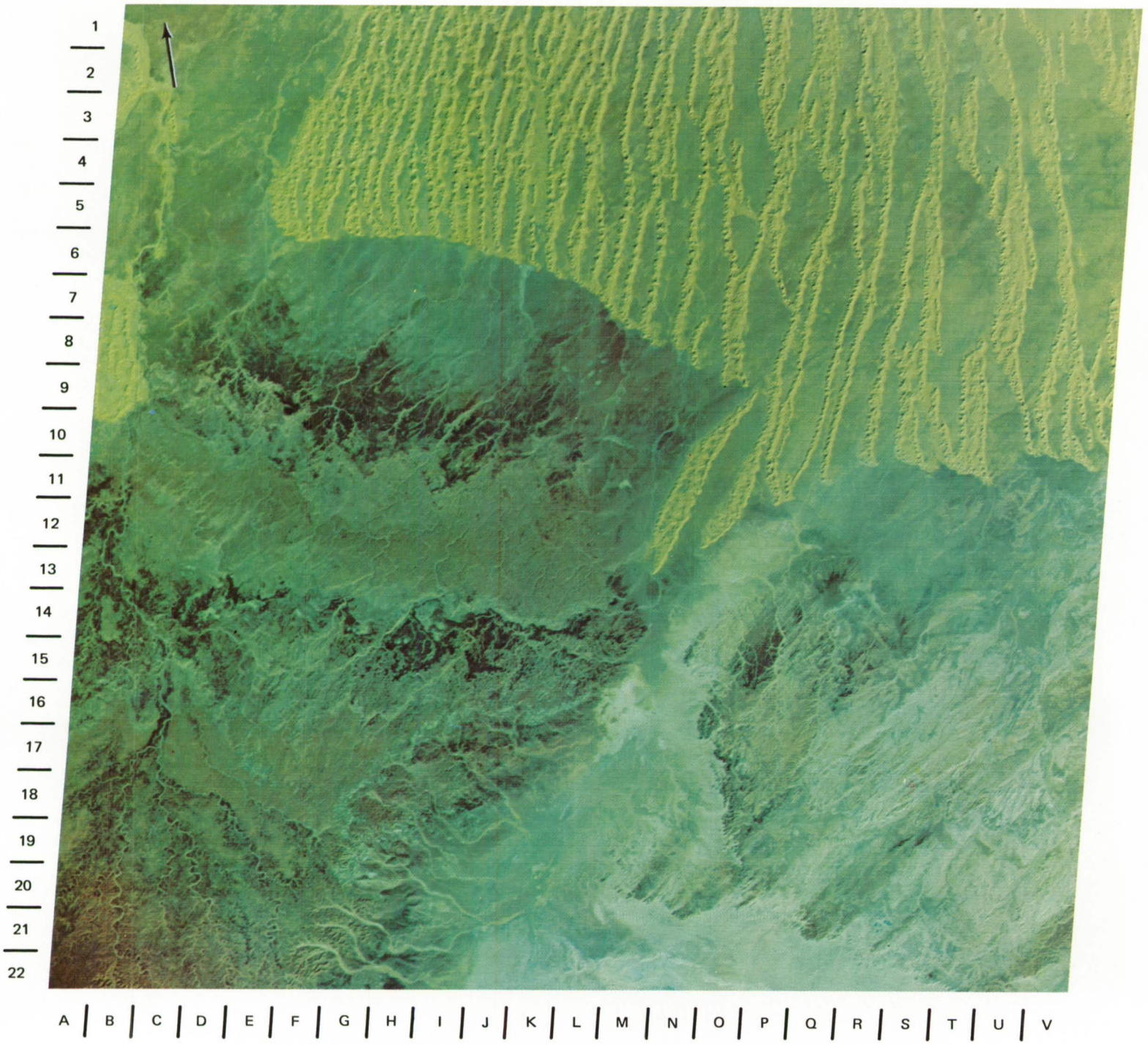
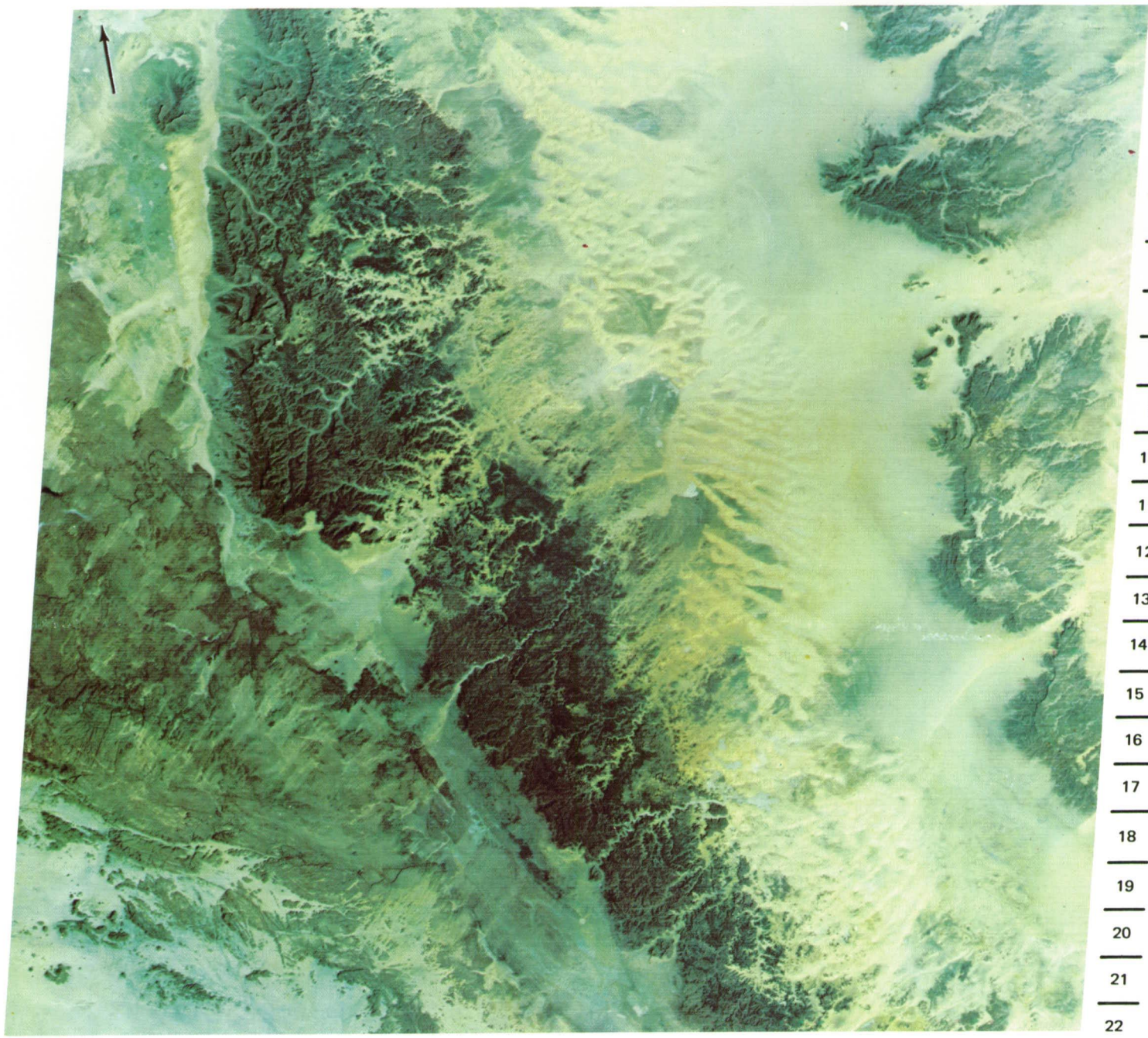


PLATE 328

ALGERIA: This area is near the center of Algeria, but is essentially uninhabitated. The only specific landmark shown on regional maps is the Hassi Msegguem (*N*–14) ("hassi" meaning waterhole in Arabic); the hassi is not visible, however. To the left is part of the Tademaït Plateau, consisting of Mesozoic sedimentary rocks forming a relatively thin, undeformed cover. To the south is the edge of the Tidikelt, a barren gravel plain. Note the intricate dendritic drainage pattern of the Tademaït Plateau, which is probably a relic from times when the Sahara had a much wetter climate (probably during the Pleistocene).

The most prominent features are the longitudinal dunes in the north half of the image. These are part of the Grand Erg Oriental, or Great Eastern Erg. The sand streaks in the lower right corner indicate that the dominant wind direction is from southwest to northeast, so the longitudinal dunes of the Grand Erg are not completely parallel to the wind direction. It appears that Landsat images of such dune fields may provide a good record of seasonal wind directions in remote areas. This should be of value in the Sahara, as development with the aid of subsurface water and oil exploration proceeds, because migrating dunes are a handicap in many deserts. The main producing region of Algeria is just a few hundred kilometers to the northeast. *1111–09442;* November 11, 1972.

PLATE 329



LIBYA AND ALGERIA: As mentioned previously, North Africa since the early Paleozoic has been affected primarily by relatively gentle vertical crustal movements, up or down, except for the Atlas and Anti-Atlas Mountains. These movements have produced "basin and swell" topography. One of the features formed this way is the Marzuq Basin of Libya, over 400 kilometers (250 miles) wide. The southwest margin of the Marzuq Basin is shown in this image, the basin itself being off the right margin. It is bounded by a series of cuestas, asymmetric ridges formed by erosion on gently dipping strata. The innermost of these is the Mesach Mellet (*S*–2 to *V*–16), consisting of Paleozoic and Mesozoic sedimentary rocks dipping to the northeast (*to the right*). To the west of this cuesta is the lower Iguidi Ouan Kasa (*L*–1 to *Q*–15), a large dune field. ("Iguidi" means dune massif in Tamahak, the Touareg language.) The dark rock area cutting across the scene (*E*–1 to *P*–21) is the Tadrart, another Tamahak word meaning simply "mountain." It too is a cuesta, formed of Paleozoic sedimentary rocks also dipping toward the Marzuq Basin. In the valley just beyond the Tadrart one can see a few small red dots marking oases; one of these at *C*–7 is the oasis and village of Ghat. The dominant vegetation in these areas is the date palm. The border between Libya (north) and Algeria (south) passes just south of Ghat. The last of the cuestas, the Tassili N'Ajjer in Algeria (*A*–11 to *L*–21), is made up of Cambro-Ordovician sedimentary rocks dipping to the upper right. This cuesta belongs more to the Hoggar Mountains (*lower left, off the image*) than to the Marzuq Basin. These mountains, also called the Ahaggar, are another massif generally similar to the Tibesti Mountains in being a broad uplifted area of Precambrian rock capped by Cenozoic volcanics. *1070–09160;* October 1, 1972.

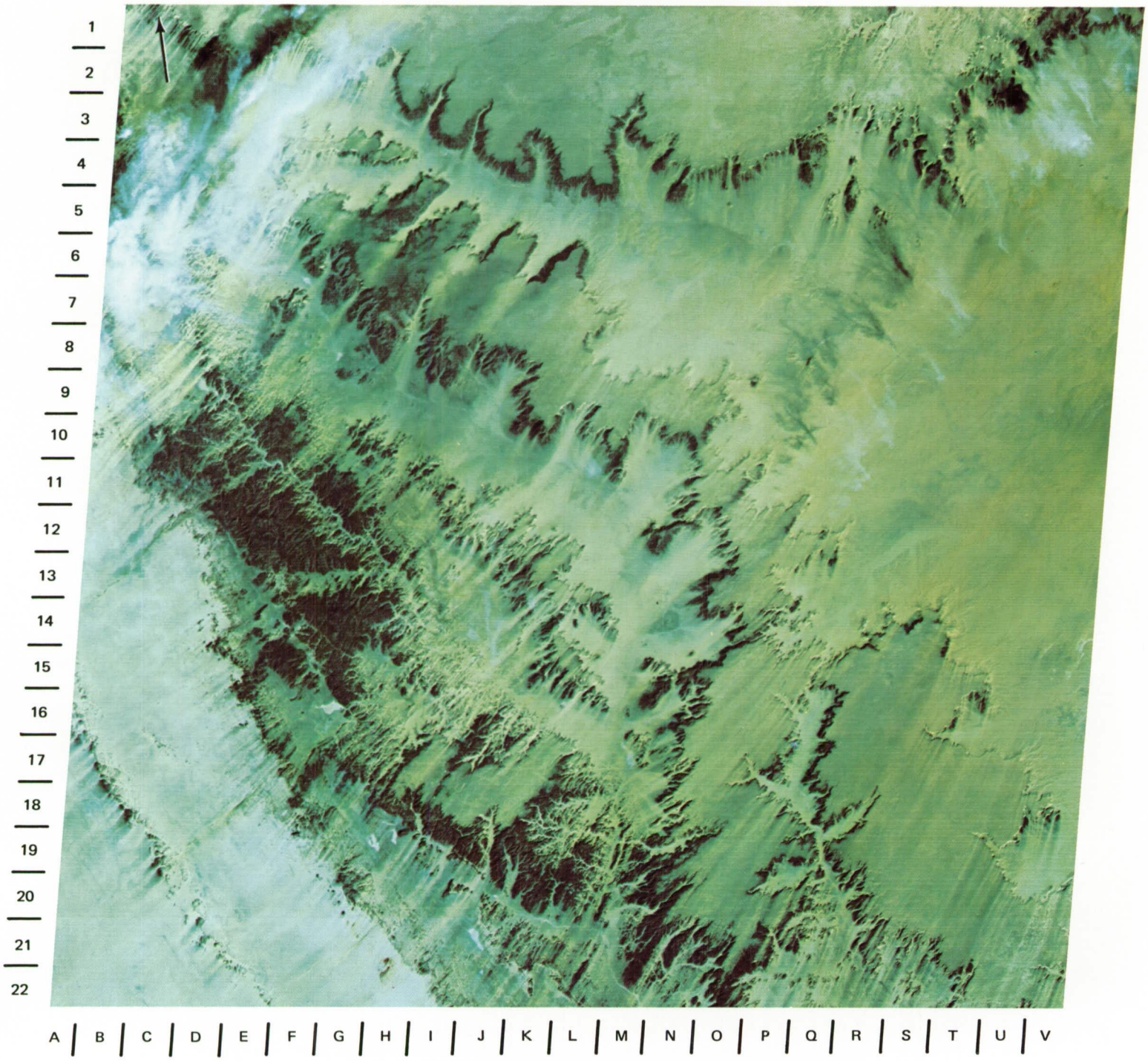


PLATE 330

NIGER: Still another part of the belt of cuestas encircling the Marzuq Basin, or sand sea, is covered by this image of northern Niger. The Marzuq Basin is to the north and the Tibesti Mountains to the northeast of this area. Visible here is the Mangueni Plateau, a deeply dissected area of gently dipping Paleozoic and Mesozoic sedimentary rock, including the Nubian sandstone. The Enneri Achelouma extends from *F*–3 to *K*–5. Two major types of geologic features are evident here. The most conspicuous is the family of sand dunes, sheets, and streaks extending from upper right to lower left. As mentioned in relation to other images of the area, the length and parallelism of these features demonstrates the strength and persistence of the regional wind pattern. The second type of feature is the intricate dendritic network of canyons eroded in the plateaus. The plateaus are considered by L. C. King to be part of the post-African, Late Cenozoic erosion surface, now being eroded laterally. Much of this erosion must date from the Pleistocene Epoch, when North Africa was much wetter, because there is too little rain at the present time. Wind erosion is also effective, although most of the landforms seen here are the result of running water. *1194–09061;* February 2, 1973.

PLATE 331



NIGER—AIR PLATEAU: This striking image of Niger shows a myriad of geologic features. The area covered is the Air Plateau, one of several Precambrian massifs in North Africa, with elevations generally between 500 and 1000 meters (1600 and 3300 feet) and individual peaks as high as 1900 meters (6200 feet). It is sparsely inhabited, but the faint red streak at *C*–21 is the location of Agadez, an oasis that is a major stop on camel routes. The areas along the bottom and right margins of the image are sandy and gravelly desert.

Turning to the Air Plateau itself, a number of dark-colored elliptical or circular mountains may be seen: Taraouadji (*J*–15), Baguezans (*L*–8), Ashkout (*L*–4), and Agalak (*J*–2). These are large granite intrusions of Late Paleozoic or Mesozoic age, thought to grade into ring dikes at depths and to have fed calderas that have now been removed by erosion. They are chemically unusual, being characterized by high alkali content. In addition, the area is rich in tin and niobium, elements that are generally associated with granitic magmas. Intrusion of these large bodies was not the last chapter in igneous activity, for there are numerous lava flows in the area, such as those at *I*–9, largely olivine basalt but with some trachytes and phonolites. All these rocks are seen against a basement complex of Late Precambrian igneous and metamorphic rocks. To add to the geologic complexity of the area, the entire Air Plateau is criss-crossed with numerous wrench faults (faults with dominantly horizontal movement); most trend northwest but some, apparently complementary, trend northeast.

This Landsat image is stimulating to the geologic imagination. For example, one of the most intriguing theories today is that volcanic and igneous activity may result, in some areas, from mantle plumes—rising columns of hot mantle material from the subcrust. The Hawaiian Islands, for example, may mark the site of such a plume over which the oceanic crust has drifted. In the Air Plateau, however, it seems clear that such drift has not occurred, at least since the Late Paleozoic, for renewed (Tertiary) volcanism is seen in the same site as that of the much earlier ring dike intrusions. *1286–09191;* May 5, 1973.

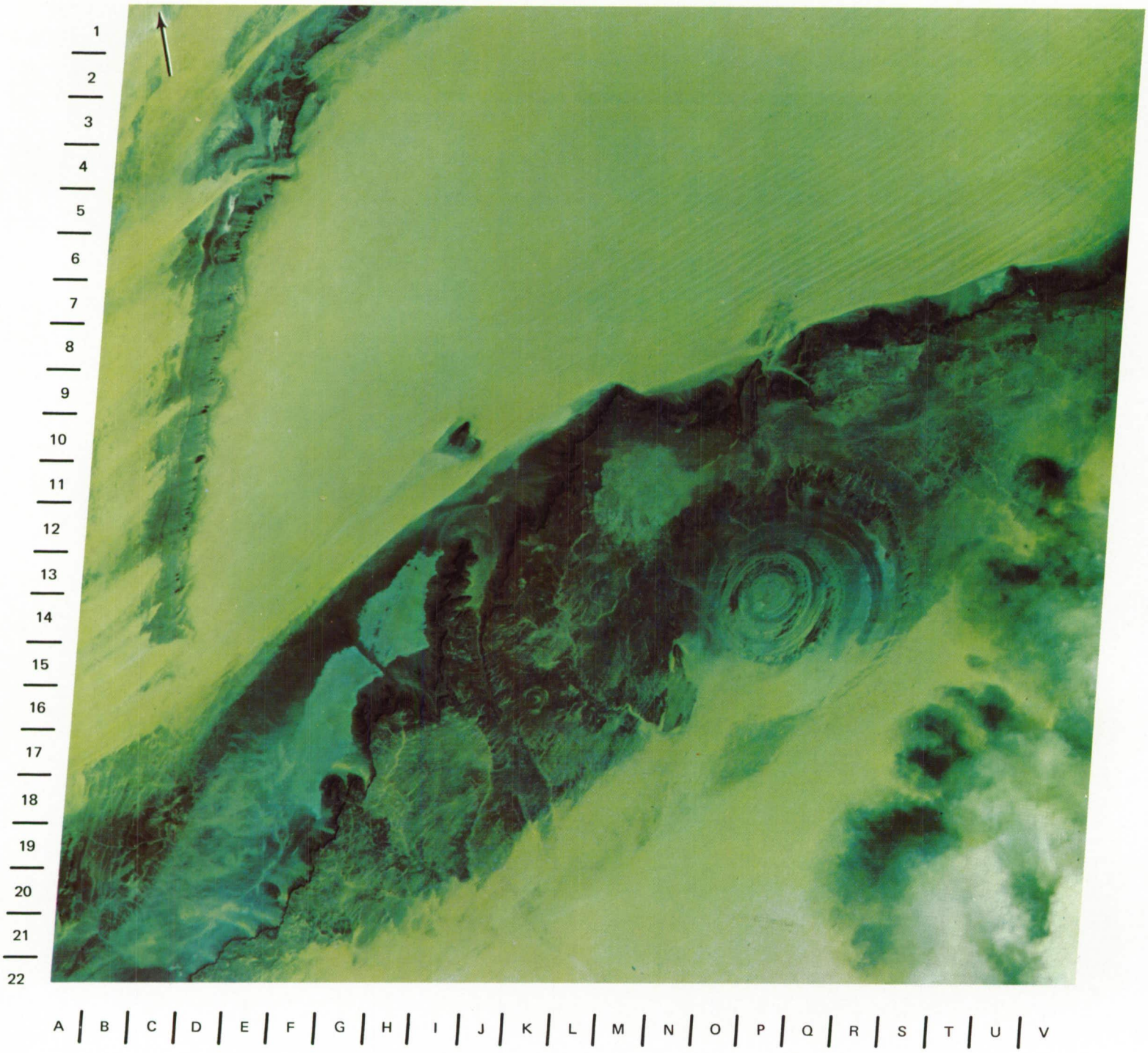


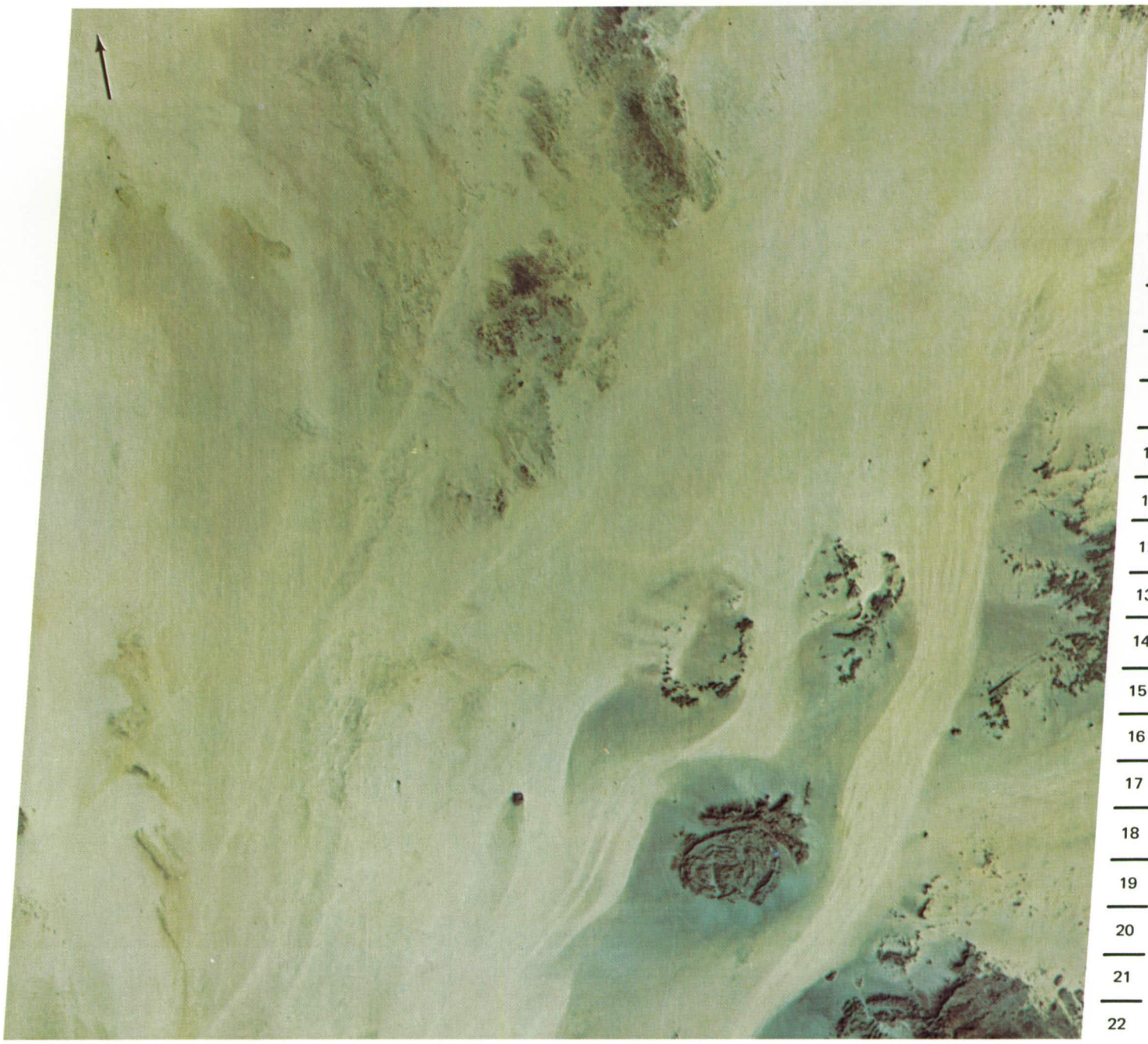
PLATE 332

RICHAT STRUCTURE: This gigantic bull's-eye is the 40- by 30-kilometer (25- by 20-mile) Richat structure. Lying in a remote part of Mauritania, it was brought to the attention of the scientific world by Gemini 4 astronauts J. A. McDivitt and E. H. White in 1965 when they passed over it and took a widely published photograph. The structure had actually been studied by French scientists before, but few had known of their studies before the Gemini picture.

The Richat structure is a series of concentric quartzite ridges averaging about 100 meters (330 feet) in height, separated by toroidal valleys underlain by less resistant rocks. The topography is clearly the result of differential erosion, but the origin of the structure itself has been a long-standing geologic problem. Its nearly circular form suggested that it might be an exhumed impact structure, similar to those in Canada and the United States; if so, it would be of major scientific interest. Stimulated by the Gemini picture, an American group headed by R. S. Dietz investigated the Richat structure and its 4-kilometer (2½-mile) wide companion, the Semsiyyat dome (*J*–15). They found no evidence at all of impact, such as high-pressure minerals or shatter cones, and concluded that the structures are definitely not of impact origin. The presence of igneous rock, as sills and dikes, suggests instead that the structures were produced by intrusion of magma, perhaps as a stock or plug. Another possibility is diapiric intrusion of shale, although the dips of the strata do not support this strongly.

The general area covered by the picture is obviously a desolate one. The only settlement, Ouadane (*M*–16), is a small oasis not even visible. The plateau in which the Richat structure is incised is the Dhar Adrar, standing about 200 meters (650 feet) above the surrounding desert. Structurally, it is an essentially flat-lying remnant of Ordovician sedimentary rocks capped by the Chinguetti sandstone; in the United States, it would be called a mesa. To the north is the Makteir dune field, an array of linear or seif dunes. The prevailing winds blow from upper right to lower left, as indicated by the sand streaks at upper right. *1103–10434;* November 3, 1972.

PLATE 333



JABAL ARKENU, LIBYA: Southeastern Libya and southwestern Egypt, one of the most remote and poorly known sections of the Sahara, are covered by this view. A small corner of the Sudan is also included, the point common to all three countries being located at the Jabal Auenat (*R*–21). This mountain, reaching 1300 meters (430 feet) above the surrounding desert, is one of several granite intrusions in the area; others include the Jabal Arkenu (*O*–18), Bahri El Jebel (*N*–14), and the Jebel Babein (*Q*–13). These intrusions, considered by Angelo Pesce, an authority on the geology of Libya, to be post-Carboniferous in age, are of considerable geologic interest. They resemble granite intrusions of similar age elsewhere in Africa, and appear to form in cratonic (i.e., stable) areas. The granite intrusions of Western Africa have potentially valuable deposits of rare earths, tin, and tungsten.

The area covered by this image is obviously a dry and barren one. Sand seas, or ergs, such as those at *R*–16 and *J*–19, show the direction of the prevailing wind to be from the north and northeast. Because of the generally unobstructed terrain, and the absence of rain, wind plays an important role in erosion in this part of North Africa, unlike the North American deserts.

Owing to its latitude and prevailing clear weather, North Africa was photographed repeatedly from Gemini spacecraft in the mid-1960's as part of the terrain photography experiment. Dr. A. Pesce and his colleagues in Libya, from these photographs, discovered an unmapped sand sea 40 by 200 kilometers (25 by 125 miles) in Libya which they named the Erg Idrisi. The erg shown here at *V*–19 appears to be a northern extension of the Erg Idrisi. *1114–08200;* November 14, 1972.

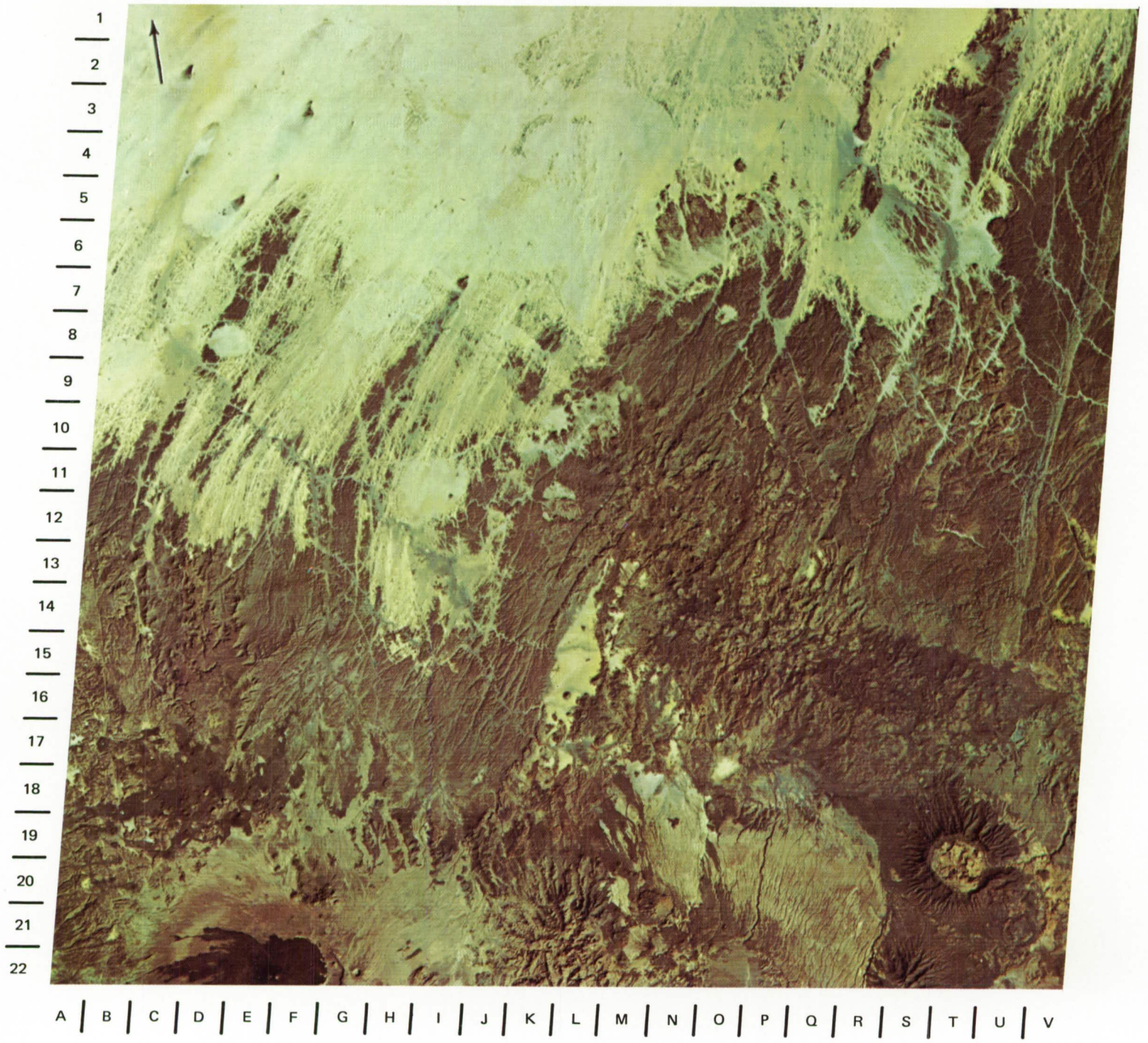


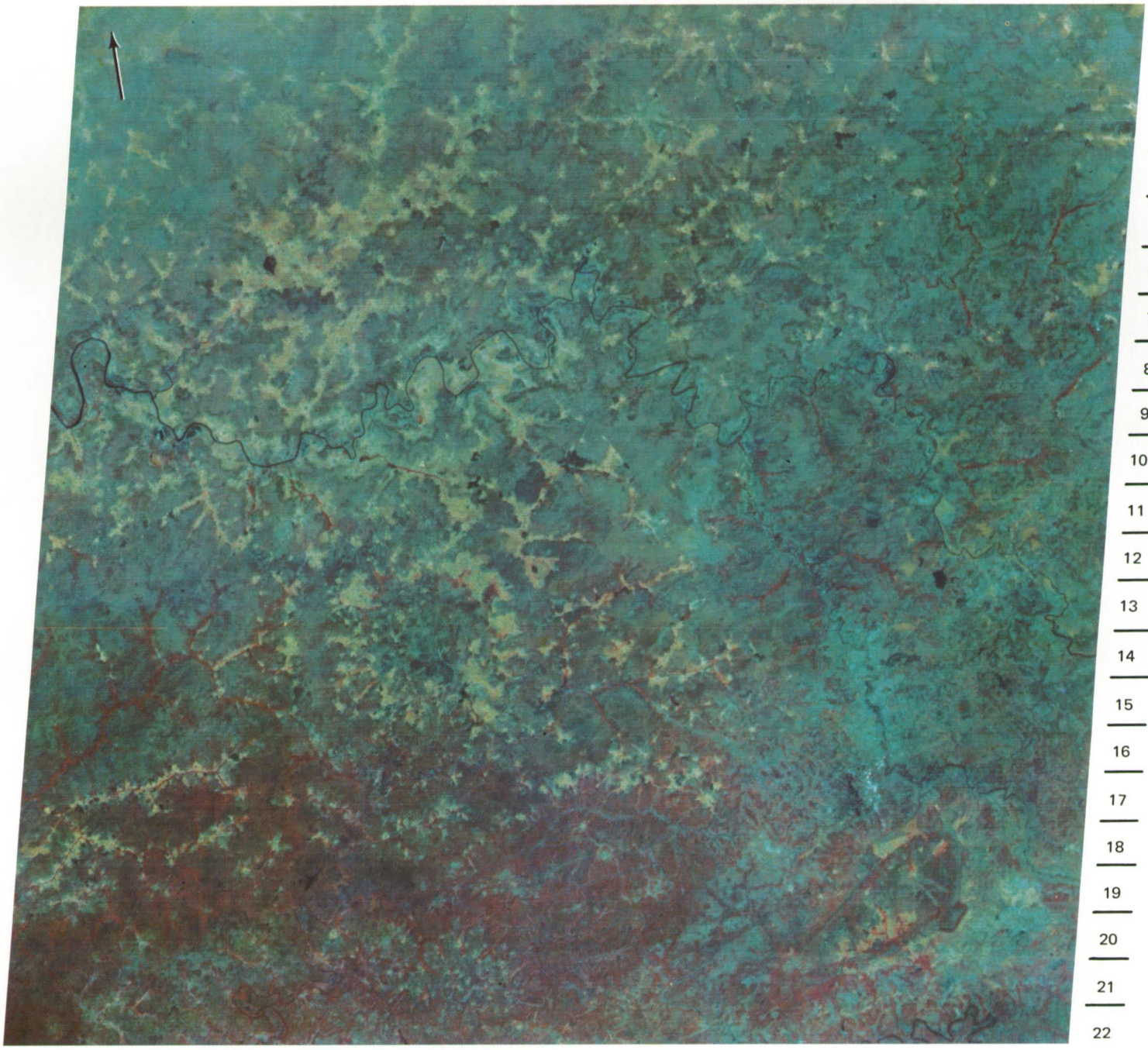
PLATE 334

TIBESTI: Turning now to the northwest sector of the Tibesti Massif, one sees a terrain of Cenozoic volcanic features superimposed on Precambrian rock. All the area shown here is in Chad; there are two small settlements, Bardai (*K*–17) and Zozou (*O*–9), but except for a trace of vegetation (red) at Bardai, both are invisible on this image. The Tibesti Mountains receive more precipitation than the surrounding Sahara because of their elevation, but they are extremely dry by ordinary standards. The light-colored area at upper left (*A*–3 to *L*–4 and northward) is part of the Serir of Tibesti, "serir" being the Arabic term for gravel plain.

The geological structure of the area is extremely well exposed. Most of the area is underlain by Precambrian rocks, except for small patches of Paleozoic and younger sedimentary rocks. The linear structure at right (*V*–4 to *U*–14) is an unconformity, according to the work of P. M. Vincent, separating older Precambrian rocks to the right from younger Precambrian rocks to the left. All in this section of the image are cut by prominent northwest- and northeast-trending faults, frequently expressed as unusually straight valleys. Along the south edge of this area lies a part of the great Tibesti volcanic field. The most prominent crater is the Tarso Toon (*T*–19), an immense caldera. The word "tarso" means, in Tedadaza (the language of the Tebu people), high plateau or gently sloping mountainside, characteristics typical of calderas. A portion of the Tarso Voon is visible at *O*–21, although most of this caldera lies to the south. The black splotch at lower left (*E*–21) is a field of andesite lava surrounding the Pic Tousidé, a crater whose height of 3265 meters (10 712 feet) makes it the second highest peak in the Tibesti Mountains.

Petrology and structure of the Tibesti have been a fertile field for investigation. P. M. Vincent, the leading authority on the subject, has concluded that the lavas, ranging in composition from basalt to rhyolite, have been formed by partial melting of the underlying mantle and crust following or accompanying uplift of the massif. It may be speculated that the massif overlies a mantle plume, inasmuch as the Tibesti Massif does not lie on a plate boundary. *1191–08485;* January 30, 1973.

PLATE 335



SENEGAL AND GAMBIA: Parts of two countries, Senegal and Gambia, are shown here. Gambia, a member of the British Commonwealth, occupies a strip some 320 kilometers (200 miles) along the Gambia River (*A*–9; *V*–14), reaching to *L*–7; however, the strip is only a few kilometers (miles) wide. The country is surrounded on all sides by Senegal, a former French territory but now independent. The Gambia River, though inconspicuous, is, in fact, a major waterway, being navigable through the entire length of the country. It should be the natural transportation route to the coast for Senegal, but this will have to wait for the frequently mentioned union of Gambia and Senegal.

The area covered by this image is all savanna. More specifically, it is a transition zone between Sudan savanna to the north and Guinea savanna to the south. The difference is largely one of the density of trees, the Guinea savanna being more densely wooded because of the increasing rainfall to the south. This Landsat image gives some indication of this vegetational transition; note the reddish color in the southern part of the scene. The rainfall is markedly seasonal, falling chiefly in July through September.

The region is level and only about a hundred meters (a few hundred feet) above sea level and is underlain by Cenozoic marine sediments. Senegal is one of the world's leading producers of peanuts, which account for about 90 percent of the country's exports. This situation is economically risky, because bad weather or low market prices can have a major effect on the entire economy. Millet, the chief food crop, is grown in rotation with peanuts. Rice is grown in Gambia along the river. *1283–10463;* May 2, 1973.

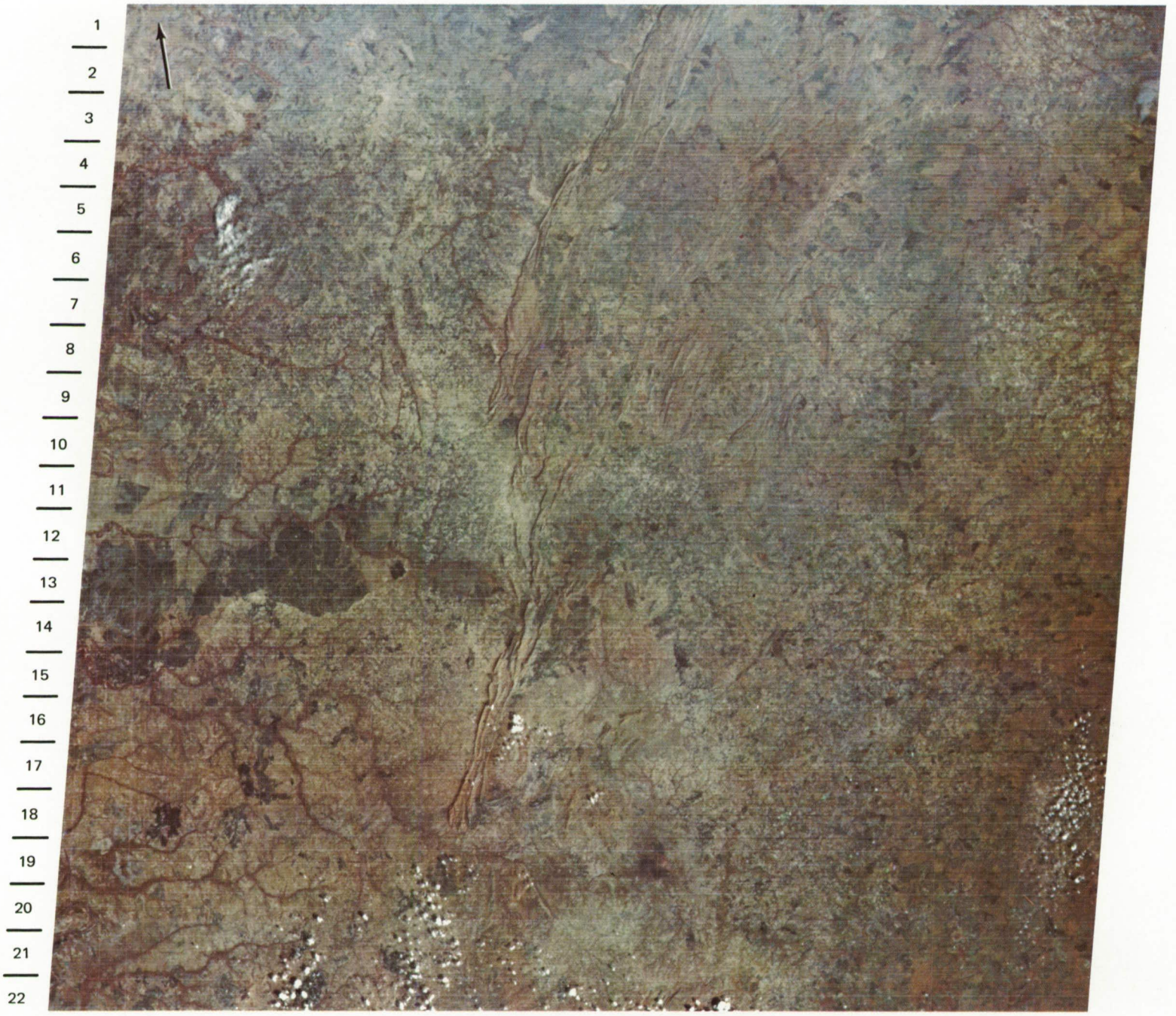


PLATE 336

AFRICAN LAND PRACTICE: This scene includes the eastern border area of Ghana (*B*–19), much of the northern half of the small country of Togo (*H*–6), and a bit of Dahomey (*U*–4), three African countries with seashores along the Gulf of Guinea in the stretch once known as the Ivory and Gold Coasts. In the past the land was once covered with a much thicker and extensive rain forest. However, the native tribes have for years been clearing these forests, replacing them with savanna grassland given to grazing of goats and cattle. It has been common practice to burn off large sections of grassland each year prior to the coming of the rainy season. Many large dark patches seen in this image represent more recent burns (*E*–13). Countless previous burns over vast areas (*D*–3; *O*–12) have combined to exert a drastic change in the ability of the soils to support seasonal grasses. Generally barren soils appear in this rendition in shades of grayish-blue to brown. The problem of maintaining adequate forage has been compounded by the extreme drought conditions in the Sahel and adjacent parts of West Africa in recent years. Still, much of the land, particularly along streams, is even now cultivated, with yams and cassava root as principal crops.

Precambrian crystalline rocks underlie the surface in the eastern part of the image. Late Precambrian and Cambrian platform sedimentary rocks occupy most of the remainder of the terrain to the west. These rocks are strongly folded in the Chaine d'Atakoara (*J*–6) and Chaine de Togo (*J*–14). *1524–09404;* December 29, 1973.

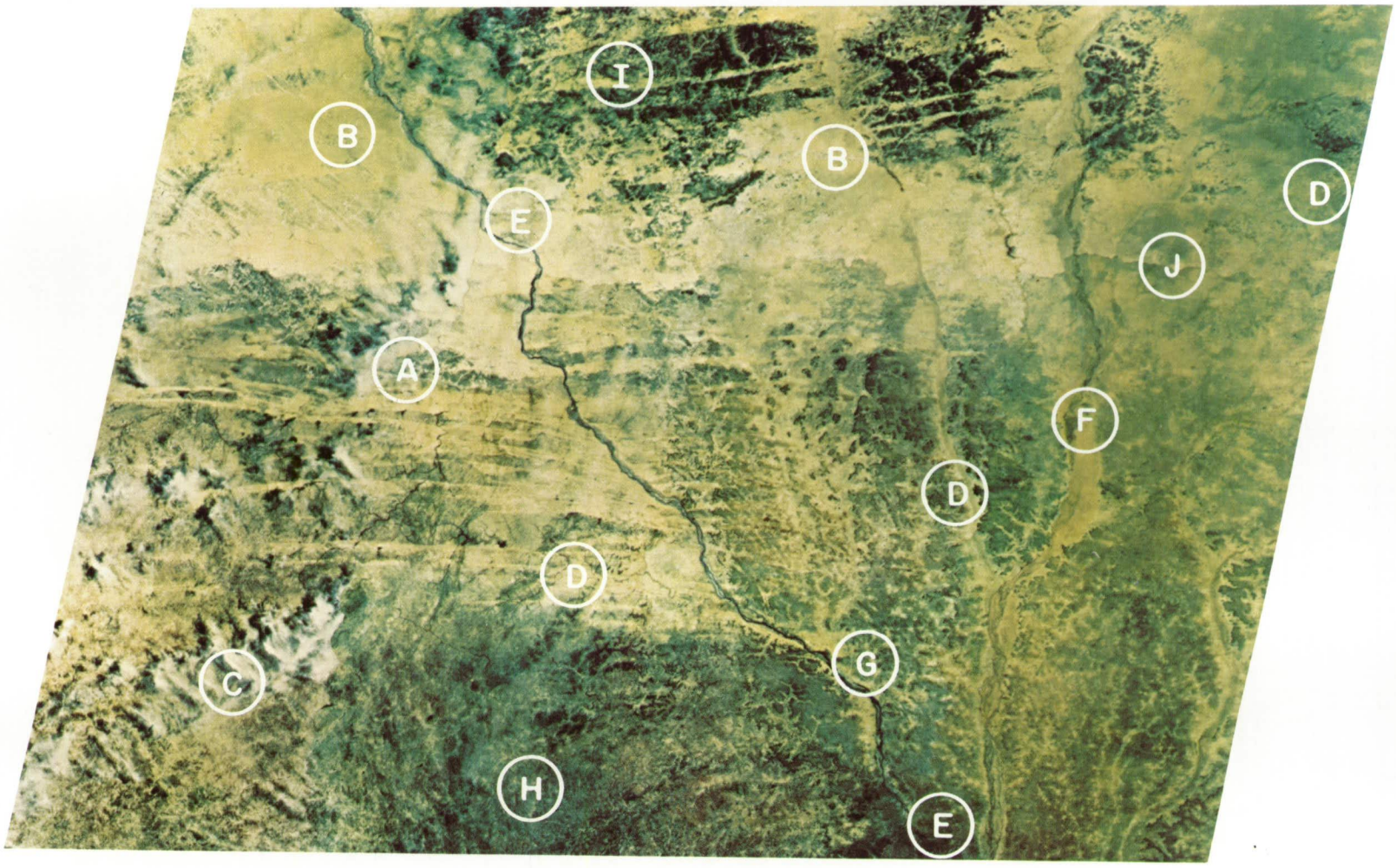


PLATE 337

MALI: Twelve Landsat 1 images from coverage between April 17 and 21, 1973, have been combined to provide this mosaic of West Africa covering the junction (*A*) of parts of three countries: Mali (*B*), Upper Volta (*C*), and Niger (*D*). The Niger River (*E*) here flows to the southeast; the other prominent river is the intermittent Dallol Bosso (*F*) and its tributaries. Both then flow through Nigeria into the Gulf of Guinea south of this mosaic. The capital of Niger, Niamey, is located on the Niger River at *G*.

This mosaic covers the transition zone between the Sahel (north) (an Arabic word meaning border) and the higher rainfall region of the Savanna (south). The darker color of the terrain to the south (*H*) is the expression of denser vegetation (grass and acacia shrub). The very dark patches in the north (*I*), however, are dissected plateaus with laterite caps. The general dryness of the area is indicated by the east to west trending dunes in the upper part of the mosaic. These are stabilized dunes, showing the former extent of the Sahara, and are now cultivated. The origin of these bands is not well understood. They may have formed in recent centuries because they are superposed on the drainage patterns. During the rainy season large ponds occur at the margins of the bands near the larger streams. Because the sediment load in the streams is heavy, the lifetimes of the ponds must be short, perhaps less than 1000 years.

The catastrophic drought of the early 1970's has caused a southward growth of the Sahara. Landsat images, when compared with previous orbital photography from Apollo and Gemini flights taken several years earlier, should permit monitoring of this process. Integration of field studies with resource analyses made possible by these images is now leading to a regional resources management plan. This planning activity is coordinated with the Liptako-Gourma Authority and other agencies established by Mali, Niger, and Upper Volta. One of the first results of Landsat-based studies was the recognition of the adverse effects of overgrazing as indicated by the discovery of better grasslands within a large polygon (*J*) in Niger. (See fig. 8 in the introductory chapter.)

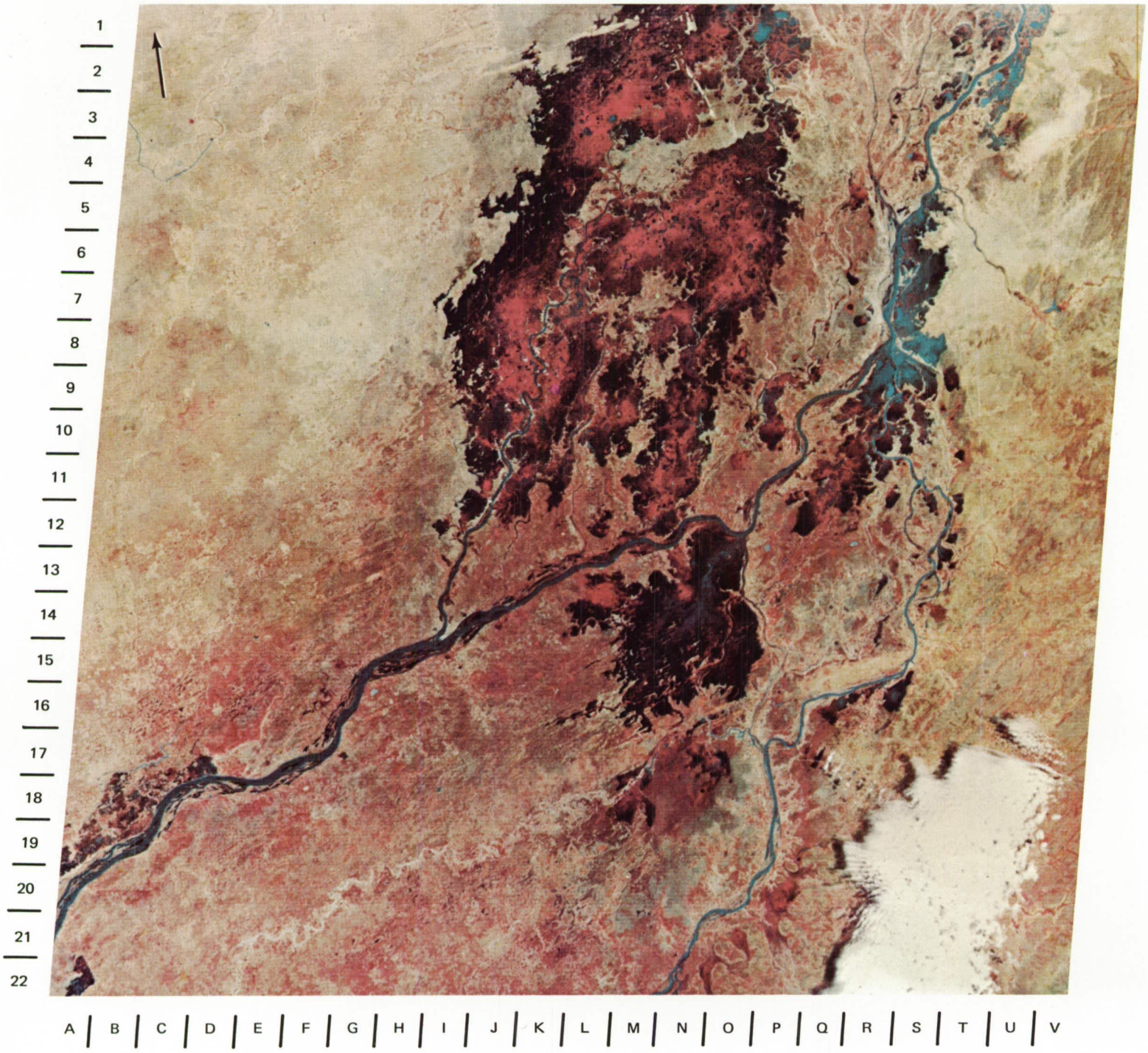


PLATE 338

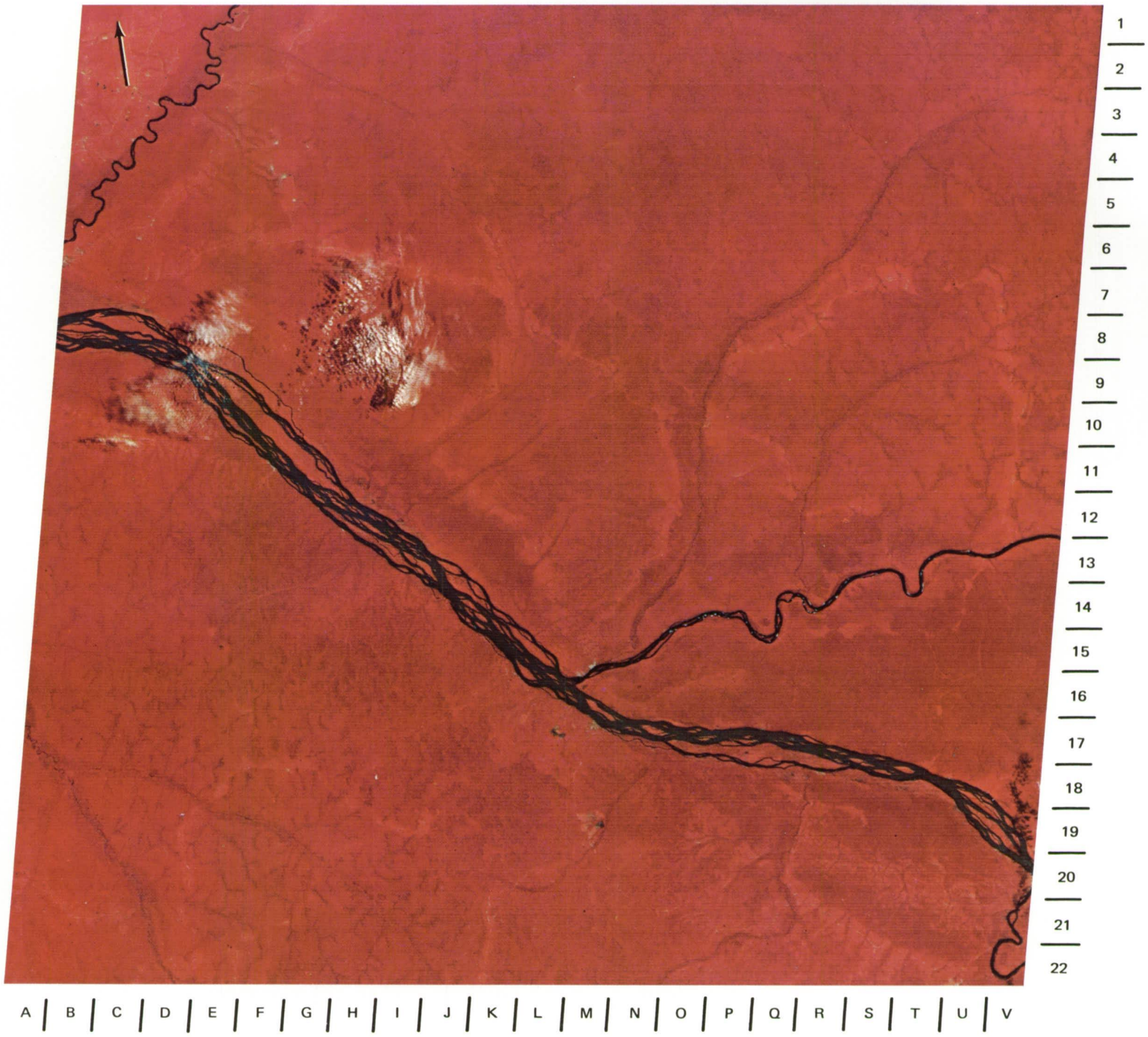
INLAND DELTA OF THE NIGER, MALI: The Niger River has been called "the life blood of Mali." The area shown here is sparsely inhabited, with most people living near the Niger River (*G*–15), where irrigation permits the growing of rice, millet, and, further to the southwest, peanuts. The Niger is being extensively dammed further upstream (to the southwest). Cattle raising is important, both for meat and hides. During the dry season, the cattle raising nomads drive their Zebu cattle to pastures in the Niger valley, but this practice now conflicts with the increasing farming of the valley area.

One of a group of tectonic basins (including Lake Chad and the Nile River's Sudd) spread east to west across the bulge of Africa, the Inland Delta occupies about 40 000 square kilometers (15 600 square miles) of south-central Mali. In September 1973, the southern Inland Delta (large blue and red feature in upper center) is at maximum flood stage. The Niger River in this region flows northeastward past Mopti (*O*–12) and the confluence with the Bani River (*R*–11).

Summer rains (between 50 and 100 centimeters (20 and 40 inches)) in the watersheds of both rivers cause an annual flood in the delta. The flood crest usually takes 3 months to pass through the marshes, lakes, and channels of the delta. In the current drought, the passage time is much shorter, bringing probable disaster to river farmers downstream. The intense reds (*M*–6) seen here are marshes, grass islands, and other uncultivated wetland vegetation. A larger area of less intense reds contains cultivated fields and grasslands. There, approximately 1 meter (3 feet) of sand overlies a hard laterite layer—a remnant of soil development under a forest cover now destroyed. The braided character of the Niger River indicates an enormous sediment load carried into the delta at the present time. The lack of meanders, normally the result of such a load, reflects a structural control of the river.

The delta region experiences other seasonal changes besides flooding. Fishing dominates during flooding (carried on by the Bozo people); cultivation of millet and other crops takes place during the preflood stage of the rainy season (Bambara people); and herders bring their cattle into the green meadows and marshes during the winter season until the next rains (Peuhl people). *1061–10104;* September 22, 1972.

PLATE 339



ZAIRE (CONGO) RIVER: "Africa" is synonymous with "jungle" to many people, but as the Landsat images demonstrate, most of Africa is desert or semiarid savanna. For that reason, and because of the generally dense cloud cover over equatorial Africa, this is one of the few Landsat images of the African jungle, or more properly, tropical rain forest. The Congo River, renamed the Zaire River in 1971, approximately bisects the picture (*A*–8; *V*–19). Other rivers include the Itimbiri (*D*–1; *A*–6), Lulu (*R*–5; *O*–13), and Aruwimi (*V*–12; *M*–15). There are numerous small villages visible, especially in the upper left corner; Stanleyville, since 1966 named Kisangani, is on the Zaire River just east of this area.

The Zaire River, one of the world's longest rivers with a length of 4373 kilometers (2718 miles), is navigable far upstream *(to the right)* from this scene, despite its intricate network of channels. This braided pattern, typical of streams with more sediment load than their gradient permits them to carry easily, reflects the fact that the Zaire River for most of its length flows through a large sedimentary basin enclosed by higher areas. Zaire is largely in this basin (formerly the Congo Basin) and has level topography generally less than 450 meters (1500 feet) above sea level. The river thus seems to be essentially an aggrading one, as opposed to a degrading, or eroding, river.

The tropical rain forest displayed so well here includes mahogany, ebony, teak, copal, palm, and cedar trees; timber and oil palm are among the major exports of Zaire. A variety of other crops, including cassava, yams, and plantains, are grown, but chiefly for local consumption. Zaire is a major mineral producer, but the mining area (Katanga) is southeast of this picture. *1237–08092;* March 17, 1973.

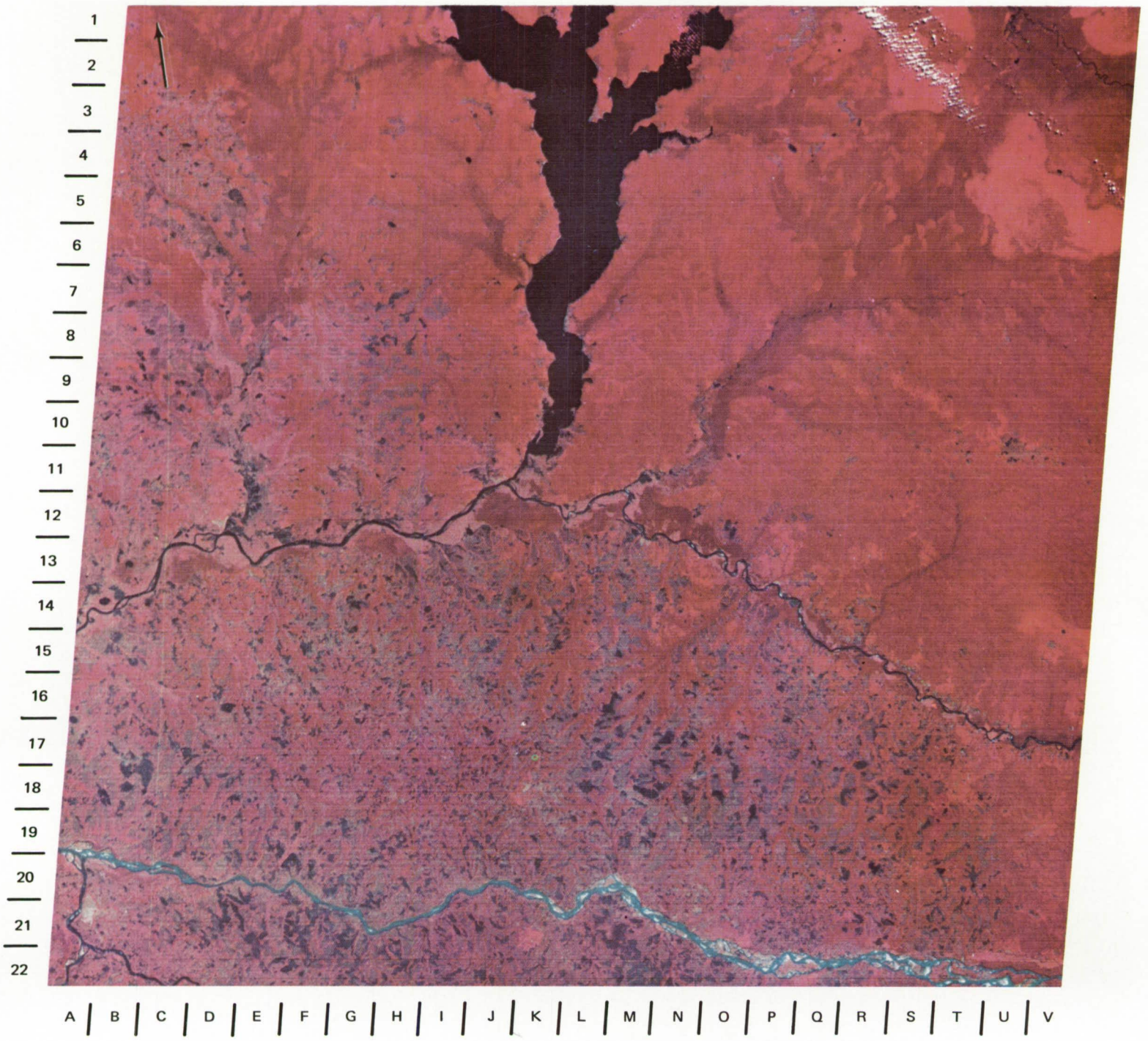
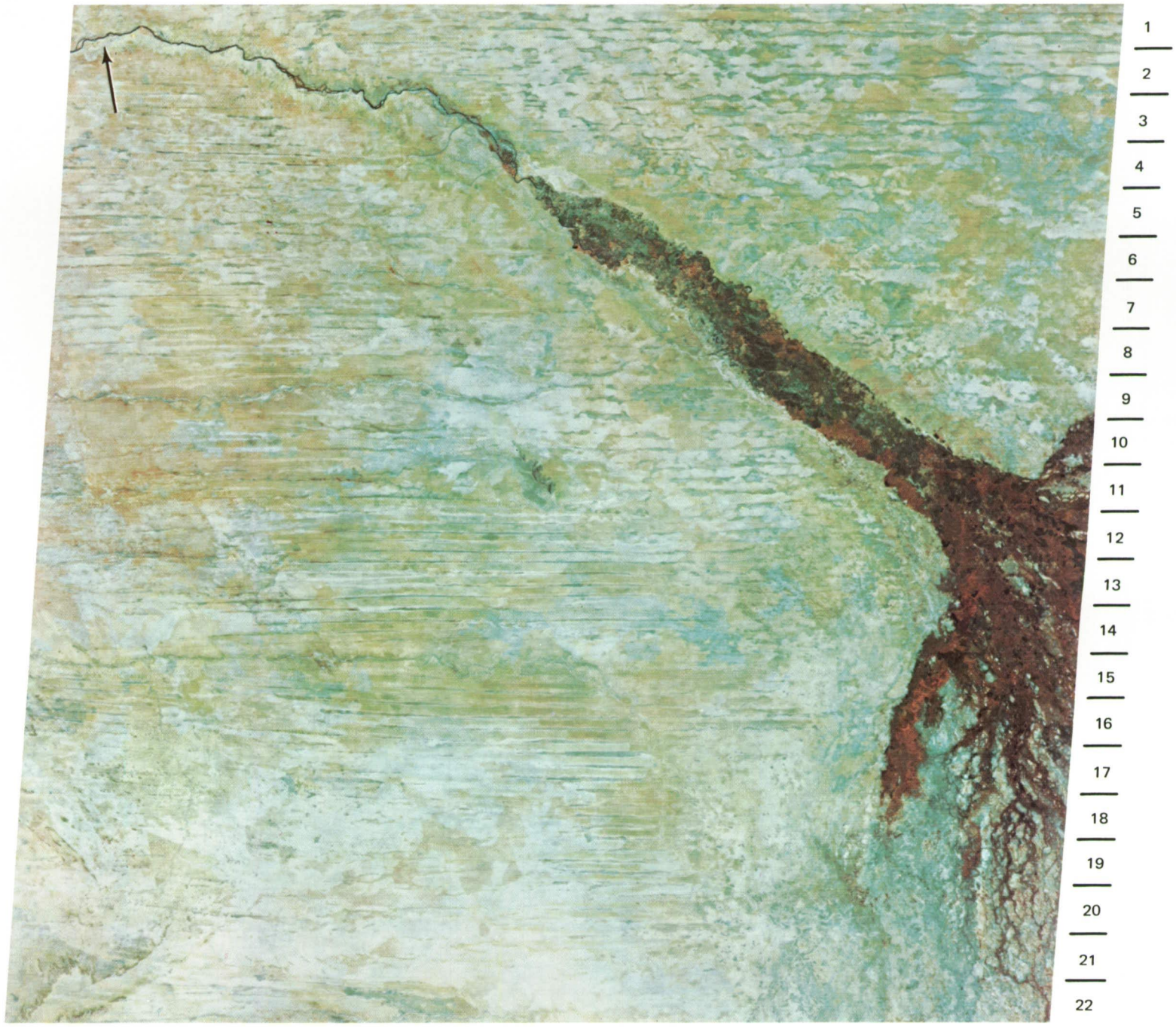


PLATE 340

KASAI RIVER, ZAIRE: This area is in western Zaire, near the rim of the Congo Basin. The Kasai River (*A*–19; *V*–21), although relatively inconspicuous in this image, is one of Zaire's major waterways, being navigable well east of this scene. It joins the Zaire River to the west. To the north are the Lukenie River (*A*–13; *V*–16), not navigable, and Lac Mai Ndombe (formerly Lake Leopold) (*K*–4). This lake is a present-day representative of the large lakes that formerly occupied the Zaire (Congo) Basin, which is largely filled with Quaternary and Tertiary lake sediments.

Zaire has essentially two major divisions. The tropical rain forest, low-lying and wet, was shown in the previous plate. This scene shows the transition from rain forest in the north to the savanna-covered plateau region in the south. Although the forest region would perhaps seem more promising for agriculture, the heavy rains leach mineral nutrients from the soil, making sustained major farming difficult. In addition, the tsetse fly, Africa's curse, renders livestock raising nearly impossible over large areas. The savanna, on the other hand, supports a variety of crops, including cotton, oil palm, and rubber, in addition to those used locally. Cattle raising is also possible in the area covered here. The natural vegetation is tall grass, including lalang grass, and a variety of trees including palm. The dark patches are the scars of bush fires, which are common on the savanna. *1348–08270;* July 6, 1973.

PLATE 341



BOTSWANA: Botswana (formerly Bechuanaland) has an area slightly greater than that of France and lies in the transition zone between desert and dry savanna. This location produces great variations in patterns and colors, both in time and space, as seen from Landsat. The following series of images has been chosen to illustrate this variability.

The first image covers the extreme northwest corner of Botswana. This area is in the Kalahari Desert. The Kalahari is one of the largest expanses of sand in the world, but the sand is generally covered with short grass or scrub. The prominent parallel bands running roughly east to west are sand dunes, now stabilized by this vegetation. Hydrologically, this area is in the Okavango Basin, one of several large basins in Africa. The Okavango River flows southeast into the Okavango Swamp, part of which is seen here. The bright red color of the river course and swamp suggests a period of heavy flow that has promoted growth of the swamp vegetation. This river drains an area much more moist than that shown here, receiving up to 130 centimeters (50 inches) of rain per year, and consequently has an average annual flow at the border of Botswana of 13 billion cubic meters (460 billion cubic feet). This diminishes rapidly to the southeast because of evaporation and infiltration. The Okavango River and the swamp represent presently untapped hydrologic resources that when used should be invaluable both for cattle raising and agriculture. *1127–08032;* November 27, 1972.

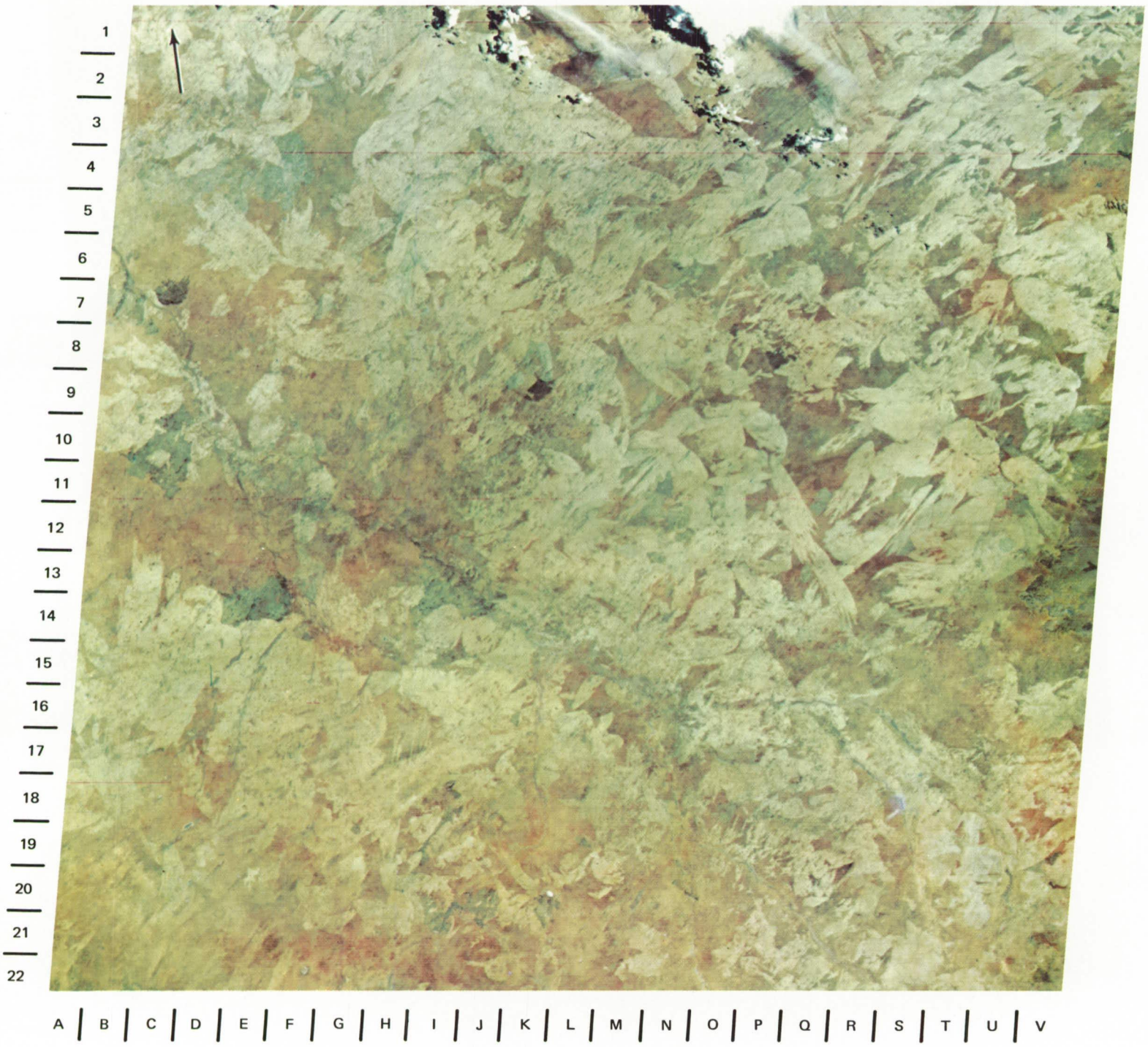


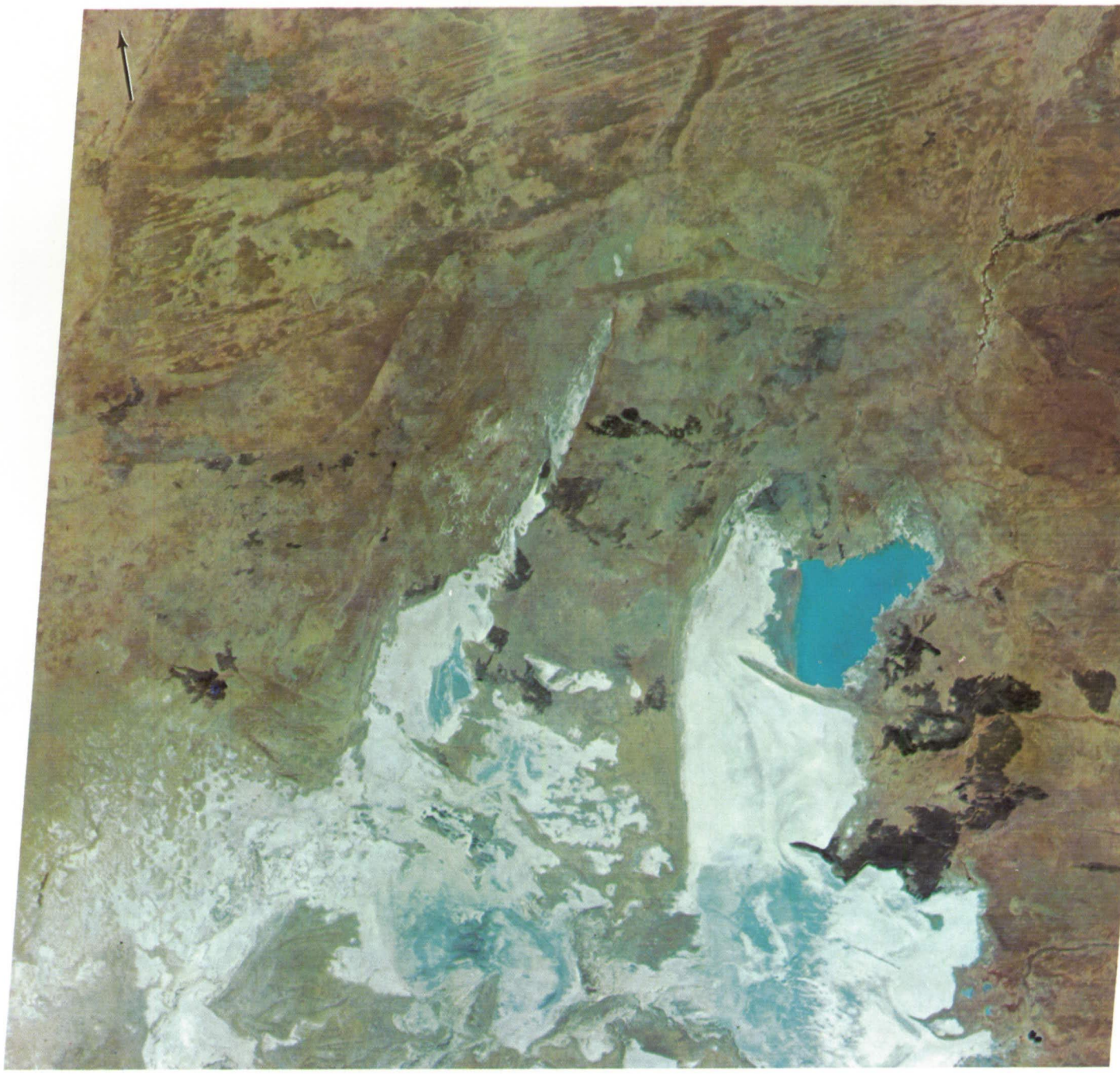
PLATE 342

BOTSWANA: Southwestern Botswana is covered by this image, the center of which is about 160 kilometers (100 miles) northwest of Gaberones, the capital. Two villages, Chachwe and Kuchwe, are in the scene, but are quite invisible. The area is dry, with annual rainfall amounting to around 30 centimeters (12 inches) per year, and the vegetation is chiefly grass with scattered trees and bushes typical of the drier parts of the savanna (or veld). This, despite the vegetative cover, is part of the Kalahari Desert.

What little rain does fall comes mainly in the summer, so that the area experiences several months of drought per year. This is partly responsible for the frequent brush fires that burn off the grass and young trees. The striking mottled pattern of the terrain results from the scars left by these fires, with the light areas (less vegetated) being the burned patches. Some of these cover hundreds of square kilometers. (It should be remembered that these images are 185 kilometers (115 miles) on a side.)

This region is marginal for agriculture and cattle raising, and is thus partly inhabited by the Kalahari Bushmen. These pre-Bantu people are among the most primitive in the world, living only by hunting antelope. They have no farms, domestic animals, or villages, but roam the veld constantly. The reader may reflect on the different levels of development represented by the Bushmen and the satellite that photographed their home; but he should ask how long he himself could survive in the Kalahari Desert. *1124–07472;* November 24, 1972.

PLATE 343



BOTSWANA: This image of the Makarikari saltpans of northeastern Botswana is presented for comparison with plate 344 to show the great seasonal changes in the appearance of the terrain between dry and wet seasons. The area covered here overlaps that of the plate on the facing page; compare the left margin of this image with the right margin of the other. This image, acquired during a dry period, shows several obvious characteristics indicating dryness. The vegetation, chiefly grass and brush, has little color. In addition, the saltpans are largely dry; compare those at *C*–18 with the corresponding area in the later image. The nature of the black patches around the saltpans is not clear. In some parts of the world, swamps look like this on Landsat imagery. However, one of these patches (*D*–14) is not visible in the other image, acquired during the wet season. They are, therefore, probably areas of recent brush fires, as indeed their prominence in a visibly dry terrain would suggest.

Geologically, this area is on the east margin of the Kalahari Basin; some Karroo system rocks are exposed in the right part of the image. The linear valley at *M*–1 to *J*–11 is shown on the International Tectonic Map of Africa as a monocline, or one-sided fold, with the east side depressed. Other linear features with the same orientation are visible, such as that north of the Nata River (*S*–6). These may be the expression of regional crustal tension associated with eruption of the Karroo volcanics.

Geologic features of a more superficial nature—stabilized sand dunes—are visible along the top of the image. The appearance of such dunes in a vegetated area suggests a drier climate existed at some time in the past. *1052–07454;* September 13, 1972.

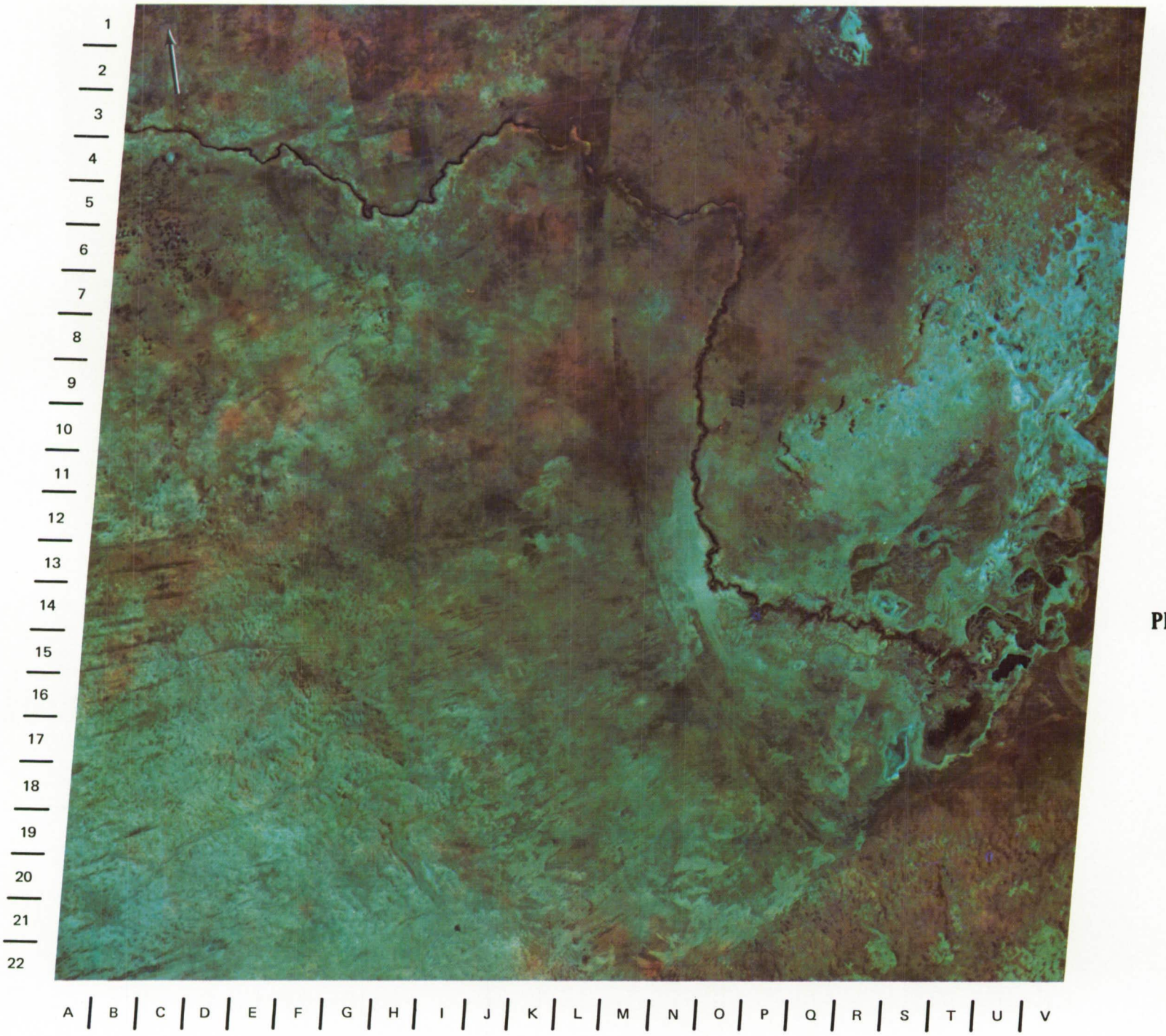


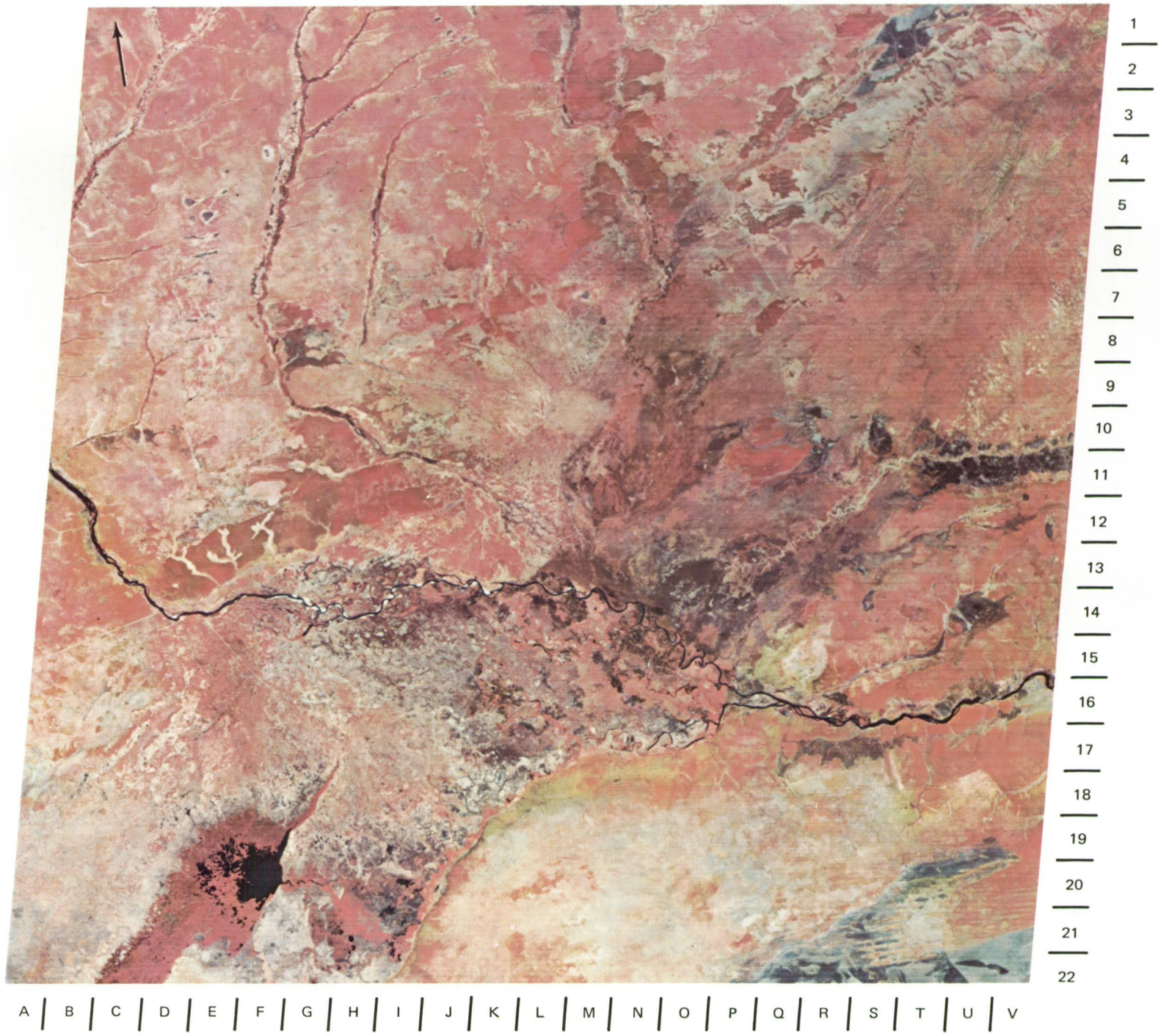
PLATE 344

BOTSWANA: Four months after the previous image was acquired by Landsat 1, rain had made striking changes in the appearance of northeastern Botswana. This scene overlaps the previous one, as described before. The most prominent landmark is the Botletle River (*F*–5; *N*–6; *O*–13); no settlements are visible. Since the previous image had been taken, the vegetation had become much greener (or redder in this color composite). The vegetation distribution is obviously not uniform; note, for example, the boundary at lower right near Lake Dow (*T*–16). The nature of the remarkably sharp vegetation boundaries, such as that at *E*–1, is not clear. Some evidently follow the limits of the former Native Reserves of Bechuanaland and probably represent the demarcation lines between areas that are overgrazed and those that are not. This is one of many Landsat images demonstrating the potential value of orbital imagery in range management.

Another obvious difference in the area since the previous image was acquired is the appearance of lakes in the Makarikari Basin at upper right. The salt deposits result, of course, from many thousands of seasons of evaporation from these ephemeral lakes. The average rainfall is well under 50 centimeters (20 inches) per year, and it falls in only a few months of the year, conditions whose effect is well shown by this pair of images.

Note also the stabilized sand dunes at lower left. *1179–07521;* January 18, 1973.

PLATE 345



ZAMBEZI RIVER: This colorful view embraces parts of four African countries: Zambia *(upper right),* Botswana *(bottom center),* Rhodesia *(lower right corner),* and South-West Africa, or Namibia *(left center).* The Zambezi River (*A*–11; *L*–13; *V*–15) forms a border in several areas and is the most prominent feature of the image. The Chobe River (*H*–20; *P*–16) separates Botswana from the Caprivi Strip of Namibia, whose northern border is visible at *B*–14. This narrow strip was acquired by Germany in 1893 to give Namibia, then a German colony, access to the Zambezi River for shipping. Such access is of little value for this purpose because, as the Landsat image shows, the Zambezi in this area is blocked by waterfalls such as Victoria Falls (just off the image to the right).

The area of this scene is part of the Kalahari Basin, but because it gets much more rain than areas farther south, it has a very different aspect from that shown by the previous Landsat images. However, some typical Kalahari features are still visible, such as the stabilized sand dunes at *T*–21. Most of the area is underlain by sand and other sediments of the Kalahari Basin, although igneous rocks of the Karroo system crop out in the eastern part of the area.

Rainfall in much of Africa is noted for its concentration in one short season. In this area, most of the rain (on the order of 64 centimeters (25 inches) per year) falls in the winter months, July being the dryest. This picture thus shows the appearance of savanna and swamps (*I*–15) at the beginning of the rainy season. *1125–07513;* November 25, 1972.

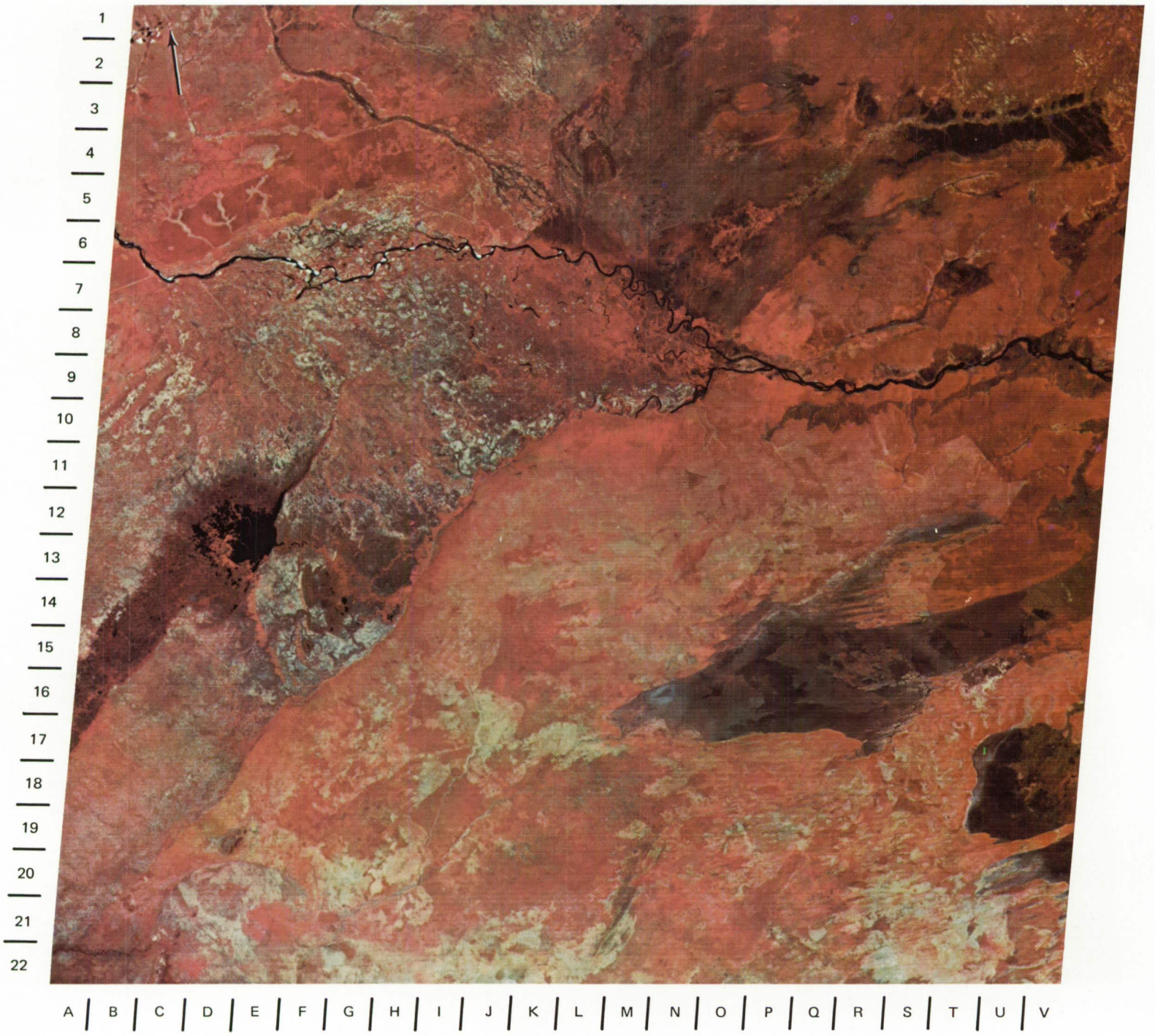
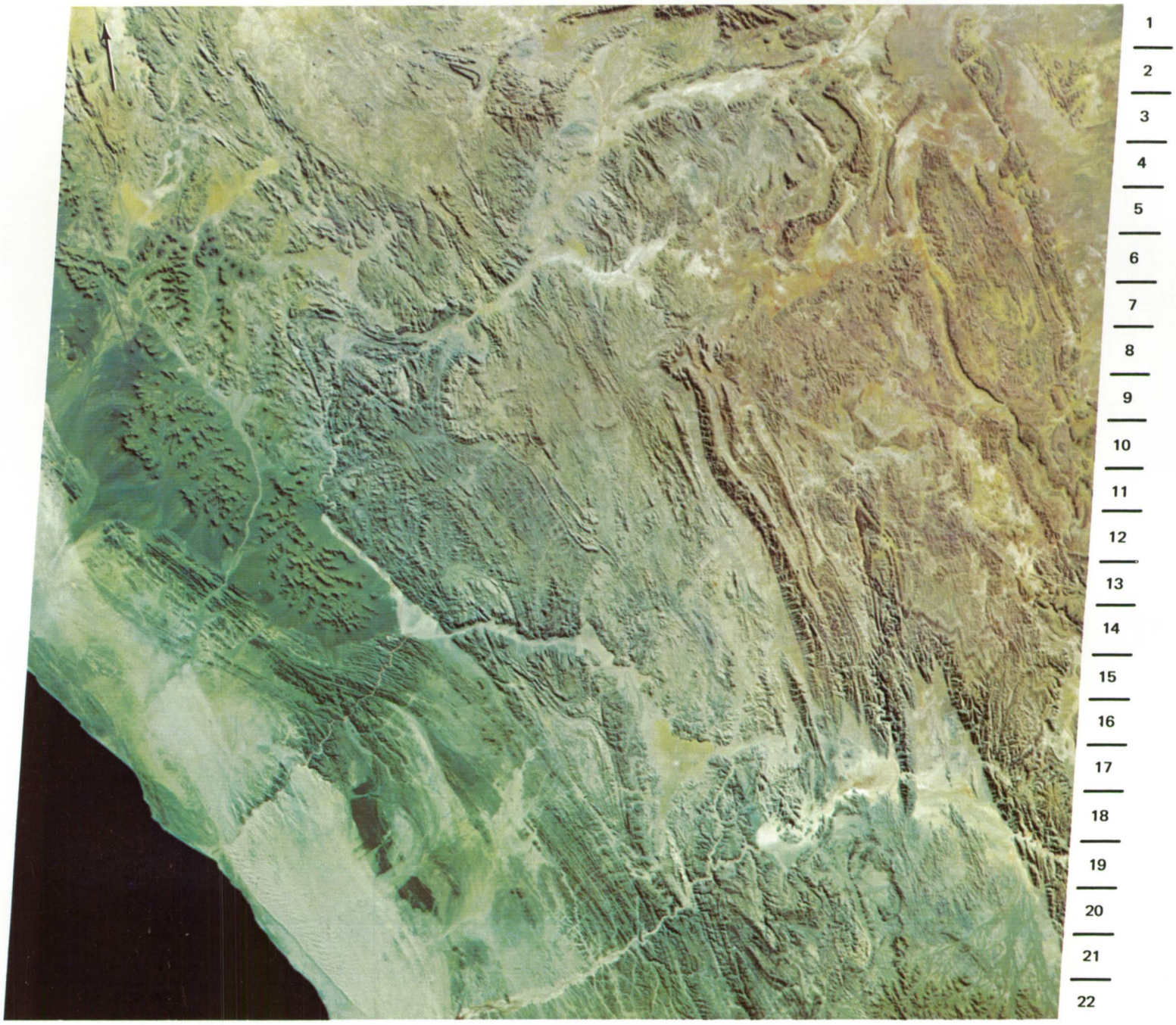


PLATE 346

ZAMBEZI RIVER: The value of the repetitive coverage provided by Landsat 1 is again demonstrated by this view of the Zambezi-Chobe River area during the rainy season, just three Landsat coverage cycles after the previous image. The vegetation changes account for most of the change in appearance, with both savanna (*E*–20; *K*–10; *V*–10; *V*–21) and swamp (*D*–16; *D*–6; *K*–9) showing marked growth. Some swampy areas (*S*–3) obviously have much more standing water than they did before. All vegetative boundaries are enhanced by this seasonal rainfall, including the burn scars of the Botswana savanna (*I*–16). The change in reflectance of vegetation from one season to the next is an invaluable aid to computer-based techniques of image interpretation, providing an additional variable for cluster analysis. Developing nations such as those of central Africa can clearly benefit from the improved vegetation and soil mapping made possible with Landsat coverage. Furthermore, roads and railroads, both of which must be expanded in this area, can also be more efficiently planned with the use of Landsat images to delineate, for example, areas flooded during the rainy season.

This region, although having an average elevation of about 1000 meters (3300 feet), is relatively level. Geological structure is generally concealed. However, linear features such as the one at *M*–20 probably represent faults or folds. This area is at the southwest end of the Zambezi-Luangwa trough, a down-faulted valley branching from the main part of the African rift system, and trending northeast from here. The Landsat image may show that the trough extends farther than had been believed. *1179–07512;* January 18, 1973.

PLATE 347



NAMIBIA: Differential erosion on folded rocks has produced an intricate, rugged landscape in the Kaoko Veld region of Namibia. The area is extremely dry, with thin soil and little vegetation, except for narrow strips along the Hoarusib (*E*–18; *H*–14) and Hoanib (*L*–21; *O*–19) Rivers. The narrow coastal strip, part of the Namib Desert, is partly covered with sand dunes. Their distribution reflects the dominant wind direction, from southeast to northwest, parallel to the Benguela current flowing north along the coast.

The dominant geologic structures are fold axes parallel to the coast. There are two main geologic units here. At upper right are rocks of the Damara System, igneous and metamorphic types of Late Precambrian age that underlie much of Namibia. The remainder of the terrain covered here is composed of igneous and sedimentary rocks of the widespread Karroo System. The Karroo System, of Paleozoic and Mesozoic age, is prominent in South Africa, underlying several tens of thousands of square kilometers and forming several major topographic features such as the Drakensberg Escarpment. However, outliers of the Karroo occur elsewhere to the north, the one shown here being one of the most distant. The dark rocks at *C*–9 to *G*–13 are basalts of the Stormberg Series. They overlie dark-colored strata that also belong to the Karroo System, consisting in this area of sandstones and tuffs, with interbedded lavas.

The origin of the fold belt shown here is interesting to speculate on. Many proponents of plate tectonics and accompanying continental drift consider folded mountains to result from continental or plate collisions. These folds appear essentially similar in scale and geometry to most other fold belts. If the collision theory is correct, there must have been a plate collision to produce these folds, But this coastline is generally considered a classic example of the scar resulting from continental fragmentation and separation, not collision. Whether this contradiction can be reconciled by continental drift enthusiasts remains to be seen; the Landsat images will certainly be of help in this task. *1007–08364;* July 30, 1972.

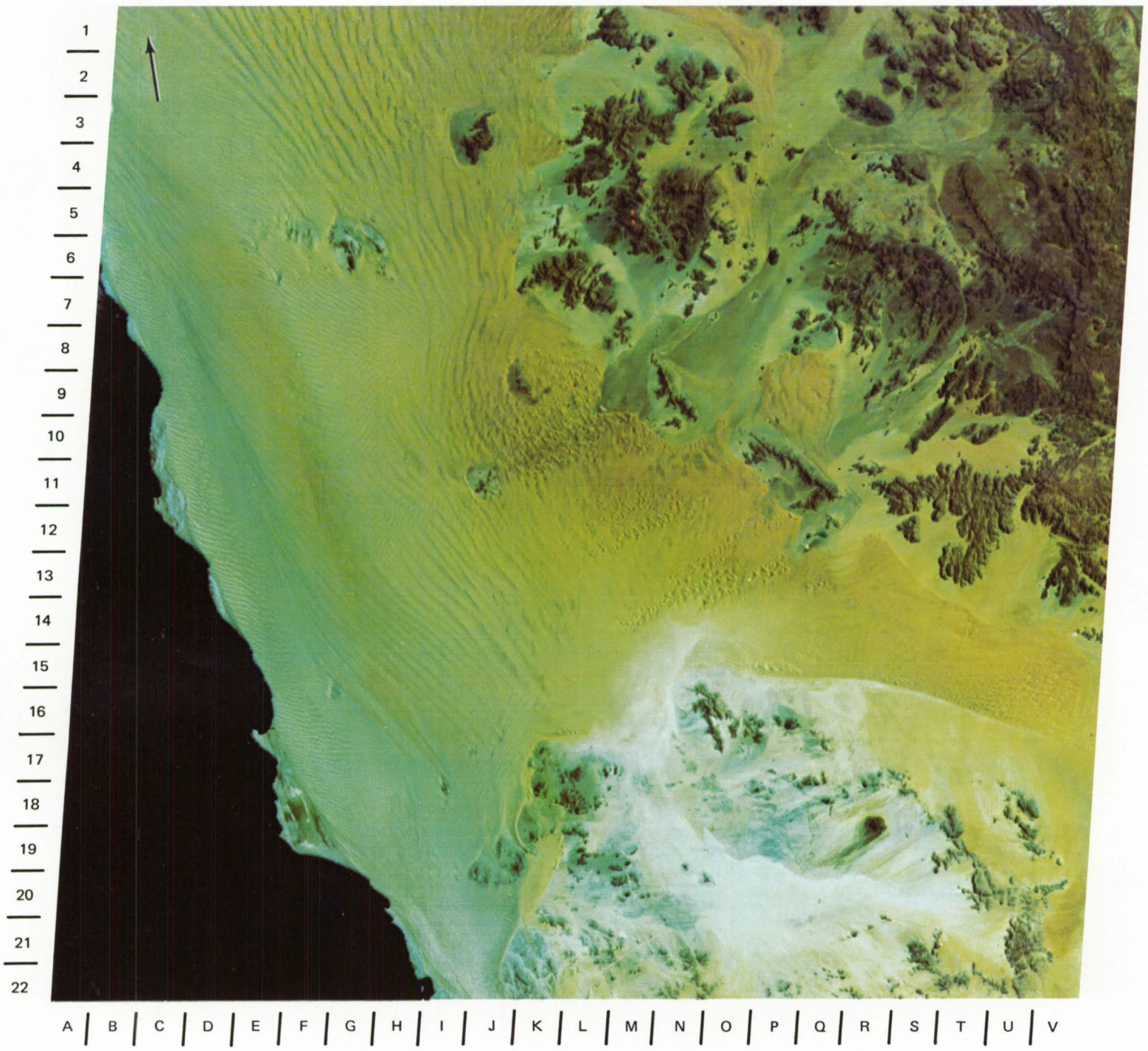
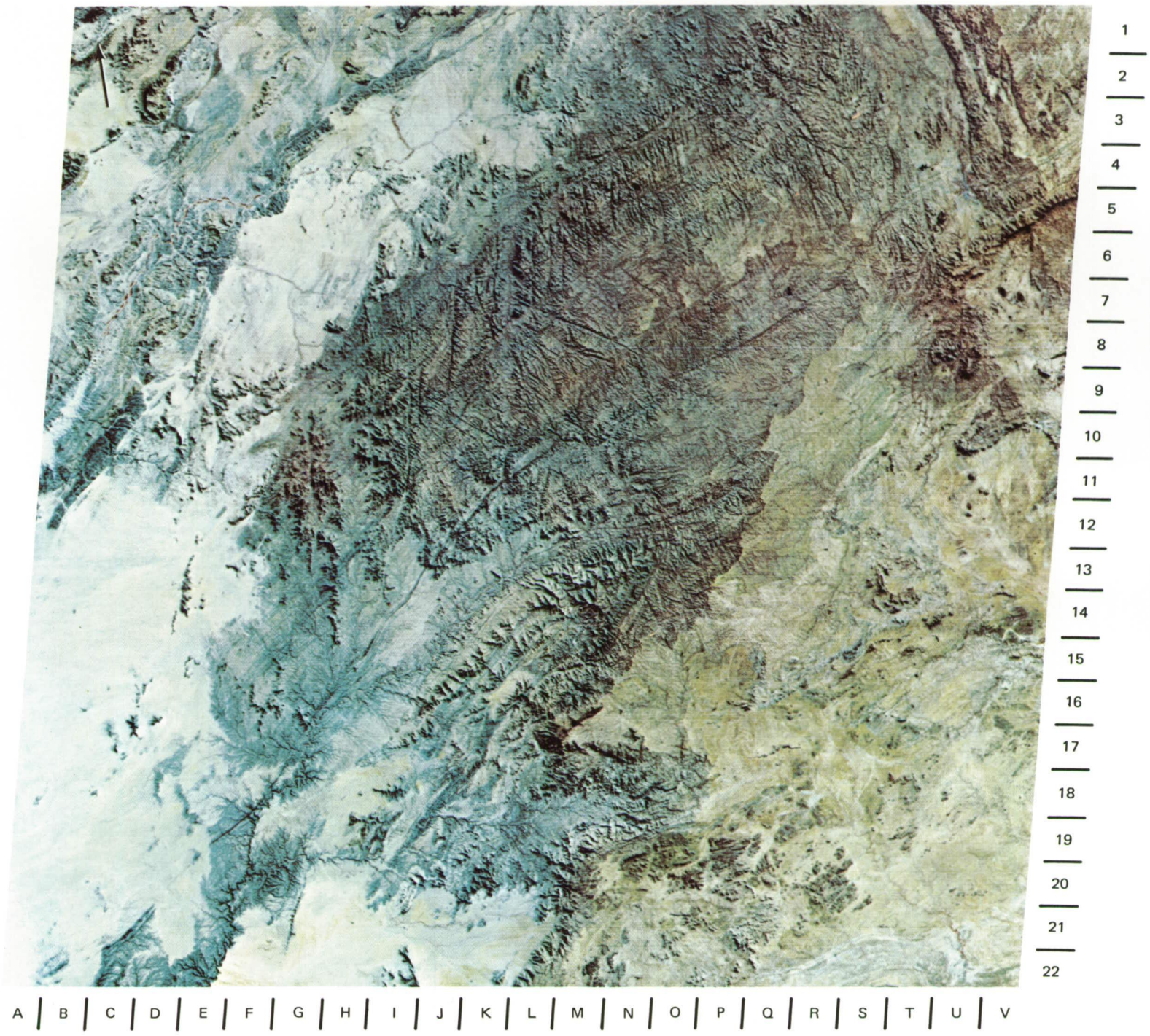


PLATE 348

NAMIB DESERT: The Namib Desert is an extremely dry area, largely because of the influence of the cool Benguela current, which flows northward along the coast of Namibia. The area shown here is just north of Lüderitz; Hottentot Bay is at *D*–15. The direction of the Benguela current is indicated by the various northward-pointing hooks and sandspits along the coast. The dominant physiographic features are, of course, the great sand dunes of the Namib Desert. As classified by E. D. McKee of the U.S. Geological Survey from Landsat imagery, there are several main types. At *F*–7 to *I*–14 are a series of parallel straight megadunes. To the north, at *F*–3, there is a field of parallel wavy megadunes. Chains of radial, or star, dunes are visible at *N*–13 and *M*–11, apparently developing from the parallel dunes. A formless sand area, or sand sheets, is at lower right (*T*–17). These dunes are much more complex than they may appear at first glance, and it is difficult to say just what wind directions they imply. The dominant dune types are longitudinal dunes, generally considered to form roughly parallel to the prevailing wind. However, there are minor dune trends cutting across the parallel dune trends, so it is unsafe to generalize about wind directions.

The area is obviously an extremely barren one. However, it has considerable mineral wealth in the form of alluvial diamonds. The cool Benguela current supports a large fishing industry, and coast cities such as Lüderitz and, to the north, Walvis Bay, depend partly on this for income. The mountains in the upper right part of the image, up to 1800 meters (6000 feet) or more in places, are all Precambrian rock. There are no known mining developments, except for diamond mining, in the area covered in this scene. *1202–08224;* February 10, 1973.

PLATE 349



WINDHOEK, NAMIBIA: The barren but geologically fascinating landscape at Namibia, about 160 kilometers (100 miles) in from the Atlantic coast, is covered by this image. Windhoek, the capital, is barely visible at *T*–4 as a small bluish-gray area. The Kuiseb River, which reaches the coast at Walvis Bay, is visible at *E*–21. Much of the region covered is mountainous, with the Auas Mountains south of Windhoek (*T*–6) reaching heights of over 2400 meters (8000 feet). The area covered by this image is essentially undeveloped economically; agriculture is practically impossible on any large scale because of the lack of water, and there is little mineral production at present.

Two major aspects of the geology of Namibia are well exhibited here. First, the bedrock geology is clearly exposed. Except for a few dune fields of the Namib Desert (e.g., *F*–21), almost the entire exposed area is Precambrian or early Paleozoic igneous or metamorphic rock. The prominent northeast-trending ridges at the center are rocks of the Damara System, a Late Precambrian mountain belt now deeply exposed. The rocks are chiefly metasediments of great thickness, presumably deposited in a former geosyncline. Since, as the Landsat image shows, they strike toward the coast at a high angle, they obviously do not represent simple lateral accretion to the present African continent.

The image also illustrates several of the successive erosional land surfaces characteristic of Africa and perhaps of other continents. In the concept advanced by L. C. King, these land surfaces have been produced by lateral erosion, with advance of scarps. However, regional uplift ("cymatogeny" in King's nomenclature) interrupts this process, so that remnants of several successively older surfaces survive. The youngest surface, designated the "Congo" Surface, of Quaternary age, is represented by the valley of the Kuiseb River (*F*–19). It is cut into the next older one, the "Post-African" Surface, which is exposed at *B*–20 to *C*–20. This surface in turn bevels the "African" Surface, the yellowish area in the lower right corner. Oldest of all is the "Gondwana" Surface, at center (*K*–15 to *P*–1), of Jurassic age. If this interpretation, and King's theory, are correct, this image shows remnants of land on which dinosaurs walked. *1382–08205;* August 9, 1973.

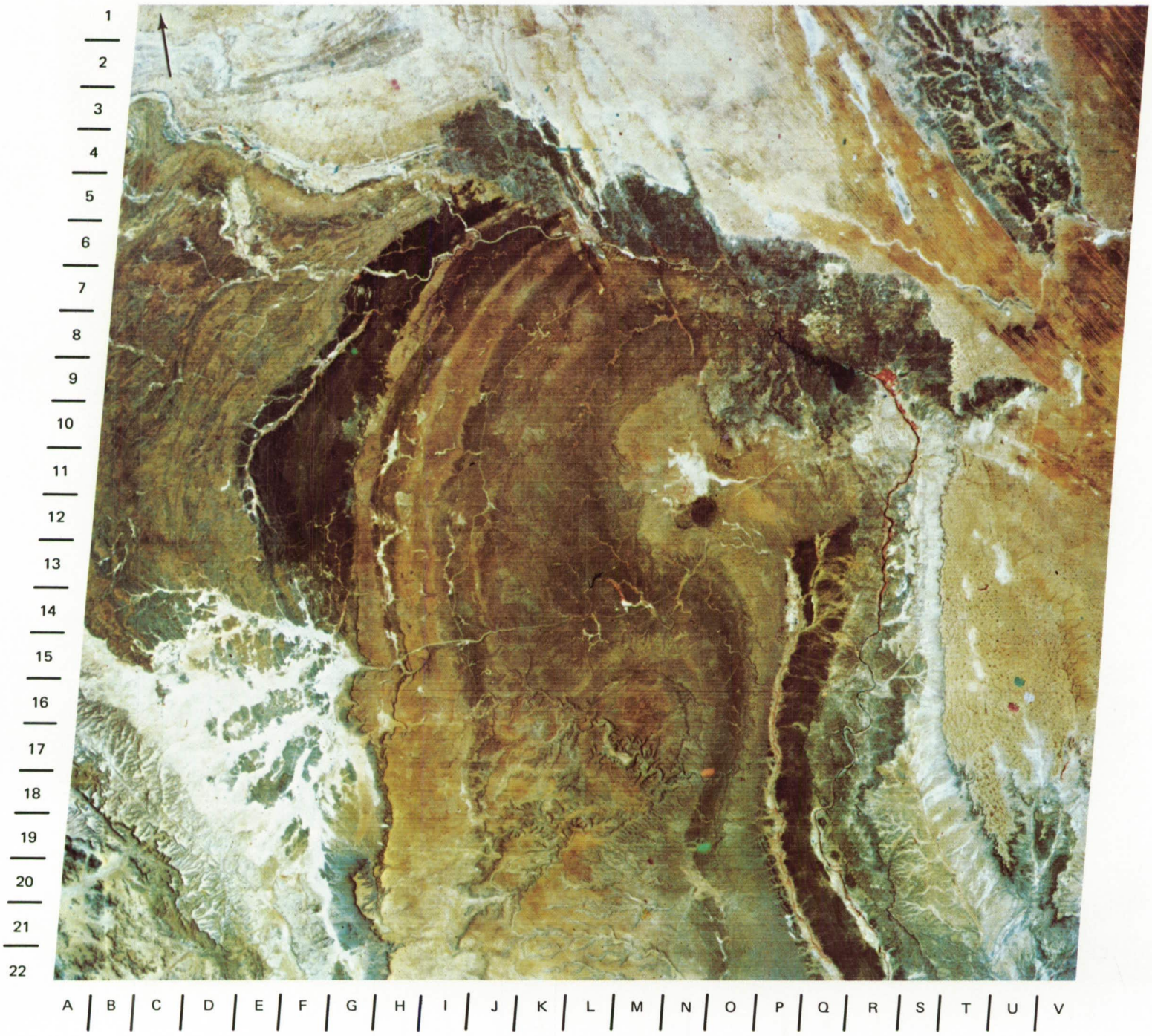
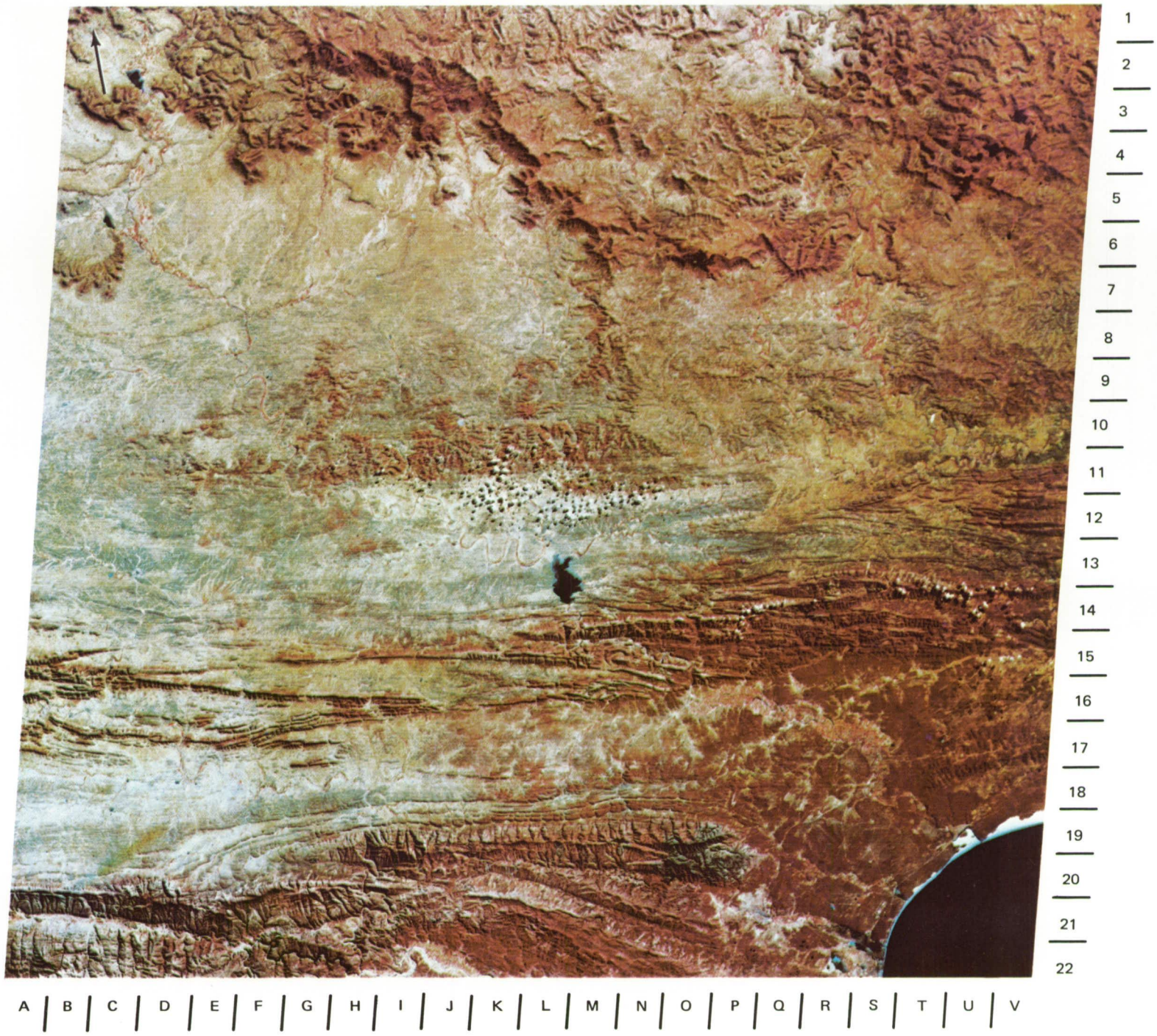


PLATE 350

NAMIBIA: The multispectral scanner brings out lithologic and structural features of this part of Great Namaland in Namibia with remarkable clarity. This area, like the rest of Namibia, is extremely dry, with little vegetation, and so the geology dominates the image. There is little evidence of habitation, although the towns of Maltahöhe (*H*–14) and Mariental (*R*–10) are barely visible. Mariental is on the Fish River (*R*–21; *R*–10), which has been impounded by the Hardap Dam (*Q*–9). Farming is possible with irrigation, as shown by the bright red areas along the Fish River, where corn, beans, potatoes, and fruit are grown. The water supply is barely sufficient for agriculture, however. The dryness of the country is suggested by the linear sand dunes of the Kalahari Desert at upper right.

The concentric banded pattern occupying the center of the image is the expression of a very large structural dome or anticline centered on *L*–17. Most of the sedimentary rocks of this dome, constituting the Nananib Plateau (*J*–15), belong stratigraphically to the Nama System of Lower Paleozoic age. The Nananib Plateau appears to be part of what L. C. King designates the African Erosion Surface of Early Cenozoic age. It is the oldest major erosion surface in the area covered by the Landsat image; the Kalk Plateau (*T*–11; *T*–17) may also be part of it. The Fish River valley (*R*–10; *R*–21) represents a younger cycle of erosion, being part of the Late Cenozoic Post-African Erosion Surface. The light-colored area at lower left probably also belongs to this cycle, with the Tsaris Mountains (*C*–19) being resistant remnants. Structurally, the area has been characterized by mild deformation, chiefly vertical, since the beginning of the Cambrian, as shown by the very low dips implied by the outcrop pattern. Some faulting has occurred, visible as the southeasterly trending lineaments at *K*–4 and *B*–17. The tectonic history of this area as expressed in its physiography is typical of the post-Cambrian history of much of Africa outside the Atlas and Cape folded belts. *1147–08163;* December 17, 1972.

PLATE 351



CAPE RANGES (SOUTH AFRICA): This image covers the southeastern coastal region of South Africa. The area shown is not densely inhabited, although the city of Port Elizabeth is just off the image to the south at *S*–21, on the shore of Algoa Bay (*U*–21). One other smaller town is visible: Uitenhage (*P*–20). Most of the area is used for farming and cattle raising. This Landsat image shows indirectly the condition most important for farming: the distribution of rainfall. Rain is strongly controlled by topography, in that major mountains or mountain chains produce rain shadows, and elevation in general has a major effect. Note in particular the reddish color of higher elevations in both the forested Cape Ranges (parallel to the bottom of the image) and the 2400-meter (8000-foot) high mountains to the north. Also note the lighter color, implying less dense vegetation, in the grassy interior valleys at upper left, due to rain shadow and elevation. Like much of southern Africa, lack of water is something of a problem; it is only in the mountains and along the coast that precipitation amounts to 65 centimeters (25 inches) (up to 130 centimeters (50 inches) in some places).

Geologically, this image is of great interest. The Cape Ranges appear to be a typical folded mountain belt, consisting of linked anticlines and synclines. They are of Paleozoic age, so that their present topography is the result of differential erosion rather than of the folding and uplift that took place earlier. There are almost no Paleozoic fold belts in all of Africa south of the Anti-Atlas Mountains until one comes to the Cape Ranges. The Cape Ranges have been considerably eroded, the erosion proceeding inward from the coast and forming a nested series of successive erosion surfaces. Summits in the Cape Ranges up to about 1500 meters (5000 feet) high are thought to date from the Jurassic Period and are labeled the "Gondwana Surface." The valleys between the various mountains in these ranges and to the north are a younger surface, the "Post-Gondwana Surface," dating from early or middle Cretaceous. Near the coast is the still younger "Coastal Plain Surface" and "Congo Surface." *1068–07380;* September 29, 1972.

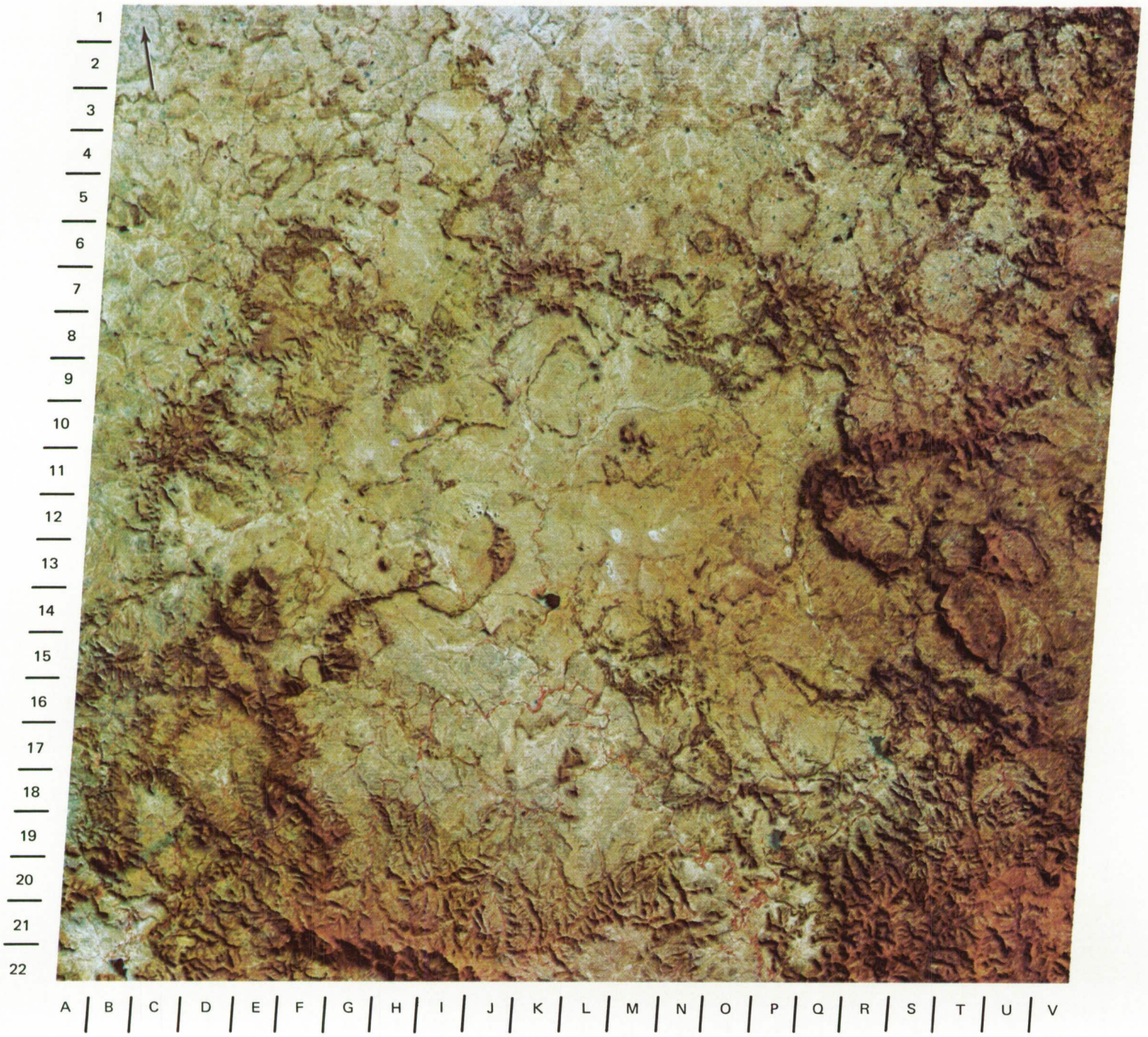


PLATE 352

CAPE PROVINCE, SOUTH AFRICA: The word "Karroo" is derived from a Hottentot word for "waterless," and crops up repeatedly in discussions of South African geology, geography, and vegetation. Several applications of the word are illustrated here. The area shown is in Cape Province, whose capital, Queenstown, is near the center of the image, though not visible. The area is obviously dry, except for high elevations, and characterized by Karroo vegetation. This association consists of small shrubs, bushes, and grass, grading into savanna in places. It is of little use for anything but sheep raising, but can carry only about six sheep per acre. Some farming is done in this area with the aid of irrigation, as along the Kei River (*L*–16). There are innumerable small reservoirs, especially along the northern part of the area covered here.

Geologically, the term "Karroo" is well known. The Karroo System is a series of Late Paleozoic to Early Mesozoic sedimentary and igneous rocks up to about 8 kilometers (5 miles) in thickness. Roughly half the area of the Republic of South Africa is underlain by the Karroo System. This image covers a region underlain by the Beaufort Series, a thick collection of sandstones and shales carrying abundant reptilian fossils. The Beaufort Series is intruded by sills and dikes of dolerite (a variety of basaltic igneous rock). The dolerite sills are somewhat undulatory, and outcrop in peculiar circular patterns (*H*–3; *K*–9; *I*–13; *O*–5), the dolerite being more resistant to erosion than the sediments it intrudes. Several dikes are visible for the same reason; a prominent one extends southeast from *G*–13 to *J*–16.

The cliffs at right are part of the Great Escarpment of South Africa, formed by lateral erosion in from the coast of an Early Cenozoic erosion surface. The rocks in the upper right part of this image include lavas of the Stormberg Series (part of the Karroo System). *1068–07373;* September 29, 1972.

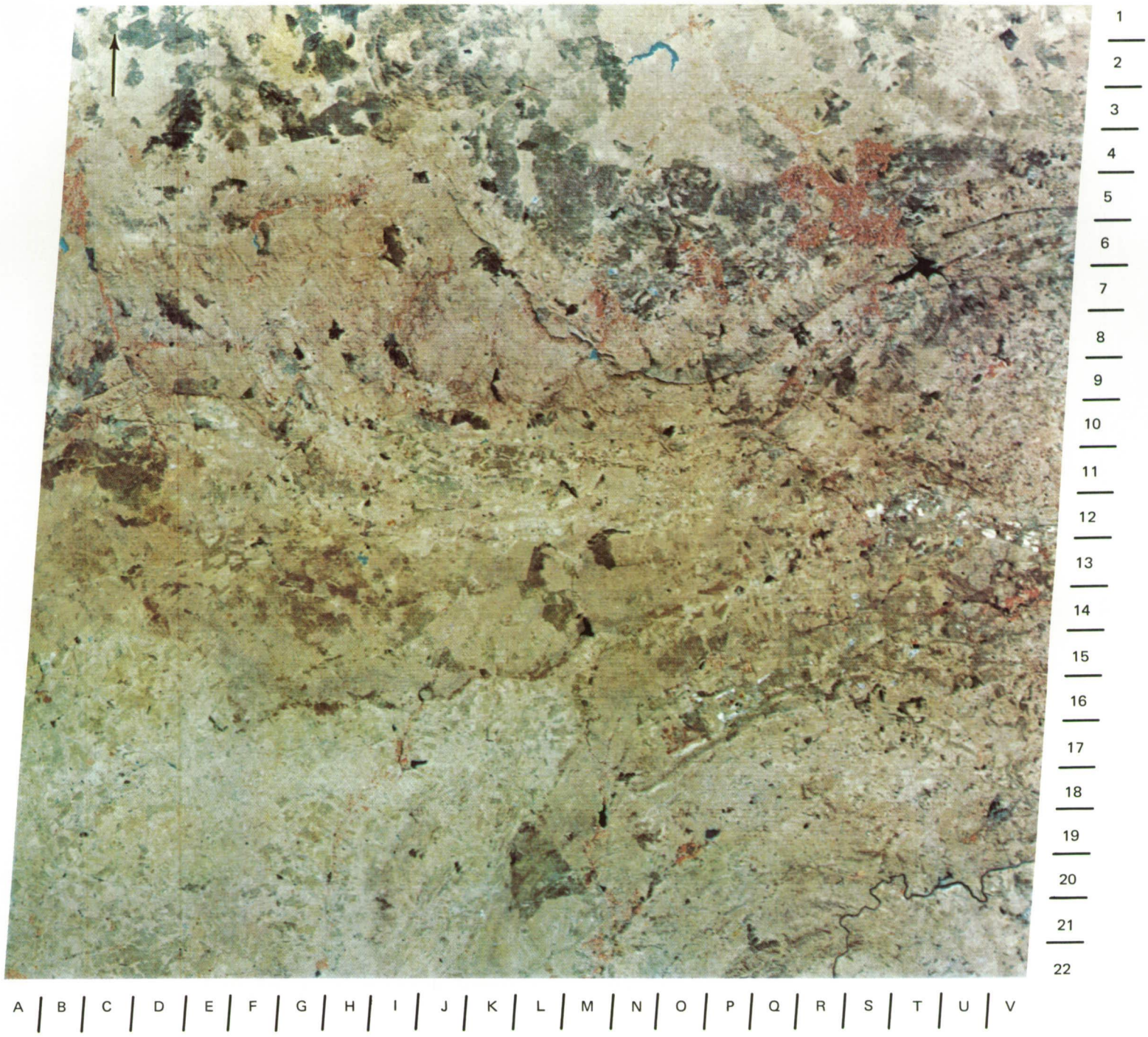


PLATE 353

SOUTH AFRICA, DRY SEASON: This image was transmitted by Landsat in September 1972 and shows the Transvaal of South Africa at the end of the dry winter season when the grasses are brown and the trees are leafless. It is presented here for comparison with the following image, acquired a few months later during the rainy summer season. This image, despite its relatively low color contrast, is nevertheless an interesting one. Johannesburg is on the right edge (*V*–12), but the chief landmarks visible at this location are the immense dumps of the Witwatersrand gold mines. The Republic of South Africa is the world's leading gold producer, accounting for two-thirds of the world's annual production, amounting to more than 800 megagrams (900 tons) per year. The gold comes from conglomerates of the Precambrian Witwatersrand System. The surface occurrences of this system have been worked out, and all production is now from underground mines. These are the world's deepest, going to depths greater than 3400 meters (11 000 feet). The gold deposits follow a syncline curving to the west and southwest from Johannesburg, as the distribution of mine dumps visible here suggests.

The geology of the area will be discussed in some detail in the next caption. However, attention should be called here to the Vredefort dome (*R*–21), appearing as a vague concentric pattern, the circular Pilanesberg intrusion (*I*–2), and the Bushveld complex in the upper right corner.

The area shown here is part of the Transvaal Bushveld (the Vaal River itself is at *S*–20), one of the interior plateaus of South Africa. The average elevation here is about 900 meters (3000 feet). Rainfall is generally 50 centimeters (20 inches) per year or less, so that most agriculture depends on irrigation. Wheat is grown in the Krokodil River area at *Q*–5; tobacco and citrus fruits are also grown in the Transvaal. Cattle raising, however, accounts for most of the agricultural income in this area. *1050–07355;* September 11, 1972.

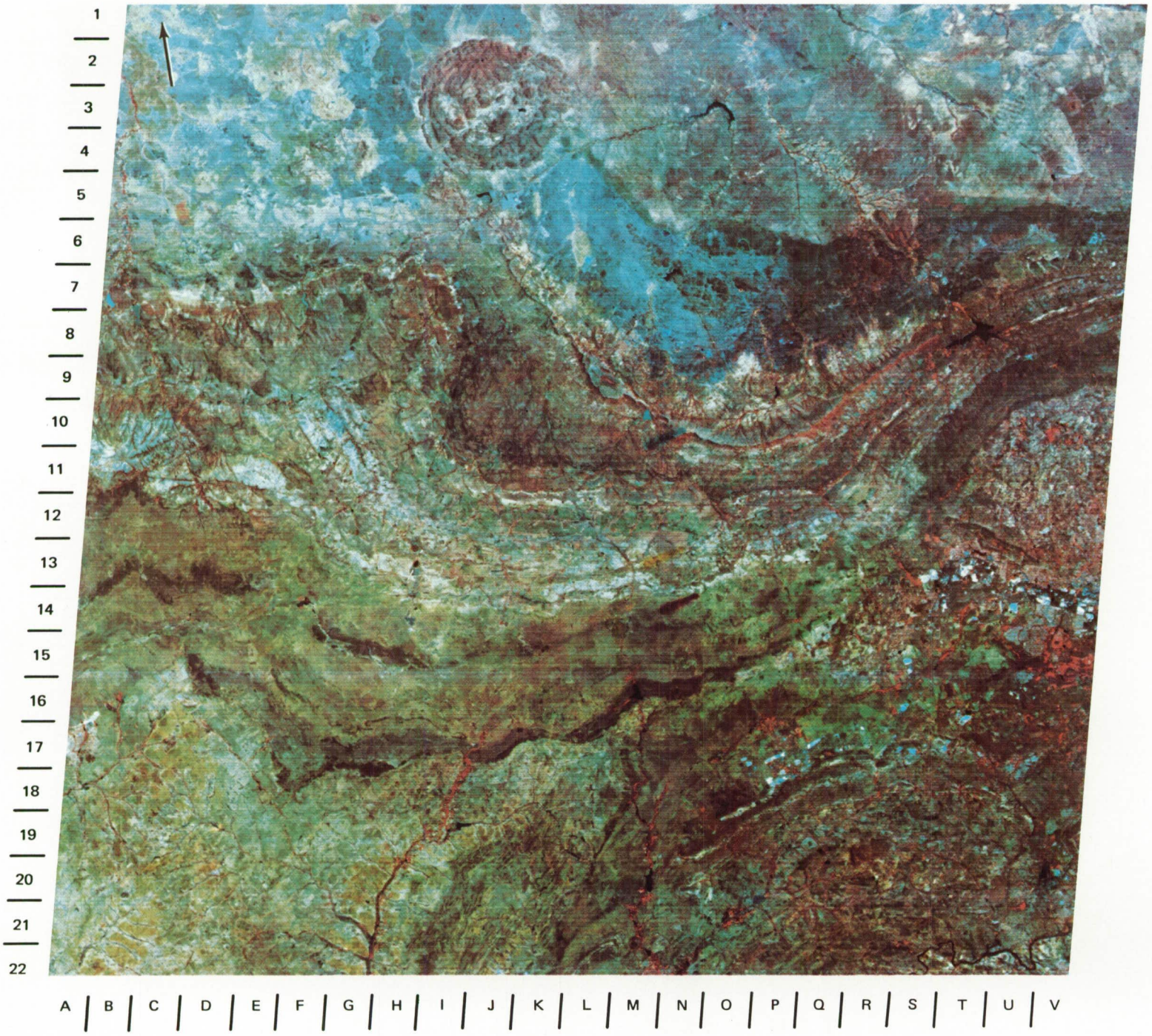


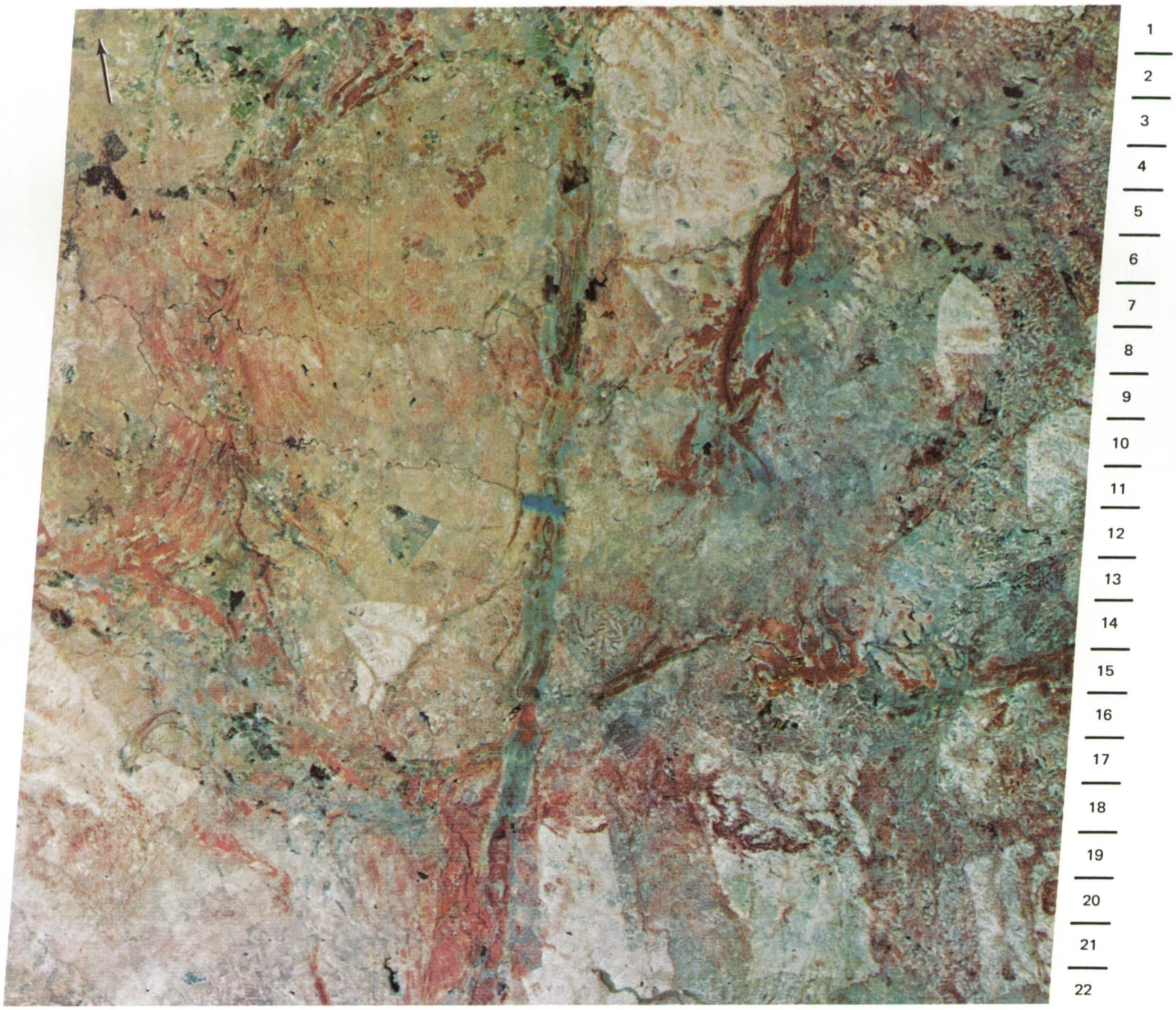
PLATE 354

SOUTH AFRICA, WET SEASON: After a few months of rain, the Transvaal takes on a strikingly different appearance, with all geologic structures and rock types being much more conspicuous than they were in the summer image. J. Grootenboer, a South African geologist, attributes this effect to the lesser amount of haze in December and secondarily to greater soil moisture and plant growth. The geology will be described as seen going from northeast to southwest across the image (upper right to lower left).

The Bushveld complex occupies the upper right corner. This is a large basinlike igneous intrusion composed of basic and ultrabasic (iron- and magnesium-rich) rocks capped by granite. The basic rocks are visible as a blue band (*J*–5; *N*–7; *S*–6); the granites are northeast of them. The Pilanesberg intrusion, composed of alkaline granites like those of the Air Mountains (plate 331), is conspicuous at *I*–3 because of the red color indicating vegetation. Southwest from the basic layer of the Bushveld complex a broad series of concentric bands roughly parallel to the edge of the complex is visible. These are sedimentary and igneous rocks of the Transvaal System. The yellow and brown units (*B*–13; *H*–15; *N*–14) are of particular interest. These are the Dolomite Series of the Transvaal System, and according to Grootenboer, had never been mapped as several units in "90 years of continuous geological activity." However, the Landsat 1 image clearly shows a number of different lithologic units, providing a striking example of the value of orbital techniques in general and repetitive coverage in particular.

Continuing the traverse, the rocks of the Witwatersrand System are visible at *J*–20, and to their right, the north part of the Vredefort dome may be seen. This dome is one of the world's great geological puzzles. It is more than 75 kilometers (47 miles) wide, with a central core of Archean granite. The discovery of shatter cones by R. B. Hargraves in rocks of the Vredefort dome indicates that it is the likely result of a meteorite impact followed by granite intrusion. But as the Landsat image suggests, the dome is in the center of the Witwatersrand Basin. Whether this is coincidental remains to be discovered. *1158–07363;* December 28, 1972.

PLATE 355



RHODESIA: Southern Africa has more than its share of geological marvels; one of the strangest of these is the Great Dike of Rhodesia, neatly bisecting this Landsat image and indeed nearly bisecting Rhodesia itself. Since the dike is about 480 kilometers (300 miles) long, only one-third of it is seen here. The term "dike" generally refers to a fissure filled with igneous rock that cuts across the enclosing rock. The Great Dike is about 6 kilometers (4 miles) wide on the average, and is better described as a series of synclines or troughs occupying a long, narrow graben (down-faulted block). Some of these synclines can be seen at *K*–12 and *K*–15; the reader may find it interesting to compare their morphology with that of the synclines in folded mountain belts such as the Atlas, Appalachian, or Ouachita Mountains. Petrologically, the Great Dike is of great scientific and economic importance. Of Precambrian age, about 2.5 billion years old, the dike is composed of basic and ultrabasic igneous rocks petrologically similar to those of the Bushveld Complex of South Africa and several other layered complexes. Like them, it has substantial concentrations of chromium and is mined in several places for this metal. Some associated gold-bearing veins are also worked.

The regional geology visible here is also of interest in relation to crustal evolution. Most of the rocks in this area are of Lower Precambrian age, about 3 billion years old and consist of great granite batholiths that have been intruded into ancient belts of gneisses and other granitic rocks. These batholiths are visible as large, light-colored elliptical masses, separated by dark schist belts and greenstones; potash-rich soils derived from these rocks support thick vegetation. The batholith outcrop patterns should not be confused with other very light patches, which are overgrazed native reserves from which most of the vegetation has been stripped (*H*–3; *T*–7; *U*–16; *L*–20). The batholiths of Rhodesia have been interpreted by African geologists as very old granite crust on which the volcanic belts (now schist belts) were deposited, after which the granite was remobilized and intruded upward. Part of the north margin of the younger Limpopo mobile belt of metamorphic rocks occupies the southeastern corner of the image. This area is in the High Veld of Rhodesia, 1200 meters (4000 feet) or more above sea level. Although receiving only about 76 centimeters (30 inches) of rain per year, it supports cultivation of corn, tobacco, and dairying. *1103–07285;* November 3, 1972.

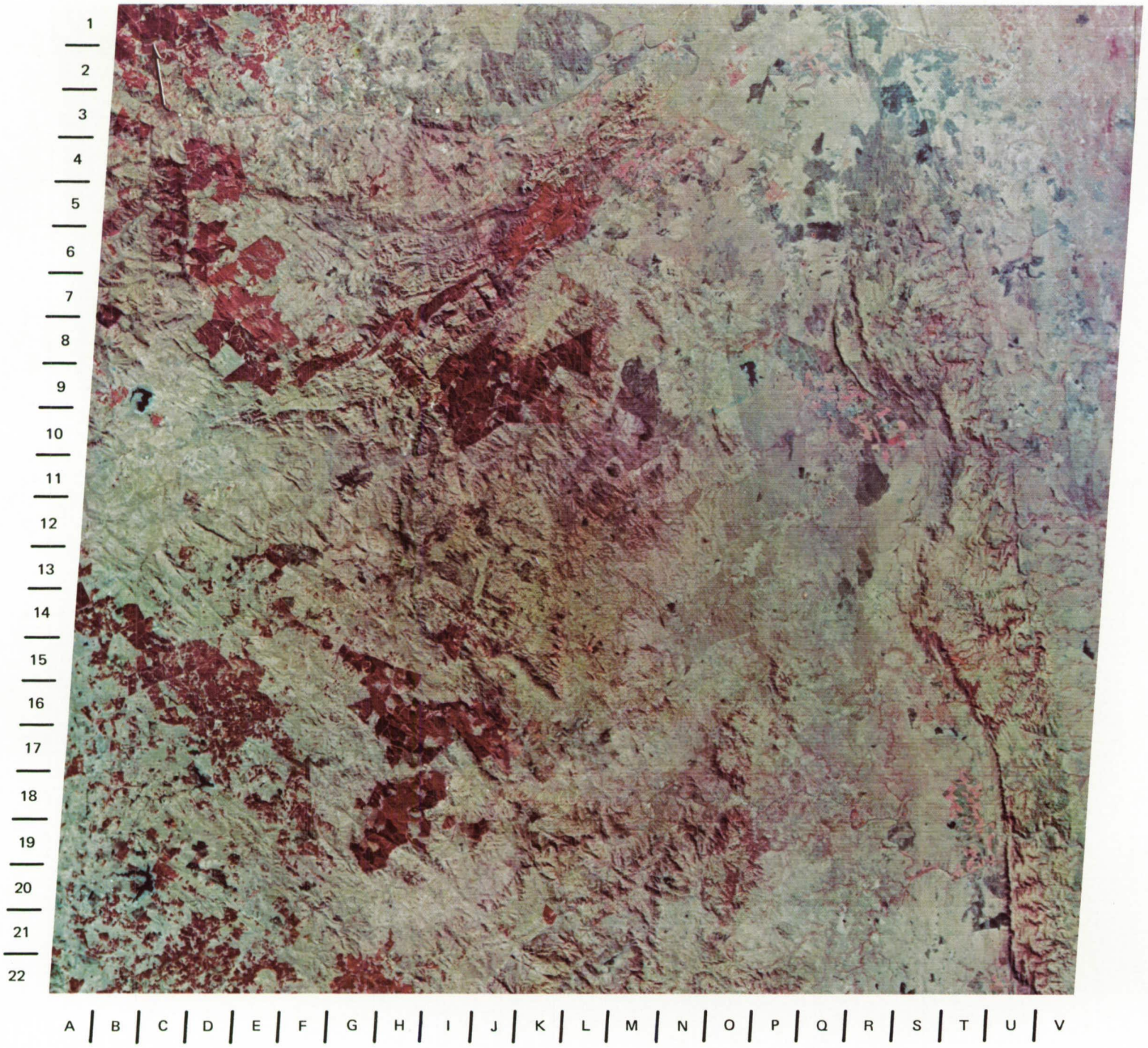
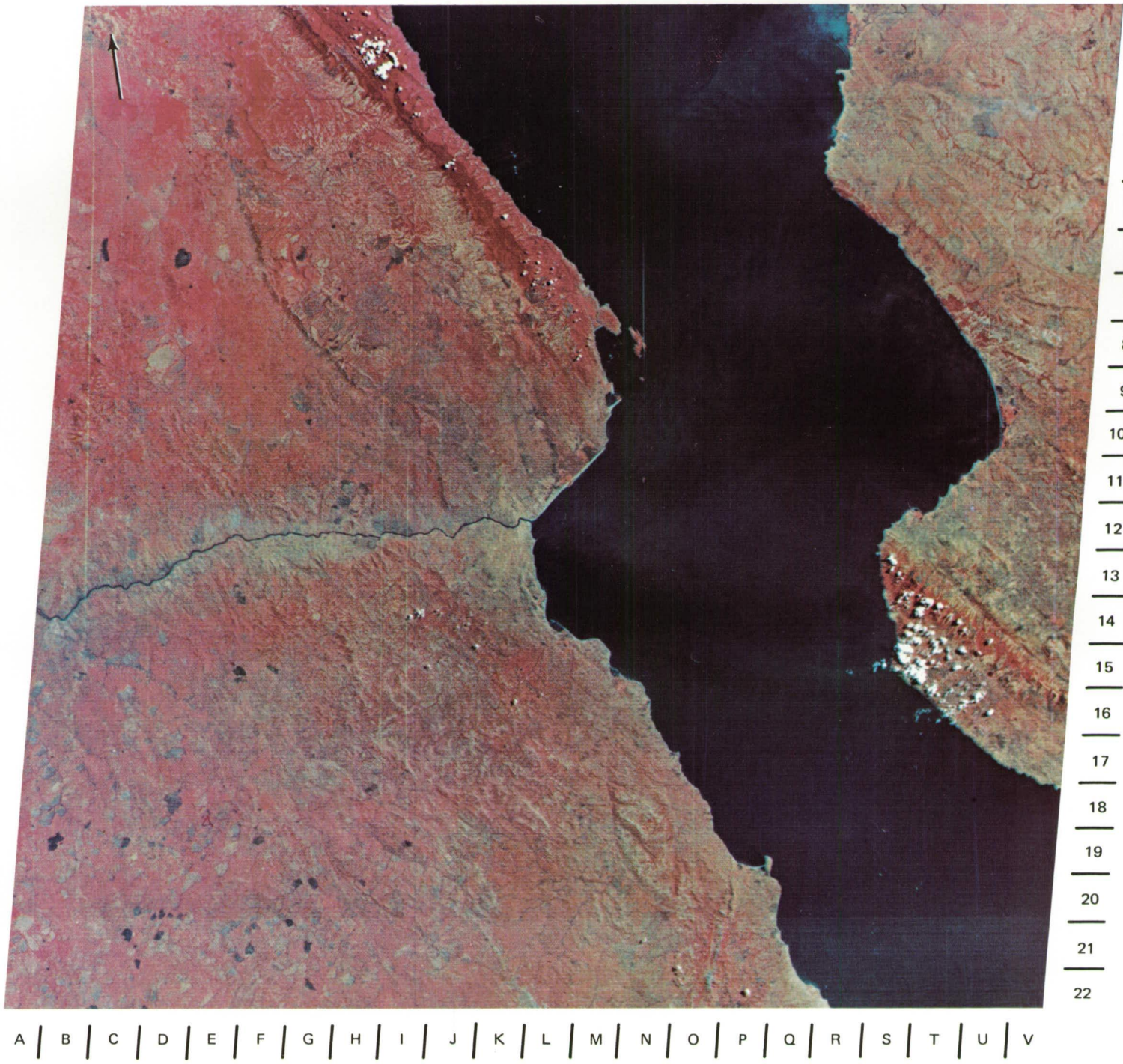


PLATE 356

SWAZILAND: Swaziland is southern Africa's smallest sovereign country, being about the size of New Jersey, and, consequently, it is not surprising that one Landsat frame includes about two-thirds of its total area. The northern border is visible at *L*–6 to *P*–8, and the capital, Mbabane, barely visible at *I*–14. The kingdom is nearly surrounded by South Africa, on the north, south, and west; Mozambique borders it on the northeast. The main physiographic regions, trending north to south, of Swaziland are easily distinguishable. At the center of the image is the High Veld, with elevations between 1000 and 1800 meters (3500 and 6000 feet) and annual rainfall of 110 to 190 centimeters (45 to 75 inches). The bright red patches at *I*–9 and *H*–16 are planted forests of pine and eucalyptus, which grow rapidly and produce large quantities of lumber. Logging roads can be resolved within these forests. To the east are the Middle Veld and Low Veld, successively; these are drier and suitable for cattle raising and farming, corn being an important crop. The High and Middle Veld regions are underlain by Precambrian rocks, largely granitic. The prominent ridge running north to south (*P*–1; *S*–13; *U*–21) is the Lebombo Mountains. Geologically, it is known as the Lebombo monocline and consists of Karroo volcanic rocks bounded by faults on the west side and dipping eastward toward the Indian Ocean.

There are many other important geological features visible. A prominent series of northwest to southeast lineaments, probably faults, can be seen in the lower left corner. Most interesting to the geologist is the Barberton Mountain Land of the South African Transvaal, in the upper left corner. The ridges trending northeast to southwest (*F*–7; *K*–3) are a greenstone belt, or folded series of Precambrian volcanic rocks, surrounded by granite. As described by M. J. and R. P. Viljoen, this is the oldest such belt known on Earth, with an age of about 3.4 billion years. Nongeologists may find it of interest that the Viljoens label rocks intruding the greenstone belt "young plutons," their age being only about 2.5 billion years. The area is important for knowledge of the early geologic evolution of the Earth's crust, providing evidence for very early differentiation of sial. *1047–07184;* September 8, 1972.

PLATE 357



LAKE TANGANYIKA: The opposite shores of Lake Tanganyika in the area shown here belong to two countries: Zaire (formerly the Republic of the Congo) on the west and Tanzania (formerly Tanganyika) on the east. Kalemi (fomerly Albertville), in the province of Katanga, is at *K*–12, on the Lukuga River (*A*–13; *K*–12). The lake, occupying part of the western rift system, is flanked by high mountains; its altitude is 772 meters (2534 feet) above sea level, while that of Kungwe Mountain (*T*–14) is 2515 meters (8250 feet). As other Landsat images have shown, the rift valleys of Africa are in general surrounded by parallel high mountains. This, and other evidence, shows that although the valleys are bounded by normal (tension) faults, they have not been formed by simple pulling apart at right angles to their length. Instead, the process is thought to have been regional uplift along linear zones, followed by down-faulting along the crest of the uplift because of the necessary crustal stretching.

The nature of the great deflection in the lake, followed by opposing coastlines, is not as it might appear. Although reminiscent of the matching coastlines of South America and South Africa, generally thought to result from continental drift, this deflection is the expression of a branching of the main depression, with one branch, not filled with water, heading southeast at *U*–12 to form the Rukwa trough.

The area is fairly well watered, with about 100 to 150 centimeters (40 to 60 inches) of rain per year. The natural vegetation in most of the area is moist savanna, except at high elevations, which are forested. Coffee is grown in the highlands, with oil palm and cotton in lower areas. The area is afflicted with the tsetse fly, so there is little cattle raising except in the highest areas. *1052–07413;* September 13, 1972.

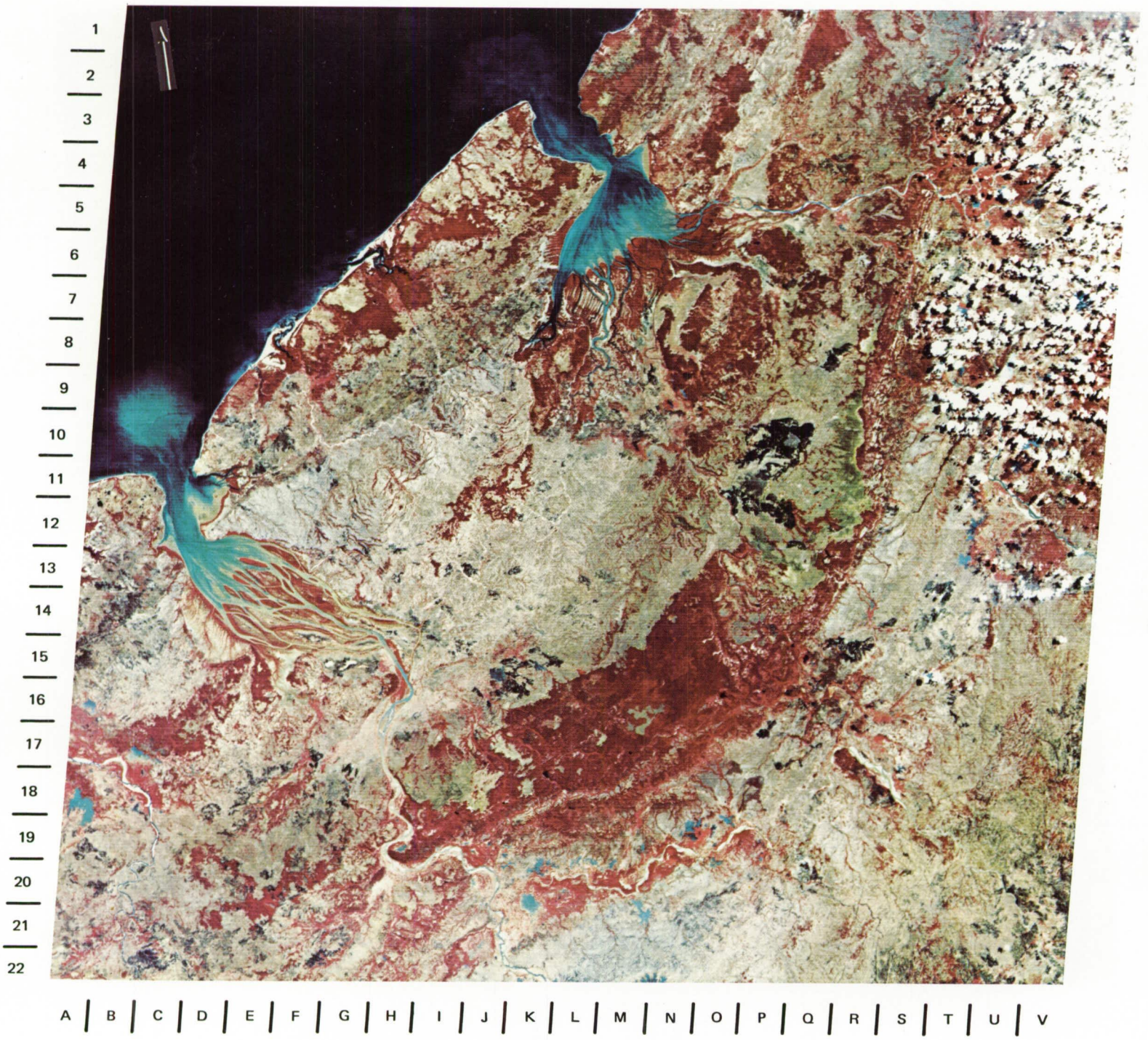


PLATE 358

MALAGASY REPUBLIC (MADAGASCAR): The island of Madagascar, constituting the Malagasy Republic, is the world's fourth largest island, having a length of nearly 1600 kilometers (1000 miles) and an average width of about 320 kilometers (200 miles). This image can thus show only a small part of it. The area covered is on the northwest coast, facing the Mozambique Channel, which separates the island from Africa by about 390 kilometers (240 miles). The port of Majunga is at *C*–11 on Bombetoka Bay. To the north is the Bay of the Mahajamba (*K*–4), named for one of the rivers that flows into it; another is the Sofia River (*N*–5; *T*–4). Both these rivers are discharging heavy sediment loads into the ocean. This is symptomatic of one of the island's problems, soil erosion caused by removal of the original forest cover and subsequent overgrazing. The braided stream patterns visible where the river splits into tributaries near the coast result from the sudden drop in velocity when the rivers reach the level plains with the high sediment load derived from the highlands to the east.

The area shown here is largely savanna, short grass with scattered trees. The chief agriculture is sugar growing and cattle raising. Malagasy is fortunate in having no tsetse flies.

The geology of this area is not well exposed because of vegetation and sedimentary cover. However, the curving feature extending from *S*–10 to *I*–21 marks the outcrop of the Karroo System so widespread in Africa. Here it consists of sedimentary rock dipping to the west. It has been down-faulted, perhaps as part of the process that formed the Mozambique Channel. West of the Karroo, the bedrock is Precambrian igneous and metamorphic types making up most of the island's area. Madagascar is composed of continental rocks of this kind, rather than the basalt or coral of which most oceanic islands consist. It is, in fact, a "micro-continent," in a geologic sense, perhaps one of the fragments of the former mega-continent of Gondwana that is thought to have broken up in the Mesozoic Era. *1074–06241;* October 5, 1972.

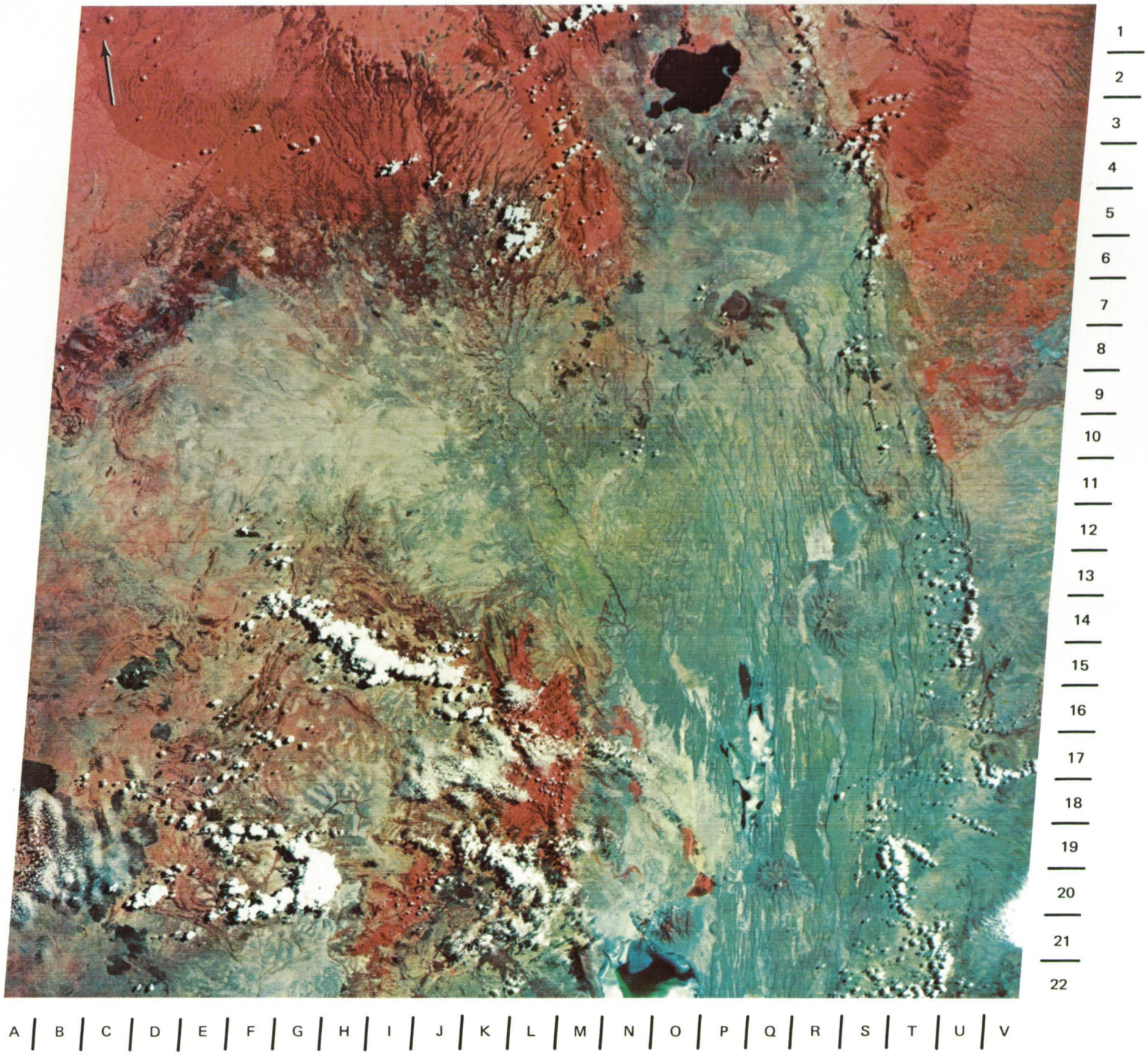


PLATE 359

NAIROBI: This image is undoubtedly one of the best orbital images ever obtained of the African rift system. It covers southern Kenya. The border with Tanzania, to the south, runs just north of Lake Natron (*N*–21). The rift itself extends from Lake Natron north to Lake Naivasha (*N*–2); the lake between them is Lake Magadi (*P*–17). The great relief of the area, more than a thousand meters (several thousand feet), accounts for the uneven distribution of vegetation, with cover ranging from near-desert to dense forest. Nairobi, the capital of Kenya, is at *V*–8. As suggested by the red color, the area north of Nairobi receives ample rain (on the order of 100 centimeters (40 inches) per year), and consequently has a fairly high population density. This is a major farming area, producing coffee and a variety of other crops. Note the cleared areas on the flanks of the Aberdare Mountains (*T*–4).

The rift itself dominates the image. Several major characteristics are well exhibited here. First, the asymmetric structure of the rift is evident; the eastern part is formed by a series of step faults, while the western part is the result of movement on a few large faults. This image should be compared with plate 366 showing the Afar Depression; the striking similarity between the step faults of each area suggests strongly that the origin of both structures is similar and that here is evident the result of incipient sea-floor spreading under continental crust. The great concentration of volcanic activity along this part of the rift is also obvious; note the many volcanoes, such as Longonot (*O*–4) and Suswa (*O*–7). The volcanic rocks of this area are notably rich in alkalis, and, in fact, the volcano Oldoinyo Lengai, just south of Lake Natron, in 1960 erupted lavas consisting chiefly of sodium and potassium carbonates. Lake Natron and Lake Magadi for this reason have great deposits of sodium carbonate, which are mined commercially. *1048–07172;* September 9, 1972.

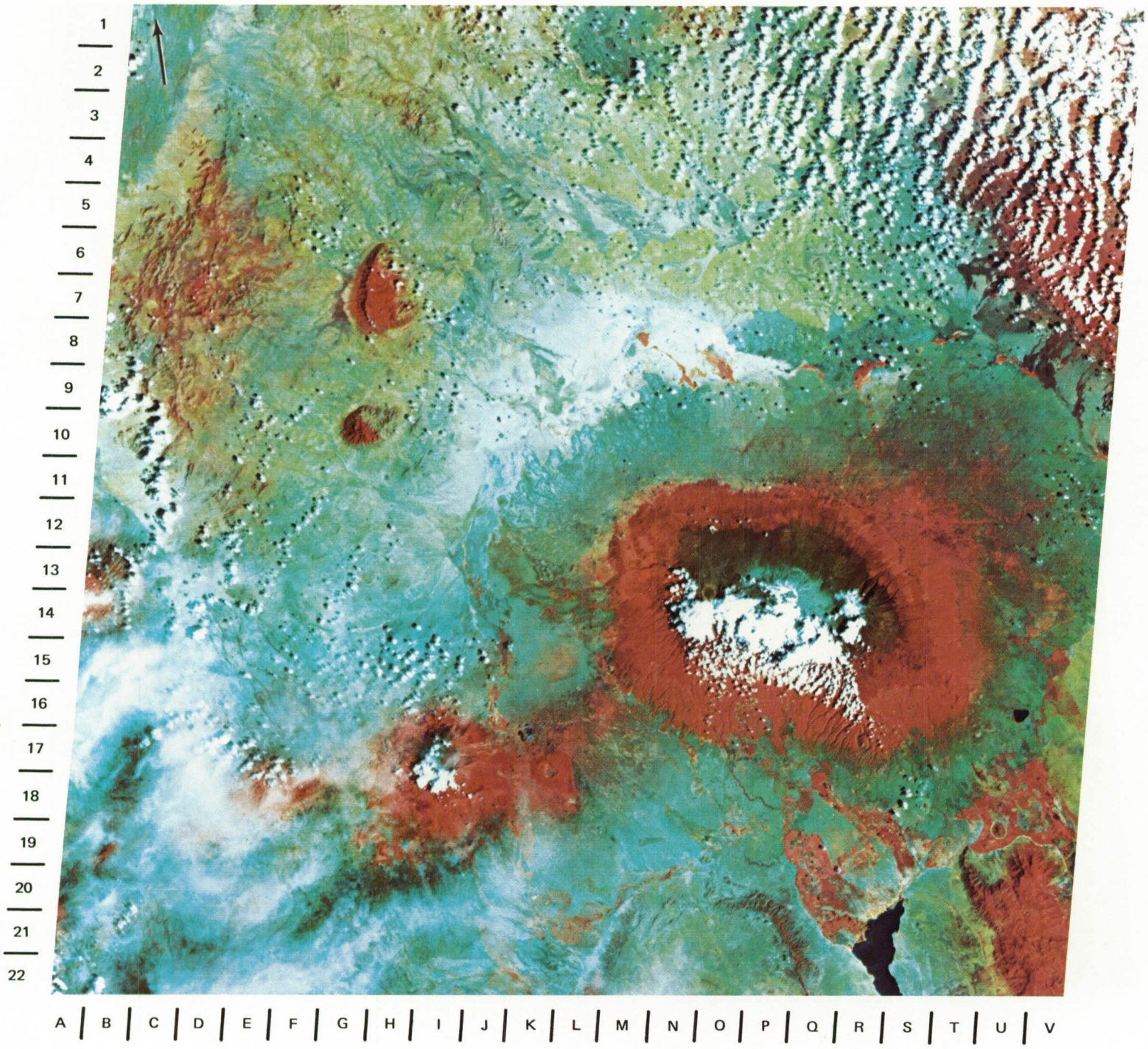
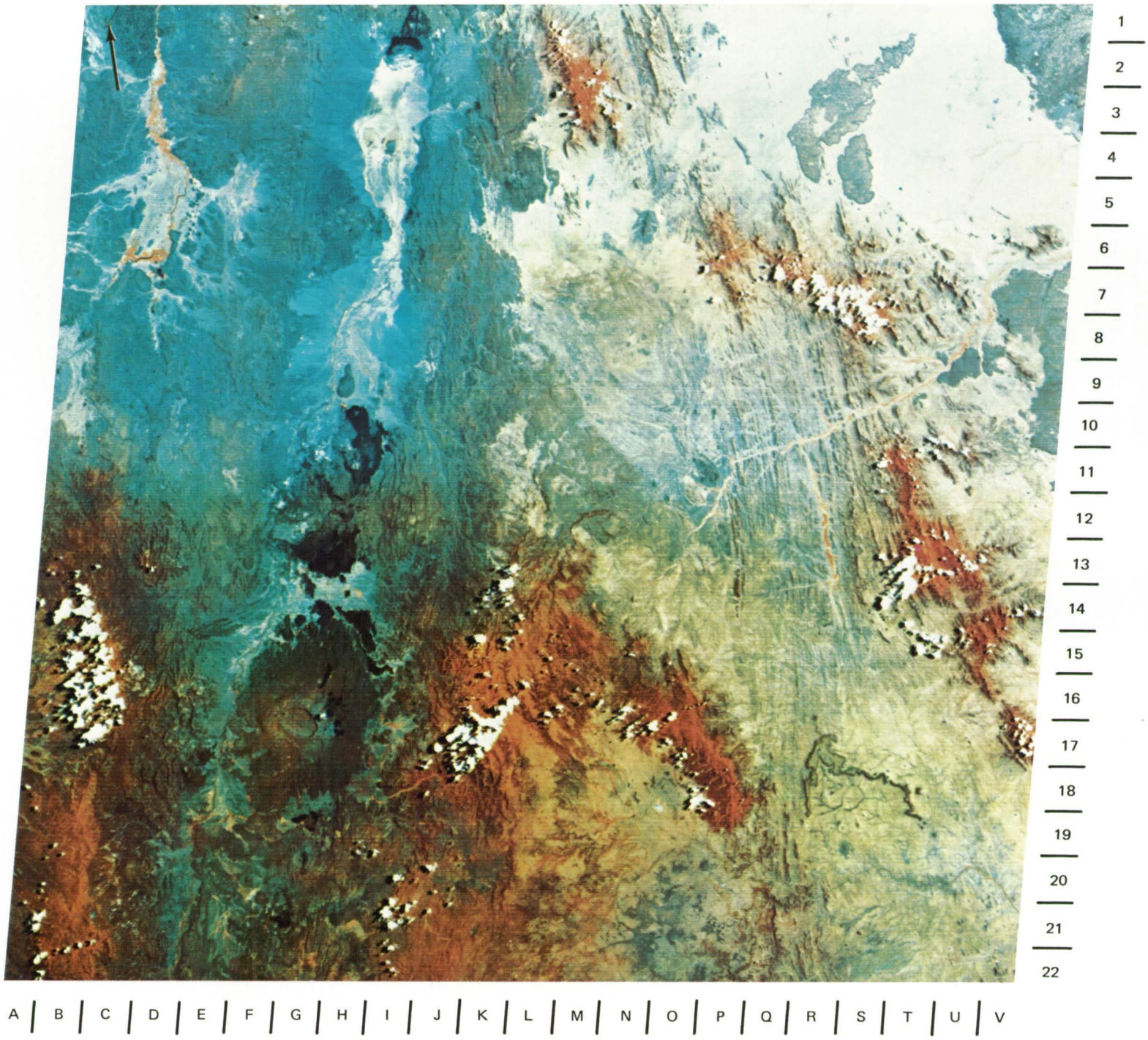


PLATE 360

MOUNT KILIMANJARO: Mount Kilimanjaro (*O*–14), with a height of 5894 meters (19 340 feet), is the highest point in Africa; it rises some 4600 meters (15 000 feet) above the surrounding countryside of Tanzania and Kenya. Consequently, in this scene an immense range of conditions can be seen, from the Nyiri Desert of southern Kenya, with dry lakes such as Lake Amboseli (*L*–8), to the glaciers of Kibo (*P*–13), one of the three eruptive centers of Mount Kilimanjaro. This image provides another striking example of the great influence elevation has on precipitation in East Africa; even the lower mountains, such as the Chyulu Range (*S*–4; *V*–7) of Kenya, are more vegetated than the adjacent lower areas. The concentric vegetation belts around Mount Kilimanjaro are, of course, the most conspicuous example; going inward (or upward), we see, successively, savanna, the cultivated zone (coffee and bananas), the montane forest, the heather zone, and the Alpine zone. On the very highest peaks, above 4900 meters (16 000 feet), there is no vegetation except for lichens and mosses. There are cultivated zones at lower elevations, using the water from Mount Kilimanjaro; note the farms of the Pangani River valley (*S*–21) around the town of Moshi (*P*–17) in northern Tanzania.

Like most Landsat images of East Africa, this one has many features of great geologic interest. Mount Kilimanjaro itself is an immense volcanic pile, measuring some 80 kilometers (50 miles) across (east to west), with three eruptive centers: Shira (*N*–13), Kibo (*P*–13), and Mawenzi (*Q*–13). The lavas are chiefly Pleistocene and Recent; the volcanoes were thought to be dormant, but vigorous fumarolic activity was discovered in Kibo Crater in 1933. As with most East African volcanic areas, Mount Kilimanjaro is characterized by notably alkalic lavas and pyroclastics, chiefly nephelinite, phonolite, and basalt. Mount Meru (*I*–17), 1391 meters (4565 feet) high, has similar rocks. The high alkali content of these lavas is probably caused by contamination of the mantle-derived magmas by sialic crustal rocks on their way to the surface. Note the closeness of the East African rift; the Ingito Hills (*B*–7) are on the edge of the rift. *1533–07091;* January 7, 1974.

PLATE 361



KENYA: South of Ethiopia, the rift system splits, one branch, the western, passing west of Lake Victoria and the eastern branch passing east of it. This image shows a northern segment of the East African Rift System in Kenya, some 320 kilometers (200 miles) north of Nairobi. The rift itself extends from *H*–1 to *F*–21; Lake Rudolf is just off the picture to the north. The Suguta River (*H*–3; *G*–8) occupies the floor of the rift valley, which is partly covered with salt deposits. Here as elsewhere the rift is bounded by highlands; Mount Nyiru (*K*–2) is 2800 meters (9200 feet) and Bukkol (*Q*–7) 2500 meters (8300 feet) high. The white area at *O*–1 to *S*–1 is the south end of the Chalbi Desert, into which flows the Milgris River (*O*–11 to *T*–8).

The strong influence of elevation on rainfall is obvious from the vegetation patterns; rainfall in this part of Kenya decreases strongly to the northeast, but even here high mountains have substantial vegetation, shown as red or pink. The area is very sparsely inhabited, chiefly because of lack of water.

The geologic features of this segment of the rift system are easily visible. The floor of the rift is occupied by volcanics, including the large volcanoes Pakka (*G*–16), and Silali (*G*–12), with a cumulative thickness of about 3000 meters (10 000 feet) (including sediments). The latter are as old as Miocene, implying that this part of the rift began to form in the Miocene Epoch. The volcanoes are Recent, and in fact slightly active. The irregular dark plateaus, such as those at *Q*–3 and *V*–8, are the remnants of lava flows flanking the rift valley. The Precambrian basement of the east margin of the rift is visible as north to south trending ridges (*M*–1; *R*–16), expressing the foliation of the crystalline rocks. The strong basement control of the much younger rift valley faults, visible at *H*–11 and elsewhere, is evident from the parallelism of these faults and the Precambrian structure. *1048–07163;* September 9, 1972.

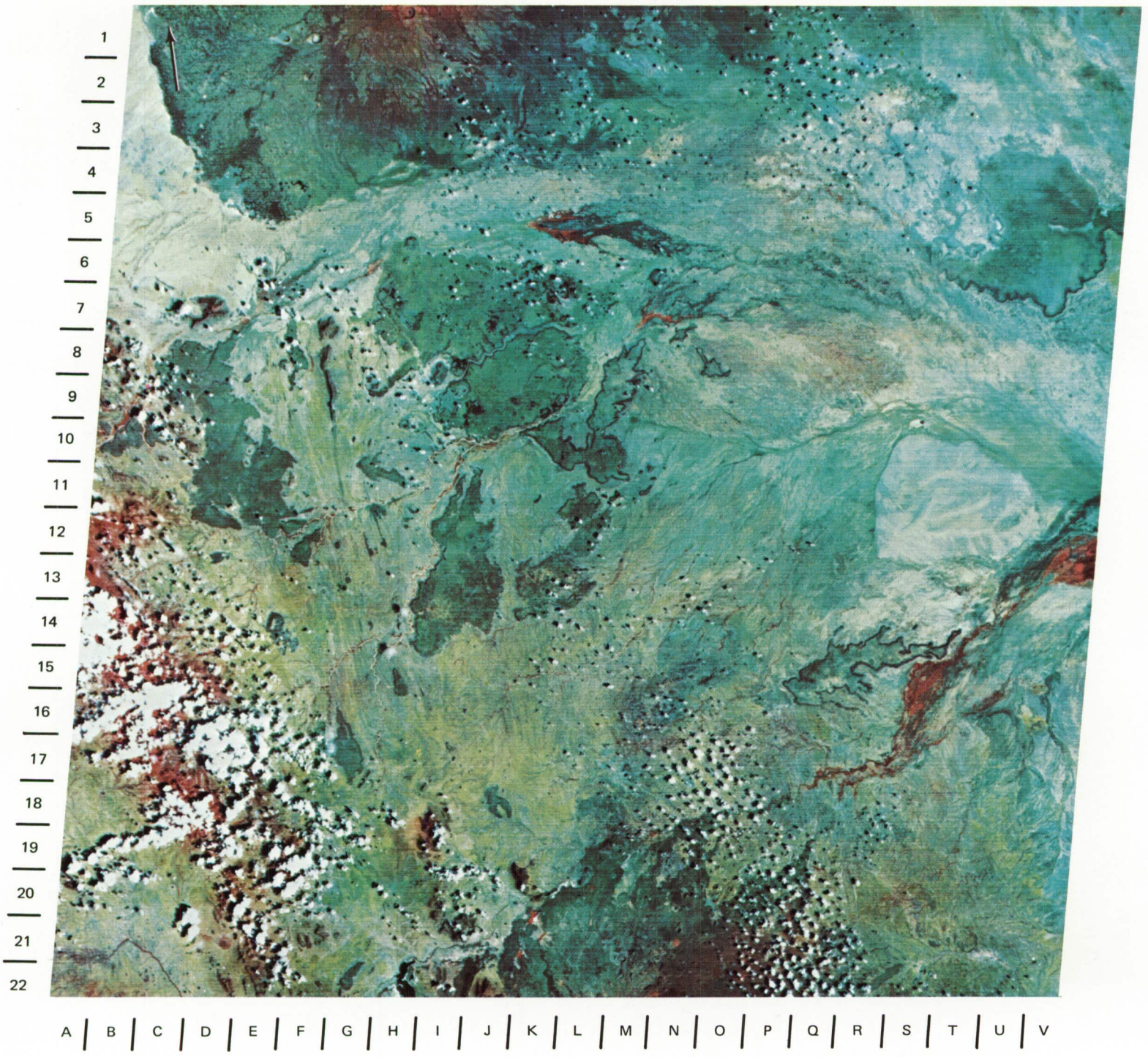
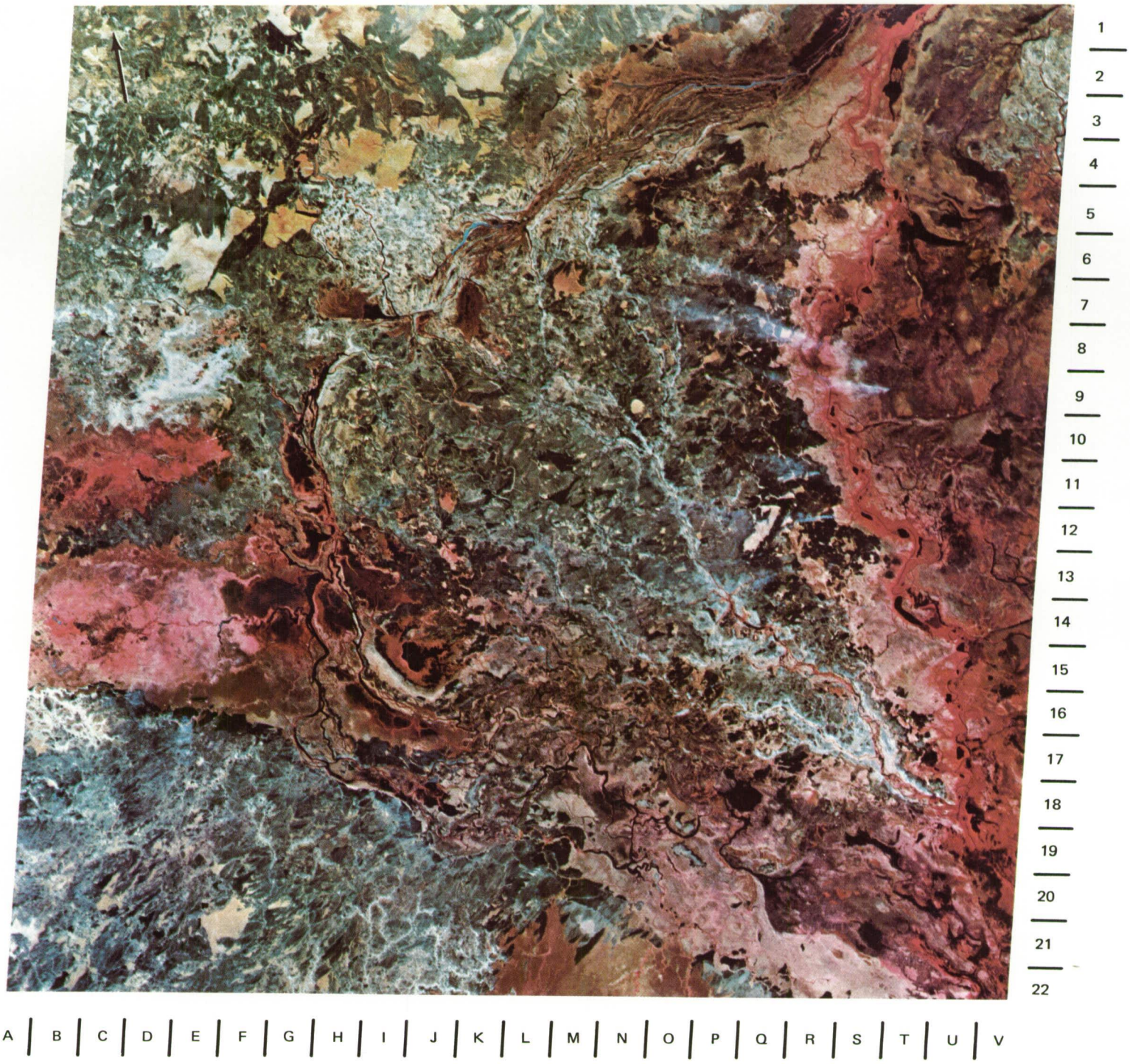


PLATE 362

KENYA: This image, overlapping the previous one (plate 361) along the left edge, shows the eastern flank of the rift valley in Kenya. The area covered is roughly between 900 and 1800 meters (3000 and 6000 feet) above sea level, but slopes off steadily to the east; it is intermediate between the Kenya Highlands *(left)* and the Intermediate Plateaus (*right*). Few well-defined landmarks are visible, the chief ones being Matthews Peak, nearly 2400 meters (8000 feet) high (*C*–16), a branch of the Dera River (*V*–10), and the Usaso Nyiro River (*T*–14). The flanks of large volcanoes just off the image are visible at *F*–1 and *O*–21. Mount Kenya is about 160 kilometers (100 miles) south of the center of the image. The area is now very sparsely inhabited, being very dry except for high elevations. It should be pointed out, however, that it *has* been inhabited for a long time; L. S. B. Leakey and his colleagues have made their famous discoveries of tool-using hominids living several million years ago just northwest of this area, along the shores of Lake Rudolf.

The geomorphology of this flank of the rift valley is of considerable interest. The irregular plateaus, such as those at *I*–8, *I*–13, and *U*–6, are erosional remnants of Cenozoic lava flows overlying Precambrian basement. According to L. C. King, the plateaus are part of the Gondwana (Jurassic) or Post-Gondwana (Cretaceous) erosion surfaces, and the Precambrian areas part of the African (Late Cenozoic) surface. This area furnished a good example of King's theory of "cymatogeny," or broad regional uplift, which he proposes initiates formation of low-relief surfaces by lateral erosion, or "pediplanation." King's concept is a controversial one that differs from classical geomorphology as developed by W. M. Davis by stressing lateral rather than vertical erosion. King considers the pediplane, or coalesced pediments, the ultimate erosion surface, rather than the peneplane. He also differs from many geomorphologists in assigning great age to some erosion surfaces; some geologists, such as Thornbury, feel that most of the world's landforms are no older than Mid-Cenozoic. Right or wrong, King's concepts are strikingly displayed in this image. *1173–07111;* January 12, 1973.

PLATE 363



THE HEADWATERS OF THE WHITE NILE: This colorful image is the first of an experimental line produced from a computer tape-controlled process developed at the Jet Propulsion Laboratory by F. Billingsley, A. F. H. Goetz, and others.

The region depicted is in the southern part of the Republic of the Sudan. Here the White Nile (*O*–8; *Q*–13), locally called the Bahr el Jebel, swings southward toward Lakes Albert and Victoria. The river is choked along its course with floating masses of vegetation or *sudd,* which jeopardize its navigability. The White Nile is joined by a major tributary, the Bahr el Ghazal (*L*–3), which itself branches into the Bahr el 'Arab (*F*–5), the Lob (*E*–6), and the Jur (*F*–4) further upstream. Because of low gradients, the streams in this region frequently spill out in floods into lowlands that are now perennial swamps. This condition is also the result of impermeable surface layers that make up the southern Clay Plains province of the Sudan. Soils in these areas are typically either heavy black (organic) clays (*K*–11) or light sandy soils (*F*–4). To the south is the higher Ironstone Plateau (*G*–19), an uplands underlain by an Archean basement complex of rocks now intensively weathered into lateritic ironstone soils.

The region is sporadically covered by savanna grasses with scattered acacias and other small trees, sections of thicker vegetation along waterways, and broad areas of treeless open country. Much deforestation is the consequence of the centuries-old practice of burning the vegetation by pastoral and farming tribes. Areas of burn are evident at *C*–5, *N*–18, and *D*–10. Several fires indicative of this practice can be seen at *P*–9. Most of the native population in this part of the Sudan is engaged in cattle raising, farming (millet and maize), and fishing. *1198–07494;* February 6, 1973.

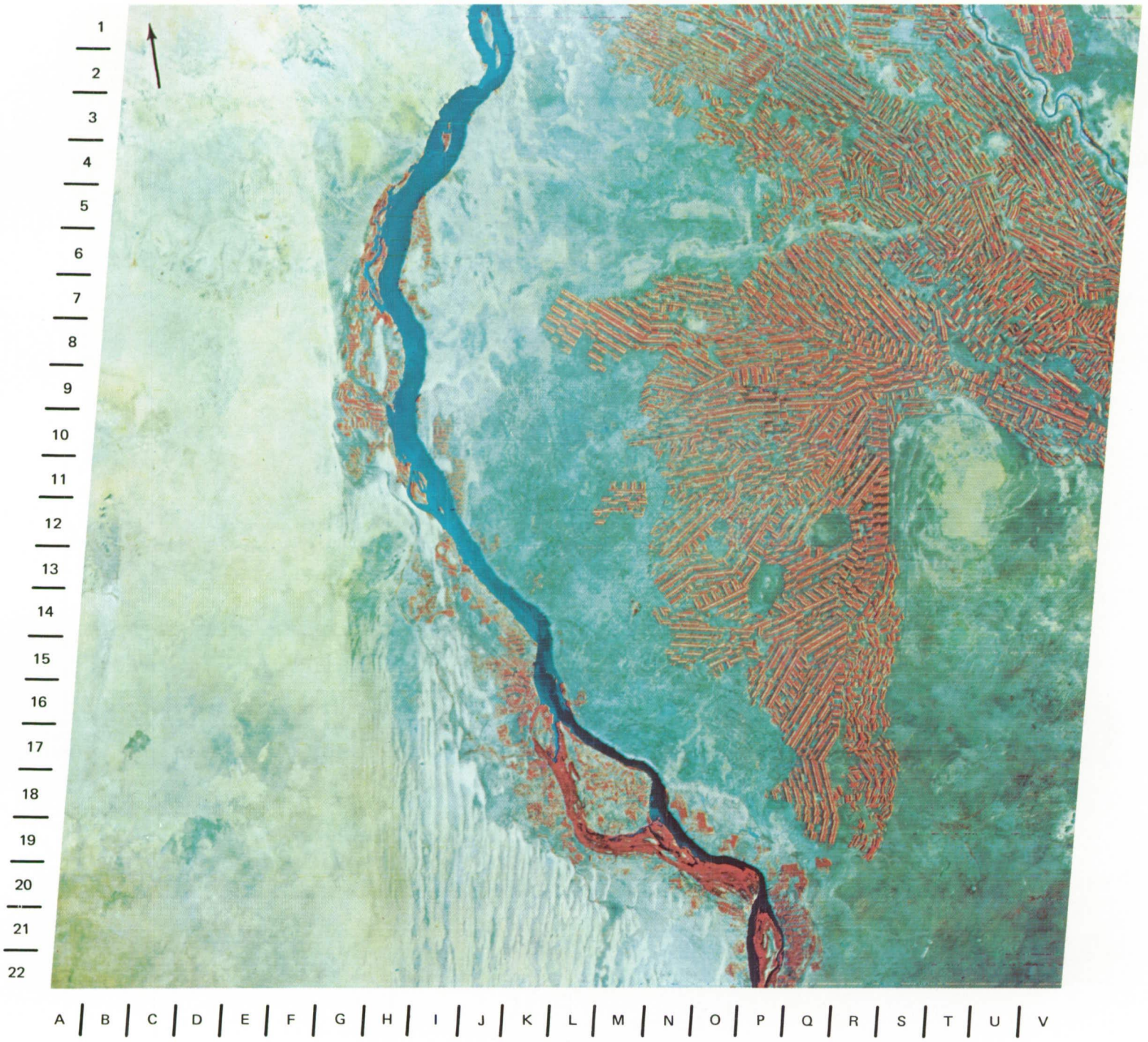


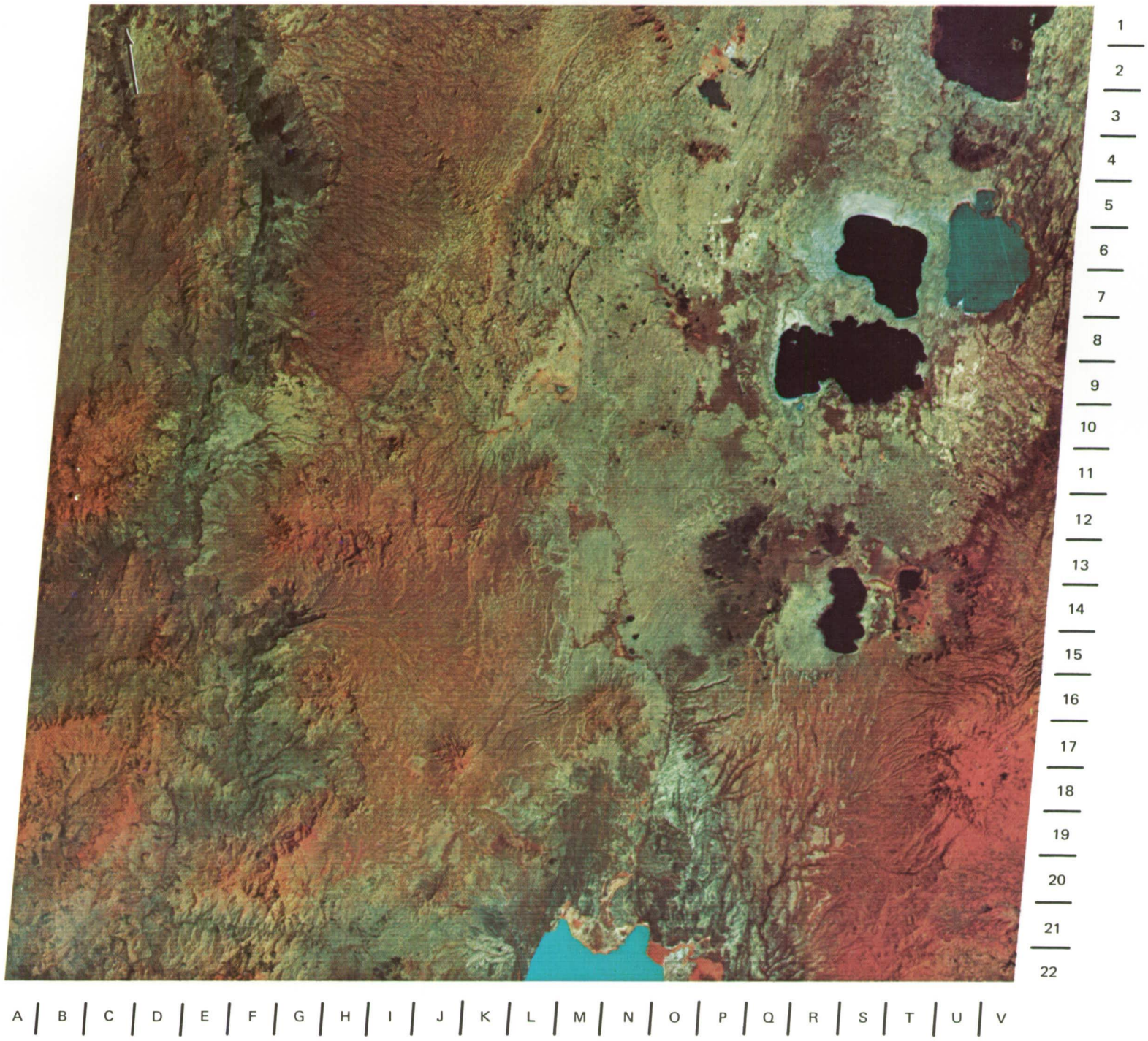
PLATE 364

SUDAN: South of Khartoum, in the Republic of the Sudan, the Nile has two branches. This image covers part of the White Nile—the western branch—and the city of Ed Dueim (barely visible at *J*–14). The region, in general, is the extremely level clay plains section of the Sudan, the name coming from the clay and silt alluvium deposited by the White Nile. The area is dry, receiving only about 20 centimeters (8 inches) of rain per year.

The striking pattern in the right half of the scene is that of two large irrigated farming areas. At upper right (*O*–1 to *U*–8) is the section developed under the Gezira Scheme, developed after the Sennar Dam was built on the Blue Nile in 1925. The section southwest of *Q*–7 is the Manaqil Extension, brought under irrigation in 1962. These areas are used for growing long-staple cotton, which is the main export from Sudan. The venture has proven highly successful to date, and further extensions are planned. Crop rotation is regularly carried out in these areas, with a given plot left fallow, or used for another crop such as millet, to help prevent plant diseases. The light part of each plot of land visible in the Landsat image probably represents a fallow surface, traditionally kept to about half the area being farmed.

The general dryness of the region is emphasized by the sand dunes south of the Nile (*J*–20). *1107–07421;* November 7, 1972.

PLATE 365



ETHIOPIA: This image covers central Ethiopia, with the center of the scene being about 120 kilometers (75 miles) due south of Addis Ababa. The East African Rift Valley, here labeled the Wonii fault belt, trends south from the upper right corner. The several lakes in the rift are Zwai (*T*–1), Langana (*T*–6), Shala (*R*–8), Hora Abyata (*R*–6), Awusa (*R*–14), and Abaya (*M*–21). There are several towns in the area covered, but none big enough to be visible, reflecting the fact that over 90 percent of the population lives in rural areas.

The area covered by the image has about 2100 meters (7000 feet) of relief between the floor of the rift and the surrounding highlands. The mountains at lower right are up to 3300 meters (10 900 feet) high and at left up to 2700 meters (8900 feet) high. There is a corresponding range of climate; the highlands in particular receive 100 centimeters (40 inches) of rain per year and the valley only about 50 centimeters (20 inches). As this Landsat image shows, there is a great difference in vegetation, ranging from Afro-Alpine forest to savanna. About 80 percent of the population lives in the highlands, living by farming and cattle raising. Grains are the chief crop, with coffee, bananas, and rubber also being grown. The term "coffee" is thought to be derived from the name of the Ethiopian province of Kefa, just southwest of this area.

The geologic structure of the rift valley is fairly well shown here. Some of the bounding faults are visible at *Q*–17 and *K*–5. The rift is characterized in this area by widespread volcanism; individual volcanoes are visible at *H*–11 and *M*–16. The highlands on both sides of the rift are underlain by lava flows, chiefly alkaline or intermediate basalts. The highlands are intricately incised by dendritic canyons, adding to the difficulties of ground transportation. To a geologist, this is a youthful landscape, one in which erosional dissection following uplift is far from complete. *1192–07153;* January 31, 1973.

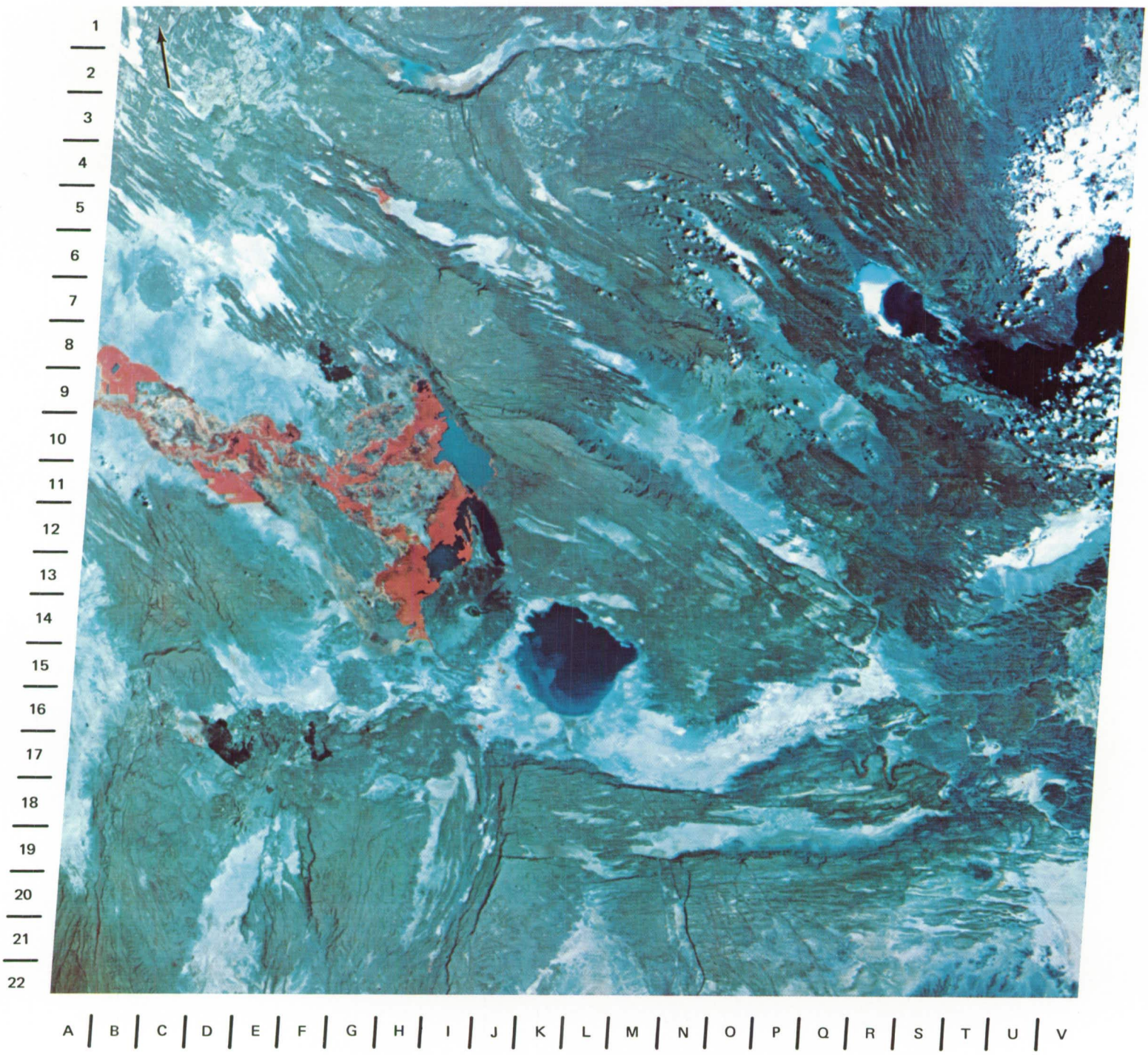
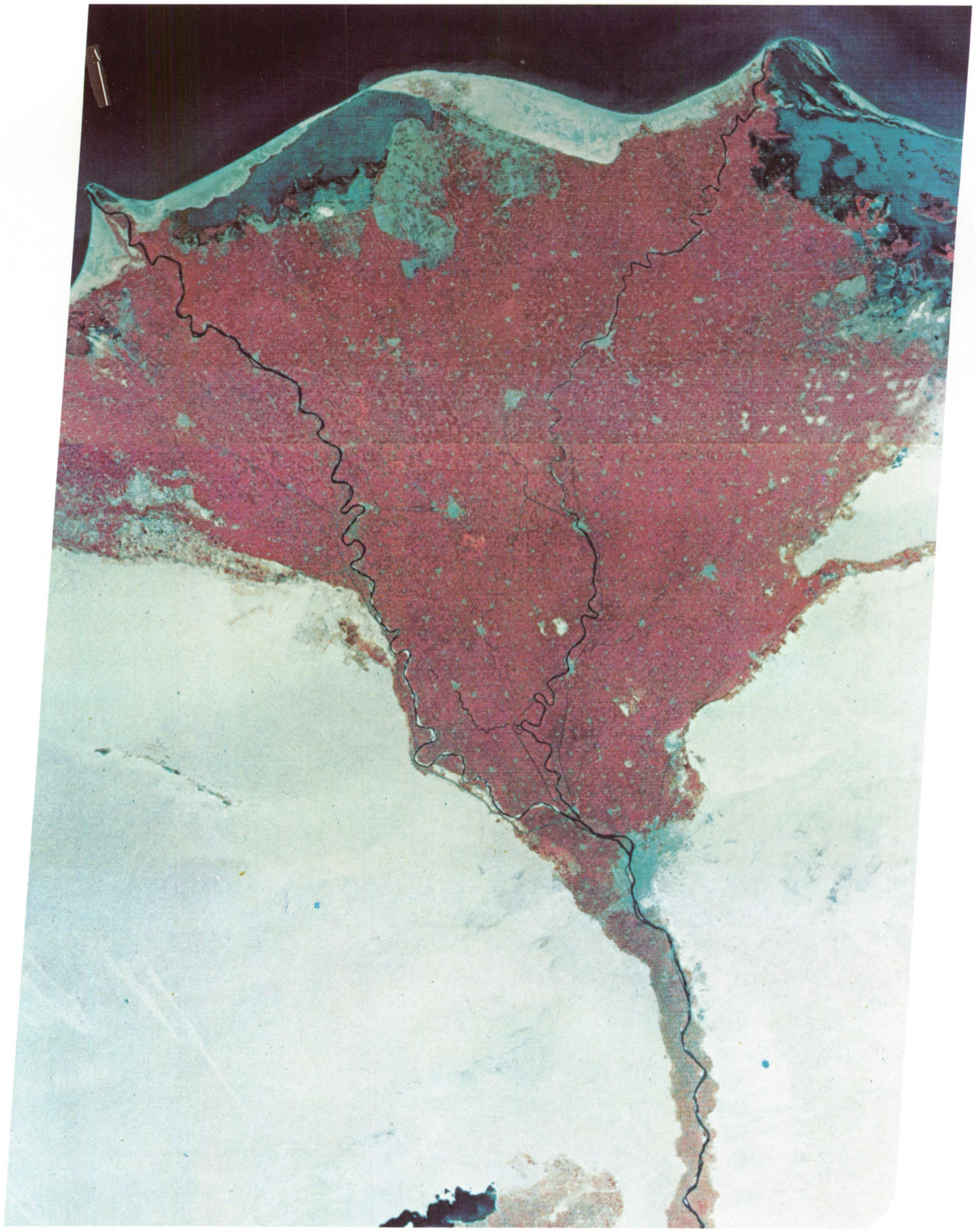


PLATE 366

AFAR DEPRESSION: So alien is the Afar Depression of Ethiopia, that this image would hardly be identified as a terrestrial landscape without the annotated information. Shown here is a triple junction of the world rift system: the intersection of rifts forming the Red Sea, the Gulf of Aden, and the East African Rift Valleys. (See plate 365.) Most of the area is in Ethiopia, but a triangular sector with the western apex at Lake Abbe (*K*–15) is the French Territory of the Afars and the Issas (formerly French Somaliland). Other landmarks are Lake Gamarri (*I*–10), the Gulf of Tadjoura (*V*–7), and Lake Assal (*R*–7). The land is an extremely harsh one, consisting of bare volcanic rock and salt flats; nevertheless it is inhabited by the Danakil people. They subsist by herding goats, sheep, cattle, and camels, and in some areas by farming. Salt is also collected for sale elsewhere in North Africa. The Awash River (*A*–9; *H*–10) region is used for growing cotton, corn, and sesame, and plans are underway to further harness the river for irrigation. The village of Aisata is at *G*–11 but is not visible.

To the geologist, this image shows an area of incipient crustal fragmentation and perhaps continental drift. The linear ridges cutting the terrain are fault scarps, produced by tension perpendicular to the scarps. This faulting is associated with extrusion of basaltic lavas from fissures and individual vents. From a broader viewpoint, the Afar Depression represents an area in which the process of sea-floor spreading is taking place on land; that is, much of this area is exposed sea floor. Similar features are visible in central Iceland (plates 219 and 220), which sits astride the Mid-Atlantic Ridge, and in Kenya (plates 361 and 362), which includes part of the East African Rift System. There is even some similarity between the faults of the Afar Depression and those of southern Oregon (plate 111). This is probably not coincidental, because that part of Oregon is at the north end of the Basin and Range province, itself thought to be caused by extension of the East Pacific Rise under the North American continent. *1100–07024;* October 31, 1972.

PLATE 367



NILE DELTA: One of the most striking space views of Africa is the Nile Delta, which, because of its intense cultivation, stands out sharply from the surrounding desert. Gemini 4 astronaut James McDivitt momentarily mistook the delta for "the world's biggest lava flow" on first seeing it; to the eye, of course, it appears dark blue-green, not red. This mosaic shows the heartland of Egypt. Cairo, with a population of over 4 million, is the biggest city in all Africa. (See plate 368.) The Nile divides into two branches above Cairo, the Rosetta Nile and the Damietta Nile. At the bottom lies the Birket Qârûn, a lake 45 meters (148 feet) below sea level, occupying the El Faiyûm depression. The adjacent area is under cultivation. The Faiyûm Depression is thought to have formed by ablation, or wind erosion; note the sand dunes that give an indication of the prevailing wind.

The land use pattern of the Nile Delta is an interesting one. The high population density is apparent; note the many small blue

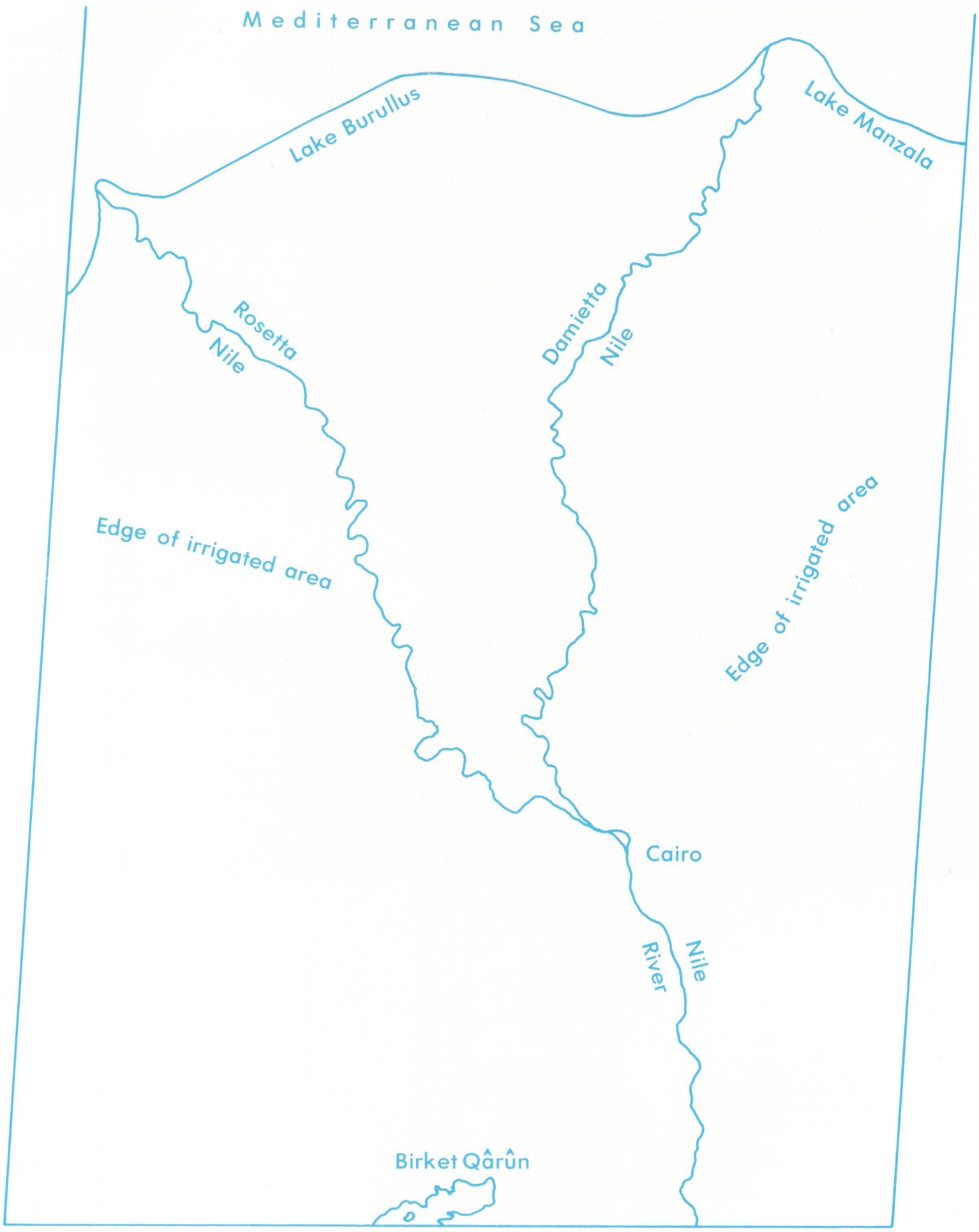
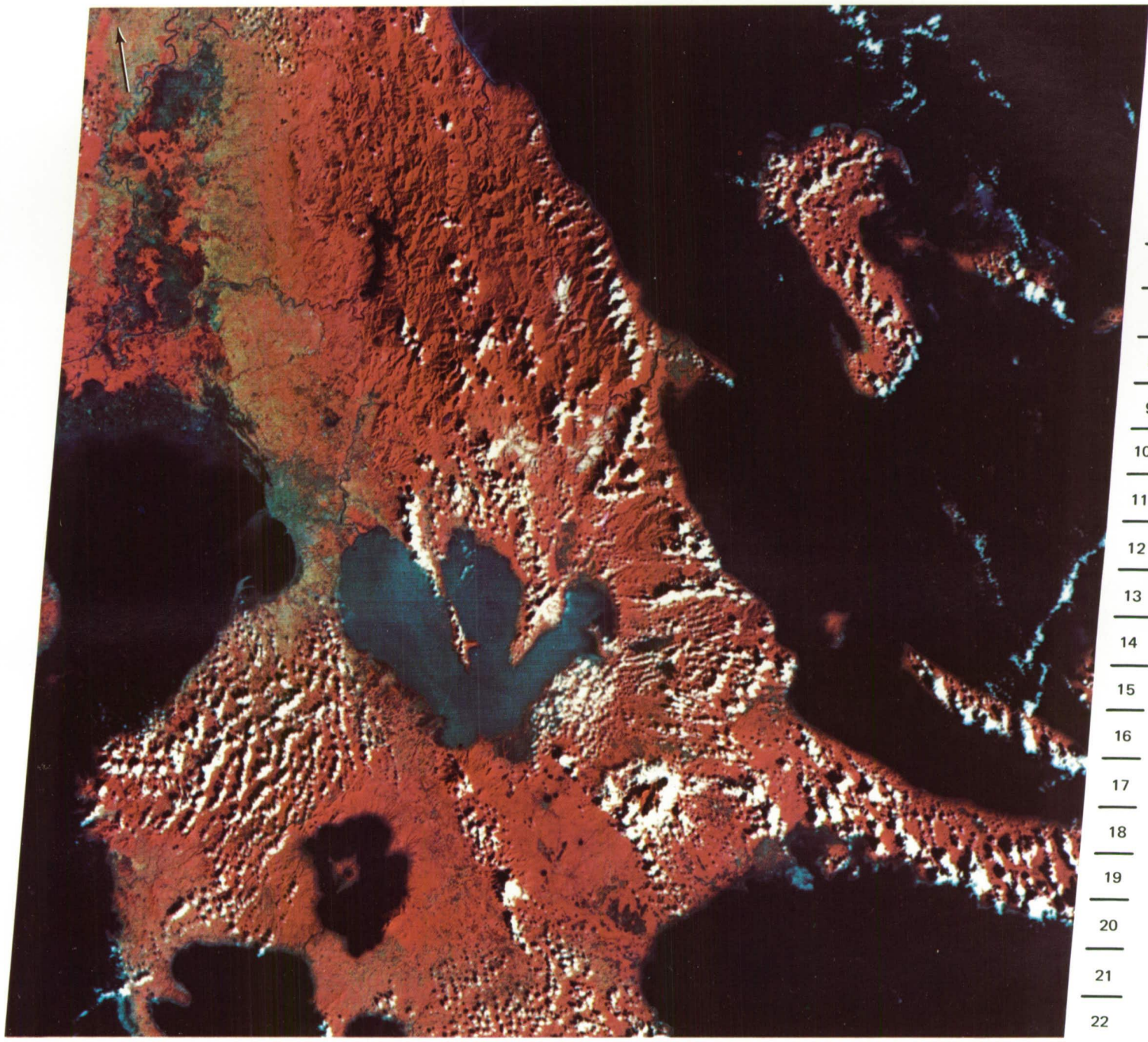


PLATE 368

patches marking the smaller towns and villages. The main crop in this part of the delta is cotton, accounting for about one quarter of the total crop area. Corn and clover follow in importance. Because rainfall is well under 25 centimeters (10 inches) per year in this area, farming is entirely dependent on irrigation, as it has been for millennia. Several of the larger canals can be seen in the mosaic. Formerly, the natural flooding of the Nile fertilized fields, but the construction of the Aswan Dam upstream has stopped that; whether artificial fertilizers can make up the loss remains to be seen.

The direction of longshore drift in the Mediterranean Sea from west to east is indicated by the sediment plumes from the two mouths of the Nile and from Lake Burullus, a brackish lagoon bordered by sand dunes and salt marshes. A similar lagoon, Lake Manzala, is to the east.

PLATE 369



SOUTHERN LUZON ISLAND, THE PHILIPPINES: Manila (*E*–11), the largest city of the Philippines, and the adjacent capital of Quezon City lie just north of a narrow strip separating Manila Bay (*C*–12) from the now landlocked Laguna de Bay (*J*–15), a former extension of the marine embayment. At the entrance to Manila Bay, just beyond the tip of the Bataan Peninsula (*A*–13), is the historic island of Corregidor (*A*–15), the last outpost of the U.S. armed forces during the invasion of the Philippines in World War II. Both the bay and the flat lowlands to the north are part of a fault-block subsidence lying between the volcanic Cabusilian and Mariveles Mountains on the Bataan Peninsula and the uplifted Mesozoic limestones of the Sierra Madre Mingan (*I*–5) to the east. In the south, an older Tertiary volcanic terrain (*N*–13) gives way to younger volcanoes. The cloud-covered 2200-meter (7100-foot) high Mount Banabas (*L*–17) is inactive. Lake Taal (*G*–19) occupies a volcanic caldera containing a small volcano (*F*–19) that erupted as recently as 1965.

Except where prevented by swamps (*B*–9; *C*–6), paddy rice and sugarcane are the principal plantings in the lowlands north of Manila. The Laguna de Bay varies greatly in water level in response to monsoon rains; rice is grown along its shores in the dry season. Coconut and palm trees are often planted in back of mangroves near the coast (*O*–18).

Coral reefs fringe parts of the coast and islands such as the Potillo Islands (*P*–5). *1153–01463;* December 23, 1972.

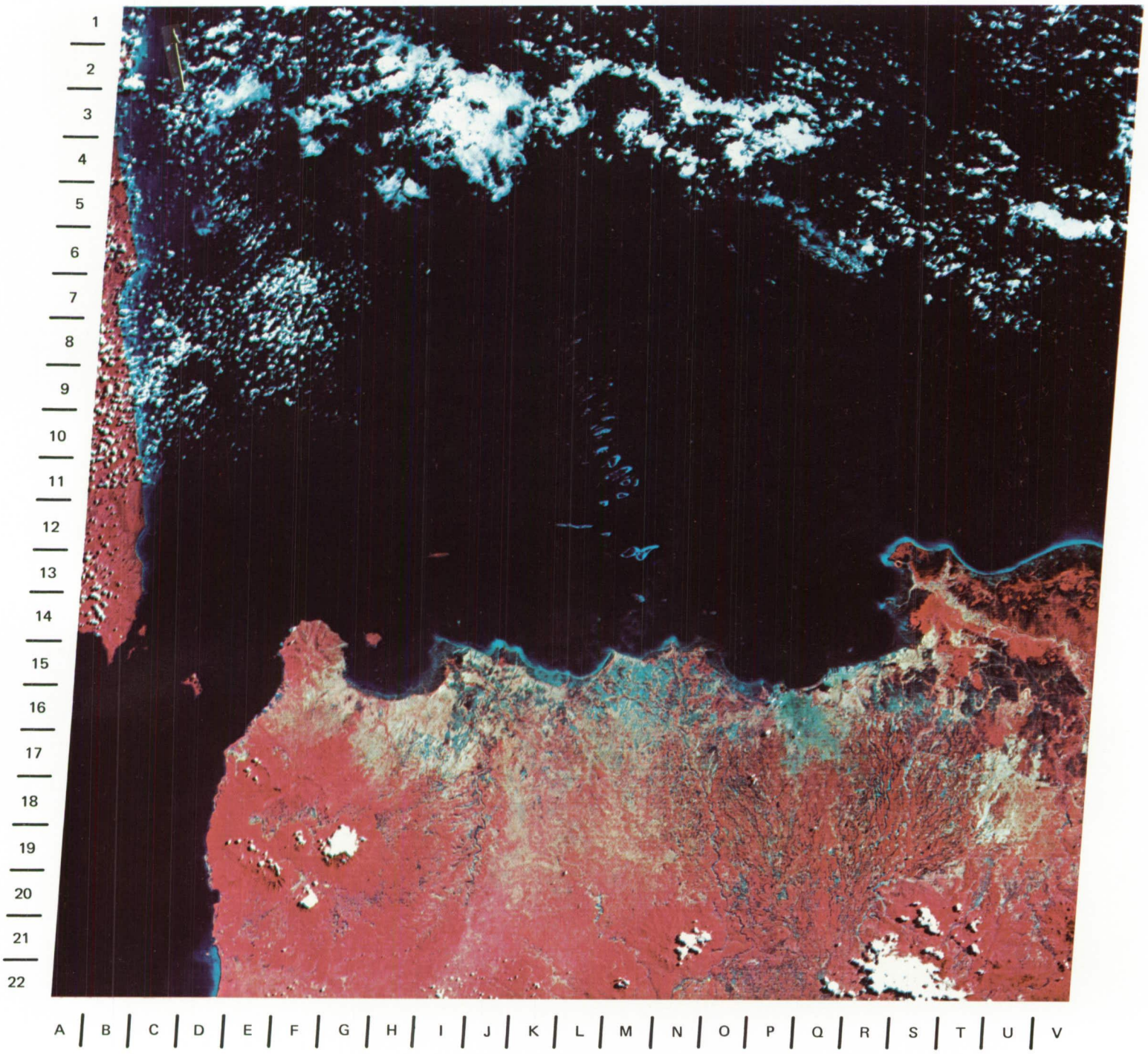
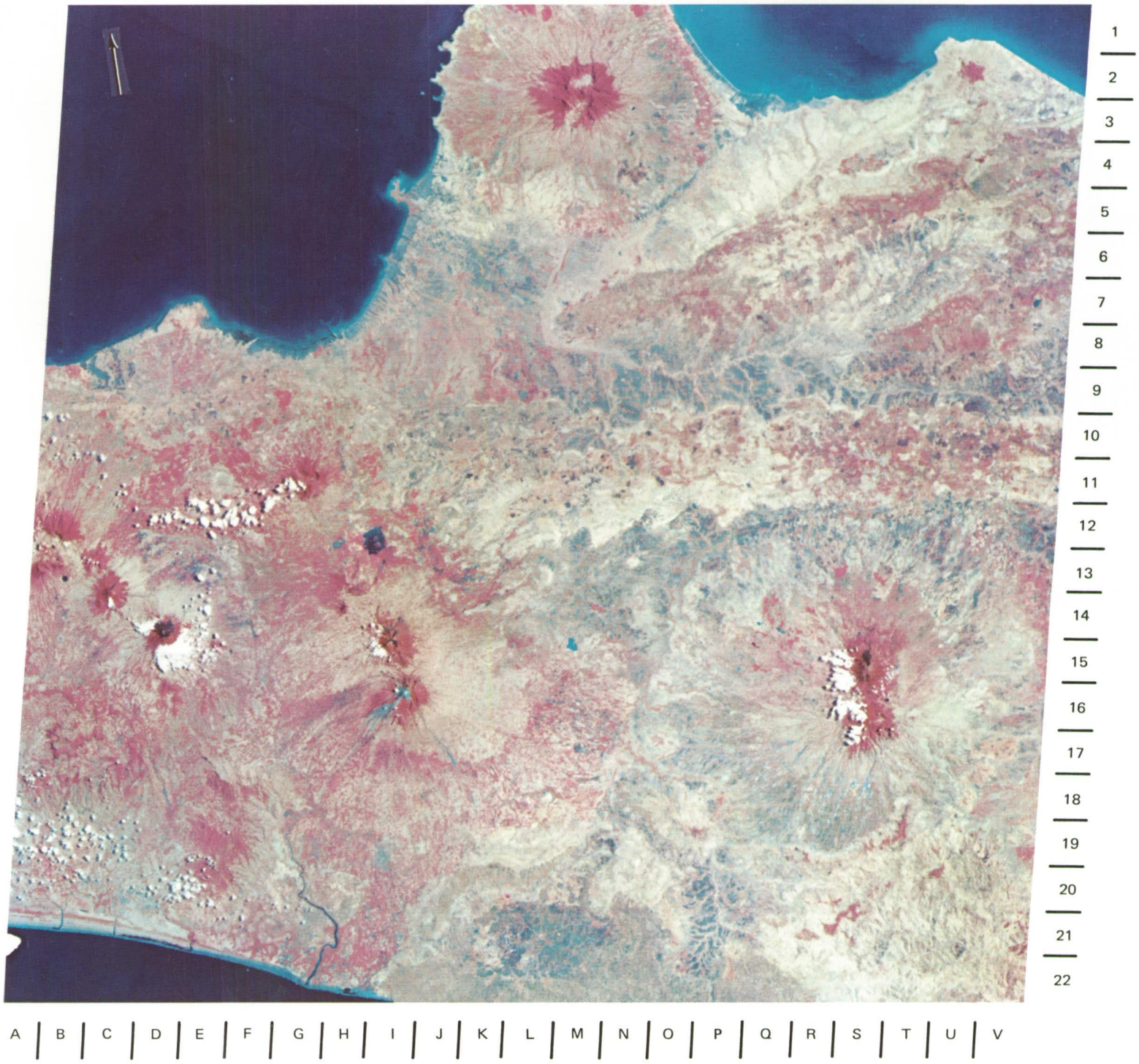


PLATE 370

WESTERN JAVA, INDONESIA: The northwest corner of Java, a slice of the easternmost coast of Sumatra (*A*–12), and the Java Sea appear in this image. Djakarta (*P*–16), the capital of Indonesia, a city with one of the highest population densities in the world, lies on a broad bay along the coast; note the large piers (*Q*–15) along its harbor. East of the town is a series of mangrove swamps (*T*–13; *T*–15) on either side of the Tarum River (*U*–16). To the west, the bluish area (*L*–15) is newly emerged land now largely used as rice paddies. Along this coast are tambaks or fishponds (*J*–15) made up of a series of connected basins that fill with tidal waters. South of the city is a great network of small streams flowing on an alluvial fan developed by drainage from the volcanic highlands further south. This area, which includes the university city of Bogor (*Q*–21), is a rich agricultural region supporting small plots of paddy (bluish patches) and terrace rice, tapioca, bananas, rubber and kapok trees, sugar, tea shrubs, and tobacco. The highlands are heavily forested (dark red), especially around the clusters of dormant volcanoes (*E*–19; *F*–15; *N*–21) of Quaternary age. Several volcanoes, just off the image, are still active. Lahars (*O*–19), mudflows of volcanic ash and debris, have spilled out over the valley east of the Udjung River (*I*–18). *1394–02313;* August 21, 1973.

PLATE 371



CENTRAL JAVA: Great stratovolcano cones, with broad aprons of ash and mudflow deposits, cover much of the middle region of the Indonesian island of Java. Among still active volcanoes are Sundoro (*B*–13), Sunbing (*C*–14), Merbabu (*H*–14), and Lawa (*S*–15). The volcano on the north coast (*L*–2) is now dormant. The richly fertile soils derived from this volcanic ash are used for dry rice along the volcanic slopes (*G*–17). Paddy rice, showing in this image as bluish, is grown in the lowlands that contain soils derived from Miocene sandstones and limestones and Quaternary alluvial deposits or in "polders," land reclaimed by the Dutch by draining coastal swamps (*J*–6; *M*–20). Other principal crops produced in this area are sugar along the north coast, tapioca, chocolate, and maize. Tea plants and rubber trees are found along lower slopes. Coconut trees are grown in plantations along the coast, such as along the old beach ridges (*A*–20) evident on the southern shores. Because fishing is a prime source of food, manmade fishponds are cultivated mainly along the north coast of the Java Sea. Urban centers in this densely populated part of Java are Semarang (*G*–8), Surakarta (*N*–15), and Jogjakarta (*H*–19). *1067–02145;* September 28, 1972.

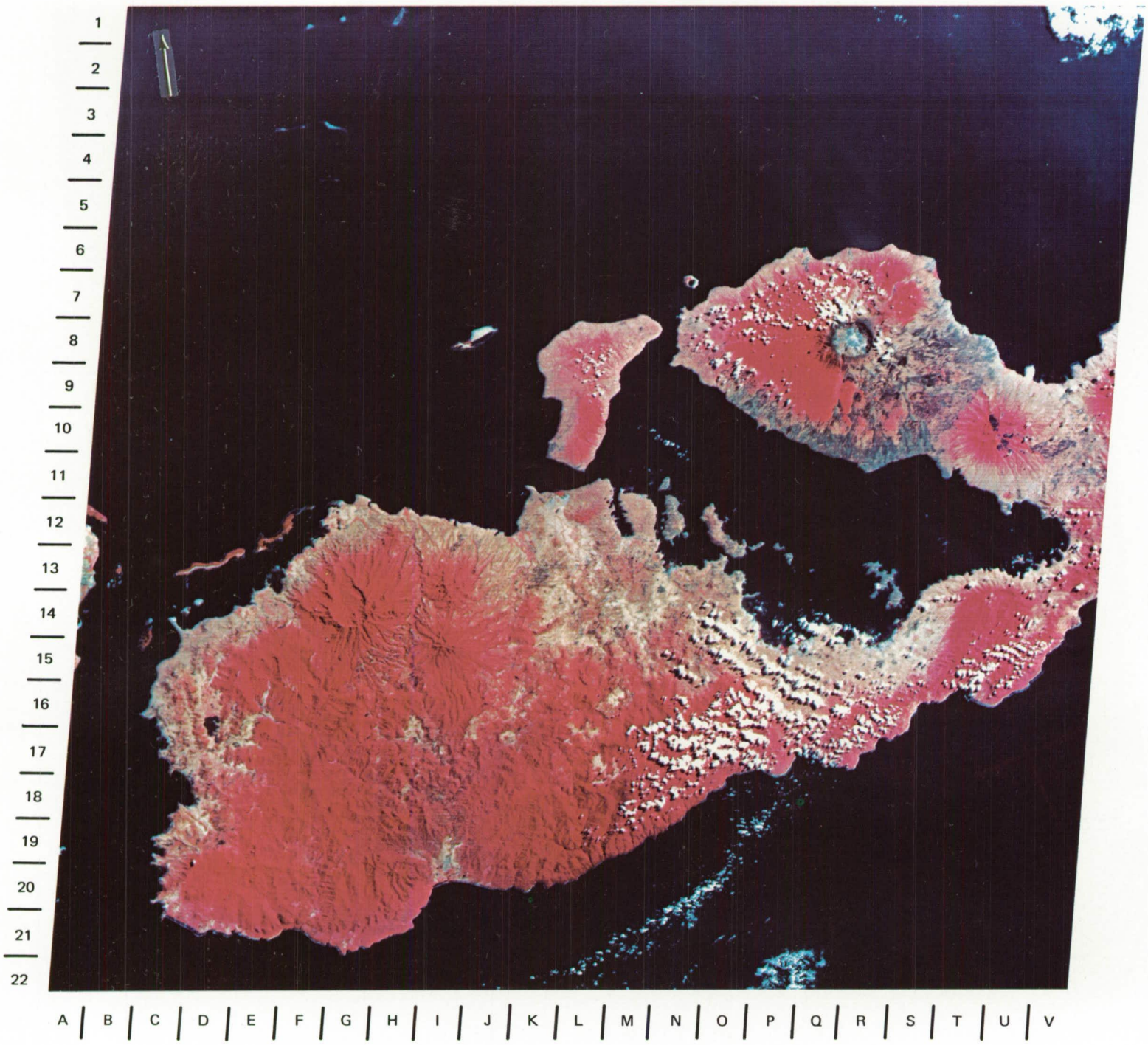
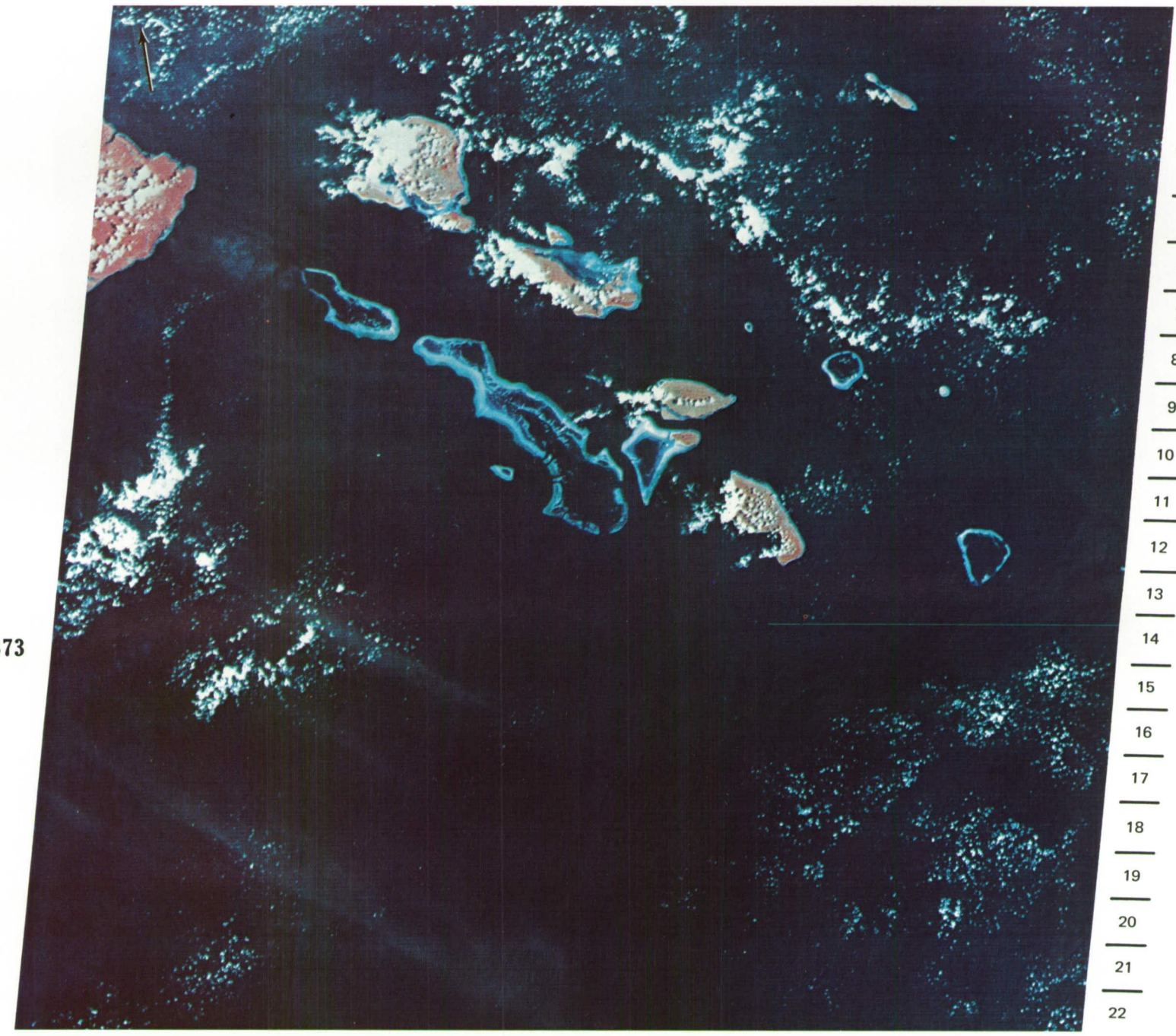


PLATE 372

SUMBAWA, INDONESIA: This heavily forested island lies to the east of Bali in the Flores Sea. The majority of its inhabitants live along the north coast where they grow some rice, sugarcane, maize, and tobacco. Fishing is another means of livelihood, especially in the Bay of Saleh (*O*–11) sheltered by Mojo Island (*K*–8). As with most of the islands in the Indonesian archipelago, Sumbawa is dotted with active and extinct volcanic cones. Recent eruptions have occurred at Tambora (*P*–8), whose central caldera rises to 2755 meters (9040 feet), from which older lava flows are visible where vegetation has not yet taken hold. The remnants of the Sangenes caldera (*E*–13), some 1900 meters (6300 feet) high, have since been fully encroached upon by jungle vegetation. Coral reef islands (*B*–13; *H*–8) are evident off the northern coast, and barrier reefs (*U*–14) are beginning to form in places along the southern coast. *1044–01464;* September 5, 1972.

PLATE 373



ATOLLS OF THE BANDA SEA: The Tukangbese group of islands lie about 80 kilometers (50 miles) southeast of Bulung (*A*–4), one of the islands of the main Celebes group in the Republic of Indonesia. The islands of Wangiwangi (*G*–4), Kaledupa (*J*–6), Tomea (*M*–8), Binongko (*O*–11), and Anano (*Q*–2) are land masses rising above the sea. Wangiwangi itself has a peak (cloud covered) more than 240 meters (800 feet) above sea level. Each of these islands is fringed with coral reefs. Coral reefs have also developed over shallow, but now submerged islands. These are classic examples of atolls—barrier reefs enclosing central lagoons—as evidenced by the more or less circular islands at *P*–8 and *S*–12. Other atolls (*F*–7; *J*–9; *L*–10) are more irregular in outline. *1112–01234;* November 12, 1972.

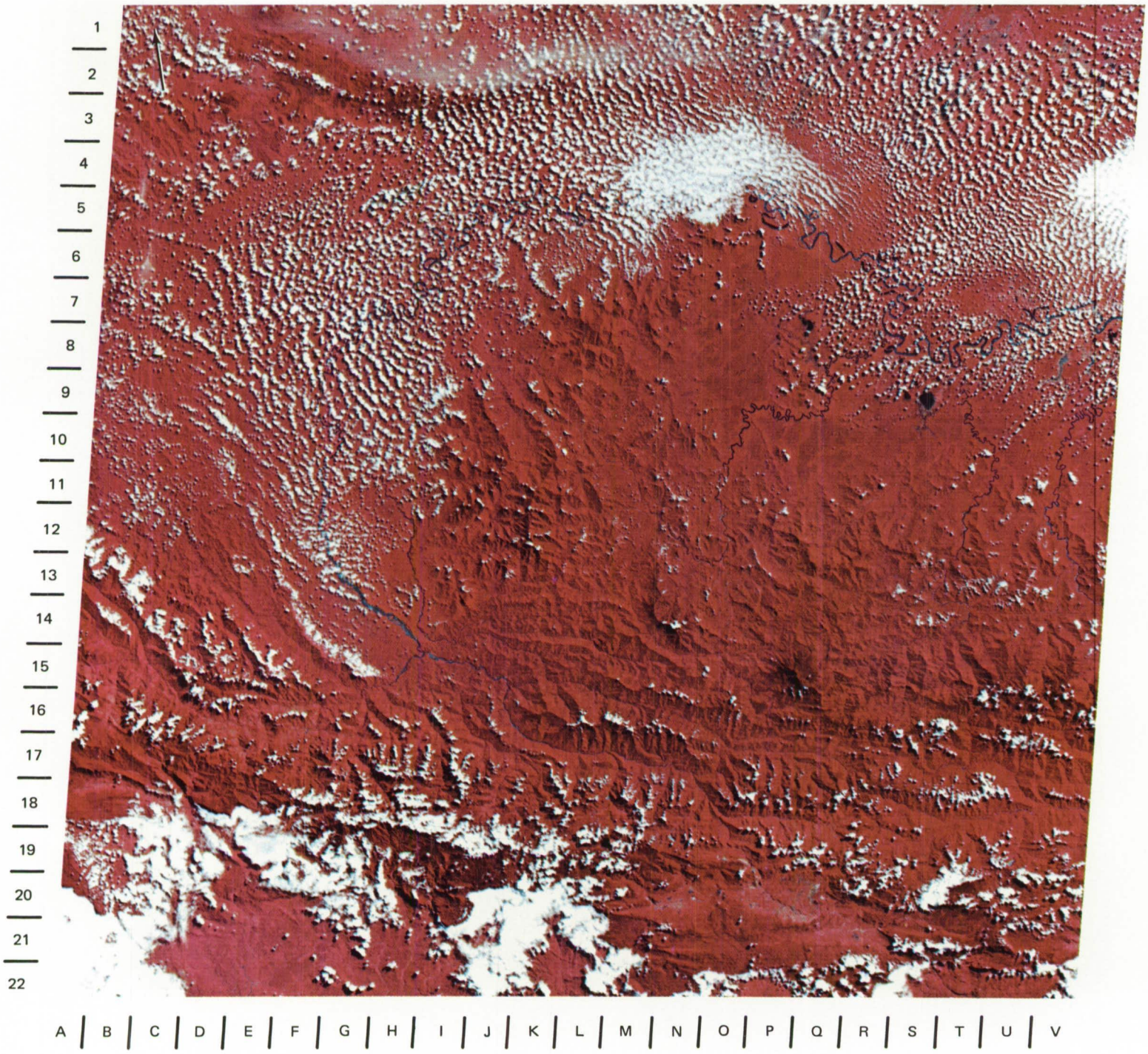


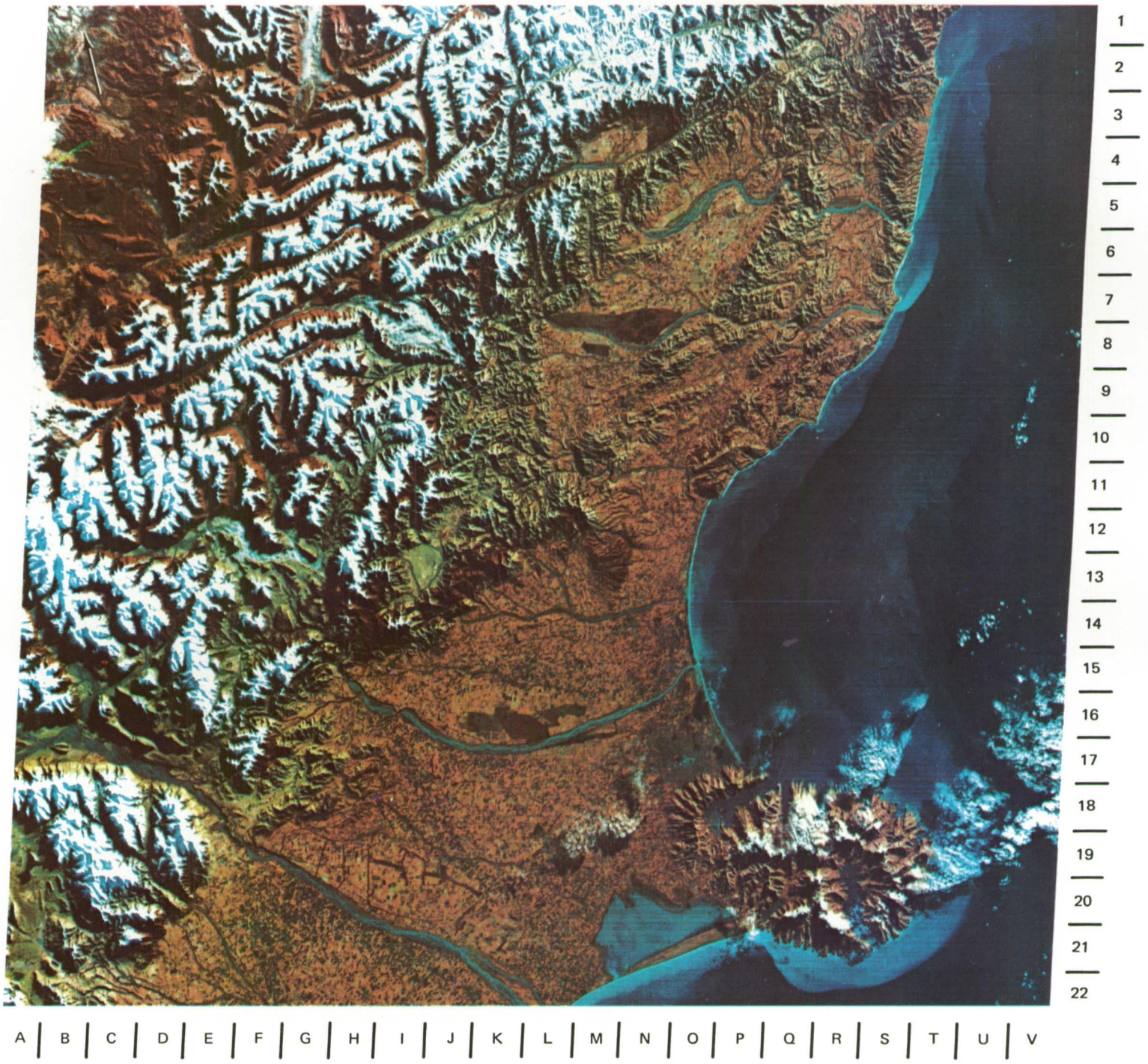
PLATE 374

CENTRAL NEW GUINEA: After World War II, the vast island of New Guinea was reorganized into three political units. The western half, once administered by the Dutch, is now West Idrian (*C*–11), a part of the Indonesian nation. Papua (*E*–22) had been ceded to Australia in 1906 and the Territory of New Guinea (*N*–8) to the north came under the trusteeship of Australia following the war.

The backbone of New Guinea is the Cordillera, a central chain of folded rocks rising to mountains as high as 4900 meters (16 000 feet) in places. In this scene, the Victor Emmanuel Range (*F*–18) on the Australian side extends to 3859 meters (12 660 feet) at Mount Capella (*K*–19) while the Sterren Range on the Indonesian side contains Antares Peak (*G*–18) at 4168 meters (13 674 feet). These ranges here consist of Tertiary and older limestones and clastic sediments. In recent years important porphyry copper deposits have been discovered in central New Guinea, including the Ok Tedi deposit (under the clouds near *K*–20) developed in a shear zone within intrusive rocks of Plio-Pleistocene age. The Thurnwald Range (*K*–8; *L*–14) further north reaches 1800 to 2400 meters (6000 to 8000 feet). These highlands are drained by the Sepik River (*F*–13; *S*–8) and its tributaries. The Sepik drops rapidly from its headwaters near the settlement of Telefomin (*P*–20) into a broad swampy plains (*F*–10; *O*–5) lying about 300 meters (1000 feet) above sea level. Several villages are built along the Sepik or in the "bush" at the edge of the swampland.

This region is typical of the jungles of the South Pacific. The entire terrain is covered by a dense tropical rain forest—annual rainfalls up to 1000 centimeters (400 inches) have been recorded in this part of the island. Swamp plants, palms, and evergreen shrubs fill the lowlands, giving way to forests of softwoods, oak, and kauri pine on the mountain slopes and beech and mosses at even higher elevations. Native clearings (*P*–20) are covered by savanna grasses. *1028–00134;* August 20, 1972.

PLATE 375



SOUTH ISLAND, NEW ZEALAND: Some of the most spectacular scenery and geology in the western Pacific is found on the two main islands of New Zealand. South Island is dominated by the Southern Alps, a chain of complexly folded, faulted, and metamorphosed rocks making up mountains that rise abruptly from the sea to altitudes in excess of 3000 meters (10 000 feet). Part of these Alps (*C*–11) appears in this image; the highest peak here is Mount Taylor (*C*–20), which reaches to 2350 meters (7640 feet). Major streams, such as the Raikaia (*J*–21), Waimakariri (*K*–17), Hurunui (*M*–8), and Waiau (*N*–5) Rivers, contain water (blue) in their flood plains from the coast inland through the Canterbury Plains (*K*–18), the rolling hills of Canterbury Downs (*L*–10), and, for several, into the higher mountains.

The Southern Alps east of the Main Divide (*G*–6) consist of deformed Triassic and Jurassic greywackes and metasedimentary rocks. To the northwest, in the Grey River (*C*–4) valley and elsewhere, the rocks are pre-Carboniferous sediments, Cretaceous intrusives, and Cenozoic sediments. These two groups of rocks form a pair of crustal blocks separated by the Alpine Fault (*C*–8; *J*–5), a great wrench or strike-slip fault along which more than 480 kilometers (300 miles) of horizontal displacement has carried the western block to the north. A thin wedge of the Otago schists lines the fault along its eastern side. The major structural movements producing the present Alps and the main faulting took place in the Miocene. Much of the rugged topography in these mountains resulted from extensive Pleistocene alpine glaciation. During the Pleistocene, two large, now extinct volcanoes (*O*–18; *R*–19) on the Banks Peninsula were breached by glaciers to form the Diamond (*P*–18) and Akarga (*R*–21) Harbors.

The plains west of the city of Christchurch (*O*–17) is given primarily to animal husbandry (sheep and dairy cattle), particularly in the higher elevations, and to wheat, some oats and barley, and fodder crops in the developed farmlands (*J*–19). Apples, pears, cherries, and apricots are grown in orchards (*L*–16), in plantations (*N*–7), and elsewhere in the vicinity of Christchurch. The arable plains (with soils derived from late Tertiary and Pleistocene marine and glacial sediments) give way to tussock grasslands in the Downs, isolated stands of conifers and polycarps in some foothills, and beech forests in rain belts within the higher mountains. *2192–21265;* August 2, 1975.

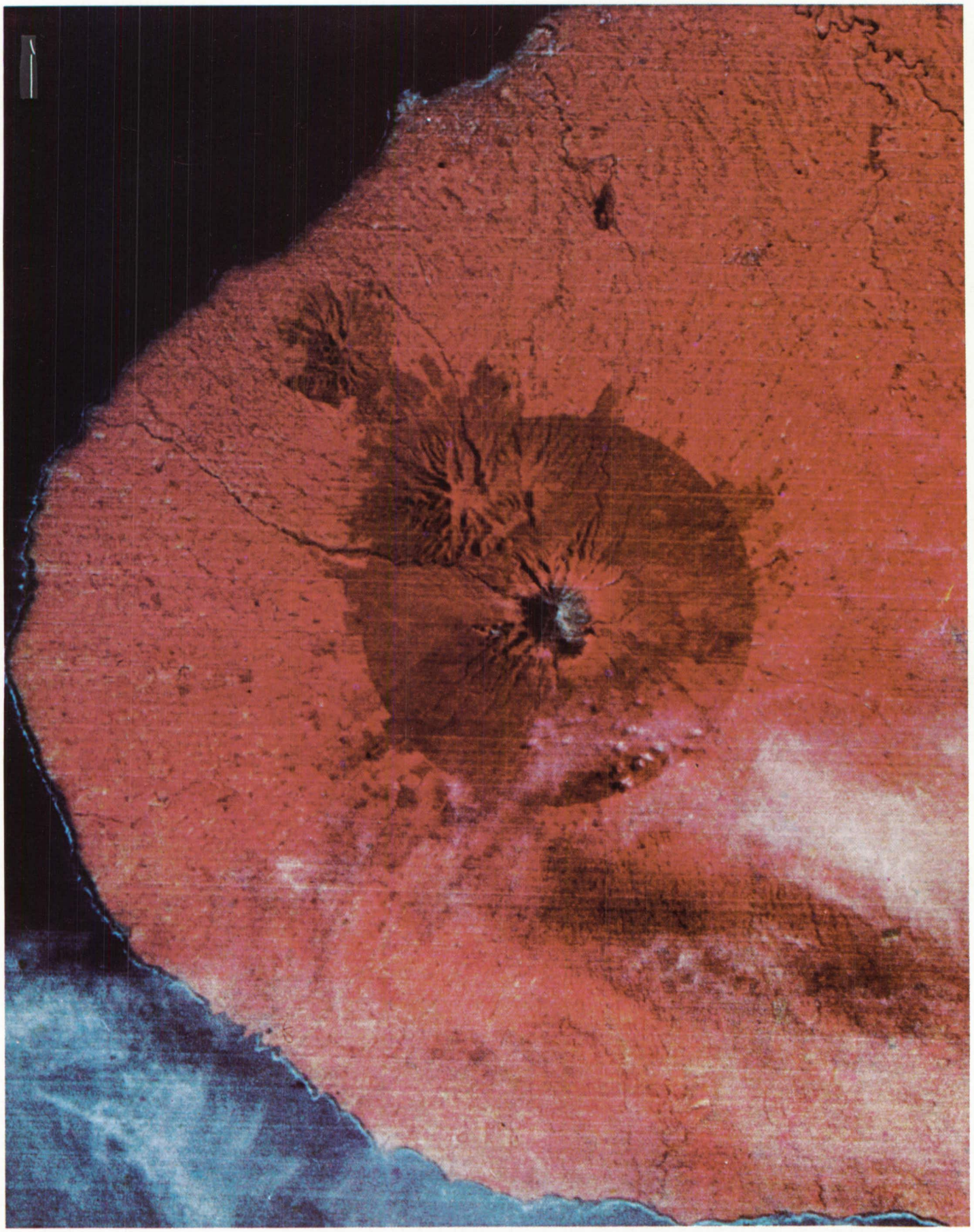
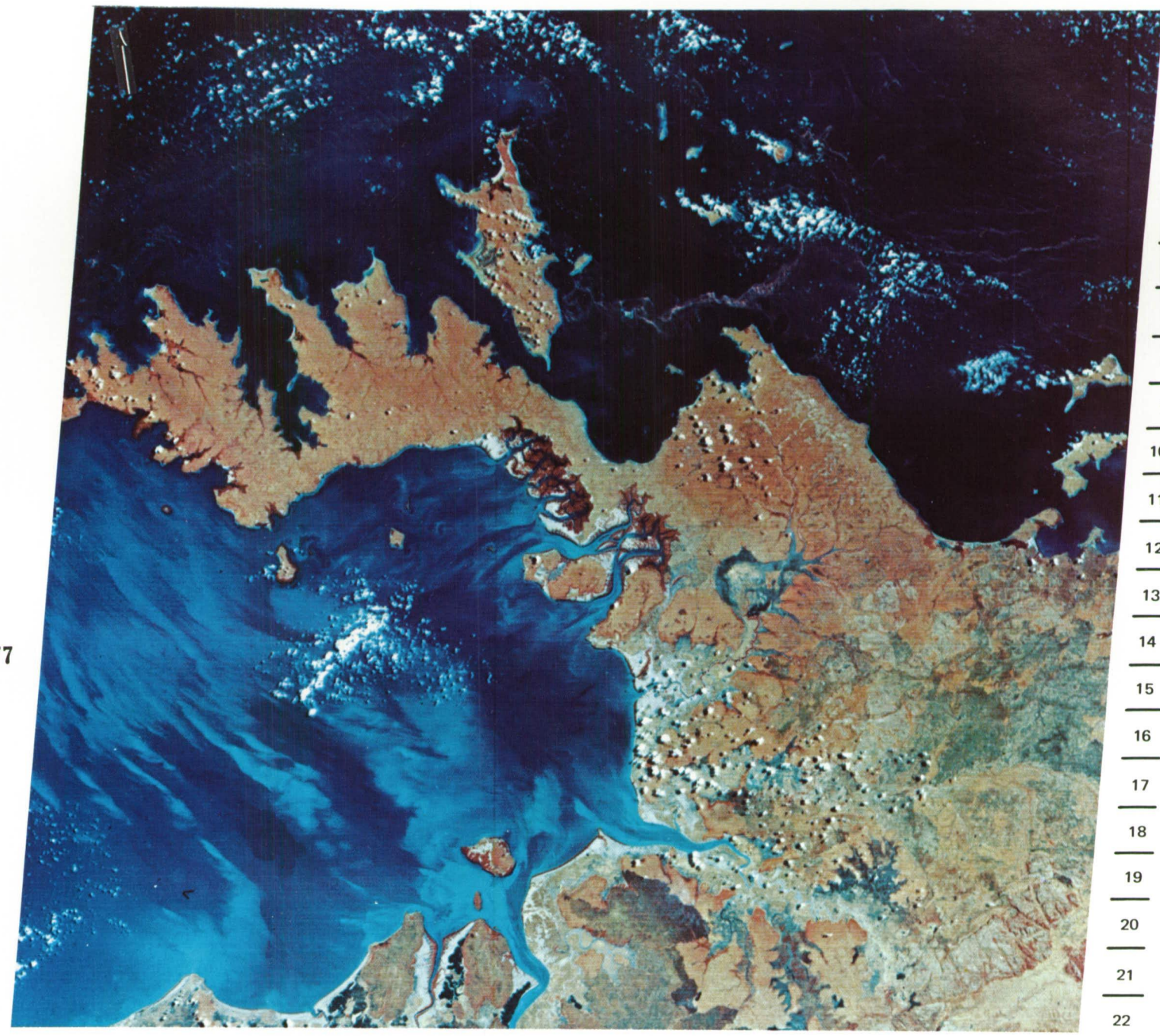


PLATE 376

MOUNT EGMONT, NEW ZEALAND: This enlargement of part of image 1556–21334 (taken on January 30, 1974, at the height of the southern hemisphere summer) to a scale of about 1:250 000 shows Cape Egmont in the southwest lowlands (plains of Taranaki, underlain by Tertiary mudstones) of the North Island of New Zealand. In the center is Mount Egmont (or Taranaki in the Maori language), one of the most perfectly shaped stratocone volcanoes in the world. This volcano rises to a height of 2630 meters (8260 feet). The area around its central peak is largely free of vegetation, exposing Late Tertiary and Pleistocene lavas, but most of the slopes are mantled by a natural forest preserve constituting the Egmont National Park. This is a dense subtropical rain forest characterized by the Tawa tree. A fence completely surrounding the park is responsible for the pronounced circular land use pattern. Beyond the fence the land has been almost totally deforested. The countryside is now covered by pasturelands, with rye grass and clover, that are devoted mainly to dairy cattle and some sheep. The region is well known for its cheeses. The small city of New Plymouth (blue area along the coast at the top of the scene) is a commercial center, a stockyards, and a shipping port. *1556–21334;* January 30, 1974.

PLATE 377



ARNHEM LAND, AUSTRALIA: One of the northernmost sections of continental Australia is the great aboriginal native preserve called Arnhem Land; it is part of the Northern Territory and stretches below the coastline of the Arafura Sea some 160 to 480 kilometers (100 to 300 miles) east of Darwin. The segment shown here is the Cobourg Peninsula (*G*–8) extending around Van Diemen Gulf (*F*–15). The peninsula consists mostly of Cretaceous rocks (*C*–8; *H*–9) with Pleistocene sediments further inland (*O*–11) and along the coasts (*M*–14; *Q*–10). The Wellington (*R*–14) and Spencer small hills (*U*–20) are outliers of Precambrian metamorphic rocks.

This scene, obtained during the dry season, shows most of the region to be covered by tall savanna grasses. Scattered rain forests (banyans, pandanus, and eucalypts) occur mainly along watercourses. Mangrove swamps develop around river estuaries (*K*–20). The nomadic aborigine tribes hunt plentiful game in this tropical zone. Kangaroo, bandicoots, wildcats, wild birds, waterfowl, and a wide variety of reptiles are typical inhabitants. The names of the two principal rivers, the East (*O*–19) and South (*K*–21) Alligator Rivers (actually populated by crocodiles), add to the junglelike flavor of the country. Domesticated animals are at a premium in Arnhem Land owing to the constant infestation by disease-bearing mosquitoes and flies.

Cloud patterns (*G*–13) mix with sediment patterns (*C*–13) in this scene. Coral islands (*J*–18) and reefs (*B*–5) are actively growing off the coast. *1069–00442;* September 30, 1972.

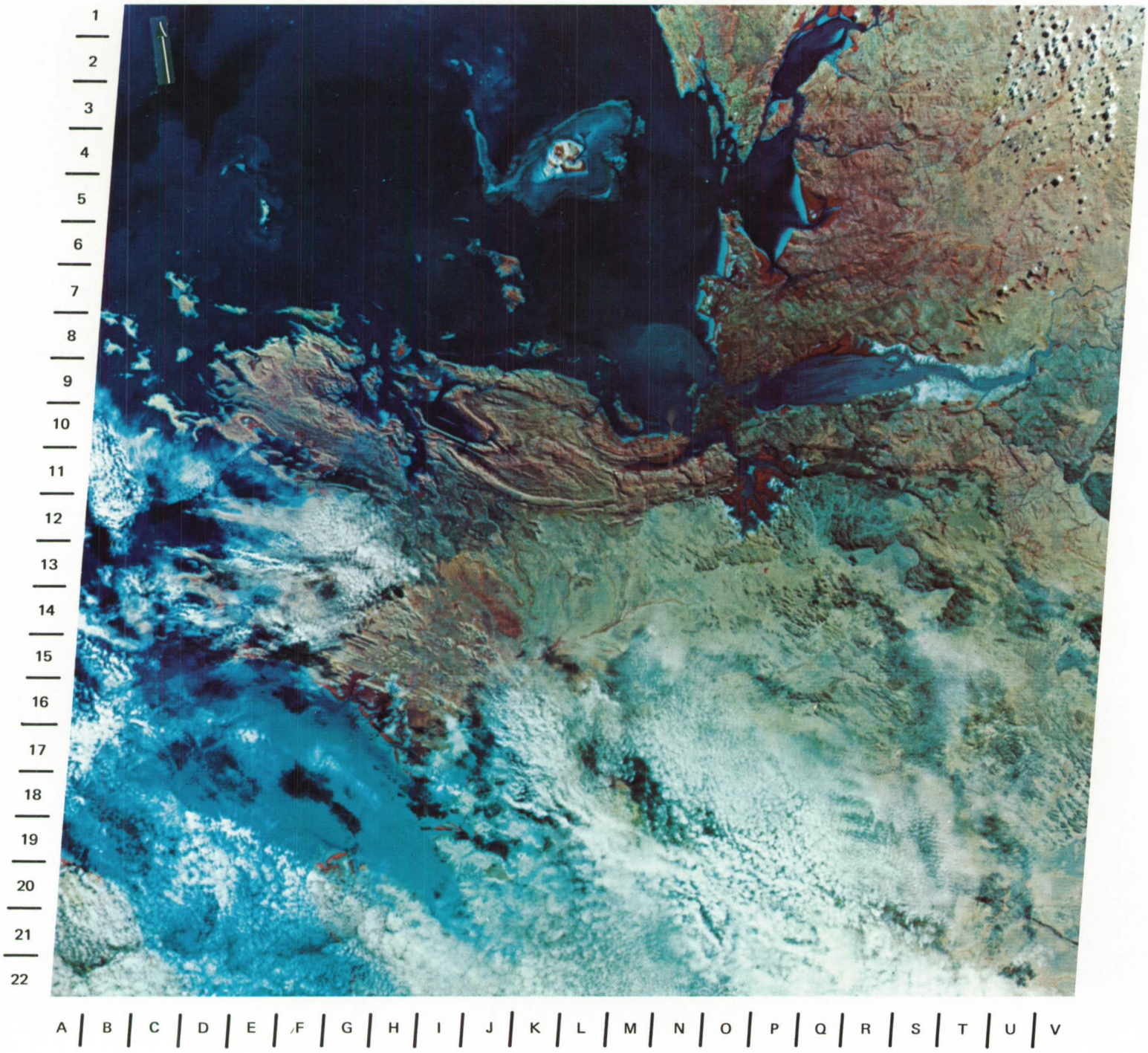


PLATE 378

NORTHWEST SUBTROPICAL COASTLANDS, AUSTRALIA: This area, at the west edge of the Kimberley Plateau and some 970 kilometers (600 miles) southwest of Darwin, receives 75 to 100 centimeters (30 to 40 inches) of rainfall per year. Mangroves (*O*–11) persist along the coast; further inland the terrain supports tall grasses with scattered trees and small forests of eucalyptus. The coast is much embayed: King Sound (*E*–16) north of Dampier Land (*C*–20), an aboriginal preserve; Collier Bay (*L*–7); Walcott Inlet (*P*–9), drained by the Isdell (*T*–10) and Charnley (*U*–8) Rivers; and Doubtful Bay (*N*–5). The Buccaneer Archipelago (*A*–8) is a cluster of islands west of Yampi Sound (*D*–11); Montgomery Island (*J*–4) is fringed with coral.

The King Leopold Range (*R*–12), rising more than a thousand meters (several thousand feet) above the sea, has a core of Proterozoic granites flanked on the north by Devonian sedimentary rocks. Folded Proterozoic rocks form distinct anticlines (*J*–11) and tilted strata (*G*–14) along the Wyndham Range (*G*–11). Proterozoic metabasalts (*S*–7) are intermixed with these and other Proterozoic sedimentary rocks north of Walcott Inlet. Cenozoic sediments cover much of the surface in the cloud-hidden part of the image. Iron deposits are being mined from several of the archipelago islands, and tin deposits occur in the King Leopold Range. Offshore oil has been discovered west of Yampi Sound. *1020–01143;* August 12, 1972.

PLATE 379



PILBARA DISTRICT, AUSTRALIA: This part of Western Australia near the west coast at Port Hedland has achieved major importance in the Australian economy because of its huge reserves of iron ore. The scene covers the area just north of the gorge-cut plateau of the Hamersley Range, highest in this section of Australia, drained by the Fortescue River (*J*–21) in the south and the Shaw (*B*–2), Coongan (*H*–2), and Nullagine (*B*–7) Rivers to the north. Vegetation is confined to tussocks of spinifex (a grass with hard spiny leaves) and other grasses and saltbush and bluebush, which support some cattle and sheep in this otherwise arid region.

Geologically this is one of the most spectacular regions of Australia. The area shown is part of the Pilbara block in which late Precambrian rocks rest on older rocks of the Archean western shield that underlies most of the north and west of Australia. Exposures (*B*–9; *E*–3; *H*–12) of Archean metabasalts (greenstones), other volcanics, and some metasedimentary rocks make up much of the terrain. These Archean rocks represent the roots of greenstone belts that remain between younger large granitic plutons (*F*–14; *J*–10; *K*–3); these intrusives were later cut by Proterozoic basalt dikes (*P*–13). A block of Archean schists, quartzites, and jaspilite (iron-ore chert) in the Nullagine Basin (*P*–12), another Archean belt (*G*–3) near Marble Bar (*G*–5), and rocks of the Chichester Range (*T*–19) were metamorphosed by these invading plutons. Intermediate to basaltic lavas and metasediments of Lower Proterozoic Age, altered at the surface to lateritic and limonitic crusts, are widely distributed (*F*–3; *L*–19; *R*–6). A narrow belt of Permian and Tertiary rocks survives along the De Grey River (*V*–10). Late Cenozoic sediments line the Fortescue River in the Ashburton Basin (*C*–22) and the Noreena Creek region (*R*–21) to the east. *1148–01282;* December 18, 1972.

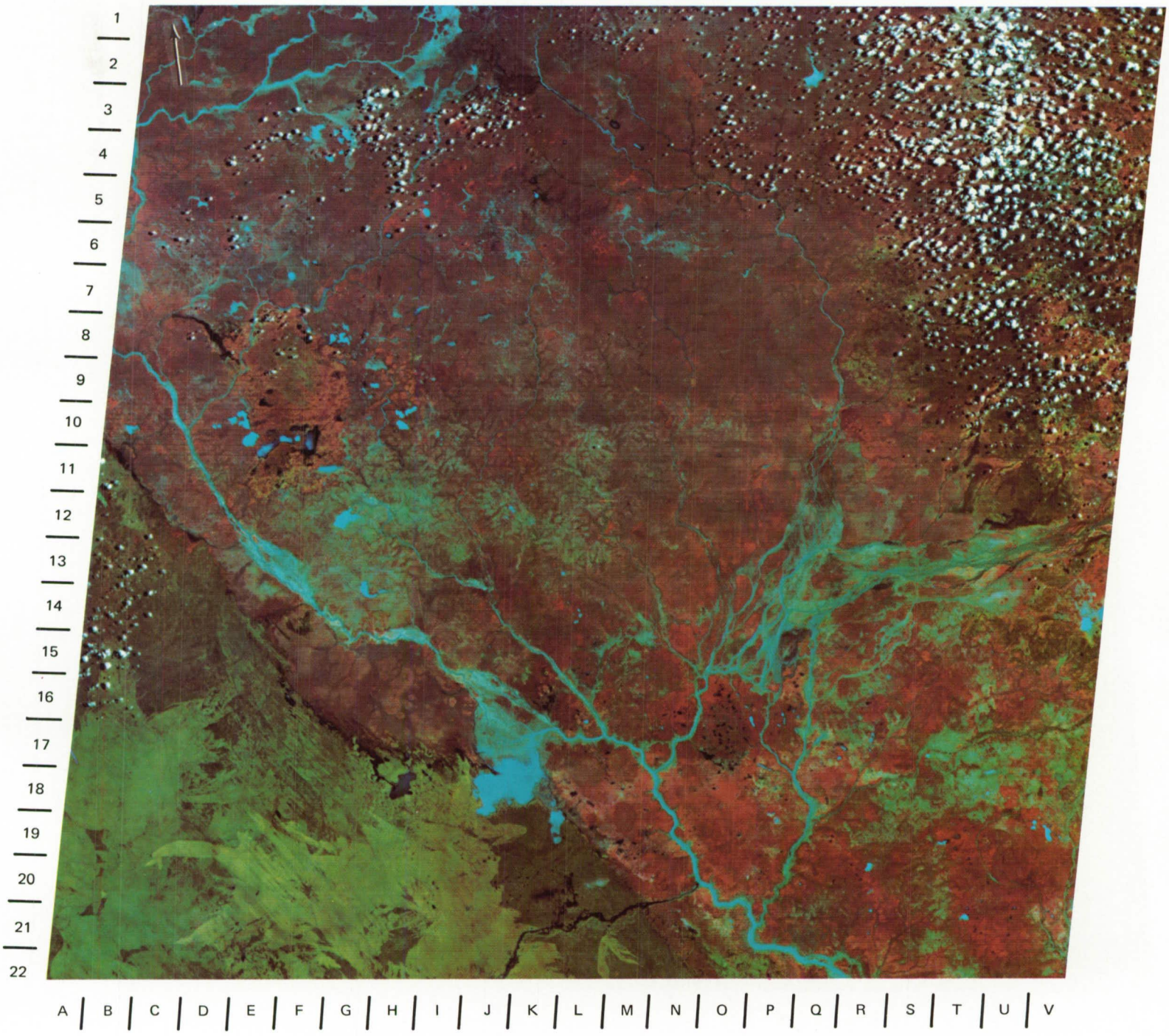
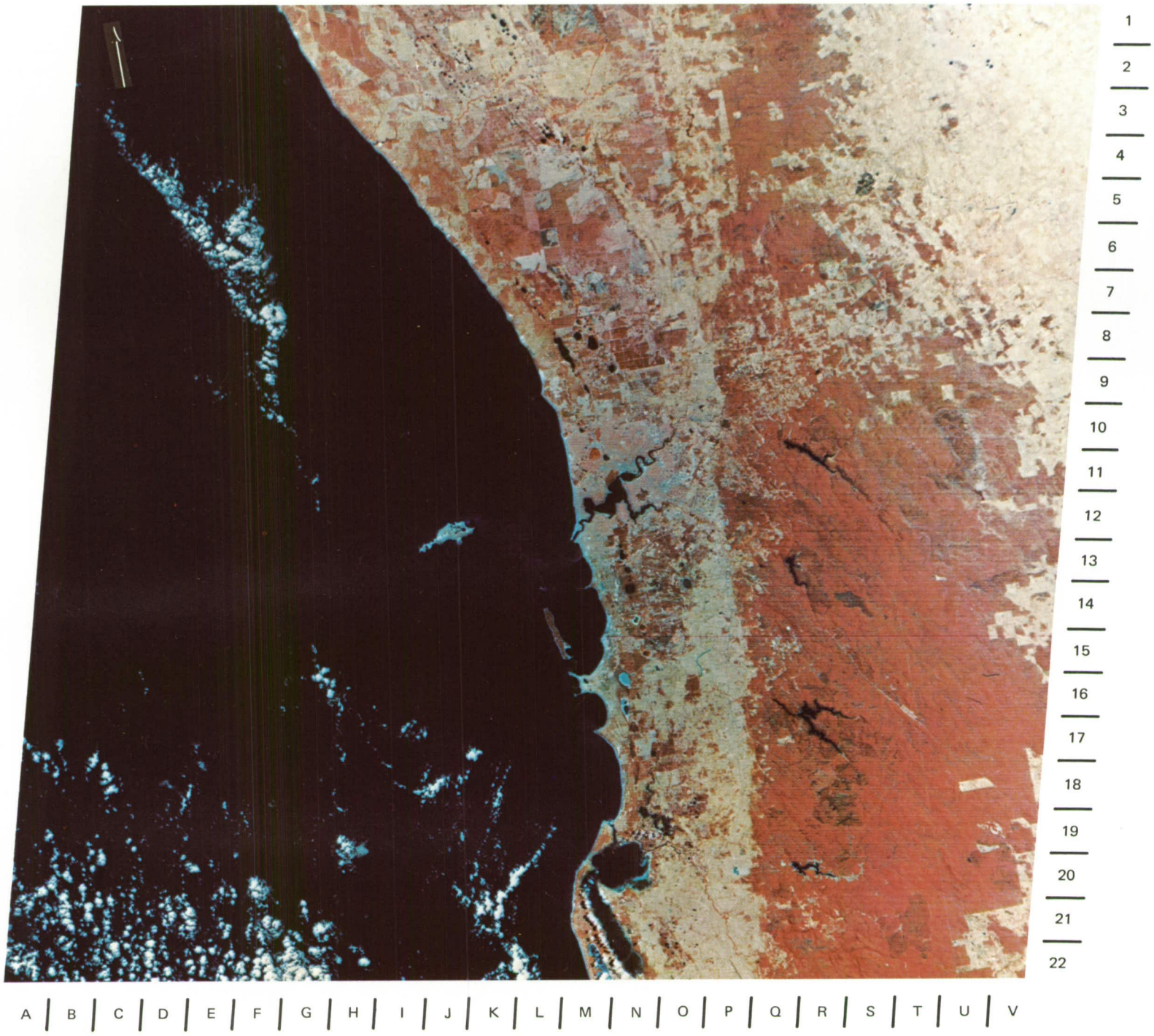


PLATE 380

NORTHERN AUSTRALIA: The border between Queensland (*T*–15) and the Northern Territory (*G*–9) runs north to south along a line passing through *N*–4 to *Q*–18. The scene shown here is centered about 350 kilometers (220 miles) south of the Gulf of Carpentaria. The area north of the Ranken River (*F*–14) is part of the Barkly Tableland, a flat plateau rising to about 430 meters (1400 feet) above sea level. Cambrian rocks underlie much of the plateau, as well as the desert sand area (*E*–19) to the southwest. Cenozoic deposits occur within a broad open area between the Ranken River and the Georgina River (*P*–9) to the east. These soft sediments are easily dissected to form a distinctive drainage network (*K*–11) of ephemeral streams in narrow gullies. Patches of Cretaceous rock are evidenced by the more yellowish-red color tones (*E*–9; *Q*–8).

The area is given over almost exclusively to raising beef cattle on the good pasture lands around the town of Camooweal (*P*–7) on the highway (*N*–8) between Darwin far to the north and Rockhampton on the east coast. Vegetation is mainly tropical grassland (Mitchell and Flinders grasses being profuse) mixed with acacias. Eucalypts begin to appear in the northern end of the scene. Heavy rains have "greened" the grasslands and filled the major rivers and their tributaries with floodwaters. Most of the "lakes" are transient and will vanish at the end of the rainy season. *1568–00142;* February 11, 1974.

PLATE 381



PERTH, SOUTHWEST AUSTRALIA: This large (700,000 people) city (*M*–11) is part of the metropolitan complex built around the Melville Sound (*M*–11), an estuary where the Swan River (*N*–10) reaches the Indian Ocean. Perth, the capital of Western Australia, is the administration, trade, and industrial center for the southwestern region of the continent. Wheat, cattle, wool, timber, oil, and minerals are shipped to other Australian cities and worldwide from the port city of Fremantle (*L*–12). The Kwinana industrial district (*M*–14) lines the coast along Cockburn Sound (*L*–14).

A flat coastal plains, built up from Tertiary and Recent sediments, abuts abruptly against the hills of the Darling Range (*T*–16) which attains heights up to 600 meters (2000 feet). Here the western edge of the great Western Shield of Precambrian rocks meets the plains along a long fault scarp (*O*–12; *P*–18) rising hundreds of feet. A wedge of Paleozoic crystalline rocks (*M*–2) separates the plains and shield to the north.

A variety of eucalypts, including the tall Tuart found only in this region and the karri gum trees, are typical of this part of Australia. Pines also occur in the Darling Range. Mallee scrub and acacia take over inland (*T*–3) where annual rainfall drops to 38 to 51 centimeters (15 to 20 inches) from highs of 130 centimeters (50 inches) in the forested hills. Wheat is the major crop in these drier lands and along parts of the coast. Sheep are raised there while dairy cattle are confined to much of the coast. Oranges are grown south of Perth. *1149–01370;* December 19, 1972.

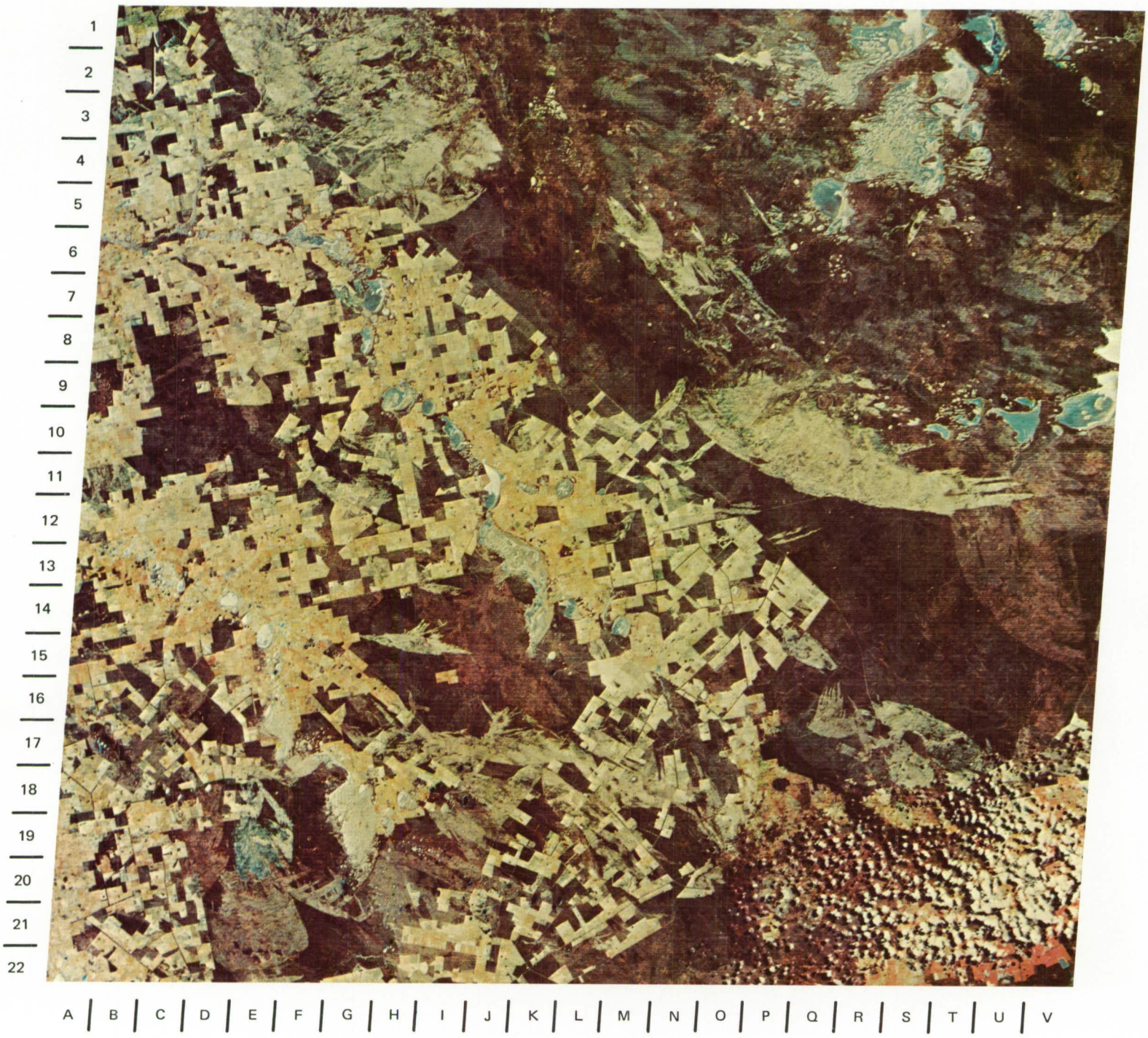
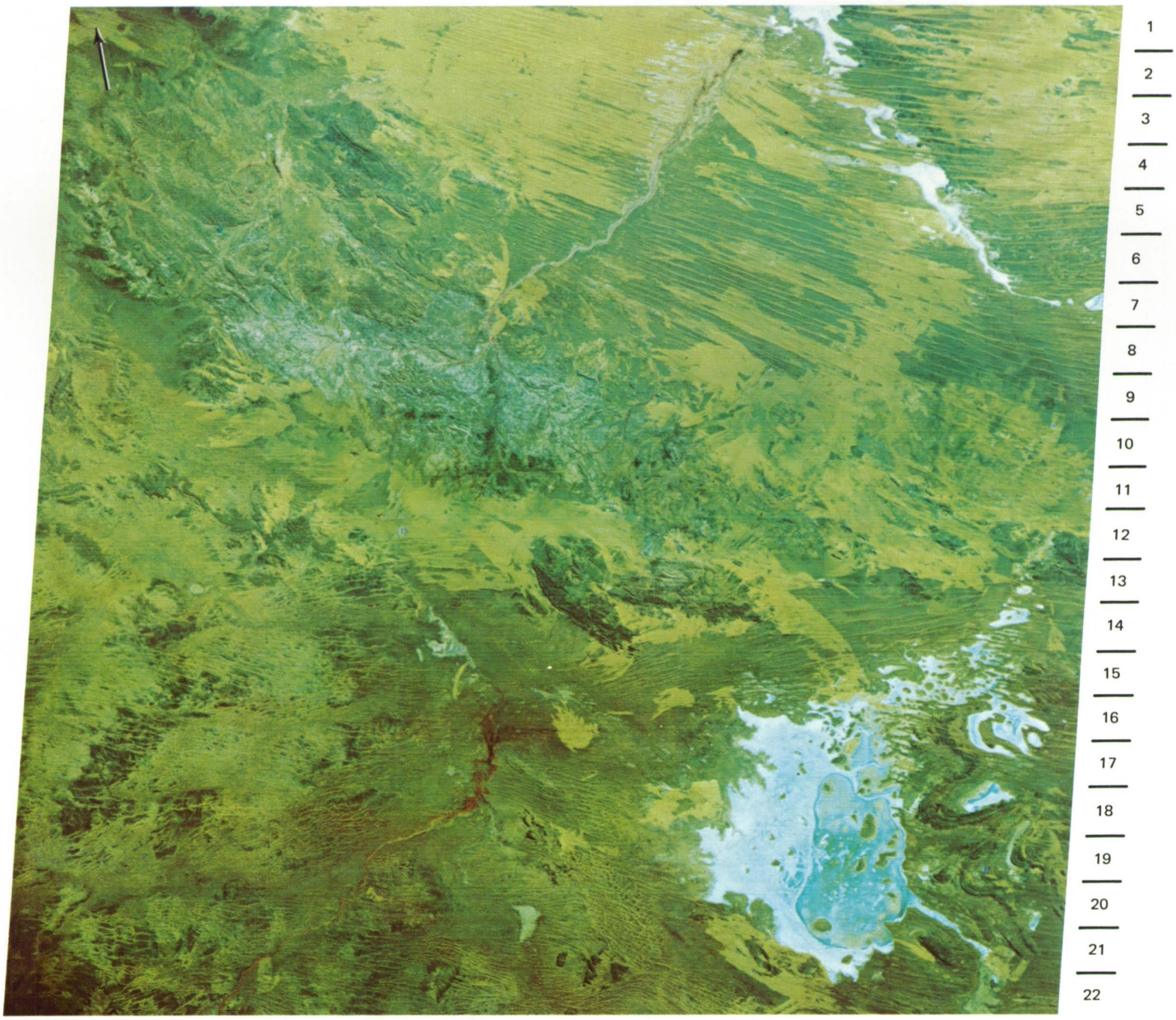


PLATE 382

SOUTHWEST AUSTRALIA: The area shown is situated about 725 kilometers (450 miles) east of Perth and 160 kilometers (100 miles) inland from the south coast. It is underlain by the Archean crystalline basement that reaches its maximum exposure in this part of Australia. A section of younger Archean rocks (*J*–3) lies within the undeveloped land occupying the upper right third of the image. The residual soils in this area, mixed with some windblown loess, are lime rich. Natural vegetation is known locally as mallee scrub, being a mixture of saltbush and bluebush with scattered dwarf eucalypts that form a heath. Much of this area is progressively cleared in places by extensive burning (*G*–3; *P*–10) and then converted to large wheat fields—the principal crop in this region. Growth of wheat is favored by this soil and a rainfall of 25 to 38 centimeters (10 to 15 inches) per year. The boundary between fields and undeveloped land here (*H*–7) coincides approximately with a "rabbit-proof" fence—one of several that run for hundreds of kilometers through southwest Australia. The Johnston Lakes (*R*–3) and Lake Tay (*V*–9) are salt lakes that remain partly filled after the winter (July and August) rainy season. The Kalgoorlie gold fields lie northeast of these lakes. *1092–01195;* October 23, 1972.

PLATE 383



DESERT COUNTRY, WESTERN AUSTRALIA: This region of Australia lies within one of the most arid parts of Australia where annual rainfalls of 20 to 30 centimeters (8 to 12 inches) are normal. The area shown is located less than 320 kilometers (200 miles) from the northwest coast along the Indian Ocean. The southwestern edge of the Great Sandy Desert (*L*–2), in the Canning Basin, extends into the upper right of the image. The Rudall River (*N*–2) is an interior stream that begins in the Broadhurst (*I*–8) and Throssel (*C*–6) Ranges, blocks of Archean metamorphic rocks forming low hills, and ends abruptly at Lake Dora (*P*–1), one of a chain of saline lakes. South of these ranges is the northwestern extension of the Gibson Desert (*M*–20). Outcrops of Permian rocks (*T*–17) occur to the east of Lake Disappointment (*Q*–18), a large saline playa deposit, as well as along the string of lakes around Lake Dora. Most of the surface in this scene is covered by Quaternary sands and alluvial deposits; parallel longitudinal dunes predominate in the northern desert while somewhat more irregular dune networks form in the southern desert. Vegetation ranges from sparse desert spinifex tussocks to dry steppe grasses. *1344–01165;* July 2, 1973.

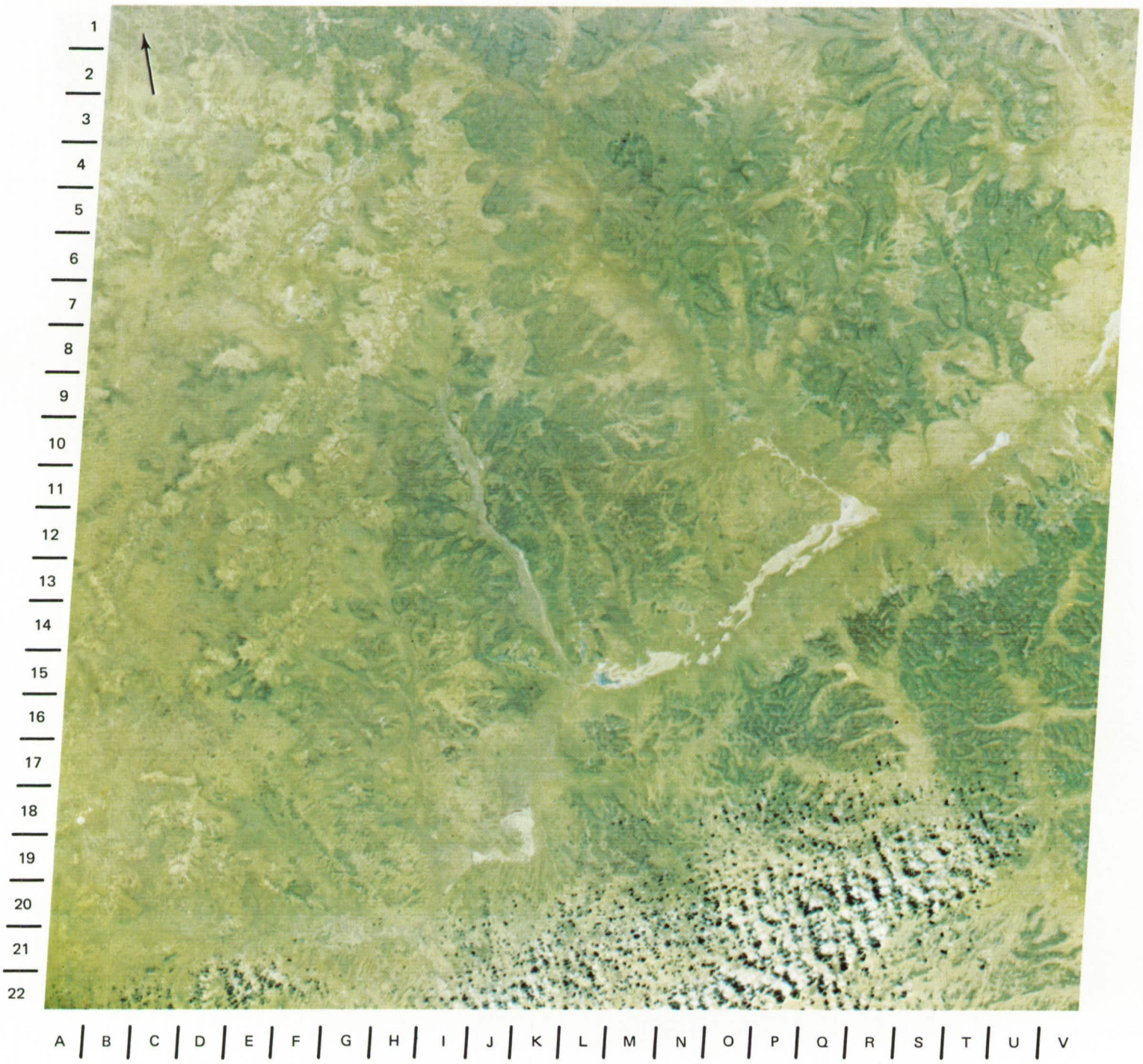
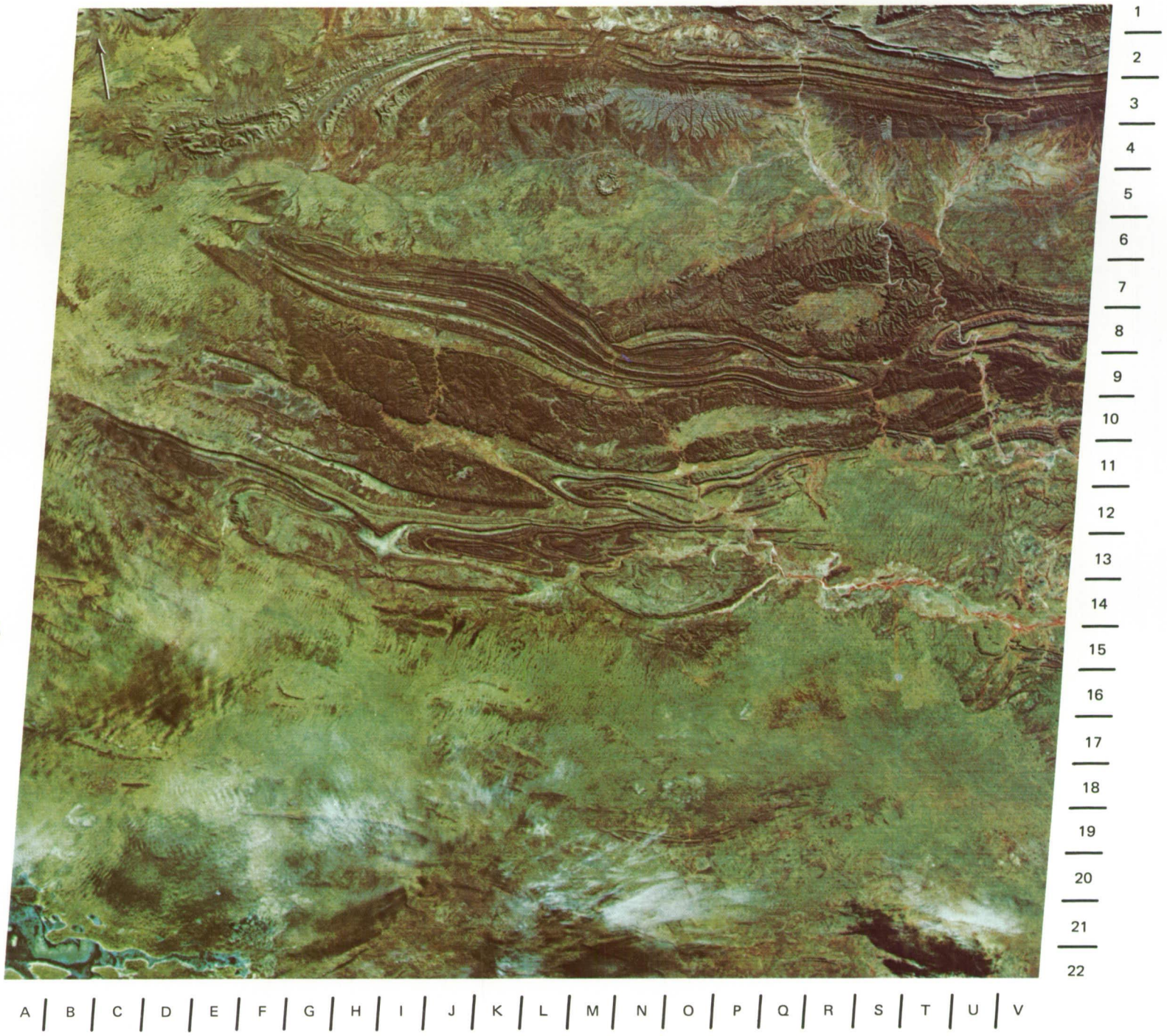


PLATE 384

THE AUSTRALIAN INTERIOR: Much of the eastern half of Western Australia is barren, without roads or settlements. This image is typical of this region, which has a desert steppe surface vegetation on the east giving way to mulga scrub, grasses, acacia, and small shrubs, on the west. Landmarks are few: the dry lakes Gillen (*L*–15) and Breaden (*P*–12); the Sutherland and the Fame (*J*–11) Ranges, consisting of Cretaceous sedimentary rocks; and the Spinifex Range (*T*–15), exposing mostly Permian rocks. Proterozoic sedimentary rocks underlie parts of the surface in the lower left corner. The region shown here is located between the southern edge of active dunes in the Gibson Desert to the north (above the image) and sands in the Great Victoria Desert to the south. *1018–01054;* August 10, 1972.

PLATE 385



MACDONNELL RANGES, AUSTRALIA: This is the only extensive east to west fold belt in Australia that is younger than the Precambrian. It is located almost in the center of the continent. Steeply dipping Cambrian and Ordovician strata (*J*–7) make up a series of tightly folded anticlines (*J*–12; *M*–11; *N*–8). More broadly folded synclines (*J*–9; *Q*–6) expose late Ordovician, Devonian, and Carboniferous sedimentary rocks. This part of the Macdonnell Ranges is subdivided into several individually named units: the Gardiner (*L*–8), George Gill (*B*–10), and Levi (*K*–2) Mountains. The south end of the higher (up to 1500 meters (5000 feet)) main range at *N*–2 is also composed of Paleozoic sedimentary rocks but Precambrian metasedimentary and crystalline rocks compose most of the central Macdonnell Range. This entire mountain system experienced its principal folding during Late Devonian and Carboniferous times.

An unusual structure not related to the folding itself appears at *L*–4. This is the Gosses Bluff astrobleme, the scar of a giant meteorite impact that produced a strongly deformed circular depression some 24 kilometers (15 miles) in diameter with a pronounced inner ring of sandstone marking a central uplift.

The mountains have been breached by several streams that probably existed before renewed uplift of these ranges. The principal channels are the Finke (*T*–8) and Palmer (*R*–13) Rivers, which join to the right of the image as a single river that flows past the Simpson Desert eventually to reach the Lake Eyre depression below sea level. The periodically filled saline Lake Amadeus is shown at *B*–2. Alice Springs lies just off the image at *V*–4. *1373–00364;* July 31, 1973.

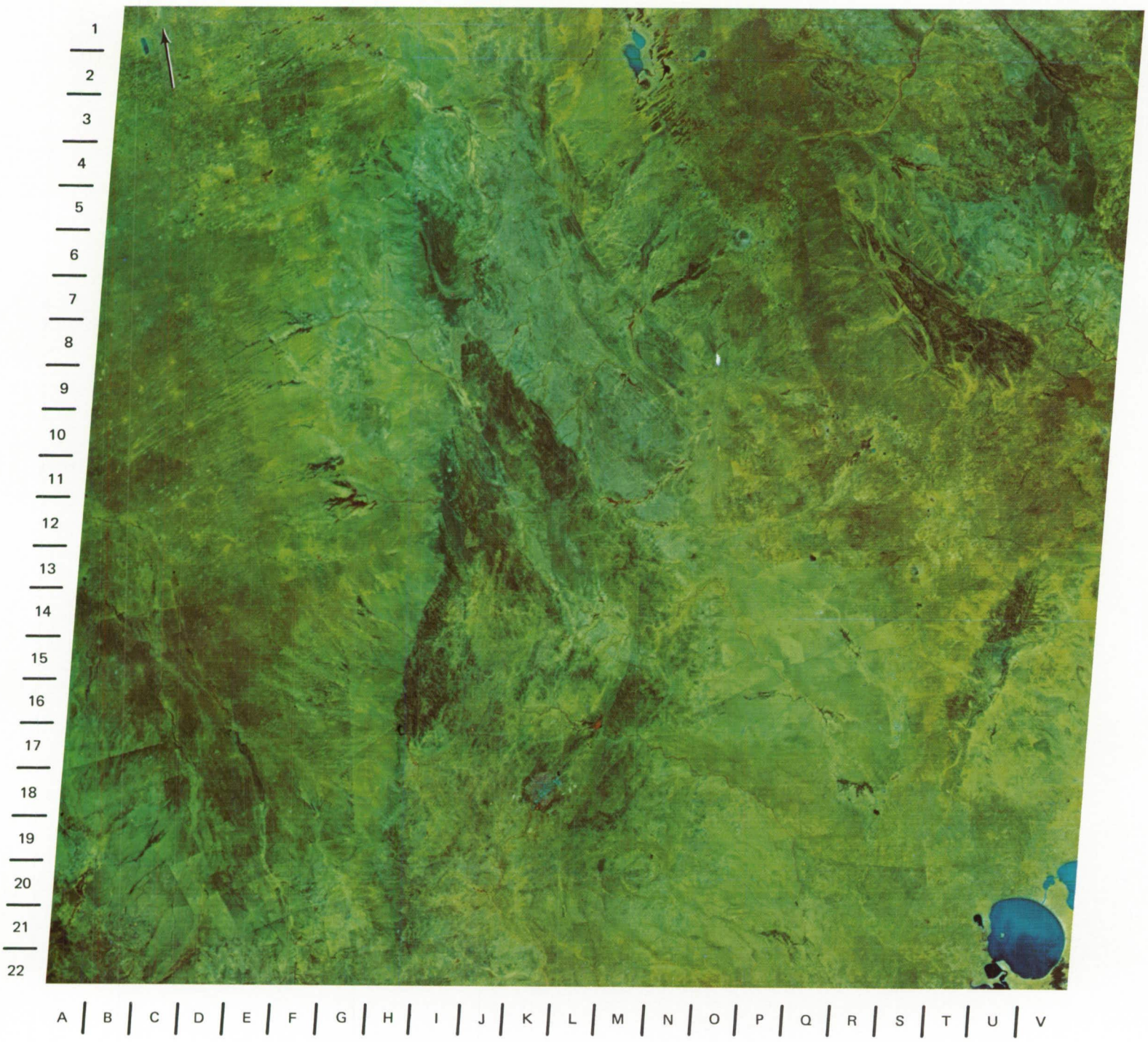


PLATE 386

THE BROKEN HILL MINING DISTRICT: The world's largest deposit of good-quality lead and zinc ore occurs in a narrow outcrop about 5 kilometers (3 miles) in length north of the city of Broken Hill (*K*–8). The deposit occurs near the east flank of the Main Barrier Range (*I*–11), a group of ancient sedimentary rocks metamorphosed by intrusive igneous rocks. The host rock consists of a distinctive brown ironstone fractured during folding into a "broken hill." Lead is the principal metal, with abundant zinc and silver, and recoverable quantities of gold and antimony. Ores are shipped by rail to Port Pirie to the south and Sydney to the east.

Broken Hill now has a population exceeding 30 000. Water is supplied from the Menindee Lakes (*V*–21) to the southeast formed along the Darling River that drains the northwest edge of the Murray River Basin. The region is semidesert, covered with arid mulga scrub or stabilized dune fields (*C*–9). The highest points are about 440 meters (1450 feet) in the Main Barrier Range and at Gnalta Peak (*S*–8). *1112–23533;* November 12, 1972.

PLATE 387



THE CHANNEL COUNTRY, AUSTRALIA: This part of east-central Australia lies within the southwest and northeast corners of the States of Queensland and South Australia, respectively. The region is part of the Great Artesian Basin of eastern Australia, structurally a vast geosyncline containing mostly Jurassic and Cretaceous rocks, which gets its name from the many water wells that tap subsurface water introduced through porous sandstones near the surface. Much of the area, including the images shown here, is a rolling plains less than 300 meters (1000 feet) above sea level covered with Quaternary sandy alluvial deposits in the lower areas (*J*–12) or with brown or gray soils developed on older rocks. In this scene, Cretaceous and Tertiary rocks underlie the Beal Range (*I*–7), which rises to nearly 460 meters (1500 feet), and occur also to the southeast (*U*–19).

The region normally receives less than 50 centimeters (20 inches) of rain per year. The low hills and plains generally are devoid of much vegetation cover, as is evident in the southern winter (July) scene. This is mulga vegetation country, marked by sparse grasses,

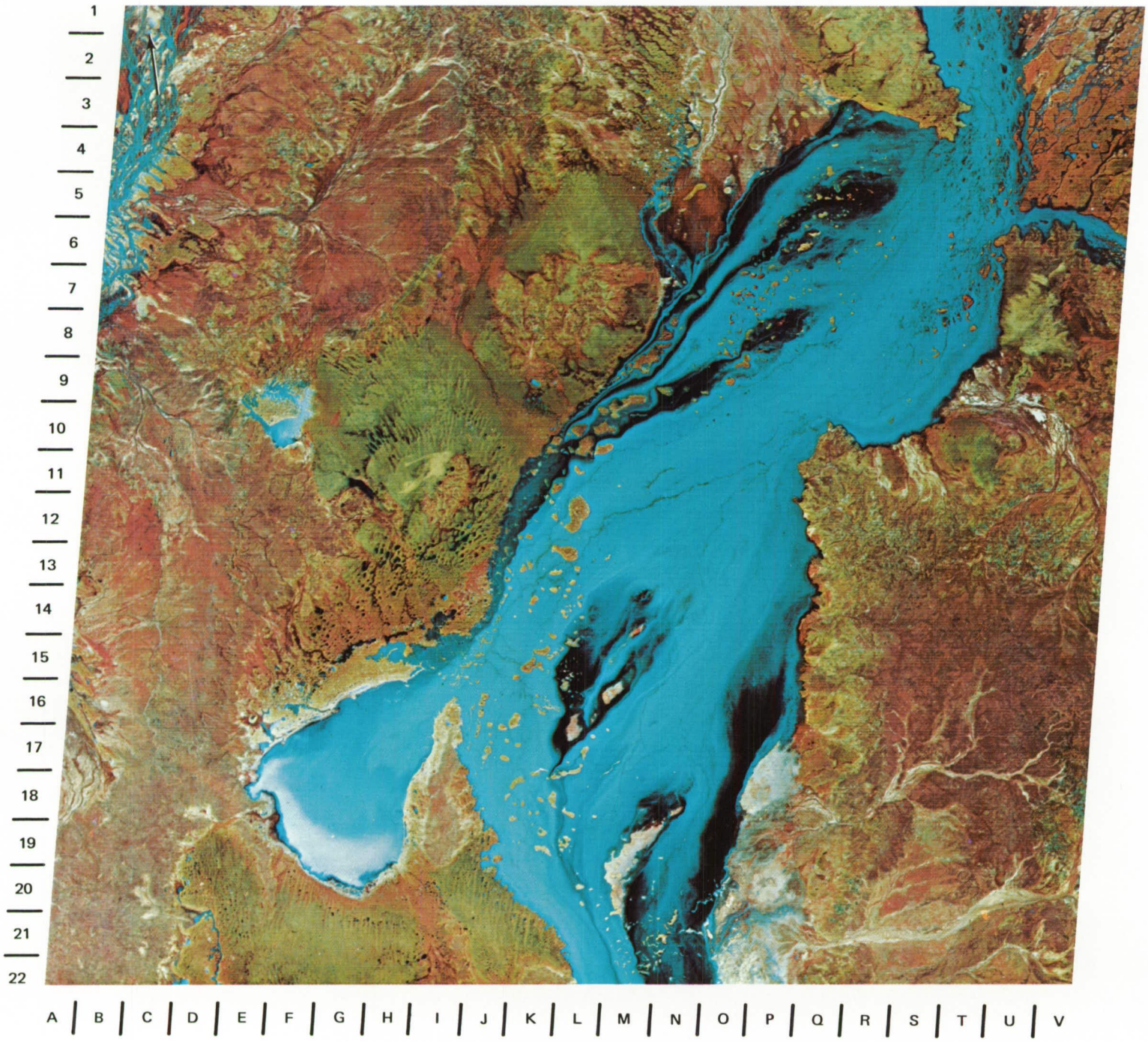
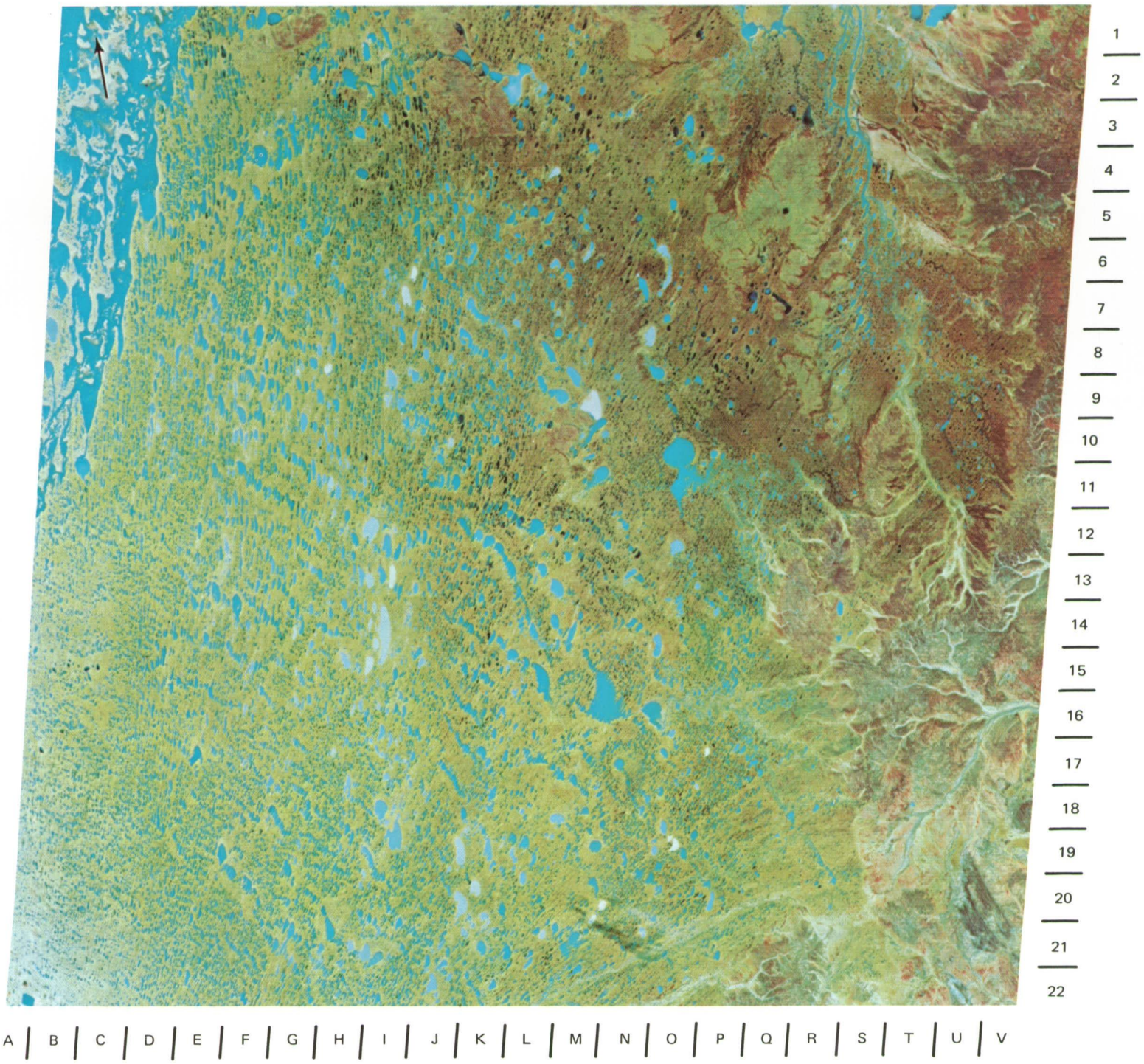


PLATE 388

small shrubs, and acacias. However, this part of Australia is especially prone to extensive flooding that results from persistent heavy rains in certain years. Water collects rapidly in low areas that can remain perennially moist. The flood plain of the Barcoo (Cooper) River (*P*–14) is subject to this condition. Grassy vegetation and even marshy plants abound, providing natural pastures for cattle grazing.

The scene on this page shows the same area during a period of major flooding in early 1974. Waters have spilled out of the immediate channel of the Barcoo River into the shallow Lake Yamma Yamma (*F*–17). The Farrars Creek (*A*–4), hard to see in the dry season image, is now a maze of flooded channels. Lake Cuddapan (*E*–9), shrunk to a nearly dry saltpan in the previous winter, has now filled from the rains. The entire countryside, except for some very sandy areas, has "bloomed" as grasses and acacias spread forth, particularly along normally dry creek beds. *1365–23570;* July 23, 1973. *1563–23530;* February 6, 1974.

PLATE 389



STURT DESERT, AUSTRALIA: This scene is located at the meeting point of the States of New South Wales (*bottom*), South Australia (*left*), and Queensland (*top and right*). The Sturt Desert (*J*–14) is a vast sand waste covered by dunes elongated in the direction of persistent winds. This desert is bounded on the east by the Grey Range (*V*–6; *V*–14), low hills of Cretaceous and Tertiary marine sedimentary rocks deposited in the Great Artesian Basin geosyncline. Water normally is available in this area only through wells sunk into sandstone aquifers underlying the Grey Range. However, at the time this image was acquired, the region had experienced a continual deluge of rains, so heavy over a short period that thousands of small lakes have accumulated in the interdunes of the desert. A network of connected "lakes" (*A*–4) has also developed within the Strzelecki Creek drainage basin. The Wary Wary River (*R*–4), which eventually flows into the Barcoo River to the north, is transporting a high volume of runoff but does not seem to be in full flood. *1563–23535;* February 6, 1974.

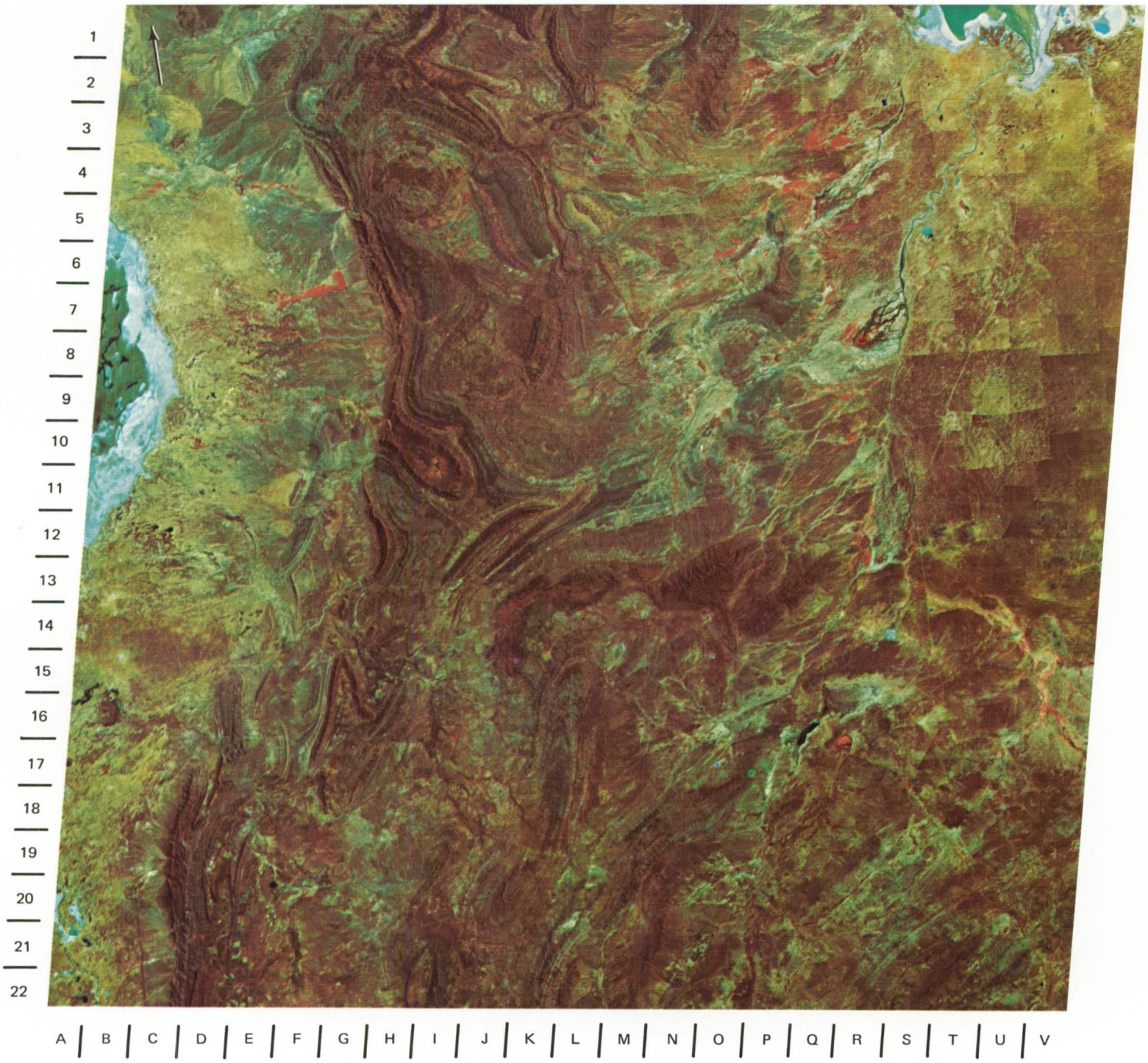
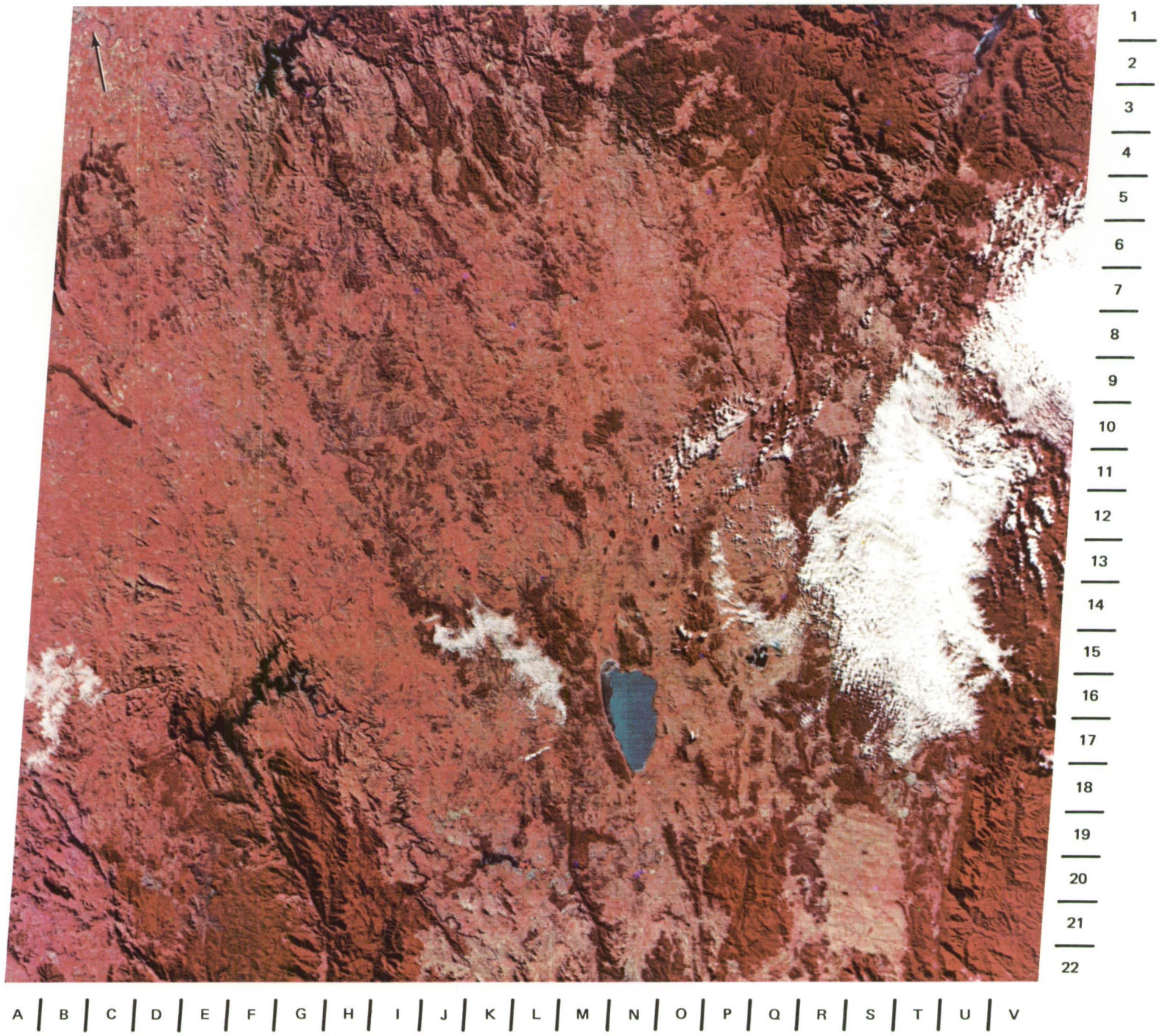


PLATE 390

FLINDERS RANGES, AUSTRALIA: The Flinders Range (*I*–4; *I*–20) is an uplifted block of Proterozoic sedimentary rocks (slightly metamorphosed) with infolded Cambrian rocks (e.g., at *H*–10 and *J*–12) that runs northward for hundreds of kilometers (several hundred miles) in the southern half of the State of South Australia some 650 kilometers (400 miles) north of Adelaide. Diapiric intrusions (*G*–5; *J*–10) are also exposed in the core of the range. The block lies along the east side of a structural trough (down-dropped fault block or graben) known as the Sunklands, which extends inland from the Spencer Gulf to Lake Torrens (*A*–9). Further to the east additional faulting separates the Flinders Range from the down-dropped Arrowie Basin (*T*–4). The range reaches heights of 900 to 1200 meters (3000 to 4000 feet) in places. Cenozoic sedimentary rocks cover the lowlands on either side of the range. Drainage into the Arrowie Basin from the Pasmore (*R*–7) and Bendieutd (*Q*–4) Rivers empties into Lake Frome (*T*–1). The rangeland in this basin has been subdivided into large ranches (*T*–9) devoted mainly to sheep but with some beef cattle; cattle also are raised on the Lake Torrens side, where some wheat is grown as well. Vineyards and fruit orchards are cultivated in the higher elevations of the Flinders Range, especially toward the south where rainfall increases. Natural vegetation is characteristic of a semidesert environment, with brown sandy soils in the south supporting saltbush and other shrubs, and desert loams further north giving rise to greater grass cover and acacia. Limited mining of uranium, gold, and zinc takes place in the Flinders Range; coal of Triassic age is mined from open cuts around Leigh Creek just north of the upper left corner.

The NASA Deep Space Receiving Station at Woomera is located about 160 kilometers (100 miles) to the west of Lake Torrens. *1565–00003;* February 8, 1974.

PLATE 391



CANBERRA, AUSTRALIA: Canberra (*K*–19), the capital of Australia, is set in a small enclave (*J*–21) called the Australian Capital Territory located near the southern limit of New South Wales. The city is actually a cluster of small town centers (blue patches) and peripheral residential areas centered about Lake Burley Griffin (*K*–19), around which are most of the Government buildings. Other nearby lakes are Lake George (*N*–16) and the smaller Lake Bathurst (*P*–15).

The region shown is part of the Eastern Highlands, low to moderately high mountains extending over almost all of Australia's east coast. These mountains are composed in part of Paleozoic sedimentary rocks that were folded and intruded by granitic rocks at the end of that era. These rocks were then buried by Mesozoic sedimentary rocks that later experienced some deformation. Finally, the whole was uplifted in Tertiary times accompanied by extensive volcanic outpourings. Most of the stratigraphic units in this scene are sedimentary rocks of Ordovician, Silurian, and Devonian age, with granitic intrusions both east and west of Canberra and Silurian volcanic rocks in lower areas just to the northeast.

The Cullaran Range (*P*–4) reaches altitudes of 900 to 1200 meters (3000 to 4000 feet) north of the lower Goulburn (*Q*–10) area through which pass the road and rail line to Sydney. The higher Gourock Range (*P*–20) is southeast of Canberra; the Captain's Flat area (*P*–22) is the site of small reserves of copper, zinc, and lead. Southwest of Canberra is the northern end of the Snowy Range (*F*–20) that forms part of the Australian Alps (reaching heights of 1800 to 2300 meters (6000 to 7500 feet), lying astride the Great Dividing Range, which forms the backbone of the Eastern Highlands. These higher ranges are covered with eucalypt (myrtle) trees, including many varieties of gum and stringybarks in the lower forests on the west and other gums, mahogany, tallowwood, and ash in the wet forests further to the east. The lower elevations are dominated by savanna grasslands and woodlands given to sheep grazing and fruit growing. Water is supplied from the Burrinjuck Reservoir (*F*–15) along the Murrumbidgee River (*I*–18) and the Macquarie Reservoir (*E*–2) in the headwaters of the Lachlan River. *1034–23192;* August 26, 1972.

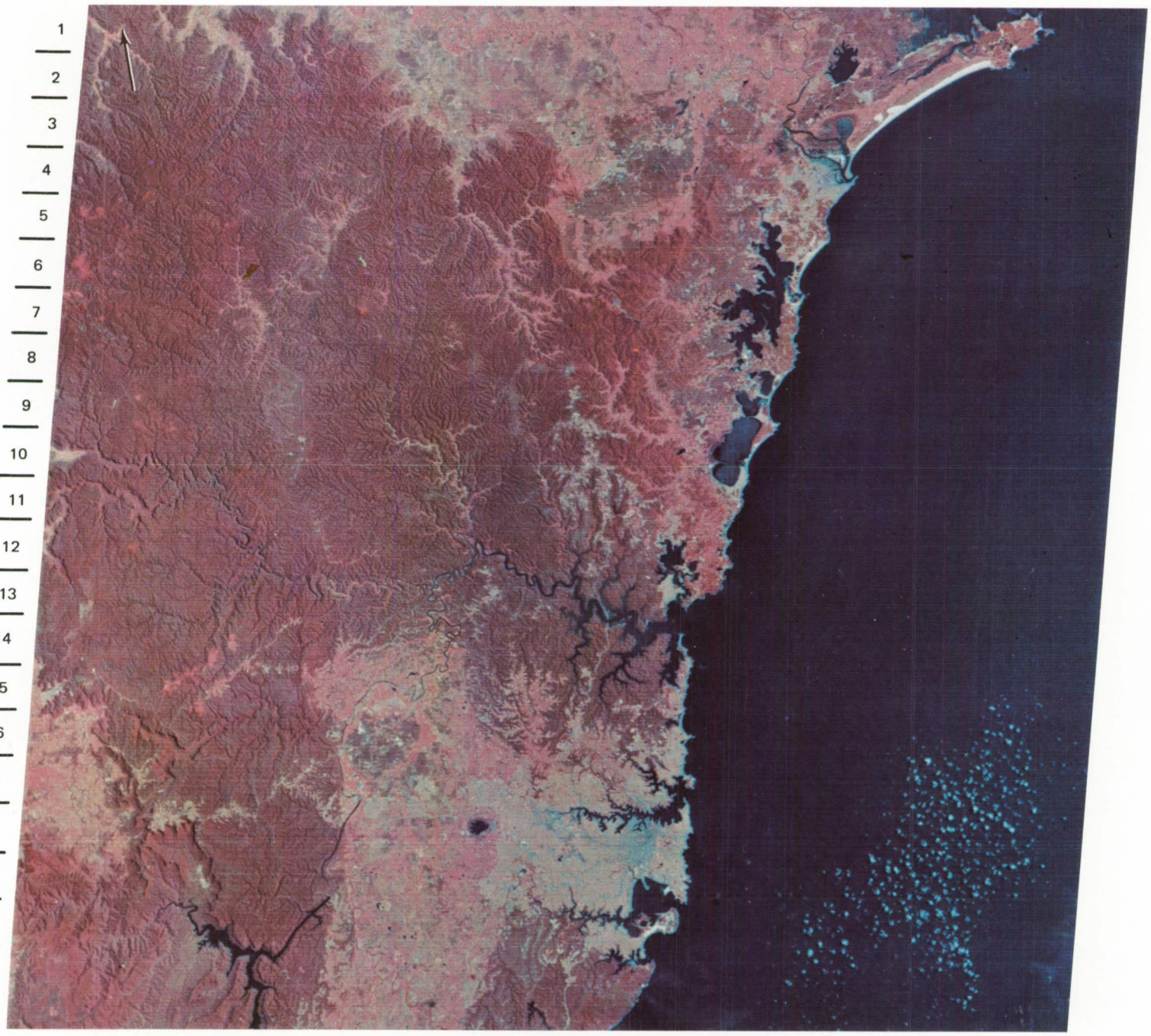
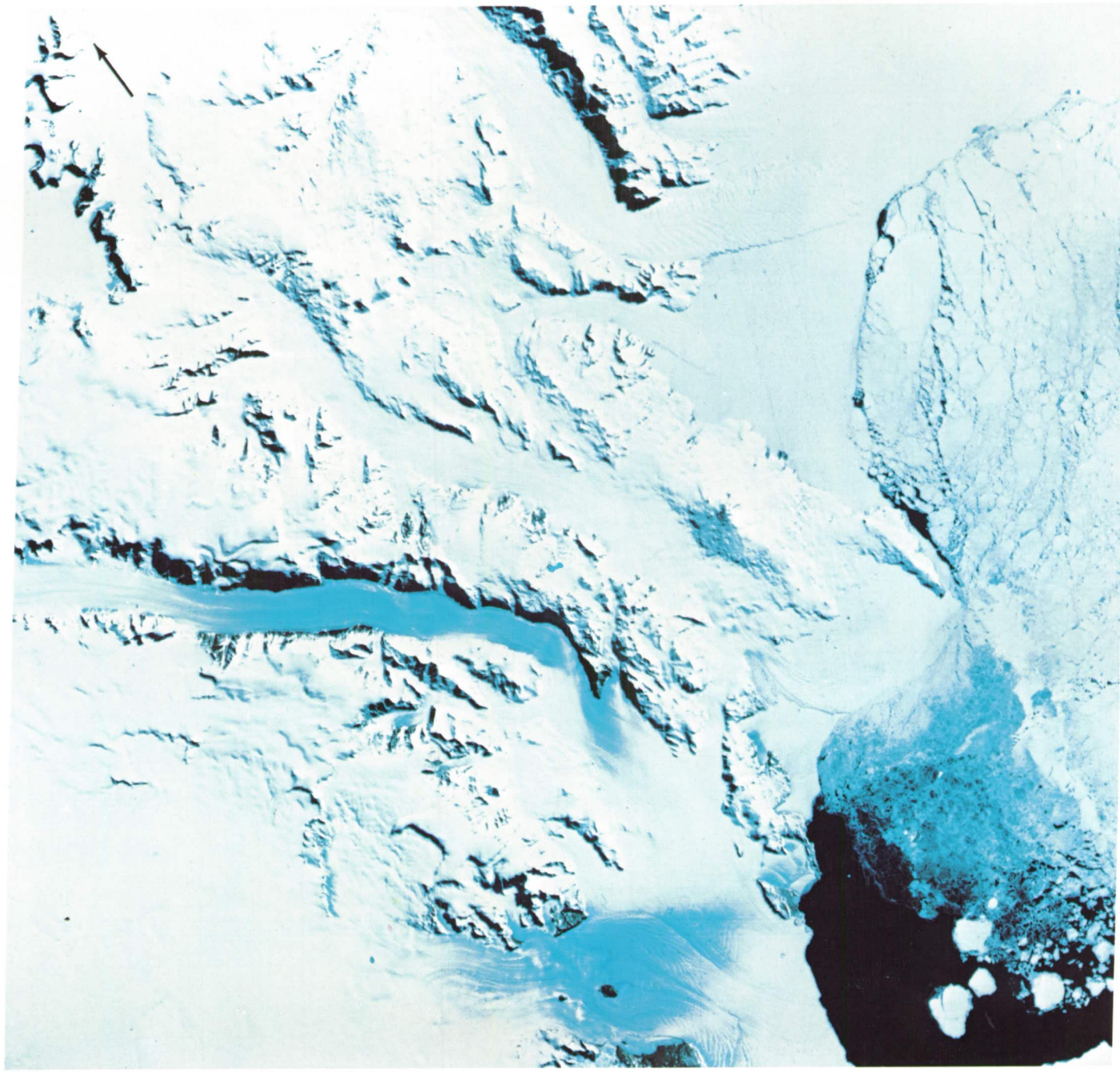


PLATE 392

SYDNEY, AUSTRALIA: The largest city (*M*–18) in Australia (nearly 3 000 000 people) is built up around Botany Bay (*M*–19) and Port Jackson (*N*–17) along the Pacific Ocean coast of New South Wales. The metropolitan area extends westward to the Prospect Reservoir (*J*–18). Sydney occupies a low plains cut into shales that are part of a gently folded (monoclinal) sequence of Triassic rocks. A thick Triassic sandstone unit makes up most of the Blue Mountains (*D*–14) and the Hunter Range (*C*–7) to the north. Rivers cutting through this plateau have produced many steep-walled narrow gorges (*B*–10). The principal stream is the Hawkesbury River (*J*–12), which begins in the Goulburn area (see plate 391) southwest of the straddling reservoir at Burragorang Lake (*E*–20) and empties into Broken Bay (*N*–14). The Nepean River (*H*–21) flows into the Hawkesbury system from the Illawarra Range (*K*–21) to the south, and the Colo River (*E*–12) passes into this drainage through canyons to the west. On the north, the Hunter River (*O*–2) flows across lowlands cut from Permian rocks en route to Newcastle (*P*–4), a steel-producing industrial center at the base of a Quaternary delta and marine spit (*R*–2) built into the ocean. Lake Macquarie (*O*–7), one of several lagoons tied to the sea, lies south of this area. The dissected plateau country west of the coast is heavily forested with eucalypts such as gum, mahogany, and ironwood and, in places nearer the coastlands, with tropical vegetation such as tree ferns, palms, and creeper vines. *1141–23140;* December 11, 1972.

PLATE 393



THE ANTARCTIC: This section of the great ice-covered continent of the Antarctic is centered approximately at 164° east longitude and 74° south latitude. The area is part of Victoria Land under the mandate of New Zealand, on the Scott coast of the Ross Sea (*U*–21). The Prince Albert Mountains line this coast, reaching a height of 2800 meters (9100 feet) here at Mount Levick (*D*–12) but a continuation of these folded ranges rises to 3700 meters (12 200 feet) in the Admiralty Mountains further north. The valleys between these high mountain spurs are now occupied by active glaciers, including Reeves (*N*–20) and Priestley (*I*–13) glaciers, which reach Terra Nova Bay (*R*–20), the Campbell glacier (*H*–9), and Aviator glacier (*K*–3), which flows out on to Wood Bay (*R*–5). The ice shelf (*S*–8) beyond these bays has begun to break up with the onset of the southern summer. *1128–20284;* November 28, 1972.

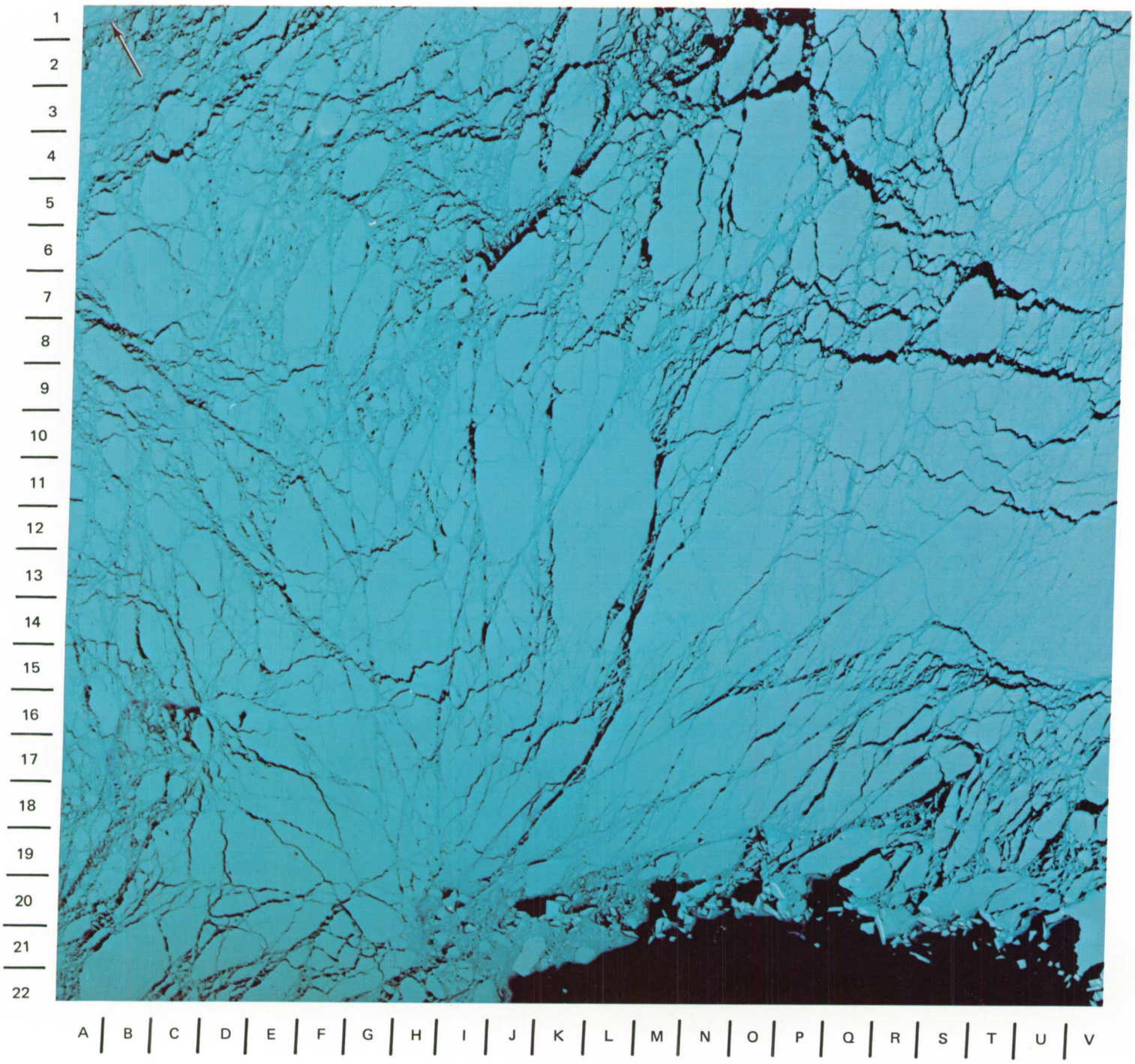


PLATE 394

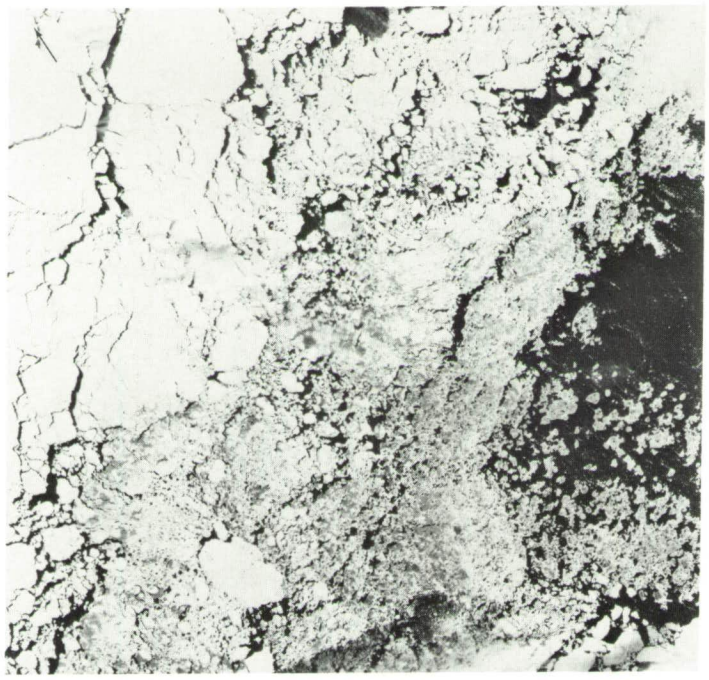
ANTARCTIC SEA ICE: This striking view shows the general breakup of sea ice off the coast of the Antarctic continent in the middle of the Austral summer. The area seen lies in the Amundsen Sea in the southeastern Pacific Ocean at a distance of about 240 kilometers (150 miles) from the coast of Marie Byrd Land, a section of the Antarctic under the jurisdiction of the United States.

Pacific Ocean currents circulate in a clockwise manner around the Antarctic (South Pole as reference). These currents tend to dislodge the continuous sea ice from the coastal waters and carry the sheets seaward and to the east. The ice breaks up along a series of long fractures or leads. The orientations of these leads is controlled in part by changes in wind directions during the breakup interval. Some leads tend to refreeze (polynyas) but eventually most large floe blocks will be broken into smaller fragments a few kilometers (miles) or less in long dimension. *2016–15062;* February 7, 1975.

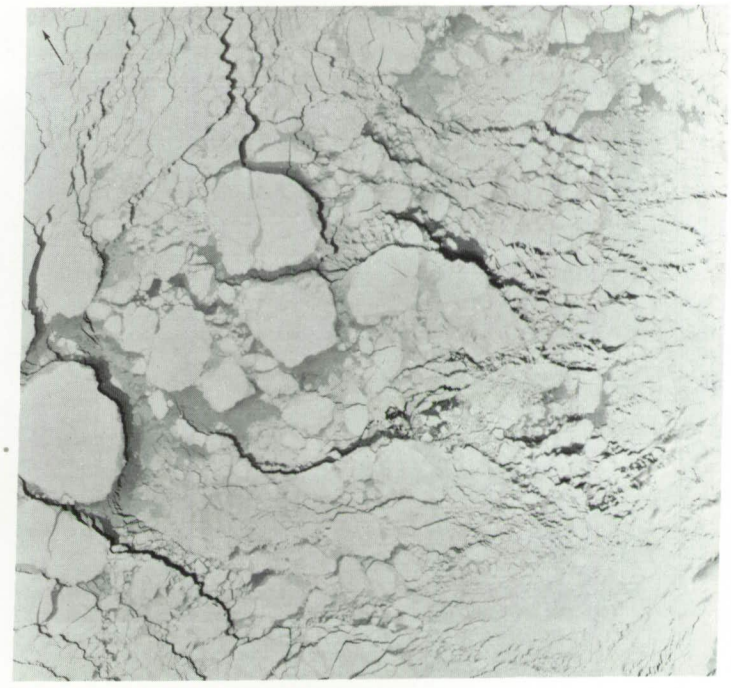
PLATE 395



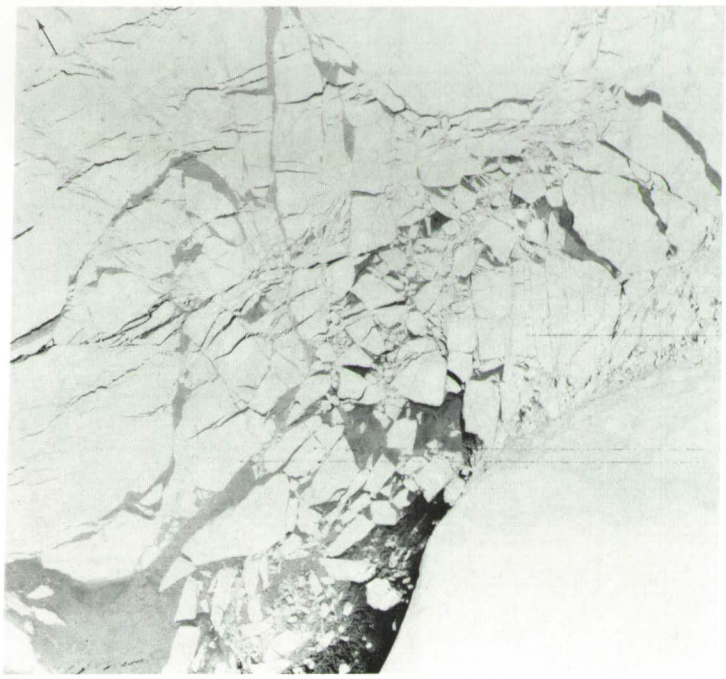
(a)



(b)

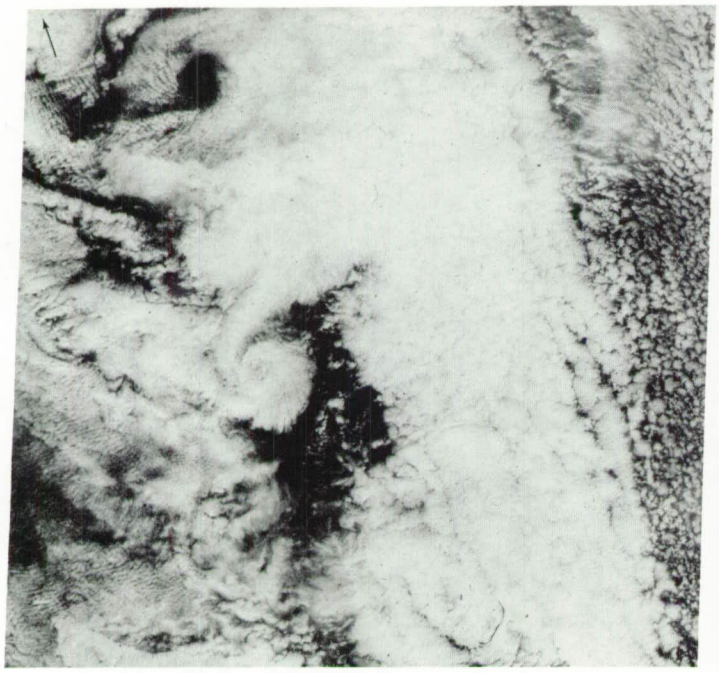


(c)

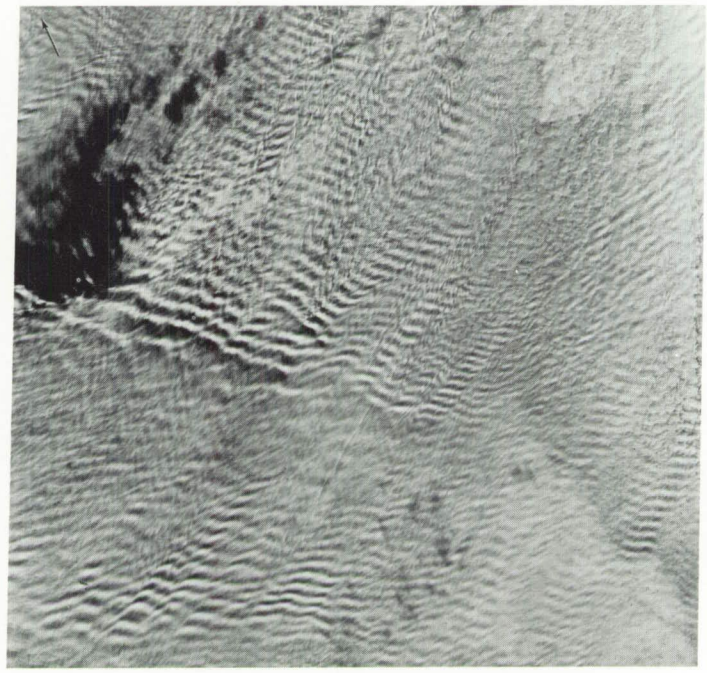


(d)

ICE: (*a*) Thin sea ice forming in the autumn off the northeast Greenland coast near Kap Broer Ruys. Swirl patterns indicate accumulation of thin ice particles caused by eddy current circulation. *1076–13023;* October 7, 1972. (*b*) Formation of open leads, refrozen leads, and ice floes due to recent divergence of sea ice near the edge of the late summer Arctic ice pack in the Siberian Sea. A mixture of small white ice floes and thin gray ice is evident in the center of the image. *1067–00082;* September 28, 1972. (*c*) Pattern of open leads, refrozen leads, and polynyas resulting from successive divergences of Arctic sea pack ice. Large multiyear ice appears at the left. *1081–23512;* October 12, 1972. (*d*) The edge of shore-fast ice and the deformation and drift of the pack ice in relation to the north coast of Alaska near Point Barrow. *1242–22032;* March 22, 1973.



(a)



(c)

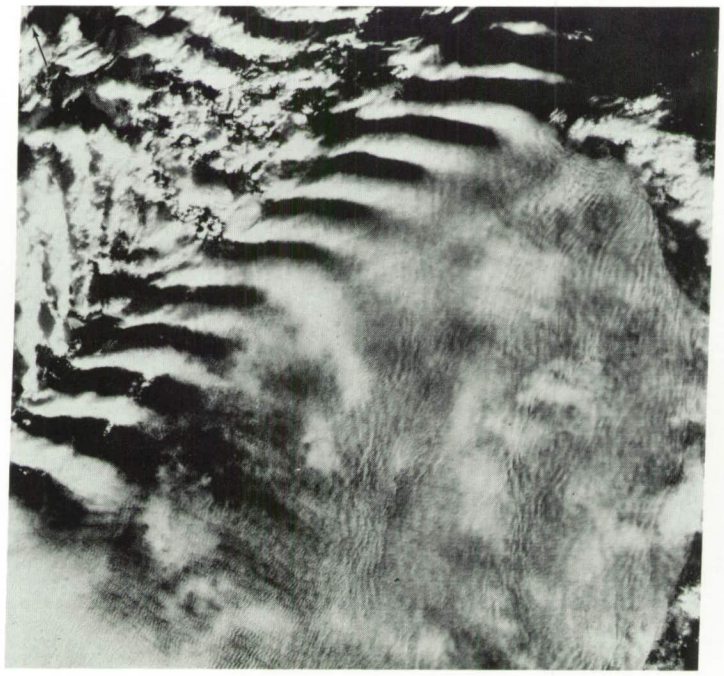


(b)

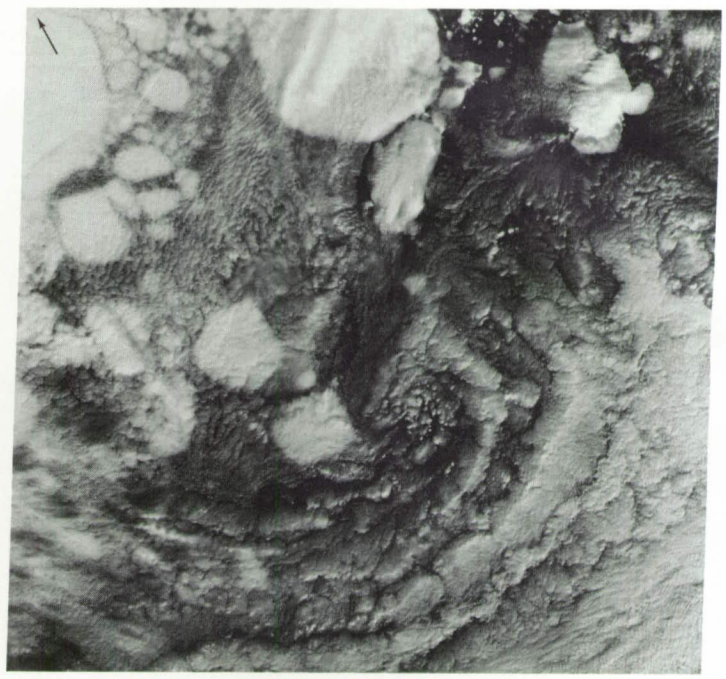


(d)

CLOUDS: (*a*) *Cumulus, stratocumulus, and cirrus*—two tightly wound vortices in the vicinity of the Shetland Islands appear to be mirror images of one another. A light surface wind perturbed by the islands may have set up this unique twin vortex pattern. *1056–11113;* September 17, 1972. (*b*) *Stratocumulus*—closed convective cells, sometimes called Bernard cells, appear northeast of Norway in the Barents Sea. This type of closed cellular pattern generally indicates weak convective mixing with a subsidence inversion to cap the convection. The cell structure is more distinct in the northeast section of the image. *1038–09245;* August 30, 1972. (*c*) *Stratocumulus* and *cirrus*—numerous waves, looking almost like receding waves on a beach, ripple across the Kola Peninsula and the Barents Sea. The fuzzy appearance of some of the waves in the lower half may be the result of thin cirrus. *1083–08344;* October 14, 1972. (*d*) *Cumulus, stratus, stratocumulus,* and *cirrus*—islands in the Bering Sea disrupt the low-level windflow producing visible shock waves on the windward side of the islands. On the lee side of these islands, lee waves are propagated that extend for many kilometers (miles) downward. Over the land, right and left center, typical convective cumulus clouds can be seen compared with the more sheetlike stratocumulus over the water. *1029–22212;* August 21, 1972.

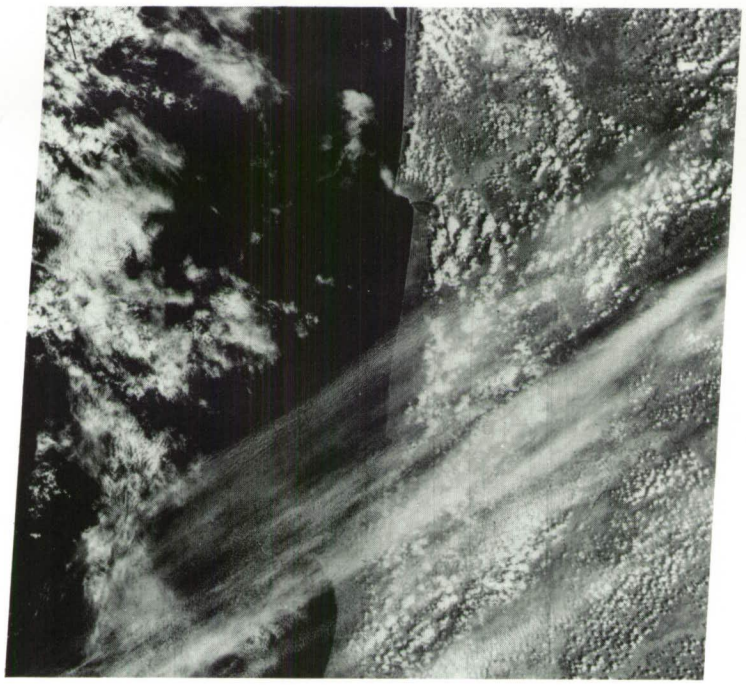


(a)

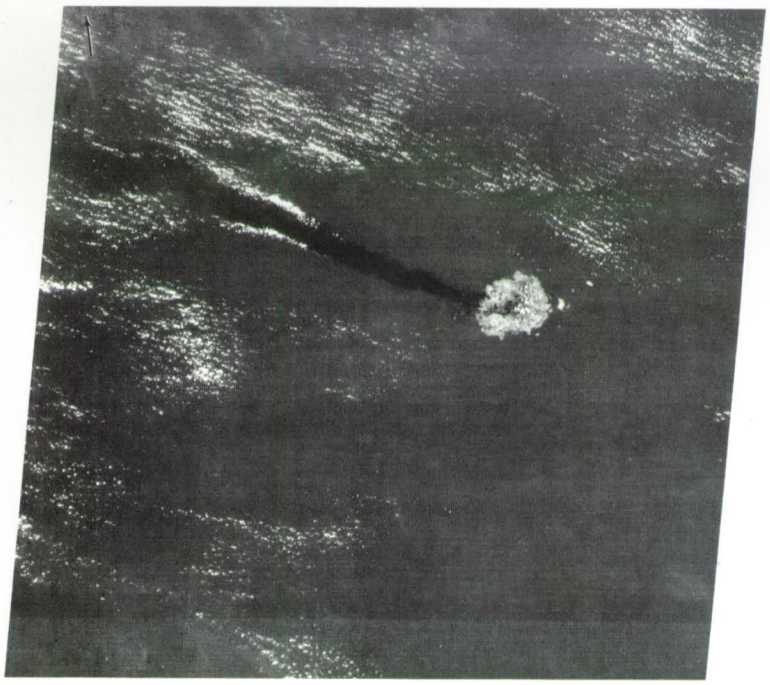


(c)

PLATE 397



(b)



(d)

CLOUDS: (*a*) *Cumulus, altocumulus,* and *altostratus*—a unique wave pattern has been set up along the east coast of Iceland. This riblike pattern of altocumulus clouds is very distinct along the coast, but becomes less so as it extends inward. Seaward the pattern merges into a more continuous altostratus layer consisting, in some areas, of small waves running normal to the general air flow. Brighter areas throughout the more continuous layer plus shadows on a group of cumulus clouds in the upper right indicate multicloud layers. *1082–11565;* October 13, 1972. (*b*) *Cirrus, cirrocumulus,* and *cumulus*—two different cloud-forming mechanisms are at work over Spain. A high-level jetstream running from the southwest to the northeast is producing bands of cirrus and cirrocumulus in the warmer air on the south side. At lower levels the effects of differential heating of the land and water plus onshore winds are evidenced by the numerous cumulus clouds formed a short distance inland. *1033–10491;* August 25, 1972. (*c*) *Cumulus* and *stratocumulus*—a collage of clouds and ice combine in this part of the Beaufort Sea north of Alaska. Wave clouds predominate over the extensive ice located in the upper left. The clouds change to smaller closed convective cells once they reach the warmer water. The arrangement of these cells suggests relatively light winds. *1064–20302;* September 25, 1972. (*d*) *Oceanic wind wake*—the peak of the central mountain on the small Bawean Island of Indonesia located in the Java Sea between Java and Borneo is about 670 meters (2200 feet) above sea level. A dark, widening strip, showing as an area of lower reflectivity (darker gray tone), extends from the island to the northwest. It is interpreted as a region of calmer water (lower sea state) that exists in a corridor of lowered wind velocity because of the blocking effect of the island mountain. This calm zone is visible for more than 105 kilometers (65 miles) downwind (leeward) from the island. Cumulus cloud lines along the edge of this wind wake, starting about 40 kilometers (25 miles) downstream of the island, are caused by aerodynamic effects associated with the wake. *1102–02093;* November 2, 1972.

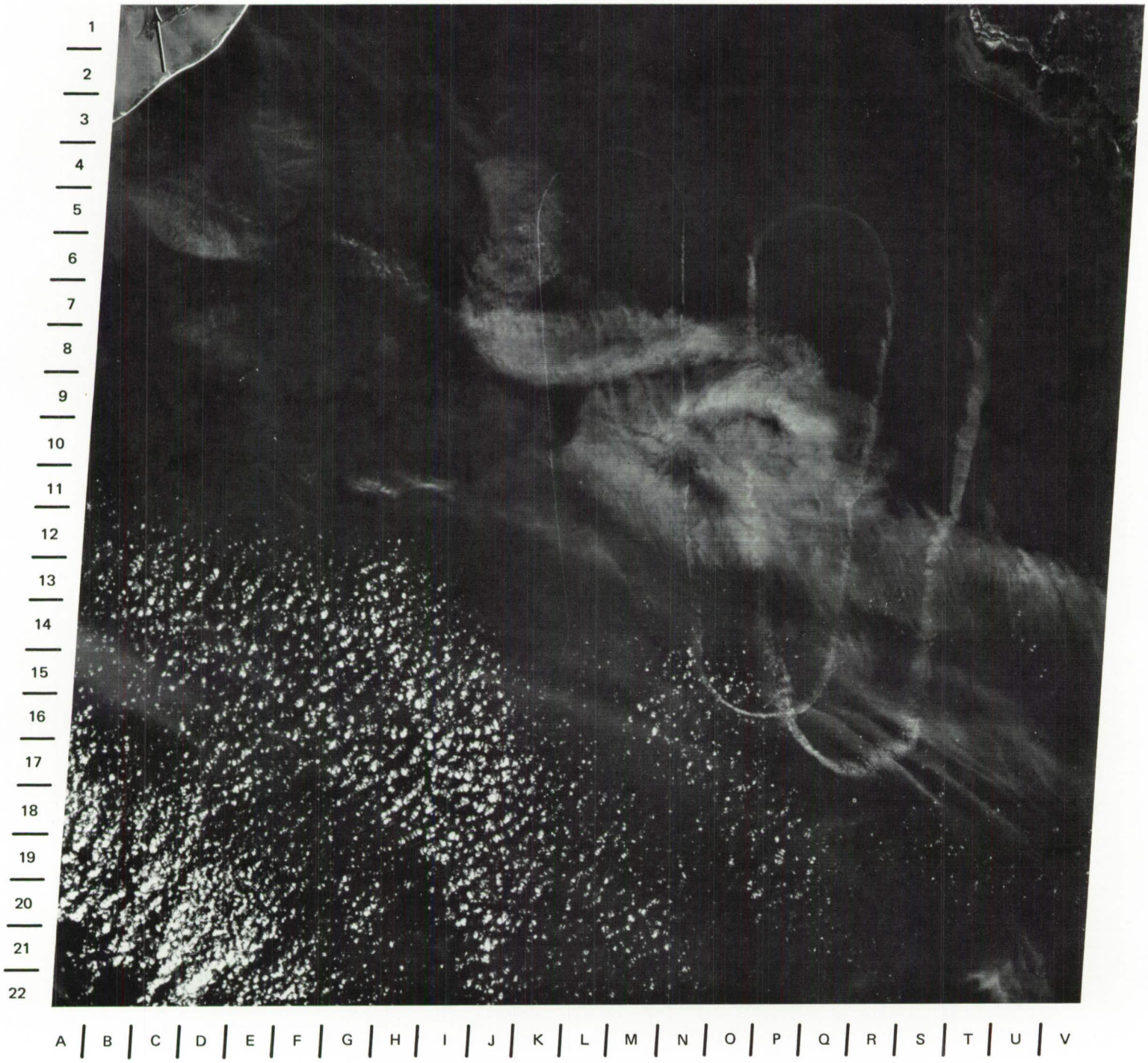
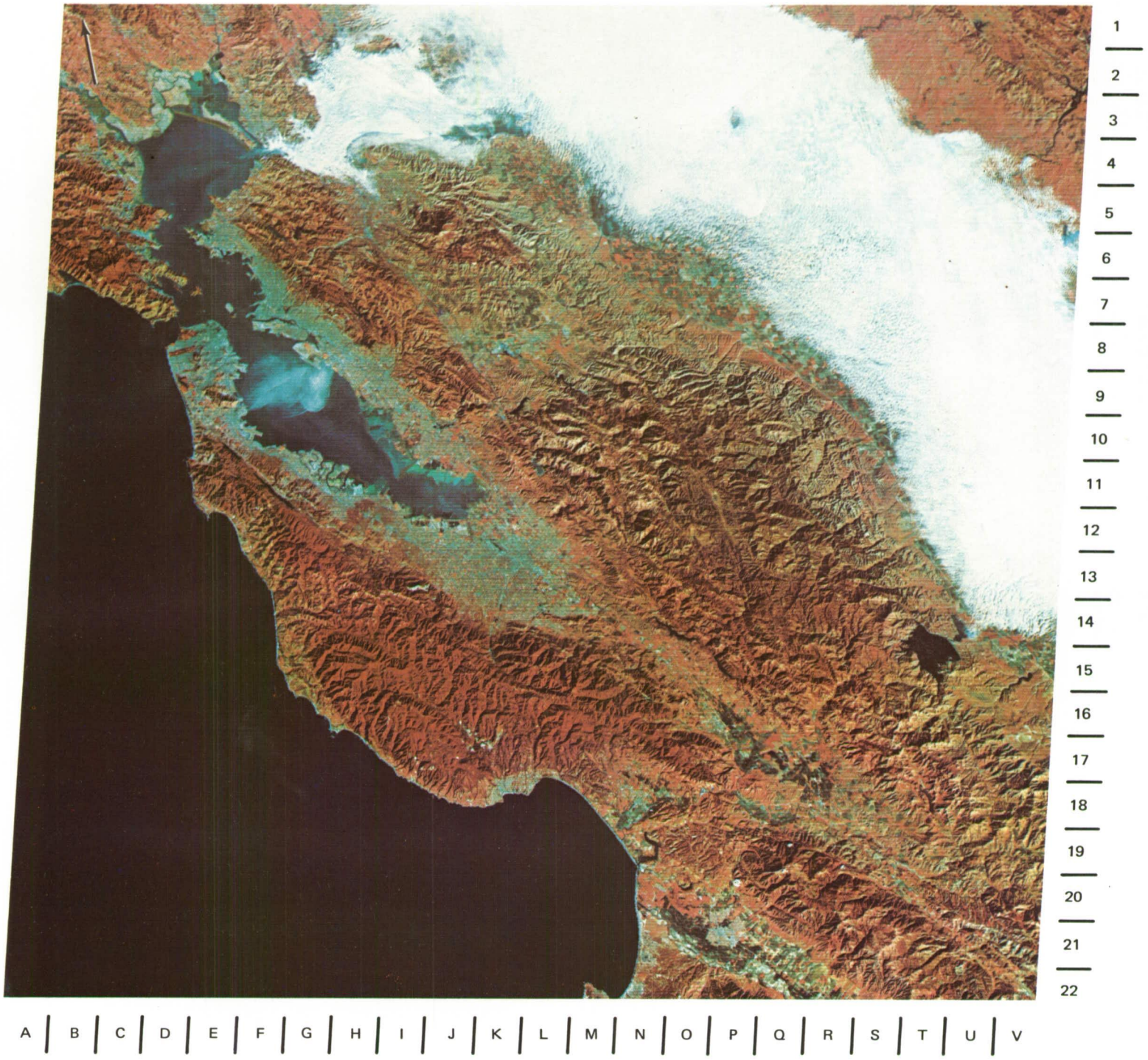


PLATE 398

THE LONGEST CONTRAIL: A condensation vapor trail from a high-flying aircraft was imaged by chance during this passage of Landsat 1 in midwinter of 1973 over the northeast part of the Gulf of Mexico. The area shown is off the northwest coast of Florida south of Apalachee Bay and Tallahassee. The plane was flying a series of approximately north to south passes, each about 80 kilometers (50 miles) in length and 24 kilometers (15 miles) apart. The contrail is first visible on the east side and can be followed for a total path length of at least 560 kilometers (350 miles). The contrail narrows in width toward the lower center of the image and appears to reach a pinpoint position, presumably where the aircraft was at the moment of image acquisition, just at the edge of the cumulus clouds in the lower left corner. Assuming the plane to be a reconnaissance jet flying at 9100 meters (30 000 feet), or higher at a speed of at least 970 kilometers per hour (600 miles per hour), the contrail has survived, even though blown southeastward and widened by upper level winds, for more than 35 minutes. It is not known whether this was a military aircraft on maneuvers, a weather monitoring aircraft, or a NASA plane engaged in obtaining "ground truth" data for a Landsat investigation. *1191–15395;* January 30, 1973.

PLATE 399



SAN FRANCISCO: Further advances in the Landsat program were assured by the successful launch of Landsat 2 on January 22, 1975. This spacecraft has identical data-gathering systems to Landsat 1. Both satellites have operated simultaneously for 12 months, providing data on a 9-day repeat cycle.

As this spectacular view of the San Francisco Bay area clearly demonstrates, the multispectral scanner on Landsat 2 functioned perfectly just after being turned on 2 days after launch to produce imagery of high quality. This midwinter scene is especially sharp because of the enhancement of topography by the low Sun angle. Comparison with images taken later in the season, as, for example, with the image in plate 126, reveals many subtle features in the Coast Ranges seen only with difficulty in those images. This is particularly well illustrated by the rolling hills just south of Mount Diablo (*I*–5). The inclined rock strata, which are expressed by linear ridges, now stand out sharply, along with a prominent north to south fault (*J*–7). The writer of this caption for several years used to drive to and from work through these hills but did not realize, until viewing this scene, the specific nature of the surface expression of the local geology there.

Other features of interest include an early morning ground fog persisting in the Sacramento Valley (*L*–1; *V*–10) and dispersing plumes of smoke (*E*–9) from an industrial area in south San Francisco. *2002–18063;* January 24, 1975.

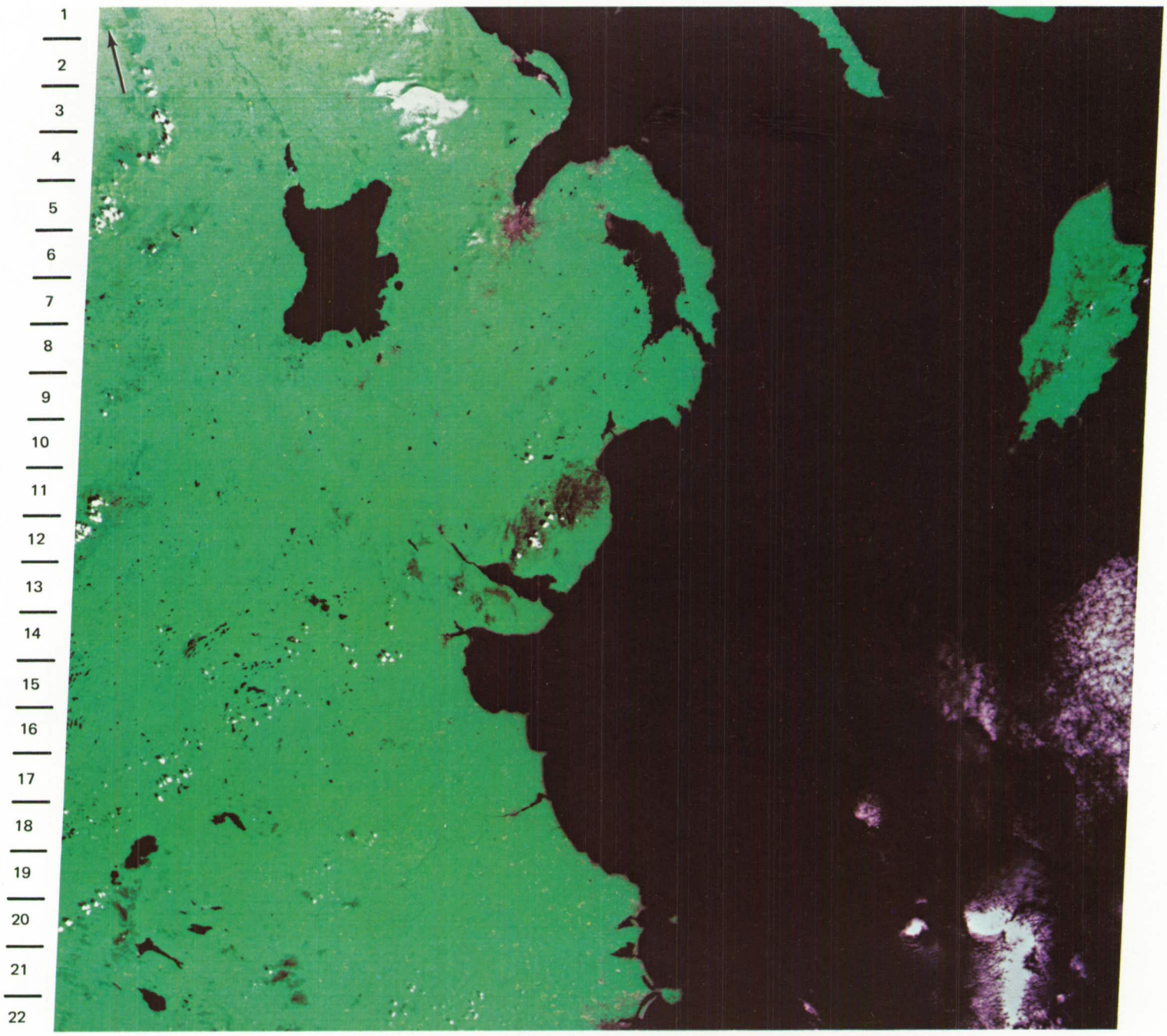


PLATE 400

IRELAND: One of the advantages of the continuity in the Landsat program, in which at least one Landsat spacecraft would "always be flying," is demonstrated by this view of the east coast area of Ireland. Efforts were made several times during the period when Landsat 1 operated alone to obtain a near-cloud-free image of the "Emerald Isle." However, each attempt was foiled by extensive cloud cover. After the launch of Landsat 2, success was finally achieved by that satellite in late spring of 1975. In this image, Ireland is shown with band 7 projected through a green instead of a red filter.

Part of both Northern Ireland (*C*–3) and Ireland (*C*–16) are shown in this scene. The city of Belfast (*J*–5), on the Belfast Lough (*J*–4), lies between the Lough Neagh (*F*–6) and Strangford Lough (*L*–6), two large inland lakes. The city of Baile Atha Cliath or Dublin (L–22) is partly visible at the bottom of the image. Most of the rolling countryside of Ireland is thickly covered with grass and pasture lands, scrub, and woodlands. The effect of this continuous carpet of vegetation is strikingly revealed in the uniformity of the red tones that express the infrared signature of plant matter. It is difficult at this time of year to separate cultivated lands from natural vegetation. Brownish-black tones in the scene are mainly vegetation-sparse hills, such as the Mourne Mountains (*K*–11), which rise to nearly 900 meters (3000 feet) close to the coast. Part of the Lake Country of central Ireland appears at the lower left.

The large island at the far right is the Isle of Man (*U*–7). Two tips of Scottish land, at the Mull of Galloway (*P*–1) and Burrow Head (*T*–1), are visible just beyond the North Channel (*M*–2). *2139–10451;* June 10, 1975.

PAGE MISSING FROM AVAILABLE VERSION

APPENDIX A

*The Landsat System**

MISSION AND SYSTEM REQUIREMENTS

The primary Landsat mission was to demonstrate the feasibility of multispectral remote sensing from space for practical Earth resource management applications. The overall system requirement was the acquisition of multispectral images, the collection of data from remotely located ground platforms, and the production of photographic and digital data in quantities and formats most helpful to potential users. In addition, it was required that these data be taken in a specific manner: namely, that repetitive observations be made at the same local time; that the images produced by the sensors be overlapping, both in and across the direction of flight; and that the images be correctly located to better than 3.7 km (2.3 miles). Periodic coverage of each area was to occur at least every 3 weeks. The operating lifespan of the spacecraft and its sensor systems was to be a minimum of 1 yr. Finally, it was necessary to process and distribute all these data to investigators in a useful form and on a timely basis.

SPACECRAFT

To accomplish these goals, the Landsat spacecraft was designed and built by the Space Division of General Electric in Valley Forge, Pa. This spacecraft, an outgrowth of the Nimbus series of meteorological satellites, was designed to carry two remote sensing systems and a system for collecting data from sensors located in remote places on the Earth (data collection system (DCS)). Some of the more pertinent parameters of the spacecraft are given in table A–1.

TABLE A–1.—*Landsat Spacecraft Characteristics*

Weight	959 kg (2100 lb)
Size	3 by 1.5 m (10 by 5 ft); 4-m (13-ft) array
Power	550 W
Attitude control	±0.7°
Attitude measurement	±0.07°
Telemetry	912 points
Commands	520 commands
Thermal	20° C
Wideband videotape recorder	30-min recording capacity each (two recorders on board)
Orbit adjust	~80 m/s

ORBIT

The Landsat 1 spacecraft was launched on July 23, 1972, and positioned in the orbit shown in figure A–1 and table A–2. It has a nominal altitude of 917 km (570 miles); a 99° orbital inclination, which makes it nearly polar; and a Sun-synchronous orbit, which means that the orbit plane precesses about the Earth at the same angular rate that the Earth moves about the Sun. This feature enables the spacecraft to cross the Equator

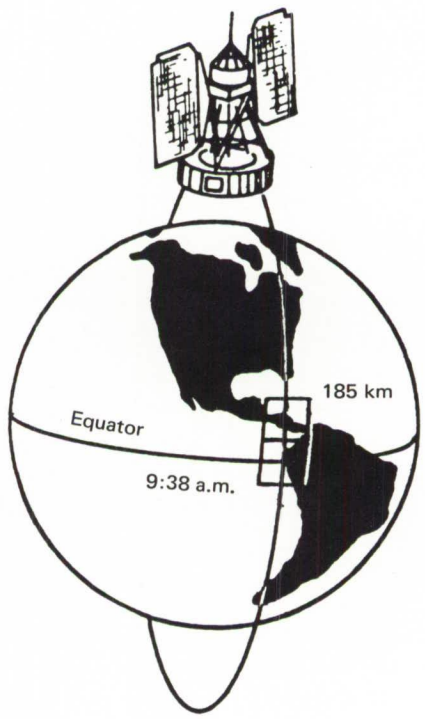


FIGURE A–1.—Landsat 1 spacecraft orbit.

at the same local time (about 9:30 to 10:00 a.m.) on the sunlit side of the Earth. Each of the two sensing systems (return beam vidicon (RBV) and multispectral scanner (MSS)) views an area 185 km (115 miles) on a side. Figure A–2 indicates how the requirement for repeat coverage is met. From one orbit to the next, the subsatellite point moves 2875 km (1785 miles) at the Equator as the Earth rotates beneath the spacecraft. The next day, 14 orbits later, it is approximately back to its original location, with orbit 15 displaced westward from orbit 1 by 159 km (99 miles) at the Equator. This continues for 18 days after which orbit 252 falls directly over orbit 1. As indicated in figure A–2, there is a sidelap of 26 km (16 miles) in coverage at the Equator from adjacent orbits on consecutive days. It is important to note that this sidelap increases with increasing latitude, to approximately 57 percent at 60°. Thus, at high latitudes, sidelap coverage is

TABLE A–2.—*Landsat 1 Orbital Parameters*

Parameter	Nominal	Initial correction	Current [a]
Altitude of apogee, km (miles)	917 (570)	912 (567)	919 (571)
Eccentricity	.0001	.0005	.0020
Apogee/perigee difference, km (miles)	1 (1.6)	9 (6)	22.7 (14.1)
Period, min	103.34	103.26	103.26
Inclination, deg	99.09	99.12	99.03
Descending node (a.m.)	9:30	9:42	9:38
Coverage cycle, days	18	18	18

[a] After 7 orbit corrections through February 4, 1974.

* Written by Stanley C. Freden, *Goddard Space Flight Center.*

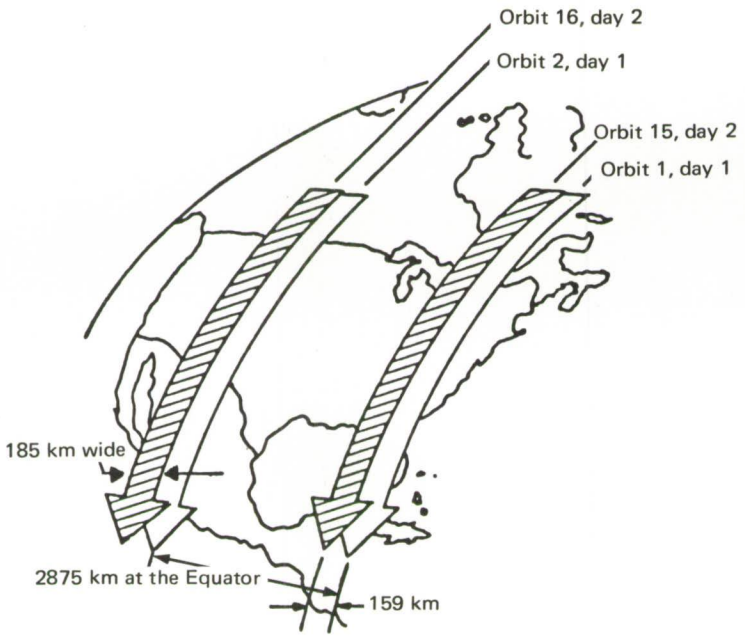


FIGURE A–2.—Landsat ground coverage pattern. There are 14 revolutions per day; global coverage is obtained in 18 days.

obtained on consecutive days over a large portion of an image. Sidelap coverage is essential for stereoscopic or three-dimensional viewing; it also permits the monitoring of changes that occur over the 1-day period. It should be noted, however, that as the area of sidelap increases with latitude, the stereoscopic viewing angle decreases.

PAYLOAD

The sensors are mounted on the bottom of the spacecraft. The RBV system consists of three television-type cameras, each covering a different spectral region; images are obtained on a frame-by-frame basis. The spectral characteristics of the RBV system are shown in table A–3. The time between picture sets is 25 s, and readout time is 3.5 s per camera. There are five exposure combinations, running from 4 to 16 ms: (1) 4, 4.8, and 6.4; (2) 5.6, 6.4, and 7.2; (3) 8, 8.8, and 8.8; (4) 12, 12, and 12; and (5) 16, 16, and 16. Data are transmitted by the vidicon cameras at 3.5 MHz FM.

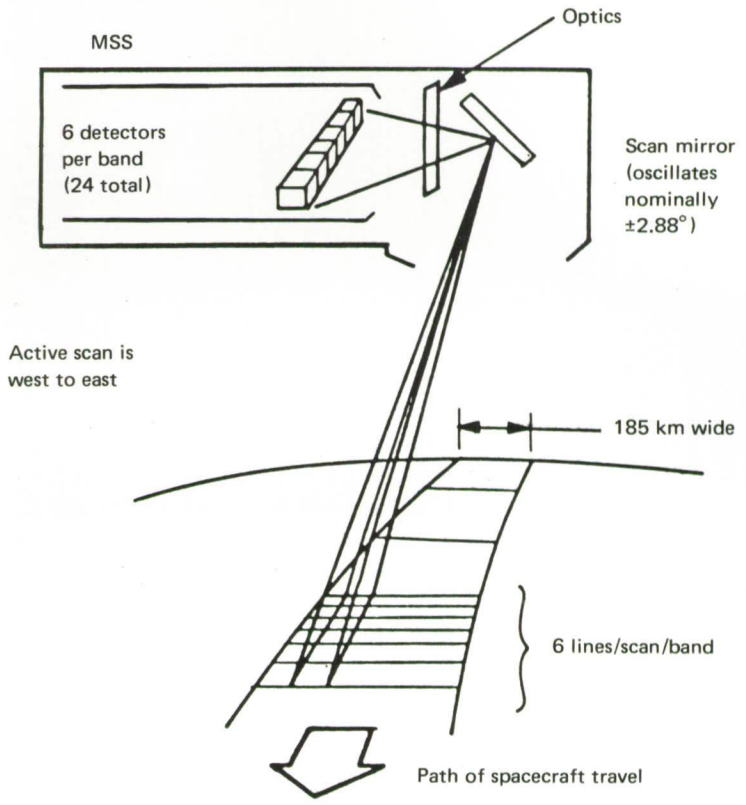


FIGURE A–3.—MSS orientation.

The three vidicon cameras are mounted on the base plate with their optical axes alined. Fiducial marks, engraved into the photoconductor of each camera, are used in the geometrical correction of the images on the ground.

Figure A–3 depicts both the concept of the MSS multidetector array and the scanning system. The scanning mirror oscillates through an angular displacement of $\pm 2.89°$. Because the angle of incidence is equal to the angle of reflection, the scanned beam is approximately 11° wide. Six parallel detectors in each of the four bands view the ground simultaneously. The instantaneous field of view on the ground of each detector is 79 m square (259 ft square). Thus, each mirror scan covers an along-track distance of approximately 480 m (1574 ft) on the ground.

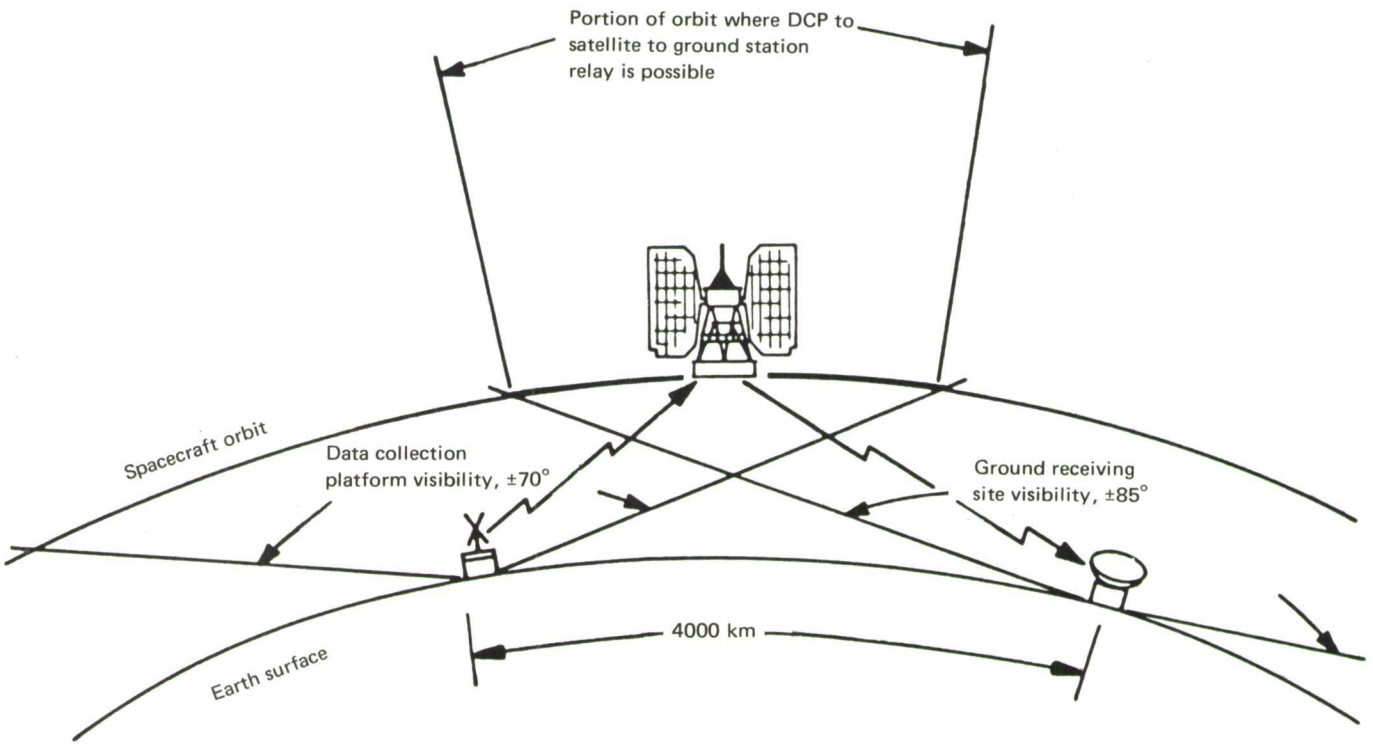


FIGURE A–4.—DCS data relay geometry. (DCP=data collection platform.)

TABLE A–3.—*Summary of Landsat 1 Payload Systems*

High resolution TV (RBV) cameras:	
Coverage	185 by 185 km (100 n. mi.)
Spectral bands:	
1	0.48 to 0.57 μm
2	0.58 to 0.68 μm
3	0.69 to 0.83 μm
Data	3.5 MHz video
4-channel MSS:	
Coverage	185 km (115 mi.) swath
Spectral bands:	
4	0.5 to 0.6 μm
5	0.6 to 0.7 μm
6	0.7 to 0.8 μm
7	0.8 to 1.1 μm
DCS:	
Ground platforms	Up to 1000
Ground platform input	8 analog or digital signals
Data	100 kHz digital

The ground resolution is effectively about 80 m (262 ft). However, the ability to distinguish adjacent objects depends greatly on their contrast. In fact, bridges over water and dirt roads passing through vegetation are visible to widths of 10 m (33 ft).

The DCS provides a mechanism for relaying data collected from remotely situated ground-based sensing platforms and retransmitting through the satellite to the receiving stations. These data are then quickly retransmitted to the data users. Each ground platform can have eight analog or digital inputs. The system has a high probability that data will be received from every platform within each 12-hr period. These sensing platforms are used to measure waterflow in rivers, water level, water quality, seismic activity, and similar phenomena. Figure A–4, showing the geometry of the DCS, demonstrates that the spacecraft must be in view of both the platform antenna and the ground receiving antenna.

Table A–3 summarizes the Landsat payload and the parameters of the three major payload systems.

GROUND DATA HANDLING

A block diagram of the total Landsat data system is shown in figure A–5. Video data from the sensors are telemetered to Earth and acquired at three data acquisition centers in the United States (Fairbanks, Alaska; Goldstone, Calif.; and Greenbelt, Md.). In addition, Canada, Brazil, and Italy have ground receiving stations for Landsat data, and several more countries are in the process of negotiating agreements with NASA to build them. The data from the U.S. stations are sent to the NASA Data Processing Facility (NDPF), which is part of the Landsat ground data handling system (GDHS) at the Goddard Space Flight Center. In the NDPF, user products—both photographic and digital tape—are produced and distributed to the various Federal data centers. Requirements for additional coverage are fed into the Operations Control Center (OCC). The OCC is responsible not only for the housekeeping management of the spacecraft, such as power budgeting, but also for command sequences that will activate and deactivate the several sensors. Because both the recording capacity of the onboard video tape recorders and the power of the spacecraft are limited, the operation of the sensors must be scheduled very carefully. Figure A–6 illustrates a typical day for this scheduling. As of this writing, both tape recorders on Landsat 1 are inoperative and one recorder is still operative on Landsat 2.

The NDPF must handle information from various sources, such as the video signals from the two instruments; the ephemeris, which is computed from the orbital tracking data; spacecraft performance (for example, attitude); and the DCS platform data. From these the NDPF generates images and photographically processes and distributes them to the various

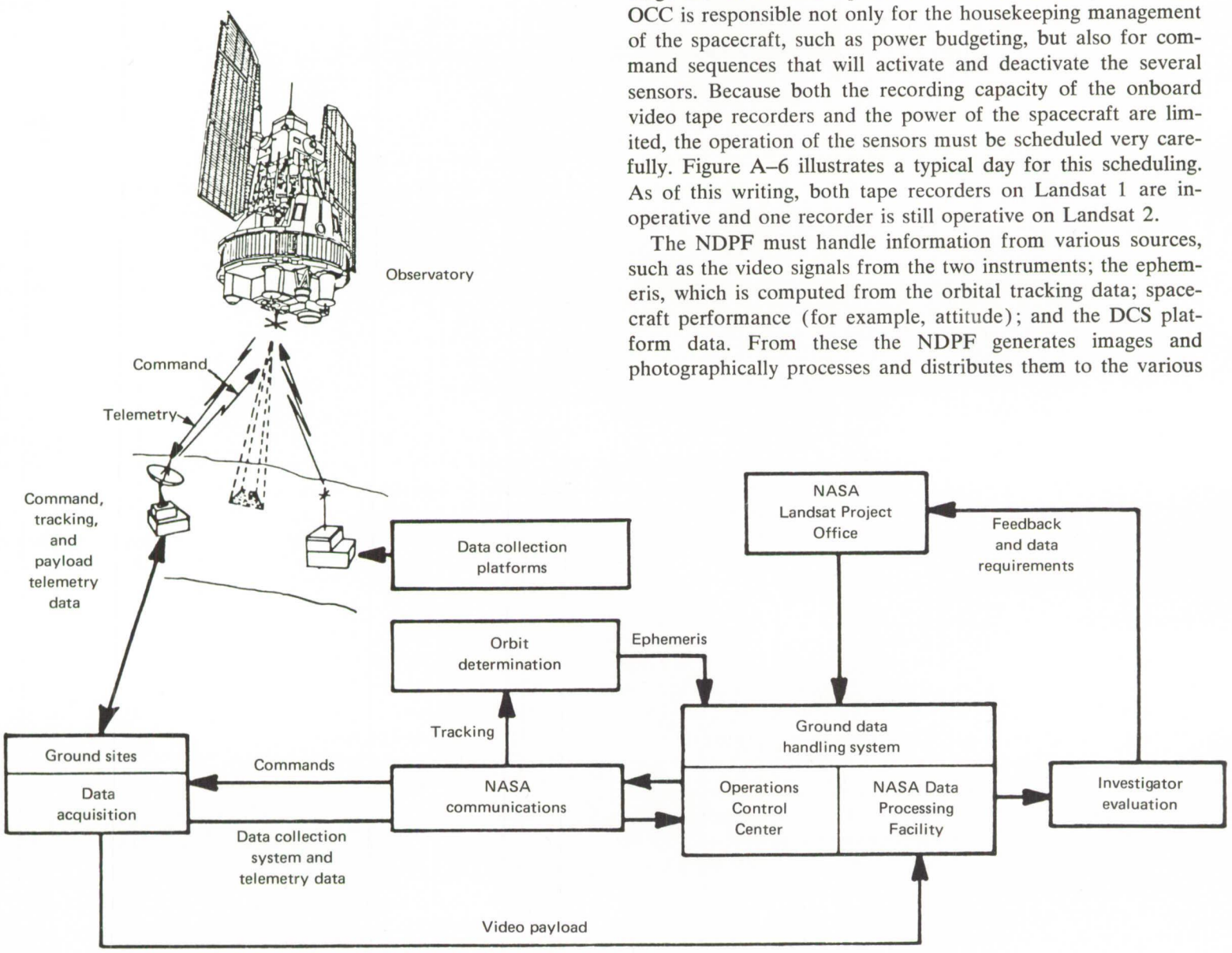


FIGURE A–5.—Landsat 1 data system.

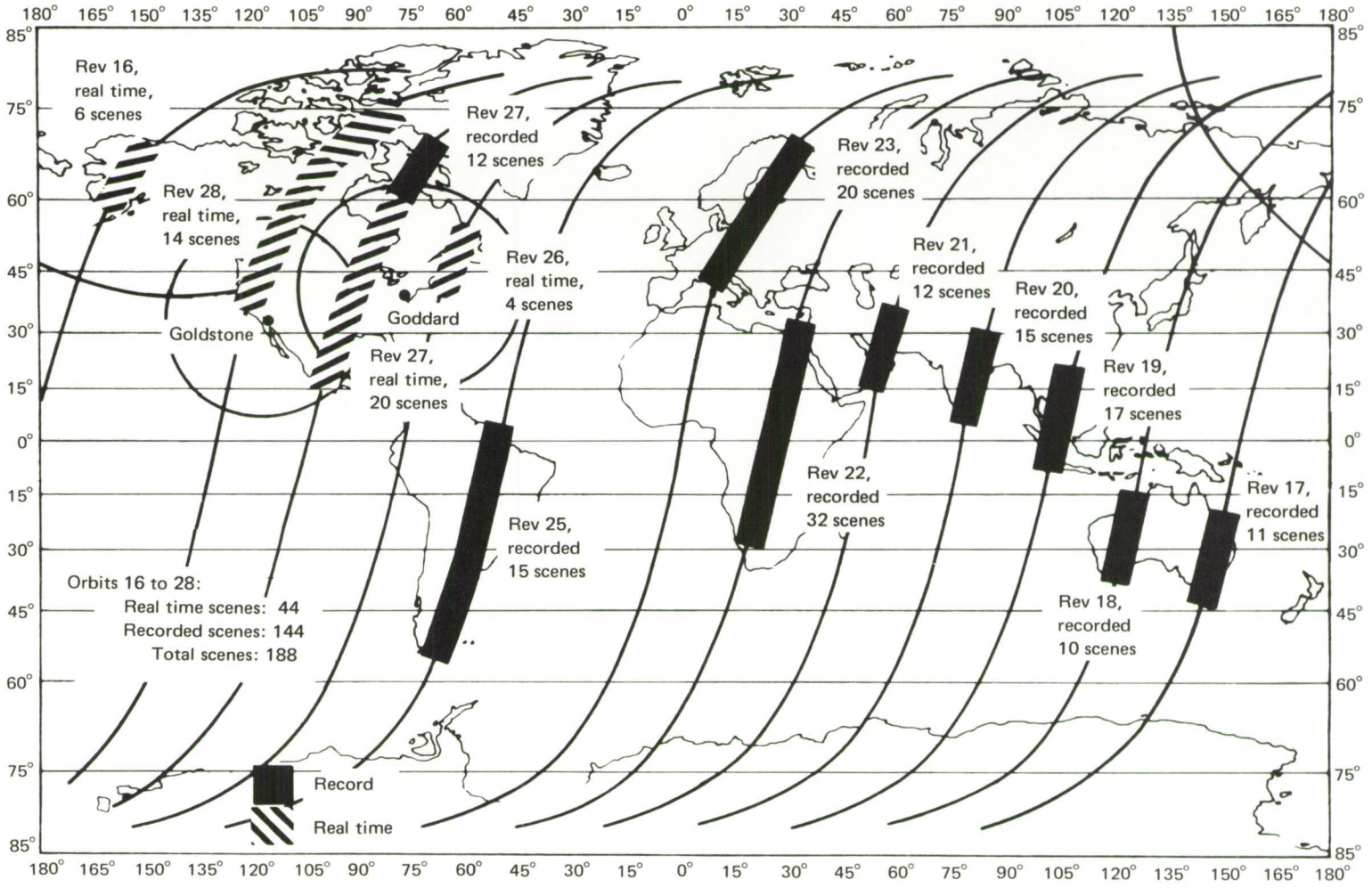


FIGURE A–6.—Typical Landsat daily coverage. (Solid bars=areas where data are recorded on wideband videotape recorders; dashed bars=areas where data are transmitted in real time to the ground.)

agencies. The NDPF provides digital tapes of these images, as well as a number of user services, such as prescreening of the data, preparation of catalogs, and cross-referencing. Some of the general requirements of the NDPF include the ability to process a total of 1500 scenes a week from the RBV and MSS systems. The facility also processes data from up to 1000 data collection platforms (DCP's) and provides 23 standard output data products. The images are corrected and scaled to a Universal Transverse Mercator (UTM) projection. They are also annotated with coordinates, gray scale, and geometric and other identifications. To generate these initial images, data are combined in what is called the initial image generation subsystem. These data include calibrations; transfer functions of radiance to voltage; and image annotation tapes containing information on the ephemeris, time of day, orbit, and location. The initial photographic images are produced on 70-mm film and then processed to produce both 70-mm and 24.1-cm (9½-in.) second-, third-, and fourth-generation products.

PRODUCTS

The NDPF must process the images rapidly, maintain a system for quick retrieval of data, and answer requests for fast delivery of products. The products produced by this system include 70-mm black and white positive and negative transparencies, 24.1-cm (9½-in.) black and white positive transparencies and prints, 24.1-cm (9½-in.) color transparencies and prints, and 7- or 9-track computer-compatible tapes (CCT's). As part of the data retrieval function, the NDPF produces catalogs containing U.S. scenes, non-U.S. scenes, and the DCS data. The *U.S. Standard Catalog,* published monthly, has maps of the continental United States with estimated cloud cover, a world map covering Alaska and Hawaii, listings of image identifiers and imagery by coordinates, and 16-mm microfilm of representative imagery. The *Non-United States Standard Catalog,* published monthly, has a world outline map depicting coverage acquired during the 18-day cycle, listings of image identifiers and imagery by coordinates, and 16-mm microfilm of representative imagery. The *DCS Catalog,* published periodically, provides summary information on DCS platforms, a list of investigators owning platforms with their addresses, and the discipline of each platform.

All Landsat data are sent to the three established federal data centers for distribution to the public. These are located at Sioux Falls, S. Dak. (U.S. Department of the Interior); Salt Lake City, Utah (U.S. Department of Agriculture); and Suitland, Md. (U.S. Department of Commerce). The data have also been distributed to over 300 principal investigators in the various disciplines as shown in table A–4.

The color composite images produced by the Landsat system are not in the normal or true colors familiar to photog-

TABLE A–4.—*Landsat 1 Investigations*

Discipline	United States	International	Total
Agriculture/forestry/range resources	37	13	50
Land use survey and mapping	27	7	34
Mineral resources, geological structure, and landform surveys	40	27	67
Water resources	27	15	42
Marine and ocean surveys	22	8	30
Meteorology	2	2	4
Environment	24	5	29
Interpretation techniques development	22	3	25
Sensor technology	4	0	4
Multidisciplinary resources survey	7	19	26
Total	212	99	311

raphers. The first MSS band, in the spectral region of 0.5 to 0.6 μm, is in the green; the second band, in the spectral region of 0.6 to 0.7 μm, is in the red. The remaining two spectral bands lie outside the visible spectrum. Thus, four black and white images (see fig. 3) are obtained from the MSS, each representing the reflected energy in one of the four spectral intervals. It is possible to combine any two, three, or four of the black and white images into a composite color image. In the most commonly used convention, the black and white image from the first band is illuminated with blue light onto a color negative; the image from the second band, with green light; and the image from the fourth band, with red light (the third band is not used). Thus, the infrared reflection is displayed as red, the red is displayed as green, and the green is displayed as blue. As a result, in a false color composite, green vegetation, which is highly reflective in the near-infrared, appears as various shades of red; clear deep water is black; cities are identified by a blue-gray color; and water with sediment in it appears as a bright blue. Rocks and soils usually range from browns, yellows, and tans to bluish groups.

Page intentionally left blank

Page intentionally left blank

APPENDIX B

*Glossary of Technical Terms**

As an aid to the reader, this informal glossary of some of the technical terms is included. For the purposes of this publication, some definitions have been simplified and/or abridged from the original sources. Because of this procedure, the glossary should be used solely as a supplement to the text of *Mission to Earth,* not as a final authority for technical definitions. For the most part, an attempt was made to include only those terms not commonly found in standard dictionaries. Information cited here was extracted from the following sources (each entry is identified by the initials of its source as indicated below; definitions not cited are the responsibility of the compilers):

Initials	*Source*
DG	W. G. Moore, *Dictionary of Geography,* Penguin, 1968
GG	*Glossary of Geology,* American Geological Institute, 1972
WNW	*Webster's New World Dictionary* (college ed.), World Press, 1962

Also included are charts presenting simplified classifications of igneous, sedimentary, and metamorphic rocks and summarizing terms associated with the geologic time scale.

ablation—all processes by which snow or ice is lost from a glacier, floating ice, or snow cover, including melting, evaporation (sublimation), wind erosion, and calving. [GG]

aeolian—*see* **eolian.**

algal matte—a clustering or concentration of floating algae.

alluvial fan—a fan-shaped accumulation of sediment deposited by a stream at the base of a hill or mountain. [GG]

alluvium—a general term for clay, silt, sand, gravel, or similar unconsolidated detrital material deposited during comparatively recent geologic time by a stream. [GG]

Alpine zone—belonging to the higher regions of a mountain system: applied in reference to the typical climate, relief (glacial features), flora, etc., of the regions (e.g., the Alpine climate). [DG]

anticline—an archlike fold in layered or foliated rock.

anticlinorium—a composite anticlinal structure of regional extent composed of lesser folds. [GG]

aquifer—a layer of rock which holds water and allows water to percolate through it. [GG]

artesian spring—a spring from which the water flows under artesian pressure, usually through a fissure or other openings in the confining bed above the aquifer. [GG]

astrobleme—an ancient impact crater or roots of a crater.

badland—extremely rough, narrowly and steeply gullied topography in arid or semiarid areas. [GG]

barrier beach—a single, narrow, elongate sand ridge rising slightly above the high-tide level and extending generally parallel with the shore, but separated from it by a lagoon or marsh. [GG]

base level—the theoretical limit or lowest level toward which erosion of the Earth's surface constantly progresses but seldom, if ever, reaches; especially the level below which a stream cannot erode its bed. [GG]

basement—a complex of undifferentiated rocks that underlies the oldest identifiable rock in an area. [GG]

batholith—a large mass of igneous rock formed by the intrusion of magma, usually granite, granodiorite, or diorite; generally consists of many individual intrusions.

bedrock—a general term for the rock, usually solid, that underlies soil or other unconsolidated, superficial material. [GG]

beheaded distributary—a branch or outlet of a main river that has been cut off and whose waters have been diverted into another drainage system. [GG]

block faulting—a type of normal faulting in which the crust is divided into structural fault blocks of different elevations and orientations. [GG]

bolson—a basin of interior drainage in an arid or semiarid region whose floor is tending to be filled by a number of alluvial fans around its flanks. The term is chiefly used in Mexico and the southwestern United States. [DG]

boreal—pertaining to the north, or located in northern regions; northern. Pertaining to the northern biotic area (or boreal region) characterized by tundra and taiga and by dominant coniferous forests. [GG]

braided stream—a network of small shallow interlaced streams derived from a single stream.

brash ice—an accumulation of floating fragments (or bits) of ice, not more than 2 m (6 ft) across, and representing the wreckage of other forms of ice; occurs especially near an icepack or floe. [GG]

breached anticline—an anticline whose crest has been deeply eroded so that it is flanked by inward-facing erosional scarps. [GG]

buffalo wallow—one of the small, subcircular, undrained very shallow depressions once common on the Great Plains of western United States, usually containing water after a rain (and often remaining as a stagnant water hole for most of the year), and generally believed to have been initially formed by the trampling and wallowing of buffalo herds in mud and dust. [GG]

butte—a flat-topped hill formed when a stratum of hard rock overlies weaker layers and protects them from being worn down. The butte is similar to but smaller than a mesa; it is characteristic of the arid plateau region of the western United States. [DG]

---

* Compiled by Paul D. Lowman, Jr., and Margaret A. Tindal, *Goddard Space Flight Center.*

calcareous—said of a substance that contains calcium carbonate. When applied to a rock name it implies that a considerable percent (up to 50 percent) of the rock is calcium carbonate. [GG]

caldera—a large, basin-shaped volcanic depression, more or less circular or cirquelike in form, the diameter of which is many times greater than that of the included vent or vents, no matter what the steepness of the walls or form of the floor. [GG]

caliche—a term applied broadly in the southwestern United States to an opaque, reddish-brown to buff or white calcareous material commonly found in layers on, near, or within the surface of stony soils of arid and semiarid regions, but also occurring as a subsoil deposit in subhumid climates. Caliche is called hardpan or calcareous duricrust (or calcrete) in some localities and kankar in parts of India. [GG]

capping layer, cap rock—a synonym of overburden, usually used for consolidated material. [GG]

carbonate—a sediment formed by the organic or inorganic precipitation from aqueous solution of carbonates of calcium, magnesium, or iron; e.g., limestone and dolomite. [GG]

Carboniferous—the Mississippian and Pennsylvanian periods, combined; also, the corresponding system of rocks. In European usage, however, the Carboniferous is considered as a single period and is divided into Upper and Lower parts. The Permian is sometimes included. *See* **geologic time scale.** [GG]

cassava—any of a number of tropical plants with edible starchy roots; also called manioc. [WNW]

chernozem—in early U.S. soil classification systems, a group of zonal soils whose upper horizon is dark and highly organic, below which is a lighter colored horizon and an accumulation of lime. It is developed under conditions of temperate to cool, subhumid climate. [GG]

cinder cone—a conical hill formed by the accumulation of cinders and other volcanic ejecta, normally of basaltic or andesitic composition.

cinnabar—a mercury sulfide; a red mineral that is the chief source of mercury metal.

cirrus clouds—a type of high cloud, made of ice crystals, and consisting of detached pieces, delicate and feathery in appearance.

clastic—pertaining to rock or sediment composed principally of mineral or rock fragments. [GG]

clear cutting—the cutting down of all the trees in a stand of timber.

cluster analysis—a statistical procedure for arranging a number of objects in homogeneous subgroups based on their mutual similarities and hierarchical relationships. [GG]

color composite—as associated with Landsat, a 24.1-cm (9½-in.) color transparency or print generated from black and white triplet sets usually using multispectral scanner bands 4, 5, and 7. The resulting colors are arbitrarily derived, hence the expression "false color."

computer-compatible tapes (CCT's)—magnetic tapes on which data are recorded in a digital mode (using a binary code language).

consequent stream—a stream that originates on a newly exposed or recently formed surface and that flows along a course determined entirely by the initial slope and configuration of that surface. [GG]

conterminous—having a common boundary at some point; contiguous. [WNW]

continental divide—a drainage divide that separates streams flowing toward opposite sides of a continent, often into different oceans; e.g., in North America, the divide separating the watersheds of the Pacific Ocean from those of the Atlantic Ocean. [GG]

continental drift—a theory, originally proposed by Wegener, that continents have moved laterally hundreds or thousands of kilometers (miles) over the past few hundred million years at very slow rates. South America, for example, was formerly continuous with southern Africa in this theory.

continental glacier—a glacier of considerable thickness completely covering a large part of a continent. [GG]

contrast—on film products refers to the degree of difference in gray level or tone between adjacent points in the image; refers also to the range of gray levels present and distinguishable in the image.

copse—a small wood or thicket.

cordillera—a comprehensive term for an extensive series of more or less parallel ranges, systems, and chains of mountains. [GG]

core—the central zone or nucleus of the Earth's interior, below the Gutenberg discontinuity at a depth of 2900 km (1800 miles). [GG]

coulee—a term applied in the northwestern United States to a dry or intermittent stream valley, especially a long, steep-walled, trenchlike gorge or valley representing an abandoned overflow channel that temporarily carried melt water from an ice sheet, as the Grand Coulee (formerly occupied by the Columbia River) in Washington State. [GG]

country rock—the rock enclosing or traversed by a mineral deposit or an igneous intrusion. [GG]

crag-and-tail morphology—an elongate hill or ridge resulting from glaciation, having at the stoss end a steep, often precipitous, face or knob of ice-smoothed, resistant bedrock (the "crag") obstructing the movement of the glacier and at the ice end a tapering, streamlined, gentle slope (the "tail") of intact weaker rock and/or till protected by the "crag."

crater lake—a lake, usually of freshwater, that has formed in a volcanic crater or caldera by the accumulation of rain and ground water. [GG]

cuesta—a hill or ridge with a gentle slope on one side and a steep slope on the other. [GG]

cumulus clouds—a cloud of considerable vertical development, though less so than in the cumulonimbus. The upper parts are dome shaped, and have cauliflower heads, while the base is practically horizontal. Two types are generally recognized: the fair-weather cumulus (small, white, detached puffs typical of fair weather) and the heavy cumulus (which has much greater depth and often develops later into cumulonimbus). [DG]

cusp, cuspate—a landform characterized by a projection with indentations of crescent shape on either side. Some examples include the cuspate delta, cuspate bar, cuspate reef, and cuspate spit. [GG]

cutoff channel—a meander cutoff. [GG]

cyclone—an atmospheric low-pressure system that is circular or nearly so, around which the wind blows in a counterclockwise direction in the Northern Hemisphere and clockwise in the Southern Hemisphere. [GG]

cymatogeny—undulating movement or warping of the Earth's crust to produce regional linear arching or doming with minimal deformation. [GG]

cypress swamp—a swamp in which cypress trees are a major constituent; found in the southeastern United States.

deciduous—said of a plant that loses its leaves annually. Said of plant parts that are lost within a year of their production. [GG]

deep focus earthquake—an earthquake originating at a depth of 300 to 700 km (190 to 430 miles). [GG]

deflation—the sorting, lifting, and removal of loose, dry, fine-grained particles (clay and silt sizes) by the wind; a form of wind erosion, producing deflation basins. [GG]

defoliation—loss of leaves, either naturally or by artificial means.

deformation—a general term for the process of folding, faulting, shearing, compression, or stretching of rocks as a result of various crustal forces. [GG]

delta—the low, nearly flat, alluvial tract of land deposited at or near the mouth of a river, commonly forming a triangular or fan-shaped plain of considerable area. [GG]

dendritic drainage pattern—a drainage pattern in which the streams branch irregularly in all directions and at almost any angle, resembling in plan the branches of a tree. [GG]

denudation—the wearing away or progressive lowering of the Earth's surface by various natural agencies that include weathering, erosion, mass wasting, and transportation. [GG]

detritus—loose rock and mineral material. [GG]

diapir—an intrusion, by plastic flow, of material such as salt, shale, or partly remobilized granite into overlying rock.

diatreme—a breccia-filled volcanic pipe that was formed by a gaseous explosion. [GG]

differential erosion—erosion that occurs at irregular or varying rates because of the differences in the resistance of surface materials: softer and weaker rocks are rapidly worn away while harder and more resistant rocks remain to form ridges, hills, or mountains. [GG]

dike—a tabular intrusion, usually of igneous rock, filling a fracture that cuts the surrounding rock.

displacement—the relative movement of the two sides of a fault, measured in any chosen direction. [GG]

dissection—the process of erosion whereby the continuity of a relatively even landscape is gradually sculptured or destroyed by the formation of gullies. [GG]

distributary—an irregular, divergent stream flowing away from the main stream and not returning to it, as in a delta or on an alluvial plain. [GG]

domal uplift—a closed anticline, or upfold, roughly circular in plan view.

dormant volcano—a volcano that is not presently erupting but that has, perhaps, done so within historic time and is considered likely to do so in the future. There is no precise distinction between a dormant and an active volcano. [GG]

downbuckle—a compressional downfolding of sialic crust, associated with oceanic trenches. [GG]

downwarping—the downward warping or subsidence of a regional area of the Earth's crust, usually as the result of isostatic pressure; e.g., geosynclinal sedimentation. [GG]

drag folds—a minor fold, usually one of a series, formed in a thinly laminated or soft (incompetent) bed lying between harder or more rigid (competent) beds and produced by relative movement of the competent beds in opposite directions relative to one another. [GG]

drift—a general term applied to all rock material (clay, sand, gravel, and boulders) transported by a glacier and deposited directly by the ice, or by running water emanating from a glacier. [GG]

ecology—the study of living organisms and their relationship to their environments.

electromagnetic spectrum—the ordered array of electromagnetic energy or radiation, extending from short wavelength cosmic rays; through gamma rays; X-rays; ultraviolet, visible, and infrared radiation; and including microwave and all other wavelengths of radio energy.

eluviation—the downward movement of soluble or suspended material in a soil from the A horizon to the B horizon, by groundwater percolation. The term refers especially but not exclusively to the movement of colloids, whereas the term "leaching" refers to the complete removal of soluble materials. [GG]

end moraine—a moraine that is being produced at the front of an actively flowing glacier at any given time; a moraine that has been deposited at the lower or outer end of a glacier. [GG]

eolian—pertaining to the wind.

ephemeris—a table giving the computed positions of bodies in space (stars, planets, and orbiting spacecraft) at some given period of time (day, minute) relative to reference point(s) on the Earth's surface.

erg—a vast region in the Sahara Desert deeply covered with shifting sand and occupied by complex sand dunes; an extensive tract of sandy desert; a sand sea. [GG]

erosion scarp—a scarp produced by erosion; e.g., a fault-line scarp or a beach scarp. [GG]

escarpment—a line of cliffs produced by erosion or faulting; essentially equivalent to scarp.

esker—a sinuous ridge of sand and gravel deposited by a stream formerly flowing under or on a glacier.

estuary—a drowned river mouth formed by the subsidence of land near the coast or by the drowning of the lower portion of a nonglaciated valley due to the rise of sea level. [GG]

eugeosyncline—a geosyncline, or regional depositional trough, in which volcanism is associated with rapid clastic sedimentation. [GG]

evaporation basin—a closed valley in which evaporation of water leaves salt deposits.

evaporite—a nonclastic sedimentary rock composed primarily of minerals produced by evaporation of a saline solution that became concentrated by evaporation of the solvent. [GG]

exhumation, exhume—the uncovering or exposure by erosion of a preexisting surface, landscape, or feature that had been buried by later deposition. [GG]

extrusive—said of igneous rock that has been ejected onto the surface of the Earth. Extrusive rocks include lava flows and pyroclastic material such as volcanic ash. [GG]

fall line—a line or belt of falls and rapids along the boundary between soft coastal plain rocks and harder rocks farther inland; applied to the eastern United States.

fallow—referring to farmland not being cultivated during a growing season.

false color composite—*see* **color composite.**

fault—a rock fracture along which there has been movement from a few centimeters (inches) to perhaps hundreds of kilometers (miles).

fault scarp—a steep slope or cliff formed directly by movement along one side of a fault. [GG]

fiducial marks—index marks inscribed on an imaging lens or plate that are transferred to image products (e.g., film) to form reference points.

flexure—a fold in rock.

flood plain—the level land along a river, produced by deposition of alluvium from the river during times of flood, when the plain is covered by water.

fold axis—in a fold, a line that connects the central points of each constituent stratum, from which its limbs bend; in a syncline, the trough; in an anticline, the crest. [GG]

foliation—a general term for a planar arrangement of textural or structural features in any type of rock; e.g., cleavage in slate or schistosity in metamorphic rock. [GG]

frazilice—fine specules or plates of ice suspended in water.

fumarole—a vent, usually volcanic, from which gases and vapors are emitted. [GG]

gabbro—a group of dark-colored, basic intrusive igneous rocks composed principally of basic plagioclase (commonly labradorite or bytownite). [GG]

gallery forest—forests growing in response to moisture available along stream courses.

gangue—the valueless rock or mineral aggregates in an ore; that part of an ore that is not economically desirable. [GG]

geologic time scale—see following tables.

Geologic Time Scale

[D. L. Eicher, *Geologic Time*, Prentice-Hall, New York, N.Y., 1969.]

Era	Period	Epoch	Time before present
Cenozoic	Quaternary	Recent (about last 5000 yr)	
		Pleistocene	2.5 million yr
	Tertiary	Pliocene	
		Miocene	
		Oligocene	
		Eocene	
		Paleocene	65 million yr
Mesozoic	Cretaceous		
	Jurassic		
	Triassic		225 million yr
Paleozoic	Permian		
	Pennsylvanian		
	Mississippian		
	Devonian		
	Silurian		
	Ordovician		
	Cambrian		570 million yr
Precambrian	Proterozoic		2500 million yr
	Archeozoic		4600 million yr
	(Archean)		(origin of Earth)

Note: Nomenclature for the Precambrian is not yet agreed upon. Dates given are very approximate.

Pleistocene Glacial and Interglacial Stages (North America)

[After A. Holmes, *Principles of Physical Geology* (2d ed.), Ronald Press, New York, 1965, 1288 p.]

Glacial	*Interglacial*
Wisconsin	
	Sangamon
Illinoan	
	Yarmouth
Kansan	
	Aftonian
Nebraskan	

geomorphic—pertaining to the form of the Earth or of its surface features; e.g., a geomorphic province. Pertaining to geomorphology; geomorphologic. [GG]

geomorphology—the science of landforms and their development.

geosyncline—a depositional basin of regional extent receiving sediments as it subsides; sometimes transformed into a folded mountain range, such as the Appalachians.

geyser—a type of hot spring that intermittently erupts jets of hot water and steam. [GG]

glacial confluence—a junction of two or more glaciers. [GG]

glacial stagnation—a condition in which a glacier has stopped receiving nourishment in its accumulation area and has essentially stopped flowing.

gneiss—a banded rock, formed by regional metamorphism, with interspersed layers of platy and granular minerals.

graben—a down-faulted crustal block; sometimes expressed as a rift valley.

ground truth—information concerning the actual state of the ground (particularly in reference to data being acquired) at the time of a remote sensing overflight.

hachures—a series of short lines used on a topographic map for shading and indicating relief (such as steepness of slopes) drawn perpendicular to the contour lines. [GG]

hammock—a term applied in the southeastern United States to a fertile area of deep, humus-rich soil generally covered by hardwood vegetation and often rising slightly above a plain or swamp; especially an island of dense tropical undergrowth in the Florida Everglades. [GG]

hinterland—an area bordering, or within, an orogenic belt on the internal side, away from the direction of overfolding and thrusting. [GG]

hogback—any ridge with a sharp summit and steep slopes of nearly equal inclination on both flanks. [GG]

homocline—a general term for a rock unit in which the strata have the same dip; e.g., one limb of a fold, a tilted fault block, a monocline, or an isocline. [GG]

horst—an up-faulted crustal block, bounded by faults; opposite of graben.

hyaloclastic—a tufflike deposit of volcanic glass formed under water.

hydrocarbon—any organic compound, gaseous, liquid, or solid, consisting solely of carbon and hydrogen. [GG]

igneous—said of a rock or mineral that solidified from molten or partly molten material; i.e., from a magma. "Igneous" rocks constitute one of the three main classes into which all rocks are divided (i.e., igneous, metamorphic, and sedimentary). (See classification at bottom of page.) [GG]

imbricate structure—a series of nearly parallel and overlapping minor thrust faults, high-angle reverse faults, or slides. [GG]

incision—the process whereby a downward-eroding stream deepens its channel or produces a narrow, steep-walled valley; especially the downcutting of a stream during, and as a result of, relative movement (uplift) of the crust. [GG]

infiltration—the movement of water or solutions, especially ore-bearing solutions, into a rock. [GG]

infrared radiation—electromagnetic radiation within the wavelength interval from about 0.7 μm to an indefinite upper boundary sometimes set at 1000 μm. The region between 0.7 and about 5.0 μm is usually referred to as the reflected infrared; the region extending to the higher wavelengths is called the thermal infrared.

inlier—an area or group of rocks surrounded by outcrops of younger age; e.g., a window, or an eroded anticlinal crest; opposite of outlier. [GG]

instantaneous field of view (IFOV)—spot size on the ground viewed at any instant of time by the sensor.

interbedded—said of beds laid between or alternating with others of different character. [GG]

interfluve—the area between rivers; especially the relatively undissected upland or ridge between two adjacent valleys containing streams flowing in the same general direction. [GG]

intermontane—situated between or surrounded by mountains, mountain ranges, or mountainous regions; e.g., the Great Basin of western United States. [GG]

intrusive—referring to material, such as molten rock, injected into other rock; may also refer to material such as salt injected by plastic flow.

isostatic rebound—crustal uplift after an imposed load, such as a glacier, is removed.

joint—a fracture in rock with no displacement along it.

karroo—a tableland found especially in South Africa that often rises to a considerable height in terraces and does not support vegetation in the dry season but that becomes a grassy plain or pastureland during the wet season. (Also spelled "karoo.") [GG]

karst—a type of topography formed by solution of limestone, dolomite, or gypsum, characterized by closed depressions or sinkholes, caves, and underground drainage. [GG]

kavir—(1) A term used in Iran for a salt desert; specifically, The Great Kavir of inner Iran, a series of closed basins noted for marshy conditions and high salinities. (2) A playa on a kavir. Synonyms: kewire; kevir. (3) A term used in Iran for a salt marsh. [GG]

kettle—a depression in a glacial outwash plain formed by melting of ice.

laccolith—a lens-shaped igneous intrusion.

lacustrine—pertaining to, produced by, or formed in a lake or lakes. [GG]

lag sand—coarse-grained sand left behind by wind or flowing water.

laterite—a highly weathered, residual red subsoil or material rich in oxides of iron, aluminum, or both, found in moist, warm to temperate climates. [GG]

lava—molten rock erupted onto the Earth's surface.

leaching—the separation, selective removal, or dissolving out of soluble constituents from a rock or ore body by the natural action of percolating water. [GG]

lee (wind)—pertaining to or located on the side sheltered from the wind; leeward. [GG]

lichens—a thallophytic plant of the order *Lichenes* that is composed of a fungus and an alga living in a symbiotic relationship. The alga is protected by the fungus, which in turn relies upon the alga for the production of food. [GG]

lime sink—a saucer-shaped solution depression in the Earth's surface, usually found in a limestone region. [DG]

lineament—straight or gently curved, lengthy features of the Earth's surface, frequently expressed topographically as depressions or lines of depressions; these are prominent on relief models, high-altitude air photographs, and radar imagery. Their meaning has been much debated; some certainly express valid structural features, such as faults, alined volcanoes, and zones of intense jointing with little displacement, but the meaning of others is

Major Igneous Rock Types

Volcanic (fine-grained)	Rhyolite	Trachyte	Andesite	Basalt	Komatiite
Intrusive (coarse-grained)	Granite	Syenite	Diorite	Gabbro	Peridotite
		Increasing Fe, Mg ⟶			
		⟵ Increasing Si, K, Na			

obscure, and their origins may be diverse, or purely accidental. Colloquial synonym: "linear." [GG]

linear fold—a narrow fold in stratified rock.

linear sand dune—long, relatively narrow sand dune.

loam—a rich soil consisting principally of a mixture of sand and clay, together with silt and humus; it has the good qualities of both sand and clay, but not their bad qualities. [DG]

Logan's Line—a boundary, in the northeast U.S. and Canada, between intensely folded and faulted Paleozoic rocks on the southeast and less deformed rocks on the northwest; in places known to be a thrust fault.

longitudinal sand dune—a long, narrow sand dune oriented parallel with the direction of the prevailing wind. [GG]

maar—a low-relief, coneless volcanic crater formed by a single explosive eruption. It is surrounded by a crater ring and is commonly filled with water. [GG]

mafic—said of an igneous rock rich in ferromagnesian, dark-colored minerals. [GG]

magma—subsurface molten rock, called "lava" when erupted.

mantled gneiss dome—a term used for a dome in metamorphic terrains that has a core of gneiss that was remobilized from an original basement and that has risen through its cover of younger, also metamorphosed rocks. [GG]

mantle plume—a hypothetical linear upward current of hot material in the Earth's mantle, thought to produce volcanoes.

marine terrace—(1) A narrow, constructional coastal strip, sloping gently seaward, veneered by a marine deposit (typically silt, sand, and fine gravel). (2) A narrow coastal plain whose margin has been strongly cliffed by marine erosion. (3) Loosely, a wave-cut platform that has been exposed by uplift along a seacoast or by the lowering of the sea level and measuring as little as 3 m (10 ft) to more than 40 m (130 ft) above mean sea level; an elevated marine-cut bench. (4) A terrace formed along a seacoast by the merging of a wave-built terrace and a wave-cut platform. [GG]

marl—a term loosely applied to an unconsolidated calcareous sediment consisting of clay and sand or silt.

massif—a highland or part of a mountain belt consisting largely of crystalline rocks.

meander cutoff—a cutoff formed when a stream cuts through a meander neck. [GG]

meander scar—a crescentic concave mark on the face of a bluff or valley wall produced by a meandering stream and indicating the abandoned route of the stream. [GG]

meandering stream—a stream having a sinuous course.

megadune—an unusually large sand dune at least a hundred meters (several hundred feet) high.

mesa—an isolated nearly level landmass standing distinctly above the surrounding country. [GG]

meta—a prefix that, when used with a rock name, indicates that the rock type has been metamorphosed; e.g., metabasalt, metasedimentary, and metavolcanic.

metamorphism—recrystallization of a rock under high pressure or temperature, or both, sometimes with compositional changes.

Major Metamorphic Rock Types

Rock type	*Antecedent rock, origin*
Marble	Limestone, recrystallized
Quartzite	Sandstone, recrystallized
Gneiss	Wide variety of igneous and sedimentary rocks, recrystallized to form coarse-grained foliated rock
Schist	Wide variety of igneous and sedimentary rocks, recrystallized to form fine-grained foliated rock
Slate	Shale, partly crystallized; cleavage developed
Greenstone	Basalts, basic igneous rocks

microcontinent—a relatively small oceanic island underlain by sialic or granitic crust, thought to be of essentially continental nature; the Seychelles are a typical example.

micrometer (μm)—the unit of length equal to one-millionth of a meter.

mine dump—the pile of material excavated from a mine.

miogeosyncline—a nonvolcanic geosyncline, typified by quartz-rich sandstones and limestones, formed by slow subsidence of a stable part of the crust.

monadnock—a hill or mountain of resistant rock rising conspicuously above the general terrain level.

monocline—a unit of strata that dips in one direction only and is not part of an anticline or syncline. It is generally a large feature of gentle dip. [GG]

monsoon—a seasonal type of wind system in which direction changes with the seasons; e.g., over the Arabian Sea the winds are from the northeast for 6 months and from the southeast for the next 6 months. [GG]

montane—of, pertaining to, or inhabiting cool upland slopes below the timberline, characterized by the dominance of evergreen trees. Synonyms: subalpine; alpestrine. [GG]

moor—a wild stretch of land, usually elevated, covered with heather, coarse grass, bracken, or similar vegetation; it sometimes includes patches of pasture grasses, and sometimes marshy hollows. [DG]

moraine—a mound, ridge, or other distinct accumulation of unsorted, unstratified glacial drift, predominantly till, deposited chiefly by direct action of glacier ice. [GG]

mosaic (photo)—an assembly of aerial photographs whose edges have been feathered (torn) or cut and matched to form a continuous photographic representation of a part of the Earth's surface; e.g., a composite photograph formed by joining together parts of several overlapping vertical photographs of adjoining areas of the Earth's surface. [GG]

mudflat—a relatively level area of fine silt along a shore (as in a sheltered estuary) or around an island, alternately covered and uncovered by the tide, or covered by shallow water; a muddy tidal flat barren of vegetation. [GG]

multiband or multispectral—the simultaneous use of two or more sensors to obtain imagery from different portions of the electromagnetic spectrum.

muskeg—a bog, usually a sphagnum bog, frequently with tussocks of deep accumulations of organic material growing in wet, poorly drained, boreal regions, often areas of permafrost. Tamarack and black spruce are commonly associated with muskeg areas. [GG]

natural levee—a long, broad, low ridge or embankment of sand and coarse silt built by a stream on its flood plain and along banks of its channel especially in time of flood. [GG]

oasis—a fertile vegetated area in the midst of a desert where the water table has come close enough to the surface for wells and springs or seepages to exist, thus making it suitable for human habitation. [GG]

oceanic rift—the valley, or canyon, found along the crest of an oceanic ridge, such as the Mid-Atlantic Ridge.

oceanization—the conversion of continental crust into oceanic crust; basification. [GG]

oil trap—the accumulation of petroleum in a reservoir rock under such conditions that its migration and escape are prevented. Sealing can be effected by the abutment of impermeable formations against the reservoir, by lateral variation within the beds to reduce permeability, or by presence of water preventing downward migration. [GG]

oolitic—pertaining to oolites, which are small round particles, generally about 1 mm (0.04 in.) in diameter, generally formed by precipitation of carbonates or oxides around sand grains.

open fold—a fold the limbs of which have been only moderately compressed. [GG]

ophiolite—a group of mafic and ultramafic igneous rocks ranging from spilite and basalt to gabbro and peridotite, including rocks rich in serpentine, chlorite, epidote, and albite derived from them by later metamorphism, whose origin is associated with an early phase of the development of a geosyncline. [GG]

orogeny—literally, the process of formation of mountains. In present geological usage, orogeny is the process by which structures within mountain areas were formed, including thrusting, folding, and faulting in the outer and higher layers, and plastic folding, metamorphism, and plutonism in the inner and deeper layers.

orographic—(1) Pertaining to mountains, especially in regard to their location and distribution. (2) Said of the precipitation (or rainfall) that results when moisture-laden air encounters a high barrier or is forced to rise over it, such as the precipitation on the

windward slopes of a mountain range facing a steady wind from a warm ocean; also, said of the lifting of an air current caused by its passage up and over a mountain. (3) Pertaining to a rain-shadow desert. [GG]

oscillatory sand dunes—a linear dune formed by winds that frequently reverse their direction.

outcrop—that part of a geologic formation or structure that appears at the surface of the Earth; also, bedrock that is covered only by surficial deposits such as alluvium. [GG]

outlier—an area or group of rocks surrounded by outcrops of older age; e.g., an eroded geosynclinal trough, or a remnant on the downthrown side of a fault. [GG]

outwash plain—a broad, outspread, flat or gently sloping, alluvial sheet of outwash deposited by melt water streams flowing in front of or beyond the terminal moraine of a glacier and formed by coalescing outwash fans; the surface of a broad body of outwash. [GG]

overthrust fault—a low-angle thrust fault of large scale, generally measured in kilometers (miles). [GG]

oxbow lake—a crescent-shaped lake occupying an abandoned stream meander.

pediment—the gently sloping erosion surfaces with a thin layer of sediment at the base of a mountain.

pediplanation—the action or process of formation and development of a pediplain or pediplains; pedimentation of regional magnitude, assisted by slope retreat. [GG]

peneplane, peneplain—a term introduced by Davis for a low, nearly featureless, and gently undulating or almost-planal land surface of considerable area that presumably has been reduced by the processes of long-contained subaerial erosion. [GG]

perennial stream—a stream or reach of a stream that flows continuously throughout the year and whose upper surface generally stands lower than the water table in the region adjoining the stream. Synonyms: permanent stream; live stream. [GG]

petrology—that branch of geology dealing with the origin, occurrence, structure, and history of rocks, especially igneous and metamorphic rocks. Petrology is broader in scope than petrography, which is concerned with the description and classification of rocks. [GG]

plankton—microscopic plants and animals found at or near the surface of water bodies.

plate tectonic theory—global tectonics based on an Earth model characterized by a small number (10 to 25) of large, broad, thick plates (blocks composed of areas of both continental and oceanic crust and mantle) each of which "floats" on some viscous underlayer in the mantle and moves more or less independently of the others. The continents form a part of the plates and move with them, like logs frozen in the ice floes. [GG]

playa, playa lake—a shallow, intermittent lake in an arid or semiarid region, covering or occupying a playa in the wet season but drying up in summer; an ephemeral lake that upon evaporation leaves or forms a playa. [GG]

plug—(1) A vertical, pipelike body of magma that represents the conduit to a former volcanic vent. (2) A crater filling of lava, the surrounding material of which has been removed by erosion. [GG]

plunging fold—a fold whose axis is inclined.

pluton—(1) An igneous intrusion. (2) A body of rock formed by metasomatic replacement. (The term originally signified only deep-seated or plutonic bodies of granitoid texture.) [GG]

polder—a generally fertile tract of flat, low-lying land (as in The Netherlands and Belgium) reclaimed and protected from the sea. [GG]

polynya—any non-linear-shaped opening enclosed in ice, especially a large expanse of water, other than a lead (ice), surrounded by sea ice, but not large enough to be called open water (ice); commonly found off the mouth of a large river. [GG]

porosity—the proportion of a rock or soil occupied by interstices.

porphyry—an igneous rock of any composition with relatively large crystals in a fine-grained groundmass. [GG]

pressure ridge—(1) An elongate uplift of the congealing crust of a lava flow, probably caused by the pressure of the underlying and still flowing lava. (2) A ridge of glacier ice, produced by horizontal pressure associated with glacier flow. (3) A rugged, irregular wall of broken floating ice buckled upward by the lateral pressure of wind or current forcing or squeezing one floe against another; it may be fresh or weathered and extend many kilometers (miles) in length and up to 30 m (100 ft) in height. [GG]

prime meridian—an arbitrary meridian selected as a reference line having a longitude of 0° and used as the origin from which other longitudes are reckoned east and west to 180°; specifically the Greenwich meridian. Local or national prime meridians are occasionally used. [GG]

pyroclastic—pertaining to clastic rock material formed by volcanic explosion or aerial expulsion from a volcanic vent; also, pertaining to rock texture of explosive origin. [GG]

radial sand dune—a dune formed by winds blowing from different directions at different times producing a star- or pyramid-shaped dune.

radiance—optical energy incident on or reflected from a unit surface area.

radiation—the process by which electromagnetic energy is propagated through free space. Also called radiant energy.

reflectance—the fraction of the total incident light reflected from a surface; varies with wavelength of light, angle of illumination, etc.

reg—a stony desert from which fine sand has been removed by the wind, leaving a sheet of gravel and small stones, as in the Algerian Sahara. [GG]

registration—point by point fitting or matching of all equivalent points or features in two or more identical images, usually of different bands.

relief—the elevations or differences in elevation, considered collectively, of a land surface.

remote sensing—acquisition of information about objects or phenomena in the surficial environment (including land, oceans, and atmosphere) through the use of sensory devices at positions separated from (remotely situated) the subject under study; involves measurements of electromagnetic radiation, acoustical energy, force fields, or nuclear radiations.

resolution—(1) Ground resolution, the minimum distance between two or more adjacent features or the minimum size of a feature that can be detected and separated from its surrounding features. (2) Image resolution is expressed in lines per millimeter for a given photographic emulsion under specified conditions.

resurgence—the point where an underground stream reappears at the surface to become a surface stream. It is usually near the point where an impermeable stratum, underlying a rock such as limestone, intersects the surface. [GG]

reverse fault—a fault with a dip of 45° or less in which the upper block appears to have moved upward relative to the lower block. Horizontal compression rather than vertical displacement is its characteristic feature. [GG]

ribbed moraine—one of a group of irregularly subparallel, locally branching, generally smoothly rounded and arcuate ridges that are convex in the downstream direction of a glacier but that curve upstream adjacent to eskers. They are most common in the continental ice sheets and are abundant in the Arctic. [GG]

ridge—a term occasionally applied to a range of hills or mountains. A top or upper part of a hill; a narrow, elongated crest of a hill or mountain. [GG]

rift (rift valley)—a rift is a narrow cleft fissure, or other opening in rock (as in limestone), made by cracking or splitting. A rift valley is a valley formed by the sinking of land between two roughly parallel faults; such a valley is long in proportion to its width.

sahel—the part of Africa lying south of the Sahara and north of the equatorial rain forest.

salar—a term used in southwestern United States and in the Chilean nitrate fields for a salt flat or for a salt-incrusted depression that may represent the basin of a salt lake. [GG]

saline—a natural deposit of common salt or of any other soluble salt; e.g., an evaporite. In this usage, a "saline" may refer to various features such as a playa, a salt flat, a saltpan, a salt marsh, a salt lake, a salt pond, a salt well, and a saltworks. [GG]

salt dome—a diapiric intrusion produced by upward plastic flow of salt.

salt marsh—flat, poorly drained land that is subject to periodic or occasional overflow. [GG]

saltpan—an undrained, usually small and shallow, natural depres-

sion or hollow in which water accumulates and evaporates, leaving a salt deposit; also, a shallow lake of brackish water occupying a saltpan. [GG]

sand sheet—a thin accumulation of coarse sand or fine gravel formed of grains too large to be transported by saltation, characterized by an extremely flat or plainlike surface broken only by small sand ripples. [GG]

sandur—Icelandic term signifying "sand," but generally adopted for outwash plain. (Plural: sandar.) [GG]

savanna—(1) An open grassy, essentially treeless plain, especially as developed in tropical or subtropical regions. Usually there are distinct wet and dry seasons; what trees and shrubs are found there are drought resistant. (2) The tall grass characteristic of a savanna. (3) Along the southeastern Atlantic coast of the United States the term (often spelled savannah) is used for marshy alluvial flats with occasional clumps of trees. [GG]

scarp—(1) A line of cliffs produced by faulting or by erosion. The term is an abbreviated form of escarpment. (2) A relatively steep and straight, clifflike face or slope of considerable linear extent. [GG]

scour—(1) The powerful and concentrated clearing and digging action of flowing air or water, especially the downward erosion by stream water in sweeping away mud and silt on the outside curve of a bend, or during time of flood. (2) A place in a streambed swept (scoured) by running water, generally leaving a gravel bottom. (3) Glacial scour. (4) Tidal scour. [GG]

scrub—low-growing or stunted vegetation growing on poor soil or in semiarid regions and which sometimes forms impenetrable masses.

sea-floor spreading—a hypothesis that the oceanic crust is increasing by convective upwelling of magma along the midoceanic ridges or world rift system, and a moving away of the new material at a rate of from 1 to 10 cm (0.4 to 4 in.) per year. This movement provides the source of power in the hypothesis of plate tectonics. This hypothesis supports the continental displacement hypothesis. [GG]

section line—the boundary line of a section in surveying.

sediment—fragmental material, either inorganic or organic, that originates from weathering of rocks. [GG]

Major Sedimentary Rock Types

	Sediment	*Rock*
Clastic rocks	Gravel	Conglomerate
	Sand	Sandstone
	Silt	Siltstone
	Clay	Shale
Organic rocks and chemical precipitates	Calcium carbonate	Limestone
	Calcium and magnesium carbonate	Dolomite
	Silica	Chert
	Sodium chloride	Salt
	Calcium sulfate	Gypsum

sediment plume—an elongated, usually open and mobile column or band of solid fragmented material that originates from weathering of rocks and is transported by, suspended in, or deposited by air, water, or ice, or that is accumulated by other natural agents.

seif dune—a very large, sharp-crested, tapering longitudinal dune or chain of sand dunes, commonly found in the Sahara Desert. [GG]

seismic—pertaining to an earthquake or Earth vibration, including those that are artificially induced. [GG]

sensor—the component of an instrument that converts an input signal into a quantity that can be measured by another part of the instrument.

shale—a fine-grained sedimentary rock with notable cleavage parallel to bedding, formed by lithification of clay and silt.

shallow-focus earthquake—an earthquake whose focus occurs at a depth of less than 50, 60, or 70 km (31, 37, or 44 miles) (there is no agreement). Most earthquake activity is of this type. [GG]

shatter cone—a distinctively striated conical fragment of rock ranging in length from less than a centimeter (half an inch) to several meters (feet), generally found in nested or composite groups in the rocks of cryptoexplosion structures, and generally believed to have been formed by shock waves generated by meteorite impact. [GG]

sheetflood—a broad expanse of moving, stormborne water that spreads as a thin, continuous, relatively uniform film over a large area in an arid region and that is not concentrated into well-defined channels.

shock metamorphism—the physical, chemical, mineralogic, and morphologic changes produced in rocks and minerals by transient high-pressure shock waves. The only known natural mechanism for producing shock metamorphic effects is the hypervelocity impact of large meteorites, but the term also includes identical effects produced by shock waves generated in small-scale laboratory experiments and in nuclear and chemical explosions. [GG]

sial—a petrologic name for the upper layer of the Earth's crust in continental areas, composed of rocks that are rich in silica and alumina. [GG]

sidelap—that portion of the sides of each of two images taken at different times that displays the same scene on the surface, allowing the two to be joined or to be examined as a stereoscopic pair.

signature—the unique reflectance or emission response over a continuous range of wavelengths characteristic of a particular object or association of features.

sill—a tabular igneous intrusion that parallels the planar structure of the surrounding rock. [GG]

siltstone—an indurated or somewhat indurated silt having the texture and composition, but lacking the fine lamination or fissility, of shale; a massive mudstone in which the silt predominates over clay; a nonfissile silt shale. [GG]

slate—a compact, fine-grained, metamorphic rock formed from such rocks as shale and volcanic ash, which possess the property of fissility along planes independent of the original bedding (slaty cleavage), whereby they can be parted into plates that are lithologically indistinguishable. [GG]

snowline—(1) The line or altitude on land separating areas in which deposited snow disappears in summer from areas in which snow remains throughout the year; on glaciers it is identical to the firn line. (2) The ever-changing extreme limit from the Equator within which no snow reaches the ground or falls unmelted. Its position depends on such physical conditions as altitude and nearness to the sea. The term is applied especially to the winter snowline in the Northern Hemisphere. [GG]

spectral region—any part of the electromagnetic spectrum that is indicated by limiting wavelengths (generally synonymous with band).

spur—a subordinate ridge or lesser elevation that projects sharply at right angles to, or in a lateral direction from, the crest or side of a hill, mountain, or other high land surface; a small hill extending from a prominent range of hills or mountains. [GG]

stabilized sand dune—a sand dune whose movement is arrested or whose form is protected from further wind action, as by a growth of vegetation or by cementation of the sand. [GG]

stack—an upstanding, steep-sided mass of rock rising above its surroundings on all sides from a slope or hill; also a small, isolated, rocky island or mass near a cliffy shore, detached from a headland. [GG]

star dune—an isolated hill of sand, its base resembling in plan a several-pointed star, and its sharp-crested ridges converging from the basal points to a central peak that may be as high as 100 m (300 ft) above the surrounding plain; it tends to remain fixed in place for centuries in an area where the wind blows from all directions. [GG]

steppe—an extensive, treeless grassland area in southeastern Europe and Asia developing in the semiarid midlatitudes of that region. Steppe areas are generally considered drier than the prairie that develops in the subhumid midlatitudes of the United States. [GG]

stock—an igneous intrusion that is less than 100 km^2 (40 sq miles) in surface exposure, is usually but not always discordant, and resembles a batholith except in size. [GG]

stratigraphy—the study of stratified (layered) rocks, mainly sedimentary.

stratovolcano—a volcano that is constructed of alternating layers of lava and pyroclastics. Viscous, acidic lava may flow from fissures radiating from a central vent, from which pyroclastics are ejected. [GG]

stratum—a layer of sediment or sedimentary rock. The term is more frequently used in its plural form, strata. [GG]

stream capture—the natural diversion of the headwaters of one stream by another stream eroding headward at a rapid rate. [GG]

stream confluence—a place of meeting of two or more streams. [GG]

strike-slip fault—a fault whose chief movement is horizontal.

string bog—a linear Pleistocene periglacial muskeg or moor with an undulating surface, occurring in the boreal needle-tree forest zone of the northern hemisphere (especially in western Siberia and the Hudson Bay area), characterized by shallow water-filled depressions and festoons of lenticular ridges (up to 1 m (3 ft) high) consisting of floating fen or moss vegetation. Its origin is controversial, but it may be related to collapse and melting of permafrost. [GG]

structural grain—a general expression for the geologic structural trends in an area.

structural high—a general term for such features as a crest, culmination, anticline, or dome. [GG]

subaerial—occurring beneath the atmosphere or in the open air; especially said of conditions and processes (such as erosion) that exist or operate on the land surface. [GG]

subduction—the process of one crustal block descending beneath another, by folding or faulting or both. The concept was originally used by Alpine geologists. [GG]

subsatellite point—the intersection with the Earth's surface of a line from the spacecraft to the center of the Earth.

subsequent drainage—drainage following belts of weak rock; i.e., following geologic structure.

Sun azimuth angle—angle in degrees measured in the horizon plane clockwise from true north.

Sun elevation—angle of the Sun above the horizon measured in degrees.

Sun-synchronous—refers to a precessing orbital path of a satellite relative to the rotating Earth such that the satellite crosses the Equator at the same local time for every successive orbital pass.

superposition—(1) The actual order in which rocks are placed or accumulated in beds one above the other, the highest bed being the youngest. (2) The process by which successively younger sedimentary layers are deposited on lower and older layers. [GG]

suspension—a mode of sediment transport in which the upward currents in eddies of turbulent flow are capable of supporting the weight of undissolved sediment particles and keeping them indefinitely held in the body of the surrounding fluid (such as silt in water or dust in air). [GG]

syncline—a troughlike fold, the core of which contains the stratigraphically younger rocks; it is concave upward. [GG]

tableland—(1) A general term for a broad, elevated region of land with a nearly level or undulating surface of considerable extent; e.g., South Africa. (2) A plateau bordered by abrupt clifflike edges rising sharply from the surrounding lowland; a mesa. [GG]

taiga—a swampy area of coniferous forest sometimes found lying between tundra and steppe regions. [GG]

tectonic—pertaining to the structure and deformation of the Earth's crust.

telemetry—the system for transmitting data or information from source to receiver or recorder; usually refers to radio or electrical signals sent over a distance.

Tennessee Valley Authority (TVA)—A Federal corporation organized in 1933 to provide cheap electrical power, flood control, improved navigation, irrigation, etc., by developing the potentialities of the Tennessee River and its tributary. Work on this project was first begun at Wilson Dam in Muscle Shoals.

terminal moraine—an end moraine, extending across a glacial valley as an arcuate or crescentic ridge, that marks the farthest advance or maximum extent of a glacier; the outermost end moraine of a glacier. It is formed at or near a more-or-less stationary edge, or at a place marking the cessation of an important glacial advance. [GG]

thrust fault—a fault with a dip of 45° or less in which the upper block appears to have moved upward relative to the lower block. Horizontal compression rather that vertical displacement is its characteristic feature. [GG]

tidal flat—an extensive, nearly horizontal, marshy or barren tract of land that is alternately covered and uncovered by the rise and fall of the tide, consisting of unconsolidated sediment (mostly mud and sand). It may form the top surface of a deltaic deposit. [GG]

till—unsorted and unstratified drift, generally unconsolidated, deposited directly by and underneath a glacier without subsequent reworking by water from the glacier, consisting of a heterogeneous mixture of clay, sand, gravel, and boulders varying widely in size and shape. [GG]

timberline—the elevation (as on a mountain) or latitudinal limits (on a regional basis) at which tree growth stops. [GG]

tombolo—a sand or gravel bar (or spit) that connects an island with the mainland or with another island. [GG]

toroid—a doughnut-shaped mold, commonly consisting of sand, of a circular scour pit made in firm, shallow water sediments (such as hard mud) by an eddy or whirlpool in flowing water. [GG]

trace—the intersection of a geological surface with another surface; e.g., the trace of bedding on a fault surface or the trace of a fault or outcrop in the ground. [GG]

transform fault—a strike-slip fault that is transformed, at its ends, into a different type of structure, such as an oceanic ridge or trench; the actual movement is the reverse of that indicated by apparent offset.

transverse dune—a strongly asymmetrical sand dune elongated perpendicular to the direction of the prevailing winds, having a gentle windward slope and a steep leeward slope standing at or near the angle of repose of sand; it generally forms in areas of sparse vegetation. [GG]

trap—any dark-colored, fine-grained, nongranitic, hypabyssal or extrusive rock such as a basalt, peridotite, diabase, or fine-grained gabbro; also, applied to any such rock used in building roads. [GG]

trellis drainage pattern—a drainage pattern characterized by parallel main streams intersected at or near right angles by their tributaries. [GG]

tributary—(1) A stream feeding, joining, or flowing into a larger stream (at any point along its course) or into a lake. Synonyms: tributary stream; affluent; feeder; side stream; contributory. (2) A valley containing a tributary stream. [GG]

tule marsh—a marsh consisting of large bulrushes, found predominantly in the Southwest.

turbid—opaque with suspended matter, such as of a sediment-laden stream flowing into a lake. [GG]

ultrabasic—said of an igneous rock rich in magnesium and iron, and having a low silica content (less than about 45 percent SiO_2). "Ultrabasic" is one subdivision of a widely used system for classifying igneous rocks on the basis of silica content; the other subdivisions are acidic, basic, and intermediate.

underfit stream—a misfit stream that appears to be too small to have eroded the valley in which it flows. It is a common result of drainage changes effected by capture, by glaciers, or by climatic variations. [GG]

uplift—a structurally high area in the crust produced by positive movements that raise or upthrust the rocks, as in a dome or arch. [GG]

upthrust—a nongeological term sometimes applied to uplifted blocks of crust or mountains; not synonymous with overthrust.

upwarping—the upward warping or uplift of a regional area of the Earth's crust, usually as the result of the release of isostatic pressure; e.g., melting of an ice sheet. [GG]

video tape—a magnetic tape designed to record and play back visual information.

vidicon camera—a TV camera used to acquire and transmit a pictorial image.

viscosity—resistance to flow.

volcanic ash—fine pyroclastic material (less than 4.0 mm (0.16 in.) in diameter; less than 0.25-mm (0.01-in.) diameter for fine ash). The term usually refers to the unconsolidated material but is sometimes also used for its consolidated counterpart, or tuff. [GG]

volcanic pipe—a vertical conduit through the Earth's crust below a volcano through which magmatic materials have passed. It is usually filled with volcanic breccia and fragments of older rock. [GG]

volcanism—the processes by which magma and its associated gases rise into the crust and are extruded onto the Earth's surface and into the atmosphere. (Alternate spelling: vulcanism.) [GG]

wadi—a term used in the desert regions of southwestern Asia and northern Africa for a streambed or channel that is usually dry except during the rainy season, and that often forms an oasis. [GG]

warp—a slight flexure or bend of the Earth's crust, either upward or downward, usually on a broad or regional scale. [GG]

watershed—a drainage basin. The original and "correct" meaning of the term "watershed" signified a "water parting" or the line, ridge, or summit of high ground separating two drainage basins. [GG]

water table—the surface between the zone of saturation and the zone of aeration; that surface of a body of unconfined ground water at which the pressure is equal to that of the atmosphere. [GG]

wave cut—carved or cut away by the action of lake or sea waves, assisted by their currents. The term is widely used in regard to marine cut features. [GG]

wavelength (λ)—the average distance between maxima or minima of a periodic or oscillating wave disturbance.

weathering—the physical and chemical distintegration of rock by atmospheric processes.

wrench fault—a strike-slip fault, or one in which the movement is chiefly horizontal.

xerophyte—a plant adapted to dry conditions; a desert plant. [GG]

yardang—a long, irregular, sharp-crested, undercut ridge in soft material carved on a plateau or unsheltered plain in a desert region by wind erosion.

Page intentionally left blank

Page intentionally left blank

APPENDIX C

*Index of Plates**

Plate number	Scene title	Image I.D. number	Date	Center coordinates	Sun angle, deg		Image source [a]	Caption author [b]
					Azimuth	Elevation		
1	Washington-Baltimore area	1080–15192	Oct. 11, 1972	38°54′ N; 76°48′ W	149	38	NDPF	NMS
2	Downtown Washington, D.C.	—	—	—	—	—	—	NMS
3	Seasonal effects around Washington, D.C.	(*a*) 1170–15193	Jan. 9, 1973	38°44′ N; 76°49′ W	150	23	GE	NMS
		(*b*) 1260–15201	Apr. 9, 1973	38°57′ N; 77°5′ W	134	50	GE	NMS
4	Delmarva Peninsula	(*a*) 1205–15141	Feb. 13, 1973	38°58′ N; 75°29′ W	145	30	GE	NMS
		(*b*) 1403–15125	Aug. 30, 1973	38°54′ N; 75°35′ W	133	51	GE	NMS
5	New York City and Philadelphia	1079–15131	Oct. 10, 1972	40°18′ N; 74°51′ W	150	38	GE	WAF
6	New York City and Long Island	1654–15013	May 8, 1974	40°20′ N; 73°41′ W	126	56	GE	NMS
7	Buffalo, N.Y., and Toronto, Canada	1407–15343	Sept. 3, 1973	43°11′ N; 79°49′ W	140	47	GE	WAF
8	Finger Lakes, N.Y.	1027–15233	Aug. 19, 1972	43°13′ N; 76°41′ W	135	51	GE	NMS
9	Adirondack Mountains, N.Y., and Green Mountains, Vt.	1079–15115	Oct. 10, 1972	44°35′ N; 73°18′ W	153	34	GE	NMS
10	Western New England	1096–15065	Oct. 27, 1972	43°3′ N; 72°30′ W	155	30	GE	NMS
11	Southern New England	1258–15080	Apr. 7, 1973	41°48′ N; 73°14′ W	138	47	NDPF	NMS
12	Boston and Cape Cod	1724–14472	July 17, 1974	41°44′ N; 70°20′ W	120	57	GE	NMS
13	Rocky coast of Maine	1220–14553	Feb. 28, 1973	44°35′ N; 69°11′ W	146	31	NDPF	NMS
14	Harrisburg, Pa.	1495–15222	Nov. 30, 1973	40°11′ N; 77°55′ W	155	24	NDPF	PDL
15	Western Appalachian Plateau	1137–15364	Dec. 7, 1972	40°10′ N; 80°46′ W	155	23	NDPF	NMS
16	Roanoke, Va.	1172–15312	Jan. 11, 1973	37°18′ N; 80°10′ W	149	24	GE	WAF
17	Knoxville, Tenn.	1084–15431	Oct. 15, 1972	36°0′ N; 83°31′ W	148	39	NDPF	WAF
18	Atlanta, Ga.	1084–15433	Oct. 15, 1972	34°34′ N; 83°58′ W	147	40	GE	HAT
19	Outer Banks, N.C.	1637–15085	Apr. 21, 1974	36°0′ N; 76°31′ W	125	54	GE	WAF
20	Cape Fear, N.C.	1080–15203	Oct. 11, 1972	34°38′ N; 78°11′ W	146	42	NDPF	WAF
21	Charleston, S.C.	1081–15264	Oct. 12, 1972	33°9′ N; 80°3′ W	145	42	GE	HAT
22	South-central Georgia	1263–15393	Apr. 12, 1973	31°49′ N; 83°37′ W	124	54	NDPF	NMS
23	State of Florida	Mosaic	Oct. 1972 to Apr. 1973	—	—	—	GE	NMS
24	State of Florida	Sketch map of mosaic	—	—	—	—	—	NMS
25	Southern Florida	1242–15240	Mar. 22, 1973	25°59′ N; 80°55′ W	124	50	NDPF	WAF
26	Cape Canaveral, Fla.	1045–15275	Sept. 6, 1972	28°45′ N; 81°21′ W	123	54	GE	WAF
27	Mobile, Ala.	1482–15541	Nov. 17, 1973	30°11′ N; 88°12′ W	149	34	EROS	HAT
28	Huntsville, Ala.	1158–15552	Dec. 28, 1972	34°37′ N; 86°49′ W	150	26	GE	PDL
29	Nashville Dome and Basin	1086–15544	Oct. 17, 1972	36°0′ N; 86°23′ W	148	39	PS	NMS
30	Louisville and Cincinnati	1086–15535	Oct. 17, 1972	38°51′ N; 85°28′ W	150	37	GE	NMS
31	Erie, Pa.	1209–15362	Feb. 17, 1973	41°46′ N; 80°16′ W	146	29	NDPF	WAF
32	Western Lake Erie	1228–15422	Mar. 8, 1973	41°47′ N; 81°45′ W	143	36	GE	NMS
33	State of Michigan	Mosaic	—	—	—	—	GE	NMS
34	State of Michigan	Sketch map of mosaic	—	—	—	—	—	NMS
35	Upper Michigan	1089–16090	Oct. 20, 1972	45°57′ N; 87°7′ W	155	30	GE	NMS
36	Lower peninsula of Michigan	1247–15474	Mar. 27, 1973	43°10′ N; 82°43′ W	141	42	NDPF	MHP
37	Detroit, Mich.	1319–15474	June 7, 1973	41°50′ N; 83°18′ W	123	61	GE	NMS
38	Chicago, Ill.	1124–16050	Nov. 24, 1972	41°40′ N; 87°24′ W	156	24	GE	PDL
39	St. Louis, Mo.	1071–16104	Oct. 2, 1972	39°0′ N; 89°37′ W	146	41	GE	NMS
40	Kansas City	5028–16075	May 17, 1975	38°50′ N; 94°20′ W	116	56	GE	NMS
41	Mississippi River flood sequence	1070–16055	Oct. 1, 1972	36°6′ N; 89°9′ W	143	44	NDPF	NMS
42	Mississippi River flood sequence	(*a*) 1214–16065	Feb. 22, 1973	36°3′ N; 89°23′ W	141	35	GE	NMS
		(*b*) 1286–16065	May 5, 1973	36°11′ N; 89°28′ W	122	59	NDPF	NMS
		(*c*) 1322–16063	June 10, 1973	36°9′ N; 89°30′ W	111	62	NDPF	NMS
		(*d*) 1394–16053	Aug. 21, 1973	36°1′ N; 89°27′ W	125	54	NDPF	NMS

* Compiled by Nicholas M. Short, *Goddard Space Flight Center.*

Note—Additional footnotes appear on last page of index.

Plate number	Scene title	Image I.D. number	Date	Center coordinates	Sun angle, deg		Image source [a]	Caption author [b]
					Azimuth	Elevation		
43	State of Louisiana	Mosaic	—	—	—	—	GE	NMS
44	State of Louisiana	Sketch map of mosaic	—	—	—	—	—	NMS
45	Yazoo Basin, Miss.	1340–16070	June 28, 1973	33°11′ N; 90°23′ W	103	62	GE	NMS
46	Texas-Louisiana Timberlands	1252–16194	Apr. 1, 1973	31°47′ N; 93°40′ W	128	51	GE	NMS
47	Mississippi Delta	1177–16023	Jan. 16, 1973	29°21′ N; 89°44′ W	145	31	EROS	HAT
48	Southern Louisiana	1286–16083	May 5, 1973	30°27′ N; 91°11′ W	112	60	GE	NMS
49	Ouachita Mountains	1128–16300	Nov. 28, 1972	34°34′ N; 95°32′ W	153	29	GE	HAT
50	Boston Mountains, Ark.	1073–16230	Oct. 4, 1972	36°6′ N; 93°29′ W	145	43	GE	NMS
51	Missouri Ozarks	1251–16122	Mar. 31, 1973	37°32′ N; 90°28′ W	135	47	NDPF	NMS
52	Upper Mississippi River	1037–16210	Aug. 29, 1972	42°46′ N; 91°11′ W	138	49	GE	NMS
53	Lake country, Minnesota	1075–16321	Oct. 6, 1972	44°35′ N; 93°24′ W	152	36	GE	NMS
54	Duluth, Minn.	1345–16313	July 3, 1973	47°24′ N; 92°35′ W	131	58	NDPF	HAT
55	North and South Dakota and Minnesota	1060–16485	Sept. 21, 1972	45°56′ N; 97°11′ W	149	40	NDPF	NMS
56	Glacial plains, North Dakota	1297–17060	May 16, 1973	48°58′ N; 100°30′ W	140	55	NDPF	NMS
57	Omaha, Nebr., and Council Bluffs, Iowa	1022–16385	Aug. 14, 1972	40°45′ N; 96°15′ W	129	54	GE	HAT
58	Western Kansas	1402–16503	Aug. 29, 1973	38°53′ N; 100°1′ W	133	51	NDPF	NMS
59	Oklahoma City and Tulsa	1003–16352	July 26, 1972	35°43′ N; 96°45′ W	114	59	GE	NMS
60	Oklahoma oil country	1257–16471	Apr. 6, 1973	36°7′ N; 99°32′ W	131	50	NDPF	NMS
61	The High Plains	2112–16515	May 14, 1975	35°52′ N; 103°33′ W	115	58	NDPF	NMS
62	Dallas-Ft. Worth	1002–16314	July 25, 1972	33°1′ N; 96°29′ W	109	59	NDPF	PDL
63	Houston, Tex.	1289–16254	May 8, 1973	30°21′ N; 95°32′ W	110	61	GE	NMS
64	South Texas coast	1092–16314	Oct. 23, 1972	27°21′ N; 97°33′ W	144	43	GE	NMS
65	Edwards Plateau, Tex.	1131–16483	Dec. 1, 1972	30°15′ N; 101°5′ W	151	32	NDPF	NMS
66	Big Bend country, west Texas	1511–16565	Dec. 16, 1973	30°15′ N; 104°0′ W	149	29	GE	NMS
67	Llano Estacado, Tex.	1330–16531	June 18, 1973	33°14′ N; 101°52′ W	103	63	NDPF	NMS
68	Pecos River, N. Mex.	1098–17043	Oct. 29, 1972	33°5′ N; 104°34′ W	149	37	NDPF	NMS
69	Southeastern Colorado	1098–17032	Oct. 29, 1972	37°21′ N; 103°12′ W	152	34	NDPF	NMS
70	Cheyenne, Wyo.	1172–17132	Jan. 11, 1973	41°36′ N; 104°32′ W	151	21	NDPF	HAT
71	Sand Hills, Nebr.	1296–17023	May 15, 1973	41°53′ N; 101°54′ W	129	58	GE	NMS
72	Western Great Plains	1711–16592	July 4, 1974	43°16′ N; 102°47′ W	121	58	EROS	NMS
73	Black Hills Region, S. Dak.	1352–17123	July 10, 1973	44°35′ N; 103°43′ W	126	58	NDPF	NMS
74	Black Hills Region, S. Dak.	1172–17123	Jan. 11, 1973	44°26′ N; 103°28′ W	153	19	GE	NMS
75	Colorado Rocky Mountains	1352–17134	July 10, 1973	40°21′ N; 105°17′ W	118	60	IBM	NMS
76	Colorado Rocky Mountains	1172–17135	Jan. 11, 1973	40°10′ N; 105°2′ W	151	22	GE	NMS
77	Uranium country, Utah-Colorado	1408–17244	Sept. 4, 1973	38°55′ N; 108°36′ W	135	49	EROS	NMS
78	North-central New Mexico	1010–17143	Aug. 2, 1972	36°2′ N; 106°26′ W	117	58	GE	NMS
79	White Sands, N. Mex.	1333–17102	June 21, 1973	33°13′ N; 106°12′ W	103	62	NDPF	NMS
80	El Paso, Tex.	1153–17105	Dec. 23, 1972	31°41′ N; 106°21′ W	150	28	NDPF	NMS
81	Tucson, Ariz.	1264–17283	Apr. 13, 1973	31°50′ N; 110°54′ W	124	55	NDPF	NMS
82	Phoenix, Ariz.	1211–17334	Feb. 19, 1973	33°11′ N; 111°46′ W	140	36	NDPF	WAF
83	North-central Arizona	1463–17300	Oct. 29, 1973	36°0′ N; 110°46′ W	150	35	EROS	NMS
84	Northwest New Mexico	1515–17180	Dec. 20, 1973	35°58′ N; 108°1′ W	151	25	NDPF	NMS
85	Canyon lands, southeast Utah	1211–17323	Feb. 19, 1973	37°29′ N; 110°25′ W	143	33	NDPF	NMS
86	6 views of canyon lands	—	—	—	—	—	—	PDL
87	Grand Canyon, Ariz.	1284–17384	May 3, 1973	36°8′ N; 112°26′ W	123	58	NDPF	WAF
88	Rock units in Arizona	1032–17373	Aug. 24, 1972	36°33′ N; 112°6′ W	128	53	—	NMS
89	Shivwits Plateau, Ariz.	1411–17424	Sept. 7, 1973	36°2′ N; 113°48′ W	133	50	EROS	WAF
90	High Plateau, Utah	1411–17422	Sept. 7, 1973	37°28′ N; 113°21′ W	135	49	GE	NMS
91	San Rafael Swell, Utah	1032–17364	Aug. 24, 1972	39°25′ N; 111°0′ W	132	52	NDPF	NMS
92	San Rafael Swell, Utah	SL2–81–014	June 5, 1973	—	—	—	JSC	NMS
93	Great Salt Lake, Utah	1015–17415	Aug. 7, 1972	40°33′ N; 112°10′ W	126	55	GE	NMS
94	Southwestern Wyoming	1014–17355	Aug. 6, 1972	41°44′ N; 110°14′ W	128	55	NDPF	NMS
95	State of Wyoming	Mosaic	—	—	—	—	GE	NMS
96	State of Wyoming	Sketch map of mosaic	—	—	—	—	—	NMS
97	Central Wyoming	1013–17294	Aug. 5, 1972	43°10′ N; 108°17′ W	130	54	GE	NMS
98	Yellowstone National Park	1015–17404	Aug. 7, 1972	44°48′ N; 110°35′ W	133	53	GE	NMS
99	Bighorn Mountains, Wyo.	1013–17291	Aug. 5, 1972	44°35′ N; 107°44′ W	132	54	GE	NMS
100	Western Wyoming and southeastern Idaho	1069–17411	Sept. 30, 1972	43°11′ N; 111°5′ W	149	39	GE	NMS
101	Southern Idaho	1035–17525	Aug. 27, 1972	43°2′ N; 114°7′ W	137	49	GE	NMS
102	Idaho Rocky Mountains	1035–17522	Aug. 27, 1972	44°27′ N; 113°35′ W	139	48	NDPF	NMS
103	Montana Rocky Mountains	1034–17461	Aug. 26, 1972	45°54′ N; 111°35′ W	140	48	NDPF	NMS
104	U.S.-Canadian border	1700–17381	June 23, 1974	48°54′ N; 110°34′ W	131	57	NDPF	NMS
105	Oregon and Washington	Mosaic	—	—	—	—	GE	NMS
106	Oregon and Washington	Sketch map of mosaic	—	—	—	—	—	NMS
107	Northwest Washington State	1006–18313	July 29, 1972	47°19′ N; 122°23′ W	134	54	GE	NMS

Plate number	Scene title	Image I.D. number	Date	Center coordinates	Sun angle, deg		Image source [a]	Caption author [b]
					Azimuth	Elevation		
108	Northwest Washington State	1006–18313 (RBV)	July 29, 1972	47°19′ N; 122°23′ W	134	54	NDPF	NMS
109	Eastern Washington	1039–18143	Aug. 31, 1972	47°21′ N; 118°10′ W	144	45	GE	NMS
110	Portland, Oreg.	1006–18315	July 29, 1972	45°56′ N; 123°2′ W	132	54	GE	NMS
111	Cascade Range, Oregon	1004–18212	July 27, 1972	42°58′ N; 121°18′ W	127	56	GE	NMS
112	Basin and Range country, Oregon and Nevada	1380–18102	Aug. 7, 1973	41°39′ N; 119°7′ W	128	55	GE	NMS
113	State of Nevada	Mosaic	—	—	—	—	APN	NMS
114	State of Nevada	Sketch map of mosaic	—	—	—	—	—	NMS
115	Elko, Nev.	1342–17594	June 30, 1973	40°22′ N; 116°48′ W	118	61	NDPF	HAT
116	Las Vegas, Nev.	1124–17495	Nov. 24, 1972	35°58′ N; 115°8′ W	153	28	NDPF	WAF
117	Reno, Nev.	1380–18104	Aug. 7, 1973	40°15′ N; 119°37′ W	126	55	GE	NMS
118	Reno, Nev.	1380–18104 (black and white)	Aug. 7, 1973	40°15′ N; 119°37′ W	126	55	USGS	NMS
119	Owens Valley, eastern California	1054–18001	Sept. 15, 1972	37°23′ N; 117°29′ W	139	47	NDPF	NMS
120	Goldfield, Nev.	—	—	—	—	—	—	NMS
121	State of California	Mosaic	—	—	—	—	GE	NMS
122	State of California	Sketch map of mosaic	—	—	—	—	—	NMS
123	Lake Tahoe, Calif.	1056–18111	Sept. 17, 1972	38°49′ N; 119°53′ W	141	46	GE	WAF
124	Mono Lake, Calif.	1397–18053	Aug. 24, 1973	37°27′ N; 119°8′ W	129	53	EROS	WAF
125	Monterey Bay	1002–18134	July 25, 1972	37°17′ N; 120°56′ W	116	59	IBM	PDL
126	Bay area, California	1075–18173	Oct. 6, 1972	37°29′ N; 121°44′ W	146	41	NDPF	NMS
127	San Francisco, Calif.	Enlargement	—	—	—	—	—	NMS
128	San Francisco, Calif.	Sketch map of enlargement	—	—	—	—	—	NMS
129	Los Angeles, Calif.	1234–18021	Mar. 14, 1973	34°34′ N; 118°37′ W	136	43	GE	WAF
130	Los Angeles aerial mosaic	—	—	—	—	—	AS	WAF
131	Santa Barbara, Calif.	1307–18073	May 26, 1973	34°43′ N; 120°1′ W	112	62	GE	WAF
132	San Diego, Calif.	1125–17563	Nov. 25, 1972	33°5′ N; 117°30′ W	152	31	GE	WAF
133	Imperial Valley, Calif.	1358–17501	July 16, 1973	33°12′ N; 116°9′ W	106	60	NDPF	WAF
134	Salton Sea, Calif.	AS9–26A–3748A	March 1969	—	—	—	PS	PDL
135	Island of Hawaii	Mosaic	—	—	—	—	GE	NMS
136	Island of Hawaii	Sketch map of mosaic	—	—	—	—	—	NMS
137	Juneau and Glacier Bay, Alaska	1307–19434	May 26, 1973	58°46′ N; 135°17′ W	152	50	NDPF	NMS
138	Wrangell Mountains area, Alaska	1422–20212 and 1422–20215	Sept. 18, 1973	61°25′ N; 144°19′ W	160	30	GE	—
139	Bend of the Yukon	1102–20441	Nov. 2, 1972	66°31′ N; 143°50′ W	171	8	NDPF	NMS
140	Fairbanks area, Alaska	Mosaic	—	—	—	—	UA	LWG
141	Cook Inlet and Anchorage area	1103–20513	Nov. 3, 1972	61°6′ N; 150°27′ W	166	12	NDPF	LWG
142	Alaska Range	1033–21020	Aug. 25, 1972	62°43′ N; 153°0′ W	159	36	GE	LWG
143	"Finger Lakes" of Alaska	1018–21200	Aug. 10, 1972	59°57′ N; 158°36′ W	153	43	NDPF	NMS
144	Brooks Range	1072–21173	Oct. 3, 1972	68°7′ N; 150°26′ W	171	17	NDPF	LWG
145	Walker Lake area, Alaska	1037–21234	Aug. 29, 1972	66°49′ N; 153°40′ W	165	31	NDPF	LWG
146	Upper Koyukuk-Kobuk River area, Alaska	1003–21355	July 26, 1972	66°13′ N; 157°15′ W	161	42	GE	LWG
147	Point Barrow, Alaska	1006–21510	July 29, 1972	70°32′ N; 155°27′ W	168	37	GE	LWG
148	Yukon Delta, Alaska	1455–21460	Oct. 21, 1973	62°51′ N; 163°23′ W	166	15	GE	NMS
149	Cape Beaufort, Alaska	1046–22143	Sept. 7, 1972	69°20′ N; 163°12′ W	170	26	NDPF	LWG
150	U.S.-Soviet border	1335–22215	June 23, 1973	65°34′ N; 169°48′ W	160	46	GE	NMS
151	Sea ice off Newfoundland	1570–13520	Feb. 13, 1974	48°43′ N; 53°3′ W	150	23	CCRS	CCRS
152	Prince Edward Island and Nova Scotia, Canada	1180–14314	Jan. 19, 1973	45°44′ N; 62°51′ W	153	20	CCRS	CCRS
153	Anticosti Island, Quebec	1073–14354	Oct. 4, 1972	49°57′ N; 62°33′ W	155	33	CCRS	CCRS
154	New Brunswick Province, Canada	1614–14373	Mar. 29, 1974	47°15′ N; 65°14′ W	143	41	CCRS	CCRS
155	Manicouagan Lake, Quebec	1636–14584	Apr. 20, 1974	51°31′ N; 69°5′ W	145	46	CCRS	CCRS
156	Clearwater Lakes, Quebec	1552–15333	Jan. 26, 1974	55°47′ N; 75°18′ W	156	13	CCRS	CCRS
157	Labrador fold belt	1438–15013	Oct. 4, 1973	55°34′ N; 66°51′ W	159	28	CCRS	CCRS
158	Akimiski Island, James Bay	1447–15534	Oct. 13, 1973	52°46′ N; 81°15′ W	158	27	CCRS	CCRS
159	Montreal	1440–15155	Oct. 6, 1973	45°40′ N; 74°26′ W	152	35	CCRS	CCRS
160	Eastern townships, Quebec	1096–15060	Oct. 27, 1972	45°53′ N; 71°23′ W	156	28	GE	NMS
161	Ottawa	1243–15235	Mar. 23, 1973	46°0′ N; 75°52′ W	144	39	NDPF	CCRS
162	Ungava Bay Region, Quebec	1027–15193	Aug. 19, 1972	57°2′ N; 70°4′ W	151	42	GE	NMS
163	Winnipeg, Manitoba	1223–16542	Mar. 3, 1973	50°16′ N; 96°55′ W	149	28	NDPF	CCRS and NMS
164	Wawa, Ontario	1376–16021	Aug. 3, 1973	48°34′ N; 84°48′ W	137	53	CCRS	CCRS

Plate number	Scene title	Image I.D. number	Date	Center coordinates	Sun angle, deg		Image source [a]	Caption author [b]
					Azimuth	Elevation		
165	Lethbridge, Alberta	1396–17560	Aug. 23, 1973	50°12′ N; 112°48′ W	144	46	NDPF	CCRS
166	Drumlin Field, north Saskatchewan	1557–17443	Jan. 31, 1974	58°33′ N; 106°33′ W	157	12	CCRS	CCRS
167	Great Slave Lake	1436–18143	Oct. 2, 1973	62°27′ N; 110°49′ W	165	23	CCRS	CCRS
168	Great Slave Lake	1436–18145	Oct. 2, 1973	61°5′ N; 111°56′ W	163	24	CCRS	CCRS
169	Horn Plateau, Northwest Territories	1423–18433	Sept. 19, 1973	62°29′ N; 117°59′ W	163	28	CCRS	CCRS
170	Forest fire south of Great Bear Lake	1372–19011	July 30, 1973	63°50′ N; 121°9′ W	157	43	CCRS	CCRS
171	Baffin Island, Northwest Territories	1404–16522	Aug. 31, 1973	70°31′ N; 81°19′ W	171	28	CCRS	CCRS
172	Coronation Gulf, Northwest Territories	1189–18432	Jan. 28, 1973	67°50′ N; 112°13′ W	166	3	CCRS	CCRS
173	Melville Island, Northwest Territories	1005–20000	July 28, 1972	76°1′ N; 114°44′ W	184	32	NDPF	NMS
174	Tuktoyaktuk Peninsula	1421–20131	Sept. 17, 1973	69°15′ N; 133°10′ W	171	23	CCRS	CCRS
175	Rocky Mountain Trench, British Columbia	2182–18183	July 23, 1975	53°12′ N; 119°44′ W	137	51	NDPF	PDL
176	Surging glaciers, northern British Columbia	1417–19532	Sept. 13, 1973	59°44′ N; 137°22′ W	159	32	CCRS	CCRS
177	Colorado River Delta, Mexico	1321–17451	June 9, 1973	31°50′ N; 115°10′ W	102	63	NDPF	WAF
178	Pinacate Volcanic Field	1410–17382	Sept. 6, 1973	31°46′ N; 113°40′ W	127	53	NDPF	PDL
179	Northern Baja California Peninsula, Mexico	1069–17450	Sept. 30, 1972	30°20′ N; 115°19′ W	138	48	NDPF	WAF
180	Ciudad Obregón, Mexico	1262–17182	Apr. 11, 1973	27°32′ N; 109°14′ W	118	56	GE	WAF
181	Mazatlán, Mexico	1079–17012	Oct. 10, 1972	23°9′ N; 105°48′ W	135	49	GE	WAF
182	Sierra Madre Occidental, Mexico	1115–17013	Nov. 15, 1972	24°31′ N; 105°32′ W	146	39	GE	WAF
183	Big Bend, Tex., and Chihuahua	1816–16430	Oct. 17, 1974	28°56′ N; 103°0′ W	139	42	NDPF	NMS
184	Sierra Madre Oriental, Mexico	1075–16380	Oct. 6, 1972	24°35′ N; 99°43′ W	134	50	GE	NMS
185	Torreón, Mexico	1078–16545	Oct. 9, 1972	26°2′ N; 103°35′ W	137	48	GE	WAF
186	Tampico, Mexico	1109–16275	Nov. 9, 1972	21°31′ N; 97°42′ W	143	43	GE	WAF
187	Mexico City, Mexico	1307–16285	May 26, 1973	18°52′ N; 98°33′ W	80	61	GE	PDL
188	Acapulco	1254–16352	Apr. 3, 1973	17°24′ N; 100°23′ W	106	56	GE	NMS
189	Bahamas Platform	1510–15093	Dec. 15, 1973	24°32′ N; 78°19′ W	146	34	GE	NMS
190	Puerto Rico mosaic	—	—	—	—	—	GE	NMS
191	Hispaniola	1523–14421	Dec. 28, 1973	18°46′ N; 72°36′ W	141	37	GE	NMS
192	Havana, Cuba	1171–15295	Jan. 10, 1973	22°57′ N; 82°54′ W	142	35	NDPF	NMS
193	Managua, Nicaragua	1243–15335	Mar. 23, 1973	11°38′ N; 85°59′ W	104	54	GE	WDC
194	Isthmus of Panama	1239–15115	Mar. 19, 1973	8°45′ N; 80°54′ W	103	54	GE	NMS
195	Caracas, Venezuela	1176–14185	Jan. 15, 1973	10°21′ N; 67°23′ W	132	43	GE	NMS
196	Orinoco Basin, Venezuela	1086–14194	Oct. 17, 1972	7°15′ N; 68°8′ W	119	56	NDPF	WAF
197	Colombian interior	1196–14325	Feb. 4, 1973	2°59′ N; 72°3′ W	118	48	GE	NMS
198	Southern Peru	1645–14255	April 29, 1974	14°22′ S; 74°44′ W	53	43	GE	NMS
199	Atacama Desert, Peru and Chile	1245–14105	Mar. 25, 1973	18°35′ S; 70°11′ W	65	46	NDPF	WAF
200	Chuquicamata and Calama, Chile	1010–14044	Aug. 2, 1972	21°52′ S; 69°21′ W	47	34	NDPF	WAF
201	Salars of Bolivia	1243–13595	Mar. 23, 1973	20°3′ S; 67°40′ W	65	46	GE	NMS
202	Serrania de Huanchaca, Brazil-Bolivia	1005–13335	July 28, 1972	14°22′ S; 60°16′ W	49	39	GE	WAF
203	Orinoco Basin	1229–14151 (band 5)	Mar. 9, 1973	5°56′ N; 67°11′ W	105	52	GE	NMS
204	Orinoco Basin	1229–14151 (band 7)	Mar. 9, 1973	5°56′ N; 67°11′ W	105	52	GE	NMS
205	Amazon River, Brazil	1008–13481	July 31, 1972	4°25′ S; 62°12′ W	56	47	GE	NMS
206	Mouth of the Amazon	1126–13013	Nov. 26, 1972	1°28′ N; 49°28′ W	128	52	GE	NMS
207	Chapada das Mangabeiras, Brazil	1050–12411	Sept. 11, 1972	10°10′ S; 46°23′ W	69	52	GE	WAF
208	Mato Grosso Plateau, Brazil	1091–13113	Oct. 22, 1972	14°22′ S; 54°35′ W	88	57	GE	WAF
209	New meteorite crater, Brazil	—	—	—	—	—	Terratek	NMS
210	Paraná River, Brazil	1088–12562	Oct. 19, 1972	21°31′ S; 52°4′ W	76	55	NDPF	WAF
211	Rio de Janeiro, Brazil	1208–12225	Feb. 16, 1973	22°55′ S; 43°55′ W	82	49	GE	NMS
212	Paraguay	1235–13151	Mar. 15, 1973	24°22′ S; 57°18′ W	66	44	GE	NMS
213	Uruguay River, Brazil and Argentina	1106–12582	Nov. 6, 1972	27°24′ S; 53°42′ W	78	55	GE	WAF
214	Humid pampa, Argentina	1073–13163	Oct. 4, 1972	32°57′ S; 59°29′ W	58	45	GE	NMS
215	Bahía Blanca, Argentina	1074–13240	Oct. 5, 1972	38°39′ S; 62°47′ W	56	41	GE	WAF
216	Tucumán, Argentina	1240–13444	Mar. 20, 1973	27°12′ S; 65°14′ W	62	42	NDPF	WAF
217	Lake Nihuil, Argentina	1241–13525	Mar. 21, 1973	35°43′ S; 69°11′ W	57	36	NDPF	WAF
218	Patagonia, Argentina	1241–13541	Mar. 21, 1973	40°2′ S; 70°36′ W	55	33	GE	NMS
219	Iceland	1392–12191	Aug. 19, 1973	64°4′ N; 20°32′ W	159	37	GE	PDL
220	Northern Iceland	1372–12080	July 30, 1973	64°7′ N; 17°38′ W	157	42	GE	PDL
221	Greenland	1064–13360	Sept. 25, 1972	75°31′ N; 20°16′ W	185	13	NDPF	PDL
222	Norway	1299–10202	May 18, 1973	62°55′ N; 8°29′ E	159	45	NDPF	PDL
223	Sweden	1345–09351	July 3, 1973	58°36′ N; 16°37′ E	148	51	NDPF	PDL
224	Denmark	1041–09471	Sept. 2, 1972	55°48′ N; 12°0′ E	153	39	GE	PDL
225	Scotland	1233–10564	Mar. 13, 1973	57°10′ N; 4°8′ W	154	27	GE	PDL
226	Nottingham—Robin Hood country	1319–10343	June 7, 1973	53°11′ N; 0°55′ W	142	55	GE	NMS
227	London	1228–10293	Mar. 8, 1973	51°40′ N; 0°6′ W	150	29	GE	PDL
228	The Netherlands	1243–10120	Mar. 23, 1973	52°59′ N; 4°55′ E	150	34	GE	PDL
229	Paris	1243–10132	Mar. 23, 1973	48°46′ N; 2°53′ E	147	37	GE	PDL

Plate number	Scene title	Image I.D. number	Date	Center coordinates	Sun angle, deg		Image source [a]	Caption author [b]
					Azimuth	Elevation		
230	Pyrenees	1028–10193	Aug. 20, 1972	42°47′ N; 0°49′ W	134	51	NDPF	PDL
231	Zaragoza, Spain	1352–10201	July 10, 1973	41°47′ N; 1°29′ W	121	59	GE	PDL
232	Madrid	1227–10271	Mar. 7, 1973	40°19′ N; 3°21′ W	142	37	GE	PDL
233	Rhone Valley, France	Mosaic	—	—	—	—	GE	PDL
234	Rhone Valley, France	Sketch map of mosaic	—	—	—	—	—	PDL
235	Lake Geneva	1078–09555	Oct. 9, 1972	45°58′ N; 6°11′ E	153	34	GE	PDL
236	Central Alps	1039–09381	Aug. 31, 1972	47°21′ N; 11°0′ E	143	45	NDPF	PDL
237	Rhine and Ruhr Valleys	1043–09595	Sept. 4, 1972	51°33′ N; 7°11′ E	149	41	GE	NMS
238	Nürnberg	1076–09431	Oct. 7, 1972	50°12′ N; 10°55′ E	156	31	GE	PDL
239	Berlin	1021–09362	Aug. 13, 1972	52°59′ N; 13°41′ E	145	47	GE	PDL
240	Vienna	1468–09184	Nov. 3, 1973	48°48′ N; 15°55′ E	158	23	GE	PDL
241	Italy	Mosaic	—	—	—	—	GE	PDL
242	Italy	Sketch map of mosaic	—	—	—	—	—	PDL
243	Sicily	1106–09130	Nov. 6, 1972	37°11′ N; 14°22′ E	153	32	GE	PDL
244	Rome	1198–09232	Feb. 6, 1973	41°46′ N; 13°5′ E	147	26	GE	PDL
245	Po Valley	1218–09341	Feb. 26, 1973	44°35′ N; 11°12′ E	146	30	NDPF	PDL
246	Dalmatian Coast of Yugoslavia	1465–09030	Oct. 31, 1973	43°10′ N; 17°55′ E	155	29	GE	NMS
247	Albania and Greece	1102–08491	Nov. 2, 1972	40°6′ N; 21°6′ E	154	31	GE	PDL
248	Athens	1010–08375	Aug. 2, 1972	37°20′ N; 23°4′ E	119	57	GE	PDL
249	Yugoslavia-Rumania	1463–08511	Oct. 29, 1973	44°31′ N; 21°23′ E	155	28	GE	PDL
250	Middle Europe	1467–09123	Nov. 2, 1973	50°17′ N; 18°3′ E	159	22	GE	NMS
251	Leningrad	1246–08435	Mar. 26, 1973	60°1′ N; 30°40′ E	157	30	NDPF	PDL
252	Moscow	1582–08052	Feb. 25, 1974	56°0′ N; 36°47′ E	153	21	GE	NMS
253	The Ukraine	1530–08200	Jan. 4, 1974	50°11′ N; 30°51′ E	156	13	NDPF	NMS
254	Bosporus, Turkey	1115–08201	Nov. 15, 1972	41°34′ N; 28°51′ E	156	26	GE	PDL
255	Armenia, Turkey	1485–07323	Nov. 20, 1973	38°47′ N; 39°16′ E	154	27	GE	PDL
256	The Lower Volga	1358–07253	July 16, 1973	50°15′ N; 45°0′ E	136	55	NDPF	NMS
257	Kara Bogaz Gol Gulf, U.S.S.R.	1134–06425	Dec. 4, 1972	41°31′ N; 53°7′ E	156	22	NDPF	WAF
258	Meeting of three countries (Iran, Afghanistan, and the U.S.S.R.)	1091–06035	Oct. 22, 1972	35°54′ N; 61°18′ E	149	37	NDPF	NMS
259	Southern Aral Sea, U.S.S.R.	1310–06192	May 29, 1973	43°16′ N; 59°16′ E	128	59	NDPF	NMS
260	World's largest lake	2150–03123	June 21, 1975	52°55′ N; 106°43′ E	136	54	GE	NMS
261	Uzbek S.S.R.	1070–05445	Oct. 1, 1972	40°23′ N; 67°11′ E	147	41	NDPF	NMS
262	Lake Balkhash, U.S.S.R.	1049–05260	Sept. 10, 1972	46°0′ N; 73°32′ E	145	43	NDPF	NMS
263	West Siberian steppes, U.S.S.R.	1309–06102	May 28, 1973	54°37′ N; 65°48′ E	146	53	NDPF	NMS
264	Vasyugan Swamp, U.S.S.R.	1126–05513	Nov. 26, 1972	59°46′ N; 73°48′ E	165	8	GE	WAF
265	Northern Urals	1211–07045	Feb. 19, 1973	64°9′ N; 58°43′ E	161	13	GE	NMS
266	Ob River, Siberia	1325–05563	June 13, 1973	61°30′ N; 73°14′ E	154	49	GE	NMS
267	Nizhnyaya Tunguska River, U.S.S.R.	1097–04465	Oct. 28, 1972	63°54′ N; 93°0′ E	168	12	GE	WAF
268	Lena-Aldan Plateau, U.S.S.R.	1089–02184	Oct. 20, 1972	59°54′ N; 126°56′ E	164	18	NDPF	WAF
269	Indigirka River system, U.S.S.R.	1097–01201	Oct. 28, 1972	63°57′ N; 144°35′ E	168	12	GE	WAF
270	Anadyr', U.S.S.R.	1073–23075	Oct. 4, 1972	64°9′ N; 177°48′ E	166	20	GE	WAF
271	Southern Red Sea	Mosaic	—	—	—	—	GE	PDL
272	Southern Red Sea	Sketch map	—	—	—	—	—	PDL
273	Northern Red Sea	Mosaic	—	—	—	—	GE	HWB
274	Northern Red Sea	Sketch map	—	—	—	—	—	HWB
275	Mideast	1054–07415	Sept. 15, 1972	33°3′ N; 36°7′ E	134	50	GE	NMS
276	Tigris and Euphrates Rivers	1153–06514	Dec. 23, 1972	30°20′ N; 48°8′ E	149	29	GE	NMS
277	Northern Saudi Arabia	1049–07145	Sept. 10, 1972	27°24′ N; 41°39′ E	124	54	NDPF	HWB
278	Western Saudi Arabia	1192–07115	Jan. 31, 1973	20°18′ N; 41°8′ E	135	39	GE	HWB
279	Arabian oil fields	1166–06252	Jan. 5, 1973	21°37′ N; 53°1′ E	142	35	NDPF	HWB
280	Arabian oil fields	1169–06411	Jan. 8, 1973	25°58′ N; 49°51′ E	144	32	GE	HWB
281	Southern Arabian Peninsula	1186–06381	Jan. 25, 1973	17°28′ N; 49°4′ E	135	40	NDPF	HWB
282	Oman Mountains	1126–06022	Nov. 26, 1972	22°55′ N; 59°2′ E	146	38	NDPF	PDL
283	Tehran, Iran	1044–06434	Sept. 5, 1972	35°55′ N; 51°19′ E	132	51	GE	NMS
284	Great Kavir, Iran	1149–06273	Dec. 19, 1972	34°35′ N; 55°9′ E	152	26	EROS	NMS
285	Dasht-E-Lut, Eastern Iran	1127–06060	Nov. 27, 1972	30°10′ N; 59°32′ E	151	33	GE	NMS
286	Dasht-E-Lut, Eastern Iran	1128–06114	Nov. 28, 1972	30°7′ N; 58°5′ E	151	32	GE	NMS
287	Southern Iran	Mosaic	—	—	—	—	ESC	NMS
288	Southern Iran	Sketch map of mosaic	—	—	—	—	—	NMS
289	Iran-Afghanistan border	1073–06042	Oct. 4, 1972	33°7′ N; 60°30′ E	142	45	NDPF	NMS
290	Makran Range, Iran	1090–06010	Oct. 21, 1972	25°55′ N; 59°49′ E	142	45	GE	NMS
291	Baluchistan Mountains, Pakistan	1068–05373	Sept. 29, 1972	26°0′ N; 65°41′ E	132	51	NDPF	NMS
292	Baluchistan Desert	1125–05545	Nov. 25, 1972	28°42′ N; 62°1′ E	150	31	IBM	NMS
293	Indus River Plains, Pakistan	1120–05270	Nov. 20, 1972	25°53′ N; 68°24′ E	148	37	NDPF	NMS
294	Rann of Kutch, India	1190–05161	Jan. 29, 1973	23°13′ N; 70°35′ E	138	37	NDPF	NMS
295	Gulf of Cambay, Western India	1242–05054	Mar. 22, 1973	21°43′ N; 72°51′ E	119	52	GE	NMS

Plate number	Scene title	Image I.D. number	Date	Center coordinates	Sun angle, deg		Image source [a]	Caption author [b]
					Azimuth	Elevation		
296	Aravalli Range, India	1134–05041	Dec. 4, 1972	25°49′ N; 74°4′ E	148	35	NDPF	NMS
297	The peninsular interior of India	1183–04373	Jan. 22, 1973	17°25′ N; 79°9′ E	136	39	NDPF	NMS
298	Top of the World	1144–04174	Dec. 14, 1972	27°20′ N; 86°1′ E	149	32	GE	NMS
299	Tibetan Plateau	(*a*) 1096–04501	Oct. 27, 1972	33°1′ N; 79°0′ E	149	38	GE	NMS
		(*b*) 1358–04031	July 16, 1973	36°4′ N; 91°15′ E	111	60	GE	NMS
		(*c*) 1482–03493	Nov. 17, 1973	35°55′ N; 94°14′ E	152	30	GE	NMS
		(*d*) 1461–03331	Oct. 27, 1973	33°8′ N; 97°46′ E	148	38	GE	NMS
300	Ganges Delta	1105–04014	Nov. 5, 1972	22°56′ N; 89°7′ E	143	43	NDPF	NMS
301	Brahmaputra River	1123–04010	Nov. 23, 1972	25°51′ N; 89°52′ E	148	37	GE	NMS
302	Eastern Burma	1531–03244	Jan. 5, 1974	20°13′ N; 97°0′ E	141	36	GE	NMS
303	Southern Burma	1099–03285	Oct. 30, 1972	17°15′ N; 96°17′ E	137	48	GE	NMS
304	Malaya and Singapore	1451–02451	Oct. 17, 1973	1°31′ N; 104°5′ E	109	57	GE	NMS
305	Southern Thailand	1221–03073	Mar. 1, 1973	13°3′ N; 100°55′ E	118	49	GE	NMS
306	Southern Cambodia	1110–02503	Nov. 10, 1972	11°25′ N; 104°56′ E	135	50	NDPF	NMS
307	Southern Vietnam	1163–02443	Jan. 2, 1973	11°33′ N; 106°25′ E	136	42	GE	NMS
308	Southwest Sinkiang Province, China	1133–04550	Dec. 3, 1972	37°15′ N; 78°56′ E	154	26	NDPF	NMS
309	Lake Baghrash, Sinkiang, China	1398–04235	Aug. 25, 1973	41°43′ N; 87°27′ E	134	51	NDPF	NMS
310	Desert Dunes, Sinkiang, China	1128–04253	Nov. 28, 1972	40°6′ N; 87°3′ E	155	24	NDPF	NMS
311	The "Great Ear" of China	1324–04135	June 12, 1973	40°21′ N; 89°43′ E	119	61	NDPF	NMS
312	Gobi Desert, Mongolia	1083–03323	Oct. 14, 1972	43°9′ N; 101°6′ E	152	34	NDPF	NMS
313	Southern Gobi Desert, Inner Mongolia	1407–03320	Sept. 3, 1973	41°44′ N; 100°26′ E	138	48	NDPF	NMS
314	Hong Kong and Canton, South China Coast	1520–02210	Dec. 25, 1973	23°2′ N; 113°30′ E	144	34	GE	NMS
315	The Yellow River, China	1524–02394	Dec. 29, 1973	37°25′ N; 111°54′ E	151	23	GE	NMS
316	Peking	1486–02280	Nov. 21, 1973	40°12′ N; 115°42′ E	155	26	GE	NMS
317	Yalu River, China and Korea	1100–01441	Oct. 31, 1972	41°34′ N; 127°45′ E	154	30	GE	NMS
318	The two Koreas	1100–01453	Oct. 31, 1972	37°17′ N; 126°16′ E	152	34	NDPF	NMS
319	Northwestern Kyūshū Island, Japan	1078–01232	Oct. 9, 1972	33°10′ N; 130°44′ E	144	43	GE	NMS
320	Osaka, Japan	1093–01060	Oct. 24, 1972	34°29′ N; 135°26′ E	149	38	NDPF	NMS
321	Tokyo, Japan	1126–00484	Nov. 26, 1972	35°53′ N; 140°9′ E	153	28	GE	NMS
322	Dormant volcano awakens	1358–00341	July 16, 1973	44°38′ N; 145°55′ E	127	57	GE	NMS
323	Southern Morocco	1247–10420	Mar. 27, 1973	28°54′ N; 9°50′ W	126	50	GE	HWB
324	Atlas Mountains	1114–09595	Nov. 14, 1972	34°18′ N; 1°59′ E	152	32	NDPF	PDL
325	Mauritania	1247–10432	Mar. 27, 1973	24°35′ N; 11°1′ W	120	52	NDPF	PDL
326	Tanezrouft, Algeria	1112–09505	Nov. 12, 1972	25°45′ N; 2°24′ E	147	39	GE	PDL
327	Tademaït Plateau, Algeria	1022–09491	Aug. 14, 1972	28°54′ N; 3°19′ E	110	58	NDPF	PDL
328	Algeria	1111–09442	Nov. 11, 1972	28°37′ N; 4°37′ E	148	37	NDPF	PDL
329	Libya and Algeria	1070–09160	Oct. 1, 1972	24°35′ N; 10°48′ E	132	51	NDPF	PDL
330	Niger	1194–09061	Feb. 2, 1973	21°42′ N; 12°47′ E	136	39	NDPF	PDL
331	Niger—Air Plateau	1286–09191	May 5, 1973	17°29′ N; 8°40′ E	87	60	NDPF	PDL
332	Richat Structure	1103–10434	Nov. 3, 1972	21°31′ N; 11°38′ W	142	45	GE	PDL
333	Jabal Arkenu, Libya	1114–08200	Nov. 14, 1972	22°51′ N; 24°33′ E	145	41	GE	PDL
334	Tibesti	1191–08485	Jan. 30, 1973	21°45′ N; 17°9′ E	137	38	NDPF	PDL
335	Senegal and Gambia	1283–10463	May 2, 1973	13°9′ N; 13°54′ W	81	59	NDPF	PDL
336	African land practice	1524–09404	Dec. 29, 1973	10°8′ N; 1°17′ E	135	42	GE	NMS
337	Mali	Mosaic	—	—	—	—	GE	PDL
338	Inland delta of the Niger, Mali	1061–10104	Sept. 22, 1972	14°23′ N; 4°43′ W	112	57	GE	PDL
339	Zaire (Congo) River	1237–08092	Mar. 17, 1973	1°32′ N; 23°35′ E	94	53	GE	PDL
340	Kasai River, Zaire	1348–08270	July 6, 1973	2°47′ S; 18°17′ E	52	46	GE	PDL
341	Botswana	1127–08032	Nov. 27, 1972	18°48′ S; 21°45′ E	100	57	NDPF	PDL
342	Botswana	1124–07472	Nov. 24, 1972	23°6′ S; 24°54′ E	92	57	NDPF	PDL
343	Botswana	1052–07454	Sept. 13, 1972	20°12′ S; 25°46′ E	60	46	NDPF	PDL
344	Botswana	1179–07521	Jan. 18, 1973	20°49′ S; 24°11′ E	96	52	NDPF	PDL
345	Zambezi River	1125–07513	Nov. 25, 1972	17°22′ S; 24°56′ E	101	57	NDPF	PDL
346	Zambezi River	1179–07512	Jan. 18, 1973	17°56′ S; 24°55′ E	100	52	NDPF	PDL
347	Namibia	1007–08364	July 30, 1972	18°36′ S; 13°17′ E	48	36	NDPF	PDL
348	Namib Desert	1202–08224	Feb. 10, 1973	25°51′ S; 15°36′ E	82	48	NDPF	PDL
349	Windhoek, Namibia	1382–08205	Aug. 9, 1973	22°59′ S; 16°15′ E	48	35	GE	PDL
350	Namibia	1147–08163	Dec. 17, 1972	24°35′ S; 17°22′ E	95	55	SA	PDL
351	Cape Ranges (South Africa)	1068–07380	Sept. 29, 1972	32°58′ S; 25°9′ E	57	43	SA	PDL
352	Cape Province, South Africa	1068–07373	Sept. 29, 1972	31°32′ S; 25°35′ E	58	44	SA	PDL
353	South Africa, dry season	1050–07355	Sept. 11, 1972	25°57′ S; 27°8′ E	55	42	SA	PDL
354	South Africa, wet season	1158–07363	Dec. 28, 1972	25°53′ S; 27°7′ E	94	54	SA	PDL
355	Rhodesia	1103–07285	Nov. 3, 1972	18°52′ S; 30°18′ E	88	58	GE	PDL
356	Swaziland	1047–07184	Sept. 8, 1972	26°7′ S; 31°24′ E	54	41	GE	PDL
357	Lake Tanganyika	1052–07413	Sept. 13, 1972	5°50′ S; 29°15′ E	75	54	GE	PDL
358	Malagasy Republic	1074–06241	Oct. 5, 1972	15°48′ S; 46°58′ E	75	54	GE	PDL
359	Nairobi	1048–07172	Sept. 9, 1972	1°25′ S; 36°0′ E	78	55	GE	PDL
360	Mt. Kilimanjaro	1533–07091	Jan. 7, 1974	2°51′ S; 37°4′ E	121	49	NDPF	PDL
361	Kenya	1048–07163	Sept. 9, 1972	1°28′ N; 36°40′ E	82	56	GE	PDL

Plate number	Scene title	Image I.D. number	Date	Center coordinates	Sun angle, deg		Image source [a]	Caption author [b]
					Azimuth	Elevation		
362	Kenya	1173–07111	Jan. 12, 1973	1°23′ N; 38°6′ E	125	47	GE	PDL
363	Headwaters of the White Nile	1198–07494	Feb. 6, 1973	8°47′ N; 29°43′ E	123	46	JPL	NMS
364	Sudan	1107–07421	Nov. 7, 1972	14°16′ N; 32°28′ E	137	48	NDPF	PDL
365	Ethiopia	1192–07153	Jan. 31, 1973	7°20′ N; 37°59′ E	124	46	GE	PDL
366	Afar Depression	1100–07024	Oct. 31, 1972	11°28′ N; 41°52′ E	131	52	NDPF	PDL
367	Nile Delta	Mosaic	—	—	—	—	GE	PDL
368	Nile Delta	Sketch map of mosaic	—	—	—	—	—	PDL
369	Southern Luzon Island, Philippines	1153–01463	Dec. 23, 1972	14°31′ N; 121°26′ E	140	41	GE	NMS
370	Western Java, Indonesia	1394–02313	Aug. 21, 1973	5°47′ S; 106°32′ E	63	49	GE	NMS
371	Central Java	1067–02145	Sept. 28, 1972	7°13′ S; 110°43′ E	82	56	IG	NMS
372	Sumbawa, Indonesia	1044–01464	Sept. 5, 1972	8°24′ S; 117°33′ E	67	51	GE	NMS
373	Atolls of the Banda Sea	1112–01234	Nov. 12, 1972	5°54′ S; 123°45′ E	113	57	GE	NMS
374	Central New Guinea	1028–00134	Aug. 20, 1972	4°24′ S; 141°28′ E	64	50	GE	NMS
375	South Island, New Zealand	2192–21265	Aug. 2, 1975	43°5′ S; 172°29′ E	46	15	GE	NMS
376	Mount Egmont, New Zealand	1556–21334	Jan. 30, 1974	38°48′ S; 173°55′ E	75	44	GE	NMS
377	Arnhem Land, Australia	1069–00442	Sept. 30, 1972	11°33′ S; 132°36′ E	77	55	GE	NMS
378	Northwest subtropical coastlands, Australia	1020–01143	Aug. 12, 1972	16°28′ S; 124°15′ E	52	40	GE	NMS
379	Pilbara District, Australia	1148–01282	Dec. 18, 1972	21°45′ S; 119°58′ E	99	55	SA	NMS
380	Northern Australia	1568–00142	Feb. 11, 1974	20°8′ S; 137°39′ E	88	49	NDPF	NMS
381	Perth, southwest Australia	1149–01370	Dec. 19, 1972	31°57′ S; 115°41′ E	86	54	GE	NMS
382	Southwest Australia	1092–01195	Oct. 23, 1972	32°59′ S; 119°44′ E	65	50	GE	NMS
383	Desert country, Western Australia	1344–01165	July 2, 1973	22°53′ S; 122°27′ E	42	30	NDPF	NMS
384	Australian interior	1018–01054	Aug. 10, 1972	25°54′ S; 124°38′ E	47	32	NDPF	NMS
385	Macdonnell Ranges, Australia	1373–00364	July 31, 1973	24°19′ S; 132°7′ E	46	32	NDPF	NMS
386	Broken Hill, Australia	1112–23533	Nov. 12, 1972	31°29′ S; 141°38′ E	75	54	NDPF	NMS
387	Channel country, Australia	1365–23570	July 23, 1973	25°45′ S; 141°47′ E	44	29	NDPF	NMS
388	Channel country, Australia	1563–23530	Feb. 6, 1974	25°56′ S; 141°57′ E	84	48	GE	NMS
389	Sturt Desert, Australia	1563–23535	Feb. 6, 1974	28°46′ S; 141°9′ E	81	47	NDPF	NMS
390	Flinders Ranges, Australia	1565–00003	Feb. 8, 1974	31°40′ S; 138°50′ E	78	46	NDPF	NMS
391	Canberra, Australia	1034–23192	Aug. 26, 1972	34°42′ S; 149°22′ E	48	30	GE	NMS
392	Sydney, Australia	1141–23140	Dec. 11, 1972	33°19′ S; 151°9′ E	83	54	GE	NMS
393	Antarctic	1128–20284	Nov. 28, 1972	74°9′ S; 163°50′ E	72	27	GE	NMS
394	Antarctic Sea ice	2016–15062	Feb. 7, 1975	71°45′ S; 112°15′ W	75	20	NDPF	NMS
395	Ice	(*a*) 1076–13023	Oct. 7, 1972	73°13′ N; 18°0′ W	180	11	NDPF	NMS
		(*b*) 1067–00082	Sept. 28, 1972	72°1′ N; 172°49′ E	177	16	NDPF	NMS
		(*c*) 1081–23512	Oct. 12, 1972	71°55′ N; 177°1′ E	178	10	NDPF	NMS
		(*d*) 1242–22032	Mar. 22, 1973	71°55′ N; 156°8′ W	172	18	GE	NMS
396	Clouds	(*a*) 1056–11113	Sept. 17, 1972	61°19′ N; 5°21′ W	161	29	GE	JO
		(*b*) 1038–09245	Aug. 30, 1972	71°59′ N; 33°34′ E	174	26	NDPF	JO
		(*c*) 1083–08344	Oct. 14, 1972	68°2′ N; 40°18′ E	172	13	NDPF	JO
		(*d*) 1029–22212	Aug. 21, 1972	65°56′ N; 169°4′ W	162	35	GE	JO
397	Clouds	(*a*) 1082–11565	Oct. 13, 1972	64°5′ N; 14°21′ W	167	17	NDPF	JO
		(*b*) 1033–10491	Aug. 25, 1972	39°53′ N; 9°0′ W	132	52	GE	JO
		(*c*) 1064–20302	Sept. 25, 1972	71°56′ N; 132°44′ W	176	16	NDPF	JO
		(*d*) 1102–02093	Nov. 2, 1972	5°49′ S; 112°20′ E	108	58	GE	JO
398	Longest contrail	1191–15395	Jan. 30, 1973	28°53′ N; 84°14′ W	141	33	NDPF	JO
399	San Francisco	2002–18063	Jan. 24, 1975	37°26′ N; 121°43′ W	145	25	GE	NMS
400	Ireland	2139–10451	June 10, 1975	54°7′ N; 5°55′ W	139	53	GE	NMS

[a] Image source abbreviations:

APN	Aerial Photographers of Nevada
AS	Aero Service, Inc.
CCRS	Canada Center for Remote Sensing
EROS	EROS Data Center, U.S. Geological Survey, Sioux Falls, S. Dak.
ESC	Earth Satellite Corp.
GE	General Electric, Beltsville, Md.
IBM	International Business Machines Corp.
IG	Indonesian Government
JPL	Jet Propulsion Laboratory
JSC	Johnson Space Center
NDPF	National Data Processing Facility
PS	Photoscience, Inc.
SA	Spectral Africa, Inc.
UA	University of Alaska
USGS	U.S. Geological Survey, Flagstaff, Ariz.

[b] Caption author abbreviations:

CCRS	Canada Center for Remote Sensing
HAT	Herbert A. Tiedemann
HWB	Herbert W. Blodget
JO	James Oversby
LWG	Lawrence W. Gatto
MHP	Melvin H. Podwysocki
NMS	Nicholas M. Short
PDL	Paul D. Lowman, Jr.
WAF	William A. Finch, Jr.
WDC	W. Douglas Carter



SPACE PORTRAIT U.S.A.
The First Color Photomosaic of the Contiguous
UNITED STATES
Produced by
GENERAL ELECTRIC COMPANY
Beltsville Photographic Engineering Laboratory
From 569 Landsat Satellite Images
In Cooperation with
The National Geographic Society and
National Aeronautics and Space Administration
© COPYRIGHT GENERAL ELECTRIC CO. 1976